

INCLUDES
access to
full text and
image bank
online!

Practical Neuroangiography

THIRD EDITION



PEARSE MORRIS



Wolters Kluwer
Health

Lippincott
Williams & Wilkins

PRACTICAL NEUROANGIOGRAPHY

Third Edition

PRACTICAL NEUROANGIOGRAPHY

Third Edition

Pearse Morris, MB, BCh

*Director of Interventional Neuroradiology
Professor of Radiology and Neurosurgery
Wake Forest University School of Medicine
Winston-Salem, North Carolina*



Wolters Kluwer | Lippincott Williams & Wilkins
Health

Philadelphia • Baltimore • New York • London
Buenos Aires • Hong Kong • Sydney • Tokyo

Senior Executive Editor: *Jonathan W. Pine, Jr.*
Senior Product Manager: *Emilie Moyer*
Production Manager: *David Saltzberg*
Senior Manufacturing Manager: *Benjamin Rivera*
Director of Marketing: *Caroline Foote*
Senior Designer: *Terry Mallon*
Production Service: *Aptara, Inc.*

© 2013 by LIPPINCOTT WILLIAMS & WILKINS, a WOLTERS KLUWER business
Two Commerce Square
2001 Market Street
Philadelphia, PA 19103 USA
LWW.com

Copyright © 2007, 1997 by Lippincott Williams & Wilkins, a Wolters Kluwer business.

All rights reserved. This book is protected by copyright. No part of this book may be reproduced in any form by any means, including photocopying, or utilized by any information storage and retrieval system without written permission from the copyright owner, except for brief quotations embodied in critical articles and reviews. Materials appearing in this book prepared by individuals as part of their official duties as U.S. government employees are not covered by the above-mentioned copyright.

Printed in China

Library of Congress Cataloging-in-Publication Data

Morris, Pearse.

Practical neuroangiography / P. Pearse Morris. — 3rd ed.
p. ; cm.

Includes bibliographical references and index.

ISBN 978-1-4511-4415-4 (alk. paper)

I. Title.

[DNLM: 1. Cerebral Angiography. 2. Cerebral Arteries—anatomy & histology. 3. Cerebrovascular Disorders—radiography. WL 141.5.C4]
616.8'107572—dc23

2012045723

Care has been taken to confirm the accuracy of the information presented and to describe generally accepted practices. However, the authors, editors, and publisher are not responsible for errors or omissions or for any consequences from application of the information in this book and make no warranty, expressed or implied, with respect to the currency, completeness, or accuracy of the contents of the publication. Application of the information in a particular situation remains the professional responsibility of the practitioner.

The authors, editors, and publisher have exerted every effort to ensure that drug selection and dosage set forth in this text are in accordance with current recommendations and practice at the time of publication. However, in view of ongoing research, changes in government regulations, and the constant flow of information relating to drug therapy and drug reactions, the reader is urged to check the package insert for each drug for any change in indications and dosage and for added warnings and precautions. This is particularly important when the recommended agent is a new or infrequently employed drug.

Some drugs and medical devices presented in the publication have Food and Drug Administration (FDA) clearance for limited use in restricted research settings. It is the responsibility of the health care provider to ascertain the FDA status of each drug or device planned for use in their clinical practice.

To purchase additional copies of this book, call our customer service department at (800) 638-3030 or fax orders to (301) 223-2320. International customers should call (301) 223-2300.

Visit Lippincott Williams & Wilkins on the Internet: at LWW.com. Lippincott Williams & Wilkins customer service representatives are available from 8:30 am to 6 pm, EST.

10 9 8 7 6 5 4 3 2 1

To Viki, as always.

Preface

to the Third Edition

Performing neuroendovascular procedures competently and ethically demands experience, specific manual skills, and the ability to make decisions with only the patient's interests in play. These attributes cannot be acquired from a book. On the other hand, they cannot be developed without the body of knowledge which I have tried to include within this textbook. The first edition of *Practical Neuroangiography* was written with the intention of being the textbook that I wished had been available at the beginning of my own fellowship. The third edition has been revised with the same goal, that is, to provide the new fellow with the background knowledge that will allow him/her to understand these procedures, the unusual variant anatomy which can be pivotally important in certain patients, and the limitations of our abilities.

This revision of *Practical Neuroangiography* retains much of the basic instruction of its predecessors but is also adapted to bring attention to new understandings of entities such as pediatric cerebral arteriopathy, cerebral vasospasm, venous occlusive disease, and radiation use, as well as dealing with technological innovations for common and rare cerebrovascular diseases.

One important measure of the success by which the field of endovascular neurosurgery/interventional neuroradiology will

be judged is the degree to which its newer generation outshines the older. If the field is to mature, then the professional goals of new trainees need to stretch far beyond simply attaining the levels of procedural competence which they witness in their mentors. The challenges facing new trainees are different from those of 20 years ago. Technologic innovations from competing vendors have become more exciting and diversified, all with the promise of greater efficacy. But when or whether to use these new devices are often open questions. Much of what we do is driven either by the availability of technology or is done in emulation of standards set in other fields, particularly those of interventional cardiology. The developments of the past 20 years have established what can be done, but they do not tell us what should be done. There is an onus on the new generation to return the focus to outcomes, patient safety, and cost-efficacy. If this textbook can play some small role in helping the new generation to get started along the road to becoming better physicians than their mentors were, then its purpose will have been well met.

Pearse Morris, MB, BCh
Wake Forest University School of Medicine

Preface

to the First Edition

The purpose of this book is to help the reader become a more competent neuroangiographer. It was created to provide a complete and concise introduction to neuroangiography and neurovascular diseases for radiology residents, a more comprehensive review for diagnostic and interventional neuroradiology fellows, and a modern perspective to readers who trained in the past. Physicians in the related fields of neurology and neurosurgery, with whom we make clinical decisions, will also find much here that is useful.

I hope that this book will save the reader a great deal of time. I endeavored to include a range of knowledge, references, practical hints, and lessons that would otherwise be time-consuming to research or acquire. It is the book that I wish had been available at the start of my fellowship. The emphasis throughout is on practicality, concision, and safety.

The past 20 years have brought great changes to the practice of neuroradiology. MRI and CT have supplanted the use of angiography and pneumoencephalography for the evaluation

of masses and other structural lesions of the central nervous system. In tandem with these changes, interventional neuroradiology has become a dominant force in the management of neurovascular and other diseases. Increasingly, the modern mission of cerebral angiography is not simply diagnostic, but instead requires the acquisition of critical data needed for decisions on how to manage patients surgically or endovascularly. Technical and anatomic discussions in the following chapters reflect this new responsibility of the neuroangiographer.

Moreover, the field of interventional neuroradiology is gathering momentum; emergency procedures are being expected of neuroradiologists who have not had such experience. The final chapters introduce the reader to fundamental interventional principles and common emergency procedures.

Pearse Morris, MB, BCh
Wake Forest University School of Medicine

Acknowledgments

A book of this nature can only be put together when one has had the privilege and good fortune to work with superbly generous friends and highly gifted colleagues over several years. My inestimable gratitude goes to current and former colleagues from the neuroradiology, neurosurgery, neurology, ENT, ophthalmology, and anesthesia departments of the Massachusetts General Hospital, Brigham and Women's Hospital, Massachusetts Eye and Ear Infirmary, Boston Medical Center, Fletcher Allen Health Care in Vermont, and Wake Forest University Medical Center in North Carolina. The patients described in this book were cared for in their

illnesses by the nursing, technical, operating room, and ICU staff of the same hospitals with universal levels of diligence and professional commitment that have been a privilege to behold. Finally, the fellows and residents of Wake Forest University School of Medicine deserve my most sincere thanks for making the work fun. It is in the hope that they might find something worthwhile within these pages that this book goes forth.

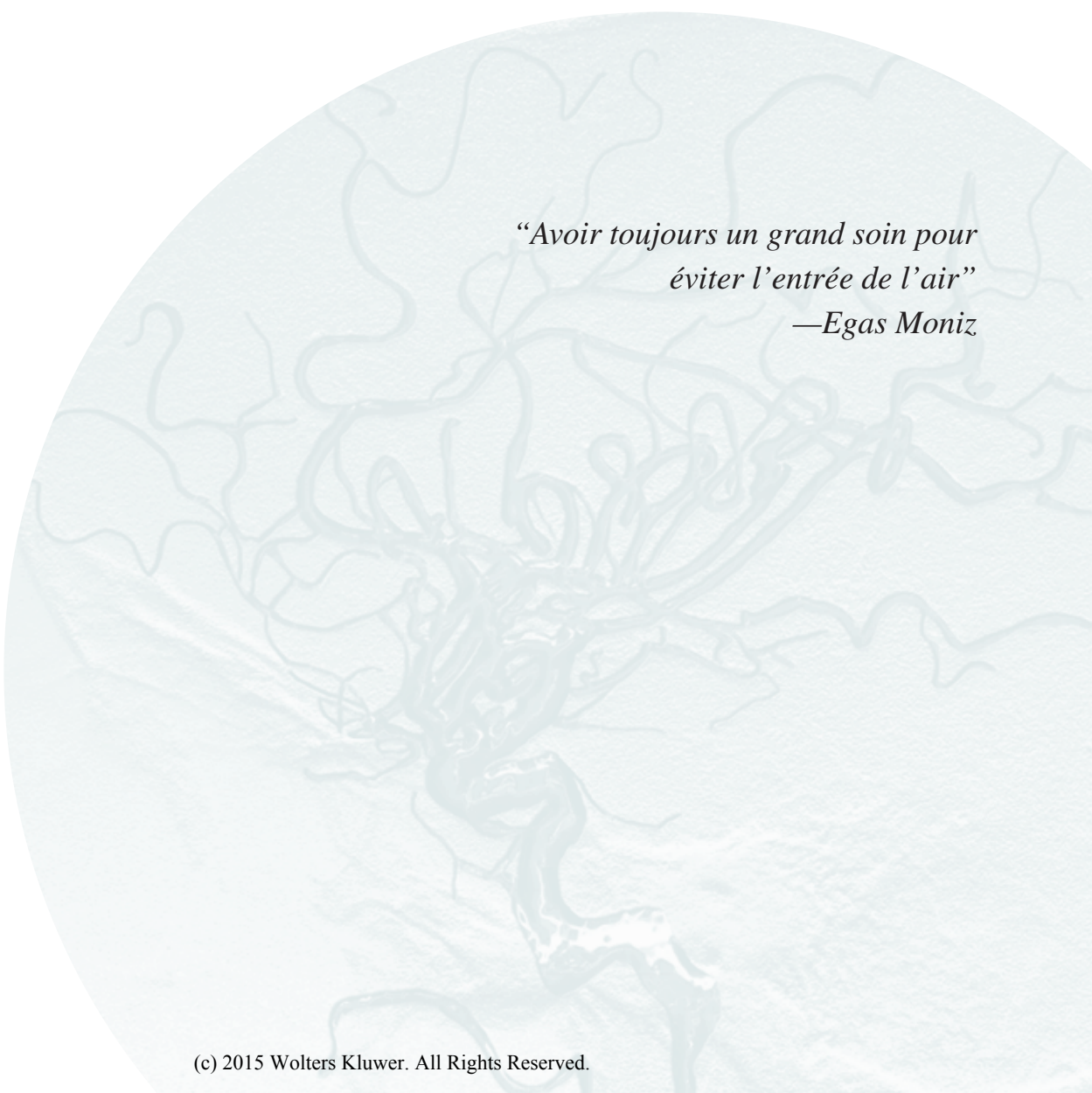
Pearse Morris, MB, BCh
Wake Forest University School of Medicine

Contents

<i>Preface to the Third Edition</i>	<i>vii</i>
<i>Preface to the First Edition</i>	<i>ix</i>
<i>Acknowledgments</i>	<i>xi</i>
SECTION I	
Techniques and Safety	1
1 History and Introduction.....	2
2 Performing a Cerebral Arteriogram.....	11
3 Spinal Angiography: Technical Aspects.....	52
4 Pediatric Neuroangiography: Technical Aspects.....	58
5 Safety and Complications.....	65
6 Radiation Risks and Safety.....	82
SECTION II	
Anatomy	99
7 Embryology of the Cranial Circulation.....	100
8 Aortic Arch.....	109
9 The Circle of Willis.....	114
10 The Internal Carotid Artery.....	132
11 The Anterior Cerebral Artery.....	161
12 The Middle Cerebral Artery.....	175
13 The Posterior Cerebral Artery.....	183
14 The Extradural Vertebral Arteries.....	195
15 The Arteries of the Posterior Fossa.....	206
16 The Venous System.....	217
17 The External Carotid Artery and Extracranial Circulation.....	231
SECTION III	
Vascular Diseases: Diagnosis and Treatment	248
18 Intracranial Aneurysms, Diagnosis and Treatment.....	249
19 Vascular Malformations of the Brain.....	291
20 Cranial Dural Vascular Malformations.....	322
21 Vascular Malformations of the Spine.....	351
22 Pediatric Ischemic Stroke and Arteriopathy.....	368
23 Carotid-Cavernous Fistulas.....	375
24 Nonaneurysmal Perimesencephalic Subarachnoid Hemorrhage.....	387
25 ENT Bleeding and Tumor Embolization.....	394
26 Reversible Cerebral Vasoconstriction Syndrome.....	426
27 Vasculitides Involving the Central Nervous System.....	434
28 Bow Hunter's Stroke.....	442
29 Dural Sinus Occlusive Disease.....	445
30 Cerebral Vasospasm.....	457
31 Angioplasty and Stenting of Atherosclerotic Disease.....	465
32 Endovascular Treatment of Ischemic Stroke.....	485
33 Vein of Galen Malformations.....	498
Index.....	505



Techniques and Safety



*“Avoir toujours un grand soin pour
éviter l’entrée de l’air”
—Egas Moniz*

1

History and Introduction

Key Points

- Willis and Moniz lived in very inauspicious times and circumstances. Using only the most primitive of tools, both left monumental legacies to medicine through their diligence, unflagging curiosity, and hard work with gifted colleagues.
- The lessons of the Thorotrast debacle are as relevant today as they were in the 1930s. Well-intentioned medical devices can be very dangerous.

► THOMAS WILLIS (1621–1675)

Thomas Willis was born on January 27, 1621, in Great Bedwyn, a small village in Wiltshire, England, and died in London on November 11, 1675, having lived his life in what the ancient Chinese maledictum refers to as “interesting times.” He had a busy and productive life, taking a Bachelor of Arts degree at Oxford in 1639 at age 18, a Master of Arts in 1642, and a Bachelor of Medicine in 1646 (1). In 1657 he married Mary Fell, thus becoming the brother-in-law of the unlovable Dr. Fell of doggerel lore. Thomas and Mary had four children, only one of whom survived to adulthood. He is buried in the north transept of Westminster Abbey.

The 17th century, which encompassed his entire life span, was a period of unparalleled political upheaval in English history, featuring several civil and religious wars, usurpation by a wart-faced tyrant, crypto-Catholicism, gunpowder plots, Long Parliaments and Rump Parliaments, regicides and restorations (2). It was a time of internal feuds and external threats. Dutch *agent provocateurs* skulked louchely behind every hedgerow, and one could not throw a stone in any corner of the kingdom without hitting some popish agent plotting sedition of one form or another. To compound the misery of the populace, adultery was declared a capital offence in 1650 by the Puritan Parliament, although, curiously, only female transgressors could be found to receive the sentence. Otherwise, the courts were clogged with proceedings related to victimless crimes such as swearing and lechery. The population declined or at least stagnated at several reprises in the latter half of the century due to the effects of disease and “warres,” while roiling epidemics of plague, smallpox, and typhus stalked the realm. In 1666, a massive fire—initially dismissed by the Mayor, Sir Thomas Bloodworth, as being of no greater merit

than “A woman might piss it out”—destroyed the City of London. Under most circumstances, such a litany of political and natural disasters might account for the decline of a nation into penury and obscurity, but the 17th century in England was an anomalous period. England entered the age in the provincial homespun of a local dominant entity in an archipelago of isles off the coast of Europe, and despite all that happened somehow emerged from it on the brink of becoming a world empire.

It was an age in which giants such as Isaac Newton, William Napier, Christopher Wren, Robert Boyle, William Harvey, and Robert Hooke milled about in gangs. As a forum for sharing their discoveries, they founded the Royal Society, putting to the sword the long stultified medieval dogmatic approach to knowledge with its exclusive emphasis on rote learning and mind-numbing Aristotelian philosophy, and laid the foundation for the growth of modern science. Willis was one of that group of intellectuals, laboring throughout at his medical practice in the town of Oxford in the midst of political turmoil, which is not to say that he was oblivious to the political events around him. His family was identified with the Royalist side, and it is known that he took a break from his studies during the first Civil War to drill with the Royalist Oxford militia. His father died in 1643 “snatched away by the Contagion of a Camp-feaver” during a siege of Oxford (3). Following this we are told that Willis the Younger “betook himself to Oxford, being the Tents of the King as well as the Muses; where listing himself a souldier in the University Legions, he received Pay for some years, until the Cause of the Best Prince being overcome, Cromwell’s tyranny afforded to this wretched nation a peace more cruel than any war” (4).

Thomas Willis began his medical studies at Oxford in 1643 at a time when the curriculum at English universities was a hide-bound 3-year course of lectures in Galenic and Aristotelian cant, declaimed every Tuesday and Friday morning at eight o’ clock by the Regius Professor of Medicine. Students had to submit evidence that they had been present at the dissection by a surgeon of two corpses, usually procured after the Lenten assizes, but medical knowledge as such was not required. Indeed, an alternative pathway to graduation was available through the offices of the Archbishop of Canterbury, who had the power to bestow a medical degree. European universities were, by comparison, considered much advanced, and ambitious students preferred to go abroad, as had, for instance, William Harvey in an earlier generation.

Fortunately for Willis, the effects of war were disruptive to this long-observed monotony of intellectual abeyance. The student population at Oxford dwindled, traditions of long usage went unobserved, and graduations grew scarce. The university buildings were converted to granaries and barracks, an epidemic of typhus ravaged the town and its hinterland, and a fire destroyed over 300 houses. The impact on Willis was to liberate him to become something of a medical autodidact, free of the pedagogic constraints that had existed hitherto. When the royal court of Charles I moved to Oxford in 1642, the royal physician William Harvey accompanied him and was appointed to the Oxford faculty, becoming a neighbor of Willis on Merton Street. His controversial and iconoclastic teachings on the circulation and other medical topics had been held in bad odor for many years by the old guard, but his arrival and appointment at Oxford at a time of such great tumult must have had an impact on the willingness of the establishment to embrace change. It seems probable that the loosening effect of the events of this period had a great influence on Willis.

From the modern coin of vantage, Willis's greatest contribution was his description of the anatomy of the brain, *Cerebri Anatome* (1664) (5), written in collaboration with Christopher Wren, Thomas Millington, and Richard Lower. This book described the anatomy of the cerebral hemispheres, brainstem, and spine with unprecedented clarity (Fig. 1-1). He cataloged the cranial nerves almost akin to how we currently enumerate them. The hippocampus, thalamus, colliculi, and superficial landmarks of the medulla

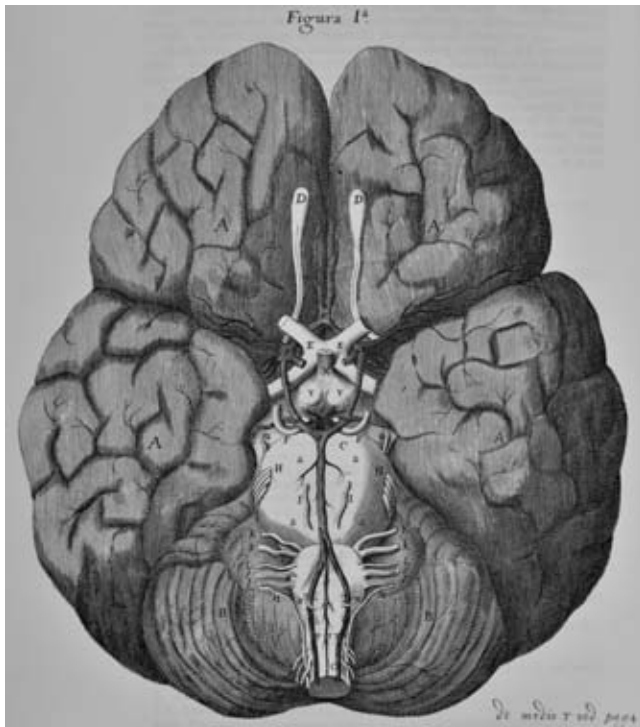


FIGURE 1-1. A diagram from Willis's 1664 textbook written in Latin, illustrated by his colleagues Richard Lower and Christopher Wren (later the architect of the rebuilt St. Paul's Cathedral in London), depicts the base of the brain in detail and is remarkably consistent with our modern understanding of this subject. The cranial nerves, thalamoperforators, mammillary bodies, anterior spinal artery, olfactory bulbs, and the circle of Willis itself are represented with astounding fidelity and clarity.

are described accurately. He speculated on the regulatory functions of the brainstem and the likelihood that the gyrated pattern of the human brain accounted for higher cognitive abilities compared with lower mammals (6). The capacity of the arterial pentagon at the base of the brain to compensate for loss of one carotid artery by compensation of flow from the other side is discussed by Willis too. The book was an immediate success for him and published in several editions in England and on the continent. This work did not, however, happen in isolation. Willis was a prolific writer of several texts throughout his professional life, demonstrating an unending curiosity about his patients and their symptoms, and exercising his ability to describe the phenomena that he witnessed in a new light, unfettered by the conventional Aristotelian wisdom. All commonplace medical symptoms were grist to his mill. He described myasthenia gravis, the sweetness of urine in diabetes (chamber-pot dropsy), schizophrenia, epilepsy, mental retardation, and scurvy. He wrote on the comparative anatomy of dogs, oysters, and earthworms. He described the phenomenon of paracuisis, which still bears his eponym. He described puerperal fever, narcolepsy, general paralysis of the insane, and whooping cough. While the medical value of these books is now severely dated, naturally, the volume and breadth of his work stand as testament to his greatness.

Willis had several key aspects of his professional life, which contributed to his well-deserved historical status and success. Primarily, he was intensely curious, and could see and describe patients and their difficulties in simple terms without a preordained bias. Secondly, he was a hard worker. His medical practice was highly successful and lucrative, not least due to his unflagging energy and willingness to make distant house calls beyond the confines of the city. In 1667, the year Willis left Oxford for London, the poll-tax records reveal that his income was 300 pounds, an enormous sum when the annual salary, for instance, of the college cook was a munificent two pounds. Thirdly, he did not work alone and was fortunate to live among friends and colleagues of a similar bent. The illustrations of *Cerebri Anatome*, for instance, are remarkably accurate and lucid, by modern standards, but these were executed by Wren and Lower. Furthermore, much of the description of comparative vascular anatomy in Willis's work, where he contrasts the human cerebral and spinal vessels and neuroanatomy with that of dogs, also owes much to his collaborators (Fig. 1-2). Based on the work of Harvey concerning the physiology of the circulation, Wren had developed, some years previously, a technique for accessing the circulation of animals using goose quills during investigation of the effects of injecting ale and opium into dogs. This technique was used by Willis and Lower for injecting India ink and alcohol pigments into the circulation of dogs and human cadaveric specimens and may also have contributed to the better preservation of his postmortem materials, compared with the inaccurate and simplistic descriptions of early writers such as Vesalius. Incidentally, a refinement of this quill technique would lead to the first instance of blood transfusion later in the same decade by Richard Lower and Edmund King (1667). Clearly, Willis's innovative contributions could not have happened without the collaboration of a remarkable coterie of friends and colleagues, all of whom were destined for greatness too in other fields of invention, science, and architecture.

By this kind of provision the Arteries about to enter the Brain are provided: yea, and the passages of the Veins, destined for the returning of the blood from thence, seem also to be disposed with a wonderful artifice. For when the anterior bosoms transfer their load into the two Laterals, which are the posterior, and they themselves end in the Jugular Veins, it is observed, that those latter bosoms have furrows or cavities insculped whereby they may settle or rest upon the hinder part of the Head: and whenas either bosom, through a proper hole, being about to go into the Jugular Vein, slides out of the Skull; nigh that hole, in the outward part of the Skull, a round and ample den is made hollow, and covered over by the extremity on either side of the same bosom, enlarged into a greater capacity, to the end, that the blood, whilst it slides forth out of the Head with a full torrent, should not rush into the Veins with too rapid and vertiginous an influx, and so make a forcible entry on the Heart it self, therefore it hath here a diversion large enough, in which estuating or boiling up, till a more free and open space may be granted to its course, it may be staid without any trouble. Certainly there can be nothing more artificial thought upon, and that can better argue the Providence of the great Creator, than this fit or convenient disposition of the blood in the brain, and without it, and the way of its reciprocation in divers Animals, accommodated to the necessity of every one. And lastly, in the dissection of Beasts, other miracles of the same nature happen, whereby shewing the finger and Divine workmanship of the Deity, a most strong and invincible Argument may be opposed to the most perverse Atheist.

FIGURE 1-2. An excerpt from Willis's textbook as "Englified" by Samuel Pordage in 1684. Apart from the observation that they all seemed to speak with a dreadful lisp back in those days, the translation has not alone a transcendent beauty in its ubiquitous poetic flourishes and stylistic paraphs, but it also introduced a wide lexicon of neuroanatomic terms that have endured to this day. Little is known of Samuel Pordage but the parlance of our profession owes him a great debt.

The most famous incident in the life of Thomas Willis concerned the ripping yarn of Anne Green, amounting to the first recorded instance of successful cardiopulmonary resuscitation (7). Anne Green was a lowly rustic wench of 22 years, toiling away in domestic service at the home of a member of the local nobility, Sir Thomas Read, when she got herself into an unfortunate state at the villainous hands of Mr. Geoffrey Read, grandson of Sir Thomas. The issue of this dilemma, a male child, was stillborn, and Anne Green was haled before the 1650 assizes on charges of infanticide, where a death sentence was handed down. Accordingly, on a cold Saturday morn in December, Anne Green was brought to the Oxford Cattle Yard, a place of execution, where "after singing a Psalme and something said in justification of herself, as to the fact for which she was to suffer and touching the Lewdness of the family wherein she lately lived, she was turn'd off the Ladder, hanging by the neck for the space of almost halfe an houre, some of her friends in the meantime thumping her on the breast, others hanging with all their weight upon her legs, sometimes lifting her up, then pulling her downe againe with a sudden jerke, thereby the sooner to dispatch her out of her paine, insomuch that the Unde-Sheriffe fearing lest they should break the rope, forebad them to do so any longer." Apparently dead, her body was placed in a coffin and "carried away in order to be anatomiz'd by some yong physitians" (8,3). According to the 1636 Royal

Charter to the university from Charles I, the Oxford professor of anatomy held claim to any corpse following an execution held within 21 miles of the town, and thus she was brought to the home of Dr. William Petty, where he, Willis, and some other local physicians were to perform an autopsy. However, when the lid of the coffin was removed, some signs of life were evident, and the party broke up into two schools of thought. The one, including the apparently incompetent executioner and some of the young men present, thought to finish her off by administering a good series of kicks in the abdomen and chest. The other, under Petty and Willis, prevailed in saving her, and after bleeding her five ounces of blood, tickling her throat with a feather to encourage breathing, and administration of restorative cordials, she was "put to bed to a warme woman." She began speaking within 24 hours, and was eating solid food at four days, recovering completely in time, except for a period of amnesia surrounding the hanging. She was granted a reprieve and subsequently a pardon, with Petty and Willis testifying on her behalf that her baby could not have survived his deformities. Anne Green lived for 15 more years apparently the object of some felicitous notoriety, married and bore three children, and lived a more comfortable life as a result of her historic adventure by virtue of her father's enterprise in charging an admission fee for curious visitors who wished to see her.

It was the sort of thing that one did in the 17th century.

► ÉGAS MONIZ (1874–1955)

António Caetano de Abreu Freire was born on November 29, 1874, in Avanca, Portugal, the eldest son of an old aristocratic family (9). While a student at the University of Coimbra, he took as pen name that of a legendary Portuguese hero, Égas Moniz, which he continued to use throughout his life. He graduated from medical school in 1899. Following studies in Bordeaux and Paris under Babinski, Pierre Marie, and Déjérine, he assumed the Chair of Neurology in Lisbon in 1911, a position he held until his retirement in 1944. Most of us would be reasonably content with as much accomplishment for one lifetime. However, Égas Moniz packed several internationally successful careers into one lifetime, to a degree that a litany of his accomplishments beggars belief. There are those who might say that early 20th-century Portugal was a less auspicious playground for providing the political and social tumult that fostered Willis's success in 17th-century England, but Moniz had the capacity to make his own times very interesting nonetheless. He died in 1955. It is fascinating to review his life accomplishments and to realize that while he was productive throughout his entire lifespan, the work for which he remains famous (cerebral angiography) and for which he won the Nobel Prize (white matter leucotomy) did not commence until he was into his 50s.

Soon after graduating from medical school, his initial interest and 1901 publication in sexual psychopathology, *A vida sexual*, shocked the public and earned the opprobrium of the Portuguese censor. A medical prescription was necessary to purchase the book. Human nature, being what it is, ordained that the book would therefore become an immediate bestseller, reaching its 10th edition by 1933. He punctuated his early medical career with several books on clinical neurology, neurologic war injuries (*A neurologia na guerra*, 1917), and several publications of a literary nature, including a biography of the hypnotist Abbé Faria (*O Padre Faria*

na história do hipnotismo, 1925) and a biography of Pope John XXI or *Petrus Hispanus*, the only physician to become pope. A social bon vivant, he was known as a lavish entertainer, a connoisseur of the arts, an epicure, a polyglot familiar with six languages, and somehow found time to dabble as a couturier, designing evening gowns for his wife and livery for his chauffeur. He was an expert in gambling and wrote a history of card games (*História das cartas de jogar*, 1942). He was also involved in a political career culminating in his appointment as Minister for Foreign Affairs and as Ambassador to Spain, and led the Portuguese delegation to the Versailles Peace Conference. He fought a duel in 1919 following a political quarrel. In 1926, a coup d'état in Portugal brought António de Oliveira Salazar to power, effectively ending democracy in Portugal for that era. These two latter events contributed to Moniz retiring from public life and facilitated a remarkable and historic reinvigoration of his medical interests at the age of 51 years. For his subsequent pioneering work of 1936 in describing the effects of prefrontal leucotomy in psychotic patients, he was awarded the Nobel Prize in medicine in 1949; but his remarkable life is better remembered now for his description of the first cerebral angiographic studies in human subjects (Fig. 1-3).

Within months of Karl Roentgen's discovery of x-rays, an angiographic study of an amputated arm was conducted successfully in Vienna using the Teichmann mixture of lime, mercuric sulfide, and petroleum (10). Building on this and on the work of other pioneers of peripheral angiography, Moniz and his colleagues, Almeida Dias and Almeida Lima, undertook a series of animal and human experiments in 1926, out of which grew the early techniques of cerebral angiography. From this period of experimentation with dogs and later with cadavers, an apocryphal anecdote survives concerning how Moniz and his colleagues were obliged to transport the human cadaveric heads across Lisbon in the trunk of his limousine to an x-ray laboratory for imaging (11). On one occasion, the limousine was unavailable, and



FIGURE 1-3. A set of postage stamps issued by the Portuguese government in 1974 to commemorate the centenary of the birth of Égas Moniz. Moniz's image has been the recipient of many such honors from the Portuguese government, appearing on stamps, coins, currency bills, and so on. On the right, an artistic rendition of one of his first cerebral angiographic images pays tribute to his major legacy to the field of modern medicine. In the center, the device depicted vaguely representing a riding crop commemorates a more dubious achievement, the one for which, ironically, Moniz was awarded the Nobel Prize in 1949. The device is a leucotome, which was inserted via a supraorbital incision into the frontal lobes where it was rotated in an authoritative manner to administer a fair old thrashing to the white matter tracts. (Image reproduced with permission from the British Medical Journal Publishing Group: Haas LF. Neurological stamp. Egas Moniz (1874–1955). *J Neurol Neurosurg Psychiatry* 2003;74(5):653.)

a taxicab was summoned to convey the materials. During the unloading of the taxi at its destination, a fumbling of the boxes resulted in a fairly dramatic spillage of several heads onto the pavement. The story goes that the incident occasioned a transport of intense emotion on the part of the taxi driver, who decamped hurriedly without awaiting his gratuity.

Moniz and his team experimented first with animals and cadavers emulating the work of Berberich and Hirsch in Germany who obtained angiographic images in 1923 of the arms, but extending this work to the cerebral vessels in living patients was an ambitious plan (12). The cadaveric work showed encouraging results depicting the intracranial vessels in a way that had not been seen before. Moniz described the curvatures of the carotid siphon and Sylvian region, terms still in use today. To obtain images in living patients, he initially attempted to use large doses of oral bromide and lithium salts, but to no avail. The notion of direct intracarotid injection of pharmaceutical agents had been familiar since the days of treatment of advanced lues, and it was to this route that Moniz turned in 1926, performing his first successful angiogram in a dog using 100% strontium bromide. In early 1927 he attempted 70% strontium bromide in patients without satisfaction. Finally on the eighth patient he was successful using 25% sodium iodide.

Immediately upon completing his cerebral angiographic studies of his first living subjects, Moniz's behavior was the exemplar of every neuroradiology fellow's instinct when coming into possession of new data, that is, parlaying the accomplishment into an instant road trip. Within a matter of days, he had hopped a train to Paris. His initial presentation of cerebral angiography in living subjects was at the Société de Neurologie in Paris on July 7, 1927, where he described two series of patients (13). A 70% solution of strontium bromide was injected directly into the internal carotid artery of the first six patients—all chronic psychiatric patients with diagnoses of general paralysis of the insane, postencephalitic parkinsonism, or brain tumors. Mechanical problems with coordination of the injection and the radiographic exposure resulted in no images with contrast being obtained in the first five patients. A Horner syndrome from perivascular extravasation of contrast developed in two patients, and a transient aphasia developed in one patient. As part of the surgical exposure of the carotid artery in the sixth patient, the internal carotid artery was ligated for 2 minutes, the better to synchronize the contrast bolus with the radiographic exposure. A successful series of four angiographic images was obtained on this patient, a 48-year-old postencephalitic parkinsonian. Ironically, the images demonstrated a thromboembolic complication of the procedure with progressive occlusion of the anterior circulation. The unnamed patient died 8 hours later.

The second series of three patients, injected with 22% to 25% sodium iodide solution, had fewer complications. Successful images were obtained in the third patient, a 20-year-old man with a diagnosis of a hypophyseal tumor causing a "Fröhlich-Babinski syndrome." The angiographic images demonstrated mass effect with displacement of the anterior cerebral artery and middle cerebral artery by the tumor. It was the capacity of this imaging technique to demonstrate the effects of tumors and masses in the intracranial cavity that would become the prime focus of clinical neuroangiography for the following decades.

Although the original presentation by Moniz has many aspects that appear quaint by modern standards—the unregulated tolerance of severe complications including at least one death, the absence of any reference to consent by the patients involved, and the cursory investigation of long-term toxicity of the contrast agents used—the body of work that he presented in 1927 is an impressive testimony to his inventive mind. His calculations of the concentration of agent necessary for visibility on film, allowing for dilution by the rapidly flowing blood of the internal carotid artery, were soundly based on a similar series of experiments performed on animals and cadavers. Out of a total of nine patients, he had successfully obtained useful angiographic images on only two, one set of which demonstrated a fatal complication of the procedure. Nevertheless, he was aware that some of the failures of the initial experiments lay with the x-ray equipment that was available to him, exposures of 0.25-second duration being too long for his purposes. He immediately foresaw the future potential of cerebral angiography for tumor characterization using stereoscopic exposures and rapid sequence cinematographically recorded injections. His paper also shows his ability to learn quickly from mistakes and his early acknowledgment of the need for technical improvements aimed at image quality and patient safety.

Moniz was severely affected all of this adult life by severe tophic gout, complications from which led to his eventual demise in 1955. All of the medical procedures that he had pioneered—cerebral angiography (1927), pulmonary arteriography (1931), and prefrontal leucotomy (1936)—were performed of necessity by assistants and colleagues, but the accomplishments of Égas Moniz in one lifetime stand as a monument to his extraordinary intellect.

A final note of biographical irony might be essayed in recounting an anecdote touching on his use (sic) of psychiatric patients for many of his medical experiments with cerebral angiography and prefrontal leucotomy. In 1939, Moniz was the target of a determined assassination attempt, in which the assailant found his mark with six bullets, four of which struck Moniz in the chest. It is not known if Moniz's reflections on this shooting, during the ample time he had for reverie over the course of a long recuperation, pondered such base ingratitude on the part of the perpetrator or the poetic retribution of class-action solidarity when his would-be assassin was identified as a "psychiatrically deranged" youth.

► THOROTRAST

Between 1927 and 1931, Moniz continued to use sodium iodide in solutions of 25% to 30%. In 1931, he and others switched to Thorotrast, a 25% colloidal solution of ^{232}Th dioxide. Despite escalating qualms over the safety of Thorotrast, this agent continued in worldwide radiologic use until after World War II, as a local or systemic contrast agent that could be imaged in virtually every body cavity. However, its use in the 1930s for cerebral angiography was associated with a high rate of thrombotic complications in the brain, as high as 60% in postmortem surgical cases (14). Local perivascular extravasation of Thorotrast in the neck was a common problem with abscess or granuloma (thorotrastoma) formation after the procedure (Figs. 1-4 and 1-5). For those patients who survived the procedure,

FIGURE 1-4. Lateral neck radiograph of a 74-year-old man who underwent carotid angiography with Thorotrast in 1946 for investigation of headaches. No specific diagnosis was made at the time. The procedure was complicated by extravasation of Thorotrast around the right carotid artery. Since that time, he had recurrent problems with a chronically draining sinus on the right side of the neck and had several rounds of chemotherapy for lymphoma. The patient's presentation almost 50 years after the initial angiogram was related to a sentinel bleed from his neck sinus, described as being sufficient to soak a large towel. Most of the Thorotrast patients are now deceased, but until recently, it was a fairly common occurrence for one of these patients' films to show up in "Stump the Chump" sessions of unknown case presentations for celebrity panels or in case reports. Abdominal films or CT examinations with dense livers and spleens were typical. In the neck, magnetic resonance images in such Thorotrastoma patients featured the unusual distinction of showing bright T1 signal from the extravasated material (28).



Thorotrast became an albatross around (and in cases of extravasation, within) their necks in later life. Procedure-related morbidity and mortality continued to follow some of these patients for years (Figs. 1-6–1-8). Thorotrast, an alpha-particle emitter with a physical half-life of 1.41×10^{10} years and a biologic half-life of 400 years (15), was sequestered particularly by the liver (60%), spleen (20%), and red marrow (12%). Exposed patients were also at risk from the decay products of ^{232}Th , including ^{226}Ra , ^{228}Th (mesothorium), and the bone-seeking radionuclide ^{224}Ra . High rates of malignant complications ensued in these target organs as well as in the neck and mediastinum adjacent to the sites of extravasation, or where it was retained in body cavities, such as the paranasal sinuses. By the time its use was discontinued around 1954, it had been adminis-

tered for a variety of radiologic procedures to perhaps as many as 2.5 to 10 million people (16–18). The fraction of patients who had intravascular administration is not known.

Follow-up studies of Thorotrast patients from Denmark (19), Germany (20,21), Portugal (22), Japan (23,24), and other countries indicate a high rate of delayed malignant disease attributable to this agent. Systemic administration of Thorotrast (15–40 mL for a typical cerebral study) has been estimated to cause a liver radiation dose of approximately 40 centigrays (cGy) per year accumulating to 16 grays (Gy) over 40 years (18). Subsequent malignancies particularly included tumors of the hepatobiliary system, which had a 200-fold increase in risk above baseline in the German and Japanese studies, and radiation-related

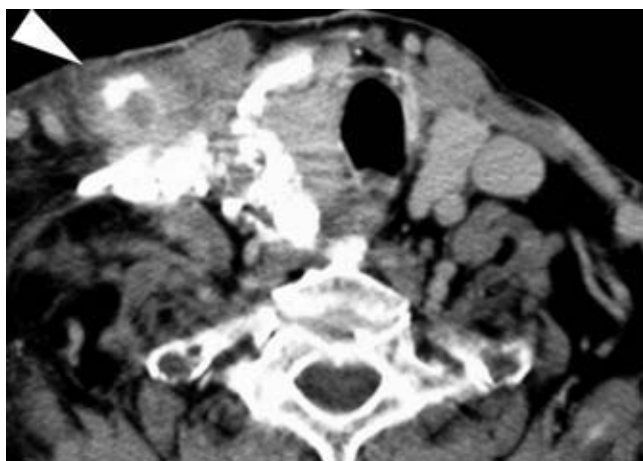


FIGURE 1-5. Neck computed tomography without contrast on the same patient as Figure 1-4 obtained from a previous admission. High-attenuation Thorotrast has dissected through the soft-tissue planes of the neck and was evident in the upper mediastinum (not shown). The patient's cutaneous sinus approximately at the level of this image is in a location marked by the arrowhead.

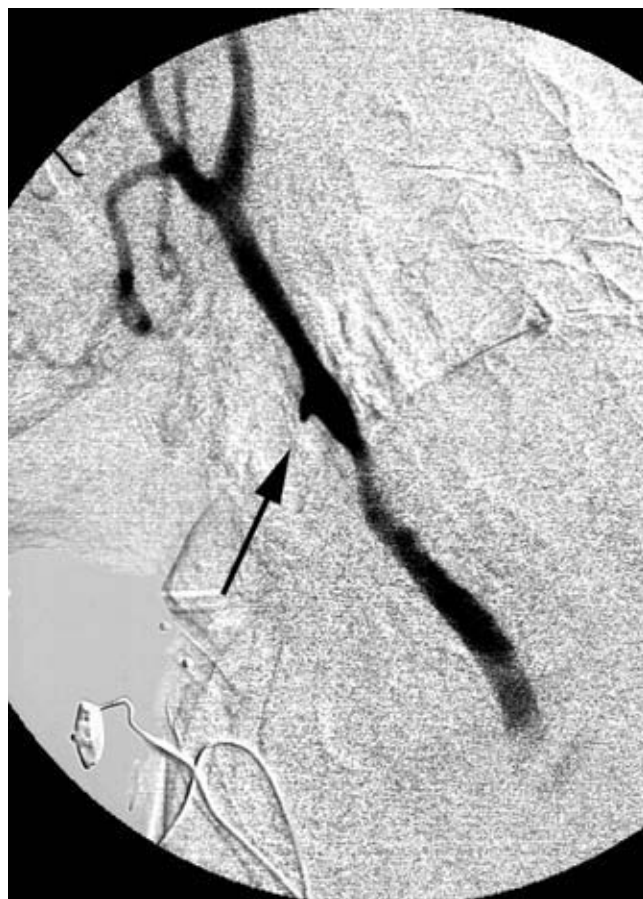


FIGURE 1-6. Right common carotid artery arteriography in the lateral plane demonstrates a pseudoaneurysm (*arrow*) of the common carotid artery close to the sinus tract, the presumed source of the sentinel bleed. There is prominent subtraction artifact over the artery due to the density of the Thorotrast.

leukemia such as the nonchronic lymphocytic type (non-CLL) (20,21) with a 10-fold increase in risk (15), in addition to other malignancies.

The ever-dwindling numbers of Thorotrast patients were studied sequentially through the 1960s and followed intermittently to the conclusion of the major cohort studies in the 1990s because their exposure and its consequences constituted a valuable and virtually unique source of data on the human effects of chronic alpha-radiation exposure. Data from these studies are still used and incorporated into guidelines and recommendations on what represents reasonably safe levels of radiation exposure for internal organs. However, other lessons to be drawn from the Thorotrast disaster might dwell on what can happen to patients in an environment of lax regulatory supervision. A dentist, Dr. T. Blum, recognized in 1924 that radium dial painters were being exposed to the risks of ingestion of radium by the practice of “tipping” their brushes—that is, pointing their wet brushes with their lips. He described the first patient with osteonecrosis of the jaw and recognized the similarity of this condition to the “phossy jaw” described in the 19th century in workers exposed to white phosphorus in match factories (25,26). The practice of tipping of brushes in radium dial painters was subsequently banned in the United States in 1926, 5 years before ^{232}Th became the standard agent for cerebral angiography. The use of ^{232}Th cannot be defended therefore, even in retrospect, by presuming that the profession was ignorant of the effects of radiation between the years of 1928 and 1954. Quite the converse. Henri Becquerel suspected early on that injuries seen in pioneer radiation workers were related to the effects of radiation, and Marie Curie—who later lost her own life to the effects of radiation exposure—was quoted in a 1927 interview deploring “the handling of such dangerous substances as radium and mesothorium in such a careless manner” (27). In the absence of regulatory oversight, the medical profession does not have a good history of policing itself adequately to assure that similar debacles cannot happen again.

If the estimate of 2.5 to 10 million patients placed at risk from Thorotrast administration is even remotely accurate, then the magnitude of this historical disaster becomes difficult to encompass. It is frequently said that until the mid-20th century, the practice of medicine killed more patients than it helped. Unfortunately, this may be true where the use of Thorotrast is concerned, and particularly so in reference to its use in neuroangiography. During the 1930s and 1940s, it was unlikely that a seriously ill patient could be cured based on information gathered from a neuroangiographic procedure alone.

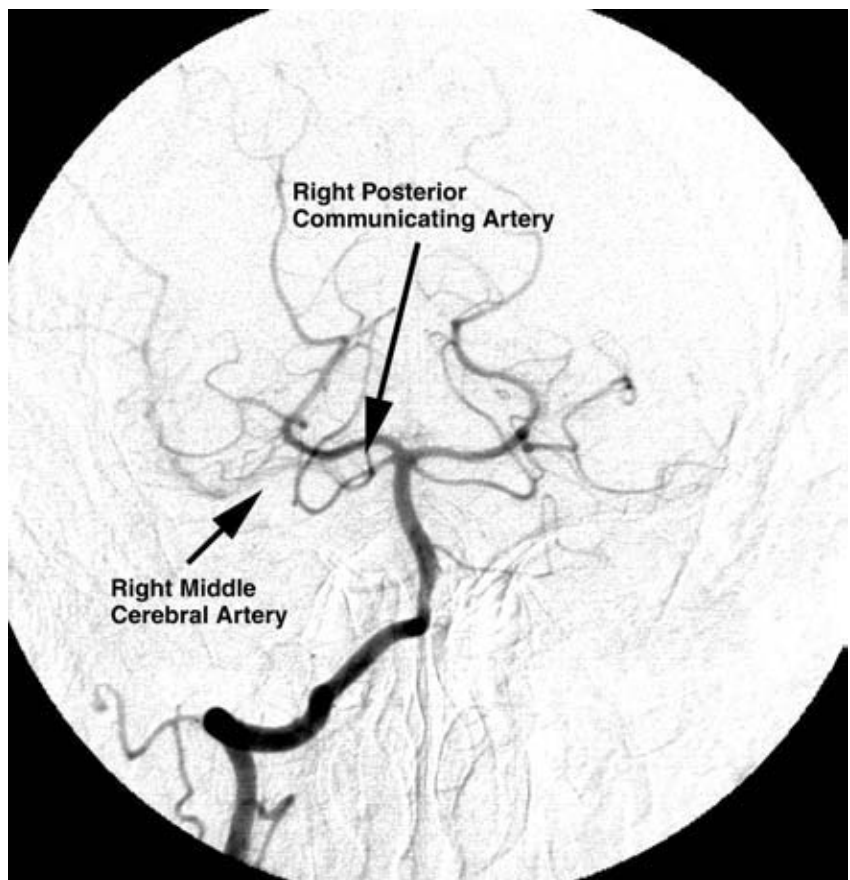
From these inauspicious beginnings, the field of neuroangiography has endured. Although the standards of equipment, material, and radiographic technique are superior today than could have been foreseen in 1927, it, nevertheless, behooves us to bear in mind that the same overarching potential for disaster, as experienced by Moniz's patients, still exists in every neuroangiographic procedure. Furthermore, an extrapolation of the Thorotrast history would counsel us to value the necessity of regulatory bodies at a governmental and institutional level. Our field is developing rapidly in the interventional domain with increasing availability of new devices and sleekly designed fluoroscopy units, and the immediate outcome is more radiation use, longer procedures, and fascinating implantable devices about which we have, at this time, a paucity of long-term data.

FIGURE 1-7. Left common carotid arteriography demonstrates prompt cross filling to the right anterior cerebral artery via the anterior communicating artery. In addition, the A1 segment (*arrow*) on the right is robust, a finding auspicious for the capacity of the circle of Willis to compensate for the intended emergency therapeutic sacrifice of the right carotid artery.



FIGURE 1-8. A shallow Townes projection of the right vertebral artery injection. The right posterior communicating artery is moderate in size and opacifies the right middle cerebral artery territory faintly. Due to previous surgical scarring and radiation-related induration of the neck, a surgical repair of the pseudoaneurysm was not possible. The patient tolerated emergency balloon occlusion of the right internal and common carotid artery, and was discharged home neurologically intact without further bleeding. (This case dates from some years ago. Today, a preferable therapeutic option would be preservation of the carotid artery through use of a covered stent at the bleeding site.)

Before being discharged, this patient was asked for his thoughts on this procedure and several decades of bad health directly related to his Thorotrast exposure—several surgically attempted repairs of his neck sinus, chemotherapy for two different types of lymphoma, and a balloon sacrifice of his right carotid artery. He considered the matter and commented dryly that “it wouldn’t have been half as bad if it hadn’t been for all those university researchers calling me weekly, asking to donate blood and marrow samples [for their work on chronic radiation exposure].”



References

1. Isler H. *Thomas Willis 1621–1675 Doctor and Scientist*. New York, London: Hafner Publishing Company; 1968.
2. Kishlansky M. *A Monarchy Transformed. Britain 1603–1714*. London: Penguin Press; 1996.
3. Willis T. *The Anatomy of the Brain and Nerves*. Montreal: McGill-Queens University Press; 1965.
4. Symonds C. *The Circle of Willis*. London: British Medical Association; 1955.
5. Willis T. *Cerebri anatome; cui accessit nervorum descriptio et usus*. London: J. Flesher; 1664.
6. Molnar Z. Thomas Willis (1621–1675), the founder of clinical neuroscience. *Nat Rev Neurosci* 2004;5(4):329–335.
7. Hughes JT. Miraculous deliverance of Anne Green: An Oxford case of resuscitation in the seventeenth century. *Br Med J (Clin Res Ed)* 1982;285(6357):1792–1793.
8. Watkins R. *Newes from the Dead*. Oxford: Robinson; 1651.
9. Ligon BL. The mystery of angiography and the “unawarded” Nobel Prize: Egas Moniz and Hans Christian Jacobaeus. *Neurosurgery* 1998;43(3):602–611.
10. Hascheck E, Lindenthal O. Ein Beitrag zur praktischen Verwethung der Photographie nach Röntgen. *Wien Klin Wochenschr* 1896;9(4):63–64.
11. Doby T. Cerebral angiography and Egas Moniz. *AJR Am J Roentgenol* 1992;159(2):364.
12. Antunes JL. Egas Moniz and cerebral angiography. *J Neurosurg* 1974;40(4):427–432.
13. Moniz E. L'encéphalographie artérielle, son importance dans la localisation des tumeurs cérébrales. *Revue Neurologique* 1927;2:72–90.
14. Eckström G, Lindren A. Gehirnschädigungen nach cerebraler Angiographie mit Thorotrast. *Z für Neurochir* 1938;2:227.
15. Andersson M, Carstensen B, Visfeldt J. Leukemia and other related hematological disorders among Danish patients exposed to Thorotrast. *Radiat Res* 1993;134(2):224–233.
16. Abbatt JD. History of the use and toxicity of thorotrast. *Environ Res* 1979;18(1):6–12.
17. Falk H, Telles NC, Ishak KG, et al. Epidemiology of thorotrast-induced hepatic angiosarcoma in the United States. *Environ Res* 1979;18(1):65–73.
18. Travis LB, Hauptmann M, Gaul LK, et al. Site-specific cancer incidence and mortality after cerebral angiography with radioactive thorotrast. *Radiat Res* 2003;160(6):691–706.
19. Andersson M, Storm HH. Cancer incidence among Danish Thorotrast-exposed patients. *J Natl Cancer Inst* 1992;84(17):1318–1325.
20. van Kaick G, Wesch H, Luhrs H, et al. Radiation-induced primary liver tumors in “Thorotrast patients.” *Recent Results Cancer Res* 1986;100:16–22.
21. van Kaick G, Wesch H, Luhrs H, et al. Neoplastic diseases induced by chronic alpha-irradiation—Epidemiological, biophysical and clinical results of the German Thorotrast Study. *J Radiat Res (Tokyo)* 1991;32 suppl 2:20–33.
22. Da Silva Horta J, Da Silva Horta M, Cayyolla de Motta Lea. Malignancies in Portuguese Thorotrast patients. *Health Phys* 1978;35:137–151.
23. Mori T, Kido C, Fukutomi K, et al. Summary of entire Japanese thorotrast follow-up study: Updated 1998. *Radiat Res* 1999;152(6 suppl):S84–S87.
24. Mori T, Kato Y. Epidemiological, pathological and dosimetric status of Japanese thorotrast patients. *J Radiat Res (Tokyo)* 1991;32 suppl 2:34–45.
25. Cherniack MG. Diseases of unusual occupations: An historical perspective. *Occup Med* 1992;7(3):369–384.
26. Miles AE. Phosphorus necrosis of the jaw: “Phossy jaw.” *Br Dent J* 1972;133(5):203–206.
27. Fry SA. Studies of U.S. radium dial workers: An epidemiological classic. *Radiat Res* 1998;150(5 suppl):S21–S29.
28. Kesava PP, Perl J, Mehta MP, et al. Thorotrast-associated oropharyngeal hemorrhage: Treatment by means of carotid occlusion with use of flow arrest and fibered coils. *J Vasc Interv Radiol* 1996;7(5):709–712.

Performing a Cerebral Arteriogram

Key Points

- New fellows in our room are often nonplussed as to why we only have two CDs for our music system. One of these is “*The Greatest Hits of Marty Robbins*” and we never play the other one. The point this detail makes is that neuroangiography is safest when practiced in a methodical, repetitive, consistent manner. Every angiogram is executed through the exact same steps, as much as possible. Certainly, there are many days when creativity, ingenuity, and improvisation are in great demand, but these moments are often best avoided and forgotten. The purpose of the music is not entertainment but providing a familiar ambiance. The priority in the room is safety.
- Safe technique can only come about through absolutely consistent practice of safe habits. In most patients, most of the time, such scrupulousness is redundant, but these habits are not aimed at the majority of cases. They are aimed at those rare, unforeseen circumstances when they will make a big difference.

► REVIEW THE PREVIOUS STUDIES

The importance of this preliminary step cannot be overemphasized. Relying on typed reports of what was seen on the previous studies, which side the findings were on, and the like, is a recipe for oversight, omission, or worse.

► EXAMINE AND TALK TO THE PATIENT

In the course of obtaining consent from the patient, a focused neurologic examination by the neuroradiologist, documented in the patient’s chart, is a worthwhile expenditure of 5 or 10 minutes. This examination should dwell on the patient’s known or suspected neurologic deficits. It should also include a baseline evaluation of those functions most likely to deteriorate in the event of angiographic misadventure. Therefore, a quick evaluation of the patient’s mental status, memory, orientation, language, visual fields and lower cranial nerve function, motor power, gait, and gross coordination should be

de rigueur during all consent interviews. An adverse event in the course of an angiographic examination is rare. However, calls to the nursing floor to evaluate a patient with minor complaints of headache or apparent change in mental state after an angiogram are common and can be dealt with quickly for having previously documented the baseline condition of the patient. Such complaints are usually trivial in nature. However, a complaint of headache and a focal neurologic deficit that may be new after a cerebral angiogram can evolve into a time-consuming process, which can be avoided.

Similarly, baseline evaluation and marking of the peripheral pulses, using a Doppler device if necessary, will help to avoid unnecessary consumption of time afterward. Prompt recognition of deterioration of a pulse can expedite a consultation with vascular surgery for suspected iliac or femoral artery dissection. On the other hand, a poor pulse obtained after an angiogram without a prior evaluation is an open-ended question.

Patients should remove all jewelry and dental prostheses before the case begins. Such devices, when left in place, have a way of projecting precisely on the area of abnormality, and their removal from the patient during the case, with a catheter already in the internal carotid or vertebral arteries, is not a benign or convenient interruption.

► PLAN THE ANGIOGRAPHIC STUDY

Many cervicocerebral angiographic studies have such a formulaic pattern that it is sometimes easy to fall into a groove and thus perform a study that does not adequately answer the question for a particular patient. Such omissions most commonly center on an oversight to study the aortic arch or to obtain images of the external carotid system when the question of a bypass procedure is being considered. Patients being studied for subclavian steal will require particular stratagems during their procedure to draw a distinction between the images obtained at rest and those obtained in a state of physiologic exertion.

Omission of an external carotid artery injection is a common oversight in cerebral angiographic studies. Most often, this shortfall only becomes apparent long after the study, when discussion of surgical options for an identified lesion

turns to the alternative of external-to-internal bypass procedures. To avoid the retrospective embarrassment of having one's work so criticized, one should anticipate questions about the external carotid circulation where bypass procedures or the possibility of involvement of the external carotid artery with disease states might be considered:

- Occlusive diseases such as Moyamoya disease, intracranial or extracranial dissections.
- Giant intracranial or otherwise inoperable aneurysms. A bypass procedure with subsequent surgical or endovascular occlusion of the parent vessel might be considered in certain difficult circumstances.
- Serpentine or dysplastic aneurysms of the middle cerebral artery.
- Cavernous aneurysms.
- Brain arteriovenous malformations (AVM) when the AVM extends to the surface of the brain, and particularly when there has been prior infraction of the dura by a surgical procedure increasing the likelihood of dural-pial anastomoses.
- Dural vascular disease as a possible cause of subarachnoid or intraparenchymal hemorrhage.

▶ WHAT CATHETER SHOULD I USE?

Use whatever catheter you have most experience and comfort with (Fig. 2-1). The calibration systems in use derive from mid-19th-century industrial standards and have not been coalesced into a modern or unified scheme, unfortunately. Catheter outer diameters (OD) are measured in the French system, inner diameters (ID) are measured in inches, percutaneous needles are measured in a Gauge system, and embolization coils are measured in millimeters. There is not an easy way to correlate all of these measurement systems except to work consistently with a proven set of instruments. Generally, the disparity of the systems of mensuration is of little significance, but it is possible for practical problems to arise. Therefore, testing the compatibility of devices before insertion into the patient is a good pragmatic solution.

Catheter tips are tapered or untapered. Untapered catheters can be inserted only through a sheath. Catheters of 4F or 5F size are the standard for diagnostic neuroangiography. A 5F cerebral catheter has an OD of 0.066 inches, with an ID up to 0.050 inches. Manufacturing techniques have

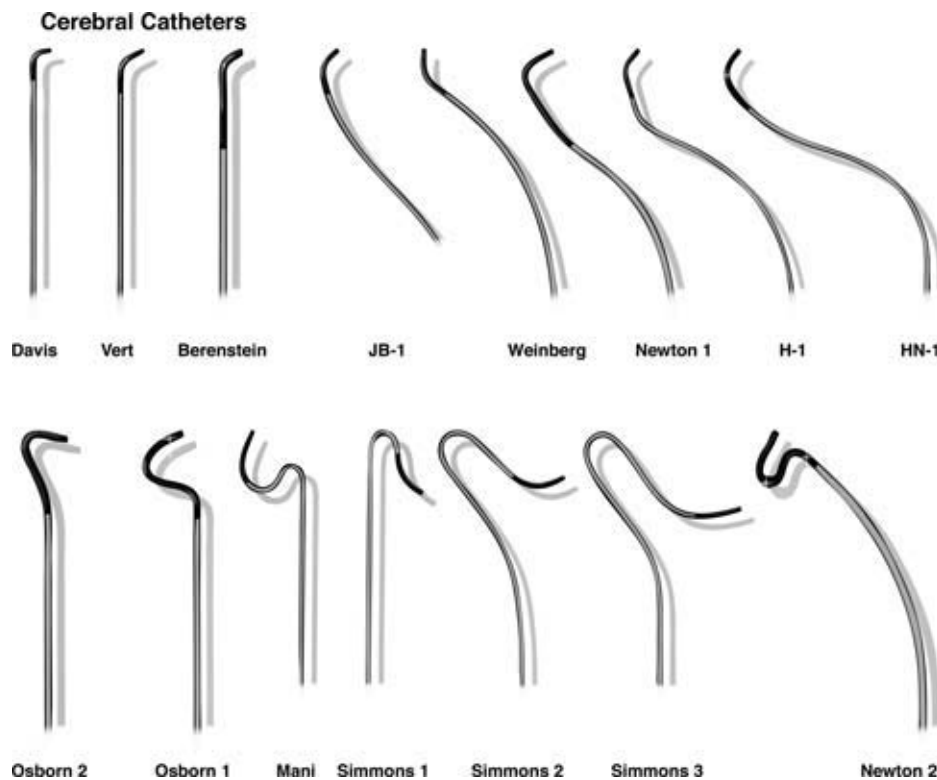


FIGURE 2-1. Cerebral catheters. A likely apocryphal legend has it that there are 25 words in the Inuit language for *snow*, so it should be no surprise, therefore, that there are as many in neuroradiology parlance for *catheter*. Just as some forms of snow are better for building an igloo than others, certain catheters are better than others in some extreme circumstances. However, the differences are marginal, and you have to know a lot about the basics of building igloos before you focus on what building materials you prefer. Catheters requiring reconstitution of their curve in the arch such as the Simmons series are more limited in their capacity for distal vessel selection. Most experienced neuroangiographers have an extremely limited repertoire of what they consider to be necessary armament for their work. Catheter length is a different matter. Most standard catheters are 100 cm long. Longer catheters (125 cm) are sometimes pivotally important for selecting difficult vessels when a larger size catheter or sheath in the vessel is the ultimate goal. Selecting the vessel with a wire and standard curve 125-cm catheter can then facilitate advancing an otherwise impossible device. Shorter catheters (60–90 cm) are also important to keep in stock for interventional cases where embolic devices might restrict the length of introducer catheter.

TABLE 2-1 Minimization of Contrast Load

The total dose of contrast needed for a particular cerebral angiogram can be reduced by 50% or more by using the following guidelines. See Figure 4-4 and accompanying caption.

- Using lowest-strength contrast where possible, for example, using 200-strength nonionic instead of 300.
- Careful planning of injection and fields of view to avoid need for repeated injections.
- Elimination of unnecessary runs, for example, aortic arch injections require 30–50 mL of contrast for a diagnostic yield so low that an aortogram is usually not warranted as a routine part of a cerebral arteriogram (1).
- Using contrast syringes on the table filled half and half with contrast and saline. Diluted contrast is adequately visualized on modern image intensifiers to allow considerable saving in contrast load through this means.
- Improving technique of roadmap acquisition; most roadmap systems respond better to a smaller-volume staccato burst of contrast than to a slow 10-cc infusion. A shorter roadmap acquisition may also eliminate artifact from respiratory motion.
- Exploiting the capacity of modern equipment to avoid roadmap acquisition in certain circumstances by overlaying previously acquired images for use as roadmap guides.
- Preloading the dead space of the catheter system with half-strength contrast and pushing it with saline when roadmaps are needed. This technique is very important in children and patients with severe renal failure and is discussed in Chapter 4.
- Aspirating contrast from the dead space of the catheter system at the completion of each run before resuming flush. This and the previous measure can save 2–3 mL of contrast per injection, which can make a critical difference in a child in a study with multiple injections.

improved in recent years so that it is now possible to perform most endovascular procedures with a 5F or 6F introducer catheter. Interventional procedures requiring larger-caliber devices, such as carotid stenting, can be performed via a long 6F sheath used in place of a catheter.

► CONTRAST

Despite its relative expense, nonionic contrast is now the standard for cerebral angiography. Nonionic contrast agents are denominated according to the content of organic iodine per milliliter; for example, Omnipaque 300 contains 647 mg of iohexol per milliliter, equivalent to 300 mg of organic iodine per milliliter. The improved performance of modern image intensifiers in digital imaging allows one to consider use of a lower concentration of contrast for cerebral angiography. Nonionic 180 to 200 preparations provide adequate vessel opacification on modern machines, with the advantage of a lower iodine total dose and a lower osmolality challenge to the blood–brain barrier (Tables 2-1 and 2-2). Lower-strength contrast has the additional advantage of a lower viscosity compared with preparations of higher concentration. This is a factor for consideration in microcatheter injections either by hand or by power injector or with reference to inflation and deflation of angioplasty balloons.

► ARTERIAL PUNCTURE AND SHEATH PLACEMENT

The arterial puncture must be made with a view to hemostasis after completion of the study. The most common error among beginners is to perform the puncture too high, above the inguinal ligament. Therefore, the angle of insertion of the arteriotomy needle is approximately 45 degrees to the skin in a line on a plane with the direction of the artery and in a site that allows compression against a bone afterward. The easiest site is at the common femoral artery on the right side (Figs. 2-2–2-8). The most critical procedure in gaining

access to the artery is the passing of the wire, which runs the risk of intimal or medial dissection. Seldinger technique with a 0.035-inch wire used to be a standard approach in adults, but the popularity of micropuncture technique is a definite improvement from every point of view. Occasionally, a very scarred or copiously endowed groin will require the support of a stiff wire such as a Rosen or Amplatz, but these impasses can be negotiated with sequential dilations once the initial access is obtained.

Wiping the wire clean of blood and clot between successive passes of the dilators, the arterial site is progressively dilated to allow smooth passage of the sheath dilator/obturator and finally of the sheath itself (Fig. 2-5). The sheath is hooked up to flush, the dilator is removed with the



FIGURE 2-2. Landmark palpation. In nonobese patients, palpating the anterior superior pubic tubercle and the anterior superior iliac spine will identify the location of the inguinal ligament. Three fingers' breadth below that line should place your right ring finger close to or on the inguinal crease. If these landmarks are concordant, it is probably not necessary to examine the groin with fluoroscopy ahead of the puncture.

TABLE 2-2 Contrast Agents Used in Cerebral Angiography

NAME	SOLUTION (mg/mL)	OSMOLALITY (mOsmol/kg water) ^a	VISCOSITY (cp at 37°C) ^b	IODINE CONTENT (mg/mL)
Isovue 200 iopamidol	408	413	2.00	200
Isovue 300 iopamidol	612	524	4.70	300
Omnipaque 180 iohexol	388	408	2.00	180
Omnipaque 300 iohexol	647	672	6.30	300
Optiray 240	509	502	3.00	240
Optiray 300	606	651	5.70	300
Optiray 320 ioversol	678	702	5.80	320
Visipaque 270	550	270	6.3	270
Visipaque 320 iodixanol	652	290	11.8	320
$\frac{\text{Weight kg} \times 5(\text{adult}) \ 4(\text{child})}{\text{Serum creatinine mg/dL}} = \text{tolerable volume of 300 nonionic contrast}$				
<p><i>Example:</i> A 75-kg adult patient who is well-hydrated with a serum creatinine of 1.5 mg/dL would tolerate an approximate total dose of 250 cc of ionic 60% or of nonionic 300 preparations, equivalent to 70.5 and 75 g of iodine, respectively. If using the lower concentrations of 43% or ionic 200 preparations, these equivalent doses calculate to an allowable volume of 349 and 375 cc, respectively. These volumes assume that the patient is adequately hydrated and that no other prevailing medical condition is present. The serum creatinine alone as an index of renal function is also increasingly fallible with advancing age. Chemistry laboratories now report estimates of creatinine clearance based on age and weight. This parameter is a more reliable indicator of the need to be cautious in planning high-dose procedures. The total volume of contrast may be extended in cases where the entire duration of contrast administration is prolonged over many hours, such as during an interventional procedure, where volumes of contrast in excess of 800 mL have been used without adverse incident (2). The pharmacokinetics of intravascular contrast materials are described as having an α phase (distribution) and an α half-life of approximately 30 min, and a β phase (elimination) with a β half-life of 1.5 to 2 hr in a patient with normal renal function and adequate hydration. Therefore, after 2 hr, about half of the contrast administered will have been excreted, allowing a commensurate recalculation of the maximum tolerable dose. In the setting of renal impairment, the β half-life becomes prolonged up to days in duration.</p>				

^aNormal human plasma osmolality, 282–295 mOsm/kg water.

^bViscosity of water is approximately 1 centipoise (cp), and that of static human blood at 37°C is about 3.5 cp.

wire, and the sheath is sutured or otherwise secured in position. While passing the sheath or dilator, a spinning motion of the advancing hand helps to twist the device into the artery smoothly and minimizes trauma to the arterial wall. Slight tension on the wire provided by an assistant helps this passage.

Difficulty with passing a dilator or sheath over the wire should prompt a pause to evaluate the tip of the device lest it should have become damaged during the attempted insertion. Examine the tip carefully. It is common to find that the plastic sheath fitted over the dilator has developed a small tear or irregularity that would possibly lacerate the vessel wall if it were forced through the arterial puncture site.

► RADIAL ARTERY ACCESS

If all cerebral angiography could be performed via a transradial approach, the world would be a sunnier and happier

place, just as it is for cardiologists. The radial artery has become the default site of access for 60% to 80% or more of cardiac catheterizations in sizes up to 7F, although 6F is considered the upper size of comfort range for most adults (3–5). The reasons for this are manifold. This route is safer with fewer hemorrhagic and other complications. Control of the artery afterward is much easier and interruption of anticoagulant or antiplatelet medication is less of an obstacle compared with a transfemoral route. One of the largest studies of the transradial approach in the cardiology world identified a 67% reduction in bleeding complications compared with the transfemoral approach (6,7), fewer delayed incidents of bleeding, and significantly fewer cases needing surgical repair of pseudoaneurysms. Patients find a transradial procedure much less intimidating and less invasive on their dignity, and mobilization afterward is not even a consideration (Figs. 2-9 and 2-10).

The radial artery approach has attracted some attention in the neuroangiography world, with universally favorable



FIGURE 2-3. Local anesthetic injection. There are several points to bear in mind with this apparently simple component:

- Agitated or confused patients will frequently jump at the first dart of the needle. Therefore, with endemic creepy-crawlies an ever-present hazard, keep your left hand away from the artery site when you are first entering the skin, in order to avoid sticking yourself with the needle.
- This is a tender area of the body. Brimming with some misguided sense of aesthetic zeal, beginning residents typically have a penchant for restricting the infiltration to 2 to 3 mL of lidocaine. “I’m saving the rest for the periosteum” goes the defensive refrain. Give the whole 10 mL, or even more!
- The nerves serving the tissues of interest sweep from lateral to medial and are thus most economically and effectively numbed by infiltration lateral to the artery. Attempts to infiltrate around the artery itself invariably meet with a successful and undesirably premature localization of the artery.
- And most important, the unwritten annals of neuroangiography are replete with unreported incidents where syringes of clear fluid on the table have been used as contrast during the case, only to discover that the remaining 7 mL of lidocaine that should have been used in the groin are now circulating in the patient’s brain announced by the abrupt onset of status epilepticus. Lidocaine syringes must be marked clearly with tape or other indicator before filling the syringe at the beginning of the case. That syringe must *always* be disposed of before the case gets under way. Leaving the syringe, marked or otherwise, on the table for later in the case is an invitation to some new fellow, resident, or assistant to do the inevitable.

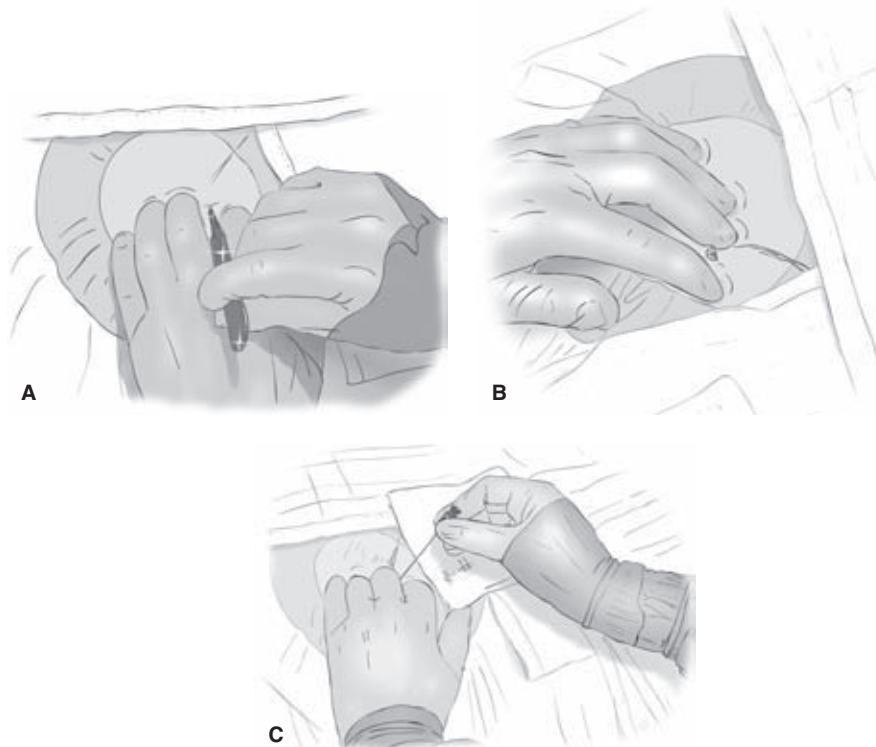


FIGURE 2-4. (A–C) Arteriotomy. A small, horizontal nick is made in the skin over the artery and opened with a tissue spreader to allow easy entry of the sheath and to facilitate escape of any subcutaneous bleeding in order to avoid accumulation of hematoma. It is quite possible to nick the artery in a thin patient or in a child. To avoid this, the nick is made with the scalpel held in a near-horizontal position with the blade pointed superiorly. The safety of the underlying artery can be preserved still more by squeezing redundant tissue between the left index and middle finger as shown, while the right hand approaches with the upward-facing scalpel (A). After the nick has been made and expanded, the artery is palpated on the points of one’s fingers exactly the way one palpates it while compressing the artery after the case (B). The index, middle, and ring fingers form a straight line pointing toward the umbilicus from a point just lateral to the ipsilateral knee. The skin wound should remain uncovered during all stages of the arteriotomy and arterial compression; its purpose is to allow blood to escape from the subcutaneous tissues in the event of bleeding. Compressing the skin wound is therefore counter to the purpose in hand. When making the puncture (C), the left hand maintains the exact same position while the needle is driven in at an angle of approximately 45 degrees. In our department at Wake Forest University Medical Center, micropuncture kits are used exclusively for arterial access. They are entirely satisfactory and less traumatic to the artery than previously used single-wall or double-wall 18G needles. Their only disadvantage is that the 0.018-inch wire does not give the biofeedback one requires to be assured that the wire is traveling retrogradely up the artery safely in all instances, and the fluoroscope is necessary to confirm this in many patients.



FIGURE 2-5. Sheath or dilator advancement (somewhat suboptimal technique). There are several lessons to be derived from this illustration. First, observe the left hand, which is in the exact same position as before except that the index finger is moved out of the way to allow advancement of the sheath. Swab the groin wound before advancing the sheath to clean up blood and clot. As mentioned earlier, the skin wound should be visible and free of encumbrances at all times. Otherwise, something is going to get pushed into the artery, most likely a redundant flap of an ill-fitting glove. Second, the positioning of the right hand in the supinated attitude illustrated here is very dainty and much favored among beginning residents. However, it does not facilitate the application of some force to the advancing sheath or dilator, and, in particular, holding the sheath supine in this manner does not facilitate rotating the device authoritatively as it advances. Grip it firmly overhand (prone), and twist into the artery. The same goes for any catheter manipulation. When using a shorter wire, such as those prepackaged with the sheath, it is vitally important for the assisting hand to follow the hub of the dilator with the tail end of the wire toward the groin once the artery has been entered. If not, there is a strong risk of the sharp dilator advancing over the wire tip into the iliac artery and perforating the vessel.

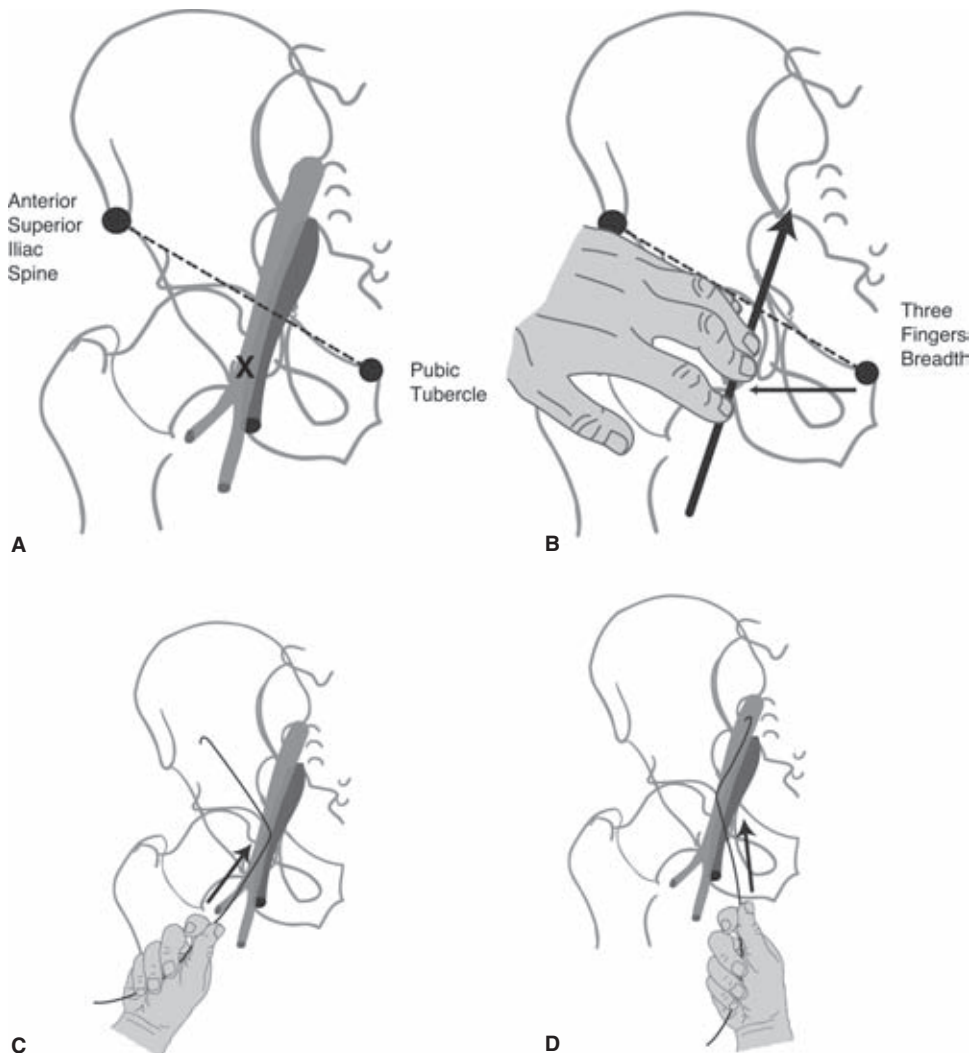


FIGURE 2-6. (A–D) Femoral arterial puncture. A line between the anterior superior iliac spine and the pubic tubercle corresponds with the inguinal ligament (A). In an adult patient, a puncture site 3 fingers' breadth below this line along the pulse of the artery provides a useful guide (arrow in B). From here, a needle thrust at 45 degrees toward the umbilicus will usually find a lie in a position suitable for compression against bone after the case (X in A). Among the difficulties encountered in passing a wire retrogradely into the femoral artery is the possibility of selecting the circumflex iliac artery (C). With a J-wire, this problem can be sidestepped counterintuitively by directing the wire toward the offending artery. The J-curve against the arterial wall will bounce the wire medially and up toward the external iliac artery (D).



FIGURE 2-7. Sharps and hazards. The only assured way of avoiding sticks and jabs from needles and syringes on the table is to have an inviolable routine for using them in every case. Uncapped needles or scalpels will cause an accident sooner or later. Therefore, once the artery has been accessed, all sharps, needles, and the lidocaine syringe should be dispensed into a secure container before the case proceeds. Trainees will need to be indoctrinated in the absolute need for single-handed recapping of sharps.

reports, certainly compared with the older transbrachial or transaxillary options (8,9), but it is technically difficult to gain access to the carotid arteries or contralateral vertebral artery from this route. Authors who have used this technique a great deal find that customized 120-cm catheters of a Simmons-type curve are the most useful, but still awkward to use, requiring a wire technique doubled back off the coronary valve for reconstitution of the Simmons curve (10).

The biggest concern with the transradial approach is injury to the radial artery and ischemic complications in the hand. The Allen test is recommended to screen for this possibility, but the predictive value of a negative (unfavorable) Allen test is questionable, so that even this test is not utilized universally in the cardiology world (6,11). Pulse oximetry is probably more sensitive and cases where cardiologists experienced in this technique back away from a transradial case are rare.

From a technical point of view, radial artery puncture is easy with a less than 5% failure rate of access (10,12).

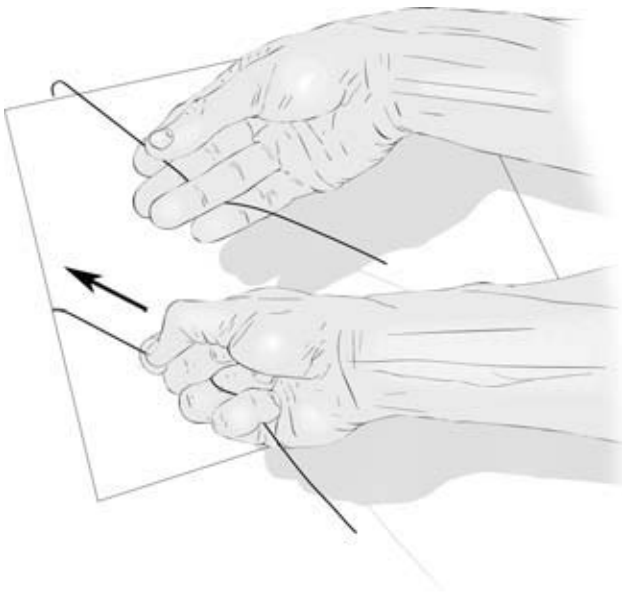


FIGURE 2-8. Wire straightening. Mandrel wires can be straightened by gripping tightly and stretching the wire. This can be done by using the fourth and fifth digits to fix the wire tightly against the palm and extending the thumb and forefinger. Alternatively, interweaving the wire shaft between the third and fourth digits can improve traction.



FIGURE 2-9. Allen test of the palmar arch. Although the risk of performing a radial artery puncture without an Allen test is unknown, and patients endure all sorts of abuse of the radial arteries in other hospital settings every day, it is probably prudent to evaluate the competence of the palmar arch before a radial approach with a larger sheath. The circulation can be evaluated by examining capillary return in the digits or nail beds, by placing a pulse-oximeter on the hand, or as illustrated by using a Doppler probe. The radial artery is compressed firmly with the thumb and maintenance of the Doppler signal via the ulnar artery is confirmed. Compression of the ulnar artery is useful too. If the patient has had previous radial artery procedures or has had some other reason for an occlusion of the radial artery higher up, the pulse one might be feeling in the radial artery might be a retrograde reconstitution via the ulnar artery. By recognizing this before the procedure, one can avoid a great deal of unnecessary and unproductive work on the occluded but still pulsing radial artery.

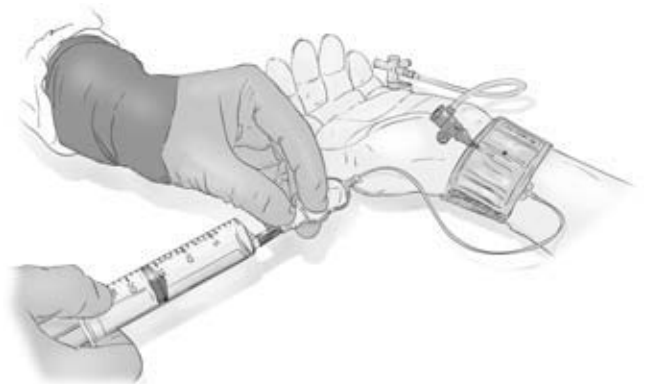


FIGURE 2-10. Terumo band for radial artery compression. A device that likely qualifies for being one of the cleverest and most elegant inventions is the pneumatically inflated Terumo band for radial artery compression. The illustration demonstrates the Velcro band, which fits snugly on the wrist with the green dot positioned over the arteriotomy. The sheath has been pulled out about a centimeter to allow the band to fit on unhindered. The balloon is inflated to a point of firm compression with about 15 to 20 mL of air and the sheath is removed. The balloon is then deflated very slowly until the very beginning of pulsating blood loss is seen through the transparent balloon at the dermatotomy site. At this point the balloon is reinflated by 2 mL and there should be complete hemostasis. Confirming distal flow with the Doppler is reassuring at this point, lest an adjustment in the pressure of inflation should be necessary. Depending on the state of heparinization of the patient, the band is left in place for 45 minutes or longer, and then deflated by 3-mL increments over 30 to 45 minutes. Patients find the process extremely easy compared with the indignity, discomfort, and immobilization of a femoral artery procedure. They can be mobilized during this process and discharged immediately afterward.

For difficult arteries advancing the needle to the backwall and then withdrawing into the lumen is very helpful. A low-profile sheath, such as the Glide Sheath offered by Terumo with a prepackaged 0.021-inch wire, precludes even the need for a dermatotomy incision. Spasm of the radial artery is a significant phenomenon and an intra-arterial dose of calcium blocker, for example, verapamil 4 mg, or nitrates, is useful to suppress this phenomenon. Heparinization of the patient after sheath insertion, or more commonly in the cardiology field, use of bivalirudin, is virtually universally recommended. Some patients are exquisitely sensitive to the application of a flush line to the radial artery sheath, possibly due to a temperature sensitivity inducing distal spasm. Many cases are more easily conducted, therefore, without an active flush line on the radial sheath and instead a bolus of heparin is inserted into the dead space for the duration. Rarely, extreme tortuosity or dissection of the brachial artery may prevent retrograde navigation even after successful transradial access has been gained.

Finally, the radial artery is easily compressed at the end of the case either by thumb, pressure dressing, or a wrist-bracelet device such as the Terumo band (Fig. 2-10). Patients can be mobilized immediately.

► AORTIC ARCH NAVIGATION

With the tip of wire leading, the catheter is advanced from the groin to the descending thoracic aorta. The wire is removed and wiped clean. In the majority of patients, a J-wire or any curved wire will advance all the way from the groin to the aortic arch without fluoroscopic monitoring in the pelvis and abdomen. If difficulties are anticipated, or if the patient has known atherosclerotic or aortic aneurysmal disease, then it is safer to monitor the progress of the wire. When particular difficulties are encountered in the iliac arteries or if they appear noticeably tortuous, it may be a

good idea to insert a longer sheath to straighten out the vascular route between the groin and the aortic arch. Similarly, when navigating a catheter in the arch, one may notice an absence of corresponding motion between the catheter tip on the fluoroscopic image and one's hands. This usually means that the catheter has become wrung, and most often, the site of kinking is at the groin or in the tortuous iliac arteries (Fig. 2-11). Great care is needed at this point to unwring the catheter slightly and to withdraw it partially from the body until the damaged section is out. Then, a wire can be passed to secure arterial access and a long sheath can be inserted.

After the catheter has been placed in the descending aorta and the wire removed, the catheter is aspirated vigorously to clear bubbles, clots, and thrombogenic debris collected as it traversed the subcutaneous tissues of the groin. The catheter is then placed on continuous heparinized flush or maintained on a meticulous hand-flush regimen for the duration of the case. For the first clearing of the catheter after insertion, a more forceful pursuit of surprisingly tenacious bubbles within the catheter is prudent. The hydrostatic pressure transmitted down the catheter from the aortic arch that allows backbleeding to occur is frequently not adequate to overcome the adhesive qualities of bubbles in the catheter. An assertive tapping of one's finger on the catheter hub and particularly at junctions such as stopcocks will often evoke an otherwise undetected shower of bubbles from the catheter. This is most common after the initial insertion of a new catheter but can be seen with surprising frequency during the case after wire removal or other manipulations.

Once the catheter is positioned in the proximal descending aorta, the angiographer rotates it until the tip is facing anteriorly toward the image intensifier, and the catheter is advanced over the aortic arch (Figs. 2-12 and 2-13). A position facing anteriorly translates into an inferior direction as the catheter is advanced over the arch. The catheter responds

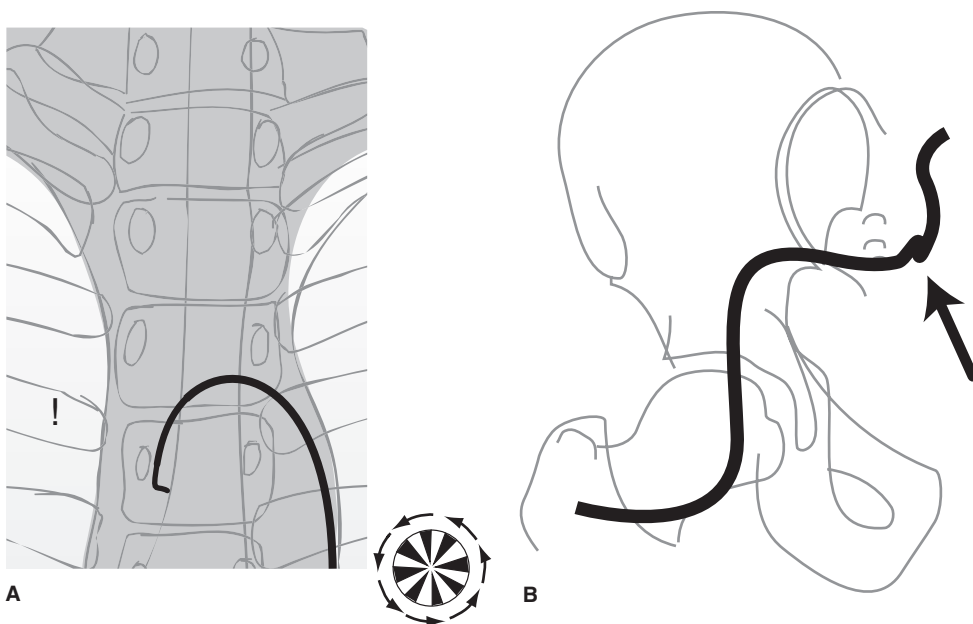
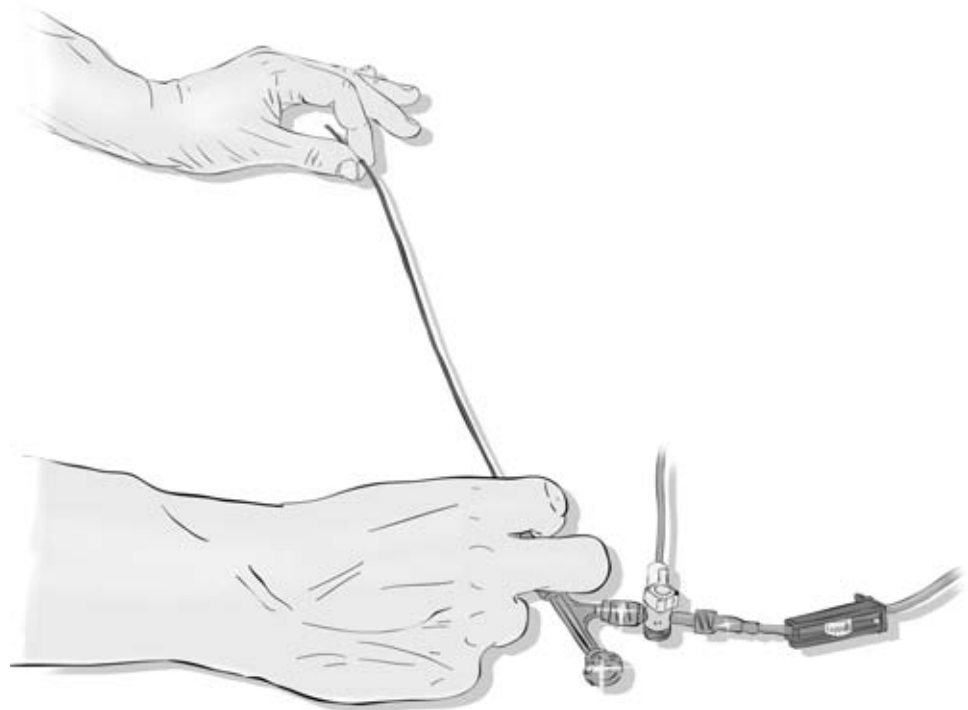


FIGURE 2-11. Catheter in the aorta is not responding: Danger of catheter kinking. The catheter tip is not responding to repeated torquing motions at the groin (A). Check for backflow and kinking. Beware of the danger of tearing the catheter or femoral artery when a tight kink (arrow in B) is present. Remove the catheter over a wire, and place a long sheath to straighten out the iliac system.

FIGURE 2-12. Catheter manipulation. The catheter is steered at the groin site by the left hand. The remainder of the catheter is kept straight outside the body to reduce counter-torque. The right hand is used to make the outside catheter move in unison with the motions of the left hand. The motion of the left hand should be a fine, delicate spinning motion between thumb and forefinger. It is not performed by flexion/extension of the wrist or elbow. It should be executed with the finesse suited to trying to pick a lock rather than the force used to turn the ignition key of a car.



best to anticlockwise rotation by a delicate, smooth spinning with the left hand at the skin entrance, and with the right hand moving in synchrony at the catheter hub. The outwardly visible catheter should be kept straight to eliminate accumulation of countertorque outside the body and to prevent any inadvertent jumps of the wire inside the body when the catheter is advanced.

Having traversed the aortic arch with the catheter tip pointing down, the major vessels are selected by gently dragging the catheter back with the tip pointed up. With the tip of the catheter pointing toward the patient's head, it is pulled back until a small flick indicates that the brachiocephalic artery is engaged (Fig. 2-14).

► CATHETER FLUSHING

Catheters can be flushed either by using a continuous irrigation system, several varieties of which are available, or by intermittently double flushing the catheter with syringes every 90 seconds. When using the double-flush syringe method, it is important that the entire length of the catheter be aspirated vigorously with the first syringe, the contents of which are then discarded, before clearing the catheter forward with fresh heparinized saline.

Using any of the systems for continuous irrigation with heparinized saline helps to free one's mind and hands from the responsibility of keeping the catheter clear of blood and allows one to concentrate on other aspects of the study. However, if not thoroughly cleared of air bubbles before the procedure and vigilantly monitored during the procedure, the supposed safety of continuous irrigation may become an illusion. Misused or neglected continuous flush systems have the potential for great calamity. There are different systems of tubing and adapters available for providing a con-

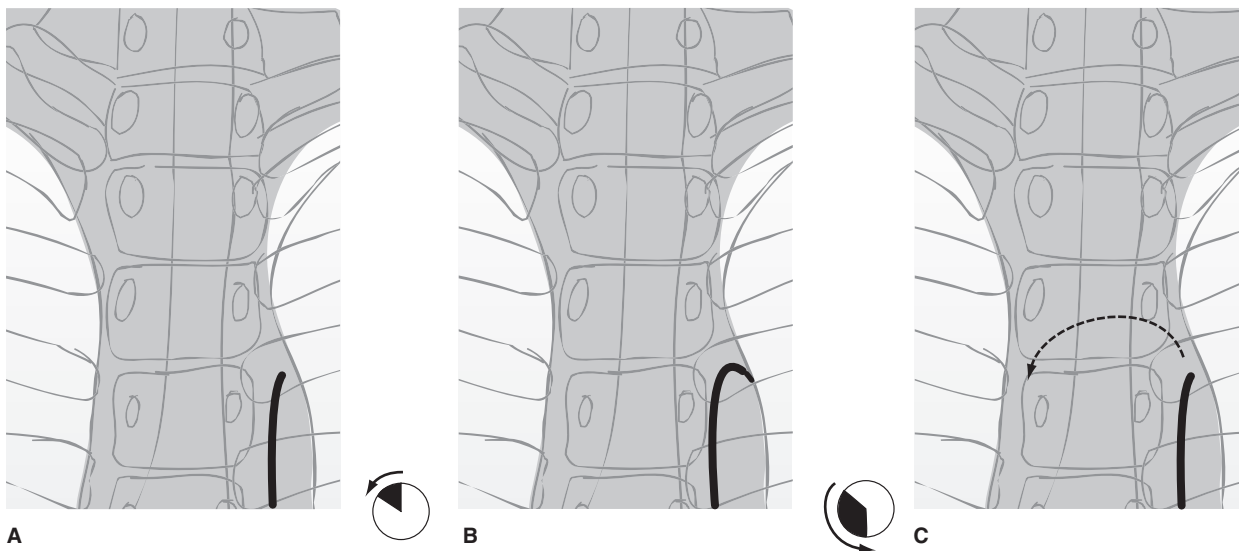
stant stream of heparinized flush (1,000 units per liter for pediatric cases, 3,000–6,000 units per liter for adults) using either a pressurized bag or an electronically driven pump. Depending on how these connect to the catheter, it may be possible using a hemostatic valve on a Y-adaptor or manifold to continue the flush while the wire is being manipulated (Figs. 2-15–2-18). This system has theoretical advantages over a system where flow of flush must be interrupted to allow insertion of the wire.

There are hidden risks in the use of a continuous irrigation system. All systems of continuous irrigation carry a risk of complication if one fails to reset flow after each hand injection or run by neglecting to reopen the stopcock immediately. A generous rate of flow of flush (150–200 mL minimum per hour) is imperative, bearing in mind that a typical catheter may have a total volume of 4 to 5 mL. With blood refluxed back to the valve, it will take at least 60 drops or 240 microdrops in a drip-chamber system to clear the catheter thoroughly from the proximal to the distal end. This does not even make allowance for laminar flow with stasis of dependent blood in the catheter, meaning that a sluggish drip rate in the flush-bag into a catheter full of blood is not a guarantee against embolic complications.

When using a pressurized bag system, the rate of forward flow is very finely balanced between one that allows adequate irrigation and one that generates a turbulent jet in the chamber, allowing bubbles to enter the tubing. Furthermore, it is easy to overestimate the actual volume of saline being advanced per minute when using a microdrop system. When acquainting oneself with such a system, it is useful to prime the tubing with saline and allow it to run at what is perceived as an adequate rate. Then, attach a dry catheter to the system. The duration

(text continues on page 22)

1. Tip is pointing posteriorly. Movement is discordant.



2. Tip is pointing anteriorly. Movement is concordant.

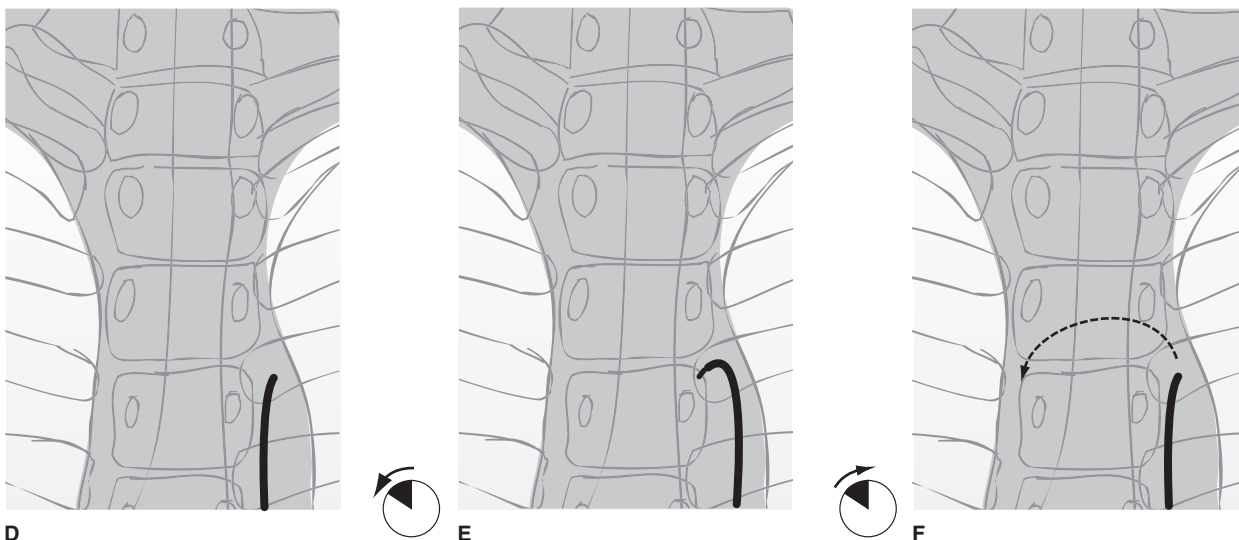


FIGURE 2-13. (A–F) Turning the catheter anteriorly in the aorta. To minimize the time that one has an obturating wire within the catheter, it is preferable to steer the catheter, if possible, to the brachiocephalic artery and select its ostium before using a wire. Most aortas will allow a hockey-stick or curved catheter to cross smoothly. To do this, the tip of the catheter needs to avoid being selected on the way over by the left subclavian and left common carotid arteries. By starting in the descending aorta with the catheter tip pointed anteriorly and pushing straight in, the catheter will sweep across the arch with the tip pointed down.

Because the fluoroscopic image is two-dimensional, it can be difficult to discern whether the tip is pointing anteriorly or posteriorly. By forming a hypothesis or assumption about the position of a randomly placed catheter and testing that assumption with an anticlockwise motion, the true position of the catheter can be perceived and a correction applied.

1. The catheter tip position is unknown. Assume that it is facing anteriorly (A). A 30- to 45-degree anticlockwise spin causes the tip to elongate toward the patient's left (B), which is discordant with an anterior position. This would indicate that the tip is facing posteriorly. The anticlockwise motion is then continued until a 180-degree turn from the original position is achieved (C). The catheter is then pushed over the arch.
2. The catheter tip position is unknown. Assume that it is facing anteriorly (D). An anticlockwise spin evokes elongation of the tip to the patient's right, concordant with an anterior position (E). Reverse the applied spin to regain an anterior position (F), and push the catheter over.

The same logic is used to achieve a posteriorly directed catheter position when performing spinal angiography.

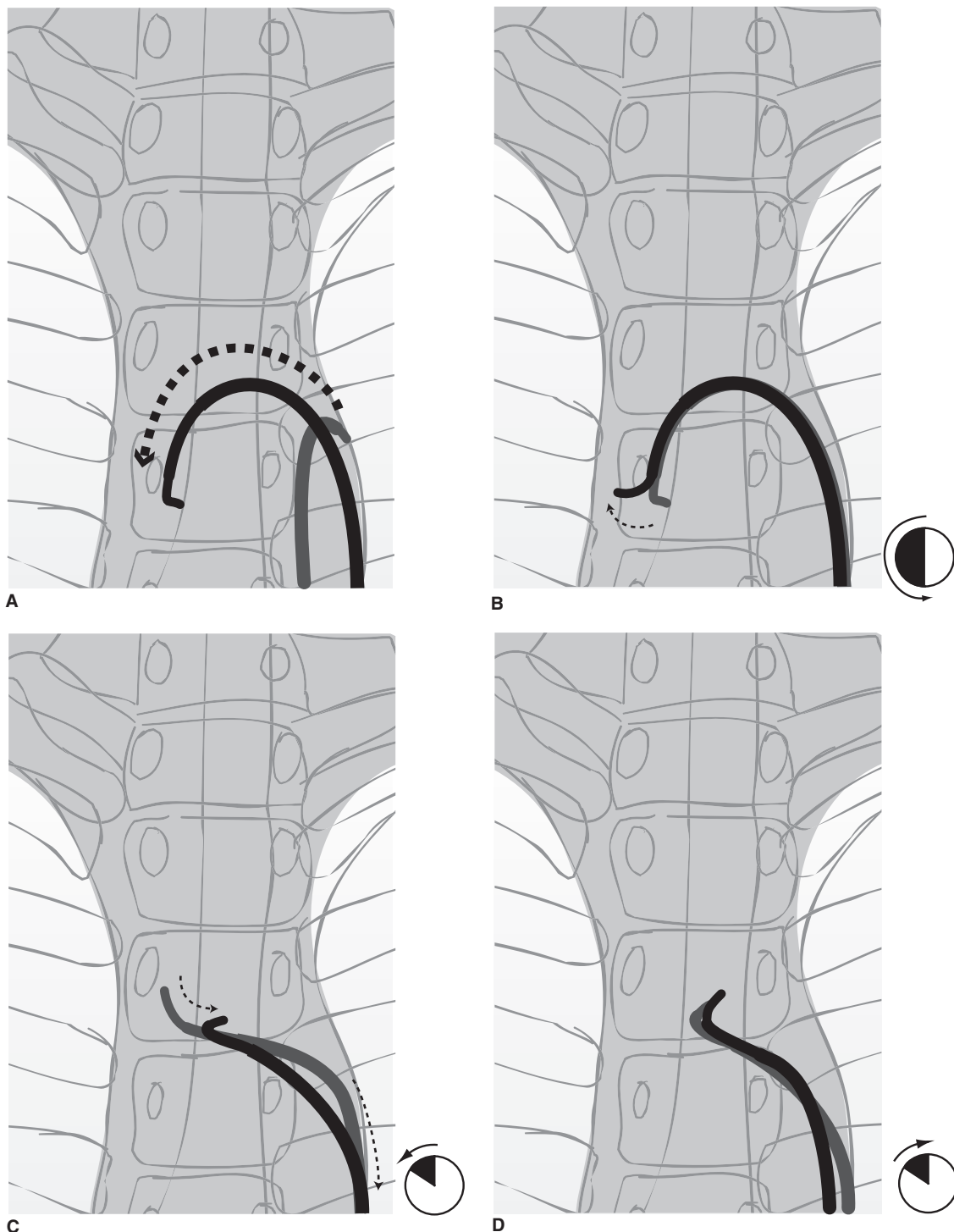


FIGURE 2-14. (A–D) **Selecting the great vessels: Establishing a stable catheter address in the left common carotid artery.** **A:** The catheter is advanced over the aortic arch by keeping the tip pointed inferiorly. This avoids trauma to the intima of the arch, and it prevents the catheter tip from becoming trapped by vessel ostia on the way over. **B:** A 180-degree spin of the catheter in the ascending arch places the tip in a vertical upright position. The catheter is gently pulled back. Usually, this motion will select the brachiocephalic artery with a discernible jump and straightening of the catheter, except in the most difficult circumstances. **C:** Pulling back from the brachiocephalic artery in a precisely vertical tip position will often cause the catheter to jump past the left common carotid artery and into the left subclavian artery. To avoid this problem, as one pulls back the catheter from the brachiocephalic artery, spin the catheter 15 to 30 degrees anticlockwise to make it point slightly anteriorly. This will select the anteriorly disposed left common carotid artery more effectively. **D:** To stabilize the catheter in this position while one prepares the wire, it is necessary to reverse the spin to the vertical position. Apply the same measure of clockwise spin to point the catheter directly into the artery and to maintain its purchase on this vessel.

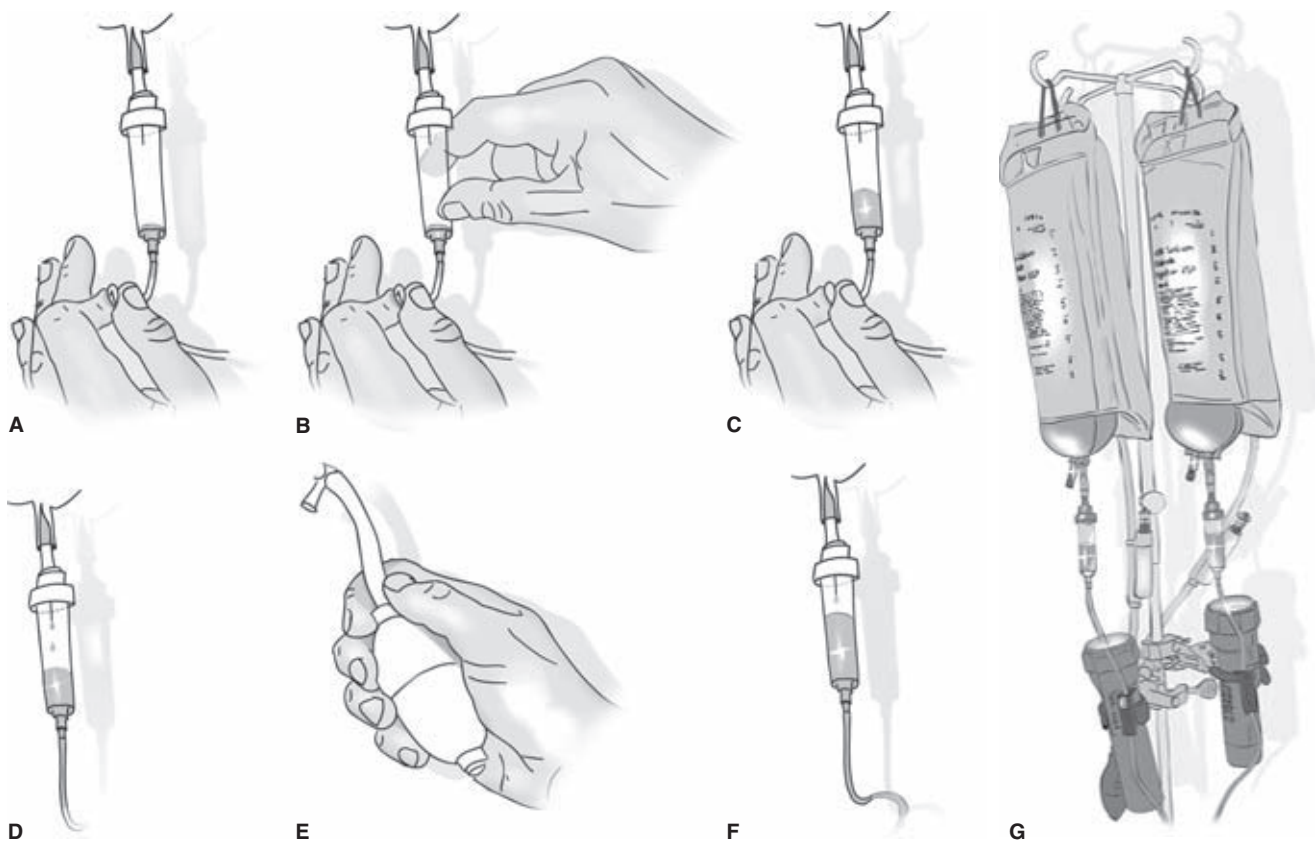


FIGURE 2-15. (A–G) Priming a flush line with a pressure-bag system. A liter bag of fluid from which all residual gas has been removed and to which 4,000 to 6,000 units of heparin has been added is prepared. For children, intraoperative cases, or patients with heparin-induced thrombocytopenia, this regimen is obviously modified. The chamber of the pressure line is plugged into the bag. The bubble-free priming of the nonsterile end of the flush line requires acquisition of a little knack on the part of technologists or assistants. Before priming the line, the distal clamp of the pressure line, that is, the end on the sterile field, is tightly closed. **A:** The line is pinched tightly by an assistant, and the chamber is squeezed (**B**) to allow inflow from the bag to fill the chamber about one-third of capacity (**C**). When the bubbles from the inside of the chamber have all been flicked away from the inner surface of the chamber, the hand pinching the line lets go slowly. Fluid will advance into the proximal part of the line from the chamber (**D**). Without having pinched the line before filling the chamber, squeezing the chamber would cause a back-and-forth movement of bubbles within the line that would make a bubble-free column of fluid difficult to attain.

E: With a clear, bubble-free column of fluid in the proximal part of the line, pressure is smoothly inflated into the bag to 300 mm Hg. This must be done with sufficient speed to allow timely completion of the task but not so fast that a jet of turbulent bubbles is generated in the chamber (**F**). This would cause bubbles to advance into the tubing. Inflation causes the air within the chamber to be compressed. A minimal volume of air is necessary to allow visualization of the drip within the chamber. Therefore, it is necessary not to overfill the chamber with fluid before the compression. Hence the recommendation for filling the chamber to only one-third of its volume in (**B**). The distal control clamp of the pressure tubing (on the sterile field) is used to advance air followed by the column of fluid all the way through the system. The line is rechecked carefully for bubbles.

G: The flush bags must be scrupulously monitored without lapse during the case. This can be facilitated by illumination of the drip chambers, each of which is color-coded for the corresponding lines on the table. In our department, the chamber illumination is accomplished inexpensively with battery-operated flashlights and a set of old chemistry clamps.

of time before one sees saline emerge from the catheter tip is usually surprisingly long and represents the same time that stagnant blood will sit in the catheter after each wire exchange at that rate of flush. This exercise is left to the reader.

With the cross-pollination of techniques from the cardiology world having an impact on neurointerventional procedures, some angiographic laboratories have switched to a manifold system, trading up to the advantage of allowing continuous blood pressure monitoring via this route but with the disadvantage that forward continuous flush within the catheter is lost.

Wire Insertion and Advancement

With a Tuohy-Borst valve system, which allows continued flow of flush during wire manipulation, it is important to realize that the rate of forward flow will be compromised by insertion of a wire into a standard catheter. Backflow of blood into the catheter to the level of the adapter is inevitable when the valve is opened to insert a wire or other device. Insertion of an obturating wire into the blood-filled catheter worsens the stagnation and increases the risk of thrombus formation. To prevent this from happening, allow

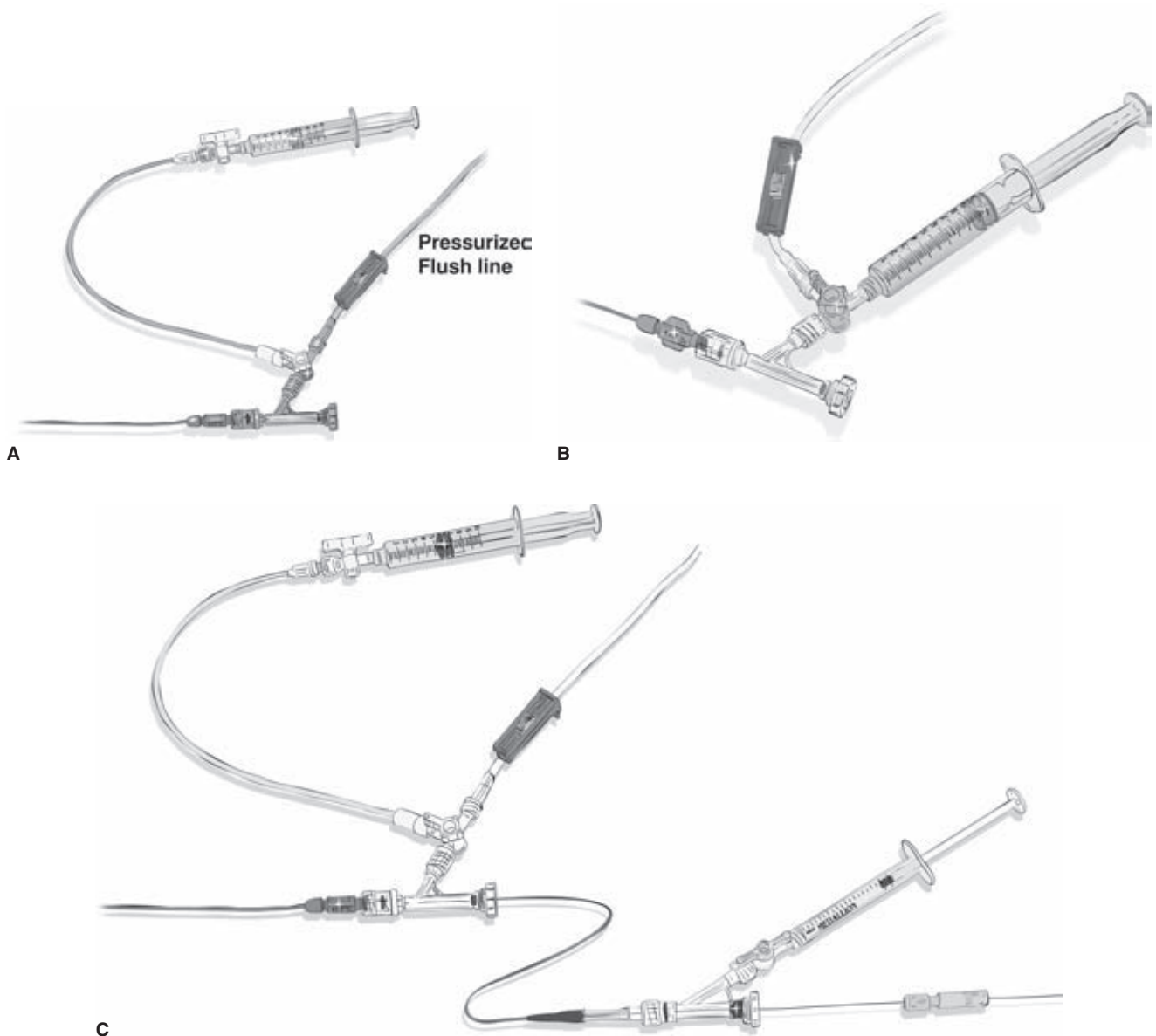


FIGURE 2-16. (A–C) Tuohy-Borst Y-valve setup for continuous flush. A commonly used system for continuous irrigation of flush is illustrated (A) as well as an alternative form (B). A pressurized flush line enters a Tuohy-Borst Y-adapter via a three-way stopcock. The other hub of the three-way stopcock can be used to attach syringes directly, but it is much more convenient to attach a short, flexible pressure line. In this way, the catheter is unlikely to be disturbed by motion at the hub when attaching syringes and the like. A two-way stopcock at the end of the 12-inch side arm can be added to provide a convenient site for attaching syringes or the tubing from the power injector. Coaxial systems of catheters or other devices can be built up as needed in this manner, each component flushed by its own pressure line (C). Parallel devices can also be inserted through a single lumen by piggybacking Y-adapter onto Y-adapter.

the catheter to flush ahead of the wire by halting the advance of the wire before it obturates the catheter, and by tightening the hemostatic valve. A pause of a few seconds is observed to allow a column of fresh flush to precede the wire into the catheter (Fig. 2-19). Then, as the wire is being advanced, the valve is adjusted to allow sealed manipulation of the wire while diverting flush into the catheter.

Leaving the hemostatic valve inadvertently unsealed after removing the wire poses the risk of air being withdrawn into the system while a syringe or injector is being

attached, and a large bolus of air could be injected intracerebrally by an inattentive hand. For this reason, a check of the valve is a mandatory automatic component of the routine whenever a syringe or injector is being attached and drawn back.

Constant vigilance by the operators and assistant staff toward the catheter flush line is necessary to avoid inadvertent closure of the flush line after arteriographic runs or hand injections. Electronic pumps carry the advantage of allowing an automatic alarm system to sound when the

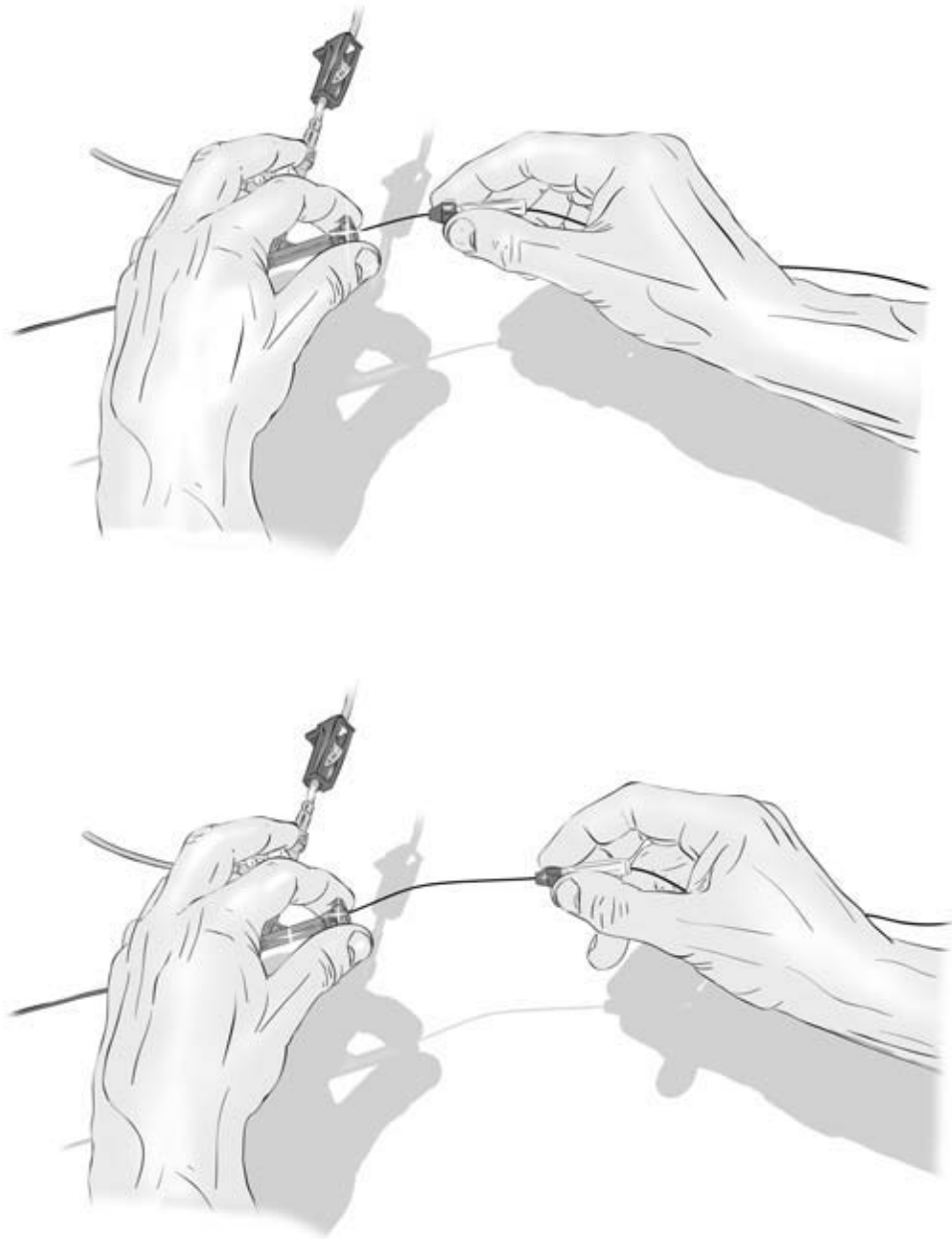


FIGURE 2-17. Torque device position. For most precise control of the wire, the torque device should be close to the hub of the valve. If not controlled from this position, torque applied to the wire is typically expended as a slewing of the wire outside the catheter with unpredictable transmission of movement to the wire tip. During wire manipulation, the valve is sufficiently tight that backbleeding from the catheter does not occur. In this manner, flush continues to be directed into the catheter around the wire.

flush is turned off. Systems operated by pressure bags can be manually adjusted and evaluated at a glance more easily by the angiographer, but without an alarm system, they have to be monitored all the more closely. A flashlight trained on the drip chamber is a useful aid. The pressure gauge should be monitored intermittently during the case to detect spontaneous deflation of the pressure bag.

An additional safety note with reference to the pressure-bag system is necessary. Most plastic saline bags have 10 to 20 cc of air within when supplied from the manufac-

turer. This air should be evacuated from the bag via a needle at the time of insertion of heparin. The reason for this is that the gravitationally dependent saline contents of the bag may expand during the course of a long case, and if undetected, the residual volume of air may then be forced into the flush line with the potential for causing a massive air embolism. The prefatory aspiration of air from the bag and insertion of heparin should be done using a needle not larger than a 19G or 20G. A hole in the rubber seal of the bag larger than this size frequently leaks when pressurized to 300 mm Hg.

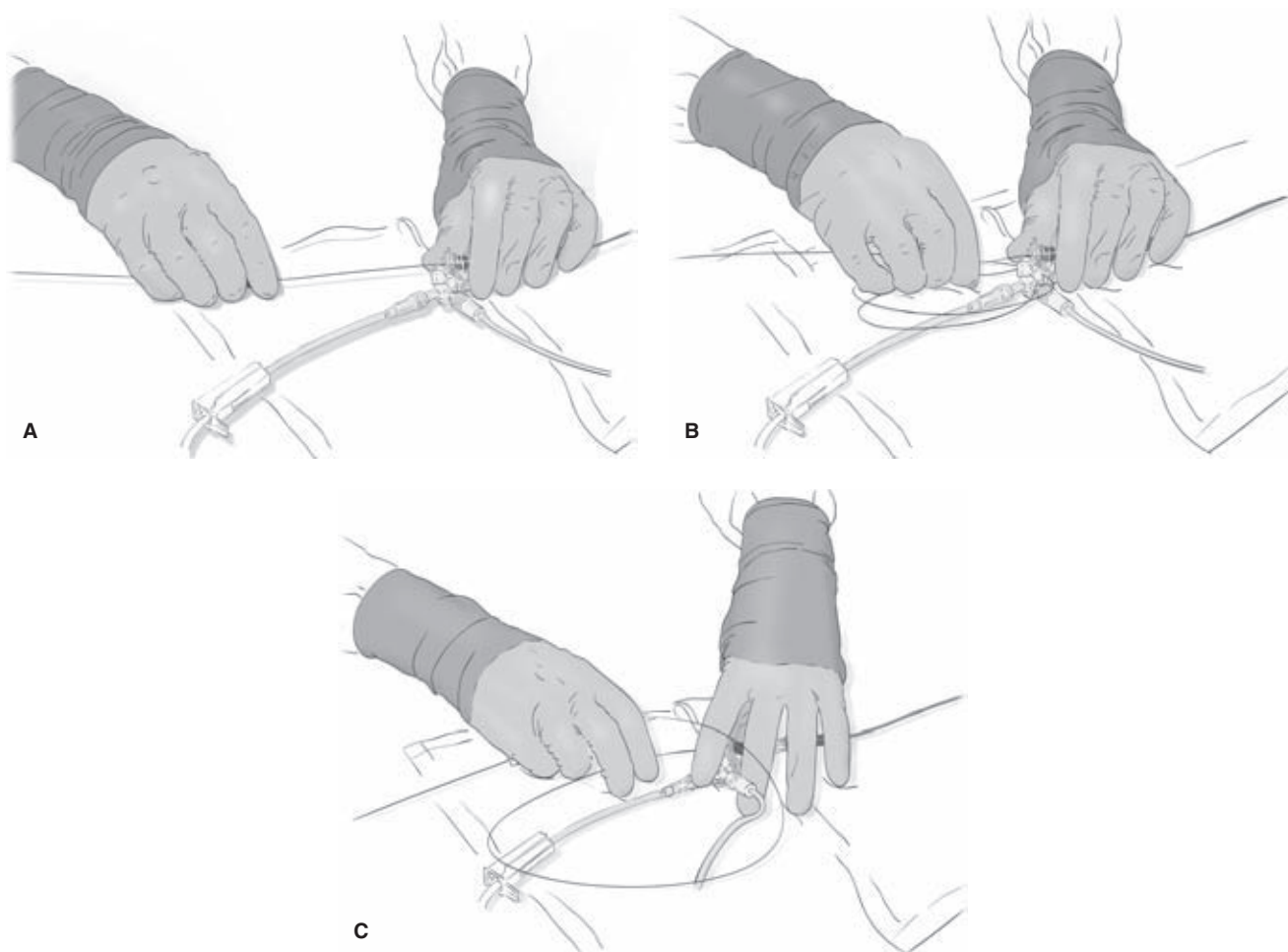
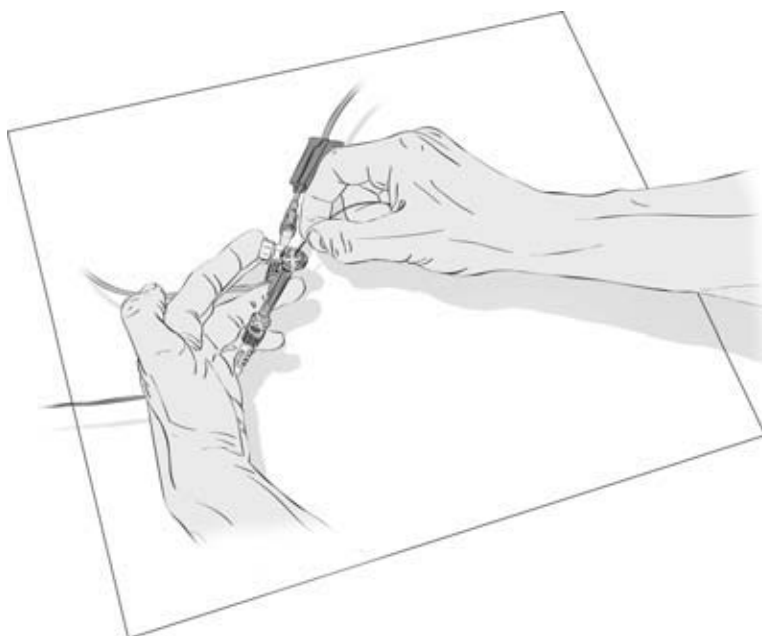


FIGURE 2-18. (A–C) Wire withdrawal. As the wire is being withdrawn from the catheter or more particularly from a microcatheter, attention is given to the Y-adaptor for evidence of generation of a negative pressure within the catheter and suction of air through the valve (A). The wire must never be whipped out quickly, and the left hand must be positioned to allow full view of the adaptor. As the loops of microwire are gathered in the right hand (B) the capacity of the wire to snag on the switch-handle of the three-way adaptor, and thus lead to kinking of the microwire, is entirely proportional to the fatigue and stress of the operator. A useful habit to cultivate (C) is to rest the left index finger on the switch as the wire is spooled in the right hand to prevent this irritating misadventure.

FIGURE 2-19. Pausing to allow the catheter to clear.

Insertion of a wire or coaxial microcatheter through the valve is inevitably going to allow some backbleeding into the catheter and adaptor. To promote clearing of the catheter before advancing the wire, seal the valve when the wire tip is inside the adaptor. This allows diversion of all flush into the catheter ahead of the wire. Gravitational dependence of blood within the adaptor can be used to clear the backwater area of the adaptor as well.



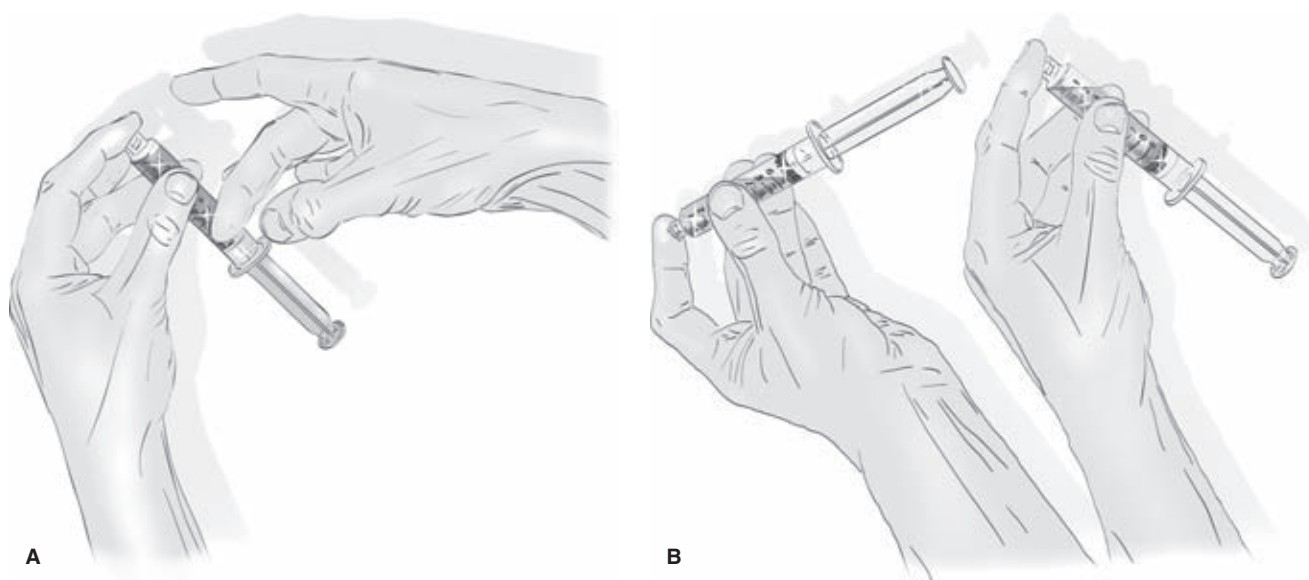


FIGURE 2-20. (A, B) Clearing bubbles from syringe while avoiding eye splashes. After filling the syringe with contrast smoothly so as not to generate bubbles, remaining air must be tapped to the top of the syringe and expelled by advancing the meniscus. To prevent eye splashing, the syringe tip should be covered as illustrated (A). This allows one to be forceful in the effort to eliminate all bubbles. Rolling a large bubble of air within the syringe will also help to clear adherent microbubbles from the wall of the syringe (B). However, even at that, there are probably still thousands of microbubbles still held in suspension in a freshly drawn-up syringe, particularly in viscous contrast. Allowing the syringes to sit for as long as possible before use may allow suspended microbubbles to coalesce and come out of suspension.

Meticulous table technique in all aspects of syringe handling is necessary to avoid generation or introduction of bubbles into the catheter (Figs. 2-20–2-22). Backflow of blood into the catheter and stasis during wire manipulation should be minimized (Figs. 2-23–2-28).

► HEPARIN AND PROTAMINE SULFATE REVERSAL

When systemic heparinization is used during a diagnostic or interventional procedure, the effectiveness of the dose can be most easily monitored by checking the activated coagulation time (ACT) with a Hemochron System (International Technidyne Corp., Edison, NJ) in the angiography suite or equivalent. An ACT level of 1.5 to 2.5 times the baseline value is desired (13,14). Usually, a heparin bolus of 3,000 to 5,000 units (40–60 U/kg) is used for adults. The ACT is then checked 5 to 10 minutes later. For long cases, checking of the ACT and hourly maintenance doses of heparin are necessary. Heparinization is commonly used as a routine precaution in children (30–40 U/kg) during transfemoral neuroangiographic procedures to reduce the likelihood of arterial occlusion at the puncture site.

When immediate reversal of heparinization is required at the end of the procedure, a dose of protamine sulfate delivered carefully over 10 minutes can be given. The dose can be calculated as 10 mg of protamine sulfate per 1,000 units of active heparin still circulating, using 1.5 to 2 hours as an approximate half-life of heparin. The ACT can be rechecked prior to removal of the arterial sheath to ensure correction of coagulation.

Catheter Positioning

Fluid dynamics at the interaction of the jet of contrast emerging from the catheter tip with the flow patterns of the catheterized vessel have an important bearing on some of the risks of angiography (Figs. 2-29 and 2-30). The patterns of flow in the major cranial vessels may dwell on a spectrum between a state of near-laminar flow on one end and various degrees of disturbed flow approaching turbulence on the other (15,16). These patterns depend on the contour of bifurcations, turns of adjacent vessels, the presence of stenotic lesions, or the distance from the aorta. For the purposes of an angiographic study, the injected bolus of contrast needs to disturb the laminar pattern of flow in the vessel enough to opacify the lumen and its territory completely. To accomplish this necessary dispersion of contrast within the vessel lumen—to prevent slipstreaming of the contrast—the velocity of flow from the catheter must significantly exceed that in the vessel. Furthermore, the streamlines of the catheter jet distal to the catheter tip must be divergent (17).

A simple formula can calculate the average velocity (U) of contrast exiting the catheter tip:

$$U_{\text{average}} = \frac{Q}{\pi R^2}$$

where Q is the volume of injection per second and R is the radius of the catheter at its exit. However, flow within the catheter, as in any long cylindrical tube, has a parabolic velocity gradient whereby peripheral flow is slower than that at the center. Mabon et al. (17) have taken the peak velocity at the center of the catheter lumen to approach $2U_{\text{average}}$. With a catheter of a 4F to 6F size commonly used in diagnostic neuroangiography, U_{average} may exceed 900 to 1,200 cm

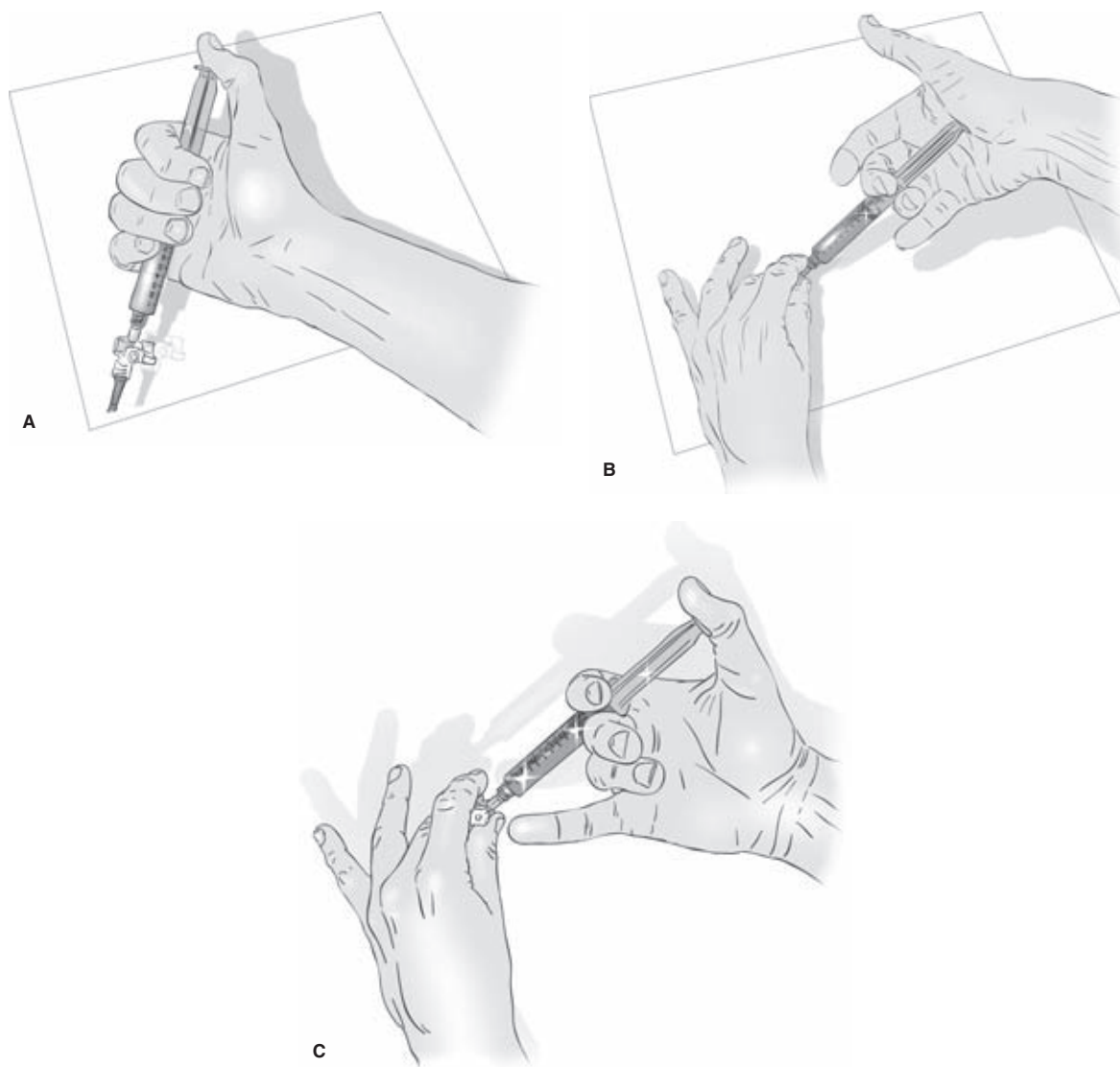


FIGURE 2-21. (A–C) Injection technique matters. A pusillanimous technique for syringe injection much favored among beginners is illustrated in (A). This technique relies completely on the flexor pollicis longus and brevis muscles for effect and, at that, in an anatomically gauche attitude of constraint. When performing an injection by hand as part of a formal run, roadmap acquisition, or test injection, it is important to be able to see the contrast on screen. Ineffective or tentative injections ultimately result in greater cumulative contrast loads because they end up having to be repeated. Make your injections definitive and, if necessary, forceful, as shown in (B) or (C).

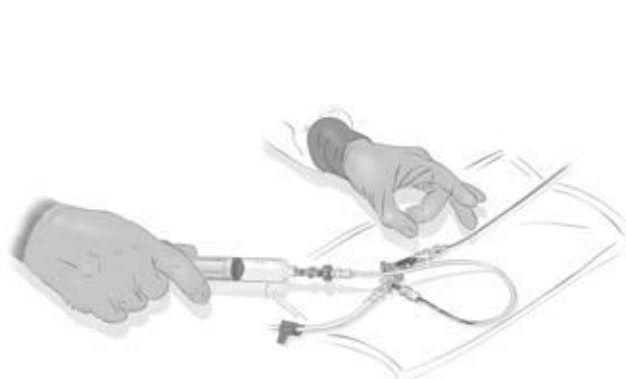


FIGURE 2-22. Keep a high suspicion for bubbles at all times. Good habits are important to cultivate from the beginning. In this image the left hand is flicking the Y-adaptor system vigorously while the right hand retracts slightly on the syringe, the better to detect and eliminate any bubbles before doing a hand-injection. Always point the syringe down at the time of injection, to reduce further any possibility of injecting air from the syringe.

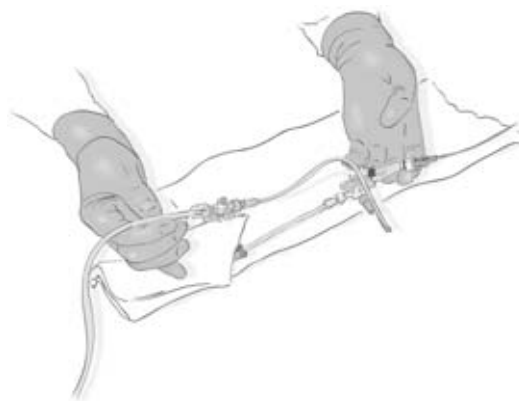


FIGURE 2-23. Clean table and clean tubing. Meticulous technique can quickly become an effortless habit, expending little precious energy or concentration during stressful or long cases. In this image the injector line has been hitched and opened to the catheter. While the technologist retracts slowly with the injector, the line is flicked and carefully examined for bubbles.

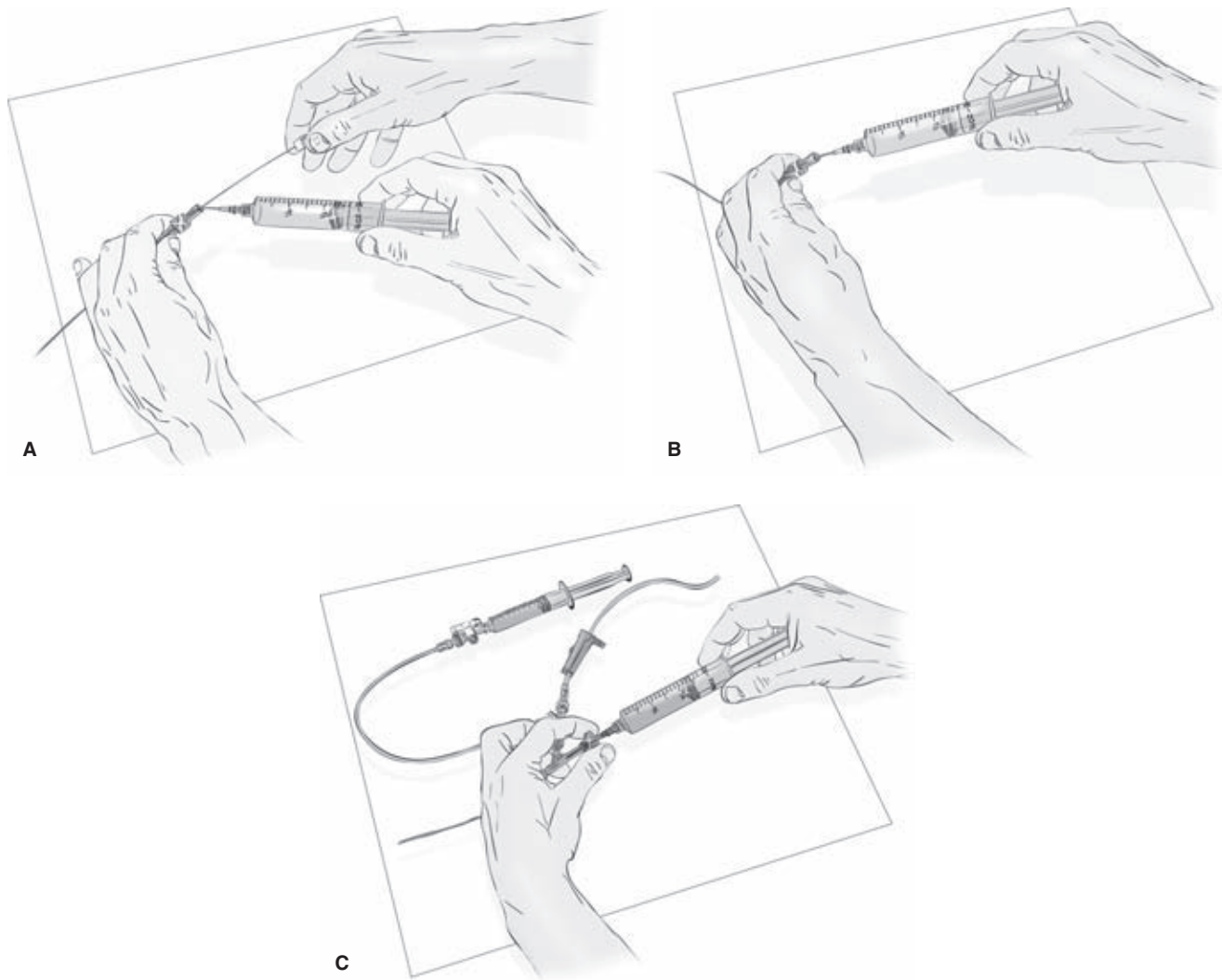


FIGURE 2-24. (A–C) The Jabbie. The best tools are the homemade ones. A useful irrigation device (aka *Jabbie*, *Son of Jabbie*, *The Jabster*, *The Winkler*) can be fashioned from components of the micropuncture sheath, an intravenous (IV) cannula, or an amputated dilator and can be pressed into yeoman's service for clearing inaccessible hubs (A), prevention of vacuum suction during microwire withdrawal (B), or winking out stagnant blood from the otherwise inaccessible dead space in the flush system (C).

per second for an 8 to 10 mL per second injection. The shear forces on the intimal wall generated by a jet of this magnitude depend greatly on the angle of incidence. They also depend strongly on the distance between the catheter tip and the wall of the vessel. With the catheter direction parallel to the axis of the flow within the vessel, injection rates of this magnitude are theoretically capable of producing shear stresses of 2,000 dynes/cm² over a 2-cm segment of vessel wall and more focal mural shear stresses as high as 5,000 dynes/cm². For comparison, reference ranges of normal physiologic stress are approximately 50 dynes/cm². Animal data indicate that high velocity flow over periods as short as 1 hour with shear stresses of approximately 380 dynes/cm² can produce intimal cell loss, cellular fragmentation, and endothelial stripping of the aorta of dogs (18).

Given these experimental results, it is clear that considerable care is necessary in catheter positioning in reference to the curvature of the vessel. Extreme care is necessary in situations where a number of injections in

a single vessel might be anticipated when interrogating a particular lesion. The shear stress on the vessel wall from a standard injection rate may be sufficient, for instance, to dislodge atheromatous plaque from the walls, causing distal emboli. Injection sites should therefore be selected away from any atheromatous irregularity seen on the roadmap images. Similarly, vulnerability of the intima to shear forces may be amplified by the presence of wire-related or catheter-induced spasm, and a tiny intimal tear could then be aggravated to a full-blown dissection by an immediately adjacent injection.

In order to minimize trauma to the intima of the catheterized vessel, it is desirable to position the catheter so that its distal curve conforms to that of a similar curve in the surrounding vessel. This avoids a situation in which an injection might be made directly against an intimal wall where the considerable kinetic force of the jet is transformed to pressure. Although there are theoretical data implying that shear forces on the intima may be less with an injection

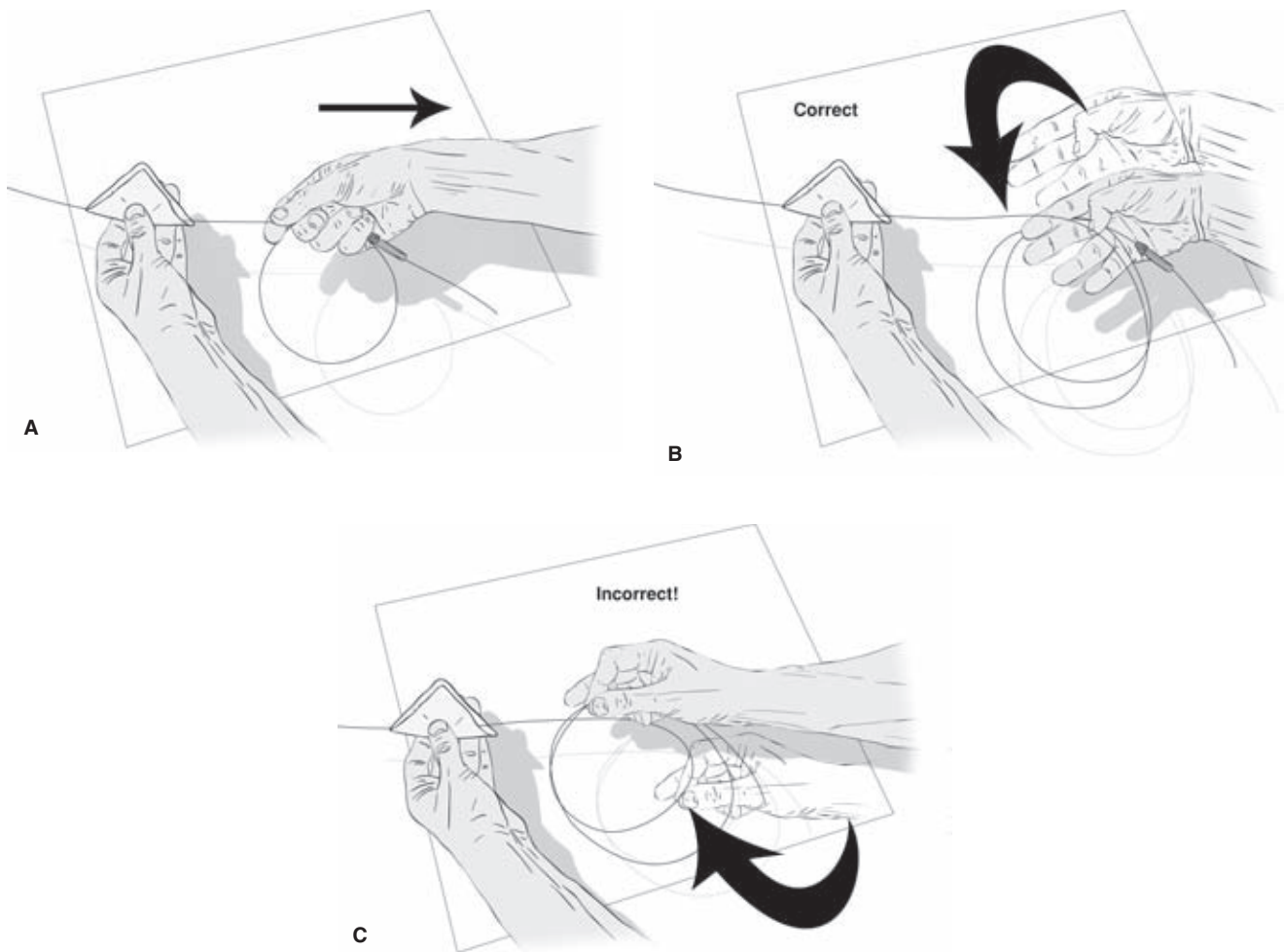


FIGURE 2-25. (A–C) Wire handling. Tense wires and microwires can be difficult to control with one hand. The most common mistake is to make the loops of the wire too small, which increases the difficulty of keeping them under control. As one retracts the wire from the catheter, wiping as one does so with the left hand (**A**), the right hand gathers the loops in by sweeping back toward the operator (**B**), not away (**C**). The higher digits and palm of the right hand open to receive the new segment of wire and then keep it pinned down, while the right thumb and forefinger then adjust position to accommodate the new loop.

perpendicular to the intima rather than parallel, the risks of a subintimal injection argue against such considerations. Usually, the common carotid artery in adults is sufficiently capacious that concern about catheter positioning is less acute than during more selective injections. In the internal carotid artery and vertebral artery, such positioning is important.

Depending on the size and appearance of the vertebral artery, two catheter positions are used most commonly. A low position at C6 prior to the vessel entering the foramen transversarium has the advantage of minimizing wire or catheter manipulation within this critical vessel. A high position at C2, at the laterally directed curve of the artery, favors compatibility between the shape of the catheter and the 90-degree lateral turn of the vessel. Furthermore, an injection at this higher level has a greater chance of refluxing the contralateral vertebral artery to opacify the contralateral posterior inferior cerebellar artery. If successful, this obviates the need to select the contralateral vertebral artery. It also offers the theoretical advantage of performing an injection distal to the site of potential

origin of the artery of cervical enlargement (anterior spinal artery), the argument being that an angiographic occlusion of the vertebral artery in the high cervical region is likely to be less damaging if supply to the anterior spinal artery is maintained. When the vertebral artery is extremely tortuous, hypoplastic, or otherwise unfavorable in appearance for catheterization, a very proximal engagement, if possible, of the vessel origin with just the tip of the catheter and a long, slow injection with a 1-second rise will be more effective in opacification than a subclavian artery injection.

Some neuroangiographers swear by the use of hand injections only and deplore the use of mechanical injectors. There are arguments on both sides of the aisle on this question. If your laboratory uses a mechanical injector, one has to be cognizant of the potential for this device to perpetuate an injury within the vessel, whereas an attentive hand might detect a problem in the course of the injection and terminate earlier. With the mechanical injector, a linear rise of the injection rate between 0.2 and 1 mL over the first second is *(text continues on page 32)*

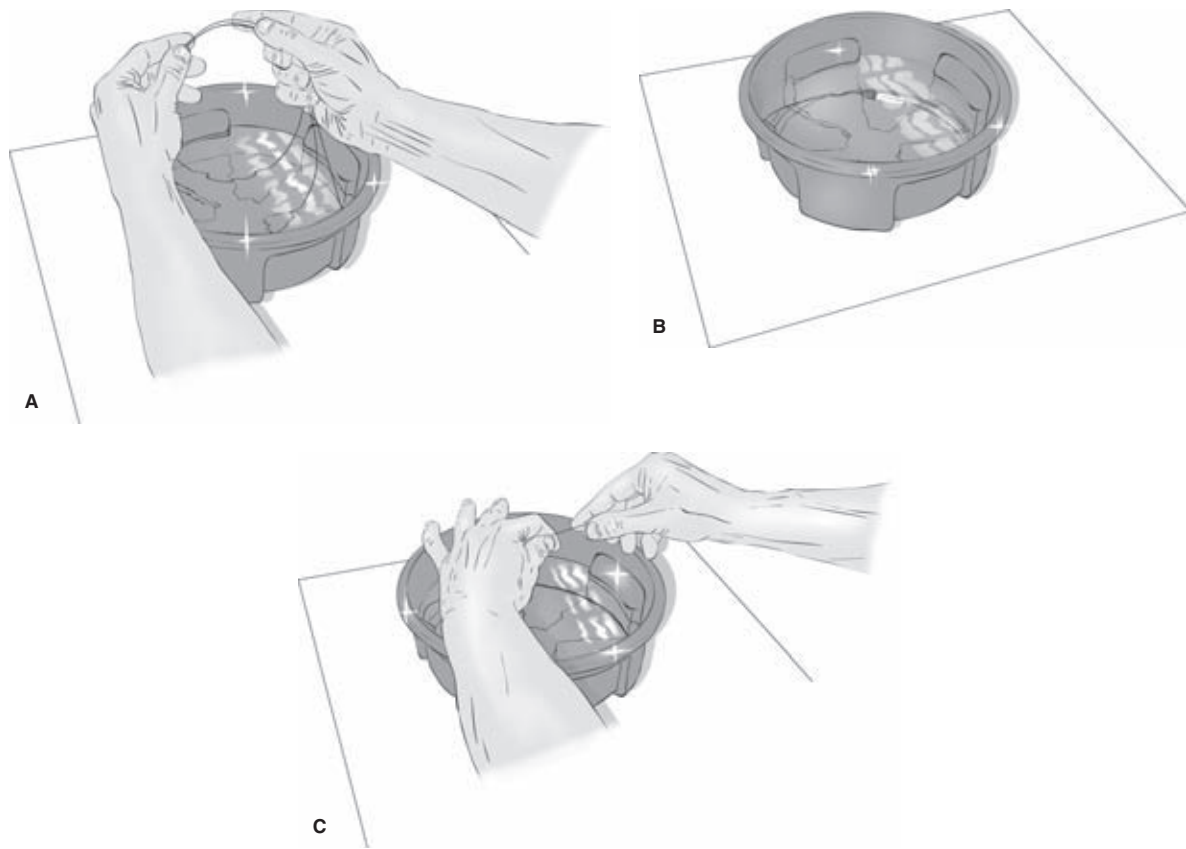


FIGURE 2-26. (A–C) Inserting and extracting a wire from the water bowl. A common difficulty for beginners is to lose control of the wire loops in the slippery environment of the water bowl. Insertion of the wire into the bowl takes two hands (**A**) to conform the wires to the floor of the basin. The wire is always placed so that it runs clockwise back to the torque handle (**B**). To extract the wire, two hands are necessary. The left hand is splayed over the bowl to discourage runaway wire loops (**C**), while the right hand pulls on the torque handle away from the bowl, gathering the wire into loops as described for Figure 2-25. The mistake beginners make is to attempt to lift all three wire loops out of the basin at once, which cannot be done, especially when there is more than one wire in the bowl.

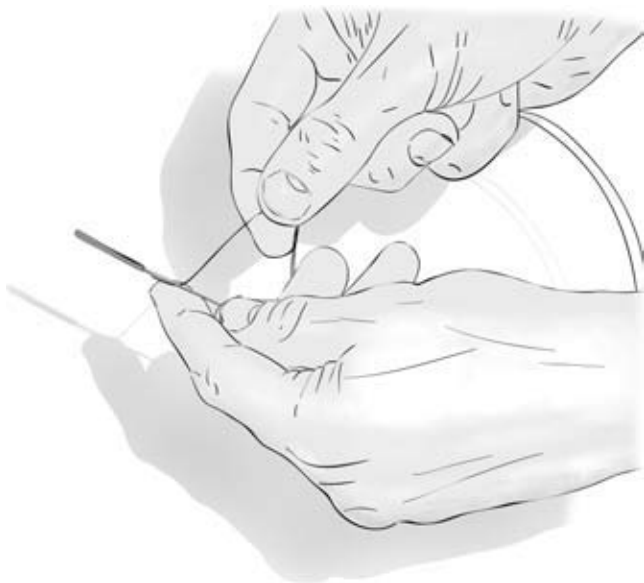


FIGURE 2-27. Microwire shaping. Microwires can be shaped easily by dragging the tip across one's finger under pressure of a shaping rod. The pressure needed for this is extremely light. Overshaped microwires are very difficult to straighten. The radius of curvature of the induced shape is related to the length of wire drawn over the rod and to the force applied. The most popular curves for microwires are a simple J-curve and a headhunter curve.

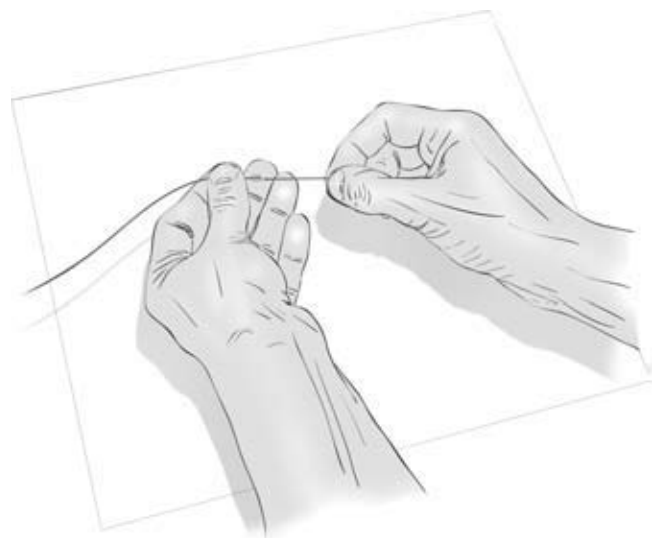


FIGURE 2-28. Make a plane from the palmar regions of the fingers. By limiting degrees of freedom of small objects, such as balloons or microcoils, one's control over them, such as when threading a delicate device, is much improved. By confining them to a working plane devised from the higher digits, manipulation becomes infinitely more controllable.

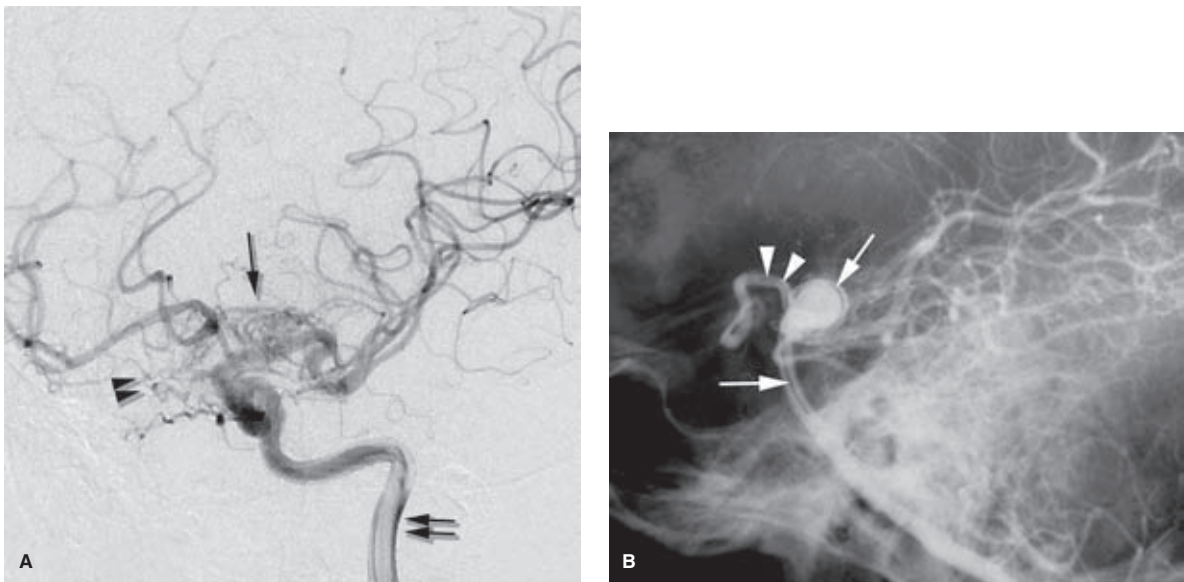


FIGURE 2-29. (A, B) Streaming of flow. **A:** An internal carotid artery injection demonstrates laminar flow toward the end of the contrast bolus (*double arrows*). This patient also demonstrates findings of the early stages of Moyamoya disease (see Chapter 22) with chaotic overgrowth of the anterior lenticulostriate vessels (*arrow*) and transthemoidal anastomotic channels from the ophthalmic artery to the frontal lobes (*double arrowheads*). **B:** A lateral view of a basilar artery aneurysm demonstrates a lucent circumferential layer within the aneurysm and within the upper basilar artery (*arrows*). This represents the unmixed blood from the noninjected vertebral artery. This also extends into the right posterior communicating artery (*arrowheads*), enlarged in this 64-year-old female with a right frontal arteriovenous malformation (not shown).

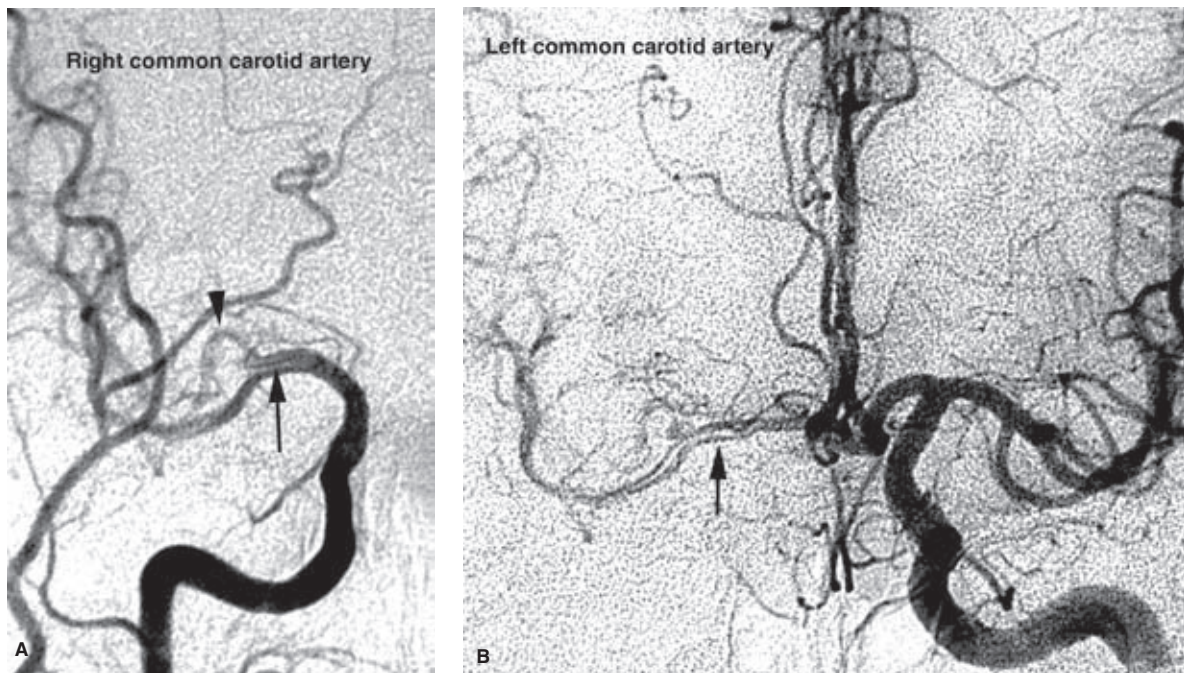


FIGURE 2-30. (A, B) Streaming of flow as a reflection of hemodynamic compromise. **A:** A right common carotid artery injection shows streaming of unopacified blood in the main stem of the right middle cerebral artery (*arrow*) with poor opacification of the superiorly directed branch (*arrowhead*). Notice that the timing of the external carotid artery circulation is ahead of the internal carotid artery, another reflection of a hemodynamic problem.

B: The left common carotid artery injection in the same patient gives a complementary view, wherein the lucent streaming in the right middle cerebral artery now derives from the unopacified right carotid inflow.

Conclusion: There is an unusual hemodynamic phenomenon present causing the left internal carotid artery to provide more flow to the right hemisphere than the right internal carotid artery. Therefore, even without knowing that this patient had a critical right internal carotid artery stenosis (off screen), one could deduce the presence of such an obstruction to flow. This deduction is corroborated by the appearance of the external carotid artery in (A). Catheter-induced spasm or a dissection could give the same hemodynamic appearance.

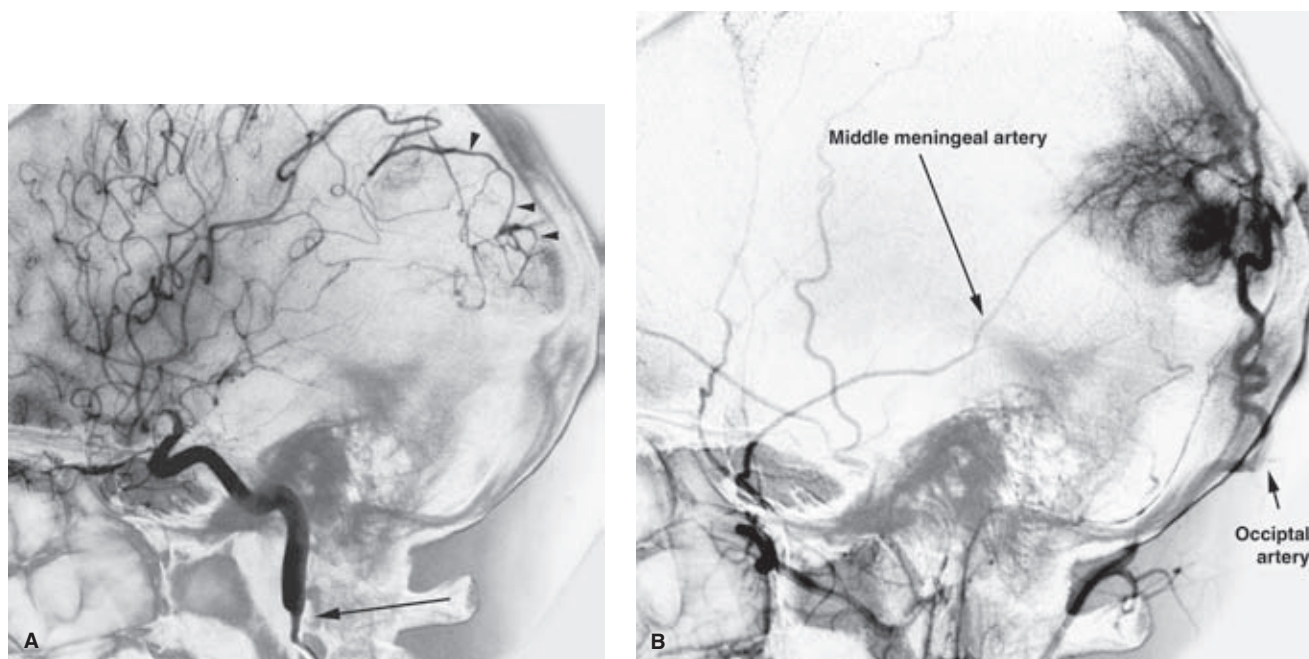


FIGURE 2-31. (A, B) Hemodynamic effects of catheter-induced vasospasm during evaluation of extra-axial hemangiopericytoma. A right internal carotid artery injection lateral plane (A) in a 34-year-old patient with a hemangiopericytoma of the right occipital region. There is spasm around the catheter tip (*arrow*). An image in the late arterial phase demonstrates a stagnant column of contrast in the cervical-cavernous internal carotid artery. One may deduce the observation of stagnation from the fact that the main stems of the anterior cerebral artery and middle cerebral artery ipsilaterally are being washed out (diluted) through collateral channels. A branch of the middle cerebral artery has been parasitized by the tumor (*arrowheads*). This tumor has a vascular pattern more disorganized and irregular than vascular meningiomas, better seen through opacification of the occipital artery and middle meningeal artery in the external carotid artery injection (B).

probably a worthwhile routine precaution for all injections to minimize the effects of shear on the intima. It will introduce the jet of contrast as a crescendo rather than as a staccato and will allow some relatively gradual displacement of the catheter away from an adjacent intimal surface before the full force of the jet is introduced. It also attenuates any whipping effect on the catheter that might displace it from a tenuous position, such as a proximally engaged vertebral artery.

A theoretical source of intimal damage during catheter injections in the major cranial vessels is the Venturi effect, by which the contrast jet may cause infolding or collapse of the arterial walls distal to the catheter tip. Doumanian and Amplatz (18) described this phenomenon at high injection rates in dogs where collapse of the vessel wall was so severe that the jet of fluid sliced the infolded vessel wall. With clinical injection rates, particularly in adult veins or occasionally in the pliable arteries of children, this phenomenon is seen in a more benign form. Because of the high rate of inflow from the aorta to the major cranial vessels, this phenomenon is unlikely to be seen during cerebral angiography. However, it could become a factor if blood flow were dampened proximally, such as might happen if one were to catheterize a vessel distal to a critical stenosis or if the catheter were to become clamped by a focus of concentric mural spasm.

Do Not Advance the Catheter All the Way to the Wire Tip

An intimal dissection most likely is initiated by the tip of a wire being inadvertently forced into a subintimal position.

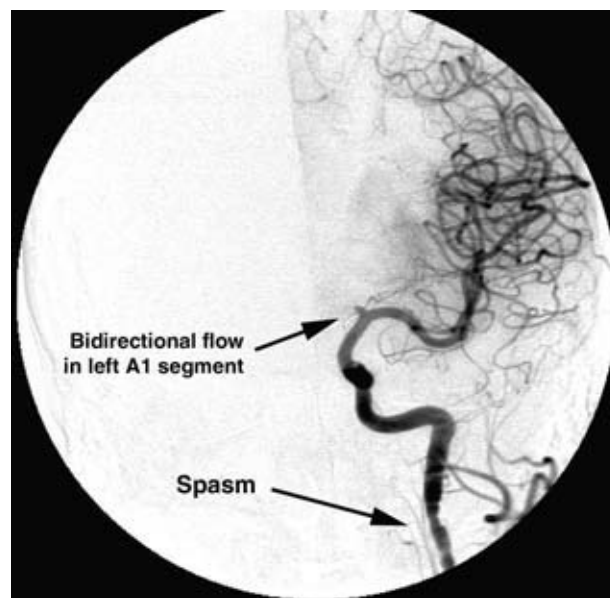


FIGURE 2-32. Hemodynamic effects of catheter-induced arterial spasm. A left internal carotid artery injection inadvertently performed in the presence of moderately severe spasm. The hemodynamic effects of spasm are evident in the appearance of prominent reflux into the external carotid artery branches. Moreover, the A1 segment is poorly opacified, even though it appears to be of robust proportions. This represents a hemodynamic effect, not an occlusion of the A1 segment. Bidirectional flow can be confirmed by looking at sequential images.

This is potentially significant, as an event such as this could prevent visualization of an aneurysm of the anterior communicating artery complex, particularly if the spasm were relieved by the time the contralateral carotid artery was studied.



FIGURE 2-33. *Standing waves*, a transient phenomenon related to the contrast injection, have a more regular corrugated appearance than a mural spasm. They do not compromise the vessel lumen significantly.

This is probably more likely to occur if the catheter tip is pushed almost to the end of the wire, causing the wire tip to lose its flexibility. If the catheter is then pushed over the end of the embedded wire, a small intimal tear will be amplified into a dissection. Therefore, always allow the distal wire to retain its flexibility by keeping the catheter position short.

Checking Catheter Position

Immediately after selecting a vessel, particularly a critical vessel such as the internal carotid or vertebral arteries, the wire is removed carefully. Attention during wire withdrawal is directed initially to the catheter tip and to ensuring that withdrawal of the wire does not have a detrimental effect on the catheter position. A bobbing motion in time with the cardiac cycle transmitted from the aortic arch along the catheter indicates that it has not become wedged in a vessel turn or area of spasm (Figs. 2-31–2-33). Attention during the latter part of the wire withdrawal is focused on the fluid meniscus in the hub of the catheter or fluid behavior in the Y-adapter. A suctioning of fluid into the catheter or a sucking sound as the wire emerges indicates the presence of a vacuum in the catheter because the catheter tip is against the arterial wall or clamped by tight spasm. Although one's immediate reflex, on hearing this sinister sound, is to pull down the catheter, it is vitally important to *open the valve of the Tuohy-Borst adapter first* to allow backflow onto the drapes. Otherwise, on resumption of flow when the catheter tip is free, the pressurized flush will push the generated bubbles in the catheter into the artery. Slowly pull down the catheter,

checking under fluoroscopy if necessary to monitor the catheter tip, until backflow is seen at the catheter hub. Suction the catheter to remove remaining air, and resume flush.

If the wire has been removed uneventfully from the catheter, the routine is to backbleed the catheter for approximately 5 to 10 seconds while tapping vigorously for bubbles, and then resume forward flush by tightening the hemostatic valve or reopening the flush line of the manifold. Before hooking up to the injector for a run, recheck the catheter position and check for spasm. This is best done with a subtracted mask on which small hand injections can be made to test flow in the vessel and to confirm that the catheter curve still conforms to the artery.

Before doing an angiographic run of any of the cranial vessels, it is very important to assess runoff first (Figs. 2-34 and 2-35). This avoids the dangers of injecting into a vessel that is atretic distally, for example, a vertebral artery ending in a posterior inferior cerebellar artery, or injecting into a

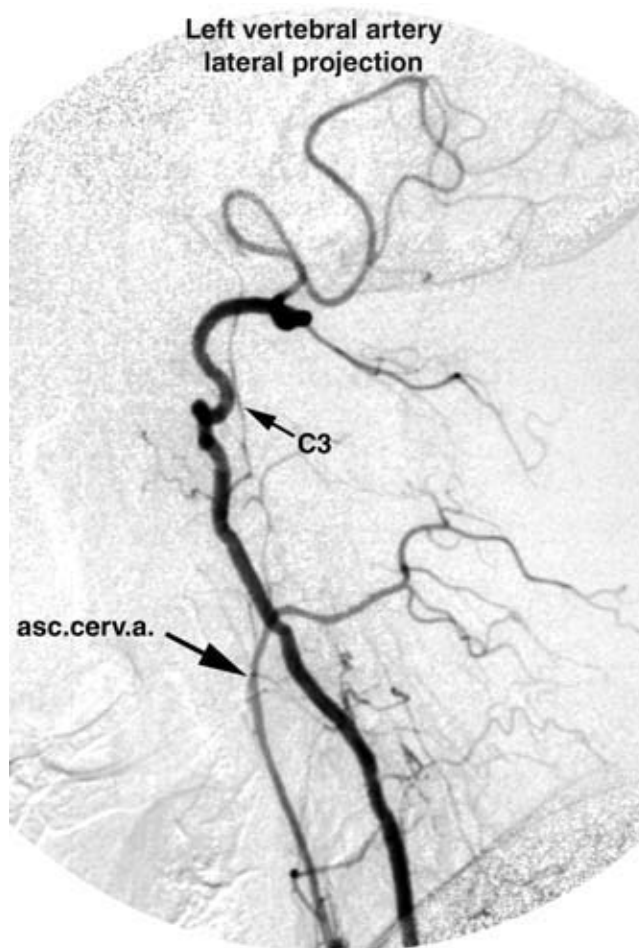


FIGURE 2-34. Importance of testing vessel runoff before performing power injections. Before doing full-volume power injections into the cerebral vessels, it is very important to assess for catheter-related spasm or dissection. Assessing runoff in the head is also vitally important. The possibility that a catheterized vertebral artery ends in a posterior inferior cerebellar artery should always be considered, as demonstrated here. The C3 anastomotic branch of the left vertebral artery is marked as is the ascending cervical artery (*asc. cerv. a.*). The ascending cervical artery is directed posteriorly to assume the territory more commonly associated with the deep cervical artery.

A full-volume injection into a hypoplastic vertebral system such as this could have severe consequences.

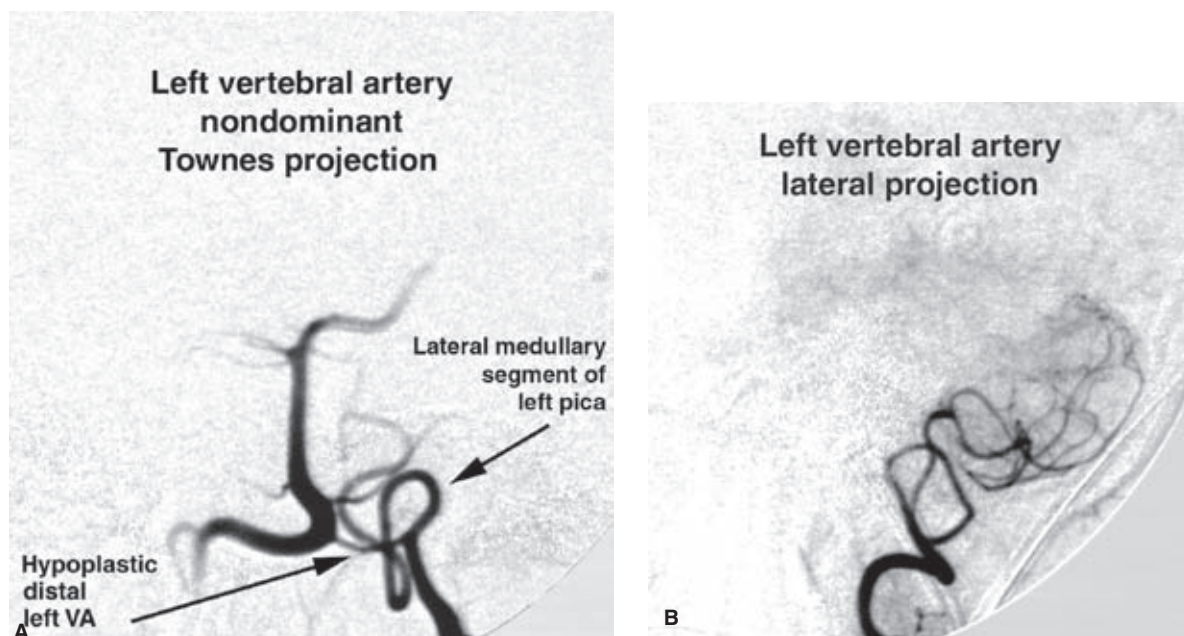


FIGURE 2-35. (A, B) Injection of a distally hypoplastic vertebral artery. **A:** A nondominant left vertebral artery was inadvertently injected. Fortunately, there was sufficient outlet through the hypoplastic distal intradural left vertebral artery. The patient tolerated the injection. However, in such instances, unless unusual circumstances prevail, the right vertebral artery should be injected. If it should be necessary to study the posterior circulation through a hypoplastic vertebral artery such as this, the injection should be performed by hand.

B: However, the patient developed prolonged spasm of the proximal left vertebral artery with the appearance of a persistent, nondiluting column of contrast extending through the territory of the left vertebral artery. Notice that the remainder of the posterior fossa opacified in (A) has already passed its venous phase. The catheter should be pulled down immediately. A roadmap image could then be obtained from the left subclavian artery to rule out an intimal dissection.

vessel with a dissection, critical aneurysm, or pseudoaneurysm in which a standard injection rate could conceivably exacerbate the problem. Alternatively, a vessel feeding a vascular malformation may need a higher rate of flow.

After positioning for the run and checking runoff, the catheter is connected to the injector. This is tightly sealed and checked carefully for bubbles with assertive tapping of the junction points as the assistant draws back until blood emerges freely from the catheter without bubbles. This is then pushed forward to clear the catheter and to prime it with contrast. With microcatheters, or when the guiding catheter is in a small vessel, it is better not to have the assistant draw back toward the power injector after the hookup. This will induce spasm or occlude the catheter. In these circumstances, have the assistant maintain forward flow during and after the hookup. Clear, audible instructions must therefore be communicated at all times to the assisting staff during the hookup in terms of the desired direction of contrast flow. A final check of contrast runoff in the head can be done at this point by watching under fluoroscopy while the assistant advances the injector. It is not rare to discover at this point that the cervical carotid or upper vertebral artery is represented by a stagnant column of contrast due to the unsuspected development of spasm.

Spasm Around the Catheter Tip

In most instances, withdrawal of the catheter from the vessel will relieve the irritation to the vessel within a few minutes. Before reflexively pulling down the catheter, however, it is worth pausing for just a moment to ask oneself how

long the catheter has been in this position and if it is possible that this spasm has been present and unknown for more than a minute or two. If this is the case, then it is probably worthwhile to aspirate vigorously 10 to 20 mL from the catheter before pulling it down lest some thrombus should have formed around the tip or in the vessel distal to it. Even in the event of severe spasm, formation of thrombus will be infinitely less likely if a generous flow rate of flush has been in place.

Wire Manipulation and Great Vessel Catheterization

Catheters and wires possess complementary behavioral characteristics that can be used to steer into the distal vascular tree from the remote vantage of the common femoral artery. Modern techniques of manufacture allow refinement of these instruments such that the wires and catheters each have a multisegmental composition, providing the theoretical versatility of being able to take advantage of a greater array of behavioral traits in a given team of instruments.

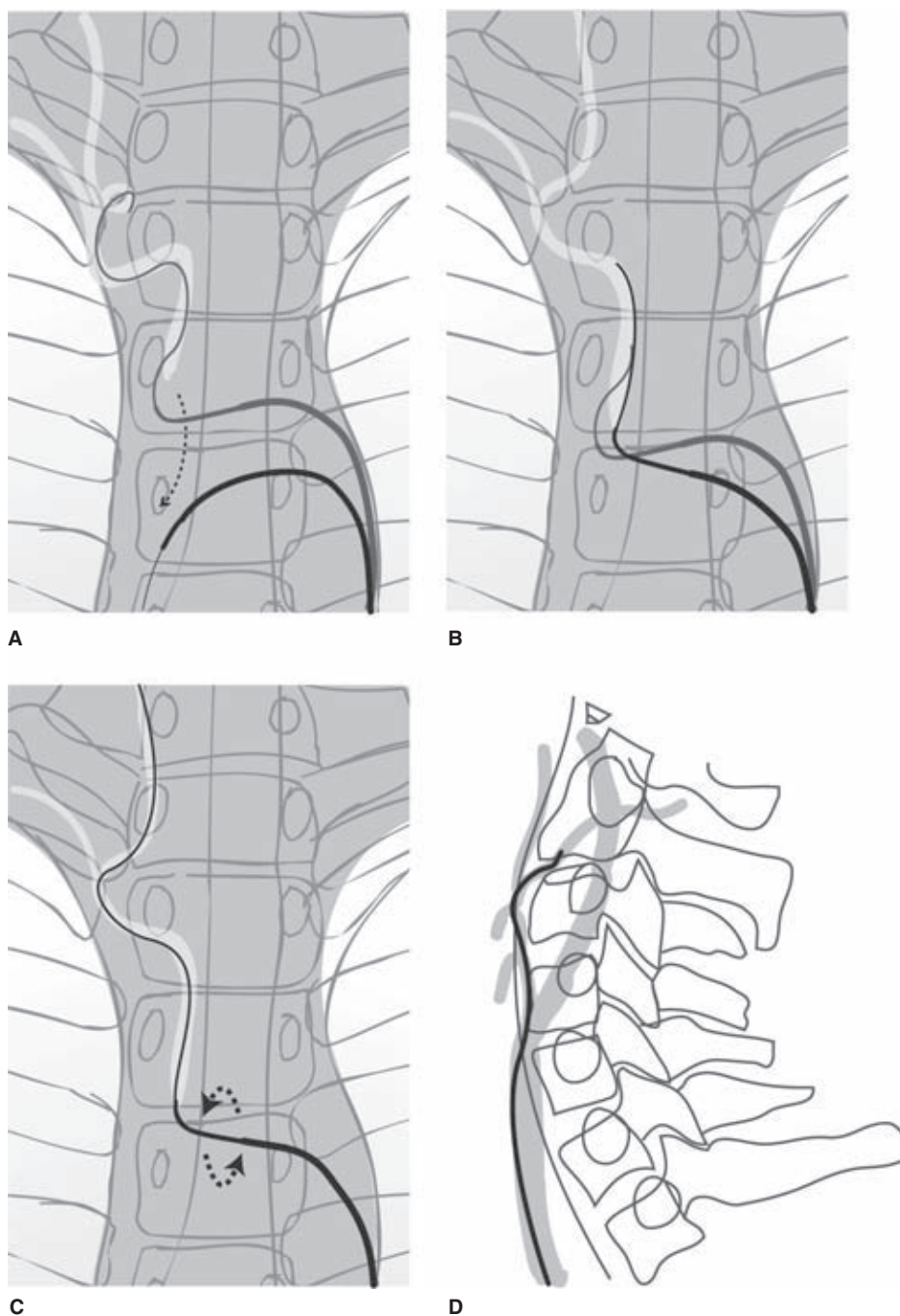
While these refinements are undoubtedly propitious, they compel the angiographer to a greater analysis of instrument behavior whenever severe navigational difficulties are encountered. Specifically, when having difficulties with catheterization of a particular vessel, the precise point of failure in the system of instruments then in hand must be identified before an intelligent modification or replacement of an instrument can be countenanced (Figs. 2-36–2-41). Exculpatory accounts that the vessels were “too tortuous” can be avoided by analyzing the precise reason for failure

FIGURE 2-36. (A–D) Difficult brachiocephalic catheterization. To improve one's chances of selecting a tortuous brachiocephalic artery and right common carotid artery, pull back the catheter to the proximal rim of the vessel and have the patient take a sustained inhalation (**B**). This will straighten the course between the descending aorta and the neck enough to make a critical difference. It may be necessary to use a long-taper pliable wire.

Advance the wire as far as possible in the external carotid artery system to improve one's purchase, particularly if using a pliable wire. Consider using a lateral road map, obtained by injecting below in the vessel ostium (**D**). This will ensure against selecting the internal carotid artery inadvertently.

Allow the patient to regain a breath. Request another sustained inhalation, but do not delay because the wire will have been in the catheter for some time now.

Spin the catheter as you advance (**C**). This will reduce friction between the catheter and the vessel wall, and between the catheter and the wire. If the catheter becomes stuck on a particular curve, ask the patient to cough, if one is completely certain that the wire is in the external carotid artery.



of the current instruments. Tortuous vessels certainly are a major problem in elderly or hypertensive patients, but they exercise this effect in different ways.

Most problems with vessel catheterization fall into a few categories:

1. *Vessel identification and selection with the catheter tip.* Most frequently, a problem with vessel selection lies with catheter positioning in the aortic arch. The tip must be pointing directly into the vessel and usually must be pulled back and perched on the closest rim of the ostium (i.e., closest to the angiographer's control). This allows the most direct route of access to the target artery. When a particular vessel or its residual stump following pathologic occlusion is not seen at all,

one must consider the possibility of anomalous vessel origins. The most commonly encountered anomalies include a common ostium or trunk for the brachiocephalic and left common carotid arteries, an aortic arch origin of the left vertebral artery, and an aberrant right subclavian artery.

The ostium of a left vertebral artery arising directly from the aortic arch can be frequently difficult to find with a catheter tip; the catheter commonly jumps from the left common carotid artery to the left subclavian artery as one withdraws. If one suspects that a left vertebral artery is arising from the aortic arch, its ostium can be sometimes found by rotating the catheter tip clockwise from the left subclavian artery while advancing slightly.

(text continues on page 39)

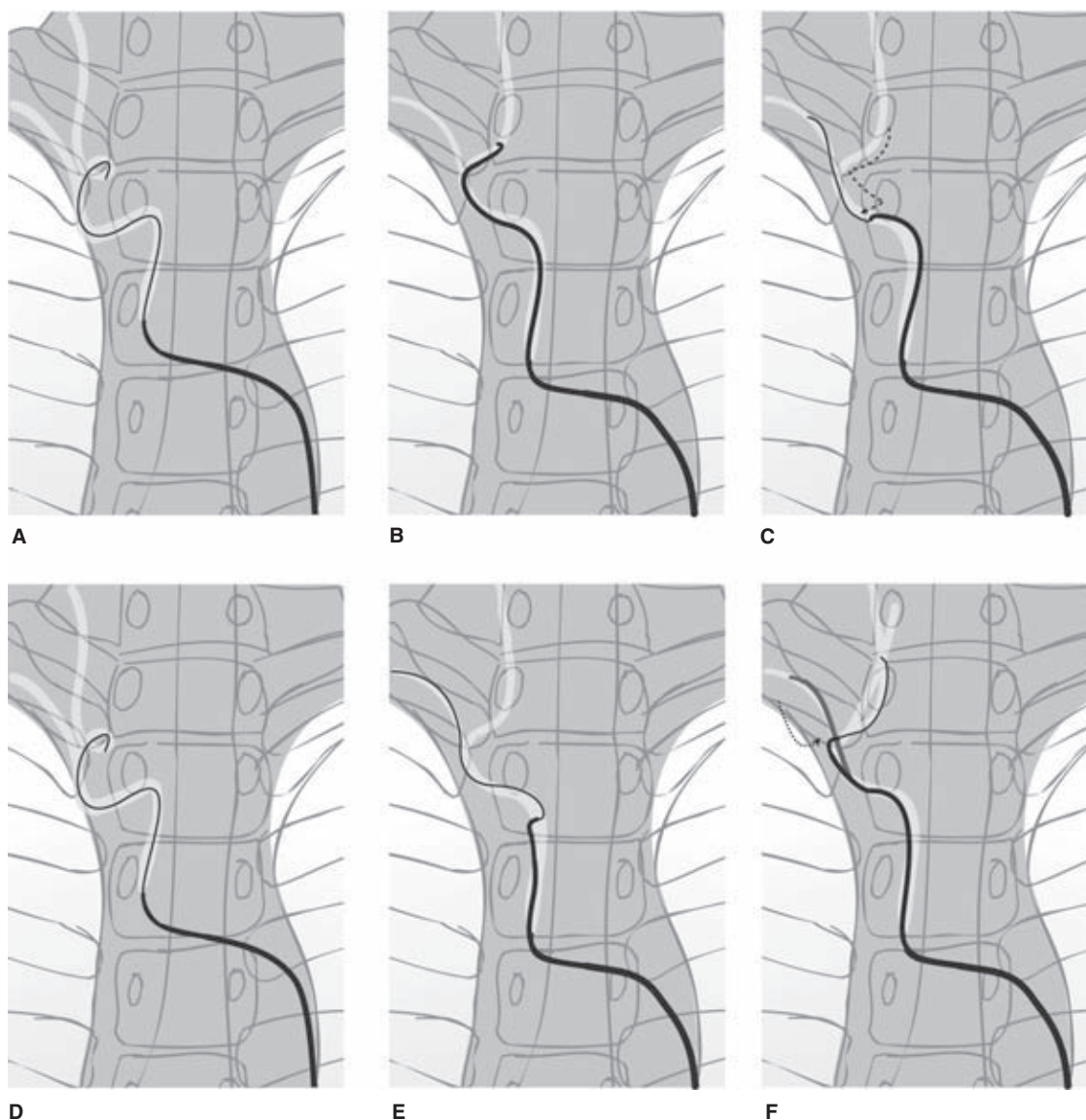


FIGURE 2-37. (A–F) Catheterizing the right subclavian artery and right vertebral artery I and II. If it is not possible to select the right subclavian artery directly from the aortic arch, then a number of possibilities might be considered.

(A) The right common carotid artery is selected and the catheter is advanced into it. The wire is withdrawn to the catheter shaft. The catheter is then torqued to point to the patient's right (B) and withdrawn slowly toward the brachiocephalic artery. A slight kick of the catheter may be seen when the subclavian ostium is reached (C), and the wire can be advanced. In a tortuous system, a catheter with a wire inside is less likely to prolapse back into the aorta as one retracts to search for a proximal vessel. A catheter with a sharper angle at its tip can make a crucial difference in searching for an elusive right subclavian artery; a headhunter or Davis A1 catheter can both be excellent in this situation.

Occasionally, it may be possible to spiral the wire within the brachiocephalic artery to select the right subclavian artery. If an apparently correct position is maintained by the catheter, but it keeps selecting the right common carotid artery, then rotating the catheter to a counterintuitive position may allow the wire to bounce into the right subclavian artery (E). In all these situations, it is very easy to lose one's position in the right subclavian artery as one retracts in searching for the right vertebral artery. Therefore, when the right subclavian artery has been selected distally, remove the wire, clean the catheter, and make a roadmap from a distal position in the right subclavian artery, aiming to opacify the right vertebral artery by reflux. Then, advance a supporting wire all the way to the catheter tip again before starting to retract to the right vertebral artery. The presence of a supporting wire will diminish the risk of collapsing the catheter out of the right subclavian artery. Notice that the wire in the vertebral artery (F) courses medial to the projected course of the common carotid artery, although it starts laterally. Confusion about the right vertebral artery versus the right common carotid artery when a wire has been passed can occur. Obliquing the intensifier may help; a vertebral wire will follow the course of the foramina transversaria. Having the patient swallow may help as well; a carotid wire should move with swallowing. For particularly difficult right subclavian arteries, there is often not an easy answer. *(continued)*

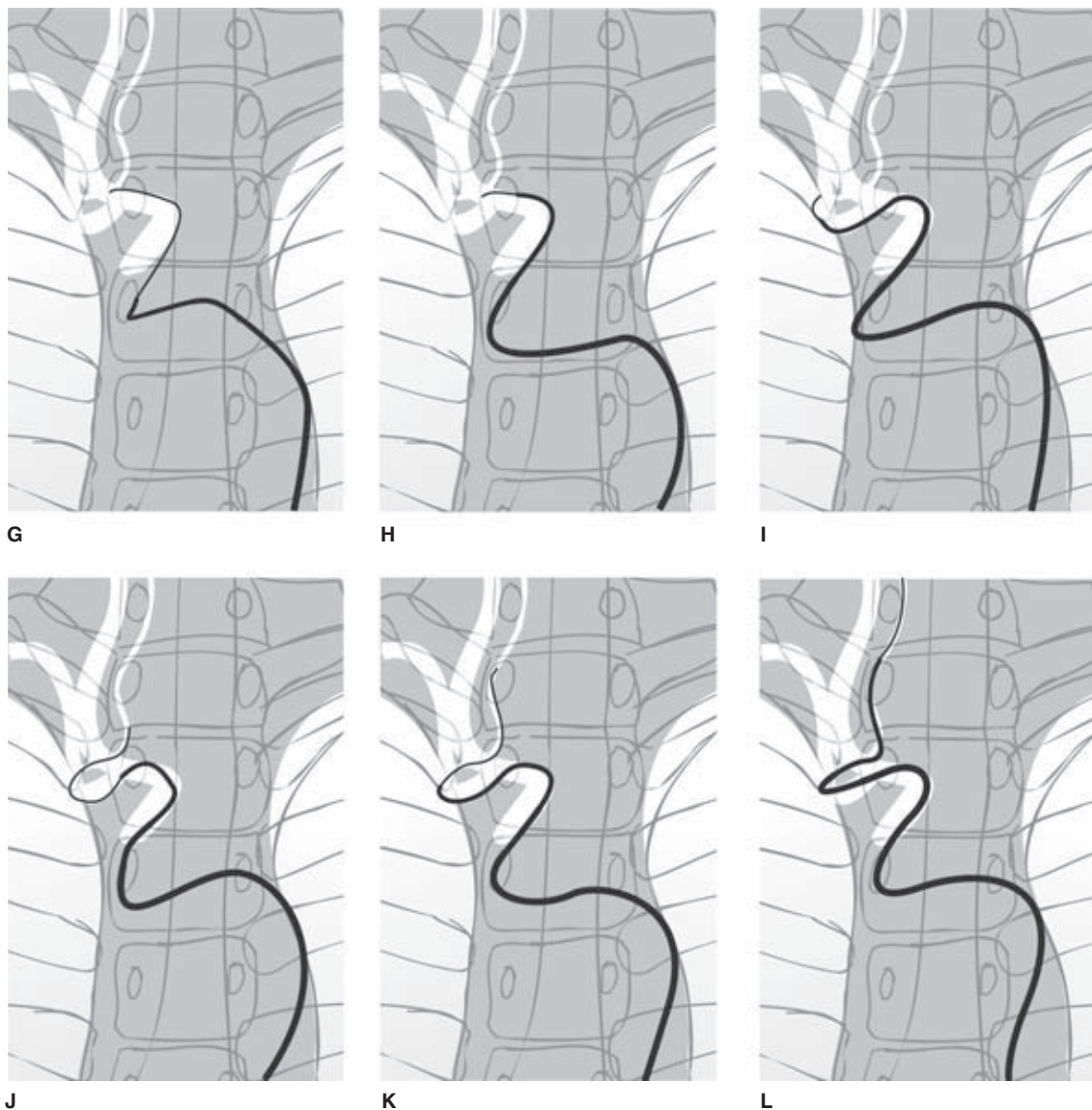
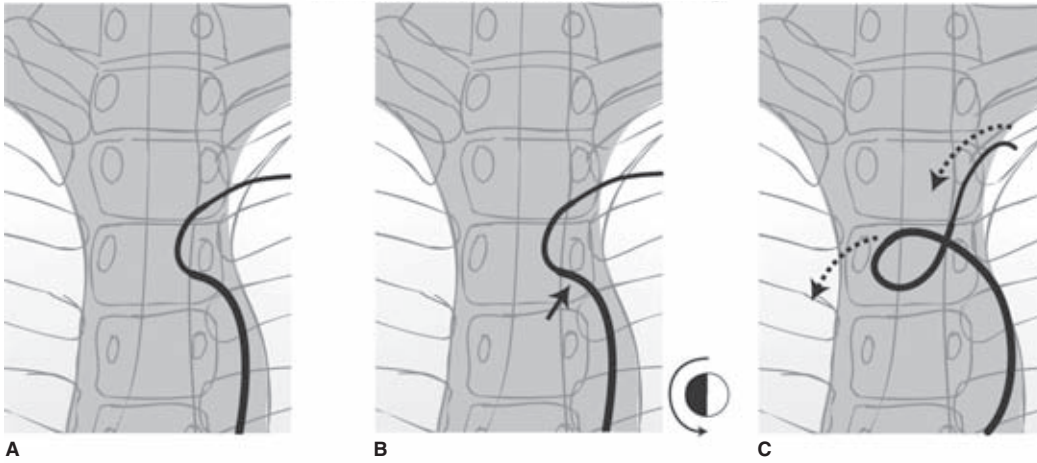


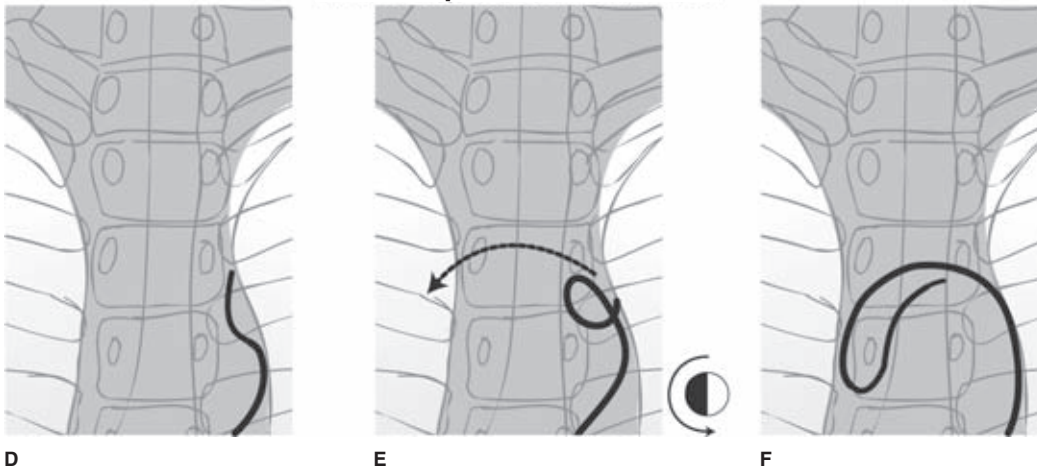
FIGURE 2-37. (CONTINUED) The most difficult cases are those in which the right subclavian artery pursues a vertically inferior course from a tortuous brachiocephalic artery (**G, H**). In these patients, the only possible solution is to find precisely the correct angle and select it with whatever curved catheters or wires one can obtain. A 30-degree right anterior oblique (RAO) road map is often extremely helpful in showing the way. A catheter such as a headhunter with a more extreme curve than a standard hockey stick is sometimes very good at finding the correct angle and at selecting the right vertebral artery subsequently (**I**). A Davis catheter usually has a tighter curve than a Berenstein catheter and frequently has the critical edge for directing a wire around a difficult ostium. A curved Bentson wire may emerge from the catheter into the brachiocephalic artery with the correct angle to select the right vertebral artery. A sustained inhalation by the patient will often straighten the proximal vessels to allow passage of a catheter or wire in an otherwise impossibly tortuous situation.

Note that the roadmap image of the vertebral artery has been illustrated as running medial to the course of the tortuous right common carotid artery. This is a point over which some confusion can occur.

1. In the left subclavian artery



2. In a capacious aortic arch



3. Off the aortic valve

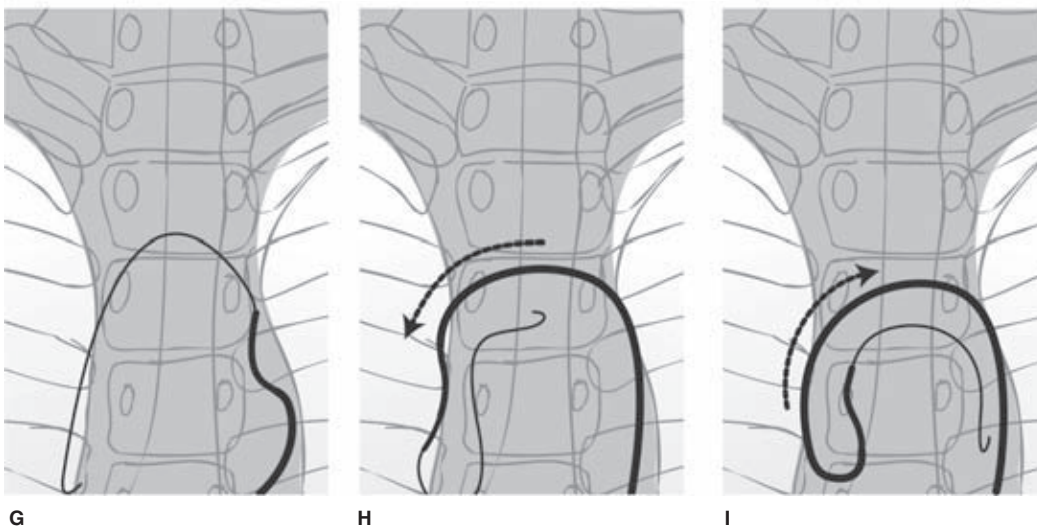


FIGURE 2-38. (A–F) Reforming a Simmons curve.

1. *Reforming in the left subclavian artery.* Generally, the unformed catheter tip will seek the ostium of the left subclavian artery without difficulty. A dirigible wire, such as a Terumo wire, or a soft curved wire, such as a Bentson, can be used to navigate the Simmons catheter tip into the subclavian artery past the vertebral artery (A). This wire can be withdrawn into the main shaft of the catheter proximal to the curve (arrow in B). Better yet, the wire can be removed and the stiff end of the Bentson wire advanced to this point, but no further, to support the catheter shaft. The next step is to create drag on the tip of the catheter by torquing the shaft in the aorta and then pushing it into the ascending arch. The success of this technique depends on having the curved section of the Simmons catheter barely in the subclavian artery so that it becomes the fulcrum of rotation when torque is applied. If the curved section is too far into the left subclavian artery, it cannot reform and the catheter will become pushed farther out the artery.
2. *In a capacious aortic arch.* In a capacious aortic arch, a Simmons catheter will usually reform itself if one can create enough drag on the tip by torquing and then pushing. This maneuver can be assisted by placing a wire within the shaft of the catheter, as in (B), for additional support.
3. *Off the aortic valve.* A 3-J wire pushed over the arch and curved off the aortic valve so that its tip is pushed as far back across the arch as possible will usually work (H). Any concerns about aortic valvular disease or coronary artery disease should preclude use of this technique.

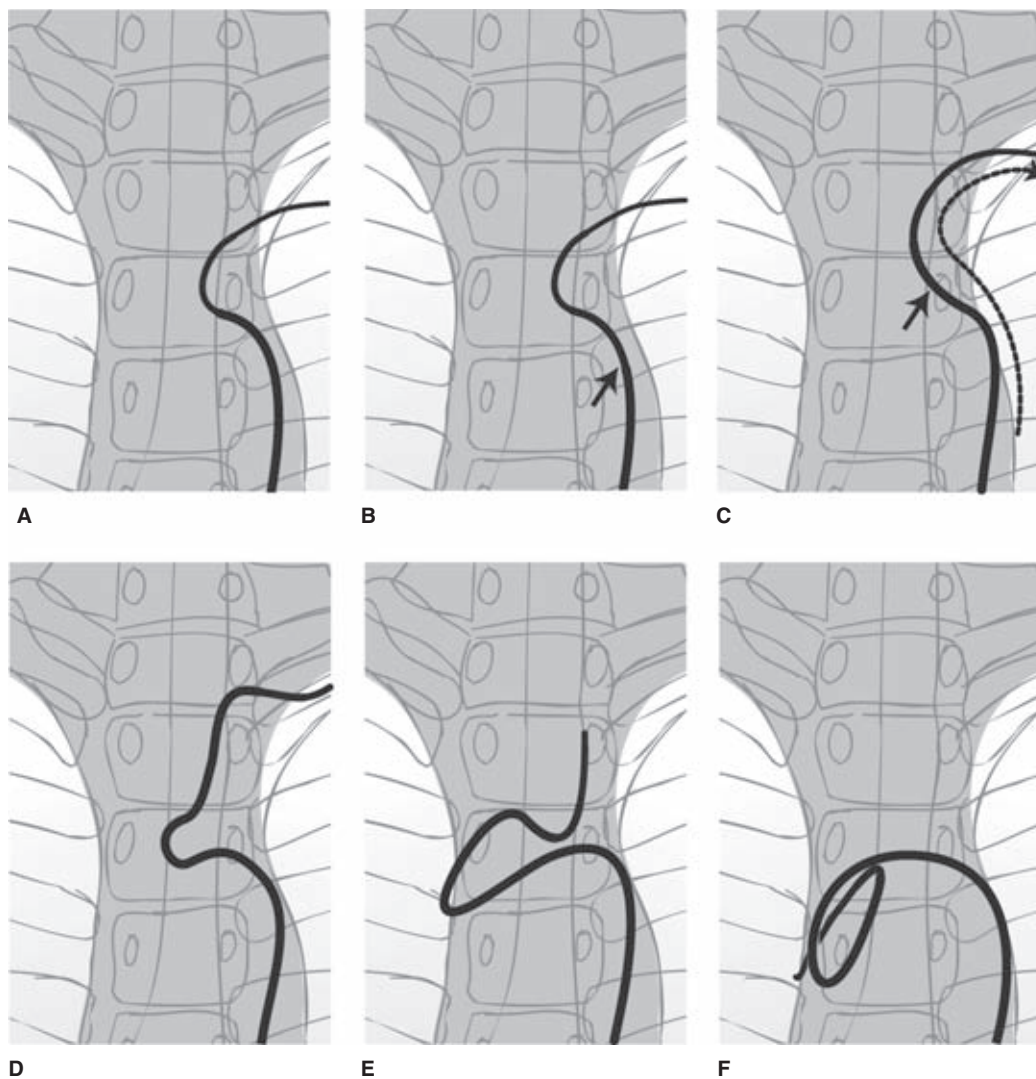


FIGURE 2-39. (A–F) Avoid forming a knot with a Simmons catheter. One of the numerous ways to form a knot with a Simmons catheter is during reformation of the catheter in the left subclavian artery. If insufficient torque or incorrect positioning is applied to the catheter, it may simply advance into the subclavian artery. This may happen by having the supporting wire too proximal in the catheter (*arrow in B*). By advancing the catheter farther, a new fulcrum point becomes established. By pushing farther, the catheter eventually folds on itself, giving the appearance of a Simmons curve. When this false loop is pushed over the aortic arch, it may drag the true curve out of the left subclavian artery. The true curve may then reform itself but does so pointing in the wrong direction. At this point, the crisscrossing segments of the Simmons catheter have the capacity to interweave and form a granny knot. If this happens, do not drag on the catheter and tighten the knot. Instead, push the catheter in as far as possible to the most capacious segment of the aorta, and straighten out the loops with as much stiff wire as the aorta will accommodate.

2. *Proximal tortuosity of the vessel impairing preliminary navigation by the wire.* When the vessel has been identified but the wire will not advance sufficiently and collapses into the aorta, then a number of possibilities should be considered. If, in fact, a tortuous vessel is at fault, then straightening the vessel with a sustained inhalation on the part of the patient, turning the patient's head, or small repeated coughs by the patient as the wire advances, can frequently be helpful (Figs. 2-36 and 2-37). Failing this, a more pliable wire may succeed in navigating the tortuous segment; it may not, however, be sufficiently robust to support the subsequent advance of the catheter. Consideration should be given to this potential problem before

calling for such a wire. A wire with a pliable, distal long taper but a stiffer proximal shaft can be an excellent compromise. For example, the long-taper stiff-shaft Terumo wire has an excellent combination of a pliable distal tip, which can engage a tortuous system, and a proximal segment, which resists deformity within the aorta as one applies forward tension to the catheter.

3. *Proximal tortuosity of the vessel impairing advancement of the catheter over the wire.* If the distal vessel can be navigated with the wire in hand but the catheter cannot be advanced over it, then maneuvers on the part of the patient to straighten the course of the vessel as mentioned earlier may be of assistance.

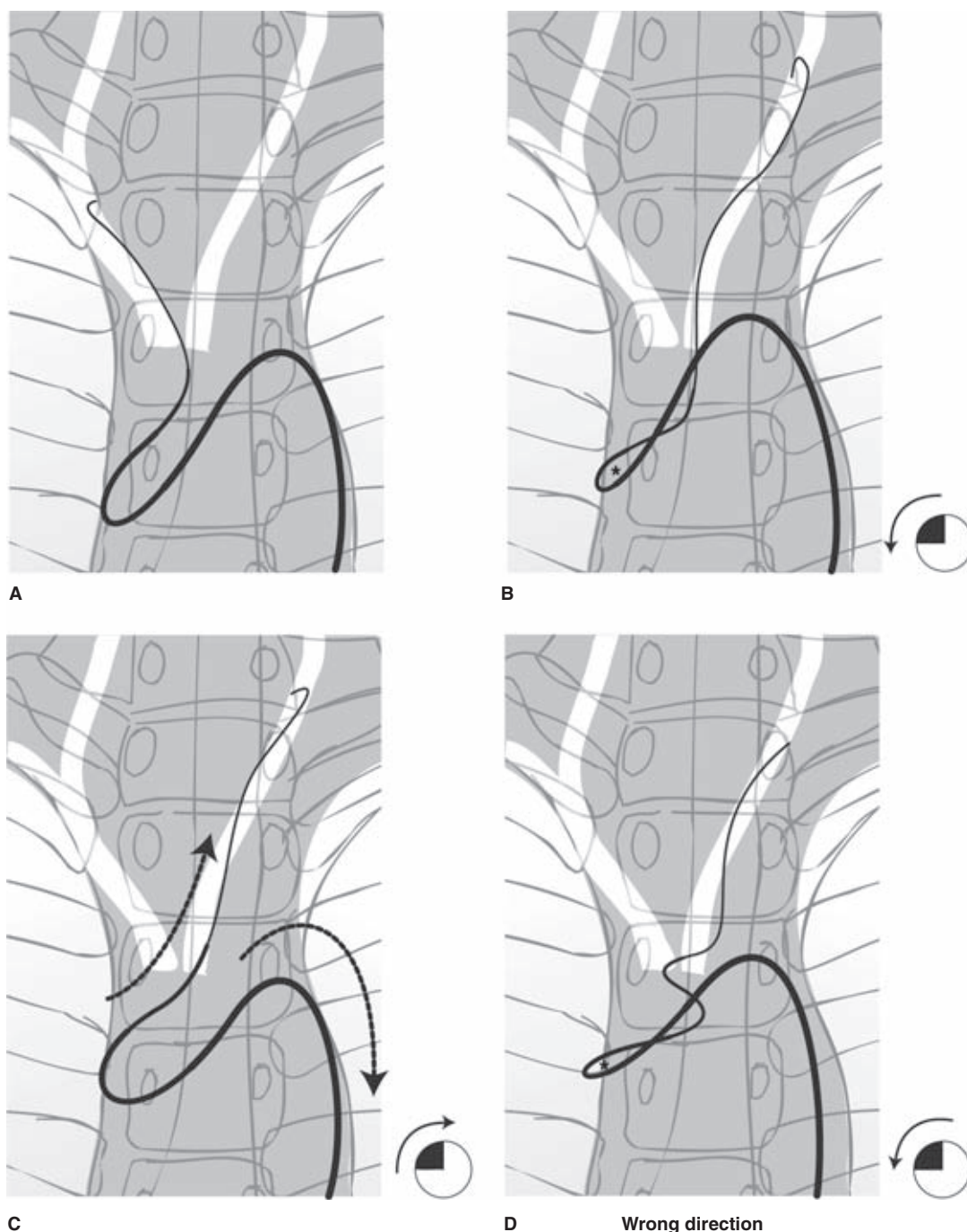


FIGURE 2-40. (A–D) Selecting the left common carotid artery with a Simmons-type curve. Generally, a reformed Simmons catheter and Bentson wire will seek the brachiocephalic artery without difficulty (A). Remember that to advance the Simmons catheter up the carotid, it must be retracted at the groin. It is safer and more effective to always lead the Simmons catheter with a soft wire.

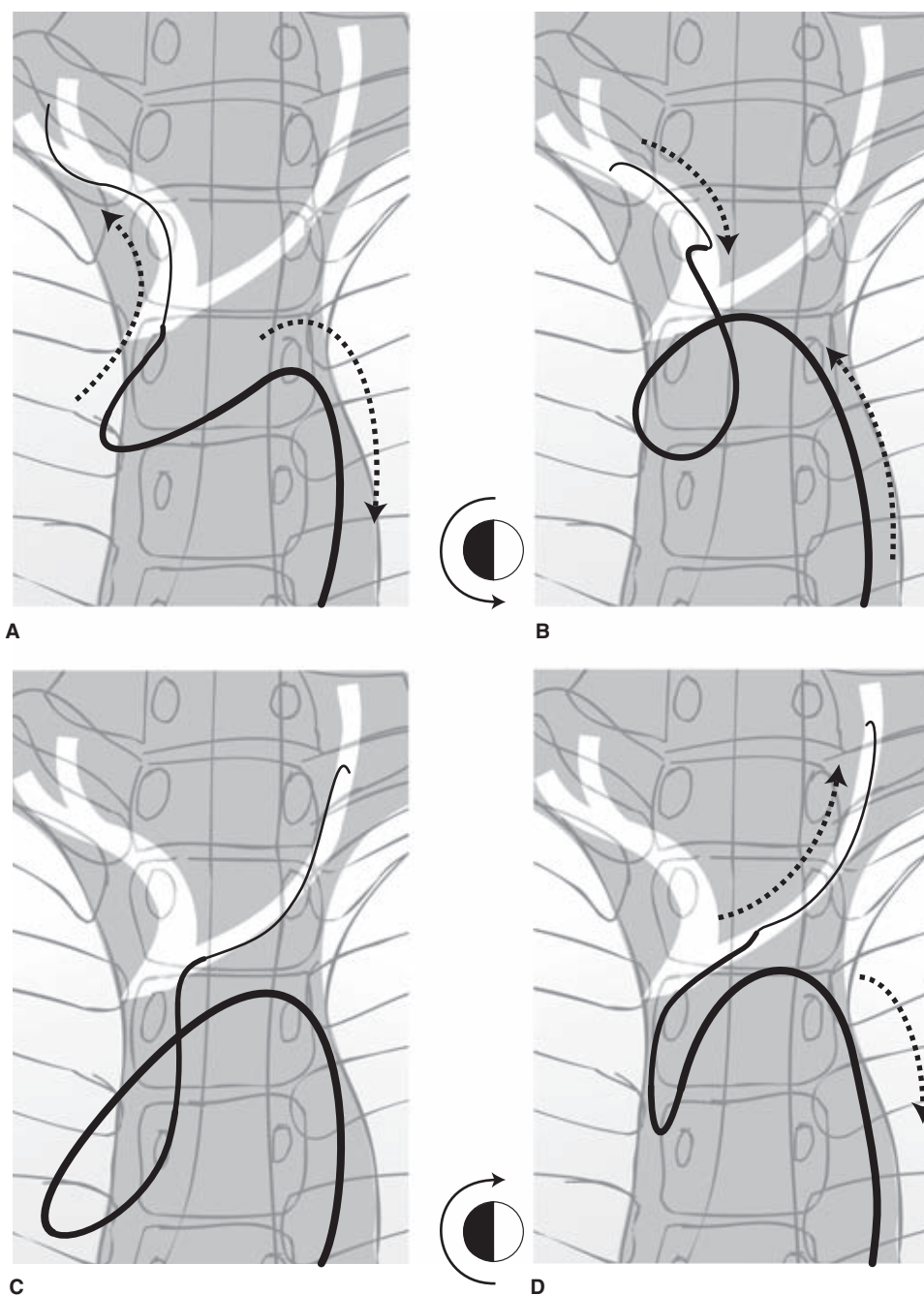
The left common carotid artery may be more difficult to select than the brachiocephalic artery. By remembering that the left common carotid artery frequently has an anterior disposition at its ostium relative to the brachiocephalic artery, one sees why rotating the catheter tip anteriorly (anticlockwise) is necessary (B). However, in older patients, the degree to which this is necessary is often surprising—the catheter may look like it is crisscrossing itself, lost somewhere in the ascending aorta (B). It is necessary to use an extreme anterior position in some patients to avoid selecting the brachiocephalic artery again as one advances the Bentson wire (B).

When the wire has found the artery, the Simmons catheter is retracted at the groin to advance it into the left common carotid artery. It may or may not open out the crossed loop in the aortic arch as it does so. Given the propensity of the Simmons catheter to knot on itself, it is better to undo the anterior turn that one has used to select the left carotid (C). The closed loop (*asterisk*) at the turn of the Simmons catheter should begin to enlarge and open if one is turning the correct way to straighten the attitude of the catheter.

In (D), the Simmons has been turned the wrong way (more anticlockwise), causing the closed loop to tighten (*asterisk*), and the twisted catheter is obstructing its own advance up the left common carotid artery.

FIGURE 2-41. (A–D) Selecting a bovine origin left common carotid artery with a Simmons-type curve.

This technique is similar to selecting a difficult, anteriorly inclined left common carotid artery with a Simmons catheter, except everything is done to a greater extreme and without leaving the brachiocephalic artery. The Simmons catheter is torqued 180 degrees to completely reverse direction in the distal brachiocephalic artery. This is called a *scissors maneuver* because of the form of the catheter at this point (B). It is then pushed in at the groin to retract it in the brachiocephalic artery. With some persistence and by keeping the very tip of the catheter pointing to the patient's left side, the left common carotid artery is selected with a Bentson wire (C). In this situation, correction of the Simmons position must be an exact reversal of the previous torquing maneuver. Otherwise, the wire and catheter will be wrapped around one another.



In addition, it may be necessary to anchor the wire more distally than usual, most often in the external carotid artery tree, to allow sufficient support for the catheter (Fig. 2-36). Generally, the tip of a steerable wire, pointing anteriorly in the common carotid artery, will select the external carotid artery as it advances and will soon thereafter give a characteristic turn as it finds the linguofacial artery. Using this deflection as a guide that the internal carotid artery has been avoided, the wire can be advanced still further into the distal external carotid artery. In patients for whom a concern about using this technique exists, such as in suspected carotid bifurcation disease, a lateral road map can illuminate potential hazards. If the vessel selection is precarious, one may wish

to work in the anteroposterior (AP) plane with a road map centered on the aortic arch. In this case, it is possible with most biplane systems to acquire a road map in the AP plane centered on the aortic arch, and then move the table to center on the neck and acquire a roadmap in the lateral plane. The two roadmaps can be alternately recentered as needed using some incidental landmark, such as dental prosthetic material or electrocardiogram (EKG) leads, when switching from one view to another.

After advancing the wire as far distally as one considers safe, the catheter can then be advanced slowly. The previously described patient maneuvers can be employed as needed. Some experienced angiographers use a *vibrato* motion of the hand to advance the catheter slowly in such

a situation; others move the catheter very slowly in time with the cardiac cycle. The most helpful maneuver in all catheter movements is a smooth counterclockwise spinning of the catheter as it advances. One's conception of advancing a catheter into a major vessel should never be one of ramming a rod up there. Rather, by spinning consistently, all friction is eliminated, and the catheter will invariably make its own progress along the wire.

Probably the common denominator in all such techniques is a reduction of friction between the catheter and the vessel wall on the outside and with the wire on the inside. Hydrophilically coated catheters and microcatheters are designed to take advantage of a lower friction coefficient with the surrounding vessel during navigation. The cost associated with such reduced friction is a lower stability of the catheter when the final position has been gained.

4. *Tortuosity of the aortic arch causing redundant loops in the catheter.* Tortuosity of a capacious aortic arch is a difficulty that can simulate many of the obstacles described earlier. It may prevent advancement of the wire or of the entire system and should be thought of whenever an advancing motion of the catheter at the groin is not met with a corresponding advance of the catheter tip on the fluoroscope. It is a common phenomenon during microcatheter advancement. Any insertion of a given length of microcatheter that is not met with a corresponding advance of the microcatheter tip should prompt consideration that a loop is prolapsing in the neck, or that the microcatheter is pushing the off-screen main catheter into the aorta. Clearly, in these situations, the vascular tree is consuming catheter length somewhere, and this is usually in the aortic arch.

A similar phenomenon can be seen with diffuse aneurysmal disease of the abdominal aorta. In this situation, the ever-increasing curvature and tension of the catheter-wire system in the redundant aorta adversely affects the angle with which the catheter addresses the great vessel, culminating in collapse of the whole system into the ascending aorta. Therefore, this may cause one to think erroneously that the problem lies in tortuosity of the proximal cephalic vessel preventing navigation of the wire or catheter.

The solution to this problem is to straighten the system proximally as much as possible. This can be done by moving to a stiffer and larger caliber catheter, adding a longer sheath, or using a stiffer wire. Moving to a larger catheter is probably the more economical and effective maneuver because a 5F catheter is very likely to continue being problematic in such a difficult aorta. When the wire-catheter system is advanced into the carotid artery from the arch, an inevitable degree of forward tension is present due to the physical forces necessary to coerce it to such a position. A relatively stiff wire used to get to this position will resist deformity from accumulated tension. In contrast, an unsupported catheter does not have this capacity to resist tension. If the wire is removed from the system without having first adjusted for the accumulated tension, then the catheter will inevitably uncoil itself within the capacious aorta, causing a retraction of the tip in the carotid artery and possibly prolapse into the arch. Therefore, after advancing the wire-catheter system of a piece into the great vessel of choice, it is necessary to retract

the system to straighten the course of the catheter before removing the wire.

The apparently "spontaneous" retraction of the catheter from the carotid or subclavian vessels due to accumulated tension after removal of the wire is precisely the opposite of the usual behavior of wire-guided microcatheters but derives from the same phenomenon. With microcatheters, there is a similar accumulation of tension during the advance, but the friction of the microwire within the microcatheter functions as a brace. A microcatheter with accumulated tension is usually confined proximally by the introducing catheter and distally by a narrow arterial tree. Therefore, the confined microcatheter system can only move in one direction—forward. When the microwire is removed, the microcatheter is freer to expend its tension by advancing forward, which it frequently does in considerable degree. Unless the same careful retraction and straightening of the wire-catheter system is used with microcatheter manipulation, severe intracranial complications can ensue from an uncontrolled microcatheter acting like a harpoon against a vessel or aneurysm wall.

On the other hand, removing tension from a microcatheter-microwire system by retraction, if overdone, can result in loss of hard-won access to a distal vessel. Using movement of the radio-opaque microcatheter tip is not a sufficiently sensitive signal. Usually, elasticity of the microcatheter is such that when the tip finally begins to move back, it will do so in excessive degree. It is often more efficacious to monitor for changes in a visible loop of the wire within the microcatheter proximally. As one retracts the system, the proximal loops shift to adjust to loss of redundancy. The microwire can then be withdrawn with a diminished risk of forward motion. In any intracranial position, but particularly critical situations, such as near an intracranial aneurysm, one should monitor the microcatheter tip closely as the wire is being withdrawn to detect any change in position (Fig. 2-37).

Another danger to consider during wire removal is the hazard of the catheter becoming kinked and occluded at a point of sharp curvature as the supporting wire is removed. This is a potentially disastrous event that can be difficult to recognize, as it frequently occurs outside of the field of view, for example, at the distal tip of the guiding catheter in the case of coaxial microcatheters, or high in the aortic arch in the case of guiding catheters. Most commonly, absence of backflow from a catheter is an indication that the distal tip is apposed against a vessel wall. Backflow can be restored by slight retraction of the catheter. However, in a difficult aortic arch, the possibility of catheter kinking should be kept in mind. This is an extremely dangerous situation because blood in the distal catheter already stagnant from a prolonged catheterization quickly thromboses and may propagate itself into the arterial tree.

Finally, it must be acknowledged that some vessels are defiant to catheterization. A recurved catheter shape, such as a Simmons type of catheter, while giving less maneuverability and flexibility in superselection of carotid branches, proves indispensable in certain patients, and is, nonetheless, an excellent way to accomplish a diagnostic study under difficult circumstances (Figs. 2-38–2-41).

A Note on Exchange-length Wires

Great pains should be taken to avoid, if at all possible, use of exchange-length wires in diagnostic cerebral angiography. During interventional procedures, the use of exchange wires

may be unavoidable, but they should probably be used only when the patient has been heparinized or premedicated with antiplatelet agents, and when the tip of the wire is in the external carotid artery circulation. Over-the-wire exchanges done in the aortic arch should be performed with the tip of the exchange wire in the descending aorta, distal to the cephalic vessels. A catheter exchange over a 300-cm wire is a time-consuming procedure no matter how smoothly it is accomplished. Even though the outer, visible portion of the wire may appear clean after being wiped, the new catheter being inserted has the opportunity to shave accumulated debris, platelets, and thrombus from the exchange wire over its full length. This debris is then free to fall from the catheter tip after removal of the exchange wire. Physicians rarely brag in journals about the instances in which they have gaffed badly. If they did, there would be a sizeable body of literature on the dangers of exchange-length wires in diagnostic procedures. They are very dangerous.

► INTRAOPERATIVE ANGIOGRAPHY

Depending on the preferences of the neurosurgeon, intraoperative angiography immediately after clip placement may be requested to assist with difficult intracranial aneurysms, particularly those in the paraclinoid area. Technically, these can be difficult angiographic procedures. It is often necessary to work in a cramped position at the patient's left groin, the television monitor may be some meters distant and behind various pieces of draped equipment, and movement of the portable fluoroscope is hampered by the paraphernalia of the sterile surgical field. The following points make the process easier:

- The surgical team must procure and remember to use a radiolucent head holder for the surgical table at the beginning of the case. The team must also remember to include the groin in the preparation of the sterile surgical field during draping. To avoid loss of time gaining arterial access to the femoral artery after the clip has been applied to the aneurysm, it is advantageous to have placed a sheath in the femoral artery on a slowly flowing irrigation system (1,000 units of heparin/L) at the beginning of the surgical procedure. Therefore, should the aneurysm clip be causing an unexpected problem, the delay until discovery by angiography is minimized.
- Use high-density (300 nonionic) contrast for maximal visibility on the portable fluoroscope.
- Vessel selection is considerably more difficult in the operating room. A Simmons-type catheter with an accompanying Bentson wire frequently proves a more efficient combination under such circumstances.

Under operating-room circumstances, hand injections of the common carotid arteries are technically adequate. Common carotid selection and injection is safer than trying to select the internal carotid artery under trying and potentially dangerous circumstances.

The utility of intraoperative and postoperative angiography has been confirmed in a number of studies. Macdonald et al. (19) found a 20% incidence of unexpected significant findings in patients who had undergone surgical clipping of aneurysms. These findings included residual aneurysm at the clipped site, other unrecognized aneurysms, or vessel occlusions. The utility of intraoperative angiography was studied

by Derdeyn et al. (20), who found that surgical technique was altered in 11% to 12% of cases in a large series, based on information gathered from the angiogram. A similar rate of clip repositioning was reported in a prospective study by Alexander et al. (21). However, they and other authors observe that intraoperative angiography does not emulate the quality of conventional studies, and that postoperative conventional arteriography may still be necessary in certain cases.

► INJECTION RATES

Visualization of an artery during an angiogram requires that injected contrast be the equivalent of approximately 30% of the volume of flowing blood. Therefore, larger arteries and vessels with faster flow will require faster injections. Immediately after cessation of the injection, a process of dilution begins such that opacification of the veins is less pronounced than that of the arteries. For this reason, in disease states where a foremost interest lies in the status of the venous system, consideration may be given to placing emphasis on a longer injection rate with a higher total volume than one might normally use.

Deciding on the rate of injection for a particular vessel depends on the caliber of the vessel, rate of flow, distal runoff, and catheter position. A useful rule of thumb suggests that when using a 10-cc syringe on a catheter with 0.038-inch ID, a forceful hand injection is the equivalent of 5 cc per second. Therefore, when testing for catheter position, reflux with a hand injection made in this fashion would indicate that a rate of less than 5 cc per second should be considered (Table 2-3). A linear rise or graded introduction of the injection into the vessel runs the theoretical risk of diluting the leading edge of the contrast bolus, but generally such an effect cannot be identified as a significant factor on the final images. Therefore, a linear rise is a good precaution, particularly in precarious or unstable catheter positions, to prevent sudden whipping of the catheter from the vessel, or in positions where the catheter does not conform to the vessel.

► MAGNIFICATION ERRORS

Precise measurement of size is important for treatment decisions regarding aneurysms and AVM. During endovascular treatment of intracranial aneurysms, it is necessary to know the dimensions of the aneurysm lumen in order to choose the correct coil size for building the initial framework. For AVM, estimations of volume and area have an important bearing on treatment decisions because the expected efficacy of radiosurgery is based on the volume of AVM being irradiated. AVM with a maximal linear diameter of 1.2 cm (22) or volume less than 4 cm³ (23) have demonstrated complete obliteration following stereotactic radiosurgery in 80% to 90% of cases at 2-year follow-up.

There are two major factors that cause significant magnification errors in calculation of lesion size based on externally applied markers such as coins and grids, or internal references such as the known diameter of a catheter tip. The relative position of the markers and lesion along the central ray generates an inherent error of geometric magnification. The latter is compounded by error related to relative position away from the central axis of the beam where the divergent nature of the beam amplifies the error of measurement. Linear measurements calculated without correcting for these

TABLE 2-3 Suggested Injection Rates for Adults

VESSEL	LINEAR RISE (s)	RATE (cc/s)	TOTAL VOLUME (cc)
Common carotid	0.2–1	7–10	10–14
Common carotid for bifurcation disease	0.2–1	6–8	6–8
Common carotid for AVM	0.2–1	10	12–14
Internal carotid	0.5–1	6–8	8–10
Internal carotid with aneurysm and acute subarachnoid hemorrhage (SAH) (may be better done with common carotid injections or hand injections to reduce the risk of rerupturing the aneurysm)	0.5–1	4–6	8
External carotid proximal to facial artery	0–0.2	3	6–8
Distal external carotid	0.5–1.0	2–3	6
Vertebral artery (may be better done by hand injection in the setting of a recently ruptured aneurysm)	0.5–1.0	4–5	10
Vertebral artery for AVM	0–0.2	5	10–12
Subclavian artery with sphygmomanometer cuff inflated	0–0.2	8–10	14–16
Costocervical and thyrocervical trunks	0–0.2	2	4–6
Facial, lingual, occipital, ascending pharyngeal arteries	0	1–2	4–6
Aortic arch	0	12–30	30–40
Intercostal, lumbar arteries	0	2	4
Internal iliac arteries	0	6–10	10–12

factors are subject to errors of 13% or greater, meaning that when such linear measurements are used to calculate area or volume, the error factor may be as great as 25% to 40% (24,25).

► WHAT IS THE VOLUME OF AN ARTERIOVENOUS MALFORMATION?

For the purposes of treatment planning, calculation of the volume of an AVM is necessary within a reasonable margin of accuracy. Different formulas are used to calculate the volume of an AVM based on the linear dimensions in three planes. A simple calculation of the volume of an assumed spherical contour is sometimes used:

$$\text{Volume} = \frac{a \times b \times c}{2}$$

Brown et al. (26) calculated the volume of an AVM as an elongated sphere:

$$\text{Volume} = \frac{4\pi(s/2)^3}{3} + \frac{\pi s^2 \cdot (L - s)}{4}$$

where s is the smallest and L the largest diameter of the AVM.

View Setup and Aneurysm Evaluation

Nostalgia is all very well, but change in most arenas of human endeavor is for the better. Specifically in the realm of optimal imaging of cerebral aneurysms, 3D angiographic and noninvasive imaging have eliminated much of the guesswork involved in fine tailoring of Caldwell, Waters, and PA angiographic positioning to individual patients. In the posterior circulation, the A-plane view used to be invariably performed in a Towne's projection, the argument being that this view optimized the visualization of the posterior cerebral arteries. However, this projection increases the radiation output of the tube and foreshortens the aspect of the basilar artery. Moreover, the undertable swing of the tube frequently clashes with lead aprons and shields. The outcome is that most of the time, obscure techniques of radiographic positioning so commonplace in days of yore have become defunct.

Nevertheless, considerations of positioning and projection have a role to play in the economical use of radiation and in the attainment of a profile view suggested by the 3D model but anatomically unreachable without some inventive preparation (Figs. 3.42–3.48). Head extension, flexion, tilting, canting, and rotation can be troublesome maneuvers at the beginning of a procedure, but essential to a safe outcome.

FIGURE 2-42. Removal of forward tension from the microcatheter prior to wire removal. In order to pull back a sufficient quantity of microwire and microcatheter (together) to reduce forward tension but not lose the position of the catheter tip, watch the position of the proximal loops of the system for motion (arrows). When the loop closest to the tip begins to move, all the tension has been removed.

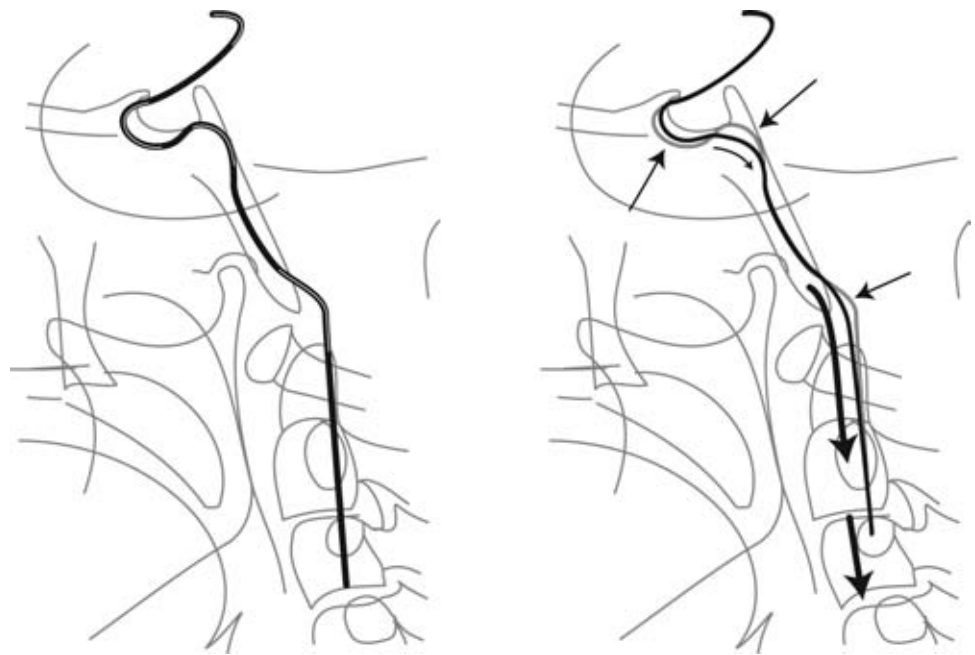


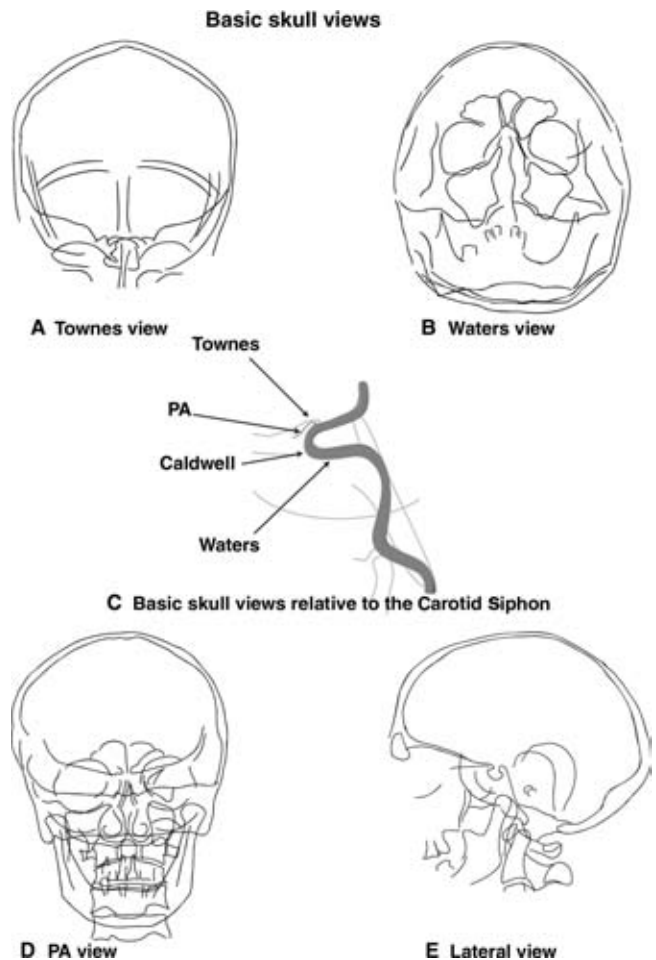
FIGURE 2-43. (A–E) Basic skull views. The frontal view of the skull can be simplified into a decision about where one wishes to place the supraorbital rims in reference to the petrous ridges.

The Townes view (A) places the orbital rims low in the field, so one is looking into the posterior fossa from a superior vantage. This is the standard initial view for the posterior fossa in the frontal plane.

The Waters view (B) places the petrous ridges low in the field. For the posterior circulation, a Waters view is frequently helpful for evaluating the basilar artery trunk or basilar tip aneurysms, particularly those that point anteriorly. For the carotid circulation, a Waters view, in combination with obliquity, is very useful for teasing apart the loops of the internal carotid artery and determining the morphology of aneurysms of the siphon.

The PA view (D) places the petrous ridges between the midsagittal plane of the orbits and as high up as behind the orbital rims. As a standard view of the internal carotid artery, this view usually provides the best overall combined view of the siphon and intracranial circulation. More angulation toward a Townes—superimposing the orbital rims on the petrous ridges—improves the evaluation of the A1 and M1 segments by eliminating subtraction artifact from the orbital rims, but at the cost of superimposing elements of the carotid siphon. Angulation in the other direction to superimpose the petrous ridges on the orbital floor—a Caldwell projection—improves the evaluation of the siphon but at the cost of foreshortening the supraclinoid segment (C). The latter projection—superimposition of orbital floor and petrous ridges combined with ipsilateral obliquity of the image intensifier—gives an excellent transorbital view of the middle cerebral artery division pattern.

In the lateral view (E), the most easily discerned landmarks on a fluoroscopic image are the orbital roofs. If necessary, the patient's head can be tilted to align these guides. Alternatively, superimposition of the external auditory meati can be a guide, although these landmarks are less easily followed on fluoroscopic images. Skewing the lateral view—elevating one orbital roof in reference to another—can be extremely helpful in evaluation of paraclinoid aneurysms. During evaluation of paraclinoid aneurysms, the internal carotid artery contour on the lateral projection can be conceptualized as the brow of a hill over which one is attempting to gain the optimal view of an aneurysm.



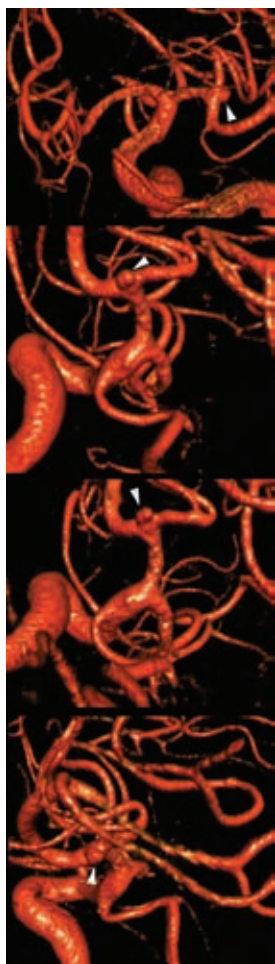


FIGURE 2-44. Left middle cerebral artery aneurysm. Rotational angiography with 3D reconstruction has fortunately supplanted much of the art of patient positioning and creative projection for aneurysm evaluation, a process that invariably involved repeated contrast injections and cumulative radiation exposures in excess of those involved with a single rotational run. This panel of surface rendered images demonstrates a bilobed sessile aneurysm of the left middle cerebral artery bifurcation (*white arrowheads*), the type of aneurysm that certainly would have been difficult to image as thoroughly—or that might well have escaped attention—using conventional techniques alone.

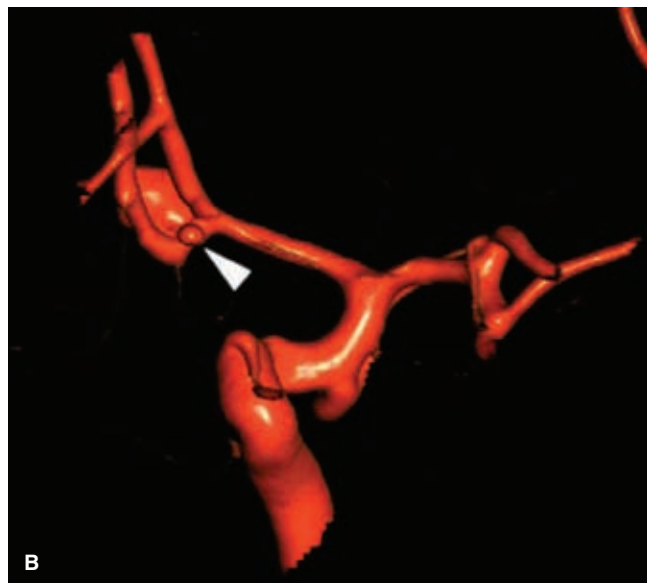


FIGURE 2-45. (A–F) Recurrence of aneurysm of the anterior communicating artery. A middle-aged patient presented with extensive subarachnoid hemorrhage (A), a Hunt and Hess grade 4 status, and was found to have a moderate-sized aneurysm of the anterior communicating artery on CTA. Rotational angiography (B) revealed a second tiny 2-mm adjacent aneurysm at the left A1–A2 junction (*arrowhead*) that could not be seen on conventional projections, until the aneurysm profile was established using the 3D data (C). (*continued*)

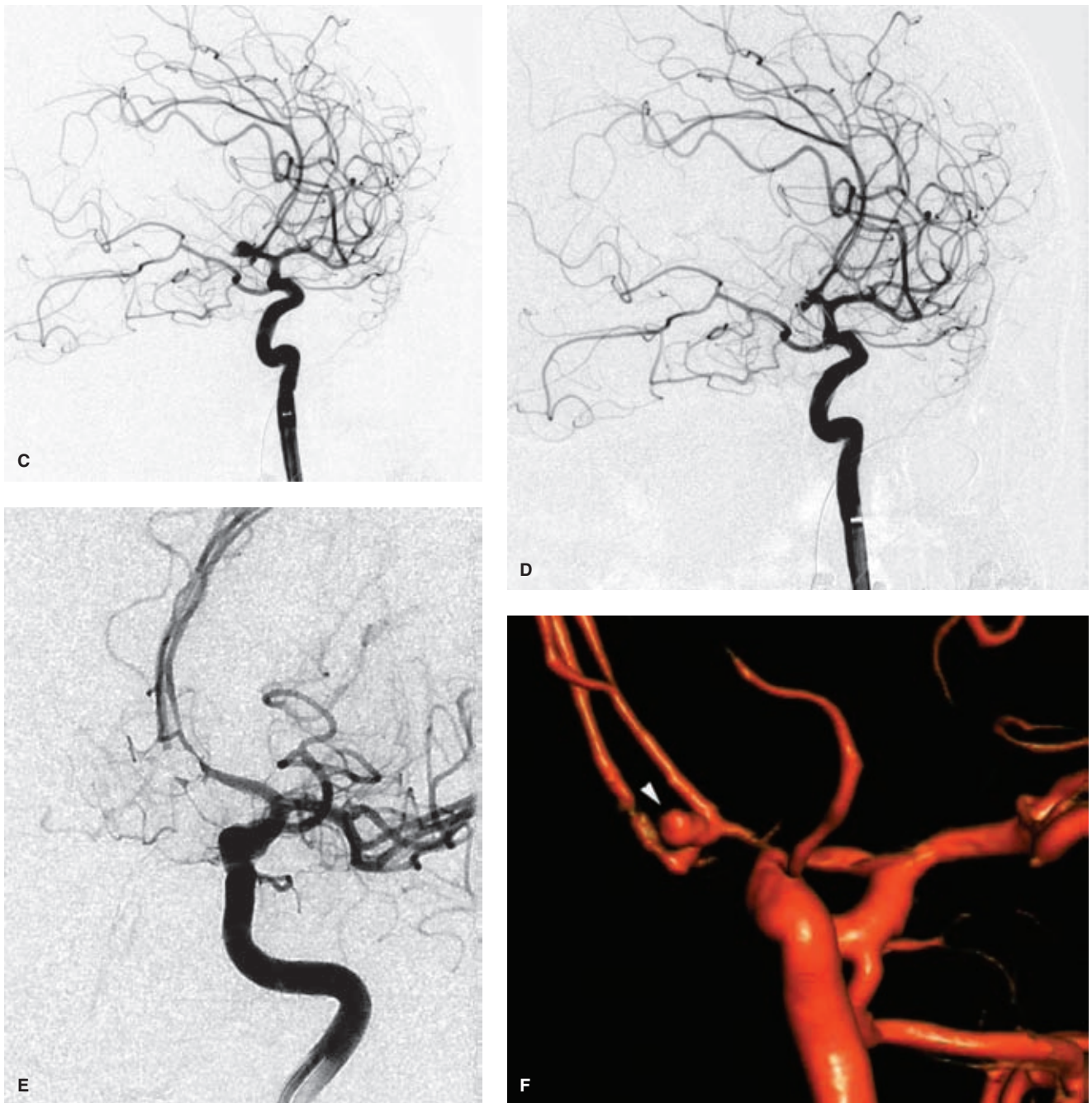


FIGURE 2-45. (CONTINUED) The larger aneurysm was addressed as the presumed site of hemorrhage, having all the hallmarks of hemorrhage—size, irregularity, apical teat—and the tiny adjacent one was left alone as inaccessible and too hazardous for endovascular catheterization on this occasion, but serendipitously both aneurysms appeared to be satisfactorily occluded at the end of the treatment (D). The patient made an excellent recovery, but returned with a severe recurrent hemorrhage 6 weeks later. The initial angiogram of the anterior communicating artery (E) showed a very satisfactory appearance of the embolization site with no evidence of recurrence. However, the 3D view (F) on which the coil mass is subtracted out, shows that the previously seen microaneurysm (*arrowhead*) has more than tripled in size since the previous treatment and now has an irregular lobulated appearance, undoubtedly representing the new site of hemorrhage. A good recovery was not forthcoming on the second occasion. This is one of those cases where the correct decisions seemed to have been made, but circumstances conspired against the patient. The complexity of the anatomy of the anterior communicating artery on both presentations would have been much more crudely informed without the 3D imaging however, and one is left to draw whatever lessons one can to help future patients.



FIGURE 2-46. (A–D) Carotid–ophthalmic aneurysm. This unruptured carotid–ophthalmic aneurysm (*arrow* in **A**) of the right carotid artery appears on several conventional views to have a configuration whereby the ophthalmic artery arose from the pointed apex of the aneurysm. The 3D surface rendered views (**B**, **C**) were extremely helpful to refute this notion and show that the ostium of the ophthalmic artery was remote from the aneurysm itself. Using the 3D data as a guide, a skewed lateral view (**D**) could then be composed to document the ophthalmic artery (*arrow*) distinct from the aneurysm profile.

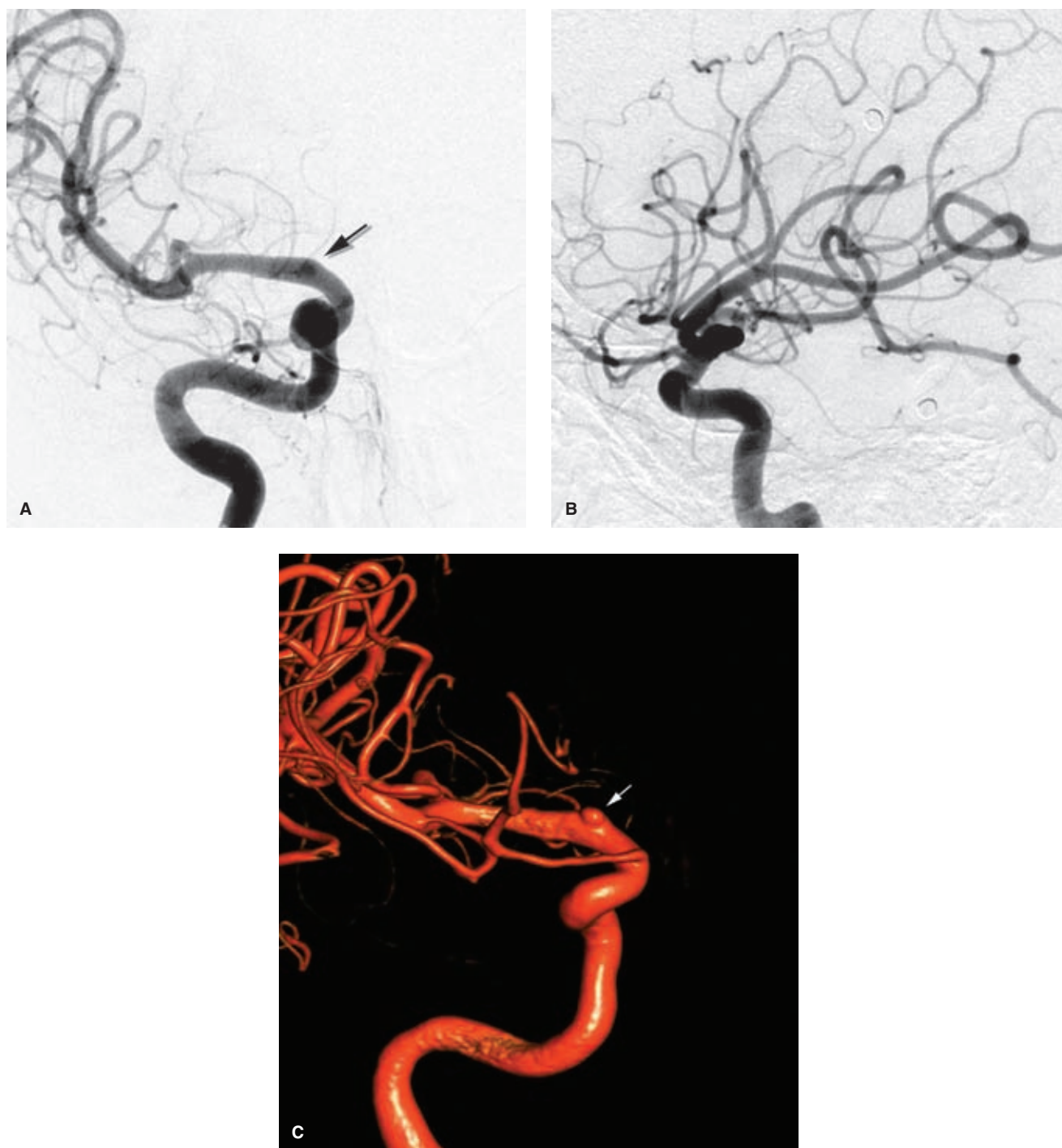


FIGURE 2-47. (A–C) Blister aneurysm of right carotid terminus. This patient's images demonstrate an example of the type of aneurysm that can be very difficult to image, even when one knows or suspects that it is there. The AP view (A) of the right internal carotid artery gives a hint—with extremely prejudiced windowing only—of a double density (arrow) at the right carotid terminus. The lateral view (B) and several other views were not helpful to guide one in attempting to understand whether exactly derived this double density. The 3D view (C) shows the aneurysm itself and the dysplasia of the adjacent artery merging into the ipsilateral M1 segment.



FIGURE 2-48. (A–D) Basilar apex aneurysm requiring a double stent Y-configuration. The AP projection of this unruptured basilar apex aneurysm (A) demonstrates many favorable aspects from the point of view of endovascular treatment. The arteries are straight. The P1 segments bilaterally are smooth and capacious. Both vertebral arteries are generously sized. However, the one crucial thing that is missing is a discernible neck on the aneurysm. Furthermore, the direction of projection of the aneurysm is difficult to discern on conventional images. The 3D images (B, C) allow a subtle alteration of the AP projection to maximize one's profile view of the aneurysm, all the more critical in a small aneurysm like this where microcatheter movement within the aneurysm is very limited and risky. An artery of Percheron variant (*arrow* in C) is noted. The patient had been premedicated with clopidogrel and aspirin in advance of the procedure and a Y-configuration of stent deployment was used. The poststent image (D) shows an interesting phenomenon. The distal tines of the Neuroform and Enterprise stents can be seen in the posterior cerebral arteries (*arrows*) and the proximal tines in the basilar artery (*arrowhead*). There is a subtle but useful difference in the anatomy of image (D) by virtue of the stents' effect. The inherent rigidity of the stents has elevated the posterior cerebral arteries bilaterally enough to squeeze the neck of the aneurysm at its base. Compare the aneurysm shape in (D) with the other images. The result of this serendipitous phenomenon was that the aneurysm coiling, originally anticipated as extremely difficult, turned out to be very smooth and easy, undoubtedly because of the effective creation of a neck by the effect of the stents.

References

1. Caplan LR, Wolpert SM. Angiography in patients with occlusive cerebrovascular disease: Views of a stroke neurologist and neuroradiologist. *AJNR Am J Neuroradiol*. 1991;12(4):593–601.
2. Rosovsky MA, Rusinek H, Berenstein A, et al. High-dose administration of nonionic contrast media: A retrospective review. *Radiology*. 1996;200(1):119–122.
3. Bertrand OF, Rao SV, Pancholy S, et al. Transradial approach for coronary angiography and interventions: Results of the first international transradial practice survey. *JACC Cardiovasc Interv* 2010;3(10):1022–1031.
4. Dauerman HL, Rao SV, Resnic FS, et al. Bleeding avoidance strategies. Consensus and controversy. *J Am Coll Cardiol* 2011;58(1):1–10.
5. Koutouzis M, Matejka G, Olivecrona G, et al. Radial vs. femoral approach for primary percutaneous coronary intervention in octogenarians. *Cardiovasc Revasc Med* 2010;11(2):79–83.
6. Jolly SS, Yusuf S, Cairns J, et al. Radial versus femoral access for coronary angiography and intervention in patients with acute coronary syndromes (RIVAL): A randomised, parallel group, multicentre trial. *Lancet* 2011;377(9775):1409–1420.
7. Rao SV, Ou FS, Wang TY, et al. Trends in the prevalence and outcomes of radial and femoral approaches to percutaneous coronary intervention: A report from the National Cardiovascular Data Registry. *JACC Cardiovasc Interv* 2008;1(4):379–386.
8. Nohara AM, Kallmes DF. Transradial cerebral angiography: Technique and outcomes. *AJNR Am J Neuroradiol* 2003;24(6):1247–1250.
9. Lee DH, Ahn JH, Jeong SS, et al. Routine transradial access for conventional cerebral angiography: A single operator's experience of its feasibility and safety. *Br J Radiol* 2004;77(922):831–838.
10. Matsumoto Y, Hongo K, Toriyama T, et al. Transradial approach for diagnostic selective cerebral angiography: Results of a consecutive series of 166 cases. *AJNR Am J Neuroradiol* 2001;22(4):704–708.
11. Barone JE, Madlinger RV. Should an Allen test be performed before radial artery cannulation? *J Trauma* 2006;61(2):468–470.
12. Yamashita T, Imai S, Tamada T, et al. Transradial approach for noncoronary angiography and interventions. *Catheter Cardiovasc Interv* 2007;70(2):303–308.
13. Cipolle RJ, Seifert RD, Neilan BA, et al. Heparin kinetics: Variables related to disposition and dosage. *Clin Pharmacol Ther* 1981;29(3):387–393.
14. Fujii Y, Takeuchi S, Koike T, et al. Heparin administration and monitoring for neuroangiography. *AJNR Am J Neuroradiol* 1994;15(1):51–54.
15. Kerber CW, Liepsch D. Flow dynamics for radiologists. II. Practical considerations in the live human. *AJNR Am J Neuroradiol* 1994;15(6):1076–1086.
16. Kerber CW, Liepsch D. Flow dynamics for radiologists. I. Basic principles of fluid flow. *AJNR Am J Neuroradiol* 1994;15(6):1065–1075.
17. Mabon RF, Soder PD, Carpenter WA, et al. Fluid dynamics in cerebral angiography. *Radiology* 1978;128(3):669–676.
18. Doumanian HO, Amplatz K. Vascular jet collapse in selective angiocardiology. *Am J Roentgenol Radium Ther Nucl Med* 1967;100(2):344–352.
19. Macdonald RL, Wallace MC, Kestle JR. Role of angiography following aneurysm surgery. *J Neurosurg* 1993;79(6):826–832.
20. Derdeyn CP, Moran CJ, Cross DT, et al. Intraoperative digital subtraction angiography: A review of 112 consecutive examinations. *AJNR Am J Neuroradiol* 1995;16(2):307–318.
21. Alexander TD, Macdonald RL, Weir B, et al. Intraoperative angiography in cerebral aneurysm surgery: A prospective study of 100 craniotomies. *Neurosurgery* 1996;39(1):10–17; discussion 17–18.
22. Betti OO, Munari C, Rosler R. Stereotactic radiosurgery with the linear accelerator: Treatment of arteriovenous malformations. *Neurosurgery* 1989;24(3):311–321.
23. Lunsford LD, Kondziolka D, Flickinger JC, et al. Stereotactic radiosurgery for arteriovenous malformations of the brain. *J Neurosurg* 1991;75(4):512–524.
24. Elisevich K, Cunningham IA, Assis L. Size estimation and magnification error in radiographic imaging: Implications for classification of arteriovenous malformations. *AJNR Am J Neuroradiol* 1995;16(3):531–538.
25. Horton JA. Sizing rings: A simple technique for measuring intracranial lesions. *AJNR Am J Neuroradiol* 1995;16(7):1449–1451.
26. Brown RD Jr, Wiebers DO, Forbes G, et al. The natural history of unruptured intracranial arteriovenous malformations. *J Neurosurg* 1988;68(3):352–357.

3

Spinal Angiography: Technical Aspects

Key Point

- The challenges of spinal angiography can be kept to a minimum by a methodical approach, careful expenditure of contrast, and a fastidious attention to details such as positioning and radiation use.

► INDICATIONS

Spinal angiography can be intimidating to beginners. However, with practice and attention to expenditure of contrast in the early part of a procedure, it is a rare patient in whom a satisfactory examination cannot be obtained safely and completely at one session. Spinal angiography is used to evaluate certain vascular diseases, or to identify the origins of the spinal arteries prior to spinal surgery. Alternatively, the study may be necessary to evaluate lesions of the spine or vertebral column in the setting of a presurgical angiogram or embolization. When a complete spinal angiogram is required to search for a possible dural arteriovenous malformation or fistula, then the study must evaluate the entire dural vasculature from the skull base to the sacrum without omission (Table 3-1). Spinal dural arteriovenous malformations are notoriously elusive and difficult to see unless a technically adequate injection is made directly into the affected pedicle. Furthermore, dural arteriovenous malformations of the spine may present with conal symptoms or myelographic findings quite remote from the site of the fistula. Except for knowing that spinal dural arteriovenous malformations are more likely to be found in the thoracic and lumbar spine than in the cervical area, there is usually no a priori way of focusing a spinal angiogram for this disease unless one happens to have a hint of the origin from magnetic resonance arteriography or myelogram. A spinal angiogram in which “most” of the vessels were injected would be the equivalent of a cerebral angiogram for aneurysm detection in which “most” of the cerebral vessels were visualized, that is, not adequate in a certain number of patients.

Spinal tumors and intramedullary arteriovenous malformations, on the other hand, are often more defined with respect to suspected location. Even in a limited examination, it is, nevertheless, always worthwhile and usually essential to extend the

study until the next neighboring uninvolved anterior spinal artery is visualized. The locations of the anterior and posterior spinal arteries are a particular concern in all situations where embolization of the paraspinous vessels is being considered.

► ANESTHESIA DURING SPINAL ARTERIOGRAPHY

Since many of the critical vessels of interest during a spinal arteriogram are of such small size, the quality of images can be significantly degraded by a slight amount of motion or respiratory artifact. Most spinal angiograms are long procedures, and it is difficult for patients to remain absolutely still during that time. Depending on the indications for the study, a spinal angiogram can be focused on a known lesion or area, or may require a diagnostic evaluation of the entire spinal axis. In either event, the procedure is invariably tedious for the patient and is best done under general anesthesia, if possible. The main purpose of this is to avoid obtaining a technically inadequate study due to motion artifact. Furthermore, under general anesthesia, respirations can be suspended for the duration of each angiographic run, eliminating respiratory artifact. Occasionally, when embolization is considered for a known focal lesion in a particularly cooperative patient, the study can be performed with a lighter degree of anesthesia. Intravenous glucagon to suppress bowel motion during the lumbar phase of the study might be considered.

► TECHNICAL CONSIDERATIONS IN SPINAL ARTERIOGRAPHY

Spinal angiography, being something of a major undertaking for all involved, must be done with an eye to technical perfection (Figs. 3-1–3-3) in order to dispel subsequent considerations of whether the study might need to be repeated because of perceived errors or omissions (1–5).

Enumerating the vertebral bodies is the first task in a complete or focused spinal study, in order to avoid miscommunication about anatomic levels. The number of rib-bearing vertebrae must be counted under the fluoroscope and collated with the number of lumbar-type bodies. In situations of an indeterminate configuration, an arbitrary decision on a system of nomenclature

TABLE 3-1 Vessels Required for a Complete Spinal Arteriogram

Vertebral arteries
Common carotid arteries
Thyrocervical trunks
Costocervical trunks (including the superior intercostal artery)
Supreme intercostal arteries (usually T2–T4)
Segmental arteries from T4–L5
Median sacral artery (midline from aortic bifurcation)
Lateral sacral arteries (from the internal iliac arteries) (Fig. 3-2)

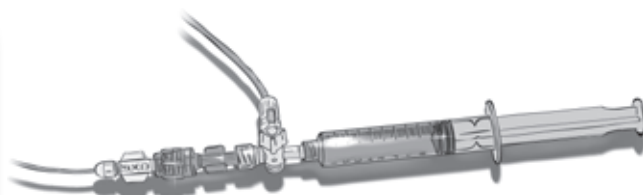


FIGURE 3-1. Setup for diagnostic spinal angiography. For diagnostic spinal angiography, a continuous flush system would generate too much dead space and, thus, excessive waste of contrast load with each injection. A three-way stopcock and a swivel adapter attached to the syringe and catheter provide an efficient means of rapidly searching for the next vessel and immediately toggling from syringe to injector tubing for the run. For coaxial spinal manipulations, a continuous flush system is used during interventional procedures.

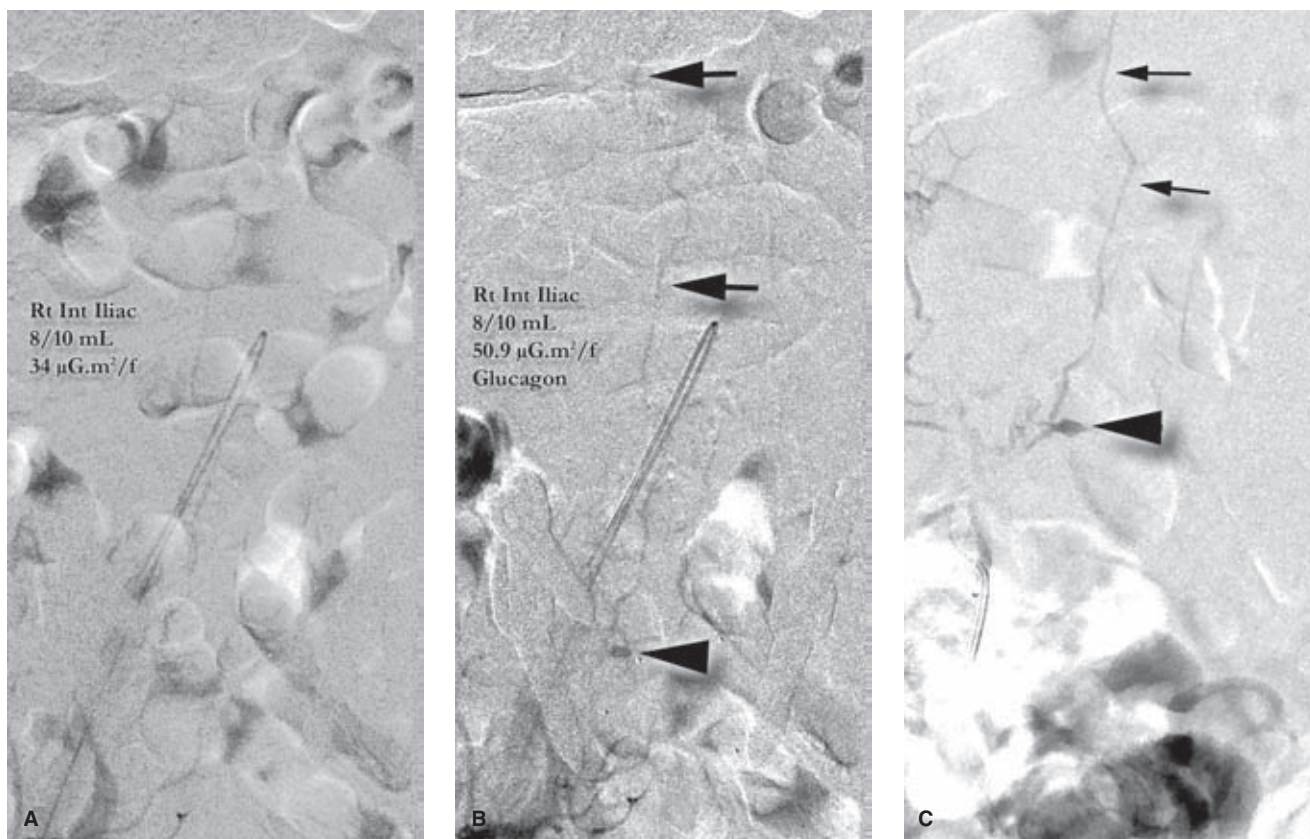


FIGURE 3-2. The many technical challenges of spinal angiography. This middle-aged patient weighed in excess of 400 lbs. Thus his MRI images were nondiagnostic due to his size and motion artifact, but they were indicative of some sort of enhancing and expansile myelopathy affecting the lower cord. His first spinal angiogram performed without general anesthesia was interpreted as negative, but appeared to have been a difficult and perhaps incomplete study. A second study under general anesthesia was planned, but appeared to be getting off to a rocky start too. The first injection (**A**) of the right internal iliac artery using a Simmons 2 catheter on a low-dose radiation protocol rendered images of poor quality. The radiation protocol was adjusted, an ampule of glucagon was administered to diminish bowel motion, and the run was repeated (**B**). Fortunately, on this run an abnormality was discernible, with a venous pouch (*arrowhead* in **B**) opacifying behind the right sacroiliac joint and draining cephalad (*arrows* in **B**) to the cord. Injection rates and dose-area product (DAP) recording per frame in each case are annotated. In retrospect, although certainly not at the time of the initial run, this abnormality could be faintly seen on image **A** after it had been tidied up and pixel shifted. This was the only vessel from the study on which the abnormality would have been evident and this second study came within an ace of missing the finding. A selective oblique microcatheter injection (**C**) performed closer to the abnormality shows the venous pouch (*arrowhead* in **C**) to better advantage, with the centripetal segmental vein draining (*arrows* in **C**) above. The pouch is likely the receiving component of the arteriovenous fistula, but the arterial feeders cannot be reliably visualized in this patient. The size of the patient and the inability to see any better than is illustrated on this image dissuaded enthusiasm for an endovascular attempt at treatment. (*continued*)

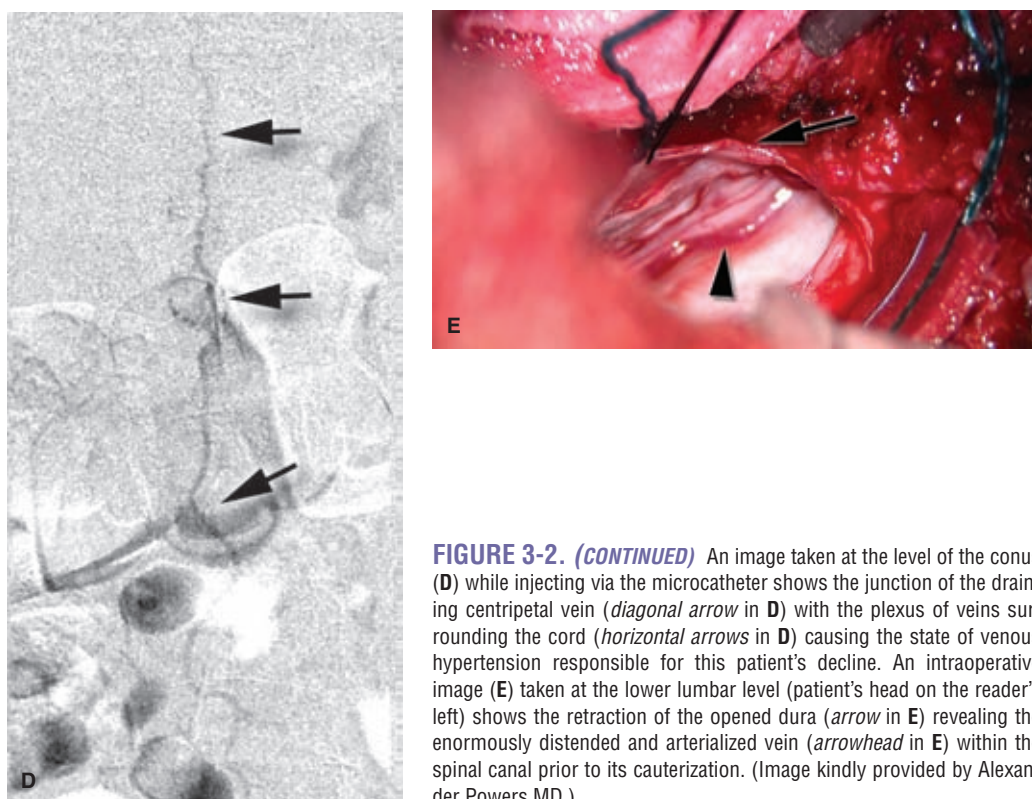


FIGURE 3-2. (CONTINUED) An image taken at the level of the conus (D) while injecting via the microcatheter shows the junction of the draining centripetal vein (*diagonal arrow in D*) with the plexus of veins surrounding the cord (*horizontal arrows in D*) causing the state of venous hypertension responsible for this patient's decline. An intraoperative image (E) taken at the lower lumbar level (patient's head on the reader's left) shows the retraction of the opened dura (*arrow in E*) revealing the enormously distended and arterialized vein (*arrowhead in E*) within the spinal canal prior to its cauterization. (Image kindly provided by Alexander Powers MD.)

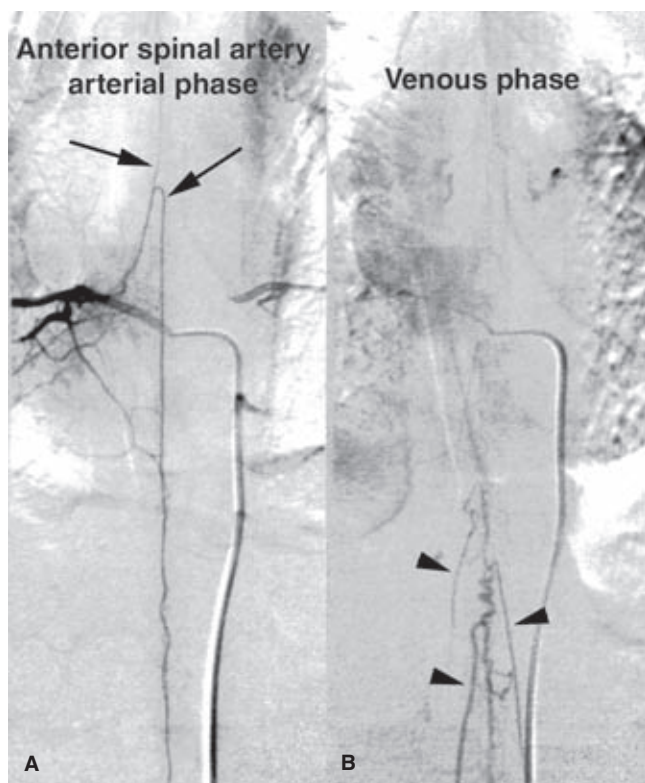


FIGURE 3-3. (A–B) Centrifugal medullary veins. A young adult was studied to exclude the possibility of a spinal dural arteriovenous fistula as a cause for atypical back pain. An injection into a lower thoracic pedicle opacifies the anterior spinal artery (*arrows in A*). Unusually prominent and tortuous veins around the conus (*arrowheads in B*) were eventually interpreted as representing a variant of normal because they opacified in normal phase with the remainder of venous structures of the injection. Drainage via the centrifugal medullary veins (*arrowheads in B*) was normal in timing and duration.

should be established and explicitly described in the report of the case, for example, “There are 11 rib-bearing vertebrae which for the purposes of this study will be numbered T1 to T11, and 5 nonrib-bearing vertebrae which will be numbered L1 to L5.” In addition, a plastic ruler included on the imaging field placed under the patient during the procedure can be helpful to avoid confusion about levels already studied and those yet needed.

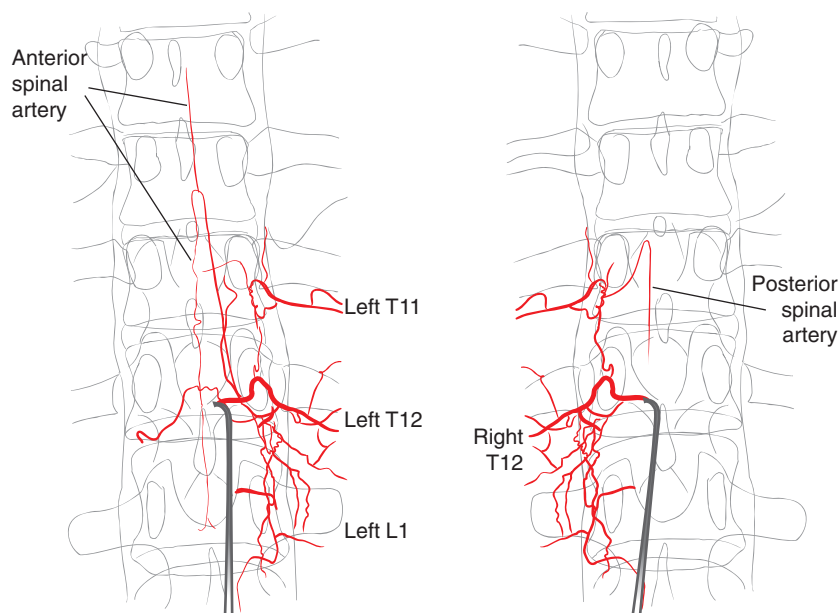
Patient positioning is the next consideration. Spinal angiography, in the thoracic and lumbar regions, is usually done using anteroposterior (AP) fluoroscopy only. It is important for the purposes of identifying the posterior and anterior spinal arteries that the imaging plane be precise. Therefore, the fluoroscope is positioned for all runs such that the spinal processes are aligned halfway between the spinal pedicles (Fig. 3-4). When a degree of rotational scoliosis is present, an adjustment of the fluoroscope may be necessary between different levels of the spine.

Minimization of the contrast volume from the very beginning of the study is critical. While it may not be apparent as a potential problem in the initial phase of a complete spinal angiogram, later technical difficulties can provoke a cumulative total dose of contrast well in excess of 400 mL on a routine basis. Standard precautionary measures, such as hydration of the patient before, during, and after the procedure with close monitoring of urine output, are therefore important.

► VESSEL SELECTION DURING SPINAL ANGIOGRAPHY

Occasionally, in a high-flow lesion, an aortogram can be helpful (Fig. 3-5) to somewhat localize the segmental arteries of interest. However, one must consider that for virtually all spinal dural AVFs the rate of flow will be inadequate to

FIGURE 3-4. Anterior and posterior spinal arteries. In selecting the spinal arterial pedicles, it is necessary to know whether one's catheter is pointing anteriorly or posteriorly. The posterior processes of the vertebrae are aligned exactly in the middle. In this manner, the precisely midline course of the anterior spinal artery can be discerned from the paramedian course of the posterior spinal artery.



allow adequate opacification and the expenditure of considerable contrast on the aortogram will be wasted.

The segmental vessels of the spinal column change orientation as one ascends the aorta. Frequently, one has to make allowance for this change by exchanging catheters during the procedure.

1. Lumbar segmental arteries are more likely than their thoracic counterparts to have a conjoined pedicle giving rise to both the left and right branches.
2. Lumbar bony pedicles and segmental arteries are more widely spaced from their superior and inferior neighbors than are their counterparts in the thoracic spine.
3. Lumbar vascular pedicles take origin from the aorta with an inferiorly directed or horizontal course. This pattern changes slowly as one ascends the aorta to a more superiorly directed course. The supreme intercostal artery (variable in territory but frequently including T2, T3, and T4) is directed with a sharply superior angle from the aorta. Furthermore, in the high thoracic levels, the concordance between the segmental artery and the similarly numbered vertebral body is lost. The number system in the thoracic region relies exclusively on counting which intercostal artery is opacified by the injection and not on the bony landmarks of the vertebral column behind.
4. The diameter of the descending thoracic aorta is greater than that in the lumbar region. The implication of this anatomic tapering is that different constraints are placed on the catheter in these two regions by the walls of the aorta. Therefore, the behavior of a particular catheter may be quite different in various locations.

During vessel selection, it is necessary for obvious reasons to be familiar with the anterior–posterior orientation of one's catheter within the aorta, the arterial ostia of the spine being posterior, or posteromedial in the thoracic aorta. Since the pattern of the arterial pedicles changes only slightly from one level to another, it is most helpful to select the vessels in a *sequential and systematic manner*, taking precautions not to miss any vessel or become confused about enumeration.

The intercostal arteries run along the inferior surface of the correspondingly numbered rib. The technologist or nurse should have a spinal angiography worksheet for recording the numbers and identifications of all the runs so that one can tell at a glance whether all the vessels have been found, and, if not, which pedicles remain to be studied.

Taking a cue from the attitude of the catheter at the vessel ostium at one level, those of the next level up or down can be divined fairly accurately, thus minimizing contrast use in blind searching. Vessel ostia, in the absence of vertebral anomalies such as hemivertebrae, tend to be extremely reliable in their alignment in the left–right and craniocaudal directions. If a particular vessel cannot be seen at all after a prolonged search of the appropriate area, the possibility that it might be occluded or congenitally hypoplastic should be considered by looking at the contiguous levels. Prominent filling of the vessels of that territory through collateral channels without evidence of washout from the unselected vessel is adequate reassurance that the missing vessel need not be pursued further.

A variety of catheter shapes are manufactured for spinal angiography (Fig. 3-6). The change in orientation of the vascular pedicles from an inferior or horizontal slant in the lumbar region to a superior inclination in the upper thoracic region is the factor that tends to be most significant in determining the optimal choice for a change of catheter shapes. Inferiorly pointing catheters such as the HS-1 are better suited in the lower aorta, while superiorly directed catheters such as the H-1-H may be more suited for the thoracic region. A particularly capacious aorta, requiring a catheter with an ample secondary curve that can span the diameter of the aorta, such as HS-2 or Mikaelsson, is another factor to consider when a stable position cannot be achieved.

There is a certain knack to stabilizing the catheter tip in the segmental artery once the ostium is selected. The catheter tip must be coaxed a little further into the vessel than it will spontaneously purchase of its own accord. By twisting the catheter tip a little further to the side of the pedicle in question, combined with a gentle forward push in the case of the HS-1 or H-1-H catheters, a subtle degree of tension can be established in the catheter that will hold it in position for

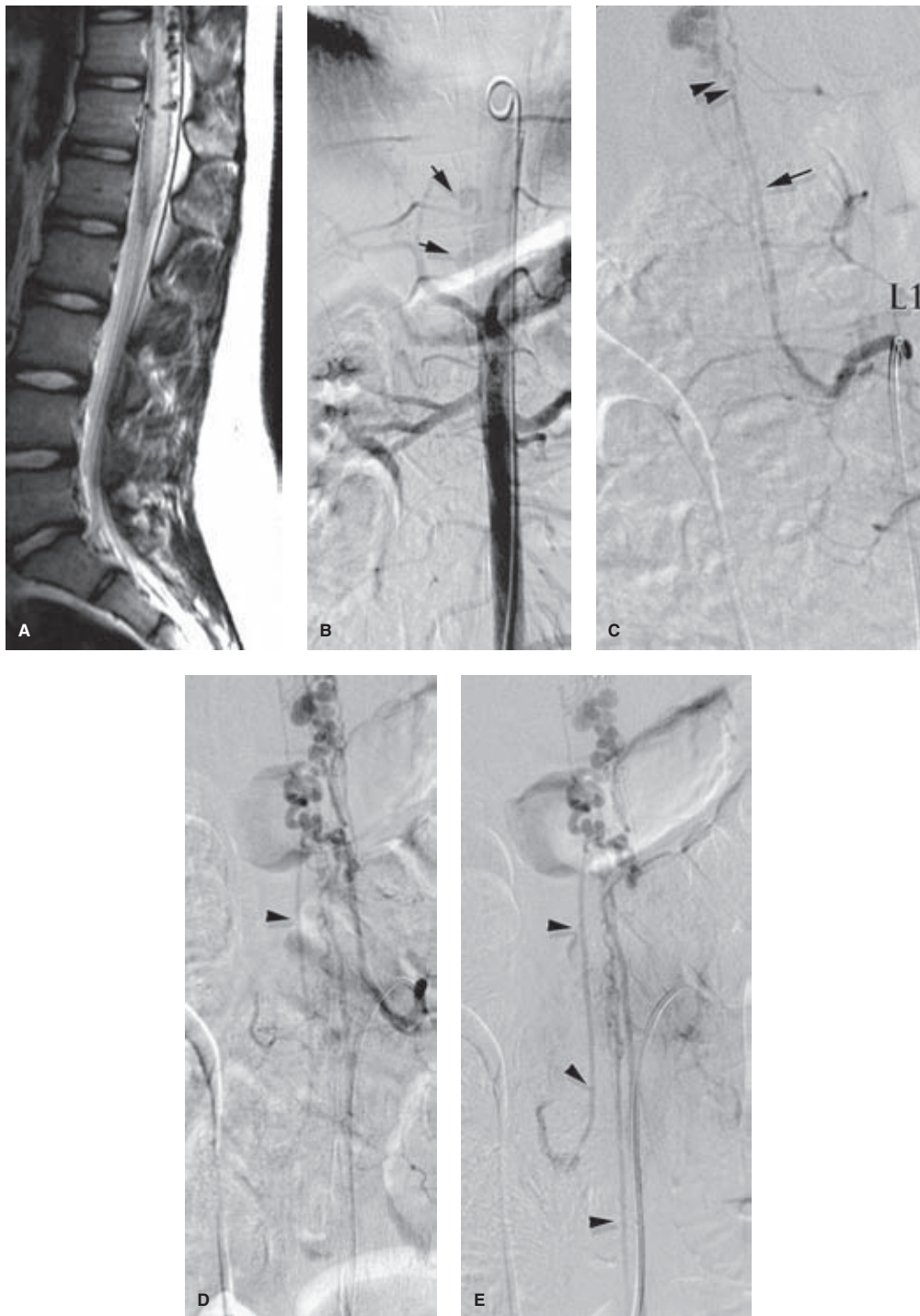


FIGURE 3-5. (A–E) Spinal angiography requires, amongst other things, knowing the difference between an artery and a vein. A middle-aged patient presented with acutely progressive decline of spinal function. The sagittal T2 MRI (A) demonstrates a markedly hyperintense and expansile appearance of the cord with prominently distended flow-voids on the pial surface of the conus. A pigtail aortogram (B) of the descending aorta faintly demonstrates some of the vessels (arrows in B) seen on the MRI, but does not help enormously otherwise. The left L1 injection (C) demonstrates an enlarged spinal artery (arrow in C) extending up to the cord where distended vascular sacs are filling rapidly at the top of the picture. Sequential images from the left L1 injection (D and E) demonstrate a massively sinuous complex of veins over the conus emanating inferiorly from a venous sac at the top of the picture, with slow centrifugal (normally directed) opacification of the segmental veins (arrowheads in D and E) to the lumbar area draining the congested cord, albeit ineffectively. This lesion is probably best understood as a perimedullary fistula (see Chapter 21). The fistula is likely close to the location of the double arrowheads in (C), with a change in caliber immediately above that level where the receiving venous component of the fistula has become aneurysmally distended. It is vitally important that at the end of a spinal angiogram there should be no confusion as to what represents an artery and what a vein on the images, particularly with reference to planned endovascular or surgical treatment. *Note: The positioning in this set of images would be much improved by centering on the region of the fistula rather than on the catheter tip. Most of the area in the lower half of the picture is wasted.*

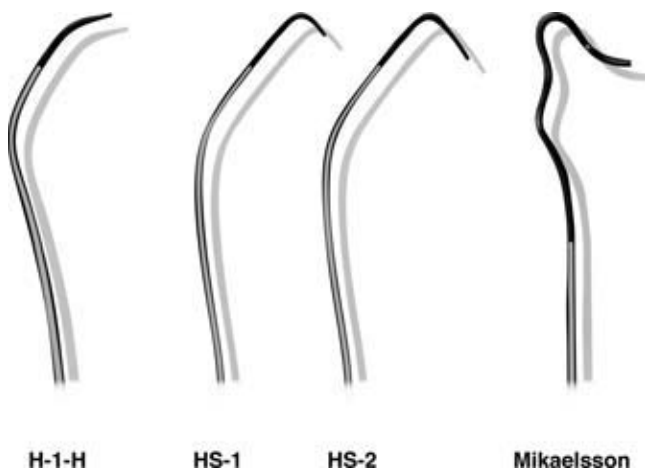


FIGURE 3-6. Catheters for spinal angiography. A few dedicated spinal catheters can be still obtained on the market or as custom-batches from certain manufacturers and are far superior to working with an improvised application of a general use catheter. Among those illustrated the Mikaelsson tends to be the most demanding in terms of contrast use while searching for vessels. However, when the vessel has been found and an embolization is contemplated, the Mikaelsson is a very stable catheter to use for coaxial introduction of a microcatheter, as it is most capable of resisting pushback into the aorta.

the subsequent run. Alternatively, with a recurved type of spinal catheter, such as the Mikaelsson shape, slight downward tension on the catheter achieves a similar end. The final step to maintaining catheter position during the injection is to assure that the external segment of the catheter, hindered by tubing and drapes outside the body, does not have a degree of

counterforce that might undo the hold that the catheter tip has on the artery. Therefore, stabilization of the outer catheter is necessary to avoid ejection of the catheter tip from the artery as contrast is injected. A linear rise to introduce the injection may reduce the risk of ejecting a precariously positioned catheter from the ostium.

In particularly difficult pedicles that can be seen on road-mapping but that are repugnant to catheterization, some further options can be considered. A soft wire might be steerable into a stable position more distally in the pedicle; this can then be used to advance the catheter further into the artery. Failing this, a roadmap image can be used to steer a wire-directed microcatheter coaxially into the pedicle, through which a run can be accomplished.

References

1. Di Chiro G, Rieth KG, Oldfield EH, et al. Digital subtraction angiography and dynamic computed tomography in the evaluation of arteriovenous malformations and hemangioblastomas of the spinal cord. *J Comput Assist Tomogr* 1982;6(4):655–670.
2. Doppman JL, Krudy AG, Miller DL, et al. Intraarterial digital subtraction angiography of spinal arteriovenous malformations. *AJNR Am J Neuroradiol* 1983;4(5):1081–1085.
3. Fanning NF, Pedroza A, Willinsky RA, et al. Segmental artery exchange technique for stable 4F guiding-catheter positioning in embolization of spinal vascular malformations. *AJNR Am J Neuroradiol* 2007;28(5):875–876.
4. Levy JM, Hessel SJ, Christensen FK, et al. Digital subtraction arteriography for spinal arteriovenous malformation. *AJNR Am J Neuroradiol* 1983;4(6):1217–1218.
5. Shi HB, Suh DC, Lee HK, et al. Preoperative transarterial embolization of spinal tumor: Embolization techniques and results. *AJNR Am J Neuroradiol* 1999;20(10):2009–2015.

4

Pediatric Neuroangiography: Technical Aspects

Key Points

- Adults are big children, but children are not small adults.
- With modification of basic techniques, the risks of endovascular procedures in children should not be any greater than that in adults, and probably less in most instances.

Neuroangiographic procedures in children are not necessarily more difficult in some ways than in adults, but the prospect of causing a complication or injury to a little one raises the operator's anxiety. In many ways, a diagnostic or interventional endovascular procedure is similar, in miniaturized form, to that of an adult. The craniocervical vessels are almost always straighter in children, which makes vessel catheterization much easier in fact. However, the differences between pediatric and adult procedures are in other ways substantial and must be considered.

► ARTERIOTOMY AND SHEATH

Quite apart from the issue of size of sheath that a pediatric femoral artery will take, the delicacy of the tissue must be taken into account (Figs. 4-1 and 4-2). A rough or forceful technique in the groin could end in a disastrous tearing or transection of the vessel. Gentle sequential dilation of the vessel to stretch the arteriotomy site is safer. Once access to the vessel is obtained, a small injection of intra-arterial calcium blocker, for example, verapamil (0.01 mg/kg), might be considered to alleviate spasm. Intra-arterial heparin and/or systemic heparinization (30–60 U/kg) are highly advised to prevent vessel thrombosis or occlusion during or following the procedure.

► GROIN COMPRESSION

Pediatric arteries are easy to compress, certainly compared with many expansive groins that the beginning fellow has to confront. Too easy, in fact. The difficulty is that one does not necessarily want to actually compress the artery completely to the point of sustained occlusion

after the first minute or two, following removal of the sheath. The priority is to encourage the re-establishment of antegrade flow in the artery as soon as possible. Therefore, a very light compression with the left hand only is usually sufficient, while the right hand palpates the distal pedal pulse or checks with a Doppler device (Fig. 4-3). A reassuring thrill under the left hand throughout the groin compression procedure is optimal, in contrast to the forceful ordeal of the adult groin.

► RADIATION PROTOCOL

The long-term consequences of the current patterns of medical x-ray use are unknown and discussed at length in Chapter 6. In all likelihood children are more sensitive to the deterministic and stochastic effects of even modest doses of radiation, and every effort should be made to reduce the dose inherent in neurovascular procedures. Furthermore, because of their small body size, an adult radiation protocol is completely unnecessary and probably counterproductive. Several pediatric specific precautions, including use of a pediatric radiation protocol, should be incorporated into the “Time-Out” checklist at the beginning of each procedure. Attention should be paid to minimizing the source image distance (SID) and consideration should also be given to removing the grid (a huge payoff—>40% reduction in radiation dose—for a small price in image quality). The greatest savings in radiation reduction are always to be had through minimization of the DSA cumulative image count. Modulation of the “frame rate per second” during the DSA run can reduce exposure by a factor of a third to a half. With reference to fluoroscopy, the biggest savings are to be made through modulation of dose per pulse, modulation of pulse rate per second, and particularly by maximal use of copper filtration options. These are all subject to manipulation in the password-protected software of the machine, but will require sitting down with the vendor engineer to change them. Vendors have an incentive to present you with images that are aesthetically pleasing and competitive. From a radiation-savings point of view, images should not be optimized; they should be adequate for the purpose in hand (1).

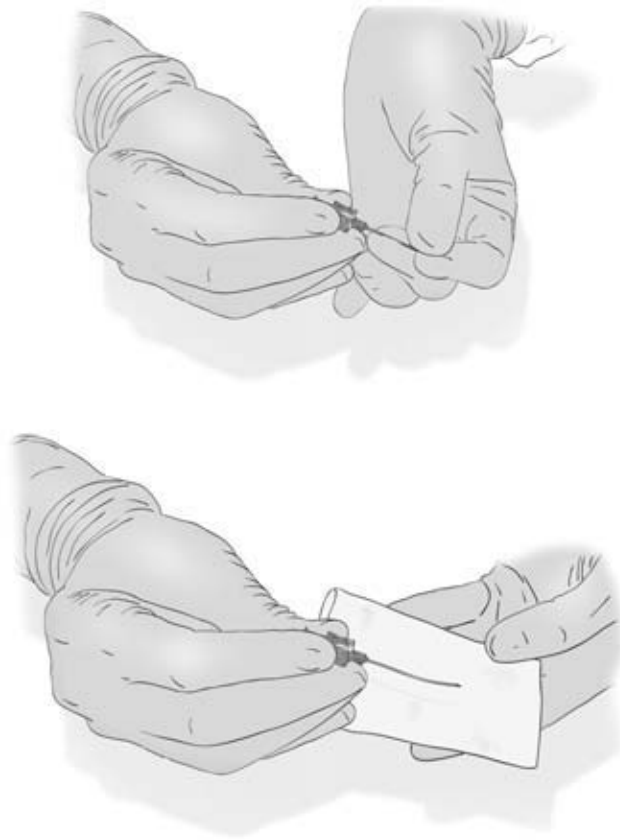


FIGURE 4-1. Pediatric needle technique. Safe access into and out of the pediatric common femoral artery is frequently the major challenge of pediatric neuroangiography, particularly for smaller children. Ultrasound guidance probably has much to recommend it, particularly when the artery is too small to palpate. Spasm, even under general anesthesia, is a big challenge, meaning that any kind of false or failed puncture will leave the operator standing there for exactly 20 minutes before the pulse normalizes and a repeat attempt can be made. A very steady hold on the needle while an assistant gently passes the wire is the best protection against losing an opportunity. A shorter 5-cm pediatric size needle is easier to hold steadily, and access of the wire to the lumen seems to be much facilitated by putting a slight bend in the distal needle by folding the needle in a piece of gauze (omitted from the diagram for illustration purposes) and bending very slightly with the left thumb.

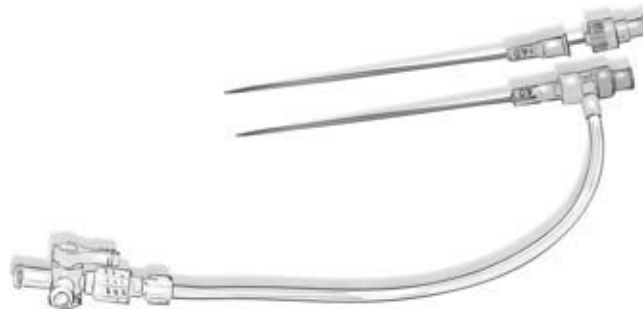


FIGURE 4-2. Pediatric sheath. Most pediatric interventional and certainly all diagnostic procedures can be accomplished via a 4F sheath (inner diameter [ID]) and will be well-tolerated in all but the smallest children, subject to standard precautions. A gentle touch with the sheath insertion is advisable, lest an arterial tear be induced. Once access is gained, heparinization of the patient to diminish any possibility of femoral artery thrombosis is generally thought prudent, and administration of a small dose of intra-arterial vasodilator, for example, verapamil, might be considered. For small infants, even a 4F (ID) sheath is going to be a challenge in terms of maintaining viability of the artery, even with these precautions. The standard 4F dilator (outer diameter [OD]) that comes with the micropuncture kit can be used as an improvised sheath to decrease the stress on the artery compared with a standard 4F (ID) sheath, and hemostatic flush maintained by attaching a standard Tuohy-Borst valve, or as illustrated the detachable side arm of an Argon sheath. With this improvised sheath system a large-lumen microcatheter, for example, Renegade or Prowler Select Plus, can be used as a catheter for diagnostic or interventional purposes.



FIGURE 4-3. Pediatric groin compression technique. It would be very easy to fall into the adult mode of prolonged 15-minute groin compression with a heavy technique, which would cause an absolute occlusion of the artery in a child for the entire duration of the process. Since the early days of transfemoral angiography concern for maintaining patency of the femoral artery in pediatric patients has been a priority due to the observation by pioneers of the field that femoral artery occlusion and leg-length discrepancy in later life were common problems. No doubt these problems are diminished with modern equipment and use of heparin, but they are best avoided. In this illustration, the fellow is compressing the femoral artery very lightly with his left hand while the right palpates the dorsalis pedis pulse, thus providing a biofeedback on the degree of compression best suited for maintaining flow and achieving hemostasis at the same time. Alternatively, a Doppler device trained on the foot pulses can make the task even easier.

► CATHETER AND WIRE LENGTH

Vendors are not as forthcoming now as was the case several years ago about making custom-sized microcatheters, and therefore one is obliged to use adult-sized devices in children. For larger children, a 4F or even 5F system might be perfectly feasible. Any standard 0.038-inch 4F diagnostic catheter will allow coaxial navigation of most microcatheters, although performing diagnostic runs with the microcatheter in place will not be possible. For very small children, these long catheters present several minor problems. Because most of the microcatheter is furled awkwardly outside the patient's body and thus not constrained by the patient's aorta, it can be very difficult to work with due to inevitable slewing across the table as one tries to advance a coil or other device. It is sometimes helpful to place the microcatheter within a shorter 60–90 cm constraining outer catheter. The latter does not enter the patient's body, but simply sits on the drapes to make the microcatheter more responsive and steerable.

For children in the middle size range, several 60-cm-length catheters in 4F denomination are available. A particular concern

with these catheters, once they are inside the body, is the possibility of absentmindedly advancing a standard-length wire close to the Tuohy-Borst valve as one does with adults. The danger of this is that due to the short length of the catheter and patient, this oversight will result in 30 or more unanticipated centimeters of wire being beyond the tip of the catheter with disastrous results, before the fluoroscopy pedal is activated. This oversight can be prevented by incorporating the placement of the torque handle on the midsection of the wire at the very beginning of the case, again as part of the “Time-Out” process.

► CONTRAST VOLUME

Although a child is proportionately smaller than an adult patient, a commensurate calculation of the contrast dose per injection cannot be performed to calculate a reasonable total dose per procedure (Figs. 4-4–4-6). For example, in a 70-kg adult one might use 6–8 mL of contrast for an internal carotid injection. In a 7-kg child, however, a 0.6–0.8-mL injection in the internal carotid artery is not going to provide a similar degree of vessel opacification, due to the relatively higher blood volume and velocity of flow in

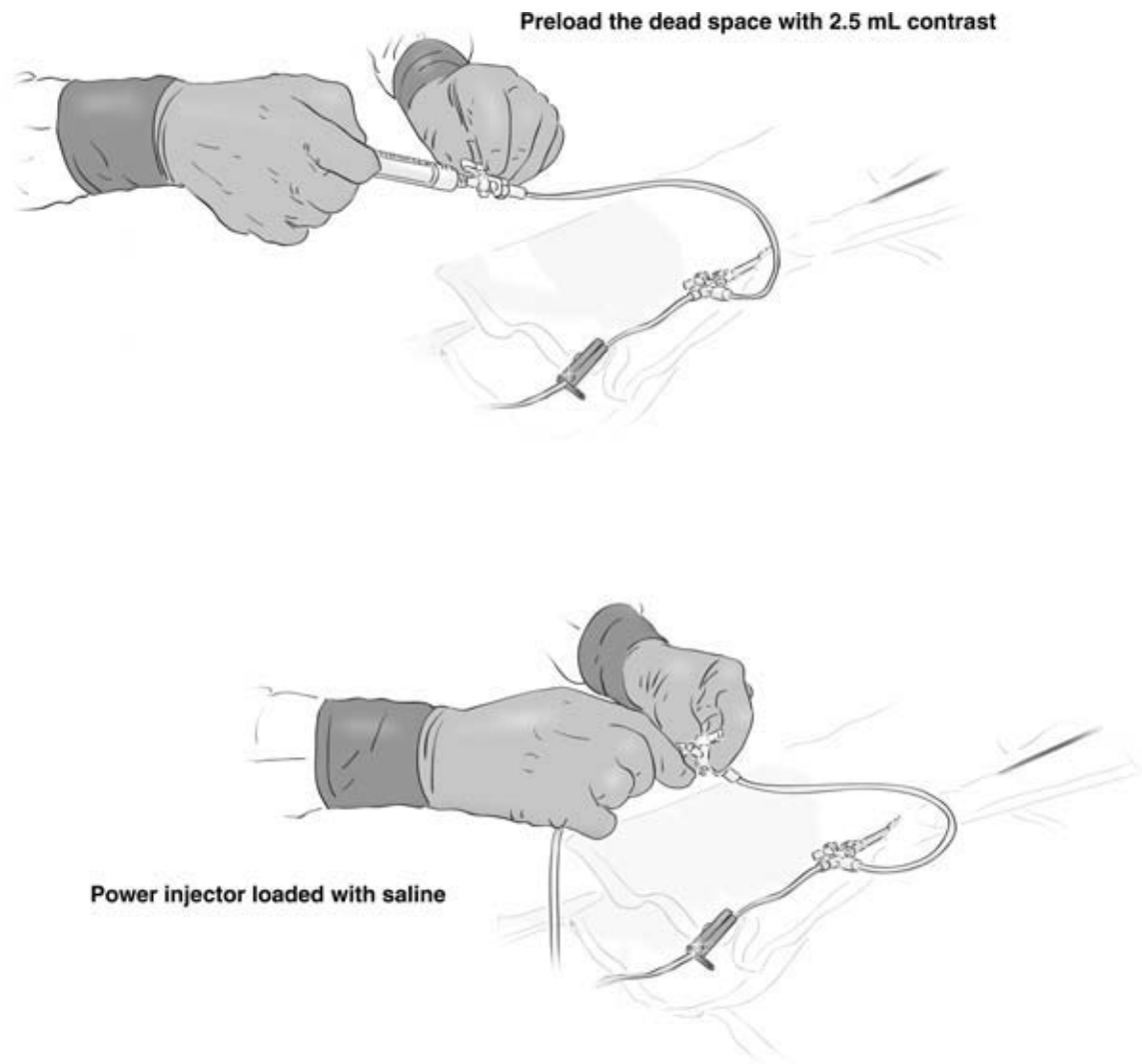


FIGURE 4-4. Contrast sparing techniques. For small children or patients with renal impairment, or any patient in whom cumulative contrast loading is a problem, technically fine images can be obtained by preloading the dead space of the Tuohy-Borst valve, side-arm, and the catheter with 2.5 mL of contrast. This can be pushed either by hand (a 5-mL syringe of saline allows a good tight push, keeping the contrast as a well-defined bolus) or with the injector that is preloaded with *saline* only. In the illustration the contrast is preloaded into the dead space. Without resuming flush from the pressurized system, the injector is hooked up. For this technique to work well, it is important for the technologist (who might be used to spinning forward a turn or two under usual circumstances to prime the catheter) to modify his/her technique. Keeping the contrast together as a tight bolus in the vessel during the injection is important to prevent compromise of signal-to-noise during imaging. Using this technique it is frequently possible to perform a technically adequate three-vessel cerebral angiogram on children or adults with as little as 9 mL of contrast ($2.5 \text{ mL} \times 3 \text{ vessels} + 0.5 \text{ mL test dose} \times 3 \text{ vessels}$).

For patients in whom such small doses of contrast per run are inadequate, using an injector filled with contrast is still an option. Considerable sparing of contrast volume can still be achieved by being very cognizant of the contrast (approximately 2 mL) that is still sitting in the dead space of the catheter and flush system at the end of each run or hand injection. This would usually be flushed antegrade into the patient when the pressurized flush system is restarted. Aspirating the dead space at the end of each DSA run and roadmap injection is a little tedious, but redounds to the patient's benefit enormously in contrast savings while still facilitating injections of near-standard volume for each DSA run. An even better alternative technique for patients in whom an injection volume of 2.5 mL is not adequate is to stay with injector loaded with saline but interpose another three-way stopcock and an additional tubing between the injector tubing and the catheter side-arm. In this way injections of up to 9 mL can be delivered by a saline push without having to deal with the issue of residual contrast in the catheter at the end of each injection.

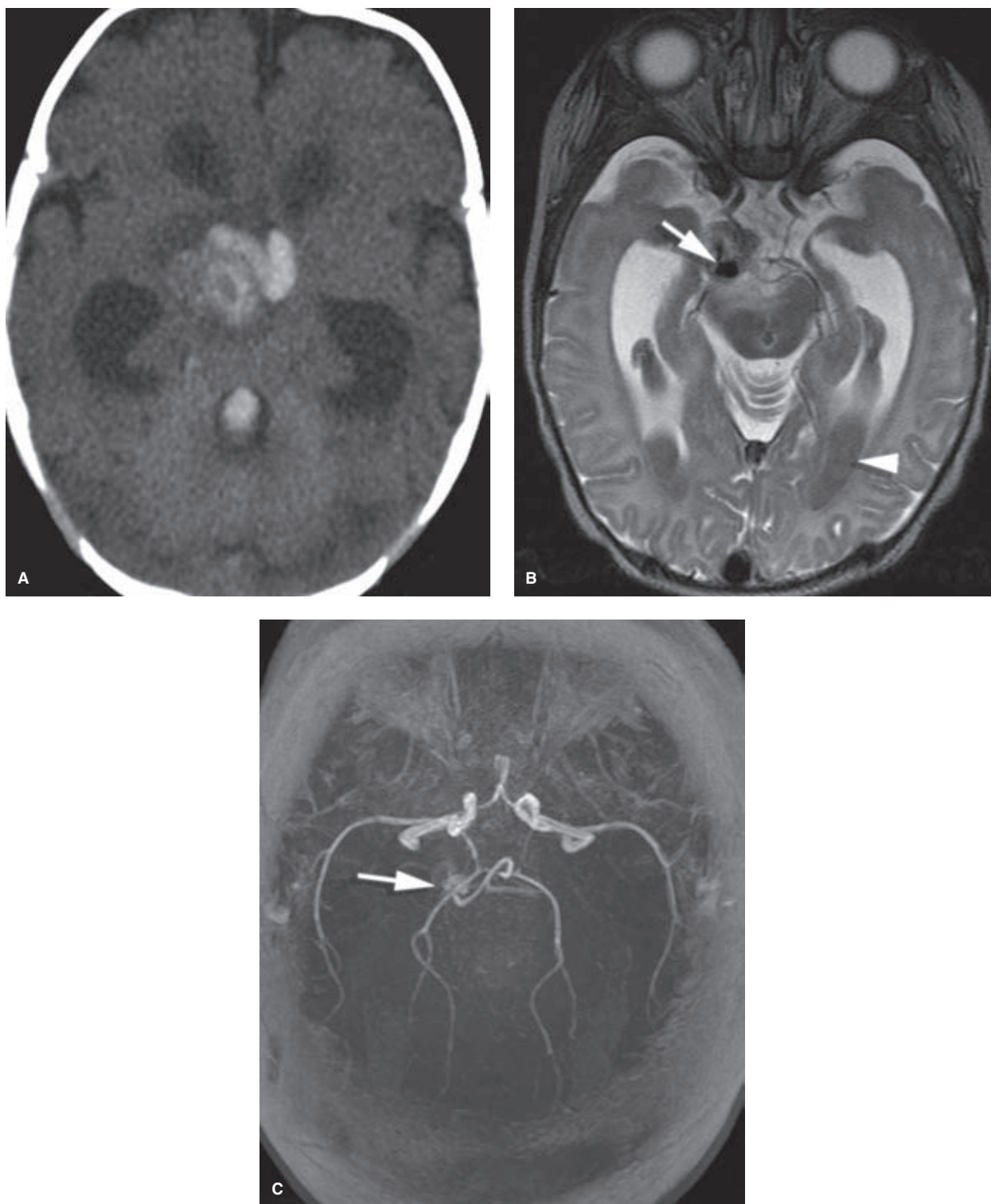


FIGURE 4-5. (A–E) **Microcatheter angiography in an infant.** This 10-week-old 6.3-kg boy demonstrates several difficulties, which could have led to a prolonged angiographic interrogation of this pseudoaneurysm and a prohibitive contrast load, if standard-sized catheters and full injections had been used. The case became very involved late in its course, and if extreme discipline on contrast use had not been observed from the very beginning, the cumulative dose would likely have become hazardous.

The patient was admitted with moderate hydrocephalus and mixed intraparenchymal/intraventricular bleeding as shown on the noncontrast head CT (A). The T2 weighted MRI (B) showed the intraventricular blood (*arrowhead* in B) and a large flow-void (*arrow* in B) with surrounding clot related to the region of the right posterior cerebral artery. The TOF MRA examination (C) appeared to confirm the likelihood that this represented an aneurysm of the posterior circulation, somehow related to the right posterior cerebral artery. The posterior circulation angiogram (not shown) performed with 2 mL of contrast via a microcatheter, however, showed no evidence whatsoever of any aneurysm. (*continued*)

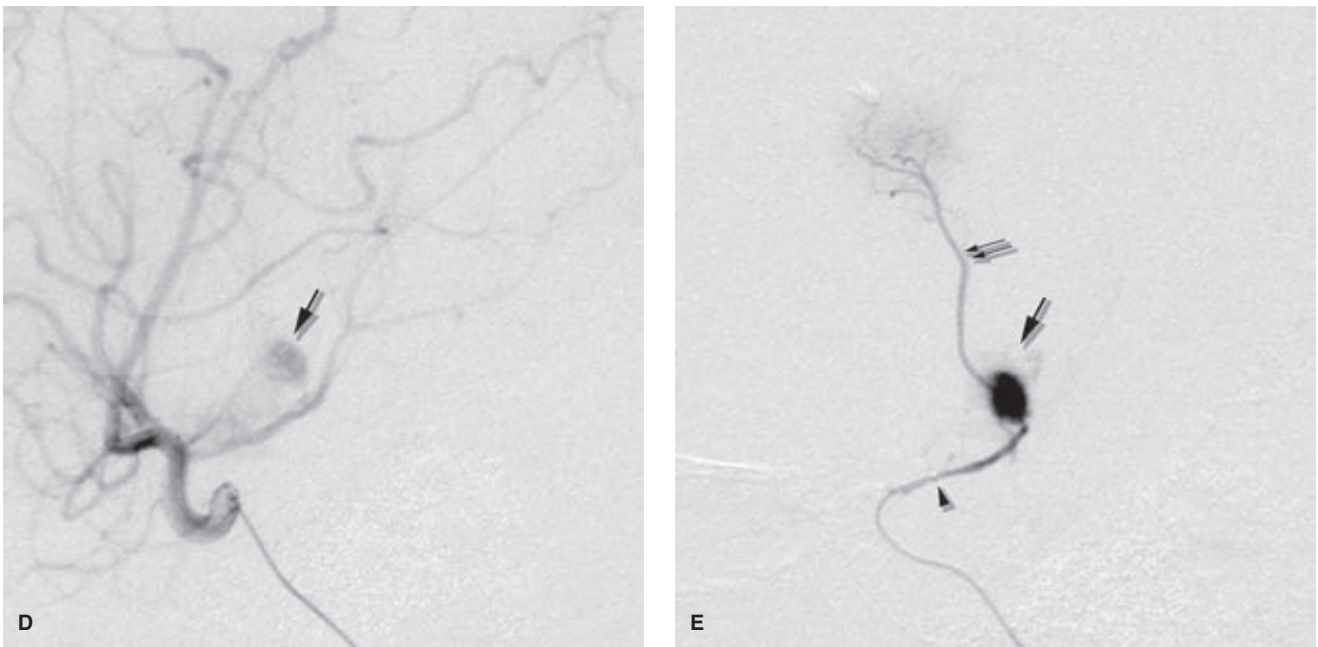


FIGURE 4-5. (CONTINUED) The right internal carotid artery injection (**D**, lateral projection) performed with 1 mL of contrast showed an ill-defined aneurysm projecting above the right posterior cerebral artery (arrow in **D**), which was difficult to understand because no such abnormality was evident on the left vertebral artery injection. A superselective injection (**E**, lateral projection) of the right posterior communicating artery with the microcatheter shows that the microcatheter tip (arrowhead in **E**) is virtually wedged in the vessel. An extremely gentle injection (0.3 mL) shows the pseudoaneurysm (arrow in **E**) to be arising from an anterior thalamoperforator vessel (double arrow in **E**), thus explaining why it was not visible from the posterior circulation. The distal posterior cerebral artery is not seen on this injection because the microcatheter is wedged and the injection is very gentle. The case became more complicated still, when successful endovascular occlusion of the thalamoperforator aneurysm with coils facilitated demonstration of yet another point of extravasation in a different anterior thalamoperforators. The final tally of contrast used was 26 mL of 240-strength nonionic, over a 2.5-hour period. For a hydrated child with normal renal function, this is probably in the reasonable range.

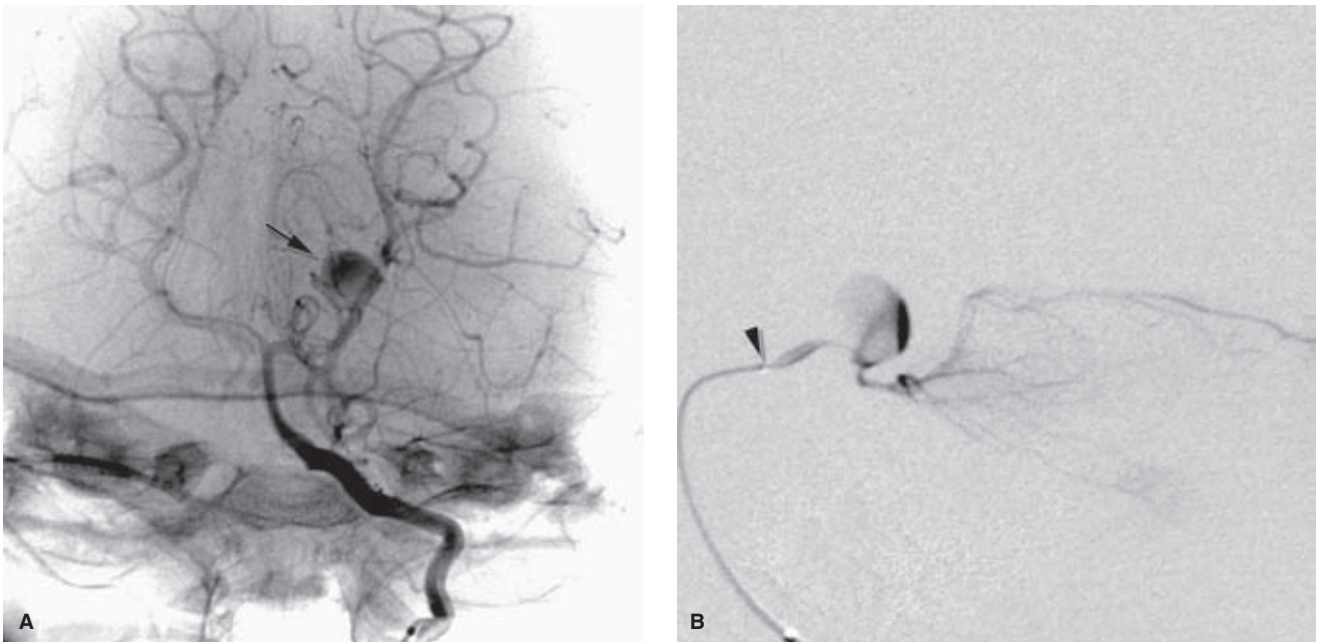


FIGURE 4-6. (A–B) Microcatheter angiography in a 10-month-old. This child suffered a subarachnoid hemorrhage into a large arachnoid cyst, which had been fenestrated surgically some weeks previously. Transfemoral angiography was performed using a 4F (OD) dilator as described above attached to an Argon valve for maintenance of flush, and a Renegade microcatheter. The left vertebral artery injection (**A**, Towne's view) performed with a hand injection of 3 mL of contrast shows a large pseudoaneurysm (arrow in **A**) of the left superior cerebellar artery. A selective injection shows the tip of the microcatheter advanced into the left superior cerebellar artery (arrowhead in **B**, lateral view) and good visualization of the aneurysm as a side-wall tear in the upper surface of the artery. The injection technique is very gentle, hence the streaming of nonopacified blood on the angiogram. In fact, the pseudoaneurysm could be seen pulsing ominously with systole during the angiogram and on roadmap imaging. Due to the high likelihood of perforation of the aneurysm with a relatively stiff microcatheter, the extremely small size of the vessels, and the uncertain nature of the pseudoaneurysm, a surgical repair was decided upon. A complete endovascular occlusion of the aneurysm without closure of the distal artery would have been improbable.

children. Therefore in children, the strategy is to image the vessel correctly the first time, and avoid a pusillanimous technique that might require repetition of the run with still further contrast and more radiation. A tight bolus of 1–2 mL of contrast, sharply delivered, will generate sufficient signal-to-noise for diagnostic-quality images. For very small children, when one is limited to a total projected volume of contrast less than 10–20 mL with which to establish a firm diagnosis or perform an endovascular procedure, careful planning of the procedure is all the more of paramount

importance. The anesthesia team may be able to promote fluid turnover through small doses of diuretics. Sometimes, it might be desirable to halt the procedure for an hour or more to allow the half-life of contrast to elapse, before resuming the procedure.

Reference

1. Kuon E, Dorn C, Schmitt M, et al. Radiation dose reduction in invasive cardiology by restriction to adequate instead of optimized picture quality. *Health Phys* 2003;84(5):626–631.

Safety and Complications

Key Points

- A methodical team-based and system-based approach to safety is becoming more established in the culture surrounding medical procedures.
- The recent reduction in the volume of diagnostic cerebral angiography due to the advent of noninvasive imaging compels trainees to learn basic skills only on complex interventional cases.

Angiographic complications share much in common with dangers in other fields touched uncommonly but dramatically by disastrous calamities. Road accidents, aviation crashes, and so on, do not happen spontaneously. They are caused when a concatenation of circumstances align at a particular point in time, and the preventive safety measures in place to avoid these accidents have either been neglected or failed to take account of the particular factors in play. Generally, however, the influential circumstances are banal rather than exotic. A driver reaches for a pen to jot down a note when speaking on his/her cell phone. Pressed for time to return home, a single-engine pilot decides to race ahead of the projected weather front moving in. Most “accidents” evolve from the mundane. Similarly, during angiographic procedures, while exotic possibilities do exist, such as a spontaneous aortic perforation by the wire in an Ehlers–Danlos patient or an anaphylactic reaction, they are extremely rare. Most complications are triggered by drearily commonplace circumstances. A tired technologist reaches for an exchange-length microwire instead of a standard-length wire. An inexperienced angiographer decides that he/she is quite capable of performing an epistaxis embolization. Thwarted by the refusal of a wire to enter a particular branch vessel, an angiographer decides that he/she is going to teach that wire a lesson it will never forget and make it go.

Prompted by a growing public awareness of the potential magnitude of the prevalence of medical errors (1), the Joint Commission (2003) (2) and subsequently the World Health Organization (WHO) (3) have released recommendations for Surgical Safety Checklists and Time-Outs, which have been implemented in operating rooms and are becoming standard in endovascular suites. Discussions of the importance of teamwork and the need to communicate clearly, due to the much hackneyed nature of these phrases, can tend to draw a response of yawning lip-service. Nevertheless, it is important to be aware that an extensive medical literature upholds the validity of intervention aimed at changing personal attitudes

and institutional culture (4). Evidence demonstrates a reduction in wrong site/wrong procedure surgeries, improved early reporting of equipment problems, avoidance of medication problems, and reduced operational costs (5). Some of these lessons are of limited value, obviously, to a field in which direct visualization of the lesion would preempt the possibility of wrong-side surgery. However, data concerning staff attitudes to and perception of the success of teamwork show a discrepancy between those of nurses, for instance, and physicians. In one study with a ring of verisimilitude to it, nurses described good collaboration as “having their input respected,” whereas physicians often described good collaboration as having nurses “who anticipate their needs and follow instructions” (4). It would not be difficult, therefore, to understand how some measure of reluctance to voice qualms during a procedure on the part of technologist or nursing staff might easily establish itself to the detriment of patient safety.

Comparisons with the culture of professional aviation confirm that a substantial lag exists in making progress within the medical profession of the type that has been wrought over 50 years of Crew Resource Management Training in the flying world. A culture of hiding errors or ignoring them as a “one-time” event still persists. In one study comparing physicians and pilots, 60% of physicians (70% of surgeons in the study) stated that even when fatigued they were capable of working with complete effectiveness at critical times, whereas the corresponding response from officer pilots was a modest 26% (6). Taking the lead from the aviation industry, the medical world is now making progress with a greater emphasis on medical team training rather than individual training and on postprocedure debriefings and analysis with open sharing of information (7).

Just as the surgical world has been lagging behind the safety standards of commercial aviation, it is safe to say that the neuroendovascular field is still further behind. At this time, no clear consensus or professional guidelines exist, for instance, on the necessity or value of prophylactic administration of antibiotics during percutaneous procedures, or use of antiembolic devices during prolonged procedures. These decisions are still made anachronistically on an institutional or individual physician basis. Furthermore, there are aspects of the field that do not lend themselves well to institutional regulatory oversight. Standards to establish or prove competence in the field in general or with particular devices are virtually nonexistent or perfunctory. While the point has been made that comparing the aviation industry track record on safety with the medical world can only go so far before the analogy breaks down (8), not least because in the aviation



FIGURE 5-1. (A–C) Why fellowship training is necessary. This young female presented with recurrent epistaxis, but was well-controlled with first aid measures and could have been transferred to a tertiary care center. A physician at her community hospital undertook to perform particle embolization of the external carotid artery bilaterally. The images of the right external carotid artery anteroposterior (AP) pre-embolization (A), lateral pre-embolization (B), and lateral postembolization (C) are presented. The patient's left-sided images are presented in Chapter 25. The images demonstrate a rare but crucial-to-recognize variant of the ophthalmic artery (*arrow*) arising from the middle meningeal artery. The distal internal maxillary artery (*double arrowheads*) demonstrates a fairly standard configuration, as it breaks up into the long and short sphenopalatine branches in the pterygo-maxillary fissure. Unfortunately for the patient, the physician embolized the internal maxillary artery in a way that occluded both the ophthalmic artery and the internal maxillary artery. The result was that the patient experienced excruciating pain in the right eye and immediate loss of vision, which prompted cessation of the case moments before embolization of the left external carotid artery was to begin.

world when there is an accident the pilot will be the first one hurt, hence the motivation factor, nevertheless, considerable room for improvement exists in our field (Figs. 5-1 and 5-2).

► NEUROLOGIC COMPLICATIONS OF CEREBRAL ANGIOGRAPHY

Since the first edition of this text, the population of patients undergoing neuroendovascular procedures has changed considerably. Diagnostic angiographic procedures have been supplanted in large measure by noninvasive imaging. On the other hand, therapeutic procedures have become more

complex and reaching in their scope. One result of this change is that the older literature pertinent to procedural complications based on patients undergoing diagnostic procedures for evaluation of carotid artery disease, subarachnoid hemorrhage, or questionably ischemic symptoms has become outdated. While some of these patients are still undergoing endovascular procedures—those with atherosclerotic disease are being catheterized with 6F to 8F introducer devices instead of what would have been previously a 5F diagnostic catheter, and subarachnoid hemorrhage patients are being treated definitively with invasive procedures involving balloon catheters, stents, and liquid or coil devices—conclusions from the older body of literature cannot be extrapolated reliably to the modern

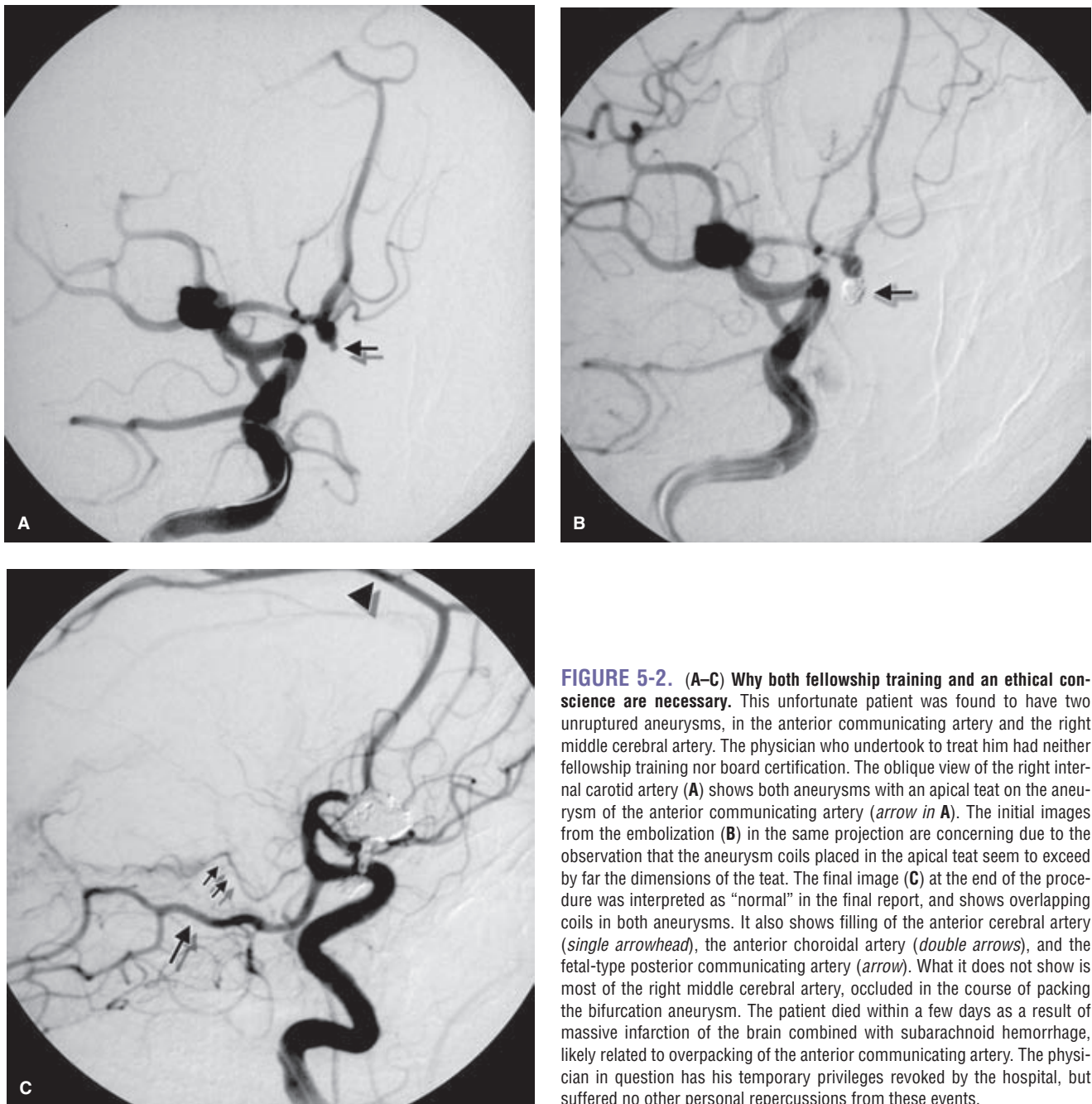


FIGURE 5-2. (A–C) Why both fellowship training and an ethical conscience are necessary. This unfortunate patient was found to have two unruptured aneurysms, in the anterior communicating artery and the right middle cerebral artery. The physician who undertook to treat him had neither fellowship training nor board certification. The oblique view of the right internal carotid artery (**A**) shows both aneurysms with an apical teat on the aneurysm of the anterior communicating artery (*arrow in A*). The initial images from the embolization (**B**) in the same projection are concerning due to the observation that the aneurysm coils placed in the apical teat seem to exceed by far the dimensions of the teat. The final image (**C**) at the end of the procedure was interpreted as “normal” in the final report, and shows overlapping coils in both aneurysms. It also shows filling of the anterior cerebral artery (*single arrowhead*), the anterior choroidal artery (*double arrows*), and the fetal-type posterior communicating artery (*arrow*). What it does not show is most of the right middle cerebral artery, occluded in the course of packing the bifurcation aneurysm. The patient died within a few days as a result of massive infarction of the brain combined with subarachnoid hemorrhage, likely related to overpacking of the anterior communicating artery. The physician in question has his temporary privileges revoked by the hospital, but suffered no other personal repercussions from these events.

practice of neuroangiography. With a few exceptions, a modern body of literature dealing with this topic has not emerged as yet. Many of the older papers referenced below, however, are still highly relevant to particular groups of patients, such as those with carotid artery disease in the setting of angioplasty and stenting procedures.

The safest endovascular procedure is the one that can be cancelled as unnecessary or that can be avoided by performing noninvasive imaging (Fig. 5-3). Complications include the possibility of killing the patient, and this risk exists with every patient who entrusts his/her welfare to your hands. The need for excellent technical training backed up by a thorough knowledge of the diseases of the neurovascular system is self-evident. Many serious complications of angiography are made worse by the effects of continuing the study, oblivious to a developing problem (Table 5-1; Figs. 5-3–5-5).

Clinically Detectable Neurologic Complications

Older studies of complications of cerebral angiography, based on clinically evident neurologic complications arising within 24 to 72 hours of transfemoral cerebral angiography, report an overall incidence of approximately 0% to 6.8% (9–22). The majority of these events are undoubtedly transient, but there is a deal of latitude in the literature as to how many permanent neurologic complications can be seen. Figures as high as 5.7% are sometimes quoted for enduring neurologic deficits, but a more realistic figure for reasonably experienced angiographers might be in the region of 1.2%, as reported in the asymptomatic carotid artery stenosis (ACAS) study (17). Studies of pediatric patients in specialized tertiary referral hospitals report a 0% complication rate in retrospective studies (23,24).

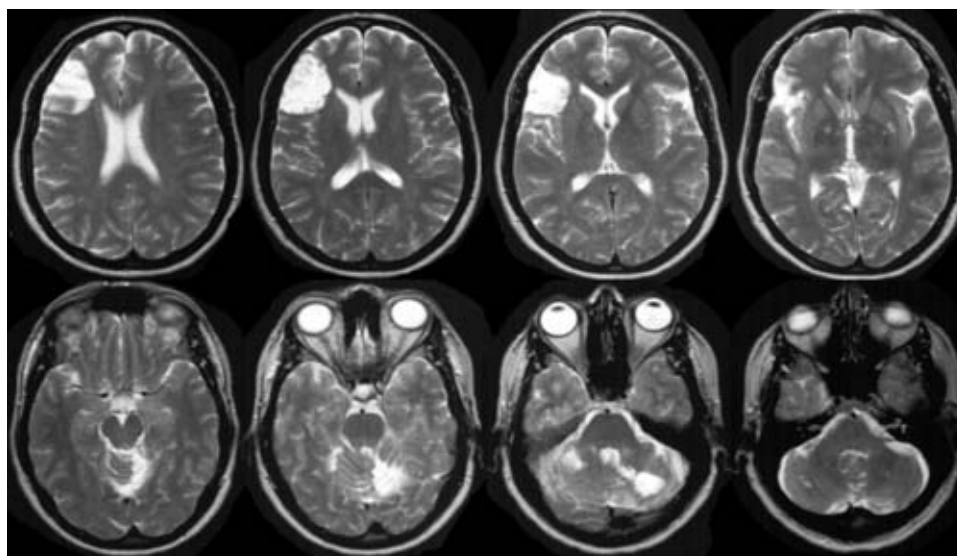


FIGURE 5-3. Dangers of cerebral angiography. A young female had a cerebral angiogram performed for complaints of headache. All noninvasive imaging up until that time was normal, with no suspicion of aneurysm, arteriovenous malformations (AVM), vasculitis, or other indication that the cerebral angiogram would yield diagnostic information. The radiologist who performed the study completed angiography of three vessels uneventfully and then used an exchange-length wire to access the right vertebral artery. This resulted in a shower of thrombus being delivered to the entire cerebral vasculature. The follow-up T2-weighted MRI shows extensive encephalomalacic change in several vascular territories, with concordant permanent clinical deficits to the patient.

Some studies contain a bias in that they consider neurologic events to be angiographic complications only if they appear to be related to the angiogram in the opinion of the investigator. Some studies (12,25,26) have managed to avoid this bias by including all neurologic deteriorations occurring within 24 hours of a cerebral arteriogram. They have found neurologic deterioration rates of approximately 9% to 14.7% for all neurologic events (18) and 0.4% to 5% for permanent events in patients referred for evaluation of recent ischemic disease. Many of the recorded complications were exacerbations of previous conditions. Earnest et al. (12) speculated that compromise of cerebral blood flow in this group of patients might be a final common pathway for many of these complications. Likely causes include inadequate hydration or normalization of blood pressure before the angiogram in patients for whom cerebral circulation is dependent on a hypertensive baseline state. On the other hand, consideration must be given to the rate of spontaneous disease-related, rather than procedure-related, events in this population over a similar period. Baum et al. (27) studied a group of patients whose angiographic examinations were canceled, and who demonstrated a similar incidence of clinical events in the time period that would have been considered in evaluation of postangiographic complications.

Variable features among studies of complications after cerebral angiography include the patient population and diseases, referral characteristics of the institution, whether the study took place at a teaching hospital, the changing practice of radiology depending on the year of the study, and whether the postangiographic evaluation was done by a radiologist or a neurologist. Risk factors for clinically evident neurologic complications in the first 24 hours after cerebral angiography include:

- Patients who are referred because of stroke or transient ischemic attacks (16,19,22).
- Patients whose angiograms demonstrate greater than 50% to 70% stenotic disease of the cerebral vessels (14,16,22,25).
- Patients older than age 70 (12,16,20,22).
- Patients whose angiograms require a higher volume of contrast (12,16,28).
- Patients whose angiograms last more than 60 to 90 minutes or require multiple catheters (9,22,28).
- Patients whose angiogram was performed by a fellow alone (22).
- Patients with systemic hypertension or renal impairment (12,28).
- Patients referred for subarachnoid hemorrhage or who are immediately postoperative (10,12,19).

The risk of cerebral angiography performed by trainees at teaching hospitals has been examined by a number of studies (9,11,13,27). Some studies (10,22,29) concluded that difficulty in catheter manipulation by inexperienced radiologists was a risk factor for the examination taking more time, possibly in turn creating a higher likelihood of neurologic complications. Moreover, there is a definite historical trend toward trainees having a lower volume of diagnostic neuroangiographic studies under supervision. Noninvasive imaging has had an impact on the volume of cases, and programs have expanded the numbers of trainees, thus changing the denominator for the available volume of cases. Gabrielsen (30) has commented that complication rates at many institutions are probably substantially higher than those quoted in medical journals, pointing out that a diminution of the workload in cerebral angiography implies that trainees and practicing neuroradiologists now gain less expertise than 20 years ago. In response to this, the American Society of Neuroradiology and allied societies in the neurovascular field issued a joint statement in 2004 suggesting that a case log of 100 patients become the minimum standard for establishing adequate training in diagnostic cervicocerebral angiography (31,32).

TABLE 5-1 General Principles for Avoiding Complications of Cerebral Angiography

Spend time with the patient ahead of the case. Avoid rushing the preangiographic evaluation. It is the source of unending bafflement how emphatically many patients will assert in the clinic or in their hospital room that they have “no allergies,” only to mention as they are climbing on the angiographic table that they “sure hope that you are not going to use any of that x-ray dye” on them that caused their heart to stop the last time they had a coronary angiogram. Rather, in the triumphalist manner of a farm carter gleefully plonking down a Jack-o’-trumps during a lunchtime hand of whist, it is not uncommon for patients to trundle out such showstoppers at the very last minute, usually with a perverse sense of pride. “They told me I was as good as dead if they ever put that dye in me again.” Wanting to strangle the patient at this point is understandable but, unfortunately, illegal in some states.

Similarly, one almost needs to adopt an inquisitional stratagem for some patients on the question of anticoagulation. Many will repeatedly deny taking any form of anticoagulant or blood thinner of any stripe, but if given the opportunity might mention the “rat poison” that they have been taking for their heart for several years. Questions of premedication for a procedure that seem blatantly obvious to us are not necessarily so to patients. Difficulty with understanding instructions and other causes of noncompliance will often interfere with your best plans. Patients need to be quizzed pointedly before a procedure about whether they have been taking their prescribed medications, in the prescribed manner, on every day.

The profundity of this problem is evident in an anecdotal experience of our department where I made a didactic point of assuring that the fellow had double-checked with the patient—a licensed RN, it needs to be stressed—that she had taken her Plavix prescription starting 5 days in advance of the procedure. The answer was a guilt-edged affirmative, as expected, and we resumed preparations for the procedure without giving it much consideration. As something of an afterthought, however, with reference to renewing the patient’s prescription for Plavix, dispensed in lots of 30, I mentioned to the patient that she should have enough supply left at home for another 25 days after discharge.

She looked baffled.

“Well,” I explained with ponderous erudition, “it’s like this. One tablet per day for five days makes five. Thirty minus five makes twenty-five. So, you should have twenty-five tablets left at home.”

She continued to appear perplexed, until a light dawned, and she smiled charitably on my gormlessness for thinking that anything in the cosmos could be so straightforward.

“Oh, no,” she replied. “I took all thirty of them the first day. It was quite an ordeal, but I got them all down over the course of about an hour.”

As Douglas Adams put it, this sort of thing probably happens all the time in the universe, and we are powerless to prevent it.

Consistency in every aspect of your work. Perform every single case with the exact same routine each time, same equipment, same standards, and same degree of ruthless consistency and diligence.

Frequently, one has a sense that certain cases have a lesser degree of urgency or legitimacy than others, either in the opinion of your team (e.g., patients who are uncooperative, abusive, intoxicated) or in your own opinion (e.g., a patient undergoing a study that you think is not warranted or of dubious merit). It is important to recognize this phenomenon in yourself and in your team members and to avoid any shortcuts in the room preparation, equipment cleaning, tray layout, and the like. It would be trite to say that every patient deserves the very best of care 100% of the time, and, without substantiation or the imposition of medical ethics, such a statement might even be open to debate. However, what will happen is that any depreciation in standards for any aspect of the team’s performance, even if only intended to be temporary, will re-establish the new lower standard as the common denominator. Group behavior from the team will balk at a fluctuating level of expectations and will seek to impose its own standards instead. This is a very bad situation to allow in your angiography suite because the group standard will always aim to sink as low as the lowest tolerated level—that of your most delinquent team member.

For instance, if you notice blood on the equipment from a previous patient as you are starting a case, you can decide to let it go and not make a fuss, or you can stop everything and declare that the current case cannot proceed until the room is fit for human habitation. One way gives you the option of being a nice, inoffensive sort of chap; the second is a little obnoxious. However, if you decide to accept the room as you find it, then it will be up to the whims of your personnel to decide from day to day what standard they feel like attaining. Similarly then, if you let it go for several months until one day you finally demand that something be done about the room, your personnel will be baffled by this sudden change in your demeanor and assume that you are off your Lithium again. On the other hand, if your staff knows that you will always insist on cleaning up blood on the machine from a previous case, putting away a dirty mop bucket leaning against the wall in plain view, or redoing a sloppily prepared tray, then your behavior and standards are merely consistent and expected by them.

Never perform a cerebral angiogram under rushed or hurried circumstances in a way that compromises your standard routine. The temptation to cut corners in this situation is insurmountable, and the patient is the only one who might pay for a slip made under these conditions.

Never perform a cerebral angiogram with a team of assistants among whom there is some current problem of interpersonal aggravation or conflict. These situations do arise from time to time, where members of the team are at a juncture where some argument or conflict has not been resolved. These events consume enormous degrees of mental and emotional energy, not just in the participants, but also in the bystanders who are inevitably stressed by witnessing what is in progress. Stop the study immediately, and break up the team to avoid this situation.

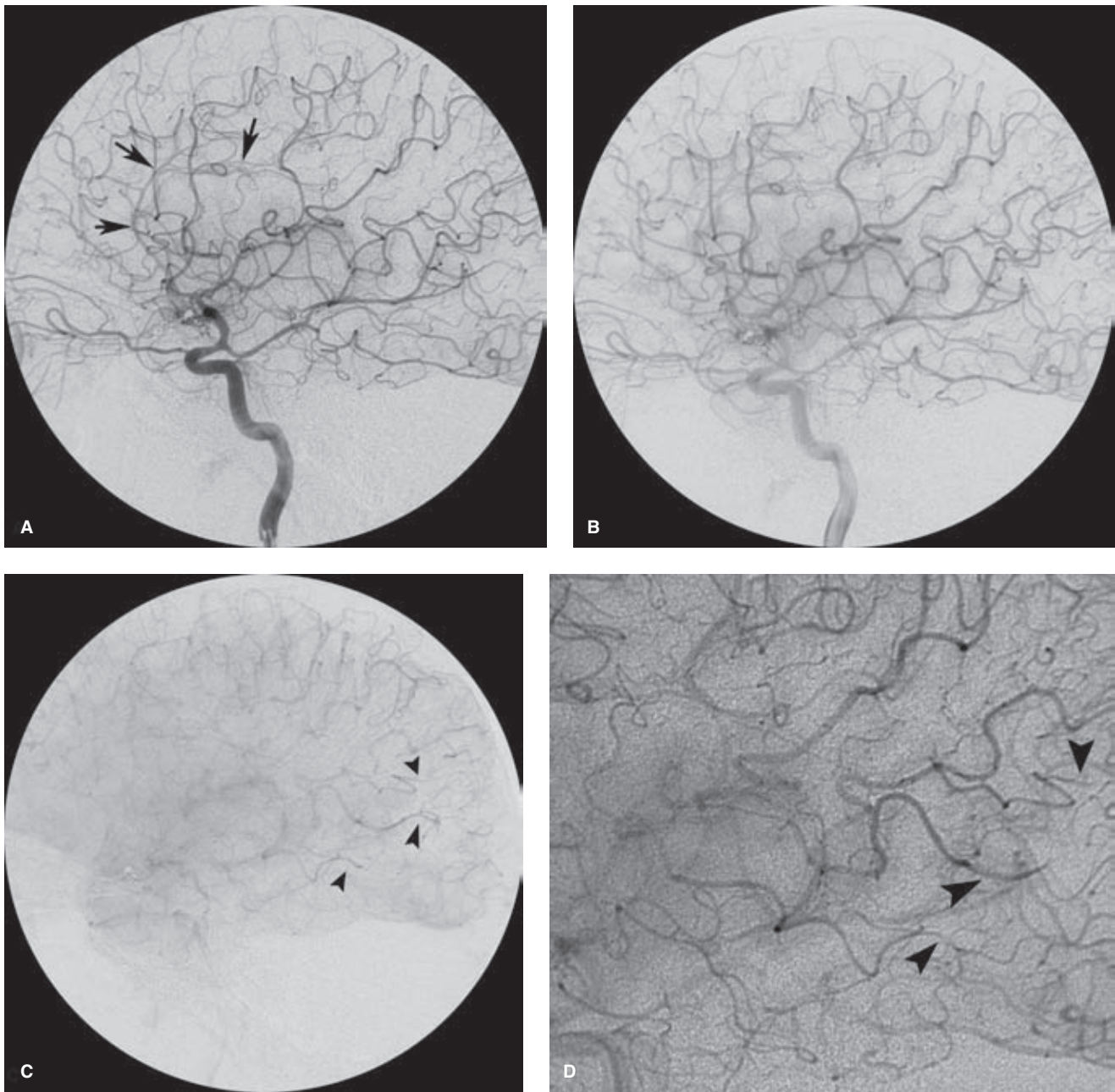


FIGURE 5-4. (A–D) Recognition of angiographic complications. Any awake medical student can recognize an M1 occlusion on an angiogram. To detect and recognize smaller emboli requires a methodical evaluation of the dynamic properties of the transit of contrast through the vascular tree. Prompt intervention through immediate removal of a suspect catheter, heparinization, thrombolysis, or blood pressure management can make a big difference to the outcome of a patient in such a predicament. Quality of imaging and competent interpretation have a tangible impact on patient outcome. In this case, a patient with altered mental status was being studied for possible vasospasm status post clipping of a rupture anterior communicating artery aneurysm. The initial left internal carotid angiogram (A) shows minimal spasm of the supraclinoidal carotid artery but poor filling of the anterior cerebral artery due to A1 spasm. The course of the pericallosal artery is also suggestive of hydrocephalus (arrows). The radiologist performing the procedure opted to infuse papaverine in the cervical internal carotid artery. The postinfusion lateral angiogram appears initially unremarkable (B), but a view (C) later in the parenchymal phase shows several posterior parietal branches that look stagnant with poor washout (arrowheads). A magnified view (D) of the affected area allows visualization of the emboli as filling defects within the arteries (arrowheads).

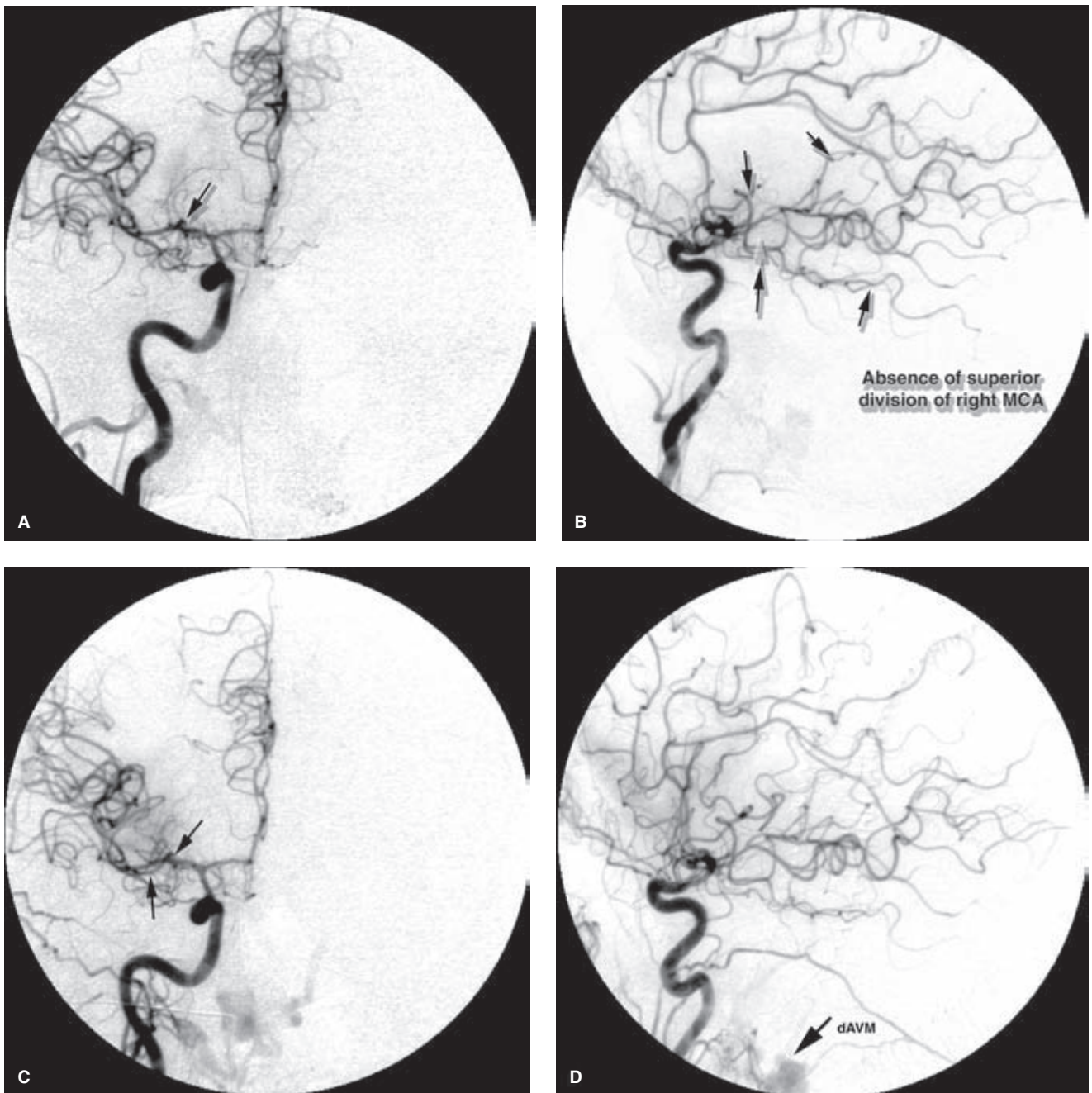


FIGURE 5-5. (A–D) Importance of prompt recognition of complications. A 65-year-old male undergoing angiographic evaluation of a posterior fossa dural AVM. A right internal carotid artery PA injection (**A**) demonstrates a stump-like density (*arrow* in **A**) off the middle cerebral artery. Although there appears to be an adequate number of middle cerebral artery branches on the PA view, the lateral view (**B**) demonstrates lucency in the window formed under the pericallosal branch of the anterior cerebral artery due to occlusion of the superior division of the right middle cerebral artery. The branches of the inferior division are present (*arrows* in **B**). This represents a procedural complication probably due to thrombus formation in the catheter. The patient was heparinized immediately, and the systolic blood pressure was elevated to 160 mm Hg. A common carotid arteriogram (**C**, **D**) done minutes later in anticipation of emergency thrombolysis demonstrated reopening of the superior division (*arrow* in **C**). Compare the lateral appearance after reopening (**D**) with the appearance during occlusion (**B**), demonstrating the sensitivity of the lateral view to branch occlusion of the middle cerebral artery. The patient recovered from this complication without clinical or imaging evidence of a related deficit. Pathologic opacification of veins in the posterior fossa is seen due to the dural AVM in the region of the foramen magnum.

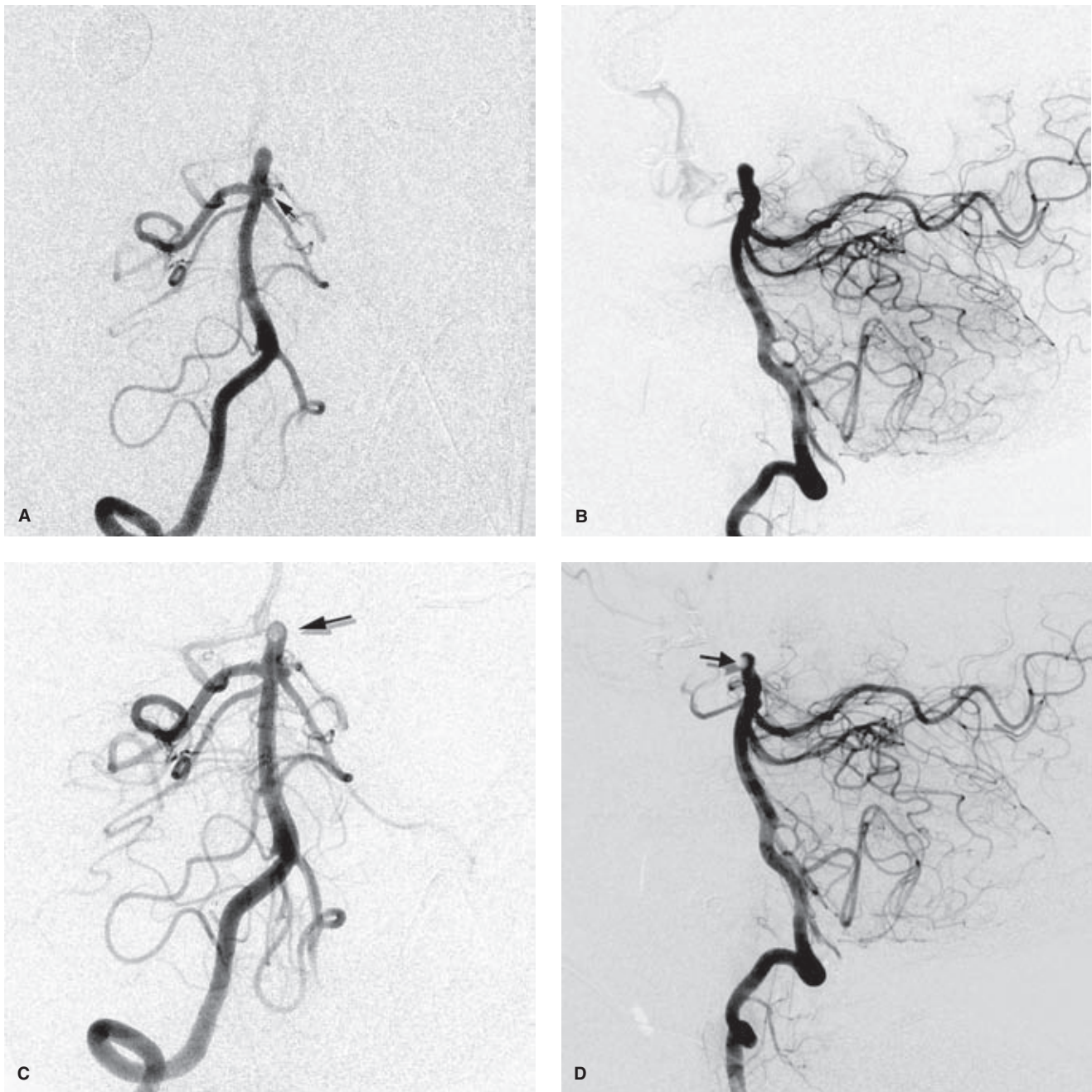


FIGURE 5-6. (A–D) Better to avoid this. Air embolism. A somewhat difficult-looking elongated aneurysm of the basilar apex is illustrated in this elective case. The patient had a clipping of a previous aneurysm in the anterior circulation complicated by ischemic complications and was keen to avoid similar complications. The right vertebral artery injection AP plane (A) and lateral plane (B) shows the aneurysm to be wide at its base and associated with a second smaller aneurysm (*small arrow* in A) lodged between the left posterior cerebral artery and the left superior cerebellar artery. Overlapping dimes on the patient's head (18 mm) are used for external sizing reference. Both vertebral arteries were catheterized and a microcatheter advanced via the left vertebral artery was jailed into the aneurysm by a Neuroform stent extending from the midbasilar artery to the right P1 segment. Unfortunately, the Neuroform stent had been inexpertly flushed and prepared in advance. Images immediately after the stent deployment (C and D) showed a sizeable bubble (*arrow*) bobbing anteriorly in the aneurysm, most likely having escaped from the stent catheter. Suction was applied (*vigorously*) to the aneurysm microcatheter and as a result of these efforts or the solvent properties of the flowing blood, the bubble disappeared and was gone when the next run was performed. No clinical sequelae were evident after the case, and many valuable lessons were learned by all.

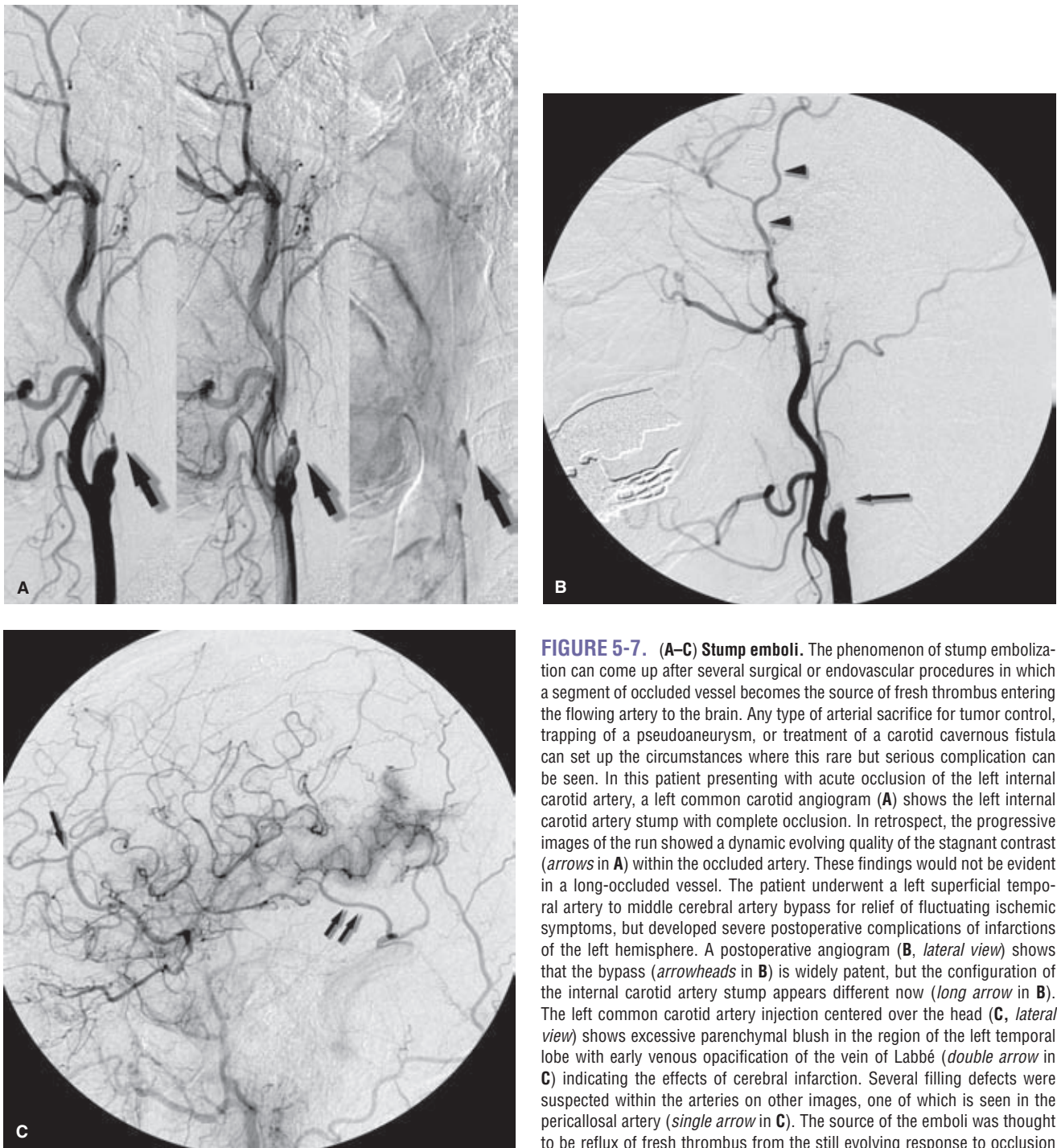


FIGURE 5-7. (A–C) Stump emboli. The phenomenon of stump embolization can come up after several surgical or endovascular procedures in which a segment of occluded vessel becomes the source of fresh thrombus entering the flowing artery to the brain. Any type of arterial sacrifice for tumor control, trapping of a pseudoaneurysm, or treatment of a carotid cavernous fistula can set up the circumstances where this rare but serious complication can be seen. In this patient presenting with acute occlusion of the left internal carotid artery, a left common carotid angiogram (**A**) shows the left internal carotid artery stump with complete occlusion. In retrospect, the progressive images of the run showed a dynamic evolving quality of the stagnant contrast (*arrows in A*) within the occluded artery. These findings would not be evident in a long-occluded vessel. The patient underwent a left superficial temporal artery to middle cerebral artery bypass for relief of fluctuating ischemic symptoms, but developed severe postoperative complications of infarctions of the left hemisphere. A postoperative angiogram (**B**, lateral view) shows that the bypass (*arrowheads in B*) is widely patent, but the configuration of the internal carotid artery stump appears different now (*long arrow in B*). The left common carotid artery injection centered over the head (**C**, lateral view) shows excessive parenchymal blush in the region of the left temporal lobe with early venous opacification of the vein of Labbé (*double arrow in C*) indicating the effects of cerebral infarction. Several filling defects were suspected within the arteries on other images, one of which is seen in the pericallosal artery (*single arrow in C*). The source of the emboli was thought to be reflux of fresh thrombus from the still evolving response to occlusion of the left internal carotid artery stump.

Microemboli and Microbubbles

Transcranial Doppler (TCD) monitoring during neuroangiographic procedures has the potential to reveal much about cerebrovascular physiology and intraprocedural events. There are different kinds of microemboli that might be detectable by TCD during diagnostic or interventional procedures with different implications for their significance. Some might be gaseous microbubbles and are probably inconsequential, leaving no trace of damage

for detection on MRI. Particulate matter, however, is more likely to cause significant ischemic injury to brain tissue.

Emboli to the brain during cerebral angiography may represent dislodged atheromatous material, thrombus from the catheter, or air bubbles (Figs. 5-6–5-9). Even if they are most often clinically silent, they may not necessarily be always benign. A retrospective review of medical records on cardiac surgery patients, for instance, might reveal a complication rate of 3.4% for altered mental state and 1% for stroke, but prospective investigation of higher motor and cognitive

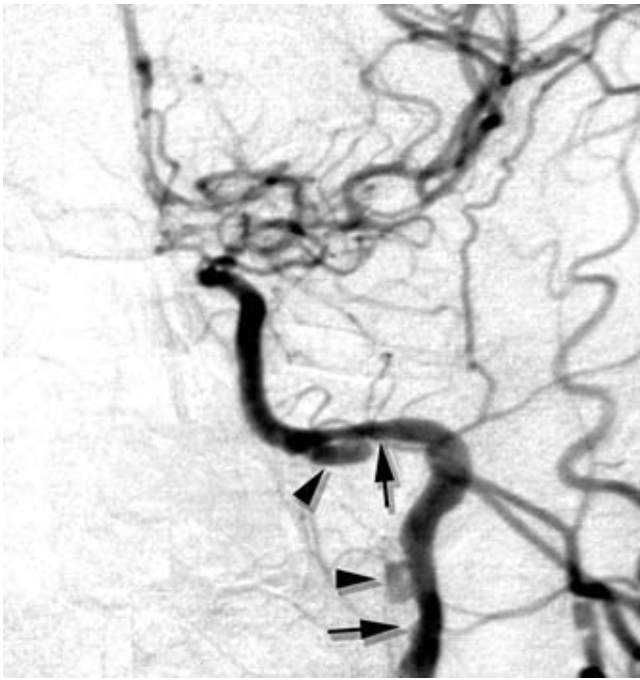


FIGURE 5-8. Catheter-related dissection. A left common carotid artery injection in a 45-year-old female with grade IV subarachnoid hemorrhage and severe intracranial spasm of the left M1 and A1 segments. Irregular narrowing (*arrows*) of the cervical and petrous internal carotid artery, with pseudoaneurysm or pouch formation (*arrowheads*), is present. This complicated dissection was probably initiated by a previous angiographic procedure and subsequently aggravated by episodes of paroxysmal hypertension. Having seen a dissection on this side, one should be all the more concerned about whether one is present on the other side. This was, in fact, the case with this patient. It is also important to consider the possibility of a covert dissection in all patients who have recently undergone angiography. High-quality road-map images should be obtained before selecting the internal carotid artery or vertebral artery in these patients.

functioning detects transient and persistent neurologic and intellectual dysfunction rates considerably higher (33–35). Terminal arteriolar or capillary focal dilatations measuring 10 to 40 μm in diameter resulting from air or fat microemboli during aortography and cardiac bypass surgery can be identified at autopsy following cardiac bypass surgery (36). These are of sufficient quantity that they could cause psychomotor dysfunction without necessarily giving histologic evidence of adjacent tissue ischemia. The importance of emboli of this size can be emphasized when one recalls that Gelfoam powder of particle size 60 μm can be used in tumor embolization when end-vessel penetration and tumor necrosis are intended. Animal experiments and clinical experience in divers with air embolism to the brain suggest that a small volume of air can be tolerated and will pass quickly through the pial capillary bed without causing cerebral dysfunction. With higher volumes, bubbles become trapped in the pial arterioles, which then dilate with rapid onset of decline in cerebral function (37). Similarly, scuba divers who have suffered decompression illness or air embolisms demonstrate MRI and CT focal deficits and problems with neuropsychological testing indicating the focal ischemic effects of gas bubbles in the cerebral circulation (38–40) (Fig. 5-6).

The number of air emboli to the brain during cardiac surgery correlates with the degree of postoperative cognitive deficit (41), and it is therefore important to eliminate or

minimize this risk during cerebral angiography, at least for bubbles of a grossly discernible size—those detectable by a careful inspection of the tubes and lines at the start of the case. Markus et al. (42) have demonstrated that Doppler-recorded events in the human middle cerebral artery, probably representing microemboli of air during cerebral angiography, are similar to those seen in sheep experiments. The authors (42) found that with higher-density nonionic contrast (340 mg/mL), the likelihood of detecting air emboli in the contrast could be reduced significantly by allowing the syringe of high-density contrast to stand for a few minutes. This phenomenon of slow clearance of air from the high-density contrast was not seen with lower-strength contrast (140 mg/mL) or saline that had been allowed to stand for a few minutes. Markus et al. (43) commented that one possible explanation for this could be that vigorous suction necessary for drawing up a syringe of higher viscosity contrast might be responsible for introducing more microbubbles. The same authors reported also that air bubbles are more likely to be introduced by a rapid injection than by a slow one.

Using diffusion-weighted MRI and TCD sonography during cerebral angiography, Bendszus et al. (44) demonstrated a statistically significant improvement in technique. By using air filters and heparinization during cerebral angiography, they demonstrated a significant reduction in Doppler events during procedures and in diffusion-weighted

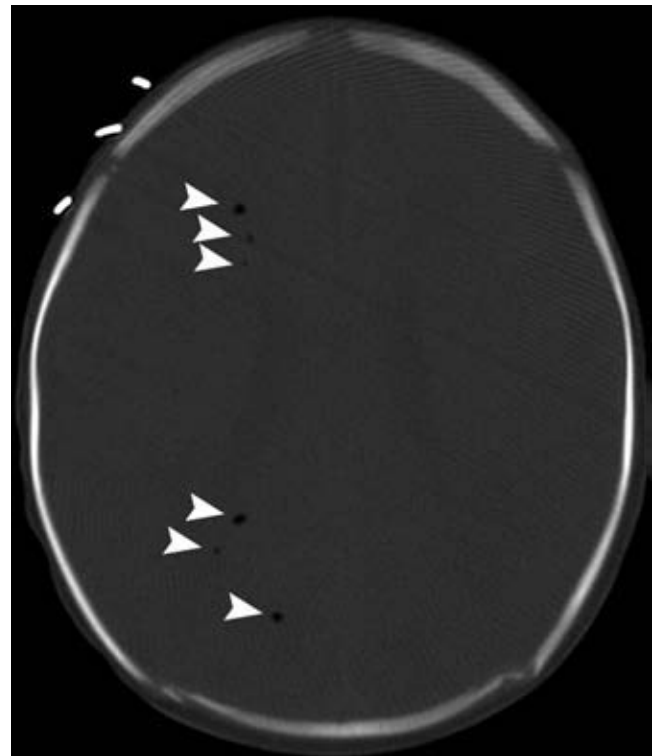


FIGURE 5-9. Air embolization on CT. A pediatric head CT scan for altered neurologic status following a noncerebral diagnostic study shows substantial air embolization within the brain parenchymal (*arrowheads*). It is possible that very small quantities of gaseous microemboli are commonplace during angiographic injections and may be tolerated by cerebral circulation (see text), but the level of embolic gas seen in this patient was undoubtedly excessive and correlated with the clinical deterioration of the patient. The observation that gaseous microemboli might be universal on TCD studies performed during cerebral angiography should not permit one to become complacent about the dangers of macroscopically visible air in lines or syringes.

imaging (DWI) abnormalities detectable on MRI within 3 days following the angiogram.

There is thus an emerging body of data from imaging outcomes, clinical outcomes, and intraprocedural use of TCD that microembolic events are common during angiographic procedures and may be responsible for some of the adverse events precipitated by this technique.

Microemboli During Cerebral Angiography and Clinically Silent Neurologic Complications

Older studies that suggested that cerebral angiographic examinations are associated with a rate of neurologic complications in the range of only 1% to 3% may be misleading. Important neurologic complications may not be clinically evident during a bedside examination. It is now understood that an incidence of DWI abnormalities on MRI following carotid interventional procedures can be found in as many as 29% to 60% of cases following carotid stenting (44–46), or cerebral aneurysm embolization (47), but most of these events are clinically silent indicating the insensitivity of clinical examination to these complications. Dagirmanjian et al. (48) have demonstrated that Doppler sonography detects an average of more than 70 microembolic events per patient during cerebral angiography, without clinical evidence of a deficit. Although the authors described these events as clinically benign, rigorous neuropsychological testing, at the very least, would probably be necessary to substantiate this. The composition of these emboli seen on TCD cannot be established, but they are more numerous during flushing and contrast injection, and less frequent during wire and catheter manipulation. Furthermore, the authors observed these embolic intracranially distal to the site of an occluded carotid artery in some patients. It is overwhelmingly likely, therefore, that TCD detected microemboli during routine angiography are mostly gaseous in nature. A consecutive series of 20 cerebral angiograms reported by Britt et al. (49) found a 0% incidence of DWI abnormalities in follow-up MRI, indicating that the phenomenon of microemboli, universal in the study by Dagirmanjian et al. (50) and thus, presumably, in all cerebral angiography patients, does not necessarily cause DWI abnormalities in all patients.

Diffusion-weighted MRI provides a powerful tool for assessing the intracranial effects of cerebral angiography. The incidence of small embolic infarcts occasionally seen on T2-weighted or diffusion-weighted MRI after diagnostic or interventional cerebral angiography procedures is variably reported in the range of 0% to 26% or as high as 66% (32,34,36,37,48–52). The likelihood of finding DWI abnormalities following a cerebral angiogram or intervention is positively correlated with the length of the procedure, difficulty of probing the vessel, the volume of contrast uses, and the need for multiple catheters—all variables that were known to correlate with clinically detectable complications in older studies (Fig. 5-8). The likelihood of a DWI abnormality following angiography also correlated with a history of vasculopathy or diseased vessels—44% versus 13% (52). It seems cogent to assume that clinically silent events are more common than the published rates of clinically evident complications. Furthermore, it is now recognized that “clinically silent” complications can be detected by neuropsychological testing in patients following cardiac bypass surgery, carotid endarterectomy (CEA), and carotid stent procedures

(53). However, it is still not clear that TCD-detectable microemboli during carotid angioplasty and stenting are necessarily all particulate and of grave consequence. Studies comparing the neuropsychological testing profile of patients following CEA and carotid angioplasty with stenting showed similar rates of decline in both groups, despite the considerably higher rates of TCD “hits” during percutaneous transluminal angioplasty (PTA) patients compared with surgical CEA patients (53).

Transient Global Amnesia and Cortical Blindness as Complications of Cerebral Angiography

Neurologic complications of cerebral angiography other than those clearly related to hemispheric ischemia may occasionally be seen and are usually transient in nature. Some of these appear to be idiosyncratic to the patient, for instance, direct toxicity in the setting of compromise of the blood–brain barrier resulting in clinical onset of cortical blindness (54), hemiballismus (55), or bilateral cochlear deafness (56). Some patients have been reported with abrupt onset of transient global amnesia after cerebral angiography (57,58). This is reported in the literature as a rare phenomenon, but it is probably more common than is acknowledged (59–65). This has been ascribed to an effect on the posterior circulation with particular reference to the medial temporal lobes. Some cases of amnesia may be related to previously diagnosed temporal lobe epilepsy, whereas others are seen in patients with atherosclerotic vertebrobasilar disease (58). Transient global amnesia after cerebral angiography usually occurs in the absence of other neurologic signs, and patients invariably recover without specific intervention within 24 to 72 hours. It can occur after use (66) of ionic and nonionic contrast, and can be seen following peripheral or cardiac studies. The possibilities of atheromatous emboli and particulate contamination of contrast have been mooted as possible explanations. Jackson et al. (67) reported an anomalous 17% incidence of transient global amnesia after vertebrobasilar angiography in a particular group of patients studied over a 24-month period. This transpired to be related to a faulty contrast warming cabinet that resulted in contrast being injected at a temperature higher than that of the body. The authors concluded that intracranial vasospasm was the explanation for their observation of transient global amnesia. The same authors included a case of transient cortical blindness within this group of patients. A migrainous phenomenon to explain these events seems plausible (66,68). Similar but lesser transient symptoms such as subjective perceptions of visual scintillations, with or without associated headache, can occasionally be reported after angiography and presumably can happen through the same mechanism.

Aneurysmal Rupture During Angiography

Probably the most severe neurologic event that can occur during cerebral angiography is rebleeding of a freshly ruptured aneurysm, associated with a mortality of at least 79% (69). For many years, it was thought that rebleeding during angiography was coincidental because it was believed there was no evidence of an increase of intracarotid or intracranial pressure during angiographic injections (70,71). However, the high prevalence of transient opacification of intracerebral

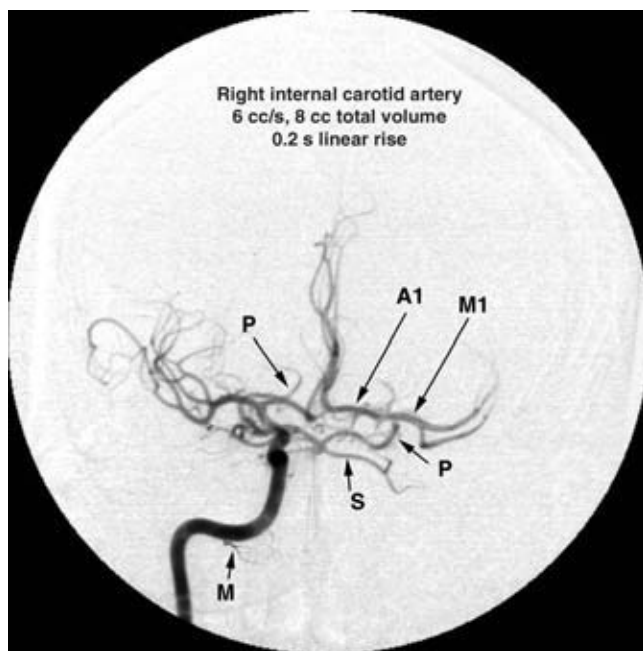


FIGURE 5-10. Nonphysiologic hemodynamic effects of internal carotid artery injections. A 27-year-old male patient presenting with dural sinus thrombosis after multiple systemic diseases, complicating an underlying diagnosis of AIDS. A 6 mL per second \times 1.3 second injection in the cervical right internal carotid artery opacifies the entire anterior and posterior circle of Willis, in the absence of occlusive arterial disease elsewhere. The superior cerebellar arteries are visualized bilaterally (*S*), as are the posterior cerebral arteries (*P*). Notice the persistent mandibuloovian artery from the right petrous internal carotid artery (*M*). With a slightly different angulation of the intensifier, one can see how the A1 and P1 segments can be directly superimposed on a frontal projection such as this. Therefore, when an internal carotid artery injection opacifies the contralateral posterior cerebral artery in this manner, it can be sometimes easy to misinterpret it as the contralateral A1 and M1 segments.

vessels through the communicating arteries during angiography would seem to argue that intracranial transmission of a substantial pressure wave is commonplace (Fig. 5-10). Other studies (72–75) have demonstrated under laboratory conditions that although an intracarotid contrast injection may cause a reflex bradycardia and mild hypotension, there is an initial 1- to 2-second period of elevated intracarotid pressure, which declines over approximately 2 to 10 seconds. Doppler sonography confirms a biphasic pattern of middle cerebral artery flow velocity during angiography (76). In the setting of an aneurysm with a recently perforated wall secured only by fresh clot and hematoma, power injections of standard rates accompanied by an increase in intravascular pressure at the level of the circle of Willis could be responsible for inducing rehemorrhage.

Koenig et al. (77) reported on 10 cases of aneurysmal rupture during angiography and reviewed the literature. They observed a 100% mortality rate in their patients and thought that this high rate (in excess of the 41% to 46% mortality observed with aneurysmal rerupture under other circumstances) was, at least in part, related to extravasation of hyperosmolar contrast around and into the brain. Moreover, they advised that consideration be given to a reduction in contrast injection rates to about 4 mL/s in patients with recent subarachnoid hemorrhage. In the setting of vasospasm or elevated intracranial pressure, such a rate should

give adequate arterial opacification and reduce the risk to the fragile aneurysm. Komiyama et al. (69) conducted an extensive review and found a rate of 79% mortality associated with aneurysmal rupture during angiography. This complication occurred in approximately 3% of all patients referred for angiography because of acute subarachnoid hemorrhage. Particular features of this group of patients were that most such angiographic bleeds occurred on day 0 after the initial subarachnoid hemorrhage and were more likely to be observed when cerebral angiography was undertaken within 6 hours of the initial bleed. Teal et al. (78) have commented that a test injection by hand can occasionally be more provocative to a constrained vascular tree than injections made with the power injector, indicating that extreme caution should be exercised regardless of the mode of injection. One of the cases reported by Koenig et al. (77) ruptured in this manner during a hand injection. Saitoh et al. (75) reported a rerupture rate for aneurysms of approximately 5% during angiography done within 6 hours of the initial bleed.

An intraprocedural rupture may not always be seen on the angiographic images (Fig. 5-11). The only warning may be changes in the patient's vital signs, subjective complaints, and deterioration in neurologic status, which should be monitored after each angiographic run. With more extreme extravasation, subtle persistence of contrast on the images or frank opacification of the subarachnoid space and ventricles may occur. With a sudden increase in intracranial pressure, diminished runoff of contrast in the internal

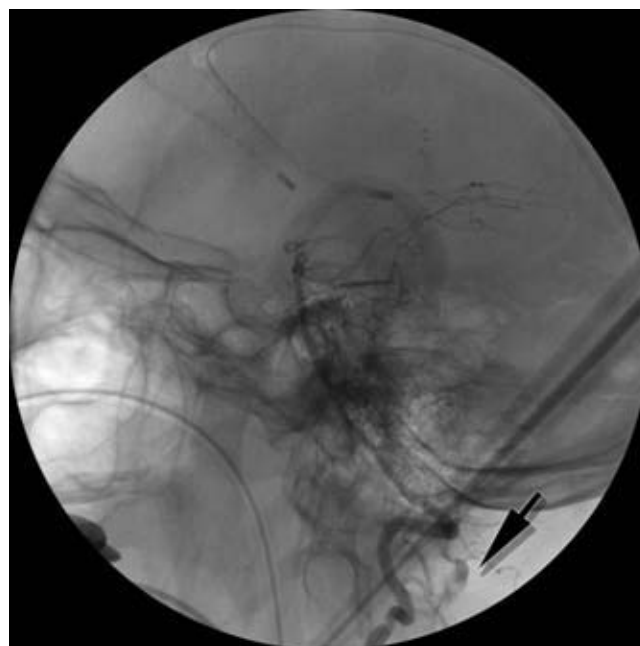


FIGURE 5-11. Aneurysm rupture during angiography. A substantial contrast extravasation during angiography of a cerebral aneurysm is easy to recognize. However, the leakage from the aneurysm can be more difficult to recognize when the degree of extravasation is less, although the consequences are just as serious to the patient's intracranial pressure. In this patient with two ventricular drains placed, an aneurysm arises from a complex duplicated origin of the left posterior inferior cerebellar artery, one limb of which derives from the C2 level of the left vertebral artery. The subtracted images gave no indication of extravasation, but there was fresh blood draining from the ventriculostomy catheter. The nonsubtracted image here demonstrates the unequivocal accumulation of intradural contrast in the CSF space (arrow) at the C1 to C2 space.

carotid artery may be seen. When stagnation of contrast in the internal carotid artery is seen, one may first think of an occluding embolus, but sudden sustained elevation of intracranial pressure can cause similar stagnation and poor runoff of contrast. Severe bradycardia or diminished cardiac output can give a similar fluoroscopic appearance. Nornes (79) reported data on the changes in internal carotid artery blood flow and pressure associated with intraoperative aneurysmal rupture. There is an initial increase in flow proportional to the amount of leakage from the aneurysm, followed by a marked reduction in flow with end-diastolic flow arrest or diastolic flow reversal. Angiographically, this pressure flux has been seen with intraprocedural aneurysm rupture as a diminished or stagnant runoff of contrast from the internal carotid artery.

Similar concerns for the status of the aneurysm and the potential for rebleeding should prompt concern about fluctuations in systemic blood pressure during intubation of the patient. This may occur if general anesthesia is being induced for an endovascular procedure or if patient agitation requires general anesthesia.

Nonneurologic Complications of Cerebral Angiography

Nonneurologic complications include, foremost, hematoma formation at the arterial puncture site. The risk of a significant hematoma is reported as high as 10.7% for femoral puncture sites depending on sheath size and use of heparinization (26,28). Higher hematoma rates for carotid and axillary/brachial sites have been reported at 25.3% and 15.7%, respectively (26), although Kerber et al. (80) reported a hematoma rate of only 6% for axillary puncture sites and a 1% complication rate of axillary artery thrombosis. Local complications during and after transbrachial punctures using a 4F catheter have been reported ranging from 2.1% to 44% (81,82). Either way, the pulse is more difficult to control in the axillary and brachial areas during compression, and these sites are more likely to be problematic than the femoral.

The risk of hematoma formation is probably influenced by a number of factors including increased age of the patient, cooperation of the patient, size of sheath or catheter used, and the presence of atherosclerotic disease. Thomson (13) found that almost all puncture-site hematomata occurred in patients older than age 60. Dion et al. (28) reported that patients older than age 70 had a hematoma rate of 18% after transfemoral cerebral angiography, of whom one third needed fluid replacement or surgical repair.

Femoral artery pseudoaneurysms are rare according to published literature with an incidence of approximately 0.05% to 0.55% (82) but with the increasingly routine use of antiplatelet agents and heparinization during and following endovascular procedures, the risk of bleeding from the femoral puncture site is likely augmented accordingly. In the event of an iliac artery dissection during an angiographic study—during the subsequent management, if possible—an angiographic image of the dissection should be obtained and pull-down pressures above and below the dissection should be recorded.

Other nonneurologic complications of cerebral angiography with an incidence of less than 1% to 2% (26,28),

but which constitute serious problems, include myocardial infarction, cardiac arrest, angina pectoris, and allergic reactions. Minor complications include nausea or vomiting, benign bradycardia or extrasystoles, fainting, paresthesia in the leg due to nerve infiltration with local anesthetic, or delayed hematoma formation after discharge home.

► PREMEDICATION FOR CONTRAST REACTION

With a patient for whom the possibility of complications such as an allergic reaction requires special consideration, extra precautions are necessary. These include more specific discussion of the risks with the patient. Additionally, premedication with corticosteroids and diphenhydramine in patients with histories of previous allergic reaction is required (83–85).

Patients with a previous episode of anaphylactoid reaction to contrast have a risk of approximately 17% to 35% of a similar reaction on subsequent re-exposure (86–88). Yocum et al. (83) found that a high-risk group of patients, so categorized on the basis of previous contrast reaction, had an 18.3% incidence of repeat reaction with intravenous or intra-arterial administration of contrast. Prior administration of diphenhydramine 50 mg intravenously (IV) reduced the rate of minor reactions in that study to 4.2%. Using a pretreatment regimen of prednisone 50 mg by mouth (PO) every 6 hours for three doses ending 1 hour before the procedure and diphenhydramine 50 mg intramuscularly (IM) 1 hour before the procedure, Greenberger et al. (84,89) demonstrated a 0.3% rate of severe reaction in a high-risk group of patients. The incidence of mild reactions was reduced to 7.1%. For emergency patients, with whom a delay in the study for extended premedication is not possible, the authors recommended hydrocortisone 200 mg IV stat and repeated every 4 hours during the procedure. Lasser et al. (85,90) found that pretreatment with methylprednisolone 32 mg PO during the 24 hours before an angiogram and repeated 2 hours before the procedure resulted in a detectable reduction in rates of adverse reaction in all patients. For high-risk patients, advance notification of the anesthesiology staff before the case gets started is good to ensure that assistance will be promptly available if airway problems develop. For these patients, the case should not get under way without having one or preferably two large-bore IV access sites established.

► HYDRATION AND DIABETIC PATIENTS

Adequate hydration of all patients, particularly those with borderline or established renal impairment, is important in the hours before the procedure when the patient is being kept NPO (no food or liquid by mouth). An IV line running at 80 to 120 mL per hour will prevent the patient from becoming dehydrated during the period of waiting.

Diabetic patients on NPO status will require modification of their insulin dose. Usually, elimination of their short-acting insulin dose and administration of half of their longer-acting dose on the morning of the procedure will suffice, with a sliding scale for the remainder of the day after the procedure. Type II diabetic patients should be questioned carefully about metformin (91).

► CONTRAST-INDUCED NEPHROPATHY

Acute contrast-induced renal injury is defined as a rise in serum creatinine of >25% above baseline or a rise of 0.5 mg/dL within 48 hours of a contrast-based procedure. It is primarily a condition of patients with a baseline creatinine clearance <47 mL/min (92), diabetic patients, congestive cardiac failure, advanced age, and pre-existent chronic renal impairment. The occurrence of contrast-induced renal injury is a marker for significantly increased in-hospital mortality, 22% compared with 1.5% in nonaffected patients, and the occurrence of contrast-induced dialysis is associated with an in-hospital mortality rate of 35% and shortened survival post discharge. Contrast-induced nephropathy accounts for as much as 10% of hospital-acquired renal failure and may be seen in as many as 14.5% of coronary catheterization patients, in up to 40% of diabetic patients undergoing angiography, or in even higher proportions in patients with established severe renal impairment (92,93). However, the episode itself is usually transient and requires long-term dialysis in less than 1% of cases. It is thought that generation of free radicals in the acidic milieu of the renal tubules accounts for the acute injury.

Identifying patients at risk for contrast-induced nephropathy in advance of a procedure is not always easy in that the serum creatinine cannot necessarily be relied on as a screening tool. Older patients with low muscle mass can have a serum creatinine level well within the normal range but at the same time have a markedly reduced creatinine clearance level (Tables 5-2 and 5-3).

The mainstays of patient management in the prevention of contrast-induced renal failure are:

- Prescreening and identification of at-risk patients. Diabetic patients, and particularly those with an estimated glomerular filtration rate (GFR) <60 mL/min, will need to discontinue using metformin for at least 48 hours following a procedure (95,96).
- Adequate hydration in preparation for the procedure, particularly the use of a bicarbonate infusion protocol, discussed below.
- Premedication with *N*-acetylcysteine.
- Use of nonionic contrast agents, particularly iodixanol (97). The validity or necessity of using iso-osmolar iodixanol compared with other low-osmolar agents is

TABLE 5-2 Cockcroft–Gault Formula for Creatinine Clearance in Adult Males

For female patients, subtract 15%.

If you are facile with a calculator and eager to impress your colleagues, you can calculate the creatinine clearance using the Cockcroft–Gault formula (94).

$$\text{Clearance Cr mL/min} = \frac{(140 - \text{age}) \times (\text{wt kg})}{72 \times \text{Serum creatinine mg/dL}}$$

Alternatively, and more reliably, you can just look up the glomerular filtration rate (GFR), corrected for age and race, as calculated by your chemistry laboratory included with the basic serum chemistry panel.

TABLE 5-3 Bicarbonate Protocol for Prevention of Contrast Nephropathy in Patients with Elevated Serum Creatinine

This procedure is much simpler than it would seem at first glance.

- Use three vials of NaHCO₃ (150 mEq) to replace a similar volume from a liter bag of D5, making a solution of 4.23% dextrose and bicarbonate.
- Give an initial intravenous infusion of 3 mL/kg per hour for 1 hr prior to the procedure.
- During the procedure, continue the infusion of the same solution at a rate of 1 mL/kg per hour and for 6 hr after the procedure.
- For the initial and subsequent infusion, a maximum weight of 110 kg is assumed.

uncertain. A meta-analysis of trials suggests that use of iodixanol can reduce the likelihood of acute renal injury from 3.5% to 1.4% in an at-risk patient, or by even more in higher-risk groups (98). Use of iodixanol has therefore become standard procedure in recent trials of strategies to attenuate the effects of contrast on renal function (99), but many recent studies on this issue also report a failure to detect a significant effect (100–103).

- In higher-risk patients with glomerular filtration rates <30 mL/min, additional use of furosemide may become standard practice according to recent studies (99).

***N*-Acetylcysteine (Mucomyst)**

N-acetylcysteine is a thiol antioxidant known to attenuate the impact of ischemic renal injury in animals. Several studies have demonstrated that in patients with mild to moderate degrees of renal impairment, premedication with oral *N*-acetylcysteine 600 mg PO twice daily the day before and the day of the procedure, in association with hydration with saline, significantly reduces the risk of adversely affecting renal function (104–106). While some randomized trials failed to demonstrate a significant benefit from *N*-acetylcysteine (107–109), a recent meta-analysis of trials evaluating the combination of *N*-acetylcysteine with bicarbonate infusion (110) has concluded that this stratagem reduces the likelihood of acute contrast-induced renal injury by 35%, although it does not seem to affect the rate of contrast-induced need for dialysis. Part of the controversy may be related to an inadvertent effect on serum creatinine levels by the introduction of *N*-acetylcysteine, independent of any putative reno-protective effect. Therefore, recent studies have incorporated an assay of cystatin C as an additional arbiter of renal status, with a broad consensus now accepting the beneficial effects of combining *N*-acetylcysteine and bicarbonate in preventing renal injury (99,111–113).

Sodium Bicarbonate

Because free radical generation is suppressed when the tubular pH is increased to the basic range, a loading infusion of bicarbonate has been proposed as a method of reducing contrast-induced nephropathy with encouraging results. Merten et al. (111) demonstrated a reduction of rates of

contrast-induced nephropathy from 13.6% in randomized patients receiving saline hydration alone to 1.7% in patients receiving a bicarbonate infusion (see Table 5-3).

Postprocedural Patient Care

Patients should leave the angiography suite with a preliminary chart or computer note indicating the procedure performed, technique used, and relevant clinical findings. There should also be a lucid set of orders for patient immobilization, groin and pulse precautions, and intravenous fluids to continue over the following 4 to 8 hours. Contingency orders for changes in neurologic status or other complications should include a telephone number at which the nurse taking care of the patient can contact the radiology team and/or referral physician. Most of the problems that arise in this time are minor. They include mild headache, hypotension from the effects of medication and prolonged fasting, or groin bleeding problems due to failure of the patient to comply with instructions. Many of these can be avoided with intravenous hydration or as-needed (PRN) medication orders for headache, nausea, vomiting, and the like as a routine component of the postangiogram paperwork.

Outpatients who are being discharged home on the same day should be given explicit instructions, as should their family members, on groin care after they return home. It is a good idea to demonstrate to them where and how exactly to compress the groin site in the event of rebleeding. Advice to recline in the car seat, to avoid strenuous activity for 24 hours, and on proper care of the groin puncture site are all routinely included with these instructions.

References

- Kohn L, Corrigan JM, Donaldson MS. *To Err is Human: Building A Safer Health Care System*. Washington, DC: National Academy Press; 1999.
- Commission J. Universal protocol for preventing wrong site, wrong procedure, wrong person surgery. 2003; http://www.jointcommission.org/standards_information/up.aspx
- Organization WH. Guidelines for safe surgery 2009. 2009; <http://www.who.int/patientsafety/en>
- Sexton JB, Makary MA, Tersigni AR, et al. Teamwork in the operating room: Frontline perspectives among hospitals and operating room personnel. *Anesthesiology* 2006;105(5):877–884.
- Wolf FA, Way LW, Stewart L. The efficacy of medical team training: Improved team performance and decreased operating room delays: A detailed analysis of 4863 cases. *Ann Surg* 2010;252(3):477–483; discussion 483–475.
- Sexton JB, Thomas EJ, Helmreich RL. Error, stress, and teamwork in medicine and aviation: Cross sectional surveys. *BMJ* 2000;320(7237):745–749.
- Awad SS, Fagan SP, Bellows C, et al. Bridging the communication gap in the operating room with medical team training. *Am J Surg* 2005;190(5):770–774.
- Andrus CH, Villasenor EG, Kettelle JB, et al. “To Err Is Human”: Uniformly reporting medical errors and near misses, a naive, costly, and misdirected goal. *J Am Coll Surg* 2003;196(6):911–918.
- Mani RL, Eisenberg RL. Complications of catheter cerebral arteriography: Analysis of 5,000 procedures. III. Assessment of arteries injected, contrast medium used, duration of procedure, and age of patient. *AJR Am J Roentgenol* 1978;131(5): 871–874.
- Mani RL, Eisenberg RL. Complications of catheter cerebral arteriography: Analysis of 5,000 procedures. II. Relation of complication rates to clinical and arteriographic diagnoses. *AJR Am J Roentgenol* 1978;131(5):867–869.
- Mani RL, Eisenberg RL, McDonald EJ Jr., et al. Complications of catheter cerebral arteriography: Analysis of 5,000 procedures. I. Criteria and incidence. *AJR Am J Roentgenol* 1978;131(5):861–865.
- Earnest Ft, Forbes G, Sandok BA, et al. Complications of cerebral angiography: Prospective assessment of risk. *AJR Am J Roentgenol* 1984;142(2):247–253.
- Thomson KR, Thomson SM. Complications of cerebral angiography in a teaching hospital. *Australas Radiol* 1986;30(3): 206–208.
- Hankey GJ, Warlow CP, Molyneux AJ. Complications of cerebral angiography for patients with mild carotid territory ischaemia being considered for carotid endarterectomy. *J Neurol Neurosurg Psychiatry* 1990;53(7):542–548.
- Warnock NG, Gandhi MR, Bergvall U, et al. Complications of intraarterial digital subtraction angiography in patients investigated for cerebral vascular disease. *Br J Radiol* 1993;66(790): 855–858.
- Heiserman JE, Dean BL, Hodak JA, et al. Neurologic complications of cerebral angiography. *AJNR Am J Neuroradiol* 1994;15(8):1401–1407; discussion 1408–1411.
- Study ECfTACA. Endarterectomy for asymptomatic carotid artery stenosis. *JAMA* 1995;273(18):1421–1428.
- Leffers AM, Wagner A. Neurologic complications of cerebral angiography. A retrospective study of complication rate and patient risk factors. *Acta Radiol* 2000;41(3):204–210.
- Dawkins AA, Evans AL, Wattam J, et al. Complications of cerebral angiography: A prospective analysis of 2,924 consecutive procedures. *Neuroradiology* 2007;49(9):753–759.
- Fifi JT, Meyers PM, Lavine SD, et al. Complications of modern diagnostic cerebral angiography in an academic medical center. *J Vasc Interv Radiol* 2009;20(4):442–447.
- Thiex R, Norbash AM, Frerichs KU. The safety of dedicated-team catheter-based diagnostic cerebral angiography in the era of advanced noninvasive imaging. *AJNR Am J Neuroradiol* 2010;31(2):230–234.
- Willinsky RA, Taylor SM, TerBrugge K, et al. Neurologic complications of cerebral angiography: Prospective analysis of 2,899 procedures and review of the literature. *Radiology* 2003;227(2):522–528.
- Burger IM, Murphy KJ, Jordan LC, et al. Safety of cerebral digital subtraction angiography in children: Complication rate analysis in 241 consecutive diagnostic angiograms. *Stroke* 2006;37(10):2535–2539.
- Wolfe TJ, Hussain SI, Lynch JR, et al. Pediatric cerebral angiography: Analysis of utilization and findings. *Pediatr Neurol* 2009;40(2):98–101.
- Faught E, Trader SD, Hanna GR. Cerebral complications of angiography for transient ischemia and stroke: Prediction of risk. *Neurology* 1979;29(1):4–15.
- Olivecrona H. Complications of cerebral angiography. *Neuroradiology* 1977;14(4):175–181.
- Baum S, Stein GN, Kuroda KK. Complications of “no arteriography.” *Radiology* 1966;86(5):835–838.
- Dion JE, Gates PC, Fox AJ, et al. Clinical events following neuroangiography: A prospective study. *Stroke* 1987;18(6):997–1004.
- McIvor J, Steiner TJ, Perkin GD, et al. Neurological morbidity of arch and carotid arteriography in cerebrovascular disease. The influence of contrast medium and radiologist. *Br J Radiol* 1987;60(710):117–122.
- Gabrielsen T. Commentary: Neurological complications of cerebral angiography. *AJNR Am J Neuroradiol* 1994;15:1408–1411.
- Connors JJ 3rd, Sacks D, Furlan AJ, et al. Training, competency, and credentialing standards for diagnostic cervicocerebral angiography, carotid stenting, and cerebrovascular intervention. *AJNR Am J Neuroradiol* 2004;25(10):1732–1741.

32. Andresen R, Roth M, Brinckmann W. Outpatient primary stent-angioplasty in symptomatic internal carotid artery stenoses. *Zentralbl Chir* 2003;128(9):703–708.
33. Shaw PJ, Bates D, Cartlidge NE, et al. Early intellectual dysfunction following coronary bypass surgery. *Q J Med* 1986;58(225):59–68.
34. Sotaniemi KA, Mononen H, Hokkanen TE. Long-term cerebral outcome after open-heart surgery. A five-year neuropsychological follow-up study. *Stroke* 1986;17(3):410–416.
35. Smith PL, Treasure T, Newman SP, et al. Cerebral consequences of cardiopulmonary bypass. *Lancet* 1986;1(8485):823–825.
36. Moody DM, Bell MA, Challa VR, et al. Brain microemboli during cardiac surgery or aortography. *Ann Neurol* 1990;28(4):477–486.
37. Helps SC, Meyer-Witting M, Reilly PL, et al. Increasing doses of intracarotid air and cerebral blood flow in rabbits. *Stroke* 1990;21(9):1340–1345.
38. Greer HD, Massey EW. Neurologic injury from undersea diving. *Neurol Clin* 1992;10(4):1031–1045.
39. Warren LP Jr., Djang WT, Moon RE, et al. Neuroimaging of scuba diving injuries to the CNS. *AJR Am J Roentgenol* 1988;151(5):1003–1008.
40. Voorhies RM, Fraser RA. Cerebral air embolism occurring at angiography and diagnosed by computerized tomography. Case report. *J Neurosurg* 1984;60(1):177–178.
41. Pugsley W, Klinger L, Paschalis C, et al. The impact of microemboli during cardiopulmonary bypass on neuropsychological functioning. *Stroke* 1994;25(7):1393–1399.
42. Markus H, Loh A, Israel D, et al. Microscopic air embolism during cerebral angiography and strategies for its avoidance. *Lancet* 1993;341(8848):784–787.
43. Markus H, Loh A, Brown MM. Computerized detection of cerebral emboli and discrimination from artifact using Doppler ultrasound. *Stroke* 1993;24(11):1667–1672.
44. Bendszus M, Koltzenburg M, Bartsch AJ, et al. Heparin and air filters reduce embolic events caused by intra-arterial cerebral angiography: A prospective, randomized trial. *Circulation* 2004;110(15):2210–2215.
45. Jaeger HJ MK, Hauth E, Drescher R, et al. Cerebral ischemia detected with diffusion-weighted MR imaging after stent implantation in the carotid artery. *AJNR Am J Neuroradiol* 2002;23(2):200–207.
46. Jaeger HJ MK, Drescher R, Hauth E, et al. Diffusion-weighted MR imaging after angioplasty or angioplasty plus stenting of arteries supplying the brain. *AJNR Am J Neuroradiol* 2001;22(7):1251–1259.
47. Soeda A, Sakai N, Murao K, et al. Thromboembolic events associated with Guglielmi detachable coil embolization with use of diffusion-weighted MR imaging. Part II. Detection of the microemboli proximal to cerebral aneurysm. *AJNR Am J Neuroradiol* 2003;24(10):2035–2038.
48. Dagirmanjian A, Davis DA, Rothfus WE, et al. Silent cerebral microemboli occurring during carotid angiography: Frequency as determined with Doppler sonography. *AJR Am J Roentgenol* 1993;161(5):1037–1040.
49. Britt PM, Heiserman JE, Snider RM, et al. Incidence of postangiographic abnormalities revealed by diffusion-weighted MR imaging. *AJNR Am J Neuroradiol* 2000;21(1):55–59.
50. Dagirmanjian A DD, Rothfus WE, Goldberg AL, et al. Detection of clinically silent intracranial emboli ipsilateral to internal carotid occlusions during cerebral angiography. *AJR Am J Roentgenol* 2000;174(2):367–369.
51. Kato K, Tomura N, Takahashi S, et al. Ischemic lesions related to cerebral angiography: Evaluation by diffusion weighted MR imaging. *Neuroradiology* 2003;45(1):39–43.
52. Bendszus M, Koltzenburg M, Burger R, et al. Silent embolism in diagnostic cerebral angiography and neurointerventional procedures: A prospective study. *Lancet* 1999;354(9190):1594–1597.
53. Crawley F, Stygall J, Lunn S, et al. Comparison of microembolism detected by transcranial Doppler and neuropsychological sequelae of carotid surgery and percutaneous transluminal angioplasty. *Stroke* 2000;31(6):1329–1334.
54. Studdard WE, Davis DO, Young SW. Cortical blindness after cerebral angiography. Case report. *J Neurosurg* 1981;54(2):240–244.
55. Komiyama M, Yasui T, Izumi T. Transient involuntary movement of the leg (monoballismus) during cerebral angiography. *AJNR Am J Neuroradiol* 1995;16(9):1942–1945.
56. Matsuoaka A, Shitara T, Okamoto M, et al. Transient deafness with iopamidol following angiography. *Acta Otolaryngol Suppl* 1994;514:78–80.
57. Wales LR, Nov AA. Transient global amnesia: Complication of cerebral angiography. *AJNR Am J Neuroradiol* 1981;2(3):275–277.
58. Pexman JH, Coates RK. Amnesia after femorocerebral angiography. *AJNR Am J Neuroradiol* 1983;4(4):979–983.
59. Akhtar N, Khatri IA, Naseer A, et al. Transient cortical blindness after coronary angiography: A case report and literature review. *J Pak Med Assoc* 2011;61(3):295–297.
60. Mentzel HJ, Blume J, Malich A, et al. Cortical blindness after contrast-enhanced CT: Complication in a patient with diabetes insipidus. *AJNR Am J Neuroradiol* 2003;24(6):1114–1116.
61. Merchut MP, Richie B. Transient visuospatial disorder from angiographic contrast. *Arch Neurol* 2002;59(5):851–854.
62. Newman CB, Schusse C, Hu YC, et al. Acute transient cortical blindness due to seizure following cerebral angiography. *World Neurosurg* 2011;75(1):83–86.
63. Niimi Y, Kupersmith MJ, Ahmad S, et al. Cortical blindness, transient and otherwise, associated with detachable coil embolization of intracranial aneurysms. *AJNR Am J Neuroradiol* 2008;29(3):603–607.
64. Till V, Koprivsek K, Stojanovic S, et al. Transient cortical blindness following vertebral angiography in a young adult with cerebellar haemangioblastoma. *Pediatr Radiol* 2009;39(11):1223–1226.
65. Vallabhaneni R, Jim J, Derdeyn CP, et al. Transient cortical blindness after thoracic endovascular aneurysm repair. *J Vasc Surg* 2011;53(5):1405–1408.
66. Juni J, Morera J, Lainez JM, et al. Transient global amnesia after cerebral angiography with iohexol. *Neuroradiology* 1992;34(2):141–143.
67. Jackson A, Stewart G, Wood A, et al. Transient global amnesia and cortical blindness after vertebral angiography: Further evidence for the role of arterial spasm. *AJNR Am J Neuroradiol* 1995;16(4 suppl):955–959.
68. Giang DW, Kido DK. Transient global amnesia associated with cerebral angiography performed with use of iopamidol. *Radiology* 1989;172(1):195–196.
69. Komiyama M, Tamura K, Nagata Y, et al. Aneurysmal rupture during angiography. *Neurosurgery* 1993;33(5):798–803.
70. Bakay L, Sweet WH. Cervical and intracranial intra-arterial pressures with and without vascular occlusion. *Surg Gynecol Obstet* 1952;95(1):67–75.
71. Greitz T. A radiologic study of the brain circulation by rapid serial angiography of the carotid artery. *Acta Radiol* 1956;46(suppl 140):1–123.
72. Lin JP, Kricheff, II, Chase NE. Blood pressure changes during retrograde brachial angiography. *Radiology* 1964;83:640–646.
73. Hayakawa K, Okuno Y, Miyazawa T, et al. The decrease of intracarotid pressure during carotid angiography. *Invest Radiol* 1994;29(suppl 2):S96–S98.
74. Saitoh H, Hayakawa K, Nishimura K, et al. Intracarotid blood pressure changes during contrast medium injection. *AJNR Am J Neuroradiol* 1996;17(1):51–54.

75. Saitoh H, Hayakawa K, Nishimura K, et al. Rerupture of cerebral aneurysms during angiography. *AJNR Am J Neuro-radiol* 1995;16(3):539–542.
76. Nornes H, Sorteberg W, Nakstad P, et al. Haemodynamic aspects of clinical cerebral angiography. Concurrent two vessel monitoring using transcranial Doppler ultrasound. *Acta Neurochir (Wien)* 1990;105(3-4):89–97.
77. Koenig GH, Marshall WH Jr., Poole GJ, et al. Rupture of intracranial aneurysms during cerebral angiography: Report of ten cases and review of the literature. *Neurosurgery* 1979;5(3): 314–324.
78. Teal JS, Wade PJ, Bergeron RT, et al. Ventricular opacification during carotid angiography secondary to rupture of intracranial aneurysm. Case report. *Radiology* 1973;106(3): 581–583.
79. Nornes H. Cerebral arterial flow dynamics during aneurysm haemorrhage. *Acta Neurochir (Wien)* 1978;41(1–3):39–48.
80. Kerber C, Mani RL, Bank WO, et al. Selective cerebral angiography through the axillary artery. *Neuroradiology* 1975; 10(3):131–135.
81. Millward SF. Routine transbrachial angiography. *Radiology* 1989;172(2):577.
82. Coley BD, Roberts AC, Fellmeth BD, et al. Postangiographic femoral artery pseudoaneurysms: Further experience with US-guided compression repair. *Radiology* 1995;194(2):307–311.
83. Yocum MW, Heller AM, Abels RI. Efficacy of intravenous pretesting and antihistamine prophylaxis in radiocontrast media-sensitive patients. *J Allergy Clin Immunol* 1978;62(5): 309–313.
84. Greenberger PA, Patterson R, Simon R, et al. Pretreatment of high-risk patients requiring radiographic contrast media studies. *J Allergy Clin Immunol* 1981;67(3):185–187.
85. Lasser EC, Berry CC, Mishkin MM, et al. Pretreatment with corticosteroids to prevent adverse reactions to nonionic contrast media. *AJR Am J Roentgenol* 1994;162(3):523–526.
86. Witten DM, Hirsch FD, Hartman GW. Acute reactions to urographic contrast medium: Incidence, clinical characteristics and relationship to history of hypersensitivity states. *Am J Roentgenol Radium Ther Nucl Med* 1973;119(4):832–840.
87. Shehadi WH. Adverse reactions to intravascularly administered contrast media. A comprehensive study based on a prospective survey. *Am J Roentgenol Radium Ther Nucl Med* 1975;124(1):145–152.
88. Fischer HW, Doust VL. An evaluation of pretesting in the problem of serious and fatal reactions to excretory urography. *Radiology* 1972;103(3):497–501.
89. Greenberger P, Patterson R, Kelly J, et al. Administration of radiographic contrast media in high-risk patients. *Invest Radiol* 1980;15(6 suppl):S40–S43.
90. Lasser EC, Lyon SG, Berry CC. Reports on contrast media reactions: Analysis of data from reports to the U.S. Food and Drug Administration. *Radiology* 1997;203(3):605–610.
91. Dachman AH. New contraindication to intravascular iodinated contrast material. *Radiology* 1995;197(2):545.
92. McCullough PA, Wolyn R, Rocher LL, et al. Acute renal failure after coronary intervention: Incidence, risk factors, and relationship to mortality. *Am J Med* 1997;103(5):368–375.
93. Briguori C, Tavano D, Colombo A. Contrast agent-associated nephrotoxicity. *Prog Cardiovasc Dis* 2003;45(6):493–503.
94. Cockcroft DW, Gault MH. Prediction of creatinine clearance from serum creatinine. *Nephron* 1976;16(1):31–41.
95. Stacul F, van der Molen AJ, Reimer P, et al. Contrast induced nephropathy: Updated ESUR Contrast Media Safety Committee guidelines. *Eur Radiol* 2011;21(12):2527–2541.
96. Thomsen HS, Morcos SK, Almen T, et al. Metformin and contrast media. *Radiology* 2010;256(2):672–673; author reply 673.
97. Aspelin P, Aubry P, Fransson SG, et al. Nephrotoxic effects in high-risk patients undergoing angiography. *N Engl J Med* 2003;348(6):491–499.
98. McCullough PA, Bertrand ME, Brinker JA, et al. A meta-analysis of the renal safety of isosmolar iodixanol compared with low-osmolar contrast media. *J Am Coll Cardiol* 2006;48(4): 692–699.
99. Briguori C, Visconti G, Focaccio A, et al. Renal Insufficiency After Contrast Media Administration Trial II (REMEDIAL II): RenalGuard System in high-risk patients for contrast-induced acute kidney injury. *Circulation* 2011;124(11):1260–1269.
100. Reed MC, Moscucci M, Smith DE, et al. The relative renal safety of iodixanol and low-osmolar contrast media in patients undergoing percutaneous coronary intervention. Insights from Blue Cross Blue Shield of Michigan Cardiovascular Consortium (BMC2). *J Invasive Cardiol* 2010;22(10): 467–472.
101. Shin DH, Choi DJ, Youn TJ, et al. Comparison of contrast-induced nephrotoxicity of iodixanol and iopromide in patients with renal insufficiency undergoing coronary angiography. *Am J Cardiol* 2011;108(2):189–194.
102. Serafin Z, Karolkiewicz M, Gruszka M, et al. High incidence of nephropathy in neurosurgical patients after intra-arterial administration of low-osmolar and iso-osmolar contrast media. *Acta Radiol* 2011;52(4):422–429.
103. Mehran R, Nikolsky E, Kirtane AJ, et al. Ionic low-osmolar versus nonionic iso-osmolar contrast media to obviate worsening nephropathy after angioplasty in chronic renal failure patients: The ICON (Ionic versus non-ionic Contrast to Obviate worsening Nephropathy after angioplasty in chronic renal failure patients) study. *JACC Cardiovasc Interv* 2009;2(5):415–421.
104. Tepel M, van der Giet M, Schwarzfeld C, et al. Prevention of radiographic-contrast-agent-induced reductions in renal function by acetylcysteine. *N Engl J Med* 2000;343(3):180–184.
105. Kay J, Chow WH, Chan TM, et al. Acetylcysteine for prevention of acute deterioration of renal function following elective coronary angiography and intervention: A randomized controlled trial. *JAMA* 2003;289(5):553–558.
106. Birck R, Krzossok S, Markowetz F, et al. Acetylcysteine for prevention of contrast nephropathy: Meta-analysis. *Lancet* 2003;362(9384):598–603.
107. Allaqaband S, Tumuluri R, Malik AM, et al. Prospective randomized study of *N*-acetylcysteine, fenoldopam, and saline for prevention of radiocontrast-induced nephropathy. *Catheter Cardiovasc Interv* 2002;57(3):279–283.
108. Durham JD, Caputo C, Dokko J, et al. A randomized controlled trial of *N*-acetylcysteine to prevent contrast nephropathy in cardiac angiography. *Kidney Int* 2002;62(6):2202–2207.
109. Rashid ST, Salman M, Myint F, et al. Prevention of contrast-induced nephropathy in vascular patients undergoing angiography: A randomized controlled trial of intravenous *N*-acetylcysteine. *J Vasc Surg* 2004;40(6):1136–1141.
110. Brown JR, Block CA, Malenka DJ, et al. Sodium bicarbonate plus *N*-acetylcysteine prophylaxis: A meta-analysis. *JACC Cardiovasc Interv* 2009;2(11):1116–1124.
111. Merten GJ, Burgess WP, Gray LV, et al. Prevention of contrast-induced nephropathy with sodium bicarbonate: A randomized controlled trial. *JAMA* 2004;291(19):2328–2334.
112. Briguori C, Airoldi F, D'Andrea D, et al. Renal Insufficiency Following Contrast Media Administration Trial (REMEDIAL): A randomized comparison of 3 preventive strategies. *Circulation* 2007;115(10):1211–1217.
113. Recio-Mayoral A, Chaparro M, Prado B, et al. The renoprotective effect of hydration with sodium bicarbonate plus *N*-acetylcysteine in patients undergoing emergency percutaneous coronary intervention: The RENO Study. *J Am Coll Cardiol* 2007;49(12):1283–1288.

6

Radiation Risks and Safety

Key Points

- Radiation safety lies in the cultivation of good habits and consistent observation of commonsense precautions.
- The risk from radiation exposure during neurointerventional procedures is probably small, but it is worth noting that trends in regulatory limits for occupational exposure are becoming more stringent.

► WHY THIS CHAPTER IS IMPORTANT

Since earlier editions of this book, two events have come to pass that have greatly enhanced the importance of this particular chapter on radiation exposure and risk. Firstly, flat detector (FD) technology has ushered in a minor revolution in the capabilities of digital angiography and fluoroscopy. Physicians have at their controls many more operator-determined variables in the modulation of beam intensity and of factors governing patient radiation dose than was possible on older image intensifiers. This renders obsolete both the older technology and the literature associated with it, and places greater responsibility in the hands of the physician for dose reduction. Secondly, the proliferation of CT technology as the primary medical screening tool for virtually all medical disorders has resulted in a quantifiable increase in the average calculated annual radiation dose among the American population, and a critical scientific and journalistic reaction to this has taken hold. A substantial body of jeremiad literature in the popular and medical press now exists expressing qualms on the potential long-term impact of what might be termed this benevolent abundance or wanton profligacy, depending on one's point of view. Alarming estimates for rates of cancer in the future being induced by current use of diagnostic radiation have been published in establishment journals, and it behooves us to pay attention (1). So far, the focus of concern by regulatory bodies has been on CT angiography and CT perfusion, but the likelihood is that the future will bring similar scrutiny to the neuroendovascular world.

There are several aspects of this problem to consider:

1. The field of radiation physics and quantification of dose in the diagnostic range is not well understood. Studies show that fewer than 50% of radiologists have an intuitive grasp of the magnitude of dose involved with a chest

x-ray, for instance, while a great majority of nonradiologists have difficulties identifying which imaging studies involve ionizing radiation or not (2).

2. Radiation dose to a patient is difficult to measure directly during a procedure, still more so when the technology involves a biplane room shifting location on the body during the procedure. Therefore we are left with indirect estimates of exposure and dose, built upon measurements of machine output and generic assumptions about factors such as body habitus and table height.
3. The chain of certainty becomes still more attenuated when one attempts to derive a conclusion on the risk extrapolated from uncertain estimates of dose. These data are, perforce, projected into regression models of risk based on epidemiologic data involving dose rates and populations very different from the individual patient in question.

The following chapter can be summarized, with the greatest parsing of language, by saying that at this time the evidence suggests that the radiation risk associated with neuroendovascular procedures is likely small.

► HISTORICAL STUDIES OF THE EFFECTS OF RADIATION

An extensive body of epidemiologic and other evidence demonstrates that radiation exposures far in excess of those used for diagnostic procedures are associated with an increased incidence of delayed malignancy. Other delayed side effects of radiation include growth retardation, cognitive impairment, lenticular opacities, premature atherosclerotic vascular disease, and mental retardation after in utero exposure. These data emerge from studies of populations intentionally or inadvertently exposed to significant doses of radiation. These studies include the following:

- Patients with ankylosing spondylitis treated with x-irradiation
- Patients exposed to Thorotrast
- Children with thymic enlargement or tinea capitis who were treated with high doses of local radiation
- Adults who were treated with high doses of local radiation to the scalp in infancy for cutaneous hemangiomas
- Uranium miners
- Radium dial painters
- Military personnel exposed during weapons testing maneuvers
- Survivors of the Hiroshima and Nagasaki bombings
- Victims of the Chernobyl disaster

From studies of exposed populations, data have been collected to give an estimate of the relationship between high radiation doses and biologic effect, with particular emphasis on carcinogenesis. Various regressions of the dose–risk curve down to radiation levels relevant to diagnostic and interventional neuroangiography can be performed on the basis of certain assumptions. The gravity of the conclusions arising from these extrapolations depends on the assumptions made about the lower end of this curve; some assumptions about the curve suggest a higher risk than do others.

To place the nature of risk from radiation in an understandable context, one must first consider that the number of known fatal malignancies following gamma or x-ray irradiation is small compared with more common fatal diseases. This does not trivialize the serious risks from radiation exposure, but places the risk in a relative context.

Concrete comparisons are probably the best medium to demonstrate that, having been exposed to diagnostic or interventional levels of radiation, a radiation-related malignancy is a highly unlikely prospect. Intuitive bias would probably lead most to believe that among atomic bomb survivors, epidemiologic studies should show a massive number of radiation-related malignancies. In fact, although the relative risks of malignancy are high, the absolute numbers are surprisingly low. It is estimated that an exposure of 1 Gy increases the risk of leukemia by a factor of 5.2 (3). To present the risk in a less alarming manner, one might point out that the average exposure of Japanese survivors has been estimated at 0.25 Gy. Of the Japanese survivors enrolled in the Life Span Study (i.e., approximately one-third of the total number of survivors), 37,800 had died by 1990. When one takes expected rates of cancer into account in a similar nonexposed population, the number of excess cancer deaths related to radiation within this group is approximately 430 (4–6). The number of radiation-related leukemia cases in the same study had reached 290 by 1987 (7). Stated otherwise, approximately 59% of those survivors who died from leukemia and 8% of the survivors who died from other malignancies did so from a radiation-related cancer (3). Some of these victims received whole body doses of up to 5 Gy (500 rad). Recent data on atomic bomb survivors indicate that a detectable risk of leukemia or lymphoma can be found in groups with exposures as low as 0.5 Gy (50 rad) (8). Although the retrospective dosimetry estimates of the gamma and neutron fluxes involved have been revised periodically, doses involved in these studies, even those revised downward, are not remotely approached by diagnostic neuroangiographic procedures.

Similarly, the absolute numbers of cases of radiation-related leukemia and other malignancies are very small in follow-up studies of other exposed populations. All of the studies that attempt to demonstrate a carcinogenic effect from whole body doses of under 0.05 Gy are of a design and size that make them vulnerable to statistical inconsistencies or methodologic oversights (4,9). Studies of human subjects in this dose range with positive findings have, on occasion, demonstrated an increased risk of malignancy in small populations. For instance, a follow-up study in 1983 (10) of the 1957 “Smoky” bomb test site in Nevada demonstrated an almost four times increased incidence of some forms of leukemia in military personnel exposed to an average of 10 mGy (1 rad) whole body dose. There was no evidence

of increased mortality from any other form of cancer. With reference to leukemia, this positive result translates to an extreme risk at variance with the relatively lower observed rates of leukemia in Japanese atomic bomb survivor studies or with risks associated with background radiation (9). Caldwell et al. (10) concluded that “this one positive finding may be either attributable to chance or the result of an unknown combination of factors . . . this conclusion cannot be generalized.” However, the Nevada test site or other similar events have entered media folklore as evidence of the severe risks of radiation exposure (11).

Epidemiologic studies of atomic bomb survivors and other groups exposed to high levels of radiation (>50 rad) have demonstrated a clear relationship between exposure and the subsequent risk of malignancy, particularly leukemia (excluding CLL) and carcinoma of the lung, ovary, thyroid, stomach, and breast (4). Exposure levels below this range, which would be of interest in evaluating possible risks to patients and medical personnel from neuroangiographic procedures, cannot be studied directly because of methodologic difficulties and because of the enormous number of subjects that such a study would require.

► DOSE–RESPONSE CURVE

Using data from populations with known or estimated high-dose exposures, an estimate of risk for low exposures can be performed by a backward regression of the relationship between exposure and outcome. However, this can only be done using assumptions about the lower end of the graph. An extrapolation of the dose–risk curve for radiation exposure below the 100-rad range can be performed in a linear, quadratic, or linear–quadratic manner (Fig. 6-1).

With a linear curve, the risk of malignancy is directly proportional to the exposure. At the lower end of the curve, the number of radiation-related tumors is obscured by the incidence of spontaneous malignancies in a given population. A quadratic curve assumes that the risk is proportional to the square of the dose and gives a curve that increases steeply with increasing doses.

Alternatively, a linear–quadratic curve, in which a linear curve at lower doses gives way to a quadratic curve at higher doses, perhaps in part related to DNA density in mammalian tissue, appears to be a more likely model based on animal studies and on data from atomic bomb survivors. Solid

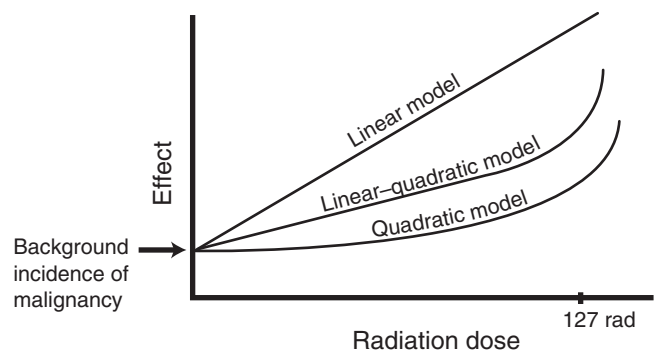


FIGURE 6-1. Dose–response curve. Common mathematical models for induction of radiation-related tumors are represented. At zero exposure, a baseline rate of cancer is still present due to the background rates of disease.

tumors and leukemia have demonstrated different dose–response curves. Furthermore, a different temporal sequence is seen for various tumors after radiation. The excess incidence of leukemia becomes apparent after 2 years and peaks at approximately 6 years, whereas the incidence of solid tumors may not peak until 15 to 20 years after exposure. A linear–quadratic curve is now most favored for describing the likely risk of most forms of carcinogenesis after radiation exposure. The curve inflection point, where it makes a transition from linear to quadratic in form, could be determined by the density of DNA in the genome (12). This means that for mammalian tissue, the curve changes from linear to quadratic at exposures of approximately 127 rad. Below this level, much of the evidence is either disputed or conjectural, and the measure of risk from an exposure of 10 rad or less is still unknown. For instance, in follow-up studies of patients exposed in infancy to radiation for “thymic enlargement”—another historic fiasco, this time visited upon an unsuspecting public in a stalwart effort to stamp out those two scourges of public health, *status lymphaticus* and *laryngospasm* in the setting of normal thymic size variation—the dose–response curve for adult onset of thyroid carcinoma demonstrated a linear regression line (13) even at fairly low doses of thyroid tissue exposure less than 0.3 Gy.

So if the bulk of evidence suggests that low-dose radiation risk is a nonstory, wherefore arises the current climate of apprehension?

One of the pivotal papers drawing attention to the altered landscape of radiation use by Brenner and Hall in 2007 (1) made a simple and clear argument that current patterns of CT use translate into a risk of radiation-induced cancer accounting for 1.5% to 2% of all cancers, up from a baseline of 0.4%. In this paper a linear regression model was assumed on the basis of the analyses of atom bomb survivors and a study of 400,000 nuclear industry workers who were exposed to an average dose of approximately 20 mSv (approximately in the range of a couple of CTA scans (14) and in whom an increased risk of cancer was identified. The paper by Brenner and Hall was criticized by several authors for using a linear regression model, for the paucity of hard evidence of risk of carcinogenesis at doses less than 50 mSv, and for not taking into account the putative phenomenon of *hormesis*. Hormesis is a term to suggest that in response to chronic low levels of radiation, an upregulation occurs in the body’s capacity to deal with free radicals (15). Authors who favor this term invoke it as an argument for a level of impunity to radiation injury, which might, one might facetiously quip, be analogous to saying that one becomes immune to the risk of melanoma by cultivating a deeply bronzed suntan. Evidence suggests that interventional cardiologists as compared with noninterventional cardiologists, for instance, demonstrate increased prevalence of somatic mutations and alterations of DNA repair genes, and while this may be offset by the presence of other markers indicating an increased relative capacity to deal with hydroxyl radicals, they were probably healthier when they were younger before they became cardiologists (16–21). Furthermore, the Brenner and Hall paper (1,22) stressed the heightened vulnerability of pediatric patients to the effects of radiation exposure and the fact that for a given examination, due to the thinner torso and

head size of children, local organ radiation doses in children are substantially higher than in adults.

► X-RAY PHYSICS REVIEW

The realm of radiation exposure and its dangers lie outside of the domain of human experience. For instance, it is difficult intuitively to understand that the energy of a cup of warm water if delivered in the form of high-energy radiation over a brief period of time would be highly lethal to one or more adult humans. Furthermore, the units used to measure and express notions of exposure are derivatives of other derivatives and thus confusing. Therefore, a brief review is necessary of the fundamental principles of radiobiology as a preamble to methods and meaning of radiation exposure.

The adverse effects of x-rays on tissue are related to a transfer of energy to the tissue by indirect ionization. With x-rays in the diagnostic range, the two processes involved, which result in ionization, are the *photoelectric effect* and the *Compton effect*. Approximately 5% of x-rays in the diagnostic range undergo *coherent scattering*. This third process is not important for transfer of energy because only a change of direction of the x-ray photon takes place, without a change in energy and without ionization. Coherent scattering contributes a little to image fogging.

In the *photoelectric process*, an incident photon interacts with and loses *all* of its energy to a K, L, or M shell electron, which is then ejected from its orbit. The ejected electron becomes a *photoelectron*. The ejected electron is replaced in its shell by an electron from an outer orbit, which releases *characteristic radiation* as it moves to the inner, more tightly bound position. The probability of a photoelectric interaction between a photon and an atom is proportional to the third power of the atomic number of the atom. A photoelectric interaction is also more likely to occur with a lower-energy photon than it is with a higher-energy beam, provided that the photon energy is greater than the binding energy of the electron. The photoelectric effect is therefore likely to occur with photons in the lower-energy range of a diagnostic beam in tissue that contains atoms with a higher atomic number, such as calcium or iodine. Therefore, photoelectric interactions are good for image quality in that they give a high contrast between soft tissue and bone or between soft tissue and iodinated contrast. However, because the photoelectric effect results in *all* of an incident photon’s energy being deposited in the patient, *the absorbed radiation dose to the patient tends to be higher when the photoelectric effect is dominant*. Therefore, to reduce patient dose, it is desirable to keep the kV setting as high as possible while maintaining adequate image contrast.

In the Compton effect, the incident photon of the x-ray beam loses *part* of its energy to an outer electron, which is ejected from its orbit. The ejected electron is referred to as the *recoil electron*. The x-ray photon continues in a variably deflected direction with a commensurately reduced energy. Compton interactions are responsible for the scatter radiation to operating personnel involved in a fluoroscopy procedure. In the diagnostic range, most of the energy of the incident photon is retained by the photon, and relatively little is transferred to the recoil electron. *The practical implication of this is that scatter radiation emanating from a patient is almost as energetic as the photons of the*

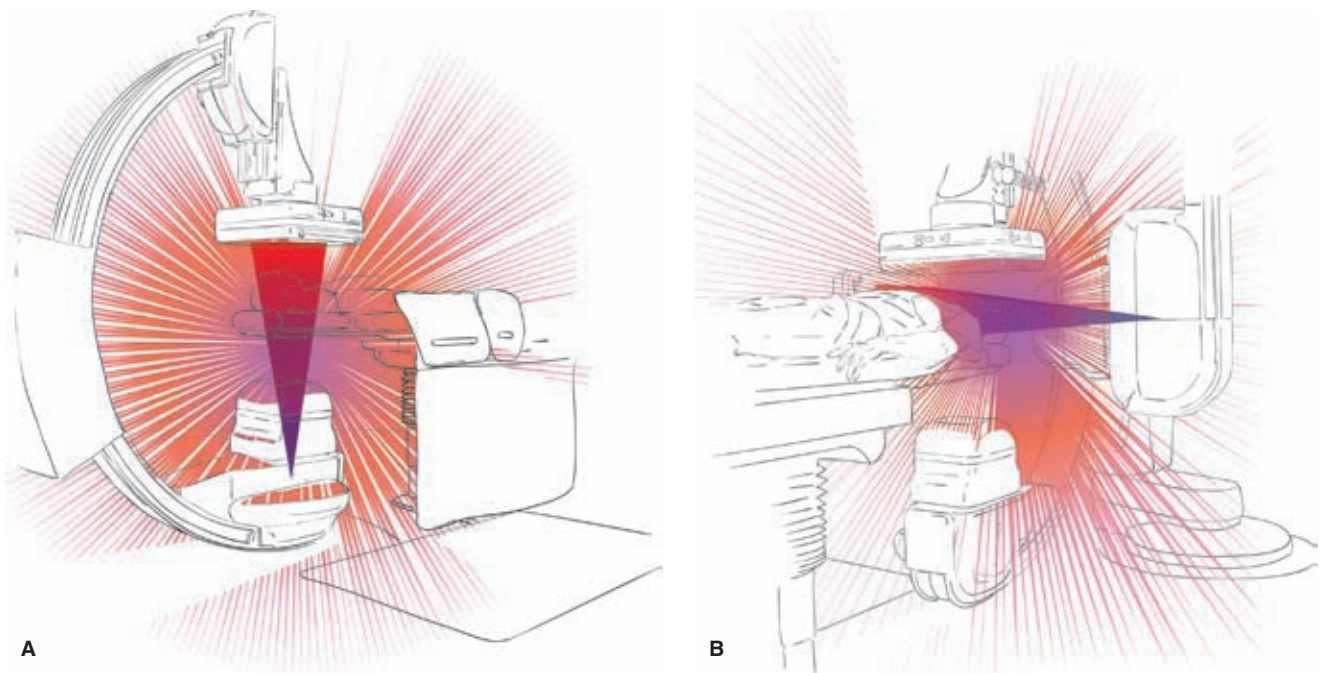


FIGURE 6-2. (A–B) Backscatter is substantial. Colorized cartoon representations of the AP plane beam (A) and the lateral plane (B) show that the backscatter can be envisaged as primarily emanating from the point of impact of the primary beam on the back and left side of the patient's head. In contrast to the tightly confined primary beam, the backscatter is virtually omnidirectional, with the only protection being distance or shielding. Furthermore, the diagrams attempt to convey the need to think of the backscatter as virtually as energetic as the primary beam. Therefore one needs to be courteous and considerate when circulating staff are making adjustments near the patient's head or when the anesthesia team is close to the patient's left side. Their fingers may not be visible on screen but if fluoroscopy is active at those moments, their exposure is almost as high as that of the patient.

primary beam. For instance, a 75-keV photon deflected by 90 degrees has an energy of 66 keV; when deflected by 180 degrees, the energy level is still a considerable 58 keV (23). Therefore, the scatter beam, which can be conceptualized as having its center at the skin-entrance site on the patient, must be taken to represent a potentially serious source of radiation to operating personnel (Fig. 6-2).

The ionizing effect of radiation in the diagnostic range is mediated by the photoelectrons and recoil electrons. They result in the formation of free radicals in tissue, which may then interact with other cellular components, particularly with DNA and RNA.

► STOCHASTIC AND DETERMINISTIC EFFECTS OF RADIATION

The detrimental effects of human radiation exposure are divided into *genetic* (placing future generations at risk—an effect that has been very difficult to confirm in population studies) and *somatic* (affecting the exposed individual). Somatic effects can be broadly classified into those related to the local tissue effects of radiation exposure (epilation, skin erythema, necrosis, retrolenticular opacities, etc.) and carcinogenic effects (see Table 6-1).

The confirmed somatic carcinogenic side effects and the putative genetic effects of radiation probably occur through common pathways involving free radical damage to DNA. The risks of these effects are sometimes termed *stochastic*,

TABLE 6-1 Somatic Deterministic Effects of Radiation (24) Skin Effects After Single-fraction Irradiation

EFFECT	SINGLE DOSE (Gy)	ONSET	PEAK
Early transient erythema	2	hours	~24 h
Temporary epilation	3	~3 wks	
Erythema ± later pigmentation	6	~10 d	~2 wks
Permanent epilation	7	~3 wks	
Dry desquamation	10	~4 wks	~5 wks
Moist desquamation	15	~4 wks	~5 wks
Secondary ulceration	0	>6 wks	
Necrosis	18	>10 wks	
Teleangiectasia	12	>1 yr	
Fibrosis	10		
Lens opacification	1–2	>1 yr	
Skin cancers	5	>4 yrs	

that is, they are best described in terms of probability. Although they are more likely to happen with increasingly higher exposures, the severity of the effect, if it happens, is not dose related. Stochastic effects are considered to be possible at all levels of exposure, that is, they do not have a threshold level. In other words, a radiation-related malignancy is more likely to occur after a higher level of exposure but may occur after a low exposure as well. The net effect to the victim is the same in either instance. A diagnosis of leukemia whether one ascribes it to a Gray or a centiGray of exposure is still leukemia.

Nonstochastic effects, sometimes called *deterministic*, are dose related and affect the exposed tissue. They involve acute or chronic complications such as epilation, ulceration, fibrosis, or lenticular opacities. Usually, they are not seen below a certain critical or threshold level of exposure.

The genetic effects of radiation exposure are probably less significant than the somatic effects. Radiation effects on the genetic material of circulating lymphocytes can be detected with exposures as low as 0.1 Sv. Such changes have been used following the Chernobyl disaster to estimate exposures retrospectively in rescue workers. However, a detectable genetic effect of radiation exposure in subsequent generations after the atomic bombings at Hiroshima and Nagasaki has been elusive. These effects are thought to be small enough to be obscured by the background noise of spontaneous mutational phenomena (4,5,25,26).

Tumor initiation after radiation exposure is the focus of most concern in evaluating the risks of radiation and is probably due to DNA point mutations, base-pair deletions, or translocations. It is not known what factors may place a particular individual at risk for such critical events, but it is known that children are more vulnerable to this effect, as are patients with certain genetic disorders. For instance, patients with some genetic disorders such as xeroderma pigmentosum and ataxia-telangiectasia are more sensitive to the carcinogenic effects of radiation than other members of the general population. Children exposed to fallout contamination after nuclear accidents are more at risk than adults for malignancies such as leukemia and thyroid neoplasia. Children treated with radiation therapy for retinoblastoma also appear to have a higher susceptibility to radiation-induced tumors than do other children or adults treated similarly for other types of tumors.

Promotional effects on tumor genesis may also be important, and these may be independent of radiation exposure. Tumor promotion may involve such factors as the hormonal or dietary status of the patient. For instance, breast tumors after fluoroscopic exposure of the chest in female children are not seen until maturity, indicating that the initiated cell(s) may remain latent until triggered by other stimuli (27–29).

► EXPOSURE QUANTIFICATION AND RADIATION “DOSE”

Quantification of radiation takes into account a number of factors, including the intensity of the source, the nature and energy of the source, and the area or particular organs of the patient exposed to the source. A lexicon of terms exists to describe the units of measurement for these variable factors. The most meaningful of these units is the “effective dose.”

Calculating the effective dose for a radiographic procedure gives a number in standardized units, which allows comparison between different procedures and permits correlation, up to a point, with probability scales from reference data. The following sections explain the somewhat convoluted derivation of the effective dose.

Quantification of Beam Intensity

Beam intensity is quantified by measuring the ionization charge induced by an x-ray beam in a given mass of air. It is a measurement of intensity that is independent of any biologic effects of the beam or of the presence of tissue in the field. Modern angiography suites are equipped with ionization chambers attached to the exit portals of the tubes. They measure the intensity of the exiting beam and give a reading expressed in units of Gray.meter² (or equivalent). By using this reading, called the dose–area product (DAP) or air kerma area product, and by calculating the attenuation of the beam between the ionization chamber and the patient, estimations of patient exposure (estimated skin dose [ESD]) can be reached.

Quantification of Energy Deposition in Tissue (“Dose”)

The “dose” of radiation to a person or a volume of tissue is a concept that can have different meanings. A purely physical notion of what constitutes a dose of radiation is the quantity of energy transferred to the tissue by the beam. Energy absorbed by tissue from an x-ray beam in the diagnostic range is measured in gray (Gy). A Gy is defined as an absorbed dose causing a deposition of 1 joule of energy in each kilogram of absorbing tissue. A Gy is the same as 100 rad.

Quantification of Biologic Responsiveness to Radiation: Dose Equivalence

Units such as the gray deal with purely physical parameters. To approach a more meaningful concept of “dose,” account must be taken of the biologic effects of these measurable physical quantities. A Gy (100 rad) of exposure may have different effects on the tissue substrate in question depending on the nature of the radiation source. To take this variable response into account, it becomes necessary to devise a quantity to measure the biologic equivalence of specified exposures. This explains the acronymic derivation of the unit devised for this purpose, the rem—“roentgen equivalent man.” The international unit now in use for expressing the biologic equivalence of radiation dose is the sievert (Sv).

Estimates of biologic dose equivalence—the “dose equivalent”—represented by sieverts are calculated by multiplying the physical dose (Gy) by a *weighting factor* (W_R).

The weighting factor (W_R) is determined by the type and energy of the radiation source. A relative weighting factor, W_R , is assigned to various radiation types to generate a scale, which reflects the biologic effectiveness of exposure to different sources. Alpha particles have an estimated W_R of 20, and neutrons 10, while photon sources have a W_R of 1. An exposure of 1 Gy from a source with a W_R of 1 gives a dose equivalent of 1 sievert.

When a tissue is exposed to different types of radiation, separate calculations using correspondingly varied values for W_R are conducted for each type of radiation involved.

These numbers are summed to give the total dose equivalent for that tissue.

Partial Body Exposure: Effective Dose Equivalent or Effective Dose (E)

How is risk to the whole person calculated when only part of the body is exposed to the radiation source? It would seem cogent, for instance, that a certain level of partial body irradiation must represent as great a risk of carcinogenesis as would some lower degree of whole body irradiation. Moreover, partial body irradiation involving the thyroid gland is more dangerous than irradiation involving the extremities only.

To generate a calculation based on partial body exposure, the International Commission on Radiological Protection (ICRP) introduced the *effective dose equivalent* (H_E), now termed the *effective dose* (E), which is also measured in sieverts.

Various tissues are assigned weighting factors depending on their respective sensitivities to radiation. For instance, thyroid tissue is assigned a *tissue-weighting factor* (W_T) of 0.04. An equivalent dose to the thyroid of 8 mSv could then be calculated to $8 \text{ mSv} \times 0.04 = 0.32 \text{ mSv}$ effective dose (H_E). In other words, an equivalent dose of 8 mSv confined to the thyroid gland represents the same risk to the individual as if the whole body had received a dose of 0.32 mSv. The most recent revision of recommendations and tissue-weighting factors by the ICRP (30) supersedes those from 1990 (31), and overall downgrades very slightly the risk of radiation-induced carcinogenesis. Some tissue-weighting factors have been altered slightly, for instance W_T for the gonads was revised from 0.2 to 0.08, while for breast tissue it was upgraded from 0.05 to 0.12 (32).

To calculate the entire risk to an individual from a quantified exposure, the effective doses for all the critical organs involved are summed to give a number, the *total effective dose*. This number can be compared with known quantities and risk tables. For instance, the effective annual dose from background radiation exposure is approximately 2.5 to 5.0 mSv, depending on altitude and geologic variables. This is a useful number to remember as a reference point for interpreting the effective dose; it gives one a scale of reference to grapple in a meaningful way with doses involved in medical procedures (Table 6-2; 25,26,33–35).

Limitations to the Application of Effective Dose Values

From a reading of medical papers concerning radiation dose and risk, one might gain an erroneous sense of certainty in using the effective dose as a common international exchange unit in the calculation of stochastic or even deterministic risk. This is a common and somewhat misleading assumption. The notion of E is best understood as a control measure, calculated with reference to a theoretical hermaphroditic model and useful for comparing one imaging technique or modality with another (36). It has therefore no real relevance to female organs or breast tissue, or indeed any real relevance to any particular patient. Its accuracy for a particular patient with confidence boundaries of 70% to 90% is probably a matter of $\pm 40\%$, that is, a wide spread of possibilities (37,38). Its application on a population-wide basis is

TABLE 6-2 Effective Doses of Diagnostic X-ray Examinations and Environmental Background Phenomena

MEDICAL PROCEDURE	EFFECTIVE DOSE (mSv) PER PROCEDURE
Chest x-ray	0.05–0.14
Lumbar spine	1.8
Thoracic spine	1.4
Barium upper gastrointestinal study	3.6
Coronary angiogram (diagnostic)	0.6–23.2 (median 4.6)
Coronary intervention	1–37 (median 6)
Barium enema	6.4
Nuclear medicine scan	5–10
Abdomen CT	8.8
Head CT	1.11–2
ENVIRONMENTAL SOURCE	EFFECTIVE DOSE (mSv) PER YEAR
Radon exposure	2.0
Cosmic radiation	0.27
Long-haul flight personnel	0.2–9.1
Ingested materials in food	0.39
Total average exposure	3.6
Regulatory dose limits for radiation workers	20

also premised on the characteristics innate to the population from which it was first derived, that is, the Japanese survivors. How applicable are those data when one considers that mortality rates and incidence of breast cancer, stomach cancer, and other malignancies in the Japanese population have changed considerably since 1945?

For neuroendovascular procedures, the best estimates of radiation exposure are the ESD and overall tube output during the case measured as dose–area product (DAP) (synonymous with air–kerma area product). The consequences of excessive doses on the ESD axis are outlined in Table 6-1. Estimates of skin dose are based on certain assumptions by the manufacturer and do not take into account factors such as table height or patient size.

The estimates of DAP are a little more difficult to grasp, but they are potentially more useful in understanding the stochastic risk from a procedure. The results are generally given in the form of $\text{Gy}\cdot\text{cm}^2$ or $\mu\text{Gy}\cdot\text{m}^2$. As to what constitutes a significant exposure level on DAP, proposals for a trigger level of 250 or 300 $\text{Gy}\cdot\text{cm}^2$ (30,000 $\mu\text{Gy}\cdot\text{m}^2$) have been proposed

(39,40), but are not yet in general use. As to the rough calculation of the effective dose of a neuroangiographic procedure, not as much progress has been forthcoming on this question as has been seen in the world of CT. Conversion factors for translating DAP into effective dose have been published and used in several papers referenced below (41,42).

► STUDIES OF X-RAY EPILATION FOR TINEA CAPITIS

From among the epidemiologic and follow-up studies of populations exposed to radiation, the most relevant to diagnostic and interventional cerebral angiography are those of children exposed in the 1940s and 1950s for treatment of tinea capitis. In some respects, these studies are the most reassuring about the long-term effects of the radiation involved in neuroangiographic procedures.

Prior to the availability of griseofulvin, treatment for childhood tinea capitis was difficult or unpleasant. Therefore, between 1910 and 1957, scalp irradiation—the Adamson–Kienbock procedure (43,44)—was used extensively to treat this condition. Children typically aged 6 to 8 years were given exposures of 300 to 400 roentgens or more in five overlapping fields to the scalp. The treatment was administered in a single dose over about 20 minutes or in divided sessions over a period of 5 days, to induce hair loss—a sort of thermonuclear buzz cut, one might say. New hair grew after approximately 6 weeks. This form of treatment ended in 1958, by which time an estimated 200,000 children had been so treated worldwide (45,46). The treatment was administered with a 100-kVp unfiltered source. Phantom reconstructions of the treatment methods estimate the skin dose to have been approximately 4.75 Gy, or as high as 6 Gy on the vertex of the scalp where the fields overlapped (47). Other retrospective estimations (48,49) calculated doses to the cranial marrow of 3.85 Gy and brain doses of 0.7 to 1.7 Gy. The thyroid gland received a mean of 0.06 Gy, the pituitary gland 0.5 Gy, and the eye 0.47 Gy (50). However, in contrast to neuroangiographic procedures of current interest, the face and neck were shielded by lead in this treatment. Therefore, the results of the tinea capitis studies cannot be completely transposed onto neuroangiographic techniques.

Follow-up studies of over 2,000 children in the United States (51) and over 10,000 children in Israel (52) have been published periodically since that time. The former study from New York demonstrated higher rates of leukemia in the irradiated group (4 cases vs. 1 in a control group), brain tumors (3 cases), parotid tumors, thyroid tumors, and skin malignancies in the irradiated field. There was also a higher rate of diverse psychiatric diagnoses among the irradiated group, at least in the US study. The Israeli follow-up study (52,53) also demonstrated a slightly higher number of leukemia cases among the irradiated group (7 vs. 5 expected) as well as statistically elevated rates of benign and malignant tumors of the head and neck, meninges, parotid, and thyroid gland. The most recent follow-up study of the treated children identifies a risk of basal cell carcinoma with a relative risk of 0.6 per Gy of exposure, but without much evidence of skin squamous carcinoma or melanoma (53). Though these observations on rates of delayed malignancy in the irradiated group appear to be valid and conform to the paradigm of radiation being a known risk factor for tumor formation, the

incidence rates within this population, nevertheless, appear to be low. The significance of elevated rates of psychiatric diagnosis in the New York cohort is unknown.

The incidence of radiation-related malignancy in these studies is very low, whereas the radiation doses involved were considerably higher than those used during cerebral angiography, at least for diagnostic studies. These studies more than any other offer some solid reassurance that the long-term risk of malignancy from angiographic procedures is vanishingly small, even in children.

Radiation Exposure during Neuroangiographic Procedures

Patient Exposure

The introduction of flat panel technology (Fig. 6-3) has rendered obsolete the analog image intensifier on which was based the previously published body of literature concerning calculation of the effective dose and skin doses to patients during neuroangiographic procedures. Nevertheless, considerable reassurance can be derived from this body of knowledge that the doses on older machines were well within a reasonable range for most patients, and have been likely considerably reduced on newer machines.

In 2006, the Joint Commission for Accreditation of Healthcare Organizations (JCAHO) established a skin dose of 15 Gy delivered over a short period of time to a single area as a “sentinel event.” It is worth emphasizing that most authorities would estimate that a skin dose of this magnitude would cause skin necrosis to a depth of several

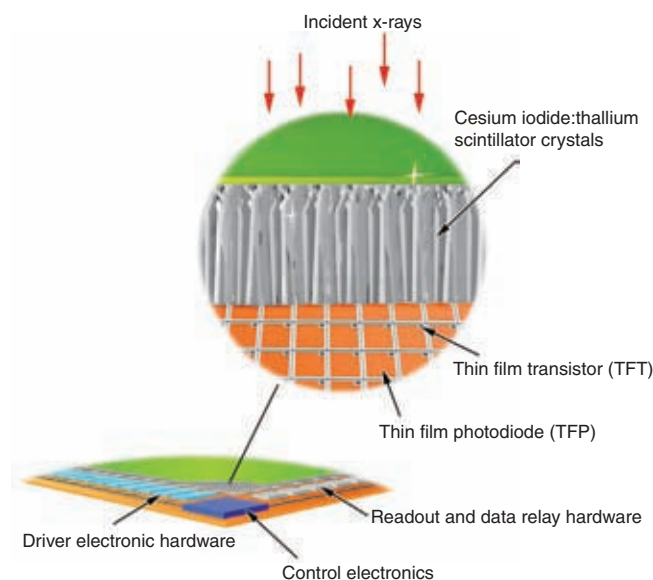


FIGURE 6-3. Flat panel technology. Flat panels eliminate the phenomenon of image intensifier distortion of the peripheral field, analogous to that of a fish-eye photographic lens, which was a problem on older technology particularly when images for gamma knife targeting were in question. In other ways too the technology offers considerable advantages over the older machines including factors such as uniformity of field, machine size, dose manipulation, imaging speed, and so on. It should be emphasized, however, that the savings on radiation dose can be nugatory or even erased if the physician operator does not familiarize himself/herself with the controllable features of the software and does not push the vendor engineers to modulate the default protocols. Based on Cowen (54,55) and Spahn (56).

centimeters (57,58). For routine diagnostic neuroangiography, deterministic effects of radiation in the adult patient are not seen because the total skin-entrance dose usually falls far below the levels where concerns about epilation (2 to 6 Gy) or lens opacification (approximately 0.5 to 2 Gy) might arise (59,60). Therefore, for adult diagnostic studies, the skin-entrance dose is less important than the effective dose because the effects of radiation that warrant consideration lie in the stochastic domain. With reference to pediatric studies, concern for the vulnerability of the skin of younger children to doses easily tolerated in adults means that one cannot dismiss the importance of the ESD so easily as in adults. Furthermore, the validity of the calculations involved with the estimation of skin dose in a pediatric patient is likely less established than in adult patients, re-emphasizing the need to keep pediatric doses to an absolute minimum at all times.

Certain general observations in older studies are still useful. In one of the most comprehensive set of papers on patient dose from interventional procedures (61–63), it was demonstrated that the wide variability of cumulative doses and fluoroscopy times involved with certain procedures means that average numbers or group data can mean very little in the cases of extreme use of fluoroscopy and DSA. Over 20% of brain/head arteriovenous malformations (AVM) and tumor treatment cases resulted in cumulative skin doses of over 5 Gy, while spine tumor treatment and spine AVM treatment cases reached this level of estimated dose in 38% and 60% of cases, respectively.

Studies based on image intensifiers suggest that the effective dose for diagnostic and interventional procedures ranged at the low end of the spectrum around 3.44 mSv (close to the annual background irradiation level in North America) (64), more generally in the range of about 10 to 36 mSv, but ranged as high as 156 mSv (59,65–67). For reference value, a CTA of the head and neck currently involves an estimate of effective dose of approximately 10 mSv in adults. With reference to the current introduction of flat panel equipment with its attendant hope of a reduction in radiation exposures, it is chastening to observe in older studies that the advent of digital imaging did not result in a reduction of patient doses from neuroangiographic procedures compared with the days of cut film. Digital imaging seemed to result in an increase in the number of images obtained, thus leveling or even overwhelming the dose-reduction capabilities of the new technology.

The typical fraction of skin dose and effective dose deriving from fluoroscopy rather than from filming during cerebral angiography varies. It depends on the difficulty of vessel selection and has been estimated at 22% to 67% of the total exposure (59,65,67). However, the proportionate measurement does not mean very much unless the size of the denominator is taken into account. If you opt to perform six DSA runs in each vessel with high magnification and a high frame rate per second and to continue each run well into the venous phase, your statistics concerning proportionate use of fluoroscopy per case will look very flattering to your technique. The overall exposure per case, however, will not be so good. It is worth remembering this disproportionate tendency of the DSA runs to rack up the exposure very quickly. Therefore, in a case where you really want to spare the radiation use, minimizing parameters of exposure on the fluoroscopy settings will help a great deal, but the big

savings can be made by eliminating unnecessary DSA runs or cutting their duration.

For long interventional procedures, deterministic effects from radiation exposure become a consideration in addition to the more concerning stochastic effects. It was not rare to see a patient who develops significant epilation and even erythema of the scalp at the site of maximal skin exposure after a long neurointerventional procedure using older II technology. Clearly, the skin injury is proportionate to the skin dose in this type of deterministic correlation. For instance, one paper calculated that a particular patient who had received a fractionated skin dose of 6.6 Gy during a long neurointerventional procedure (a dose that is at the highest end of the range of exposures used in this type of procedure) had an approximately 0.3% risk of carcinogenesis deriving from the procedure (60). Radiation physicists, however, exercise a great deal of patience in reminding us that extrapolation of data estimates for a particular patient to the epidemiologic domain is misleading and likely erroneous (36). It is still reassuring to recall that most neurointerventional cases involve exposures of less than 2 Gy (200 rad) skin-entrance dose per plane. Kuwayama et al. (68) estimated that the skin exposure to the typical neurointerventional patient would probably be of the same order as that used in the 1940s and 1950s for treatment of tinea capitis (discussed earlier).

Pediatric Patient Exposure

References to studies of pediatric patients are beset with the same limitations seen in adult studies, that is, wide variability in the technique and difficulty of cases and documentation using outdated machines. Using conversion factors to calculate effective dose and ESD from recordings of DAP during pediatric diagnostic and interventional procedures, Raelson et al. (69) reported a mean DAP of 280.5 Gy.cm² per case equating with a mean effective dose of 28.1 mSv, but with a long tail extending to 289.9 mSv. Estimated skin doses were reported at 150 mGy for diagnostic procedures and 580 mGy for interventional procedures. A different study (70), which looked at mostly diagnostic pediatric cases, but which used a custom-installed 0.2-mm Cu filter, reported consistently reasonable skin doses for neuroangiographic procedures with a mean ESD of 68.1 mGy in the anteroposterior (AP) plane (max 924 mGy) and 40.9 mGy in the lateral plane (max 397.1 mGy). The same group of authors later reported peak ESD figures for diagnostic cerebral angiography of 149.9 mGy on the AP plane and 101.6 mGy on the lateral plane (71) (Figs. 6-4–6-6).

Personnel Exposure

All in all, the literature on radiation exposure of personnel during neuroangiographic procedures is sparse and confusing, and dated by technologic innovation. References involving cut-film technique, continuous-mode fluoroscopy, or angiography rooms with the output tube above the patient or on the operator side are of very limited value today.

As a rule of thumb, the radiation dose to the exposed areas of the angiographer can be calculated as between 1/100 to 1/1,000 (66,72) that of the patient. This is a variable relationship depending on the setup of a particular room and the angiographer's techniques and position.

Berthelsen et al. (66) estimated that the effective dose to the angiographer and assisting personnel ranges from 3 to

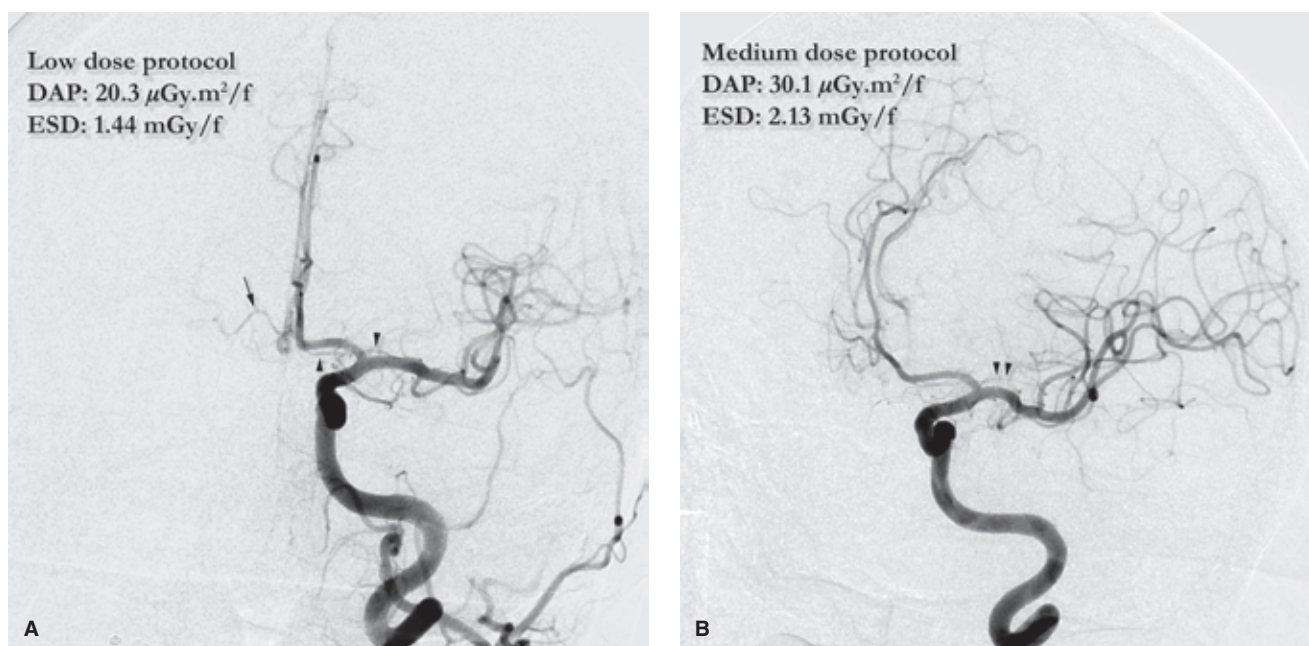


FIGURE 6-4. (A–B) Reducing dose does not need to compromise in image quality. Two images from the left internal carotid artery evaluation of an adult patient for possible vasculitis. The first image (A) was taken from a DSA run with some customized modulations to dose, principally in copper filtration and dose-per-frame settings, while the oblique view (B) was taken with the same FOV and a less drastically curtailed derivative of a factory protocol. The recorded DAP and ESD per frame are annotated showing a substantial increase in both parameters from (A) to (B). Admittedly, the obliquity of the second view imposes a geometric variable in the comparison, which will by itself drive up the dose, but this is a relatively minor increment (based on phantom measurements). The second image (B) is clearly an improvement over (A) for the definition of the distal MCA branches, hence the modulation of the dose for the second run in this protocol for evaluation of vasculitis. However, the difference is marginal, one might argue. Notice the reasonably clear definition of the recurrent artery of Heubner on the left (*arrowheads*) and right (*thin arrow*). At what point does demand for pure aesthetic appeal and clarity of the image, obtained at the cost of increased exposure, obscure the mundane utilitarian and diagnostic mission of the study? One might say that the dose increment for the better image is small and for most studies the final dose estimates will still be reasonable, no matter what I do; 50% additional increment onto a small number is still a smallish number *for most cases*. However, as I have consistently informed the fellows of our department, nobody will ever thank you for the six kids you remember to bring home from the mall. All they ever want to talk on and on about is the one you forgot. Thus, when you get yourself into a situation of a bad radiation burn, nobody will compliment you for having done a reasonable job on all the other patients you treated that month. The extreme cases are avoided by cultivating habits exercised during all diagnostic and interventional cases, so that these measures don't become an imposition when the extremely difficult cases present themselves.

Note: the images taken with protocol B in this example represent a substantial modification of a factory-set adult protocol recommended by the vendor at installation. A true comparison here would have been between image (A) and the original factory protocol, which would likely have made the comparative dose increments closer to 100% (based on personal phantom recordings).

86 μSv per case or approximately 5 mSv per year, assuming a caseload of about 200 embolizations. A study specifically looking at neurointerventional procedures estimated that the mean effective dose to the operator was 32 μSv , with a mean dose to the eye and thyroid of 80.6 and 28.8 μGy , respectively (73). A similar range of figures for an annual caseload of 120 coronary angiography procedures has been reported by Gustafsson (74). This figure would represent an estimation of dose similar to that received from undergoing a barium enema (4.06 mSv) and a CT scan (1.11 mSv) each year, or the difference in cosmic radiation involved in living in Denver, Colorado (altitude 1,610 m), instead of at sea level for 17 years (4,25).

These estimates of personnel exposure during neuroangiography are slightly higher than the mean annual H_E dose (measured under the collar) for general interventional radiologists. The annual effective dose for this group, approximately 3.16 to 10.1 mSv, has been calculated to represent

a risk of excess fatal cancer of approximately 1 per 10,000 careers (75). Niklason et al. (75) also emphasized the importance of wearing a thyroid collar during interventional cases by pointing out that a typical dose to the unshielded thyroid of the angiographer increases the calculated effective dose by a factor of 2. In other words, a thyroid collar provides half of one's protection during angiography.

Several studies have shown that doses to personnel within the room are beyond the limits of detection for single-case exposure, with the exception of the principal operator's forehead and left hand, where dose estimates vary by orders of magnitude between 14 to 240 μGy and 19 to 440 μGy , respectively (65). The lower figures are the equivalent of the cosmic radiation involved in a round-trip flight from Los Angeles to New York (76). Estimated exposures to the left hand and eye of operating during embolization procedures vary between 0.05 and 3.55 mSv (68). It becomes apparent that discrepancies

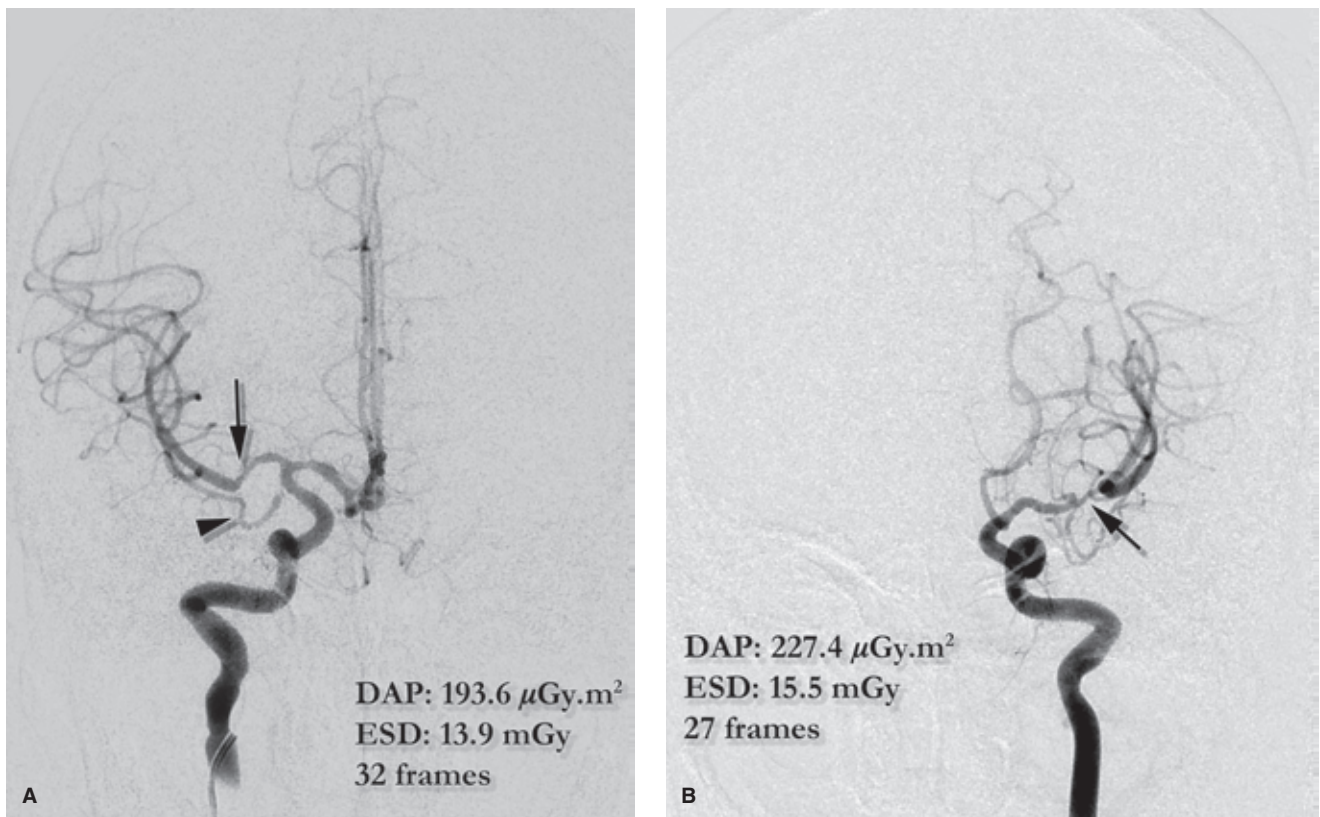


FIGURE 6-5. (A–B) Low-dose pediatric DSA protocol. Two images from the diagnostic evaluation of a small-stature teenage female patient with hemispheric ischemic symptoms in the setting of known sickle cell disease. The grid was in place for both images. Image (A) was taken with the lowest-dose pediatric protocol, and although the image background is somewhat grainy, the image quality is good. A moderate stenosis of the distal right M1 segment is well studied (*arrow* in A). An accessory middle cerebral artery (*arrowhead* in A) is also well delineated. Image (B) was taken with an older low-dose pediatric protocol (also reduced below vendor default) with slightly higher-exposure settings. A long irregular arteriopathic stenosis of the left middle cerebral artery is demonstrated (*arrow* in B). Image (B) demonstrates sharper vessel definition and greater detail on small vessels, such as the lenticulostriate branches, compared with (A). However, none of these differences had any bearing on the interpretation of the images or on the management of this particular patient. Annotations indicate the recorded DAP and ESD for each run with the number of frames.

exist between studies of at least one order of magnitude. It is probable that various measures of radiation protection, room design, and improvements in machine performance may explain some of the differences between these studies, but in older studies it was clear that busy neuroangiographers could easily exceed recommended annual dose limits to the hand (500 mSv/yr) and eye (150 mSv/yr) (68), and lens opacities were documented even in radiologists whose annual overall dose did not exceed 5 mSv (77). Most of these older studies were performed either with the undesirable configuration of having the lateral plane tube/emitter on the operator side (i.e., more backscatter to the operator), or, worse still, with the AP tube above the table. These configurations have been eliminated on modern equipment, but the concerns remain relevant, particularly to personnel such as the anesthesia team who are likely working on the tube side of the patient and without much in the way of under-the-table protection.

Protection of the Anesthesiology Team

For many years, it seems, the presence of the anesthesia team in the room was overlooked in discussions of radiation

safety and exposure. Recent improvement in machine design has reconfigured the lateral beam entry point to the left side of the table, which spares the angiographer a significant deal of backscatter, but instead throws it back at the anesthesiology team. Furthermore, most tables are designed with hanging aprons and shields on the right side of the patient, but without any equivalent protection on the left (Fig 6-2). The result is that the radiation dose per unit of time in the room can be substantially higher for neuroanesthesiologists than it is for the primary operating physician. One study showed that the dose to the face of the anesthesiology staff was $\times 6$ times that to the radiologist (78). This issue is gaining some attention in anesthesiology journals (79,80), and should be incorporated into the thinking of physicians operating a biplane room with a multitude of staff from different backgrounds in attendance. The peaks of radiation exposure to the anesthesiology team are likely related to those occasions when they are reaching under the covers to gain access to IV lines or muscle-twitch devices. These exposures could be substantially reduced by communication among personnel in the room.



FIGURE 6-6. (A–B) Effect of grid removal. Two images from an adult patient both taken with a low-dose protocol DSA setting. The right vertebral artery (**A**) was taken first and shows an atherosclerotic fusiform area of aneurysmal change in the distal intradural right vertebral artery proximal to the vertebrobasilar junction. The left vertebral artery image (**B**) was taken for the sake of completeness of the evaluation, but based on noninvasive imaging was not expected to add new information at this point. Therefore, the grid was removed for the duration of the injection. Certainly the edge sharpness and level of clarity in the background of image (**B**) is less appealing. Notice the definition of the transverse pontine or inferior cerebellar branches (*arrowheads*) in (**A**), which are virtually nondiscernible in (**B**). However, for the purposes of this patient, image (**B**) was perfectly adequate and involved an exposure and dose reduction of more than 40% compared with image (**A**).

Summary

In terms of routinely quantifying or even approximately defining the risk of stochastic effects from low-level radiation exposure, the data are incomplete. Some stochastic risk is thought to exist at whole body entrance dose levels above 0.1 Gy (10 rad) and more certainly above 1 Gy (100 rad). Extrapolation of the probability curve below the 0.1 Gy mark rests on uncertainty. In the face of this uncertainty, the general admonition is to keep exposure “as low as reasonably achievable” (ALARA).

Radiation exposure to a particular patient undergoing a diagnostic or interventional procedure depends on some factors that are outside of the angiographer’s apparent control but for which he or she may be expected to assume some legal responsibility. Given the increasing number of fluoroscopically guided interventional procedures being done, in the future, some spontaneous malignancies may be blamed on these procedures. A written record of one’s departmental conformity with nationally endorsed recommendations and of a periodic quality assurance program for equipment maintenance may be the best defense in such a situation.

The Potential Impact of FD Technology

If radiation beams could be focused like visible light, medical imaging would be much easier. Because we are com-

pelled, however, to use imaging plates of a dimension similar to the body part of interest, the capacity to develop large area active matrix arrays of electronic components took some time. Current technology in FD uses a thin layer of hydrogenated amorphous silicon a-Si:H (Fig. 6-3). A high-resolution array of diodes, capacitors, and transistor switches is integrated at each pixel location, coordinated with metal lines for control and data relay. On top of this rests a layer of x-ray fluorescent material, most commonly thallium-activated cesium iodide (CsI:Tl) with $Z = 55$ and 53, respectively. The CsI:Tl layer has an innate crystalline structure arrayed perpendicular to the a-Si:H plate, which creates an effective fiber-optic composition for transmission of light downward with reduction of spread laterally (the latter being responsible for blur) (54–56). FDs, when used to best advantage, have the potential to offer higher spatial resolution, elimination of geometric distortion, and elimination of problems with contrast and flare artifact inherent to older image intensifiers. They also demonstrate an improved ability to detect photons and convert them to signal (improved detective quantum efficiency [DQE]), which should translate into lower radiation doses for equivalent conditions of imaging compared with older machines. However, this is not necessarily an automatic benefit and depends very much on the physician operator taking advantage of the FD flexibility to reduce dose (Fig. 6-7).

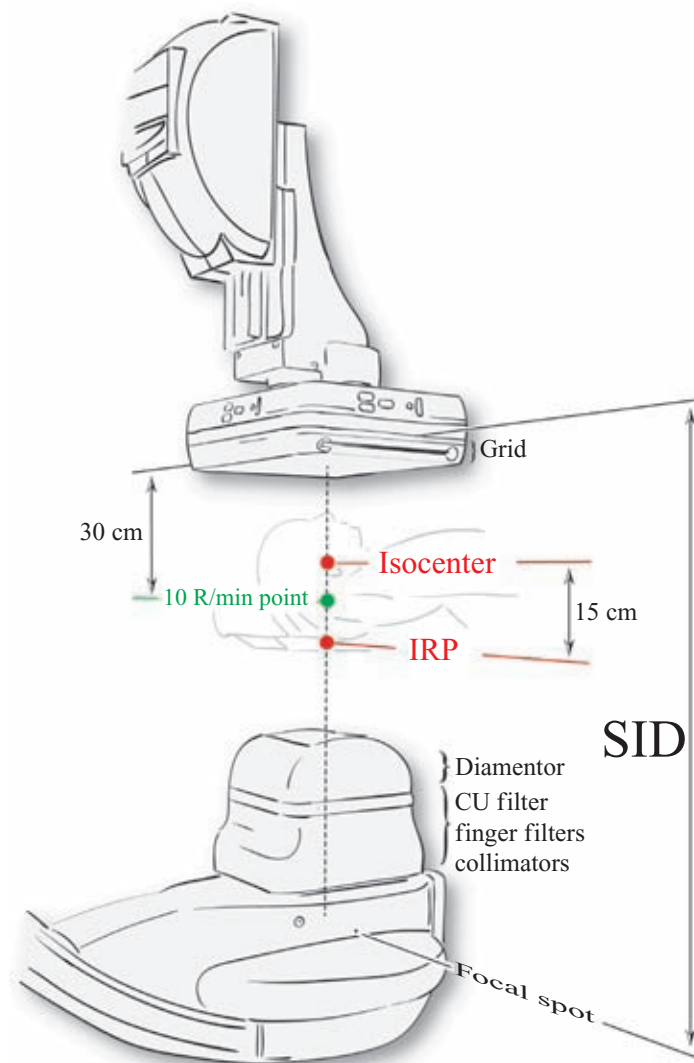


FIGURE 6-7. Interventional reference point (IRP) and estimated dose calculation. Although modern biplane units are very sophisticated, they cannot tell precisely where the patient is, what size is the patient, or what body part is being imaged, all of which would be among the many factors necessary to be taken into allowance in the calculation of effective dose or even just skin dose. The best they can do is work on certain assumptions of where the patient's entrance skin surface will be in relation to the equipment. From the manufacturer's point of view there are some nonnegotiable points in space between the tube and the image panel. The 10 R point, 30 cm below the panel, is a regulatory limit whereby under normal working circumstances the exposure at that point cannot exceed 10 R/minute. An assumption on the part of the manufacturer establishes where the likely isocenter of imaging (center of the head) will be, and skin dose calculations are then focused on the Interventional Reference Point (IRP) 15 cm on the tube side of the isocenter. The Estimated Skin Dose (ESD) provided by the manufacturer assumes that the machine is being operated under standard geometric circumstances, in which arrangement the IRP and the 10 R point are very close to one another. However, consider how the manufacturer's calculations can be confounded (and the estimated dose report become significantly understated) if the machine is operated with the SID extended through having the imaging panel elevated to an SID of 110 or 120 cm. Similarly, if the patient table is dropped closer to the tube, actual skin dose (but not reported ESD) is significantly augmented. Machines are checked with reference dosimeters periodically and dose estimates are expected to be accurate within 10% of reference readings. Manufacturers like to have their equipment calibrated on the "safe" side, that is, it is better from the point of view of their reputation and commitment to safety to have a machine slightly overestimate the patient doses than to underestimate. However, if the geometric assumptions built into the manufacturer's calculations are not practiced, the dose estimates may become significantly inaccurate to an increment of at least 20%. (Based on diagrams and data generously provided by Dr. Markus Lendl, Ph.D. of Siemens, Inc.)

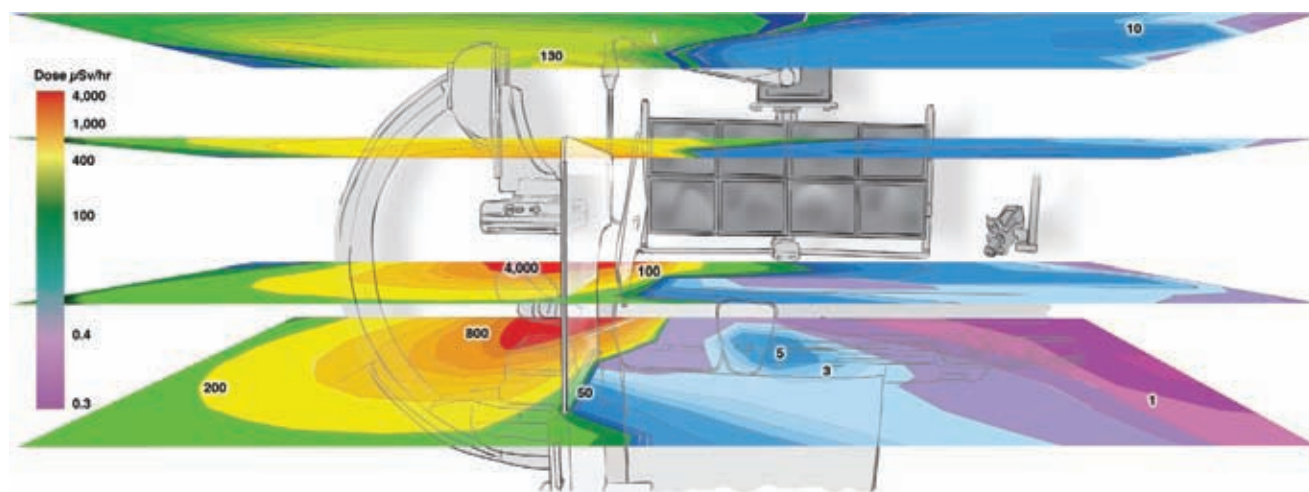


FIGURE 6-8. Distance and shielding matter. The superimposed colorized data presented are based in part on those published by Kuon et al. (87) for exposures using a single-plane machine in the coronary domain, with planes of color-coded isodose estimates illustrated at heights of 50, 100, 150, and 200 cm from the floor. The image demonstrates the enormous attenuation of beam intensity achieved by the interposition of the rolling and/or hanging glass shield. Big gaps around or under the lead shields eliminate the protecting attenuation illustrated here. Consider how the colorized isodose lines would be different on the lower end of the table without the interposed shields. Also, the images attempt to illustrate the relatively high exposures involved to individuals working at the patient's head, such as the anesthesia team, and therefore emphasize the importance of encouraging the anesthesia team to use a second shield during interventional cases.

If standard or default protocols are used, then the dose performance of FD technology compared with image intensifiers is indifferent (81,82) or even worse than a well-tuned II system (83). However, when used to advantage in patients or in phantoms, radiation dose reduction of 50% or more is possible (84–86). Understanding an FD biplane system takes a deal of time sitting with the vendor engineers and asking questions about variables that can be altered behind the scenes, which the physician who is accustomed to II technology may not be aware of. The software password accesses a netherworld of possibilities. Fluoroscopy dose per pulse, dose per DSA frame, Cu filtration levels, frame rate per second, and roadmap dose per pulse can all be manipulated into custom protocols made available on the tableside menus.

Practical Conclusions

The total duration of fluoroscopy depends on the nature of the case, but the angiographer can strive to reduce this time and other factors contributing to the total exposure considerably. Modern biplane fluoroscopy units have a theoretically maximal output range equivalent to a skin dose of 10 R per minute, equating with a theoretical maximal skin dose of 87.8 mGy/min (Fig 6-7). However, poor technique, incorrect table height, or activation of Fluoro+ (high dose permitted by the FDA with a warning bell) can exceed even this figure. Vendors need to compete with one another on the basis of image quality, and therefore unless you push them to scale back on the tube output to a degree

with image quality is noticeably affected, they are likely to install the machine with middle-of-the-road default protocols. Vendors will not push you to get yourself accustomed to grainy images or jumpy fluoroscopy rates of 2 or 3 pulses per second. Therefore, with default protocols doses will tend to add up quickly.

In one of the most thorough studies of personnel exposure in the cardiac angiography suite, Kuon et al. (87) have demonstrated—by scrupulous draping of the patient with lead shielding and use of rolling and ceiling-mounted lead protection—that it is possible to reduce personnel and patient exposure to a quarter or less of what it would otherwise have been (88). For those readers who require extra motivation in this matter, these authors discovered that without particular attention to radiation leaks between barriers, an exposure at the *gonadal* level of the operator of 897 μ Sv per hour could be eliminated by use of supplementary 1-mm Pb equivalent flaps above and below the patient table. The isodose line diagrams calculated by these authors argue convincingly for tight application of a contoured lead shield to the patient's trunk during all procedures (Fig. 6-8).

A definitive conclusion on the risks posed to patients and angiographers from diagnostic and interventional procedures is not attainable using current data and statistical methods. It is overwhelmingly likely that the risk to the patient and operating personnel is small. The reader is strongly encouraged to prioritize the development of personal routines and habits for improved manipulation of those variables under his or her direct control, which will reduce this exposure (Table 6-3).

TABLE 6-3 Reducing Radiation Exposure

A conscious effort to reduce radiation exposure and attention to the ongoing cumulative dose during a case can reduce patient exposure by 38–50% (89) and personnel exposure by 80% (87) without much effort. Remember that anything that is good for reducing the exposure of the patient is generally good for the operating personnel.

- Fluoroscopy time, in itself, is not a helpful indicator of patient dose. What matters more are the parameters in place for the fluoroscopy protocol, that is, pulse per second, dose per pulse, and so on, and the geometric conditions. Physicians should be conversant with the meaning of the numbers indicating cumulative kerma area product (synonymous with Dose Area Product) and Estimated Skin Dose (ESD) during a case. One should also be mindful that the ESD is an approximation based on the geometry of machine design. The machine does not know where the patient is and makes no allowances for focus-skin distance or patient size. Therefore, conditions can easily be construed where the ESD and actual skin dose become very divergent.
- On flat panel machines, magnification of the image involves a seesaw effect on the skin dose and DAP. Skin dose increases linearly with magnification, while DAP due to the smaller cross-sectional area of the beam decreases. Although the stochastic risks of the procedure are proportional to the DAP, nevertheless, the best recommendation is to keep magnification at a low level.
- Collimate as much as possible to reduce scatter as well as the size of the beam entering the patient. A small degree of collimation can reduce the area of the beam substantially, with a proportionate reduction in dose. This will also reduce backscatter to the personnel.
- Increasing the distance that the beam has to traverse through the patient will drive up beam strength and increase patient dose significantly. The shortest routes are a straight AP and lateral view. Be aware that with extreme angulation of either C-arm, beam strength and scatter patterns are going to be altered in an unfavorable direction.
- Fluoroscopy dose can be reduced by minimizing magnification, reducing the time with one's foot on the pedal, reducing the dose per pulse, and minimizing the pulse rate per second. Roadmapping involves settings on your machine that are likely higher by default than the fluoroscopy settings and will need to be calibrated separately.
- During diagnostic angiography, DSA accounts for approximately 70–90% of the total radiation dose. DSA dosage can be minimized by minimizing the number of runs, curtailing the length of all runs if possible, adjusting the frame rate per second for imaging during DSA, and adjusting the dose per frame (usually done by the service engineer in the password-protected software). Variable frame rates are possible on modern machines, for example, 2 frames per second (fps) for the first 3 s, and 1 fps thereafter, or variations thereon, so that the cumulative frame count per run can be minimized without compromising the quality of one's imaging.
- Use lead screens, thyroid collars, and shields at all times. Even though they are extremely cumbersome, it is safer to wear lead goggles or glasses too. After many years of assuming that the risk of radiation-induced lens opacities in medical staff of angiography suites was low, several trends of evidence suggest otherwise with data indicating a substantially higher risk in airline pilots, angiography technologists and nurses, and interventional cardiologists (90–93). A growing chorus of concern has arisen that sensitivity of the eye to radiation may lie below the current limit of 150 mSv/yr, and eye protection is increasingly endorsed for operating personnel (94–96). Older interpretations of the atomic bomb survivor data suggested that lens opacities were not a concern under 2 Gy or certainly less than 1 Gy of exposure. It is likely that the updated figure will be half of that, 0.5 Gy, adding to the likelihood that limits for occupational exposure of the eye will also be reduced (97,98).
- Bring the AP panel down as much as possible and the lateral panel in. Leaving the SID at 120 cm involves an unnecessary increase in patient dose of approximately 40% as compared with an SID of 100 cm.
- Remember to use pediatric low-dose protocols consistently. Inadvertent use of an adult protocol on a child can more than double or triple the dose from a procedure, depending on the settings.
- Removal of the grid may be possible for some pediatric and adult procedures, with only minimal subjective compromise of image quality. This will reduce the dose to the patient by approximately 40% and will reduce beam backscatter to staff by an equivalent degree.
- As a general rule, excellent imaging quality can only be achieved by use of radiation photons in sufficient quantities. Modern flat detector machines are so sensitive and well engineered that the emphasis now should be on achieving “adequate” rather than “excellent” image quality (99).

References

1. Brenner DJ, Hall EJ. Computed tomography—An increasing source of radiation exposure. *N Engl J Med* 2007;357(22):2277–2284.
2. Lee RK, Chu WC, Graham CA, et al. Knowledge of radiation exposure in common radiological investigations: A comparison between radiologists and non-radiologists. *Emerg Med J* 2011.
3. Schull W. *A Half-Century of Studies from Hiroshima and Nagasaki*. 1st ed. New York: Wiley-Liss; 1995.
4. Mettler F, Upton A. *Medical Effects of Ionizing Radiation*. 2nd ed. Philadelphia: W.B. Saunders; 1995.
5. UNSCEAR. UNSCEAR 2000. The United Nations Scientific Committee on the Effects of Atomic Radiation. *Health Phys* 2000;79(3):314.
6. Preston DL, Shimizu Y, Pierce DA, et al. Studies of mortality of atomic bomb survivors. Report 13: Solid cancer and noncancer disease mortality: 1950–1997. *Radiat Res* 2003; 160(4):381–407.
7. Preston DL, Kato H, Kopecky K, et al. Studies of the mortality of A-bomb survivors. 8. Cancer mortality, 1950–1982. *Radiat Res* 1987;111(1):151–178.
8. Preston DL, Kusumi S, Tomonaga M, et al. Cancer incidence in atomic bomb survivors. Part III. Leukemia, lymphoma and multiple myeloma, 1950–1987. *Radiat Res* 1994;137(2 suppl):S68–S97.

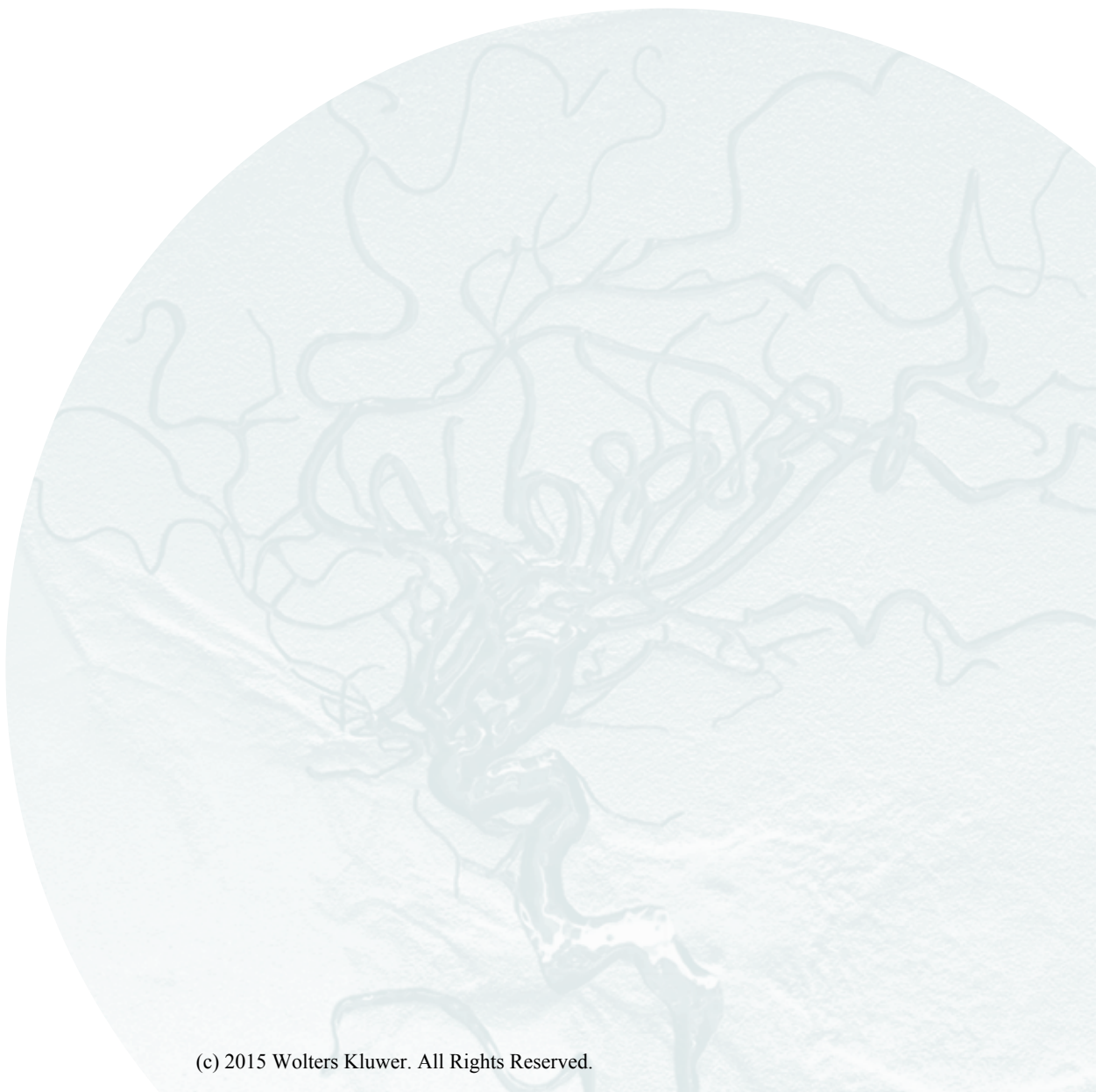
9. Webster EW. Garland Lecture. On the question of cancer induction by small x-ray doses. *AJR Am J Roentgenol* 1981;137(4):647–666.
10. Caldwell GG, Kelley D, Zack M, et al. Mortality and cancer frequency among military nuclear test (Smoky) participants, 1957 through 1979. *JAMA* 1983;250(5):620–624.
11. Johnson CJ. Cancer incidence in an area of radioactive fallout downwind from the Nevada Test Site. *JAMA* 1984;251(2):230–236.
12. Brown JM. The shape of the dose–response curve for radiation carcinogenesis. Extrapolation to low doses. *Radiat Res* 1977;71(1):34–50.
13. Shore RE, Hildreth N, Dvoretzky P, et al. Thyroid cancer among persons given x-ray treatment in infancy for an enlarged thymus gland. *Am J Epidemiol* 1993;137(10):1068–1080.
14. Smith-Bindman R, Lipson J, Marcus R, et al. Radiation dose associated with common computed tomography examinations and the associated lifetime attributable risk of cancer. *Arch Intern Med* 2009;169(22):2078–2086.
15. Gori T, Munzel T. Biological effects of low-dose radiation: Of harm and hormesis. *Eur Heart J* 2011;33(3):408–414.
16. Andreassi MG, Cioppa A, Botto N, et al. Somatic DNA damage in interventional cardiologists: A case-control study. *Faseb J* 2005;19(8):998–999.
17. Andreassi MG, Cioppa A, Manfredi S, et al. *N*-acetyl cysteine reduces chromosomal DNA damage in circulating lymphocytes during cardiac catheterization procedures: A pilot study. *Int J Cardiol* 2011.
18. Andreassi MG, Cioppa A, Manfredi S, et al. Acute chromosomal DNA damage in human lymphocytes after radiation exposure in invasive cardiovascular procedures. *Eur Heart J* 2007;28(18):2195–2199.
19. Andreassi MG, Foffa I, Manfredi S, et al. Genetic polymorphisms in XRCC1, OGG1, APE1 and XRCC3 DNA repair genes, ionizing radiation exposure and chromosomal DNA damage in interventional cardiologists. *Mutat Res* 2009;666(1–2):57–63.
20. Andreassi MG, Sagliano I, Cioppa A, et al. Chronic low-dose radiation exposure from interventional cardiology procedures induces chromosomal abnormalities in originally genetically identical twins. *Int J Cardiol* 2007;118(1):130–131.
21. Russo GL, Tedesco I, Russo M, et al. Cellular adaptive response to chronic radiation exposure in interventional cardiologists. *Eur Heart J* 2011.
22. Hall EJ, Brenner DJ. Cancer risks from diagnostic radiology. *Br J Radiol* 2008;81(965):362–378.
23. Curry TS, Dowdey JE, Murray RC. *Christensen's Physics of Diagnostic Radiology*. 4th ed. Philadelphia: Lea and Febiger; 1990.
24. Wagner LK EP, Geise RA. Potential biological effects following high x-ray dose interventional procedures. *J Vasc Interv Radiol* 1994;5:71–84.
25. UNSCEAR. Effects of ionizing radiation. Volume I. Report to the general assembly with scientific annexes A and B. United Nations Office, Vienna 2008.
26. UNSCEAR. Effects of ionizing radiation. Volume II. Report to the general assembly with scientific annexes C, D, and E. United Nations Office, Vienna 2009.
27. Moolgavkar SH. Hormones and multistage carcinogenesis. *Cancer Surv* 1986;5(3):635–648.
28. Lindell B. Radiation protection—A look to the future: ICRP perceptions. *Health Phys* 1988;55(2):145–147.
29. Sinclair WK. Radiation protection recommendations on dose limits: The role of the NCRP and the ICRP and future developments. *Int J Radiat Oncol Biol Phys* 1995;31(2):387–392.
30. ICRP. ICoRP. The 2007 Recommendations of the International Commission on Radiological Protection. ICRP publication 103. *Ann ICRP* 2007;37(2–4):1–332.
31. ICRP. ICoRP. Recommendations of the International Commission on Radiological Protection (ICRP publication 60). *Ann ICRP* 1991;21:1–3.
32. Wrixon AD. New recommendations from the International Commission on Radiological Protection—A review. *Phys Med Biol* 2008;53(8):R41–R60.
33. Bacher K, Bogaert E, Lapere R, et al. Patient-specific dose and radiation risk estimation in pediatric cardiac catheterization. *Circulation* 2005;111(1):83–89.
34. Bakalyar DM, Castellani MD, Safian RD. Radiation exposure to patients undergoing diagnostic and interventional cardiac catheterization procedures. *Cathet Cardiovasc Diagn* 1997;42(2):121–125.
35. Friedberg W, Faulkner DN, Snyder L, et al. Galactic cosmic radiation exposure and associated health risks for air carrier crewmembers. *Aviat Space Environ Med* 1989;60(11):1104–1108.
36. McCollough CH, Christner JA, Kofler JM. How effective is effective dose as a predictor of radiation risk? *AJR Am J Roentgenol* 2010;194(4):890–896.
37. Martin CJ. Effective dose: How should it be applied to medical exposures? *Br J Radiol* 2007;80(956):639–647.
38. Martin CJ. The application of effective dose to medical exposures. *Radiat Prot Dosimetry* 2008;128(1):1–4.
39. Bogaert E, Bacher K, Lemmens K, et al. A large-scale multicentre study of patient skin doses in interventional cardiology: Dose–area product action levels and dose reference levels. *Br J Radiol* 2009;82(976):303–312.
40. Struelens L, Vanhavere F, Bosmans H, et al. Skin dose measurements on patients for diagnostic and interventional neuroradiology: A multicentre study. *Radiat Prot Dosimetry* 2005;114(1–3):143–146.
41. McParland BJ. Entrance skin dose estimates derived from dose–area product measurements in interventional radiological procedures. *Br J Radiol* 1998;71(852):1288–1295.
42. McParland BJ. A study of patient radiation doses in interventional radiological procedures. *Br J Radiol* 1998;71(842):175–185.
43. Kienböck R. Über radiotherapie der haarkrankungen. *Arch Dermatol Syph Wien* 1907;83:77–111.
44. Adamson H. A simplified method of x-ray application for the cure of ringworm of the scalp; Kienböck's method. *Lancet* 1909;1:1378–1380.
45. Albert RE, Omran AR. Follow-up study of patients treated by x-ray epilation for tinea capitis. I. Population characteristics, posttreatment illnesses, and mortality experience. *Arch Environ Health* 1968;17(6):899–918.
46. Albert RE, Omran AR, Brauer EW, et al. Follow-up study of patients treated by x-ray epilation for tinea capitis. II. Results of clinical and laboratory examinations. *Arch Environ Health* 1968;17(6):919–934.
47. Shore RE, Albert RE, Reed M, et al. Skin cancer incidence among children irradiated for ringworm of the scalp. *Radiat Res* 1984;100(1):192–204.
48. Schulz RJ, Albert RE. Follow-up study of patients treated by x-ray epilation for tinea capitis. 3. Dose to organs of the head from the x-ray treatment of tinea capitis. *Arch Environ Health* 1968;17(6):935–950.
49. Werner A, Modan B, Davidoff D. Doses to brain, skull and thyroid, following x-ray therapy for tinea capitis. *Phys Med Biol* 1968;13(2):247–258.
50. Harley NH, Albert RE, Shore RE, et al. Follow-up study of patients treated by x-ray epilation for tinea capitis. Estimation of the dose to the thyroid and pituitary glands and other structures of the head and neck. *Phys Med Biol* 1976;21(4):631–642.
51. Shore RE, Albert RE, Pasternack BS. Follow-up study of patients treated by x-ray epilation for tinea capitis; resurvey of

- post-treatment illness and mortality experience. *Arch Environ Health* 1976;31(1):21–28.
52. Modan B, Baidatz D, Mart H, et al. Radiation-induced head and neck tumours. *Lancet* 1974;1(7852):277–279.
 53. Shore RE, Moseson M, Xue X, et al. Skin cancer after x-ray treatment for scalp ringworm. *Radiat Res* 2002;157(4): 410–418.
 54. Cowen AR, Davies AG, Sivanathan MU. The design and imaging characteristics of dynamic, solid-state, flat-panel x-ray image detectors for digital fluoroscopy and fluorography. *Clin Radiol* 2008;63(10):1073–1085.
 55. Cowen AR, Kengyelics SM, Davies AG. Solid-state, flat-panel, digital radiography detectors and their physical imaging characteristics. *Clin Radiol* 2008;63(5):487–498.
 56. Spahn M. Flat detectors and their clinical applications. *Eur Radiol* 2005;15(9):1934–1947.
 57. Balter S, Miller DL. The new Joint Commission sentinel event pertaining to prolonged fluoroscopy. *J Am Coll Radiol* 2007; 4(7):497–500.
 58. Balter S, Moses J. Managing patient dose in interventional cardiology. *Catheter Cardiovasc Interv* 2007;70(2):244–249.
 59. Feygelman VM, Huda W, Peters KR. Effective dose equivalents to patients undergoing cerebral angiography. *AJNR Am J Neuroradiol* 1992;13(3):845–849.
 60. Huda W, Peters KR. Radiation-induced temporary epilation after a neuroradiologically guided embolization procedure. *Radiology* 1994;193(3):642–644.
 61. Miller DL, Balter S, Cole PE, et al. Radiation doses in interventional radiology procedures: The RAD-IR study. Part II: Skin dose. *J Vasc Interv Radiol* 2003;14(8):977–990.
 62. Miller DL, Balter S, Cole PE, et al. Radiation doses in interventional radiology procedures: The RAD-IR study. Part I: Overall measures of dose. *J Vasc Interv Radiol* 2003;14(6): 711–727.
 63. Balter S, Schueler BA, Miller DL, et al. Radiation doses in interventional radiology procedures: The RAD-IR study. Part III: Dosimetric performance of the interventional fluoroscopy units. *J Vasc Interv Radiol* 2004;15(9):919–926.
 64. Bergeron P, Carrier R, Roy D, et al. Radiation doses to patients in neurointerventional procedures. *AJNR Am J Neuroradiol* 1994;15(10):1809–1812.
 65. Marshall NW, Noble J, Faulkner K. Patient and staff dosimetry in neuroradiological procedures. *Br J Radiol* 1995;68(809): 495–501.
 66. Berthelsen B, Cederblad A. Radiation doses to patients and personnel involved in embolization of intracerebral arteriovenous malformations. *Acta Radiol* 1991;32(6):492–497.
 67. Gkanatsios NA, Huda W, Peters KR. Adult patient doses in interventional neuroradiology. *Med Phys* 2002;29(5):717–723.
 68. Kuwayama N, Takaku A, Endo S, et al. Radiation exposure in endovascular surgery of the head and neck. *AJNR Am J Neuroradiol* 1994;15(10):1801–1808.
 69. Raelson CA, Kanal KM, Vavilala MS, et al. Radiation dose and excess risk of cancer in children undergoing neuroangiography. *AJR Am J Roentgenol* 2009;193(6):1621–1628.
 70. Swoboda NA, Armstrong DG, Smith J, et al. Pediatric patient surface doses in neuroangiography. *Pediatr Radiol* 2005;35(9): 859–866.
 71. Glennie D, Connolly BL, Gordon C. Entrance skin dose measured with MOSFETs in children undergoing interventional radiology procedures. *Pediatr Radiol* 2008;38(11):1180–1187.
 72. Bushong SC. Hazards evaluation of neuroangiographic procedures. *AJNR Am J Neuroradiol* 1994;15(10):1813–1816.
 73. Bor D, Cekirge S, Turkay T, et al. Patient and staff doses in interventional neuroradiology. *Radiat Prot Dosimetry* 2005; 117(1–3):62–68.
 74. Gustafsson M, Lunderquist A. Personnel exposure to radiation at some angiographic procedures. *Radiology* 1981;140(3): 807–811.
 75. Niklason LT, Marx MV, Chan HP. Interventional radiologists: Occupational radiation doses and risks. *Radiology* 1993; 187(3):729–733.
 76. Wallace R. Measurements of the cosmic radiation dose in subsonic commercial aircraft compared to the city-pair dose calculation. *Lawrence Berkley Report No. 1505*. 1975.
 77. Vano E, Gonzalez L, Beneytez F, et al. Lens injuries induced by occupational exposure in non-optimized interventional radiology laboratories. *Br J Radiol* 1998;71(847):728–733.
 78. Anastasian ZH, Strozyk D, Meyers PM, et al. Radiation exposure of the anesthesiologist in the neurointerventional suite. *Anesthesiology* 2011;114(3):512–520.
 79. Dagal A. Radiation safety for anesthesiologists. *Curr Opin Anaesthesiol* 2011;24(4):445–450.
 80. Amis ES Jr., Anesthesiologists in the neurointerventional suite: What is appropriate radiation protection? *Anesthesiology* 2011;114(3):477–478.
 81. Davies AG, Cowen AR, Kengyelics SM, et al. Do flat detector cardiac x-ray systems convey advantages over image-intensifier-based systems? Study comparing x-ray dose and image quality. *Eur Radiol* 2007;17(7):1787–1794.
 82. Grewal RK, McLean ID. Comparative evaluation of an II based and a flat panel based cardiovascular fluoroscopy system within a clinical environment. *Australas Phys Eng Sci Med* 2005;28(3):151–158.
 83. Prasan AM, Ison G, Rees DM. Radiation exposure during elective coronary angioplasty: The effect of flat-panel detection. *Heart Lung Circ* 2008;17(3):215–219.
 84. Suzuki S, Furui S, Kobayashi I, et al. Radiation dose to patients and radiologists during transcatheter arterial embolization: Comparison of a digital flat-panel system and conventional unit. *AJR Am J Roentgenol* 2005;185(4):855–859.
 85. Geijer H, Beckman KW, Andersson T, et al. Image quality vs. radiation dose for a flat-panel amorphous silicon detector: A phantom study. *Eur Radiol* 2001;11(9):1704–1709.
 86. Korner M, Weber CH, Wirth S, et al. Advances in digital radiography: Physical principles and system overview. *Radiographics* 2007;27(3):675–686.
 87. Kuon E, Schmitt M, Dahm JB. Significant reduction of radiation exposure to operator and staff during cardiac interventions by analysis of radiation leakage and improved lead shielding. *Am J Cardiol* 2002;89(1):44–49.
 88. Kuon E, Glaser C, Dahm JB. Effective techniques for reduction of radiation dosage to patients undergoing invasive cardiac procedures. *Br J Radiol* 2003;76(906):406–413.
 89. Norbash AM, Busick D, Marks MP. Techniques for reducing interventional neuroradiologic skin dose: Tube position rotation and supplemental beam filtration. *AJNR Am J Neuroradiol* 1996;17(1):41–49.
 90. Chodick G, Bekiroglu N, Hauptmann M, et al. Risk of cataract after exposure to low doses of ionizing radiation: a 20-year prospective cohort study among US radiologic technologists. *Am J Epidemiol* 2008;168(6):620–631.
 91. Jacob S, Michel M, Spaulding C, et al. Occupational cataracts and lens opacities in interventional cardiology (O'CLOC study): Are x-rays involved? Radiation-induced cataracts and lens opacities. *BMC Public Health* 2010;10:537.
 92. Rafnsson V, Olafsdottir E, Hrafnkelsson J, et al. Cosmic radiation increases the risk of nuclear cataract in airline pilots: A population-based case-control study. *Arch Ophthalmol* 2005; 123(8):1102–1105.
 93. Vano E, Kleiman NJ, Duran A, et al. Radiation cataract risk in interventional cardiology personnel. *Radiat Res* 2010;174(4): 490–495.
 94. Mrena S, Kivela T, Kurtio P, et al. Lens opacities among physicians occupationally exposed to ionizing radiation—A pilot study in Finland. *Scand J Work Environ Health* 2011;37(3): 237–243.

95. Shore RE, Neriishi K, Nakashima E. Epidemiological studies of cataract risk at low to moderate radiation doses: (Not) seeing is believing. *Radiat Res* 2010;174(6):889–894.
96. Shore RE, Neriishi K, Nakashima E. Epidemiological studies of cataract risk at low to moderate radiation doses: (Not) seeing is believing. *Radiat Res* 2010. [Epub ahead of print].
97. Ainsbury EA, Bouffler SD, Dorr W, et al. Radiation cataractogenesis: A review of recent studies. *Radiat Res* 2009;172(1):1–9.
98. Neriishi K, Nakashima E, Minamoto A, et al. Postoperative cataract cases among atomic bomb survivors: Radiation dose response and threshold. *Radiat Res* 2007;168(4):404–408.
99. Kuon E, Dorn C, Schmitt M, et al. Radiation dose reduction in invasive cardiology by restriction to adequate instead of optimized picture quality. *Health Phys* 2003;84(5):626–631.



Anatomy



7

Embryology of the Cranial Circulation

Key Point

- Embryologic development explains the many anatomic variants of the cerebrovascular circulation.

A rudimentary description of the embryonic origins of the cranial vessels will assist in understanding the variants and anomalies that may be seen during cerebral angiography. The terminology and nomenclature of embryologic literature can be very intimidating and obscurantist to say the least; however, the major events that describe the vascular embryology of the brain are simple to understand. Moreover, such an understanding, rather than a memorization of categorically distinct variants, will allow flexibility in one's thinking about these anomalies. Archetypal variations are easily recognized in textbooks; for the interpretation of angiograms, however, it is necessary to realize that numerous intermediate anomalous states may coexist and are rarely, if ever, exactly similar in different cases. The following synopsis of the embryology of the cranial vasculature is based largely on the classic papers by E. D. Congdon (1) and D. H. Padget (2–6).

► PRIMITIVE AORTIC ARCHES

The embryologic development of the aortic arch and great vessels is described in two stages (1). A branchial stage (3- to 14-mm crown–rump length) corresponds with the arterial pattern seen in lower vertebrates, similar to that supplying the gill apparatus (*branchia = gill*). A postbranchial phase describes the evolution of the adult arterial pattern from the remnants of the branchial components.

The six pairs of primitive aortic arches—the existence of the fifth arches being inconstant or contentious—fill a developmental role in association with the development of the pharyngeal pouches (Fig. 7-1). This occurs by virtue of the initially cephalic location of the primitive heart and the interruption, by the pharyngeal structures, of the route between the ventral aortic sac and the dorsal paired aortae. To circumvent the pharyngeal pouches, the aortic outflow interdigitates between the pouches starting with the first set of aortic arches. As the cardiac structures migrate into

the thorax, the primitive aorta is drawn caudally so that the cephalically located aortic arches, being uneconomical in disposition, regress and are replaced by other successively forming and regressing sets of arches. Not all six pairs of arches are present at a single time, as represented by synoptic diagrams.

From a point of interest in the cephalic vessels, the major events in the postbranchial phase are:

- Regression of the left dorsal aorta between the third and fourth arches, such that the residuum of the left dorsal aorta becomes the source of the major carotid branches off the aortic arch (Fig. 7-1G).
- Derivation of the subclavian arteries from the sixth intersegmental arteries, themselves branching from the fourth aortic arches bilaterally. The subclavian arteries assume the supply of the caudal end of the vertebral arterial network. This allows evolution of the most common adult configuration whereby the vertebral arteries, deriving from the sixth intersegmental arteries, enter the foramina transversaria of the C6 vertebral body (Fig. 7-1F).
- Attenuation of the right fourth aortic arch to a caliber commensurate with a role of supplying the right subclavian artery. The right fourth dorsal aorta regresses caudad to that point, leaving the adult right subclavian artery to derive supply from the brachiocephalic artery (a remnant of the third and fourth arches), except in instances of an aberrant right subclavian artery (Fig. 7-1H).

► ARTERIAL EMBRYOLOGY

The cranial arterial vasculature in its adult form evolves in early fetal life through a number of simultaneous or overlapping steps. Primitive embryonic vessels without an adult derivative usually regress completely but are of interest by virtue of occasional anomalous persistence. Their closure results in hemodynamic changes that contribute in part to the genesis of other permanent vessel derivatives from the embryonic plexi. These derivatives emerge with an economic regression of the otiose remaining plexal components. Anomalies associated with early events, such as failure of regression of the primitive maxillary or hypoglossal arteries, are more rarely seen than those with later events, such as persistence of a trigeminal artery or failure of normal diminution of the territory of the anterior choroidal artery.

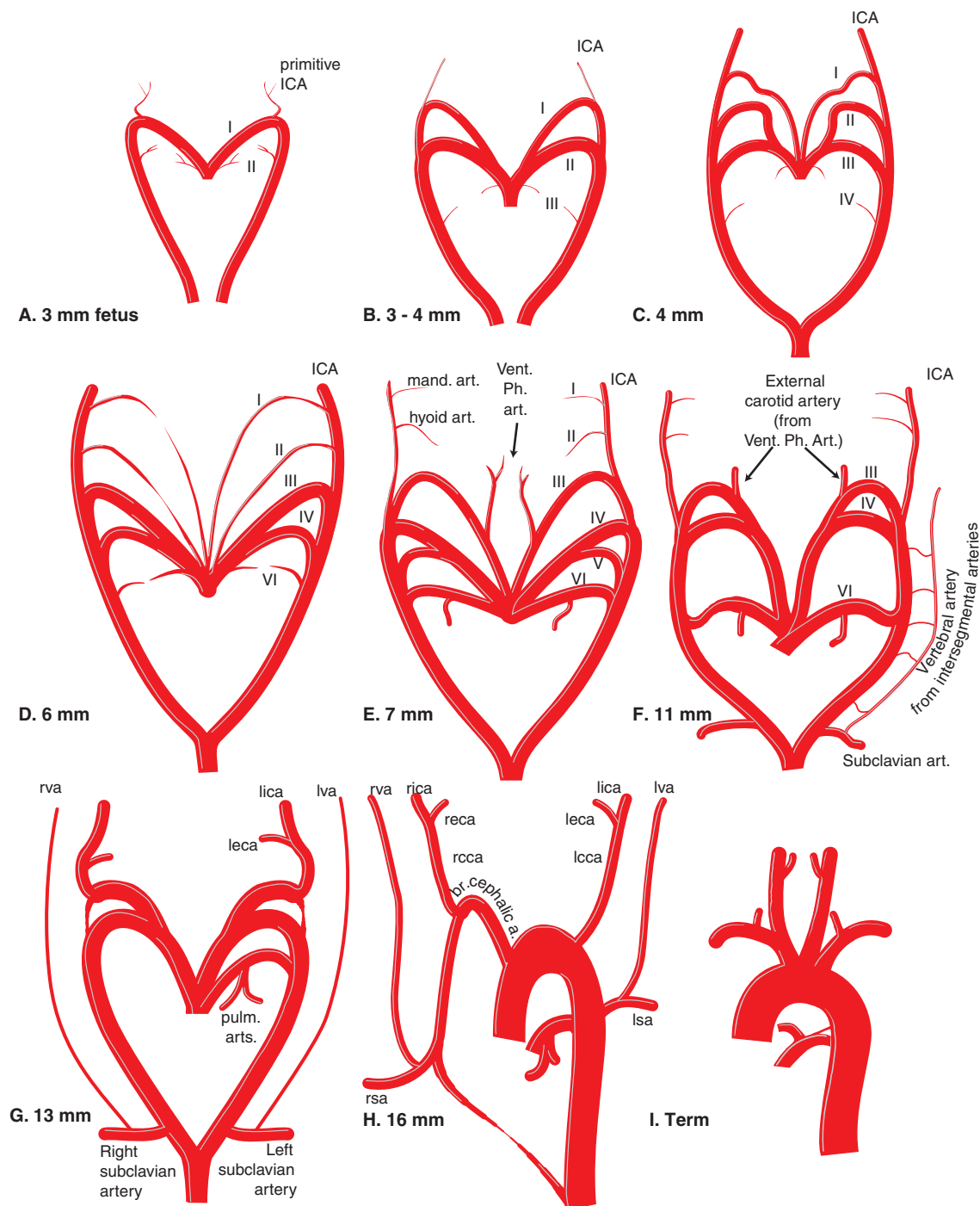


FIGURE 7-1. (A–I) Schematic unscaled diagram of the evolution of the embryonic aortic arches. (Labels: ICA, internal carotid artery; eca, external carotid artery; sa, subclavian artery; cca, common carotid artery; va, vertebral artery; vent. ph. art., ventral pharyngeal artery; mand. art., mandibular artery; Roman numerals, primitive aortic arches; l, left; r, right.)

The 4-mm Fetal Stage

At the 4-mm fetal stage, the first and second aortic arches are involuting and their remnants, the *mandibular* and *hyoid arteries*, respectively, become incorporated as branches of the third arch (Fig. 7-2). The third arch is the precursor of the internal and common carotid artery. The hyoid artery is discussed later.

The mandibular artery has a less complicated evolution than the hyoid artery, and, in Padgett's opinion, is associated with the superficial petrosal nerve, thus represented in adult form by the artery of the Vidian canal. The mandibular artery is frequently seen in children, particularly in the setting of a hypervascular mass in the external carotid artery territory, such as a juvenile angiofibroma (7) or tonsillar hyperplasia (8).

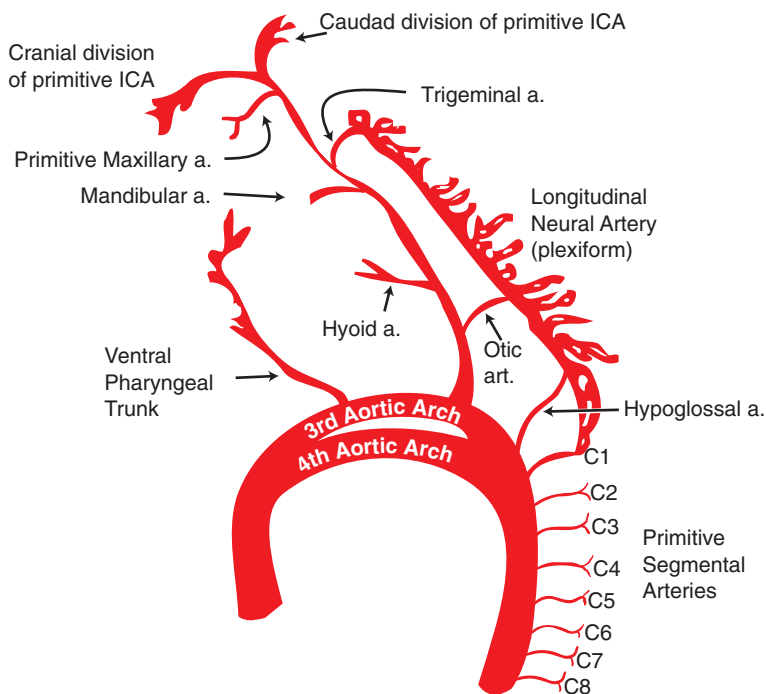


FIGURE 7-2. Embryologic development of cranial arteries at the 4- to 6-mm stage. See text for discussion. Allowing for variability in timing between fetuses, parts of this diagram correlate with Figure 7-1E.

The primitive internal carotid artery continues cephalad and gives a major anastomosis to the posterior circulation, the *primitive trigeminal artery*, at the level of the trigeminal ganglion. Further along its course, the primitive internal carotid artery gives a branch adjacent to the Rathké pouch, the *primitive maxillary artery*, which courses ventrally to the base of the optic vesicle. The primitive maxillary artery later regresses to assume a more mesial course and likely corresponds with the inferior hypophyseal artery in adults. An occasional case of an intrasellar cross-carotid anastomosis, usually in the setting of a unilateral carotid agenesis is most likely a representation of the primitive maxillary artery (9–12).

The primitive internal carotid artery forms two divisions at its most cephalad branching point:

- Cranial division (*the primitive anterior cerebral artery*) curves around and in front of the optic vesicle to reach the olfactory area;
- Caudal division (*precursor of the posterior communicating artery*) ends in the region of the developing mesencephalon.

Phylogenetic comparisons indicate that the cranial division of the internal carotid artery in humans is homologous with the medial olfactory artery in lower orders, such as fish and reptiles. This vessel is seen to evolve into the anterior cerebral artery as one ascends the phylogenetic hierarchy, implying that the anterior cerebral artery in humans is the direct embryonic continuation of the internal carotid artery, whereas the middle cerebral artery is a secondary branch of this vessel (12).

In the hindbrain area, the arterial vasculature consists initially of paired, separate, *longitudinal neural plexi* supplied cranially by the trigeminal artery and caudally by the first cervical artery. The caudal supply from the C1 segmental artery is supported by input from the *otic artery* at the level of the acoustic nerve and from the *primitive hypoglossal artery* at the level of the XII nerve. These latter two vessels are highly transient and regress early.

The 5- to 6-mm Fetal Stage

The first arch derivative, the mandibular artery, is diminishing in this stage, but the second arch derivative, the hyoid artery, continues to be robust and goes on to play an important role in the genesis of the middle meningeal artery and ophthalmic artery.

A vessel in the area ventral to the first two aortic arches, and which originates from the third arch, becomes prominent and is termed the *ventral pharyngeal artery* (1). This vessel is the precursor of much of the proximal external carotid artery vasculature (Fig. 7-3).

In the hindbrain, the caudal division of the internal carotid artery forms anastomoses with the cranial end of the bilateral—and as yet separate—longitudinal vascular plexi (*longitudinal neural arteries*). These anastomoses will form the posterior communicating artery, and as they emerge, the trigeminal arteries begin to regress. During this stage, the *primitive (lateral) dorsal ophthalmic artery* originating from the proximal internal carotid artery is becoming identifiable. This is one of the two embryonic sources of vascular supply to the developing eye discussed later.

The 7- to 12-mm Fetal Stage

The ventral pharyngeal system becomes more extensive; lingual and thyroidal branches are identifiable (Fig. 7-4). The ventral pharyngeal artery can be conceived of as the precursor of the lower or proximal external carotid artery. The upper portion of the external carotid artery evolves later from the hyoid artery.

In the posterior neck, longitudinal anastomoses between the cervical segmental arteries begin to fuse and form the longitudinally disposed vertebral arteries. Whereas they ultimately form a single dominant vessel, that is, the primitive vertebral artery, ipsilateral parallel longitudinal vertebral channels can persist, which explains the etiology of duplications of the vertebral arteries. More cephalad, the

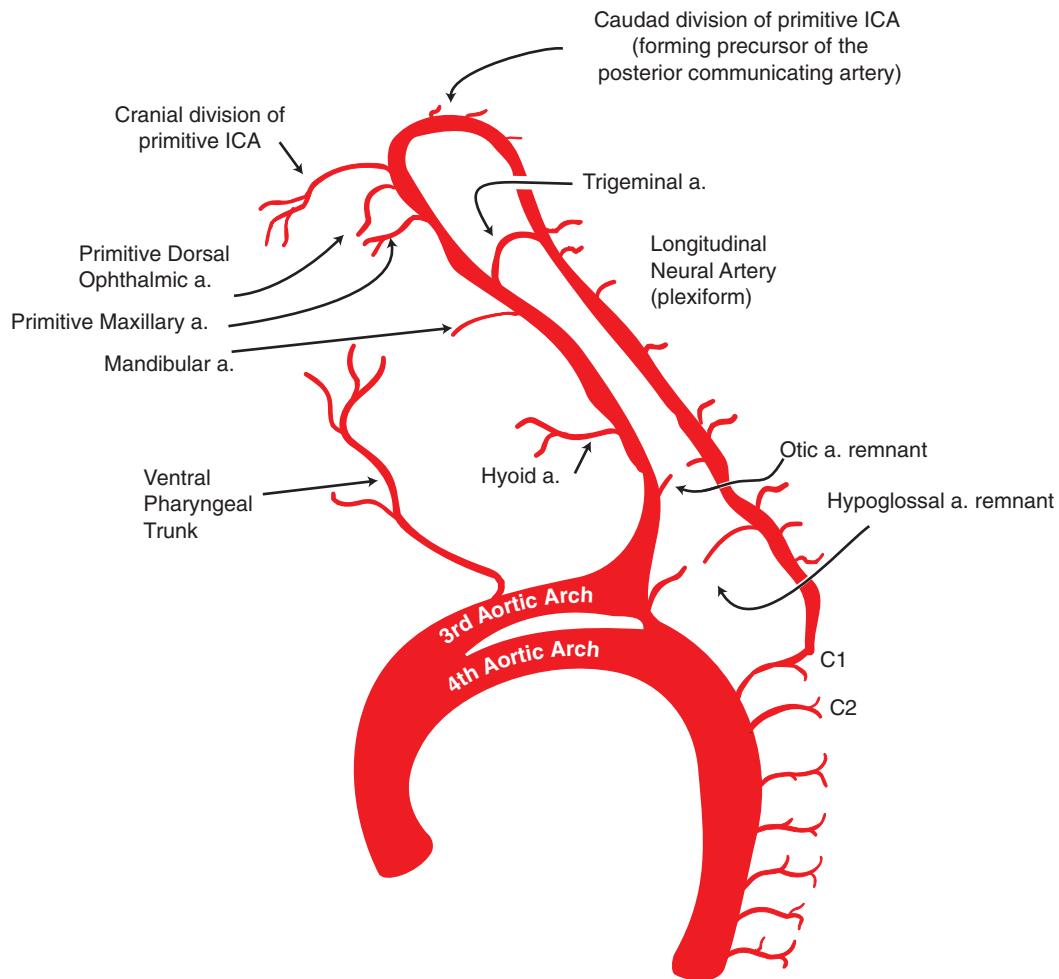


FIGURE 7-3. Embryologic development of cranial arteries at the 5- to 7-mm stage. See text for discussion. Allowing for variability in timing between fetuses, parts of this diagram correlate with Figure 7-1E and F.

longitudinal neural arteries of the hindbrain are still separate from one another for the most part but have begun to form prominent anastomoses across the midline.

The cranial division of the internal carotid artery (i.e., that part thought of in adult form as distal to the origin of the posterior communicating artery) gives a branch with prominent diencephalic supply (i.e., the primitive *anterior choroïdal artery*). More distally, the *middle cerebral artery* is first recognized as multiple twigs branching from the cranial division of the internal carotid artery (i.e., from the anterior cerebral artery). Coalescence of these twigs into a single branch to form the middle cerebral artery trunk occurs later. Persistence of a twig separate from the middle cerebral artery trunk can explain the anomaly of an accessory middle cerebral artery arising from the proximal anterior cerebral artery. A striate artery with a long phylogenetic history is consistently seen arising from the anterior cerebral artery at the level of the anterior communicating artery. It represents the *recurrent artery of Heubner* (13). This represents the supply of the anterior cerebral artery, well recognized in many lower species, to the medial and anterior parts of the paleostriatum.

The cranial division (anterior cerebral artery) also gives a branch, the *ventral (nasal) primitive ophthalmic artery*, directed toward the cranial and ventral parts of the optic

plexus. By a process of anastomotic connections, the origin of the primitive ventral ophthalmic artery later migrates proximally from the anterior cerebral artery to the internal carotid artery to assume the paraclinoid location typically seen in adult life.

The 12- to 14-mm Fetal Stage

The developments of the hyoid artery and, in particular, of its principal branch, the stapedial artery, shape the appearance of the distal external carotid artery circulation and middle meningeal artery. The fate of the stapedial artery also determines the nature, location, and extent of anastomotic connections between the middle meningeal artery and the ophthalmic artery (Fig. 7-5).

The arterial plexus supplying the eye coalesces into two main trunks at this stage. The dorsal ophthalmic artery gives a temporociliary artery supplying the caudodorsal aspect of the optic cup with a hyaloid branch (later to become the central retinal artery) to the fetal ocular cleft. The primitive ventral ophthalmic artery is still in the process of proximal migration and gives a common nasal–ciliary artery as its main trunk.

A plexiform anastomosis between the anterior cerebral arteries is identified at around this time, which will evolve into the anterior communicating artery. When this plexus

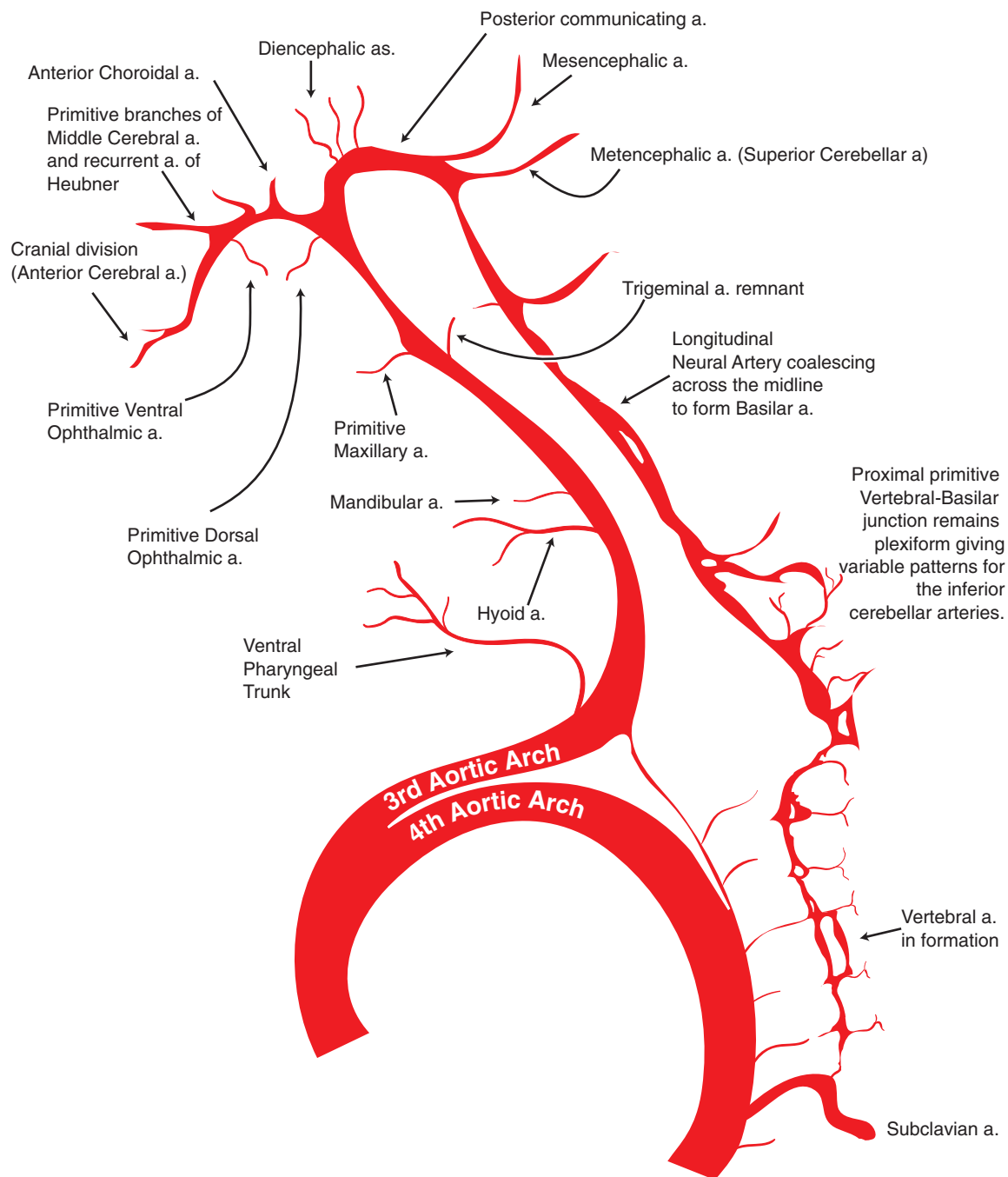


FIGURE 7-4. Embryologic development of cranial arteries at the 9-mm stage. See text for discussion. This diagram correlates with parts of Figure 7-1F and G.

fails to regress into a single channel, the possibility of multiple variations, duplications, or fenestrations of the anterior communicating artery becomes evident.

The 16- to 18-mm Fetal Stage

Fate of the Stapedial Artery

The stapedial artery is now at the zenith of its development. The stapedial artery arises from what will become the proximal intracranial internal carotid artery and runs between the crura of the primitive stapes (Fig. 7-5). In most placental mammals, the stapedial artery is a dominant source of vascular supply to the nonneural structures of the face, orbit,

and dermatocranium for at least some period of time during ontogeny. It may persist into adult life for some species, such as the European hedgehog (14). The fate of the stapedial artery in humans is to undergo a very proximal trunk regression in association with an annexation of its territories by the ventral pharyngeal trunk (external carotid artery) and by the ophthalmic artery.

The stapedial artery arises near the middle ear promontory, and after supplying the back wall of the middle ear cavity, stapedius muscle, and mastoid region, it travels anterolaterally through the intercrural foramen toward the tympanic roof, anterior to the epitympanic recess (14,15).

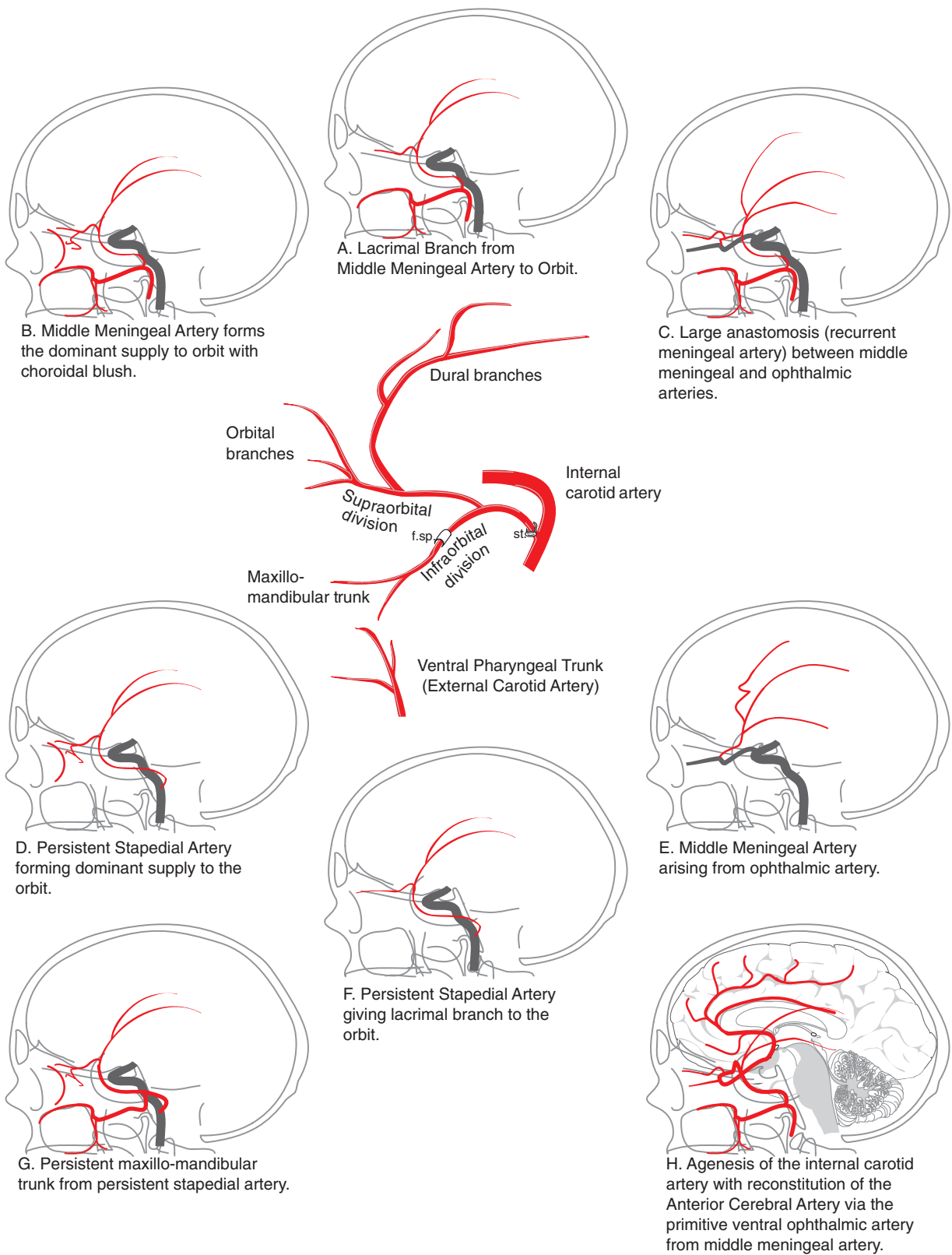


FIGURE 7-5. Development of the hyoid–stapedial artery. A schematic illustration of the hyoid–stapedial artery at its zenith (approximately 20-mm stage) is represented in the center. The maxillomandibular trunk exits from the primitive cranium via a route that will later represent the foramen spinosum (*f.sp.*). The maxillomandibular trunk is annexed by the ventral pharyngeal artery and becomes the distal external carotid artery. The hyoid artery regresses at the level of the stapes (*st.*). The stem of the infraorbital division reverses direction of flow through the foramen spinosum and becomes the trunk of the middle meningeal artery. The orbital branches of the supraorbital division are annexed in varying degrees by the ophthalmic artery. Numerous outcomes are possible in terms of the variability of vessel regressions necessary to achieve the “normal state.” Of the variants illustrated, (D), (G), and (H) are extremely rare.

It divides into a *superior (supraorbital) ramus* and *inferior (infraorbital) ramus*.

Infraorbital Ramus of the Stapedial Artery

The inferior ramus runs in company with the lesser superficial petrosal nerve and exits from the floor of the middle cranial fossa to the infratemporal fossa to support a large area of dermatocranial supply through its large *maxillomandibular branch*. This trunk forms prominent anastomoses with the ventral pharyngeal trunk (proximal external carotid artery), which therefore becomes the dominant supply to this territory when the stapedial artery undergoes proximal regression at the level of the middle ear. The segment of vessel representing the transcranial connection between the inferior ramus of the stapedial artery and the exocranial territory will reverse flow after this annexation and corresponds in adult life with the stem of the middle meningeal artery traversing the foramen spinosum. The stem of the hyoid trunk and stapedial artery proximal to the point of regression becomes the caroticotympanic branch of the internal carotid artery. The segment of the stapedial artery immediately distal to the point of regression will reverse flow after the annexation and corresponds with the tympanic branch of the middle meningeal artery in adult life (16).

Supraorbital Ramus of the Stapedial Artery

The superior (supraorbital) ramus of the stapedial artery supplies a large territory of the developing orbit and the primitive dural coverings of the brain. The dural supply is assumed by the external carotid artery when the stapedial artery regresses proximally and corresponds with the territory of the middle meningeal artery. The territory of the supraorbital ramus or artery in the region of the orbit undergoes further changes that influence the development of the ophthalmic artery and its connections with the middle meningeal artery territory.

Evolution of the Dorsal and Ventral Primitive Ophthalmic Arteries

At approximately the 18-mm stage, the ventral primitive ophthalmic artery (from the anterior cerebral artery) has gained the upper hand in dominance of supply to the optic apparatus, and the dorsal ophthalmic artery has begun to regress. By adult life, the dorsal ophthalmic artery is usually represented by an anastomosis, a recurrent meningeal branch, between the ophthalmic artery and the inferolateral trunk of the cavernous internal carotid artery. When the dorsal ophthalmic artery persists or is the dominant vessel, the ophthalmic artery demonstrates a site of origin from the cavernous segment of the internal carotid artery.

With reference to the anastomoses between the ophthalmic artery and supraorbital artery, various patterns may be seen. When the orbital branch of the supraorbital artery divides proximally within the middle cranial fossa, the sphenoid bone, which ossifies later, will allow more than one transosseous route for these vessels. Most commonly, the supraorbital artery (later to become the middle meningeal artery) connects with the ophthalmic artery through the superior orbital fissure via a proximal vessel called the *sphenoidal artery* or *recurrent meningeal artery* (16) or *orbital branch of the middle meningeal artery* (17). In approximately 50% of dissected specimens, there is an additional transosseous foramen (multiple in 5% to 15% of specimens)

lateral to the superior orbital fissure, which allows anastomoses between the middle meningeal artery and the lacrimal division of the ophthalmic artery (17–19). This foramen has been given various names including the *foramen meningo-orbitale* (17,18), the *foramen of Hyrtl* (20), and the *cranio-orbital foramen* (20), and the vessel that traverses it is most commonly called the *meningolacrimal artery* (19). Variable points of regression in the genesis of the middle meningeal artery and the ophthalmic artery can therefore lead to anomalous states, whereby the ophthalmic artery gives rise to the middle meningeal artery or vice versa. Alternatively, the middle meningeal artery may be the dominant source of supply to the ophthalmic artery (the most common arrangement in some species such as the rabbit), or only the lacrimal area of the orbit may be supplied dominantly by the middle meningeal artery. The middle meningeal artery may connect proximally with the ophthalmic artery through the superior orbital fissure and distally through the foramen meningo-orbitale in the same dissection specimens, prompting some authors to deduce that these are separate entities and not variant courses of a single vessel. By recalling that the ventral primitive ophthalmic artery originally arises from the cranial division of the primitive internal carotid artery (i.e., the anterior cerebral artery), the highly unusual possibilities of the ophthalmic artery arising from the anterior cerebral artery (21) and of the anterior cerebral artery being supplied by the orbital branches of the middle meningeal artery can be explained (22) (Fig. 7-5H).

Evolution of the Posterior Circulation

Over a variable period of development between the 9- and 40-mm stages, the *basilar artery* is formed by a midline coalescence of transverse anastomoses between the paired longitudinal neural arteries. Numerous islands or interruptions of this midline fusion can persist into adult life as fenestration of the basilar artery. Variability in the origins and course of the cerebellar arteries is commonly seen in adults, particularly those of the posterior inferior cerebellar artery and anterior inferior cerebellar artery, which form later than the superior cerebellar artery. For instance, a persistent remnant of the primitive trigeminal artery together with an anomalous pattern of regression of the longitudinal neural arterial plexus can combine to give an origin of the anterior inferior cerebellar artery or posterior inferior cerebellar artery from the internal carotid artery. The possibilities and combinations of variations are numerous.

As a general rule (13), origin of the posterior cerebral artery circulation switches from the internal carotid artery to the basilar artery with ascending phylogenetic rank. The form and pattern of the posterior cerebral artery becomes settled in human ontogeny later than that of the other major vessels. As part of the phylogenetic vacillation surrounding this process, variants, in which the posterior cerebral circulation derives from the anterior choroidal artery, the internal carotid artery, and the basilar artery, can be seen. Most commonly, a posterior cerebral artery arising from the internal carotid artery, predominantly or exclusively, is described as being of “fetal origin.”

► VENOUS EMBRYOLOGY

Padgett’s quotation of an earlier author (23) “there is no overstatement in Mall’s picturesque comment that the history

of the arteries is relatively simple when compared with the gyrations the veins undergo” summarizes the complexity of cranial venous embryology. However, the following points can be abstracted in the interests of simplification.

- Unlike the arteries that reach a form resembling the adult configuration at the 40-mm fetal stage, the veins do not reach such a semblance until the 80-mm stage or later. Evolution of the venous system continues into the postnatal period such that an infant may display sinuses or veins not usually seen in adults, for example, the sphenobasal vein or various tentorial sinuses. Alternatively, connections or veins seen in adults may not be identifiable in infants, for example, the cavernous sinus may not yet drain to the superior petrosal sinus, and the lateral mesencephalic vein may not be present at birth. Furthermore, when a prenatal vascular malformation is present, such as a vein of Galen aneurysm or arteriovenous malformation, primitive venous channels or sinuses that normally regress before birth may be present giving the malformation a bizarre venous pattern with unfamiliar connections (24,25).
- With development of the telencephalon at a rate disproportionate to the rest of the brain, expansion posteriorly of the cerebral hemispheres results in a displacement and stretching of the arachnoidal veins posteriorly relative to their site of insertion into the superior sagittal sinus. According to Padget, this phenomenon explains the observation that many draining cortical veins of the cerebral hemispheres drain into the superior sagittal sinus *against* the direction of flow. Additionally, their derivation by a process of being drawn away from the sinus across the cortical surface explains why the major cortical draining veins of the cerebral hemisphere are *superficial* to the pial arteries, in contrast to the smaller pial veins, which lie *beneath* the arteries.
- The torcular Herophili evolves from a venous dural plexus and frequently has a configuration such that the superior sagittal sinus predominantly drains to the right side while the straight sinus may drain to the left. This and other asymmetries favoring accelerated development of the venous system on the right side were ascribed by Padget (5,6) and Okudera (26) to the venous anatomy of the thorax in which venous drainage is more prompt from the right side, in contrast to the left, which is routed via the sinus venosus.
- The cavernous sinus and inferior petrosal sinus develop from the pro-otic sinus, which evolves in association with the venous drainage of the orbit. Initially, it has no part in the venous drainage of intracranial structures, effectively being a rerouting of craniofacial drainage via an intracranial channel. Therefore, venous drainage of areas considered to be associated with the cavernous sinus and its related tributaries in the adult must have an alternative embryologic pathway before connections to the cavernous sinus are established. These pathways are dural sinuses related to the primitive tentorium, which can sometimes persist into adulthood. When the sphenoparietal sinus, for instance, does not connect medially with the cavernous sinus, it may drain posteriorly via a tentorial sinus, sometimes called the *sphenobasal sinus*, *sphenotemporal sinus*, or *ophthalmomeningeal sinus*, to the superior petrosal sinus or transverse sinus. Alternatively, transsphenoidal venous pathways via the foramen

ovale or foramen of Vesalius may connect to the pterygoid plexus.

- The basal vein of Rosenthal is fragmented in its genesis and connects late to the Galenic system. It does not become recognizably formed until the 60- to 80-mm stage and represents the longitudinal confluence of primary pial channels seen in lower vertebrates, which correspond with telencephalic, diencephalic, mesencephalic, metencephalic, and myelencephalic veins. Its drainage is initially laterally (infratentorially) via a “trigeminal vein,” corresponding with the superior petrosal sinus of adulthood, toward the tentorial sinuses. Drainage of the basal vein of Rosenthal primarily to the tentorial sinuses may be seen in adults. The lateral anastomotic mesencephalic vein is a postnatal structure.
- Variant or minor dural sinuses seen occasionally in adults, such as the occipital sinus (extending from the torcular Herophili inferiorly toward the foramen magnum) or the marginal sinus (surrounding the foramen magnum), may be typically prominent at birth and during childhood (26).

▶ ETYMOLOGY OF THE PROATLANTAL AND OTIC ARTERIES

For an artery that is rarely seen, the proatlantal artery draws a great deal of attention to itself and is discussed in a later chapter. The otic artery, considering that it is an urban legend and likely no more, is seen on board examinations, but no place else. Published case reports are somewhat difficult to decipher and appear universally reducible to being a variant of the trigeminal or stapedia systems (27,28). It is, nonetheless, important to recognize primitive carotid–basilar anastomotic variants as their presence can drastically alter the risk profile of a planned surgical or endovascular procedure.

The term *proatlantal* derives from comparative anatomy. The *proatlas* is a rudimentary vertebral structure in some animals intercalated between the atlas and the occipital bone. It is occasionally seen in man. The segmental vessel in this area—the C1 segmental artery—later in development becomes designated as the *proatlantal intersegmental artery*. When this artery persists in adulthood as a major route of supply to the posterior circulation, this variant is called a *proatlantal artery*.

References

1. Congdon ED. Transformation of the aortic-arch system during the development of the human embryo. *Contrib Embryol* 1922; 14:47–110.
2. Padget DH. Designation of the embryonic intersegmental arteries in reference to the vertebral artery and subclavian stem. *Contrib Embryol* 1948;32:205–262.
3. Padget DH. The development of the cranial arteries in the human embryo. *Contrib Embryol* 1948;32:205–262.
4. Padget DH. Designation of the embryonic intersegmental arteries in reference to the vertebral artery and subclavian stem. *Anat Rec* 1954;119(3):349–356.
5. Padget DH. The cranial venous system in man in reference to development, adult configuration, and relation to the arteries. *Am J Anat* 1956;98(3):307–355.
6. Padget DH. The development of the cranial venous system in man, from a viewpoint of comparative anatomy. *Contrib Embryol* 1957;37:80–140.
7. Davis KR. Embolization of epistaxis and juvenile nasopharyngeal angiofibromas. *AJR Am J Roentgenol* 1987;148(1):209–218.

8. Jinkins JR. The vidian artery in childhood tonsillar hypertrophy. *AJNR Am J Neuroradiol* 1988;9(1):141–143.
9. De La Torre E, Mitchell OC, Netsky MG, et al. Anatomic and angiographic study of the vertebral–basilar arterial system in the dog intracranial and extracranial circulations in the dog: Anatomic and angiographic studies. *Am J Anat* 1962;110:187–197.
10. Tracy PT. Unusual intercarotid anastomosis associated with anterior communicating artery aneurysm. Case report. *J Neurosurg* 1987;67(5):765–767.
11. Kishore PR, Kaufman AB, Melichar FA. Intrasellar carotid anastomosis simulating pituitary microadenoma. *Radiology* 1979;132(2):381–383.
12. Smith RR, Kees CJ, Hogg ID. Agenesis of the internal carotid artery with an unusual primitive collateral. Case report. *J Neurosurg* 1972;37(4):460–462.
13. Abbie AA. The morphology of the fore-brain arteries with especial reference to the evolution of the basal ganglia. *J Anat* 1934;68:28–470.
14. Wible JR. The eutherian stapodial artery: Character analysis and implications for superordinal relationships. *Zoological J Linnean Soc* 1987;91:107–135.
15. Diamond MK. Homologies of the stapodial artery in humans, with a reconstruction of the primitive stapodial artery configuration of Euprimates. *Am J Phys Anthropol* 1991;84(4):433–462.
16. Lasjaunias P, Moret J, Manelfe C, et al. Arterial anomalies at the base of the skull. *Neuroradiology* 1977;13(5):267–272.
17. Royle G. A groove in the lateral wall of the orbit. *J Anat* 1973;115(3):461–465.
18. Georgiou C, Cassell MD. The foramen meningo-orbitale and its relationship to the development of the ophthalmic artery. *J Anat* 1992;180(pt 1):119–125.
19. Diamond MK. Homologies of the meningeal–orbital arteries of humans: A reappraisal. *J Anat* 1991;178:223–241.
20. Lasjaunias P. *Craniofacial and Upper Cervical Arteries: Functional Clinical and Angiographic Aspects*. 1st ed. Baltimore: Williams and Wilkins; 1981.
21. Hassler W, Zentner J, Voigt K. Abnormal origin of the ophthalmic artery from the anterior cerebral artery: Neuroradiological and intraoperative findings. *Neuroradiology* 1989;31(1):85–87.
22. Lasjaunias P, Berenstein A. *Surgical Neuroangiography: Functional Anatomy of Craniofacial Arteries*. Berlin: Springer-Verlag; 1987.
23. Mall FP. On the development of the blood vessels of the brain in the human embryo. *Am J Anat* 1904;4:1–18.
24. Mullan S, Mojtahedi S, Johnson DL, et al. Cerebral venous malformation–arteriovenous malformation transition forms. *J Neurosurg* 1996;85(1):9–13.
25. Mullan S, Mojtahedi S, Johnson DL, et al. Embryological basis of some aspects of cerebral vascular fistulas and malformations. *J Neurosurg* 1996;85(1):1–8.
26. Okudera T, Huang YP, Ohta T, et al. Development of posterior fossa dural sinuses, emissary veins, and jugular bulb: Morphological and radiologic study. *AJNR Am J Neuroradiol* 1994;15(10):1871–1883.
27. Bhattacharya JJ, Lamin S, Thammaroj J. Otic or mythic? *AJNR Am J Neuroradiol* 2004;25(1):160–162; author reply 162.
28. Croft HJ. Persistent otic artery. *AJNR Am J Neuroradiol* 2004;25(1):162; author reply 162.

Aortic Arch

Key Points

- The challenges posed by complex aortic anatomy demand specific considerations in choice of introducer catheters.
- It must be emphasized that catheter manipulation in atherosclerotic arches is likely a significant source of embolic complications.

Cerebral angiography can usually be performed without the need for an aortic arch injection. Considering the time, effort, difficulty, and contrast load involved in a pigtail catheter injection in the ascending aorta, and then replacing that catheter with one suitable for selective angiography, the undertaking is usually not worthwhile on a routine basis (1). However, an arch aortogram may prove necessary in the setting of proximal great vessel stenosis, tortuosity, or anatomic variations. This can be accomplished with 30 to 50 mL of contrast. The best projection is usually 30 to 40 degrees in a left anterior oblique projection. It should be considered prospectively in patients in whom proximal stenotic disease is suspected, particularly with cases such as subclavian steal phenomenon, or in patients with congenital heart disease. Additionally, during catheterizations that are proving exceptionally difficult, resorting to an arch aortogram can clarify the anatomy immediately.

The many possible variations of the aortic arch can prove a challenge for catheterization (Fig. 8-1). The most common variations, a bovine arch (Fig. 8-1B and C), origin of the left vertebral artery from the arch (Fig. 8-1H), and an aberrant right subclavian artery (Fig. 8-1K), can be quickly recognized and catheterized without an arch injection.

► BI-INNOMINATE ARTERY

This is a rare entity. The aortic arch has a symmetric appearance with each innominate artery giving a common carotid and subclavian artery (Fig. 8-1D).

► ABERRANT RIGHT SUBCLAVIAN ARTERY

This is a common anomaly and has an association with trisomy 21. The term usually refers to origin of the right subclavian artery from a point distal to the left subclavian artery

(Figs. 8-1K and 8-2). The right vertebral artery will usually arise from the right subclavian artery. The aberrant right subclavian artery may arise from an aortic diverticulum (Kommerell) and pursue a retroesophageal course. It can frequently be recognized by the unusual course taken by the wire and catheter from the thoracic aorta. Frequently, with a simple curved catheter, such as a Berenstein or Davis, it is necessary to park the catheter in the descending aorta pointing toward the origin of the aberrant right subclavian artery, which can then be selected by probing with the wire from a distance. However, be careful as such an appearance of the wire crossing the midline can also be seen with inadvertent catheterization of a right supreme intercostal artery.

With rarer forms of aberrant origin of the right subclavian artery from points more proximal in the aortic arch, the right vertebral artery may arise separately from the arch.

► BICAROTID TRUNK

The right and left carotid arteries may share a common trunk (Figs. 8-3 and 8-4). This is particularly likely in the setting of an aberrant origin of the right subclavian artery. In such instances, the left carotid artery may have a steep recurrent course, making catheterization more difficult.

► DOUBLE AORTIC ARCH

This has a variable anatomy (Fig. 8-5). From an angiographic viewpoint, important factors include the relative size of the two arches, the side of descent, the position of the ductus arteriosus, and the possibility of atresia. Usually, each arch will give off a common carotid artery and a subclavian artery (Fig. 8-1O and P).

► RIGHT AORTIC ARCH

This may be an incidental finding or may be associated with known congenital heart disease or a vascular ring (Fig. 8-6). The descending aorta may be right- or left-sided. The branching pattern is described as a mirror image (Fig. 8-1M) (with a high associated rate of congenital heart disease) or a nonmirror image (Fig. 8-1N) (with an aberrant left subclavian artery). This variant is one of the greatest challenges for cerebral angiography when it is encountered in late adulthood. The carotid vessels can be very proximal in their origin on the aorta and very difficult to catheterize. A curved catheter such as a

(text continues on page 112)

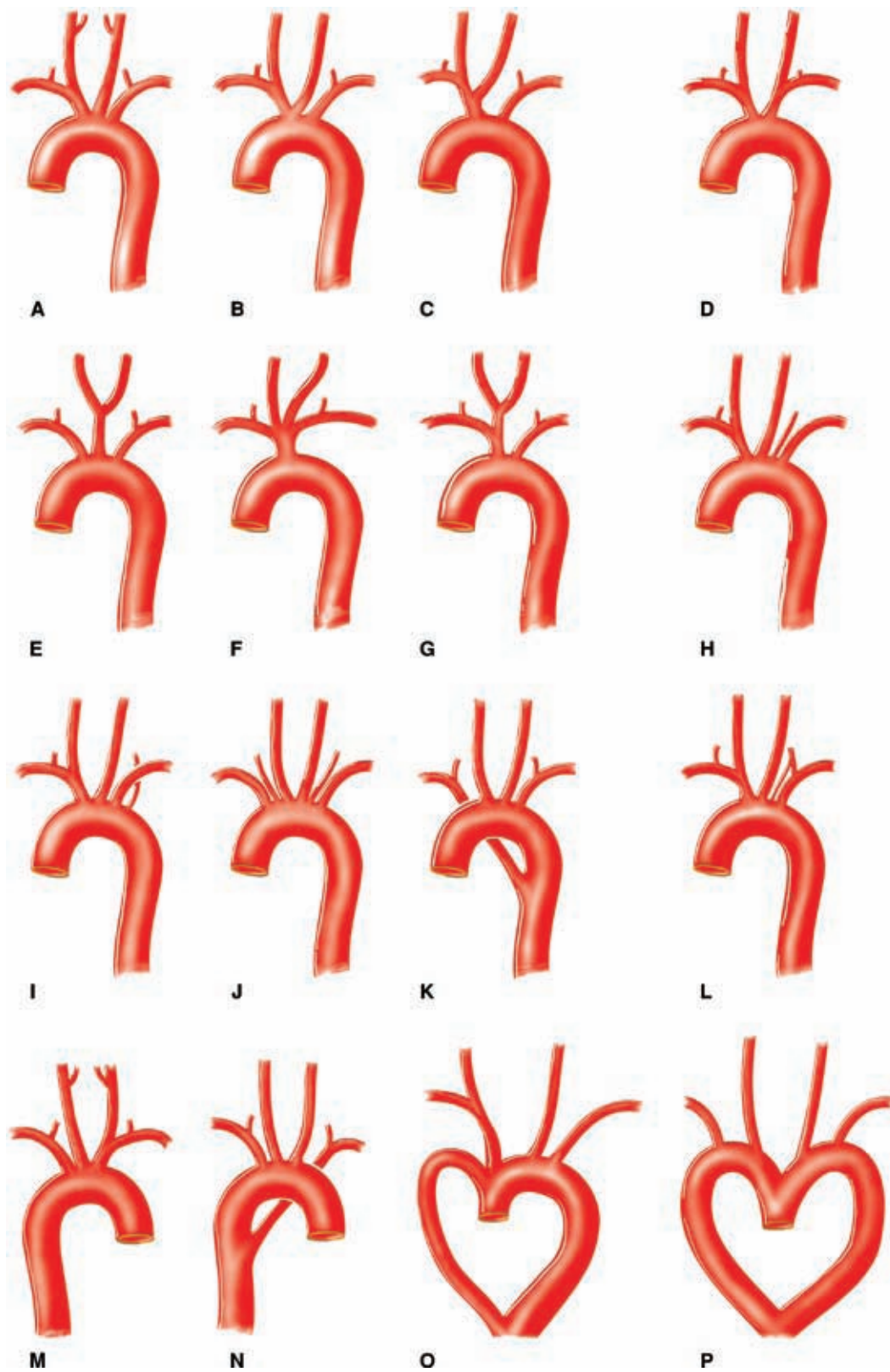


FIGURE 8-1. (A–P) Aortic arch variations and anomalies. Schematic illustration of the major groups of aortic anomalies.



FIGURE 8-2. Aberrant right subclavian artery. Probably the most common variant after a bovine arch. This corresponds with Figure 8-1K.



FIGURE 8-4. Bicarotid trunk with aberrant right subclavian artery. This variant combines with Figure 8.1K and E.



FIGURE 8-3. Bicarotid trunk. Both carotid arteries share a common trunk, distinct from those of the subclavian arteries. This corresponds with Figure 8-1E.



FIGURE 8-5. Double aortic arch. This variant corresponds with Figure 8-1P.



FIGURE 8-6. Right side aortic arch with mirror imaging. This variant corresponds with Figure 8-1M. This variant can be one of the most difficult for selective catheterization because the left-sided branches frequently arise at an extremely sharp angle from the ascending aortic arch.

Simmons I might be the best option. The vessels' ostia can be so close to the aortic valve that there is insufficient space for manipulating a longer tip, such as a Simmons II.

► CAROTID BIFURCATION

The right common carotid artery is usually slightly shorter than the left. The carotid bifurcation is usually at the C3 to C4 level but can occur from C2 down to T2 vertebral levels. From a practical point of view, the angle of the mandible is a useful landmark for initial placement of the tip of the wire during carotid catheterization. In more than 75% of patients, the internal carotid artery lies posterolateral to the external carotid trunk. This means that an ipsilateral anterior oblique projection will usually be the best view for evaluation of the carotid bifurcation in single-plane fluoroscopy rooms.

► VERTEBRAL ARTERY VARIANTS

The vertebral artery is usually the first branch of the subclavian artery (Fig. 8-7). The level at which the vertebral artery enters the canal of the foramen transversarium is determined by which cervical intersegmental artery persists as the vertebral artery. In more than 95% of cases, the left vertebral artery enters the foramen transversarium at the C6 vertebral level. Alternative sites of entry will be seen in cases of variant origin of the left vertebral artery. A left vertebral artery

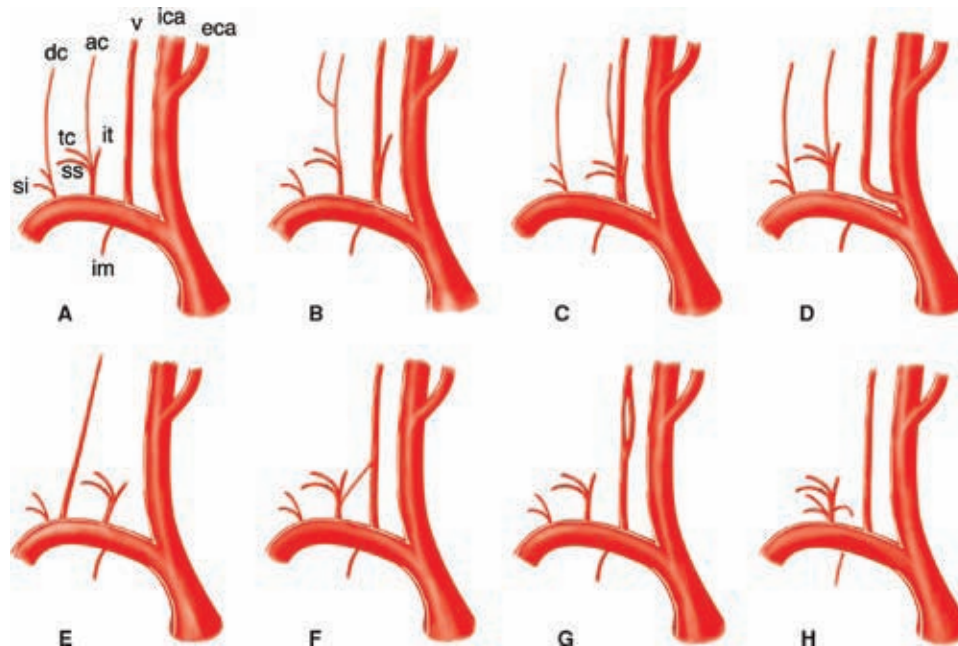


FIGURE 8-7. (A-H) Subclavian artery and cervical trunk variations. A schematic representation of the major variations of the branches of the proximal right subclavian artery of concern during neuroangiographic procedures is provided. (Labels: ica, internal carotid artery; eca, external carotid artery; v, vertebral artery; it, inferior thyroidal artery; ac, ascending cervical artery; dc, deep cervical artery; tc, transverse cervical artery; ss, suprascapular artery; si, superior intercostal artery; im, internal mammary artery.) Variant (A) represents the standard description in which the thyrocervical trunk and the costocervical trunk arise distal to the vertebral artery. In (B), the inferior thyroidal artery shares a common trunk with the vertebral artery, whereas the deep cervical territory is taken over by the ascending cervical artery. In (C), the vertebral artery is represented as a branch of the thyrocervical trunk. In (D), the vertebral artery arises from the proximal common carotid artery. The vertebral artery arises from the right subclavian artery distal to the thyrocervical trunk in (E). In (F), the vertebral artery has a duplicated origin, with a smaller distal limb arising from the thyrocervical trunk. In (G), the vertebral artery has a duplicated segment more distally. In (H), the thyrocervical and costocervical arteries share a common trunk.

arising directly from the aortic arch usually enters the foramen at approximately the C4 level. With a proatlantal intersegmental origin of the vertebral artery from the internal carotid artery (proatlantal artery type I), origin of the vertebral artery from the internal carotid artery joining the usual course of the vertebral artery at C1 will be seen (2). With origin of the artery to the posterior fossa from the external carotid artery corresponding with the C2 level, this is termed a *proatlantal type II artery*. A less common variation is persistence of the C7 intersegmental artery entering the canal at the C7 level and giving an arch origin for the left vertebral artery distal to the left subclavian artery. With the exception of a C4 verte-

bral artery arising from the aortic arch, these variations are rare (3) (see Chapter 14).

References

1. Caplan LR, Wolpert SM. Angiography in patients with occlusive cerebrovascular disease: Views of a stroke neurologist and neuroradiologist. *AJNR Am J Neuroradiol* 1991;12(4):593–601.
2. Legre J, Tapias PL, Nardin JY, et al. Embryonic intersegmental anastomosis between the external carotid and vertebral arteries. Classification problems of the proatlantal artery. *J Neuroradiol* 1980;7(2):97–104.
3. Lippert H, Pabst P. *Arterial Variations in Man*. Munich: J.F. Bergmann Verlag; 1985.

9

The Circle of Willis

Key Point

- An understanding of the variant anatomy and flow dynamics of the Circle of Willis is crucial in many of the treatment decisions we make. Rare variations, on occasion, can represent considerable risks for particular patients.

Although a schema of the circle of Willis is easy to remember, there is enormous interindividual variation in the configuration of this arterial ring. Most intracranial saccular aneurysms occur on the circle of Willis or on the major branches close by. Of these, 82% to 85% occur anterior to a transverse line bisecting the posterior communicating arteries, with the single most common site being the region of the anterior communicating artery complex.

► ANATOMIC RELATIONSHIP TO SURROUNDING STRUCTURES

The relationships of the circle of Willis and particularly those of the anterior cerebral artery and anterior communicating artery to surrounding cisternal and neural structures can be more easily envisioned if it is remembered that the optic structures and the infundibulum are subtended anteriorly *through* the ring of the circle (Figs. 9-1–9-3). The image of the arterial circle as a crab reaching around the optic chiasm with its claws may help to recall this relationship. The optic apparatus enters this ring at an angle that sweeps from posterosuperior to anteroinferior as the optic nerves make their way toward the optic canals. Optic nerve and chiasm displacement or compression with visual field deficits may be frequently seen with aneurysms of the anterior circle of Willis. In fact, Wilbrand's knee (1), the genu of nasal fibers that loop into the posterior aspect of the contralateral optic nerve before continuing posteriorly in the optic tract, was described in 1915 in the setting of optic nerve compression by an aneurysm (although the existence of this loop is disputed (2,3)). The relationship of the optic chiasm to the anterior communicating artery is then easily remembered, as is the way that it derives perforator feeders from the *inferior* aspect of the anterior communicating artery and A1 segments. The tight apposition of the optic tracts and the basal forebrain can be easily remembered and underscore that the anterior choroidal artery must travel

posteromedially *under* the optic tract before turning laterally into the choroidal fissure. The optic tracts will therefore receive perforators from the medial and superior aspects of the anterior choroidal artery and posterior communicating artery below.

The posterior communicating artery usually joins the posterior cerebral artery in front of the midbrain by leaving the posteromedial aspect of the internal carotid artery and ascending posteriorly, superiorly, and slightly medially. The oculomotor nerve lying between the posterior cerebral artery and superior cerebellar artery is a fairly constant relationship; therefore, it follows that the posterior communicating artery is usually superior or superomedial to the oculomotor nerve. Aneurysms in the region of the posterior communicating artery may present frequently with III nerve signs.

The position of the mammillary bodies in front of the midbrain allows one to recall that they are suspended above the posterior aspect of the ring of the circle of Willis. The posterior communicating artery sends between four and eight anterior perforating vessels superiorly toward the diencephalon. The sites of origin of these vessels are more frequently in the anterior half of the posterior communicating artery. The largest identifiable perforator in 80% of dissection specimens terminates between the mammillary bodies and the tuber cinereum. Therefore, this vessel is sometimes called the *pre-mammillary artery* or *thalamotuberous artery* (4).

► VARIATIONS IN THE CIRCLE OF WILLIS

The propensity of the circle of Willis for anomalies and variations is of interest in that the hemodynamic stresses associated with these variations combined with defects in the media at vessel junctions predispose to aneurysm formation (Figs. 9-4 and 9-5). Patients with aneurysms are more likely to have asymmetries or anomalies of the circle of Willis (5). Berry or saccular aneurysms form at a turn or curve in the artery, usually at a bifurcation point (6,7). The impact of hemodynamic stresses on bifurcations in the formation of aneurysms is reflected in the observation that aneurysms most often point in the direction in which flow would have traveled had its course not been deflected by the arterial wall. It is therefore cogent that in the setting of an anterior communicating artery aneurysm with asymmetry of the A1 segments, the aneurysm will point along the line of hemodynamic thrust from the dominant A1 segment.

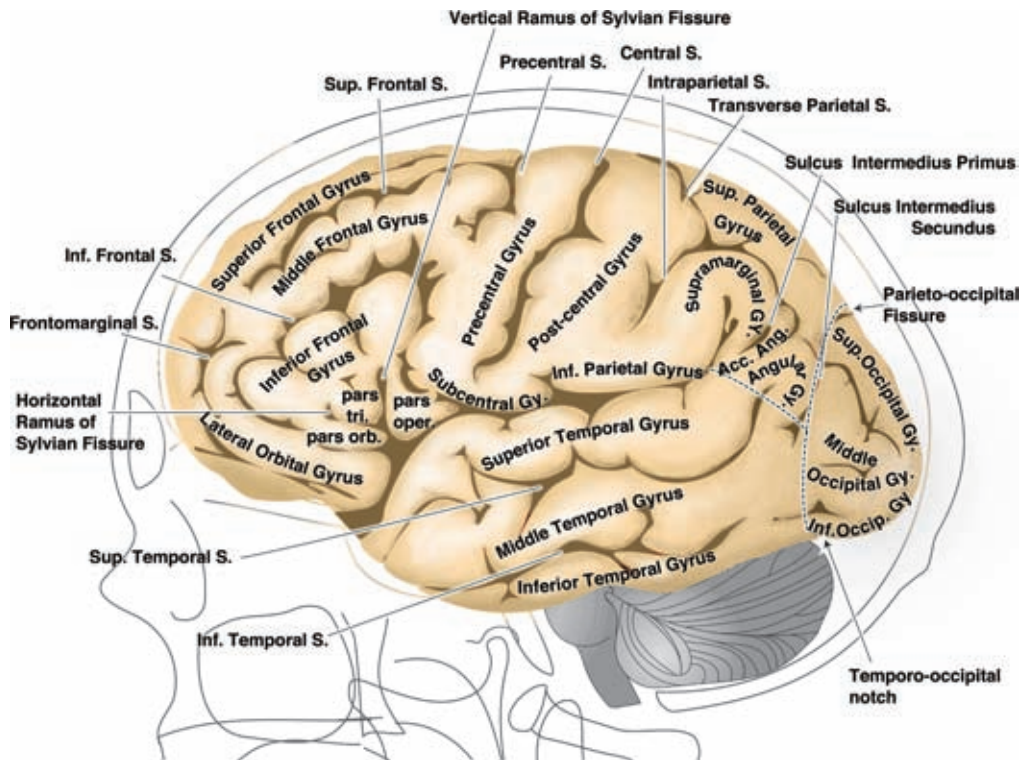


FIGURE 9-1. Lateral view of the brain. Illustration of the lateral aspect of the brain used as a template in subsequent diagrams (S., sulcus; Gy., gyrus; Sup., superior; Inf., inferior; pars orb., pars orbitalis; pars tri., pars triangularis; pars oper., pars opercularis; acc. ang., accessory angular gyrus (variant)).

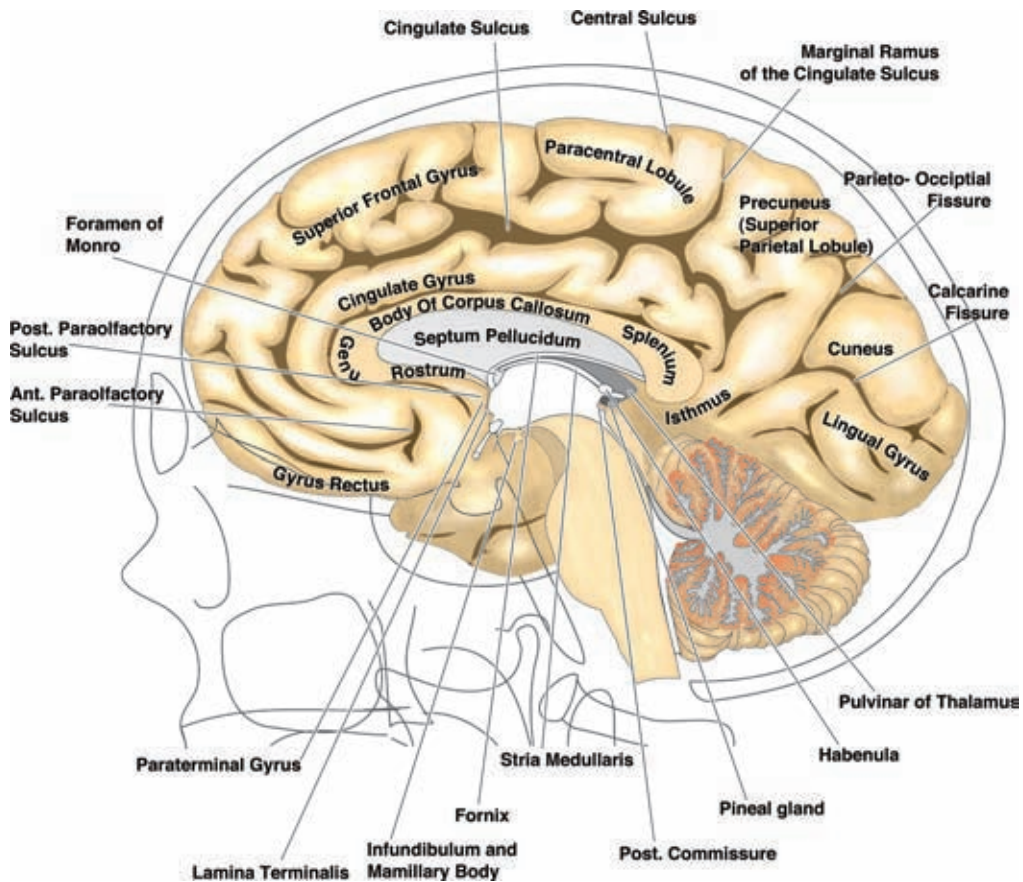


FIGURE 9-2. Midline view of the brain. Illustration of median view of the brain used as a template in later diagrams. Notice in particular the marginal ramus of the cingulate sulcus. This defines the posterior margin of the paracentral lobule, providing a useful means of identifying the central sulcus on sagittal MRI images.

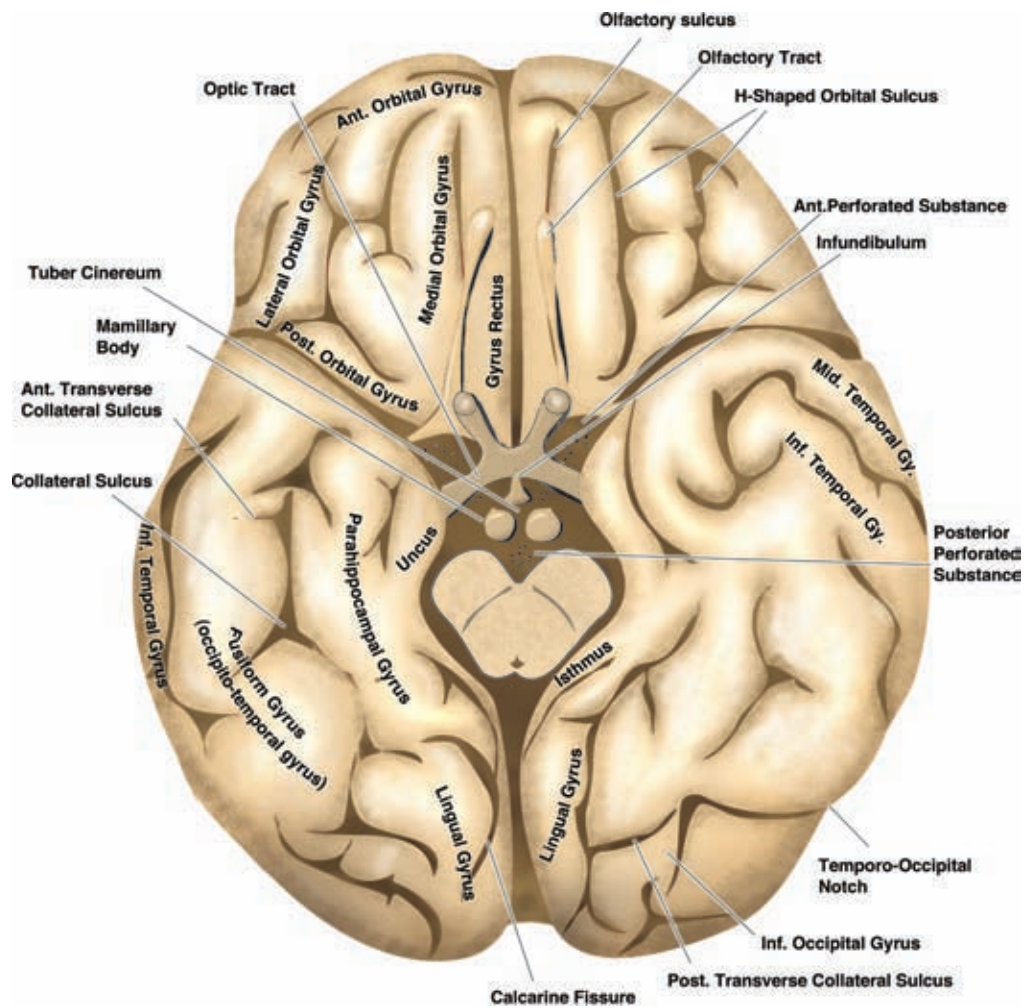


FIGURE 9-3. Base of the brain. Illustration of the base view of the brain used in subsequent diagrams. Notice in particular the relationship of the anterior perforated substance to the olfactory tract. The lenticulostriate arteries enter the base of the brain via the anterior perforated substance and are divided into medial and lateral groups by a line extended posteriorly along the line of the olfactory tracts.

In this circumstance, the aneurysm will project anteriorly and away from the side of the dominant A1, a relationship that is the case in the majority of such aneurysms. Some degree of A1 asymmetry is found in the majority of anterior communicating artery aneurysms (8). Similarly, the effects of hemodynamic stresses contribute, at least in part, to the formation of aneurysms at the sites of variant vessel origins. Aneurysms are associated with anomalous vessels or in situations with higher than usual rates of flow. Aneurysms are seen more frequently than one would expect by coincidence in the setting of variant carotid–vertebrobasilar anastomoses, arterial feeders of arteriovenous malformations, or after occlusion of cranial vessels by balloon closure, surgical ligation, or disease. For instance, an azygous anomaly of the anterior cerebral artery, seen in less than 1% of brains, is associated with a higher than usual rate of aneurysm formation (9–11).

Vessel Size

The circle of Willis is formed by a communication between the left and right carotid intracranial circulations at the

anterior communicating artery and by bilateral communications between the carotid and vertebrobasilar circulations through the posterior communicating arteries. Because of the large number of embryologic steps involved in the evolution of the circle (12) and of each of its many components, variations and anomalies are common. Of these, the most common are those related to size of individual segments. Variability in the circle of Willis is not chaotic but has an order that conforms to hemodynamic principles, replicated in mathematical models (13,14). Therefore, for instance, an inverse relationship in size between the P1 segment of the posterior cerebral artery and the diameter of the posterior communicating artery is commonly seen. Similarly, the anterior communicating artery tends to be largest in the setting of unilateral hypoplasia of an A1 segment. Hillen et al. (15,16) demonstrated that the relationship curve of flow versus vessel diameter is steepest in the 0.5- to 2-mm range. This implies that compensatory hemodynamic effects can be predicted when a component of the circle of Willis is less than 2 mm in diameter.

A “typical” circle of Willis—in which all components are robust in diameter and symmetric—is unusual, being present

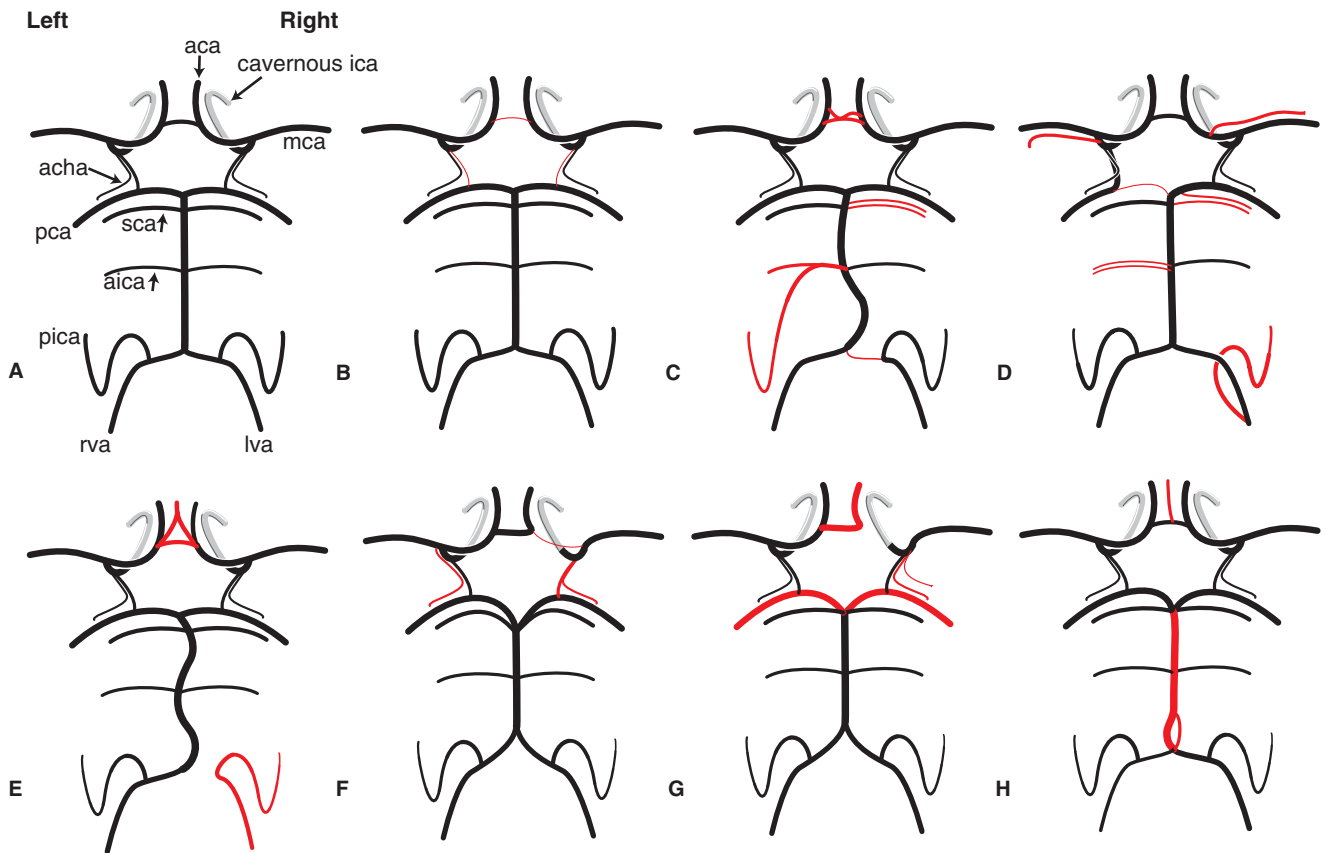


FIGURE 9-4. (A–H) Circle of Willis variations and anomalies. Schematic representation of most of the anomalies and variants discussed in the subsequent chapters. The view is from above; therefore, the anatomic right is on the reader's right. (Labels: aca, anterior cerebral artery; mca, middle cerebral artery; acha, anterior choroidal artery; pca, posterior cerebral artery; sca, superior cerebellar artery; aica, anterior inferior cerebellar artery; pica, posterior inferior cerebellar artery.) **A:** Symmetric pentagonal circle of robust components. **B:** Hypoplastic posterior communicating arteries and anterior communicating artery. **C:** Fenestration/duplication of the anterior communicating artery; duplication of the right superior cerebellar artery; left aica/pica artery; hypoplastic distal right vertebral artery; curve of the basilar artery is with the direction of inflow from the dominant vertebral artery. **D:** Duplicated left middle cerebral artery from internal carotid artery; accessory right middle cerebral artery from A1 segment; fetal left posterior communicating artery coursing more laterally than usual, and related hypoplastic elongated left P1 segment; duplicated right superior cerebellar artery with upper branch arising from P1 segment; duplicated left anterior inferior cerebellar artery; extradural origin of right posterior inferior cerebellar artery. **E:** Fenestrated anterior communicating artery with "triplicated A2"; right vertebral artery terminates in a posterior inferior cerebellar artery. **F:** Hypoplasia of right A1 segment; left anterior choroidal artery arises from left middle cerebral artery; right anterior choroidal artery arises from right posterior communicating artery; low bifurcation of the basilar artery with common stem for right posterior cerebral artery and right superior cerebellar artery. **G:** Complete absence of right A1 segment (rare); duplication of right anterior choroidal artery; low bifurcation of basilar artery. **H:** Triplicated A2; low basilar artery bifurcation; fenestration of the basilar artery. (continued)

on macroscopic examination in only 21% of autopsy specimens (17). When bilateral small posterior communicating arteries are allowed as part of the normal symmetric configuration, only 30% would be "typical" (18); or, if asymmetry of vessel size is allowed with all vessels in the polygon measuring 1 mm or more, the proportion of "normals" is approximately 52% (19). A fetal-type posterior communicating artery, that is, a posterior communicating artery larger than the P1 segment of the posterior cerebral artery or one supplying the bulk of flow to that territory, is seen in 22% to 26% of cases. A 15% incidence of a more definitive fetal posterior cerebral artery is seen (19), whereas a hypoplastic posterior communicating artery is seen in 32% (4,20). When there is a fetal-type

posterior communicating artery present, the P1 segment of the posterior cerebral artery is often longer and more tortuous. In these instances, the course of the fetal posterior communicating artery is more directly posterior off the internal carotid artery or posterolateral compared with the usual posteromedial course of the nonfetal posterior communicating artery. This alters the relationship of the posterior communicating artery to the oculomotor nerve. Instead of running superomedial to the oculomotor nerve, the fetal posterior communicating artery takes a more superior or superolateral course.

Complete absence of the posterior communicating artery is rare during dissection, 0.6% or less (19), although it is more common during angiographic interpretation not to be

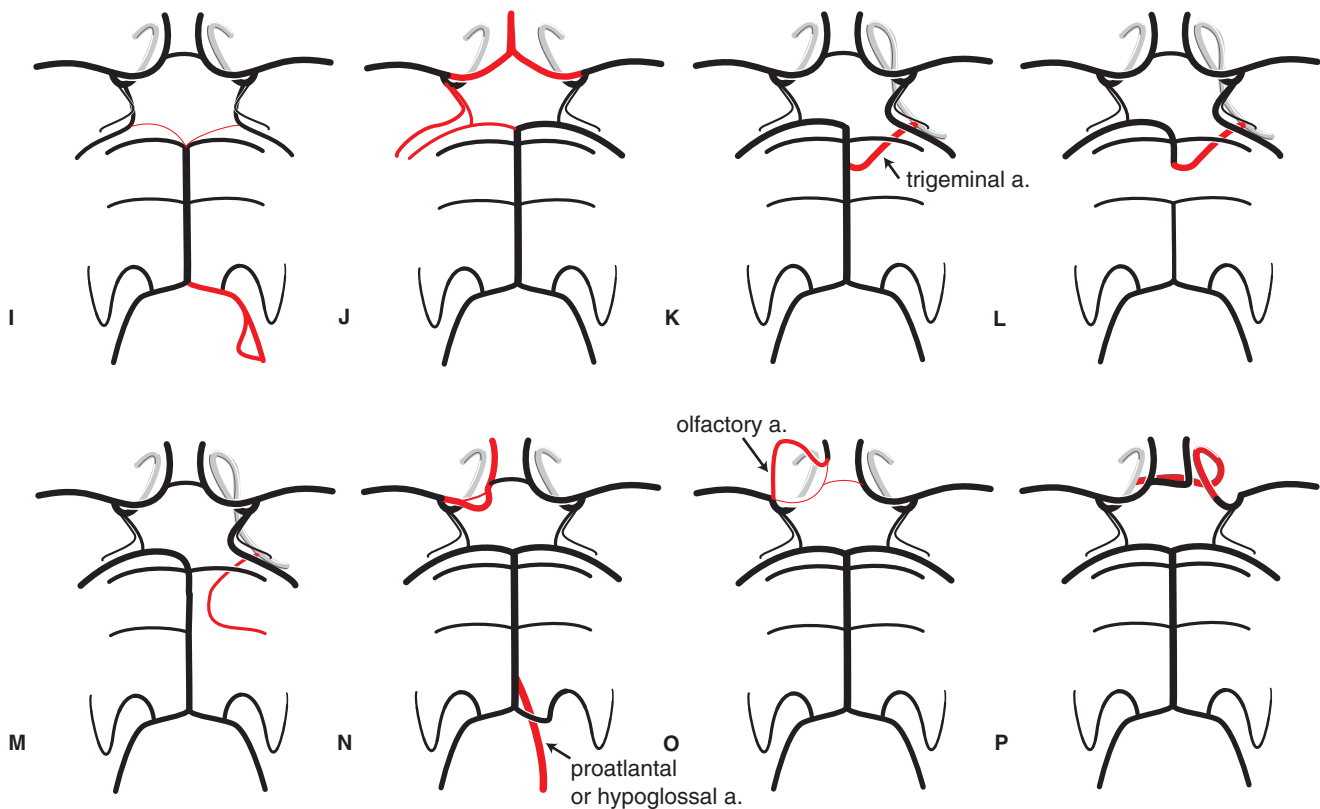


FIGURE 9-4. (CONTINUED) **I:** Bilateral fetal posterior communicating arteries; bilateral hypoplastic P1 segments; duplication of distal right vertebral artery. **J:** Azygous anterior cerebral artery; dominant anterior choroidal artery supply to left hemisphere (duplication of posterior communicating artery). **K:** Trigeminal artery variant with continuity of upper and lower basilar arteries; ipsilateral fetal posterior communicating artery. **L:** Trigeminal artery variant with discontinuity between upper basilar artery and lower basilar artery. **M:** Trigeminal variant giving origin to right anterior inferior cerebellar artery; unrelated origin of right anterior choroidal artery from right posterior communicating artery. **N:** Persistent carotid–vertebral circulation (proatlantal or hypoglossal artery); unrelated duplication of left A1 segment, the larger channel representing an infraoptic course. **O:** Primitive olfactory artery giving dominant supply to anterior cerebral artery. **P:** Agenesis of right internal carotid artery with reconstitution via cavernous branch from left internal carotid artery, most likely representing a persistent primitive maxillary artery.

able to see any evidence of a hemodynamically significant posterior communicating artery.

Alone or in combination with other variations of the circle, a hypoplastic A1 segment may be seen in 12% of autopsy specimens, a hypoplastic P1 segment in 18%, and a hypoplastic anterior communicating artery in 20% (17).

Other Anomalies

Anomalies other than those related to vessel size fall into three general categories: Unusual vessels, duplications of normally present vessels, and origins of normally present vessels from unusual sites.

The anterior communicating artery complex is probably the single most common site in the circle of Willis for anomalous configurations. Duplications or fenestrations of this complex are seen in 9% to 40% of dissections (8,19). Alpers et al. (5,19) found a total incidence of duplications of vessels in the polygon of 19% (Figs. 9-6 and 9-7). A more unusual variant of the anterior communicating artery complex is the *superior anterior communicating artery*, which is occasionally seen more superiorly joining the A2 segments of the distal anterior cerebral arteries.

Duplication of the anterior choroidal artery is reported in 4% of specimen dissections (21). The anterior choroidal artery, alternatively, may share a common origin with or be a branch of the posterior communicating artery. Up to 24% of anterior choroidal arteries may arise from atypical origins, such as the middle cerebral artery, posterior communicating artery, or posterior cerebral artery with some measure of interracial variation (21,22). A more unusual configuration of the anterior choroidal artery is seen when this vessel retains a portion of its embryologic circulation pattern, continuing to supply much of the posterior cerebral hemisphere (Figs. 9-8 and 9-9). The appearance of this large vessel arising distal to the posterior communicating artery from the internal carotid artery with such a cerebral territory is termed by some authors as a *duplicated posterior cerebral artery* or *duplicated posterior communicating artery*. This configuration may explain some or most of the reported cases of “duplication” of the posterior communicating artery because true duplication of the posterior communicating artery is not reported in the microanatomical studies of 50 cadaver brains by Saeki and Rhoton (4). Origin of the posterior communicating artery



FIGURE 9-5. Fenestration of the proximal basilar artery predisposing to aneurysm formation. Aneurysms of the proximal basilar artery of the nature illustrated are frequently associated with fenestrations of the proximal basilar artery. The distal limbs (*arrows*) are partially seen behind the aneurysm dome. They can be difficult to see on 2D imaging, but 3D rotational angiography can be very helpful in these instances. The presence of the fenestration is important with a view to planning of endovascular treatment whether this involves stent placement or balloon assistance.



FIGURE 9-7. Duplicated right middle cerebral artery. A patient presenting with a subarachnoid hemorrhage related to an aneurysm of the anterior communicating artery (*arrow*) demonstrates a “duplicated” appearance of the middle cerebral artery (*arrowheads*). In effect, this is a very proximal bifurcating pattern of the middle cerebral artery but, nevertheless, constitutes an anomaly that might have specific implications for patient treatment in various situations. Note the mandibular artery remnant (*squiggly arrow*) arising from the petrous segment.

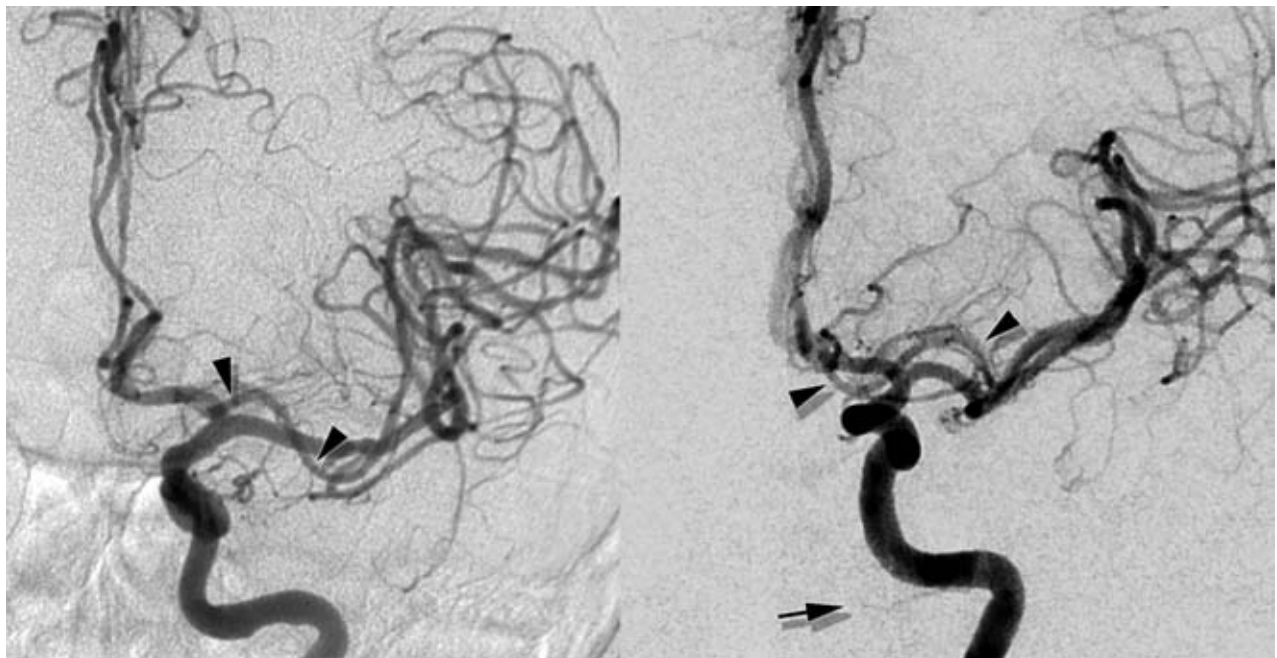


FIGURE 9-6. Accessory left middle cerebral arteries. Two patients demonstrate a variant of the left middle cerebral artery territory with a large vessel (*arrowheads*) arising from the region of the anterior communicating artery and extending laterally parallel to the A1 and M1 segments. The image on the right also demonstrates a small mandibulovidian artery (*arrow*) arising from the petrous carotid artery.

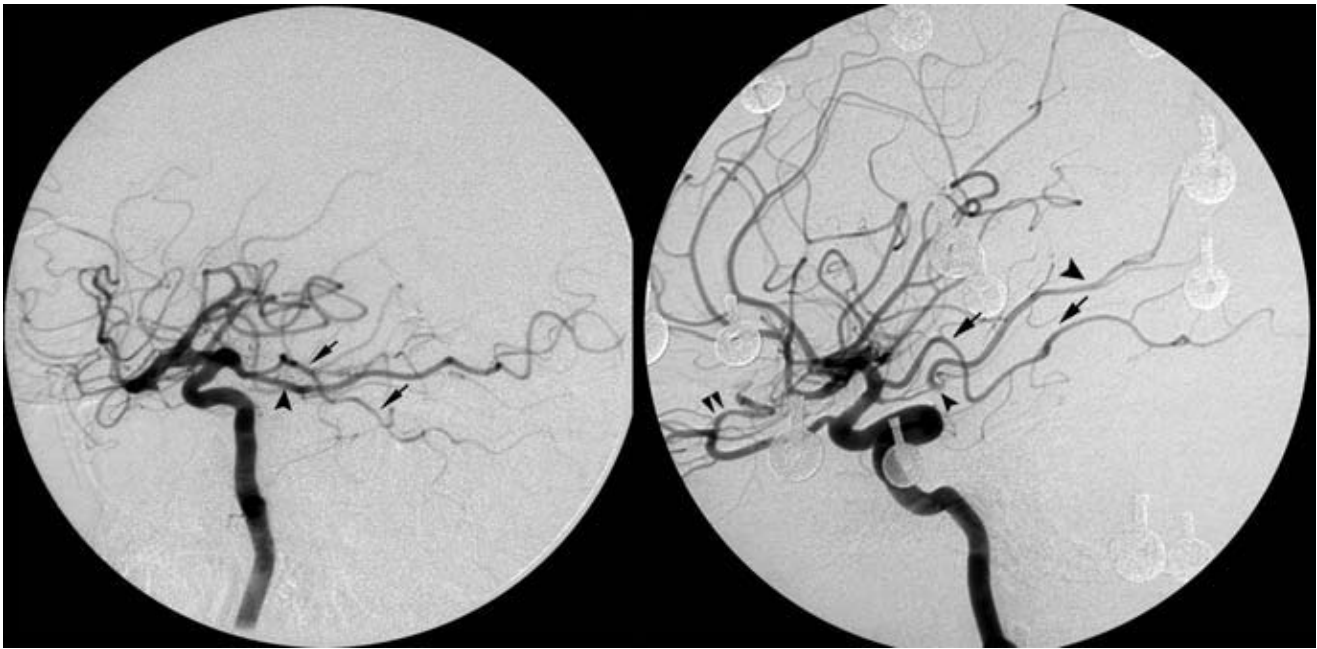


FIGURE 9-8. Duplicated posterior communicating artery. Two patients demonstrate a fairly common variation of the anterior choroidal artery, although not much discussed in the literature. In both cases the posterior communicating artery (*single arrowhead*) arises from the supraclinoid segment of the carotid artery, the one on the reader's left being a fetal type, the right being a hypoplastic posterior communicating artery. The anterior choroidal artery (*arrow*) in both patients is larger than is conventionally seen extending to supply an extended territory of the temporo-occipital region. The patient on the right also shows the middle meningeal artery (*double arrowhead*) arising from the ophthalmic artery.

from the ophthalmic artery during dissection has also been described (23).

Other anomalies of the circle of Willis include the anomalous relationship of the A1 segments to the optic chiasm or nerve, which they usually surmount (Fig. 9-10). Rarely, the A1 segment of one or both sides may loop under the optic structures or may do so in the setting of anomalous origin of the A1 segment from a more proximal point than usual on the supraclinoid internal carotid artery (24). The latter variant probably represents an unusual persistence of the embryologic origin of the ventral ophthalmic artery from the A2 segment, which normally establishes a connection with the supraclinoid internal carotid artery en route to the orbit. The proximal portion of the primitive ventral ophthalmic artery usually regresses, but if there should be a prenatal occlusion of the proximal A1 segment, the primitive ventral ophthalmic artery may persist as this rare infraoptic anomalous course of the anterior cerebral artery.

Prenatal or developmental occlusions of the internal carotid artery are rare and have differing angiographic manifestations (Figs. 9-11 and 9-12). With an occlusion proximal to the usual site of origin of the ophthalmic artery, flow to the ipsilateral hemisphere will most often be supplied by the contralateral carotid and the vertebrobasilar systems. Congenital absence of the internal carotid artery can occasionally be bilateral (25–27).

Fenestrations

Fenestrations of the circle of Willis are due to developmental anomalies of vessel fusion, resulting in a segmental separation of the vessel lumen by a pillar or bridge of varying length (Figs. 9-13–9-15). The gross, anatomic appearance may range from that of two parallel vessels to a subtle dimple on the adventitial surface. Fenestrations of the vertebrobasilar junction are said to be uncommon during clinical angiography, being seen in less than 1% of published studies (28,29) (but if one looks out for them, they are much more common than this given figure). However, fenestrations can be seen in 5% of postmortem angiographic studies (30) and in 7% to 16% of autopsy dissections (6,31). Fenestrations or duplications of the anterior communicating artery complex are seen in up to 40% of dissections (5).

Fenestrations of the other intracranial vessels besides the anterior communicating artery and basilar artery are more commonly seen now than in years past, with modern DSA and rotational angiography including the proximal anterior cerebral artery (32–34), middle cerebral artery (32,35), and rare cases of duplication or fenestration of the internal carotid artery (36–38).

Fenestrations or duplications of the extracranial vessels, particularly of the vertebral artery, have the potential to be confused with different types of carotid–basilar anastomoses

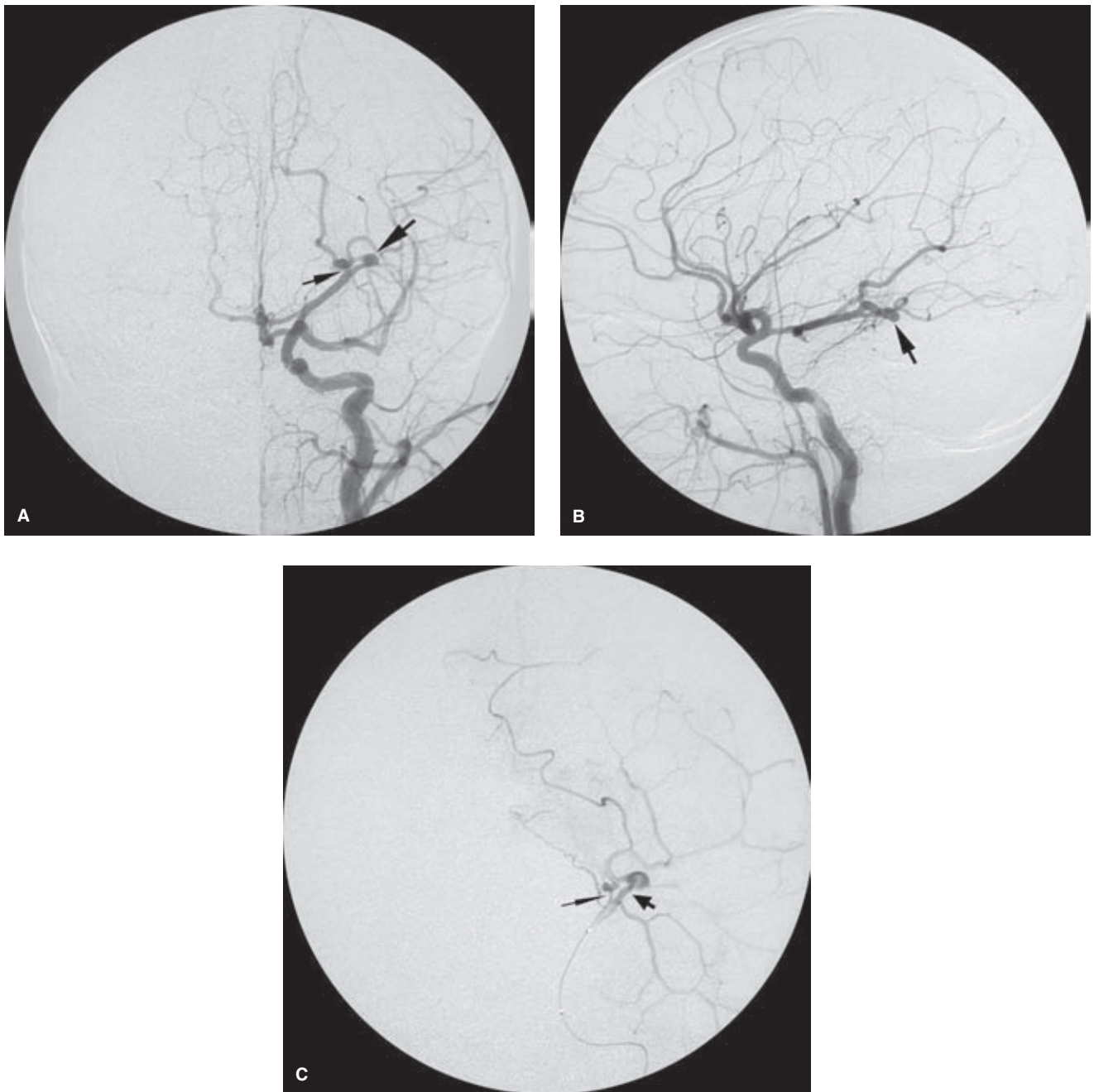


FIGURE 9-9. (A–C) Duplication of the distal posterior cerebral artery. A rarer variant is demonstrated in this patient who presented with a subarachnoid hemorrhage from a dysplastic aneurysm on a knuckle of an arterial moiety of an unusual duplication of the distal cortical branches of the left posterior cerebral artery. The AP (A) and lateral (B) views show a confusing appearance of the posterior cerebral artery filling from a fetal-type posterior communicating artery. The AP view suggests that there are two vessels involved (*arrows* in A) in creating the appearance of a knuckle seen on the lateral view (*arrow* in B). The microcatheter injection (C) more convincingly demonstrated that duplicated nature of this segment of the posterior cerebral artery, with the smaller medial branch (*smaller arrow* in A and C) appearing intact, while the larger dysplastic component (*larger arrow* in A and C) demonstrates the aneurysm.

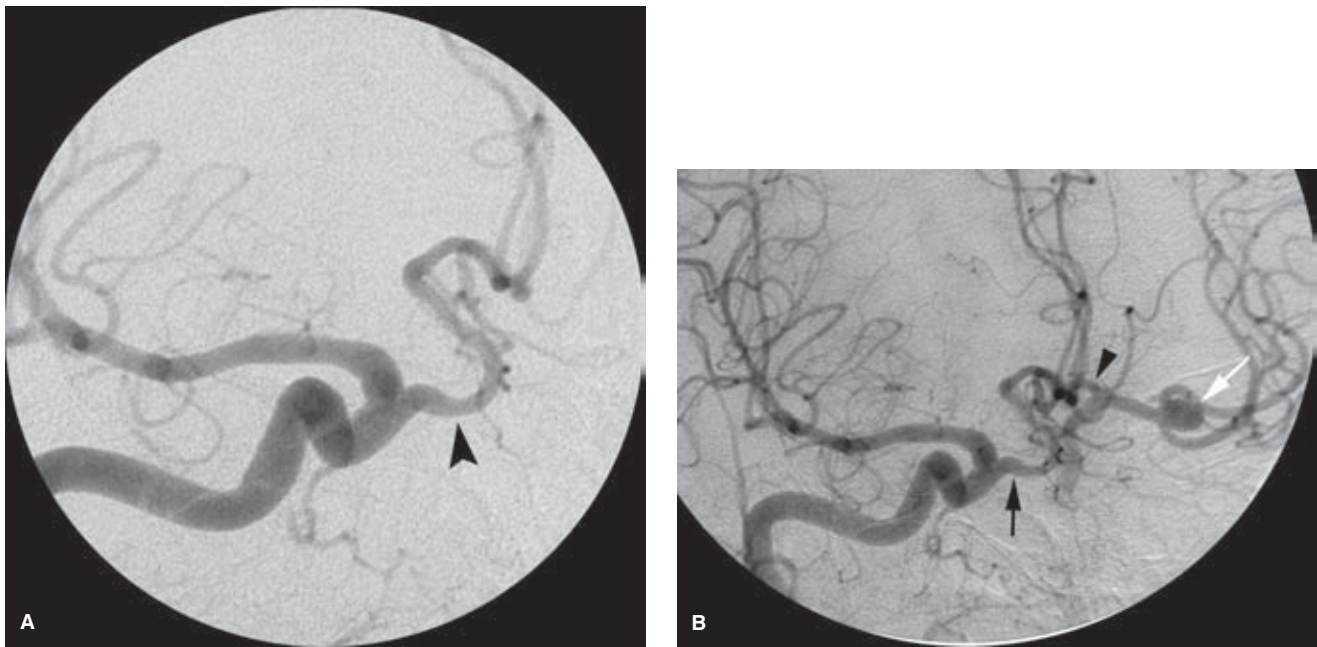


FIGURE 9-10. (A–B) Infraoptic course of the A1 segment of the anterior cerebral artery. An RAO view of the right internal carotid artery in this patient (**A**) shows an unusual appearance of the anterior cerebral artery origin more proximally on the supraclinoid carotid artery (*arrowhead* in **A**). The cross-compression view (**B**) allows comparison between this anomalous A1 (*black arrow* in **B**) and the normal contralateral A1 segment (*arrowhead* in **B**). The right-sided anomaly represents the appearance of an infraoptic A1, unlike the normal supraoptic contralateral homolog. Occasionally, this variant may even pierce the optic nerve or chiasm to gain the suprachiasmatic cistern. Failure to recognize this variant can cause considerable difficulties when the aneurysm being operated on is on the anterior communicating artery. In this instance, the aneurysm was on the contralateral middle cerebral artery bifurcation (*white arrow* in **B**). This variant corresponds partially with Figure 9-4N.

(Figs. 9-16–9-19). In a true fenestration of the vertebral artery—a rare anomaly—both limbs lie within the vertebral canal. Persistent carotid–basilar anastomoses are described more fully in Chapter 10.

► VARIABILITY OF THE TERRITORIES OF THE CEREBRAL ARTERIES

An assumption that the major cerebral arteries have consistent, easily identifiable territories of distribution on axial imaging is probably not correct. When considering whether particular ischemic events may be embolic or related to distal hypoperfusion of the watershed zone at the periphery of a territory, an understanding of the territorial boundaries of each of the major vessels is involved. A watershed infarct is one located in the border zone between two vascular areas, and is related to diminished perfusion of one or both territories (39). If the territories of individual vessels are injected with a marking material, leptomeningeal anastomoses may exaggerate the territory of the injected vessel, an observation known from Heubner (40). Using a technique to inject the three major vessels simultaneously, van der Zwan et al. (41–43) have demonstrated that there is enormous asymmetry and interindividual variability in the cortical and subcortical territories of the major cerebral arteries

(Figs. 9-20–9-22). This variability is directly related to the proximal diameters and peripheral resistance of the major vessels (42). Therefore, in considering the possibility of watershed infarcts on axial images or the possible clinical sequelae of a particular single artery occlusion, one must incorporate a degree of latitude into the understanding of the potential location of the border zone. For instance, using this technique, van der Zwan et al. (43) demonstrated that in approximately 25% of brains, the anterior cerebral artery does not perfuse the anterior limb of the internal capsule or lateral segment of the lentiform nucleus, in which cases the middle cerebral artery territory will be correspondingly larger. Also, the superior part of the precentral gyrus concerned with trunk and leg motor function was supplied by the middle cerebral artery in 4% and by the posterior cerebral artery in 2% of cases, implying that lower extremity weakness is not an exclusive feature of anterior cerebral artery infarction.

With a decrease in perfusion of two neighboring vessels, the location of a distal territory infarct will be different from that caused by a decrease in peripheral perfusion confined to only one of the vessels. The territorial boundaries in life will shift in response to changes in vessel perfusion. They are therefore considered to be dynamic rather than static phenomena.

(text continues on page 130)

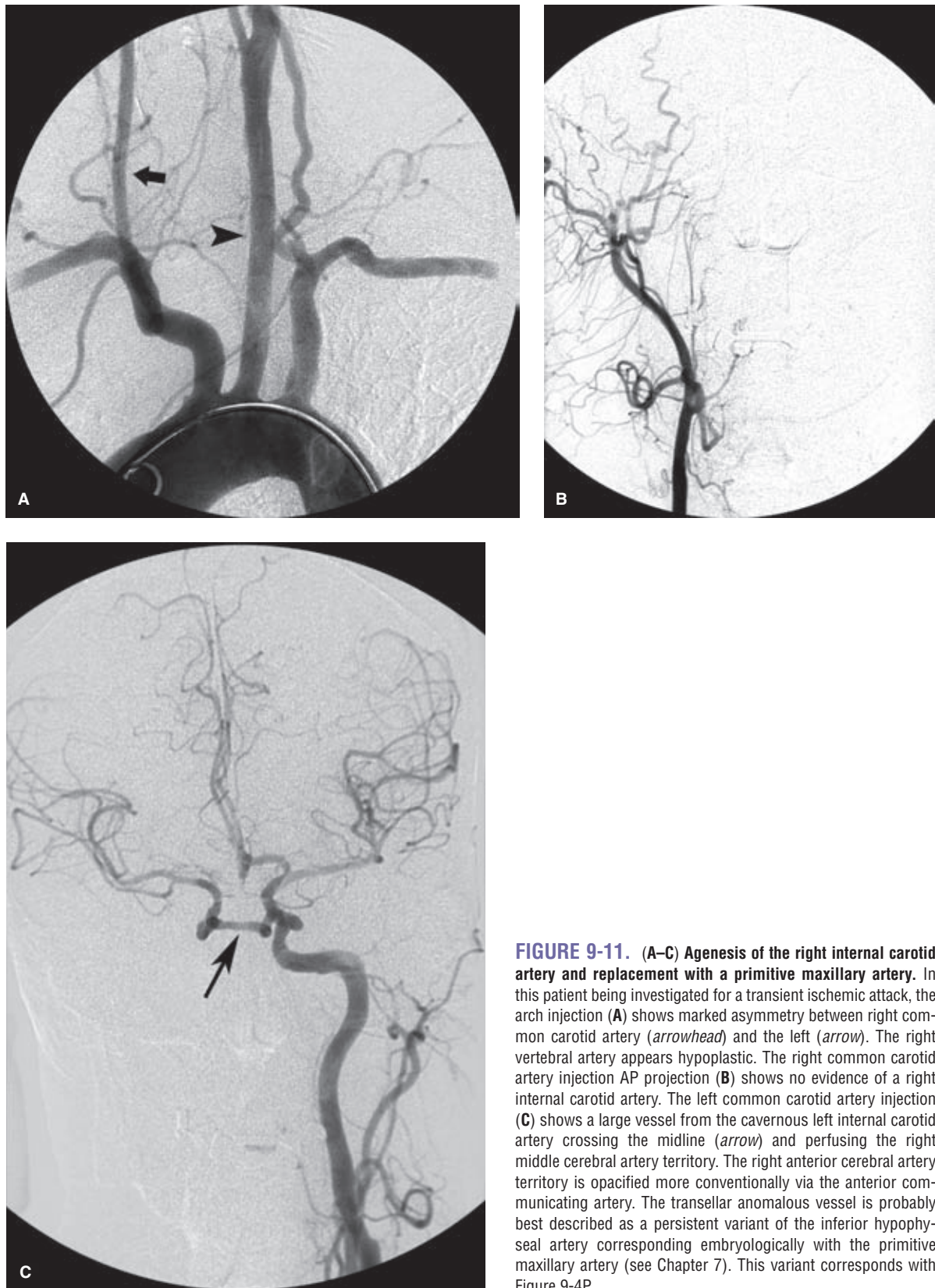


FIGURE 9-11. (A–C) Agenesis of the right internal carotid artery and replacement with a primitive maxillary artery. In this patient being investigated for a transient ischemic attack, the arch injection (A) shows marked asymmetry between right common carotid artery (*arrowhead*) and the left (*arrow*). The right vertebral artery appears hypoplastic. The right common carotid artery injection AP projection (B) shows no evidence of a right internal carotid artery. The left common carotid artery injection (C) shows a large vessel from the cavernous left internal carotid artery crossing the midline (*arrow*) and perfusing the right middle cerebral artery territory. The right anterior cerebral artery territory is opacified more conventionally via the anterior communicating artery. The transellar anomalous vessel is probably best described as a persistent variant of the inferior hypophyseal artery corresponding embryologically with the primitive maxillary artery (see Chapter 7). This variant corresponds with Figure 9-4P.

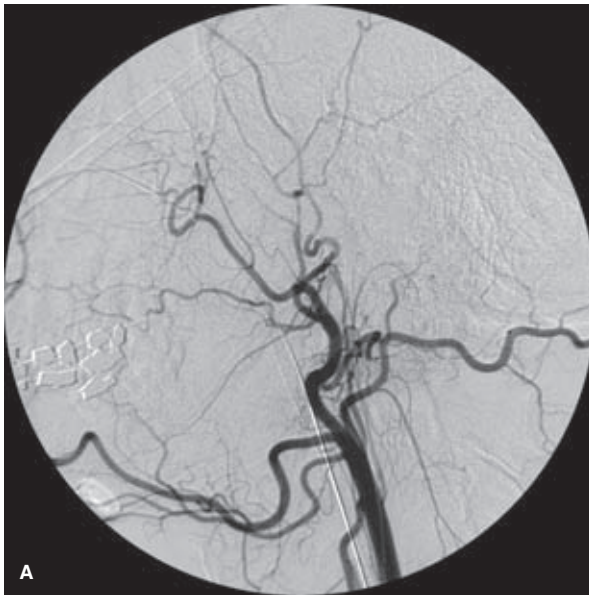
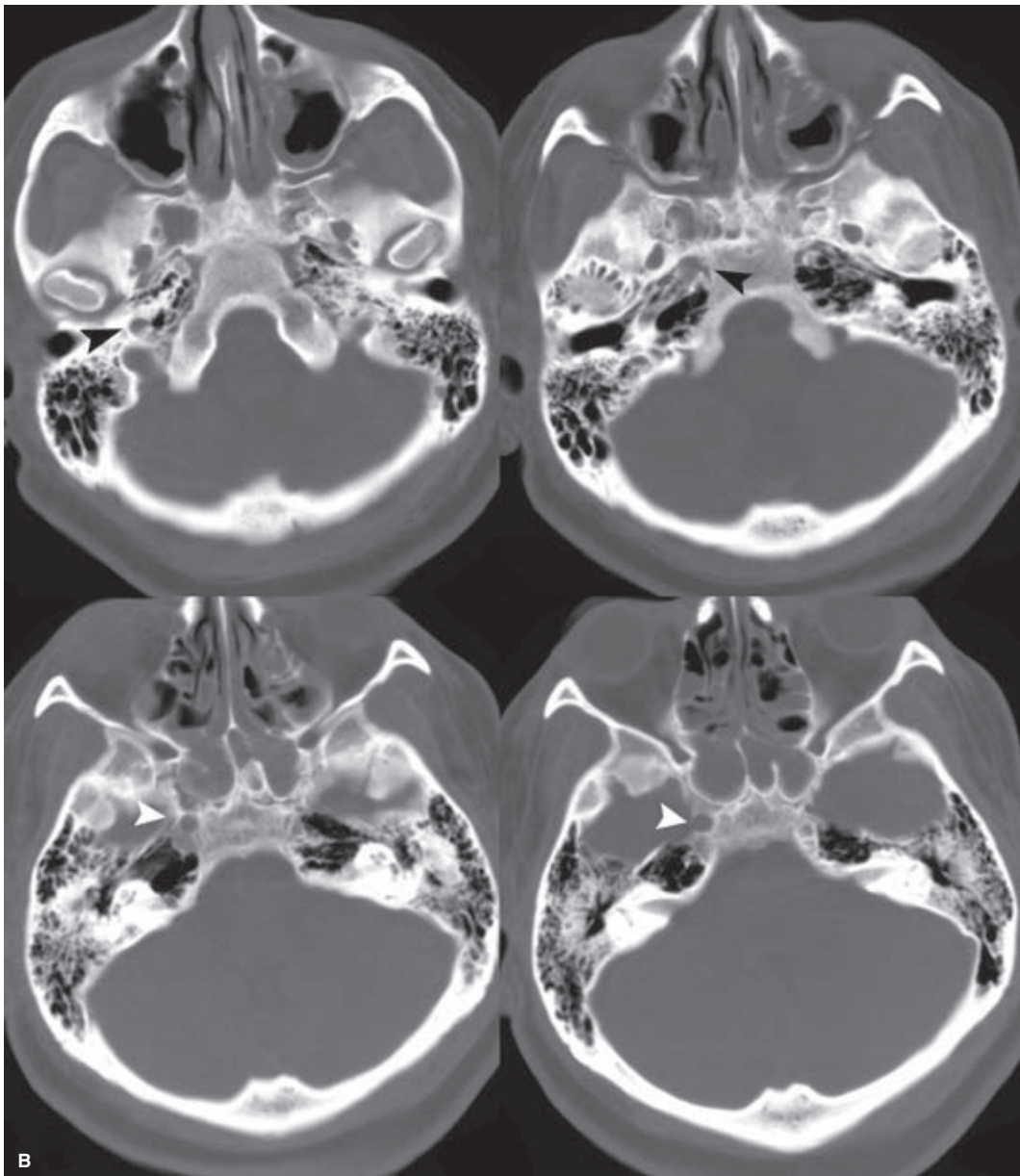


FIGURE 9-12. (A–B) Agenesis of the left internal carotid artery. In this patient, the left common carotid artery injection, lateral view (**A**), shows no evidence of an internal carotid artery. A long-standing occlusion or dissection could have allowed remodeling and healing of the artery to take place to a degree where no angiographic clue to the lost vessel might be apparent, although this would be unusual. In this patient, the CT scan of the skull base (**B**) shows a normal appearance of the bony landmarks for the carotid canal (*white and black arrowheads*) and foramen lacerum on the right, while those landmarks are absent on the left side, indicating that this is likely related to a prenatal event.



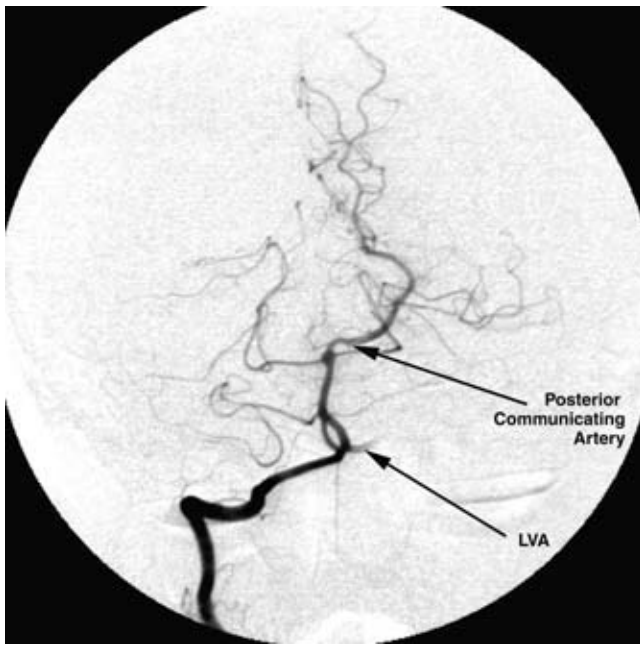


FIGURE 9-13. Fenestration of the basilar artery. An injection of the right vertebral artery demonstrates a fenestration of the proximal basilar artery. The left vertebral artery is briefly opacified (LVA). The right P1 segment is not seen. The left P1 segment is slightly hypoplastic with evidence of widening of the caliber of the posterior cerebral artery distal to the insertion of the posterior communicating artery. In the distal left posterior cerebral artery, there is streaming from posterior communicating artery inflow.



FIGURE 9-15. Fenestration of the left middle cerebral artery. In this patient being evaluated for an aneurysm of the carotid–ophthalmic regions (arrowhead), the proximal M1 segment demonstrates a fenestrated appearance (arrow). A proximal division of the middle cerebral artery with wrapping or overlap of the two arteries could give this appearance on a single view, but the fenestration was confirmed on other images. The implications of a fenestration such as this on a situation such as angioplasty or stenting of the M1 artery for whatever reason are self-evident. Either limb of the fenestrations would be prone to rupture by overexpansion of a device to the expected diameter of the nonfenestrated segment of artery.

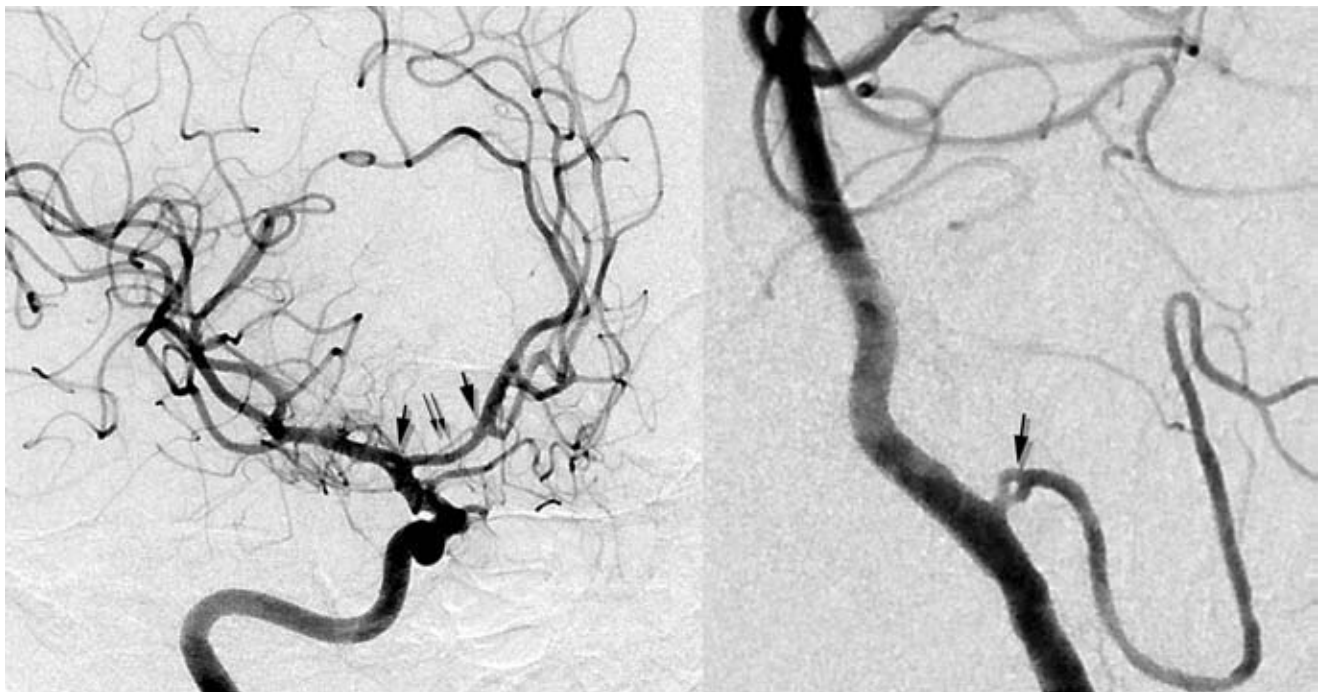


FIGURE 9-14. Fenestrations are commonplace. With improvement quality of DSA imaging and rotational angiography, fenestrations are more commonly seen than before. Frequently they consist of a subtle pillar of intima interrupting the lumen. These two patients show fenestrations of the right A1–A2 junction, the right M1 origin, and the origin of the posterior–inferior cerebellar artery (arrows). The oblique view of the right carotid on the reader's right also gives an unusually clear view of the recurrent artery of Huebner (double arrow) arising from the proximal A2 segment just past the fenestration.

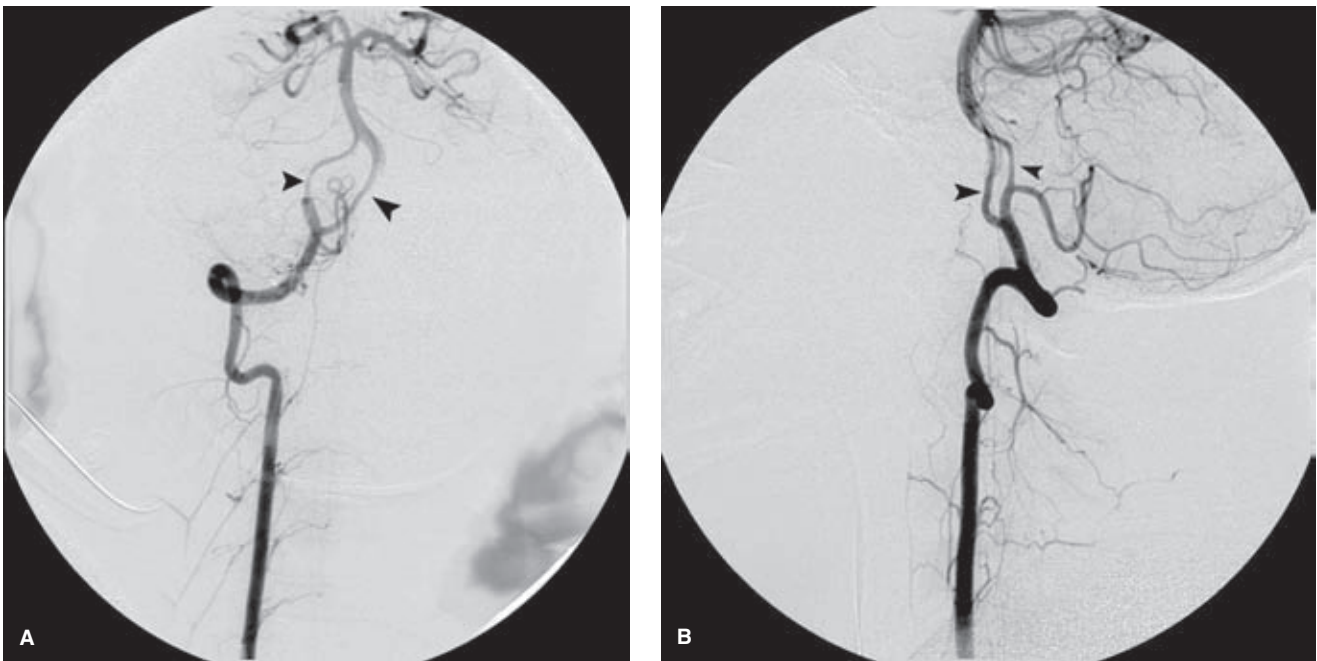


FIGURE 9-16. (A–B) Duplication of the intradural vertebral artery. In this patient, the AP (A) and lateral (B) views of the right vertebral artery injection show an unusual duplication of the vertebral artery (*arrowheads*) distal to the origin of the posterior inferior cerebellar artery, implying that the right vertebral artery has two junctions with the basilar artery. Although this is an unusual variant, it is merely one of degree because it represents the same failure of coalescence of the basilar artery plexus as seen in Figures 9-13 and 9-14. (A microcatheter is present in the basilar artery for an unrelated procedure.)

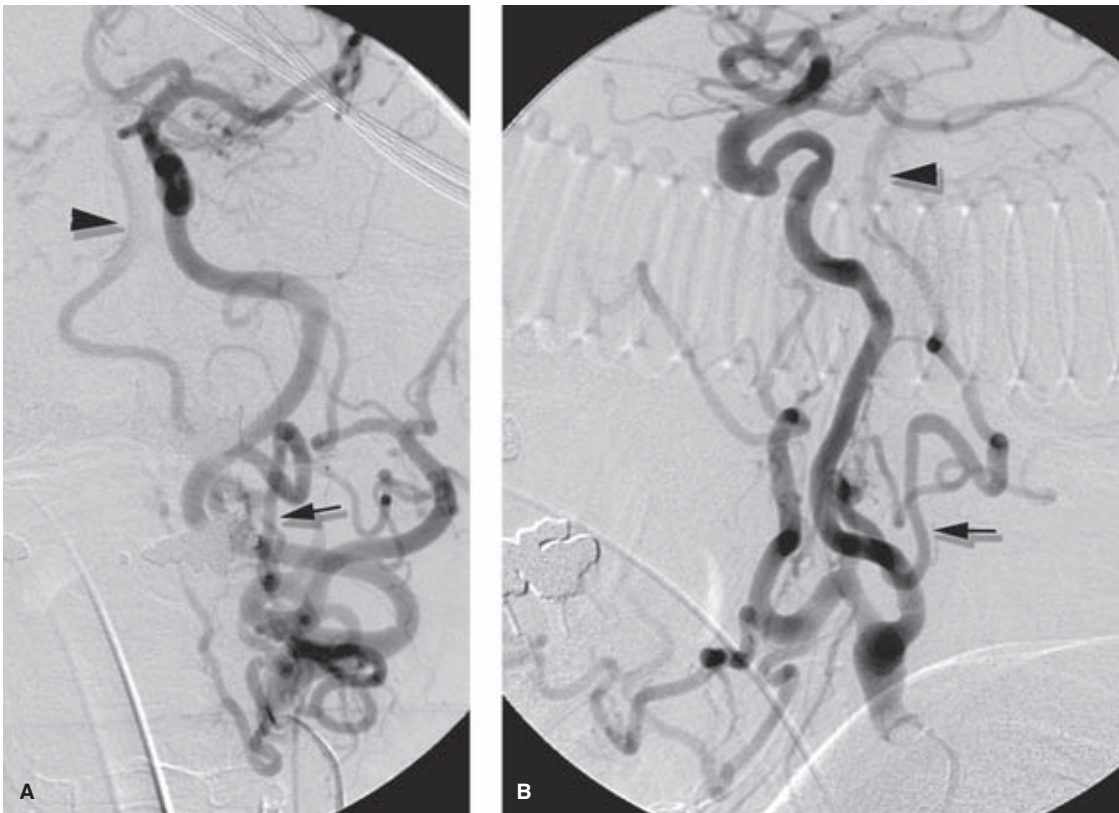


FIGURE 9-17. (A–B) Proatlantal artery. In these AP (A) and lateral (B) views of the left common carotid artery, unusual opacification of the basilar artery is seen (*arrowhead*) due to filling by a branch (*arrow*) of the external carotid artery joining the expected course of the ipsilateral vertebral artery at the C1–C2 level. Carotid–basilar anastomoses are discussed more fully in Chapter 10.

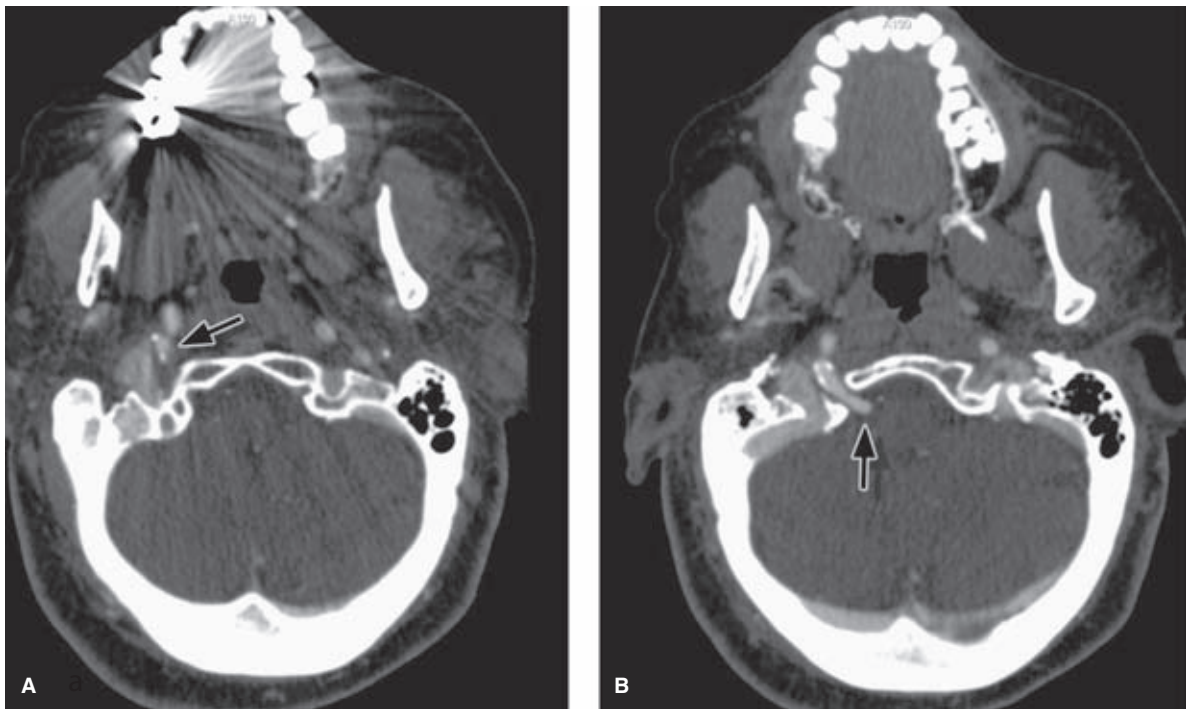


FIGURE 9-18. Hypoglossal artery. Two axial images from a CTA examination demonstrate an unusual vessel arising from the cervical segment of the internal carotid artery and entering the skull through the hypoglossal foramen (*arrow*).

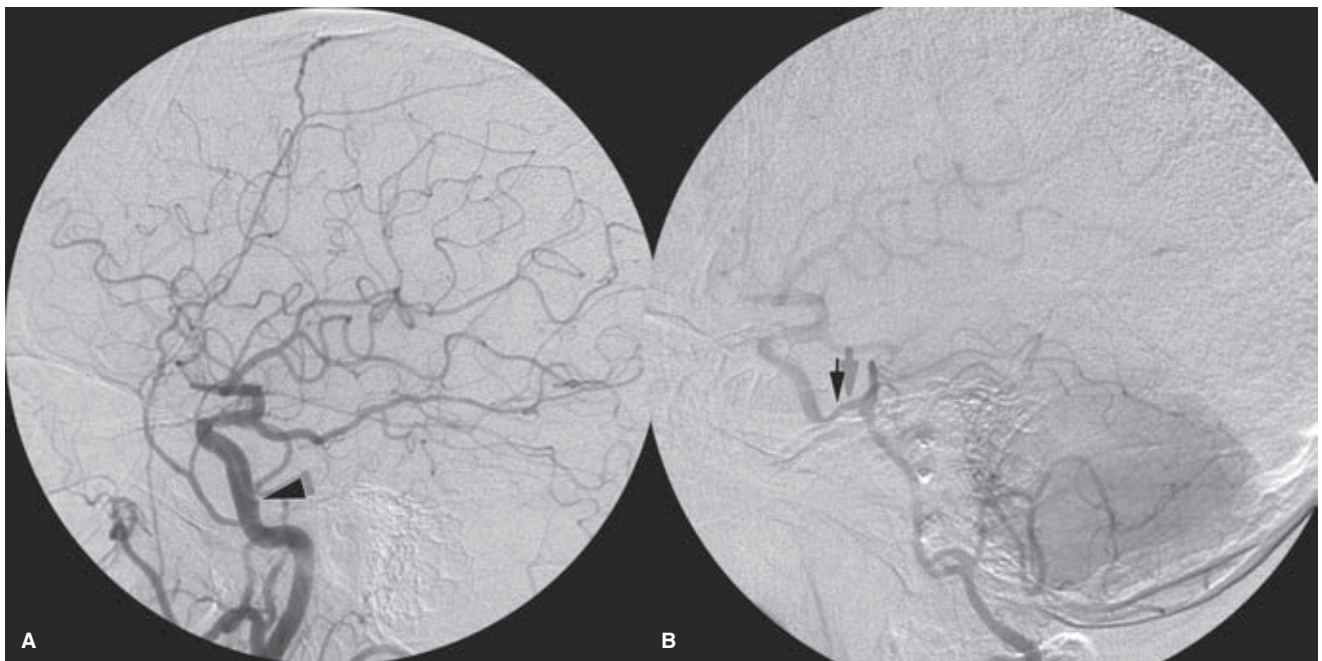


FIGURE 9-19. (A–B) Trigeminal artery. An unconventional view of a trigeminal artery is demonstrated in the patient with a critical stenosis of the right internal carotid artery origin. By virtue of the hemodynamic effect of the carotid stenosis flow in this trigeminal artery is from posterior to anterior, contrary to the usual dynamic state. The inflow from the trigeminal artery causes a flap-like artifact in the carotid artery (*arrowhead*). The lateral view of the left vertebral artery (**B**) demonstrates the complementary view to that of image (**A**) with the trigeminal artery (*arrow*) partially filling the compromised carotid artery.

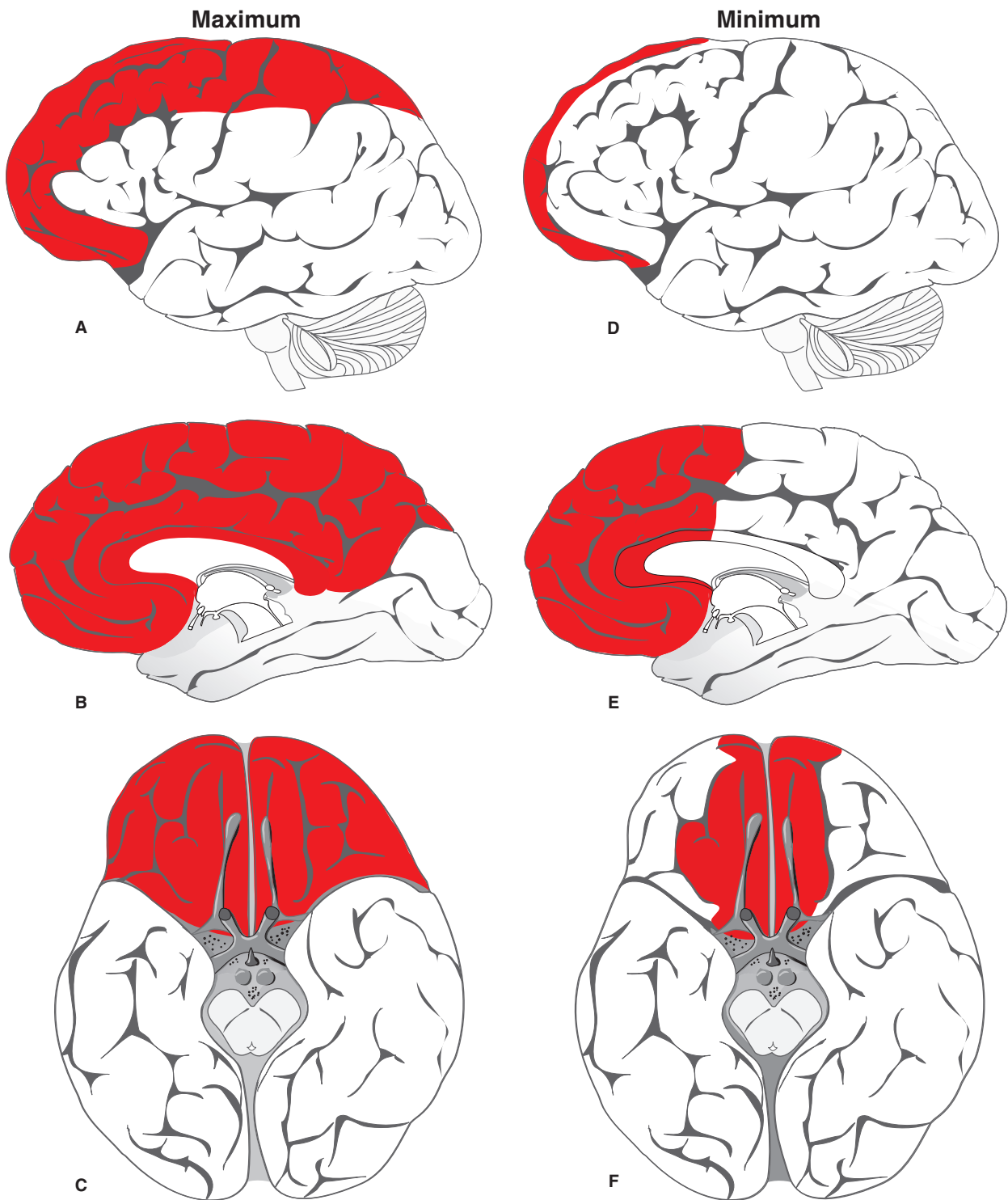


FIGURE 9-20. Extremes of territorial distribution of the anterior cerebral artery. See text for discussion. (Based on Reference 43.)

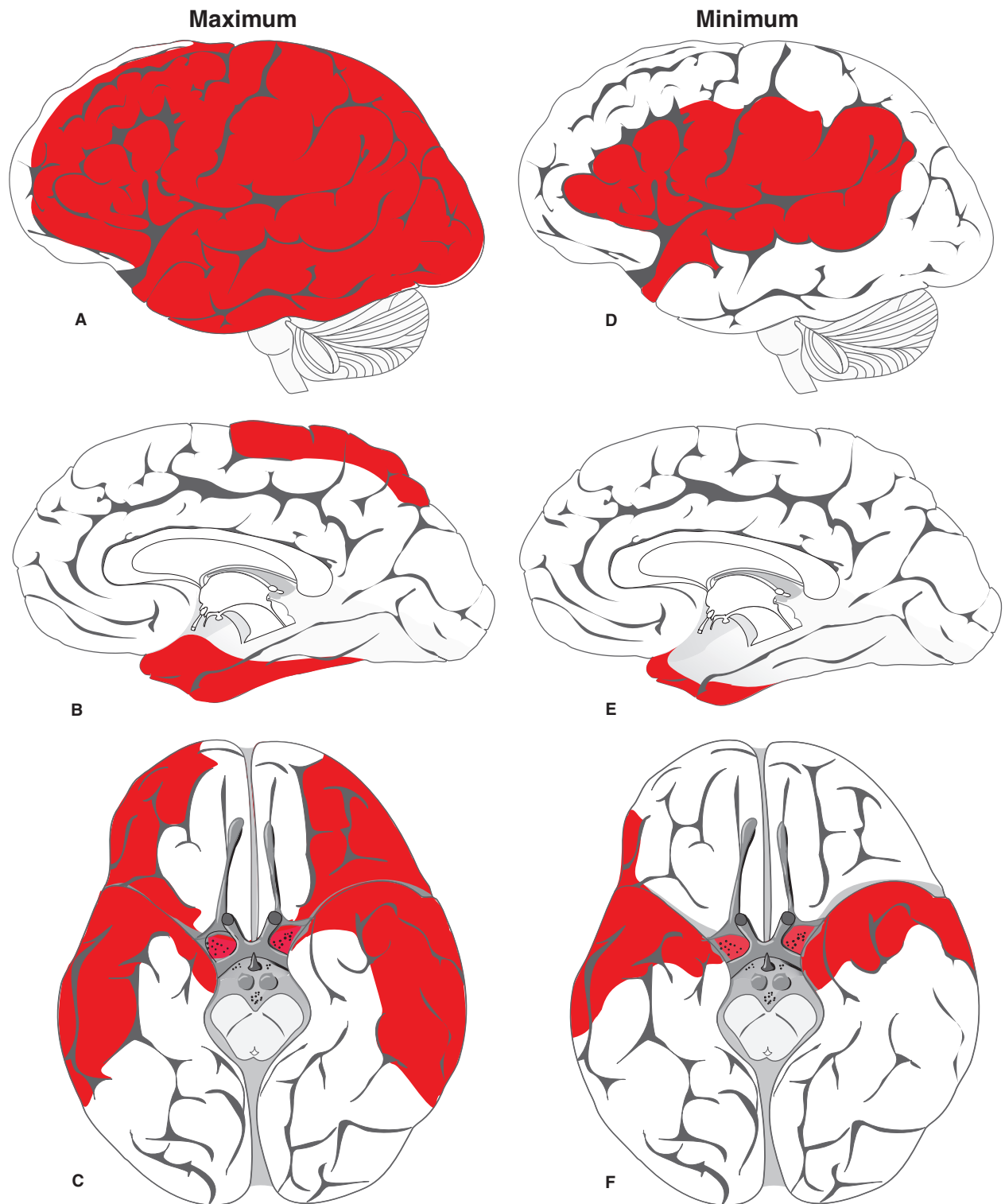


FIGURE 9-21. Extremes of territorial distribution of the middle cerebral artery. See text for discussion.
(Based on Reference 43.)

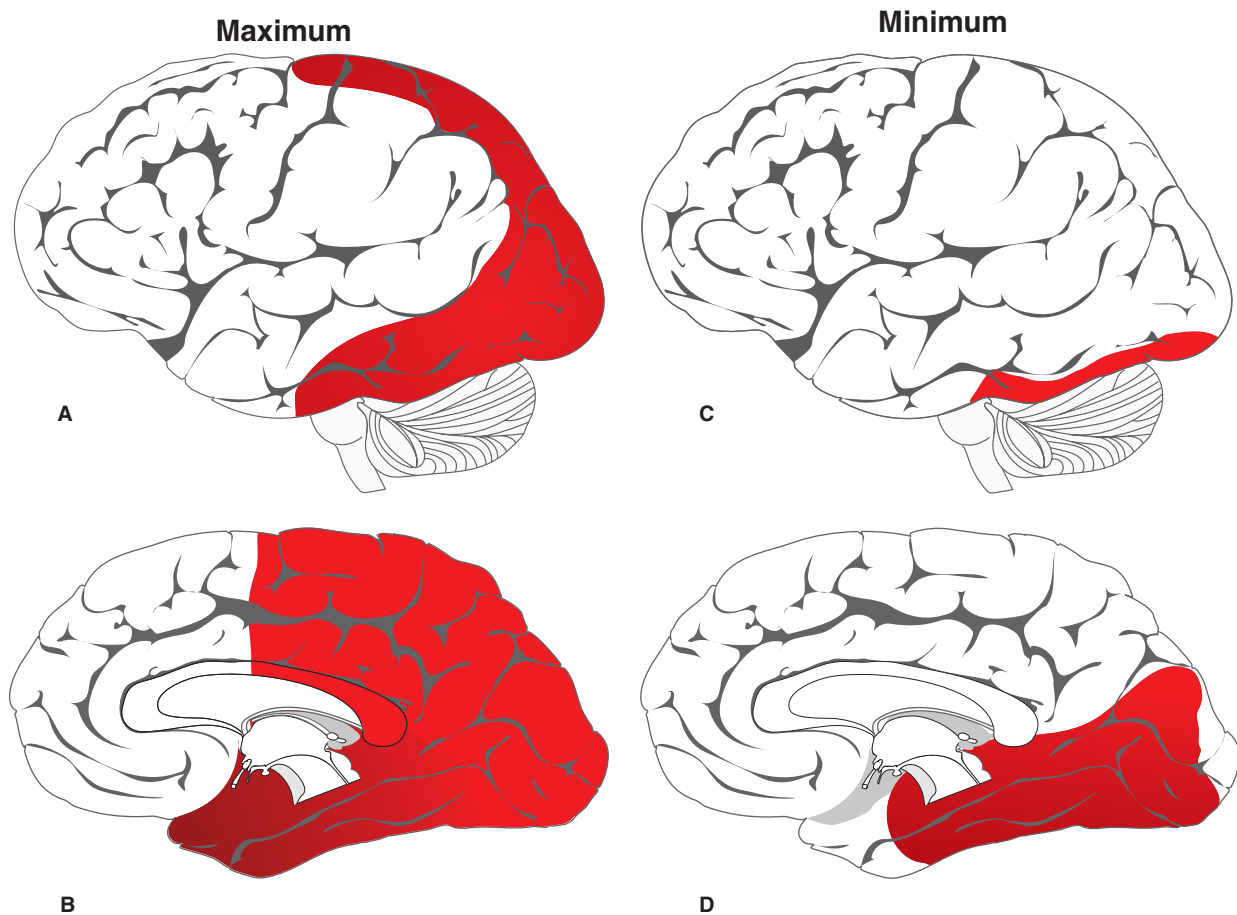


FIGURE 9-22. Extremes of territorial distribution of the posterior cerebral artery. See text for discussion. (Based on Reference 43.)

References

1. Wilbrand H, Saenger A. *Die Neurologie des Auges* 1915.
2. Horton JC. Wilbrand's knee of the primate optic chiasm is an artefact of monocular enucleation. *Trans Am Ophthalmol Soc* 1997;95:579–609.
3. Lee JH, Tobias S, Kwon JT, et al. Wilbrand's knee: Does it exist? *Surg Neurol* 2006;66(1):11–17; discussion 17.
4. Saeki N, Rhoton AL Jr. Microsurgical anatomy of the upper basilar artery and the posterior circle of Willis. *J Neurosurg* 1977;46(5):563–578.
5. Alpers BJ, Berry RG. Circle of Willis in cerebral vascular disorders. The anatomical structure. *Arch Neurol* 1963;8:398–402.
6. Hassler O. Morphological studies on the large cerebral arteries, with reference to the aetiology of subarachnoid haemorrhage. *Acta Psychiatr Scand Suppl* 1961;154:1–145.
7. Rhoton AL Jr. Anatomy of saccular aneurysms. *Surg Neurol* 1980;14(1):59–66.
8. Perlmutter D, Rhoton AL Jr. Microsurgical anatomy of the anterior cerebral-anterior communicating-recurrent artery complex. *J Neurosurg* 1976;45(3):259–272.
9. LeMay M, Gooding CA. The clinical significance of the azygous anterior cerebral artery (A.C.A.). *Am J Roentgenol Radium Ther Nucl Med* 1966;98(3):602–610.
10. Nardi PV, Esposito S, Greco R, et al. Aneurysms of azygous anterior cerebral artery. Report of two cases treated by surgery. *J Neurosurg Sci* 1990;34(1):17–20.
11. Nishio S, Matsushima T, Fukui M, et al. Microsurgical anatomy around the origin of the ophthalmic artery with reference to contralateral pterional surgical approach to the carotid-ophthalmic aneurysm. *Acta Neurochir (Wien)* 1985;76(3–4):82–89.
12. Padgett DH. The development of the cranial arteries in the human embryo. *Contrib Embryol* 1948;32:205–262.
13. Hillen B. The variability of the circulus arteriosus (Willisii): Order or anarchy? *Acta Anat (Basel)* 1987;129(1):74–80.
14. Hillen B, Hoogstraten HW, Van Overbeeke JJ, et al. Functional anatomy of the circulus arteriosus cerebri (Willisii). *Bull Assoc Anat (Nancy)* 1991;75(229):123–126.
15. Hillen B. The variability of the circle of Willis: Univariate and bivariate analysis. *Acta Morphol Neerl Scand* 1986;24(2):87–101.
16. Hillen B, Gaasbeek T, Hoogstraten HW. A mathematical model of the flow in the posterior communicating arteries. *J Biomech* 1982;15(6):441–448.
17. Riggs HE, Rupp C. Variation in form of circle of Willis. The relation of the variations to collateral circulation: Anatomic analysis. *Arch Neurol* 1963;8:8–14.
18. Fisher CM. The circle of Willis: Anatomical variations. *Vasc Dis* 1965;2:99–105.
19. Alpers BJ, Berry RG, Paddison RM. Anatomical studies of the circle of Willis in normal brain. *AMA Arch Neurol Psychiatry* 1959;81(4):409–418.
20. Wollschlaeger G, Wollschlaeger PB. *The Circle of Willis*. Vol 2. St. Louis: CV Mosby; 1974;1171–1201.
21. Otomo E. The anterior choroidal artery. *Arch Neurol* 1965;13(6):656–658.

22. Carpenter MB, Noback CR, Moss ML. The anterior choroidal artery; its origins course, distribution, and variations. *AMA Arch Neurol Psychiatry* 1954;71(6):714–722.
23. Bisaria KK. Anomalies of the posterior communicating artery and their potential clinical significance. *J Neurosurg* 1984;60(3):572–576.
24. Given CA 2nd, Morris PP, Given CA 2nd, et al. Recognition and importance of an infraoptic anterior cerebral artery: Case report. Congenital absence of the internal carotid artery: Case reports and review of the collateral circulation. *AJNR Am J Neuroradiol* 2002;23(3):452–454.
25. Moyes PD. Basilar aneurysm associated with agenesis of the left internal carotid artery. Case report. *J Neurosurg* 1969;30(5):608–611.
26. Tangchai P, Khaoborisut V. Agenesis of internal carotid artery associated with aneurysm of contralateral middle cerebral artery. *Neurology* 1970;20(8):809–812.
27. Given CA 2nd, Huang-Hellinger F, Baker MD, et al. Congenital absence of the internal carotid artery: Case reports and review of the collateral circulation. *AJNR Am J Neuroradiol* 2001;22(10):1953–1959.
28. Takahashi M, Tamakawa Y, Kishikawa T, et al. Fenestration of the basilar artery. Report of three cases and review of the literature. *Radiology* 1973;109(1):79–82.
29. Sanders WP, Sorek PA, Mehta BA. Fenestration of intracranial arteries with special attention to associated aneurysms and other anomalies. *AJNR Am J Neuroradiol* 1993;14(3):675–680.
30. Wollschlaeger G, Wollschlaeger PB, Lucas FV, et al. Experience and result with postmortem cerebral angiography performed as routine procedure of the autopsy. *Am J Roentgenol Radium Ther Nucl Med* 1967;101(1):68–87.
31. Ito J, Washiyama K, Kim CH, et al. Fenestration of the anterior cerebral artery. *Neuroradiology* 1981;21(5):277–280.
32. Ito J, Maeda H, Inoue K, et al. Fenestration of the middle cerebral artery. *Neuroradiology* 1977;13(1):37–39.
33. Baptista AG. Studies on the arteries of the brain. II. The anterior cerebral artery: Some anatomic features and their clinical implications. *Neurology* 1963;13:825–835.
34. Baptista AG. Studies on the arteries of the brain. 3. Circle Of Willis: Morphologic features. *Acta Neurol Scand* 1964;40:398–414.
35. Teal JS, Rumbaugh CL, Bergeron RT, et al. Angiographic demonstration of fenestrations of the intradural intracranial arteries. *Radiology* 1973;106(1):123–126.
36. Killien FC, Wyler AR, Cromwell LD. Duplication of the internal carotid artery. *Neuroradiology* 1980;19(2):101–102.
37. Chess MA, Barsotti JB, Chang JK, et al. Duplication of the extracranial internal carotid artery. *AJNR Am J Neuroradiol* 1995;16(7):1545–1547.
38. Hasegawa T, Kashihara K, Ito H, et al. Fenestration of the internal carotid artery. *Surg Neurol* 1985;23(4):391–395.
39. Zuelch KJ. [On the pathogenesis and localization of cerebral infarction.]. *Zentralbl Neurochir* 1961;21:158–178.
40. Heubner O. Zur Topographie der Ernährungsgebiete der einzelnen Hirnarterien. *Zentralb Med Wissen* 1872;10:816–821.
41. van der Zwan A, Hillen B. Review of the variability of the territories of the major cerebral arteries. *Stroke* 1991;22(8):1078–1084.
42. van der Zwan A, Hillen B, Tulleken CA, et al. A quantitative investigation of the variability of the major cerebral arterial territories. *Stroke* 1993;24(12):1951–1959.
43. van der Zwan A, Hillen B, Tulleken CA, et al. Variability of the territories of the major cerebral arteries. *J Neurosurg* 1992;77(6):927–940.

10

The Internal Carotid Artery

Key Points

- The extracranial and ophthalmic branches of the internal carotid artery exist in a state of actual or potential exchange with distal branches of the external carotid artery. During endovascular interventions one must be ever attentive to the possibility of inadvertent reflux of embolic material in the wrong direction through these routes. The greatest of these risks is with the ophthalmic artery.
- Minor or rare variants of the branches of the internal carotid artery are important to recognize in every patient so that catastrophic surgical and endovascular calamities can be avoided.

The common carotid artery usually bifurcates at the C3–C4 level into an external carotid artery trunk and an internal carotid artery. The bifurcation may be lower, occasionally being seen as low as T2–T3, although such extremes are rare (Fig. 10-1) (1). Most carotid angiograms are performed on older patients in whom the possibility of atherosclerotic change demands an evaluation of the bifurcation before catheterization of the internal carotid artery (Fig. 10-2). There are other situations in which it is prudent or imperative to perform an angiogram of the common carotid bifurcation before further catheterization or wire manipulation. Some of these are obvious and include questions related to the cervical internal carotid artery itself, for example, dissection, pseudoaneurysm, tumor involvement, and the like (Figs. 10-3–10-6). Others are less obvious but encompass any situation in which the final interpretation of the angiogram might be seriously compromised by the presence of a minimal amount of cervical carotid spasm induced by the wire, for example, evaluation of subtle tumor encasement or traumatic injury (Figs. 10-7–10-9).

► ANATOMY OF THE INTERNAL CAROTID ARTERY

The anatomy of the internal carotid artery is described in segments between the common carotid bifurcation in the neck and the supraclinoid internal carotid bifurcation. In ascending order, these consist broadly of the cervical, petrous, precavernous, cavernous, paraclinoid, and supraclinoid segments (Fig. 10-10).

Cervical Segment

This segment spans the common carotid bifurcation to the skull base. At the base of the skull, the internal carotid artery lies anteromedial to the internal jugular vein with which it shares a neurovascular sheath. This sheath also encloses the IX, X, XI, and XII cranial nerves and post-ganglionic sympathetic fibers. The pharyngeal wall lies directly anteromedial to the carotid artery. Instrumentation or biopsy of the Rosenmuller fossa carries a risk of internal carotid injury. Such injuries are also more likely in the setting of unsuspected pharyngeal loops of the internal carotid artery, particularly where these loops have a more medial or directly submucosal course (sometimes confusingly referred to as an aberrant carotid artery, not to be confused with the more important variant by the same name taking a route through the middle ear). Parapharyngeal infections may involve the wall of the carotid artery at this level with a risk of pseudoaneurysm formation. At the exocranial ostium of the carotid canal, the carotid sheath splits into two layers. The inner layer becomes the periosteum of the carotid canal; the outer becomes the exocranial periosteum. The cervical segment usually does not have any branches (Fig. 10-11).

Petrous Segment and Laceral Segment

The petrous segment of the internal carotid artery consists of a vertical and a horizontal portion (Fig. 10-12). It enters the skull base at the exocranial opening of the carotid canal, ascends approximately 1 cm, and then turns anteromedially until it enters the intracranial space at the foramen lacerum. The laceral segment is a continuation of the petrous segment ending at the petrolingual ligament (2,3). The artery is accompanied along its course by the sympathetic fibers of the stellate ganglion and by a venous plexus (4,5). Some of the sympathetic fibers part company from the internal carotid artery at the foramen lacerum and form the deep petrosal nerve. The deep petrosal nerve joins the parasympathetic fibers of the greater superficial petrosal nerve to become the Vidian nerve. This nerve travels anteriorly to the pterygopalatine fossa via the Vidian (pterygoid) canal. Angiographically, branches of the petrous internal carotid artery are uncommon, but at least three possible branches are worth remembering: The carotico-tymppanic branch, the mandibulovidian branch, and the variant stapedia artery.

(text continues on page 137)



FIGURE 10-1. Unusually low bifurcation of the left common carotid artery close to the thoracic inlet. Such anomalies are rare. Variants such as this can be confusing when the catheter is advanced obliviously into the distal external carotid artery without the benefit of an aortic arch injection ahead of time. One can then be deceived into thinking that the vessel injected is the sequelae of an internal carotid artery occlusion or agenesis, unless one retracts the catheter very proximally to find the bifurcation.

FIGURE 10-2. Measurement of carotid artery stenosis. The formula for calculation of the percentage stenosis of the internal carotid artery is illustrated according to the North American Symptomatic Carotid Endarterectomy Trial (NASCET) criteria. In situations of advanced stenosis, the distal diameter of “normal” vessel, (D), is attenuated or underopacified, leading to an underestimation of the percentage stenosis. (Label: N , diameter of stenosis segment at the most severe point.)

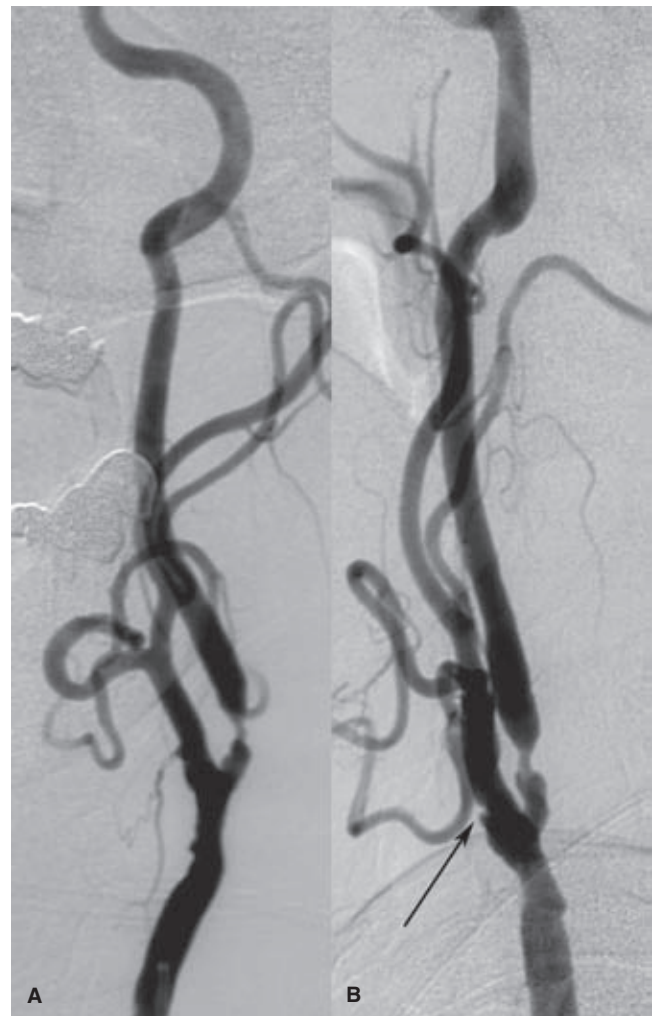
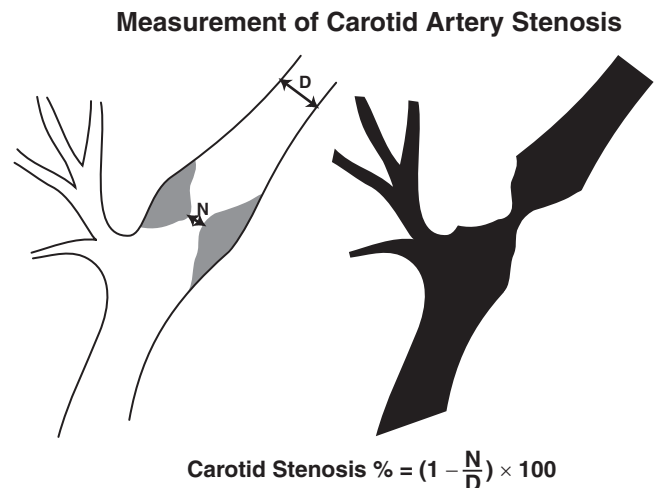


FIGURE 10-3. (A–B) Recurrent left internal carotid artery stenosis following previous endarterectomy. This 81-year-old patient was referred for left carotid angioplasty and stenting with asymptomatic recurrent disease 2 years after a previous endarterectomy with Doppler estimates of 90% stenosis. The hints that this is a previously operated-on artery include the extension of irregularity into the external carotid artery with a “cuff” or shelf-like appearance (*arrow in B*). As is frequently the case, the final calculation of the degree of stenosis depends very much on where one places the calipers, but the calculation should always be done on the view showing the degree of stenosis at its most severe—in this instance, the AP view (*A*).



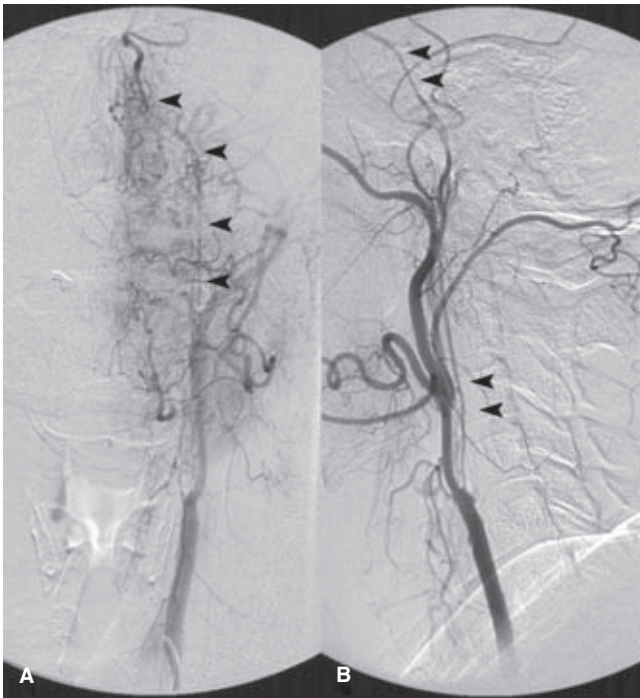


FIGURE 10-4. (A–B) String sign of preocclusive carotid disease. In this patient, the internal carotid artery opacification (*arrowheads*) happens later than expected in the film sequence due to the advanced degree of stenosis with contraction of the lumen of the artery. (Labels: A, AP view, B, lateral view.) When a string sign such as is seen here is demonstrated, it can be very important to verify that the flow is antegrade in the internal carotid artery (indicating the viability of the still patent vessel) and that the occluded artery is not filling retrogradely from above, through cavernous or ophthalmic collaterals.



FIGURE 10-5. Carotid ulceration. A factor not taken into account by a simple calculation of the degree of stenosis of a carotid artery is the quality or thrombogenic potential of the substrate of the stenosis. In this case, the degree of stenosis as measured by NASCET criteria would be approximately 50% to 60%. However, the prominent ulcer (*arrow*) suggests that this is a more troublesome lesion than a smooth, inactive 50% stenosis in another patient. Presumably, the ulcerated appearance is the remnant of a prior plaque rupture, followed by excavation and pitting of the plaque site.

FIGURE 10-6. Complete occlusion of the carotid artery with retrograde flow to the petrous segment. In this patient, the internal carotid artery (*ica*) is already occluded. The external carotid artery fills the middle meningeal artery (*mma*), which gives a big collateral branch to the ophthalmic artery (*oph*). The ophthalmic artery flows retrogradely to the internal carotid artery, where there is antegrade and retrograde opacification of the carotid vessel. Note the density change as the ophthalmic artery enters the carotid artery due to dilution.

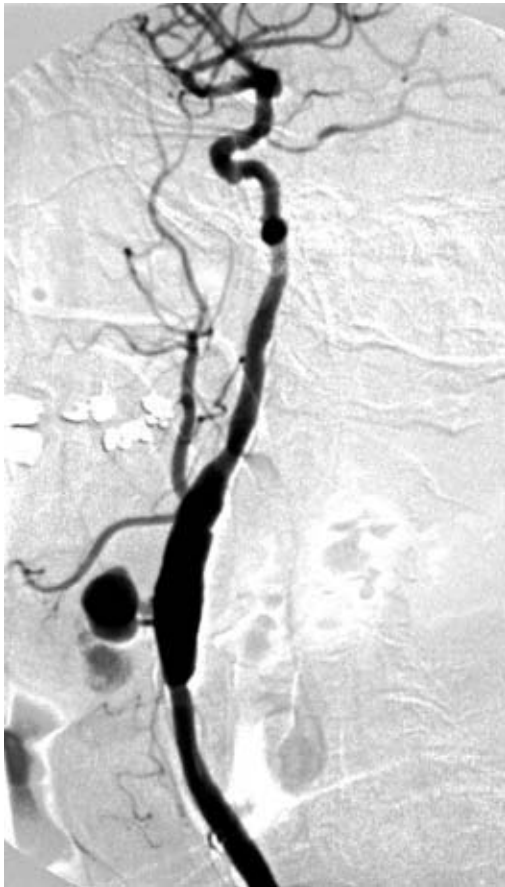
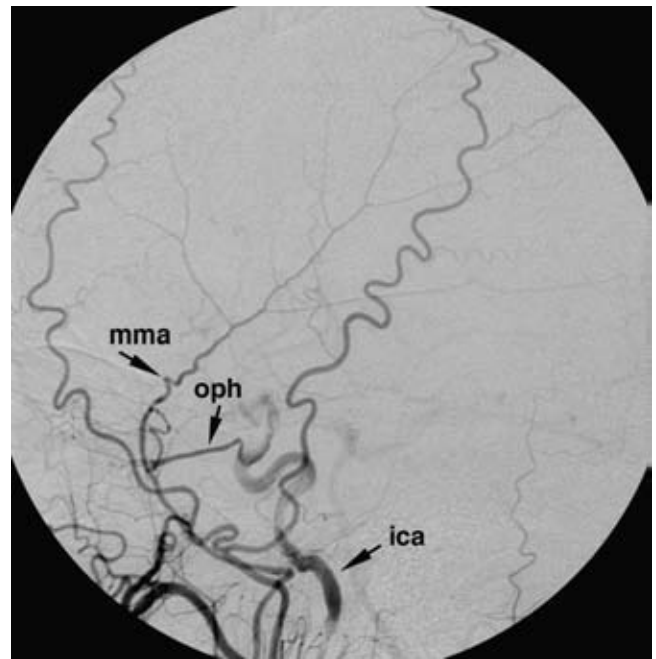


FIGURE 10-7. Anastomotic breakdown in a left carotid graft. A jet of contrast directed anteriorly fills a multilobulated pseudoaneurysm, which is presented as a pulsatile mass.

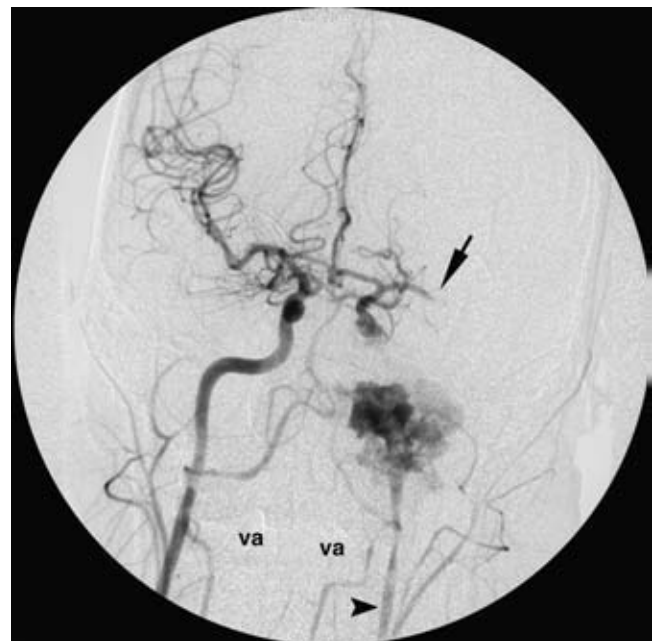


FIGURE 10-8. Laceration of the internal carotid artery. Frontal view of the head during an arch aortogram showing a complete transection of the left internal carotid artery and absence of flow in the left middle cerebral artery (*arrow*). There is reflex spasm or collapse of the walls of the left internal carotid artery (*arrowhead*). *va*, vertebral artery.

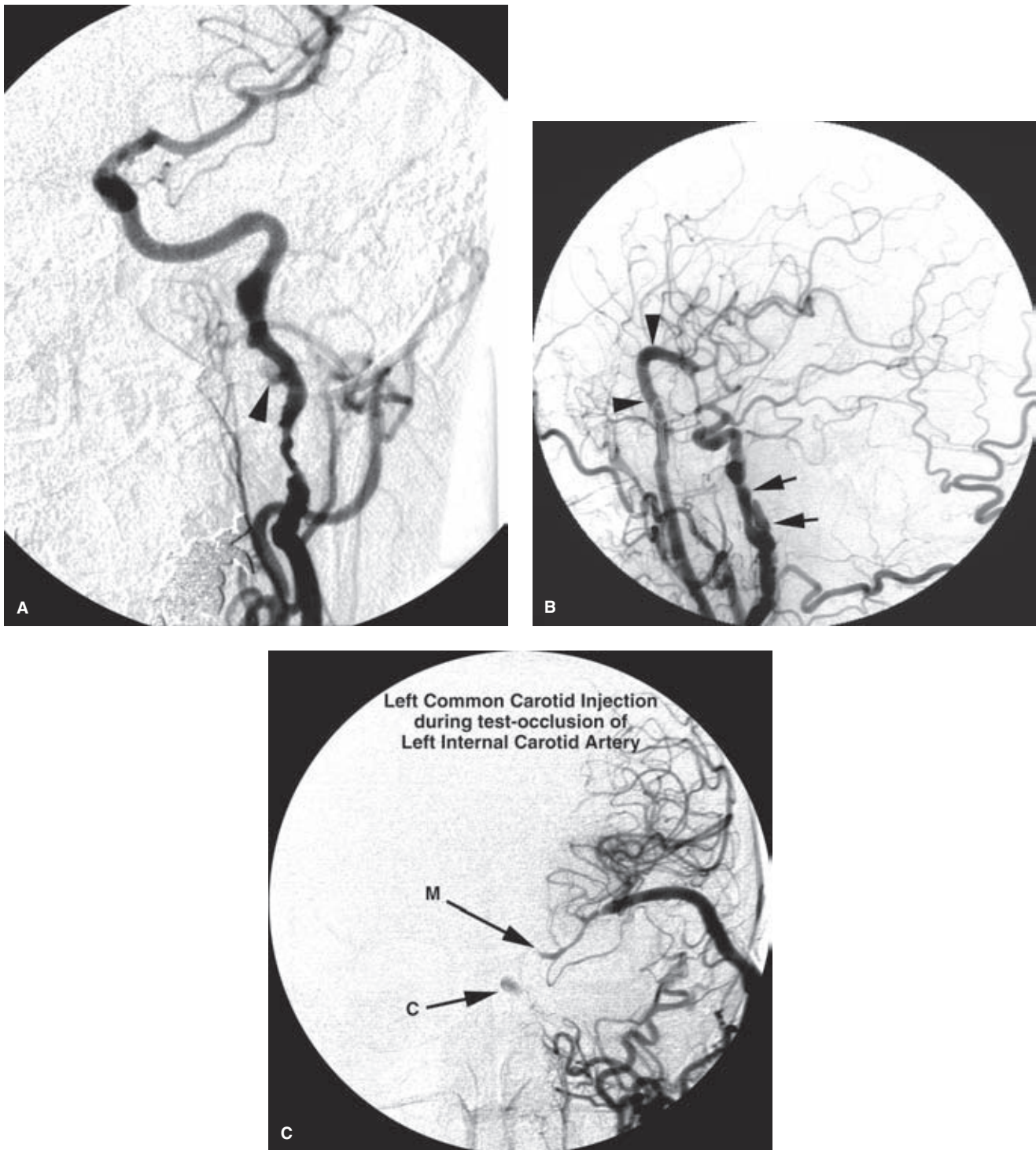


FIGURE 10-9. (A–C) Dissecting pseudoaneurysms of the internal carotid artery. A: A middle-aged female with angiographic and clinical evidence of deterioration in a left internal carotid artery dissection, even with adequate anticoagulation. A left common carotid artery injection demonstrates irregular attenuation of the artery with pseudoaneurysm or pouch formation at the skull base (*arrowhead*). Significant other observations on this image include the absence of collateral flow through the circle of Willis. The marginal degree of collateral flow was confirmed on injections of the other cerebral vessels. The patient was advised to undergo a bypass procedure to the left hemisphere, to be followed by endovascular occlusion of the left internal carotid artery. **B:** A left common carotid artery injection, lateral projection, after a venous graft bypass (*arrowheads*) from the left external carotid artery to the left middle cerebral artery. The complex architecture of the pseudoaneurysms can be seen on this oblique projection (*arrows*). **C:** A frontal projection of a left common carotid artery injection made proximal to an occluding test balloon placed proximally in the left internal carotid artery. Reconstitution of the left cavernous internal carotid artery (**C**) via collaterals from the external carotid artery is seen. The M1 segment of the left middle cerebral artery (**M**) opacifies retrogradely from the anastomotic site.

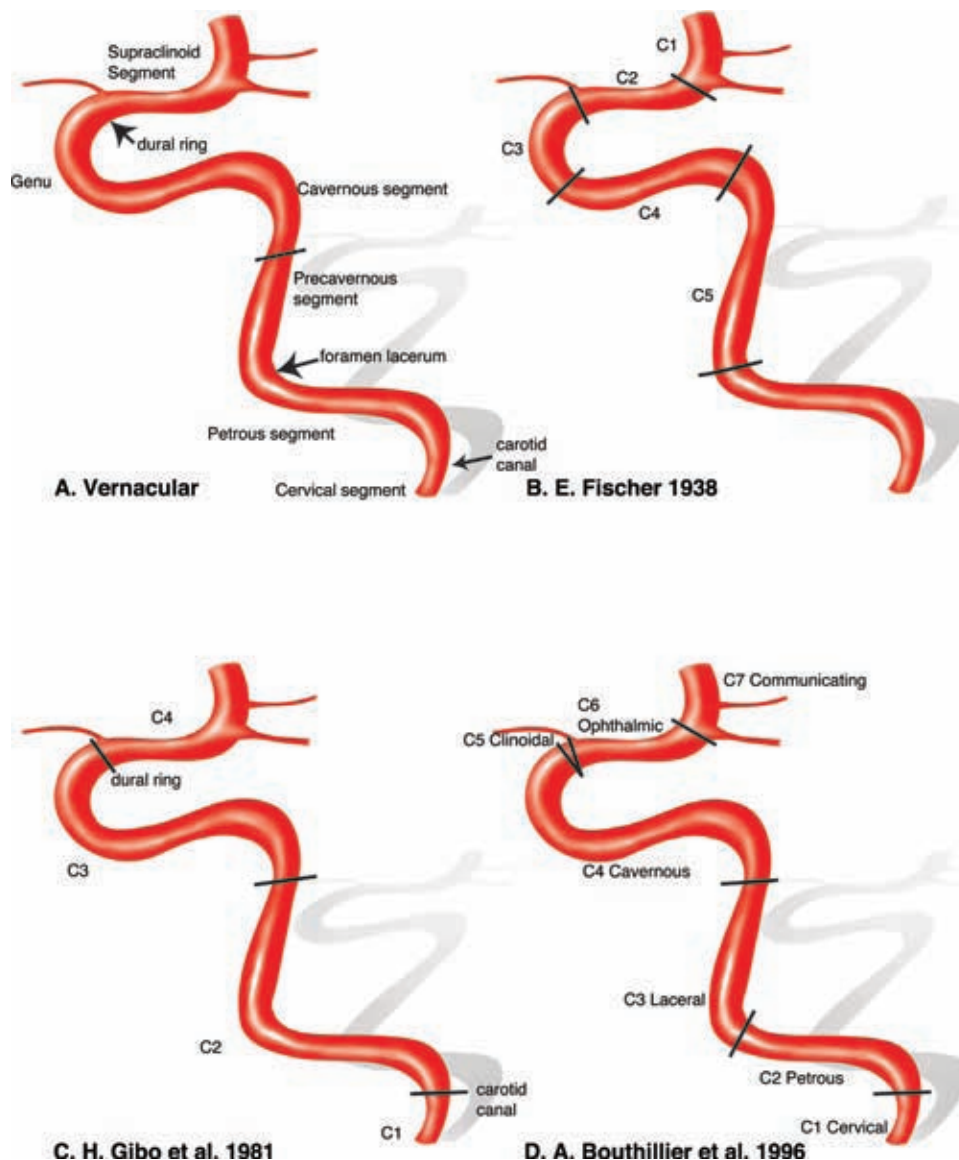


FIGURE 10-10. (A–D) Segmental nomenclature of the internal carotid artery. Several numbering schemes (71,21,2) have been canvassed for anatomy of the internal carotid artery, which can be very confusing. It is easiest to stick to the vernacular version (A).

Caroticotympanic Branch of the Petrous Internal Carotid Artery

This branch of the petrous internal carotid artery is usually too small to see or is obscured by dense petrous bone. It is a vestige of the course of the hyoid artery. Apart from its role as a vestigial remnant in understanding vascular anomalies of the middle ear, the importance of the caroticotympanic artery lies in its potential supply to vascular tumors of the middle ear.

Mandibulovidian Branch of the Petrous Internal Carotid Artery

This artery is usually too small to see but may enlarge quickly in the setting of occlusive disease (see Fig. 10-13). It is unusual to see this artery in adults. When seen, it is usually in children with a vascular mass of the nasopharynx, for example, a juvenile angiofibroma. It has an origin from

the horizontal portion of the petrous carotid artery. The Vidian branch is described as more horizontal and medial than the inferolateral direction of the mandibular branch. The Vidian artery has a straight course along the skull base, anastomosing with branches of the internal maxillary artery anteriorly (5).

Variant Stapedial Artery

Discussed below are the variants of the carotid artery (Figs. 10-14 and 10-15).

Cavernous Segment

From the foramen lacerum, the internal carotid artery ascends vertically and medially to the sella, where it turns anteriorly within the structures of the cavernous sinus. Anteriorly, the carotid artery makes a 180-degree turn, pierces

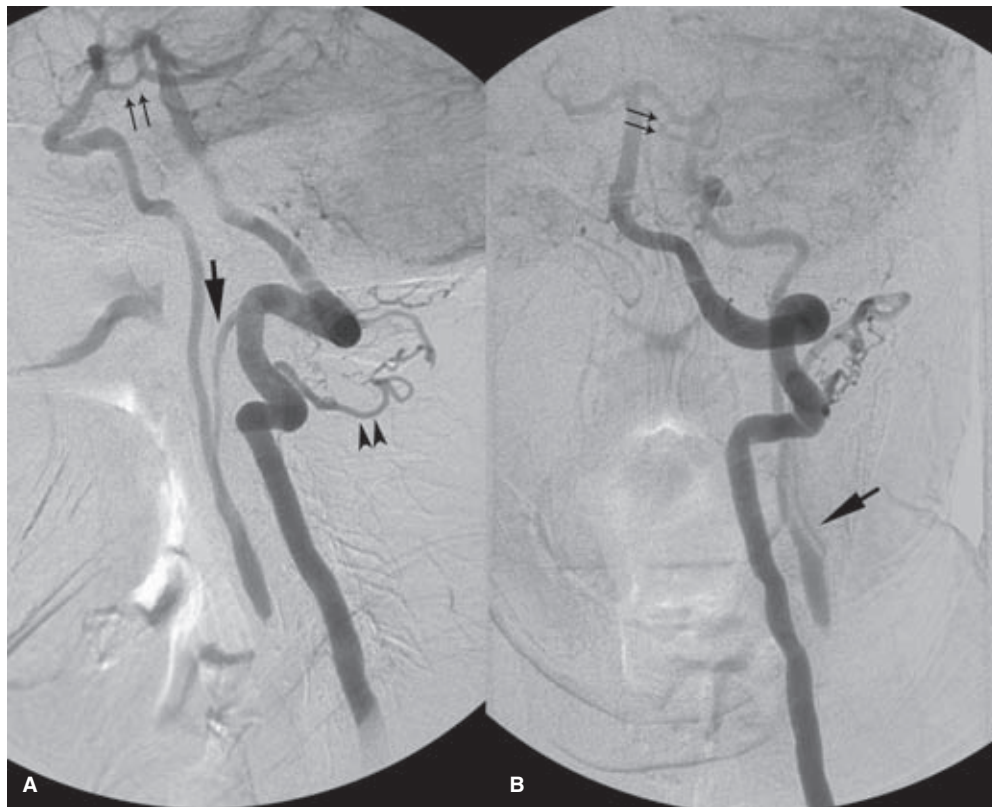


FIGURE 10-11. (A–B) Origin of the occipital artery from the internal carotid artery. This patient has an established occlusion of the left internal carotid artery at the level of the carotid bulb. This left vertebral artery injection fills the occipital artery (*single arrow* in **A** and **B**) retrogradely mainly via the C2 muscular branch (*arrowheads* in lateral view **A**). The occipital artery then flows retrogradely to fill the internal carotid artery, which then flows antegradely to the intracranial circulation. The left anterior intracranial circulation is also assisted by the posterior communicating artery (*double arrows*).

the proximal dural ring at the level of the anterior clinoid process, and becomes the clinoidal segment. The level of tortuosity of the carotid artery in this region is variable. Children have a straighter course than adults. In older patients, redundant superimposed loops present problems from the point of view of catheterization, visualization of the anatomy of aneurysms, and arterial injury during transphenoidal surgery.

Branches of the juxtaseptal internal carotid artery are frequently seen with modern digital technology and may become enlarged in the presence of collateral flow or pathologic conditions (Fig. 10-16). These branches are among the most important for consideration during external carotid artery embolization. They constitute a dangerous system of anastomoses between the external carotid and internal carotid artery systems. Therefore, whether or not they are seen on an initial angiogram, embolization is always done with the cautious assumption that they are present.

The branches of the cavernous internal carotid artery supply the pituitary gland and the adjacent dura. They have important anastomoses with the distal external carotid artery and with the ophthalmic artery. They play an important role in the arterial component of dural arteriovenous malformations (AVMs). They are sometimes described as being seen as two major trunks: The *meningohypophyseal trunk* posteriorly and the *inferolateral trunk* anteriorly and laterally

(Figs. 10-16–10-20). The most consistently present branches from this site are as follows.

The Marginal and Basal Tentorial Arteries

The *tentorial arteries* (Fig. 10-18) from this segment of the internal carotid artery are described as marginal, that is, running medially and superiorly along the margin of the tentorial incisura, or basal, that is, running laterally and inferiorly along the insertion of the tentorium along the petrous ridge.

The *marginal artery of the tentorium*, regardless of its many possible sites of origin, is sometimes referred to eponymously as the artery of Bernasconi and Cassinari (6). In contrast, the *basal tentorial artery* does not ascend in the same manner but rather diverges laterally along the course of the tentorial insertion on the petrous ridge. Along the petrous ridge and sigmoid sinus, it has anastomoses with the middle meningeal artery and dural arteries of the posterior fossa.

The Posterior Inferior Hypophyseal Artery

The *posteroinferior hypophyseal artery* is directed medially from the cavernous segment. It supplies the neurohypophysis and peripheral adenohypophysis of the pituitary gland. It anastomoses with the superior hypophyseal artery (from the supraclinoidal segment), and with its contralateral

(text continues on page 143)

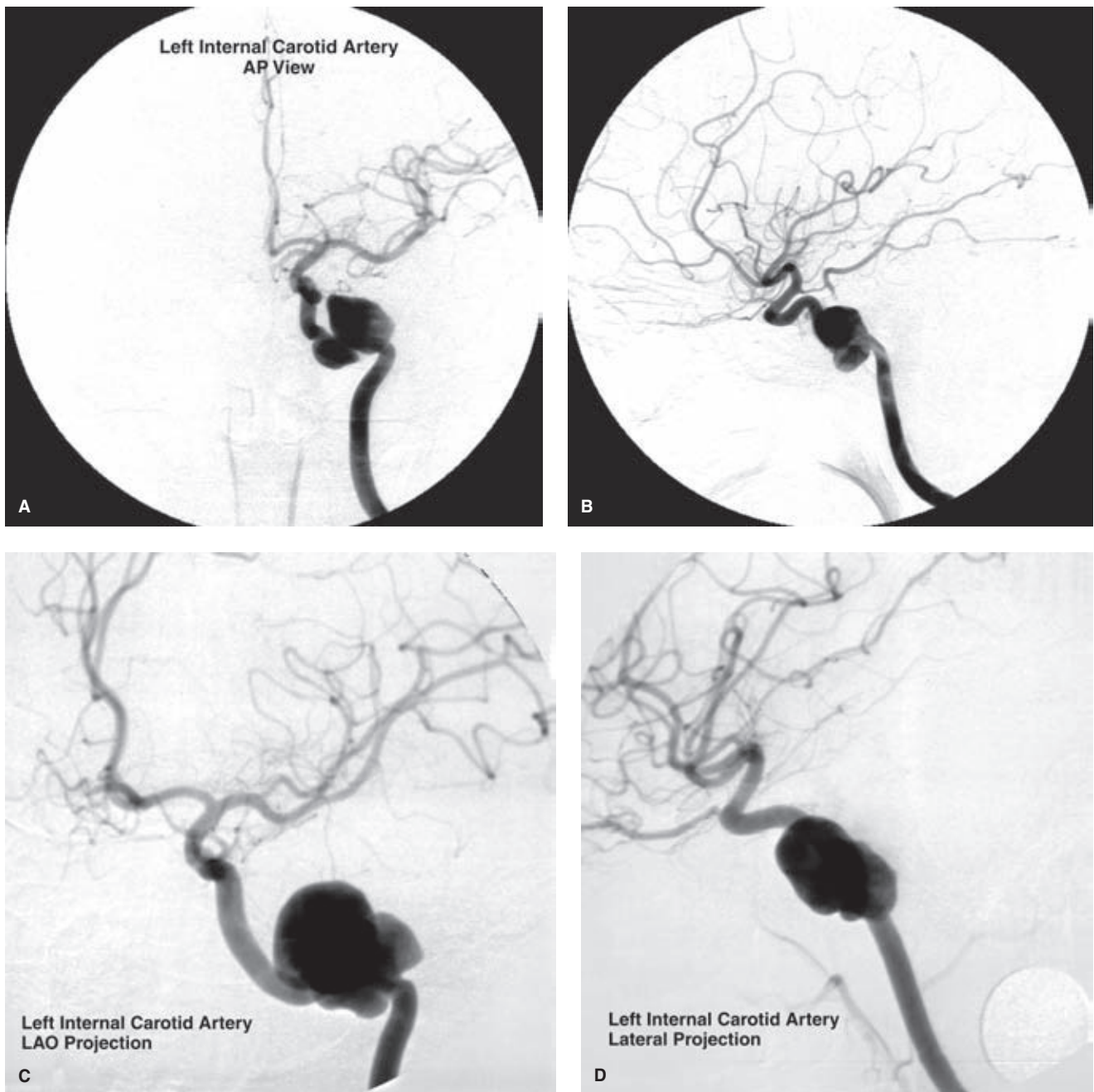


FIGURE 10-12. (A–D) Aneurysms of the petrous internal carotid artery. A–B: A young adult presented with symptoms of intolerable headache and left V nerve irritation. A lobulated aneurysm of the left petrous internal carotid artery was exercising considerable mass effect in the left middle cranial fossa. Previous skull trauma or petrous apicitis might be considered as possible etiologies for aneurysms in this location. A small posterior communicating artery is present (B), but the anterior communicating artery was small or absent (A). This demonstrates a need for a surgical bypass procedure before endovascular occlusion of the left internal carotid artery. The complex nature of the aneurysm, better seen on (A), presented considerable difficulties during balloon navigation, but the internal carotid artery was finally occluded at the cavernous segment. **C–D:** A young adult female presented with throbbing headache worsening over months. A complex aneurysm of the left petrous internal carotid artery was discovered. This patient tolerated a test occlusion of the left internal carotid artery due to the presence of a robust anterior communicating artery. However, balloon navigation of the complex lobulations of the aneurysm proved impossible, and occlusion was performed proximal to the aneurysm. Both of these cases would likely be treated today with flow-diverting devices.

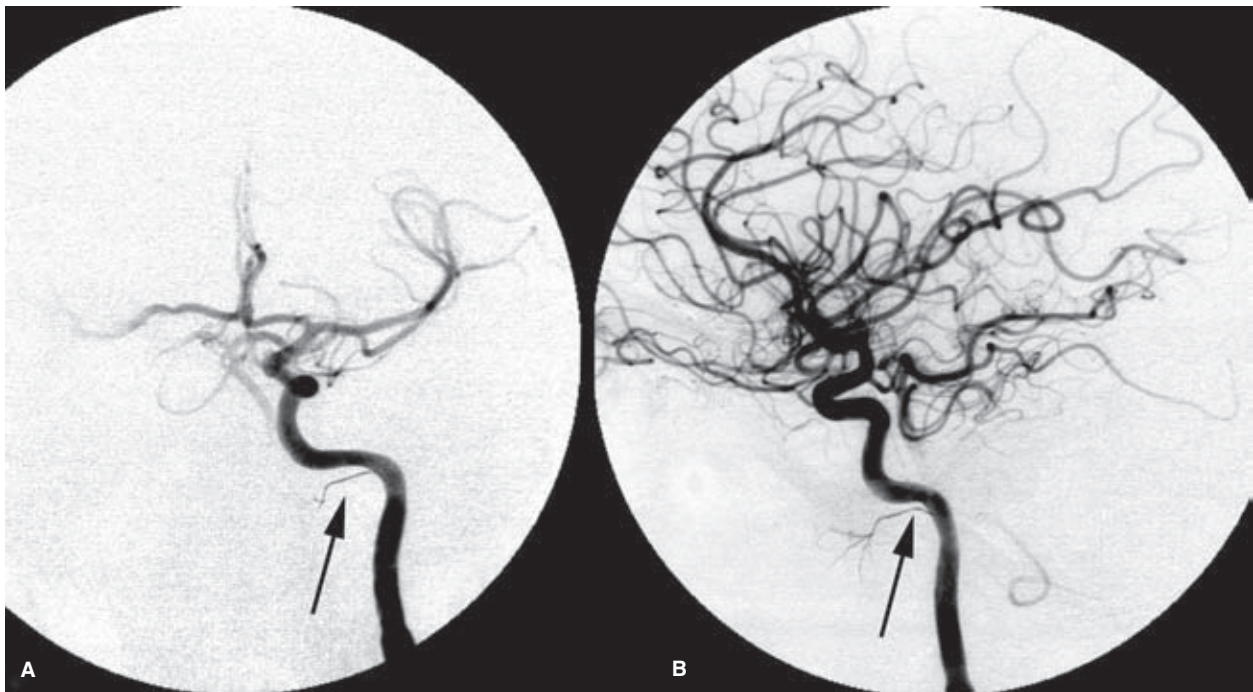


FIGURE 10-13. (A–B) Persistent mandibulovidian trunk. AP (A) and lateral (B) views of the left internal carotid artery in a child with a juvenile angiofibroma. An unusual branch of the petrous internal carotid artery (arrows) represents a persistent mandibular or mandibulovidian artery.

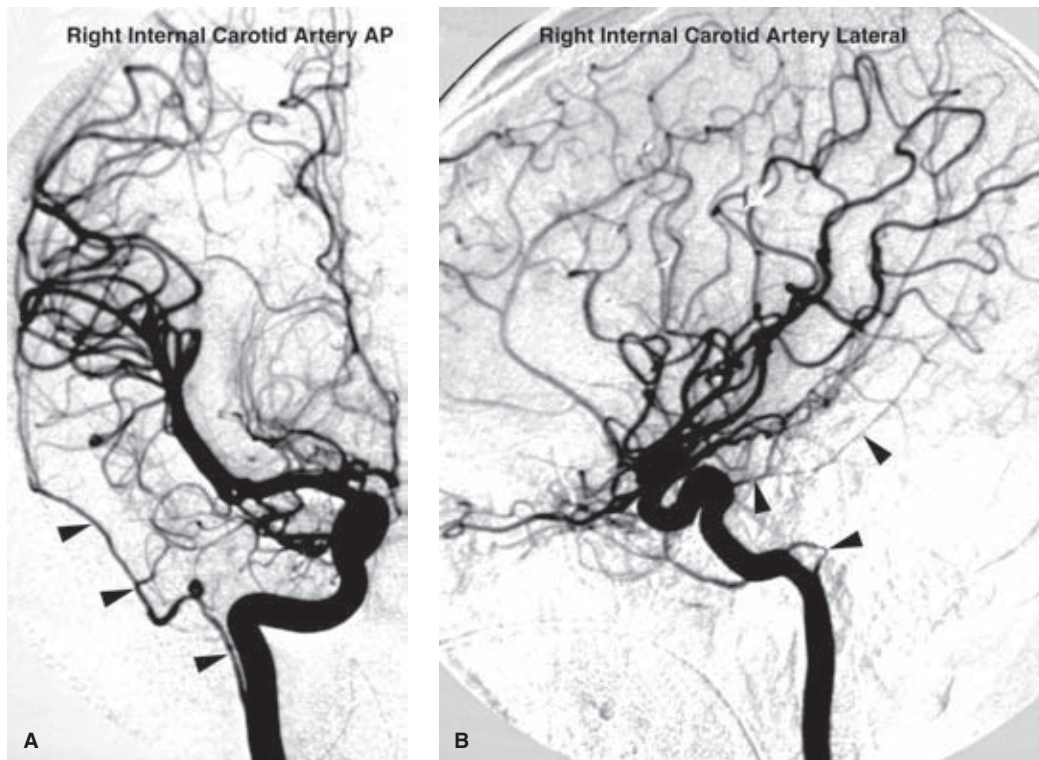


FIGURE 10-14. (A–B) Persistent stapedia artery variant. An AP and lateral view of the right internal carotid artery in a young adult undergoing angiography because of penetrating injury by metallic fragments after a gunshot wound. Notice the displacement of the anterior cerebral artery by hematoma on the AP view and artifact from fragments on the lateral view. An unusual vessel (arrowheads) arises from the high cervical internal carotid artery and becomes the middle meningeal artery intracranially. The lateral aspect is redolent of the curve evident when the inferior tympanic artery re-forms the petrous internal carotid artery in cases of an aberrant internal carotid artery. This particular variant has, therefore, been termed the *pharyngotympanostapedial* artery.



FIGURE 10-15. Variant origin of the middle meningeal artery from the petrous internal carotid artery. This patient shows a prominent and unusual variant (*arrowhead*) on this AP view of the left internal carotid artery. The site of origin from the petrous carotid is suggestive of this being a mandibulovidian remnant, but embryologically, the middle meningeal artery is more likely to derive variant origin through persistence of a hyoid–stapedial anomaly.

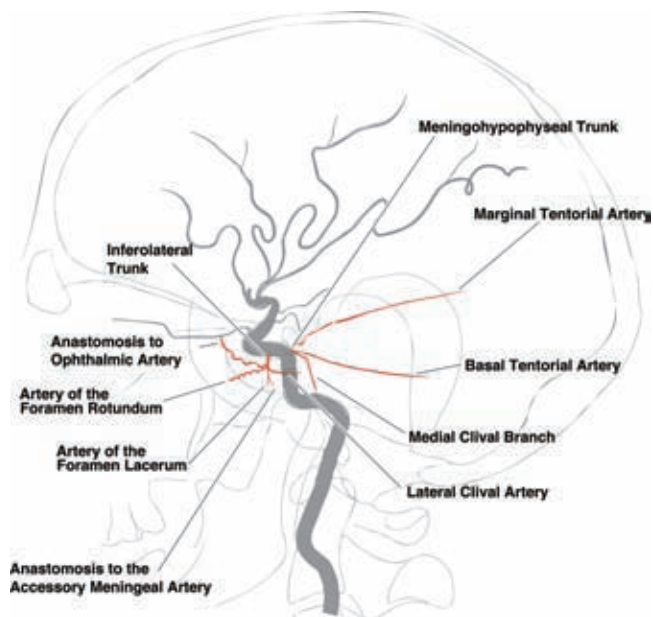


FIGURE 10-16. Angiographically visible branches of the cavernous internal carotid artery.



FIGURE 10-17. Meningohypophyseal trunk of the internal carotid artery. A lateral projection of the left internal carotid artery in a 60-year-old female with a large meningioma of the tentorium and petrous region. Part of the vascular supply to the tumor derives from the meningohypophyseal trunk (*MHT*), which supplies the tumor via the lateral clival branch.

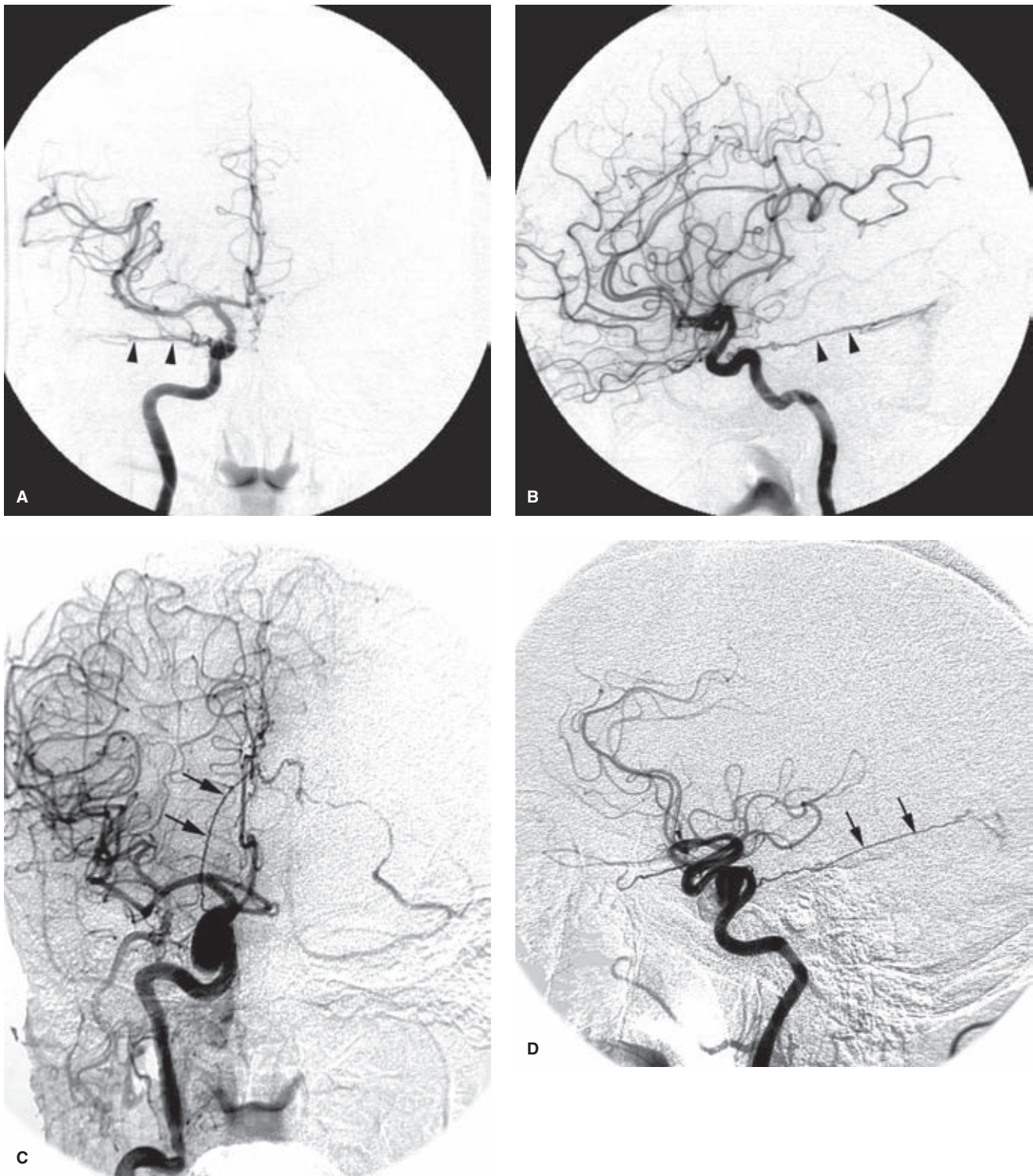


FIGURE 10-18. (A–D) Basal and marginal tentorial arteries. **A–B:** Basal tentorial artery. PA view and lateral views of the right internal carotid artery in a patient with a symptomatic dural AVM in the region of the right sigmoid and transverse sinuses. The basal tentorial artery (*arrowheads*) extends laterally and horizontally along the petrous ridge. This could be confirmed by looking at the course of the artery on a nonsubtracted image. **C–D:** Marginal tentorial artery. PA and lateral views of the right internal carotid artery in a different patient being studied for symptoms related to a cavernous internal carotid artery aneurysm. An incidental dural AVM of the tentorial margin is present. The marginal tentorial artery (*arrows*) follows the tentorial incisura posteriorly and superiorly. Compare with the course of the basal tentorial artery in **(A)** and **(B)**.



FIGURE 10-19. Reconstitution of the left internal carotid artery. A PA view of a right common carotid artery injection in the setting of occlusive disease of the left internal carotid artery. Early reconstitution of the cavernous left internal carotid artery (*lica*) is demonstrated. Small collateral vessels (arrows) cross the midline through the sella (inferior hypophyseal arteries) and along the clivus (clival branches from the internal carotid artery and ascending pharyngeal artery).

fellow. These branches cause a characteristic early neurohypophyseal blush on carotid angiography. The posteroinferior hypophyseal artery also gives a medial clival branch, which runs near the midline along the clivus to meet the ascending clival branch from the hypoglossal artery (a branch of the neurovascular trunk deriving from the ascending pharyngeal artery). This connection explains the occasional visualization of the pituitary blush on ascending pharyngeal artery injections.

Lateral Clival Artery

The lateral clival artery gives lateral and inferomedial branches along the course of the superior and inferior petrosal sinuses, respectively (7) (Fig. 10-17).

The Recurrent Artery of the Foramen Lacerum

The recurrent artery of the foramen lacerum is important in clinical practice by virtue of its anastomosis in the foramen lacerum with the carotid branch of the superior pharyngeal branch of the ascending pharyngeal artery.

Persistent Trigeminal Artery

The persistent trigeminal artery is discussed below with carotid basilar anastomoses.

Capsular Arteries of McConnell

The capsular arteries of McConnell in the normal state are rarely if ever seen during angiography. However, they may represent one possible site of cavernous internal carotid artery aneurysm formation. Medially directed aneurysms in this location can occupy the sella and are thought to represent a more serious variant of cavernous aneurysms. Their rupture into the sella can penetrate the diaphragm sellae and cause subarachnoid hemorrhage (Fig. 10-21). Sella-occupying

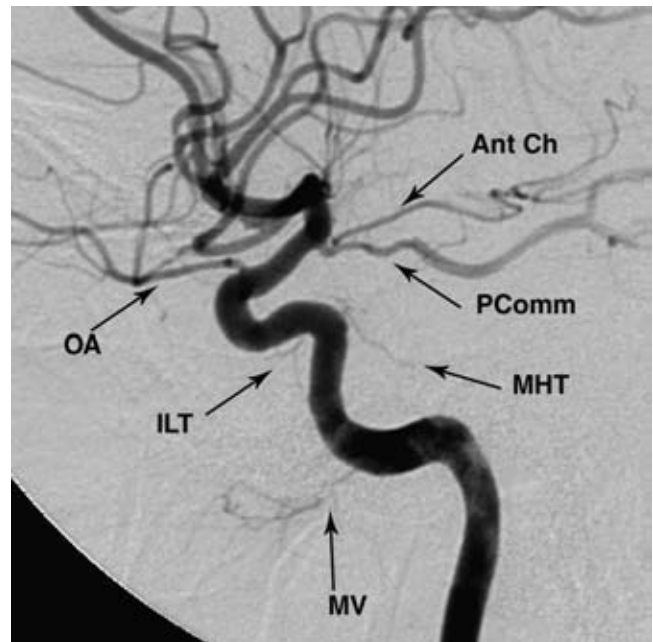


FIGURE 10-20. Normal anatomic branches around the carotid siphon.

A lateral arteriogram in a young adult demonstrates the standard configuration most commonly seen. In the normal state, the mandibulovidian artery (*MV*), inferolateral trunk (*ILT*), and meningohypophyseal trunk (*MHT*) are commonly difficult to see. The dural ring can be assumed to be just proximal to the origin of the ophthalmic artery (*OA*), sometimes demonstrated by a cincture or subtle waist in the contour of the artery as it pierces the ring. The posterior communicating artery (*PComm*) and anterior choroidal artery (*Ant Ch*) are shown arising from their typical location. The junction of the posterior communicating artery with the posterior cerebral artery is identifiable where the vessel changes caliber, and also typically by the appearance of streaming of unopacified blood within the vessel due to laminar mixing with unopacified blood from the basilar artery.

aneurysms may also cause hypopituitarism as the presenting clinical problem.

Inferolateral Trunk

The inferolateral trunk (8), sometimes referred to as the artery of the inferior cavernous sinus (7), is the remnant of the embryonic dorsal ophthalmic artery. It is present in more than 80% of microsurgical dissections (9) (Figs. 10-16–10-23). Its reach includes branches to the tentorium, the superior orbital fissure (potentially connecting with the ophthalmic territory), the foramen rotundum (connecting to the internal maxillary artery), the foramen lacerum (where it can anastomose with the ascending pharyngeal artery), and the foramen ovale. Very rarely, the dorsal ophthalmic artery may persist beyond embryonic life and be the dominant arterial supply to the orbit (Fig. 10-24). When a dual ophthalmic artery supply to the orbit is present (Fig. 10-25), variations in the pattern of anastomosis between the two arteries may be seen, including the possibility of a complete or partial arterial ring around the optic nerve (10).

Cavernous Carotid Aneurysms

Aneurysms of the cavernous segment of the internal carotid artery account for approximately 5% of intracranial aneurysms and are more likely to be detected in female patients (Fig. 10-26). Idiopathic aneurysms in this location have a

(text continues on page 146)

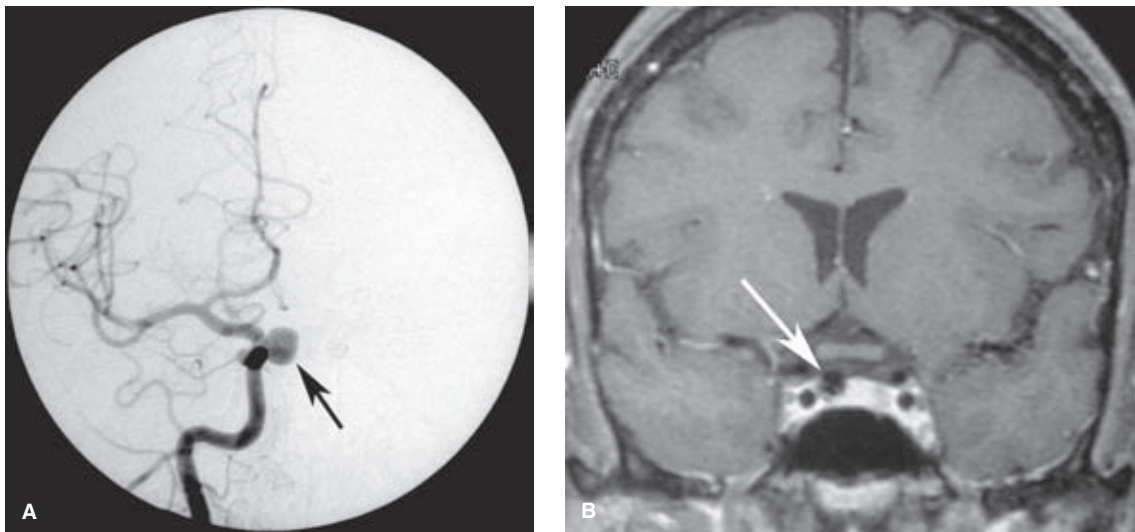


FIGURE 10-21. (A–B) Intrasellar aneurysm from the cavernous internal carotid artery. A PA angiographic view (A) of a right internal carotid artery injection in a middle-aged female with multiple aneurysms. A medially directed aneurysm from the cavernous internal carotid artery is present (arrow). Aneurysms in this location are thought to correspond with the hypophyseal or capsular branches. The intrasellar location was confirmed on a coronal T1-weighted, gadolinium-enhanced MRI study (B). Although this particular aneurysm was asymptomatic, endovascular treatment was recommended. Intrasellar aneurysms that rupture can leak into the subarachnoid space, causing significantly greater morbidity than rupture of cavernous aneurysms in other positions.



FIGURE 10-22. Enlarged extracranial branches of the cavernous internal carotid artery. This teenager presented with nasal stuffiness and was found to have a hypervascular mass arising from the pterygomaxillary fissure, with prominent vascularity demonstrated on the ipsilateral external carotid artery injection (not shown). The internal carotid artery injection provided here shows a prominent vessel from the cavernous segment, most likely an inferolateral trunk (ilt), which contributes substantially to the posterior aspect of the tumor (arrowhead). The importance of this finding is of some interest to the operating surgeon for prediction of bleeding. However, it is very important for planned embolization of the external carotid artery as well because a large connector to the internal carotid artery can be the source of retrograde embolization into the internal carotid artery, if the embolic material is pushed too hard in the external carotid artery branches, which invariably interconnect within or around the tumor with ILT branches. This is termed *intratumoral anastomosis of feeding vessels* and is a common phenomenon in all types of hypervascular lesions.

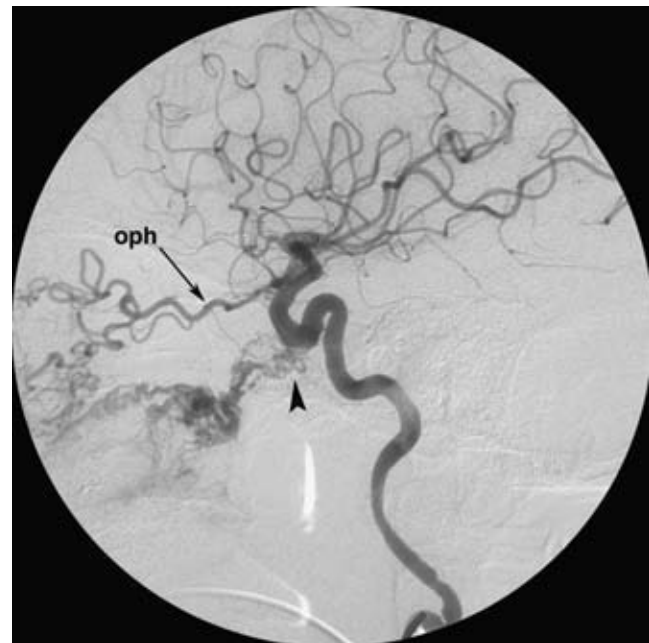


FIGURE 10-23. Enlarged artery of the foramen rotundum. This patient has a large facial AVM. Several years previously, an attempt at treatment included ligation of the ipsilateral branches of the external carotid artery. This stratagem did not work well for the patient because it was ineffective for eliminating the AVM, but blocked subsequent endovascular access to the AVM. The AVM is now deriving prominent supply from the ipsilateral internal carotid artery via the inferolateral trunk via the artery of the foramen rotundum (arrowhead) and the ophthalmic artery (oph).

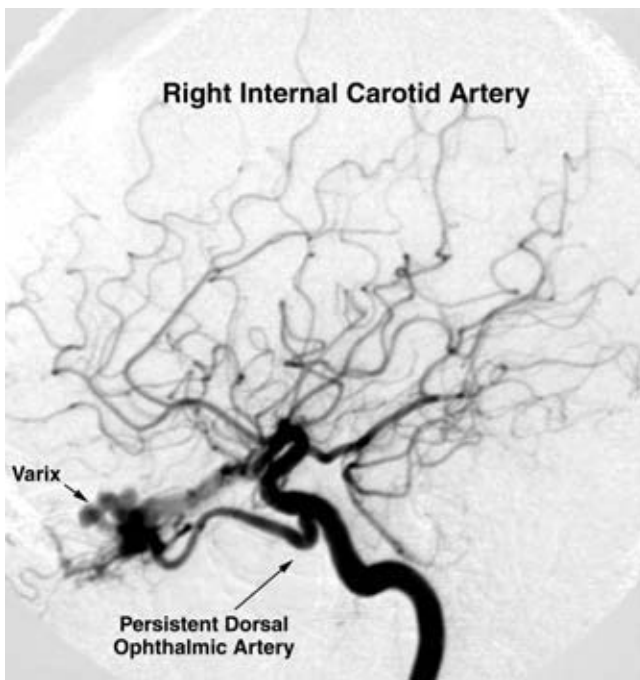


FIGURE 10-24. Persistent dorsal ophthalmic artery. A persistent primitive dorsal ophthalmic artery is present in this middle-aged female who presented with headaches related to a dural AVM of the anterior cranial fossa. The origin of this unusual vessel from the horizontal cavernous internal carotid artery corresponds with that of the inferolateral trunk. Most commonly, the dorsal ophthalmic artery regresses to become an anastomotic twig, the deep recurrent ophthalmic artery, between the ophthalmic artery and the inferolateral trunk. Dural AVMs of the anterior cranial fossa in this location are typically supplied by ethmoidal branches of the ophthalmic arteries. Because of a propensity for subarachnoid or cortical venous drainage, they are thought to have a high risk of becoming complicated early by subarachnoid hemorrhage.



FIGURE 10-25. Dual ophthalmic artery. Unusual persistence of dual ophthalmic supply from the internal carotid artery to the orbit is seen in association with an aneurysm of the cavernous horizontal segment. The ventral ophthalmic artery (*arrowheads*) arises from the usual paraclinoidal location; the dorsal ophthalmic artery (*arrow*) is larger and has a cavernous origin.

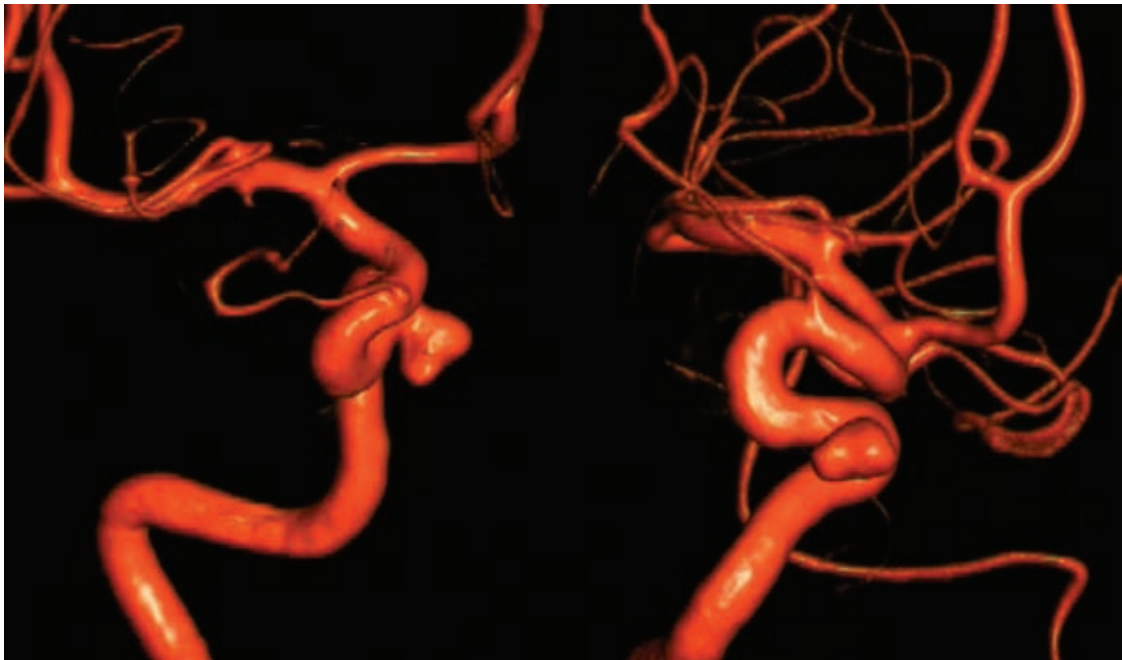


FIGURE 10-26. Medially projecting aneurysm of the cavernous carotid artery. Cavernous aneurysms are extradural. They require treatment if they are causing specific symptoms such as oculoplegia or headache. Occasionally, medially projecting aneurysms appear to burrow their way into the sella where there is a theoretical risk of subarachnoid hemorrhage through the diaphragm sellae should they rupture. However, this phenomenon is exceedingly rare.

strong association with hypertension and advancing age, whereas posttraumatic aneurysms or pseudoaneurysms may be seen in any age group. Approximately 50% of cavernous aneurysms occur anteriorly adjacent to the carotid genu, and 16% can be giant aneurysms, that is, greater than 2.5 cm in diameter (11,12). Most cavernous aneurysms seen during angiography are incidental, asymptomatic lesions that usually warrant no further evaluation or treatment (13). Symptoms may develop due to compression of adjacent structures causing cranial nerve deficits, headache, embolic events, or aneurysmal rupture.

Aneurysms close to the genu and the optic nerve frequently present with retro-orbital headache and visual symptoms of blurring or field deficits. Aneurysms of the horizontal cavernous segment are more likely to affect the III, IV, and VI nerves. There is some debate about whether cranial nerve ischemia, rather than compression by mass effect, may play a role in the etiology of the cranial neuropathies associated with cavernous aneurysms. However, mass effect seems to be the most likely explanation.

When cavernous aneurysms rupture, which is an uncommon event, symptoms are related to the carotid–cavernous fistula (14), massive epistaxis (15), and subdural (16) or subarachnoid hemorrhage (17,18). Most spontaneous direct carotid–cavernous fistulas are thought to be related to rupture of a cavernous aneurysm into the surrounding venous structures. The risks of subarachnoid hemorrhage are greatest with anterior aneurysms at the genu. Anterior aneurysms may breach the dural ring and expand superiorly

into the subarachnoid space. Medially directed aneurysms from the horizontal segment are also thought to represent a risk of subarachnoid hemorrhage if they have an intrasellar location.

Clinoidal Segment

The clinoidal segment of the internal carotid artery is a short wedge-shaped area of the artery between the proximal and distal dural rings. Some authors refer to the lateral aspect of this ring as the clinoidal segment and to the medial aspect as the carotid cave. Aneurysms on the lateral aspect of this segment are extracavernous and, strictly speaking, extradural. However, because of the difficulty in precisely defining the dural margin on angiographic images, aneurysms in this location are treated with a great deal of caution, as if they were subarachnoid. Medial to the carotid genu a redundant fold of dura insinuates itself between the artery laterally and the carotid sulcus of the sphenoid bone medially, thus extending the inferior reach of the intradural space along the medial aspect of the artery.

Ophthalmic Segment

The ophthalmic segment extends from the distal dural ring to the origin of the posterior communicating artery, thus including the territory referred to as supraclinoidal in some references. There are two major branches of the ophthalmic segment: The ophthalmic artery and the superior hypophyseal artery (Figs. 10-27–10-29).

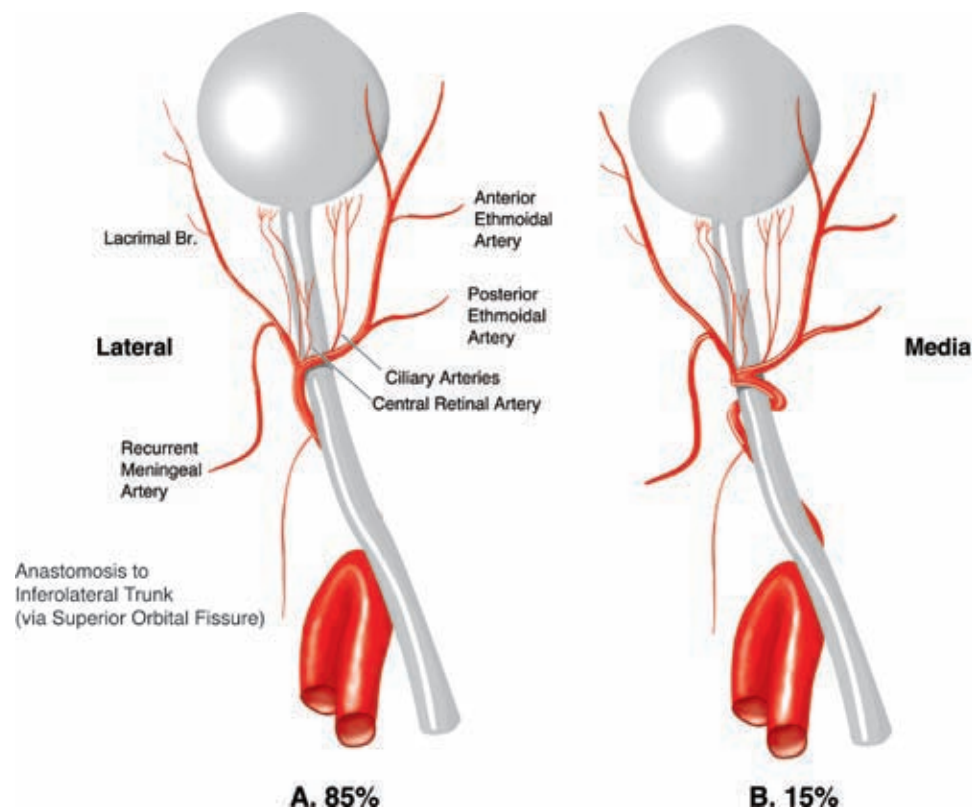


FIGURE 10-27. Course of the left ophthalmic artery: Superior view. Seen from above, the ophthalmic artery courses under the optic nerve external to the optic nerve sheath. In 85% of the population, the ophthalmic artery curves around the lateral aspect of the nerve to swing medially over the nerve (A). In 15%, the artery courses under the nerve and curves to the upper aspect of the optic nerve along the medial side (B) (20).

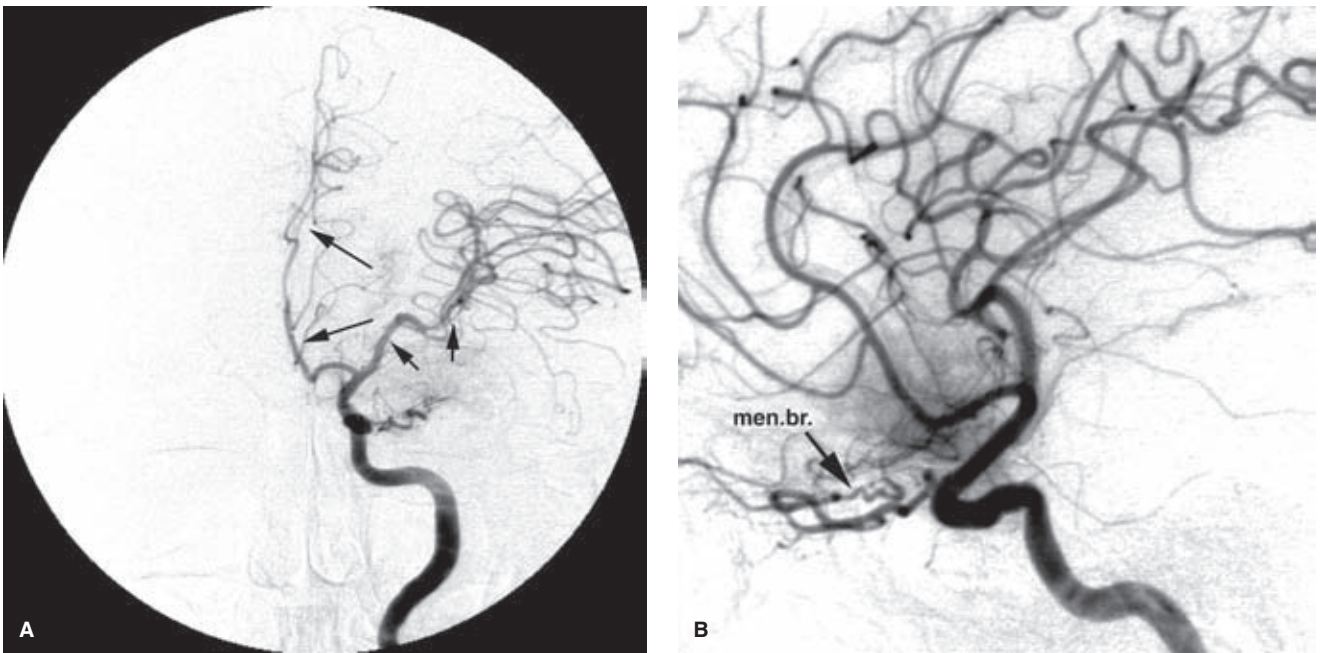


FIGURE 10-28. (A–B) Sphenoid wing meningioma. A late-middle-aged female with a symptomatic large left sphenoid wing meningioma. On the PA view (A), there is marked mass effect on the course of the middle cerebral artery (*small arrows*) and shift of the anterior cerebral artery (*long arrows*). On the lateral view (B), a characteristic blush of the meningioma is seen on the internal carotid artery injection. The predominant supply to the tumor is via the recurrent meningeal branch of the ophthalmic artery (*men.br.*) reaching the tumor via the superior orbital fissure.

Ophthalmic Artery

As described by Padget (19), the ophthalmic artery has two major sources of embryologic derivation: The primitive ventral ophthalmic artery from the anterior cerebral artery and the primitive dorsal ophthalmic artery from the internal carotid artery (corresponding with the inferolateral trunk).

The important named branches of the ophthalmic artery (20) include the central retinal artery, the anterior and posterior ethmoidal branches (enlarged in the setting of vascular tumors of the anterior cranial fossa or dural AVMs), and connections with the middle meningeal artery, which can be either afferent or efferent (Fig. 10-30).



FIGURE 10-29. Ethmoidal and dural branches of the ophthalmic artery. A large meningioma of the anterior cranial fossa displaces the anterior cerebral arteries posteriorly and superiorly (*small arrows*). It derives supply from the ethmoidal branches of the ophthalmic artery (*long arrow*) via the cribriform plate. The anterior artery of the falx cerebri is also enlarged (*arrowhead*).



FIGURE 10-30. Origin of the middle meningeal artery from the ophthalmic artery. It can be easy to overlook this variant due to the multiple overlapping vessels seen on a lateral view. However, the manner in which the relatively straight course of the middle meningeal artery and its branches (*arrows*) cross the intracranial vessels without joining should catch the eye. This is an example of how vessels that are in different planes cross one another on an angiographic projection without communicating. The course of the middle meningeal artery is buckled at the level of the lowest arrow, where it describes a recurrent course through the superior orbital fissure.

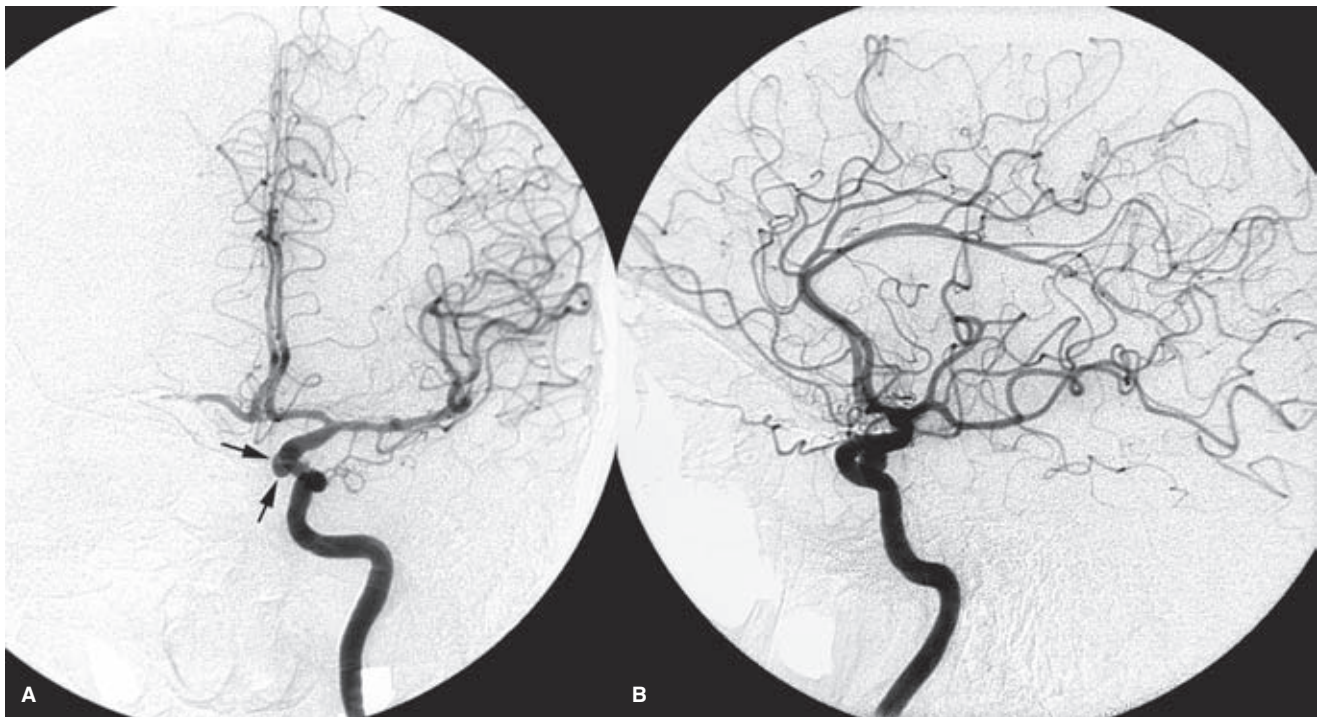


FIGURE 10-31. (A–B) Superior hypophyseal aneurysm. Aneurysms projecting medially from the supraclinoidal internal carotid artery (A) distal to the ophthalmic artery and proximal to the posterior communicating artery are most commonly described as being hemodynamically related to the superior hypophyseal arteries. On the lateral view (B), the origin of this particular aneurysm is easy to discern, although the dome overlaps with the horizontal segment of the cavernous internal carotid artery. When such aneurysms enlarge, the precise site of origin can be difficult to clarify. Superior hypophyseal aneurysms may extend proximally and mimic paraclinoidal aneurysms.

Superior Hypophyseal Arteries

The superior hypophyseal arteries are the most consistent branches of the supraclinoidal segment of the internal carotid artery. They may arise as a single trunk or be up to five in number (9,21,22), up to 500 μm in diameter. Branches to the upper infundibulum anastomose with branches from the contralateral superior hypophyseal arteries and from the posterior communicating arteries to form a circuminfundibular anastomosis. Some of these branches continue superiorly and supply the hypothalamic structures adjacent to the floor of the third ventricle. Other branches include a recurrent anterior branch along the optic nerve, branches to the inferior part of the optic chiasm, and inferiorly directed branches to the diaphragm sellae and pituitary gland. The branch(es) to the optic nerve may be the dominant vascular supply to the intradural segment of the optic nerve, implying that care must be taken to preserve this artery during resection of sellar and suprasellar tumors.

The optic chiasm, on the other hand, typically has vascular supply from many sources in addition to that from the superior hypophyseal artery. These include the anterior communicating artery, posterior communicating artery, and even the basilar artery. A bitemporal visual field cut seen with superiorly directed pituitary tumors may be due to compromise of the superior hypophyseal artery supply to the lower aspect of the optic chiasm rather than to mechanical compression of the chiasm (23). Care with neurotoxic agents such as dimethylsulfoxide (DMSO) in this region is necessary on this account.

Aneurysms of the supraclinoidal internal carotid artery that are directed medially are usually considered to be hemodynamically related to the superior hypophyseal arteries

(Fig. 10-31). It is thought that aneurysms in this location are somewhat more likely to bleed at a smaller diameter than subarachnoid aneurysms of a similar size in other locations. Patients with aneurysms in this location may be more prone than other patients to have aneurysms in multiple sites, particularly of the contralateral subarachnoid internal carotid artery, cavernous internal carotid artery, and posterior communicating artery. Superior hypophyseal aneurysms project medially in two patterns. They may extend medially inferior to the optic chiasm and simulate a suprasellar mass. Alternatively, superior hypophyseal aneurysms may extend inferiorly underneath the anterior clinoid process. In this position, they may be misinterpreted as paraclinoidal in location or even as carotico-ophthalmic (24). Aneurysms on the more proximal curve of the carotid genu, medially, are known as “carotid cave” aneurysms and are significant for the difficulty in determining their relationship to the dura (Fig. 10-32).

Anterior Choroidal Artery

Origin of the Anterior Choroidal Artery

The anterior choroidal artery arises from the posterior wall of the internal carotid artery as the most consistently identifiable branch between the posterior communicating artery and the internal carotid bifurcation (Figs. 10-33 and 10-34). It arises most commonly 2 to 4 mm distal to the origin of the posterior communicating artery. It usually measures about 1 mm in diameter. It is duplicated in approximately 4% of dissection specimens, and its absence is rare (25,26). Smaller lenticulostriate branches may arise from the carotid artery between the posterior communicating artery and the anterior

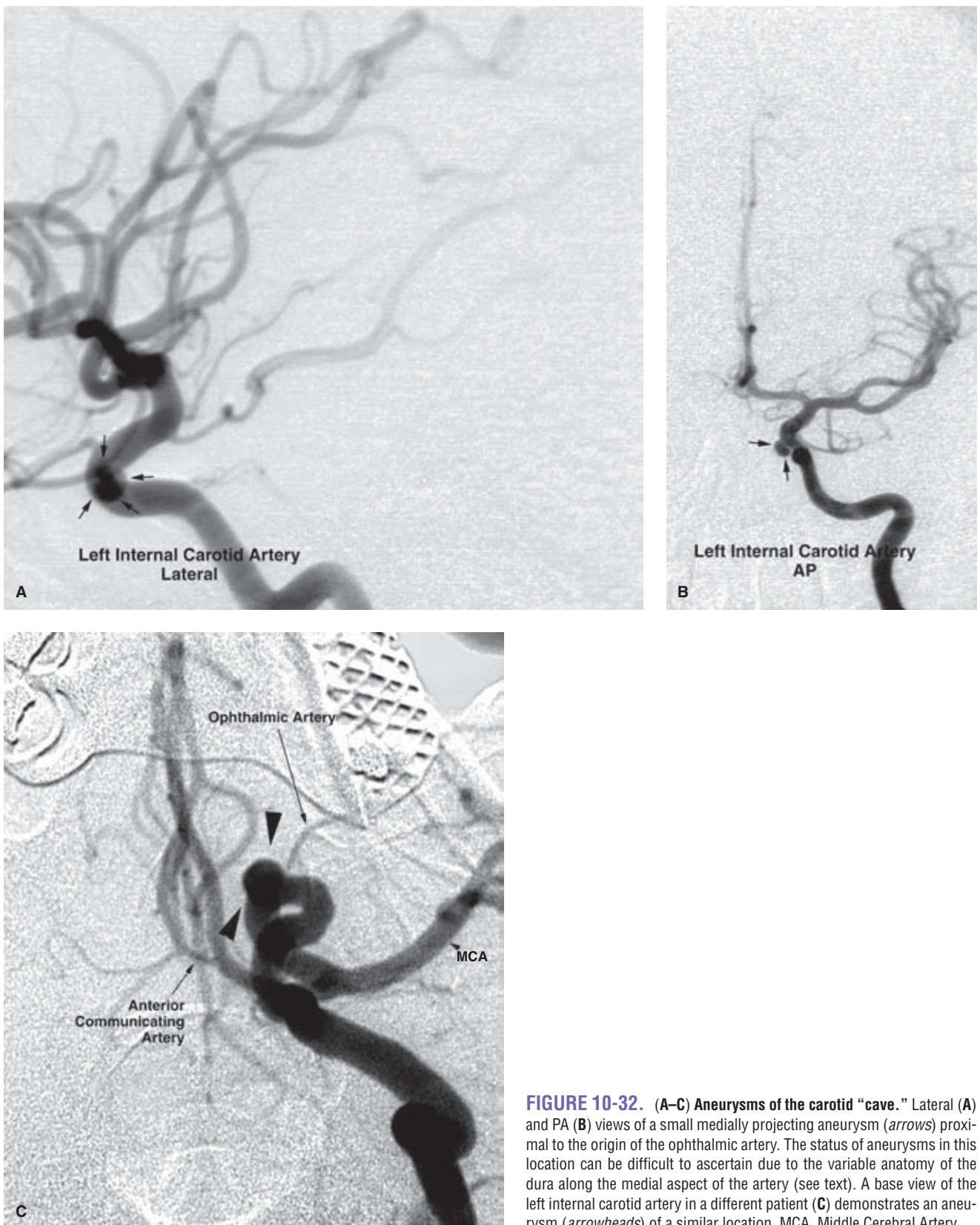


FIGURE 10-32. (A–C) Aneurysms of the carotid “cave.” Lateral (A) and PA (B) views of a small medially projecting aneurysm (arrows) proximal to the origin of the ophthalmic artery. The status of aneurysms in this location can be difficult to ascertain due to the variable anatomy of the dura along the medial aspect of the artery (see text). A base view of the left internal carotid artery in a different patient (C) demonstrates an aneurysm (arrowheads) of a similar location. MCA, Middle Cerebral Artery.

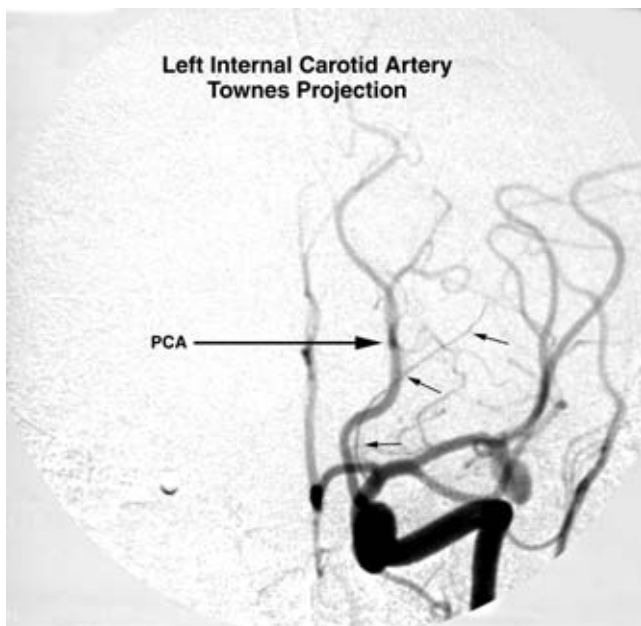


FIGURE 10-33. Origin and course of the anterior choroidal artery in reference to that of the posterior cerebral artery. A Townes projection performed in the evaluation of a left middle cerebral artery aneurysm. There is a fetal posterior communicating artery (*PCA*) present. The more lateral origin of the anterior choroidal artery (*arrows*), its initially medially directed course, and its broad curve into the choroidal fissure are well demonstrated.



FIGURE 10-34. Course of the left anterior choroidal artery. In this selective left internal carotid artery injection of a patient with a left hemispheric AVM, the course of the anterior choroidal artery (*arrowheads*) is clearly demonstrated sweeping slightly medially in its distal segments and then laterally through the choroidal fissure. Note the unusual fenestration of the A1 origin (*arrow*).

choroidal artery. Origin of the anterior choroidal artery from the middle cerebral artery or posterior communicating artery has been reported at angiography and at dissection with a frequency of 2% to 11% (27–29). Rarely, the origin of the anterior choroidal artery may be proximal to that of the posterior communicating artery (30).

Territory of the Anterior Choroidal Artery

The anterior choroidal artery territory consists of a critical area of the diencephalon and mesencephalon, making it a focus of risk evaluation in planning surgical or interventional treatments. In the embryologic stage, the anterior choroidal artery has a more extensive distribution than is seen in adult angiographic studies. The common pattern of anterior choroidal supply includes the uncus, piriform cortex, much of the tail of the caudate nucleus, hippocampus, amygdala, thalamus, lateral geniculate body, optic tract, some of the cerebral peduncle, the subthalamic nucleus, and genu and posterior limb of the internal capsule. The importance of the anterior choroidal artery as well as the high risk of severe morbidity related to infarction of this distribution is self-evident (29). Ischemic infarcts of the anterior choroidal artery are not common and when they do occur are most likely to involve the posterior two thirds of the posterior limb and the retrolenticular segment of the internal capsule. An anterior choroidal artery occlusion, accounting for approximately 3% of cerebral ischemic infarcts (31), may cause a clinical syndrome with variable degrees of contralateral hemiplegia, hemianesthesia, and hemianopsia with memory loss and somnolence (32). Hemiplegia is due to involvement of the posterior two thirds of the posterior limb of the internal capsule; the sensory deficit is due to interruption of thalamocortical fibers; and hemianopsia is due to involvement of the optic tract, the lateral geniculate body, or the geniculocalcarine fibers. This syndrome was not a consistent outcome, however, in all patients who underwent surgical clipping of the anterior choroidal artery in the 1950s for Parkinson disease, a procedure since abandoned (33). Some patients can have a favorable outcome from a proximal occlusion of the anterior choroidal artery due to distal collateral flow. However, surgical dissection and preservation of the anterior choroidal artery at surgery is considered a priority.

The anterior choroidal supply exists in balance with a surrounding system of collateral choroidal and parenchymal anastomoses from the anterior, middle, and posterior cerebral arteries. Pathologic lesions or congenital diminution of the adjacent territories account for the variable degree of prominence that the anterior choroidal artery may demonstrate. When the anterior choroidal artery retains a portion of its embryologic territory in the posterior cerebrum, the posterior cerebral artery will be correspondingly smaller (Fig. 10-35). The anterior choroidal artery can have a large posterior and inferior temporal cortical supply, potentially extending to the occipital lobe, described in Chapter 9.

▶ ANATOMIC VARIANTS OF THE INTERNAL CAROTID ARTERY

A number of common vessels with sites of origin usually found elsewhere can be seen occasionally arising from the internal carotid artery, including the ascending pharyngeal artery, the occipital artery, and other more obscure vessels (34).

FIGURE 10-35. Variant territory of the anterior choroidal artery. A middle-aged male was referred for Wada testing because of a frontal lobe glioma. Note the artifacts from EEG leads and the taut, displaced appearance of the pericallosal artery. A fetal-type posterior communicating artery (*arrow-head*) is present. Another vessel (*double arrow*) with an extensive temporal and occipital territory arises from the internal carotid artery above the posterior communicating artery. This represents a persistence of the embryologic territory of the anterior choroidal artery encompassing much of the temporal and temporo-occipital region. It is sometimes named a *duplicated posterior communicating artery*.



Agenesis of the Internal Carotid Artery

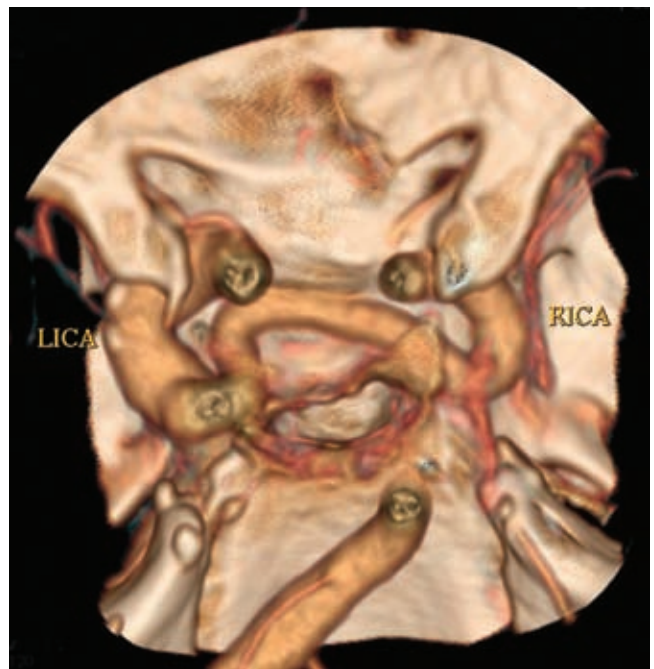
Rare cases of bilateral or unilateral agenesis of the internal carotid artery have been reported. In this condition, depending on the site of segmental agenesis, the ipsilateral hemispheric circulation may be reconstituted via the contralateral internal carotid artery through a trans-sellar anastomosis thought to correspond with the primitive maxillary artery (35,36) (Figs. 10-36 and 10-37). Alternative routes include the ipsilateral inferolateral trunk, predominantly through the accessory meningeal artery, the artery of the foramen rotun-

dum, persistent stapedia artery, and other routes (34,37,38); the contralateral internal carotid artery via the anterior communicating artery; or the posterior circulation via the posterior communicating artery or via unusual carotid–basilar anastomoses, such as a persistent trigeminal artery (39).

Aberrant Internal Carotid Artery

This unusual but important condition may be an incidental finding or may present with pulsatile tinnitus. An error to avoid is misdiagnosis of this condition as a middle

FIGURE 10-36. Trans-sellar anastomosis in the setting of ICA agenesis. A CTA image from this patient with absence of the petrous and cervical segments of the right internal carotid artery shows a large-caliber connection crossing the midline via the sella and reconstituting the right internal carotid artery at the cavernous level. This is probably an embryologic derivative of the primitive maxillary artery discussed in Chapter 7.



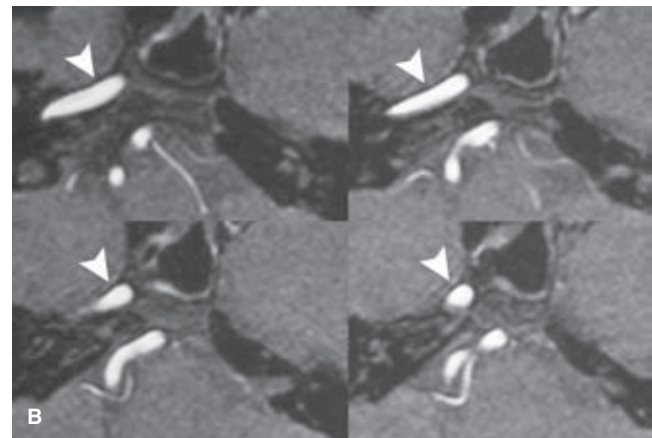
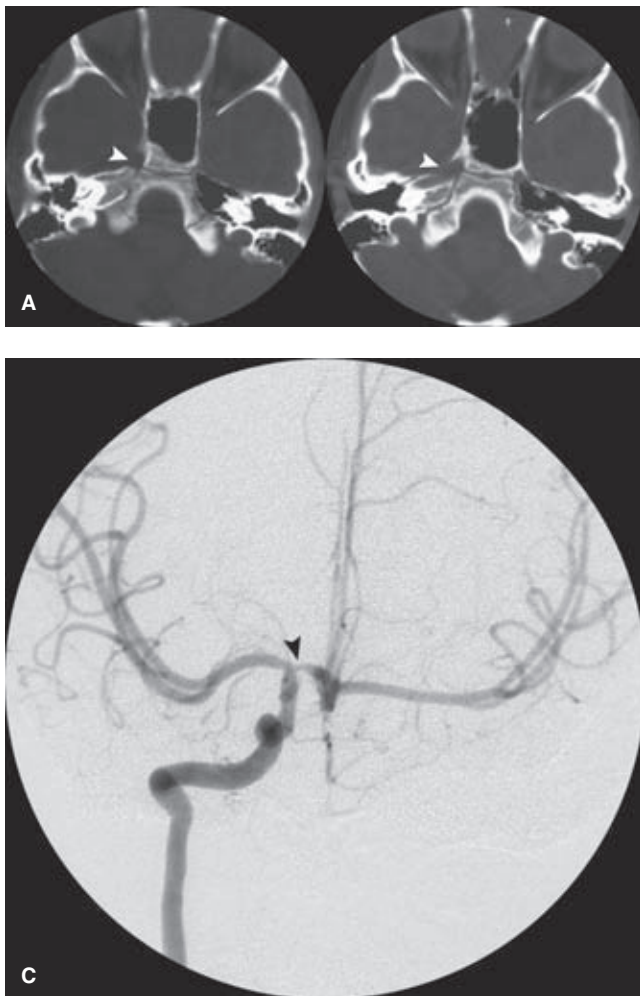


FIGURE 10-37. (A–C) Agnesis of the left internal carotid artery. A 9-year-old child with intermittent ischemic symptoms in the left hemisphere with demonstration of agnesis of the left internal carotid artery. The CT scan bone windows of the skull base demonstrate a normal carotid bony canal (*arrowheads*) on the right side, but no such corresponding structures on the left. The time-of-flight magnetic resonance angiography (TOF MRA) (**B**) confirms the normal-appearing right internal carotid artery (*white arrowheads* in **B**), but no left internal carotid artery. Subsequent cerebral angiography demonstrated no evidence of an internal carotid artery on the left side, representing presumed agnesis or early pre/perinatal occlusion. The right internal carotid artery AP view (**C**) shows prompt cross filling via the anterior communicating artery to the left hemisphere, but unfortunately, there is evidence of early stenosis or narrowing of the right A1 segment (*arrowhead* in **C**), which was thought to be the explanation of her development of new symptoms.

ear mass on axial images with subsequent biopsy, severe bleeding, and pseudoaneurysm formation (40,41) (Fig. 10-38). This is a rare condition, but because of the surgical risks involved through inadvertent biopsy, it is necessary to be familiar with it. It may occasionally be seen bilaterally (42,43).

This condition is thought to relate to atresia or regression of the cervical portion of the internal carotid artery. In these cases, what appears to be the internal carotid artery represents an enlarged inferior tympanic branch of the ascending pharyngeal artery. This usually tiny vessel enters the tympanic cavity through the inferior tympanic canaliculus (which it shares with the Jacobson tympanic branch of the IX nerve). With reconstitution of the petrous internal carotid artery through this route, the vessel has a more lateral and posterior location than the usual carotid canal. This location in association with a pinched contour of the vessel causes a characteristic angiographic appearance. Lapayowker et al. (44) described the vestibular line on the AP view, which is a vertical line dropped from the most lateral aspect of the vestibular apparatus. The petrous internal carotid artery normally lies medial to this line but swings lateral to it in the setting of an aberrant internal carotid artery.

Persistent Stapedial Artery

A persistent stapedial artery represents a rare anomalous derivative of the hyoid–stapedial artery (see Chapter 7). Usually, this artery regresses at the level of the stapes, becoming the carotico-tympanic branch of the petrous internal carotid artery. A persistent stapedial artery traces a course through the middle ear. Therefore, it represents a surgical hazard during middle ear exploration or biopsy (Fig. 10-15). Most commonly, a persistent stapedial artery retains as its territory the dural branches of the primitive hyoid artery. Therefore, the middle meningeal artery in these cases is supplied by the petrous internal carotid artery, with an accompanying diminution or absence of the foramen spinosum (45). Still rarer cases have been described where the persistent stapedial artery from the internal carotid artery retains the territory of the maxillomandibular trunk of the hyoid artery, that is, that territory usually subsumed by the distal external carotid artery (46).

Primitive Maxillary Artery

This is an extremely rare variant of the cavernous segment of the internal carotid artery (C5) that arises at approximately the same level as a persistent trigeminal artery. Unlike the latter, which is directed posteriorly, a primitive maxillary

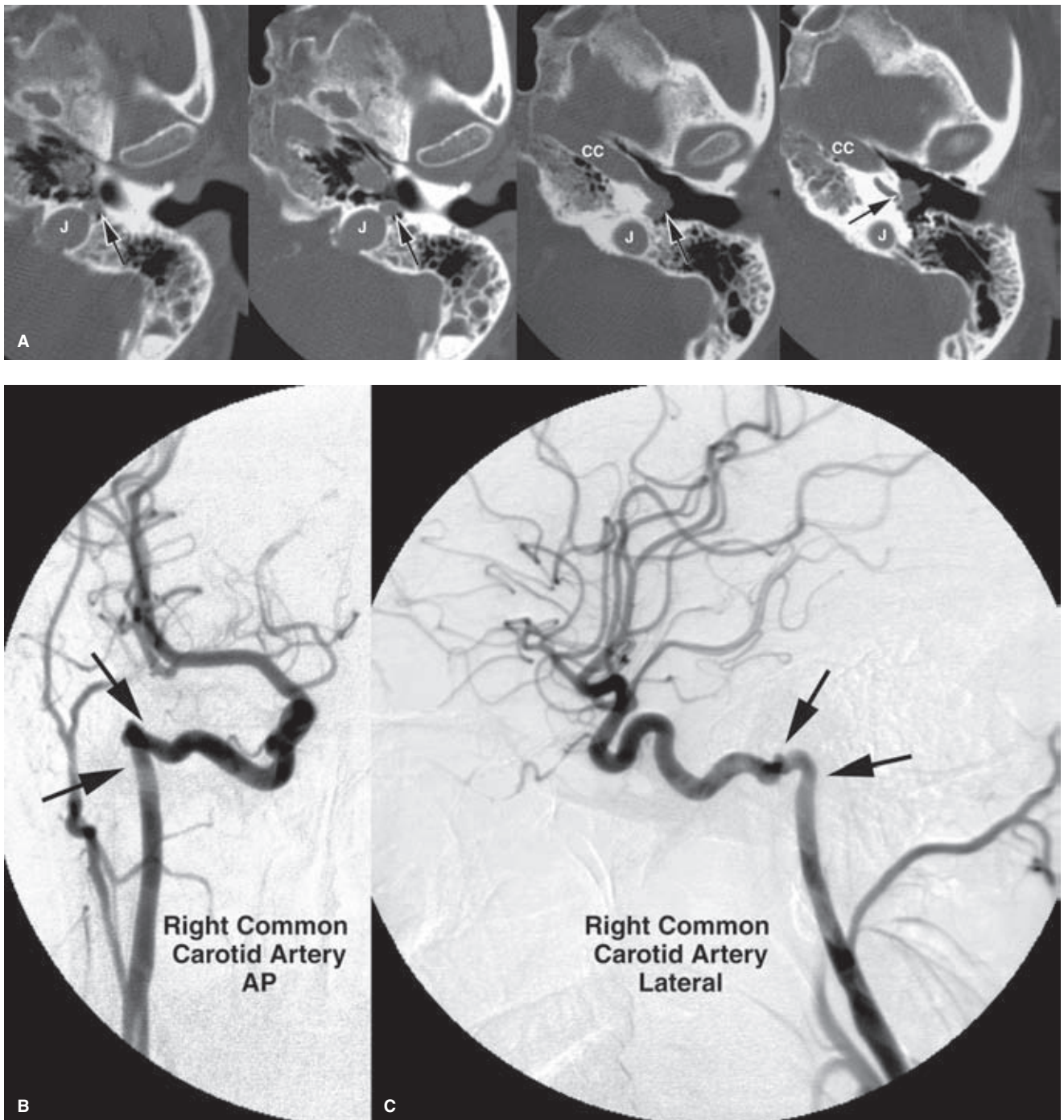


FIGURE 10-38. (A–C) Aberrant internal carotid artery. An elderly female was studied for evaluation of otosclerosis. A diagnosis of middle ear mass was reached. The “mass” was biopsied with a 22G needle, causing profuse bleeding. Axial CT images (**A**) from inferior to superior demonstrate absence of an exocranial ostium of the carotid canal (*CC*) in the usual location. An unusually large bony canal (*arrow*) is seen adjacent to the jugular bulb (*J*). Followed from one slice to the next, this canal becomes a tubular soft tissue structure joining the carotid canal (*CC*). At its apex in the middle ear, the afferent and efferent components of this vessel cannot be perceived on a single image explaining why this entity is sometimes misinterpreted as a mass. Notice how it lies lateral to the semicircular canals of the vestibular apparatus. This is a typical CT appearance of an aberrant internal carotid artery. Right common carotid arteriography demonstrates the typical angiographic appearance of an aberrant internal carotid artery. The artery extends more posteriorly than usual on the lateral view (**C**) with a constrained, knuckled appearance (*arrows*). On the AP view (**B**), it projects more laterally than does the usual course of the internal carotid artery. Fortunately, for this patient, a pseudoaneurysm at the biopsy site was not found.

artery is directed medially, where it gives branches to the clivus, dorsum sellae, and hypophysis. Inferiorly, it anastomoses with the clival branches of the ascending pharyngeal artery and medially with its contralateral fellow. It is through the latter route that reconstitution of the contralateral internal carotid artery may take place in cases of prenatal carotid occlusion, giving the appearance of a cavernous origin of the contralateral carotid artery (47) (Figs. 10-36, Fig. 9-11).

► CAROTID–BASILAR ANASTOMOSES

Persistent Trigeminal Artery

This unusual vessel, seen in approximately 0.3% of cerebral angiograms, extends from the presellar segment of the internal carotid artery to the basilar system (48,49). It is most commonly seen in two predominant patterns (50). First, it may connect with the upper part of the basilar trunk and supply the posterior cerebral artery and superior cerebellar artery territories. In this instance, the inferior part of the posterior circulation below the level of the anterior inferior cerebellar artery is separated from the upper part. Alternatively, there may be one or two fetal-type posterior cerebral artery origins present restricting the trigeminal artery supply to the posterior fossa. Other possible variants include origin of a single cerebellar artery from the trigeminal site (51) (Figs. 10-39–10-42).

It is important to recognize the trigeminal artery in situations such as Wada testing to avoid embolization or infusion of barbiturates into the posterior fossa. The trigeminal artery may also have an intrasellar course and could be mistaken for a pituitary mass or cyst (52). A persistent trigeminal artery may be a site of aneurysm formation (49,53). A

ruptured aneurysm in this location may leak into the subarachnoid space. Alternatively, leakage into the cavernous sinus presents as a carotid–cavernous fistula. Treatment by endovascular or surgical techniques for fistulas in this location can be undertaken using the same methods as those for carotid–cavernous fistulas in more usual locations (49). However, clarify the vascular anatomy of the posterior fossa before undertaking treatment of a lesion related to a persistent trigeminal artery. In cases in which there is midbasilar atresia or hypoplasia, it is vitally important to preserve the trigeminal artery as a source of flow to the posterior circulation.

Proatlantal Intersegmental Arteries

The proatlantal intersegmental arteries represent a persistent embryologic connection between the anterior and posterior circulations, whereby the vertebrobasilar circulation derives supply either from the internal or external carotid arteries (54). These are extremely rare anomalies of which only a handful have been reported with modern imaging techniques (Figs. 10-43 and 10-44, Fig. 9-17). They are probably associated in embryologic development with the formation of the occipital artery. Therefore, many of the published examples demonstrate a common origin with the occipital artery (55). Kolbinger et al. (56) reported on 39 cases. They observed that the proatlantal artery usually takes origin at the C2–C3 level and is associated with aplasia or hypoplasia of the ipsilateral or both vertebral arteries in about 50% of cases. Cases arising from the external carotid artery are slightly more common than those from the internal carotid artery. The finding of such an anomalous vessel is usually incidental

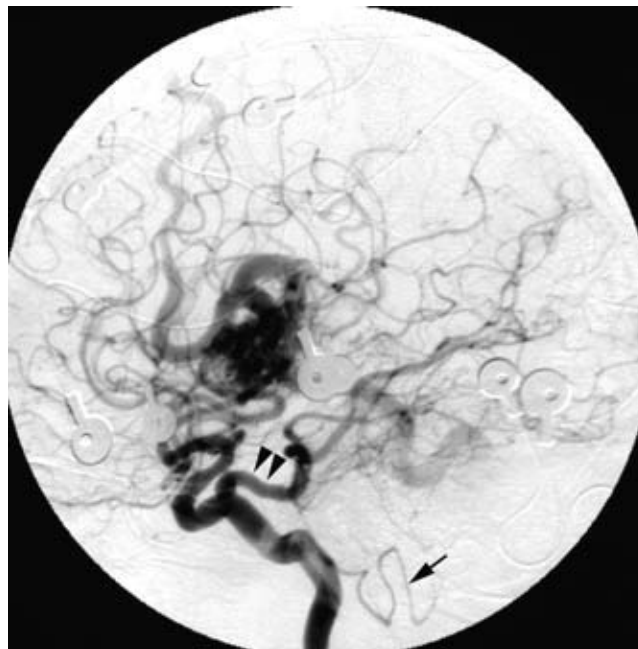


FIGURE 10-39. Trigeminal artery in a patient for Wada testing. A middle-aged female with a left hemispheric AVM referred for preoperative Wada testing. A preliminary internal carotid artery injection demonstrates a persistent trigeminal artery (*arrowheads*) perfusing the posterior circulation as far as the posterior inferior cerebellar artery (*arrow*). To perform a Wada test safely in this patient, the infusion of amobarbital must be made above the carotid–basilar connection in order to avoid perfusing the posterior circulation. This requires heparinization of the patient and coaxial passage of a microcatheter to the supraclinoid internal carotid artery.

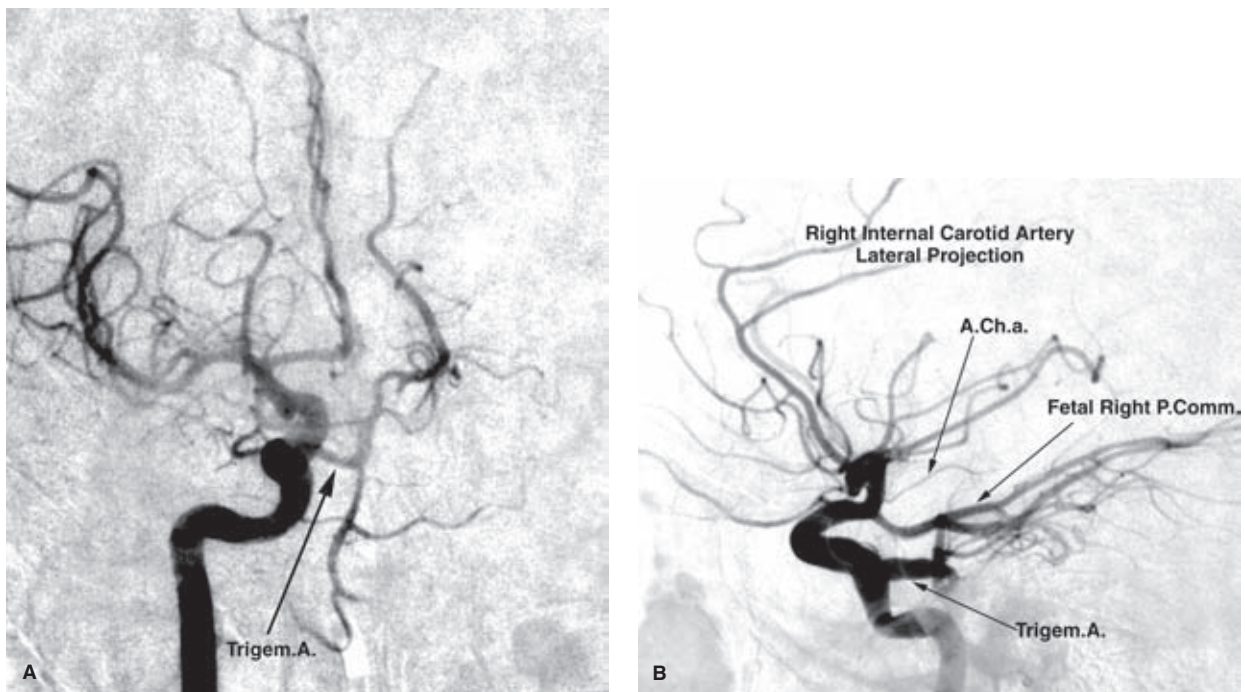


FIGURE 10-40. (A–B) Trigeminal artery. A variant of the trigeminal artery is demonstrated. An associated ipsilateral fetal posterior communicating artery is present. On the lateral view, confusion over the identity of posteriorly directed vessels from the carotid artery must be avoided by discerning clearly between the posterior communicating artery and anterior choroidal artery (*A.Ch.a.*), which arise from the supraclinoid internal carotid artery, and the persistent trigeminal artery (*Trigem.A.*), which arises from the cavernous internal carotid artery. As the trigeminal artery enters the basilar artery it frequently makes a loop or turn, well demonstrated in this case. However, in many instances, this turn may simulate the appearance of an aneurysm on the lateral view.

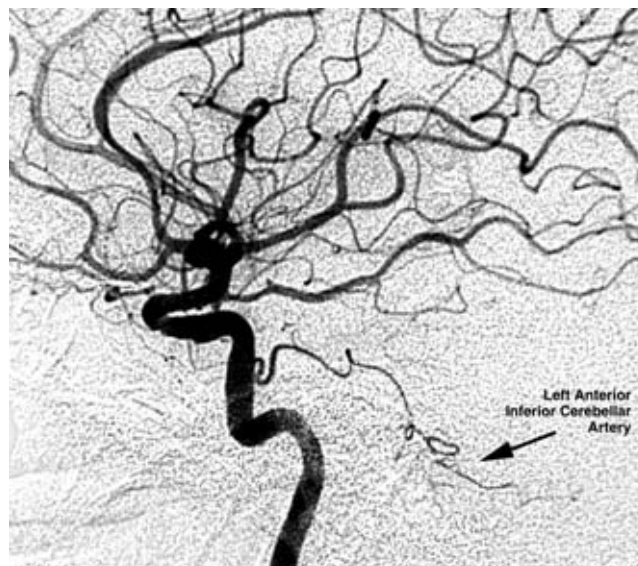


FIGURE 10-41. Trigeminal variant to anterior inferior cerebellar artery. Incidental finding of a trigeminal variant giving supply to the territory of the ipsilateral anterior inferior cerebellar artery. Cases of posterior inferior cerebellar artery supply in a similar manner have been reported.

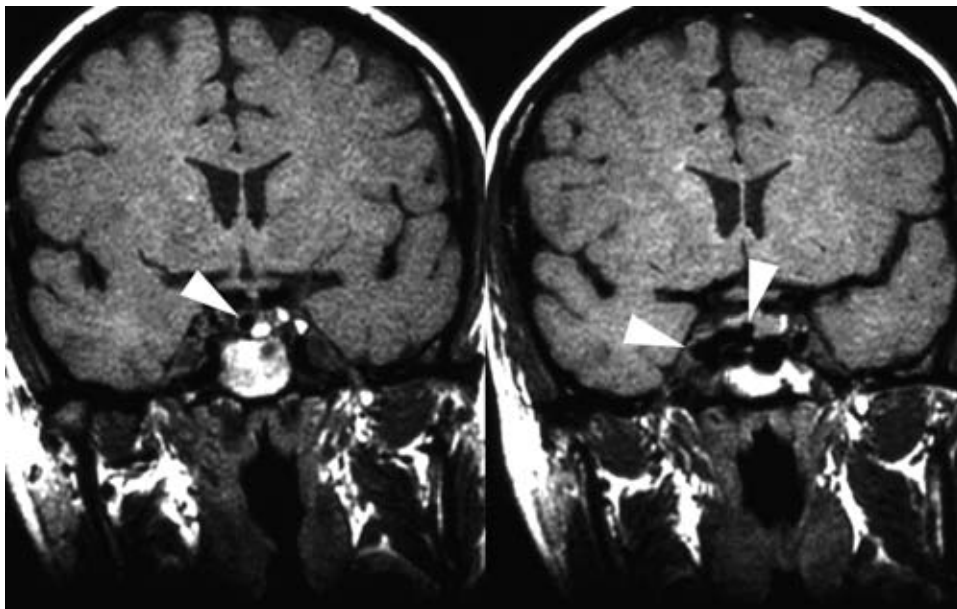
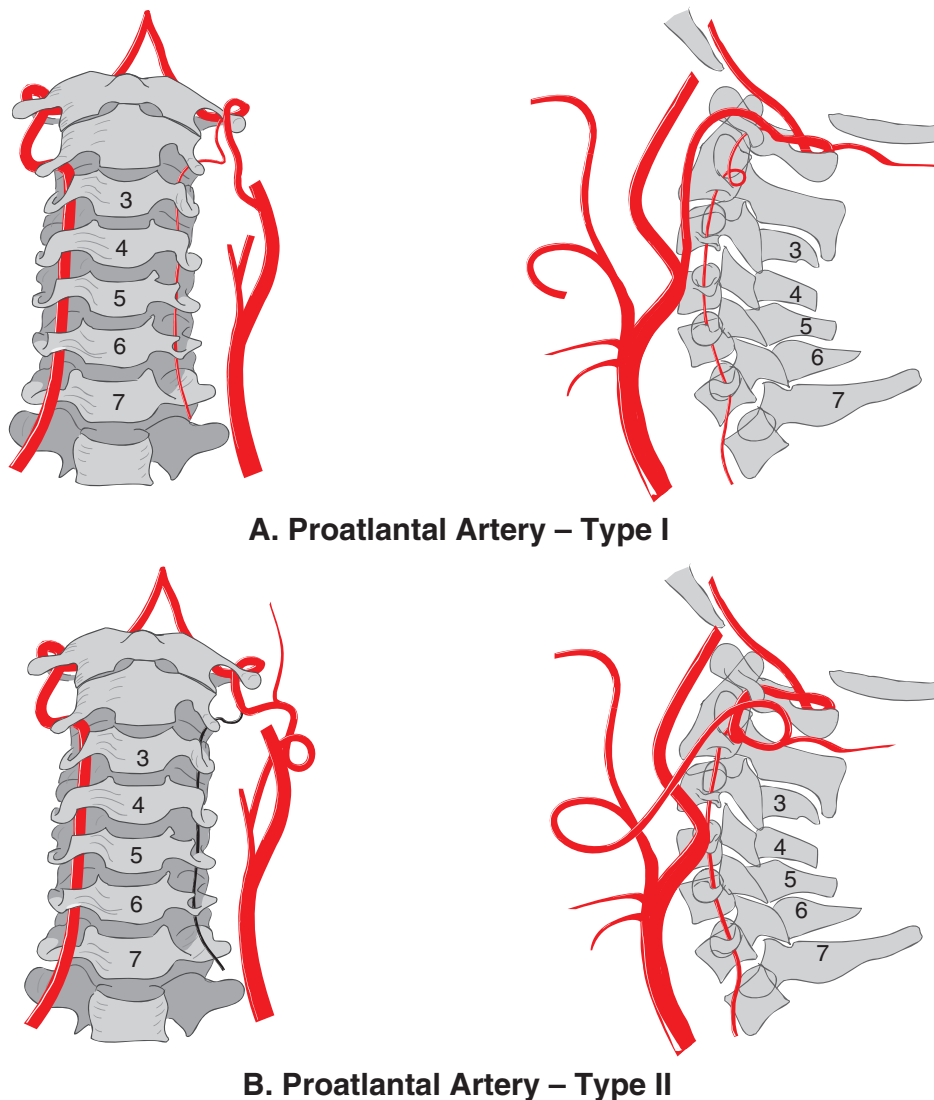


FIGURE 10-42. Intrasellar course of a persistent trigeminal artery. Coronal T1-weighted images demonstrate an intrasellar course of a carotid–basilar anastomotic vessel (*white arrowheads*). The importance of discerning this entity from intrasellar masses or cysts in which surgery might be considered is self-evident.

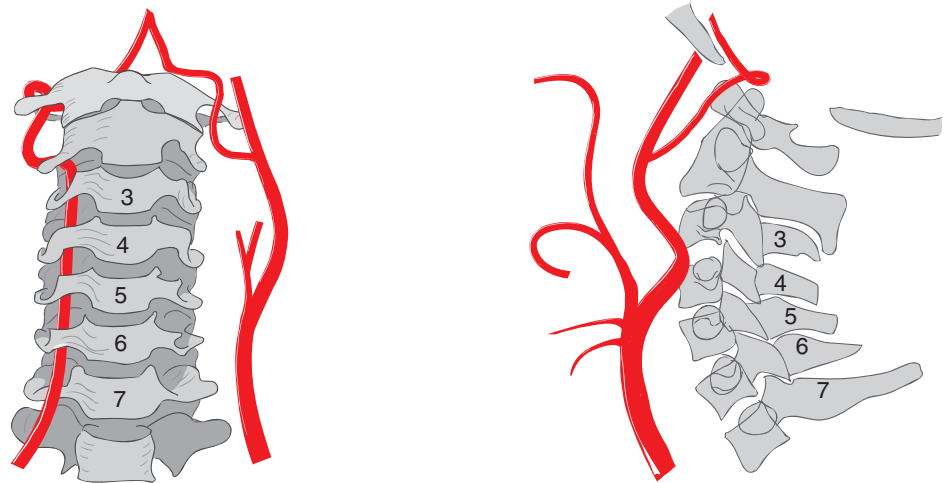


A. Proatlantal Artery – Type I

B. Proatlantal Artery – Type II

FIGURE 10-43. (A–C) Proatlantal and hypoglossal artery variants. Proatlantal arteries, types I (A) and II (B), and a persistent hypoglossal artery (C) are illustrated. For the sake of didactic contrast, hypoplastic ipsilateral vertebral arteries are included, but they are not usually seen in reported clinical examples. Discerning among these variants depends on identifying where they join the normal course of the vertebrobasilar circulation. (*continued*)

FIGURE 10-43. (CONTINUED)



C. Hypoglossal Artery

but may warrant specific consideration when associated with ischemic disease or when an endarterectomy or angioplasty is being planned (57,58).

A persistent proatlantal intersegmental artery type I is said to take origin from the internal carotid artery and is connected to the vertebral artery at the atlanto-occipital space (Fig. 10-44). The type I does not traverse a foramen transversarium. A type II persistent proatlantal intersegmental artery, usually associated with the external carotid artery,

joins the normal course of the vertebral artery at the C1–C2 interspace (Fig. 9-17).

Persistent Hypoglossal Artery

The rare hypoglossal artery has its origin from the internal carotid or common carotid artery between the expected level of the carotid bifurcation and C1–C2 (Figs. 10-43, 10-45, 10-46, Fig. 9-18). In contrast to the proatlantal intersegmental arteries, which join the extracranial vertebral

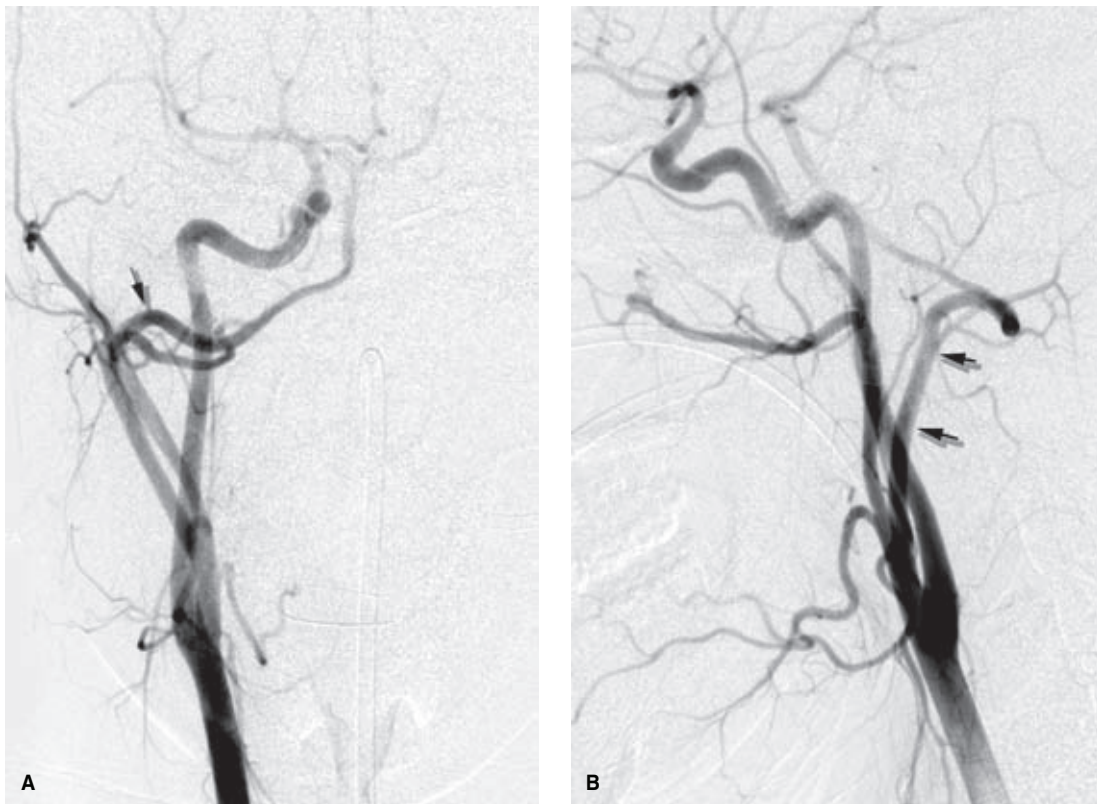


FIGURE 10-44. (A–B) Proatlantal artery. This young patient was studied for the cause of a cerebellar bleed. Her right common carotid angiogram demonstrates an unusual artery (*arrow*) from the external carotid artery to the C1 level reconstituting the ipsilateral expected course of the vertebral artery. The observation that this proatlantal artery arises from the external carotid artery and joins the vertebral artery at the C1 level calls into question the long promulgated classification of this rare anomaly into type I and type II. See also Figure 9-17.



FIGURE 10-45. (A–B) Persistent hypoglossal artery. PA (A) and lateral (B) views of an incidentally discovered hypoglossal artery. See text for features contrasting this with proatlantal anomalies.

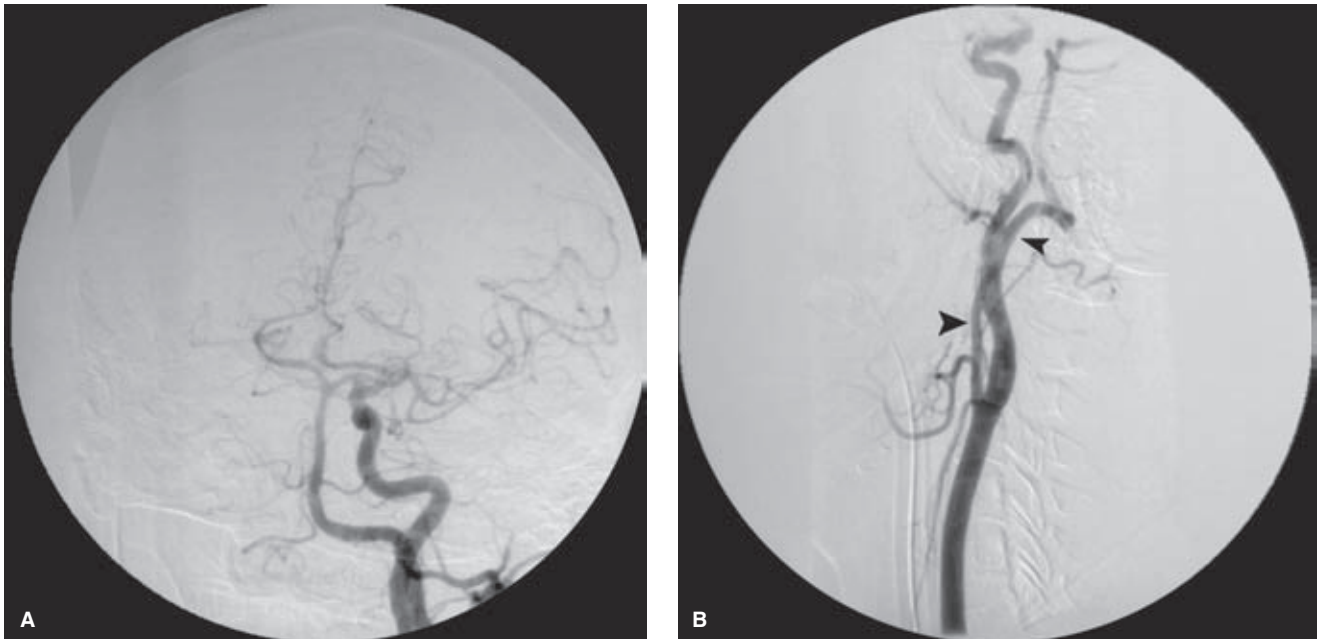


FIGURE 10-46. A–B: Persistent hypoglossal artery. A PA view (A) centered on the head and lateral (B) view centered on the neck demonstrate a typical hypoglossal artery (*arrowheads*) reaching the intracranial space via the hypoglossal foramen. In this instance, the neuroradiologist had the presence of mind to recognize the variant while the examination was in progress and thus obtained tailored views. However, frequently one is so accustomed to seeing opacification of the basilar artery through reflux during common carotid artery views that it often does not immediately occur to the angiographer that something odd is afoot.

system gaining access to the intracranial cavity via the foramen magnum, the hypoglossal artery enters the skull via the hypoglossal (anterior condylar) canal (59,60). The hypoglossal artery has been described on the AP view as having a more medial and direct course in the neck toward the hypoglossal canal, compared with the proatlantal artery, which must join the more laterally disposed course of the cervical vertebral artery (61,62). On the lateral view, the hypoglossal artery does not have the posterior loop in the atlanto-occipital space seen with both variants of the proatlantal artery (57,59,63–66). Rare cases of bilateral primitive hypoglossal arteries or trigeminal arteries have been reported (67,68).

Otic Artery

The otic artery is probably an example of how difficult it is to purge a black pearl from the literature. Every purported case that has ever been published is either filmed on ancient equipment or more accurately understood as a trigeminal variant or remnant (69,70).

References

- Vitek JJ, Reaves P. Thoracic bifurcation of the common carotid artery. *Neuroradiology* 1973;5(3):133–139.
- Bouthillier A, van Loveren HR, Keller JT. Segments of the internal carotid artery: A new classification. *Neurosurgery* 1996;38(3):425–432; discussion 432–423.
- Umansky F, Elidan J, Valarezo A. Dorello's canal: A microanatomical study. *J Neurosurg* 1991;75(2):294–298.
- von Overbeeke JJ, Dujovny M, Dragovic L, et al. Anatomy of the sympathetic pathways in the carotid canal. *Neurosurgery* 1991;29(6):838–843; discussion 843–834.
- Paullus WS, Pait TG, Rhoton AI Jr. Microsurgical exposure of the petrous portion of the carotid artery. *J Neurosurg* 1977;47(5):713–726.
- Bernasconi V, Cassinari V, Gori G. Diagnostic value of the tentorial arteries of the carotid siphon. (Angiographic study of a case of falcotentorial angioma). *Neurochirurgia (Stuttg)* 1965;62:67–72.
- Harris FS, Rhoton AL. Anatomy of the cavernous sinus. A microsurgical study. *J Neurosurg* 1976;45(2):169–180.
- Lasjaunias P, Moret J, Mink J. The anatomy of the inferolateral trunk (ILT) of the internal carotid artery. *Neuroradiology* 1977;13(4):215–220.
- Krisht AF, Barrow DL, Barnett DW, et al. The microsurgical anatomy of the superior hypophyseal artery. *Neurosurgery* 1994;35(5):899–903; discussion 903.
- Ogawa T, Miyauchi T, Kato T, et al. Internal carotid origin of double ophthalmic arteries. *Neuroradiology* 1990;32(6):508–510.
- Linskey ME, Sekhar LN, Hirsch W Jr, et al. Aneurysms of the intracavernous carotid artery: Clinical presentation, radiographic features, and pathogenesis. *Neurosurgery* 1990;26(1):71–79.
- Linskey ME, Sekhar LN, Hirsch WL Jr, et al. Aneurysms of the intracavernous carotid artery: Natural history and indications for treatment. *Neurosurgery* 1990;26(6):933–937; discussion 937–938.
- Kupersmith MJ, Hurst R, Berenstein A, et al. The benign course of cavernous carotid artery aneurysms. *J Neurosurg* 1992;77(5):690–693.
- Obrador S, Gomez-Bueno J, Silvela J. Spontaneous carotid-cavernous fistula produced by ruptured aneurysm of the meningo-hypophyseal branch of the internal carotid artery. Case report. *J Neurosurg* 1974;40(4):539–543.
- Teitelbaum GP, Halbach VV, Larsen DW, et al. Treatment of massive posterior epistaxis by detachable coil embolization of a cavernous internal carotid artery aneurysm. *Neuroradiology* 1995;37(4):334–336.
- McLaughlin MR, Jho HD, Kwon Y. Acute subdural hematoma caused by a ruptured giant intracavernous aneurysm: Case report. *Neurosurgery* 1996;38(2):388–392.
- Nishioka T, Kondo A, Aoyama I, et al. Subarachnoid hemorrhage possibly caused by a saccular carotid artery aneurysm within the cavernous sinus. Case report. *J Neurosurg* 1990;73(2):301–304.
- Lee AG, Mawad ME, Baskin DS. Fatal subarachnoid hemorrhage from the rupture of a totally intracavernous carotid artery aneurysm: Case report. *Neurosurgery* 1996;38(3):596–598; discussion 598–599.
- Padgett DH. The development of the cranial arteries in the human embryo. *Contrib Embryol* 1948;32:205–262.
- Hayreh SS. The ophthalmic artery, III. Branches. *Br J Ophthalmol* 1962;46:212–247.
- Gibo H, Lenkey C, Rhoton AL Jr. Microsurgical anatomy of the supraclinoid portion of the internal carotid artery. *J Neurosurg* 1981;55(4):560–574.
- Gibo H, Kobayashi S, Kyoshima K, et al. Microsurgical anatomy of the arteries of the pituitary stalk and gland as viewed from above. *Acta Neurochir (Wien)* 1988;90(1–2):60–66.
- Bergland R. The arterial supply of the human optic chiasm. *J Neurosurg* 1969;31(3):327–334.
- Day AL. Aneurysms of the ophthalmic segment. A clinical and anatomical analysis. *J Neurosurg* 1990;72(5):677–691.
- Rhoton AL Jr, Fujii K, Fradd B. Microsurgical anatomy of the anterior choroidal artery. *Surg Neurol* 1979;12(2):171–187.
- Rhoton AL Jr, Saeki N, Perlmutter D, et al. Microsurgical anatomy of common aneurysm sites. *Clin Neurosurg* 1979;26:248–306.
- Carpenter MB, Noback CR, Moss ML. The anterior choroidal artery; its origins course, distribution, and variations. *AMA Arch Neurol Psychiatry* 1954;71(6):714–722.
- Morello A, Cooper IS. Arteriographic anatomy of the anterior choroidal artery. *Am J Roentgenol Radium Ther Nucl Med* 1955;73(5):748–751.
- Herman LH, Fernando OU, Gurdjian ES. The anterior choroidal artery: An anatomical study of its area of distribution. *Anat Rec* 1966;154(1):95–101.
- Moyer DJ, Flamm ES. Anomalous arrangement of the origins of the anterior choroidal and posterior communicating arteries. Case report. *J Neurosurg* 1992;76(6):1017–1018.
- Paroni Sterbini GL, Agatiello LM, Stocchi A, et al. CT of ischemic infarctions in the territory of the anterior choroidal artery: A review of 28 cases. *AJNR Am J Neuroradiol* 1987;8(2):229–232.
- Foix CH, Chavany H, Hillemand P. Oblitération de l'artère choroïdienne antérieure. Ramollissement cérébrale, hémiplégié, hémianesthésie, et hémianopsie. *Société d'Ophthalmologie* 1925;27:221–223.
- Cooper IS. Surgical occlusion of the anterior choroidal artery in parkinsonism. *Surg Gynecol Obstet* 1954;92(2):207–219.
- Teal JS, Rumbaugh CL, Segall HD, et al. Anomalous branches of the internal carotid artery. *Radiology* 1973;106(3):567–573.
- Kishore PR, Kaufman AB, Melichar FA. Intracavernous carotid anastomosis simulating pituitary microadenoma. *Radiology* 1979;132(2):381–383.
- Staples GS. Transsellar intracavernous intercarotid collateral artery associated with agenesis of the internal carotid artery. Case report. *J Neurosurg* 1979;50(3):393–394.
- Beresini DC, Hieshima GB, Mehringer CM, et al. Bilateral absence of the internal carotid artery with sellar enlargement due to anomalous vascularity. *Surg Neurol* 1981;16(1):9–16.
- Dilenge D, Geraud G. Accessory meningeal artery. *Acta Radiol (Suppl)* 1975;347:63–69.
- Lasjaunias P, Santoyo-Vazquez A. Segmental agenesis of the internal carotid artery: Angiographic aspects with embryological discussion. *Anat Clin* 1984;6(2):133–141.

40. Cole RD, May JS. Aberrant internal carotid artery. *South Med J* 1994;87(12):1277–1280.
41. Goldman NC, Singleton GT, Holly EH. Aberrant internal carotid artery presenting as a mass in the middle ear. *Arch Otolaryngol* 1971;94(3):269–273.
42. Campbell G, Renner G, Estrem SA. Bilateral aberrant internal carotid arteries. *Otolaryngol Head Neck Surg* 1992;107(1):124–128.
43. Glasscock ME 3rd, Seshul M, Seshul MB Sr. Bilateral aberrant internal carotid artery case presentation. *Arch Otolaryngol Head Neck Surg* 1993;119(3):335–339.
44. Lapayowker MS, Liebman EP, Ronis ML, et al. Presentation of the internal carotid artery as a tumor of the middle ear. *Radiology* 1971;98(2):293–297.
45. Guinto FC Jr, Garrabrant EC, Radcliffe WB. Radiology of the persistent stapedia artery. *Radiology* 1972;105(2):365–369.
46. Rodesch G, Choi IS, Lasjaunias P. Complete persistence of the hyoido-stapedial artery in man. Case report. Intra-petrous origin of the maxillary artery from ICA. *Surg Radiol Anat* 1991;13(1):63–65.
47. Midkiff RB, Boykin MW, McFarland DR, et al. Agenesis of the internal carotid artery with intercavernous anastomosis. *AJNR Am J Neuroradiol* 1995;16(6):1356–1359.
48. Tomsick TA, Lukin RR, Chambers AA. Persistent trigeminal artery: Unusual associated abnormalities. *Neuroradiology* 1979;17(5):253–257.
49. Debrun GM, Davis KR, Nauta HJ, et al. Treatment of carotid cavernous fistulae or cavernous aneurysms associated with a persistent trigeminal artery: Report of three cases. *AJNR Am J Neuroradiol* 1988;9(4):749–755.
50. Saltzman GF. Patent primitive trigeminal artery studied by cerebral angiography. *Acta Radiol* 1959;51(5):329–336.
51. Siqueira M, Piske R, Ono M, et al. Cerebellar arteries originating from the internal carotid artery. *AJNR Am J Neuroradiol* 1993;14(5):1229–1235.
52. Richardson DN, Elster AD, Ball MR. Intrasellar trigeminal artery. *AJNR Am J Neuroradiol* 1989;10(1):205.
53. McKenzie JD, Dean BL, Flom RA. Trigeminal–cavernous fistula: Saltzman anatomy revisited. *AJNR Am J Neuroradiol* 1996;17(2):280–282.
54. Lasjaunias P, Theron J, Moret J. The occipital artery. Anatomy—normal arteriographic aspects—Embryological significance. *Neuroradiology* 1978;15(1):31–37.
55. Suzuki S, Nobechi T, Itoh I, et al. Persistent proatlantal intersegmental artery and occipital artery originating from internal carotid artery. *Neuroradiology* 1979;17(2):105–109.
56. Kolbinger R, Heindel W, Pawlik G, et al. Right proatlantal artery type I, right internal carotid occlusion, and left internal carotid stenosis: Case report and review of the literature. *J Neurol Sci* 1993;117(1–2):232–239.
57. Fantini GA, Reilly LM, Stoney RJ. Persistent hypoglossal artery: Diagnostic and therapeutic considerations concerning carotid thromboendarterectomy. *J Vasc Surg* 1994;20(6):995–999.
58. Ouriel K, Green RM, DeWeese JA. Anomalous carotid–basilar anastomoses in cerebrovascular surgery. *J Vasc Surg* 1988;7(6):774–777.
59. Anderson RA, Sondheimer FK. Rare carotid–vertebrobasilar anastomoses with notes on the differentiation between proatlantal and hypoglossal arteries. *Neuroradiology* 1976;11(3):113–118.
60. Brismar J. Persistent hypoglossal artery, diagnostic criteria. Report of a case. *Acta Radiol Diagn (Stockh)* 1976;17(2):160–166.
61. Wardwell GA, Goree JA, Jimenez JP. The hypoglossal artery and hypoglossal canal. *Am J Roentgenol Radium Ther Nucl Med* 1973;118(3):528–533.
62. Resche F, Resche-Perrin I, Robert R, et al. [The hypoglossal artery. A new case report—Review of the literature]. *J Neuro-radiol* 1980;7(1):27–43.
63. Bahsi YZ, Uysal H, Peker S, et al. Persistent primitive proatlantal intersegmental artery (proatlantal artery I) results in “top of the basilar” syndrome. *Stroke* 1993;24(12):2114–2117.
64. Lui CC, Liu YH, Wai YY, et al. Persistence of both proatlantal arteries with absence of vertebral arteries. *Neuroradiology* 1987;29(3):304–305.
65. Hutchinson NA, Miller JD. Persistent proatlantal artery. *J Neurol Neurosurg Psychiatry* 1970;33(4):524–527.
66. Obayashi T, Furuse M. The proatlantal intersegmental artery: A case report and review of the literature. *Arch Neurol* 1980;37(6):387–389.
67. Karasawa J, Kikuchi H, Furuse S, et al. Bilateral persistent carotid–basilar anastomoses. *Am J Roentgenol* 1976;127(6):1053–1056.
68. Oertel H. Über de Persistenz embryonaler Verbindungen zwischen der A. Carotid interna und der A. Vertebralis cerebrealis. *Verhandlungen der Anatomischen Gesellschaft* 1922;31:281–295.
69. Bhattacharya JJ, Lamin S, Thammaroj J. Otic or mythic? *AJNR Am J Neuroradiol* 2004;25(1):160–162; author reply 162.
70. Croft HJ. Persistent otic artery. *AJNR Am J Neuroradiol* 2004;25(1):162; author reply 162.
71. Fischer E. Die Lageabweichungen der vorderen Hirnarterien Gafässbild. *Zentralbl Neurochir* 1938;3:300–313.

The Anterior Cerebral Artery

Key Points

- Selecting the A1 segment with a wire and microcatheter is often very difficult. Therefore, to force the microcatheter to make this difficult turn, a great deal of forward tension will build up in the microcatheter. Be attentive to the tip of the wire lest a small medial lenticulostriate or cortical branch might perforate as the microcatheter finally advances.
- Do not underestimate the capacity of the A1–A2 junction to occlude itself during an endovascular procedure. Anticipate this scenario and think of backup strategies ahead of time, for example, bilateral carotid catheters, balloon reconstruction assistance, balloon angioplasty.

The anterior cerebral artery arises from the medial aspect of the internal carotid bifurcation below the anterior perforated substance. It courses anteromedially toward the interhemispheric fissure. The usual route that it takes is above the optic chiasm or nerve, meaning that the optic structures therefore slope *through* the ring of the circle of Willis. At the level of the interhemispheric fissure, the anterior cerebral artery is joined to its contralateral counterpart via the anterior communicating artery in the suprachiasmatic cistern. The anterior communicating artery represents the most common site of intracranial aneurysms, accounting for approximately 30% in most series (1).

► SEGMENTAL ANATOMY OF THE ANTERIOR CEREBRAL ARTERY

The A1 segment of the anterior cerebral artery extends from the internal carotid artery bifurcation to the anterior communicating artery; the A2 segment extends from there to the junction of the rostrum and genu of the corpus callosum; the A3 extends around the genu until the artery turns sharply posteriorly. The A4 and A5 segments above the corpus callosum are separated by the plane of the coronal fissure (2–4) (Figs. 11-1 and 11-2).

► VARIATIONS OF THE ANTERIOR CEREBRAL ARTERY–COMMUNICATING ARTERY COMPLEX

Variations in the region of the anterior communicating artery are not just common, but are to be expected.

The term *anterior cerebral artery–communicating artery complex* is frequently used in clinical parlance. As elsewhere in the circle of Willis, alterations in hemodynamics due to the presence of anomalous vessels are thought to explain the high-frequency vulnerability in patients with aneurysms in this region. The extreme variability of the anatomy in this region, due to redundancy of vessel loops, vessel duplication, and early bifurcation of the A2 segment, can make the anterior communicating artery complex one of the most difficult areas to evaluate angiographically (3) (Figs. 11-3–11-6). Fortunately, 3D angiography has eliminated the need for performing multiple DSA runs in varying obliquity in the hope of finding an optimal profile view of an anterior communicating artery or aneurysm.

Usually, the anterior cerebral arteries join the anterior communicating artery superior to the optic chiasm (70%). When the A1 segments are longer or redundant, this union may occur more anteriorly above the optic nerves. Fenestrations or duplications of the A1 portion of the anterior cerebral artery are common. More rare anomalies include an interoptic or infraoptic course of the A1 segment (5–10), or even perforation of the optic nerve by the A1 segment (11). One possible embryologic explanation for an infraoptic course of the anterior cerebral artery suggests that the A1 segment in these instances represents a persistence of the ventral primitive ophthalmic artery taking origin from the internal carotid artery and flowing retrogradely to the anterior cerebral artery.

Variations in the relative size of the A1 segments and the anterior communicating artery are common. Using a diameter of 1.5 mm or smaller as a definition for hypoplasia, approximately 10% of brains demonstrate hypoplastic A1 segments (3,12,13). The anterior communicating artery varies in length up to 7 mm, may be quite tortuous, and measures up to 3.4 mm in diameter. There is a positive correlation between the diameter of the anterior communicating artery and the degree of asymmetry of the A1 segments. This is to compensate hemodynamically for hypoplasia of the smaller vessel. Asymmetry of the A1 segments has an important impact on the likelihood of aneurysm formation in the anterior communicating artery region (Fig. 11-7). The end-on hemodynamic impact of pulsatile flow in the larger A1 segment directed against the anterior wall of the anterior communicating artery is thought to explain the higher rate of aneurysm formation under these circumstances. Up to 80% of anterior communicating artery aneurysms have significant A1

(text continues on page 164)

Segmental anatomy of the anterior cerebral artery (Fischer, 1938)

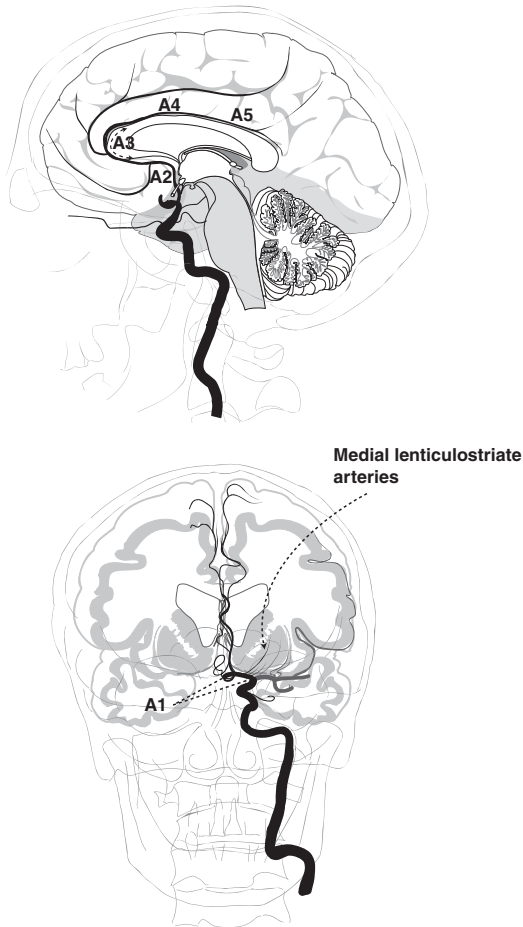


FIGURE 11-1. Segmental anatomy of the anterior cerebral artery.



FIGURE 11-2. Isolated anatomy of the anterior cerebral artery. A lateral view from an internal carotid artery injection in the setting of acute ischemic stroke treatment for complete occlusion of the middle cerebral artery affords an uninterrupted view of the territory and branches of the anterior cerebral arteries in the midline, similar to that depicted in Figure 11-1.

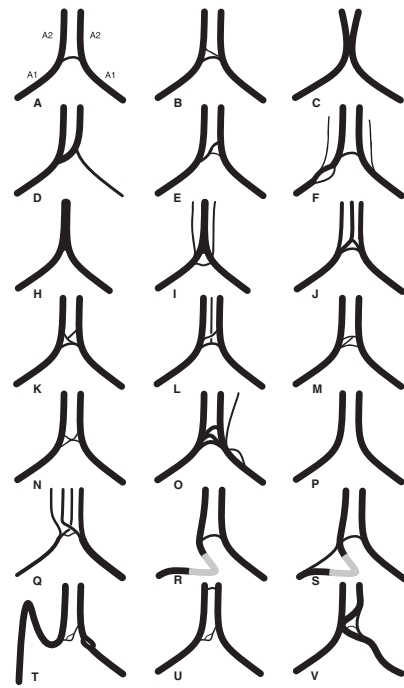


FIGURE 11-3. (A–V) Variations in the anterior communicating artery complex. Numerous variants of the junction of the anterior cerebral arteries in the region of the anterior communicating artery make this a difficult area to interrogate angiographically. Schematic illustrations of a range of common and rare variants are represented. Variants R and S represent an infraoptic course of the A1 segment. Variant T represents a persistent primitive olfactory artery.



FIGURE 11-4. Fenestration of the anterior communicating artery. Fenestrations or duplications of the anterior communicating artery such as in this example are commonly incompletely evaluated during angiography due to the complexity of the anatomy and overlap of vessels. Therefore, this example (arrow) is more unusual by virtue of the clarity of its depiction on this film than by its structure, which is probably a commonplace.

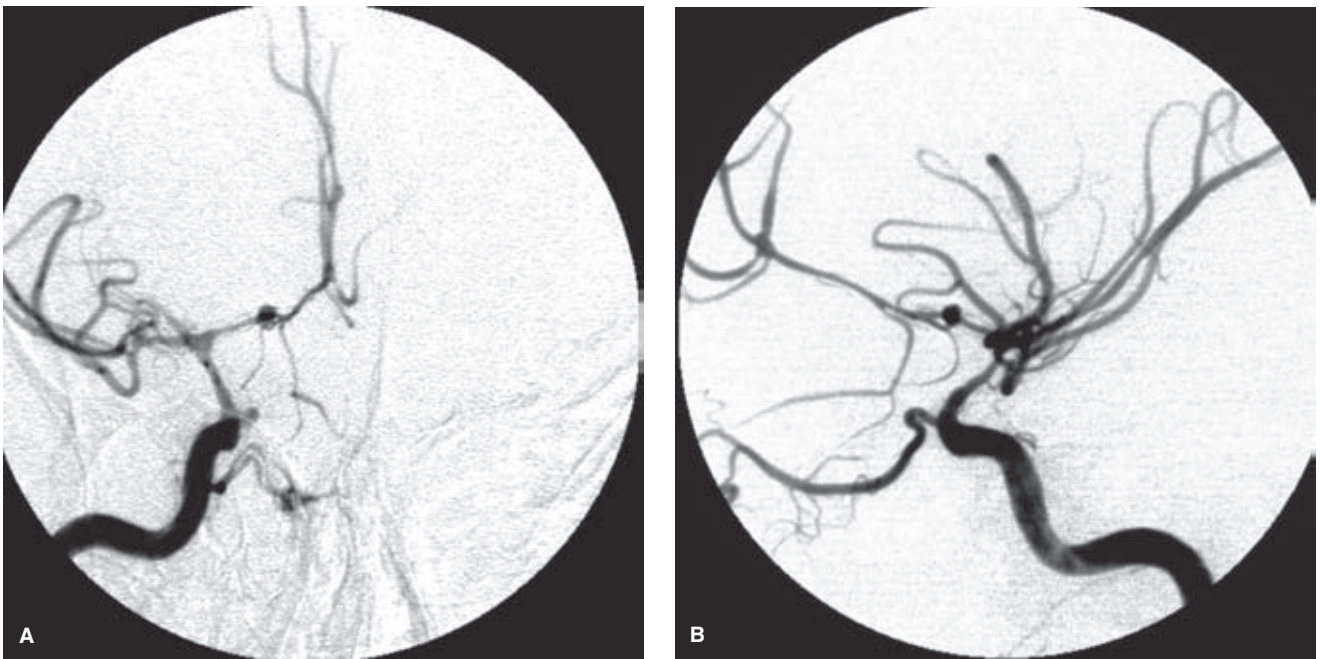
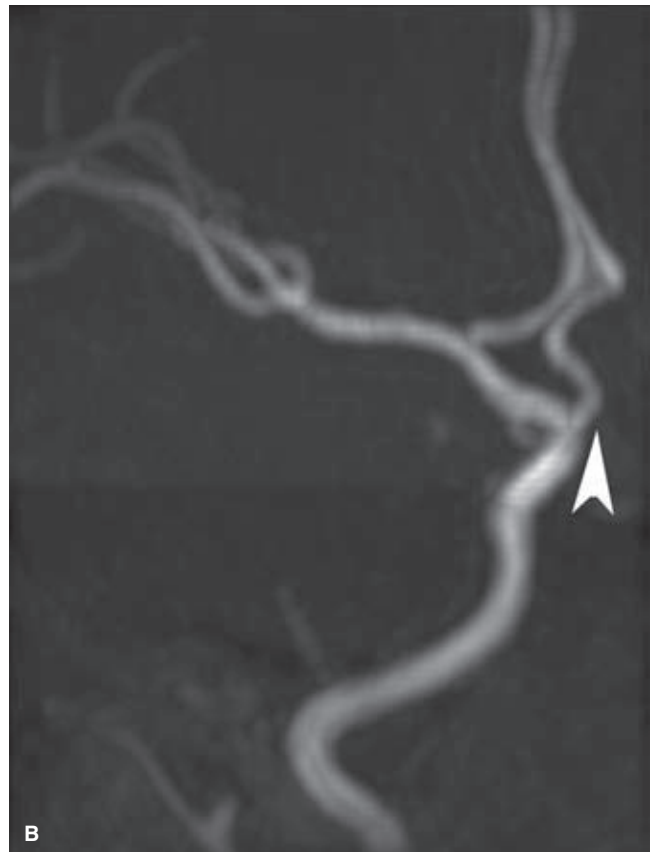
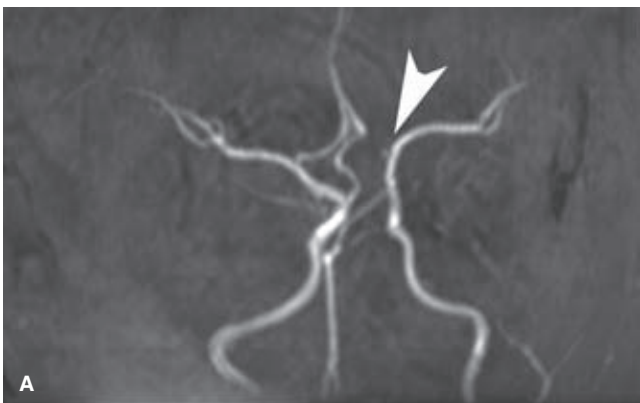


FIGURE 11-5. (A–B) A1 fenestration with associated aneurysm. A 3-mm ruptured aneurysm extends from the proximal end of a fenestration of the right A1 segment (A). Evidence of mild intracranial vasospasm is seen in the distal anterior cerebral artery circulation (B).

FIGURE 11-6. (A–B) Contralateral carotid origin of the left anterior cerebral artery. A rare anomaly is seen on this TOF MRA in a child. The AP view (A) demonstrates no evidence of an A1 segment on the left (*arrowhead in A*). The left anterior cerebral artery (*arrowhead in B*) arises from the right supraclinoid carotid artery, where it pursues an infraoptic course before entering the interhemispheric fissure. The oblique restricted view (B) confirms the anomalous vessel origin corresponding with where the right ophthalmic artery might be expected to arise.



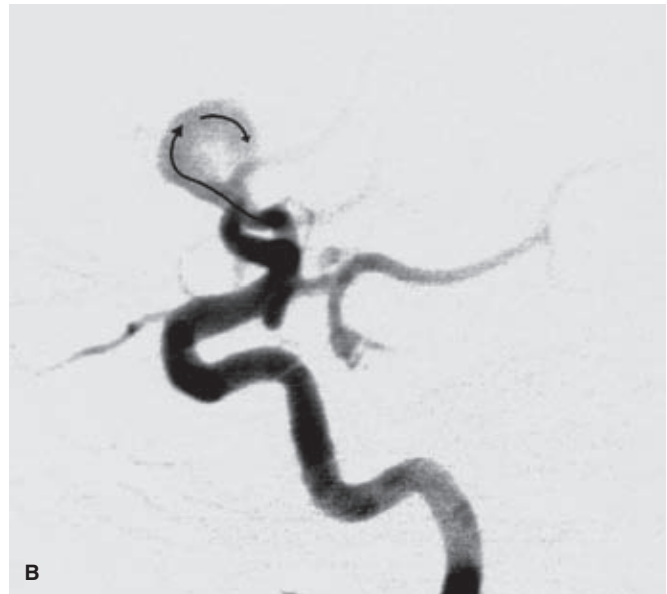
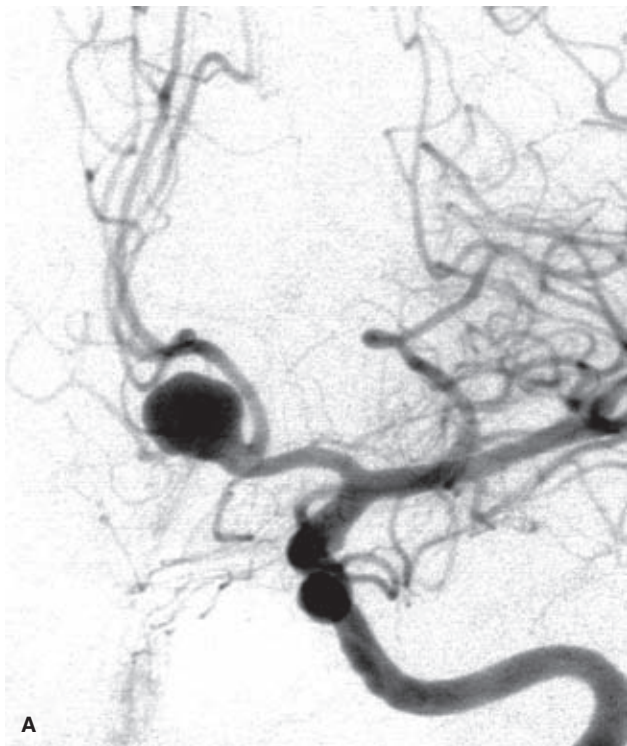


FIGURE 11-7. (A–B) Hemodynamic determination of the profile of aneurysms of the anterior communicating artery complex. In the majority of aneurysms of the anterior communicating artery region, inflow to the aneurysm is along the line of thrust from the dominant A1 segment. This, in turn, determines the direction of projection of the aneurysm dome, which in most cases is anterior and toward the opposite side. An early arterial image (B) demonstrates the opacified jet as it strikes forward within the aneurysm and is deflected off the dome.

asymmetry. This hemodynamic force also explains why approximately 70% of such aneurysms here project anteriorly (14,15) (Figs. 11-8–11-10). Altered hemodynamics in the anterior communicating artery after therapeutic occlusion of an internal carotid artery are also associated with an increased likelihood of delayed aneurysm formation.

Other common variations in this area include the presence of two or more anterior communicating arteries in 11% to 43% of brains (14,16,17). This may take the form of a fenestration of the anterior communicating artery or complete duplication or triplication (3,18). Another angiographic difficulty in imaging this area occurs when the anterior cerebral arteries are not exactly parallel; the anterior communicating artery must run an oblique course to connect the two. This calls for flexibility in one's positioning for imaging of this region.

A rare variant of the proximal anterior cerebral artery is a persistent olfactory artery that runs anteriorly from the internal carotid artery bifurcation along the olfactory groove. It may supply the territory of the anterior cerebral artery distally (19). Fenestrations of the distal A1 segment, an anomaly that is embryologically difficult to explain in this location, may represent an incomplete fusion of the anterior cerebral artery with the primitive olfactory artery (20).

► BRANCHES OF THE PROXIMAL ANTERIOR CEREBRAL ARTERY

Anterior Perforator Vessels

From the A1, proximal A2, and anterior communicating artery, two groups of perforator branches are seen. An inferiorly directed group supplies the optic chiasm and nerve. A superiorly directed group of medial lenticulostriate arteries supplies the anterior hypothalamus, septum pellucidum, the medial part of the anterior commissure, the pillars of the fornix, and the anterior aspect of the striatum. Between 2 and 15 basal arteries arise from the A1 segment, usually from the superior and posterior surfaces, particularly from the lateral half of the A1 segment (3). They enter the anterior perforated substance in the basal forebrain (21). Aneurysms of the A1 segment of the anterior cerebral artery, proximal to the anterior communicating artery, have a high likelihood of being related either to a lenticulostriate origin or cortical branch from this segment of vessel or to a fenestration of the vessel (22).

Anterior communicating artery perforator branches are directed toward the fornix, septal region, anterior cingulum, and corpus callosum (23). Similar to the disposition of the A1 segment, perforators from the anterior communicating artery arise from the posterosuperior aspect of the communicating



FIGURE 11-8. (A–C) Difficulty of evaluating the anterior communicating artery with conventional angiography. This middle-aged patient presented with a subarachnoid hemorrhage related to an aneurysm of the anterior communicating artery (A). The 3D rotational angiography view (B) showed an additional 2-mm aneurysm (arrow) at the base of the larger aneurysm. Even with the information from the 3D view the smaller aneurysm could not be seen on DSA very well, and certainly not on roadmap at all, due to its small size and location. It was considered too small and hazardous to coil at the time of treating the larger aneurysm (presumed to represent the site of hemorrhage at that time). One month later she presented with an even larger hemorrhage. The 3D view (C), on which the coils from the first procedure are subtracted from the reconstruction, shows that the previously seen inaccessible aneurysm has grown considerably in the interim with a lobulated contour, undoubtedly representing the site of new hemorrhage.

artery. This argues well in terms of surgical risk for aneurysms that project anteroinferiorly rather than those that point posteriorly. Bilobed anterior communicating artery aneurysms, in which one lobe projects posteriorly, warrant specific preoperative consideration due to the difficulty of visualizing the posterior aneurysmal lobe during surgery.

Particular neurologic and psychiatric syndromes have been described when the anterior basal perforators of the anterior cerebral artery–communicating artery complex are compromised by vasospasm, clipping, or effects of coiling. For example, diminished perfusion of the hypothalamus can result in altered personality, agitation, hypokinesia, and changes in affective state (24,25). Following a rupture of an anterior communicating artery aneurysm patients often have a prolonged recovery of subtle symptoms related to hypo-

thalamic dysfunction such as sleep-cycle regulation, heat regulation, and attention.

Recurrent Artery of Heubner

A prominent laterally directed lenticulostriate vessel arising in the region of the anterior communicating artery complex is referred to as the recurrent artery of Heubner (26). It doubles back on the course of its parent vessel. It is directed laterally above the A1 and M1 segments (Figs. 11-11 and 11-12). It supplies the anteroinferior portion of the caudate nucleus, anterior limb of the internal capsule, the paraterminal gyrus, and anterior third of putamen (24). It is considered to be an important vessel to identify and preserve during surgery. It arises most often (49% to 78%) proximally from the A2 segment, or from the anterior

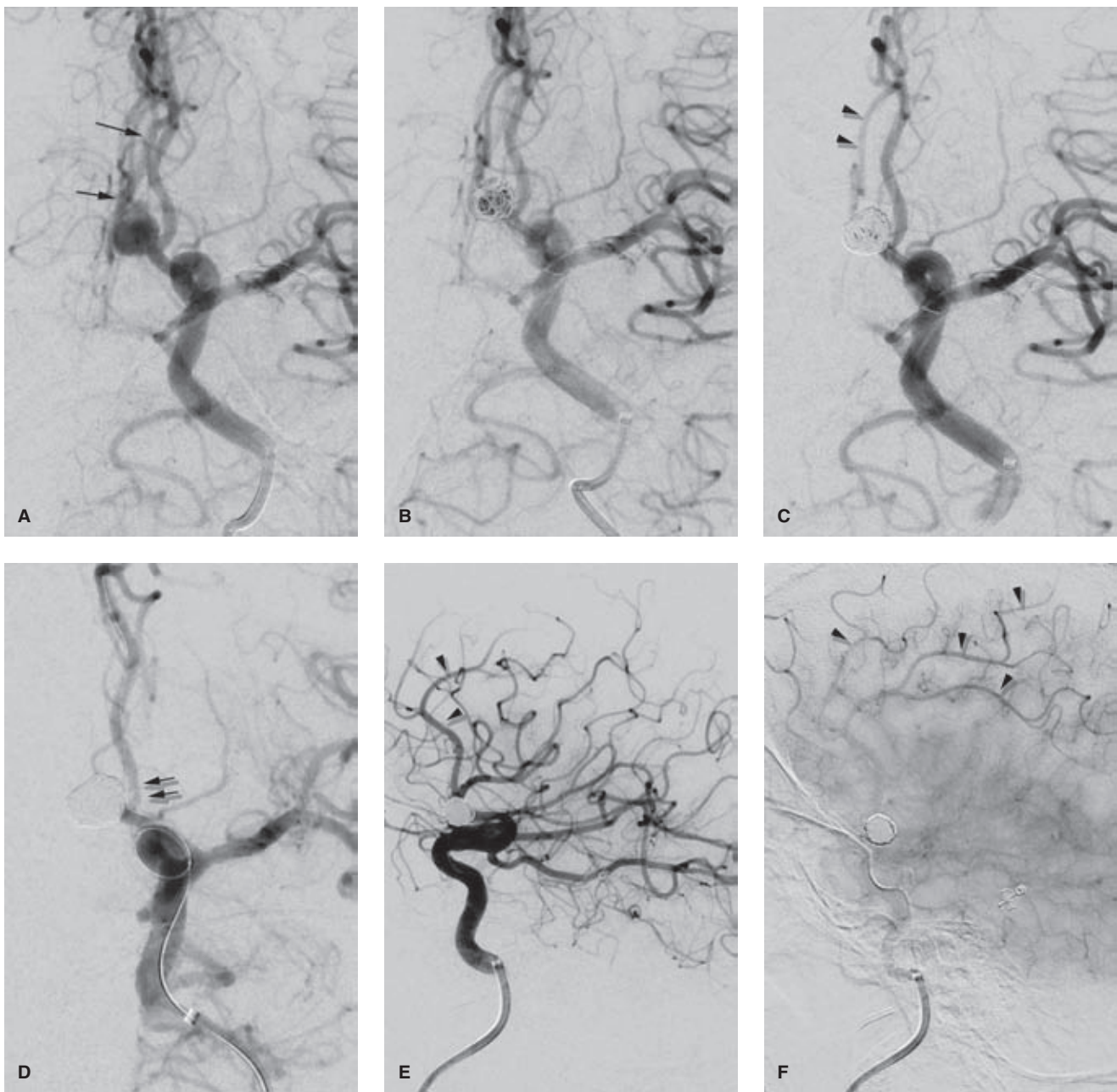


FIGURE 11-9. (A–F) Complexity of anatomy in the anterior communicating artery region. Sequential AP submentovertex views (A–C) during an embolization of an anterior communicating artery aneurysm show how easily a vessel occlusion can sneak up on you during such a procedure. The dominant left A1 fills the right ACA (arrows) via the communicating artery, and the coiling appears to be doing well after several coils have been placed. However, the complexity of the anatomy obscured a subtle change in the degree of opacification of the right ACA (B), and even when the vessel was completely occluded (C) it was obscured by the overlap of the distal left pericallosal artery (arrowheads). Concern before the case has been centered principally on the left A2, as fortunately there was enough capacity in the right A1 to supply the right ACA (confirmed with a previously placed right carotid catheter). Propagating thrombus can be seen advancing into the proximal left A2 (double arrows in D). Notice carefully in (E) that the left pericallosal artery seems to fill well (arrowheads), but the degree of hemodynamic compromise is clearly shown in the later images (F) where slow filling and stagnation are evident. Fortunately, this occlusion responded well to balloon angioplasty of the left A1–A2 junction, but the patient developed mild, transient ischemia of the left recurrent artery of Heubner after the procedure clearing after 2 to 3 days on heparin.

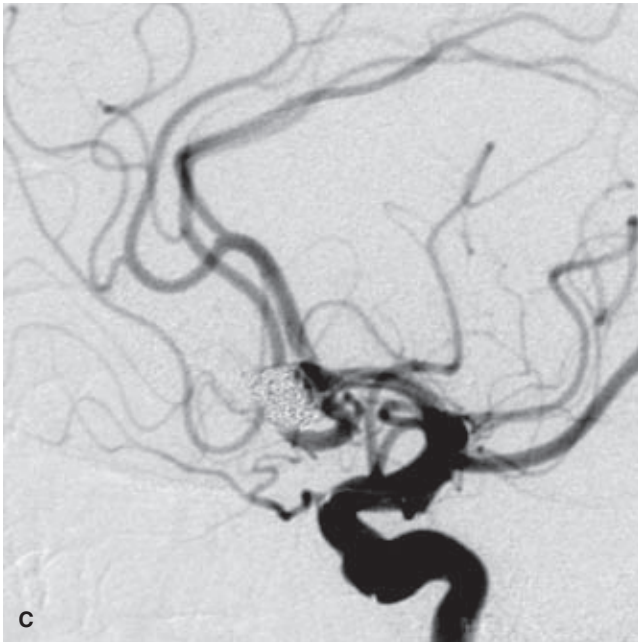
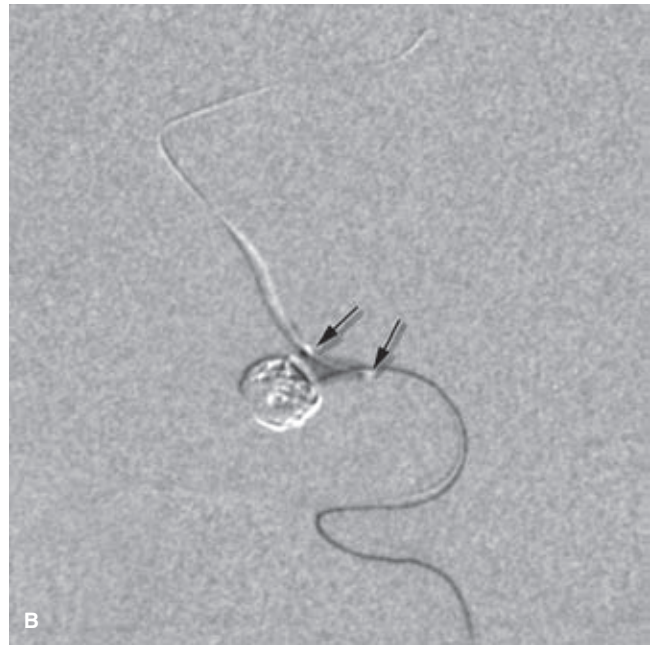


FIGURE 11-10. (A–C) Anatomic challenges of the anterior communicating artery. A typical configuration of a dominant A1 segment with a T-junction forming the basis for a widely based aneurysm is shown (A). The angles of the superiorly directed left A2 and inferiorly directed right A2 (arrowhead) are unfavorable for easy bypass of the aneurysm with a wire or device for stent or balloon assistance. Therefore, when one can gain access through a challenging junction, in this instance a balloon (arrows in B) was used to assist coiling of the aneurysm, one must remember that the anatomic configuration will be altered by the presence of this device, sometimes favorably, sometimes not. While vessel irritation from the balloon, with resulting spasm, can certainly be a problem during the procedure, when the balloon is removed the vessel may relax in a way that occludes the A1–A2 junction. In this instance (C) an underaggressive coiling of the aneurysm proved adequate in the long-term, and avoided short-term procedural complications too.

communicating artery or A1 segment, or even adjacent cortical branches of the anterior cerebral artery (3,4,14,27). It may occasionally be absent (3%) or duplicated (12%). Usually, it follows a recurrent course along the superior or anterosuperior surface of the A1 segment to which it is attached by arachnoid strands. Less commonly, it may run more posteriorly or within the anterior perforated substance. As it moves laterally, it frequently gives olfactory, frontal, and Sylvian branches and may have a total length along its course of up to 38 mm. It enters the lateral aspect of the anterior perforated substance (i.e., lateral to a sagittal plane described by the olfactory nerve) as a single vessel or with as many as 12 branches. Less commonly, it enters the medial anterior perforated substance. It is thought to represent an important route for preservation of blood flow to the basal

ganglia during occlusion of the middle cerebral artery. On the lateral projection, its area of distribution is the anteroinferior portion of the lenticulostriate blush or fan. Because it hugs the course of the A1 segment closely and because of its small size, usually just under 1 mm in diameter, the vessel is not seen as consistently at angiography as it is during surgery. In fact, a contralateral carotid injection usually demonstrates the recurrent artery of Heubner better by virtue of cross filling via the anterior communicating artery. Preservation of the artery of Heubner is a concern during anterior communicating artery aneurysm clipping. Occlusion of the recurrent artery of Heubner causes a hemiparesis that is most prominent in the upper extremity and face. Despite its proximity, the recurrent artery does not play a significant role in supply of the optic apparatus.

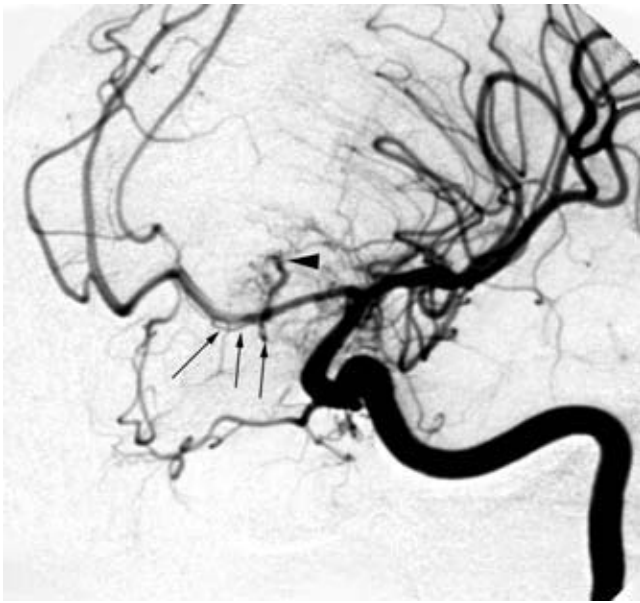


FIGURE 11-11. Inferior frontal AVM supplied by the recurrent artery of Heubner. A tiny AVM nidus along the undersurface of the left anterior perforated substance (*arrowhead*) is opacified by a thin recurrent artery from region of the A1–A2 junction (*arrows*).

► DISTAL ANTERIOR CEREBRAL ARTERY

Aneurysms of the anterior cerebral artery distal to the anterior communicating artery account for approximately 3% of intracranial aneurysms, and most of these occur at the junction of the pericallosal and callosomarginal arteries

(28) (Fig. 11-13). They are thought to be prone to a greater volume of hemorrhage than their typically small size would suggest, possible due to relative absence of surrounding arachnoid membranes (29). Posttraumatic pseudoaneurysms of the distal anterior cerebral artery where it crosses the course of the falx cerebri are sometimes seen after a shearing motion against the immobile falx.

Early Division of the Distal Anterior Cerebral Artery

A large number of variations are possible in terms of which anterior cerebral artery branches may arise proximally. The importance of these vessels is that their presence makes the anatomic and angiographic interrogation of the anterior communicating artery more difficult. It is sometimes impossible to discern between the anterior communicating artery and the pericallosal–callosomarginal junction. The presence of such multiple vessels may also make surgical exploration here extremely difficult.

► BRANCHES OF THE DISTAL ANTERIOR CEREBRAL ARTERY

The A2 and more distal segments of the anterior cerebral artery begin at the anterior communicating artery. It extends from the suprachiasmatic cistern to the cistern of the lamina terminalis and curves around the corpus callosum in the sagittal plane. Usually, the anterior cerebral arteries are not side by side here, but rather are staggered in the sagittal plane such that one lies within the concavity of the other. The main trunk

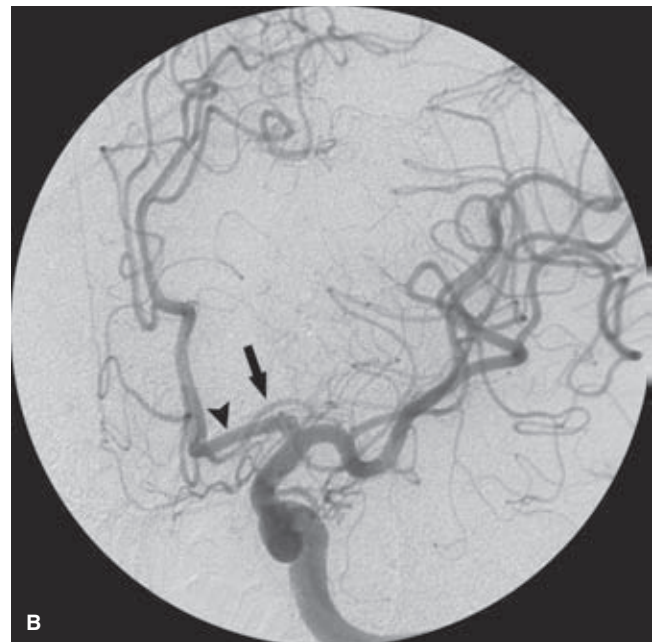
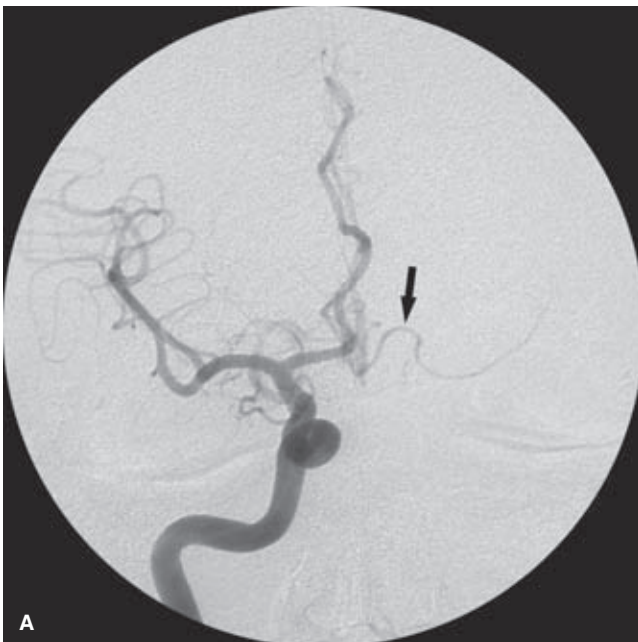


FIGURE 11-12. (A–B) Recurrent artery of Heubner demonstrated from the contralateral side. On this right internal carotid artery injection (A), one could be forgiven for thinking at first that the vessel (*arrow*) filling to the left hemisphere via the anterior communicating artery is a hypoplastic A1 segment on the other side. However, the contralateral left internal carotid artery view (B) shows that the left A1 segment (*arrowhead*) is robust. The more slender vessel seen from the right injection is seen again (*arrow*) coursing parallel to the left A1 but in a different direction. This is the recurrent artery of Heubner filling from the A2 segment just beyond the anterior communicating artery.

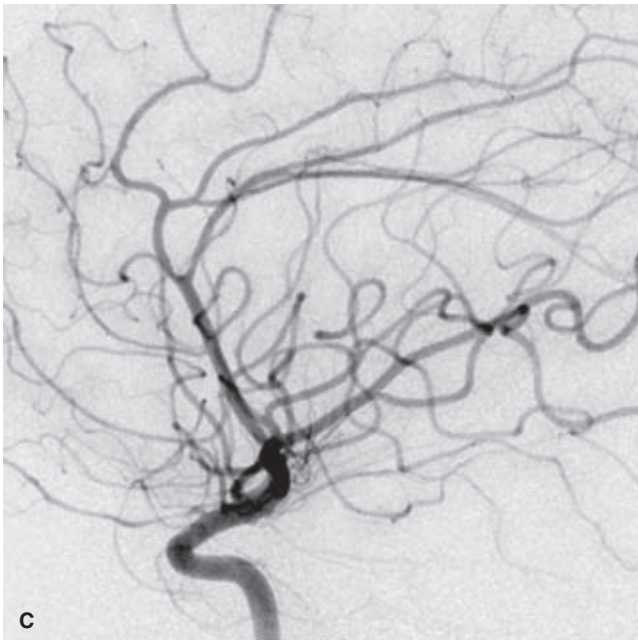
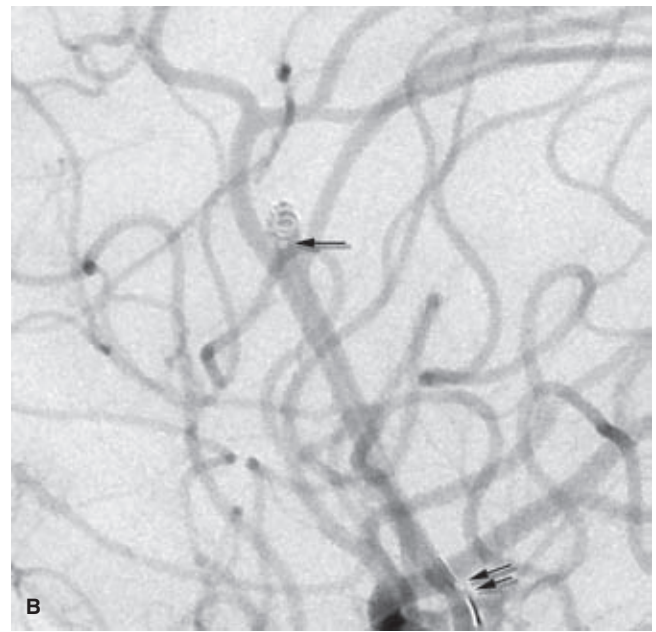
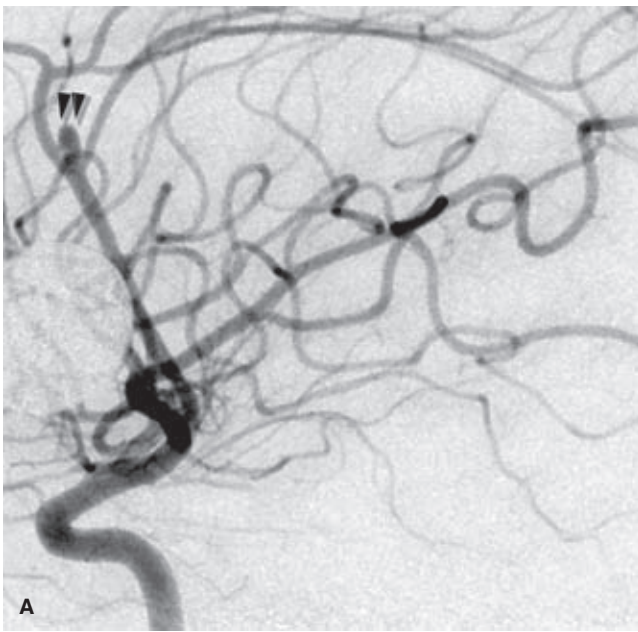


FIGURE 11-13. (A–C) Aneurysms of the distal anterior cerebral artery.

A small aneurysm at the junction of the pericallosal and callosomarginal artery (*arrowheads in A*) presented with interhemispheric hemorrhage. Berry aneurysms of the distal anterior cerebral artery often occur in this location. This small aneurysm illustrates one of the important lessons in dealing with lesions of this size. They are extremely delicate. It is often prudent to go past them with the wire/microcatheter at first, get a feel for the tensions at play in approaching the aneurysm, pull back, and *barely enter the aneurysm*. Take all the tension out of the wire/microcatheter combination before removing the wire; otherwise the microcatheter will harpoon forward. It is far preferable to fall back out of this aneurysm repeatedly than to rupture it by going too far in. Image **(B)** shows soft coils being advanced very gingerly into the dome of the aneurysm. The 6-month follow-up image **(C)** is provided to illustrate the contrast with image **(A)** and shows a normalized contour of the anterior cerebral artery, which showed signs of hydrocephalus on the first image.

of the anterior cerebral artery continues posteriorly as the pericallosal artery in the epicallosal cistern, which gives cortical and callosal branches as it proceeds. Most authors use the term *pericallosal artery* as being synonymous with the anterior cerebral artery distal to the anterior communicating artery. Others prefer to define it as originating at the division of the anterior cerebral artery into pericallosal and callosomarginal branches. In either event, approximately 18% of hemispheres do not have a definable callosomarginal branch (4).

The anterior cerebral artery supplies all of the medial aspect of the frontal lobes, most of the anteromedial aspect of the parietal lobes, and a portion of the parasagittal cortex of both lobes, including cortical territories related to motor and sensory functions. Distal anterior cerebral artery occlusion is most prominently associated with contralateral lower extremity weakness or plegia.

Cortical Branches of the Anterior Cerebral Artery

The distal branches are named according to the territory perfused. As is the case elsewhere in the cerebrovascular circulation, the configuration is variable and the nomenclature is at best a shorthand argot for purposes of communication. The named territories are best described in diagrammatic format (Figs. 11-14 and 11-15).

► PERICALLOSAL ARTERY

The pericallosal artery is the most important named branch of the distal anterior cerebral artery. Its course on the lateral view is an indicator of ventricular size and of the AP view is an important landmark for midline shift.

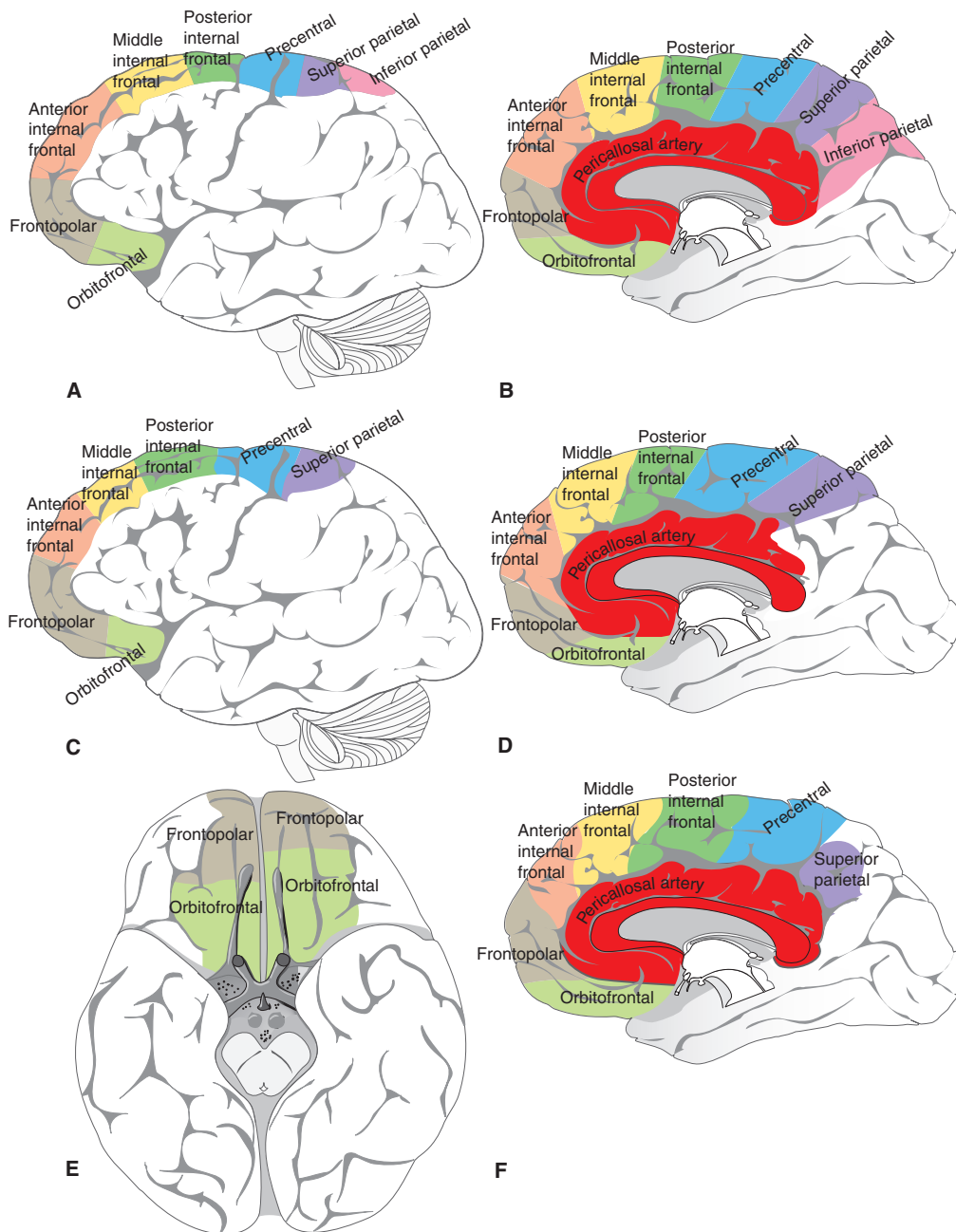


FIGURE 11-14. Named cortical territories of the anterior cerebral artery. The most typically named branches of the anterior cerebral artery are indicated.

Distal anastomoses between the pericallosal artery and the posterior cerebral artery via the perisplenial branches are an important angiographic sign of nonphysiologic collateral flow indicative of compensation for insufficient perfusion on one artery or the other (Fig. 11-16). For instance, the anterior cerebral artery may thus supply the posterior choroidal area in the presence of hypervascular lesions of the third and lateral ventricles. The embryologic basis for this relationship is expressed most vividly in the degree to which prominent anterior cerebral artery supply is frequently seen in vascular malformations of the vein of Galen (30).

► CALLOSOMARGINAL ARTERY

This is the biggest branch of the pericallosal artery. It runs posteriorly in the cingulate sulcus giving named branches to the frontal lobe, precentral area, and anterior parietal lobe.

► CALLOSAL BRANCHES OF THE ANTERIOR CEREBRAL ARTERY

Small perforating branches of the pericallosal artery are directed toward the corpus callosum (31). These usually take the form of “short callosal arteries.” Up to 20 such

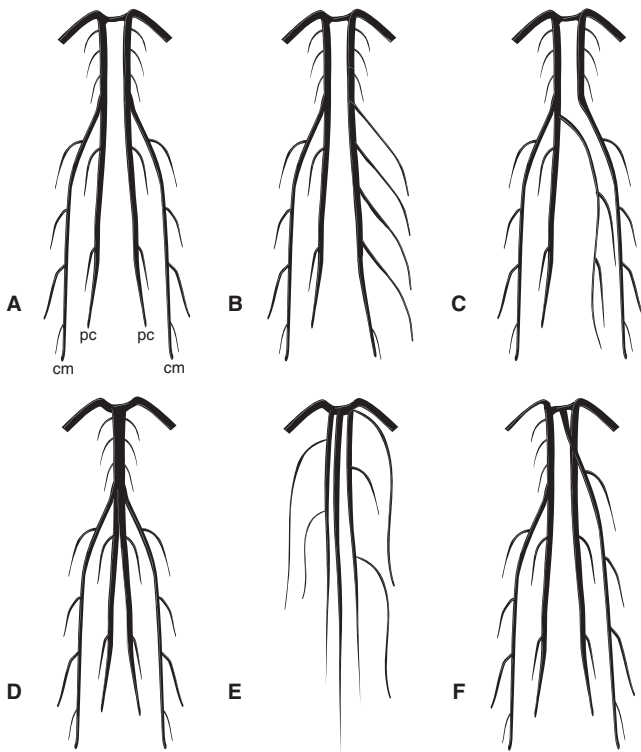


FIGURE 11-15. Distal anterior cerebral artery variations. Schematic illustrations of the range of possible distribution patterns of the distal anterior cerebral arteries are depicted. (Labels: *pc*, pericallosal; *cm*, callosomarginal.) Based on Baptista AG (31).

vessels per hemisphere may be present. They traverse the corpus callosum to supply the septum pellucidum, anterior pillars of the fornix, and the anterior commissure. “Long callosal arteries” may be seen that supply the corpus callosum, adjacent cortex, and septal structures. This artery or arteries may sometimes be called the *median artery of the corpus callosum*.

► DURAL BRANCHES OF THE ANTERIOR CEREBRAL ARTERY

Dural supply may be seen from two sources off the anterior cerebral artery. Anteriorly at the cribriform plate, small arteries may cross the dura with the olfactory fibers and anastomose with the ethmoidal arteries. In addition, the pericallosal artery may give a dural branch to the inferior rim of the falx cerebri, which runs along the course of the inferior sagittal sinus.

► VARIATIONS IN THE DISTAL ANTERIOR CEREBRAL ARTERY

Variations of the A2–A4 circulation are common in terms of the degree of bihemispheric supply, which may be present from one anterior cerebral artery. Using microsurgical techniques, bihemispheric supply can be found in some measure in up to 64% of hemispheres (4), with macroscopically evident bihemispheric supply in 12% (31). An azygous anterior cerebral artery is a rare (0.3%) anomaly, in which only one A2

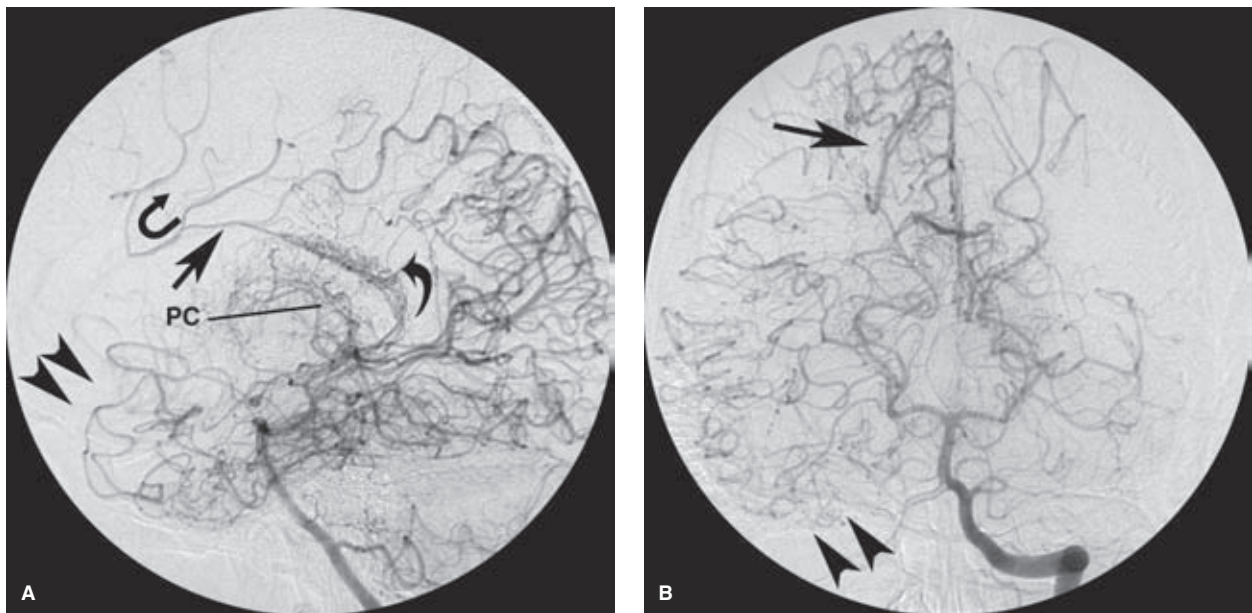


FIGURE 11-16. (A–B) Reconstitution of the right anterior cerebral artery through pial–pial collaterals from the posterior cerebral artery. A lateral (A) and AP (B) view of the left vertebral artery injection in a patient with Moya-Moya of the right internal carotid artery demonstrates chronic autoregulatory changes with a profusion of collateral vessels attempting to compensate for the loss of perfusion pressure in the right anterior circulation. In (A), the pericallosal artery (*big straight arrow*) reconstitutes retrogradely via the perisplenial artery (*curved arrow*) and flows back to the bifurcation with an internal frontal branch, which then flows antegrade (*U-shaped arrow*). Part of the typical Moya-Moya angiographic appearance in this patient is created by the proliferation of posterior chorioidal branches (*PC*), but the AP view (B) suggests that these are more prominent on the left side, also affected by this disease. The *double arrowheads* in (A) indicate the degree of retrograde reconstitution of the inferior division of the right middle cerebral artery through pial collaterals. The AP view (B) demonstrates the hyperplastic appearance of the distal branches of the right posterior cerebral artery and the shift of the watershed in response to the hemodynamic sump throughout the right hemisphere.

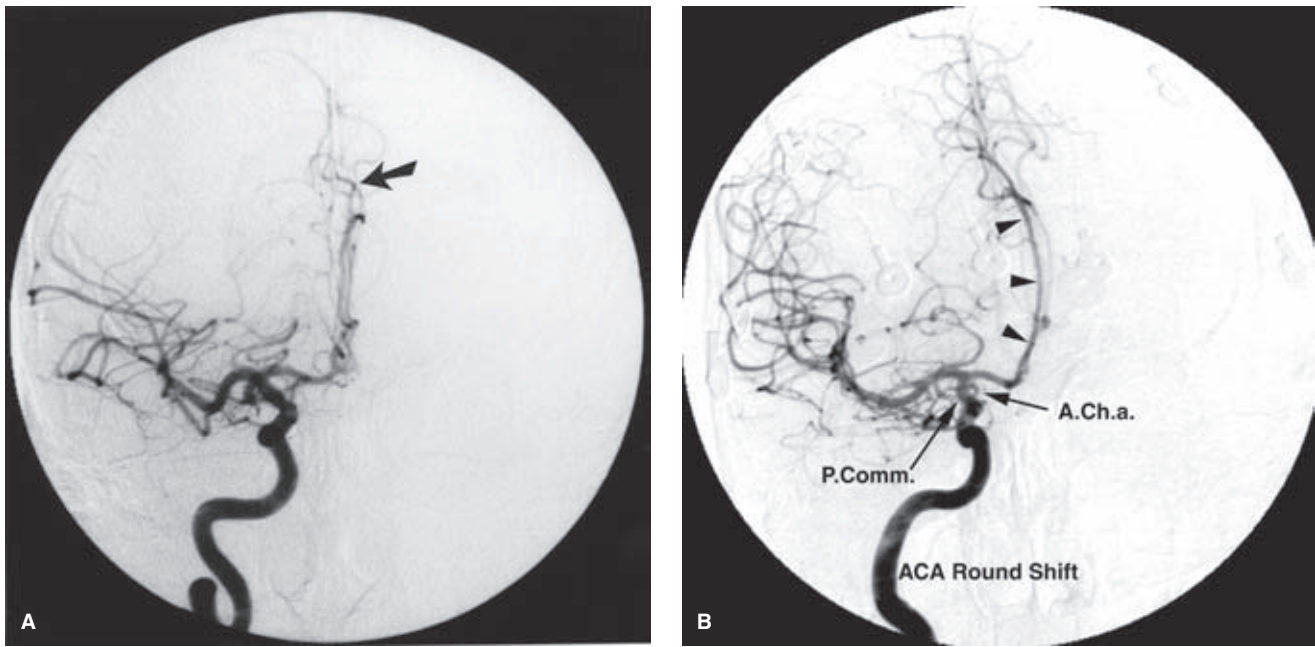


FIGURE 11-17. (A–B) Anterior cerebral artery shift. **A:** Midline shift of the anterior cerebral artery to the left is present due to a right hemispheric mass. An abrupt steplike correction (square shift) of the course of the distal anterior cerebral artery is seen at its intersection with the immobile falx cerebri (*arrow*). **B:** Round shift of the anterior cerebral artery in a different patient (*arrowheads*). An unusual appearance of vessels is seen behind the internal carotid artery. This is the PA appearance of the variant territory of the anterior choroidal artery (*A.Ch.a.*) seen in lateral projection on Figure 10.35.

trunk is present throughout the interhemispheric distribution area (Fig. 11-15). It can be seen in variants of the holoprosencephalic spectrum of congenital disorders. More commonly in situations of bihemispheric supply (32), one anterior cerebral artery will be dominant, and a pericallosal branch of one anterior cerebral artery will have bilateral supply in its distal aspect.

These developmental variants of the distal anterior cerebral artery may be associated with an increased propensity for distal anterior cerebral artery aneurysm formation, particularly at the bifurcation of the pericallosal and callosomarginal arteries. This appears to be especially so for true azygous anterior cerebral artery variants. In a retrospective study of pericallosal aneurysms, which normally constitute 5% or less of all intracranial berry aneurysms, about a quarter of them occur at the bifurcation of an unpaired pericallosal trunk (33).

Occasionally, a communication exists between the anterior cerebral arteries near the callosal genu and has been termed the *superior anterior communicating artery* (28,34).

► ANTERIOR CEREBRAL ARTERY SHIFT

Although the use of cerebral angiography as a primary means for detection of intracranial masses is now of historical interest, it behooves the modern neuroangiographer to be familiar with this body of knowledge. There are still situations in which a careful analysis of vessel location is of vital interest to surgical planning for a particular patient. Hydrocephalus arising as a complication during neuro-interventional procedures is an important phenomenon to recognize in a patient under general anesthesia where a

ventriculostomy might be malfunctioning or not yet placed. Intracranial collections or hemorrhages occasionally avoid detection when alternative processes such as spasm or infection are commanding clinical attention, and it is vitally important to recognize these unexpected findings during angiography.

Moreover, an understanding of these phenomena can help prevent misinterpretation of normal variants on obliqued films. Succinctly, angiographic shift of the anterior cerebral artery occurs when mobile median or paramedian structures are displaced. The angiographic signs of shift are analyzed by juxtaposition of the appearance of displaced and fixed structures (Figs. 11-17 and 11-18). The most mobile and, thus, most sensitive paramedian structure is the pericallosal artery. The mobility of the anterior two thirds of this artery relates to the position of the falx cerebri anteriorly. The falx is more remote from the genu of the corpus callosum than it is relative to the splenium posteriorly. Therefore, the pericallosal artery is highly mobile throughout much of its course until it becomes suddenly immobile posteriorly at the point where it crosses the falx. The descriptive categorizations of round, square, or central shift relate to the point of maximal impact of mass effect on the course of the anterior cerebral artery and whether an abrupt steplike deformity of the pericallosal artery can be seen posteriorly at the point of falcine constraint. An understanding of the diffuse impact of such mass effect should prevent a meandering anterior cerebral artery with relatively smooth turns from being misperceived as displaced. In addition, a smooth posterior course of the pericallosal artery without a steplike deflection and a normal appearance of the pericallosal venous mustache will help in recognition on oblique films. Gross

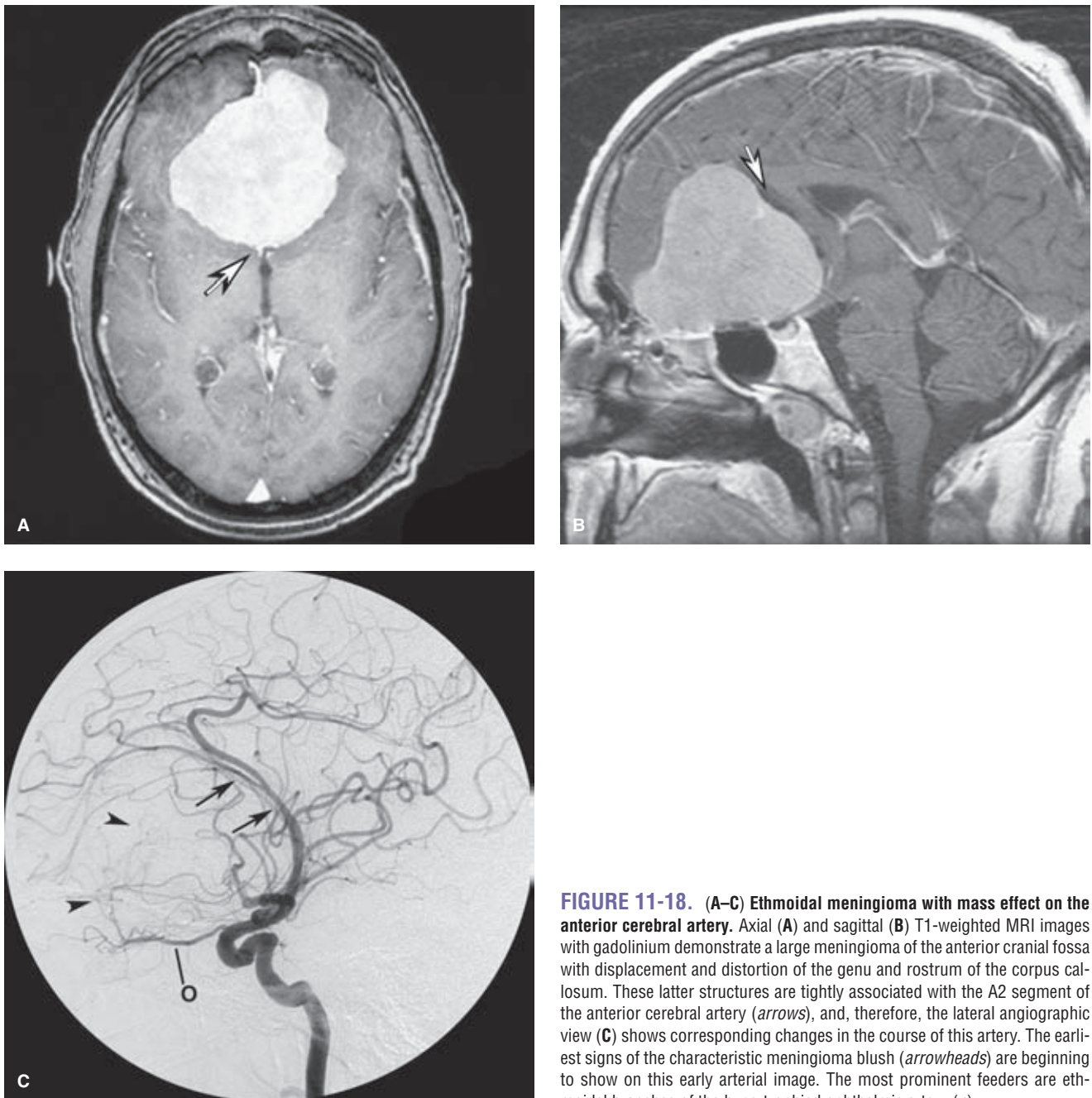


FIGURE 11-18. (A–C) Ethmoidal meningioma with mass effect on the anterior cerebral artery. Axial (A) and sagittal (B) T1-weighted MRI images with gadolinium demonstrate a large meningioma of the anterior cranial fossa with displacement and distortion of the genu and rostrum of the corpus callosum. These latter structures are tightly associated with the A2 segment of the anterior cerebral artery (arrows), and, therefore, the lateral angiographic view (C) shows corresponding changes in the course of this artery. The earliest signs of the characteristic meningioma blush (arrowheads) are beginning to show on this early arterial image. The most prominent feeders are ethmoidal branches of the hypertrophied ophthalmic artery (o).

midline shift will always be accompanied by venous signs of mass effect.

References

1. McKissock W, Walsh L. Subarachnoid haemorrhage due to intracranial aneurysms: Results of treatment of 249 verified cases. *Br Med J* 1956;32(4992):559–565.
2. Fischer E. Die Lageabweichungen der vorderen Hirnarterien Gefäßbild. *Zentralbl Neurochir* 1938;3:300–313.
3. Perlmutter D, Rhoton AL Jr. Microsurgical anatomy of the anterior cerebral–anterior communicating–recurrent artery complex. *J Neurosurg* 1976;45(3):259–272.
4. Perlmutter D, Rhoton AL Jr. Microsurgical anatomy of the distal anterior cerebral artery. *J Neurosurg* 1978;49(2):204–228.
5. Given CA 2nd, Morris PP, Given CA 2nd, et al. Recognition and importance of an infraoptic anterior cerebral artery: Case report. *Congenital absence of the internal carotid artery: case reports and review of the collateral circulation.* *AJNR Am J Neuroradiol* 2002;23(3):452–454.
6. Friedlander RM, Oglivly CS. Aneurysmal subarachnoid hemorrhage in a patient with bilateral A1 fenestrations associated with an azygos anterior cerebral artery. Case report and literature review. *J Neurosurg* 1996;84(4):681–684.
7. Klein SI, Gahbauer H, Goodrich I. Bilateral anomalous anterior cerebral artery and infraoptic aneurysm. *AJNR Am J Neuroradiol* 1987;8(6):1142–1143.
8. Fujimoto S, Murakami M. Anomalous branch of the internal carotid artery supplying circulation of the anterior cerebral artery. Case report. *J Neurosurg* 1983;58(6):941–946.
9. Stevenson CB, Chambless LB, Rini DA, et al. Bilateral infraoptic A1 arteries in association with a craniopharyngioma: Case report and review of the literature. *Surg Neurol Int* 2011;2:89.

10. Turkoglu E, Arat A, Patel N, et al. Anterior communicating artery aneurysm associated with an infraoptic course of anterior cerebral artery and rare variant of the persistent trigeminal artery: A case report and literature review. *Clin Neurol Neurosurg* 2011;113(4):335–340.
11. Maurer J, Maurer E, Perneczky A. Surgically verified variations in the A1 segment of the anterior cerebral artery. Report of two cases. *J Neurosurg* 1991;75(6):950–953.
12. Alpers BJ, Berry RG, Paddison RM. Anatomical studies of the circle of Willis in normal brain. *AMA Arch Neurol Psychiatry* 1959;81(4):409–418.
13. Nathal E, Yasui N, Sampei T, et al. Intraoperative anatomical studies in patients with aneurysms of the anterior communicating artery complex. *J Neurosurg* 1992;76(4):629–634.
14. Wilson G, Riggs HE, Rupp C. The pathologic anatomy of ruptured cerebral aneurysms. *J Neurosurg* 1954;11(2):128–134.
15. VanderArk GD, Kempe LC. Classification of anterior communicating aneurysms as a basis for surgical approach. *J Neurosurg* 1970;32(3):300–303.
16. Gomes FB, Dujovny M, Umansky F, et al. Microanatomy of the anterior cerebral artery. *Surg Neurol* 1986;26(2):129–141.
17. Avci E, Fossett D, Erdogan A, et al. Perforating branches of the anomalous anterior communicating complex. *Clin Neurol Neurosurg* 2001;103(1):19–22.
18. Fisher CM. The circle of Willis: Anatomical variations. *Vasc Dis* 1965;2:99–105.
19. Tsuji T, Abe M, Tabuchi K. Aneurysm of a persistent primitive olfactory artery. Case report. *J Neurosurg* 1995;83(1):138–140.
20. Minakawa T, Kawamata M, Hayano M, et al. Aneurysms associated with fenestrated anterior cerebral arteries. Report of four cases and review of the literature. *Surg Neurol* 1985; 24(3):284–288.
21. Rosner SS, Rhoton AL Jr, Ono M, et al. Microsurgical anatomy of the anterior perforating arteries. *J Neurosurg* 1984; 61(3):468–485.
22. Suzuki M, Onuma T, Sakurai Y, et al. Aneurysms arising from the proximal (A1) segment of the anterior cerebral artery. A study of 38 cases. *J Neurosurg* 1992;76(3):455–458.
23. Dunker RO, Harris AB. Surgical anatomy of the proximal anterior cerebral artery. *J Neurosurg* 1976;44(3):359–367.
24. Ostrowski AZ, Webster JE, Gurdjian ES. The proximal anterior cerebral artery: An anatomic study. *Arch Neurol* 1960;3: 661–664.
25. Webster JE, Gurdjian ES, Lindner DW, et al. Proximal occlusion of the anterior cerebral artery. *Arch Neurol* 1960;2:19–26.
26. Heubner O. Zur Topographie der Ernährungsgebiete der einzelnen Hirnarterien. *Zentralb Med Wissen* 1872;10:816–821.
27. Gomes F, Dujovny M, Umansky F, et al. Microsurgical anatomy of the recurrent artery of Heubner. *J Neurosurg* 1984; 60(1):130–139.
28. Yasargil MG, Carter LP. Saccular aneurysms of the distal anterior cerebral artery. *J Neurosurg* 1974;40(2):218–223.
29. Sekerci Z, Sanli M, Ergun R, et al. Aneurysms of the distal anterior cerebral artery: A clinical series. *Neurol Neurochir Pol* 2011;45(2):115–120.
30. Mullan S, Mojtahedi S, Johnson DL, et al. Embryological basis of some aspects of cerebral vascular fistulas and malformations. *J Neurosurg* 1996;85(1):1–8.
31. Baptista AG. Studies on the arteries of the brain. II. The anterior cerebral artery: Some anatomic features and their clinical implications. *Neurology* 1963;13:825–835.
32. Moniz E. *Die Cerebral Arteriographie und Phlebographie*. Berlin: Springer-Verlag; 1940.
33. Huber P, Braun J, Hirschmann D, et al. Incidence of berry aneurysms of the unpaired pericallosal artery: Angiographic study. *Neuroradiology* 1980;19(3):143–147.
34. Laitinen L, Snellman A. Aneurysms of the pericallosal artery: A study of 14 cases verified angiographically and treated mainly by direct surgical attack. *J Neurosurg* 1960;17: 447–458.

The Middle Cerebral Artery

Key Points

- Variants of the middle cerebral artery, such as accessory branches or duplications, represent a substantial risk for misadventure during endovascular embolization or blind navigation during treatment of ischemic stroke. Probe gently.
- The AP angiographic view can be very misleading as to the state of perfusion of the middle cerebral artery. Always review the DSA runs well into the parenchymal and venous phases, particularly on the lateral view, to search for late filling or slowly draining vessels, an indicator of distal embolic complications.

The vascular territory of the middle cerebral artery includes some of the most eloquent cortical areas for motor and sensory functions. It encompasses the receptive and expressive components of language, abstract thought, and other faculties of higher cognitive functioning. In addition, perforating branches of the proximal middle cerebral artery supply the basal ganglia and important descending and corticospinal tracts.

► SEGMENTAL ANATOMY OF THE MIDDLE CEREBRAL ARTERY

The M1 (horizontal/sphenoidal) segment of the middle cerebral artery extends from the bifurcation of the internal carotid artery to the limen insulae, where the middle cerebral artery makes a turn or genu superiorly into the insula (Fig. 12-1). The M2 (insular) segment extends from the genu to the circular sulcus of the insula, and the M3 (opercular) extends from the circular sulcus to the opercular turn of the middle cerebral artery branches. The M4 (cortical) segments are those visible on the lateral convexity of the hemisphere (1,2).

► BRANCHING PATTERNS OF THE MIDDLE CEREBRAL ARTERY

The middle cerebral artery can divide in up to four described patterns: a single trunk with no main division, a bifurcation, a trifurcation, or a quadrifurcation. Of these, the most common is a bifurcation pattern seen in 64% to 90% of hemispheres (2–4). Most neurology literature presupposes this pattern (5), and the terminology of *superior* and *inferior*

divisions of the middle cerebral artery is in ubiquitous clinical use. A trifurcation pattern may be seen in 12% to 29% of hemispheres, with other patterns being less common.

Variability within the bifurcation pattern can be evident at microanatomical examination and in the clinical syndromes associated with a division occlusion. It is slightly more common (32%) for the inferior division to be *dominant*, covering a more extensive cortical area than the superior division. The superior division is dominant in 28% of hemispheres (Fig. 12-2). Balanced division is seen in approximately 18% of hemispheres (2), in which cases, the superior division spans the orbitofrontal to the posterior parietal areas.

► PERFORATING BRANCHES

The anterior perforated substance is the flat surface at the base of the brain bound medially by the interhemispheric fissure, laterally by the limen insulae, anteriorly by the division of the olfactory tract into the medial and lateral olfactory striae, and posteriorly by the optic tract and temporal lobe. It is divided along the sagittal plane into medial and lateral components by a line drawn posteriorly from the axis of the olfactory tract (6). This line divides the medial from the lateral anterior perforator or lenticulo-striate vessels, which penetrate the perforated substance.

There are between 1 and 21 lenticulo-striate branches per hemisphere, with an average of 10 (6–8). Approximately 80% arise usually from the posterosuperior aspect of the artery proximal to the middle cerebral artery division. The remainder arises from the proximal branches of the middle cerebral artery, particularly from the superior division (Fig. 12-3).

The lateral lenticulo-striate arteries have a slightly larger diameter than the medial group. The lateral group in particular describes a recurrent curve before entering the anterior perforated substance. The lateral lenticulo-striate arteries arise from the M1 or M2 segments of the middle cerebral artery. On AP projection, they have an S (on the right side) or reverse S (on the left side) shape. From their origin, they follow a sharp posterior and medial turn in the cisternal segment to assume a more lateral curve as they enter the anterior perforated substance. Here, they initially course around the lateral aspect of the putamen and fan out to give an important supply to the lateral aspect of the anterior commissure, internal capsule, dorsal aspect of the head of caudate nucleus, putamen, lateral globus pallidus, and substantia innominata. Blood supply to more lateral structures including the claustrum and external capsule derives from insular branches.

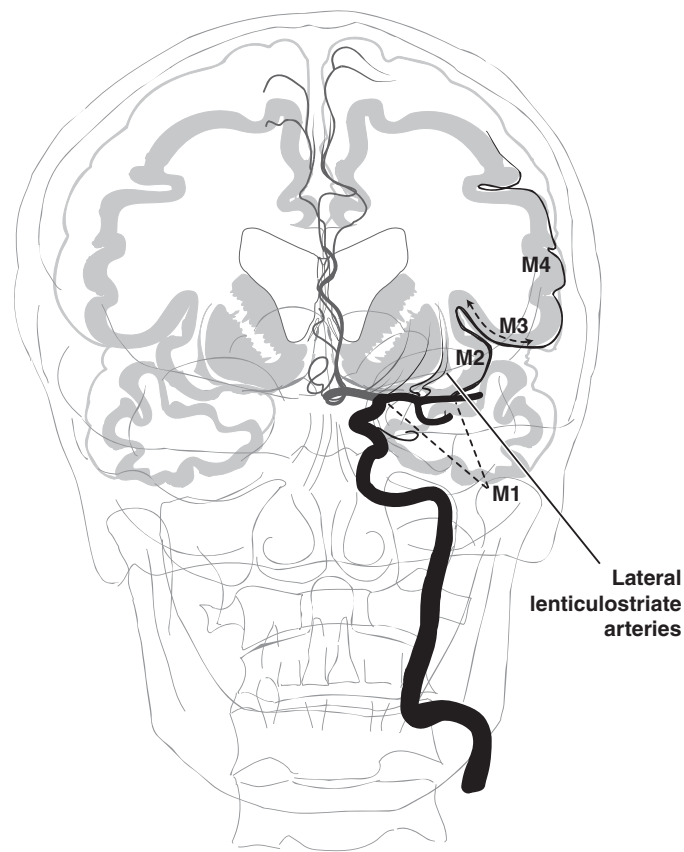


FIGURE 12-1. Segmental anatomy of the middle cerebral artery. The segmental anatomy of the middle cerebral artery is illustrated. Although the M1 segment was originally defined as extending from the carotid bifurcation to the limen insulae, in clinical parlance, the term *M1* is most frequently applied to the main stem of the middle cerebral artery extending to the principal division.

More than 70% of all aneurysms of the middle cerebral artery occur at its division, while aneurysms of the M1 trunk of the middle cerebral artery represent 10% of MCA aneurysms. They tend to arise either from the superior wall of the artery, in which case they are associated with the lenticulostriate arteries, or from the inferior surface—that is, associated with the anterior temporal branches (9).

► CORTICAL BRANCHES OF THE MIDDLE CEREBRAL ARTERY

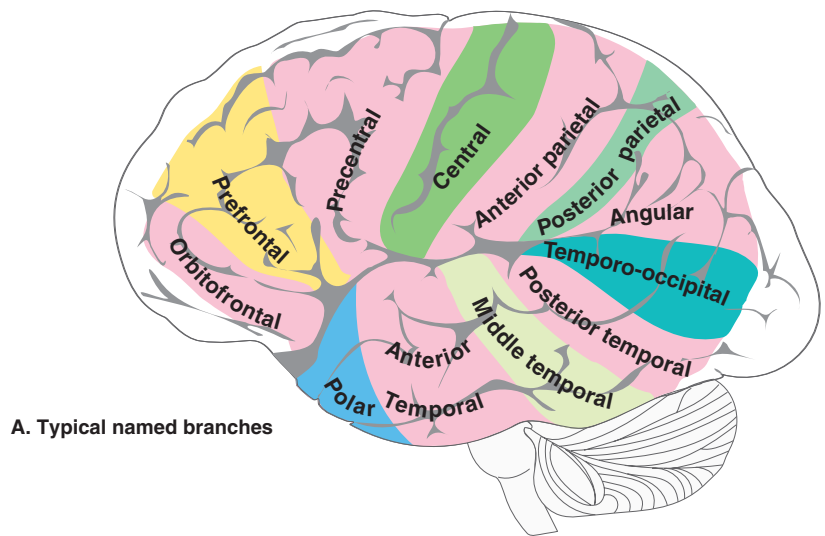
The insula is a fan-shaped area of cortex obscured from lateral view by the frontal, temporal, and parietal opercula. Seen in coronal section, it has a laterally convex aspect and is higher posteriorly. At the lowest point of the fan is the limen insulae, from which the sulci and gyri of the insula radiate superiorly and posteriorly. In correspondence with these sulci, the branches of the middle cerebral artery extend until their course is deflected by the circular sulcus or sulcus limitans of Reil. Within the sulcus limitans, the middle cerebral artery branches change direction 180 degrees and curve around the operculum. They then undergo another 180-degree turn to start coursing along the surface of the cerebral convexity. The frontal branches of the M2 segments have a shorter insular course than the posterior frontal and parietal branches. The appearance on the lateral projection of the middle cerebral artery branches within the insula

turning in the sulcus limitans describes a straight line. This line forms the base of an upturned triangle with the limen insulae at its apex, termed the *Sylvian triangle* (Fig. 12-4). The highest angiographic point posteriorly in this triangle is the Sylvian point. These angiographic phenomena were used for detection and description of middle cerebral artery shift and mass effect. An understanding of the route taken by each middle cerebral branch is still valuable, however, in understanding the anatomy of the middle cerebral artery and identifying its individual branches.

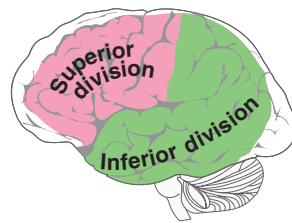
The cortical branches of the middle cerebral artery supply most of the lateral convexity of the cerebral hemisphere, the insular and opercular cortex, the lateral part of the orbital surface of the frontal lobe, and the lateral inferior surface of the temporal lobe anteriorly. The border region between the distribution of the middle cerebral artery and the adjacent cerebral arteries is termed the *watershed zone*, meaning that it is at the interface of different circulations. This region is therefore most at risk when conditions of hypoperfusion exist, such as might be due to proximal occlusive disease or systemic hypotension. *Shift of the watershed zone* is an angiographic observation due to adaptive changes in the cerebral circulation when the interface between two territories moves to compensate for a state of hypoperfusion in one territory. It is often most clearly demonstrated in the presence of chronic adaptation.

Approximately 10 to 12 named cortical branches of the middle cerebral artery are described, with much variability.

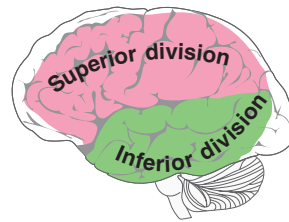
FIGURE 12-2. (A–D) Branching pattern of the middle cerebral artery. The most commonly named branches of the middle cerebral artery and division patterns are illustrated.



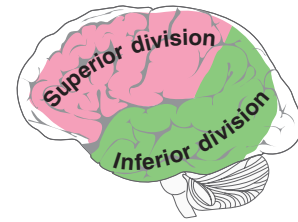
A. Typical named branches



B. Inferior division dominant (32%)



C. Superior division dominant (28%)



D. Equal bifurcation (18%)

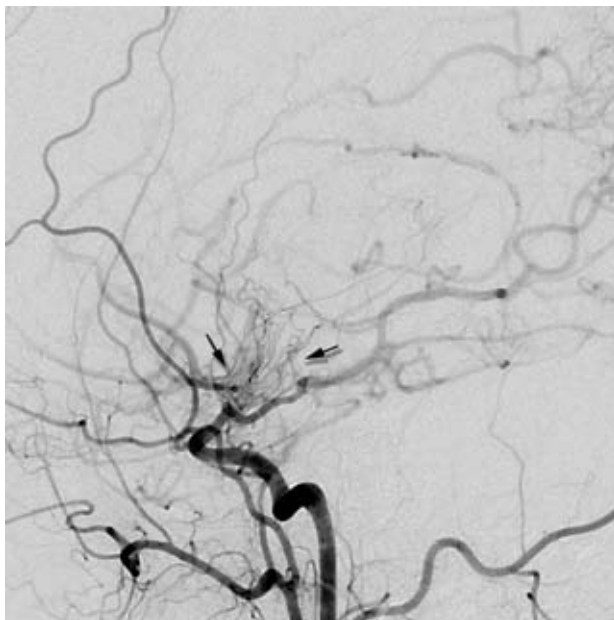


FIGURE 12-3. Lenticulostriate arteries. A lateral view of a common carotid artery injection in this patient with Moya-Moya syndrome demonstrates a prominent fan-shaped array of enlarged lenticulostriate vessels (*arrows*) compensating for the near occlusion of the ipsilateral middle cerebral artery.

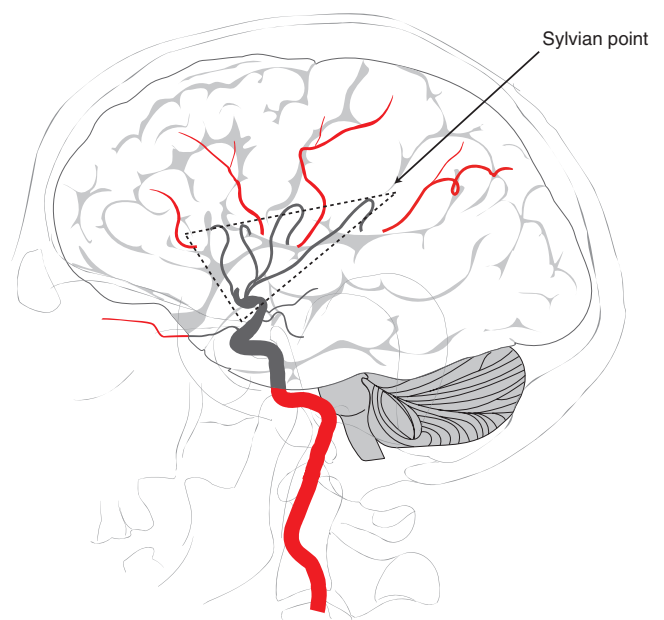


FIGURE 12-4. Sylvian triangle. The angiographic appearance of the Sylvian triangle is created by deflection of the buried insular branches of the middle cerebral artery by the sulcus limitans to a course that brings them around the opercula to the cerebral convexities. The course of each individual vessel is then made more tortuous by undulation into sulci and over gyri along its course.



FIGURE 12-5. Anterior temporal branch. A typical appearance of an anterior temporal branch of the middle cerebral artery proximal to the main bifurcation is indicated with the *arrow*.

They may arise as common trunks. Particular named branches may not be individually identifiable in every patient. The largest branches, and thus those most useful when an external to internal carotid bypass procedure is performed, are usually the angular (3) or the temporo-occipital branches (2,10).

The anterior temporal branch arises proximally as a separate branch from the horizontal portion of the M1

(Fig. 12-5). Alternatively, it can share a common trunk with the orbitofrontal branch or may arise as part of a middle cerebral artery trifurcation (Fig. 12-6). When a middle cerebral artery bifurcation is present, this vessel usually belongs to the inferior division. It supplies the anterior portion of the temporal pole with a variable degree of supply to the lateral aspect of the anterior temporal lobe.



FIGURE 12-6. Anterior temporal artery origin from the inferior division of the middle cerebral artery. In contrast to Figure 12-5, the middle cerebral artery in this patient has a short main stem ending in a bifurcation where a sessile unruptured aneurysm (*arrow*) is identified. Due to the complex pattern of overlying vessels on planar imaging, this aneurysm was very difficult to see before the 3D images. The anterior temporal artery (*double arrowheads*) arises from the inferior division.

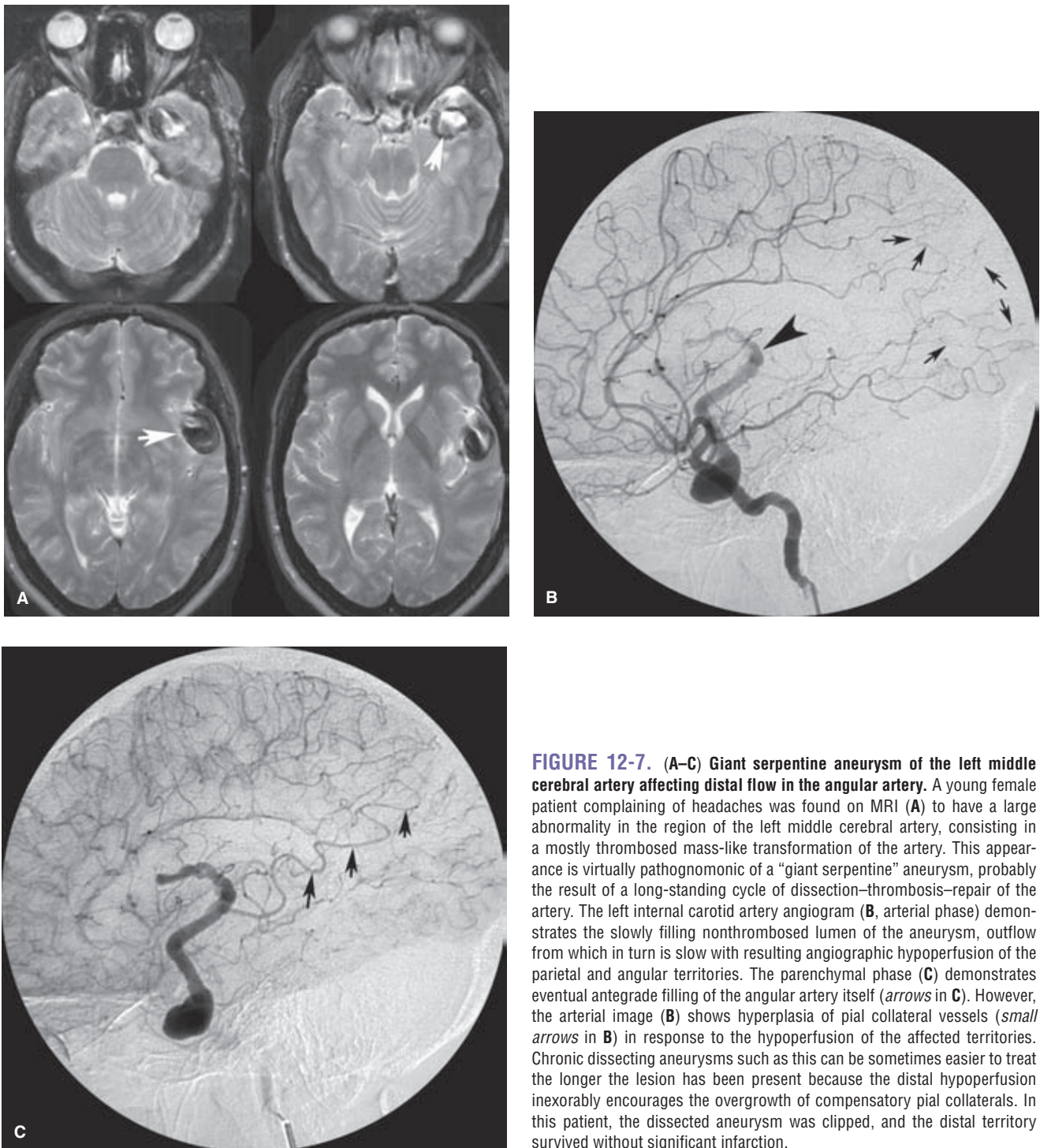


FIGURE 12-7. (A–C) Giant serpentine aneurysm of the left middle cerebral artery affecting distal flow in the angular artery. A young female patient complaining of headaches was found on MRI (A) to have a large abnormality in the region of the left middle cerebral artery, consisting in a mostly thrombosed mass-like transformation of the artery. This appearance is virtually pathognomonic of a “giant serpentine” aneurysm, probably the result of a long-standing cycle of dissection–thrombosis–repair of the artery. The left internal carotid artery angiogram (B, arterial phase) demonstrates the slowly filling nonthrombosed lumen of the aneurysm, outflow from which in turn is slow with resulting angiographic hypoperfusion of the parietal and angular territories. The parenchymal phase (C) demonstrates eventual antegrade filling of the angular artery itself (arrows in C). However, the arterial image (B) shows hyperplasia of pial collateral vessels (small arrows in B) in response to the hypoperfusion of the affected territories. Chronic dissecting aneurysms such as this can be sometimes easier to treat the longer the lesion has been present because the distal hypoperfusion inexorably encourages the overgrowth of compensatory pial collaterals. In this patient, the dissected aneurysm was clipped, and the distal territory survived without significant infarction.

The remaining named cortical territories are illustrated in Figure 12-2. The pattern described by the orbitofrontal and prefrontal branches was sometimes compared with the fanciful appearance of a candelabra, hence the term the *candelabra group*. The significance of the individual arteries lies only in the territories supplied by each, with particular neurologic deficits and syndromes occurring with occlusive states. For instance, the prefrontal and orbitofrontal branches usually supply the Broca speech area, the frontal eye fields,

and the premotor strip, meaning that an expressive aphasia will be a prominent component of the clinical syndrome in a dominant hemispheric lesion involving these branches. The clinical syndrome of a motor deficit with involvement of the central branches is self-evident, while infarctions of the dominant angular branch cause a classic neurologic syndrome (Fig. 12-7). Infarctions of the supramarginal gyrus are associated with ideomotor apraxia, and those of the angular gyrus of the dominant lobe are associated with alexia and agraphia.

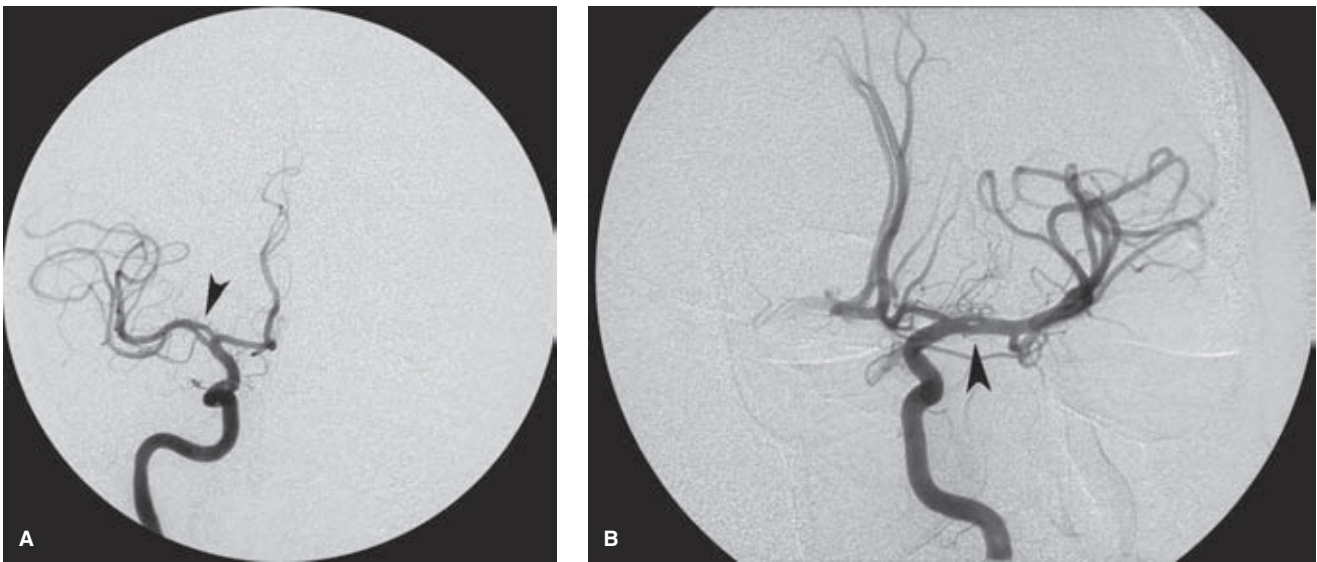


FIGURE 12-8. (A–B) Fenestrations of the middle cerebral artery. Two cases demonstrate a variable appearance of fenestration of the proximal M1 segment (*arrowheads*). In these patients, it is an inconsequential finding. However, when endovascular treatment of a nearby lesion is planned, the presence of an anomaly such as this can be very significant. Fenestrations of the vertebrobasilar junction are associated with a high risk of aneurysm formation, but fenestrations of the middle cerebral artery are so uncommon that an association with aneurysmal formation is not known.

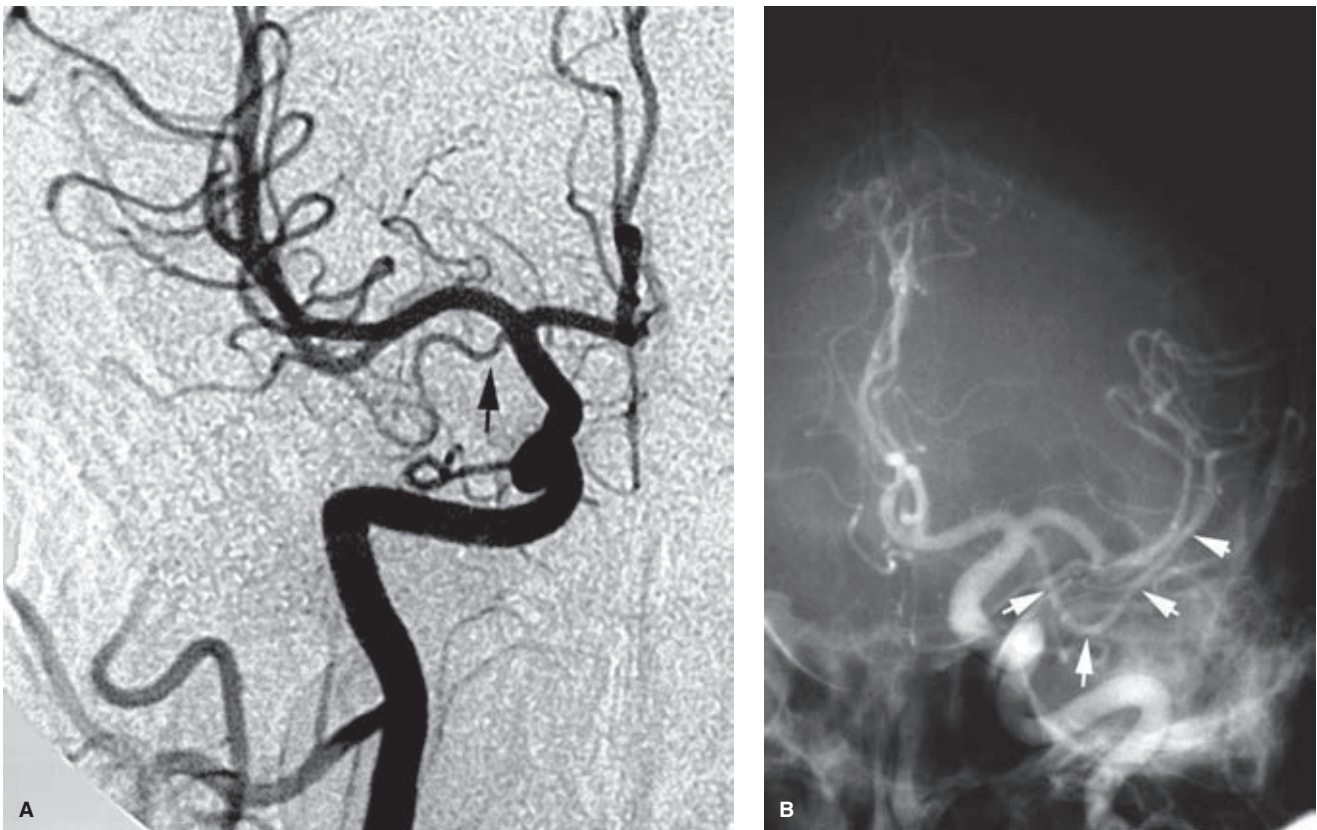


FIGURE 12-9. (A–B) Duplicated middle cerebral arteries. **A:** A temporal branch of the right middle cerebral artery territory (*arrow*) has its origin from the supraclinoid internal carotid artery, distinguishing this vessel as a duplicated middle cerebral artery. An incidental finding in this patient, it would, however, be important to clarify such an anomalous finding if treatment of an adjacent aneurysm were contemplated. **B:** A similar anomaly is seen (*arrows*) from the left internal carotid artery in another patient.

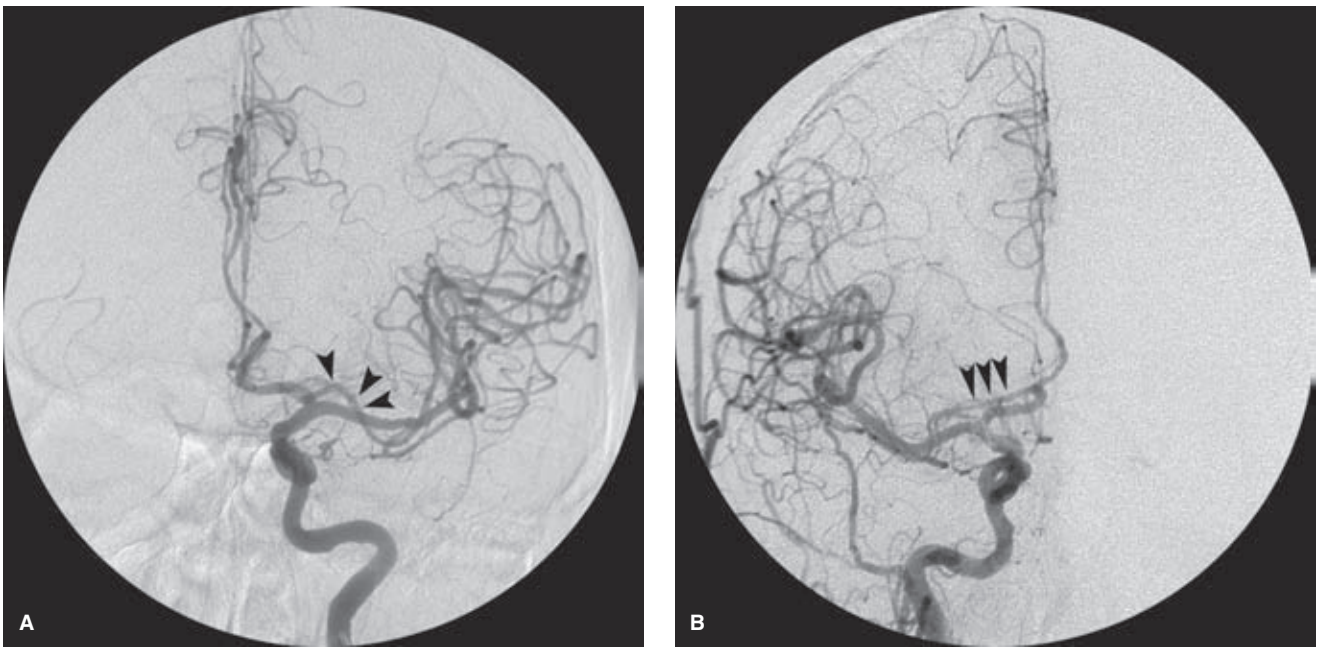


FIGURE 12-10. (A–B) Bilateral accessory middle cerebral artery. In this patient, an anomalous vessel (arrowheads) to the middle cerebral artery territory arises on each side from the A1–A2 region, qualifying as accessory middle cerebral arteries in each instance. However, some authors would argue this vessel is only a hyperplastic variant of the recurrent artery of Heubner.

▶ ANOMALIES OF THE MIDDLE CEREBRAL ARTERY

Anomalies of the middle cerebral artery are more rare than those of the other intracranial vessels. They are seen in approximately 0.6% to 3% of dissected hemispheres in microanatomical studies (2–4,11) but less commonly during angiography (12). Anomalies of the middle cerebral artery encompass:

- Rare instances of fenestrations (Fig. 12-8)
- Duplications arising from the internal carotid artery (Fig. 12-9)
- An accessory middle cerebral artery from the anterior cerebral artery (Figs. 12-10 and 12-11)

Many authors consider that these anomalous vessels may be prone to aneurysm formation (13–15). The nature and nomenclature of these anomalous vessels is debated. Although the accessory middle cerebral artery may have lenticulostriate branches, it is distinguished by some authors from a recurrent artery of Heubner by the fact that it has a predominantly cortical distribution. Moreover, it has been seen during dissections to be distinct from Heubner's artery (3,16–19).



FIGURE 12-11. Accessory middle cerebral artery from the A1 segment. A middle-aged patient was having ischemic symptoms in the right hemisphere. At angiography, the only lesion explaining her symptoms was this stenosis (arrow) at the origin of this accessory middle cerebral artery variant.

References

1. Fischer E. Die Lageabweichungen der vorderen Hirnarterien Gafässbild. *Zentralbl Neurochir* 1938;3:300–313.
2. Gibo H, Carver CC, Rhoton AL Jr, et al. Microsurgical anatomy of the middle cerebral artery. *J Neurosurg* 1981;54(2):151–169.
3. Umansky F, Juarez SM, Dujovny M, et al. Microsurgical anatomy of the proximal segments of the middle cerebral artery. *J Neurosurg* 1984;61(3):458–467.
4. Jain KK. Some observations on the anatomy of the middle cerebral artery. *Can J Surg* 1964;55:134–139.
5. Fisher CM. Clinical syndromes in cerebral thrombosis, hypertensive hemorrhage, and ruptured saccular aneurysm. *Clin Neurosurg* 1975;22:117–147.
6. Rosner SS, Rhoton AL Jr, Ono M, et al. Microsurgical anatomy of the anterior perforating arteries. *J Neurosurg* 1984; 61(3):468–485.
7. Grand W. Microsurgical anatomy of the proximal middle cerebral artery and the internal carotid artery bifurcation. *Neurosurgery* 1980;7(3):215–218.
8. Umansky F, Gomes FB, Dujovny M, et al. The perforating branches of the middle cerebral artery. A microanatomical study. *J Neurosurg* 1985;62(2):261–268.

9. Hosoda K, Fujita S, Kawaguchi T, et al. Saccular aneurysms of the proximal (M1) segment of the middle cerebral artery. *Neurosurgery* 1995;36(3):441–446.
10. Chater N, Spetzler R, Tonnemacher K, et al. Microvascular bypass surgery. Part 1: Anatomical studies. *J Neurosurg* 1976;44(6):712–714.
11. Crompton MR. The pathology of ruptured middle-cerebral aneurysms with special reference to the differences between the sexes. *Lancet* 1962;2:421–425.
12. Teal JS, Rumbaugh CL, Bergeron RT, et al. Anomalies of the middle cerebral artery: Accessory artery, duplication, and early bifurcation. *Am J Roentgenol Radium Ther Nucl Med* 1973;118(3):567–575.
13. Stabler J. Two cases of accessory middle cerebral artery, including one with an aneurysm at its origin. *Br J Radiol* 1970;43(509):314–318.
14. Tacconi L, Johnston FG, Symon L. Accessory middle cerebral artery. Case report. *J Neurosurg* 1995;83(5):916–918.
15. Takahashi T, Suzuki S, Ohkuma H, et al. Aneurysm at a duplication of the middle cerebral artery. *AJNR Am J Neuroradiol* 1994;15(6):1166–1168.
16. van der Zwan A, Hillen B. Review of the variability of the territories of the major cerebral arteries. *Stroke* 1991;22(8):1078–1084.
17. van der Zwan A, Hillen B, Tulleken CA, et al. A quantitative investigation of the variability of the major cerebral arterial territories. *Stroke* 1993;24(12):1951–1959.
18. van der Zwan A, Hillen B, Tulleken CA, et al. Variability of the territories of the major cerebral arteries. *J Neurosurg* 1992;77(6):927–940.
19. Takahashi S, Hoshino F, Uemura K, et al. Accessory middle cerebral artery: Is it a variant form of the recurrent artery of Heubner? *AJNR Am J Neuroradiol* 1989;10(3):563–568.

The Posterior Cerebral Artery

Key Points

- The vessels along the basilar trunk and at the basilar apex are delicate and can be easily perforated or injured with a wire or microcatheter.
- The proximal segment of the posterior cerebral artery runs in the perimesencephalic cistern, but so do many other smaller parallel arteries. A wire may look on roadmap as though it is in the posterior cerebral artery but may actually be in a much smaller vessel. Be attentive to what the tip of the wire might be telling you and if there is inexplicable difficulty in advancing the wire, reconsider where you might be.

The embryologic origin of the posterior cerebral artery is from the internal carotid artery, but by the time of full development, the dominant supply to the posterior cerebral artery is usually from the basilar artery (1). A *fetal posterior communicating artery* configuration implies origin of posterior cerebral artery flow from the internal carotid artery.

The posterior cerebral artery serves the posterior cerebral hemisphere, thalamus, midbrain, and structures in the walls of the third ventricle and choroidal fissure (Figs. 13-1–13-3). Vascular injury to the posterior cerebral artery or its branches causes a range of debilitating deficits, of which the most severe are those related to the realm of vision. These include functions of a higher order for cortical and subcortical integration of visual perception, interhemispheric integration of visual fields, and relay of visual information to the visual association cortex. Ocular functions served by the posterior cerebral artery include many aspects of eye movement, pupillary reflexes, and eye coordination. Other sites of injury to the posterior cerebral artery may result in devastating neurologic syndromes related to thalamic infarction. Other deficits relate to disruption of afferent pathways in the medial lemniscus and of efferent pathways in the corticospinal tracts. Alterations in levels of arousal and consciousness occur with involvement of the midbrain reticular activating system; memory and endocrine disturbances occur with involvement of the hippocampal and hypothalamic vascular supply.

► SEGMENTAL NOMENCLATURE

Various shorthand schemes for segmental description of the posterior cerebral artery have been proposed, two of which

are most commonly used. A descriptive scheme (2) identifies:

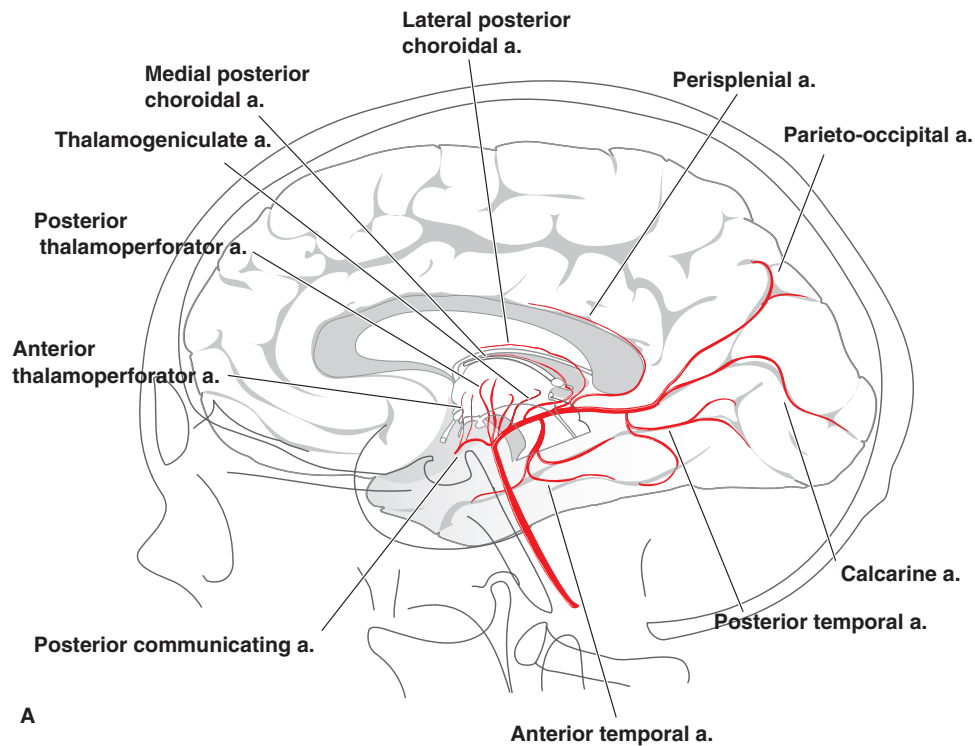
- The *peduncular segment* coursing around the peduncle and bisected by the posterior communicating artery (Fig. 13-4).
- The *ambient segment* lying between the midbrain and the hippocampal gyrus.
- The *quadrigeminal segment* running in the cistern of that name.

More commonly, a symbolic scheme is used (3–6), wherein the P1 segment extends from the basilar tip to the posterior communicating artery insertion, the P2 segment extends from there to the back of the midbrain, and the P3 segment runs through the lateral aspect of the quadrigeminal cistern around the pulvinar and divides into named branches at the anterior end of the calcarine fissure. The patterns of the proximal branches of the posterior cerebral artery vary and cannot always be exclusively assigned to one segment or another.

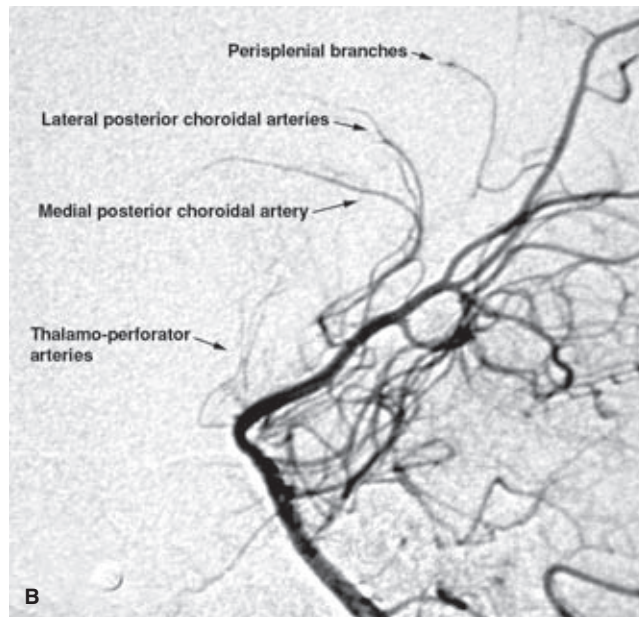
► HERNIATION THROUGH THE TENTORIAL INCISURA

As the posterior cerebral artery and some of its circumflex branches curve around the midbrain, they course parallel and inferior to the basal vein of Rosenthal and to the geniculate bodies. The posterior cerebral artery is separated from the superior cerebellar artery below by the oculomotor nerve medially and the trochlear nerve laterally. Its usual position is superomedial to the tentorium. In the setting of severe asymmetric mass effect or temporal lobe herniation, the midbrain may become compressed against the tentorium. This causes a classically described indentation in the midbrain contralateral to the mass effect, the *Kernohan notch* (7), with an occlusion of the interposed posterior cerebral artery or its branches. Therefore, the clinical phenomenon of a “false localizing sign” occurs with hemiparesis ipsilateral to the side of the tumor or mass lesion. In addition to occlusion of the contralateral posterior cerebral artery by compression between the midbrain and tentorium, occlusion of the posterior cerebral artery ipsilateral to the side of mass effect may occur as well. This can happen when this vessel or its branches are stretched around the tentorial edge (8,9).

(text continues on page 186)



A



B

FIGURE 13-1. (A–B) Lateral view of the posterior cerebral artery. The principal angiographically identifiable branches of the posterior cerebral artery are illustrated. The curve described by the lateral posterior choroidal artery conforms to the posterior surface of the pulvinar, thus serving as a useful angiographic marker for the anterior margin of the atrium. The curve of the medial posterior choroidal artery depicts the location of the velum interpositum (as does the internal cerebral vein). The calcarine artery demonstrates the position of the calcarine fissure; the parieto-occipital artery lying in the fissure of that name separates the parietal from the occipital lobes. The posterior curve of the splenium is illustrated angiographically by the perisplenic artery (**B**). These and other relatively fixed angiographic–anatomic relationships can be extremely useful when collating data from angiograms with MRI or CT images where these anatomic structures are identifiable through other techniques.

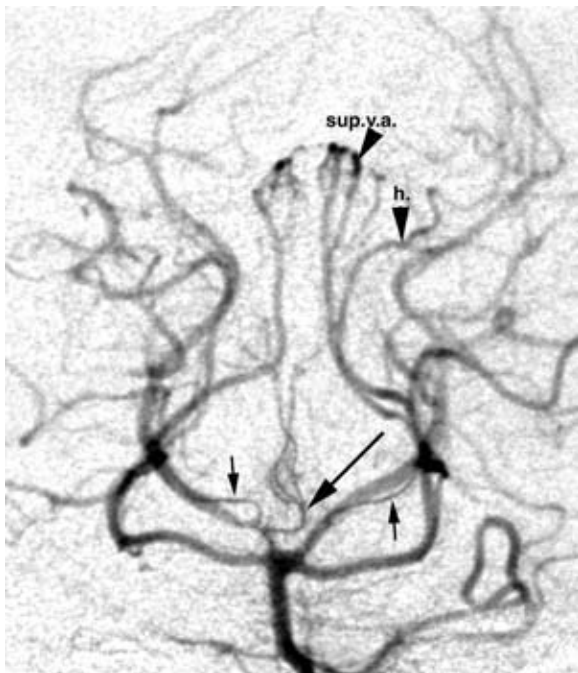


FIGURE 13-2. Townes view of basilar artery tip: artery of Percheron. A hypoplastic right P1 segment is seen, which widens in the P2 segment with dilution (wash-in) indicating that an unseen right posterior communicating artery of substantial size is present. A single midline vessel (Percheron) (*longer arrow*) arises from the right P1 segment and supplies bilateral thalamoperforator vessels. However, even though its course is midline, its origin is off midline—that is, from the P1 segment rather than from the basilar artery itself. Proximal branches of the P1 segments bilaterally (*shorter arrows*), probably representing medial posterior choroidal arteries or circumflex branches, parallel the course of the posterior cerebral artery.

The superior vermian branches of the superior cerebellar artery (*sup.v.a.*) describe the peaked surface of the superior vermis. Sloping laterally, the superior surface of the cerebellum is outlined by the medial hemispheric branches (*h.*) of the superior cerebellar artery.



FIGURE 13-4. Variant of the P1 trunk. In this patient the P1 segment of the posterior cerebral artery bilaterally incorporates the superior cerebellar arteries, giving a somewhat unusual appearance, particularly on the right, to this fairly common variant.

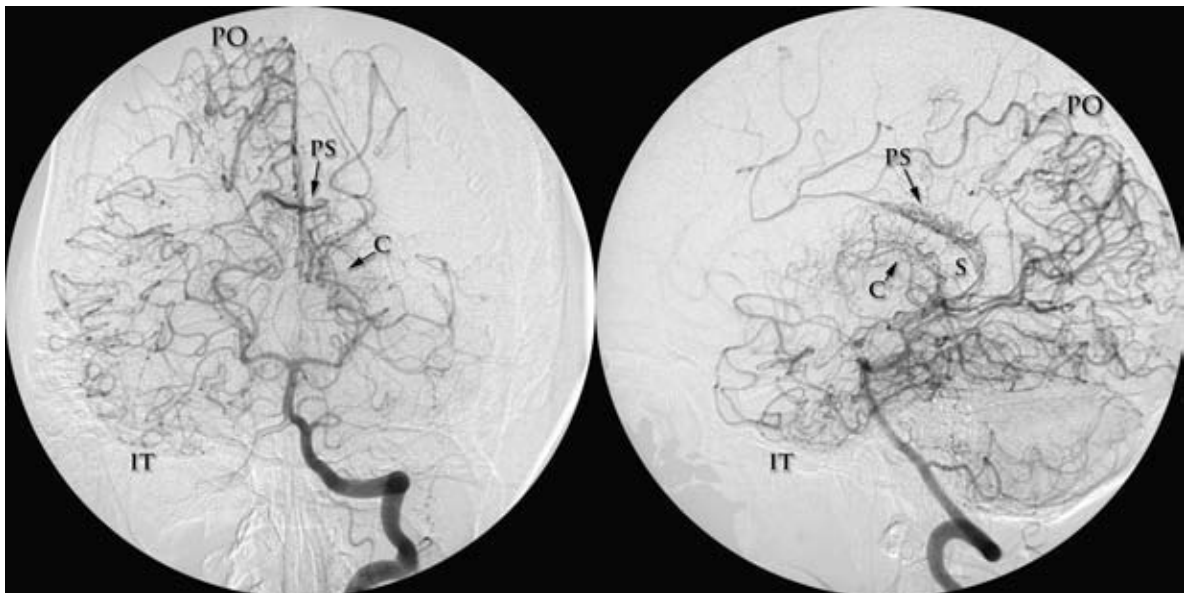


FIGURE 13-3. Collateral potential of the posterior cerebral artery. An AP and lateral view of the right vertebral artery injection in this patient with advanced Moya-Moya of the anterior circulation gives a view of the capacity for collateral flow from the posterior cerebral artery induced over a prolonged period. The relatively avascular outline of the splenium (*S*) is flanked by the perisplenial branches (*PS*) to the anterior cerebral artery and enlarged posterior choroidal branches (*C*), while the parieto-occipital artery (*PO*) and inferior temporal branches (*IT*) compensate toward the superior and inferior divisions, respectively, of the middle cerebral artery.

► POSTERIOR CEREBRAL ARTERY BRANCHES

For purposes of description, three broad categories of branches from the posterior cerebral artery are identified (10):

1. Direct or circumflex perforating branches to the brainstem and thalamus
2. Ventricular branches winding around the brainstem to the choroidal fissure
3. Cortical branches

Occasionally, in the setting of a meningioma or a dural arteriovenous malformation of the tentorium or posterior fossa, evidence of dural arteries from the posterior cerebral artery may be seen. Small dural branches from the distal cortical and choroidal branches of the artery, normally too small to image angiographically, can supply the falx cerebri (the artery of Davidoff and Schechter) (11,12).

Brainstem and Thalamic Branches of the Posterior Cerebral Artery

These centrally directed branches fall into two patterns:

1. Direct branches arise from the posterior cerebral artery and enter the brainstem immediately. This pattern includes the posterior thalamoperforator arteries from the P1 segment directed superiorly, the thalamogeniculate arteries from the P2 segment directed superiorly and laterally, and the peduncular perforating branches from the P1 and P2 segments directed centrally into the peduncle and brainstem.
2. Circumflex branches encircle the brainstem in a course parallel to that of the posterior cerebral artery for variable distances before entering the thalamus or mesencephalon.

► THALAMIC PERFORATOR ARTERIES OF THE POSTERIOR CEREBRAL ARTERY

The anterior thalamoperforator arteries, 7 to 10 in number, arise from the superolateral aspect of the posterior communicating arteries. The anterior group of thalamoperforator arteries supplies the thalamic nuclei, the posterior aspect of the optic chiasm, the proximal part of the optic radiations, the posterior hypothalamus, and part of the cerebral peduncle. Having traversed the thalamus, they may give a variable supply to the ependyma of the lateral ventricle and anastomose there with the choroidal vessels (13).

Up to eight posterior thalamoperforator and thalamogeniculate arteries arise from the posterior or posterosuperior aspect of the P1 segment of the posterior cerebral artery. They enter the brain via the posterior perforated substance, the recess of the interpeduncular fossa, and the medial walls of the cerebral peduncles. Together, they supply the thalamus, subthalamic nucleus, and the nuclei and tracts of the upper midbrain, including the substantia nigra, red nucleus, oculomotor and trochlear nuclei, posterior portion of the internal capsule, and the cisternal segment of the oculomotor nerve (2,14,15). Occasionally, posterior thalamoperforator arteries may arise predominantly or exclusively from one side. When a dominant thalamoperforating vessel is seen giving bilateral supply, it is sometimes referred to as the *artery of Percheron* (Fig. 13-2) (16,17).

Surgical or occlusive injury to thalamoperforating branches may result in a number of midbrain or thalamic syndromes due to involvement of the substrates of cranial nerves III and IV, with hemiplegia, hemiballismus, cerebellar ataxia, and choreiform movement disorders (Figs. 13-5 and 13-6). The number and size of thalamoperforating vessels arising from the posterior communicating arteries and P1 segments is fairly constant, even when one or the other is hypoplastic (5,10). This implies that midbrain and thalamic morbidity is still a consideration and risk if sacrifice or compromise of a hypoplastic P1 segment or a hypoplastic posterior communicating artery is contemplated.

► PEDUNCULAR PERFORATING BRANCHES OF THE POSTERIOR CEREBRAL ARTERY

Up to six branches from the P1 and P2 segments enter the cerebral peduncle directly to supply the corticospinal and corticobulbar tracts, substantia nigra, and red nucleus. They also supply the tegmental and cisternal portions of the oculomotor nerve (5,18). Close to the midline, up to six perforator branches course posteriorly to supply the median portion of midbrain back to the aqueduct. Therefore, occlusion of these medial vessels has a profound impact on the nuclear and fascicular substrates of extraocular movement.

► CIRCUMFLEX BRANCHES OF THE POSTERIOR CEREBRAL ARTERY

One or more short circumflex branches arise from the P1 segment or, less commonly, from the P2 segment. They encircle the brainstem, coursing deep to the medial posterior choroidal artery and posterior cerebral artery. En route as far back as the geniculate bodies, they send small twigs to the lateral aspects of the peduncles and the tegmentum.

► VENTRICULAR BRANCHES OF THE POSTERIOR CEREBRAL ARTERY

Two groups of branches directed toward the choroid plexus and its adjacent structures arise from the posterior cerebral artery.

Medial Posterior Choroidal Arteries

The medial posterior choroidal artery is multiple in up to 40% of hemispheres (10), with two or three vessels seen per hemisphere (Figs. 13-7 and 13-8). The most common site of origin is from the P2 segment, slightly more proximal on the posterior cerebral artery than the dominant sites of origin of the lateral posterior choroidal arteries. The medial posterior choroidal artery may also arise from the parieto-occipital, calcarine, and splenic branches of the posterior cerebral artery, or even from the basilar artery (19). As it courses around the ambient cistern, cisternal branches contribute to the vascular supply of midbrain, tectal plate, pineal gland, posterior thalamus, the habenula, and medial geniculate body. It then curves over the quadrigeminal plate slightly lateral to the pineal gland (19) to enter the roof of the third ventricle, where it becomes the *plexal segment*. The plexal segment of the medial posterior choroidal artery runs anteriorly within

(text continues on page 190)

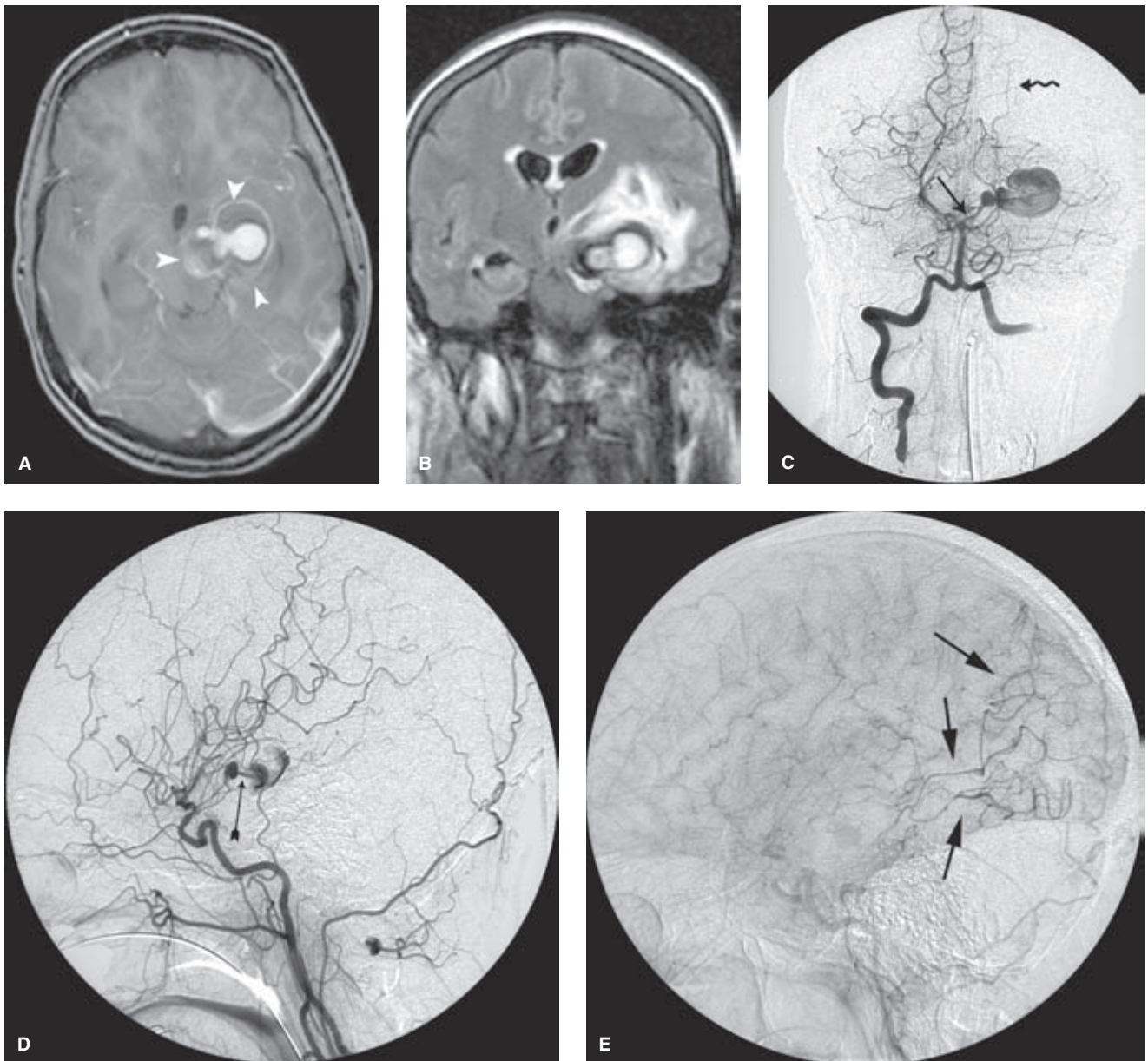


FIGURE 13-5. (A–E) Dissecting aneurysm of the left posterior cerebral artery I. A young adult presented with right-sided hemiplegic symptoms, oculoplegic disturbance, and a visual field cut. The T1 gadolinium-enhanced MRI (A) and FLAIR sequence (B) demonstrate that the enhancing component of the large aneurysm in the perimesencephalic cistern is only a fraction of the overall aneurysm size (*arrowhead* in A). There is considerable surrounding edema and mass effect in the brainstem, thalamus, and internal capsule accounting for her symptoms. The Townes view of the posterior circulation (C) shows elevation and stretching (*straight arrow* in C) leading to filling of a complex multilobulated aneurysm, beyond which there is slow filling of the distal posterior cerebral artery territory (*wavy arrow*). The aneurysm is also seen on the left common carotid artery injection (D), where a pronounced jet of inflow to the distal aneurysm (*arrow* in D) is seen. This jet pattern probably accounts for the bizarre multilobulated and partially thrombosed appearance of the aneurysm. The compromised flow in the distal posterior cerebral artery is a commonly seen feature of long-standing dissecting aneurysms, and this can work to the patient's advantage in that this compromise can encourage development of pial–pial or other collaterals to the distal territory over time. In (E), the patient is undergoing a temporary balloon occlusion of the left posterior cerebral artery, while a simultaneous contrast injection is performed in the left common carotid artery. The parenchymal phase of the injection shows prominent retrograde collaterals (*arrows* in E) to the posterior cerebral artery territory, arguing that the patient should be able to tolerate an endovascular occlusion of the dissected segment of vessel as definitive therapy for this aneurysm.

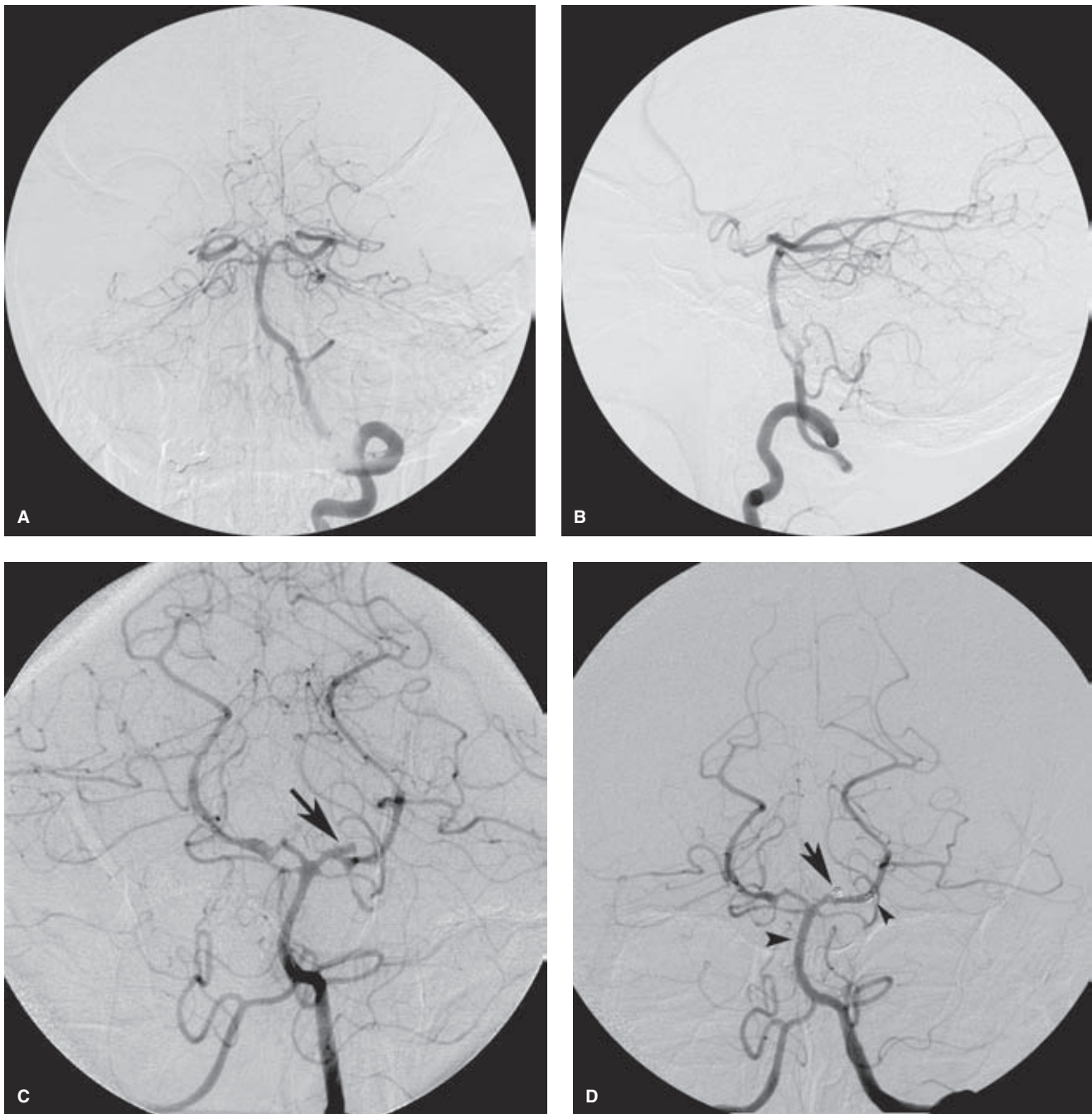


FIGURE 13-6. (A–D) Dissecting aneurysm of the posterior cerebral artery II. A middle-aged female patient presented with mild subarachnoid hemorrhage, and her cerebral angiogram and noninvasive imaging showed no evidence of an aneurysm. Her initial AP (**A**) and lateral (**B**) views of the posterior circulation showed a normal appearance of the left posterior cerebral artery. The patient made a good recovery and was discharged home with a presumed diagnosis of perimesencephalic hemorrhage, but with the provision that a follow-up angiogram would be performed in the short term. The need for this repeat angiogram was forced by events when the patient returned to the hospital with deterioration of her neurologic status. A repeat angiogram (**C**) 10 days following the initial angiogram shows development or reemergence of an aneurysm (*arrow* in **C**) of the P1 segment of the left posterior cerebral artery. Because of its unusual location and elongated appearance, it was presumed to be dissecting in nature. This aneurysm was treated by an endovascular approach, in part in deference to the risk posed to the perforator vessels along that segment by conventional surgical clipping. Additionally, because of the time frame of her return to the hospital, vasospasm was thought to be a factor in the genesis of her new symptoms. Her postembolization image (**D**) shows satisfactory coil obliteration of the aneurysm (*arrow*). The coils are retained within the aneurysm by a Neuroform stent extending from the posterior cerebral artery to the midbasilar artery (tines marked by *arrowheads* in **D**).

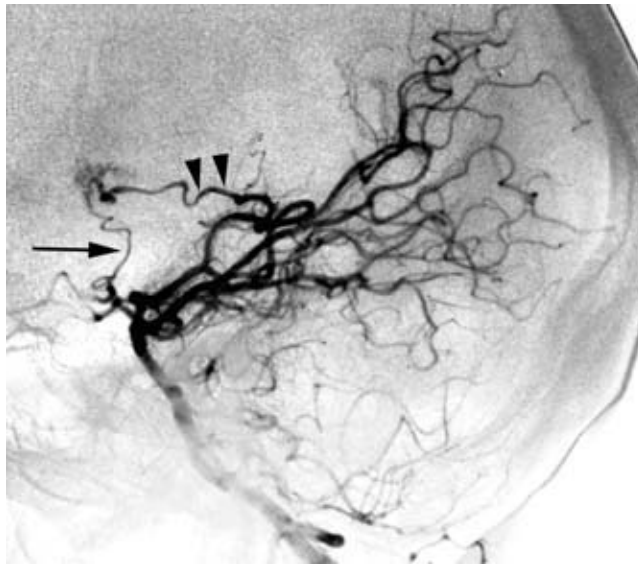


FIGURE 13-7 Arteriovenous malformation of the foramen of Monro. A lateral projection of the posterior fossa demonstrates an enlarged medial posterior choroidal artery (*double arrowhead*) and an anterior thalamoperforator/thalamotuberal artery (*arrow*) directed toward an arteriovenous malformation nidus in the region of the foramen of Monro. The identity of the medial posterior choroidal artery can be confirmed by superimposing the arterial image on the venous. The medial posterior choroidal artery and the internal cerebral vein both course within the cistern of the velum interpositum.

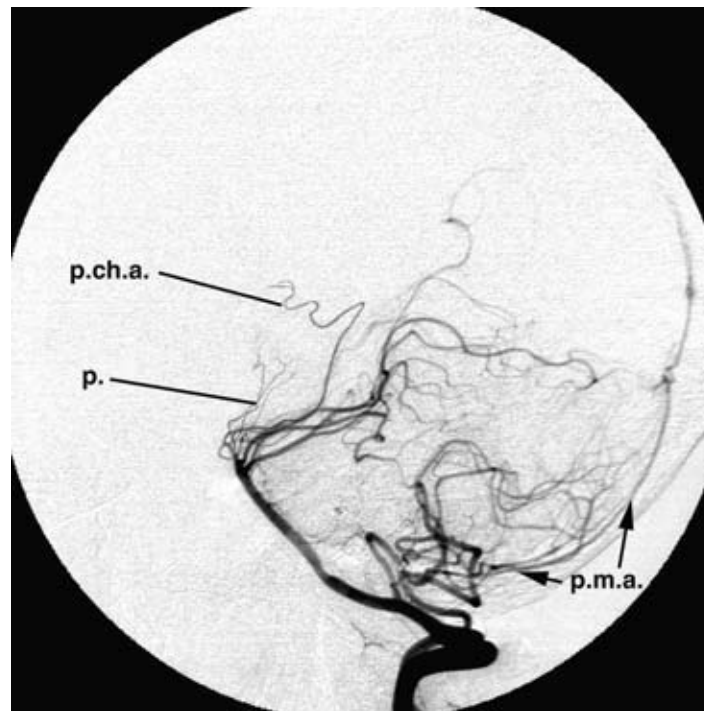


FIGURE 13-8 Variant origin of the posterior choroidal arteries. A posterior fossa injection in a patient with bilateral fetal posterior communicating arteries affords an unobstructed view of the transmesencephalic, thalamoperforator, and circumflex branches of the upper basilar artery (*p.*), without superimposed posterior cerebral arteries. A medial posterior choroidal artery (*p.ch.a.*) appears to arise from the basilar artery, a variant that has been described. However, this could also be due to preferential opacification of this vessel via a hypoplastic P1 segment. The course of the posterior meningeal artery (*p.m.a.*) clinging to the inner table of the skull is well seen.

the velum interpositum toward the foramen of Monro, supplying the ipsilateral choroid plexus of the third ventricle. Its terminal branches are directed anteriorly toward the foramen of Monro, where they anastomose with the terminal branches of the lateral posterior choroidal artery.

Lateral Posterior Choroidal Arteries

The lateral posterior choroidal arteries, up to nine per hemisphere, arise typically from the P2 segment of the posterior cerebral artery slightly more distal in origin than the medial posterior choroidal arteries. However, up to 48% can be identified arising from more distal branches of the posterior cerebral artery including the hippocampal, temporal, parieto-occipital, and other arteries (5,20). Before entering the choroidal fissure lateral to the ambient cistern, the lateral posterior choroidal arteries may give peduncular or tegmental branches. The lateral posterior choroidal arteries most commonly enter the lateral ventricle posteriorly at the level of the atrium. The posterior wall of the pulvinar defines the medial anterior edge of the ventricular atrium, which is therefore accurately described

on a lateral angiogram by the curve of the lateral posterior choroidal artery. This used to be an important marker for thalamic masses and shift, but it can still be useful with modern axial imaging, serving as an easily transposed landmark from one imaging modality to the other. The anastomoses between the lateral posterior choroidal artery and medial posterior choroidal artery anteriorly sometimes serve as a useful angiographic reference point for the foramen of Monro.

► CORTICAL BRANCHES OF THE POSTERIOR CEREBRAL ARTERY

Cortical branches of the posterior cerebral artery are the temporal arteries to the inferior surface of the temporal lobe, parieto-occipital artery, calcarine artery, and splenial artery. During posterior fossa arteriography, they are frequently superimposed on each other and on the thalamic, midbrain, and superior cerebellar artery branches. They are therefore most clearly seen on a lateral view of a carotid artery injection in the setting of a fetal posterior cerebral artery origin (Figs. 13-9–13-12).

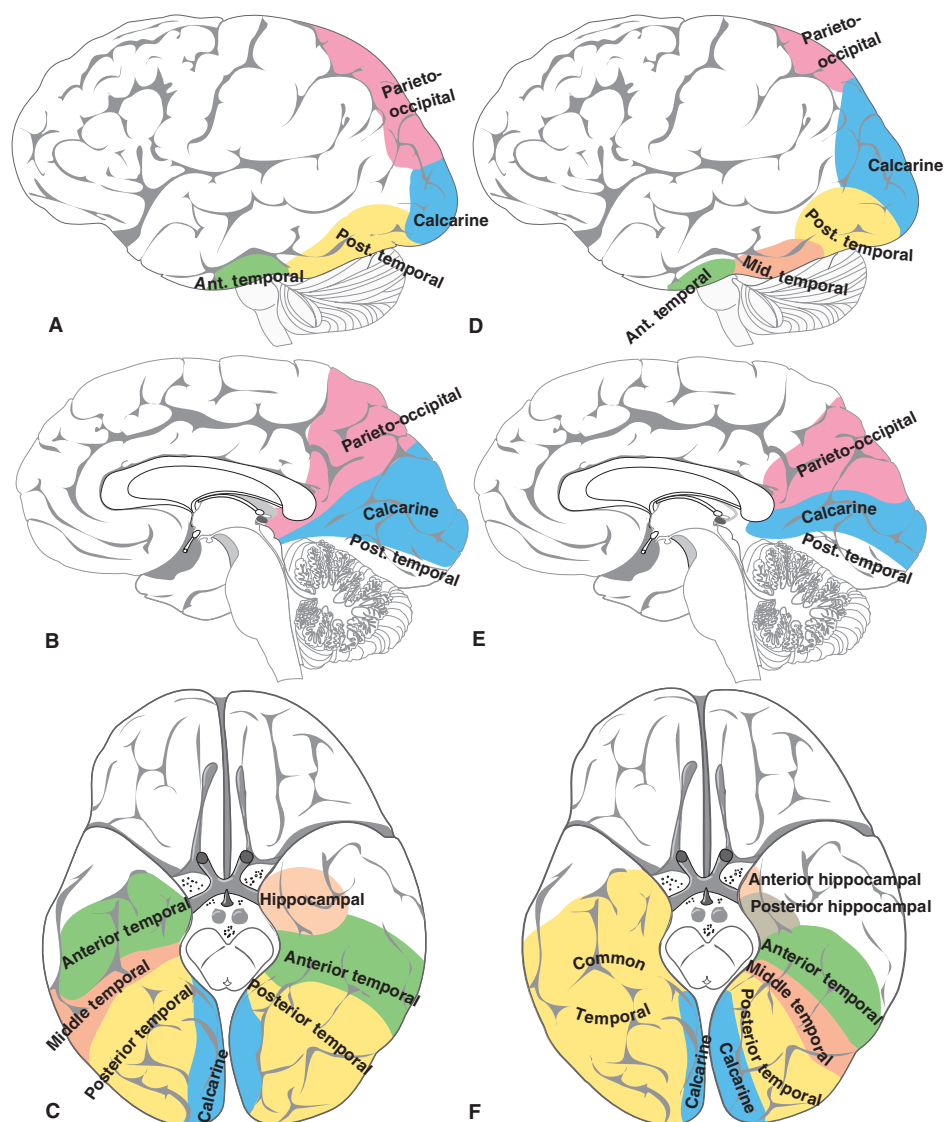


FIGURE 13-9. Named cortical branches of the posterior cerebral artery. Common division patterns and assigned nomenclature of the cortical branches of the posterior cerebral artery are illustrated.

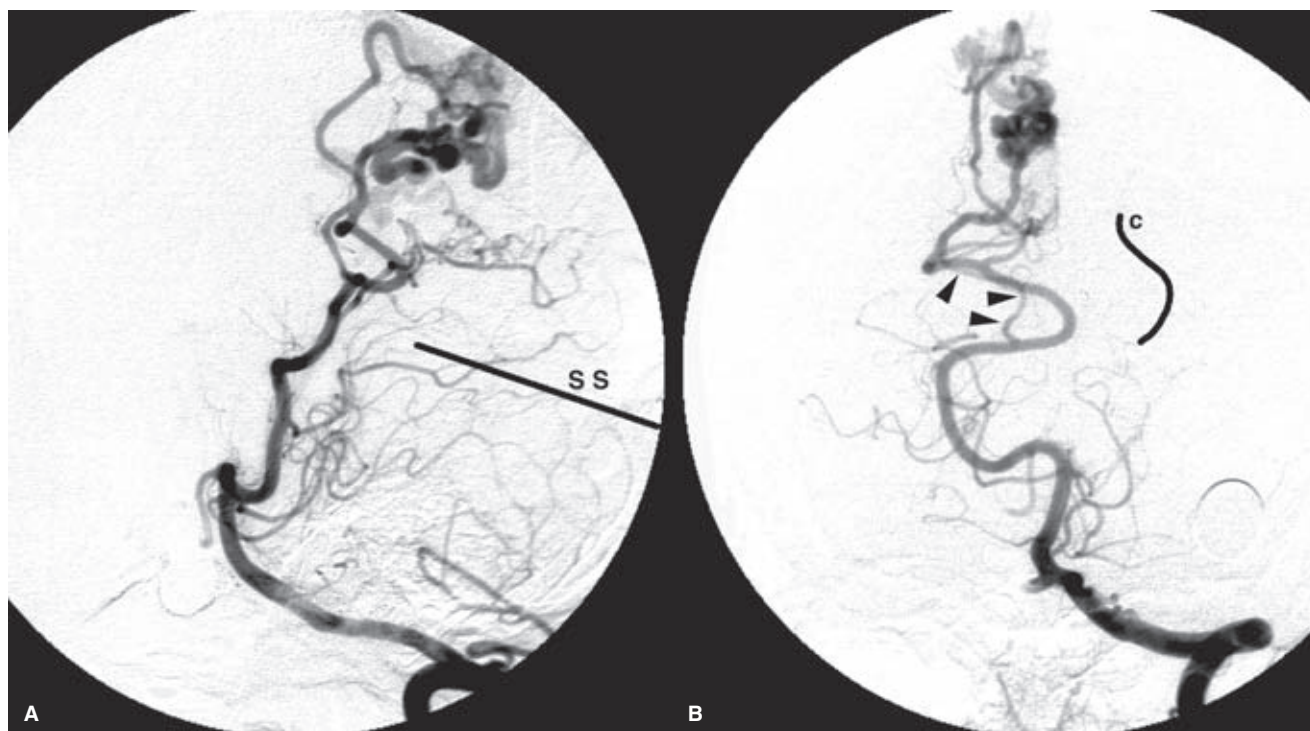


FIGURE 13-10. (A–B) Parieto-occipital arteriovenous malformation. A right parieto-occipital arteriovenous malformation is opacified in this patient without superimposition on the lateral view (A) because of the presence of a left fetal posterior communicating artery. The course of the straight sinus (S.S.) is depicted by the black line (A). On the Townes view (B), the arrowheads on the patient's right indicate the course of the calcarine artery as it deviates more laterally than the near midline course of the parieto-occipital artery. This is because the calcarine artery usually lies within the depths of the calcarine fissure; it therefore usually projects more laterally, as illustrated by line c. on the patient's left side.

Temporal and Hippocampal Branches of the Posterior Cerebral Artery

The temporal branches of the posterior cerebral artery, sometimes called the *inferior temporal branches* in distinction from the superior temporal branches of the middle cerebral artery, vary in number (10,21). Approximately 10% of hemispheres have a full complement of temporal posterior cerebral artery branches, including anterior temporal, middle temporal, posterior temporal, and hippocampal branches.

The hippocampal artery (64% of hemispheres) is the most proximal temporal branch arising from the P2 segment of the posterior cerebral artery. It supplies the medial temporal lobe, specifically the uncus, hippocampal gyrus, and the dentate gyrus. It may send branches anteriorly to the temporal pole, which anastomose with temporal polar branches of the middle cerebral artery.

The posterior temporal artery is a large branch that runs posteriorly toward the occipital pole and supplies the posterior undersurface of the temporal lobe and the occipital lobe. It supplies the lingual gyrus and gives collateral or accessory vessels to the calcarine fissure in 10% to 20% of brains. This accessory route of calcarine supply is posed as one explanation for central visual field sparing after a distal posterior cerebral artery occlusion.

Parieto-occipital Artery

This is the largest and most readily identified terminal branch of the posterior cerebral artery, present in more than

96% of hemispheres, running in the parieto-occipital fissure. It supplies the cuneus, part of precuneus, and lateral occipital gyrus, and may occasionally extend to the medial aspects of the precentral gyrus and superior parietal lobule.

Calcarine Artery

This important vessel to the primary visual cortex buried deep in the calcarine fissure may arise from the posterior cerebral trunk, from the parieto-occipital branch, or from the posterior temporal branch. Accessory calcarine vessels may be present from the posterior temporal or parieto-occipital arteries in 10% to 20% of hemispheres (10). The calcarine artery supplies the cortex in the reaches of the calcarine fissure and gives branches extending to the surface of the fissure to supply the lingual gyrus and cuneus. Unilateral occlusion of the calcarine artery is associated with homonymous hemianopsia with a variable degree of macular sparing. Bilateral calcarine artery occlusion can cause Anton syndrome, in which there may be confabulatory denial of blindness.

Splenial Artery

This vessel (or vessels) arises most often from the parieto-occipital branch of the posterior cerebral artery but can arise from the temporal and calcarine branches. It can form a common trunk with the medial posterior choroidal artery or can arise directly from the main trunk of the posterior cerebral artery. It is sometimes called the *posterior pericallosal artery* and represents an important source of collateral

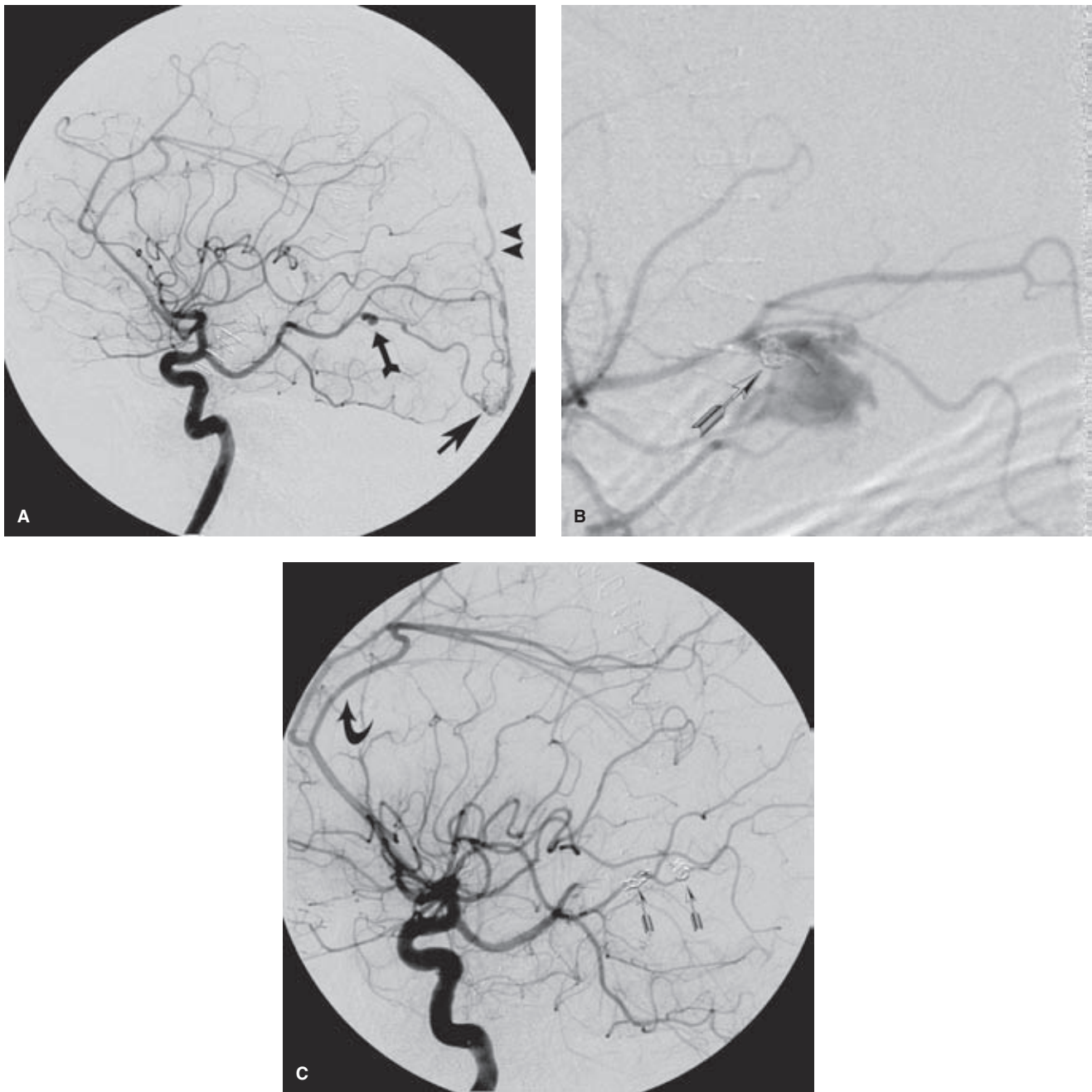


FIGURE 13-11. (A–C) Occipital arteriovenous malformation with aneurysm of the origin of the calcarine artery. A middle-aged female presented with massive intraparenchymal and subarachnoid hemorrhage centered on the right occipital area. An angiogram of the right internal carotid artery shows a fetal-type posterior cerebral artery with an AVM (*arrow*) in the right occipital pole and venous drainage (*arrowhead*) toward the superior sagittal sinus. Despite the fact that a ventriculostomy has already been performed, notice the tense appearance of the pericallosal branch of the anterior cerebral artery with buckling of the vessel along its midcourse. An aneurysm (*feathered arrow*) that is the likely site of hemorrhage is identified at the origin of what is presumed to be the calcarine artery, enlarged in this patient by virtue of the flow to the AVM. Aneurysms on arteries feeding an AVM are often assumed to be in part promoted by the hemodynamic shear stress induced by the high-flow state in such vessels. Out of concern for the visual cortex in this patient, an attempt was made initially to embolize the aneurysm with coils while preserving flow in the calcarine artery and parieto-occipital artery. However, the aneurysm proved extremely fragile and ruptured in response to the stress of the advancing coil (*feathered arrow* in **B**). Prominent extravasation of contrast surrounds the coil site in (**B**). The posterior cerebral artery was then hurriedly occluded with a second coil nidus (*feathered arrows* in **C**), resulting in elimination of flow in that segment of the artery. In the final image (**C**), the increased appearance of distension and bowing of the pericallosal artery (*curved arrow*) should prompt concerns that the ventriculostomy is either closed, malfunctioning, or is overwhelmed by the new hemorrhage from the intraprocedural rupture.

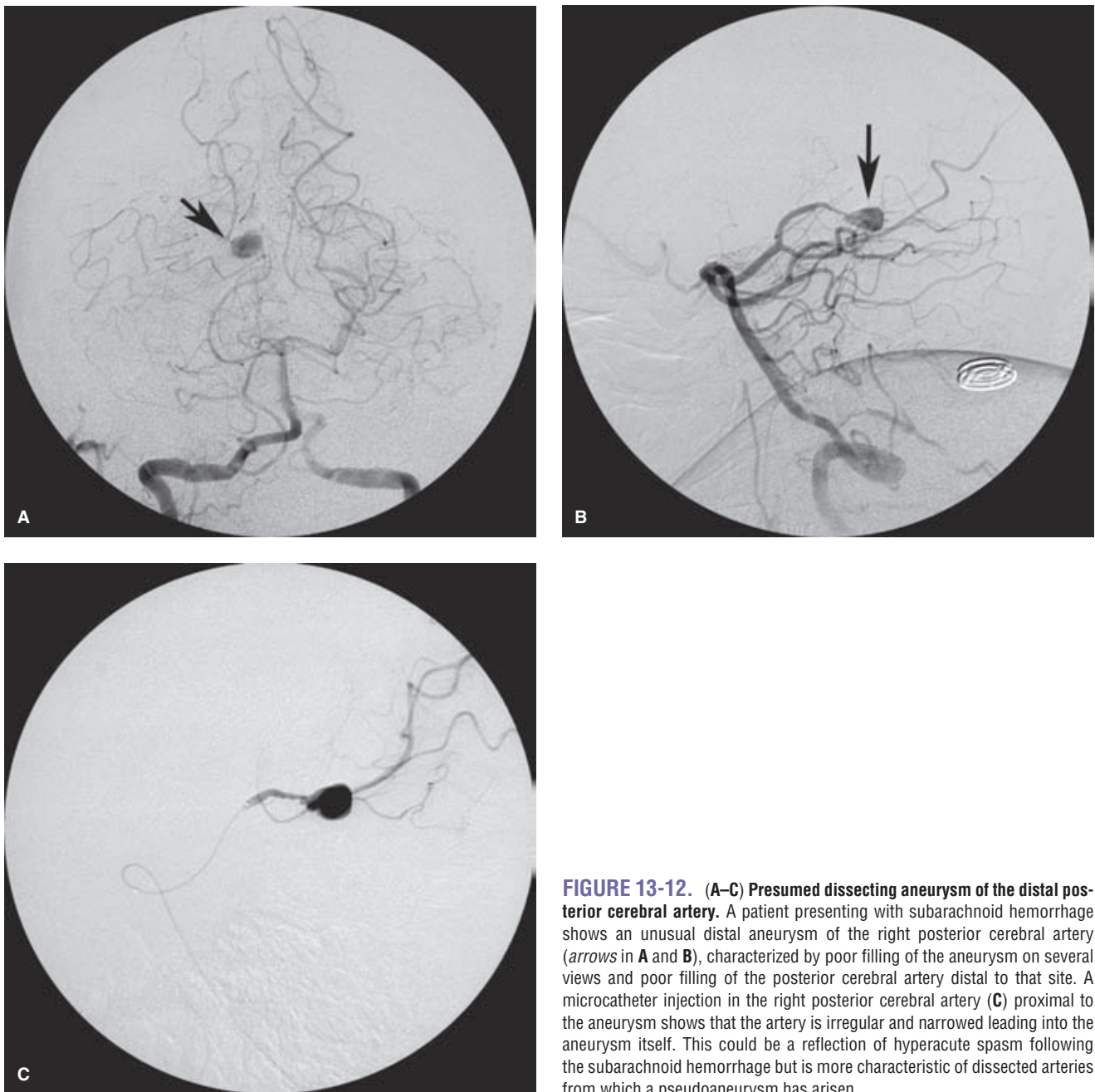


FIGURE 13-12. (A–C) Presumed dissecting aneurysm of the distal posterior cerebral artery. A patient presenting with subarachnoid hemorrhage shows an unusual distal aneurysm of the right posterior cerebral artery (arrows in A and B), characterized by poor filling of the aneurysm on several views and poor filling of the posterior cerebral artery distal to that site. A microcatheter injection in the right posterior cerebral artery (C) proximal to the aneurysm shows that the artery is irregular and narrowed leading into the aneurysm itself. This could be a reflection of hyperacute spasm following the subarachnoid hemorrhage but is more characteristic of dissected arteries from which a pseudoaneurysm has arisen.

supply from the posterior to anterior cerebral arteries. It sometimes has a recurrent branch to the fornix, which anastomoses with the medial posterior choroidal arteries.

References

1. Padget DH. The development of the cranial arteries in the human embryo. *Contrib Embryol* 1948;32:205–262.
2. Margolis MT, Newton TH, Hoyt WF. Gross and roentgenologic anatomy of the posterior cerebral artery. In: Newton TH, Potts DG, eds. *Radiology of the Skull and Brain*. Vol II. St. Louis: C.V. Mosby; 1974:1551–1576.
3. Fischer E. Die Lageabweichungen der vorderen Hirnarterien Gafässbild. *Zentralbl Neurochir* 1938;3:300–313.
4. Krayenbühl HA, Yasargil MG. *Cerebral Angiography*. 2nd ed. Philadelphia: J.B. Lippincott; 1968.
5. Saeki N, Rhoton AL Jr. Microsurgical anatomy of the upper basilar artery and the posterior circle of Willis. *J Neurosurg* 1977;46(5):563–578.
6. Parraga RG, Ribas GC, Andrade SE, et al. Microsurgical anatomy of the posterior cerebral artery in three-dimensional images. *World Neurosurg* 2011;75(2):233–257.
7. Kernohan JW, Woltman HW. Incisura of the crus due to contralateral brain tumor. *Arch Neurol Psychiat* 1929;21:272–287.
8. Ono M, Ono M, Rhoton AL Jr, et al. Microsurgical anatomy of the region of the tentorial incisura. *J Neurosurg* 1984;60(2):365–399.
9. Blinkov SM, Gabibov GA, Tanyashin SV. Variations in location of the arteries coursing between the brain stem and the free edge of the tentorium. *J Neurosurg* 1992;76(6):973–978.

10. Zeal AA, Rhoton AL Jr. Microsurgical anatomy of the posterior cerebral artery. *J Neurosurg* 1978;48(4):534–559.
11. Wollschlaeger PB, Wollschlaeger G. [An infratentorial meningeal artery]. *Radiologe* 1965;5(11):451–452.
12. Weinstein M, Stein R, Pollock J, et al. Meningeal branch of the posterior cerebral artery. *Neuroradiology* 1974;7(3):129–131.
13. Kaya AH, Dacinar A, Ulu MO, et al. The perforating branches of the P1 segment of the posterior cerebral artery. *J Clin Neurosci* 2010;17(1):80–84.
14. Lazorthes G, Salamon G. The arteries of the thalamus: An anatomical and radiological study. *J Neurosurg* 1971;34(1):23–26.
15. Uz A, Tekdemir I. Relationship between the posterior cerebral artery and the cisternal segment of the oculomotor nerve. *J Clin Neurosci* 2006;13(10):1019–1022.
16. Westberg G. Arteries of the basal ganglia. *Acta Radiol Diagn (Stockh)* 1966;5:581–596.
17. Percheron G. The anatomy of the arterial supply of the human thalamus and its use for the interpretation of the thalamic vascular pathology. *Z Neurol* 1973;205(1):1–13.
18. Marinkovic S, Milisavljevic M, Kovacevic M. Interpeduncular perforating branches of the posterior cerebral artery. Microsurgical anatomy of their extracerebral and intracerebral segments. *Surg Neurol* 1986;26(4):349–359.
19. Berland LL, Houghton VM. Anomalous origin of posterior choroidal artery from basilar artery. *AJR Am J Roentgenol* 1979;132(4):674–675.
20. Fujii K, Lenkey C, Rhoton AL Jr. Microsurgical anatomy of the choroidal arteries: Lateral and third ventricles. *J Neurosurg* 1980;52(2):165–188.
21. Yamamoto I, Kageyama N. Microsurgical anatomy of the pineal region. *J Neurosurg* 1980;53(2):205–221.

The Extradural Vertebral Arteries

Key Points

- The anterior spinal artery is a major focus of concern in all vertebral artery catheterizations and embolizations.
- Anastomotic connections between the vertebral arteries and the external carotid arteries are universally present, whether they are angiographically evident or not, and may become the basis for misadventurous embolization of the posterior circulation in various circumstances.

The vertebral arteries derive from eight paired segmental vessels that correspond with the embryologic cervical somites. As the vertebral bodies differentiate, the vessels become intersegmental in location and are so designated thereafter in the embryologic literature, with each numbered to correspond with the vertebral body above. In the embryologic literature, the first segmental artery is therefore displaced from the numbering scheme and is then termed the *proatlantal intersegmental artery* (1). However, in angiographic parlance, anastomotic branches of the vertebral artery are numbered according to the corresponding cervical nerve root. For example, the C2 branch of the vertebral artery emerges between the C1 and C2 vertebral bodies (Figs. 14-1 and 14-2).

The plexus, which is formed cranially by the segmental arteries during embryonic life, anastomoses at the level of the hypoglossal nerve with the paired longitudinal neural plexi, which form the basilar artery. The cervical vertebral artery forms from a longitudinal anastomosis between the segmental cervical arteries. A concurrent partial regression of the proximal portions of each of the upper segmental arteries takes place.

It should be theoretically possible for any of the segmental arteries to become the dominant feeder to the forming longitudinal anastomosis, which will become the ipsilateral vertebral artery. Usually the proximal vertebral trunk off the subclavian artery corresponds with the sixth intersegmental artery and enters the foramen transversarium below the C6 vertebral body. When the left vertebral artery arises directly off the aorta proximal to the subclavian artery, the vertebral artery corresponds most commonly with the fourth intersegmental

vessel and enters the foramen under the C4 body. Other derivations of the intersegmental arteries such as the proatlantal intersegmental artery are rare (discussed in Chapter 10) (2).

The formation of the vertebrobasilar system from the fusion of two sets of vascular embryologic plexi explains the propensity of the vessels in this region to emerge with variable patterns. The vertebral artery itself may retain flow through two parallel channels, giving the appearance of a duplication (Figs. 14-3–14-5). Duplications can be seen at any level of the vertebral artery in 0.7% of studies (3–7). Alternatively, ectasia or looping in the high cervical area may result in the vertebral artery assuming an intradural course at a level as low as the C2 body. This can be an incidental finding but can also be associated with cord or root compression symptoms (8) and may be seen particularly with somal disorders affecting the cervical area such as Klippel–Feil syndrome (9). An anomalous pattern of regression of elements of the longitudinal neural plexi (in the posterior fossa) and of the cervical plexus can also explain a C1 or C2 origin of the posterior inferior cerebellar artery (Fig. 14-6).

The anatomy of the vertebral artery is sometimes described in four parts (Fig. 14-7).

1. The first segment extends from the subclavian artery to the foramen transversarium of the C6 vertebral body.
2. The second segment ascends vertically within the foramina transversaria from C6 to the atlas.
3. The third segment leaves the transverse foramen of the atlas and extends posteriorly and horizontally on the superior surface of the posterior arch of the atlas.
4. The fourth segment pierces the atlanto-occipital membrane and the dura in turn, and then enters the intracranial cavity via the foramen magnum.

Within the foramina transversaria, the vertebral artery in its usual configuration ascends surrounded by the vertebral venous plexus. It runs immediately adjacent to the uncinat processes medially and the ventral rami of the cervical nerves posteriorly. Above the axis, the artery courses laterally and posteriorly before turning sharply cephalad. It then passes through the foramen transversarium of the atlas, which is located more laterally than those below. It courses postero-medially in a horizontal direction, imprinting a groove on the superior surface of the posterior arch of the atlas. In a minority

(text continues on page 199)

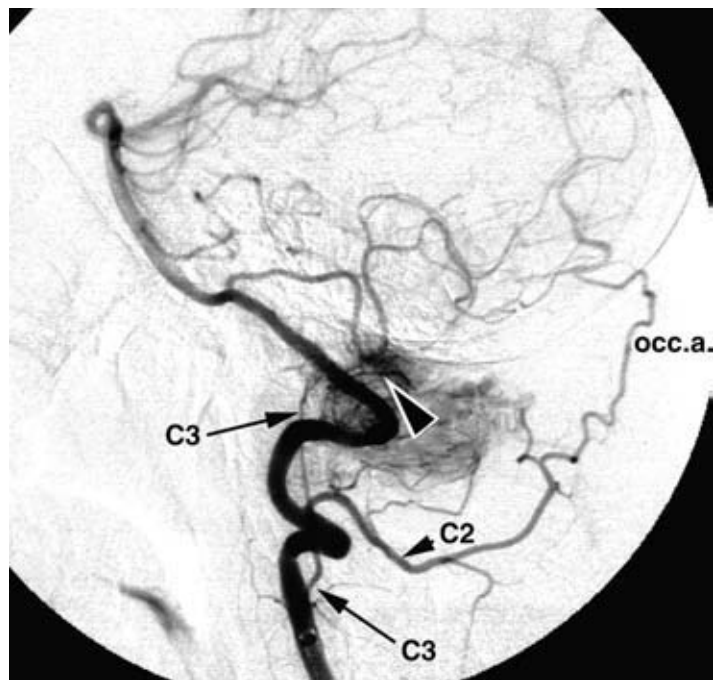


FIGURE 14-1. Anastomotic branches of the upper vertebral artery. A left vertebral artery injection in a patient with a vascular tumor of the C1 vertebral body. The C1 branches (*large arrowhead*) of the vertebral artery supply the center of the mass directly. The vertebral artery at the C1 level is irregular and narrowed, indicating encasement. The C2 branch of the vertebral artery also gives supply to the tumor and has prominent anastomotic connection with the occipital artery (*occ.a.*). The C3 anastomotic branch of the vertebral artery ascends medially behind the vertebral bodies of C2 and C1 close to the midline and is also involved with supply to the tumor.

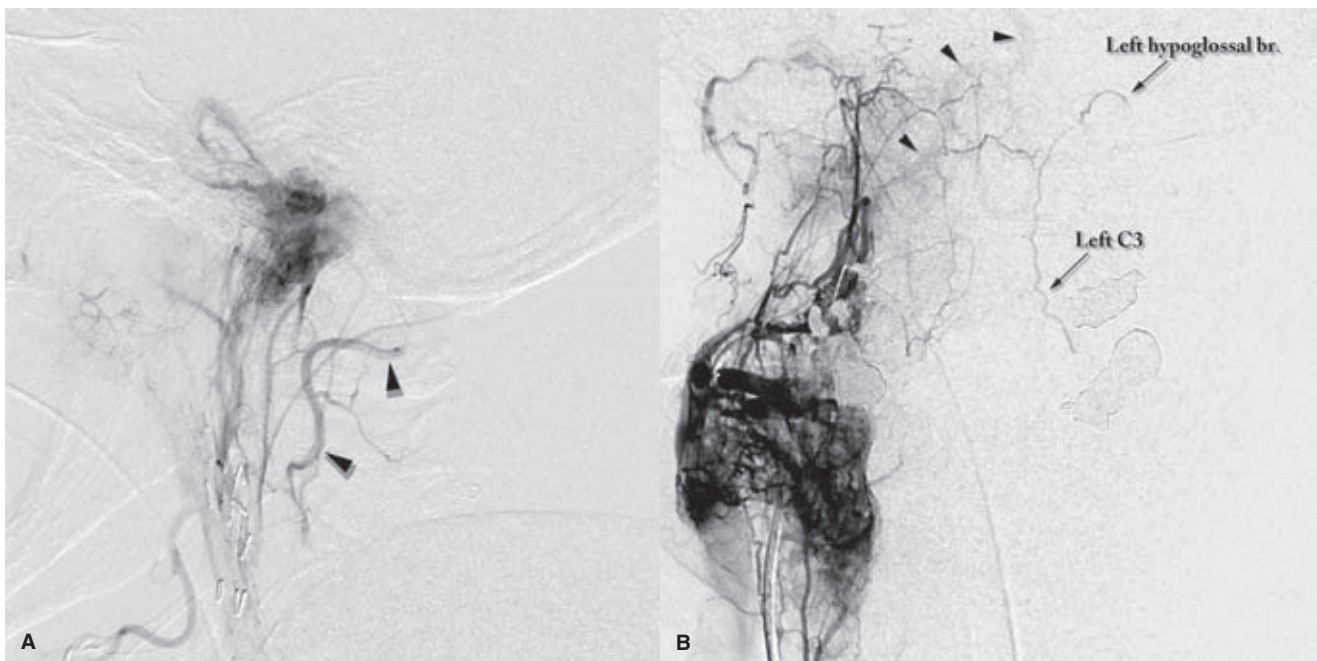


FIGURE 14-2. Anastomotic dangers to the vertebral artery. Lateral (A) and AP (B) views of injections in the ascending pharyngeal artery in two different patients, each with a paraganglioma of the jugular bulb and carotid body respectively. Each image shows the extreme ease with which access to the ipsilateral vertebral artery and subsequently the basilar artery (*arrowheads*) can be established, even when the anastomotic connections are not particularly enlarged. The C3 anastomoses to the vertebral arteries bilaterally are shown well in image (B) accessed via the hypoglossal branch of the neuromeningeal trunk on the right side, and refluxing contralaterally to the left-sided counterparts.



FIGURE 14-3. Segmental duplication of the right vertebral artery. Lateral views of a right vertebral artery demonstrating an incidental finding of a duplicated segment.



FIGURE 14-4. Duplicated upper segment of vertebral artery I. A left vertebral artery Townes projection demonstrates an incidentally discovered duplication of the upper segment. The medial limb of such duplications frequently pursues a medial intradural course, similar to instances of C1 or C2 origins of a posterior inferior cerebellar artery.

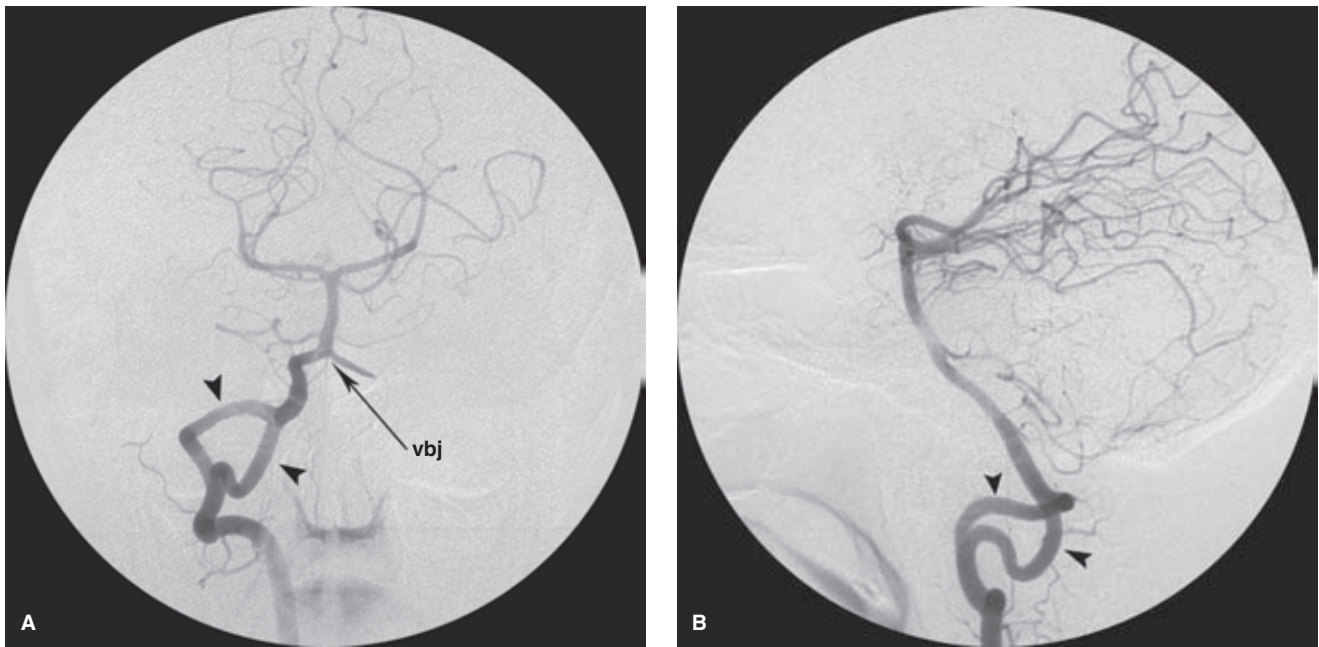


FIGURE 14-5. (A–B) Duplicated upper segment of right vertebral artery II. AP (A) and lateral (B) projections demonstrate a similar anatomic anomaly as in Figure 14-4. vbj, vertebrobasilar junction.



FIGURE 14-6. Cervical origin of the left posterior inferior cerebellar artery. On this Townes projection, the posterior inferior cerebellar artery (*arrowheads*) arises at the C1 level of the left vertebral artery. The dural margin is demonstrated by the cincture (*arrows*) of the vertebral artery above this level.

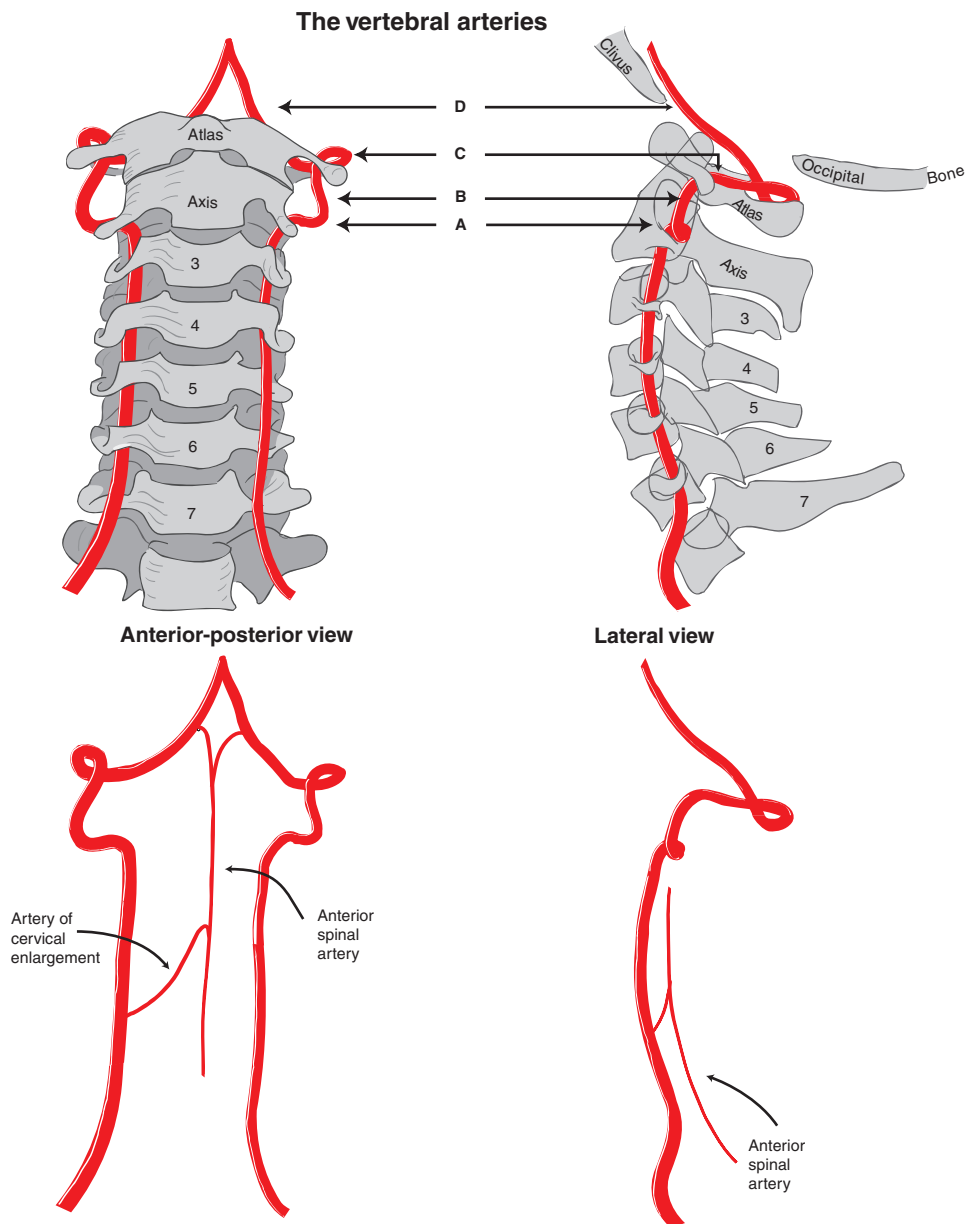


FIGURE 14-7. Vertebral arteries. The course of the vertebral arteries with and without related bony structures is illustrated, as seen on angiographic images. The turns of the vessel at the C1–C2 level are difficult to correlate on direct AP and lateral views without having a mental image of the four turns that the vertebral artery makes in this region. The course of the anterior spinal artery lying anteriorly within the spinal canal is illustrated.

of anatomic specimens, the rims of this groove on the superior atlantal surface become a circumferential bony ring. At the margin of the C1 posterior arch, the vertebral artery turns abruptly anteromedially and pierces the atlanto-occipital membrane to enter the dura where a waistlike impression on the contour of the vessel may be seen angiographically. The vertebral artery then fuses with its counterpart anterior to the medulla to form the basilar artery. This junction is usually at or within a few millimeters of the inferior rim of the clivus.

The distal intradural portion of the vertebral artery may be hypoplastic or absent, implying that the vertebral artery effectively ends with a posterior inferior cerebellar artery as a terminal branch. Although this is uncommon (<5%), the consequences of performing a full-volume injection into a vertebral artery terminating in a posterior inferior cerebellar

artery could be devastating, due to the risk of vessel rupture or infarction. Evaluating the distal runoff from a vertebral artery to exclude this possibility is a routine consideration before performing any vertebral artery injection.

The anterior spinal artery in the cervical area is sometimes referred to as the *artery of cervical enlargement*. It is a major focus of concern during embolization of the cervical region, particularly in vessels with anastomotic connections to the C4–C6 level (Figs. 14-8 and 14-9). The artery of cervical enlargement usually arises from the vertebral arteries, often bilaterally. Other origins are frequently seen, particularly from branches of the thyrocervical trunk. During all embolizations or therapeutic vessel occlusions in the low cervical area, it is important to identify and preserve the source of the artery of cervical enlargement.

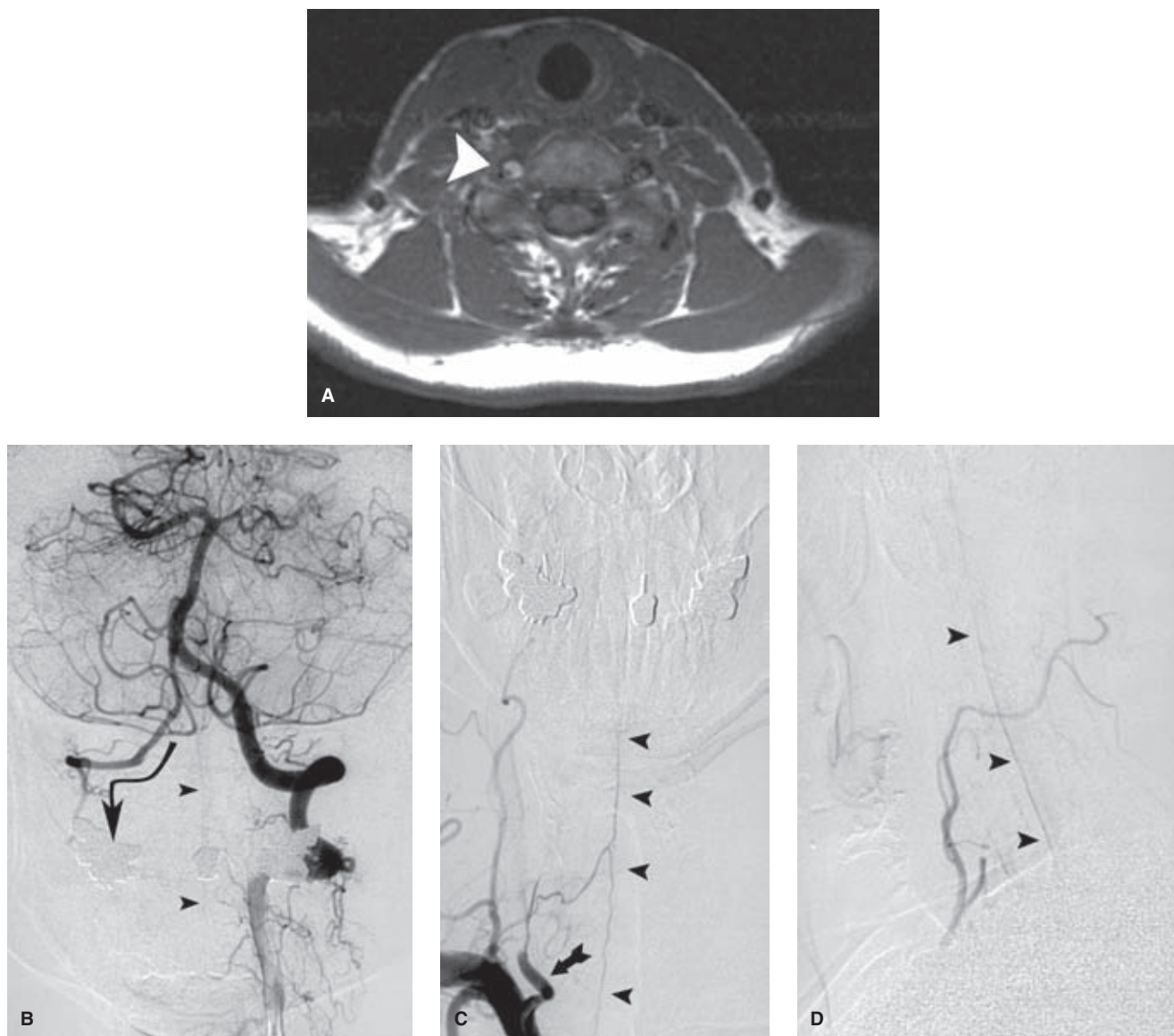


FIGURE 14-8. (A–D) Vulnerability of the anterior spinal artery. A middle-aged female complained of neck pain, assumed to be musculoskeletal in origin. When she developed lower extremity fluctuating paraplegia, cord compression from a disc herniation was suspected. However, an MRI demonstrated (*arrowhead* in **A**) a flow abnormality in the right vertebral artery suspicious for dissection. An angiogram of the left vertebral artery (**B**, AP view) showed retrograde opacification down the right vertebral artery that did not wash away, indicating compromise of flow in the right vertebral artery. The anterior spinal artery (*arrowheads* in **B**) was prominently seen on this injection, filling down from the vertebrobasilar junction. The right vertebral artery injection (**C**, AP view; **D**, lateral view) shows that the artery (*arrow* in **C**) terminates in a ragged taper, indicating the intraluminal presence of clot. Out of this tapered segment of artery arises the anterior spinal artery (*arrowheads*). In this case, the anterior spinal artery is larger than the average, suggesting that if the ischemia that had brought this patient to attention had become permanent, she probably would have sustained an extensive infarction of the spinal cord.

► DISSECTION OF THE VERTEBRAL ARTERIES

Like dissection of the internal carotid artery, dissection of the vertebral artery is thought to have a similar pathogenesis. With the exception of systemic angiopathic syndromes discussed later, most cases of vertebral artery dissection are either of spontaneous origin or are seen following neck trauma. A variety of traumatic etiologies for vertebral artery dissection have been reported, particularly after sport and

vehicular accidents (Fig. 14-10). Iatrogenic traumatic etiologies include vessel catheterization, percutaneous needle placement, and chiropractic manipulation. Spontaneous vertebral artery dissection occurs most commonly in middle-aged females (10). Many cases of “spontaneous” vertebral artery dissection in middle-aged females may be related to fibromuscular dysplasia (11) or paroxysmal hypertension, with 30% of cases being bilateral (Fig. 14-11).

The incidence of subclinical or mildly symptomatic vertebral artery dissection is unknown. An MRI study of

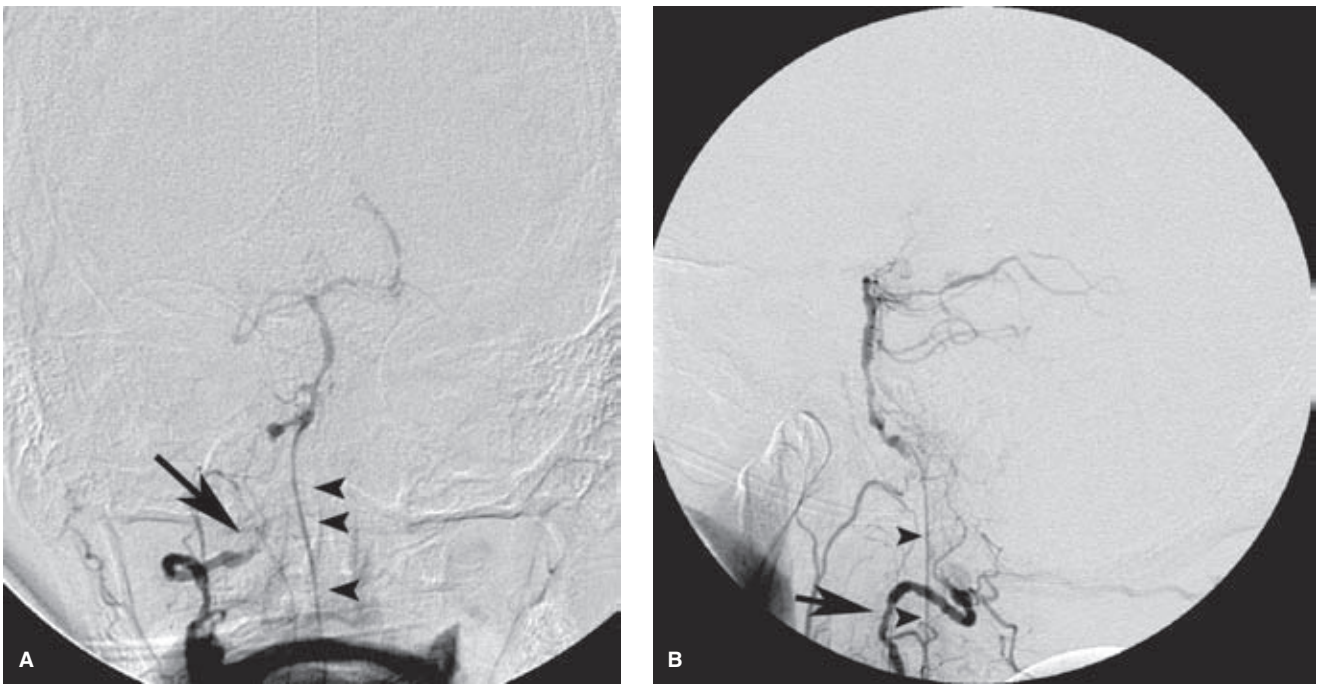


FIGURE 14-9. (A–B) Anterior spinal artery as collateral circulation to the basilar artery. This elderly female patient presented with left hemispheric ischemic symptoms due to critical left internal carotid artery stenosis. However, her angiogram (A, AP view; B, lateral view) also showed that her left vertebral artery was completely occluded, and the right vertebral artery (arrow) demonstrated virtually complete occlusion, with the anterior spinal artery (arrowheads) constituting the major route of supply to the basilar artery via retrograde flow from the lower cervical region. The intracranial vessels demonstrate diffuse atherosclerotic disease.

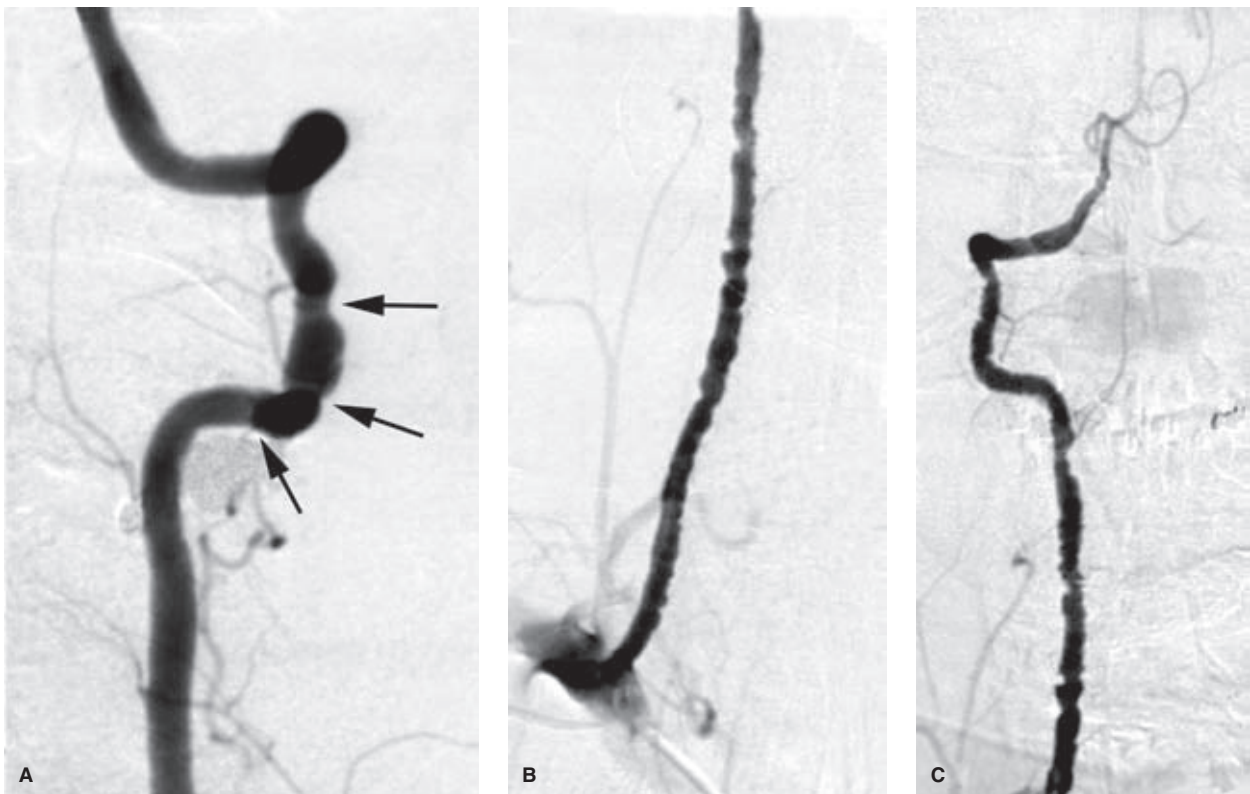


FIGURE 14-10. (A–C) Traumatic dissection of the vertebral arteries. A young adult female involved in a vehicular accident with severe cervical trauma developed complications from a right internal carotid artery dissection and a right Wallenberg syndrome. MRA demonstrated a normal appearance of the vertebral arteries. During angiographic evaluation of the carotid arteries, injection of the left vertebral artery (A) and right vertebral artery (B, C) demonstrated multiple areas of intimal irregularity representing dissection and spasm (arrows).

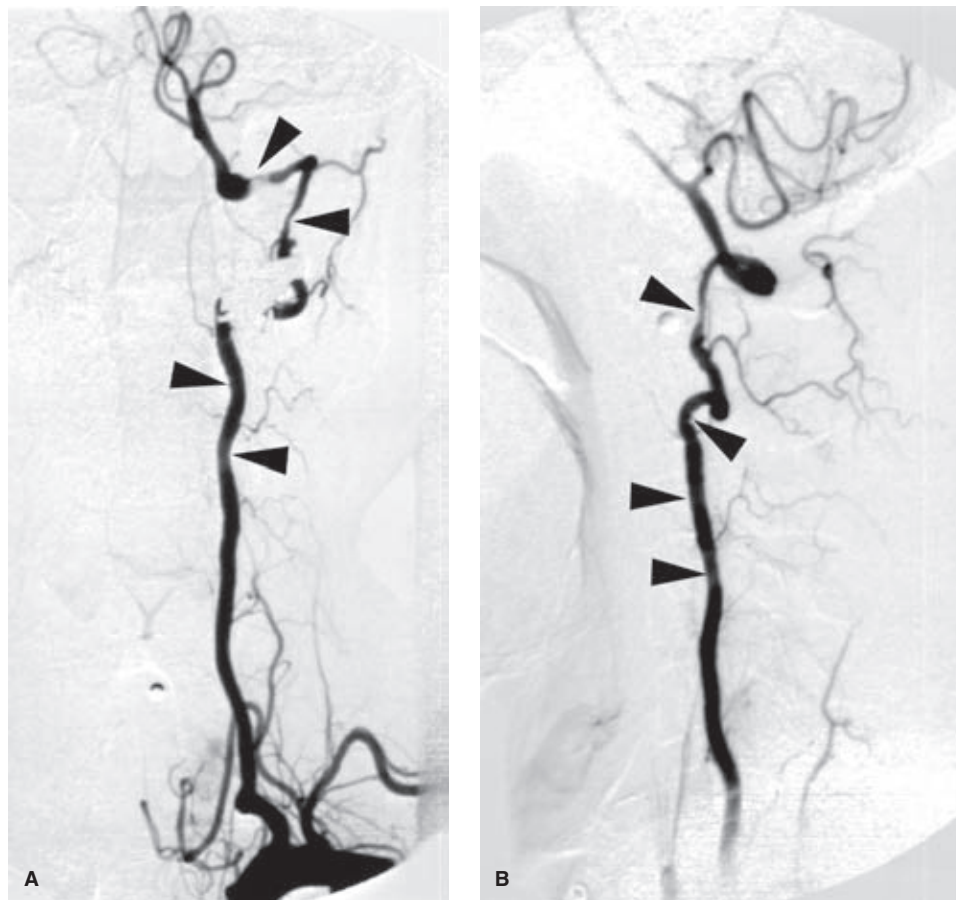


FIGURE 14-11. (A–B) Vertebral artery dissection with presumed fibromuscular dysplasia. A middle-aged patient with malignant hypertension was found to have renal artery dissections and renal infarcts during angiography. A presumptive diagnosis of fibromuscular dysplasia was established. Subsequent complaints of headache and neck pain were evaluated by cerebral angiography, which demonstrated carotid and vertebral artery irregularities and dissections (*arrowheads*).

patients who had suffered major cervical nonpenetrating trauma indicated that at least 24% of such patients had sustained an arterial injury to the vertebral arteries, most of which remained asymptomatic (12). An angiographic study of patients with blunt cervical injuries and significant vertebral instability had a 46% rate of major vascular injuries involving the vertebral arteries (occlusion, intimal flap, pseudoaneurysm formation, or dissection), most of which were clinically silent (13). These studies would suggest that many patients who sustain similar or lesser injuries may have arterial dissections or occlusions that do not become clinically relevant.

Moreover, the symptoms of vertebral artery dissection can be difficult to discern from musculoskeletal pain. Neck ache and headache are a prominent symptom in approximately 70% of patients with this disorder (10). Pain may be localized to the neck and occiput, or it may give the sensation of a diffuse headache. Therefore, unless the patient develops neurologic symptoms, the possibility of a vertebral artery dissection may be overlooked in many instances.

The neurologic complications of extracranial vertebral artery dissection can be severe or even fatal. Frequently,

neurologic symptoms are preceded by pain for a period ranging from hours to weeks. Ischemia of the posterior circulation may be related to embolic events or to complete vessel occlusion in the setting of inadequate collateral circulation. A lateral medullary (Wallenberg) infarct is a typical presenting syndrome.

Angiographic findings of vertebral artery dissection include long, irregular luminal narrowing; vessel occlusion; a double lumen or intimal flap; and pseudoaneurysm formation. The vertebral artery is most vulnerable to external traumatic injury or to spontaneous dissection, where it is most mobile, that is, after it leaves the foramen transversarium of C2. Above this level, the normal vertebral artery must conform to physiologic rotational maneuvers of the C1–C2 articulation. Narrowing or transient occlusion of flow related to head position or head traction can be seen angiographically at this level and may be symptomatic (see Chapter 28).

Traumatic injuries of the vertebral artery that are due to penetrating injuries or catheter manipulations correspond with the site of injury (Figs. 14-12 and 14-13). Those related to unsuccessful attempts at percutaneous jugular vein catheterization are typically seen at the C5–C6 level and may be associated with a vertebrovenous fistula.

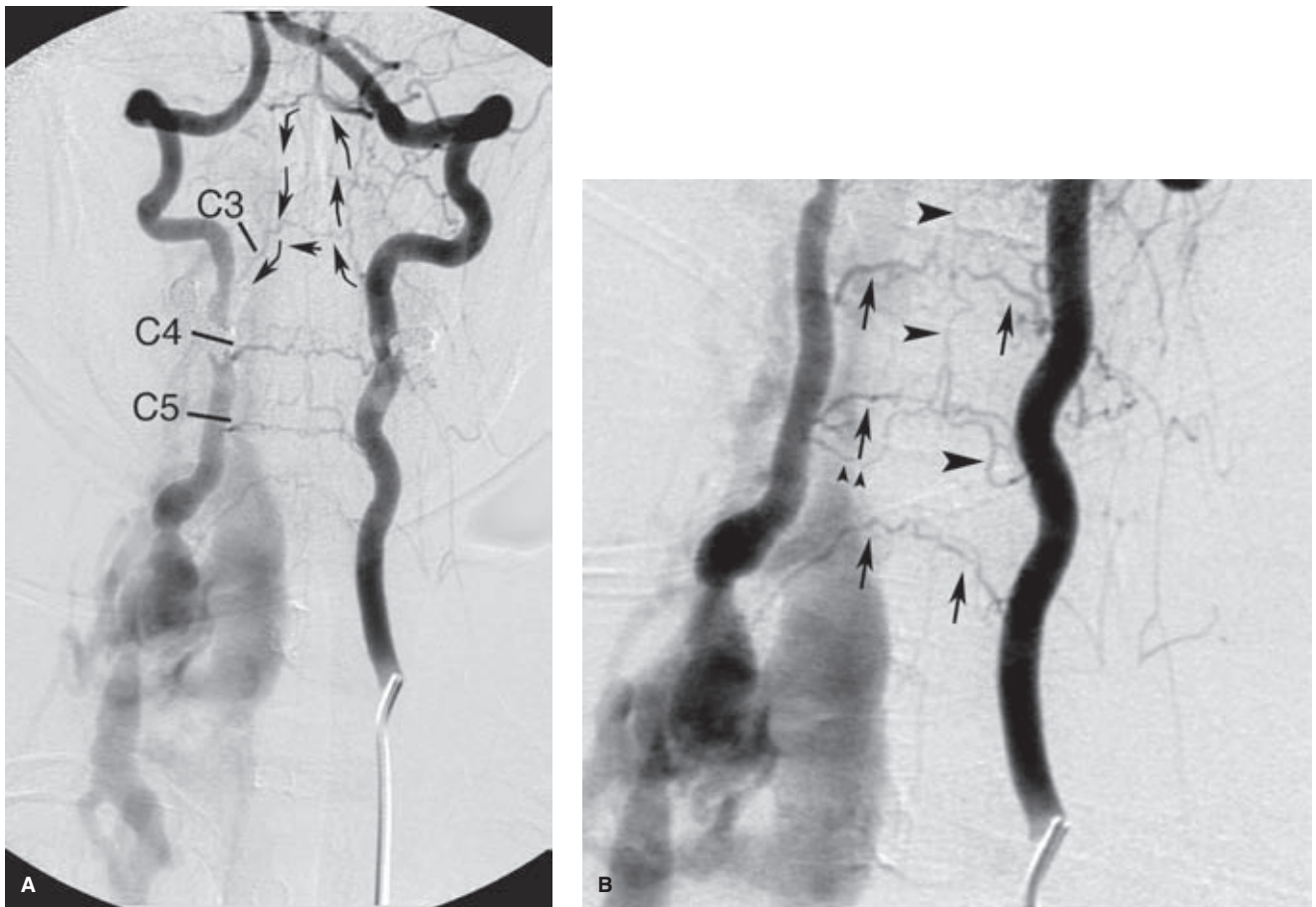


FIGURE 14-12. (A–B) Spontaneous fistula of the right vertebral artery in a patient with neurofibromatosis type I. A young female presented with sudden onset of pulsatile right-sided tinnitus, which was related to a spontaneous fistula in the lower right vertebral artery. The AP view (A) and detailed magnification view (B) show that the best imaging of the precise fistula site was from the contralateral side, whereas from the ipsilateral side, the venous opacification engulfed the angiographic image. View (A) demonstrates prompt retrograde opacification of the right vertebral artery from the vertebrobasilar junction and also left-to-right anastomoses via muscular and segmental collaterals crossing the midline. Prominent among those is the C3 anastomotic arch (*curved arrows*) arising at the interspace between the C2 and C3 vertebral bodies. This particular anastomotic pathway is vitally important for understanding the connections between the vertebral artery and the ipsilateral ascending pharyngeal artery (see Chapter 17). As shown here, it also has the capacity for robust anastomotic collaterals to its contralateral fellow in any high-flow or occlusive disease state.

Of particular importance in this case is the location of the anterior spinal artery. The right vertebral artery fistula was thought difficult to occlude with coils or liquid embolic material, and the artery was too large for any available covered stents. Therefore, a sacrifice of the right vertebral artery was proposed, but obviously, an inadvertent occlusion of the anterior spinal artery would have to be avoided scrupulously. The magnification view (B) shows the anterior spinal artery (*arrowheads*) arising from the left vertebral artery. However, still closer scrutiny shows that the anterior spinal artery also connects with the right vertebral artery (*small double arrowheads*). The dynamic observation that flow in this segment was retrograde—from left to right—gave the assurance that occluding the right vertebral artery would not therefore represent a risk to the patient.

Notice that the anterior spinal artery overlaps with muscular collaterals (*arrows*) without communicating with them, an indication—as with all angiographic representation of overlapping vessels—that these arteries lie in a different anatomic plane.

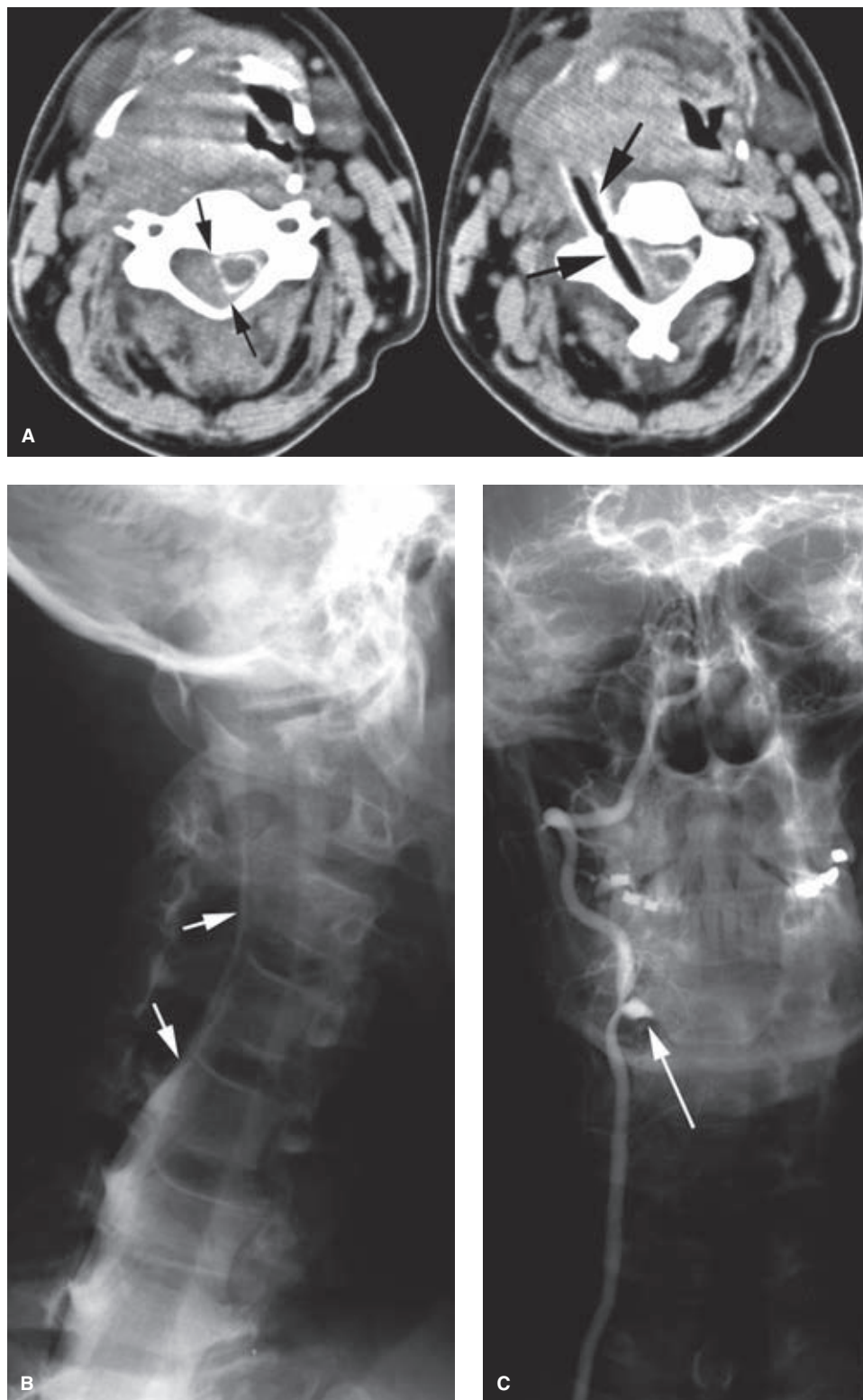


FIGURE 14-13. (A–C) Pseudoaneurysm of the right vertebral artery due to wooden foreign body. **A:** CT myelographic images in a middle-aged patient with a history of a fall on deck lumber. A soft tissue mass representing an infected hematoma displaces the airway toward the patient's left. There is soft tissue (hematoma) within the spinal canal displacing the thecal sac (*small arrows*). A linear structure of air density (*larger arrows*) representing a wooden fragment projects directly through the foramen transversarium of C3, narrowly missing the spine. **B:** Oblique myelographic image demonstrates displacement of the thecal sac by epidural hematoma (*white arrows*). **C:** A PA angiographic image of the right vertebral artery demonstrates a pseudoaneurysm of the right vertebral artery at the site of the wooden missile (*arrow*). The artery was sacrificed using balloon occlusion before surgical evacuation of the hematoma.

References

1. Padget DH. Designation of the embryonic intersegmental arteries in reference to the vertebral artery and subclavian stem. *Anat Rec* 1954;119(3):349–356.
2. Legre J, Tapias PL, Nardin JY, et al. Embryonic intersegmental anastomosis between the external carotid and vertebral arteries. Classification problems of the proatlantal artery. *J Neuro-radiol* 1980;7(2):97–104.
3. Takasato Y, Hayashi H, Kobayashi T, et al. Duplicated origin of right vertebral artery with rudimentary and accessory left vertebral arteries. *Neuroradiology* 1992;34(4):287–289.
4. Rieger P, Huber G. Fenestration and duplicate origin of the left vertebral artery in angiography. Report of three cases. *Neuro-radiology* 1983;25(1):45–50.
5. Suzuki S, Kuwabara Y, Hatano R, et al. Duplicate origin of left vertebral artery. *Neuroradiology* 1978;15(1):27–29.
6. Hashimoto H, Ohnishi H, Yuasa T, et al. Duplicate origin of the vertebral artery: Report of two cases. *Neuroradiology* 1987; 29(3):301–303.
7. Eisenberg RA, Vines FS, Taylor SB. Bifid origin of the left vertebral artery. *Radiology* 1986;159(2):429–430.
8. Sharma RR, Parekh HC, Prabhu S, et al. Compression of the C-2 root by a rare anomalous ectatic vertebral artery. Case report. *J Neurosurg* 1993;78(4):669–672.
9. Tokuda K, Miyasaka K, Abe H, et al. Anomalous atlantoaxial portions of vertebral and posterior inferior cerebellar arteries. *Neuroradiology* 1985;27(5):410–413.
10. Hinse P, Thie A, Lachenmayer L. Dissection of the extracranial vertebral artery: Report of four cases and review of the literature. *J Neurol Neurosurg Psychiatry* 1991;54(10):863–869.
11. Chiras J, Marciano S, Vega Molina J, et al. Spontaneous dissecting aneurysm of the extracranial vertebral artery (20 cases). *Neuroradiology* 1985;27(4):327–333.
12. Friedman D, Flanders A, Thomas C, et al. Vertebral artery injury after acute cervical spine trauma: rate of occurrence as detected by MR angiography and assessment of clinical consequences. *AJR Am J Roentgenol* 1995;164(2):443–447; discussion 448–449.
13. Willis BK, Greiner F, Orrison WW, et al. The incidence of vertebral artery injury after midcervical spine fracture or subluxation. *Neurosurgery* 1994;34(3):435–441; discussion 441–432.

15

The Arteries of the Posterior Fossa

Key Points

- Perforator branches of the brainstem are difficult to see angiographically but injury to them can be the mechanism of devastating ischemic deficits to the patient.
- The proximal segments of the cerebellar arteries frequently give important perforator and circumflex branches to the brainstem before reaching the cerebellum itself.

The basilar artery forms by fusion of the left and right vertebral arteries. It runs from the vertebrobasilar junction at the pontomedullary sulcus to the interpeduncular cistern, where it bifurcates behind the dorsum sellae. The level of the basilar bifurcation in reference to the posterior clinoid processes can have an important bearing on the surgical approach to basilar tip aneurysms (Fig. 15-1). More than 70% of basilar bifurcations lie level with or above the posterior clinoid processes (1). The other major anatomic determinant of surgical difficulty in approaching a basilar tip aneurysm is the attitude of the aneurysm to the artery in terms of whether it inclines anteriorly or posteriorly. An anteriorly pointing basilar tip aneurysm high above the clinoidal level is more favorable for surgical access. Aneurysms at a low basilar bifurcation or those that point posteriorly are considered inaccessible or hazardous.

The vertebrobasilar system gives vascular supply to the posterior cerebral arteries and three pairs of named branches to the cerebellum. Smaller perforating and circumflex branches throughout its length supply the upper spine, medulla, pons, midbrain, and thalamus (Figs. 15-2–15-4). The posterior circulation is more prone than the anterior to demonstrate developmental anomalies or variants that can frequently be of clinical significance in the genesis of vascular pathology or during therapeutic procedures.

► INTRACRANIAL SEGMENT OF THE VERTEBRAL ARTERY

In approximately 60% of cases, the left vertebral artery is “dominant” or significantly larger than the right. Hypoplasia

of the distal nondominant vertebral artery can be seen in varying degrees in approximately 5% to 10% of cases, underscoring the need to check the intracranial runoff before doing a full-volume power injection in a vertebral artery (Fig. 15-3). After traversing the atlanto-occipital membrane, the vertebral artery pierces the dura and enters the subarachnoid space usually in the lateral medullary cistern.

From the lateral medullary cistern, the vertebral arteries on their respective sides wind around the medulla oblongata anteriorly into the premedullary cistern. They fuse close to the midline with an angle of incidence between 30 and 90 degrees. Their meeting is most commonly at or within a few millimeters of the pontomedullary junction (2,3). The blood supply of the medulla is therefore predominantly from the intracranial segment of the vertebral arteries proximal to the vertebrobasilar junction, and to a lesser extent from small recurrent basilar artery branches that loop inferiorly.

Medially directed branches of the intracranial segment of the vertebral arteries supply the anterior medulla and pyramid. The most prominent of these vessels is the anterior spinal artery (Figs. 15-5–15-7), directed inferiorly along the anterior median sulcus (3). The anterior spinal artery is absent unilaterally in approximately 20% of postmortem angiograms (4). Moreover, the ideal appearance of bilateral symmetric spinal arteries fusing in the anterior median sulcus is frequently replaced by the configuration of a dominant vessel from one side supplying the major portion of flow. A connecting vessel between the left and right anterior spinal arteries can be seen occasionally at dissection and is termed the *anterior spinal communicating artery*.

The foramen cecum, also known as the Schwalbe foramen or the foramen of Vicq d’Azyr, is a median triangle-shaped fossicle on the anterior surface of the medulla at the pontomedullary junction at the superior end of the ventral median sulcus (5). This fossa fills a role analogous to that played by the anterior and posterior perforated substance at the base of the brain, in that it is traversed by a number of small (<1 mm) perforator vessels. These vessels penetrate the brainstem to provide vascular supply as far back as the tegmentum and floor of the IV ventricle. The brainstem perforators observe a sharp demarcation of the midline and do not give bilateral supply. Compromise of these vessels is responsible for the long tract or nuclear substrate

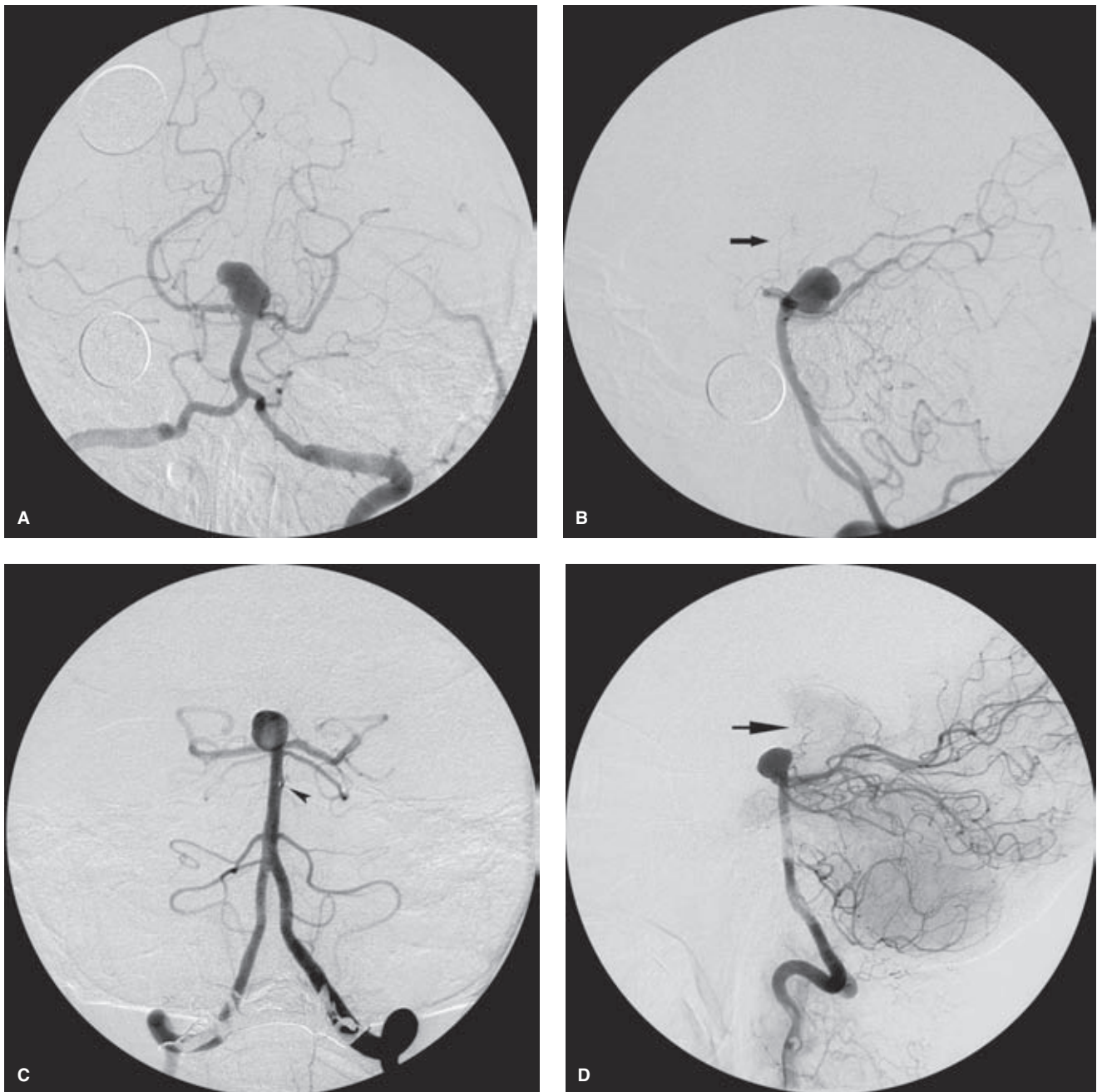


FIGURE 15-1. (A–D) Anterior and posterior projections of basilar tip aneurysms. In the first of two patients, a posteriorly projecting aneurysm is demonstrated in (A) and (B), with the thalamoperforators (*arrow*) depicted in front of the aneurysm, hampering surgical access to the neck of the aneurysm. By contrast, in (C) and (D), an anteriorly projecting aneurysm is shown with the thalamoperforators (*arrow*) behind the aneurysm. Note the small fenestration of the midbasilar artery in (C) (*arrowhead*).

of brainstem syndromes associated with occlusive infarcts there.

The lateral branches of the intracranial segment of the vertebral artery include the posterior inferior cerebellar artery and circumferential branches to the inferior cerebellar peduncle, lateral medulla, and the olivary structures. The posterior inferior cerebellar artery usually arises from the vertebral artery at the level of the olive, but may be either absent, hypoplastic, or arise from the basilar artery. It may alternatively arise more proximally from the vertebral artery as low as the C2 vertebral body and have an initially extradural course. Rarely, the

posterior inferior cerebellar artery may arise from an alternative source in the suboccipital region such as the occipital artery or ascending pharyngeal artery, or from the internal carotid artery as a remnant of the trigeminal artery (6–9). The medullary segment of the posterior inferior cerebellar artery also gives medullary branches, which anastomose with those arising directly from the vertebral artery.

The lateral spinal artery of the upper cervical cord may take origin from the intradural segment of the vertebral artery or from the posterior inferior cerebellar artery posterior to the medulla (8). The lateral spinal artery is usually

(text continues on page 210)

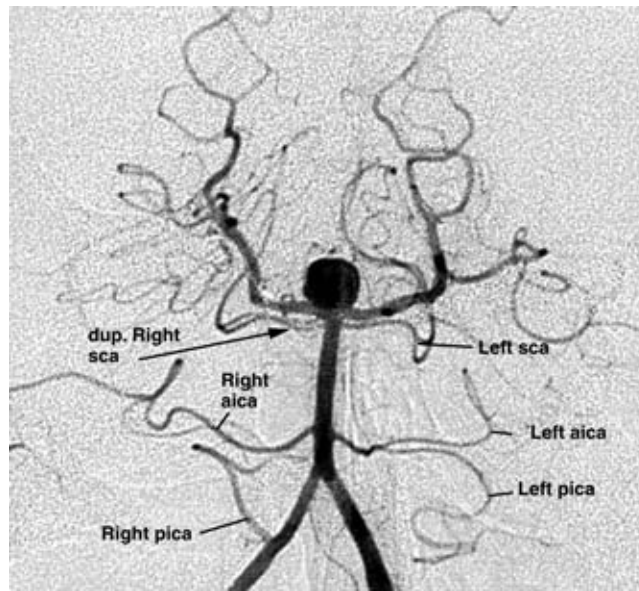


FIGURE 15-2. Townes projection of the posterior fossa. A young adult male presented with headache and anxiety and was found to have an unruptured basilar artery tip aneurysm. A Townes projection demonstrates common examples of the variability in the configurations of the vessels of the posterior fossa. The left posterior inferior cerebellar artery (*pica*) territory is supplied by the left anterior inferior cerebellar artery (*aica*). The right anterior inferior cerebellar artery and posterior inferior cerebellar artery have a balanced distribution. The right superior cerebellar artery (*sca*) has a duplicated origin, the upper branch arising from the posterior cerebral artery.

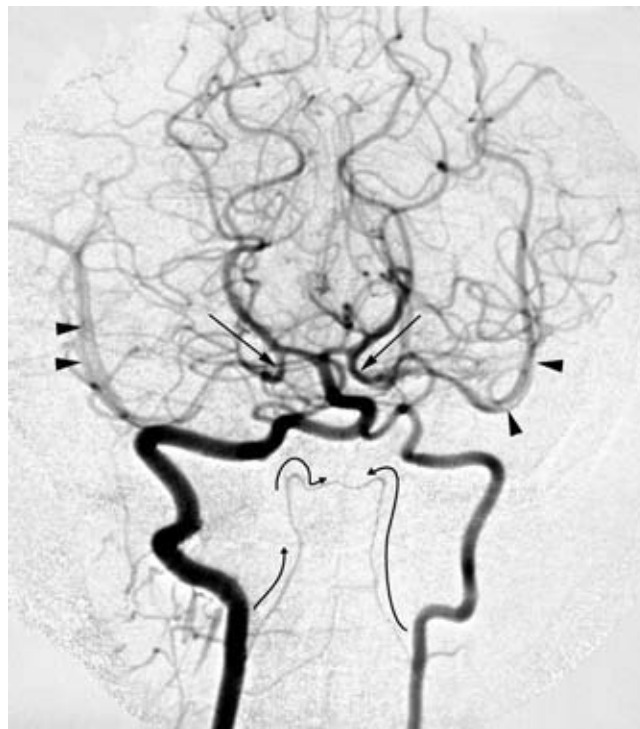


FIGURE 15-3. Dominant right vertebral artery. An injection into the right vertebral artery refluxes the left vertebral artery. To interpret this Townes projection, recall that one is looking at the posterior fossa from above. Therefore, the posterior communicating arteries (*long arrows*) course across the superior cerebellar arteries bilaterally and opacify the middle cerebellar arteries (*arrowheads*) bilaterally. The arcade of the odontoid process is well seen in this image filling from the C3 branches of the vertebral arteries bilaterally (*curved arrows*).

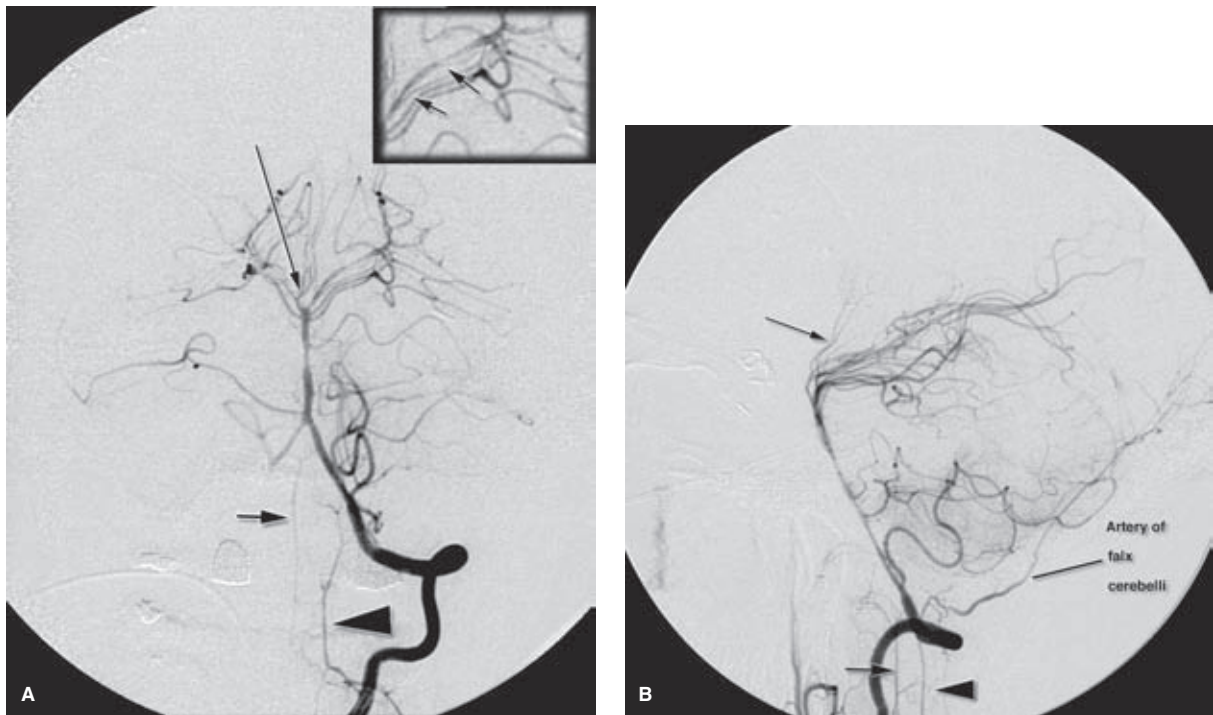


FIGURE 15-4. (A–B) Visualization of anatomy enhanced by background vasospasm. This AP (A) and lateral (B) view of the left vertebral artery injection in the setting of severe vasospasm gives a prominence to smaller branches normally obscured in one's perception by larger vessels. The C3 anastomotic branch of the vertebral artery (*arrowhead*) is to be distinguished from the anterior spinal artery (*short arrow*). In this instance a balanced origin of the anterior spinal artery from both vertebral arteries can be seen. A cluster of thalamoperforator vessels from the right posterior cerebral artery represents a nice example of an artery of Percheron (*long arrow*). The inset in image (A) represents a magnified view of the left posterior cerebral artery. This shows not just a duplicated left superior cerebellar artery, but at least two circumflex branches (*short arrows*) from the proximal posterior cerebral artery. Thus one can understand how a wire-tip can sometimes look on a roadmap as if it is within the P1 or P2 but is actually in a much smaller and more vulnerable vessel. This is a point of extreme caution when a wire inexplicably does not advance in the posterior cerebral artery or a following device such as a balloon or microcatheter appear to be having difficulty following the wire.

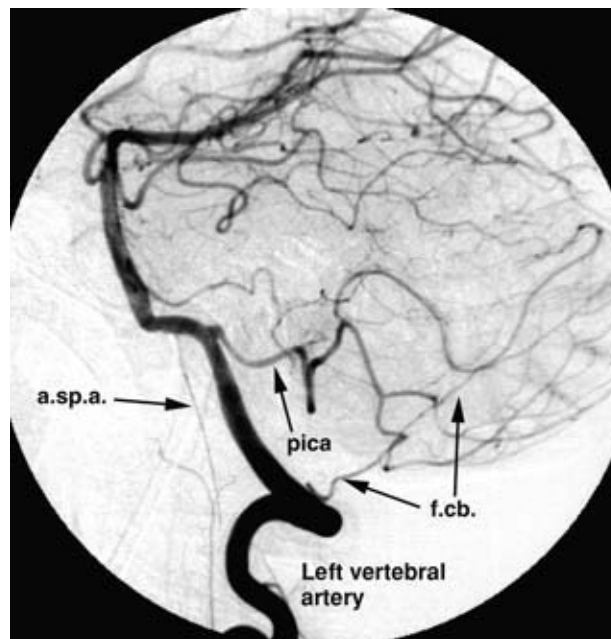


FIGURE 15-5. Anterior spinal artery and artery of the falx cerebelli. A lateral projection of the left vertebral artery demonstrates a well-visualized anterior spinal artery (*a.sp.a.*) directed inferiorly along the anterior surface of the medulla and spine. The left posterior inferior cerebellar artery (*pica*) has a relatively high origin off the intradural left vertebral artery. The artery of the falx cerebelli (*f.cb.*) arises from the extracranial vertebral artery. It courses diagonally toward the torcular deviating away from the inner table of the skull.

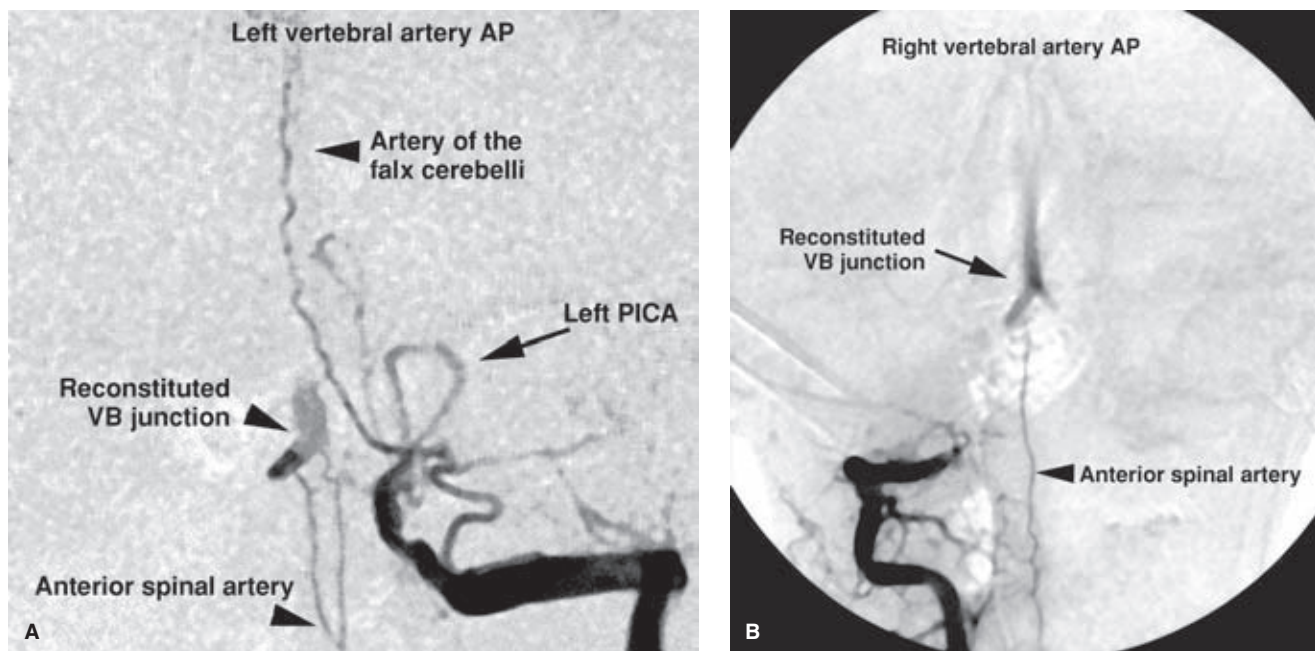


FIGURE 15-6. (A–B) Anterior spinal artery collateral flow to the basilar artery. PA views of the left vertebral artery (A) and right vertebral artery (B) in a patient with bilateral distal vertebral artery occlusions and ischemia of the basilar artery territory. The left vertebral artery is occluded distal to the origin of the left posterior inferior cerebellar artery. However, the artery of cervical enlargement lower in the neck opacifies the anterior spinal artery, which has collateralized the vertebrobasilar junction. The midline course of the artery of the falx cerebelli is well seen. The right vertebral artery (B) is occluded just proximal to the dural margin. The anterior spinal artery is seen again from this side flowing retrogradely to opacify the intracranial circulation.

small and difficult to see during angiography. Augmentation of the vascular territory of the lateral spinal artery can be seen in congenital diminutive variations of the suboccipital vertebral artery and of the posterior inferior cerebellar artery origin. This vessel usually runs caudally posterior to the dentate ligament and anterior to the posterior nerve roots of the upper four cervical levels. Below this point, it joins or is replaced by the posterior spinal artery.

► BASILAR ARTERY

From its formation at the pontomedullary junction to its division into the P1 segments of the posterior cerebral arteries, the basilar artery measures approximately 32 mm in length (range: 15–40 mm) with a normal adult diameter of approximately 4 mm (10,11) (Fig. 15-8). The basilar artery is sometimes narrowest at the level of the superior cerebellar arteries, which is a reflection of how this point represents the embryologic junction between the anterior and posterior circulations. The basilar artery frequently has a tortuous course, particularly in older patients or patients with hypertension, and demonstrates a curve away from the side of the dominant vertebral artery inflow. When inflow is balanced from each vertebral artery, the basilar artery can demonstrate slip-streamed laminar flow. This phenomenon sometimes causes appearances that raise concerns about whether vessel occlusion has occurred.

Brainstem Branches of the Basilar Artery

An average of 17 perforator branches arise from the basilar artery between the vertebrobasilar junction and the origins

of the superior cerebellar arteries (2). These fall into two patterns. Median branches enter the pons close to the midline in the median sulcus and penetrate to the floor of the IV ventricle. Short and long circumflex or transverse branches encircle the brainstem and eventually penetrate the surface more laterally (12). Anastomoses may occur within the brainstem between arteries of the same side but do not typically cross the midline. Although these perforator vessels are difficult to see at angiography, they nevertheless play a vital role as they supply the corticospinal and corticobulbar tracts, pontine nuclei, and the lemnisci, fasciculi, and motor nuclei of the midbrain and pons. Diminished perfusion of the reticular activating system is thought to explain the alterations in levels of consciousness seen in cerebral vasospasm, which affects the basilar artery after subarachnoid hemorrhage (13).

Basilar Artery Bifurcation

Approximately 10% to 18% of intracranial saccular aneurysms occur in the posterior circulation, of which more than half occur at the basilar bifurcation (14).

The perforator vessels in the region of the basilar artery bifurcation fall into two categories. The posterior aspect of the upper centimeter of the basilar artery frequently gives horizontally and posteriorly directed branches to the midbrain (Fig. 15-9). These form a complex arterial network or arcade in the interpeduncular fossa mingling with mesencephalic and thalamoperforator branches from the posterior and superior surfaces of the P1 segments (10,13). The distal centimeter of the basilar artery can have on average about eight perforating vessels, and the proximal P1 segment an

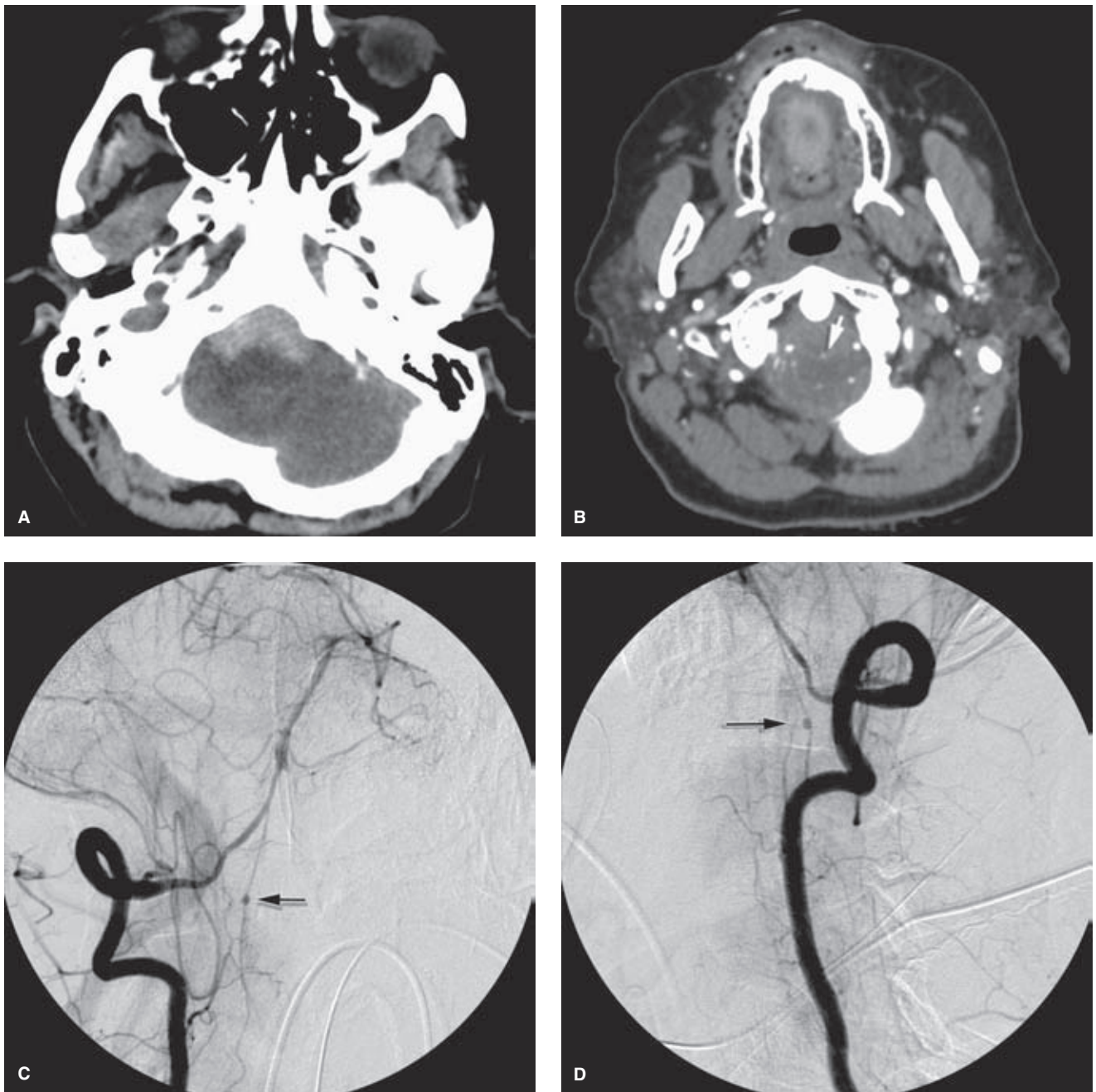


FIGURE 15-7. (A–D) You only see what you look for; you only look for what you know. Sometimes, it can be very difficult to recognize or even perceive things on an angiogram when you have never seen them before. One near miss was this example of an aneurysm of the anterior spinal artery. This patient presented with a distribution of blood on the CT (A) closely related to the foramen magnum, prompting concern about spinal pathology such as an AVM or spinal ependymoma. The CTA examination (B) was read as negative, but in retrospect a subtle enlargement of the size of the anterior spinal artery (*white arrow*) could be seen on a single slice. The right vertebral artery injection (C and D) showed spasm of the posterior circulation and an unusual aneurysm of the anterior spinal artery (*black arrow*). Notice that the angiographic images are centered lower than usual because of the suspicion of spinal pathology, but even at that the subtle finding was difficult to perceive at first because the eye was searching for findings of a more dramatic or familiar nature.

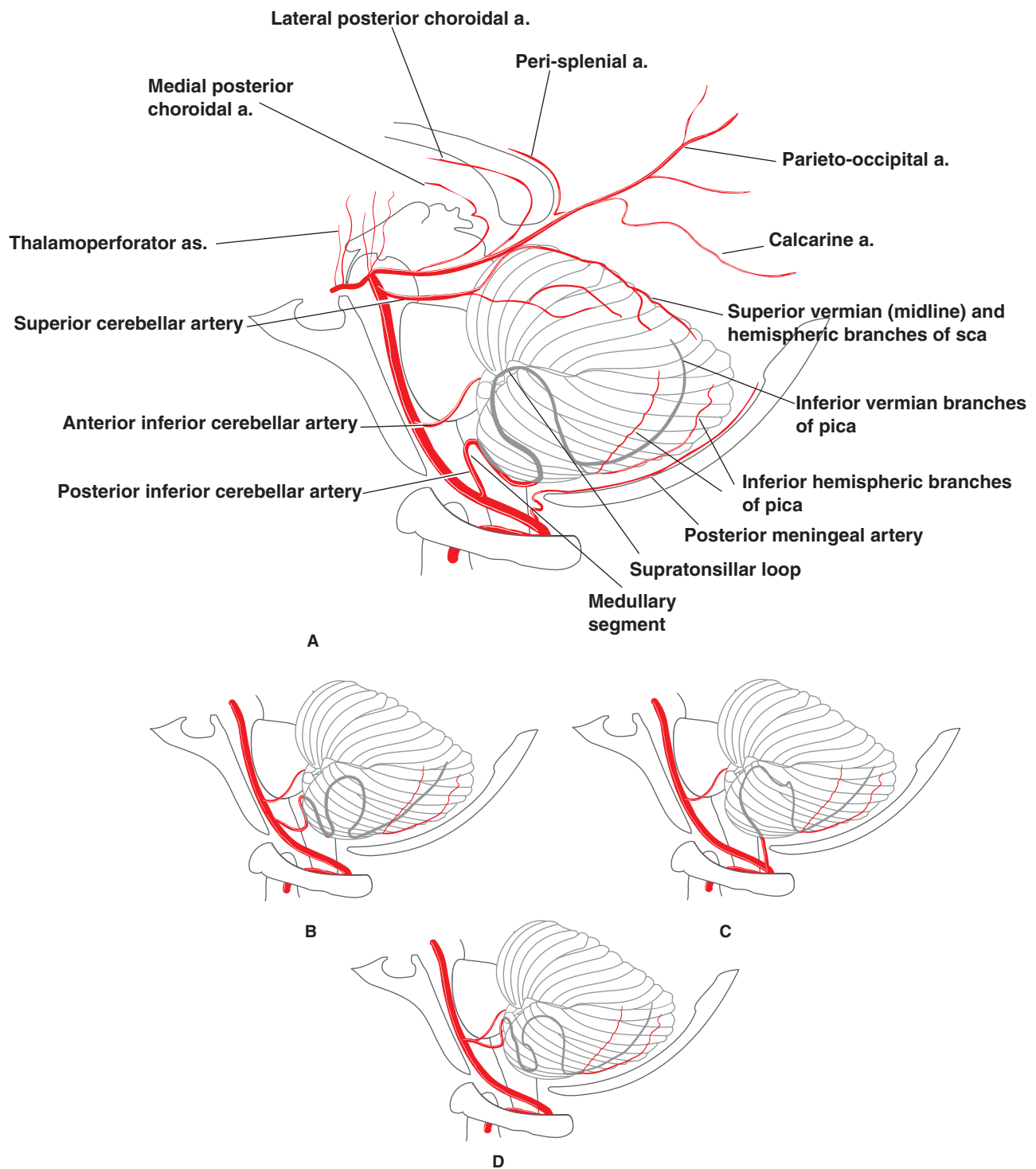


FIGURE 15-8. (A–D) Lateral projection of the posterior circulation. Variations of the posterior inferior cerebellar artery. The major angiographically identifiable vessels of the posterior fossa are illustrated (A). Variability in the course of the posterior inferior cerebellar artery leads to numerous appearances on the lateral projection (B–D). In all configurations, the posterior inferior cerebellar artery circumvents the medulla first and the cerebellar tonsil second, to perfuse finally the inferior cerebellar hemisphere and inferior vermis.



FIGURE 15-9. Basilar artery aneurysm and perforator vessels. A lateral view of a basilar artery tip aneurysm demonstrates separation of the dome of the aneurysm from the adjacent small vessels with unusual clarity. The reason for this is that the thalamoperforator arteries and circumflex branches (*arrows*) of the posterior cerebral artery are displaced away from the aneurysm by mass effect from unopacified circumferential thrombus within the aneurysm.

average of two to four. They measure 200 to 800 μm in diameter (15). The basilar artery tip itself and proximal 2 to 3 mm of the P1 segments are most often free of vessels, implying that aneurysms in this location can be treated without necessarily threatening an occlusion of the perforator branches. However, the microanatomy of these vessels is extremely complex as some of the perforator vessels often have origin from other posterior cerebral artery branches in this area, such as the medial posterior choroidal artery and collicular artery. Before perforating the peduncular wall or posterior perforated substance, some of the mesencephalic or thalamoperforator vessels in the interpeduncular fossa give supply to the mammillary bodies and the oculomotor nerves.

► ARTERIES OF THE CEREBELLUM

The cerebellum can be described as a three-surfaced organ lying behind the brainstem. The superior or tentorial surface is supplied predominantly by the superior cerebellar artery. The surface facing anteriorly against the anterior wall of the posterior cranial fossa is called the *petrosal surface* and is dominantly supplied by the anterior inferior cerebellar artery (Fig. 15-8). The inferiorly projecting or suboccipital surface has the most complex topography and is supplied by the posterior inferior cerebellar artery. All of the cerebellar arteries provide important perforating vessels to the brainstem along their early course. They demonstrate a high degree of variability in their origins, rates of absence or duplication, and in the extent of their territories (16).

Posterior Inferior Cerebellar Artery

The posterior inferior cerebellar artery is the most complex and variable of the cerebellar arteries. It supplies the lower medulla and the inferior aspects of the fourth ventricle, tonsils, vermis, and inferolateral cerebellar hemisphere. An infarction of the entire territory of the posterior inferior cerebellar artery is termed a *lateral medullary syndrome* or the *Wallenberg syndrome* (17–19). This includes ipsilateral trigeminal nerve sensory loss, ipsilateral sympathoplegic symptoms, ipsilateral bulbar and pharyngeal paresis, ipsilateral cerebellar symptoms, contralateral hemiplegia, and contralateral numbness to pain and temperature. More distal posterior inferior cerebellar artery infarctions involve only the cerebellar symptoms with sparing of the medullary tracts and nuclei.

The size of the territory of the posterior inferior cerebellar artery is in inverse proportion to that of the ipsilateral anterior inferior cerebellar artery, the larger of the two being referred to as “dominant” in the patois of angiographic interpretation. It is common for a dominant posterior inferior cerebellar artery to arise from the larger of the vertebral arteries with a small ipsilateral and a dominant contralateral anterior inferior cerebellar artery. When a posterior inferior cerebellar artery is absent, its territory is most often assumed by the caudal branch of the ipsilateral anterior inferior cerebellar artery discussed below, in which case the artery is colloquially termed an *aica-pica complex*. When the anterior inferior cerebellar artery is absent, its territory is taken over by the tonsillohemispheric branch of the ipsilateral posterior inferior cerebellar artery. An even more extensive distribution of the posterior inferior cerebellar artery is seen in approximately 14% of brains when the vermian

branches of the posterior inferior cerebellar artery cross the midline to establish a bilateral supply, which may include some of the contralateral hemisphere (20). The medullary segments of the posterior inferior cerebellar artery may also give rise to the anterior and lateral spinal arteries.

The posterior inferior cerebellar artery arises from the distal vertebral artery, at or above the level of the foramen magnum in more than 80% of brains, usually at or immediately below the level of the inferior olive. It may arise below that level as far caudally as C2. Rare origins from alternative sources, such as the occipital artery, ascending pharyngeal artery, or the internal carotid artery as a variant remnant of a persistent trigeminal artery can be seen (6,21,22). The posterior inferior cerebellar artery may be absent or hypoplastic unilaterally in 4% to 25%, and absent bilaterally in approximately 2% of cases (23–25). Rarely, it may be duplicated (26).

Meningeal Branches of the Posterior Inferior Cerebellar Artery

The posterior meningeal artery and artery of the falx cerebelli may arise from the vertebral artery, the posterior inferior cerebellar artery, or from another source such as the occipital artery. The artery of the falx cerebelli is distinguished by its near-midline course on the AP angiogram. On the lateral projection, its straight course along the falx cerebelli away from the inner table of the skull is like a taut bowstring.

The posterior meningeal artery has a more lateral location. Its curved course conforms in close apposition to the inner table.

Anterior Inferior Cerebellar Artery

The anterior inferior cerebellar artery arises from the proximal or middle third of the basilar artery. It courses laterally and inferiorly to embrace the belly of the pons. It runs

superior or inferior to the VI cranial nerve root and divides into a rostral (lateral) branch and a caudal (medial) branch. The artery of the internal auditory meatus usually arises from the proximal trunk or loop of the anterior inferior cerebellar artery and supplies the nerve roots of the internal auditory canal and the sensory structures of the inner ear. Less frequently, this artery may arise directly from the basilar artery distal to the origin of the anterior inferior cerebellar artery. The anterior inferior cerebellar artery and its branches may become displaced by or involved in supply to tumors of the posterior fossa, such as meningioma or vestibular schwannoma, or tumors that have invaded the posterior fossa—for example, glomus tumors, craniopharyngioma, chordoma. For this reason, angiographic evaluation of the posterior circulation in certain situations can be very helpful to confirm that intradural extension of a tumor has occurred, as represented by involvement of the anterior inferior cerebellar artery.

During chemotherapy infusions in the posterior circulation, the anterior inferior cerebellar artery is taken as an important landmark for microcatheter placement. The catheter infusion must be made above the origin of the anterior inferior cerebellar artery because of the vulnerability of the cochlear structures to injury by some chemotherapeutic agents resulting in permanent deafness.

Superior Cerebellar Artery

The superior cerebellar artery supplies the lower midbrain, upper pons, upper vermis, and superior aspects of the cerebellar hemispheres. It has a duplicated origin in 14% to 28% of cases (25,27–30) (Figs. 15-10 and 15-11). With a similar frequency, it may share a common ostium with the ipsilateral posterior cerebral artery. Less commonly, it arises from the P1 segment. The main trunk of the superior cerebellar artery runs in the perimesencephalic cistern

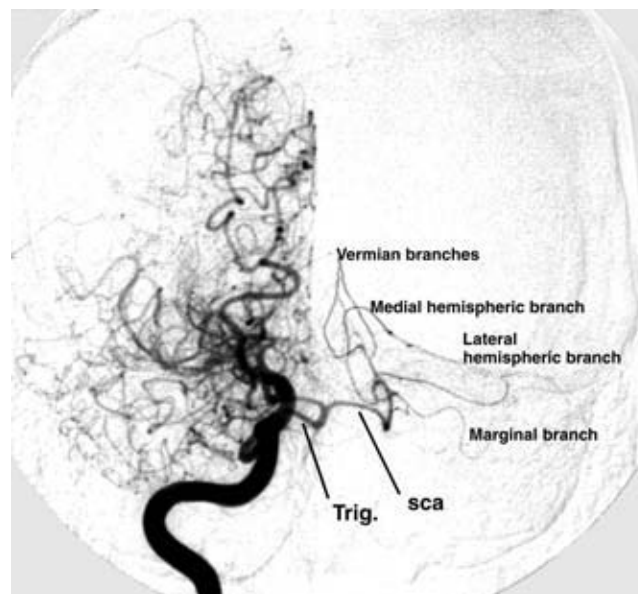


FIGURE 15-10. Moyamoya disease of the right hemisphere with a persistent trigeminal variant. A right internal carotid artery injection opacifies both superior cerebellar arteries (*sca*) via a persistent trigeminal artery (*Trig.*). The slope of the superior cerebellar surface is depicted by the superior vermian and hemispheric branches of the left superior cerebellar artery. A fetal posterior cerebral artery is present on the right side. The anterior and the middle cerebral artery flow have been supplanted by a moyamoya (“haze”) pattern of lenticulostriate and perforator collateral flow.

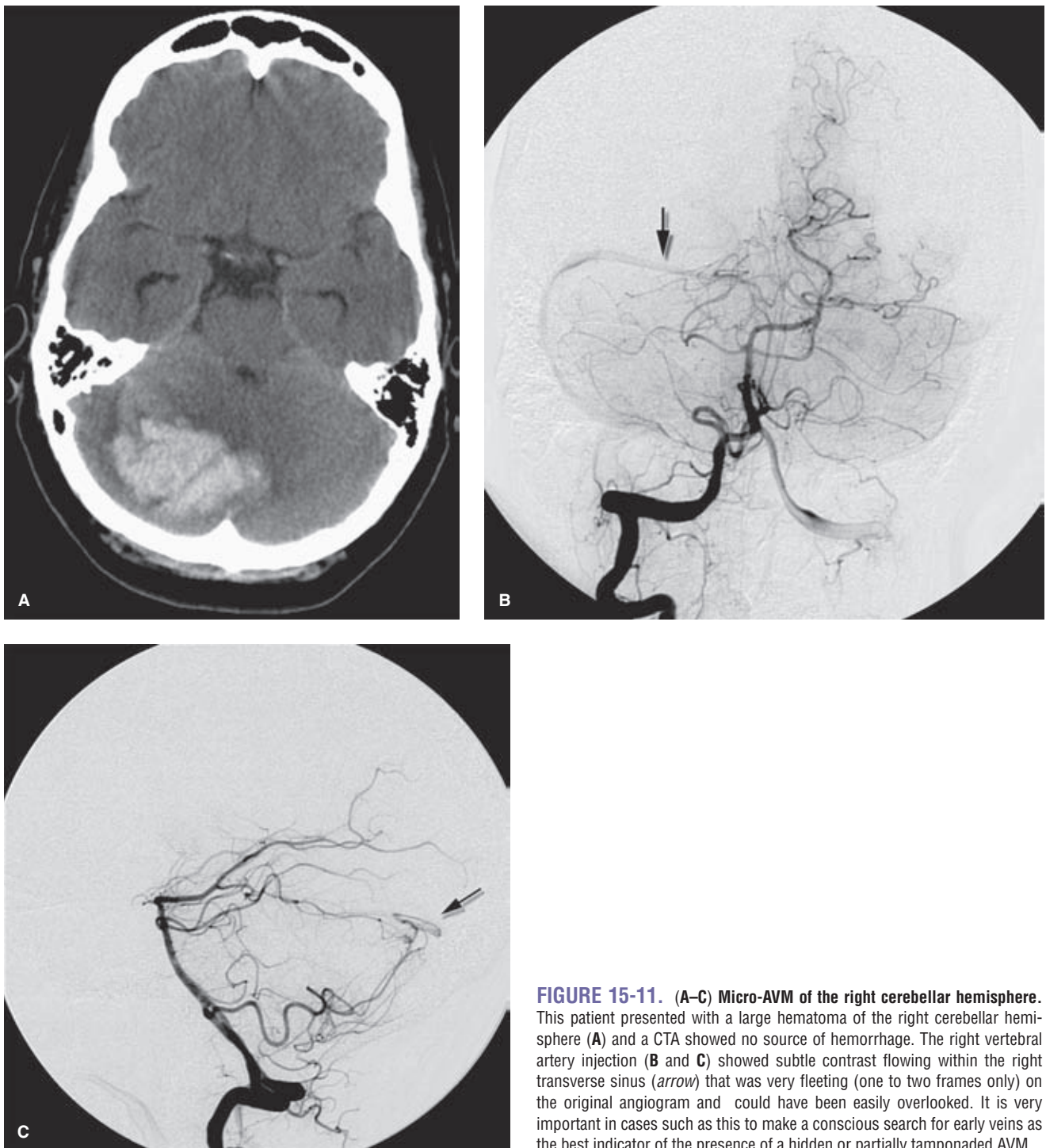


FIGURE 15-11. (A–C) Micro-AVM of the right cerebellar hemisphere. This patient presented with a large hematoma of the right cerebellar hemisphere (A) and a CTA showed no source of hemorrhage. The right vertebral artery injection (B and C) showed subtle contrast flowing within the right transverse sinus (arrow) that was very fleeting (one to two frames only) on the original angiogram and could have been easily overlooked. It is very important in cases such as this to make a conscious search for early veins as the best indicator of the presence of a hidden or partially tamponaded AVM.

above the trigeminal nerve at the pontomesencephalic junction. It is separated from the P1 segment of the posterior cerebral artery above by the oculomotor nerve medially and by the trochlear nerve more laterally. The trigeminal nerve roots come in contact with the superior cerebellar artery in approximately 50% of anatomical dissections or with the anterior inferior cerebellar artery in 8% (29). When neurovascular contact of a pronounced degree produces distortion of nerve roots in patients with tic douloureux, some

authors have advocated surgical decompression at the site of distortion (31).

The cortical cerebellar branches are described as marginal (lateral), hemispheric, and vermian (Fig. 15-12). Anastomoses between the superior vermian and hemispheric branches of the superior cerebellar artery and the inferior counterparts from the posterior inferior cerebellar artery are commonly seen. They constitute an important route of flow in situations of midbasilar occlusive disease.

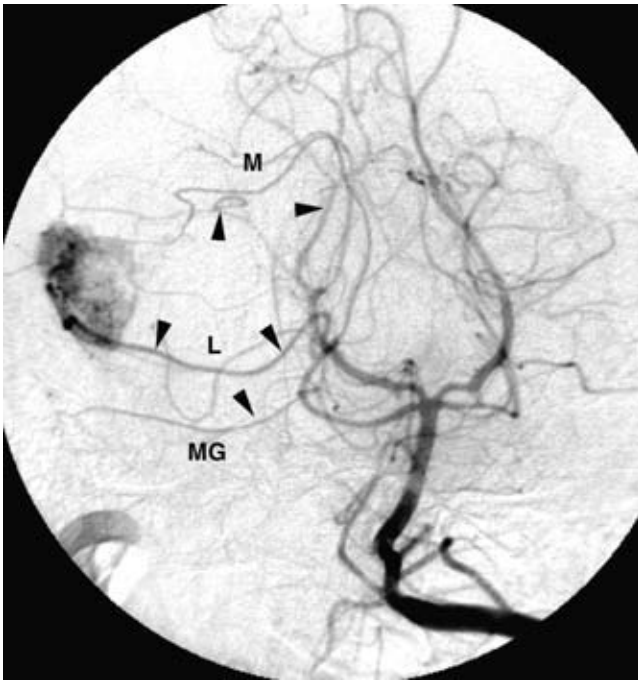


FIGURE 15-12. Hemangioblastoma of the right cerebellar hemisphere. A left vertebral artery injection in a patient with a hemangioblastoma. The vascular tumor nodule projects in the lateral aspect of the right cerebellar hemisphere. The tumor is supplied by medial hemispheric (*M*) and lateral hemispheric (*L*) branches of the right superior cerebellar artery. The presence of a large cystic component of the tumor can be deduced from the marked mass effect (*arrowheads*) on the surrounding hemispheric and marginal branches (*MG*) of the superior cerebellar artery.

References

- Caruso G, Vincentelli F, Giudicelli G, et al. Perforating branches of the basilar bifurcation. *J Neurosurg* 1990;73(2):259–265.
- Torche M, Mahmood A, Araujo R, et al. Microsurgical anatomy of the lower basilar artery. *Neurol Res* 1992;14(3):259–262.
- Akar ZC, Dujovny M, Slavin KV, et al. Microsurgical anatomy of the intracranial part of the vertebral artery. *Neurol Res* 1994;16(3):171–180.
- Wollschlaeger G, Wollschlaeger PB, Lucas FV, et al. Experience and result with postmortem cerebral angiography performed as routine procedure of the autopsy. *Am J Roentgenol Radium Ther Nucl Med* 1967;101(1):68–87.
- Mahmood A, Dujovny M, Torche M, et al. Microvascular anatomy of foramen caecum medullae oblongatae. *J Neurosurg* 1991;75(2):299–304.
- Ito J, Takeda N, Suzuki Y, et al. Anomalous origin of the anterior inferior cerebellar arteries from the internal carotid artery. *Neuroradiology* 1980;19(2):105–109.
- Lasjaunias P. *Craniofacial and Upper Cervical Arteries: Functional Clinical and Angiographic Aspects*. 1st ed. Baltimore: Williams and Wilkins; 1981.
- Lasjaunias P, Vallee B, Person H, et al. The lateral spinal artery of the upper cervical spinal cord. Anatomy, normal variations, and angiographic aspects. *J Neurosurg* 1985;63(2):235–241.
- Manabe H, Oda N, Ishii M, et al. The posterior inferior cerebellar artery originating from the internal carotid artery, associ-

- ated with multiple aneurysms. *Neuroradiology* 1991;33(6):513–515.
- Saeki N, Rhoton AL Jr. Microsurgical anatomy of the upper basilar artery and the posterior circle of Willis. *J Neurosurg* 1977;46(5):563–578.
- Shrontz C, Dujovny M, Ausman JI, et al. Surgical anatomy of the arteries of the posterior fossa. *J Neurosurg* 1986;65(4):540–544.
- Hassler O. Arterial pattern of human brainstem. Normal appearance and deformation in expanding supratentorial conditions. *Neurology* 1967;17(4):368–375 passim.
- Pedroza A, Dujovny M, Ausman JI, et al. Microvascular anatomy of the interpeduncular fossa. *J Neurosurg* 1986;64(3):484–493.
- Schievink WI, Wijdicks EF, Piepgras DG, et al. The poor prognosis of ruptured intracranial aneurysms of the posterior circulation. *J Neurosurg* 1995;82(5):791–795.
- Marinkovic S, Milisavljevic M, Kovacevic M. Interpeduncular perforating branches of the posterior cerebral artery. Microsurgical anatomy of their extracerebral and intracerebral segments. *Surg Neurol* 1986;26(4):349–359.
- Rodriguez-Hernandez A, Rhoton AL Jr, Lawton MT. Segmental anatomy of cerebellar arteries: A proposed nomenclature. Laboratory investigation. *J Neurosurg* 2011;115(2):387–397.
- Senator H. Apoplektische bulbärparalyse mit wechselständiger empfindungslähmung. *Arch f Psychiatri* 1881;11:713.
- Wallenberg A. Acute bulbar affections. Embolie der art. cerebellar post. inf. sinistra. *Arch f Psychiatri* 1895;27:504.
- Merritt H, Finland M. Vascular lesions of the hind-brain (lateral medullary syndrome). *Brain* 1930;53:290–305.
- Fujii K, Lenkey C, Rhoton AL Jr. Microsurgical anatomy of the choroidal arteries. Fourth ventricle and cerebellopontine angles. *J Neurosurg* 1980;52(4):504–524.
- Ahuja A, Graves VB, Crosby DL, et al. Anomalous origin of the posterior inferior cerebellar artery from the internal carotid artery. *AJNR Am J Neuroradiol* 1992;13(6):1625–1626.
- Ogawa T, Fujita H, Inugami A, et al. Anomalous origin of the posterior inferior cerebellar artery from the posterior meningeal artery. *AJNR Am J Neuroradiol* 1991;12(1):186.
- Fujii K, Lenkey C, Rhoton AL Jr. Microsurgical anatomy of the choroidal arteries: Lateral and third ventricles. *J Neurosurg* 1980;52(2):165–188.
- Margolis MT, Newton TH. The posterior inferior cerebellar artery. In: Newton TH, Potts DG, eds. *Radiology of the Skull and Brain*. Vol. II. St. Louis: C.V. Mosby; 1974:1710–1774.
- Salamon G, Huang YP. *Radiologic Anatomy of the Brain*. Berlin: Springer-Verlag; 1976.
- Lister JR, Rhoton AL Jr, Matsushima T, et al. Microsurgical anatomy of the posterior inferior cerebellar artery. *Neurosurgery* 1982;10(2):170–199.
- Mani RL, Newton TH, Glickman MG. The superior cerebellar artery: An anatomic–roentgenographic correlation. *Radiology* 1968;91(6):1102–1108.
- Huang YP, Wolf BS. Angiographic features of fourth ventricle tumors with special reference to the posterior inferior cerebellar artery. *Am J Roentgenol Radium Ther Nucl Med* 1969;107(3):543–564.
- Hardy DG, Peace DA, Rhoton AL Jr. Microsurgical anatomy of the superior cerebellar artery. *Neurosurgery* 1980;6(1):10–28.
- Hardy DG, Rhoton AL Jr. Microsurgical relationships of the superior cerebellar artery and the trigeminal nerve. *J Neurosurg* 1978;49(5):669–678.
- Jannetta PJ. Arterial compression of the trigeminal nerve at the pons in patients with trigeminal neuralgia. *J Neurosurg* 1967;26(1):Suppl:159–162.

The Venous System

Key Points

- Venous anatomy can vary a great deal meaning that the clinical impact of venous pathology or excessive venous flow can be very variable from one patient to another.
- Many of the venous connections between the petrosal sinuses and the pial veins have an arcane nomenclature, but these connections are very important in the genesis of venous complications from remote arteriovenous fistulae.

The venous system of the intracranial and extracranial structures of the neck and head is most easily described in separate spaces or compartments. However, it is important to understand the remarkable potential of these layers to communicate. The variable pattern of free communication through certain channels, in combination with selective flow restriction through others, forms the basis for the pathophysiology of some vascular diseases of the brain and its coverings. A small shunt or fistula in a certain setting can have a catastrophic clinical effect on one patient; another patient with a large shunt in the same location may be asymptomatic and may even be best left untreated.

► EXTRACRANIAL VEINS

The scalp and face are highly vascular structures with a rich network of large veins throughout. The superficial temporal vein corresponds with the artery of the same name and runs down anterior to the ear to the posterior aspect of the parotid gland (Figs. 16-1 and 16-2). Here, it usually joins with the internal maxillary vein to form the retromandibular vein. The retromandibular vein joins the internal jugular vein. The anterior facial vein may also join the retromandibular vein or may empty directly into the internal jugular vein. The angular vein is formed at the junction of the frontal and supraorbital veins and forms an important anastomosis posteriorly with the superior ophthalmic vein. Although it usually drains inferiorly into the facial vein, it can drain into the cavernous sinus if flow is reversed and can become a conduit for propagation of infection or thrombosis. The occipital vein drains inferiorly into the deep cervical or vertebral veins. It may connect with the posterior auricular vein, and then to the external jugular vein.

The intracranial and extracranial venous systems communicate via emissary veins through skull foramina. Important emissary veins connect the superior sagittal sinus and transverse sinus with the suboccipital veins. The pterygoid plexus lies outside the skull base but has a number of important connections with the cavernous sinus via the foramina of the middle cranial fossa, notably the foramen of Vesalius, the foramen ovale, and other foramina innominata (Figs. 16-3 and 16-4). The pterygoid plexus usually drains to the facial vein. It may also connect superiorly into the orbit via the inferior orbital fissure through which it drains part of the inferior ophthalmic vein.

The internal jugular vein runs inferiorly in a position lateral to the internal carotid artery. The internal jugular vein receives input from the inferior petrosal sinus, the facial vein, the lingual vein, the pharyngeal veins, and the thyroidal veins. In the thoracic inlet, it joins with the subclavian vein to form the brachiocephalic vein.

The external jugular vein receives venous outflow from the scalp, occipital region of the neck, and part of the face. It forms in the parotid gland and runs inferiorly superficial to the sternocleidomastoid muscle.

The vertebral vein forms at the level of atlas and runs as a plexus in the foramina transversaria surrounding the vertebral artery. A single outlet vein runs inferiorly and then joins the brachiocephalic vein.

► MENINGEAL VEINS

Meningeal veins accompany their respective meningeal arteries. The anterior meningeal vein joins the superficial Sylvian vein to form the sphenoparietal sinus. The sphenoparietal sinus then passes below the lesser wing of the sphenoid bone to join the cavernous sinus. Alternatively, it may course posteriorly in the middle cranial fossa to join the lateral sinus.

► DURAL SINUSES

The dural sinuses are venous channels enclosed between two layers of dura. They do not have valves.

The superior sagittal sinus extends from the foramen cecum to the torcular herophili (Fig. 16-2). Occasionally, the superior sagittal sinus may bifurcate above the internal occipital protuberance. The superior sagittal sinus drains the superficial cerebral veins from the lateral and medial surfaces of the cerebral hemispheres. The largest such

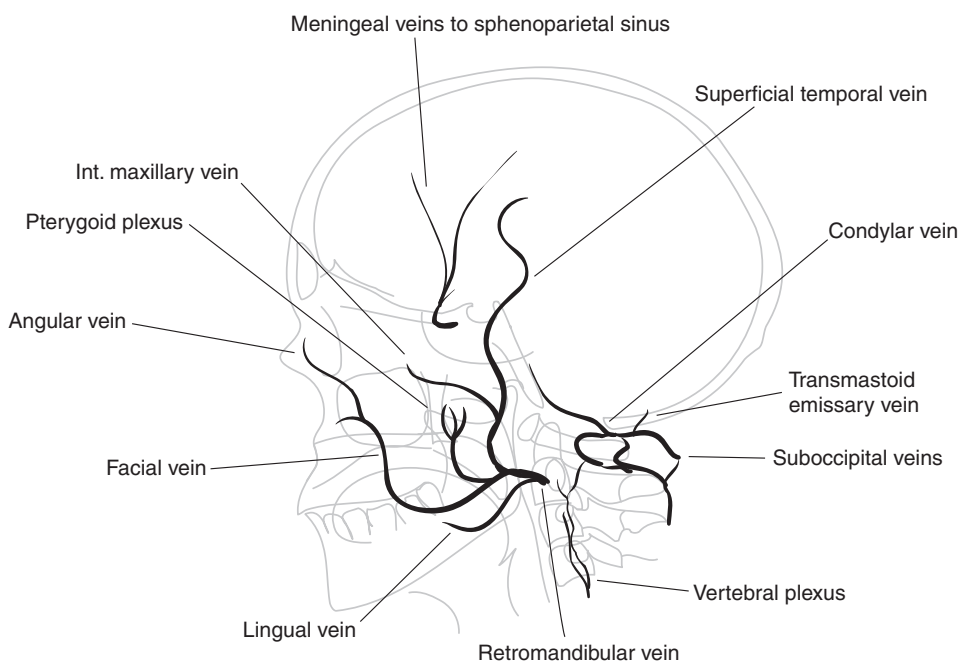


FIGURE 16-1. Superficial extracranial and middle meningeal veins.

named vein is the vein of Trolard. Venous lacunae along the course of the superior sagittal sinus contain arachnoid granulations, which become more prominent with age. They may form filling defects within the sinus itself. Veins entering the superior sagittal sinus often appear constrained at the point of entry, giving a false appearance of venous stenosis.

The torcular herophili, named for its similarity to the handle of a manually operated winepress (1), is the confluence of the superior sagittal sinus, the straight sinus, and the occipital sinus. It drains into the two transverse sinuses. The drainage is usually bilateral. If unilateral or asymmetric, the right transverse sinus is usually larger (2).

The inferior sagittal sinus lies along the inferior edge of the falx cerebri. It drains the anterior part of the corpus callosum, the medial portions of the cerebral hemispheres, and the falx. It joins with the internal cerebral vein to form the vein of Galen.

The straight sinus extends posteriorly from the junction between the falx cerebri and the tentorium, where it collects the vein of Galen and related tributaries. It drains to the torcular posteriorly.

The occipital sinus is inconstantly seen (Figs. 16-2B and 16-5). It usually drains upward to the torcular. It may flow inferiorly and bevel laterally to join the sigmoid sinus or connect with a sinus around the foramen magnum, termed the *marginal sinus*. The occipital and marginal sinuses are most commonly seen in young children. They diminish in size with age.

The transverse (lateral) sinuses curve laterally in the perimeter of the tentorium until they turn inferiorly to form the sigmoid sinuses. The transverse sinus receives a number of important supratentorial veins from the temporal and occipital lobes, notably the vein of Labbé. Infratentorial veins also drain to the transverse sinus, and it also receives the drainage of the superior petrosal sinus.

The sigmoid sinus represents the anterior, medial, and inferior continuation of the transverse sinus. It becomes the

internal jugular vein in the jugular fossa and may receive direct venous channels from the pons and medulla. It communicates with the scalp veins via the mastoid and condylar veins.

The superior petrosal sinus runs from the posterior aspect of the cavernous sinus along the petrosal ridge to the junction of the sigmoid and transverse sinuses within the basal attachment of the tentorium. It receives venous channels from the supratentorial and infratentorial compartments and from the tympanic structures. It may lie either adjacent to or surround the roots of the trigeminal nerve.

The inferior petrosal sinus runs inferiorly and laterally from the posterior part of the cavernous sinus to join the jugular vein in the pars nervosa, which it shares with the glossopharyngeal nerve. The inferior petrosal sinus may receive channels from the medulla, cerebellum, and internal auditory veins.

The sphenoparietal sinus drains the superficial Sylvian vein into the cavernous sinus along the lesser wing of sphenoid behind the orbit. It receives variable contributions from meningeal, orbital, medial anterior temporal (uncal), and inferior frontal veins. Less commonly, this venous system may not reach the cavernous sinus. Alternatively, it can turn posteriorly in a sinus, most commonly referred to as the sphenopetrosal sinus (3), running along the floor of the middle cranial fossa to drain along the tentorium and into the superior petrosal sinus. An alternative variant drains into the pterygoid plexus and bypasses the cavernous sinus.

The cavernous sinus represents the most important site of confluence of intracranial and extracranial venous structures. Variations in the configuration of the outlets from the cavernous sinus are of little significance in the normal state. However, in the setting of pathologically increased blood flow through the sinus, the varied nature of the resulting clinical conditions is determined by the restrictions on venous outflow from the cavernous sinus.

Orbital venous drainage is via the superior and inferior ophthalmic veins, normally in an anterior to posterior direction.

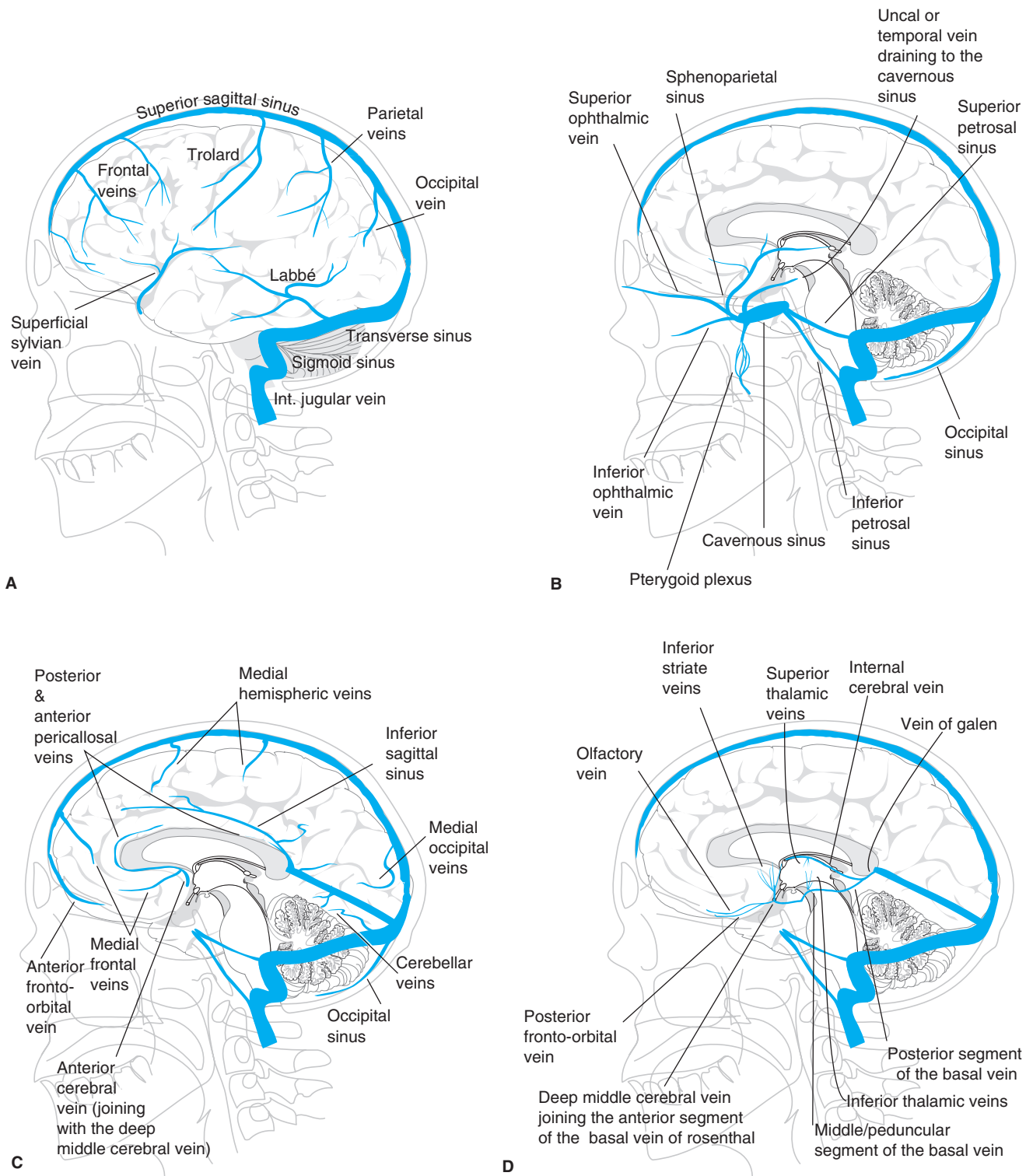


FIGURE 16-2. (A–D) Intracranial dural sinuses and veins. A: Superficial cortical veins of the left hemisphere are illustrated. A balanced arrangement of the superficial Sylvian vein, vein of Trolard, and vein of Labbé is depicted. **B:** The left hemisphere has been removed from the illustration. The left superficial Sylvian vein is still in place (from **A**) to illustrate its relationship to the cavernous sinus. An understanding of the variability of the connections to and from the cavernous sinus is important to explain the clinical and angiographic consequences of arteriovenous shunting in this structure. The most common connection of clinical consequence is to the superior ophthalmic vein. A sinister possibility is the presence of connections from the cavernous sinus to the basal vein. Venous hypertension transmitted through this route accounts for the most serious complications of such disorders. **C:** Superficial veins close to the midline are illustrated. The anterior pericallosal vein becomes the anterior cerebral vein. This vein may communicate across the midline via the anterior communicating vein. The anterior cerebral vein usually joins the anterior segment of the basal vein. **D:** The major components of the deep venous system are illustrated. (continued)

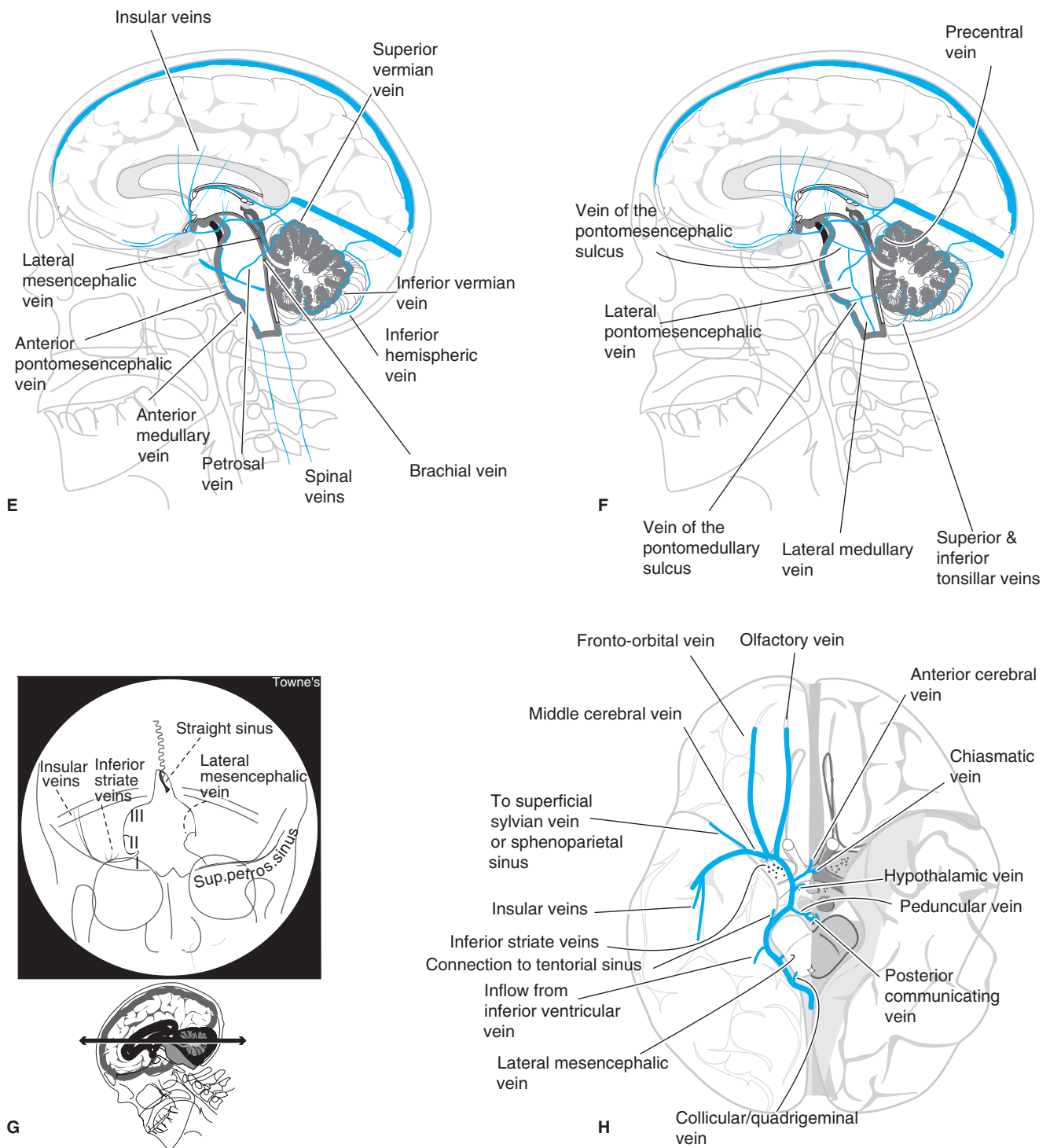


FIGURE 16-2. (CONTINUED) E-H: The insular veins, which are defining tributaries of the middle cerebral vein, usually superimpose on the inferior striate veins and are illustrated in **(E)** and **(H)**. The internal cerebral vein runs in the velum interpositum; it should therefore be superimposed on the course of the medial posterior choroidal artery from the arterial phase of the posterior circulation. **E** and **F:** The insular veins are demonstrated without the underlying inferior striate veins. The major anastomotic vessels of the posterior fossa are illustrated. **G:** A schematic illustration of the shape of the basal vein and middle cerebral vein as seen on a Townes projection. The segments of the basal vein are numbered I, II, and III. The lateral mesencephalic vein slopes medially along the surface of the midbrain. Therefore, it usually has a characteristically medial course relative to the basal vein, demonstrated on the anatomic left side here. It drains to the superior petrosal sinus via the petrosal vein. **H:** A base view of the brain demonstrates the complete territory of the basal vein. In reality, it is common for the basal vein to be a fragmented structure with preferential drainage through alternative pathways other than the vein of Galen. (*continued*)

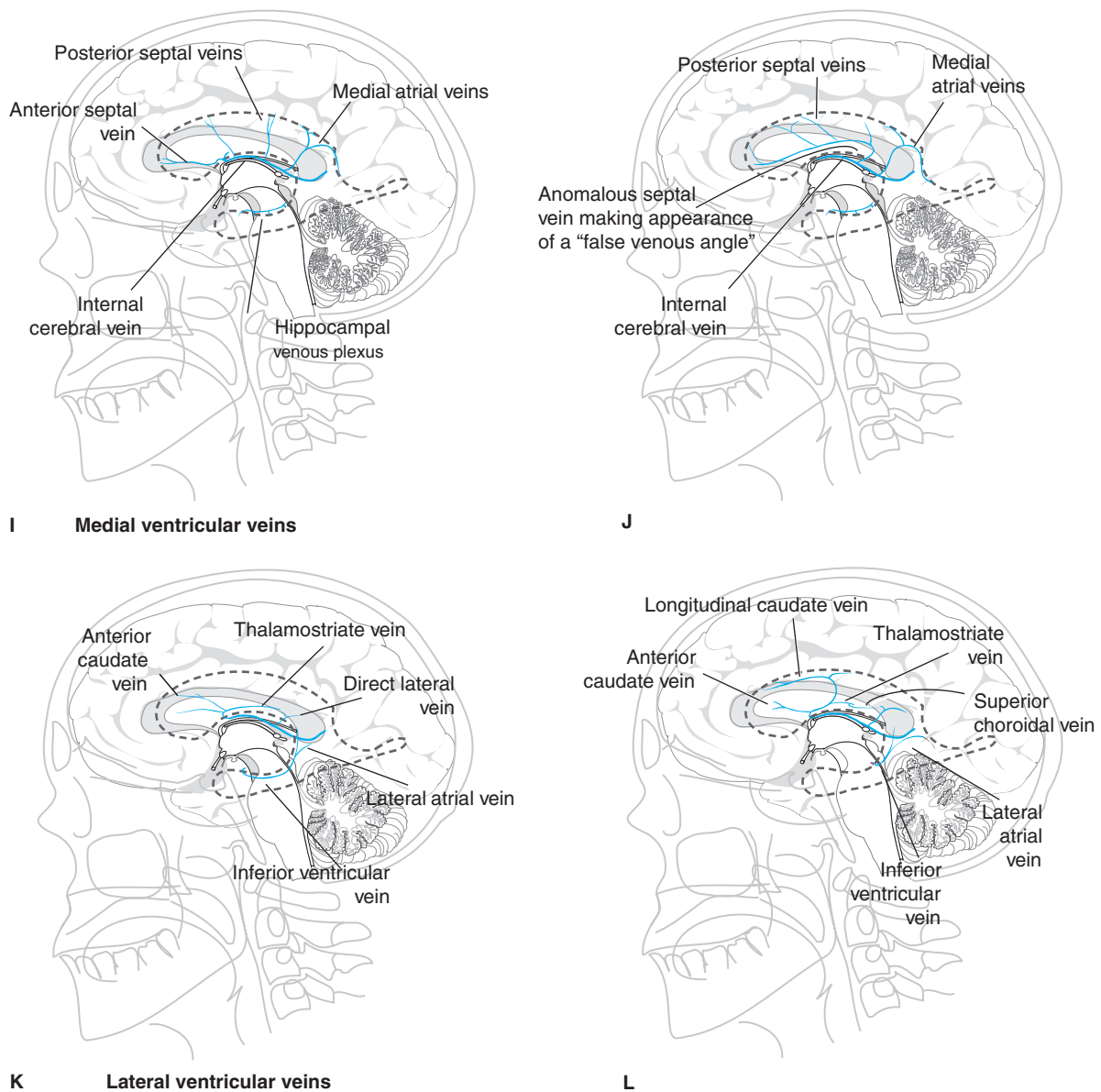


FIGURE 16-2. (CONTINUED) I–L: I, J: The outline of the lateral ventricle is depicted by the dotted line. The medial ventricular veins are demonstrated in lateral appearance. It is rare to identify the hippocampal veins unless there is a high flow state such as might be related to the presence of an AVM. The inferior ventricular vein runs in the roof of the temporal horn and connects with the veins on the lateral wall of the atrium. **K and L:** The lateral ventricular veins of the deep system are illustrated in lateral projection.

There are important variable anastomoses anteriorly with angular branches of the facial vein and frontal veins. The superior ophthalmic vein communicates posteriorly with the cavernous sinus and occasionally with the sphenoparietal sinus. The inferior ophthalmic vein also connects anteriorly with the facial vein and drains posteriorly to the cavernous sinus separate from or after joining the superior ophthalmic vein. It also connects inferiorly via the inferior orbital fissure with the pterygoid plexus.

The cavernous sinuses are multicompartmental extradural spaces that lie on either side of the sella on the surfaces of the greater wing of the sphenoid bone. They are interconnected by the anterior and posterior coronary (intercav-

ernous) sinuses under the diaphragm sellae and by variable sinuses on the clivus (Fig. 16-3). Anteriorly, they accept venous drainage from the ophthalmic veins and the sphenoparietal sinus. Posteriorly, they can accept parenchymal draining channels from the temporal lobe, particularly the uncal vein or middle cerebral vein. They also receive flow from the hypophyseal veins.

Outflow from the cavernous sinuses is mainly posteriorly to the petrosal sinuses. There are also draining connections to the pterygoid plexi through the foramina of the middle cranial fossa. The superior petrosal sinus and inferior ophthalmic vein may be either afferent to or efferent from the cavernous sinus.

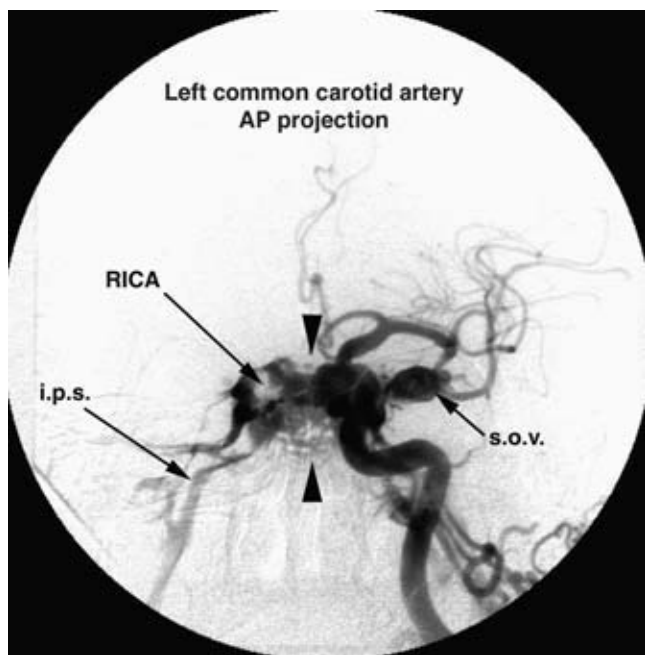


FIGURE 16-3. Intercavernous venous connections in a dural AVM of the left cavernous sinus. A left common carotid artery injection opacifies a multitude of venous structures in the region of the left cavernous sinus through involved branches of the external carotid artery. Prominent intercavernous connections through the sella and along the clivus connect across the midline (*arrowheads*) to opacify the right cavernous sinus. Within the latter, lucency is preserved by the course of the unopacified right internal carotid artery (*RICA*). Prompt drainage to the right inferior petrosal sinus (*i.p.s.*) is seen. On the left side, the superior ophthalmic vein (*s.o.v.*) is massively dilated. It projects foreshortened along the plane of viewing.

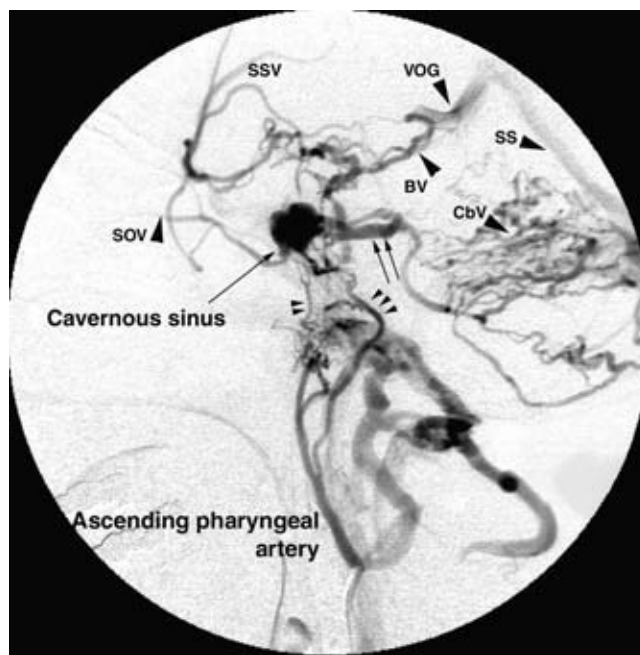


FIGURE 16-4. Venous hypertension due to restricted outflow from the cavernous sinus. Unlike the patient in Figure 16-3, this patient with the same diagnosis, dural AVM of the cavernous sinus, does not have ready outflow from the cavernous sinus to the contralateral side or to the superior ophthalmic vein. At least, this is the case for the involved compartment of the cavernous sinus. This injection is made into the ascending pharyngeal artery in the lateral projection. There is early opacification of the cavernous sinus via the carotid branch of the pharyngeal trunk (*double arrowhead*) and clival branches (*triple arrowhead*) from the neuromeningeal trunk. The superior ophthalmic vein (*SOV*) is small. The cavernous sinus decompresses itself via the basal vein (*BV*) with connections to the Sylvian veins (*SSV*), the vein of Galen (*VOG*), and the straight sinus (*SS*). There is prominent opacification of cerebellar veins (*CbV*) in the posterior fossa. This is because of drainage from the cavernous sinus via the superior petrosal sinus (*double arrow*). The patient's symptoms were related to venous hypertension of the posterior fossa.

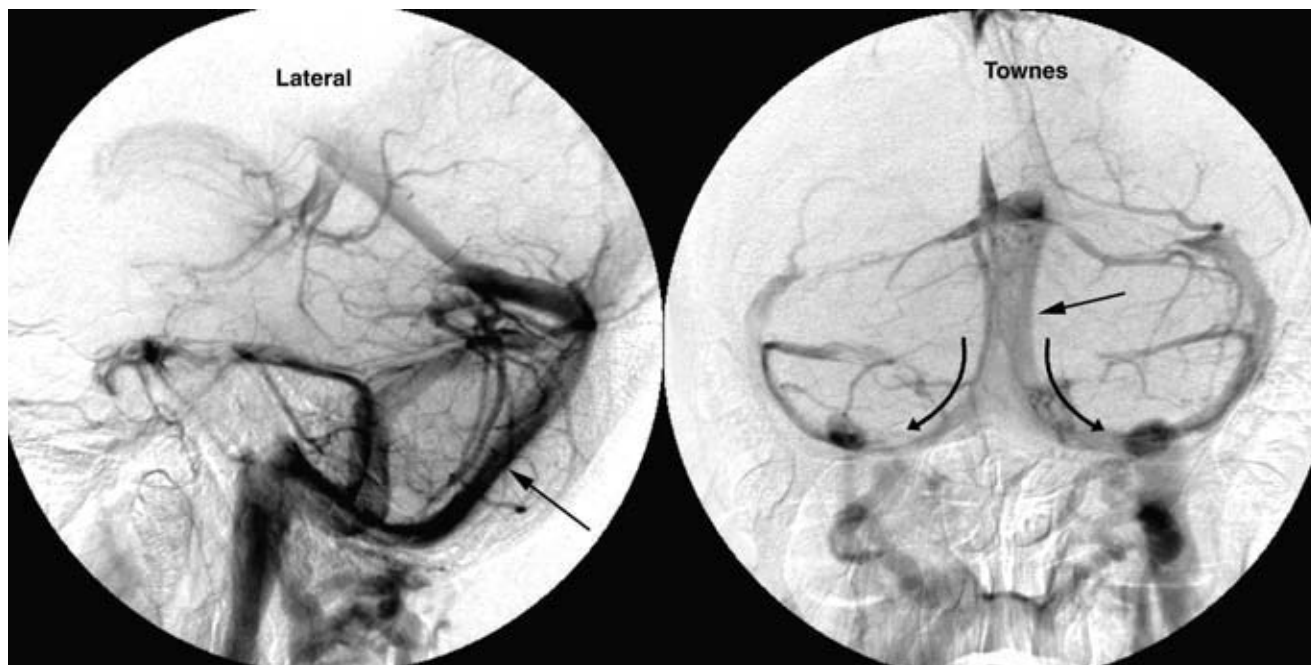


FIGURE 16-5. Prominent occipital sinus. An incidental observation of a large occipital sinus in an adult patient. The occipital sinus (*arrows*) descends along the falx cerebelli and divides into the marginal sinus around the foramen magnum joining the jugular foramen on each side. The transverse sinuses are correspondingly hypoplastic.

► SUPRATENTORIAL INTRADURAL VENOUS SYSTEM

The venous drainage pattern of the supratentorial structures is described as having a superficial system and a deep system. This is a useful division, but there are some superficial areas of cortex that drain via veins of the deep system. In the setting of anomalous or pathologic venous flow, the distinction between the two systems becomes blurred. Nevertheless, where surgery is planned, it is important to be able to recognize the major veins and sinuses present and to describe their direction of flow. Sacrificing major cortical veins or subdural bridging veins carries some risk of venous infarction and is therefore kept to a minimum during surgery (Fig. 16-6).

Superficial Supratentorial Cortical Veins

The superficial veins lie on the surface of the cerebral cortex. On the basal surface of the brain, many of the surface veins drain to the basal vein of Rosenthal and are considered part of the deep drainage system (Fig. 16-2). The superficial veins of the cerebral convexities drain to four major destinations or groups of bridging veins (4):

1. Superior sagittal sinus
2. Sphenoparietal sinus and cavernous sinus
3. Inferior sagittal sinus and vein of Galen
4. Tributaries of the sinuses related to the tentorium cerebelli

The superficial surface veins of the cerebral hemispheres drain the outer 1 to 2 cm of cortex and white matter. They have no muscle layers or valves. As they approach their sinus of destination, they assume a fibrous layer. When seen from a particular angle, they may give an appearance of constriction or pseudostenosis at the point of piercing the dura. Bridging veins of varying length may assume a tortuous course in the subdural space. They frequently fuse with meningeal veins to form common conduits before joining a major sinus.

Medial Hemispheric Superficial Veins

Anteriorly and superiorly in the frontal and parietal areas, superficial veins named for their respective sulci are directed

superiorly and anteriorly toward the superior sagittal sinus. The superficial medial veins curve around the superior rim of the hemispheres and join with the superficial veins from the convexities to form common subarachnoid veins, which then pierce the dura (5). Collecting veins may run for variable distances in the subdural space. They may run within the falx itself, particularly posteriorly.

Not all the venous drainage from the medial aspect of the hemispheres enters the superficial system. Veins from the anterior cingulate gyrus and paraterminal gyrus are collected toward the anterior pericallosal vein, the paraterminal vein, and the anterior cerebral vein, which become tributaries of the basal vein. More posteriorly, veins from the central frontal and parietal lobes drain to the inferior sagittal sinus and posterior pericallosal vein, both of which join the vein of Galen. In the occipital lobe, peripherally disposed veins drain centrifugally toward the superior sagittal sinus, while more central veins drain to the straight sinus, to the vein of Galen, or to lesser tentorial sinuses.

Convexity Hemispheric Veins

Veins of the lateral hemispheric convexities drain via three major routes.

1. Veins adjacent to the Sylvian fissure collect into a common channel, the superficial Sylvian vein, which usually drains along the lesser sphenoid wing as the sphenoparietal sinus. The sphenoparietal sinus most often drains to the anterior part of the cavernous sinus.
2. Superiorly directed veins, up to 14 in number per hemisphere (6), empty into the superior sagittal sinus. The largest of these veins usually has an anastomosis with the Sylvian system and is called the *anastomotic vein of Trolard* (Fig. 16-7).
3. Inferiorly disposed veins are directed toward the transverse sinus and other smaller dural sinuses of the middle cranial fossa. The largest of these, again with anastomosis to the Sylvian system, is termed the *anastomotic vein of Labbé*.

Of the three major anastomotic veins—the vein of Labbé, the vein of Trolard, and the superficial Sylvian vein—usually only one or two are present to a substantial degree. The vein of Labbé is most frequently prominent in the dominant hemisphere, and the vein of Trolard is so in the

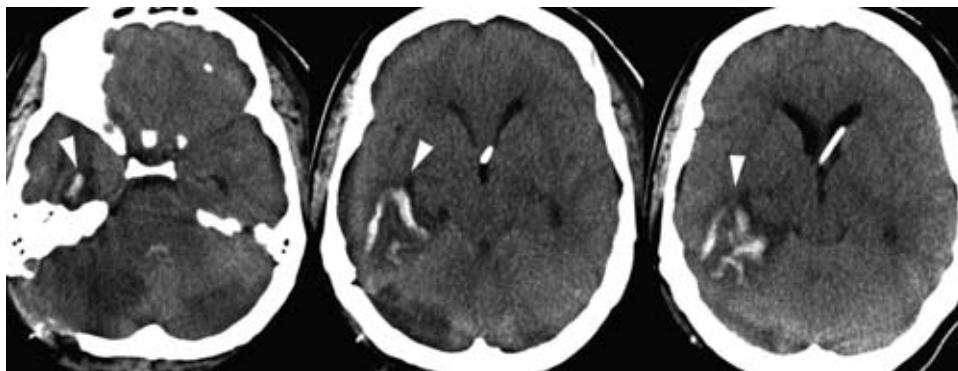


FIGURE 16-6. Venous infarction after surgery. An infratentorial surgical approach to a ruptured aneurysm in the posterior fossa was complicated by presumed occlusion of the right transverse sinus. Hypodensity of the infratentorial tissues may represent effects of retraction during surgery. However, a supratentorial hemorrhagic infarct is seen with a serpentine density representing a thrombosed vein and/or hemorrhage (*white arrowheads*). The findings probably relate to compromise of the right vein of Labbé.

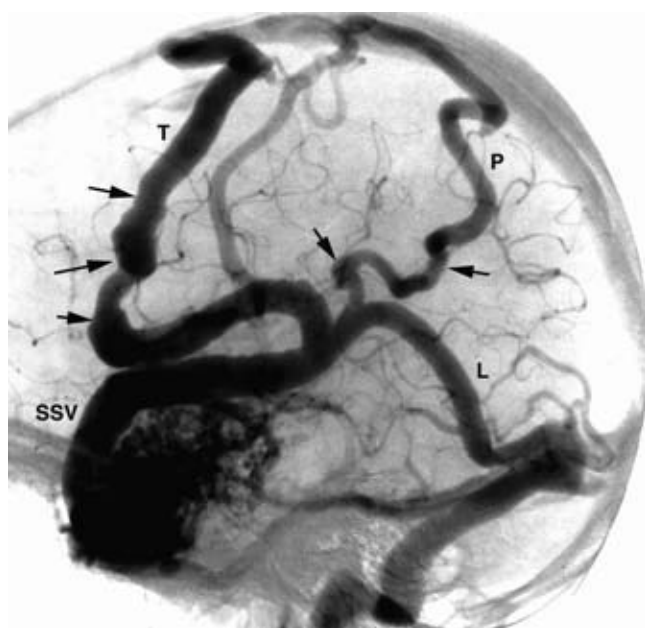


FIGURE 16-7. Superficial anastomotic veins. A brain AVM of the left temporal lobe drains predominantly through superficial convexity veins. The superficial Sylvian vein (SSV) drains retrogradely from the AVM to the superiorly directed vein of Trolard (*T*), a lesser parietal convexity vein (*P*), and an anastomotic vein of Labbé (*L*). The observation that venous outflow from this AVM is through a single channel (SSV) is concerning because this has some correlation with the risk of hemorrhage. Furthermore, the vein of Trolard (*T*) and parietal vein (*P*) demonstrate signs of early stenotic change or venous aneurysm formation (*arrows*).

nondominant hemisphere (7). The superficial Sylvian vein is relatively constant in its location lying along the length of the superficial aspect of the Sylvian fissure. The vein of Trolard, by definition the largest anastomotic channel connecting the superficial Sylvian vein with the superior sagittal sinus, most commonly corresponds with the level of the postcentral sulcus. It can be represented as far forward as the anterior frontal convexity veins or as far posteriorly as the anterior parietal veins. It may be duplicated. The vein of Labbé is defined as the largest channel crossing the temporal lobe convexity from the superficial Sylvian vein to the transverse sinus. It usually crosses the middle third of the temporal lobe but can be inconstant in location or duplicated.

The superficial hemispheric veins of the convexities are frequently described as making an acute angle against the direction of flow as they address the sinus. This appearance is most prevalent posteriorly and is thought by Padget (2) to be a mechanical stretching of the superficial veins away from their site of dural drainage by expansion of the cerebral hemisphere during forebrain development, resulting in a pattern of insertion by the veins into the superior sagittal sinus altering from anterior to posterior (5). Anterior veins have a superolateral insertion site; posterior veins approach the superior sagittal sinus inferiorly along or within the falx cerebri.

► BASAL HEMISPHERIC SUPERFICIAL VEINS

Veins from the basal or inferior surface of the frontal lobes may drain in two directions, which can be especially obvious

with the patterns of venous drainage from anterior cranial fossa dural arteriovenous malformations (AVMs). Anterior orbitofrontal branches drain into the superior sagittal sinus. Posteriorly directed veins—the posterior orbitofrontal and olfactory veins—join the confluence of veins under the anterior perforated substance and so become tributaries of the middle cerebral veins (Fig. 16-2). The veins in this area may also drain to the cavernous sinus or sphenoparietal sinus.

Veins from the basal surface of the temporal lobes are divided into medial and lateral according to their direction. Laterally directed veins drain to the tentorial sinuses. Medially directed veins may drain to the superior petrosal sinus or to the basal vein of Rosenthal. With the typical configuration of the basal vein, this implies that the medial temporal lobe structures are drained usually to the vein of Galen. However, the basal vein of Rosenthal varies in its configuration, and the anterior territory of this vein may drain to the cavernous sinus. Therefore, in the setting of a high-flow state through the cavernous sinus, such as a carotid cavernous fistula or dural AVM, venous hypertension of the temporal lobes may be an alarming complication of the disease with a risk of seizures or venous infarction.

The inferior surface of the occipital lobe is drained by occipitobasal veins, which can be directed either to the transverse sinus or toward the basal vein.

Deep Supratentorial Veins

The deep venous system consists of the internal cerebral vein, the basal vein of Rosenthal, and their tributaries (8). The tributary branches of these veins are either ventricular or cisternal in location. The deep veins are concerned with the venous drainage of the central structures of the hemispheres, basal ganglia, corpus callosum, pineal region, mid-brain, parts of the limbic system, and thalamus.

The intraventricular veins initially have a subependymal location. They used to be the most reliable angiographic indicators of central or deep mass lesions. In modern times, their relative importance for detection of mass effect has decreased. They remain a strong consideration in analysis of the drainage patterns of AVMs and for surgical planning. They are also used as landmarks for endoscopic navigation of the ventricles, particularly when other landmarks have been obliterated by the effects of hydrocephalus.

The earliest venous pattern seen embryologically is almost exclusively centrifugal to the pial veins. With enlargement of the brain, the deep, centripetal venous structures develop and become prominent, but being late in development are prone to anomalous configurations.

The deep white matter of the hemispheres is drained by medullary veins, which are characteristically straight in appearance. This appearance is thought to be related to the centrifugal pattern of migration of cells from the germinal matrix. The medullary veins collect in subependymal veins, which run along the surface of the lateral ventricles. For purposes of description, the deep ventricular veins are divided into lateral and medial groups. The ventricular veins drain toward the choroidal fissure and eventually join either the internal cerebral vein in the roof of the third ventricle or the basal vein of Rosenthal (Fig. 16-8). The medial group of ventricular veins passes through the outer or forniceal edge of the choroidal fissure; the lateral ventricular group passes through the thalamic or inner edge of the fissure (9). The

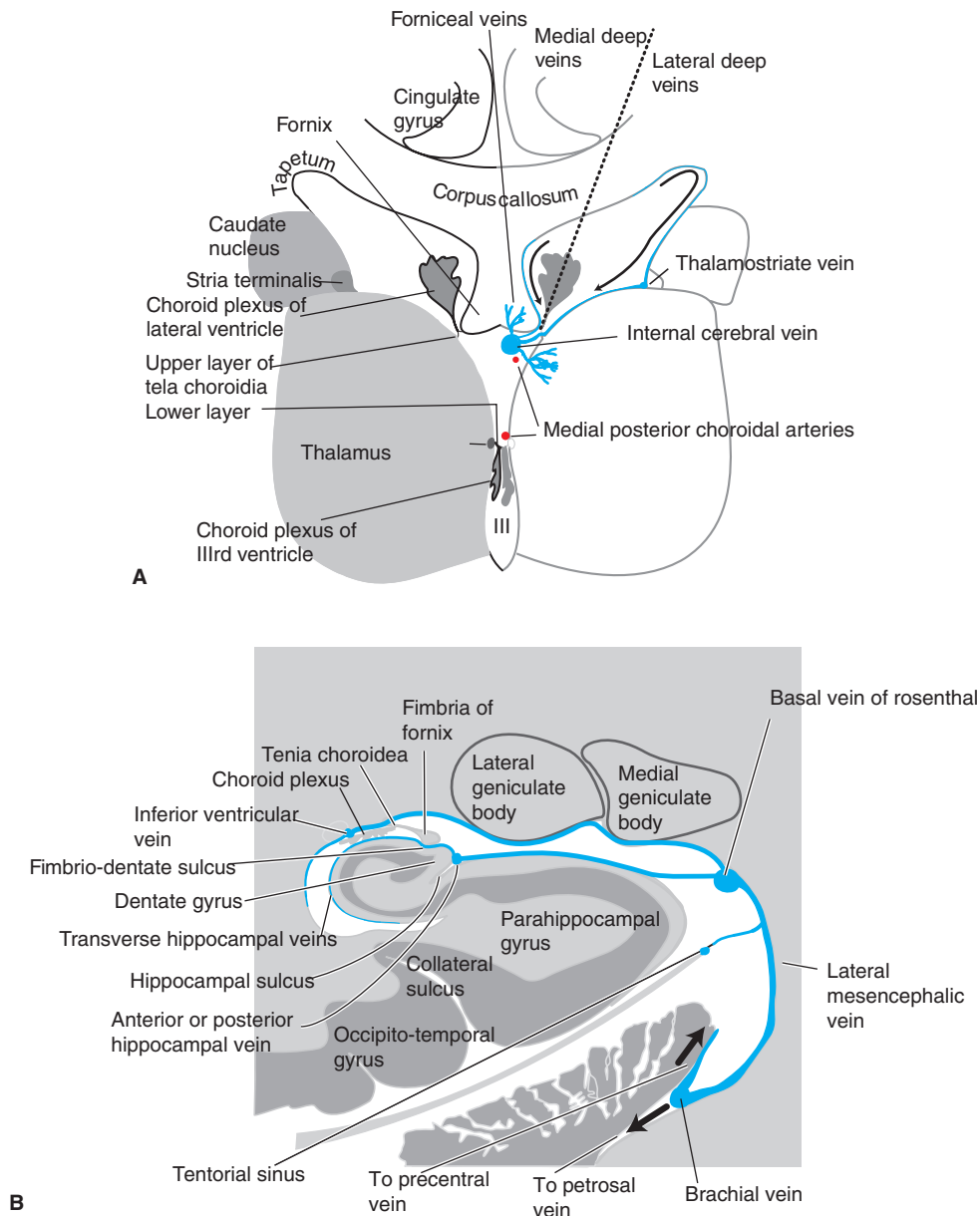


FIGURE 16-8. (A–B) Deep ventricular veins and the choroidal fissure. A: A coronal illustration of the cistern of the velum interpositum at the level of the thalami demonstrates the internal cerebral vein and choroidal arteries, which run within this space or potential space. The velum interpositum is defined on each side by the medial walls of the thalami and superiorly by the fornices. The cleavage between the fornix and thalamus on each side represents the uppermost extension of the choroidal fissure. The fissure is bridged by tela choroidea from which is suspended the choroid plexus of the ventricles. The floor of the velum interpositum is composed of a layer of tela choroidea extending between the stria medullaris on each side. The choroid plexus of the third ventricle below is suspended from this layer of tela choroidea. The *dotted line* in (A) runs through the choroidal fissure separating the medial from the lateral ventricular veins. The medial veins run close to the fornix, the lateral group close to the thalamic side of the fissure. Notice the shape of the epicallosal cistern or sulcus between the cingulate gyrus and the corpus callosum. Venous opacification in this space causes the “mustache” appearance on a direct PA view. Asymmetric hydrocephalus or midline shift causes a tilting of the venous mustache. **B:** An illustration in the coronal plane of the choroidal fissure at the level of the perimesencephalic cistern. Because of embryologic torsion in the formation of the choroidal fissure, the lateral ventricular veins correspond with those in the roof of the temporal horn, that is, the inferior ventricular vein. The hippocampal plexus of veins drains on the other side of the choroidal fissure via the fimbriodentate sulcus to the hippocampal vein in the hippocampal sulcus. Notice how the lateral mesencephalic vein bevels medially from the basal vein, corresponding with its appearance in Townes projection in Figure 16-2G.

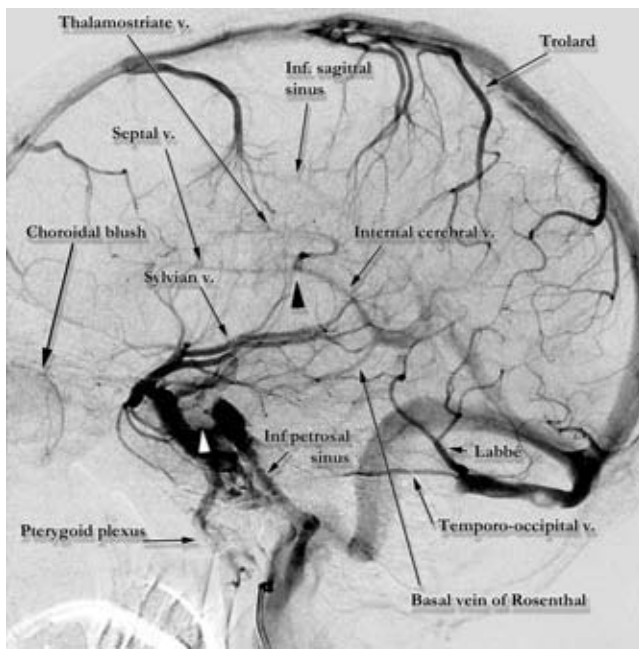


FIGURE 16-9. Venous angle. The venous angle (*arrowhead*) is formed by the junction of the thalamostriate vein and anterior septal vein. This junction usually occurs within a few millimeters of the posterior rim of the foramen of Monro.

medial group of ventricular veins drains the inner surface of the corpus callosum, septum pellucidum, the fornix, and the hippocampus. The lateral group drains the body, floor, and lateral wall of the lateral ventricle and roof of the temporal and occipital horns (Figs. 16-9 and 16-10).

► CHOROIDAL VEINS OF THE DEEP VENOUS SYSTEM

There are two named choroidal veins that receive drainage only from the choroid plexus.

The superior choroidal vein runs from posterior to anterior in the floor of the body of the lateral ventricle in a course medial to the thalamostriate vein and lateral to the fornix. It drains to the thalamostriate vein or directly to the internal cerebral vein.

The inferior choroidal vein drains the choroid plexus of the temporal horn. It also runs from posterior to anterior and joins the inferior ventricular vein or runs directly to the basal vein.

► THALAMIC VEINS

The superior thalamic vein is a centrally directed structure that emerges from the thalamus above the pineal gland. It

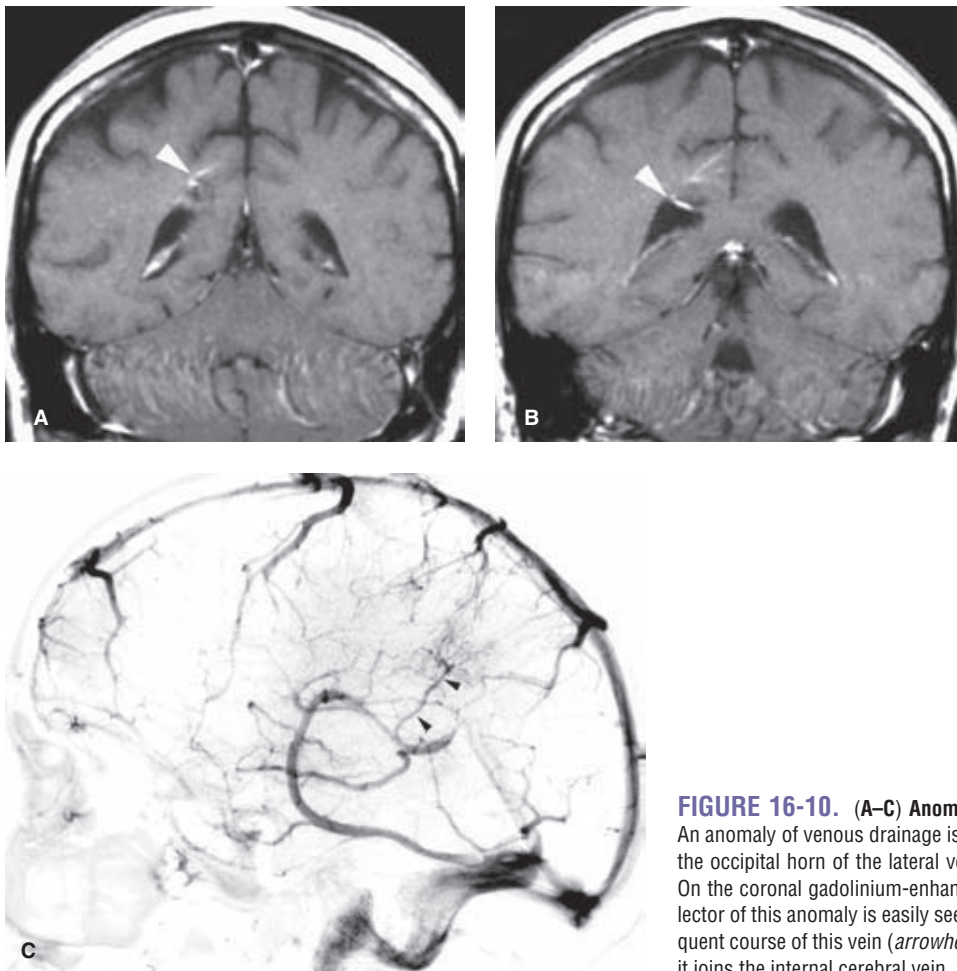


FIGURE 16-10. (A–C) Anomaly of venous drainage to an atrial vein. An anomaly of venous drainage is seen as an incidental finding in the roof of the occipital horn of the lateral ventricle above the calcar avis (*arrowhead*). On the coronal gadolinium-enhanced images (A, B), the subependymal collector of this anomaly is easily seen. On a cerebral angiogram (C), the subsequent course of this vein (*arrowheads*) is evident on the late venous phase as it joins the internal cerebral vein.

enters the most posterior aspect of the internal cerebral vein or the vein of Galen.

The anterior thalamic vein lies medially and anteriorly and becomes a tributary of the thalamostriate vein, septal vein, or internal cerebral vein.

The inferior thalamic veins are very fine vessels that exit inferiorly through the posterior perforated substance to the posterior mesencephalic vein. They drain the inferomedial portion of the thalamus.

The posterior thalamic veins drain the posterolateral portion of the thalamus to the posterior mesencephalic vein or basal vein of Rosenthal. Superficial thalamic veins drain along the ventricular surface of the thalamus or on the surface contiguous with the cistern of the velum interpositum. They join the tributaries of the internal cerebral vein anteriorly or may join atrial veins posteriorly.

► INTERNAL CEREBRAL VEINS

The paired internal cerebral veins run from anterior to posterior in the roof of the third ventricle enclosed between two layers of tela choroidea. This potential space between the two layers is called the *cistern of the velum interpositum*. As this space emerges into the suprapineal area, the veins diverge from one another to run around the pineal gland and then reconverge. Underneath the tip of the splenium, they unite into the great cerebral vein of Galen.

► GREAT CEREBRAL VEIN OF GALEN

This is a midline, unpaired, subarachnoid structure. Its length is from 5 to 20 mm. It forms below the tip of the splenium around which it then curves posteriorly. In addition to the internal cerebral veins, it receives tributaries from the basal vein of Rosenthal, the inferior sagittal sinus, the posterior pericallosal vein, the internal occipital veins, and veins from the posterior fossa.

► BASAL CEREBRAL VEIN OF ROSENTHAL

The standard configuration of the basal vein forms under the anterior perforated substance and runs posteriorly on the undersurface of the brain to its termination with the vein of Galen or the internal cerebral vein. It is the collector of venous output from an extensive distribution of tissue encompassing the orbital surface of the frontal lobe, insula and medial temporal lobe, hypothalamus, striatum, thalamus, and midbrain. It has important anastomoses with the superficial Sylvian vein, the veins of the posterior fossa, and the petrosal and cavernous sinuses.

The formation of the basal vein is defined as the junction of the inferior striate veins with the middle cerebral vein under the anterior perforated substance (Fig. 16-11). The venous system of the brain is characterized by a closer adherence of venous channels to the adjacent brain structures than is seen with the arterial counterparts, thus making the veins a more precise adumbration of anatomic landmarks. Unlike the lateral lenticulostriate arteries, which weave medially in the subarachnoid space before entering the anterior perforated substance, the inferior striate veins have a shorter subarachnoid stem and immedi-

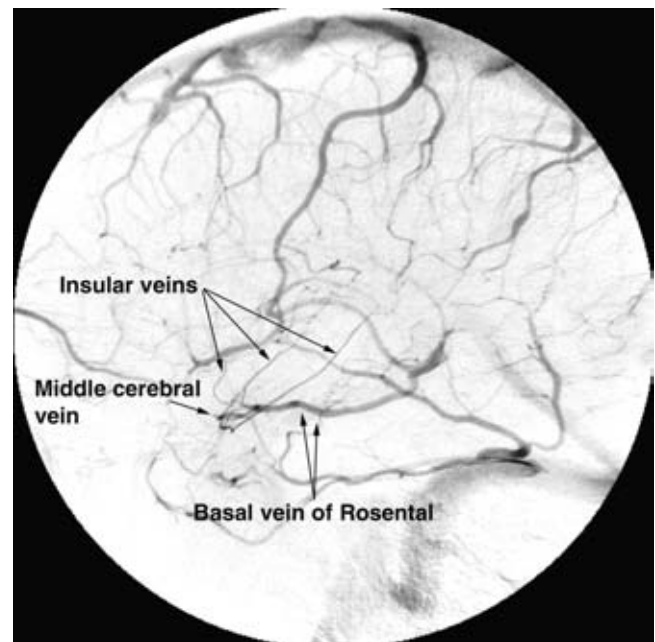


FIGURE 16-11. Basal vein of Rosenthal, insular veins, and middle cerebral vein. In this example, the superficial Sylvian vein is not well seen. This affords an unobstructed view of the insular veins. The insular veins course along the sulci of the insular triangle, forming the middle cerebral vein at their confluence around the limen insulae. The middle cerebral vein collects the inferior striate veins along the anterior perforated substance to form the anterior segment of the basal vein of Rosenthal. A deflection in the course of the basal vein is frequently seen (between the *arrows*) as it circumvents the cerebral peduncle.

ately enter the basal vein. The basal vein is described in three segments.

1. The first (anterior or striate) segment runs from the anterior perforated substance to the anterior margin of the cerebral peduncle.
2. The second (peduncular) extends from there to the lateral mesencephalic sulcus on the lateral aspect of the midbrain.
3. The third (posterior mesencephalic) segment continues to the junction with the great vein of Galen. By evaluating each of these segments, the adjacent anatomy outlined by the basal vein and its tributaries can be more easily inferred.

Furthermore, in variant configurations of the basal vein, where the venous collecting system is not united into a single channel, these segments form the basis for alternative collectors and their respective outflow channels.

Anatomic Variants in the Basal Vein

Variations are common in the configuration of the basal vein and relate to the degree to which the various segments of the basal vein fail to unite, and to alternative outflow routes draining parts or all of this venous system (10).

When there is failure of communication between the anterior and middle segments, venous outflow from the anterior segment is preserved through routes usually directed anteriorly to the cavernous sinus. Union of the middle cerebral vein and the inferior striate veins forms

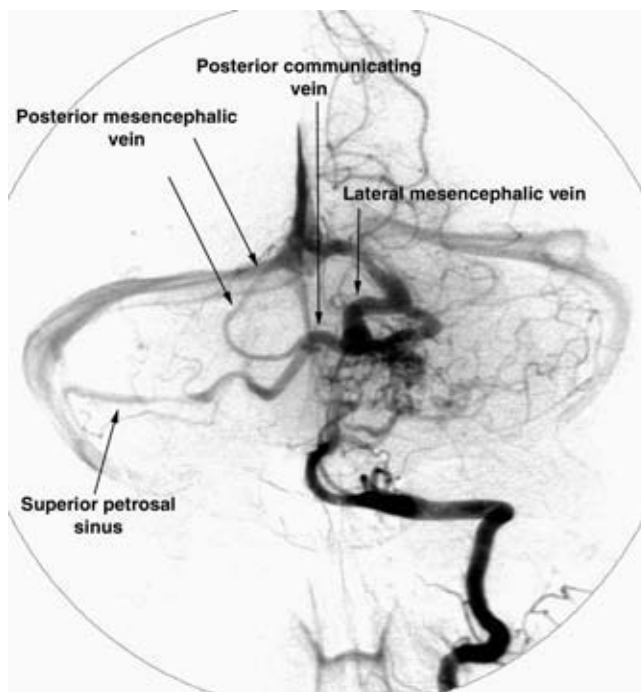


FIGURE 16-12. Venous drainage of a posterior fossa AVM. A Townes view of an AVM in the region of the left middle cerebellar peduncle. The route of venous drainage is superiorly through the lateral mesencephalic vein, which is considerably distended in this patient. When it reaches the posterior mesencephalic vein (synonymous with the basal vein), flow is directed posteriorly to the galenic system. Flow is also directed anteriorly around the peduncle and opacifies the contralateral posterior mesencephalic vein via the posterior communicating vein. The right side also decompresses via the petrosal vein to the right superior petrosal sinus.

the uncus vein with other tributaries from the frontal and temporal lobes. This vein most commonly drains directly to the cavernous sinus or may do so indirectly by draining laterally to the superficial Sylvian vein and the sphenoparietal sinus. More posteriorly, alternative outflow routes include drainage via the lateral mesencephalic vein to the superior petrosal sinus (via the petrosal vein). The basal system may drain alternatively via tentorial sinuses to the transverse and superior petrosal sinuses (Figs. 16-12 and 16-13).

► SEQUENCE OF DEEP VENOUS FILLING

After a carotid injection, the earliest deep venous structures to fill are the thalamostriate and internal cerebral veins, at the same time as the posterior frontal veins. The septal vein fills last, at the same time as the dural sinuses, vein of Trolard, and the occipital veins. The basal vein normally has an intermediate timing. On vertebral artery injections, the transit time for the thalamic circulation is shortest, which means that thalamic veins will be seen during the time that the cerebellum and posterior hemispheres are still in the capillary phase (11,12).

► INFRATENTORIAL VENOUS SYSTEM

The elegance of angiographic depiction of the veins of the posterior fossa lies in the close relationship between the more constant members of this group and their associated anatomic landmarks. More importantly, the functional significance of the configuration of these veins derives from the multitude of possible connections to and from the venous

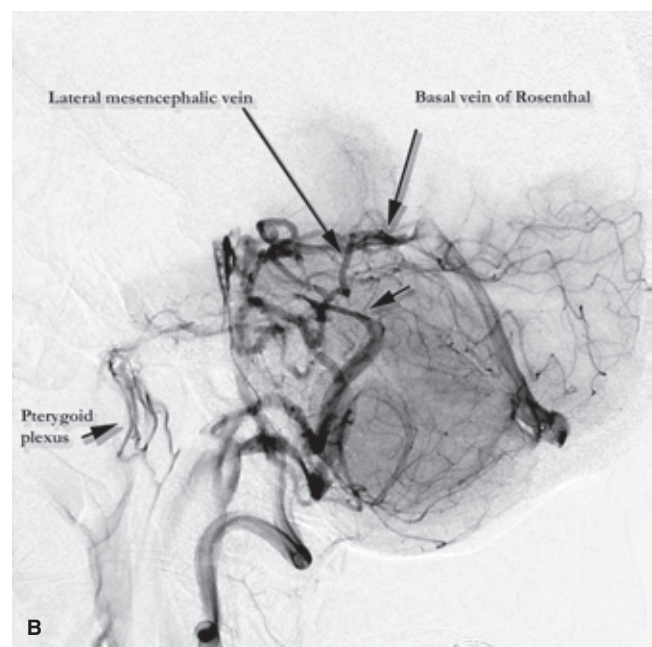
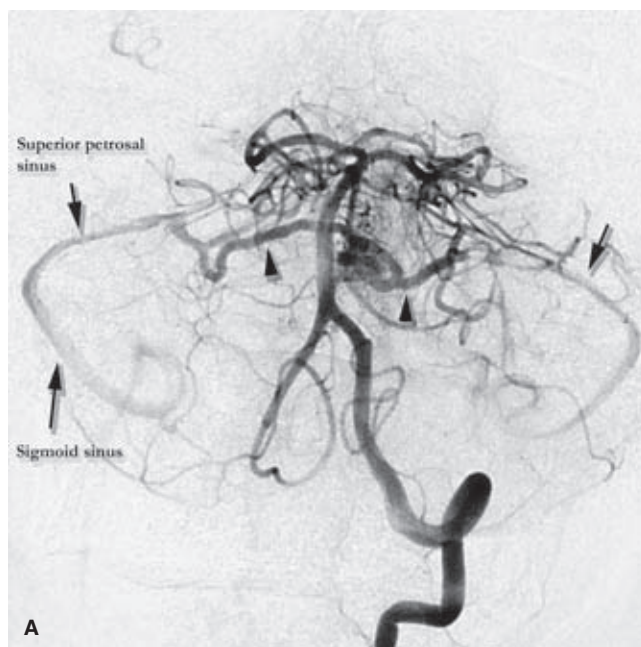


FIGURE 16-13. (A–B) Venous drainage of a pontine AVM. An AP (A) and lateral (B) projection of a left vertebral artery injection in a patient with an AVM in the region of the left middle cerebellar peduncle. The principal route of drainage is through a large transverse pontine vein extending bilaterally (arrowheads) to the superior petrosal sinuses (arrows). The lateral mesencephalic vein also serves a role in drainage toward the Basal vein of Rosenthal.

system of the supratentorial space and that of the spinal cord. Therefore, more germane than the enumeration of tiny, obscure veins encountered in this enclosed space is knowledge of these connections. This prompts an evaluation of the effects of vascular lesions of this area on local and remote venous fields. Conversely, an evaluation of the effects of vascular lesions elsewhere may include examination of effects on the venous system of the posterior fossa. For instance, a carotid–cavernous fistula or dural AVM of the cavernous sinus can present only with symptoms of posterior fossa venous hypertension. An AVM of the posterior fossa may mimic a spinal dural arteriovenous fistula and present with symptoms of conal myelopathy.

The veins of the posterior fossa collect to three principal destinations (13–15): The petrosal sinuses, the Vein of Galen and related tributaries, and the dural sinuses bordering on or between the leaves of the tentorium cerebelli.

No single configuration is typical, but certain members of these veins are more commonly and clearly visualized, and certain connections between these three groups will be seen in typical locations (Figs. 16-2, 16-3, 16-12, and 16-13).

Anatomic variations can be seen in the drainage of the basal vein of Rosenthal to the dural sinuses, and these will affect the pattern of drainage seen in the posterior fossa. Persistence of embryonic venous sinuses may be seen through which the basal vein may drain to the lateral mesencephalic vein or tentorial sinuses (16).

► VEINS RELATED TO THE SURFACE OF THE BRAINSTEM

The major veins related to and named correspondingly with the structures of the brainstem are easily identified on normal angiograms. They frequently act as collectors for smaller cerebellar veins. They are named according to their relationship to the mesencephalon, pons, or medulla and according to whether they lie in a transverse or longitudinal disposition.

At the interpeduncular fossa, the inferior thalamic veins exit the posterior perforated substance and join with mesencephalic veins to form the peduncular vein. This vein skirts anteriorly around the peduncle from medial to lateral to enter either the basal vein or the posterior mesencephalic vein in the ambient cistern.

On the lateral aspect of the midbrain, the lateral mesencephalic vein runs in a cephalad–caudad direction in the lateral mesencephalic sulcus, draining superiorly to the posterior mesencephalic vein or basal vein (16).

The anterior pontomesencephalic vein runs from the peduncular vein in the interpeduncular cistern in a longitudinal direction in approximately the midline along the anterior rim of the pons. It frequently connects with its inferior midline counterpart, the anterior medullary vein, which in turn connects inferiorly with the anterior spinal vein.

► CEREBELLAR VEINS

The complex anatomy of the cerebellum can be simplified into a description that allows three surfaces (17): Anterior (petrosal), tentorial, and suboccipital.

Within the cerebellomesencephalic fissure, lying on the lateral aspect of the cerebral peduncle runs the lateral mes-

encephalic vein. This connects above with the basal vein of Rosenthal. Anterior drainage from this point via a vein sometimes named the *brachial vein* (because of its relation to the brachium pontis and brachium conjunctivum) connects to the petrosal vein and thus to the superior petrosal sinus (17). Posteriorly, the cerebellomesencephalic fissure extends behind the brainstem to the midline, where it continues as the fissure in front of the central lobule of the vermis. The vein in this fissure was called the *precentral cerebellar vein* by Huang and Wolf (14) and was a major angiographic landmark of mass effect in the old days. It usually drains superiorly and posteriorly to enter the galenic vein after receiving superior hemispheric and superior vermian tributaries. In situations of reversed venous flow, this route back into the cerebellomesencephalic fissure allows drainage of these regions into the confluence on the superior aspect of the cerebellar peduncles and thus toward the petrosal vein or other veins.

The tentorial surface of the cerebellum is drained by the superior hemispheric and the superior vermian veins. The more peripheral superior hemispheric veins drain centrifugally to the transverse sinus and torcular. Centrally, the superior hemispheric veins may drain anteriorly to the superior petrosal sinus, or centripetally to join the superior vermian vein or the veins in the cerebellomesencephalic fissure, and ultimately the galenic system. The superior vermian veins drain anteriorly to the galenic system or posteriorly to the torcular or straight sinus.

The suboccipital surface of the cerebellum is drained by the inferior hemispheric veins and the inferior vermian veins. The latter also drain the superior and inferior tonsillar veins. The inferior hemispheric veins may drain to the adjacent transverse or tentorial sinuses. Alternatively, they may be collected by tributaries to the vein of the cerebellomedullary fissure and ultimately become part of the petrosal drainage system.

References

1. Scatliff JH, Clark JK. How the brain got its names and numbers. *AJNR Am J Neuroradiol* 1992;13(1):241–248.
2. Padget DH. The development of the cranial venous system in man, from a viewpoint of comparative anatomy. *Contrib Embryol* 1957;37:80–140.
3. Wolf BS, Huang YP, Newman CM. The superficial sylvian venous drainage system. *Am J Roentgenol Radium Ther Nucl Med* 1963;89:398–410.
4. Oka K, Rhoton AL Jr, Barry M, et al. Microsurgical anatomy of the superficial veins of the cerebrum. *Neurosurgery* 1985;17(5):711–748.
5. Piffer CR, Horn Y, Hureau J, et al. [Anatomical study of the superior cerebral veins]. *Anat Anz* 1985;160(4):271–283.
6. Andrews BT, Dujovny M, Mirchandani HG, et al. Microsurgical anatomy of the venous drainage into the superior sagittal sinus. *Neurosurgery* 1989;24(4):514–520.
7. Di Chiro G. Angiographic patterns of cerebral convexity veins and superficial dural sinuses. *Am J Roentgenol Radium Ther Nucl Med* 1962;87:308–321.
8. Wolf BS, Huang YP. The subependymal veins of the lateral ventricles. *Am J Roentgenol Radium Ther Nucl Med* 1964;91:406–426.
9. Ono M, Rhoton AL Jr, Peace D, et al. Microsurgical anatomy of the deep venous system of the brain. *Neurosurgery* 1984;15(5):621–657.
10. Babin E, Megret M. Variations in the drainage of the basal vein. *Neuroradiology* 1973;6(3):154–161.

11. Bub B, Ferris EJ, Levy PS, et al. The cerebral venogram: A statistical analysis of the sequence of venous filling in cerebral angiograms. *Radiology* 1968;91(6):1112–1118.
12. El-Banhawy A, Walter W. Incidence and significance of early filling of veins in normal internal carotid angiography. *J Neurosurg* 1961;18:717–729.
13. Huang YP, Wolf BS. The veins of the posterior fossa—Superior or galenic draining group. *Am J Roentgenol Radium Ther Nucl Med* 1965;95(4):808–821.
14. Huang YP, Wolf BS. Precentral cerebellar vein in angiography. *Acta Radiol Diagn (Stockh)* 1966;5:250–262.
15. Huang YP, Wolf BS, Antin SP, et al. The veins of the posterior fossa—Anterior or petrosal draining group. *Am J Roentgenol Radium Ther Nucl Med* 1968;104(1):36–56.
16. Wolf BS, Huang YP, Newman CM. The lateral anastomotic mesencephalic vein and other variations in drainage of the basal cerebral vein. *Am J Roentgenol Radium Ther Nucl Med* 1963;89:411–422.
17. Matsushima T, Rhoton AL Jr, de Oliveira E, et al. Microsurgical anatomy of the veins of the posterior fossa. *J Neurosurg* 1983;59(1):63–105.

The External Carotid Artery and Extracranial Circulation

Key Points

- The anatomy of the extracranial circulation is in many ways more challenging than that of the intracranial system. Proficiency in this domain is essential for the prevention of severe complications from endovascular procedures, including tissue necrosis, cranial nerve injury, and blindness.
- Anastomotic connections between the extracranial vessels and the intracranial circulation are an ever-present danger during extracranial embolizations and should always be evaluated before proceeding.

The branches of the external carotid system are named according to their respective territories without regard to the site of origin of the vessel or pattern of division of the external carotid artery. Certain patterns of branching can be seen as characteristic and, when present, will help in identification of named vessels. The capacity of the external carotid artery to compensate for a restriction on flow in one branch by developing collateral flow through a number of other pathways becomes a major consideration in interventional procedures. The preocclusion angiogram does not necessarily indicate which anastomoses are lying dormant waiting to assume a greater hemodynamic role. In a vascular field being embolized, potential anastomoses with dangerous collateral pathways to the internal carotid artery or ophthalmic artery may not fill during the initial part of the procedure. However, as the outflow from the field becomes restricted by progressive embolization, previously unseen pathways emerge, turning what may have initially seemed a safe embolization procedure into a dangerous one.

Therefore, in learning the anatomy of the external carotid system, flexibility must be incorporated into one's conception of the arborization of the vessel. The territory of destination is the factor that determines the nomenclature of a vessel; its relationship to bony structures and tissue planes helps to confirm its identity. A vessel's location and identity guide the interpreter toward an awareness of the potentially dangerous anastomoses that may be relevant. One's thinking should also take reckoning of nonvisualization of supply to a particular area. An assumption that the supply is coming from an alternative source must be entertained.

On the AP view of the external carotid artery, most of the proximal vessels are superimposed on the outer aspect of the face in an area that is prone to technical overexposure. For these reasons, and because most of the branches of the external carotid artery run in an AP plane, most images of the proximal external carotid artery branches are depicted in the lateral plane. An important component for understanding the angiographic anatomy of the external carotid artery is the tissue plane in which a particular vessel lies. Vessels that cross one another on the angiographic image without anastomosing lie in different anatomic planes. Vessels that appear to cross a bony barrier, such as the skull base, without a deflection in their course, must lie in a more superficial tissue plane.

► BRANCHES OF THE EXTERNAL CAROTID ARTERY

Superior Thyroidal Artery

In approximately 75% of patients, the external carotid system arises as a common trunk in an anteromedial relationship to the internal carotid artery between C3 and C5. It usually divides quickly, giving an inferiorly directed superior thyroidal artery as the first branch (Figs. 17-1 and 17-2). In the normal state, this is a small, tapered vessel projecting anteriorly and medially with a number of branches to the larynx and related structures, thyroid gland, and parathyroid glands. If injected directly, the normal thyroid gland will give a discernible dense blush. The superior thyroidal artery may arise as a common trunk with other branches of the external carotid artery or from the common carotid artery. There are rich anastomoses within and around the thyroid gland between the superior and inferior thyroidal arteries. The inferior thyroidal artery is a branch of the thyrocervical trunk or, less commonly, of the vertebral artery, subclavian artery, or common carotid artery. The thyroid ima artery arises from the aortic arch.

Ascending Pharyngeal Artery

The ascending pharyngeal artery is usually a long, needle-thin vessel arising from the posterior aspect of the proximal external carotid trunk. Variant sites of origin include a

(text continues on page 234)

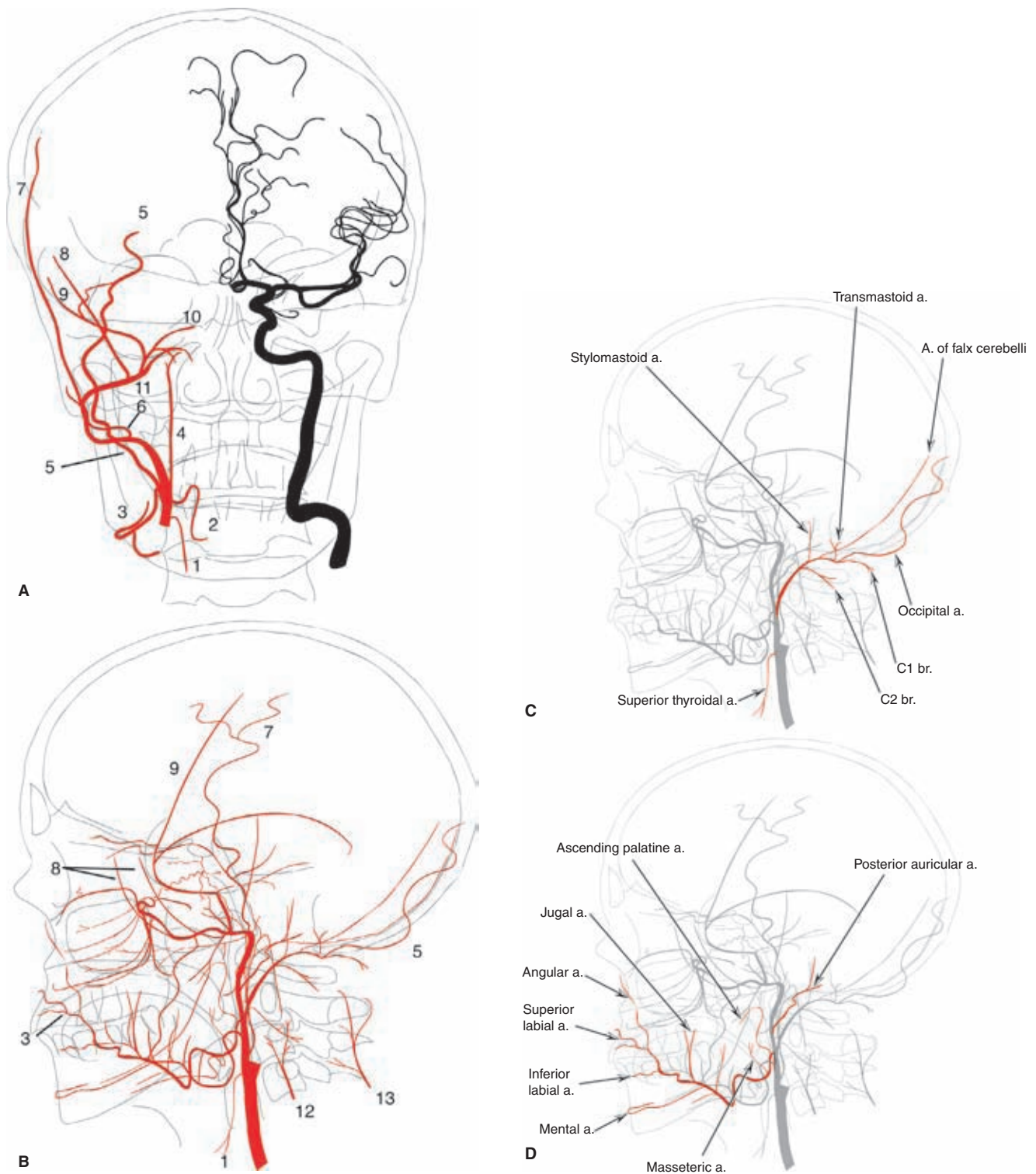


FIGURE 17-1. (A–D) External carotid artery. A and B: PA and lateral illustrations of the external carotid artery circulation, while the internal carotid artery is illustrated on the anatomic left side for reference. (1, superior thyroidal artery; 2, lingual artery; 3, facial artery; 4, ascending pharyngeal artery; 5, occipital artery; 6, posterior auricular artery; 7, superficial temporal artery; 8, deep temporal artery; 9, middle meningeal artery; 10, accessory meningeal artery; 11, internal maxillary artery; 12, ascending cervical artery (from thyrocervical trunk); 13, deep cervical artery from the costocervical trunk.) **B:** Template for subsequent illustrations of individual arteries. **C:** The superior thyroidal artery and occipital artery are highlighted. The C1 and C2 branches of the occipital artery are indicated, as are the stylomastoid and transmastoid branches of the occipital artery. The stylomastoid and transmastoid branches may arise from other external carotid branches. The occipital artery may also give rise frequently to the neuromeningeal trunk, which is illustrated in Figure 17-1H in its more common form as a branch of the ascending pharyngeal artery. The occipital artery is illustrated giving rise to the artery of the falx cerebelli. This dural artery more commonly arises from the vertebral artery or posterior inferior cerebellar artery. **D:** The facial artery and posterior auricular artery are highlighted. The branches of the facial artery are labeled. The shepherd's hook appearance of the ascending palatine artery illustrated here is characteristic of this vessel. It is often this curve that catches one's attention when this territory is filled via collateral flow. In (A), notice the superficial course of the posterior auricular artery relative to the occipital artery. They may occasionally arise together as a common trunk. The curve of the posterior auricular artery in (A) is characteristic of the vessel. It can be difficult to cannulate if the external carotid artery proximal to that point is tortuous.

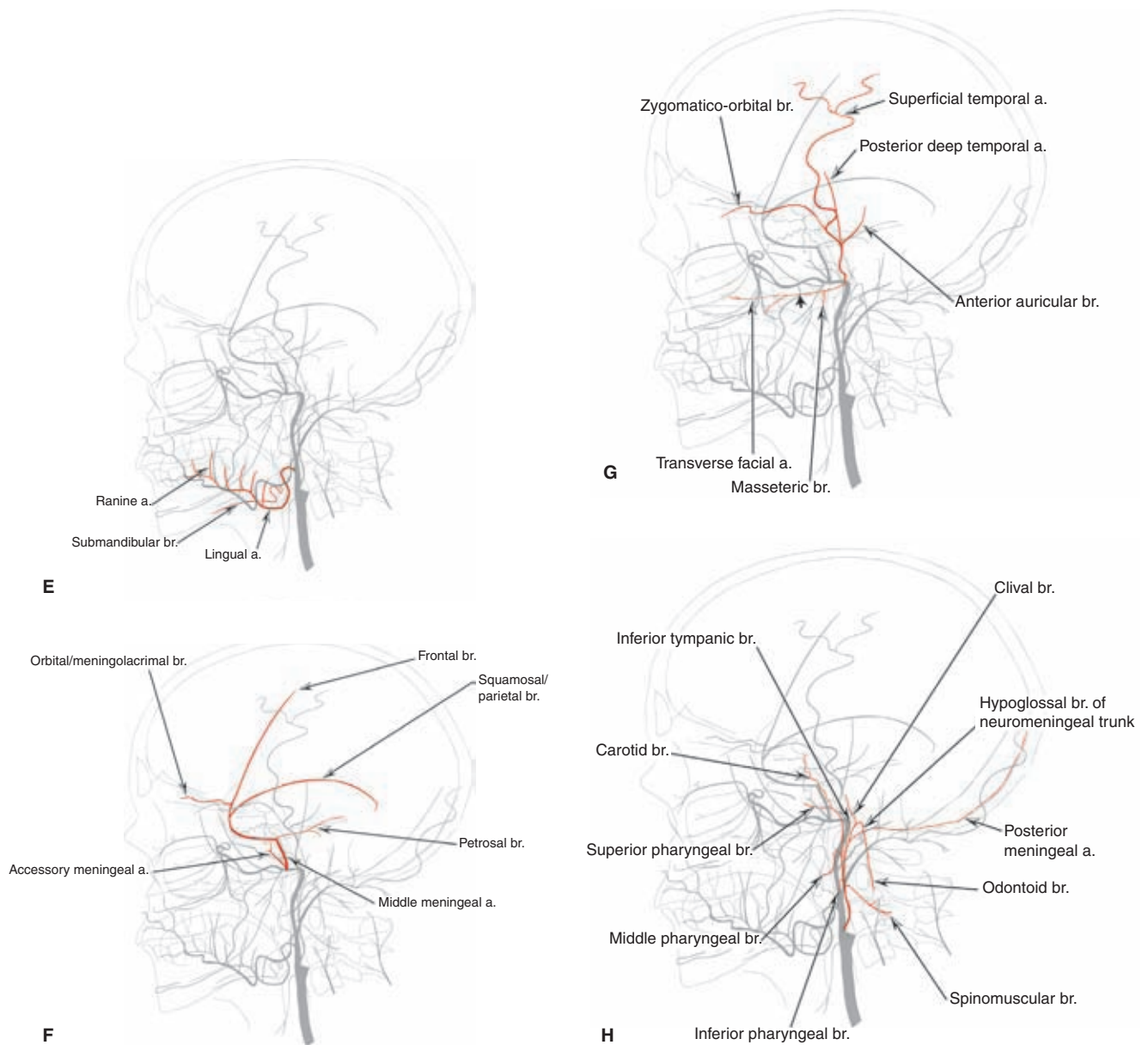
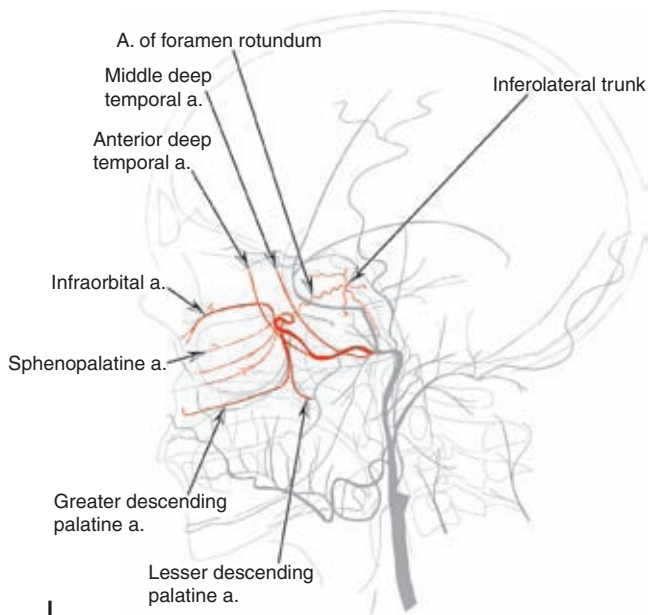
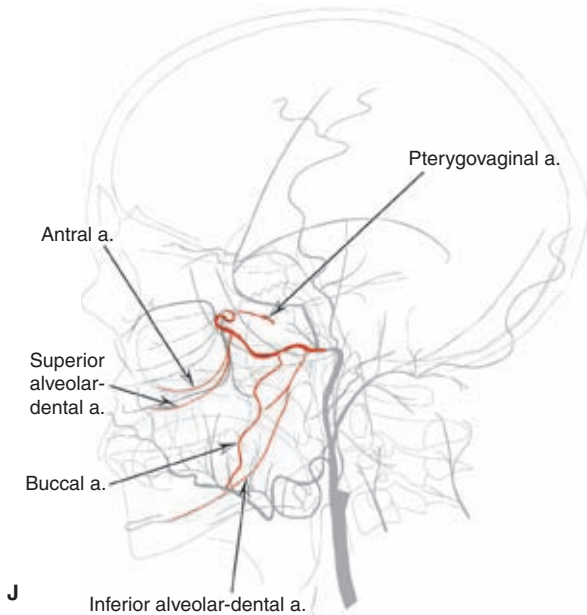


FIGURE 17-1. (CONTINUED) (E–H) E: The lingual artery is highlighted. The dorsal artery of the tongue with its ranine branches is a characteristic feature. Its circulation at the floor of the mouth and around the submandibular gland is in variable balance with the adjacent branches of the facial artery. F: The middle meningeal artery is highlighted. It is illustrated here with a common exocranial trunk shared by the accessory meningeal artery. However, the accessory meningeal artery may have a separate origin from the internal maxillary artery. The branches of the middle meningeal artery are indicated (petrous branch (a dangerous vessel during embolization as it can supply the vasa nervorum of the VII nerve in the middle ear); lacrimal branch to the orbit (variable); frontal branch; squamous branch). G: The superficial temporal artery and related arteries are highlighted. These include the posterior deep temporal artery, anterior auricular artery, transverse facial artery, and masseteric branches of the latter. The *arrow* indicates the characteristic intersection of the transverse facial artery and the underlying buccal artery. The zygomatico-orbital branch of the superficial temporal artery is indicated because this is an important branch for superficial temporal artery to ophthalmic artery reconstitution. When the zygomatic branch is prominent, the transverse facial artery is not well seen, and vice versa. H: The lateral appearance of the ascending pharyngeal artery is illustrated. The main branches of the ascending pharyngeal artery are labeled (see text for discussion). (continued)



I



J

FIGURE 17-1. (CONTINUED) (I–J) I: Various branches and anastomotic relations of the internal maxillary artery are highlighted (anterior deep temporal; middle deep temporal; artery of the foramen rotundum connecting to the inferolateral trunk, lesser descending palatine artery supplying the soft palate; greater descending palatine artery; sphenopalatine arteries; infraorbital artery). The deep temporal arteries are sometimes described as having a “pseudomeningeal appearance,” which refers to their smooth straight course. However, they do not deflect at the skull base, as is the case of the middle meningeal artery. Furthermore, they have a very straight superficial course on the PA view (see A). The tortuous appearance of the artery of the foramen rotundum is very characteristic as it directs itself toward the floor of the sella. This is one of the most important anastomoses in internal maxillary artery embolization. The infraorbital artery is easy to recognize. It has the shape of an upturned boat hull, giving a small orbital branch directed superiorly as indicated. The lateral (short) sphenopalatine arteries conform to the curves of the turbinate bones. **J:** More branches of the internal maxillary artery are labeled (pterygogovaginal artery; inferior alveolar (dental) shown here arising from a common trunk with the middle deep temporal artery, a common variant; antral branch arising as a common alveoloantral trunk with the superior alveolar artery, buccal artery connecting the facial and internal maxillary arteries).

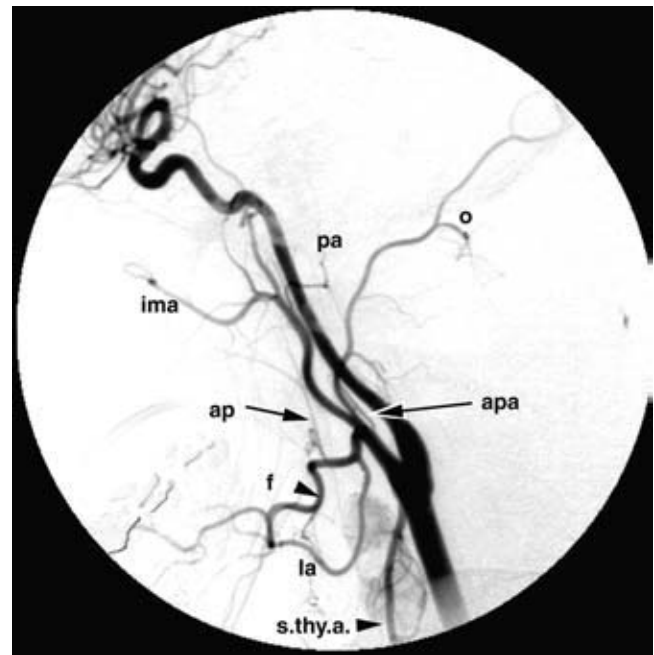


FIGURE 17-2. Superior thyroidal artery. A common carotid injection in a patient with a thyroid adenoma. A hypervascular blush is seen from an enlarged superior thyroidal artery (*s.thy.a.*). (ap, ascending palatine artery; apa, ascending pharyngeal artery; o, occipital artery; ima, internal maxillary artery; pa, posterior auricular artery; f, facial artery; la, lingual artery.)

common trunk with the occipital artery or origin from the internal carotid artery.

The ascending pharyngeal artery is directed superiorly in a straight course toward the posterior nasopharynx, appearing to lie in front of or on the vertebral column on the lateral view, and in a position medial to the main external carotid trunk on the AP view. It is an important supply route to the pharynx, dura, and lower cranial nerve foramina of the skull base, and to the middle ear. The ascending pharyngeal artery usually divides into a number of identifiable branches or trunks, several of which have important collateral anastomoses to intracranial vessels:

1. Pharyngeal trunk
 - Superior pharyngeal branch
 - Middle pharyngeal branch
 - Inferior pharyngeal branch
2. Neuromeningeal trunk
 - Hypoglossal branch
 - Jugular branch
3. Inferior tympanic artery
4. Musculosplinal artery

The configuration is prone to variability. The pharyngeal trunk may not have all three branches present in an identifiable form. The inferior tympanic artery may be a branch of one of the other trunks. Some components or the entire neuromeningeal trunk may be a branch of the occipital artery.

The pharyngeal branches of the ascending pharyngeal artery can be most easily seen on the lateral view anterior to the ascending pharyngeal artery itself and are described and frequently seen as three in number: Superior, middle, and inferior (Fig. 17-3). These can be thought of as corresponding with the nasopharynx (Eustachian tube region), oropharynx (and soft palate), and hypopharynx, respectively.

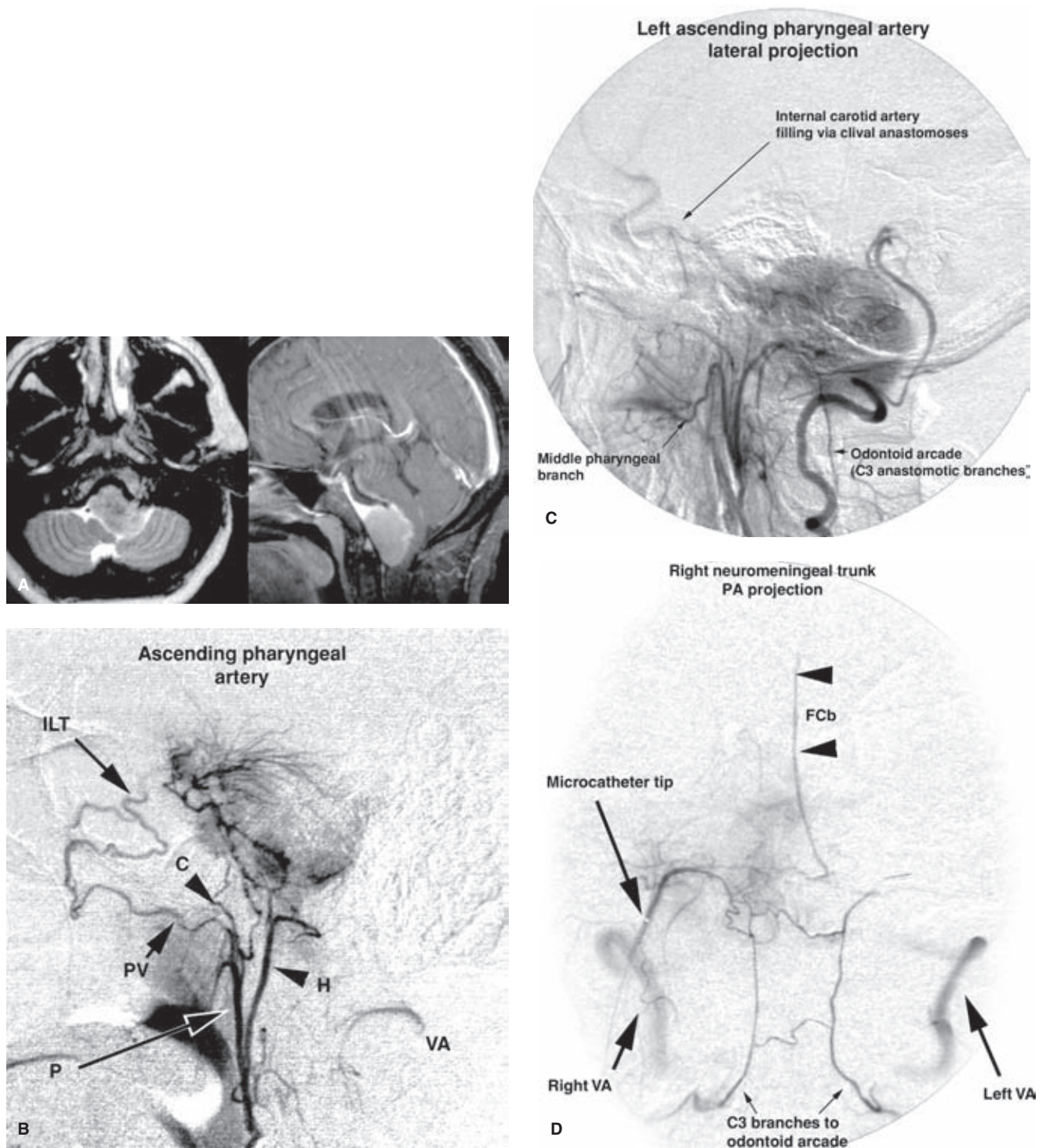


FIGURE 17-3. (A–B) **Ascending pharyngeal artery.** **A:** Axial T2-weighted and sagittal T1-weighted (fat-saturation postgadolinium) MRI images demonstrate a typical appearance of a near midline clival meningioma. There is pronounced deformity of the structures of the posterior fossa. A dural tail of enhancement extends up to the dorsum sellae. **B:** A microcatheter injection of the right ascending pharyngeal artery, lateral projection, demonstrates a pronounced tumor blush corresponding with the sagittal appearance of the tumor. The pharyngeal trunk (*P*) and hypoglossal branch (*H*) of the neuromeningeal trunk are well seen. The superior pharyngeal branch of the pharyngeal trunk anastomoses to the territory of the internal maxillary artery via the pterygoglossal artery (*PV*). This results in opacification of the inferolateral trunk (*ILT*) via the artery of the foramen rotundum. The superior pharyngeal artery may also connect with the middle cranial fossa via the foramen lacerum through its carotid branch (*C*). The vertebral artery (*VA*) is transiently opacified on this injection. (C–E) **C:** A lateral projection of the left ascending pharyngeal artery injection demonstrates a tumor blush with a tail extending to the dorsum sellae. Faint opacification of the internal carotid artery is seen, probably through clival anastomoses. The left vertebral artery is compressed by the tumor and shows slow runoff. It is opacified by the odontoid arcade from the neuromeningeal trunk. **D and E:** A selective PA injection (**D**) and lateral view (**E**) of an injection in the neuromeningeal trunk of the right ascending pharyngeal artery demonstrates the odontoid arcade and its anastomoses across the midline. Both vertebral arteries are opacified by this injection through the C3 branches. A midline artery extends high above the sella on this view; therefore, it represents the artery of the falx cerebelli (*FCb*).

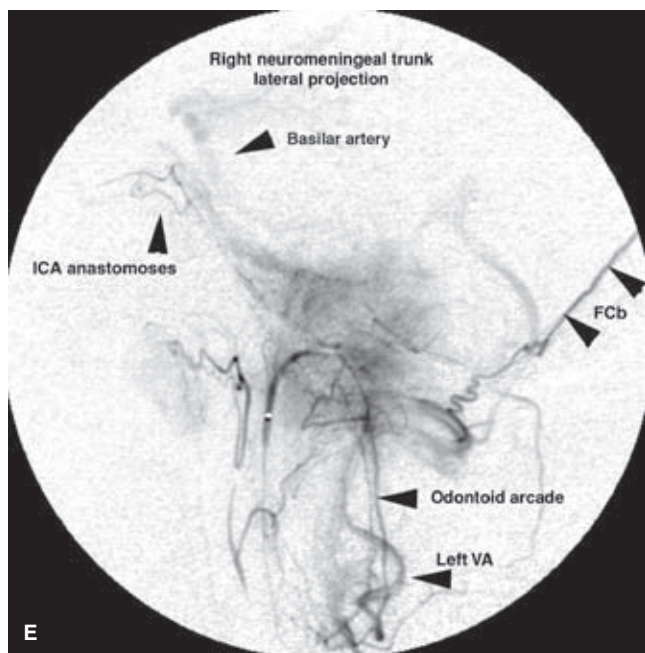


FIGURE 17-3. (CONTINUED)

The superior pharyngeal branch gives an important intracranial anastomosis through the foramen lacerum, the carotid branch, which anastomoses with the recurrent lateral branch of the inferolateral trunk of the internal carotid artery. In the posterior nasopharynx, the superior pharyngeal branch anastomoses with the internal maxillary artery system via the pterygovaginal artery. The superior pharyngeal branch also makes variable anastomoses with pharyngeal branches of the accessory meningeal artery and with the mandibular artery, when present.

The neuromeningeal trunk is also a long straight artery diverging posteriorly from the pharyngeal trunk, ascending to overlap the foramen magnum on the lateral view. Its major posteriorly directed branches are the hypoglossal artery and the jugular artery, which access the endocranial space through the respectively named foramina. The hypoglossal artery is the more medial of the two branches on the AP view.

The hypoglossal branch of the neuromeningeal trunk is an extremely important vessel. Its normal function is to supply the neural structures of the hypoglossal canal and a variable dural territory in the posterior fossa. It may give rise to the artery of the falx cerebelli, the posterior meningeal artery, or rarely, the posterior inferior cerebellar artery. Its important anastomotic branches can be divided into those that ascend along the back of the clivus, and those that descend through the foramen magnum and along the back of the body of the C2 vertebral body where it meets the C3 branch of the ipsilateral vertebral artery. This bilateral connection between the vertebral artery and the ascending pharyngeal artery behind the body of C2 is called the *arcade of the odontoid process*.

Clival branches of the hypoglossal branch of the neuromeningeal trunk ascend the dorsum of the clivus to meet with medial clival branches from the meningohypophyseal trunk or equivalent internal carotid artery hypophyseal branches

(Fig. 17-3). Thus, opacification of the posterior aspect of the pituitary gland can be seen occasionally during superselective injections of the ascending pharyngeal artery. More importantly, this route of collateral flow from the ascending pharyngeal artery to the internal carotid artery can form the basis for dangerous anastomoses during embolization. Alternatively, flow through this route may be visible on the lateral angiogram, allowing reconstitution of the cavernous internal carotid artery. In this manner, clival branches of the neuromeningeal trunk may simulate the “string sign” for persistent internal carotid artery flow in the setting of internal carotid artery occlusive disease.

The jugular branch of the neuromeningeal trunk supplies the neural structures and adjacent dura of the jugular foramen. It is prominently seen in the setting of vascular tumors, such as glomus jugulare, in the region of the jugular foramen. In the normal state, it may also send branches anteromedially toward the Dorello canal containing cranial nerve VI. It anastomoses in this region with lateral clival branches of the internal carotid artery. Dural branches of the jugular branch of the neuromeningeal trunk directed toward the sigmoid sinus may have prominent anastomoses with dural branches of the middle meningeal artery and transosseous dural branches of other sources from the external carotid artery.

The inferior tympanic artery is usually a tiny vessel and steers a middle course between the neuromeningeal and pharyngeal trunks on the lateral view. It may arise from either trunk. It gains access to the middle ear via the inferior tympanic canaliculus, which it shares with the Jacobson branch of the glossopharyngeal nerve. It is therefore prominently involved in glomus tympanicum tumors. Within the middle ear, the inferior tympanic artery anastomoses with:

1. The stylomastoid branch of the occipital artery, which enters the middle ear via the canal of that name, running with the VII nerve.
2. The petrosal branch of the middle meningeal artery.
3. The caroticotympanic branch of the internal carotid artery.

The musculospinal branch of the ascending pharyngeal artery is directed posteriorly and inferiorly on the lateral view at the level of the third cervical space. It supplies the cervical musculature, cranial nerve XI, and the superior sympathetic ganglion. It has important anastomoses to the ascending and deep cervical arteries and with the vertebral artery.

Lingual Artery

The lingual artery supplies the tongue, floor of mouth, and suprahyoid area. The largest branch is the terminal dorsal artery of the tongue, which is most easily identified on the lateral view. It extends toward the tip of the tongue and gives characteristic parallel ranine branches to the musculature of the tongue (Fig. 17-1E). Particle or other embolization in the lingual artery needs to be performed conservatively because the tongue has no alternative route of arterial supply, and iatrogenic tongue injuries can be very debilitating to the patient. In the floor of the mouth, the lingual artery has rich anastomoses with the facial artery. The facial artery territory in the region of the mandible, floor of mouth, and lower face may be supplanted completely by the lingual artery. The lingual artery contributes in varying degrees to the supply

of the submandibular and sublingual salivary glands. The lingual artery and facial artery may arise as a common linguofacial trunk. These two arteries are hemodynamically balanced; hypoplasia of one is compensated by dominance of the other.

Facial Artery

The facial artery arises more distally than the lingual artery, or they may share a common origin from the external carotid artery (Fig. 17-4). The usual musculocutaneous distribution of the facial artery is extensive, and its many branches have rich anastomoses to territories supplied by other external carotid artery branches. Therefore, when these other branches are prominent or “dominant,” the facial artery will be correspondingly smaller or hypoplastic. The facial artery usually arises medial to the angle of the mandible. To gain access to the facial structures outside the plane of the mandible, the facial artery must make an inferiorly and laterally directed loop to course around the body of the mandible. This point corresponds with the anterior edge of the masseter muscle insertion (Fig. 17-1D). To make this loop on the lateral projection, it must dip below the level of the lingual artery, creating potential confusion between the two vessels at this point.

The ascending palatine artery arises from the proximal deep segment of the facial artery or adjacent external carotid artery. It ascends toward the soft palate along the levator palati muscle with a very characteristic shepherd’s crook configuration. It anastomoses with the other arteries to the soft palate, particularly the middle branch of the pharyngeal trunk of the ascending pharyngeal artery, the lesser descending palatine artery from the internal maxillary artery, and the pharyngeal

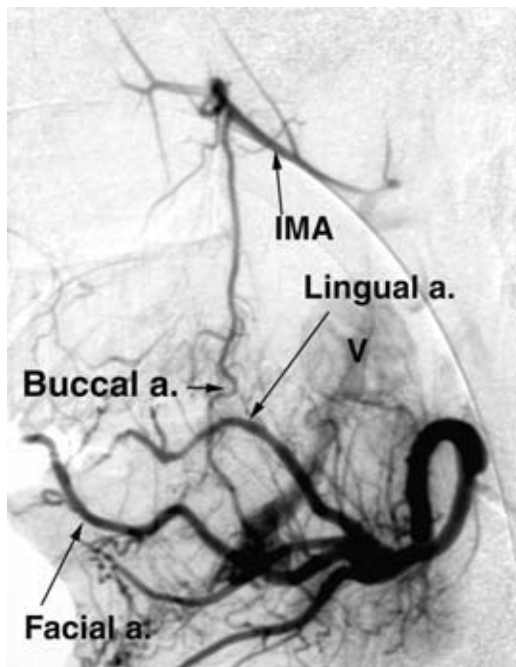


FIGURE 17-4. Linguo-facial trunk and buccal artery. A lateral projection of an injection in the left linguo-facial trunk of a teenager with an arteriovenous malformation of the floor of the mouth. Early venous opacification is seen directed to a large varix (V). A prominent buccal artery allows opacification of the internal maxillary artery (IMA) from the facial artery.

branch of the accessory meningeal artery. In cases of delayed post-tonsillectomy bleeding, this is the most likely site of injury due to necrosis or sloughing of the tonsillar bed.

The facial artery supplies the superficial facial structures, giving named branches to the submandibular gland, the submental foramen, the mandible (mental branch), the superior and inferior labial area, the cheek (jugal branches), and the ala of the nose (alar branch). It terminates as a nasoangular branch tapering along the lateral aspect of the bridge of the nose, or alternatively as a naso-orbital branch when directed toward the inner canthus of the eye.

The jugal vessels may arise as a common trunk or as separate anterior, middle, and posterior branches from the facial artery. The jugal branches are directed superiorly toward the muscles of the cheek and masseter muscle. A prominent buccal branch may be seen connecting this system to the internal maxillary artery superiorly (Fig. 17-1J). Identification of the buccal artery can be assisted sometimes by identifying how it crosses deep to the transverse facial artery without intersecting with it at the level of the pterygoid plates. The buccal artery and posterior jugal artery may be the site of origin of lower masseteric branches from the facial artery.

The labial vessels are termed *superior* and *inferior*, and they have rich anastomoses with adjacent territories. The superior labial arteries may have a considerable circulation to the nasal septum in the midline, raising the possibility of anastomoses with the ethmoidal branches of the ophthalmic artery and with the long sphenopalatine arteries.

In the setting of a proximal ligation or congenital hypoplasia of the facial artery, the surrounding vascular territories will be enlarged to assume supply to the facial distribution. These territories particularly include the following:

- Infraorbital artery, which can assume supply equivalent to the anterior jugal branches of the facial artery
- Buccal branch of the internal maxillary artery
- Transverse facial branch of the superficial temporal artery (very common)
- Lingual artery
- Palatine arteries
- Masseteric branches of the external carotid trunk

Occipital Artery

The occipital artery is a posteriorly directed branch of the external carotid artery, which has an extensive musculocutaneous, meningeal, and scalp distribution at the craniocervical junction and above. It runs medial to the sternocleidomastoid muscle, where it cuts a prominent groove in the undersurface of the temporal bone, medial to that cut by the posterior belly of digastric muscle. Like its more anterior counterpart, the superficial temporal artery, the occipital artery may have a sinuous appearance. The occipital artery is embryologically related to the first segmental artery of the cervical vasculature, and therefore it may arise from the internal carotid artery as a *forme fruste* of a proatlantal intersegmental artery. In the setting of rare cases of a persistent proatlantal intersegmental artery, the occipital artery usually arises from this variant vessel. The occipital artery, in the normal state, has important anastomotic relationships with the C1, C2, C3, and C4 anastomotic systems. In the C1 and C2 spaces, it anastomoses freely with the equivalent branches of the ipsilateral vertebral artery. At the C3 and C4

levels, the occipital artery frequently anastomoses with the distal field of the deep cervical artery. It may also anastomose in the third space with the musculospinal branch of the ascending pharyngeal artery (Fig. 17-1C and H).

It gives two named endocranial branches: the stylomastoid artery and the transmastoid branch. The stylomastoid artery is a superiorly directed straight vessel along the anterior aspect of the mastoid process in the stylomastoid canal, thus identifying the course of the distal canal of the VII nerve. The stylomastoid artery is an important supply route to the middle ear and a potential site of VII nerve morbidity during embolization. More posteriorly, the artery of the mastoid foramen (transmastoid branch) describes a transosseous route to gain access to the dura of the posterior fossa. It is an important route of supply to vascular lesions of the dura in this region, including tumors and dural vascular malformations. The mastoid branch is one of the most frequently involved vessels seen in high-flow vascular lesions or tumors in the posterior fossa floor. In this capacity, the possibility of anastomoses with the subarcuate branch of the ipsilateral anterior inferior cerebellar artery should be considered. These two named endocranial branches of the occipital artery may have alternative sites of origin—from the ascending pharyngeal artery or from the posterior auricular artery—and therefore are not dependent on the occipital artery for their nomenclature. Alternatively, other endocranial vessels usually associated with other sites of origin may arise from the occipital artery, for example, the posterior meningeal artery and artery of the falx cerebelli.

Posterior Auricular Artery

The posterior auricular artery may arise separately from the external carotid artery, or it may share a common auriculo-occipital trunk with the occipital artery (Fig. 17-1D). In either event, it can be thought of as a scalp vessel existing in hemodynamic balance with the occipital artery posteriorly and with the superficial temporal artery anteriorly. It usually supplies the superficial structures of the outer ear. It runs behind the ear, where it can sometimes be palpated under the skin against the mastoid bone. It may be the source of origin for the artery of the stylomastoid canal.

The denomination of “posterior” obviously connotes the presence of an “anterior” auricular artery. The latter is a branch of the superficial temporal artery, which anastomoses with the posterior auricular artery above the ear, forming an arcade of vessels in the scalp. A more superficial arcade in the earlobe may be seen in superselective magnification views.

Superficial Temporal Artery

The superficial temporal artery, as its name describes, runs on the outer surface of the temporalis muscle for much of its course, giving named terminal branches to the frontal and parietal areas of the scalp (Fig. 17-1G). More proximally, it makes a turn around the zygomatic arch, where it gives posteriorly directed branches. The anterior auricular branch was described earlier. The posterior deep temporal artery runs deep to the temporalis muscle along the surface of the skull. Anteriorly directed named branches from the superficial temporal artery at the level of the zygomatic arch include the zygomatico-orbital branch superiorly toward the lateral rim of the orbit, and the more inferior alternative, the transverse facial artery (Figs. 17-5 and 17-6). The zygomatico-orbital artery may be most prominently seen

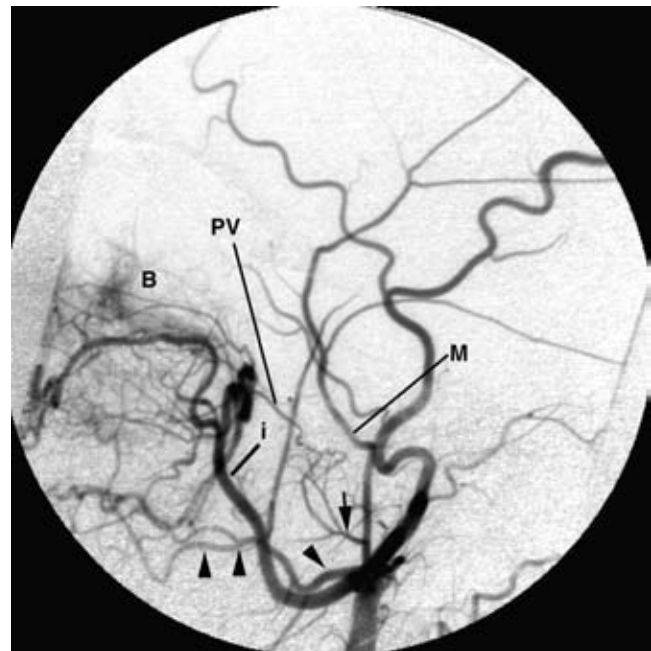


FIGURE 17-5. Transverse facial artery. A lateral, slightly skewed, projection of the distal external carotid artery in a patient being studied for intractable epistaxis. There is pronounced blush (*B*) of nasal mucosa in the territory of the distal internal maxillary artery (*I*). A characteristic 90-degree turn of the middle meningeal artery (*M*) is seen as it enters the foramen spinosum. The accessory meningeal artery (*single arrow*) is seen as a proximal branch of the middle meningeal artery; its branches in the nasopharynx can be seen extending forward to meet the pterygovaginal branch (*PV*) of the internal maxillary artery. A prominent vessel running anteriorly crosses the course of the internal maxillary artery. This is the transverse facial artery (*arrowheads*).

when the frontal branch of the more distal superficial temporal artery is diminutive or weak. Being directed to the lateral aspect of the orbit, it has important anastomoses with the palpebral and lacrimal arteries.

The transverse facial artery lies slightly lower along the lower rim of the zygomatic arch or along the parotid duct. The transverse facial artery supplies the superficial area of the temple bridging the transition between face and scalp. It carries particular supply to the upper masseteric muscles. Being in this transitional position, it can be thought of as a vessel that will be prominently seen when one or more of the vessels in the adjoining areas is weak, that is, the zygomatico-orbital above or distal facial artery or internal maxillary artery below. When seen, it has a characteristic relationship with the buccal artery, which it crosses at a near 90-degree angle, the buccal artery lying in a deeper plane of the cheek.

Internal Maxillary Artery

The internal maxillary artery and its branches constitute a distribution of vessels emanating from or best understood in relationship to the sphenopalatine fossa. The sphenopalatine fossa is a slitlike cavity defined by the curve of back wall of the maxillary sinus anteriorly and the pterygoid plates of the greater wing of the sphenoid bone posteriorly. In addition to serving as a focal point for the arterial anatomy of the central face and skull base, it also functions as a distribution point for the neural branches of the maxillary division of the V nerve and parasympathetic fibers of the superior salivatory nucleus, which synapse in the sphenopalatine ganglion.

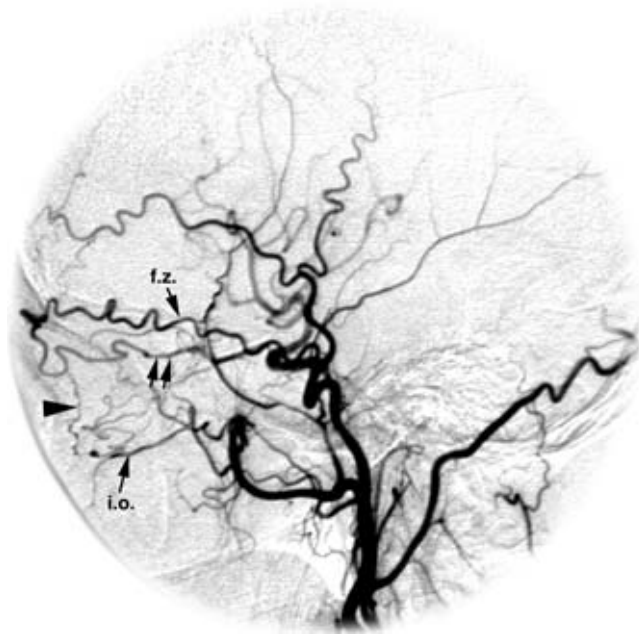


FIGURE 17-6. Superficial temporal artery to ophthalmic artery anastomoses. A lateral projection of a common carotid artery injection in the setting of occlusive internal carotid artery disease. It demonstrates that a frontozygomatic (*f.z.*) branch of the superficial temporal artery contributes significantly to retrograde opacification of the ophthalmic artery (*double arrow*). A lesser degree of input is seen from the orbital branch (*arrowhead*) of the infraorbital artery (*i.o.*). Notice that the timing of external carotid artery opacification is ahead of that of the internal carotid artery, an indication of incipient hemodynamic failure of the internal carotid artery.

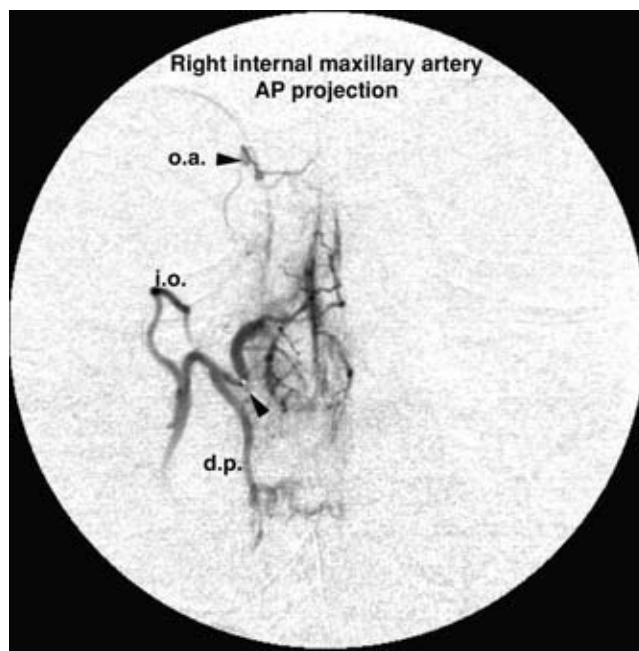


FIGURE 17-7. Ethmoidal branches of the sphenopalatine arteries. An AP view of a microcatheter (*arrowhead*) injection in the distal internal maxillary artery. In this projection, the infraorbital artery (*i.o.*) is in the plane of projection and foreshortened. The descending palatine artery (*d.p.*) in the greater palatine canal turns at the palate into the plane of imaging. Beading and irregularity of the sphenopalatine vessels is a typical finding in patients with long sphenopalatine arteries to the ophthalmic artery result in opacification of the ophthalmic artery (*o.a.*), prompting caution during embolization.

The named arterial branches of the internal maxillary artery number between 14 and 16. Their nomenclature follows that of the surrounding osseous structures and bony foramina (Figs. 17-7 and 17-8). See Table 17-1.

Middle Meningeal Artery

The middle meningeal artery arises from the internal maxillary artery on the lateral angiogram soon after the origin of the superficial temporal artery. However, this appearance is deceptive, and it is frequently necessary to demonstrate the origin of the middle meningeal artery on an AP view for catheterization (Fig. 17-1A, F). On this view, the middle meningeal artery is medial to and at some distance from the superficial temporal artery. The middle meningeal artery enters the cranium via the foramen spinosum. This foramen is hypoplastic or absent in variants where the middle meningeal artery has origin from an alternative source, such as a persistent stapedia artery (Chapter 7). The middle meningeal artery is easily recognized by the sharp turn it makes along the floor of the middle cranial fossa after entering via the foramen spinosum (Fig. 17-9). Furthermore, its course along the inner aspect of the skull is characterized, for the most part, by smooth curves, in contrast to the sinuous course of the overlapping superficial temporal artery.

The middle meningeal artery supplies named dural branches to the frontal area, temporal squamous region, petrous area, parietal dural convexity, and to the region of the sigmoid and transverse sinuses. The latter branches may

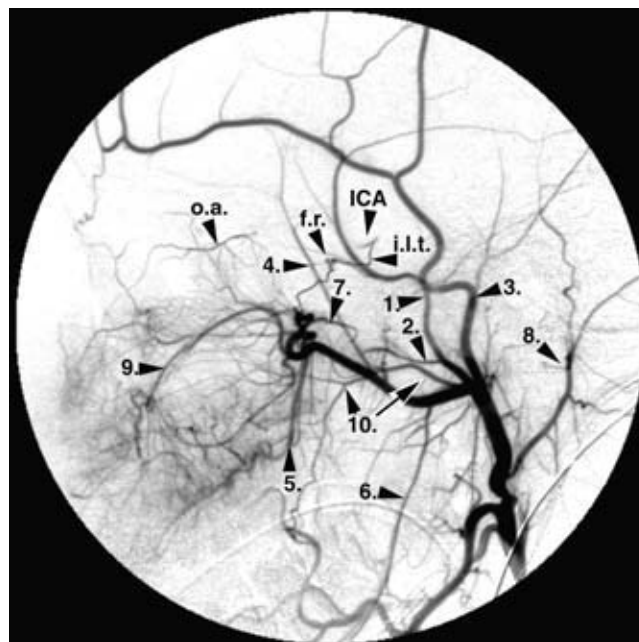


FIGURE 17-8 Anatomy of the distal external carotid artery. A lateral projection of the distal external carotid artery anatomy presents a typical angiographic appearance. However, the image must be inspected closely to reveal dangerous anastomoses to the ophthalmic artery (*o.a.*) and the internal carotid artery (*ICA*) via artery of the foramen rotundum (*f.r.*), and the inferolateral trunk (*i.l.t.*). (1, middle meningeal artery; 2, accessory meningeal artery; 3, superficial temporal artery; 4, middle deep temporal artery; 5, greater descending palatine artery; 6, inferior alveolar artery; 7, pterygovaginal artery; 8, posterior auricular artery; 9, infraorbital artery; 10, transverse facial artery.)

TABLE 17-1 Pterygopalatine Fossa

WALL	FORAMINA	ARTERIAL CONTENTS	NEURAL CONTENTS
Posterior	Foramen rotundum Pterygovaginal canal Vidian canal	Artery of the foramen rotundum Pterygovaginal artery Vidian artery	Maxillary division V_b of the V nerve Pharyngeal branches of V_b Parasympathetic fibers from the superior salivatory nucleus, i.e., greater superficial petrosal nerve from VII Deep petrosal nerve (sympathetic fibers) leaving the carotid sheath
Superior	Inferior orbital fissure	Infraorbital artery	Infraorbital nerve
Medial	Lesser sphenopalatine foramen Greater sphenopalatine foramen	Lesser/short sphenopalatine arteries Greater/long sphenopalatine arteries	Short sphenopalatine nerves Long sphenopalatine nerves
Lateral	Pterygomaxillary fissure	Internal maxillary artery	
Inferior	Greater palatine canal Lesser palatine canal	Greater descending palatine artery Lesser descending palatine artery	Greater palatine nerve Middle and posterior palatine nerves

also give supply to hypervascular lesions of the tentorium cerebelli and posterior fossa. The middle meningeal artery also supplies the dura in the area of the middle cranial fossa adjacent to the cavernous sinus, where it can give rise to prominent orbital branches as described elsewhere. The middle meningeal artery may also give origin to the marginal tentorial artery. At the level of the superior sagittal sinus, the middle meningeal artery anastomoses with the artery of the falx cerebri, and together they supply the dural layers of the falx and associated lesions.

Accessory Meningeal Artery

The accessory meningeal artery arises from a common trunk with the middle meningeal artery, or it may arise distal to the middle meningeal artery from the internal maxillary artery (Fig. 17-1A, F). On the lateral view, it has a more oblique, anterior slant in contrast to the straight course of the exocranial trunk of the middle meningeal artery. On the AP view, the accessory meningeal artery is slanted medially toward the cavernous sinus and specifically toward the point of arborization of the inferolateral trunk (Figs. 17-10–17-13).

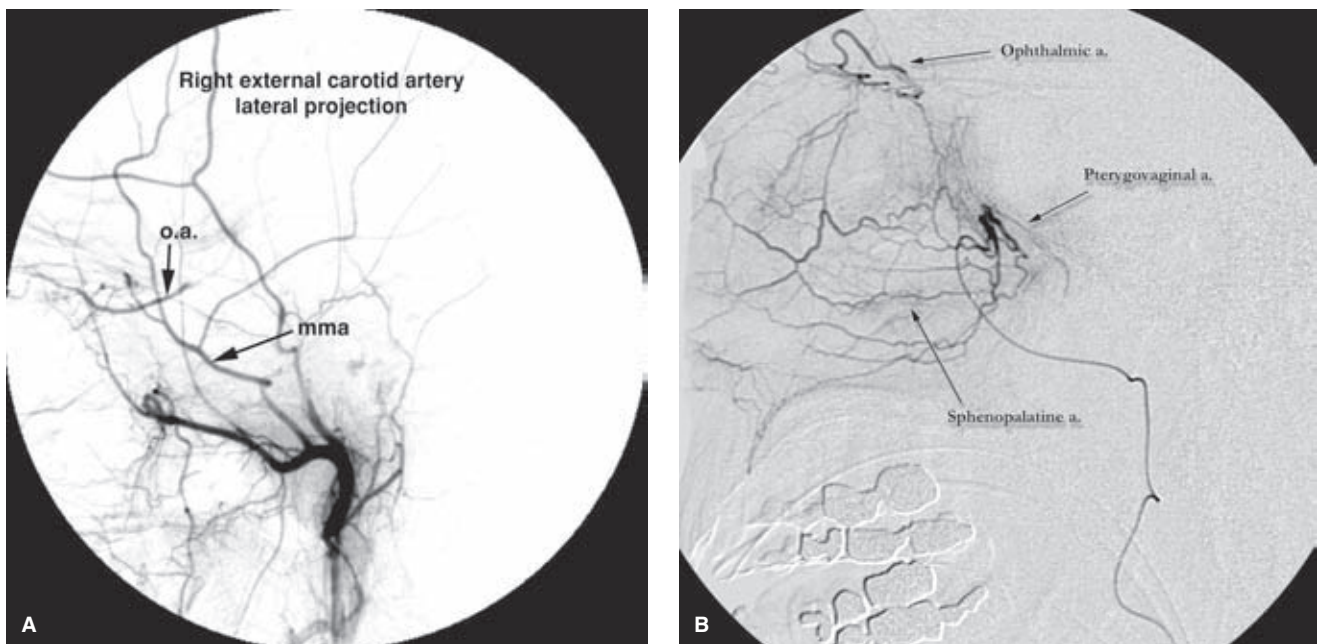


FIGURE 17-9. (A–B) Orbital anastomoses (two patients). Every embolization of the distal external carotid artery must be preceded by a review for possible anastomoses to the ophthalmic artery. In patient A there is prompt opacification of the ophthalmic artery (*o.a.*) via the middle meningeal artery (*mma*), probably through the superior orbital fissure or Foramen of Hyrtl. In patient B, the injection is made more distally in the internal maxillary artery prior to an epistaxis embolization. The ophthalmic artery is prominent opacified, likely by ethmoidal branches along the superior septum.

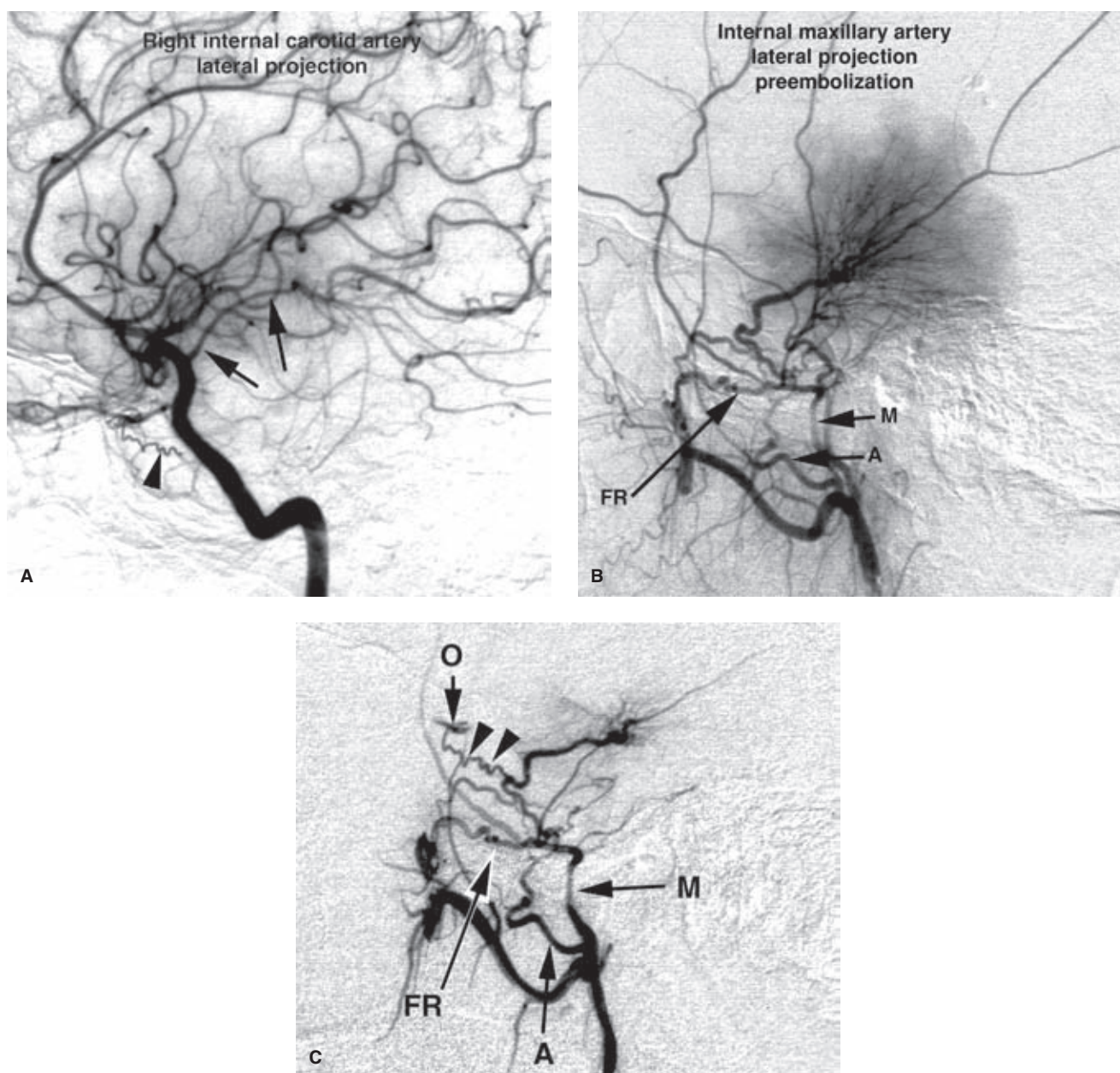


FIGURE 17-10. (A–C) Dangers to the inferolateral trunk during external carotid artery embolization. **A:** A pre-embolization right internal carotid artery injection in a patient with a large meningioma behind the orbit demonstrates some deformity of the course of siphon but no evidence of internal carotid artery supply to the tumor. Notice the draped appearance of the posterior communicating artery (*arrows*). However, a tortuous little vessel is seen (*arrowhead*) near the genu. The precise identity of this vessel became evident later in the case. **B:** A pre-embolization injection of the distal external carotid artery demonstrates a complex network of vessels in the paracavernous area supplying the tumor. (*M*, middle meningeal artery; *A*, accessory meningeal artery; *FR*, artery of the foramen rotundum.) The characteristic appearance of the inferolateral trunk is not specifically identified, but its presence must be suspected. **C:** A lateral projection of a microcatheter injection in the internal maxillary artery to check on the interim effects of careful embolization. It demonstrates a change in the hemodynamics of the vascular network feeding the tumor. A tortuous vessel (*double arrowheads*) is now seen in the upper anterior aspect of the network opacifying the ophthalmic artery (*O*), which immediately washes out the opacification. Therefore, the tortuous vessel seen on the internal carotid artery injection (*arrowhead* in **A**) represents the deep recurrent ophthalmic artery, which anastomoses the ophthalmic artery to the inferolateral trunk. Therefore, the margin for error in this situation is extremely narrow. The chances of damaging the ophthalmic artery by forceful injection of emboli are considerable.

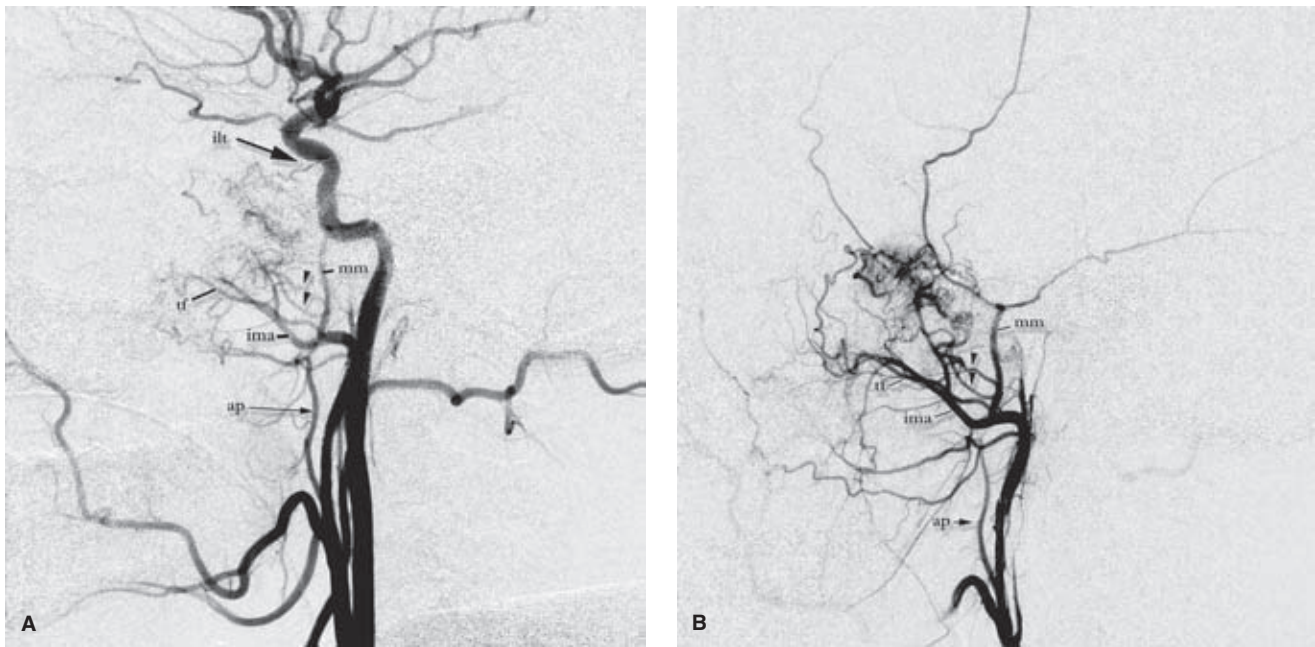


FIGURE 17-11. (A–B) Ever-present proximity of dangerous anastomoses. The right common carotid arteriogram (A) and selective external carotid arteriogram (B) in this patient with recurrence of a juvenile angiofibroma show some of the same vessels under different physiologic conditions. The tumor has been previously embolized and operated upon; hence the ipsilateral internal maxillary artery (*ima*) is stunted and the ipsilateral transverse facial artery has become hyperplastic (*tf*). For reference the middle meningeal (*mm*) and ascending palatine (*ap*) arteries have been labeled in both images. The recurrent component of tumor is heavily supplied by the enlarged accessory meningeal arteries (*arrowheads*). However, one must be cognizant of the enlarged inferolateral trunk (*ilt*) from the internal carotid artery, which is also supplying the upper aspect of the recurrent tumor. Just because the inferolateral trunk is not seen directly on the external injection does not mean that it might not be accessible later in the embolization when flow dynamics have changed.

The dominant territory of supply of the accessory meningeal artery is exocranial. Ascending and descending branches supply the tensor veli palatini, pterygoid muscles, distal Eustachian tube, and soft palate. Therefore, this artery is considered in vascular lesions of the nasopharynx and palatal region. Its principal exocranial anastomoses are with the superior and middle pharyngeal branches of the ascending pharyngeal artery, the ascending and descending palatine arteries, the mandibulovidian artery, and the pterygovaginal branch of the internal maxillary artery.

The mandibulovidian artery arises from the petrous internal carotid artery. It may anastomose with the accessory meningeal artery, particularly in the setting of juvenile angiofibroma or other hypervascular lesions in children.

A small fraction of the flow of the accessory meningeal artery reaches the endocranial circulation via the foramen ovale or, less commonly, via the foramen of Vesalius. In this location, it anastomoses with the internal carotid artery via the inferolateral trunk. It is frequently involved in paracavernous tumors and dural arteriovenous malformations.

Sphenopalatine Arteries

The long and short sphenopalatine arteries are directed medially through the sphenopalatine foramen into the nasal cavities, where they supply the septal and lateral surfaces of the ipsilateral nasal airway. On the lateral view, the arteries on the lateral wall—the short sphenopalatine

arteries—describe a curve parallel to that of the turbinates (Fig. 17-11). Medially, branches of the sphenopalatine arteries near the roof of the nasal cavity may be directed superiorly along the ethmoidal air cells and anastomose with inferiorly directed ethmoidal branches of the ophthalmic artery. Anteriorly, the long sphenopalatine arteries contribute to the Kiesselbach plexus on the septum. This is the site of idiopathic venous epistaxis in younger patients. Along the nasal septum, the long sphenopalatine vessels anastomose with distal branches of the descending (greater) palatine artery, which have reentered the nasal cavity from the oral cavity via the incisive canal of the hard palate.

Greater Descending Palatine Artery

The descending palatine artery is easy to recognize on the lateral arteriogram as it conforms closely to the osseous anatomy of the greater palatine canal and hard palate (Fig. 17-11). From the sphenopalatine fossa, it descends directly inferiorly and enters the oral cavity at the greater palatine foramen posterolaterally. It makes a 90-degree turn anteriorly, seen from the lateral view, and from there runs in the roof of the mouth directly anteromedially to the incisive foramen. At the incisive foramen, it makes a direct 90-degree turn superiorly to reenter the nasal cavity close to the midline. In the nasal cavity, its distal branches along the septum anastomose with those of the long sphenopalatine arteries and ethmoidal arteries.

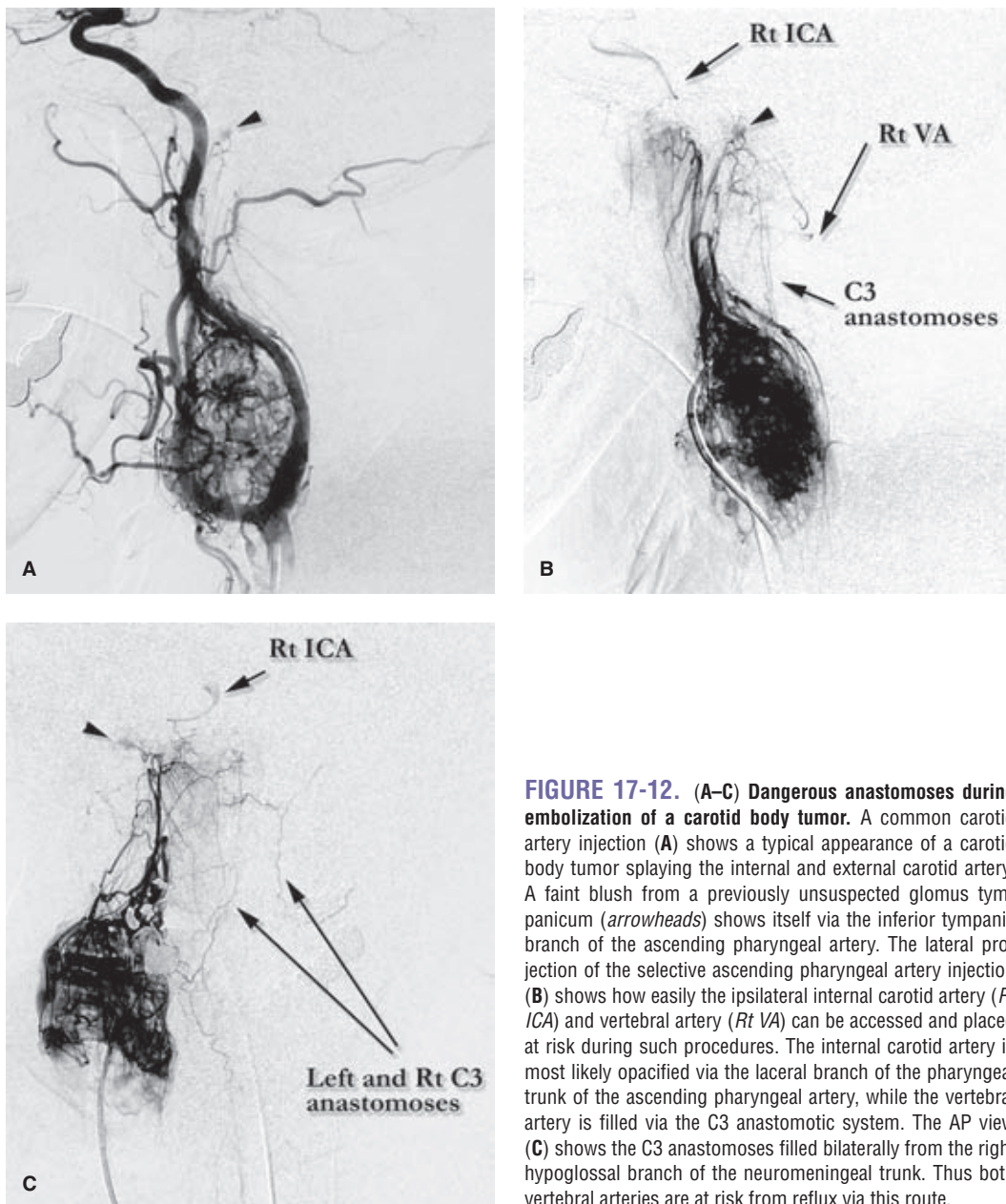


FIGURE 17-12. (A–C) Dangerous anastomoses during embolization of a carotid body tumor. A common carotid artery injection (A) shows a typical appearance of a carotid body tumor splaying the internal and external carotid artery. A faint blush from a previously unsuspected glomus tympanicum (*arrowheads*) shows itself via the inferior tympanic branch of the ascending pharyngeal artery. The lateral projection of the selective ascending pharyngeal artery injection (B) shows how easily the ipsilateral internal carotid artery (*Rt ICA*) and vertebral artery (*Rt VA*) can be accessed and placed at risk during such procedures. The internal carotid artery is most likely opacified via the laceral branch of the pharyngeal trunk of the ascending pharyngeal artery, while the vertebral artery is filled via the C3 anastomotic system. The AP view (C) shows the C3 anastomoses filled bilaterally from the right hypoglossal branch of the neuromeningeal trunk. Thus both vertebral arteries are at risk from reflux via this route.

Lesser Descending Palatine Artery

The lesser palatine artery in the lesser palatine canal parallels the initial course of the greater palatine artery. At the lesser palatine foramen on the oral surface of the hard palate, it turns directly posteriorly (Fig. 17-11). Here, it supplies the soft palate and upper faucial area and has potentially significant anastomoses with the other vessels that supply this area, particularly the middle pharyngeal branch of the ascending pharyngeal artery, the accessory meningeal artery, and ascending palatine artery.

Infraorbital Artery

The infraorbital artery enters the orbit through the inferior orbital fissure and describes a characteristic curve like an upturned boat hull on the lateral view (Fig. 17-11). In the anterior third of the orbit, it temporarily enters the infra-orbital canal curving inferiorly onto the anterior aspect of

the maxillary bone. Anterolaterally, its zygomatic branches anastomose with the adjacent branches of transverse facial and facial arteries. Medially, palpebral and naso-orbital branches anastomose with terminal branches of the ophthalmic artery. Although it is in the orbit itself for much of its early course, its importance as a source of collateral reconstitution of the ophthalmic artery is minor compared with other collateral vessels.

Deep Temporal Arteries

The deep temporal arteries are usually three in number. They lie along the outer skull surface deep to the temporalis muscle. The anterior and middle deep temporal arteries arise from the internal maxillary artery, while the posterior deep temporal artery arises from the proximal superficial temporal artery (Fig. 17-1G, I). The deep temporal arteries share with the middle meningeal artery a quality of having

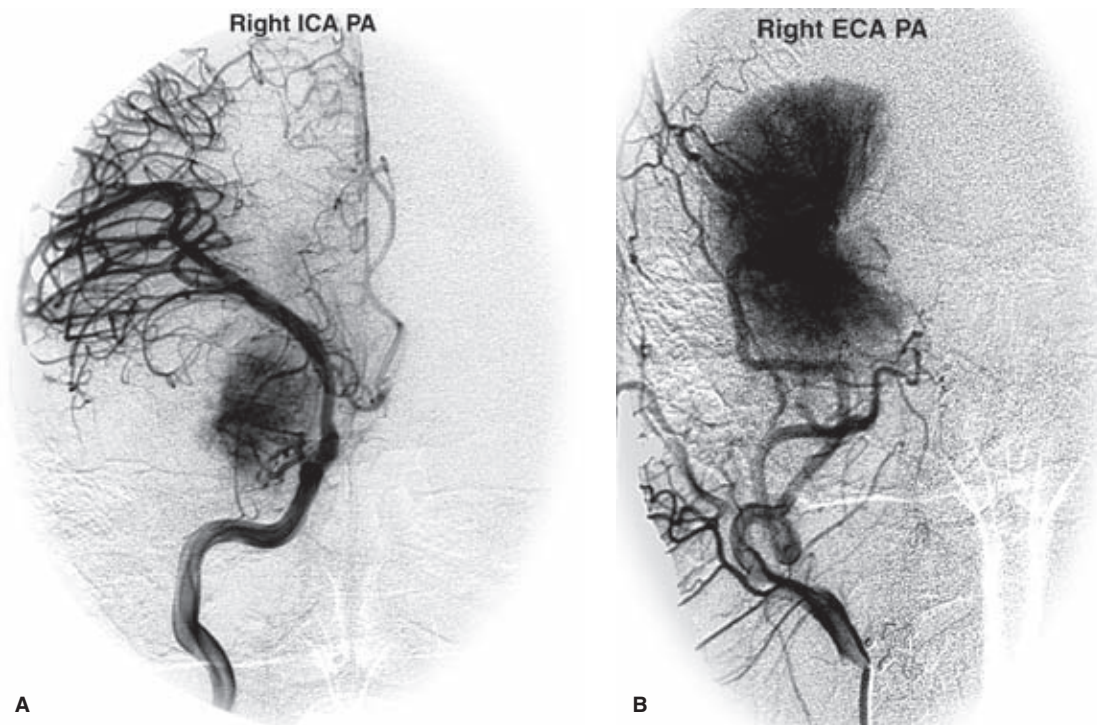


FIGURE 17-13. (A–B) Tumor compartments. A right sphenoid wing meningioma in a middle-aged male presenting with severe right-sided proptosis demonstrates the angiographic appearance of tumor compartmentalization. The right internal carotid artery injection (**A**) opacifies the superior medial quadrant of the tumor via the recurrent meningeal branch of the ophthalmic artery. There is pronounced mass effect on the course of the middle cerebral artery. The anterior cerebral artery is displaced to the left. The external carotid artery injection (**B**) opacifies the remainder of the tumor via the middle meningeal artery. The images are complementary.

smooth unbroken curves, referred to as a *pseudomeningeal* appearance, best perceived in contrast to the tortuosity of the surrounding extracranial and intracranial vessels. Unlike the meningeal vessels, the deep temporal arteries do not change course as they cross the skull base—they lie outside the skull. The anterior deep temporal artery is of most practical importance because it contributes an important branch to the lateral aspect of the orbit. A branch of the anterior deep temporal artery reaches the orbit via the inferior orbital fissure or by penetrating the malar bone along the lateral aspect of the orbit, where a large anastomosis to the lacrimal vascular territory may be seen. This is a frequent route for retrograde collateral flow into the ophthalmic artery in the setting of carotid occlusive disease.

Masseteric Branches

Masseteric arteries fall into four groups: Superior, middle, inferior, and deep. The superior arises from the transverse facial artery, the middle from the distal external carotid artery or internal maxillary artery, the inferior from the facial artery, and the deep from the internal maxillary artery. These vessels follow the course of the masseter muscle and therefore on the AP view project lateral to the ramus of the mandible.

Inferior Alveolar (Dental) Artery

The inferior alveolar artery arises proximally from the internal maxillary artery either alone or in a common trunk with

other vessels, particularly the middle deep temporal artery. On the medial surface of the mandible, it enters the mandibular canal. As it runs forward to anastomose with the mental branches of the facial artery via the submental foramen, it supplies the roots of the lower teeth.

Superior Alveolar (Dental) Artery

The superior alveolar artery supplies the roots of the upper teeth. This branch arises from the internal maxillary artery and gives an antral branch to the floor of the maxillary sinus (Fig. 17-1J). The superior alveolar artery may arise in a common trunk with other branches of the internal maxillary artery (Fig. 17-1I).

Buccal Artery

The buccal artery is frequently seen as an almost straight vessel connecting the facial artery with the internal maxillary artery. It is characterized by a 90-degree overlap with the transverse facial artery (Figs. 17-1G, J and 17-4). It is an important route of reconstitution of the facial artery after a proximal ligation.

Pterygovaginal Artery

The pterygovaginal artery projects posteriorly from the distal internal maxillary artery on the lateral view within the pterygovaginal canal to the region of the Eustachian tube (Figs. 17-1J and 17-5). Here, it exists in balance and

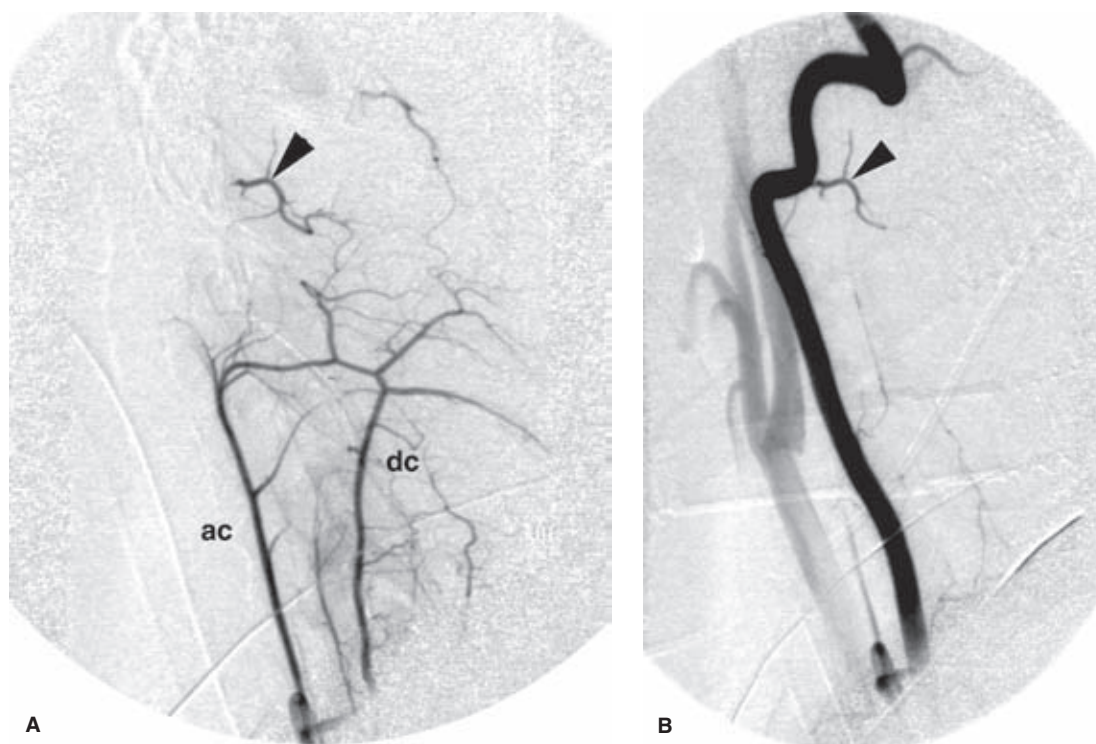


FIGURE 17-14. (A–B) Ascending and deep cervical arteries. A lateral projection (A) of an injection in the right costocervical trunk demonstrates an anastomotic arcade between the deep cervical artery (*dc*) and the ascending cervical artery (*ac*). The vertebral artery is not seen directly. However, careful comparison with the injection of the right vertebral artery (B) demonstrates that the entire C2 branch (*arrowhead*) of the vertebral artery is visible on the cervical injection. Important anastomoses are often recognized in this fashion by comparing the curves, positions, and branching patterns of vessels seen on different runs.

anastomoses with the pharyngeal branches of the accessory meningeal artery, the ascending pharyngeal artery, and the mandibulovidian artery when present.

Mandibulovidian Artery

The mandibulovidian artery lies within the Vidian canal connecting the anterior wall of the foramen lacerum and the sphenopalatine fossa. It may be opacified via an injection of the internal maxillary artery or through the petrous internal carotid artery. The artery of the Vidian canal derives from the embryologic mandibular artery.

Artery of the Foramen Rotundum

The artery of the foramen rotundum is a posteriorly directed branch of the internal maxillary artery. It forms one of the most dangerous collateral pathways directly to the inferolateral trunk. It is recognized by its tortuous course directed at the base of the sella (Figs. 17-11 and 17-8).

► CERVICAL ARTERIES

In addition to the branches of the external carotid artery, when considering angiographic evaluation of the upper neck and skull base, it is necessary to include the ascending cervical artery, usually from the thyrocervical trunk of the subclavian artery, and the deep cervical artery, usually from the costocervical trunk (Fig. 17-1B). These trunks will also be of vital interest in evaluation of cervical spinal lesions.

In the upper cervical levels, there is a system of anastomotic connections between the ascending and deep cervical

arteries, the occipital artery, the vertebral artery, and the ascending pharyngeal artery. Because of this propensity for anastomotic collateral flow, the area is an important route for vessel reconstitution in the setting of occlusive disease. It is also an area of critical concern during neurointerventional procedures. The dangers of inadvertent embolization to the posterior circulation are real. Embolization with sclerosing agents in the upper cervical level may also threaten the vasa nervorum of the lower cranial nerves (Fig. 17-14).

On the lateral projection, the ascending cervical artery is a straight vessel that lies at about the level of the vertebral bodies (Fig. 17-1B). The deep cervical artery lies more posteriorly close to a level with the spinous processes. Frequently, one or the other will be absent higher in the neck.

The branch vessels in this region are named according to the cervical space or neural foramen with which they correspond, that is, a vessel lying between the bodies of vertebrae C4 and C5 will be the C5 branch. The vertebral artery has segmental branches at each level corresponding with the neural foramina. The C1 and C2 branches of the vertebral artery have a particular propensity to anastomose with the occipital artery. The deep cervical artery is also likely to be involved in the C2, C3, and C4 anastomoses posteriorly. At levels C3 and C4, the anastomoses are also likely to involve respective branches of the vertebral artery with the ascending cervical artery and the ascending pharyngeal artery (Figs. 17-15–17-17).

Due to the possibility of the artery of cervical enlargement taking origin from the cervical trunks, embolization in these vessels proximally should be done with extreme caution.

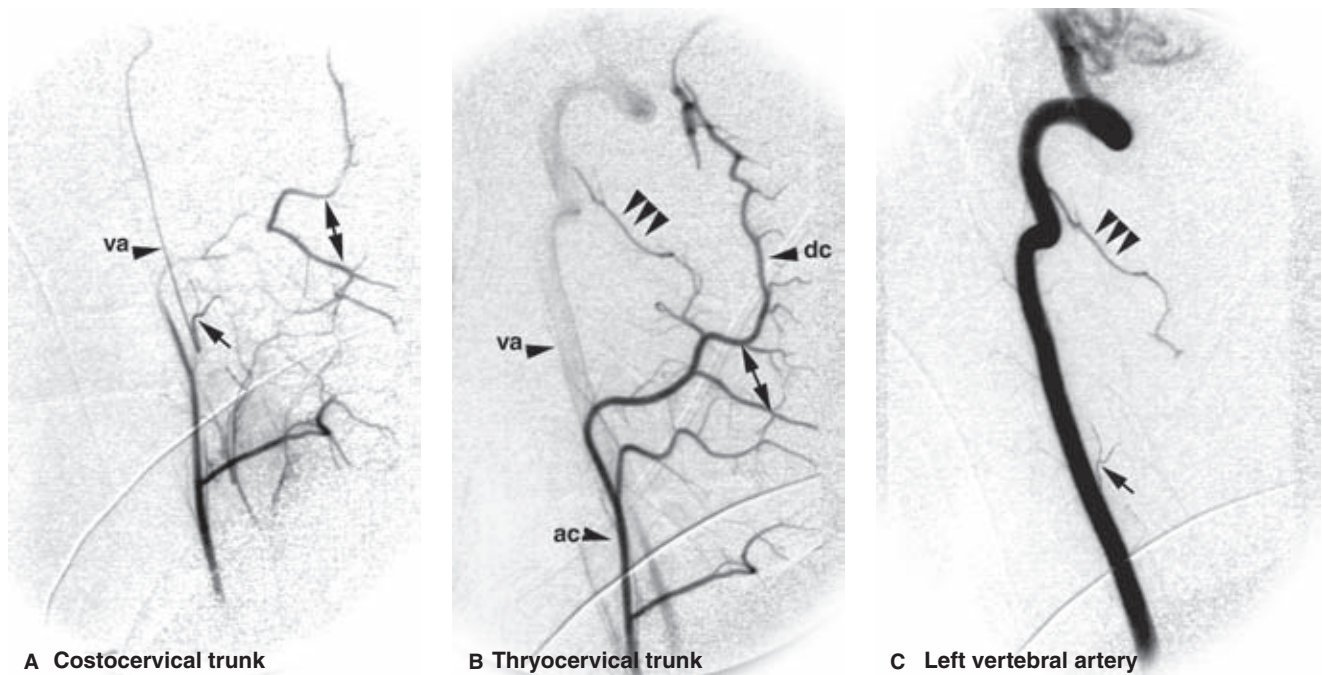


FIGURE 17-15. (A–C) Cervical anastomoses. Lateral projections of the left costocervical trunk (A), left thyrocervical trunk (B), and left vertebral artery (C), performed in that order, are presented. Only by collating all three runs can the potential anastomotic vessels be identified. In (B), the ascending cervical artery (ac) has taken over the distal deep cervical (dc) territory. In (A), the ascending cervical artery (ac) was opacified therefore by reflux or by muscular anastomoses off-screen. The anastomotic branch that opacifies the vertebral artery in (A) (arrow) is seen again in (C). The apparent caliber of the vertebral artery in (A) is due to slipstreaming of flow along the posterior wall of the vertebral artery.

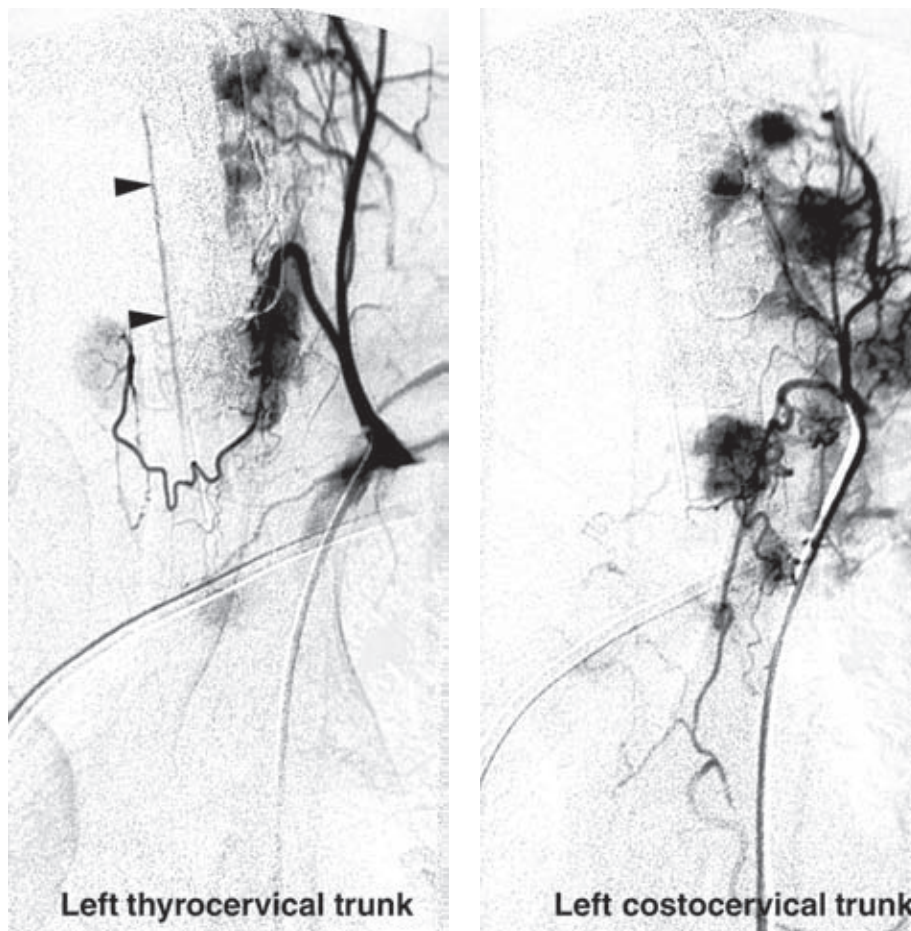


FIGURE 17-16. Dangers of cervical embolization. AP projections of the left thyrocervical trunk and left costocervical trunk in a young adult with metastatic paraganglioma. Hypervascular metastases were evident on virtually every injection of this spinal embolization being performed preoperatively to reduce vascularity in a T3 spine compression. Nevertheless, dangerous vessels must be identified and avoided. The artery of cervical enlargement arose from the left thyrocervical trunk and was only faintly evident in the midline (arrowheads).

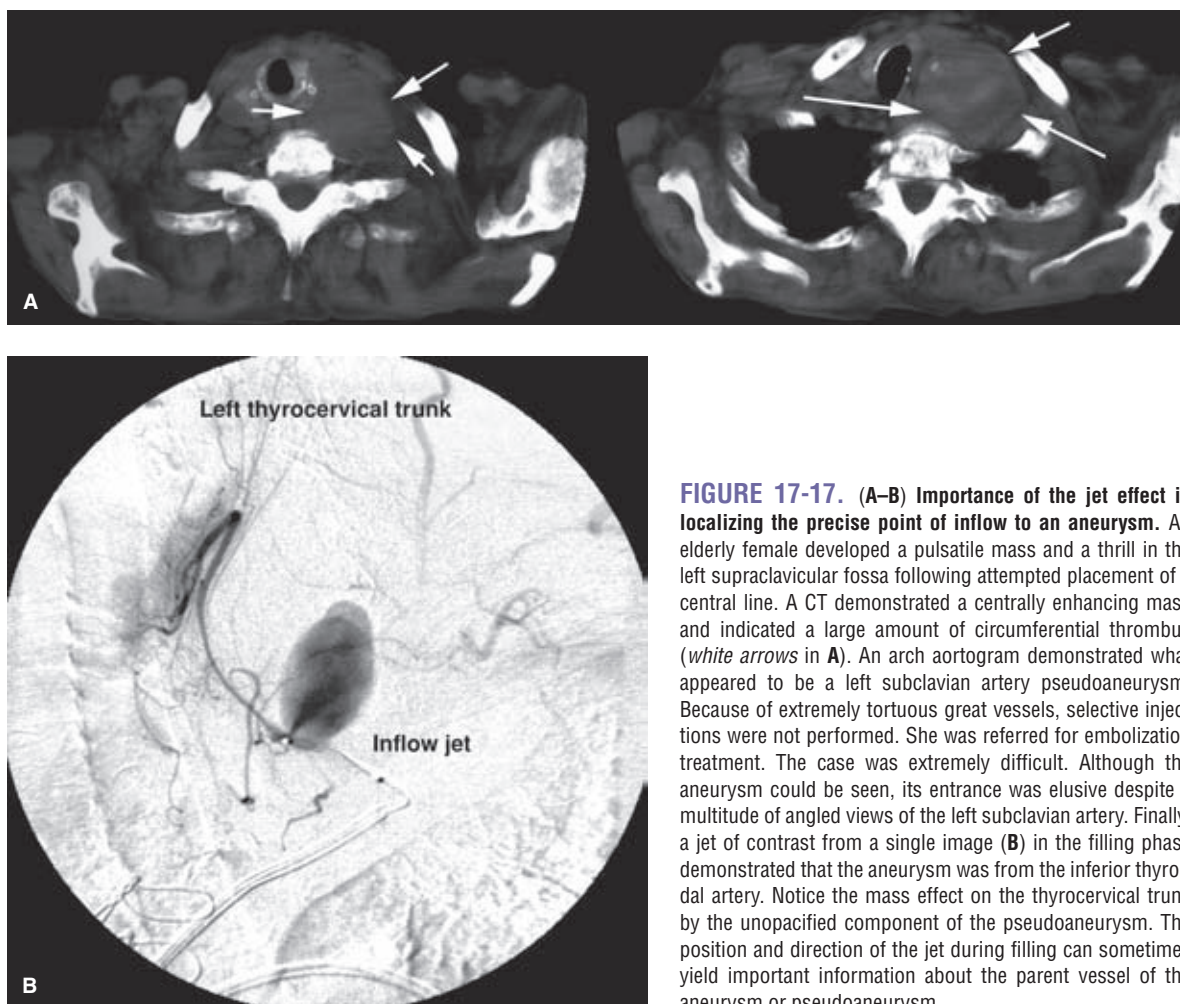


FIGURE 17-17. (A–B) Importance of the jet effect in localizing the precise point of inflow to an aneurysm. An elderly female developed a pulsatile mass and a thrill in the left supraclavicular fossa following attempted placement of a central line. A CT demonstrated a centrally enhancing mass and indicated a large amount of circumferential thrombus (*white arrows in A*). An arch aortogram demonstrated what appeared to be a left subclavian artery pseudoaneurysm. Because of extremely tortuous great vessels, selective injections were not performed. She was referred for embolization treatment. The case was extremely difficult. Although the aneurysm could be seen, its entrance was elusive despite a multitude of angled views of the left subclavian artery. Finally, a jet of contrast from a single image (*B*) in the filling phase demonstrated that the aneurysm was from the inferior thyroidal artery. Notice the mass effect on the thyrocervical trunk by the unopacified component of the pseudoaneurysm. The position and direction of the jet during filling can sometimes yield important information about the parent vessel of the aneurysm or pseudoaneurysm.

The involvement of the ascending pharyngeal artery in the upper cervical vascular system is twofold:

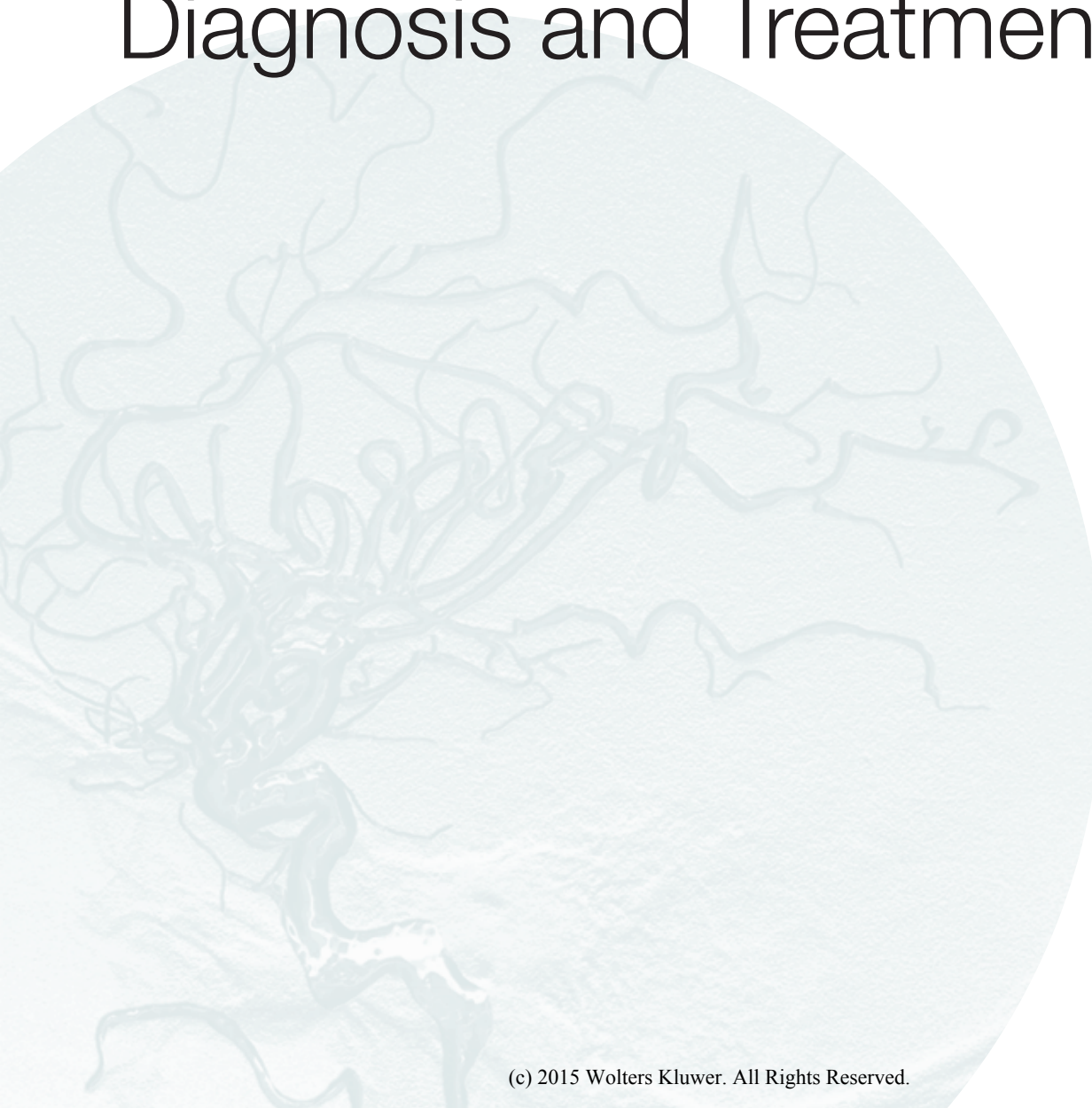
1. The C3 anastomotic branch of the vertebral artery ascends within extradural space of the spinal canal behind the odontoid process to anastomose with the descending branch of the hypoglossal branch of the neuromeningeal trunk.
2. More laterally, the musculospinal branch of the ascending pharyngeal artery anastomoses with the C3 branches of the vertebral artery.

Suggested Readings

- Djindjian R, Merland JJ. *Superselective Arteriography of the External Carotid Artery*. Berlin: Springer-Verlag; 1978.
- Lasjaunias PL. *Craniofacial and Upper Cervical Arteries: Functional Clinical and Angiographic Aspects*. Baltimore: Williams & Wilkins; 1981.
- Lasjaunias P, Berenstein A. *Surgical Neuroangiography: Functional Anatomy of Craniofacial Arteries*. Vol. 1. Berlin: Springer-Verlag; 1987.
- Lasjaunias P, Guibert-Tranier F, Braun JP. The pharyngo-cerebellar artery or ascending pharyngeal artery origin of the posterior inferior cerebellar artery. *J Neuroradiol* 1981;8:317–325.
- Lasjaunias P, Moret J. The ascending pharyngeal artery: Normal and pathological radioanatomy. *Neuroradiology* 1976;11:77–82.
- Lasjaunias P, Moret J, Mink J. The anatomy of the inferolateral trunk of the internal carotid artery. *Neuroradiology* 1977;13:215–220.
- Lasjaunias P, Theron J, Moret J. The occipital artery: Anatomy—normal arteriographic aspects—embryologic significance. *Neuroradiology* 1978;15:31–37.
- Lasjaunias P, Vignaud J, Hasso AN. Maxillary artery blood supply to the orbit: Normal and pathological aspects. *Neuroradiology* 1975;9:87–97.
- Osborn AG. The Vidian artery: Normal and pathologic anatomy. *Radiology* 1980;136:373–378.



Vascular Diseases: Diagnosis and Treatment



Intracranial Aneurysms, Diagnosis and Treatment

Key Points

- Intracranial aneurysms are delicate structures prone to procedural rupture or perforation. Treat them very gently.
- Rotational 3D angiography has improved enormously the angiographic interrogation of complex intracranial anatomy. Small or blister aneurysms are difficult to see on conventional planar views and a low threshold for performing a 3D run during diagnostic studies is a good policy.

The term *aneurysm* usually refers to a persistent pathologic dilatation of an arterial wall. In certain diseases, particularly arteriovenous malformations, the possibility of aneurysms affecting venous structures must be considered as well. Arterial aneurysms may be described according to configuration as fusiform, when the whole vessel circumference is involved (Figs. 18-1 and 18-2), or saccular, when the lesion is eccentric. Mild dilatation of a segment of vessel is called *ectasia*. The point at which diffuse ectasia becomes an extended fusiform aneurysm is often difficult to define objectively. The term *pseudoaneurysm* is used when the circumferential containment of the lumen by the arterial wall is lost to a substantial degree and is dependent on an improvised barrier of clot, adventitia, or surrounding tissues.

▶ EXTRADURAL ANEURYSMS AND PSEUDOANEURYSMS

Extradural aneurysms are unlikely to cause subarachnoid hemorrhage, unless they rupture with particular force against the dura. They are therefore, usually considered to be less immediately life-threatening than subarachnoid aneurysms. The commonest location for true aneurysms of the extradural carotid artery is in the cavernous segment.

Aneurysms of the Petrous and Cervical Segments of the Internal Carotid Artery

Aneurysms of the petrous and cervical segments are uncommon. They are sometimes seen in patients with connective tissue diseases. However, pseudoaneurysms in these areas are

encountered more frequently. They can be related to complications of posttraumatic or idiopathic dissection, parapharyngeal infection, infection of the petrous air cells, skull fracture, surgical or traumatic laceration, or tumor invasion. When complications of bleeding or embolic phenomena in the internal carotid artery territory occur, these lesions can constitute a serious risk to life. Bleeding from a petrous aneurysm may occur when erosion of the adjacent supporting bone permits rupture of the aneurysm into the middle ear or sphenoid sinus. These aneurysms or pseudoaneurysms may also present with mass effect as they bulge into adjacent structures, particularly the floor of the middle cranial fossa where they may compress branches of the trigeminal nerve.

Aneurysms of the Cavernous Segment of the Internal Carotid Artery

Aneurysms in this location are relatively common and are seen particularly in older patients. They may be fusiform or have a relatively defined neck. Frequently, there are variable degrees of intraluminal thrombus and atherosclerotic mural changes. They are often giant in size (>25 mm), in which case they are likely to present with mass effect and neuropathy of the paracavernous cranial nerves. They may rupture into the cavernous sinus and establish a carotid-cavernous fistula. It is uncommon for them to rupture into the subarachnoid or subdural spaces.

Cavernous aneurysms projecting medially into the sella turcica are thought to carry a particular risk of subarachnoid hemorrhage if they rupture, but even this phenomenon for aneurysms in this particular location is rare. Additional care is advised for large cavernous aneurysms when the support of the sphenoid sinus wall has become eroded. Rupture of an aneurysm in this direction is life-threatening due to exsanguinating epistaxis, a feature to bear in mind when reading the CT bone windows.

Most small cavernous aneurysms are incidental observations on angiographic or axial examinations. Asymptomatic cavernous aneurysms are usually not treated unless there is compelling evidence of imminent complications.

▶ FALSE ANEURYSMS OF THE INTRACRANIAL CIRCULATION

Cerebral aneurysms can be classified according to location, size, etiology, or configuration. When classified by



FIGURE 18-1. Fusiform aneurysm. A fusiform aneurysm (*arrows*) of the right middle cerebral artery involves the entire circumference of an extended segment of vessel. With an irregular appearance over a long segment of vessel, it is fairly probable that a dissection mechanism played a role in the genesis of this aneurysm.

the integrity or otherwise of their mural components, they can be separated into true aneurysms (intima and adventitia intact) or pseudoaneurysms. A pseudoaneurysm is one in which the wall of the artery has been perforated. The apparent lumen of the opacified aneurysm is contained by an organized extraluminal hematoma.

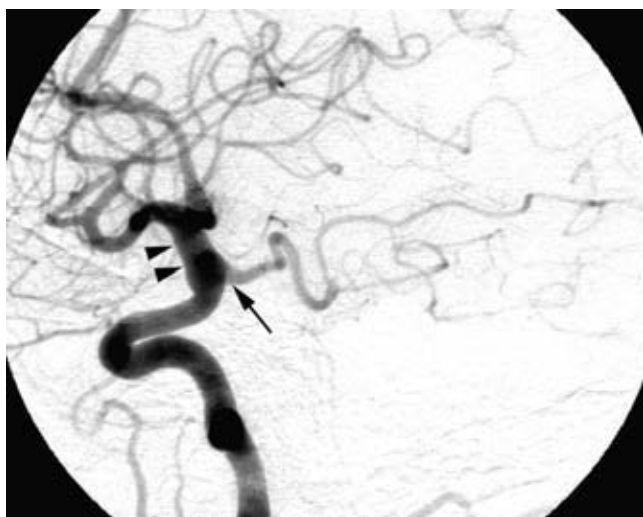


FIGURE 18-2. Mild dysplasia. The communicating segment of the supraclinoidal right internal carotid artery in this patient demonstrates mild ectasia (*arrowheads*) and an alteration in caliber, in contrast to the more proximal internal carotid artery. Infundibular widening (*arrow*) of the origin of the posterior communicating artery extends posteriorly from this segment.

Postsurgical Pseudoaneurysms

False aneurysms of the proximal or distal intracranial vessels after surgery are rare. They have been seen following vessel injury in the course of open or endoscopic sinus surgery (1–4), transsphenoidal pituitary procedures (5,6), stereotactic biopsy (7), or craniotomy for a variety of reasons (8).

Traumatic Intracranial Aneurysms

Pseudoaneurysms of the intracranial circulation may be seen as a result of penetrating or nonpenetrating head injuries (9), impaction on the vessel by bone fragments (10), or following surgical injury (11,12). They are typically seen in young males after severe injury to the head (Figs. 18-3 and 18-4), but more than 30% are identified in children (13,14). Posttraumatic lacerations of intracranial major vessels are often fatal, and in the past it would have been unusual for a patient so injured to reach medical attention.

A consistent theme in the literature dealing with posttraumatic pseudoaneurysms is that their discovery depends entirely on the index of suspicion of the managing physician. Without angiography, they frequently elude early detection. They can be present with subacute or delayed rebleeding or other complications, typically after a period of 1 or 2 weeks but possibly as long as months (9,15).

These injuries can be seen in the anterior or posterior circulation (16) and most frequently have a contiguous or related bone injury. Their discovery is usually associated with penetrating injuries in which the missile impact has scattered numerous fragments of bone or metal in diverging trajectories, particularly when fragments are seen close to the skull base (17).

Pseudoaneurysms in the setting of closed head injury have also been seen where no violation of the dura or skull is present (18). Pseudoaneurysms may be seen with closed head injury, particularly in children, when frontolateral shear injuries cause significant impaction of the pericallosal and callosomarginal branches against the falx cerebri, or of the middle cerebral artery against the sphenoid ridge (19). Traumatic aneurysms may account for 14% to 39% of intracranial aneurysms in the pediatric population (20). Traumatic intracranial pseudoaneurysms may be a more significant problem in military experience than in civilian life. While they were described as rare in the Korean and Vietnamese wars (21,22), experience in Lebanon and in the Iran–Iraq wars in the 1970s and 1980s indicates an incidence higher than once supposed (9,17,23,24), a trend that has become even more prominent with the high incidence of blast and penetrating head injuries casualties returning from the Iraq and Afghanistan wars (25–28). As many as 35% of military casualties from these conflicts who undergo cerebral angiography for vascular problems demonstrate intracranial or extracranial pseudoaneurysms, as well as other cerebrovascular complications such as vasospasm (29), vessel occlusions, or late development of carotid-cavernous fistulas (30).

Intracranial pseudoaneurysms also feature prominently in low-velocity civilian injuries, such as in South Africa where stabbing injuries to the head are more commonplace than in the Occidental urban experience. In stabbing victims, vascular injuries to the head may reach an incidence of

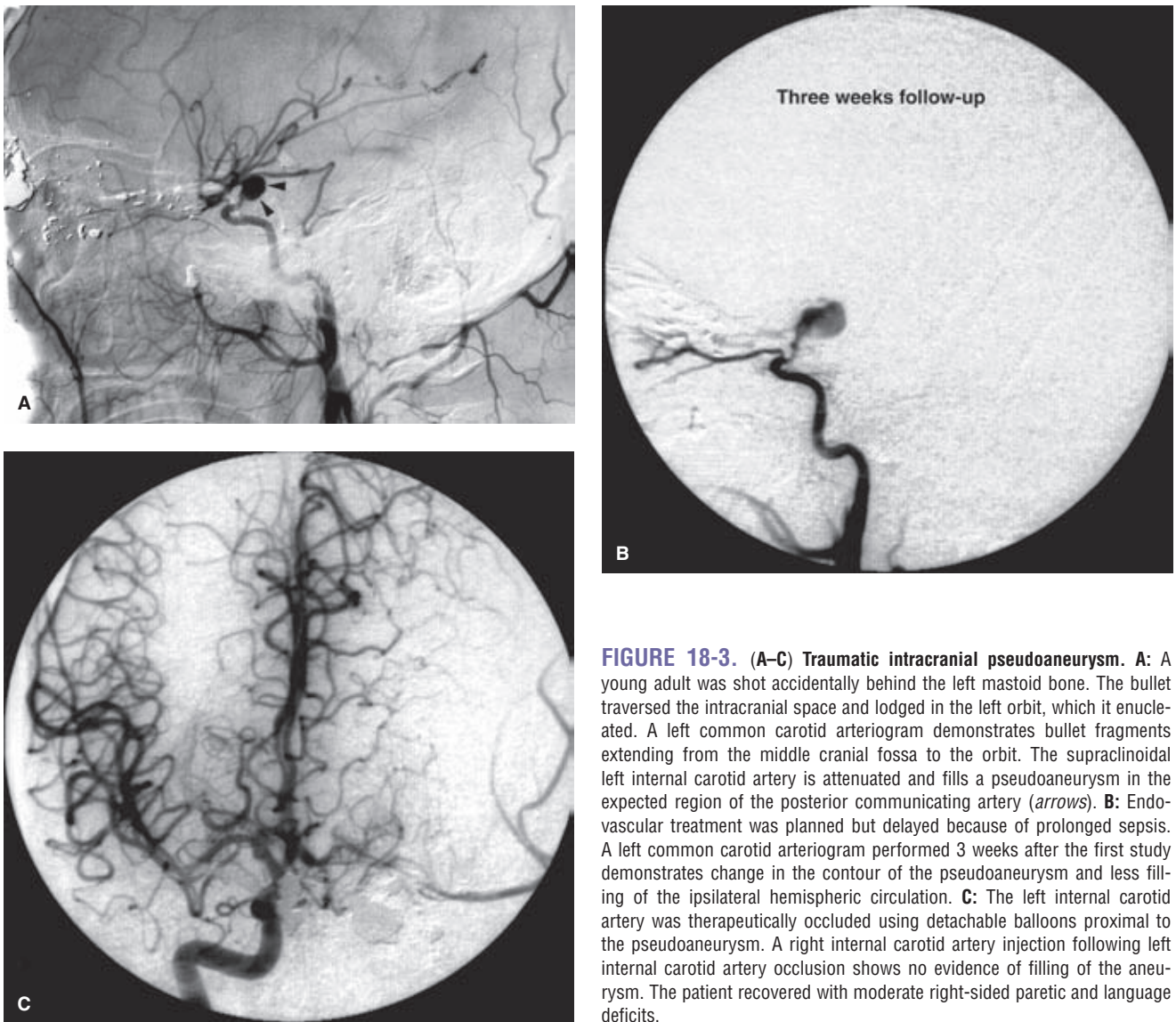


FIGURE 18-3. (A–C) Traumatic intracranial pseudoaneurysm. **A:** A young adult was shot accidentally behind the left mastoid bone. The bullet traversed the intracranial space and lodged in the left orbit, which it enucleated. A left common carotid arteriogram demonstrates bullet fragments extending from the middle cranial fossa to the orbit. The supraclinoidal left internal carotid artery is attenuated and fills a pseudoaneurysm in the expected region of the posterior communicating artery (*arrows*). **B:** Endovascular treatment was planned but delayed because of prolonged sepsis. A left common carotid arteriogram performed 3 weeks after the first study demonstrates change in the contour of the pseudoaneurysm and less filling of the ipsilateral hemispheric circulation. **C:** The left internal carotid artery was therapeutically occluded using detachable balloons proximal to the pseudoaneurysm. A right internal carotid artery injection following left internal carotid artery occlusion shows no evidence of filling of the aneurysm. The patient recovered with moderate right-sided paretic and language deficits.

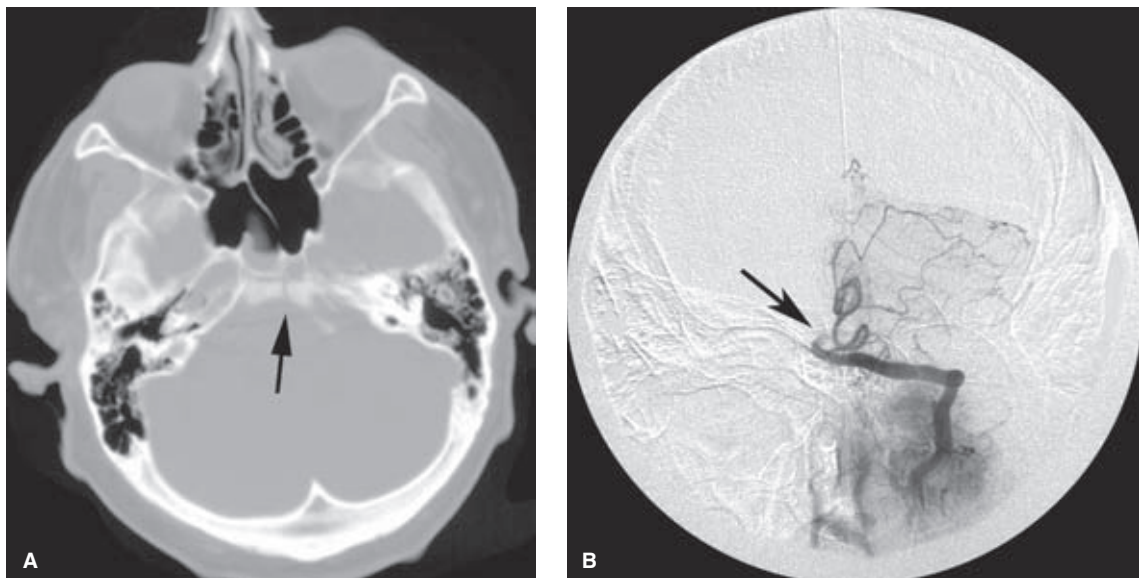


FIGURE 18-4. (A–B) Traumatic dissection and occlusion of the basilar artery. A young adult male involved in a high-velocity motor vehicle accident demonstrates a sagittally oriented fracture of the clivus (*arrow* in **A**). His left vertebral artery arteriogram demonstrated complete occlusion of the basilar artery (*arrow* in **B**) in its proximal segment, an injury from which no likelihood of a neurologic recovery could be countenanced.

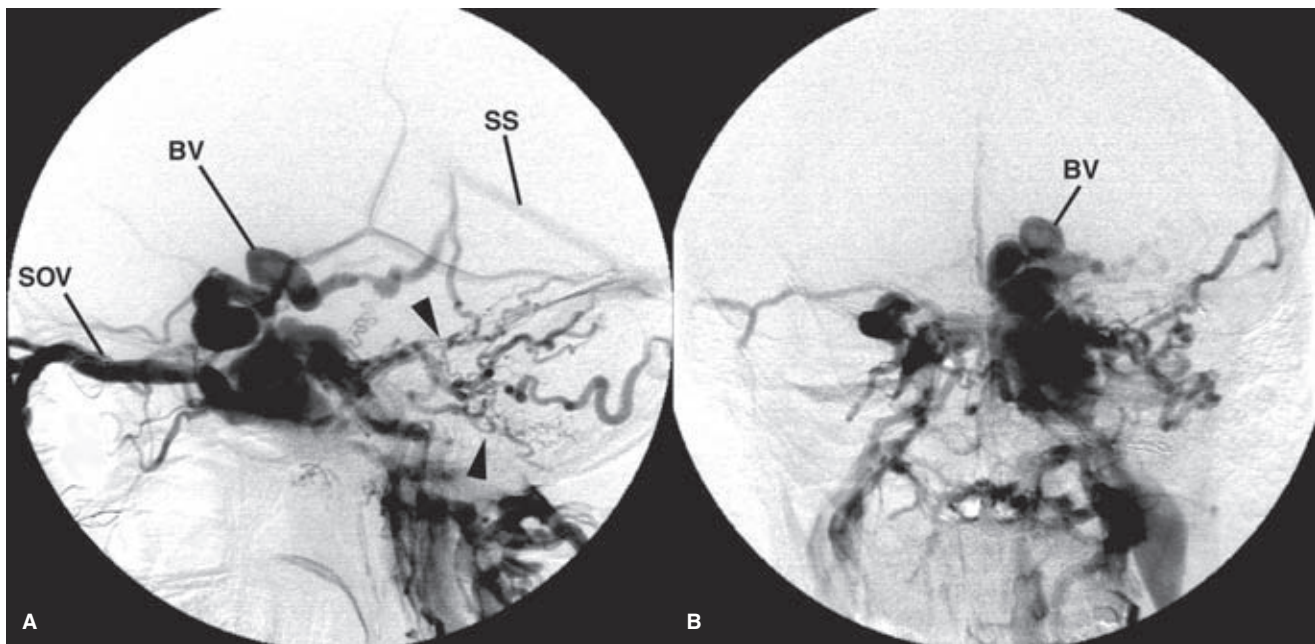


FIGURE 18-5. (A–B) Carotid cavernous fistula following trauma. Lateral (A) and PA (B) views of the left internal carotid artery injection in a young adult following severe head trauma. There is immediate and profuse opacification of venous structures due to fistulous flow from the cavernous internal carotid artery. Intercavernous connections fill the contralateral cavernous sinus. Although his symptoms were relatively mild, the angiographic appearance of varicose distention of the anterior segment of the basal vein (BV) and opacification of parenchymal veins of the posterior fossa (arrowheads) suggest that complications of venous hypertension may be imminent (SOV, superior ophthalmic vein; SS, straight sinus.)

30%, including pseudoaneurysms, dissections, fistulae, and occlusions (31).

Complications specifically related to false aneurysms include delayed rupture; mass effect on adjacent brain or cranial nerves; or an associated intraparenchymal, sub-arachnoid, or subdural hemorrhage. Delayed presentation may be seen months or even years following the initial injury (32). Acute or delayed complications of carotid injuries in the sphenoidal region include carotid cavernous fistulae and massive epistaxis from the sphenoidal sinus (Figs. 18-5 and 18-6).

Posttraumatic aneurysms represent a difficult management problem, as there is a significant risk of profuse bleeding at surgery when the dura is opened. Trapping of the pseudoaneurysm or occlusion of the parent vessel proximal to the laceration by surgical or endovascular means may represent the best therapeutic option in certain circumstances (25,27,33).

Immediate angiography for patients with penetrating head injuries is likely prudent as approximately 12% to 35% of such patients will have an intracranial pseudoaneurysm (29,34). Follow-up angiography may be necessary for patients in whom spasm or other vascular abnormalities preclude adequate evaluation.

► FUSIFORM INTRADURAL ANEURYSMS

Fusiform aneurysms are frequently associated with vessel tortuosity, hypertension, atherosclerosis, and advancing age. They typically affect the cavernous or supraclinoidal internal carotid artery and the basilar trunk. They often

present with symptoms related to mass effect (Fig. 18-7). With large aneurysms, stagnation of blood can lead to thrombus formation, and patients may present with embolic stroke (35,36). Rupture is not common when the condition is mild (37). Surgical management of a ruptured fusiform

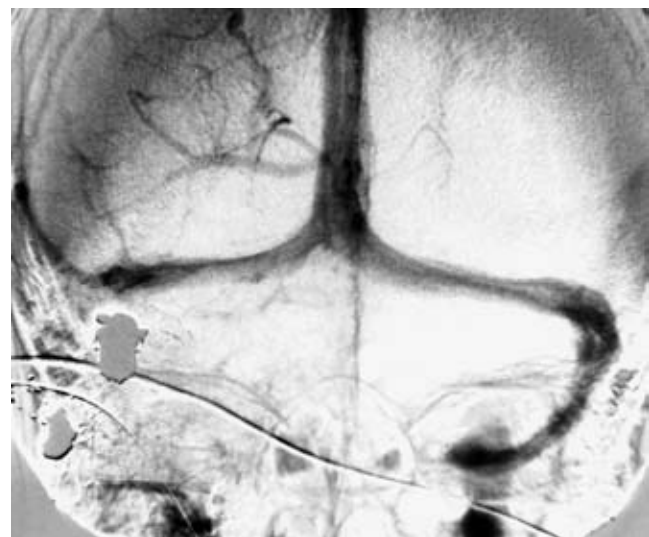


FIGURE 18-6. Remember to examine the venous structures when evaluating penetrating missile injuries. Venous injury may follow penetrating injuries. In this patient, the right transverse sinus has been occluded by bullet fragments lodged in the right mastoid bone.



FIGURE 18-7. Fusiform dysplasia/aneurysm of the basilar artery. Changes of this degree are frequently associated with a history of longstanding hypertension. Vessel changes may be more extreme than indicated on an angiogram. Circumferential thrombus augments the degree of mass effect on surrounding structures.

segment of vessel can be difficult (38). Techniques, including wrapping, proximal occlusion, or bypassing, must make allowance for preserving important perforator vessels, which might take origin from the dysplastic segment (39). Endovascular treatment with flow-diverting stents, such as Pipeline or Silk, will undoubtedly play more of a role in the treatment of these difficult lesions in the future (40–43).

When ectasia of the basilar artery reaches bizarre proportions, the terms *megadolichobasilar anomaly* or *giant fusiform aneurysm* are used (Fig. 18-8) (36,44). They represent less than 1% of intracranial aneurysms. Although they are classically described as affecting the vertebrobasilar circulation, giant fusiform or serpentine aneurysms are also seen in the anterior circulation (39) (Fig. 18-8). This group of usually elderly patients typically presents with mass effect, brainstem compression, cranial nerve deficits, obstructive hydrocephalus, subarachnoid hemorrhage, and embolic strokes due to stagnation of blood. Underlying, partially healed dissection likely explains the genesis of many of these aneurysms (45). Furthermore, long-term clinical follow-up of this group of patients indicates a poor prognosis due to recurrent subarachnoid hemorrhage or progressive mass effect.

▶ MYCOTIC AND INFLAMMATORY ANEURYSMS

Mycotic aneurysms are classically described as occurring distally in the cerebral circulation and as being not necessarily related to vessel bifurcation points. They may be subtle in appearance and are frequently best seen in the parenchymal phase of the injection when the arteries are already washing out.

Intracranial aneurysms of inflammatory origin may be of several types: Bacterial; syphilitic (Heubner arteritis); related to angiocentric organisms such as mucormycosis, aspergillus (46), or other fungi; or associated with systemic arteritides such as giant cell arteritis, human immunodeficiency virus (HIV), and polyarteritis nodosa (Fig. 18-9).

In the modern era, an increased incidence of aneurysms related to HIV or its associated infections has been described. This may be primarily due to a necrotizing vasculitis related to the virus itself, particularly in congenital infections, or due to acquired diseases such as tuberculosis or syphilis (47–49).

Presentation and Incidence of Mycotic Aneurysms

Mycotic intracranial aneurysms present most commonly with acute subarachnoid hemorrhage or intraparenchymal hematoma developing as a complication of already established septic disease. Occasionally, young patients may present with an embolic neurologic deficit, such as hemiplegia, as the presenting event of bacterial endocarditis (Figs. 18-10 and 18-11) (50). Other common presentations include seizure or focal neurologic signs due to vasculitis or vegetative emboli in an area of the brain distal to a silent aneurysm (51). Direct vessel invasion from adjacent infected paranasal sinuses may also be seen (Figs. 18-12 and 18-13).

Although mycotic aneurysms are typically described as being found in unusual peripheral locations, multiple in number, and not necessarily related to vessel bifurcations, this archetype is not always valid (52). They may be single in presentation and centrally located. Mycotic aneurysms can be seen in the cavernous carotid artery when a systemic illness is complicated by cavernous thrombophlebitis (53). When an aneurysm is seen in an unusual peripheral location, the possibility of an infectious embolic etiology should be considered, but not all mycotic aneurysms are atypical in appearance or location.

Bacterial aneurysms were typically associated with bacterial endocarditis when this disease was more common but can be seen with any septicemic state, particularly with respiratory infections. Older studies suggest that the incidence of intracranial aneurysms in patients with endocarditis varies between 4% and 15% or perhaps higher, and many of these aneurysms remain asymptomatic (53,54).

Mycotic aneurysms are related to impaction of a septic embolus in the intima of a peripheral cerebral artery with development of a resulting arteritis, focal mural necrosis, and aneurysm formation. This explains the friable nature of the wall of these lesions and their propensity to bleed spontaneously or during surgery.

(text continues on page 256)

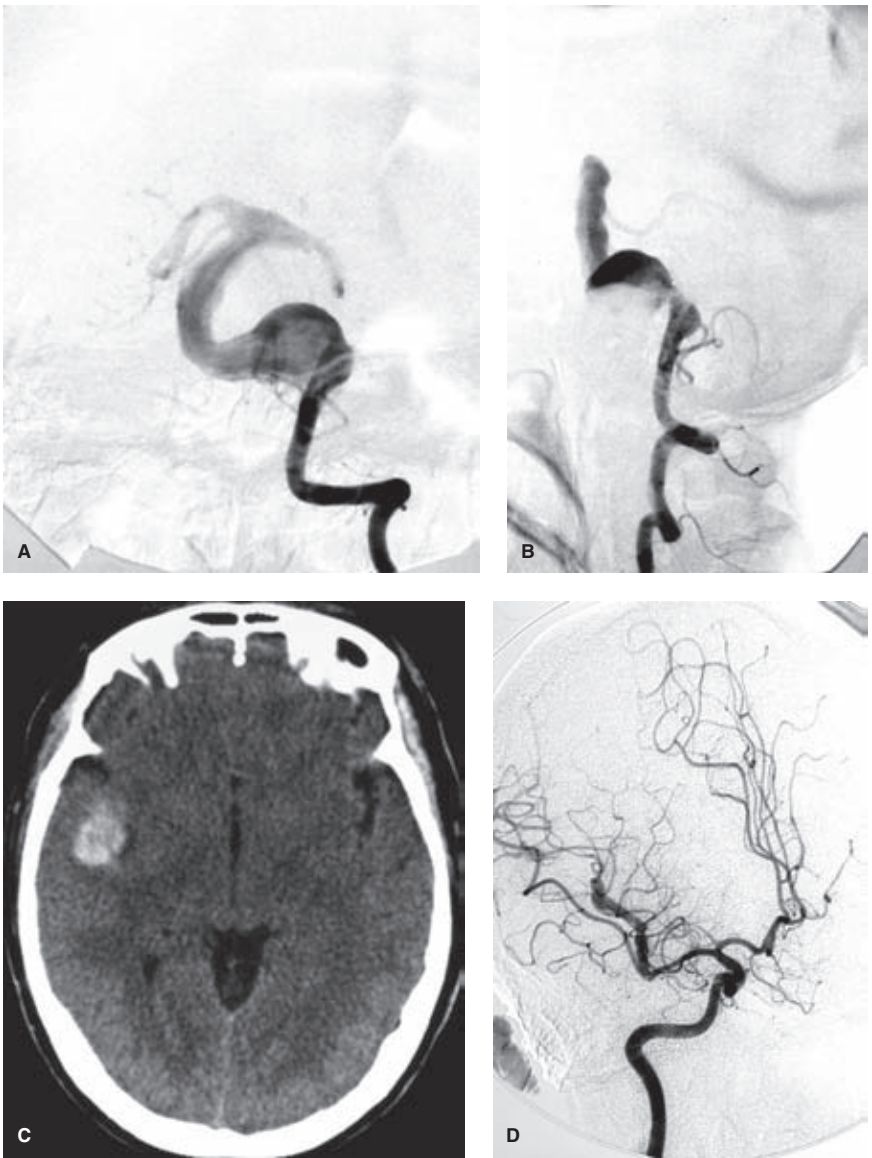


FIGURE 18-8. (A–D) Megadolichoectatic basilar artery and serpentine aneurysm. (Two cases) Townes (A) and lateral (B) projections of a megadolichoectatic basilar artery in an elderly hypertensive patient. A CT scan of the head (C) in a young adult presenting with sudden headache demonstrates a focal collection of blood in the right Sylvian fissure. An oblique RAO view (D) of the right internal carotid artery injection demonstrates an elongated fusiform or “serpentine” aneurysm of the parietal branch of the right middle cerebral artery.

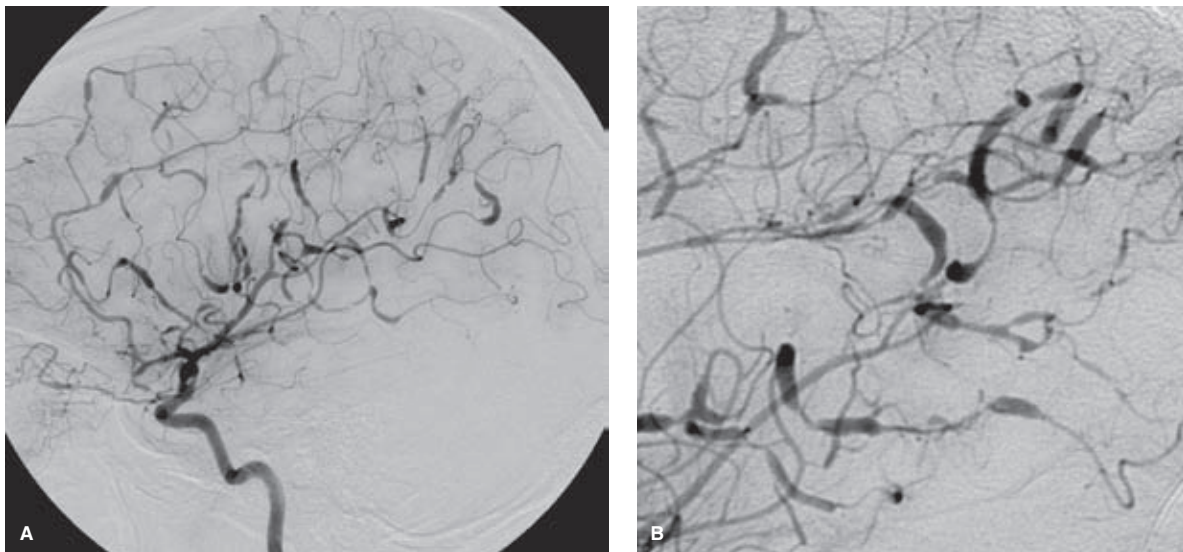


FIGURE 18-9. (A–B) HIV-associated arteriopathy. A middle-aged patient with advanced complications of HIV and fluctuating neurologic deficits showed subtle pial enhancement on a gadolinium enhancement MRI (not shown) but no confirming evidence of a meningitis or cerebritis could be found. An angiogram of the left internal carotid artery (A) and magnification view of the right internal carotid artery (B) showed diffuse arterial disease characterized by aneurysmal dilatation of multiple segments of arteries through the anterior circulation. In the absence of an identifiable other cause, this arterial disease was assumed to be a direct effect of the HIV virus itself.

FIGURE 18-10. (A–B) Mycotic aneurysm of the right middle cerebral artery. A young patient with known bacterial endocarditis had a change in mental status and a CT scan (A) demonstrated a hemorrhagic masslike region in the parietal lobe of the right hemisphere. A right common carotid artery angiogram (B) demonstrates a mycotic aneurysm of the parietal branch of the right middle cerebral artery, which was assumed to be embolic from the primary site of endocarditis.

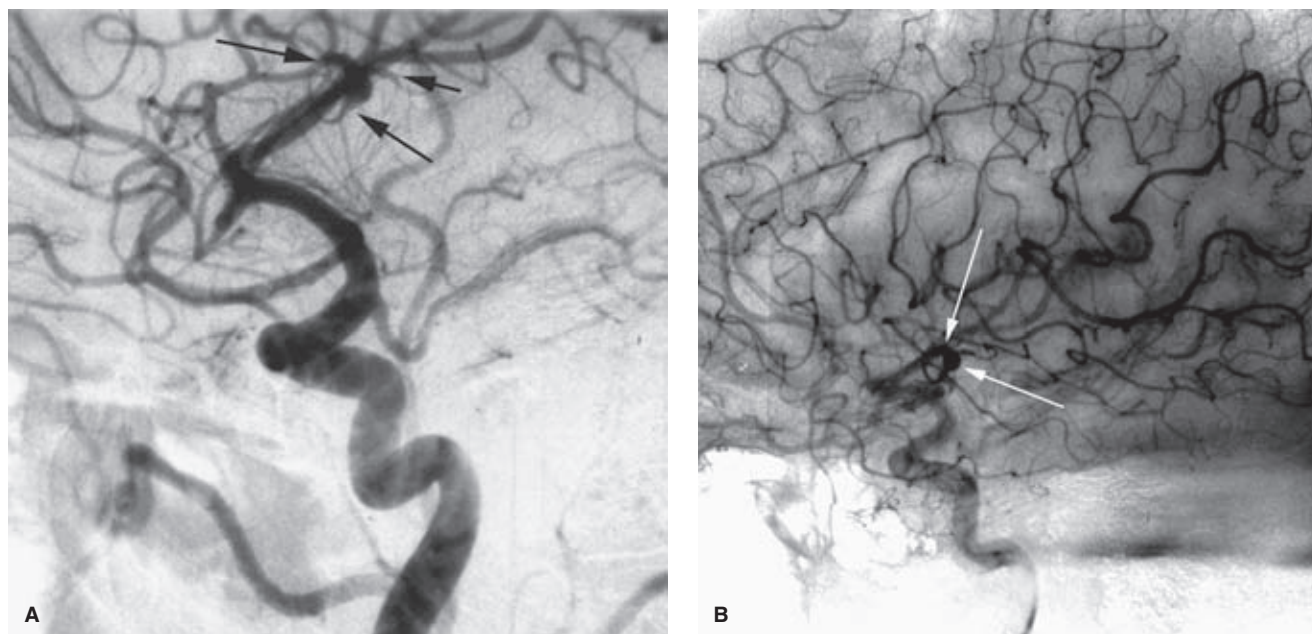
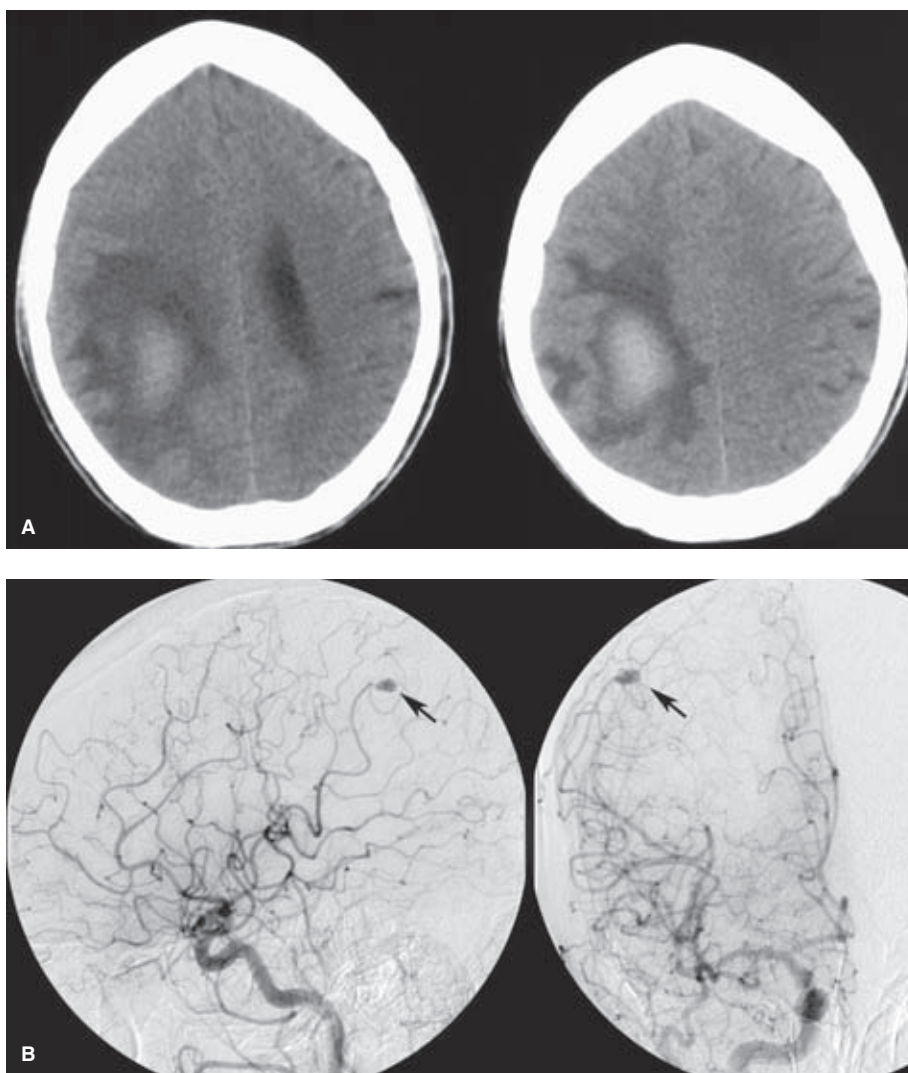


FIGURE 18-11. (A–B) Mycotic aneurysm of the right middle cerebral artery. This peripheral aneurysm (arrows) in a patient with infective endocarditis is demonstrated on a skewed lateral view (A). The aneurysm has a fusiform, tapered appearance extending into adjacent branches. Small peripheral mycotic aneurysms are frequently best seen on a late arterial phase when the main arterial structures have begun to lose density (B).

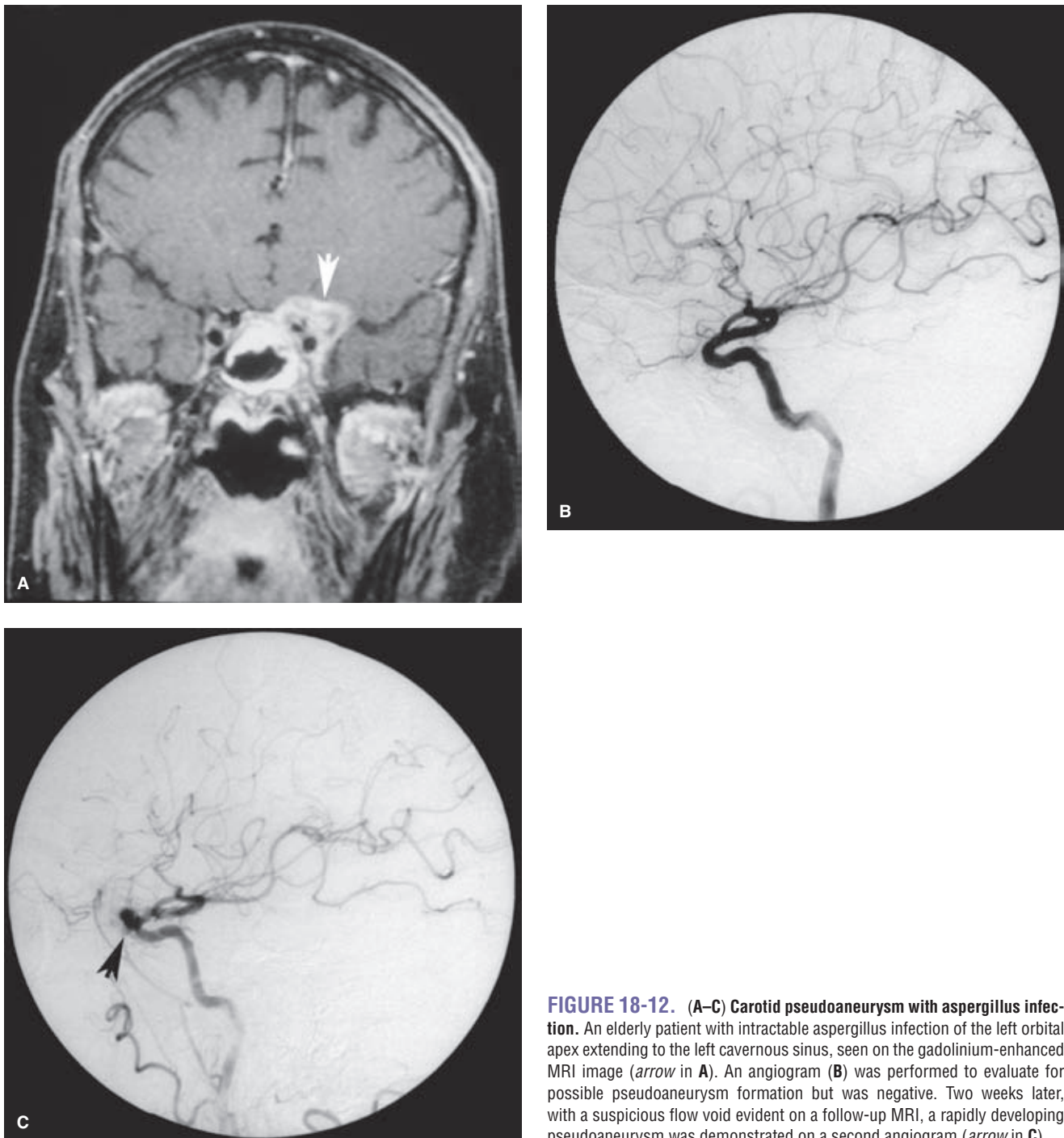


FIGURE 18-12. (A–C) Carotid pseudoaneurysm with aspergillus infection. An elderly patient with intractable aspergillus infection of the left orbital apex extending to the left cavernous sinus, seen on the gadolinium-enhanced MRI image (*arrow* in **A**). An angiogram (**B**) was performed to evaluate for possible pseudoaneurysm formation but was negative. Two weeks later, with a suspicious flow void evident on a follow-up MRI, a rapidly developing pseudoaneurysm was demonstrated on a second angiogram (*arrow* in **C**).

Role of Endovascular Intervention in Management of Mycotic Aneurysms

Some inflammatory aneurysms, a third or more in some series, tend to regress with treatment of the primary infection (45–47) (55–57). Possibly as many as a third of them will resolve spontaneously with medical treatment alone (52,55). Better results are seen in patients with single, unruptured aneurysms. Sequential angiography in patients with infective endocarditis may be reasonable where a high index of suspicion for development of lesions, even in the

setting of active treatment, much be maintained. Surgical evacuation of ruptured aneurysms with hematoma and endovascular treatment of unruptured aneurysms are typically necessary when medical management fails (51,58–60).

► ONCOTIC INTRACRANIAL ANEURYSMS

Invasion of the intracranial vessel wall with destruction of the internal elastic lamina and cavitation with aneurysm or pseudoaneurysm formation is a rare but well-recognized event from metastatic deposits of atrial myxoma,

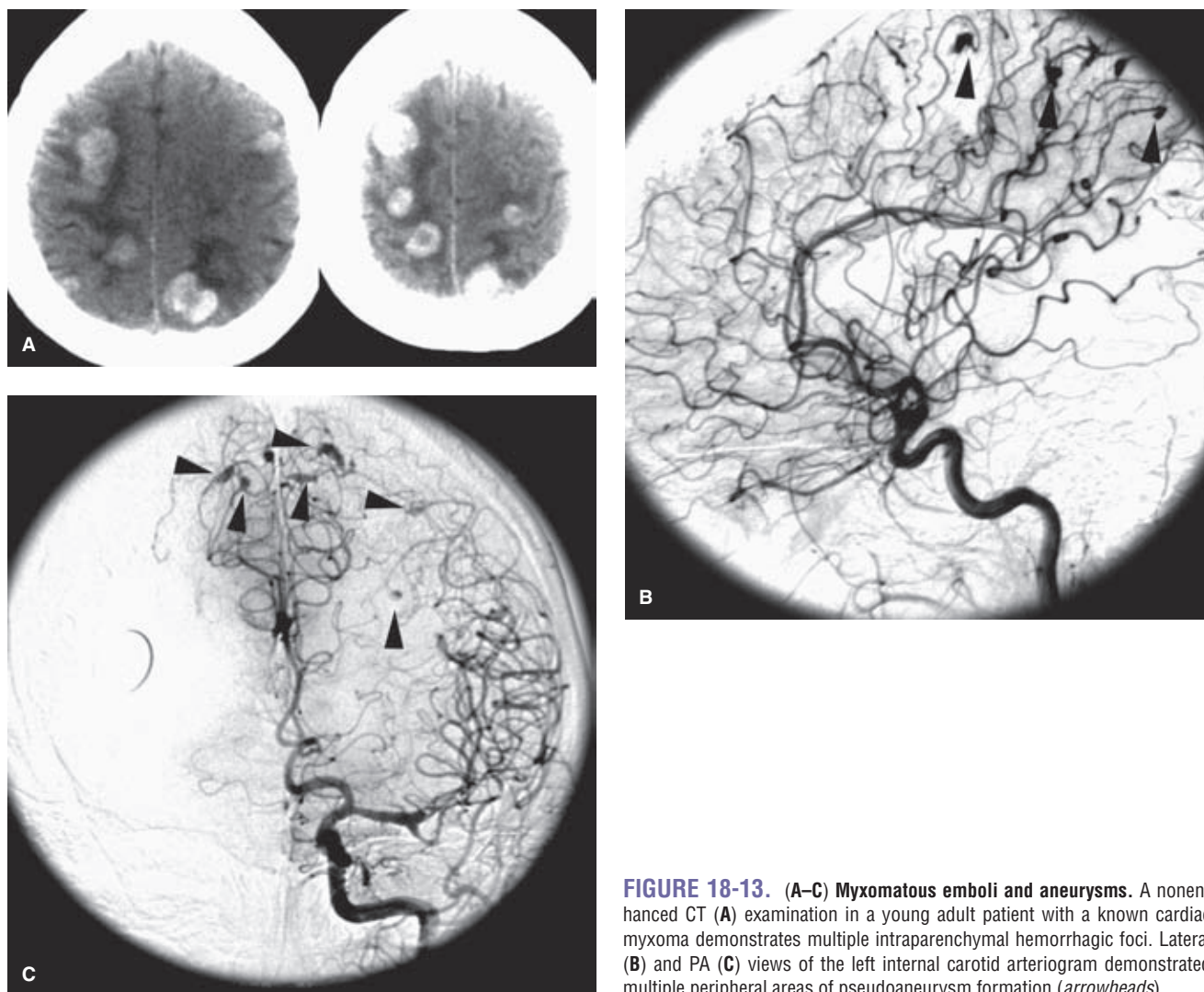


FIGURE 18-13. (A–C) Myxomatous emboli and aneurysms. A non-enhanced CT (A) examination in a young adult patient with a known cardiac myxoma demonstrates multiple intraparenchymal hemorrhagic foci. Lateral (B) and PA (C) views of the left internal carotid arteriogram demonstrated multiple peripheral areas of pseudoaneurysm formation (*arrowheads*).

choriocarcinoma (61,62), renal cell carcinoma, or bronchogenic carcinoma (63–65). Invasion of arteriolar walls by gliomatous tumors may explain the very rare association of false aneurysms with primary brain tumors (66). Features shared by oncotic aneurysms are that they may be delayed at the onset (i.e., they may not be seen on an initial angiogram), may be multiple, may grow rapidly, or may thrombose spontaneously. They may resolve with chemotherapy for the primary lesion (67).

Left atrial myxoma may be complicated by or present with neurologic symptoms related to arterial obstruction by myxomatous emboli or intracranial aneurysmal rupture with subarachnoid or intraparenchymal hemorrhage (Fig. 18-13) (68–70). The destructive and invasive nature of the histologic findings with embolization of cardiac myxoma is ascribed to the high degree of elaboration of matrix metalloproteinases and interleukin-6 by this tumor (71,72). Although this is a rare clinical presentation, it is a treatable disease that can be seen in otherwise healthy young patients. Systemic emboli from myxoma have been reported in up to 45% of patients, one-half of these going to the cerebral circulation (73). The diagnosis may be delayed due to the initially small size of the cardiac tumor (74). Angiographic

features described in these patients include intraluminal filling defects, fusiform or saccular peripheral aneurysms, vessel occlusions, and delayed passage of contrast. Some peripheral aneurysms may be extremely subtle and could be missed if not looked for carefully on the late arterial or parenchymal angiographic phase.

▶ INTRACRANIAL DISSECTIONS AND DISSECTING ANEURYSMS

Dissection of intracranial vessels, once considered an extremely rare disease (75), is now a more recognized entity representing as many as 3% to 7% of patients presenting with nontraumatic subarachnoid hemorrhage and possibly as many as 50% of aneurysms in the younger pediatric age group (76–81). In general this phenomenon is a devastating disease when the presentation is hemorrhagic with a mortality rate between 17% and 46% or more (78,82). Intracranial dissections are usually clinically idiopathic but have been reported after head trauma, electrocution, with syphilitic and other arteritides of the intracranial vessels, and with conditions such as polyarteritis nodosa, fibromuscular



FIGURE 18-14. Intracranial dissection in a child. Dissections (*arrows*) in children have a predilection for the supraclinoid internal carotid artery. They may be idiopathic or follow trauma. Hemispheric ischemia is the most common presenting event in this age group.

dysplasia, and migraine (Figs. 18-14–18-17). Before 1950, more than one-half of recognized cases were associated with the meningovascular phase of syphilis (Heubner endarteritis), a disease seen now as a result of the AIDS epidemic. Some cases of intracranial dissection in older patients might be related to rupture of intramural arteriosclerotic plaques, but this is unlikely to be an explanation for this disease in younger patients (83).

Intracranial dissections are more common in the posterior than in the anterior circulation (Fig. 18-18). Patients typically present in two different ways, either with an acute subarachnoid hemorrhage related to rupture of the arterial pseudoaneurysm or with nonhemorrhagic complication such as suboccipital headache, mass effect, focal neurologic deficits, or ischemic complications (84). Patients presenting with nonhemorrhagic complications have a much better outcome, whereas those with pseudoaneurysms or subarachnoid bleeding account for most of the mortality associated with this disease. The media and adventitia of the intradural vertebral and carotid arteries are thinner than in the extracranial vessels. Therefore, arterial rupture with subarachnoid hemorrhage as a complication of intracranial dissections is more likely to develop than is the case with extracranial dissections. Intracranial vessels lack an external elastic membrane and have fewer elastic fibers in the media (85).

Furthermore, the intracranial arteries are relatively deficient in vasa vasorum (86). Poor healing of intracranial vessels due to the lack of vasa vasorum may be part of the explanation for the greater likelihood of complications in many diseases of these vessels compared with extracranial vessels. In autopsy specimens of intracranial dissection with subarachnoid hemorrhage, extension of clot between the media and adventitia is seen with destruction of all three mural layers (77,87). Intracranial dissections usually affect the major vessel trunks of the circle of Willis, less commonly in the distal vessels (88).

Dissections in the anterior domain of the circle of Willis are less common than in the posterior, and have a predilection for the carotid terminus in children and young adults (76,89,90). Patients may have a variable course after the initial ictus of hemispheric ischemia. Massive infarction and swelling with herniation is the mechanism of death when the deterioration is rapid (91). When vascular occlusion is only partial, patients can survive with variable deficits (Fig. 18-19).

Intracranial dissections can be recognized angiographically by an irregular tapering of the vessel lumen, a linear filling defect within the lumen, retention of contrast within the wall of the vessel, or by the presence of an irregular aneurysm or pseudoaneurysm associated with focal luminal narrowing or irregularity (92–94). The angiographic and MRA appearance of the dissected vessel is sometimes described as a “pearl and string” sign, referring to the appearance of fusiform dilatation interrupted by segments of stringlike narrowing (Figs. 18-16 and 18-17). In a small number of patients, a double set of parallel lumens may be seen angiographically (75).

It is important to distinguish dissecting aneurysms from saccular bifurcation aneurysms, as the treatment may be different. Even with good-quality angiography, the signs of intracranial dissection may be subtle. The possibility of a dissection as a source for subarachnoid hemorrhage should be borne in mind during aneurysm search studies. The disease may be bilateral in the vertebrobasilar system in 5% to 10% of cases (95). Optimal treatment for dissecting extradural and intradural aneurysms sometimes involves altering or eliminating, if possible, the flow pattern in the vessel around the pseudoaneurysm. This hemodynamic alteration will suppress the inflow jet. This can be done by surgical clipping of the vessel or vessel reimplantation (96). Endovascular techniques include coiling of the pseudoaneurysm, stenting the vessel, trapping the pseudoaneurysm or occluding the parent vessel proximally, if the patient’s collateral flow will tolerate such a procedure (Fig. 18-20) (97–105). It is important to perform this occlusion as close as possible to the aneurysm to eliminate the possibility of continued anterograde flow through collateral vessels (106). Without treatment, dissecting aneurysms with subarachnoid hemorrhage have a rebleed risk reported to be between 30% and 70% (78,107–109). Therefore, immediate treatment of intracranial dissecting pseudoaneurysms is advised bearing in mind that ruptured dissecting aneurysms are extremely fragile with a significant risk of intraprocedural rebleeding. The possibility of spasm from subarachnoid hemorrhage related to this disease may affect the efficacy of collateral vessels where vessel occlusion is planned. Dissections without subarachnoid hemorrhage may do well without surgical intervention, *(text continues on page 264)*

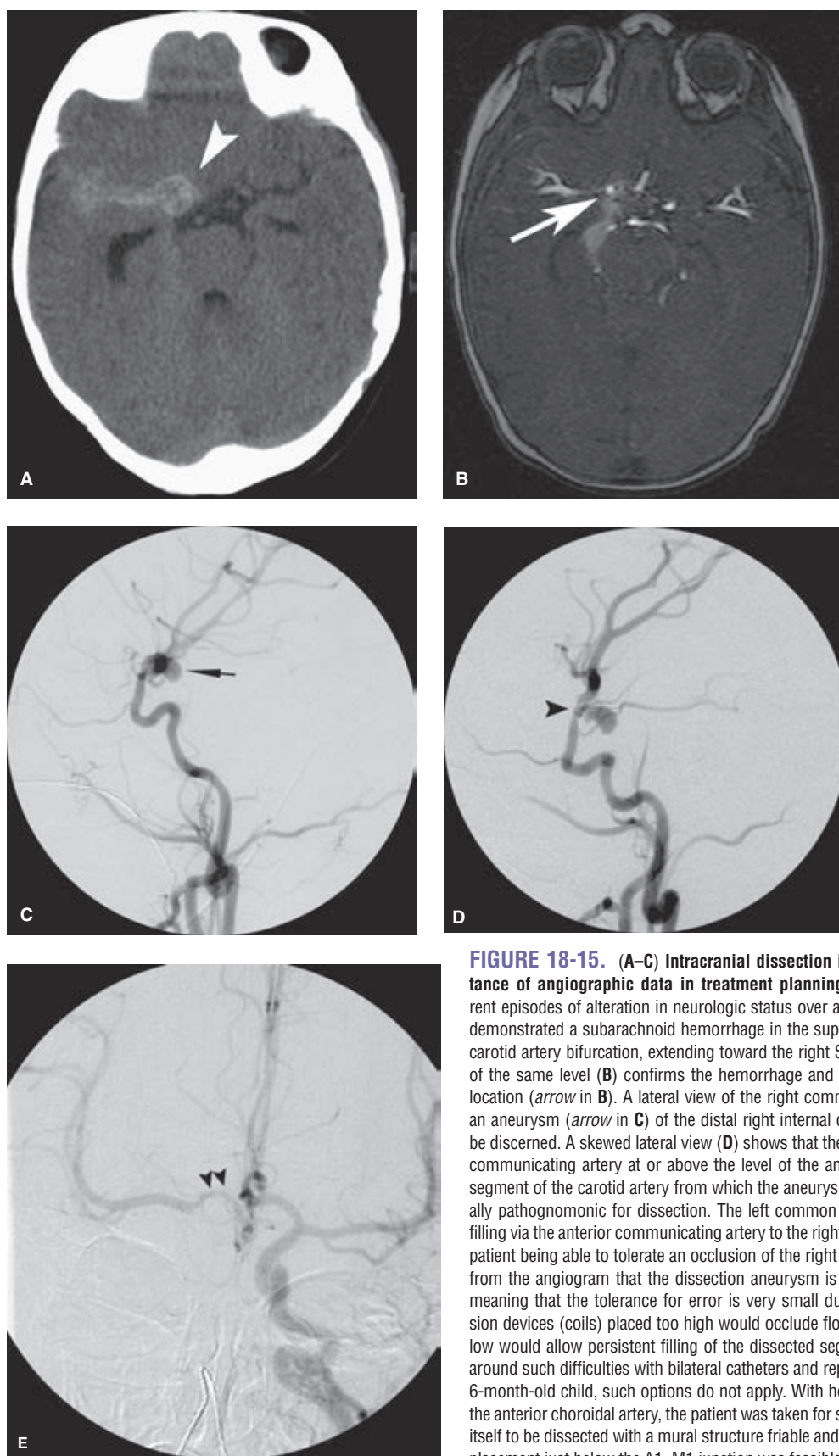


FIGURE 18-15. (A–C) Intracranial dissection in a 6-month-old child and the importance of angiographic data in treatment planning. A young infant presented with recurrent episodes of alteration in neurologic status over a 2-week period. Her second CT scan (A) demonstrated a subarachnoid hemorrhage in the suprasellar cistern close to the right internal carotid artery bifurcation, extending toward the right Sylvian region (*arrowhead* in A). An MRA of the same level (B) confirms the hemorrhage and raises suspicion of an aneurysm in that location (*arrow* in B). A lateral view of the right common carotid artery angiogram (C) shows an aneurysm (*arrow* in C) of the distal right internal carotid artery, but its exact origin cannot be discerned. A skewed lateral view (D) shows that the aneurysm is arising above the posterior communicating artery at or above the level of the anterior choroidal artery. Furthermore, the segment of the carotid artery from which the aneurysm arises is narrowed and irregular, virtually pathognomonic for dissection. The left common carotid artery injection (E) shows cross filling via the anterior communicating artery to the right A1 (*arrowheads* in E), auspicious for the patient being able to tolerate an occlusion of the right internal carotid artery. It can be deduced from the angiogram that the dissection aneurysm is very close to the right A1–M1 junction, meaning that the tolerance for error is very small during an endovascular procedure. Occlusion devices (coils) placed too high would occlude flow to the middle cerebral artery while too low would allow persistent filling of the dissected segment. In an adult patient, one can work around such difficulties with bilateral catheters and repeated test injections of contrast, but in a 6-month-old child, such options do not apply. With hopes of preserving the carotid artery and the anterior choroidal artery, the patient was taken for surgical exploration, but the artery proved itself to be dissected with a mural structure friable and tattered beyond repair. Fortunately, a clip placement just below the A1–M1 junction was feasible with a successful outcome.

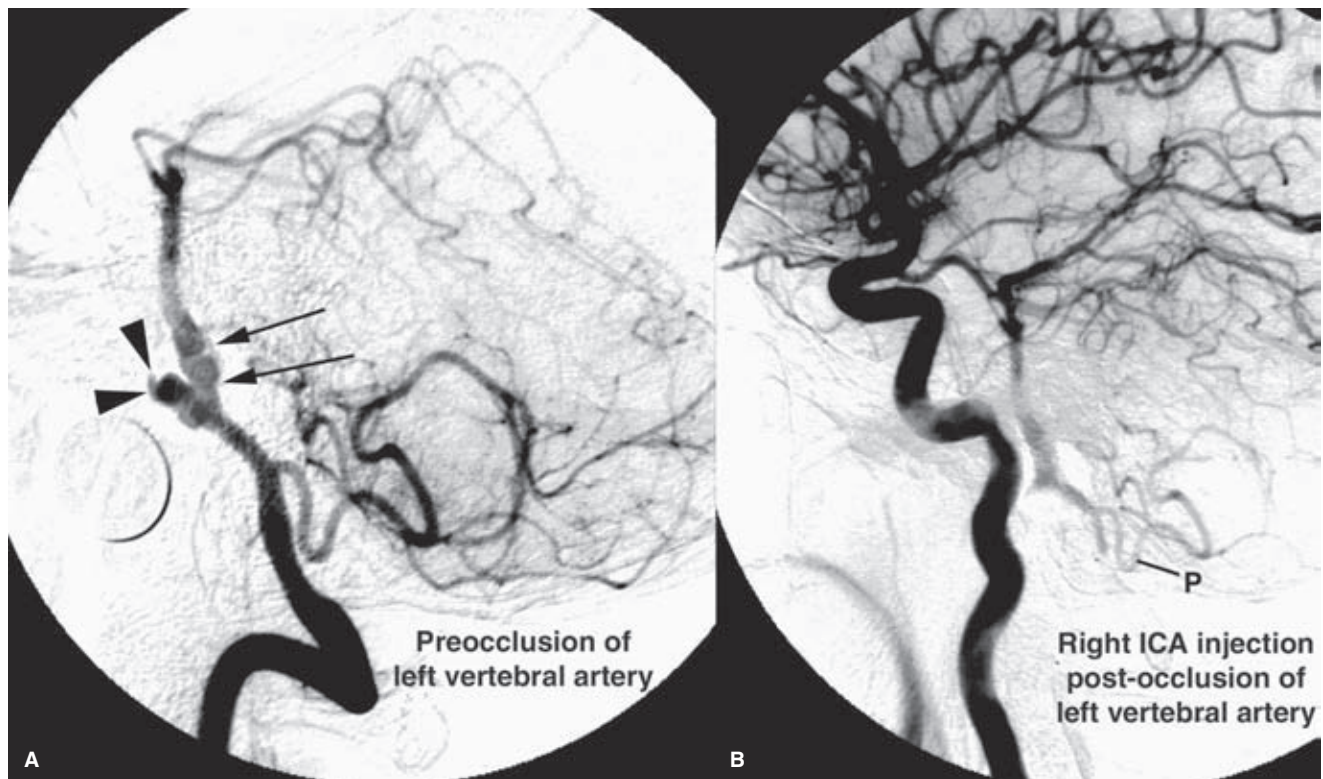


FIGURE 18-16. (A–B) Dissecting aneurysm of the distal left vertebral artery. A middle-aged male presenting with Grade II subarachnoid hemorrhage was found to have a sharply cornered aneurysm (*arrowheads*) projecting from an irregular segment (*arrows*) of the vertebrobasilar junction, indicating a dissection. The right vertebral artery did not supply flow to the basilar artery. The patient was treated successfully by balloon occlusion of the left vertebral artery. This resulted in reversal of flow down the basilar artery altering the hemodynamic stress on the ruptured dissection. The procedure jeopardized supply to the left posterior inferior cerebellar artery (*P*). A right carotid injection during placement of the first balloon in the left vertebral artery (prior to detachment) demonstrated adequate filling of the posterior inferior cerebellar artery, and the patient showed no neurologic deficit to suggest posterior fossa ischemia. Consequently, balloon occlusion of the left vertebral artery was executed. The patient made an excellent recovery.

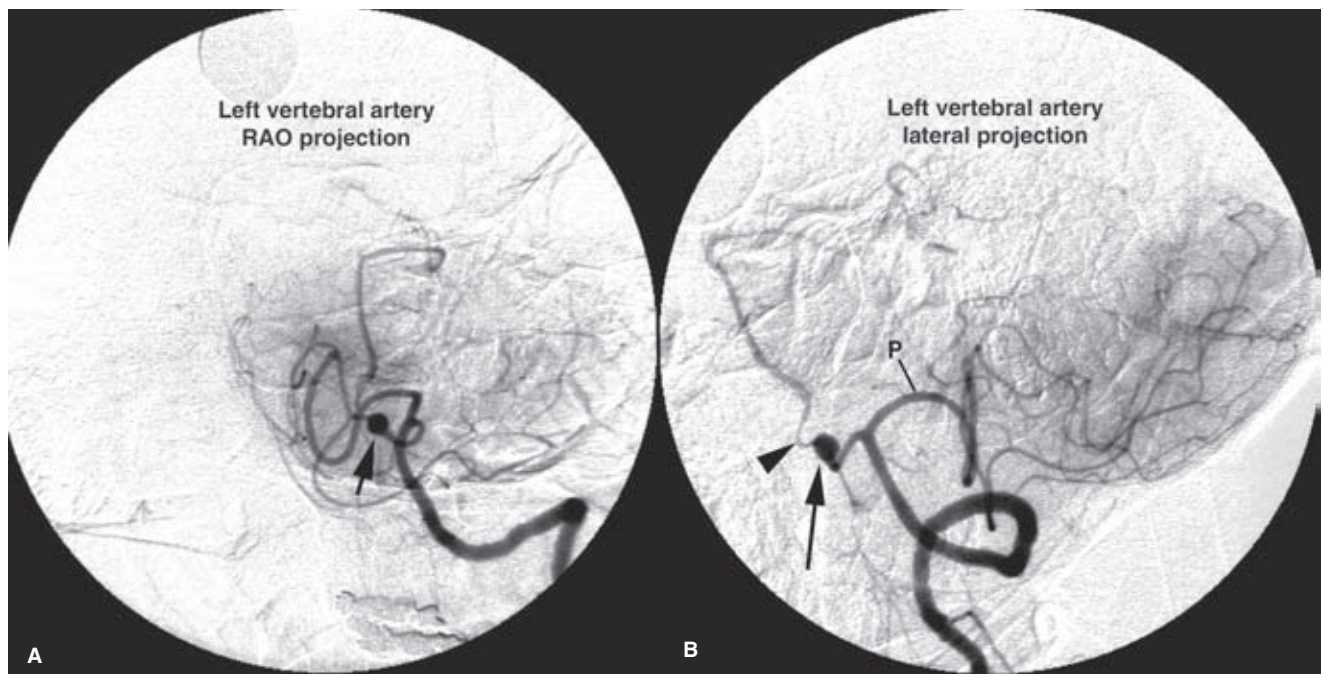


FIGURE 18-17. (A–B) Unruptured left vertebral artery dissection. A middle-aged female with complaints of headaches was found to have a suspicious flow void on MRI examination (not shown). A dissection at the vertebrobasilar junction demonstrated a focal area of aneurysmal widening (*arrow*) associated with extreme narrowing of the proximal basilar artery (*arrowhead*) above that level (“string and pearl”). The overlapping posterior inferior cerebellar artery (*P*) made the standard PA and Townes views difficult to interpret. The anatomy of the vertebrobasilar junction was clarified by these obliqued and skewed images.

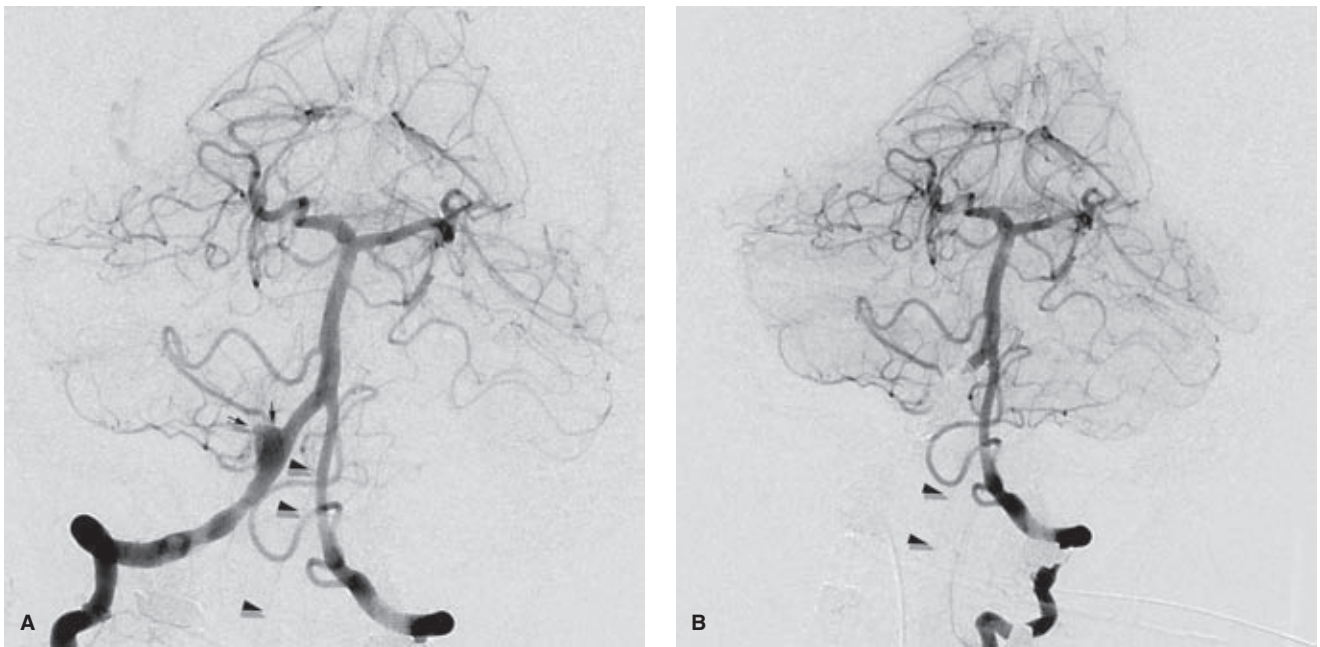


FIGURE 18-18. (A–B) Dissecting aneurysm of the right vertebral artery treated by trapping. A middle-aged female patient presented with a severe subarachnoid hemorrhage related to an irregular aneurysm (*small arrows* in **A**) of the right vertebral artery. The location and configuration are typical of intracranial dissecting aneurysms. The aneurysm was thought too fragile to withstand stent and coil occlusion. In planning a sacrifice of the right vertebral artery, the absence of a right posterior inferior cerebellar artery on the diseased segment was fortunate, although the status of the anterior spinal artery (*small arrowheads* in **A**) had to be considered. Following coil occlusion of the disease segment on the right, a left vertebral artery injection (**B**) shows reflux into the right vertebral artery stump, but no evidence of penetration into the coil mass. The anterior spinal artery (*arrowheads* in **B**) has been preserved. The patient made a promising recovery from the acute presentation and procedure, but eventually succumbed to complications of severe cerebral vasospasm and bowel strangulation.

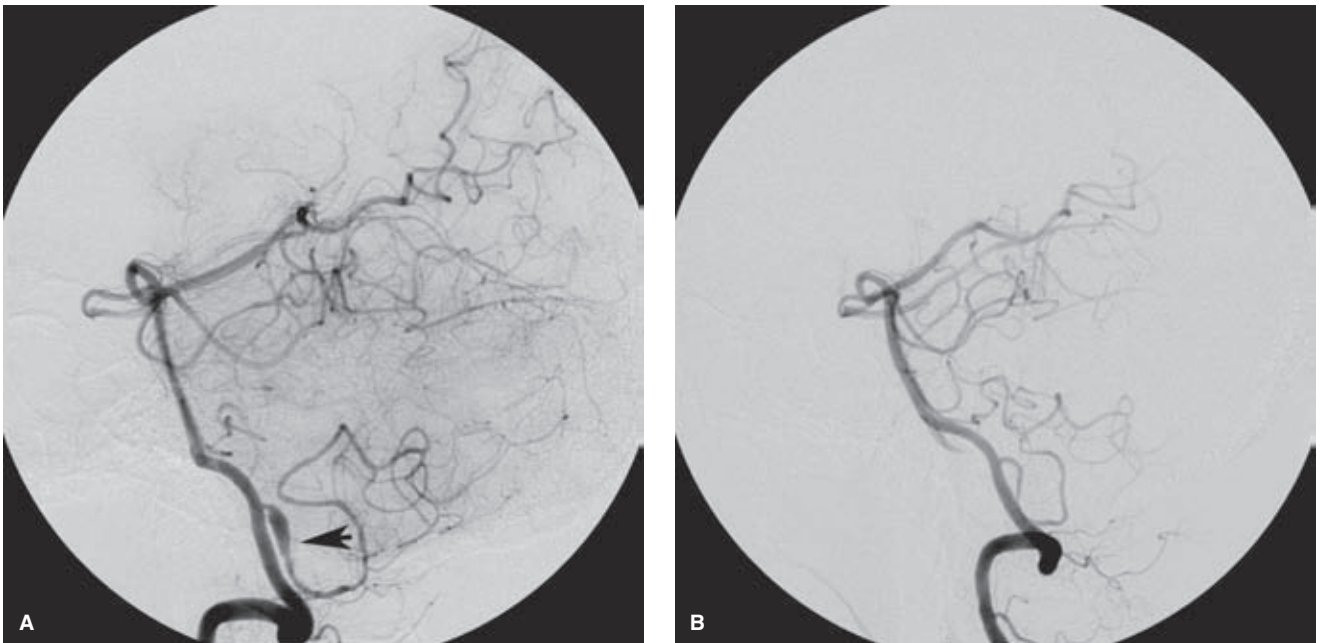


FIGURE 18-19. (A–B) Three-month follow-up of an unruptured dissection of the left posterior inferior cerebellar artery. A middle-aged female presented with the worst headache of her life. A workup for subarachnoid hemorrhage was negative, but an angiogram was performed nonetheless. This showed a fusiform, presumed dissection of the left posterior inferior cerebellar artery on the left vertebral artery injection (*arrow* in **A**). Distal to the dilatation, the posterior inferior cerebellar artery lumen continues to be irregular and slightly beaded over a short segment, suggesting that the diseased segment is quite long. A decision was made with the patient to take a chance on managing her conservatively. Her symptoms resolved and a follow-up angiogram (**B**) after 3 months shows a normal appearance with no new symptoms since that time.

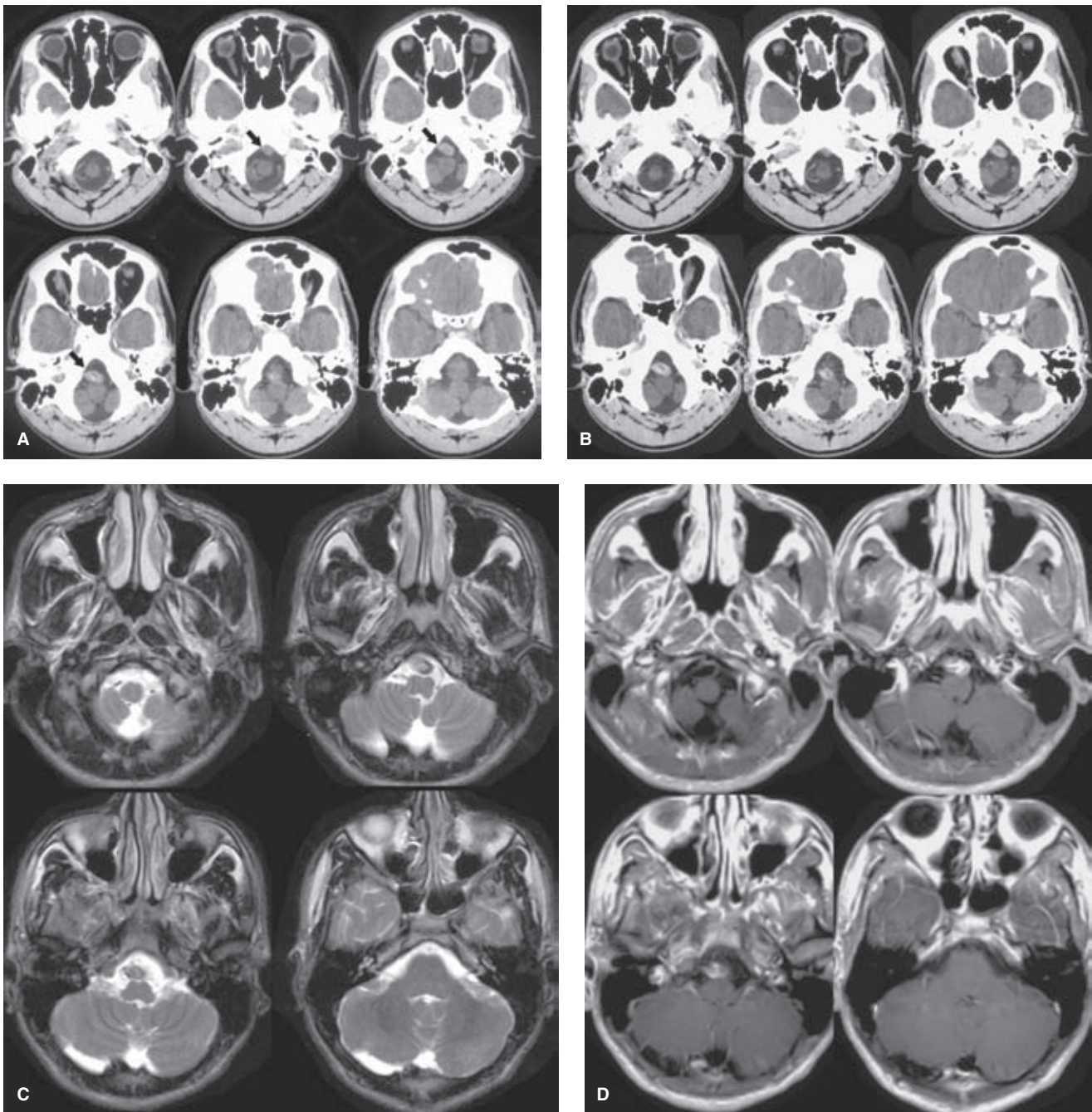


FIGURE 18-20. (A–H) Vertebral-basilar dissection in a teenager presenting with mass effect. A teenager presented with a 3-week history of syncopal episodes, headache, and fluctuating degrees of left-sided hemiparesis and sensory disturbance. The likely diagnosis is that of a dissecting aneurysm of the vertebral-basilar junction. The high-density appearance on the noncontrast CT examination (**A**) is suggestive of intramural or laminar thrombus, confirmed on the contrast-enhanced CT (**B**) and MRI (**C and D**) images with evidence that enhancing lumen is only a small component of the mass formed. The principal concern for this lesion in the acute phase is progression to rupture or extension of the dissection higher in the basilar artery with probable injury to the brainstem. Rupture with subarachnoid hemorrhage from an aneurysm in this location would carry a substantial morbidity and mortality in any circumstance, but the likelihood of further hemorrhage from a dissecting aneurysm is probably higher than that of a berry aneurysm. Surgical or endovascular treatment for a ruptured dissecting aneurysm is probably more hazardous than for a berry aneurysm due to the possibility of disintegration of the aneurysm from any type of manipulation. The fragility of a dissecting aneurysm in this location would probably demand that even angiographic images should be obtained gingerly with gentle hand injections of contrast. (*continued*)

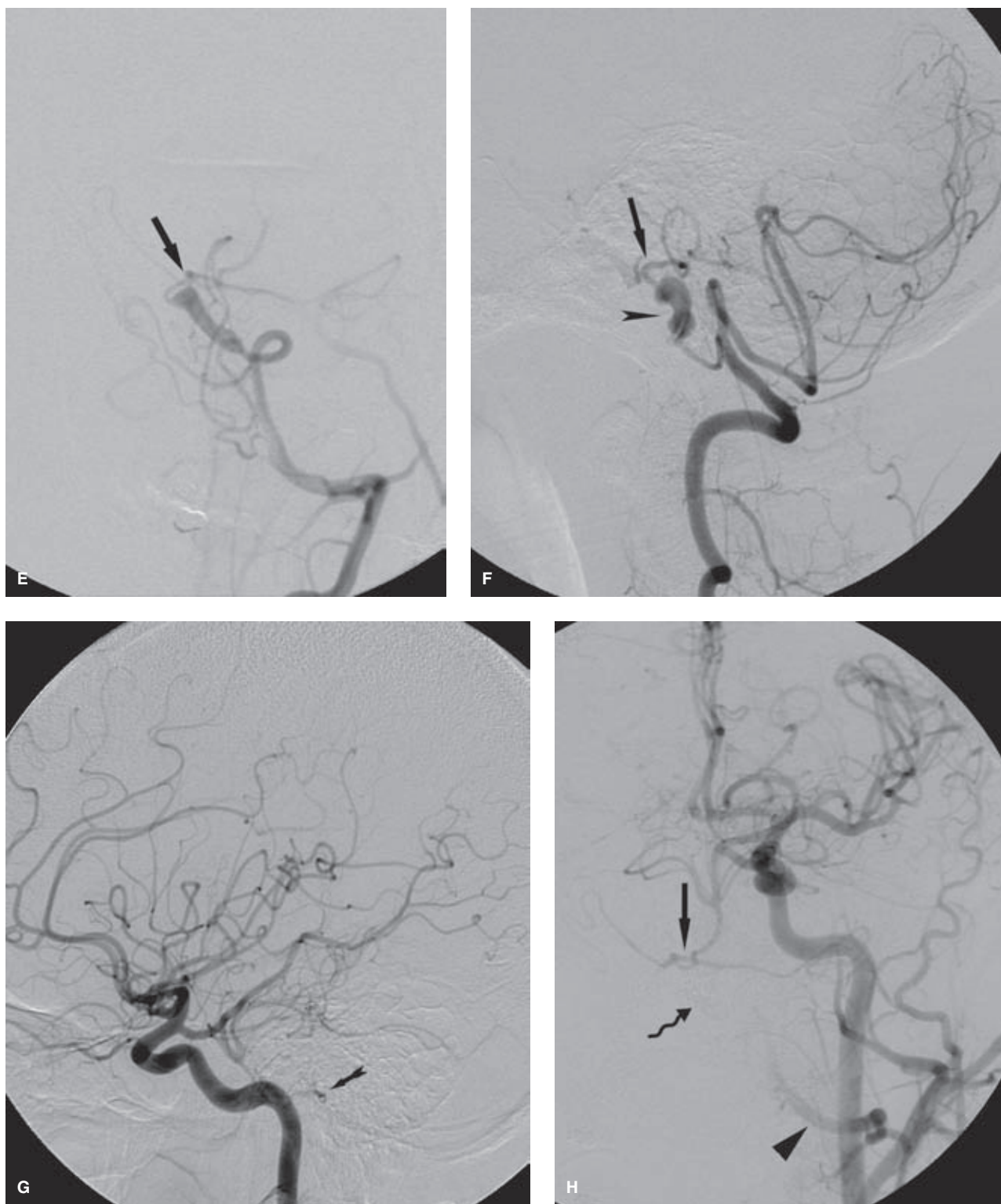


FIGURE 18-20. (CONTINUED) In addition to defining the anatomy of the dissected segment, which in this instance extends up from the vertebrobasilar junction to the origin of the left anterior inferior cerebellar artery (*arrow* in **E** and **F**), some of the important findings from this angiogram include the identification of prompt collateral flow from the anterior circulation from the carotid arteries.

In this patient, a test occlusion of the collateral circulation was performed with the plan to preserve flow in the vertebral arteries proximal to the dissection, thus maintaining perfusion of the posterior inferior cerebellar arteries, medullary perforators, and anterior spinal artery below the dissection. The basilar artery above the dissection would then rely on the collateral flow from the anterior circulation for perfusion (*straight arrows* in **G–H** post occlusion). Coils within the disease segment are indicated with a corrugated arrow in (**H**). Furthermore, the preserved segment of the left vertebral artery below the coils (*arrowhead* in **H**) is opacified via the occipital artery representing the vital preservation of flow to the left posterior inferior cerebellar artery, lower brainstem, and upper spinal cord.

although some of these patients may progress to a chronic fusiform dilatation of the vertebrobasilar system (93) and may ultimately need surgical or endovascular treatment. An important discriminator for the clinical effects of the disease seems to be whether extension to the basilar artery from the vertebral artery occurs. When the disease is more confined and there is no subarachnoid hemorrhage, patients have a far more favorable outcome, and most will resolve their symptoms and angiographic findings within a few months (82,103,110,111).

► SACULAR (BERRY) ANEURYSMS

The cognomen “berry” for saccular intracranial aneurysms was introduced in 1931 by Collier (112) because of the fanciful resemblance of these aneurysms with their shining coats to berries hanging from the arterial tree. The perfect berry-shaped aneurysm with a spherical contour and confined neck is uncommon. Many aneurysms have a more complex structure, often with more than one distinct compartment or lobule and a neck that can be of variable size. A congenital defect in the arterial media may be one of the explanations for later development of this acquired disease.

Histopathologic examination demonstrates that unruptured small aneurysms have a thin wall measuring 30 to 150 μm in thickness, composed of endothelium and adventitia similar to that of the parent vessel (113). As the aneurysm enlarges, some portions of the wall become collagenized and thickened with endothelial cells, fibroblasts, and elastic fibers. More attenuated portions become points of potential rupture. When an aneurysm ruptures, it is usually assumed that it is the dome that has given way, but this is not always the case. The wall at the neck may sometimes be the most fragile segment. After the aneurysm ruptures and stabilizes, the rupture point is supported by weak fibrin nets for approximately the first 3 weeks. This correlates with the clinically observed period of high risk for rerupture. After 3 weeks, the wall becomes infiltrated with capillaries. Stronger collagen is incorporated into the healing wall with a diminishing risk of rerupture (114).

Intracranial saccular aneurysms have a population prevalence between 0.2% and 8.9%, based on angiographic and autopsy studies. The higher number refers to more lenient histopathologic definitions of what constitutes an aneurysm. Approximately 15% to 30% of patients with aneurysms have more than one (113). The majority of all aneurysms likely remain small and asymptomatic during life. Aneurysms become symptomatic due to rupture with subarachnoid hemorrhage, expansion with mass effect on surrounding structures, or development of thrombus and embolic events.

Risk factors for development of intracranial aneurysms include factors such as polycystic kidney disease; smoking; hypertension; aortic coarctation; α_1 -antitrypsin deficiency (115); connective tissue diseases, for example, Ehlers–Danlos syndrome Type IV (100–102, 116–118); fibromuscular dysplasia (119,120); and a family history of berry aneurysms.

Some families have been identified with a genetically heterogeneous pattern of inheritance of intracranial aneurysms. Within this group of patients, most will have only one other affected family member, usually a sibling (121). Screening of asymptomatic patients with polycystic kidney disease detects an aneurysm prevalence of approximately

12%, but the prevalence increases to 25% when there is also a family history of intracranial aneurysms (122,123).

Among all patients with aneurysmal subarachnoid hemorrhage, as many as 20% have a first- or second-degree relative with a similar history. First-degree relatives of a patient with aneurysmal subarachnoid hemorrhage have a risk of subarachnoid hemorrhage that is four times that of the general population (124). In some families with more than one proband, first-degree relatives have a 17% to 44% incidence of aneurysms detectable by screening (121,125). Therefore, screening of family members with a strong family history of intracranial aneurysms is recommended, at least with noninvasive imaging (126). The question of screening of asymptomatic family members is confounded by not knowing the patterns of aneurysm growth and when aneurysms are more likely to bleed. Screening may only detect stable unruptured aneurysms. Dangerous aneurysms that may rupture later in the relative’s lifetime may not yet have formed at the time of screening. However, most patients (80% to 90%) with aneurysms do not fall into this familial category.

Nevertheless, familial aneurysms form an important subgroup of aneurysm patients. There is evidence (127–129) that familial aneurysms compared with nonfamilial aneurysms demonstrate the following features:

- More likely to rupture at a smaller size.
- More likely to be multiple.
- Show a preponderance in females even greater than is the case for sporadic aneurysms.
- Less likely than sporadically occurring aneurysms to be found at the anterior communicating artery complex.
- More likely to rupture at a younger age, occur in the same arterial tree, and rupture in the same decade as the proband.

Aneurysm Formation following Vessel Sacrifice

Another group of patients at risk for intracranial aneurysm formation requiring particular consideration are those who have undergone therapeutic proximal carotid occlusion or ligation for treatment of intracranial aneurysms. It is thought by some authors that altered hemodynamic forces affecting the circle of Willis, and the anterior communicating artery in particular, are responsible for a delayed rate of de novo aneurysm formation that may approach 4% or higher in incidence (130–133). In a series of 27 patients who had been treated with surgical occlusion of a carotid artery and followed over a 3- to 22-year period, Fujiwara et al. (132) reported two complications related to rupture of new aneurysms of the anterior communicating artery and two fatal ruptures of preexisting aneurysms ipsilateral to the remaining carotid artery, so this phenomenon of delayed aneurysm formation is probably similar in magnitude to the likelihood of metachronous aneurysm formation in any patient who has undergone a previous treatment.

Sites of Aneurysm Formation

The most common sites of aneurysm formation are at stress points on the circle of Willis and on the proximal major intracranial vessels where branches bifurcate. Approximately 85% of aneurysms occur in the anterior portion of

the circle of Willis as divided by a line transecting the posterior communicating arteries (113). The anterior communicating artery complex represents the single most common site. Between 5% and 10% of intracranial aneurysms occur in the posterior fossa. When they rupture, they have a considerably poorer prognosis than those of the anterior circulation (134).

► NATURAL HISTORY OF UNRUPTURED INTRACRANIAL ANEURYSMS

Precise data on the natural history of asymptomatic aneurysms are scant, but some series suggest that for patients with unruptured aneurysms, the most valuable predictors of rupture are patient age and aneurysm size. Asymptomatic aneurysms less than 7 mm in diameter have a small risk of rupture, close to 0% in the anterior circulation and 2.5% in the posterior communicating artery and posterior circulation in 5-year cumulative data (135–137). Corresponding figures for aneurysms of 7 to 12 mm were 2.6% and 14.5%, respectively; for aneurysms 13 to 24 mm, 14.5% and 18.4%; and for aneurysms 25 mm and greater, 40% and 50%, respectively. While some nuances of the methodology involved with these data are disputed, it has been accepted in the field that these figures have at least some validity.

A troublesome observation continues to be the fact that most aneurysms presenting with subarachnoid hemorrhage are small, even by the criteria of the International Study of Unruptured Intracranial Aneurysms (USUIA). Aneurysms may expand rapidly at the time of initial formation, at which time they are presumably most likely to rupture (138), but there is evidence casting doubt on this explanation too. Presumably there is a dominant cohort of aneurysms that endure an initial phase of expansion without rupturing and can then stabilize and fortify their walls. This would explain the observation that most ruptured aneurysms are small (<10 mm) in clinical practice and would also explain the epidemiologic observation that for larger aneurysms, the risk of rupture appears linked to aneurysm diameter. However, cases of long-standing small aneurysms proceeding to rupture have been well documented (139,140). Furthermore, if rupture of small intracranial aneurysms is such a rare event, then the prevalence of unruptured aneurysms should vastly overwhelm that of ruptured aneurysms, but this is not the case in reality. This translates into a great deal of uncertainty as to how to advise a young patient with an incidentally discovered intracranial aneurysm.

Other factors thought to contribute to a risk of aneurysm formation or subarachnoid hemorrhage include atherosclerosis, female sex, smoking, use of oral contraceptives, alcohol consumption, asymmetry of the circle of Willis, viral infections, pituitary tumors, and deficiency of some human leukocyte antigen-associated factors (140–143). Higher rates of subarachnoid hemorrhage are also seen in some geographic areas. For example, Japan and Finland have an annual incidence of almost 24 per 100,000 persons (144). The USUIA has demonstrated that approximately 77% of enlisted patients are current or former smokers and that 18% of patients have a family history of aneurysms (137). Factors predisposing to the formation of multiple aneurysms include female gender, smoking, family history, use of oral contraceptives, drug use, and associated diseases such as hypertension, coarctation, and neurofibromatosis.

The cost-effectiveness of the treatment, surgical and endovascular, of unruptured intracranial aneurysms has been addressed, but a consensus is stymied by the uncertainties concerning the natural history of the disease. It is estimated that elective surgery for unruptured, asymptomatic, intracranial aneurysms is cost-effective if the patient has a life expectancy of at least 13 years (145). Similar conclusions on the irrationality of treating small, asymptomatic aneurysms in patients over 70 years with endovascular coiling have also been reached (146).

► NATURAL HISTORY AND OUTCOME OF RUPTURED INTRACRANIAL ANEURYSMS

The statistics on outcome of patients with subarachnoid hemorrhage depend on whether the data were collected at referral centers or based on population registers. More than 10% to 17% (147) of patients with subarachnoid hemorrhage in most studies die immediately and do not become part of a hospital-based experience. Tertiary centers are also more likely to be referred patients with better-grade subarachnoid hemorrhage who have survived the initial triage and who will then be likely to have a better ultimate outcome (148). Of those who make it to a hospital, a further 25% die, and only 42% to 58% return to a pre-morbid level of function at 6 months. In population studies, aneurysmal subarachnoid hemorrhage has an overall 30-day survival of 40% to 57% (134). Survival for ruptured posterior fossa aneurysms is considerably poorer in population-based studies, 11% at 30 days (134). This is probably due to devastating mass effect in the confined space of the infratentorial compartment. For treated patients with anterior circulation aneurysms with Hunt and Hess Grades I, II, and III, 30-day survival is approximately 70% and for Grades IV and V is less than 20% (149). With modern aggressive management, including use of endovascular techniques for management of cerebral vasospasm, these statistics for anterior circulation aneurysms with good clinical grades are even better. Among patients with Hunt and Hess Grades I to III, 86% return to independent functioning, this figure being 96% for Grade I patients (150).

After the initial rupture, vasospasm and recurrent rupture are the important determinants of outcome (151). Older patients, patients with prior hypertension, and those with intracerebral hematoma have a poorer prognosis, as do patients with depressed levels of consciousness at presentation, thick layers of subarachnoid clot on CT, pre-existing medical conditions, and basilar aneurysms (152). In round figures, the risk of immediate rebleeding from an untreated ruptured aneurysm, Grades I to III (153), is taken as 2% to 4% per day for the first 10 days, 30% during the first 30 days, and 2% to 4% per year thereafter (Box 18-1).

The major source of delayed mortality derives from rebleeding. The risk of rerupture is highest immediately after the subarachnoid hemorrhage and declines over the following weeks. It is postulated that subarachnoid clot from the first hemorrhage deflects the new blood toward the brain parenchyma or into the ventricular system. This accounts for the more grave implications and effects of a rebleed, which is less likely to confine itself to the subarachnoid space (154).

BOX 18-1 Hunt and Hess Scale for Clinical Grading of Subarachnoid Hemorrhage (153)

This scale is a useful tool for triage and communication at initial presentation. Its importance lies in the correlation between the patients' grade and the likelihood of a favorable outcome from surgical intervention. Grades I–III are considered to be “good” grades.

Grade I: Asymptomatic, minimal headache, or slight nuchal rigidity.

Grade II: Moderate to severe headache, nuchal rigidity, neurologic deficit confined to cranial nerve palsy.

Grade III: Drowsiness, confusion, or mild focal deficit.

Grade IV: Stupor, moderate to severe hemiparesis, possible early decerebrate rigidity, and vegetative disturbances.

Grade V: Deep coma, decerebrate rigidity, moribund appearance.

Of those who survive the initial rupture, the probability of a favorable outcome depends on the following:

- *Elimination of risk of rebleeding by treatment of the aneurysm.* For instance, among patients presenting to the hospital, almost one-third present with an initial minor or sentinel leak followed by a more devastating hemorrhage within 24 hours to 4 weeks with a mortality rate of over 50% (155). The question of timing of aneurysm surgery has been a matter of debate for some years (152), but this consideration has been virtually eliminated by the advent of endovascular treatment options.
- *Management of vasospasm.* Early occlusion of the aneurysm can facilitate aggressive use of hypertension as part of the Triple-H therapy for vasospasm—hypertension, hypervolemia, hemodilution, in combination with nimodipine therapy. Without prophylactic and active management, the morbidity of neurologic deficits due to vasospasm becoming evident from days 4 to 14 after a subarachnoid hemorrhage can approach that related to the hemorrhage itself. The Fisher scale (156) is occasionally mentioned in reference to the CT appearance of subarachnoid hemorrhage and prediction of the risk of vasospasm. A CT done within 24 hours of the hemorrhage, that is, before the blood can disperse, which demonstrates large subarachnoid clots in the basal cisterns or extensive blood in the vertically oriented subarachnoid spaces, is a helpful predictor of a high risk of vasospasm compared with milder degrees of subarachnoid blood (157).
- *Management of intracranial pressure.* In the absence of focal mass effect, a cerebral perfusion pressure of 60 mm Hg (mean arterial pressure minus intracranial pressure) is a desirable target to prevent brain ischemia.
- *Management of hydrocephalus.* This complication can occur in 20% to 67% of patients following subarachnoid hemorrhage, of whom 13% become symptomatic (158).
- *Management of other complications.* Complications such as hyponatremia (10% to 25%) may occur, possibly due

to increased secretion of atrial natriuretic factor (159), a condition that can aggravate cerebral ischemia.

- *Monitoring of EKG abnormalities and myocardial dysfunction, due to coronary artery spasm or catecholamine release (160,161).* This can be complicated by the need for sympathomimetic agents to elevate blood pressure in the treatment of vasospasm.

Giant Aneurysms

Giant aneurysms are defined as those greater than 25 mm in diameter. Ironically, compared with smaller aneurysms, they may have a somewhat diminished risk of rupture if the lumen is surrounded by laminar thrombus. However, the character and thickness of this layer of clot is probably in constant flux, and the possibility of rupture should still be considered as significant. When the aneurysm is almost completely thrombosed, a sinusoidal, residual lumen may be seen. This subtype is sometimes referred to as a *giant serpentine aneurysm* (162–164). Mass effect is the typical presentation of such aneurysms and may respond to steroid therapy.

Giant aneurysms are seen most commonly arising from the internal carotid artery (57%) and in the posterior circulation (24%). They are less common in the middle cerebral artery (9%) and anterior cerebral artery (10%) (13). Because of their size, distortion, and involvement of surrounding vessels as well as overlapping contrast density, they are difficult to study angiographically or during craniotomy with respect to defining the afferent and efferent parent vessels.

The presence of calcification in the walls of giant aneurysms as well as in smaller saccular aneurysms must be noted, as this represents a technical difficulty for satisfactory neurosurgical application of a clip across the neck. Without treatment, the 5-year outcome for more than 80% of patients with symptomatic giant aneurysms is poor due to mass effect, thrombosis of important vessels, or subarachnoid hemorrhage (165–167), whereas with surgical bypass and arterial reconstruction or endovascular reconstruction, a good outcome can be seen in as many as 60% to 80% of patients (168–170). However, periprocedural or perioperative mortality is very high (10% to 20% mortality) even in the most upbeat of case series concerning this group of patients.

Note: A particular danger with giant aneurysms is the possibility of fulminant acute thrombosis and rupture following apparently successful surgical or endovascular intervention. A small degree of expansion of the aneurysm or stress on the wall can precipitate an acute rupture in the first 24 to 48 hours following treatment, even when the aneurysm has been previously unruptured. Prolongation of anticoagulation following a therapeutic procedure may be worth considering to attempt some measure of control of the rate of thrombosis, but this will have the disadvantage that if a rupture does supervene, its effects will be all the more severe.

► CEREBRAL ANEURYSMS IN CHILDREN

Intracranial aneurysms in children are rare, accounting for less than 5% of all aneurysms and they are never found as incidental lesions in pediatric autopsies (171,172). It is fairly axiomatic, then, that all cerebral aneurysms in children are symptomatic. In children, aneurysms are less likely

to be multiple or to be associated with a family history than is the case in the adult population, and they are more likely to be fusiform or elongated in morphology (173,174). They are more likely to be distal in location and more likely to be at the carotid terminus or in the posterior circulation than is the case in adults. Moreover, aneurysms in young children are more likely to be associated with an identifiable etiology, and have a male predominance. Underlying dissection is likely the most common etiology for genesis of intracranial aneurysms in about 50% of younger children. Up to 10% to 39% of aneurysms in children may be associated with a history of trauma (20). Traumatic pseudoaneurysms are often associated with the anterior cerebral artery due to impaction against the falx cerebri, and they have a characteristic tendency to present 2 to 4 weeks following the trauma with a delayed hemorrhage. Other etiologies include infection with mycotic aneurysms. HIV infection with necrotizing vasculitis may need to be considered (48). As many as 15% of pediatric aneurysms are infectious or mycotic in etiology. They can be peripheral when the mechanism is embolic or centrally related to spread of infection from the skull base to the large vessels of the circle of Willis.

The spectrum of presentation and symptoms seen in younger children differs from that of adults and is more likely a reflection of the underlying dissection than of the aneurysm itself in many cases. Focal neurologic deficits, mass effect, headaches, and epilepsy are more common in the younger group than hemorrhage as an immediate cause for presentation. When the underlying etiology is a dissection, the complications may be seen in the acute phase as previously listed, but may also extend into a more chronic presentation with genesis of giant serpentine or fusiform aneurysms or other bizarre patterns of failed healing.

The treatment of intracranial aneurysms in children differs therefore from the situation with berry aneurysms in adults. Vessel sacrifice (Fig. 18-20), trapping of the pseudoaneurysm, liquid embolic embolization, or coil embolization of distal vessels are more likely to play a role, in keeping with the underlying mechanism of dissection (76,84,101)

Endovascular Treatment of Aneurysms

The endovascular treatment of aneurysms has a long and interesting history. In the 19th century and before, aortic aneurysms related to late complications of syphilitic infections were a very common problem with a high mortality and a poor likelihood of effective therapy. Aortic ligation was the limit of possible intervention with poor results. In 1864, the English physician Moore (175) noted that a bullet in the postmortem thoracic aorta of a sailor was enmeshed in clot and conceived the notion of treating aortic aneurysm by “filipuncture,” that is, the spooling of a metal wire into the aneurysm from without to induce thrombosis. Several variations on this followed, including the induction of a current through the wire delivery apparatus by Corradi in 1879 to promote the process still further. The “Moore–Corradi” technique was never fully eclipsed by rival techniques that came and went over the years such as the “Gallagher Pilojector” for shooting horsehairs, catgut, hog-bristle, or fishing line into aneurysms (176) or stereotactic magnetic control of iron particles within aneurysms (177). Eventually the “electothermic procedure”

saw a resurgence of interest with refined materials in 1938 by Blakemore and King in the treatment of aortic aneurysms. A New York physician, Sidney C. Werner, collaborated with these researchers in performing the first such case of direct puncture of an intracranial aneurysm on April 13, 1939, in a 15-year-old schoolgirl (178,179). The direct puncture approach to aneurysm consolidation in otherwise inoperable cases with wire embolization was promoted further in the 1960s by Mullan (180) using copper wire. The modern endovascular approach followed soon afterward with the publication of Serbinenko’s papers from the USSR on balloon embolization (181) and the invention of the microcatheter.

► EFFICACY OF ENDOVASCULAR TREATMENT FOR RUPTURED ANEURYSMS

Two prospective, randomized trials have examined the outcomes of endovascular treatment of ruptured aneurysms versus surgical clipping (Fig. 18-21).

The first study from Finland (182,183) randomized 109 patients with acute subarachnoid hemorrhage who were suitable for either modality of therapy to surgery or endovascular coiling. Angiographic outcomes in the anterior cerebral artery distribution were significantly better for surgery, while those in the posterior circulation were significantly better following endovascular treatment. Angiographic outcomes in the middle cerebral artery and internal carotid artery distribution were similar in both groups. Clinical outcomes (Glasgow Outcome Scale) were equivalent between the two groups at 3 months. Mortality for technical reasons during surgery (4%) was twice that of the endovascular group (2%). Early rebleeding was seen in one endovascular patient following incomplete coiling of the aneurysm.

The second study was the International Subarachnoid Trial (ISAT) (184–186), in which over 2,000 patients with subarachnoid hemorrhage in several countries who, in the judgment of the treating team were in a situation of clinical equipoise, that is, suitable for either modality of treatment, were randomized to endovascular coiling or surgical clipping. Outcome analysis on the basis of death or dependency at 2 months and 1 year (modified Rankin score 3 to 6) was the primary parameter of interest in the first publication in 2002, while more extended follow-up was published in 2005 and 2009. At 1-year postprocedure, 250 of 1,063 (23.5%) endovascular patients were dead or dependent, while following surgery the outcome was 326 of 1,055 (30.9%). This represents an absolute risk reduction of 7.4% for those treated by endovascular means, or 74 patients for every 1,000 treated avoiding death or dependency at 1 year. Delayed rebleeding was more common with the endovascular group, which in many cases was attributable to obviously incomplete treatments and regrowth of the original aneurysm or development of a new separate aneurysm. In either event, rebleeding in the endovascular group was still so infrequent that its occurrence failed to subvert the clinical difference in outcomes between the two groups (186). Seizures and cognitive impairment were seen less commonly in the endovascular group at delayed follow-up (185,187).

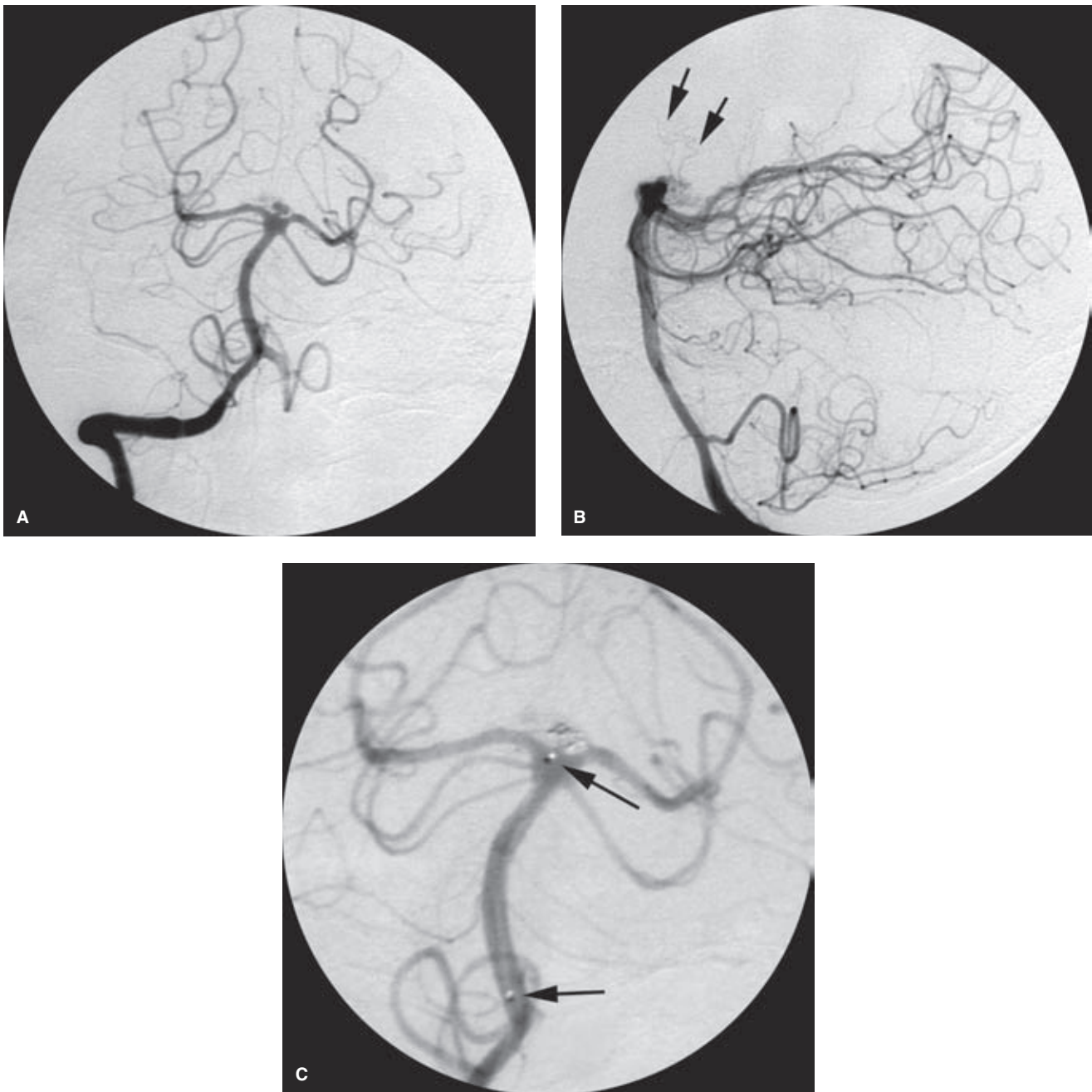


FIGURE 18-21. (A–C) Embolization of a ruptured basilar tip aneurysm. An 84-year-old female presented with a Grade I subarachnoid hemorrhage related to a tiny heart-shaped aneurysm of the basilar apex (A). Despite the fact that the neck looks well defined in this patient, implying that the aneurysm should hold the coils well, this apparent advantage could work to the detriment of the patient very easily. First, the small size of the aneurysm itself poses a risk of intraprocedural rupture due to the smaller margin for error between stress on the wall of the aneurysm and a size mismatch for the choice of coils. Second, the small size leaves no room for error in the advance of the microcatheter into the aneurysm as the microwire retracts. Any harpooning of the microcatheter forward will almost certainly stress the aneurysm excessively and provoke a rupture. Furthermore, the relatively confined space within the aneurysm means that as the coils prolapse within the aneurysm, they may become “trapped” by the hard shoulders of the aneurysm, and instead of finding a way to escape through the mouth of the aneurysm, the stress may all be transferred to the weak wall of the aneurysm. The lateral view (B) shows that the perforator vessels (*arrows*) all lie on a plane behind the aneurysm, which is itself obscured between the two zeniths of the posterior cerebral arteries.

To avoid the dangers described above, the aneurysm was not catheterized directly. The straight microcatheter was advanced into the left posterior cerebral artery and then retracted slowly until it “popped” back into the very ostium of the aneurysm, from which position a single 2-mm diameter was deployed very slowly with the result shown (C). The distal marker of the microcatheter (*upper arrow*) has been pushed back from the aneurysm by the detachment segment of the coil, but the result is satisfactory. The proximal marker (*lower arrow*)—important for knowing how far one can advance the coil—has also moved back.

The ISAT study was initially criticized vociferously on a number of grounds, chief among them being the fact that over three times as many patients were not randomized into the study as were actually included. The subtext of this criticism would seem to imply that patients were “cherry-picked” for the study to reflect favorably on endovascular treatment, but this does not hold up to scrutiny. The ISAT study does not include the typical array of cases usually thought favorable for endovascular therapy—basilar apex aneurysms, aneurysms of the posterior inferior cerebellar artery origin, and the like—because these patients were screened out of the randomization process based on the preference for endovascular therapy in these instances. In other words, equipoise did not apply in situations where typically endovascular treatment would be the obvious modality of choice. Therefore, posterior circulation aneurysms were not heavily represented within the ISAT study, explaining why 97.3% of those patients randomized had aneurysms in the anterior circulation. The impact of the ISAT study on the treatment of cerebral aneurysms, particularly ruptured aneurysms, has been monumental in changing the emphasis on the treatment of aneurysms from open craniotomy to endovascular in the majority of patients. Despite equivocations about recruitment biases in the ISAT study, it is accepted that the results of the study can be generalized (188,189).

► EFFICACY OF ENDOVASCULAR TREATMENT FOR UNRUPTURED ANEURYSMS

In contrast to the methodologically robust evidence showing the efficacy of endovascular treatment versus that of surgical clipping of ruptured aneurysms, the evidence in the case of unruptured aneurysms does not benefit from the availability of studies that are both randomized and prospective. A review of modern large clipping and coiling trials, most of which were retrospective and nonrandomized, was published in 2005 (190) in which a cumulative adverse outcome for endovascular coiling was estimated at 8.8% and for clipping at 17.8%. Data from the International Study of Unruptured Intracranial Aneurysm (USUIA) (137) similarly indicate that adverse outcomes were less common with endovascular treatment (9.3%) than with surgery (13.7%), but even at that, the study, being nonrandomized, showed data based on endovascular treatments that included more elderly and larger or posterior fossa aneurysms, all factors known to increase the risk of treatment. Surgical adverse outcomes in the USUIA study correlated with patient age greater than 50 years, aneurysm size greater than 12 mm, location in the posterior circulation, previous ischemic cerebrovascular disease, and symptoms of mass effect from the aneurysm, while endovascular outcomes were less clearly influenced by these factors. Several other single-center or meta-analytical studies of the treatment of unruptured aneurysms have been published, all with a consistent outcome: Surgical clipping results in a better angiographic appearance of aneurysm obliteration, but endovascular treatment results in better clinical outcome, immediate and delayed, and better quality of life (191–195).

In summary, for as long as prospective, randomized trials of treatments of unruptured aneurysms are wanting, the

literature will continue to consist in a methodologically less robust canon, which is vulnerable to a variety of publication biases. The need for scientific studies in this domain is self-evident.

► RECURRENCE RATES FOLLOWING ANEURYSM EMBOLIZATION

As mentioned earlier, there is no doubt that there is a higher risk of aneurysm recurrence, regrowth, and rebleeding after endovascular treatment than is the case following a surgical clipping (185,186). A great deal of fuss is made out of this technical shortcoming of coil embolization, but the question might well be asked whether it really matters when the long-term clinical outcome data of the ISAT study are so patently favorable toward endovascular treatment. Operator evaluation of the degree of aneurysm occlusion is a somewhat subjective parameter and difficult to quantify precisely. Estimates of the degree of complete aneurysm occlusion at follow-up vary between 66% and 74% (185,196). While estimates of the proportion of patients requiring retreatment or who have significant or symptomatic recurrences vary as high as 20% in retrospective studies (197), only 8% of patients in the ISAT study showed persistent aneurysm filling beyond the degree of a neck remnant at follow-up (26% if one counts a neck remnant or subtotal occlusion). Factors that likely influence the likelihood of significant aneurysm recurrence or regrowth include aneurysm size, treatment following an acute rupture, aneurysm neck wider than 4 mm, and aneurysm location at a hemodynamically stressed junction or terminus such as the basilar apex. A relationship between the proportionate volume of the aneurysm replaced or filled by platinum or coil material and the likelihood of recurrence has also been established (198), meaning that more tightly packed aneurysms are less likely to regrow.

In summary, propensity toward aneurysm regrowth and recurrence are certainly problems with endovascular treatment of aneurysms, but in the ISAT study, these weaknesses of the technology, even with some rebleeds, did not translate into a tangible detraction from the overall outcome of the study. This weakness of the endovascular option cannot be rationally used as an argument against the treatment modality as a whole. The importance of this phenomenon lies with the ongoing management of individual patients, who must be followed with noninvasive imaging or angiography to monitor the status of their aneurysm, particularly those of a hemodynamically stressed configuration or location.

► COMPLICATIONS AND SAFETY

The major safety concerns during endovascular coil embolization include:

- Thromboembolic complications from the introducer catheter, from the microcatheter, or from the aneurysm (Fig. 18-22).
- Perforation of the aneurysm or arterial wall by the microwire, microcatheter, or coil (Fig. 18-23).

(text continues on page 272)

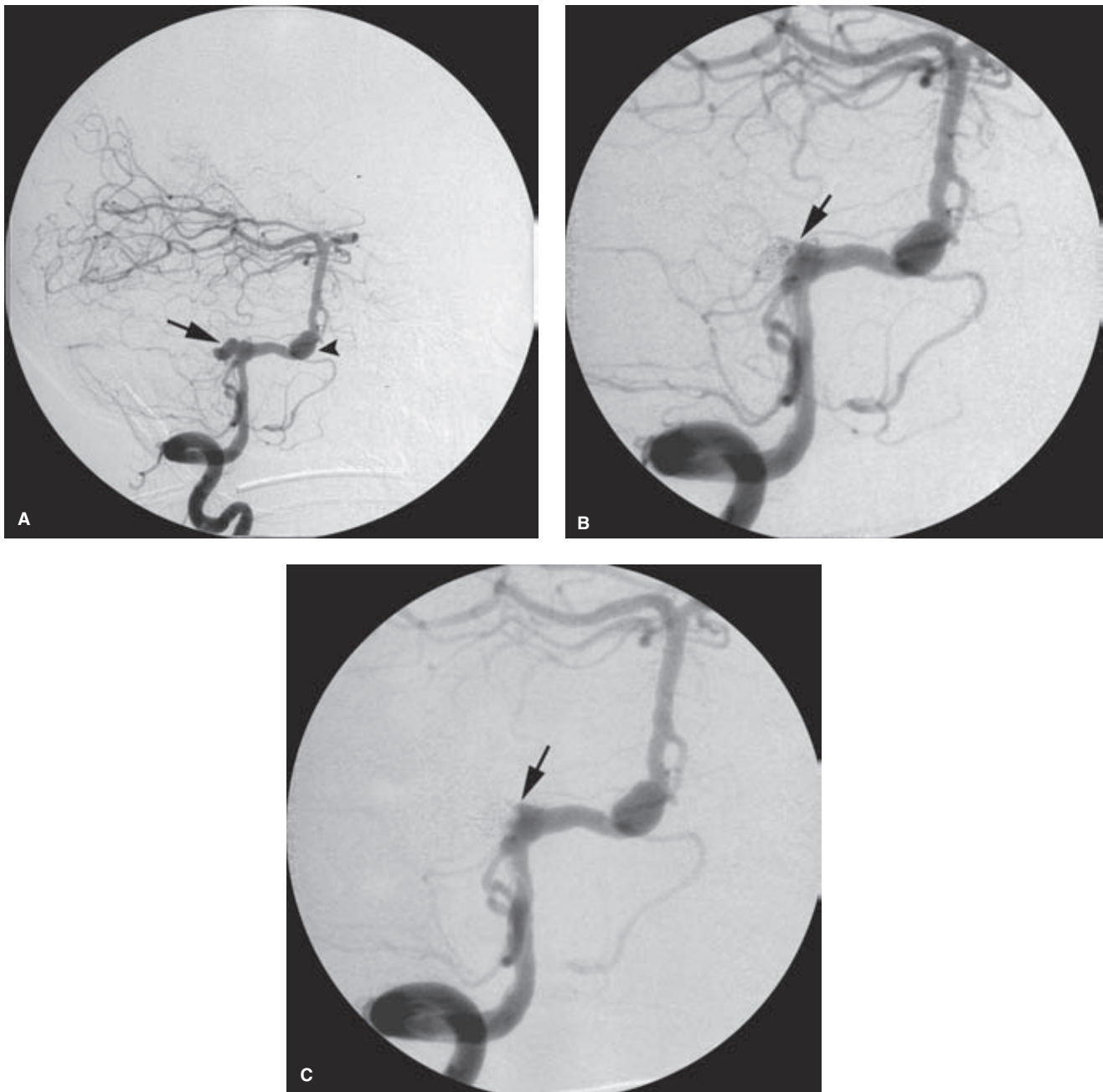


FIGURE 18-22. (A–C) Sudden nature of acute thrombus formation during aneurysm embolization. The dysplastic nature of the right vertebral artery along the segment giving origin to the posterior inferior cerebellar artery and this wide-based aneurysm (*arrow* in **A**) suggest that the case will be technically difficult. A stent along that segment of artery might help, but the aneurysm was acutely ruptured, and the use of antiplatelet agents in a patient with acute subarachnoid hemorrhage can be problematic. There is a second dysplastic aneurysm of the vertebrobasilar junction (*arrowhead*), which was thought less likely as the site of hemorrhage. Another possibility would be a supportive balloon within the artery during the coiling, but the vertebral artery was small and would admit only a 5F catheter. Fortunately, the coils sat auspiciously within the aneurysm with a fairly satisfactory result (**B**). Along the interface between aneurysm and artery (*arrow* in **B**), a single errant loop extends toward the artery, but after several difficulties with coil insertion, this was taken as a reasonable result, and the final coil was detached. There is still contrast within the interstices of the aneurysm, but it can be assumed that the aneurysm will thrombose and occlude satisfactorily in the near-term future, especially when the heparinization from the procedure wears off. The next run performed within a few minutes (**C**) shows how abruptly this can happen. The sharp interface between the coils and the artery is now replaced by an indistinct and fuzzy margin. The opacifying interstices are no longer seen. A layer of acute thrombus has accumulated abruptly along the aneurysm–artery interface. An event such as this should prompt caution and vigilant monitoring over the subsequent minutes to ensure that the process does not propagate or embolize. Fortunately, in this case, the phenomenon seemed self-contained, but heparinization was continued for another 24 hours following the procedure. A thromboembolism would raise the dilemma of deciding between mechanical thrombolysis (balloon angioplasty), thrombolytics, or glycoprotein IIb – IIIa inhibitors.

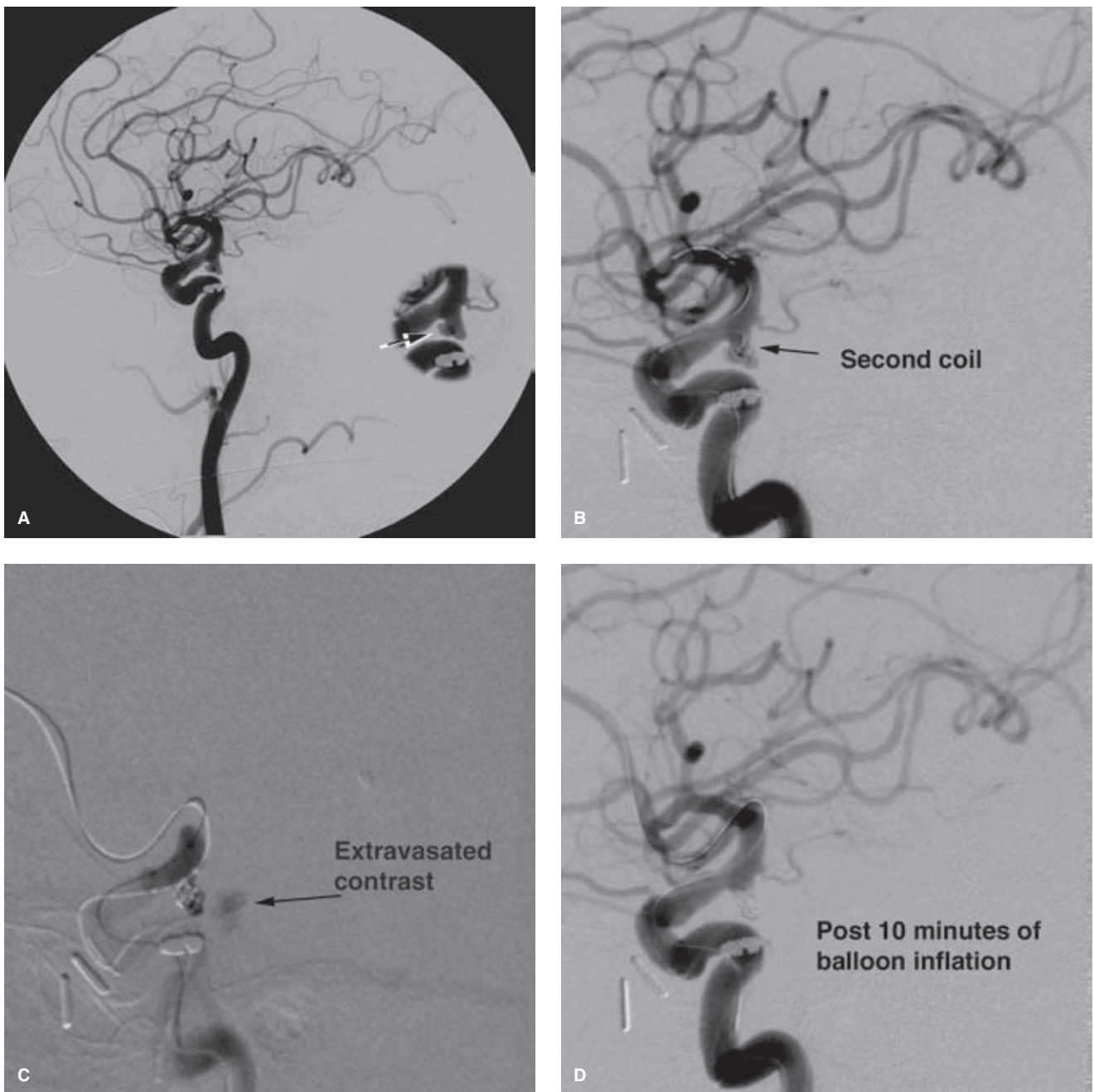


FIGURE 18-23. (A–D) Extravasation from an aneurysm during embolization. This elderly patient presented with a rupture of this left posterior communicating aneurysm (A). The magnified insert in (A) shows the pseudoaneurysm or daughter sac along the anterior surface of the aneurysm (arrow). Because of the uneven shape of the aneurysm, balloon reconstruction technique was opted for, and matters seemed to be progressing well by the time the second coil was detached (B). The third coil transgressed the wall of the aneurysm posteriorly, showing extravasation of the roadmap image (C). This was contained by reinflation of the Hyperform balloon across the mouth of the aneurysm. After almost 10 minutes of balloon inflation and reversal of the heparinization, the next run demonstrated containment of the leakage (D) and thrombosis of the aneurysm. However, the microcatheter was still in the aneurysm at this point and had to be withdrawn. (continued)

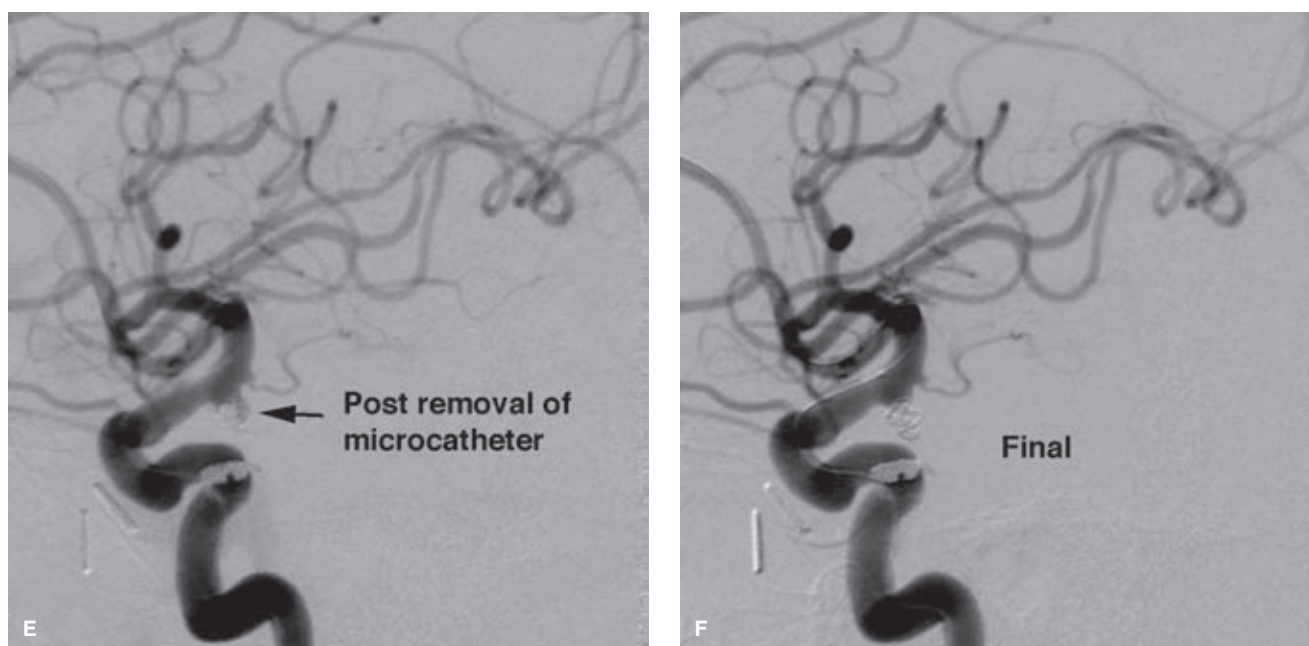


FIGURE 18-23. (CONTINUED) E–F: This was done with the balloon inflated to avoid disturbing any of the coils or thrombus, but the next run (E) showed a new aspect to the contour of the aneurysm (arrow in E), which seemed to lie outside of the contour of the aneurysm on the first run and therefore likely represented fresh extravasation rather than recanalization of the original lumen. A further few minutes of balloon inflation eliminated this new episode of extravasation (F), and the patient had no further bleeding from this aneurysm.

- Compromise of the parent vessel or branch vessel by either inadvertent progressive coil packing in an anatomically hazardous pattern or sudden prolapse of coils into the parent artery due to coil instability or during attempts to remove a damaged or ensnared coil (Fig. 18-24).

Published procedural or technical complications rates are consistently higher for ruptured than for unruptured aneurysms. Combined morbidity and mortality rates related to procedural problems for ruptured aneurysms range up to 13.5% (199) and for unruptured aneurysms from 2.8% to 11.3% (200), but not all events counted in these statistics are of permanent consequence to the patient. Several authors have identified clinically overt and silent thromboembolic DWI+ complications following endovascular aneurysm embolization in 20% to 71% of patients, but these are mostly retrospective small case series with inconsistent use of antiplatelet medication (201–204).

Technical Aspects of Safety and Efficacy

Without any doubt, the technical innovations brought to market over the past decade in device design, coil configuration, bioactive coating of coils, endovascular stent delivery, and the like have all been influential in moving the field forward, but before focusing on these factors, it is worthwhile reiterating that the major advances in safety have derived from much more fundamental and less expensive components of the patient's care. Chief among these is the awareness of the importance of antiplatelet medication for reducing thromboembolic complications during an endovascular procedure (Fig. 18-25). The most commonly used combination is aspirin 81 mg or 325 mg per day and clopidogrel 75 mg per day

for at least 5 days in advance of an elective procedure (205). The phenomenon of a substantial minority of the population (5% to 45%) developing resistance to aspirin and thienopyridine drugs is gaining increasing recognition (206,207), with an awareness in the cardiology field that increased postprocedural complications can be seen more frequently in this segment of the population (208–210). Aspirin and Plavix resistance and heterogeneity of response can develop from a variety of clinical, cellular, and genetic factors. A number of laboratory assays are now available for detecting functional response of platelets to aspirin and clopidogrel, and their use has become standard. In patients who are allergic or resistant to clopidogrel, an alternative thienopyridine, prasugrel, is now available, but has the disadvantage of inducing an extreme state of platelet inhibition associated with higher rates of intracranial hemorrhage and severe bleeding should surgery become necessary (211,212).

Variability in individual response to heparin is another potential major problem. Vigilant heparinization to an activated clotting time (ACT) of approximately 250 to 300 seconds for most patients is universally advocated but a little more difficult to achieve without meticulous attention during a procedure. Patients can be extremely variable in their response to heparin, and simply giving a standard bolus of heparin calculated by body weight without subsequent ACT checks every hour is not going to be adequate for many patients.

Advances in device design have focused either on achieving a denser volumetric packing of the aneurysm with coils or on provoking a histologic response within the aneurysm to promote healing through use of coated or “bioactive” coils. There is predictable overlap between vendors in all these categories, but the salient user options that the reader

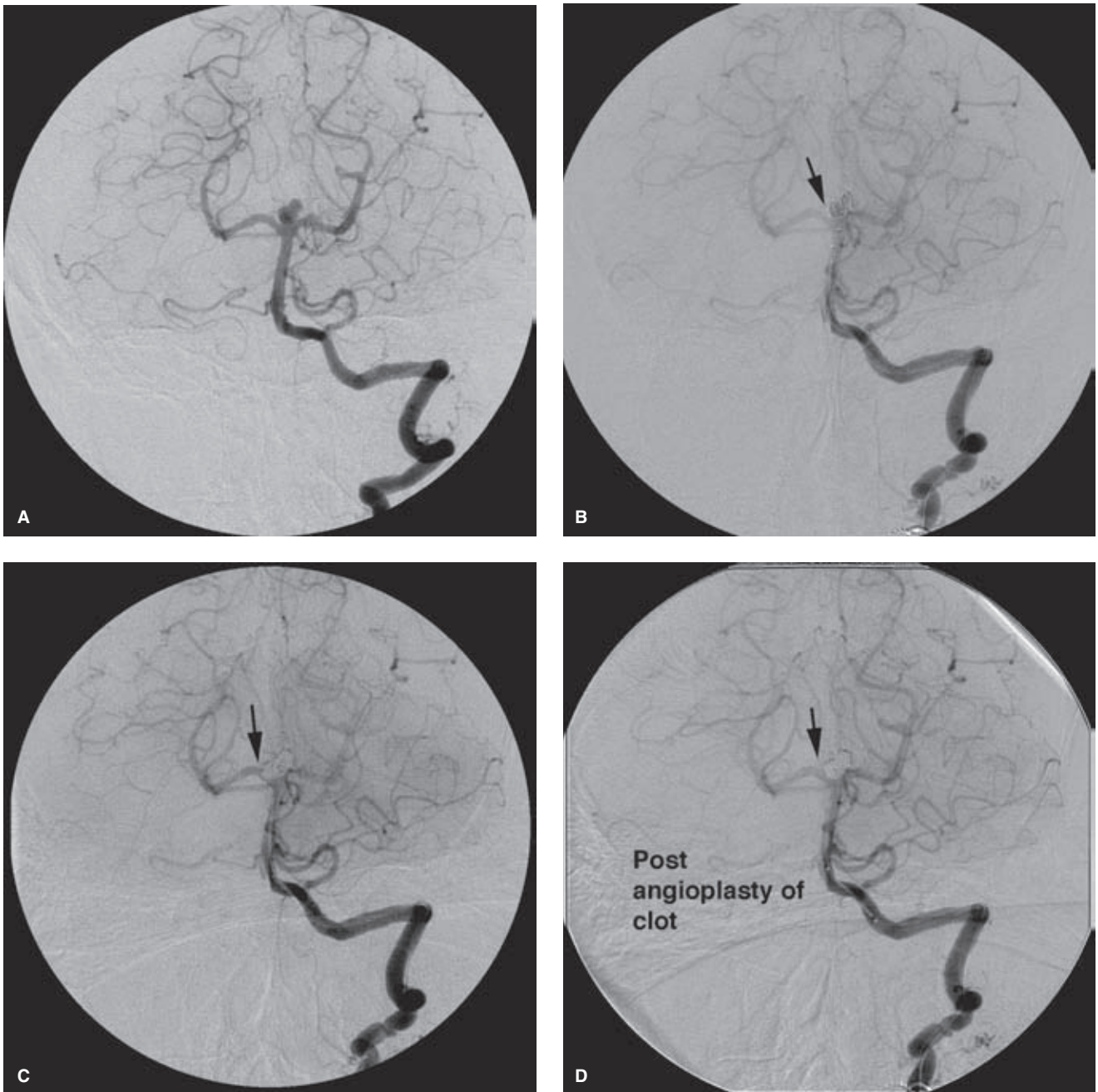


FIGURE 18-24. (A–D) Subtle appearance of acute thrombus from an aneurysm compromising the parent artery. This ruptured basilar tip aneurysm (A) has a lobule or daughter sac eccentrically on the left, but the relationship of its neck to the posterior cerebral arteries is balanced. A soft, compliant balloon was used in this case to stabilize the microcatheter during coil deployment and to reconstruct the neck of the aneurysm. The parallel microcatheter and balloon shaft induced a significant degree of vasospasm in the left vertebral artery, so the run performed after the second coil (B) was suboptimal. In retrospect, the origin of the right posterior cerebral artery has a fuzzy appearance (*arrow*) betokening the early formation of thrombus, although this was not realized at the time. The next run (C) shows definite compromise of the right posterior cerebral artery due to acute thrombus. In this patient, with the balloon immediately available, a curved Transend 10 wire was used within the balloon to direct it into the compromised vessel, which was then angioplastied. The result (D) was sustained by increasing the heparinization and administration of intravenous antiplatelet agents, and the thrombus did not reaccumulate. No distal thromboembolic complications were evident angiographically or clinically.

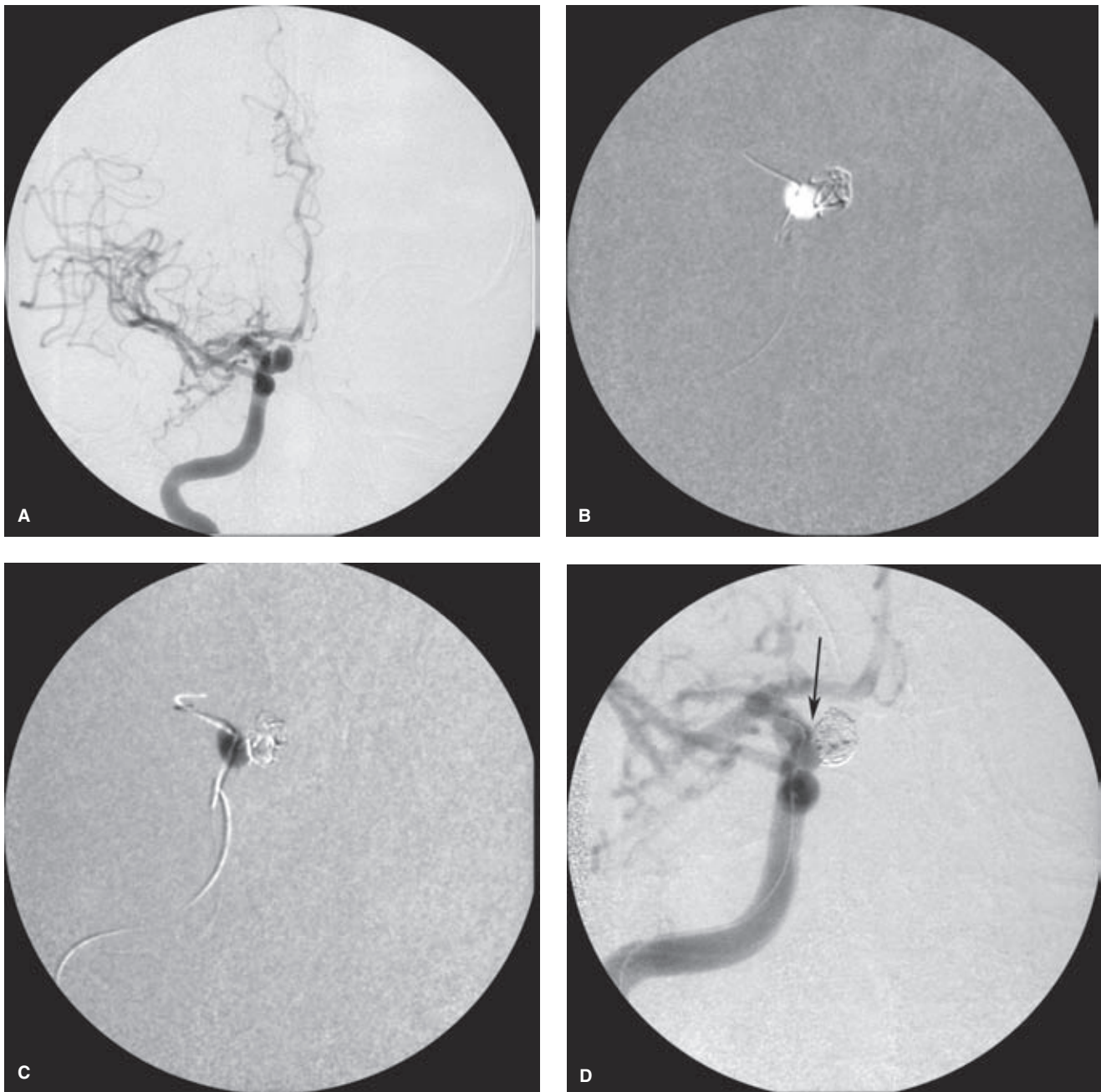


FIGURE 18-25. (A–C) Balloon reconstruction technique in an unruptured elective aneurysm and the importance of antiplatelet medication. This middle-aged patient presented with headache in the right retro-orbital area and an aneurysm of the superior hypophyseal segment of the right internal carotid artery (A). The aneurysm looks widely based, or at least does not appear to have sufficient shoulders that would confidently predict technically easy confinement of coils to the aneurysm without spillage into the parent artery. The patient was premedicated with clopidogrel and aspirin, and her preprocedure PFA-100 (platelet function analysis) indicated a satisfactory response. She was consented for possible use of a stent, but an attempt was made at first to coil the aneurysm using balloon reconstruction technique. This technique is very reassuring to the operator during the case because it gives much more control than an unsupported case using only a microcatheter and greater visibility than when using a stent. The roadmap mask (B) obtained after the first coil is inserted is acquired before the balloon is deflated. The deflated balloon (Hyperform 4 × 7 mm) leaves a white ghost on the mask, but the stable coil remains subtracted without indication of motion as the balloon deflates. Thus, the operator is assured that the coil can be detached safely. If the first coil deploys itself in a way that encompasses the entire contour of the aneurysm, roadmap masks can then be used for subsequent coils. This was the case with this aneurysm. The next image (C) shows a mask of the second detached coil acquired before the balloon was reinflated. Now, the third coil is about to emerge from the microcatheter, and the balloon has been inflated to stabilize the microcatheter and the coil mass. The final result (D) appeared satisfactory, but in comparison to the unsubtracted view of the coil mass from the same run (E), the upper margin (arrow in D) of the coil–artery interface appears suspicious for thrombus formation. This problem did not propagate or cause imaging or clinical sequelae, but the possibility of calamitous results in patients who have not responded to antiplatelet measures or who have been noncompliant with their prescription can be assumed.

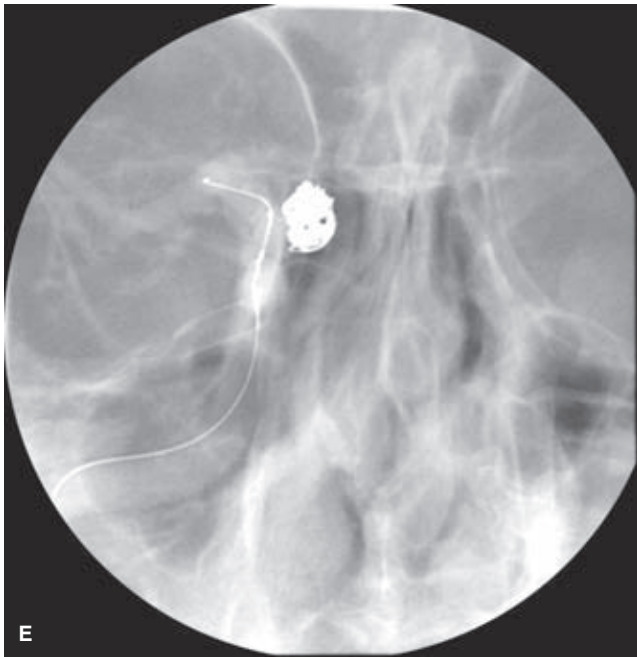


FIGURE 18-25. (CONTINUED)

may encounter during rotations in the neurointerventional suite, regardless of the favored vendor, are as follows:

Coil Geometric Configurations

The first platinum coils were all simple helices of a fixed diameter and length, for example, a 3 × 30 coil is 3 mm in diameter and 30 mm long. To encourage the first loop of coil to tumble within the aneurysm without finding the outflow of the neck into the parent artery, some coils (2D) were designed with an initial helical loop smaller than the rest, constraining its behavior somewhat. The next design was to make a coil that tumbled and configured itself into a sphere, rather than a flat series of loops, and these are the 3D coils, marketed under various proprietary legends. There are two hypothetical narratives accompanying these coils. Firstly, some vendors like to advocate a Russian doll approach, whereby successive coils of ever-diminishing size onionskin inside one another to fill the aneurysm centripetally. Other vendors promote the capacity of their form-filling coils to “seek out” the remaining spaces within the aneurysm. Whether either of these scenarios is valid in the chaotic happenstance of coil extrusion into aneurysms, particularly in the later stages of a case, is left to the discretion of the reader (Fig. 18-26).

Detachment Configurations

Various vendors have offered a variety of electrolytic, electrothermal, and hydraulic detachment mechanisms for their various coils. All have theoretical advantages of their own, but the margin between them is probably very slim (Fig. 18-27).

Coil Coating

In order to promote more active smooth muscle cell invasion and fibrosis at the mouth or neck of the aneurysm after

coil embolization, vendors offer lines of coils coated with a variety of agents designed to have this effect. There is evidence in animals of the efficacy of these coils in experimental aneurysms, but the case for their efficacy in patients is less convincing (213,214). Obliteration rates appear to be higher with bioactive coils with fewer recurrences, but at the cost of higher rates of symptomatic hydrocephalus, possibly due to a chemical meningitis (215–217).

Endovascular Stents for Aneurysm Reconstruction

Several widely porous, self-expanding stents are available as adjunctive devices during treatment of intracranial aneurysms, of which the Neuroform (Fig. 18-28) and Enterprise stents are the most commonly used (218–220). The stent sits astride the mouth of the aneurysm and permits coil deployment within the aneurysm without compromise of the parent vessel (Fig. 2.48, Figs. 18-29 and 18-30). While these devices have a major impact on cases that were completely impossible for endovascular coiling previously, data from randomized trials are not available. Clinical outcomes, aneurysm obliteration rates, and in-stent stenosis rates all appear to be satisfactory in the case series published to date (221–223).

A new generation of endovascular stent devices approaches the problem of aneurysm obliteration from a slightly different perspective. A more tightly wound mesh on the Pipeline (Fig. 18-31) and Silk devices induces a rheologic pattern of flow disruption along its margins such that eventual autothrombosis of the excluded aneurysm may take place, while perforator or branch vessels that have been jailed by device continue to flow (40–43).

Balloon Remodeling Technique

The technique of using a balloon intermittently as a buttress within the parent artery during coil embolization of an aneurysm was described by Moret et al. (224,225). Short inflations (<2 minutes) in patients under general anesthesia have not had discernible deleterious effects in complication rates in most studies, while contributing enormously to the potential of coil embolization to deal with otherwise difficult aneurysm configurations (Figs. 18-32 and 18-33). Since the advent of dedicated stents for this purpose, it is likely that this technique is less commonly used, but the benefits to patients of this change have not been clarified. Moreover, while the majority of publications comparing unsupported coiling with balloon remodeling have reported similar complication rates for both techniques (225,226), much attention has been given to reports that the use of an adjunctive balloon is associated with higher rates of thromboembolic complications or aneurysm rupture (227,228). These qualms—but perhaps more so the novelty of using intravascular stents—have somewhat eclipsed the balloon-remodeling technique in the endovascular treatment of aneurysms, perhaps unjustifiably. The balloon technique has several important advantages over stent-assisted coiling (Figs. 18-28–18-30):

- The microcatheter is pinned down within the artery, which prevents it from backing out of the aneurysm prematurely, further contributing to the density of packing achieved with this technique (Fig. 18-34). (This immobilization of the microcatheter could become a disadvantage too in *(text continues on page 282)*)

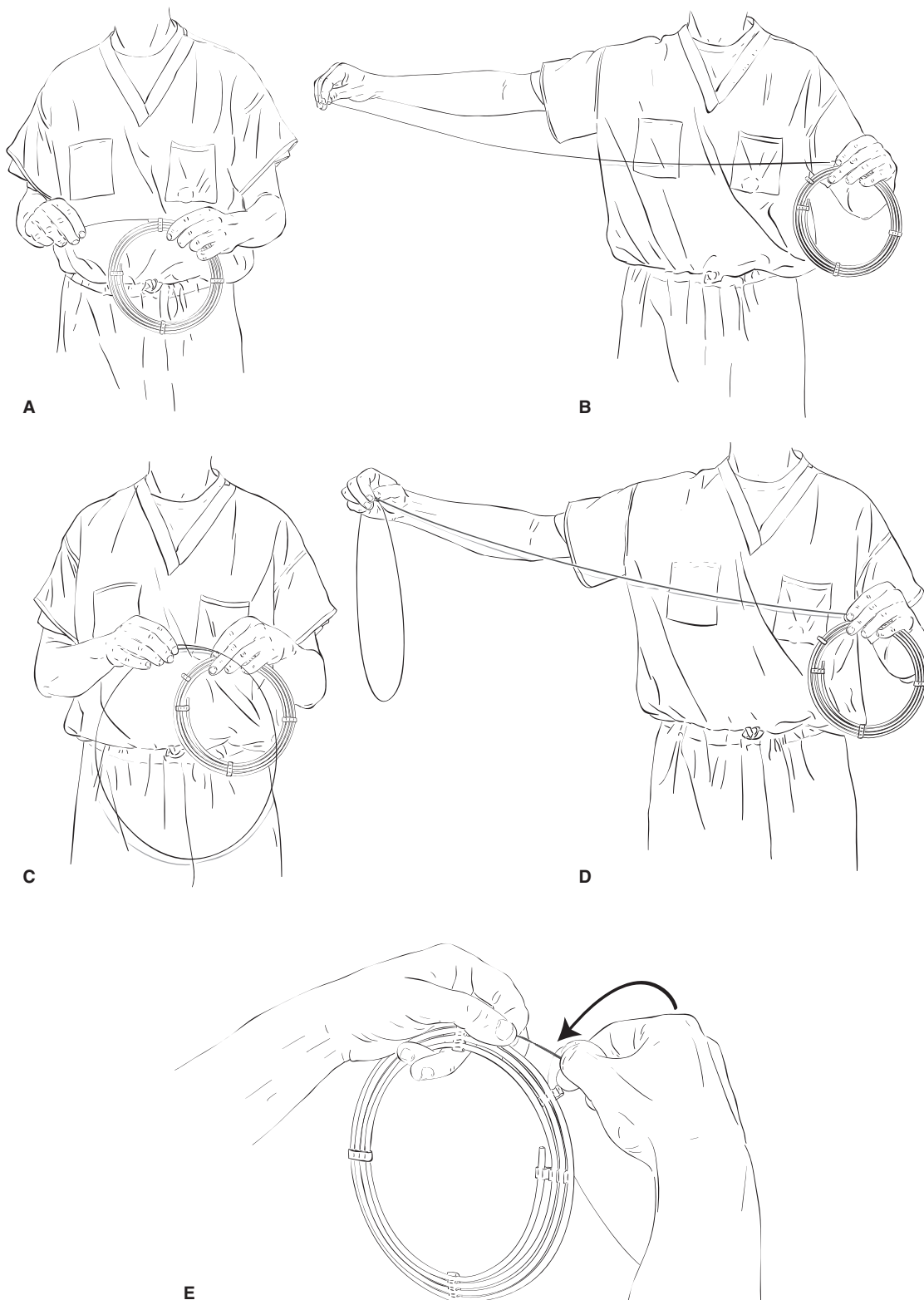


FIGURE 18-26. (A–E) Coil handling. All of the vendors' coils have one thing in common, which is that beginners get themselves into knots of anxiety about how to hold and handle such an expensive item when it seems to have such an affinity for springing free and hitting them in the eye or falling on the floor. The difficulty comes in making the loops too tight. In the diagram (**A and B**), the coil—in this case a Stryker GDC—is pulled from its housing tube with a long, relaxed sweep of the arm, until the plastic yellow or green introducer emerges into view. Then (**C and D**), the right hand reaches in and pinches where the metal meets the plastic of the introducer tube and retracts again forming a second loop, until the end of the coil is secured by the left thumb and forefinger. The housing tube can be allowed to fall to the tabletop, and the coil is under perfect control. The Stryker coils have a crimping on the back end of the introducer tube that must be loosened with an anticlockwise twist of the right hand (**E**), but all the coils from every vendor can be considered equivalent in their ease of handling. The key is to *Relax!* It is only a coil.

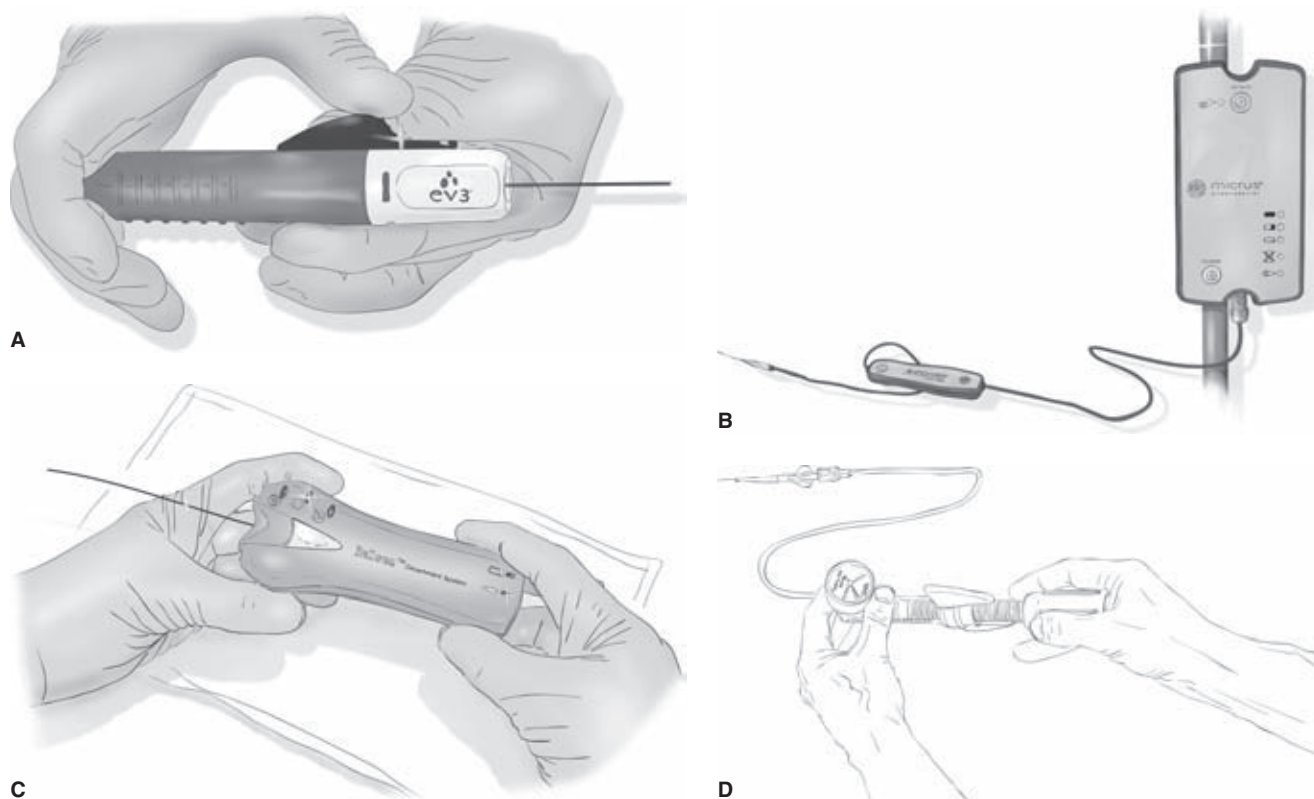


FIGURE 18-27. (A–D) Coil detachment mechanisms. Despite the best efforts of legions of patent lawyers, a remarkable confluence of technology is evident in the detachment mechanisms of the various coils on the market. These fall into two major groups: Electrolytic/electrothermal and hydraulic/mechanical. Many of the detachment boxes appear similar, but the technologies are all proprietary, and wires and boxes are not interchangeable during cases. Despite promises of the sales representatives, all of these mechanisms have idiosyncrasies and quirks peculiar to themselves with the occasional failure of detachment or other reasons for failure to advance the coil. Company names are so evanescent that one hesitates to mention them, but illustrated are the detachment mechanisms for EV-3 (A), Micrus (B), Stryker (C), and Micrus-Trufill (D).



FIGURE 18-28. Nitinol Neuroform stent. The basic mechanism of the Neuroform stent is a nitinol self-expanding structure, confined within a larger-caliber Renegade Hi-Flo microcatheter. Popular opinion is fairly unanimous that a Marksman microcatheter has several competitive features that make it the microcatheter of choice for delivery of the Neuroform stent. The Enterprise stent is delivered through a Prowler Select Plus catheter. A stabilizer or pusher device is fixed in position by the right hand, and the constraining microcatheter is retracted over it, exposing the stent. The learning curve for these devices is deceptively longer than one would anticipate.

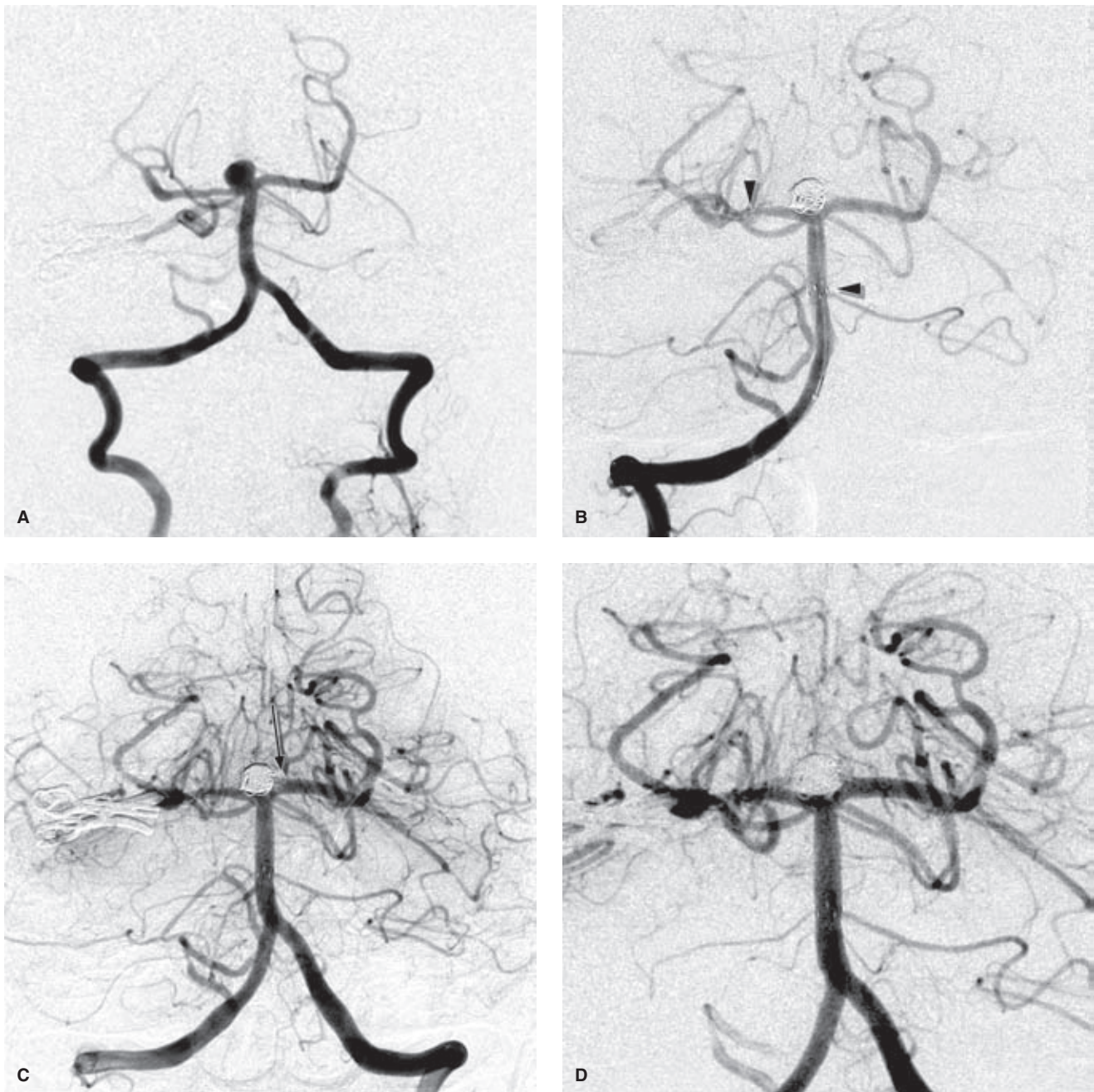


FIGURE 18-29. (A–D) Stent-supported aneurysm embolization complicated by sudden thrombus formation.

A middle-aged patient already taking clopidogrel and aspirin for coronary artery disease was admitted with subarachnoid hemorrhage. The pretreatment right vertebral arteriogram (A) showed that the base of the aneurysm was wide and incorporated into the right posterior cerebral artery. A statutory attempt to coil the aneurysm with balloon assistance proved unfruitful and stent assistance was used with a Neuroform stent on the pretext of the fortuitous happenstance that the patient was already premedicated. Bilateral vertebral artery catheters were placed. A satisfactory result (B) appeared imminent. Arrowheads indicate the proximal tines of the stent in the basilar artery and distal tines in the right posterior cerebral artery. One of the features of endovascular treatment of aneurysms is the potential for the case to turn sour in an instant, for several reasons. In this case, image (C) taken a few minutes later via the left vertebral artery, after removal of the microcatheter from the right, shows a fluffy, indistinct contour of the contrast in the left posterior cerebral artery (arrow in C). This is a typical appearance of early thrombus formation and it can progress very quickly to vessel occlusion at which point it can become much more resistant to treatment. Early recognition of this complication is very critical. Options to deal with such problems include balloon angioplasty of the clot (difficult in this case due to the stent jailing the left posterior cerebral artery), intraarterial thrombolytic (hazardous due to the recent subarachnoid hemorrhage), or intra-arterial use of a small dose of glycoprotein IIb to IIIa inhibitor (used in this case). A successful response was seen (D) on the final images. After the case a platelet function analysis suggested that the patient, a heavy smoker, was insufficiently responsive to her antiplatelet medications. Her antiplatelet regimen was doubled and no subsequent complications of this procedure were seen.

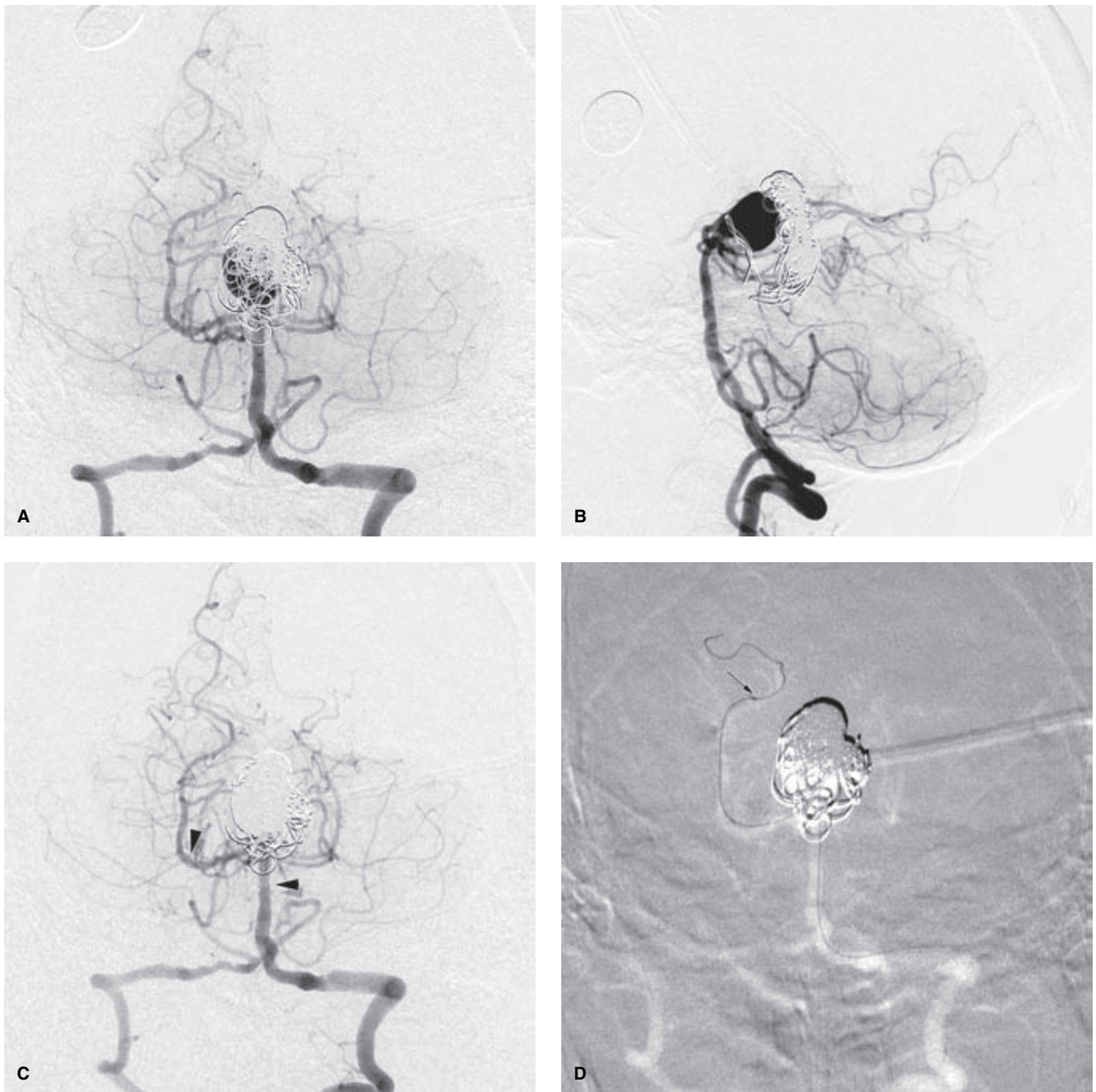


FIGURE 18-30. (A–D) Giant aneurysm recurrence of the basilar artery. Some years after previous endovascular treatment at an outside hospital this elderly lady returned with recurrence of a mass effect from this partially thrombosed giant basilar apex aneurysm. The original procedure had caused a large infarction of the left posterior cerebral artery. The wide base of the aneurysm, difficult vessels, and obscuration of the neck of the aneurysm by the previously placed coils (**A and B**) all contributed to the usual degree of difficulty with such an aneurysm embolization. Overlying coins for reference measure 18 mm. The final image (**C**) shows a reasonably satisfactory result that could certainly not have been anticipated without the use of a Neuroform stent (*arrowheads* in **C**). More germanely, this case illustrates one of the most difficult features of navigating past a giant or large aneurysm. It is often impossible to bypass the large aneurysm without looping through the aneurysm body (frequently hazardous if there has been a recent rupture) and then navigating out of the aneurysm and into the distal artery. The frustration comes when one attempts to pull back the microcatheter loop out of the aneurysm, in order to form a configuration of bridging the mouth of the aneurysm in preparation for the stent. Sometimes the microcatheter is very difficult to straighten and will preferentially backtrack itself through the aneurysm loop, regardless of whatever wire one has within it or not. The obvious need is to pin the distal microcatheter in the distal artery, so as to exert drag on the redundant loop. It might be possible to create this effect with a parallel balloon in the distal artery, for instance, and this technique has been described. In this patient, success was achieved by creating sufficient drag in the distal artery on the tip of the microcatheter (*arrow* in **D**) with a long 30-cm aneurysm coil deployed distally in the right posterior cerebral artery. The trick is in using a long coil such that there is plenty of coil in the distal artery to create friction and yet still enough length of coil within the aneurysm loop to be soft and pliable in that segment. The pusher wire of a shorter coil within the redundant loop would prevent this maneuver from working. The other component of the trick is to realize that the stiffness of a Renegade Hi-Flo or Marksman microcatheter would also stymie this maneuver. Therefore, this is more likely to work with a softer microcatheter, for example, an SL10 microcatheter as in this case. Once the microcatheter is straightened across the mouth of the aneurysm, an exchange-length microwire can be deployed for navigation of a stouter microcatheter and subsequent delivery of the stent.

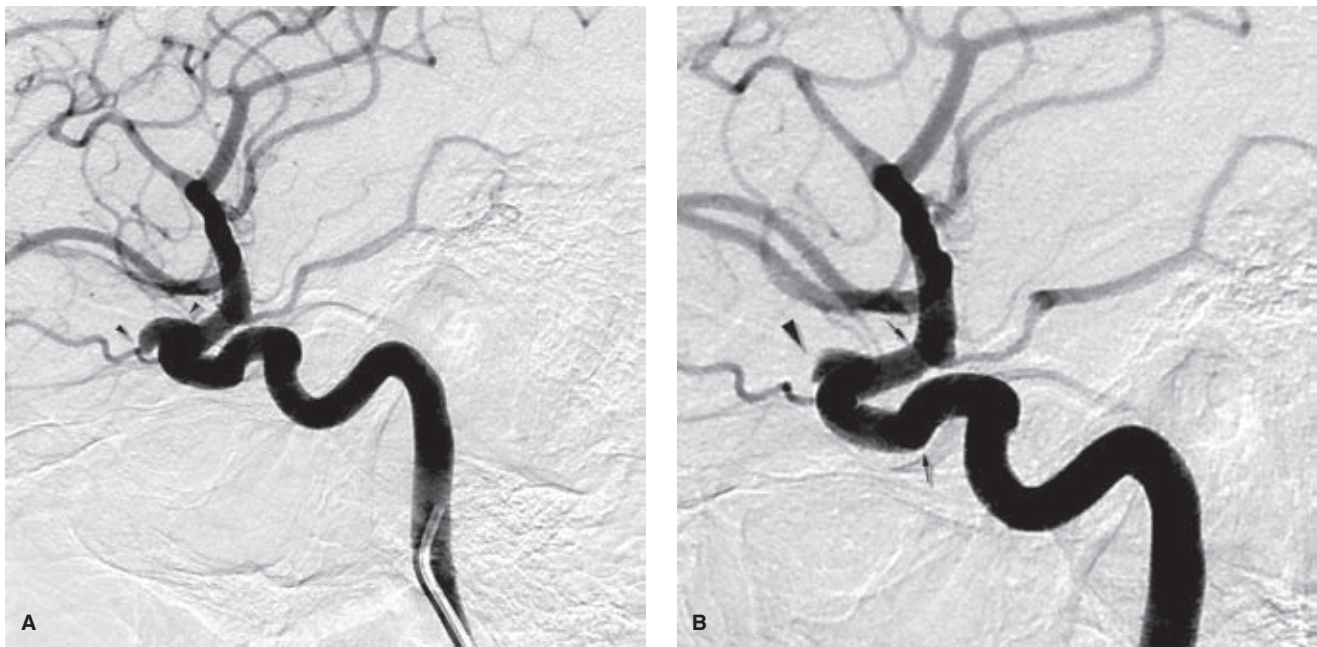


FIGURE 18-31. (A–B) Pipeline stents used for treating a left carotid–ophthalmic aneurysm. A middle-aged female complaining of vague symptoms was found to have an aneurysm, probably unrelated, of the left carotid–ophthalmic region. The diagnostic evaluation of this aneurysm illustrated the value of 3D rotational angiography in establishing that the aneurysm was separate from the origin of the ophthalmic artery, confirmed on the skewed lateral view (**A**). The aneurysm has a somewhat widely based configuration and an apex that overhangs the carotid genu (*arrowheads* in **A**), promising to be a moderately awkward technical procedure in terms of coil conformation, and almost certainly requiring a supporting stent within the artery. The patient opted to go to another hospital and have the aneurysm treated with the Pipeline device.

Embolization was performed using a brace of Pipeline devices, cupped inside one another, and the patient was discharged uneventfully. However, she returned to our hospital after 4 days with progressive ischemic symptoms in the left hemisphere. Angiography (**B**) at that time showed no identifiable clot in the stents or distally. While the aneurysm is still filling outside the stent (stent margins indicated with *small arrows* in **B**), stagnation in the anterior dome is already evident (*arrowhead* in **B**), suggesting that the rheologic impact of the stent is beginning to work. Unfortunately, the next day she developed a massive hematoma of the left hemisphere that required surgical evacuation, leaving the patient with major neurologic deficits. Whether this patient might have done better with a more established stent device and aneurysm coiling will never be known but is worth considering in view of the fact that this was likely an asymptomatic aneurysm.

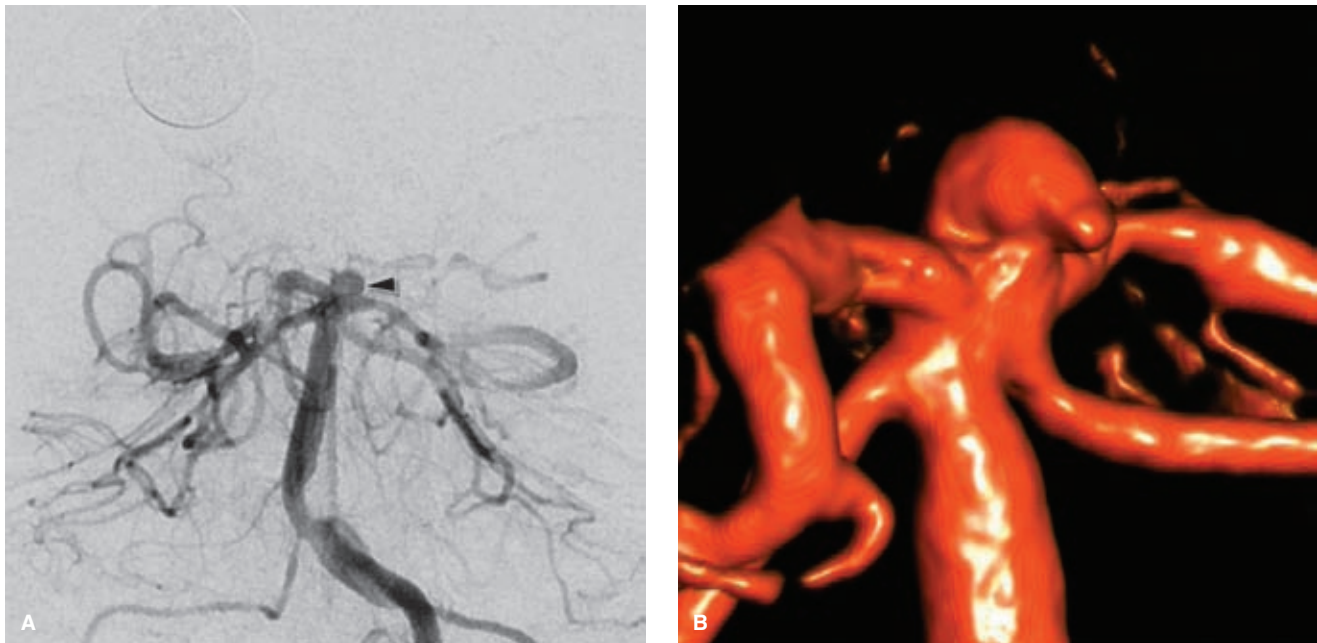


FIGURE 18-32. (A–F) Difficult ruptured basilar apex aneurysm treated with balloon reconstruction technique. This case is selected to demonstrate two principles. Firstly, very daunting-appearing aneurysms can sometimes yield surprisingly satisfactory results without resorting to use of a stent. You cannot predict how things will go unless you at least try the less invasive maneuver first. Secondly, small movements of microcatheters must be anticipated and kept to a minimum by being attentive to the degree of forward tension in the microcatheter. An AP view (**A**) of the basilar apex (*arrowhead* in **A**) shows a very difficult-looking wide-based basilar aneurysm, although the 3D view (**B**) suggests that much of the body of the aneurysm projects anterior to the basilar apex, effectively elongating the aneurysm and raising one's hopes that coils might find a stable purchase within the aneurysm without the necessity of a stent. (*continued*)



FIGURE 18-32. (CONTINUED) A roadmap image (**C**) shows the first coil in progress, while a Hyperform balloon (*arrowheads* in **C**) is gently inflated at the mouth of the aneurysm to encourage stability of the coils. Image (**D**) is taken later in the case after a coil has been placed but not detached. Arrowheads in (**D**) indicate the microcatheter markers. The distal marker has almost backed itself out of the aneurysm under the force of the final loop of coil. Slight registration artifact (*arrows* in **D**) of the markers from the deflated balloon is noted. The coil shows no such artifact and thus has not shifted with balloon deflation. At this point, the question is whether to advance the microcatheter back into the aneurysm, so as not to lose access to the aneurysm for the final coil. Sometimes, it is better to avoid this temptation and to take one's chances. It is a very small, recently ruptured aneurysm, and it can be very difficult to gauge what exactly will happen when the coil detaches and releases that tension. Image (**E**) illustrates the reason for this caution. This is taken a few seconds after image (**D**) and shows that with coil detachment, the proximal marker system (*small double arrows* in **E**) has shifted considerably on the roadmap, and the distal marker has moved back up out of view into the aneurysm of its own volition. To have given the microcatheter additional tension to force it back up into the aneurysm before coil detachment would have elevated the risk of this potential hazardous moment even further. The final image (**F**) shows a satisfactory final result without all the attendant postprocedure concerns of antiplatelet complications that would have come about with use of a stent.

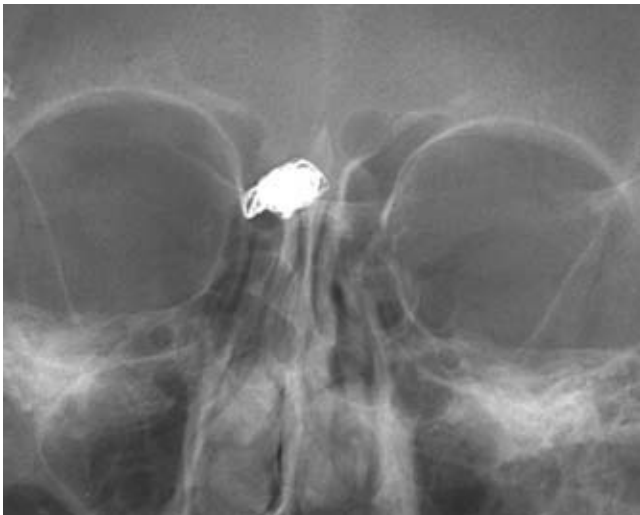


FIGURE 18-33. Follow-up of a right carotid ophthalmic aneurysm treated with balloon reconstruction. This 6-month follow-up angiogram demonstrated no evidence of coil compaction or aneurysm regrowth since the original procedure. The sharp interface between aneurysm and artery sculpted by the effect of the balloon is sustained and stable. There was persistent but unchanged minor contrast opacification of the aneurysm neck along its lateral aspect. The point of this case is to make the argument that a better result than this would have been unlikely with the use of a stent of any design, whereas the risk of the stent may well have augmented the risk and expense of the case for no clear benefit.

smaller spaces if the pressure of the extruding coil on the aneurysm wall became critically elevated.)

- The balloon is inflated with contrast and is therefore visible, unlike the nitinol stents. One can be much assured by being able to see what is what during a case and knowing that the balloon is performing its function in a discernible manner. With stents, it is often difficult to be certain whether all loops of the coils are on the aneurysm side of the “fence” or not.
- A balloon across the neck of an aneurysm is a good thing when the aneurysm ruptures during the case.
- The balloon technique does not leave a permanent device within the artery after the procedure.
- The balloon technique does not create the dilemma of whether one needs to continue antiplatelet agents after the procedure in a patient with a ruptured aneurysm. This can be a particular conflict for insertion and management of ventricular drains when they become necessary. In addition, balloon remodeling is considerably less expensive than a stent-based procedure.

Liquid Embolic Agents Onyx HD-500

Onyx HD-500 is a highly viscous preparation of an ethylene vinyl alcohol copolymer dissolved in dimethylsulfoxide with suspended tantalum for opacity (Fig. 18-35). By occluding the mouth of an aneurysm with a balloon, a slow injection of this liquid agent can be eased into the aneurysm

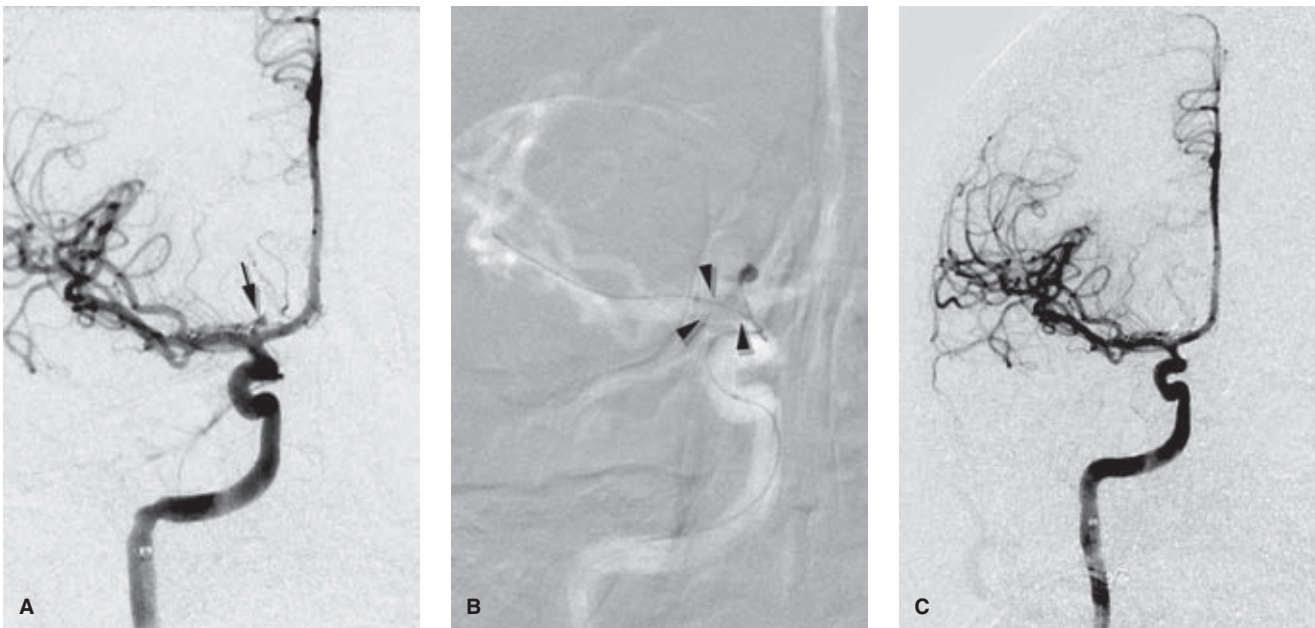


FIGURE 18-34. (A–C) Carotid terminus microaneurysm with balloon reconstruction, catheter stabilization, and aneurysm protection. This ruptured aneurysm is selected to illustrate a number of technical aspects in which the use of the adjunctive balloon played a mostly positive role. Small aneurysms can be among the most hazardous from the point of view of intraprocedural rupture due to the constraints imposed by Laplace’s law of surface tension. A minor overestimation in coil size selection is easily accommodated in a big aneurysm, but in a small aneurysm this can result in untenable stress on the aneurysm wall. Furthermore, the presence of a balloon can aggravate this problem. The balloon pins down the microcatheter and prevents it from backing out of the aneurysm in response to the stress of the coil on the aneurysm wall. Therefore, even though the presence of a balloon in the parent artery is undoubtedly welcomed when one has an aneurysmal perforation by a coil loop, one must be cognizant of the stresses against the aneurysm wall at all times in such a confined space. This particular aneurysm (arrow in A) looks like a strong candidate for an intraprocedural rupture. It is irregular in outline and appears to be possibly a pseudoaneurysm off a small sessile aneurysm body from the carotid terminus. It proved impossible to catheterize the aneurysm in a stable manner until an adjunctive balloon was deployed (arrowheads in B). This allowed the microcatheter to sit at the entrance to the aneurysm and facilitate coil extrusion into the upper lobule. The final image (C) shows some looseness of coils at the base of the aneurysm, but is otherwise satisfactory considering the difficulty of the case. Notice the grainy quality of the images related to the low radiation settings in use for most of the case. The images are perfectly satisfactory from a procedural and diagnostic point of view. Higher radiation settings would have contributed to the case only in an aesthetic way.

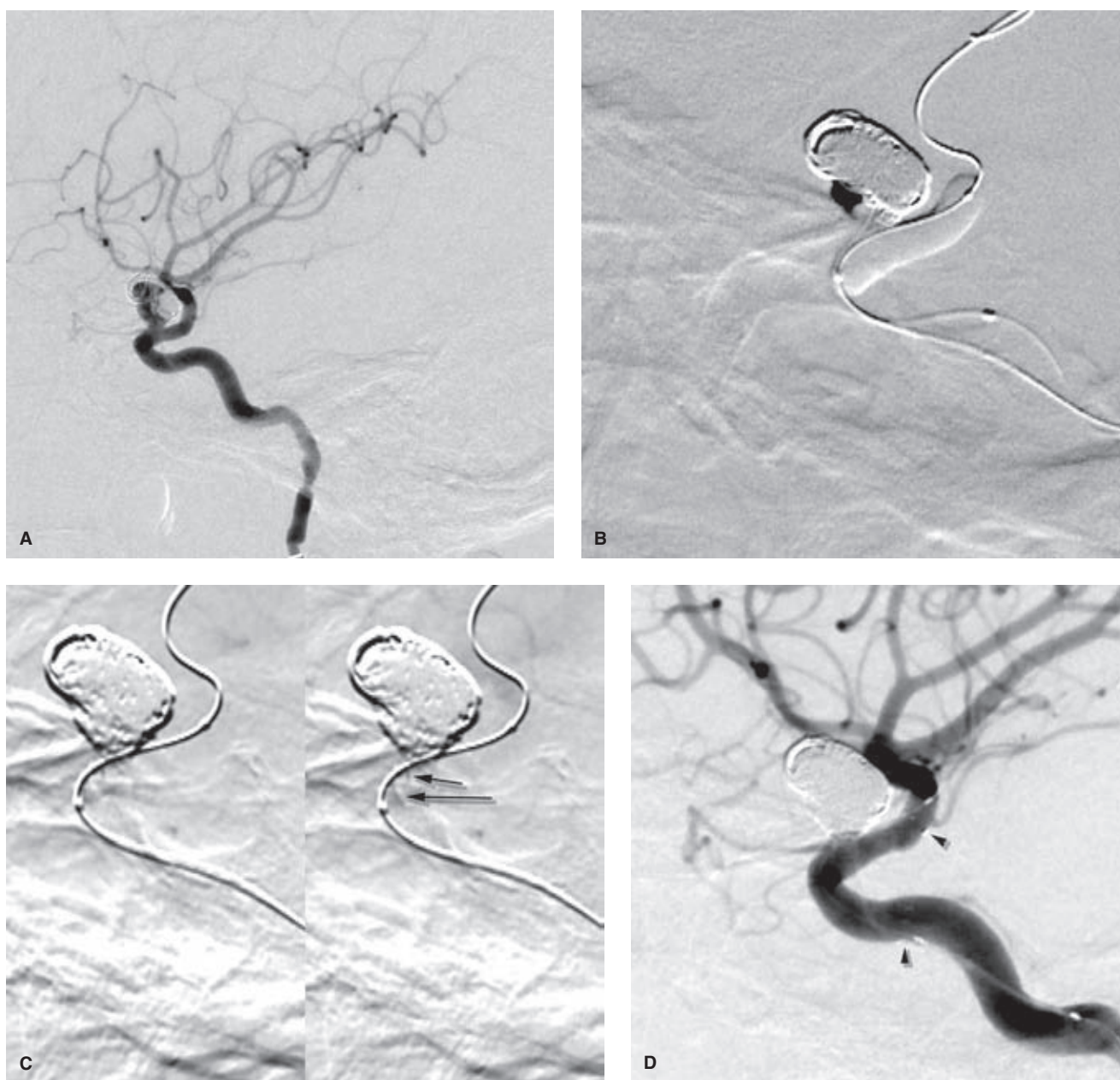


FIGURE 18-35. (A–D) Onyx HD-500 treatment of a recurrent carotid–ophthalmic aneurysm. A young adult returned with short-term recanalization and regrowth of a previously ruptured left carotid–ophthalmic aneurysm. The overall aneurysm dome–neck ratio is reasonably favorable, but the older coils within the aneurysm effectively change this calculation somewhat so that bridging the neck of the aneurysm with initial framing coils might be difficult (A). In this case the decision was to treat the patient with HD-500. A Hyperglide balloon (DMSO compatible) was inflated across the mouth of the aneurysm and a seal test was performed through a Rebar microcatheter. Once a good seal of the aneurysm was ensured, embolization of the aneurysm proceeded using some new coils in the dome and then Onyx HD-500. On the roadmap image, freshly extruded Onyx (*black* in B) can be seen confined within the aneurysm sealed by the balloon in the carotid artery. Part of the technique recommended by the vendors is to leave the microcatheter in place within the aneurysm for several minutes to allow the Onyx to solidify before final withdrawal of the microcatheter. This is done using the inflated balloon as a brace to discourage dislodgement of the Onyx. After microcatheter withdrawal in this case (C) dynamic images at the end of the DSA run show motion artifact (*arrows* in C) related to strands of Onyx flapping within the artery and moving like seaweed in the tide. These were satisfactorily stabilized by deployment of a Neuroform stent within the artery (*arrowheads* in D). Could this case have been treated less expensively with balloon reconstruction alone, or perhaps with stent and coil embolization alone, or even just coils alone without adjunctive devices?

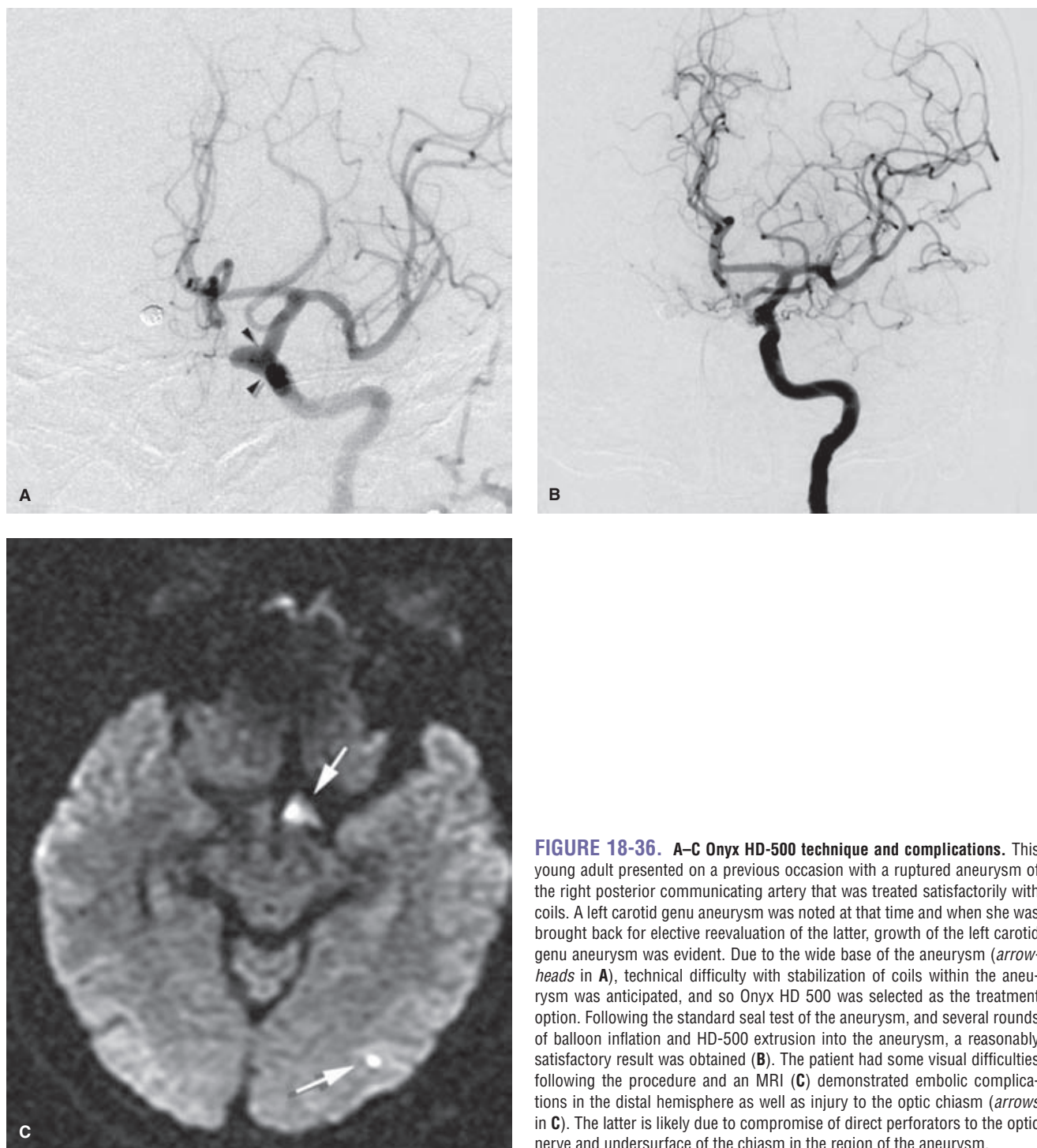


FIGURE 18-36. A–C Onyx HD-500 technique and complications. This young adult presented on a previous occasion with a ruptured aneurysm of the right posterior communicating artery that was treated satisfactorily with coils. A left carotid genu aneurysm was noted at that time and when she was brought back for elective reevaluation of the latter, growth of the left carotid genu aneurysm was evident. Due to the wide base of the aneurysm (*arrowheads in A*), technical difficulty with stabilization of coils within the aneurysm was anticipated, and so Onyx HD 500 was selected as the treatment option. Following the standard seal test of the aneurysm, and several rounds of balloon inflation and HD-500 extrusion into the aneurysm, a reasonably satisfactory result was obtained (**B**). The patient had some visual difficulties following the procedure and an MRI (**C**) demonstrated embolic complications in the distal hemisphere as well as injury to the optic chiasm (*arrows in C*). The latter is likely due to compromise of direct perforators to the optic nerve and undersurface of the chiasm in the region of the aneurysm.

over the period of a few minutes, followed by deflation of the balloon and reperfusion of the distal arterial territory. This cycle is repeated until the aneurysm is obliterated. A few published case series suggest a reasonable profile of efficacy and outcome in large or wide-mouth aneurysms, with procedure morbidity between 7% and 8% and mortality of 0% and 3% (229–232). Concerns about the embolic risks posed by the liquid nature of the preparation coupled with the likelihood that this device has been overtaken technologically by rheologic stents, at least in the domain of difficult or unusual aneurysms unsuitable for more conventional means of therapy, will likely continue to limit its use (Fig. 18-36).

References

1. Sachdev VP, Drapkin AJ, Hollin SA, et al. Subarachnoid hemorrhage following intranasal procedures. *Surg Neurol* 1977; 8(2):112–115.
2. Wakai S, Yoshimasu N, Eguchi T, et al. Traumatic intracavernous aneurysm of the internal carotid artery following surgery for chronic sinusitis. *Surg Neurol* 1980;13(5):391–394.
3. Yamaura A, Makino H, Hachisu H, et al. Secondary aneurysm due to arterial injury during surgical procedures. *Surg Neurol* 1978;10(5):327–333.
4. Hudgins PA, Browning DG, Gallups J, et al. Endoscopic paranasal sinus surgery: Radiographic evaluation of severe complications. *AJNR Am J Neuroradiol* 1992;13(4):1161–1167.

5. Ahuja A, Guterman LR, Hopkins LN. Carotid cavernous fistula and false aneurysm of the cavernous carotid artery: Complications of transphenoidal surgery. *Neurosurgery* 1992; 31(4):774–778; discussion 778–779.
6. Cabezedo JM, Carrillo R, Vaquero J, et al. Intracavernous aneurysm of the carotid artery following transphenoidal surgery. Case report. *J Neurosurg* 1981;54(1):118–121.
7. Sahrakar K, Boggan JE, Salamat MS. Traumatic aneurysm: A complication of stereotactic brain biopsy: Case report. *Neurosurgery* 1995;36(4):842–846.
8. Connaughton PN, Williams JP. Iatrogenic intracranial aneurysms. *Acta Radiol Suppl* 1976;347:59–62.
9. Aarabi B. Management of traumatic aneurysms caused by high-velocity missile head wounds. *Neurosurg Clin N Am* 1995;6(4):775–797.
10. Loop JW, White LE Jr, Shaw CM. Traumatic occlusion of the basilar artery within a clivus fracture. *Radiology* 1964;83:36–40.
11. Overton MC 3rd, Calvin TH Jr. Iatrogenic cerebral cortical aneurysm. Case report. *J Neurosurg* 1966;24(3):672–675.
12. Lassman LP, Ramani PS, Sengupta RP. Aneurysms of peripheral cerebral arteries due to surgical trauma. *Vasc Surg* 1974; 8(1):1–5.
13. Fox AL. *Intracranial Aneurysms*. New York, Berlin, Heidelberg: Springer-Verlag; 1983.
14. Buckingham MJ, Crone KR, Ball WS, et al. Traumatic intracranial aneurysms in childhood: Two cases and a review of the literature. *Neurosurgery* 1988;22(2):398–408.
15. Parkinson D, West M. Traumatic intracranial aneurysms. *J Neurosurg* 1980;52(1):11–20.
16. Quintana F, Diez C, Gutierrez A, et al. Traumatic aneurysm of the basilar artery. *AJNR Am J Neuroradiol* 1996;17(2):283–285.
17. Amirjamshidi A, Rahmat H, Abbassioun K. Traumatic aneurysms and arteriovenous fistulas of intracranial vessels associated with penetrating head injuries occurring during war: Principles and pitfalls in diagnosis and management. A survey of 31 cases and review of the literature. *J Neurosurg* 1996;84(5):769–780.
18. Holmes B, Harbaugh RE. Traumatic intracranial aneurysms: A contemporary review. *J Trauma* 1993;35(6):855–860.
19. Nakstad P, Nornes H, Hauge HN. Traumatic aneurysms of the pericallosal arteries. *Neuroradiology* 1986;28(4):335–338.
20. Ventureyra EC, Higgins MJ. Traumatic intracranial aneurysms in childhood and adolescence. Case reports and review of the literature. *Childs Nerv Syst* 1994;10(6):361–379.
21. Ferry DJ Jr, Kempe LG. False aneurysm secondary to penetration of the brain through orbitofacial wounds. Report of two cases. *J Neurosurg* 1972;36(4):503–506.
22. Carey ME, Young HF, Rish BL, et al. Follow-up study of 103 American soldiers who sustained a brain wound in Vietnam. *J Neurosurg* 1974;41(5):542–549.
23. Rahimizadeh A, Abtahi H, Daylami MS, et al. Traumatic cerebral aneurysms caused by shell fragments. Report of four cases and review of the literature. *Acta Neurochir (Wien)* 1987;84 (3–4):93–98.
24. Haddad FS. Wilder Penfield Lecture: Nature and management of penetrating head injuries during the civil war in Lebanon. *Can J Surg* 1978;21(3):233–237, 240.
25. Bell RS, Ecker RD, Severson MA 3rd, et al. The evolution of the treatment of traumatic cerebrovascular injury during wartime. *Neurosurg Focus* 2010;28(5):E5.
26. Bell RS, Vo AH, Roberts R, et al. Wartime traumatic aneurysms: Acute presentation, diagnosis, and multimodal treatment of 64 craniocervical arterial injuries. *Neurosurgery* 2010;66(1):66–79; discussion 79.
27. Cohen JE, Gomori JM, Segal R, et al. Results of endovascular treatment of traumatic intracranial aneurysms. *Neurosurgery* 2008;63(3):476–485; discussion 485–476.
28. Risdall JE, Menon DK. Traumatic brain injury. *Philos Trans R Soc Lond B Biol Sci* 2011;366(1562):241–250.
29. Armonda RA, Bell RS, Vo AH, et al. Wartime traumatic cerebral vasospasm: Recent review of combat casualties. *Neurosurgery* 2006;59(6):1215–1225; discussion 1225.
30. Vadivelu S, Bell RS, Crandall B, et al. Delayed detection of carotid-cavernous fistulas associated with wartime blast-induced craniofacial trauma. *Neurosurg Focus* 2010;28(5):E6.
31. Kieck CF, de Villiers JC. Vascular lesions due to transcranial stab wounds. *J Neurosurg* 1984;60(1):42–46.
32. Soria ED, Paroski MW, Schamann ME. Traumatic aneurysms of cerebral vessels: A case study and review of the literature. *Angiology* 1988;39(7 pt 1):609–615.
33. Davis JM, Zimmerman RA. Injury of the carotid and vertebral arteries. *Neuroradiology* 1983;25(2):55–69.
34. du Trevou MD, van Dellen JR. Penetrating stab wounds to the brain: The timing of angiography in patients presenting with the weapon already removed. *Neurosurgery* 1992; 31(5):905–911; discussion 911–902.
35. Cohen MM, Hemalatha CP, D'Addario RT, et al. Embolization from a fusiform middle cerebral artery aneurysm. *Stroke* 1980;11(2):158–161.
36. Little JR, St Louis P, Weinstein M, et al. Giant fusiform aneurysm of the cerebral arteries. *Stroke* 1981;12(2):183–188.
37. Bederson JB, Zabramski JM, Spetzler RF. Treatment of fusiform intracranial aneurysms by circumferential wrapping with clip reinforcement. Technical note. *J Neurosurg* 1992;77(3):478–480.
38. Wakui K, Kobayashi S, Takemae T, et al. Giant thrombosed vertebral artery aneurysm managed with extracranial–intracranial bypass surgery and aneurysmectomy. Case report. *J Neurosurg* 1992;77(4):624–627.
39. Anson JA, Lawton MT, Spetzler RF. Characteristics and surgical treatment of dolichoectatic and fusiform aneurysms. *J Neurosurg* 1996;84(2):185–193.
40. Fischer S, Vajda Z, Aguilar Perez M, et al. Pipeline embolization device (PED) for neurovascular reconstruction: Initial experience in the treatment of 101 intracranial aneurysms and dissections. *Neuroradiology* 2011;54(4):369–382.
41. McAuliffe W, Wycoco V, Rice H, et al. Immediate and mid-term results following treatment of unruptured intracranial aneurysms with the Pipeline embolization device. *AJNR Am J Neuroradiol* 2011;33(1):164–170.
42. Tahtinen OI, Manninen HI, Vanninen RL, et al. The silk flow diverting stent in the endovascular treatment of complex intracranial aneurysms: Technical aspects and mid-term results in 24 consecutive patients. *Neurosurgery* 2011;70(3): 617–623.
43. Wagner A, Cortsen M, Hauerberg J, et al. Treatment of intracranial aneurysms. Reconstruction of the parent artery with flow-diverting (Silk) stent. *Neuroradiology* 2011;54(7): 709–718.
44. Boeri R, Passerini A. The megadolichobasilar anomaly. *J Neurol Sci* 1964;11:475–484.
45. Mizutani T. A fatal, chronically growing basilar artery: A new type of dissecting aneurysm. *J Neurosurg* 1996;84(6): 962–971.
46. Radhakrishnan VV, Saraswathy A, Rout D, et al. Mycotic aneurysms of the intracranial vessels. *Indian J Med Res* 1994; 100:228–231.
47. Sinzobahamvya N, Kalangu K, Hamel-Kalinowski W. Arterial aneurysms associated with human immunodeficiency virus (HIV) infection. *Acta Chir Belg* 1989;89(4):185–188.
48. Lang C, Jacobi G, Kreuz W, et al. Rapid development of giant aneurysm at the base of the brain in an 8-year-old boy with perinatal HIV infection. *Acta Histochem Suppl* 1992; 42:83–90.

49. Marks C, Kuskov S. Pattern of arterial aneurysms in acquired immunodeficiency disease. *World J Surg* 1995;19(1):127–132.
50. Lerner PI, Weinstein L. Infective endocarditis in the antibiotic era. *N Engl J Med* 1966;274(5):259–266 contd.
51. Ducruet AF, Hickman ZL, Zacharia BE, et al. Intracranial infectious aneurysms: A comprehensive review. *Neurosurg Rev* 2010;33(1):37–46.
52. Corr P, Wright M, Handler LC. Endocarditis-related cerebral aneurysms: Radiologic changes with treatment. *AJNR Am J Neuroradiol* 1995;16(4):745–748.
53. Cates JE, Christie RV. Subacute bacterial endocarditis. *Q J Med* 1951;20:93–120.
54. Jones HR Jr, Siekert RG, Geraci JE. Neurologic manifestations of bacterial endocarditis. *Ann Intern Med* 1969;71(1):21–28.
55. Bohmfalk GL, Story JL, Wissinger JP, et al. Bacterial intracranial aneurysm. *J Neurosurg* 1978;48(3):369–382.
56. Bingham WF. Treatment of mycotic intracranial aneurysms. *J Neurosurg* 1977;46(4):428–437.
57. Morawetz RB, Karp RB. Evolution and resolution of intracranial bacterial (mycotic) aneurysms. *Neurosurgery* 1984;15(1):43–49.
58. Phuong LK, Link M, Wijdicks E. Management of intracranial infectious aneurysms: A series of 16 cases. *Neurosurgery* 2002;51(5):1145–1151; discussion 1151–1142.
59. Scotti G, Li MH, Righi C, et al. Endovascular treatment of bacterial intracranial aneurysms. *Neuroradiology* 1996;38(2):186–189.
60. Khayata MH, Aymard A, Casasco A, et al. Selective endovascular techniques in the treatment of cerebral mycotic aneurysms. Report of three cases. *J Neurosurg* 1993;78(4):661–665.
61. Hove B, Andersen BB, Christiansen TM. Intracranial oncotic aneurysms from choriocarcinoma. Case report and review of the literature. *Neuroradiology* 1990;32(6):526–528.
62. Pullar M, Blumbergs PC, Phillips GE, et al. Neoplastic cerebral aneurysm from metastatic gestational choriocarcinoma. Case report. *J Neurosurg* 1985;63(4):644–647.
63. Ho KL. Neoplastic aneurysm and intracranial hemorrhage. *Cancer* 1982;50(12):2935–2940.
64. Kochi N, Tani E, Yokota M, et al. Neoplastic cerebral aneurysm from lung cancer. Case report. *J Neurosurg* 1984;60(3):640–643.
65. Reina A, Seal RB. False cerebral aneurysm associated with metastatic carcinoma of the brain. Case report. *J Neurosurg* 1974;41(3):380–382.
66. Barker CS. Peripheral cerebral aneurysm associated with a glioma. *Neuroradiology* 1992;34(1):30–32.
67. Fujiwara T, Mino S, Nagao S, et al. Metastatic choriocarcinoma with neoplastic aneurysms cured by aneurysm resection and chemotherapy. Case report. *J Neurosurg* 1992;76(1):148–151.
68. Tamuleviciute E, Taeshineetanakul P, Terbrugge K, et al. Myxomatous aneurysms: A case report and literature review. *Interv Neuroradiol* 2011;17(2):188–194.
69. Markel ML, Waller BF, Armstrong WF. Cardiac myxoma. A review. *Medicine (Baltimore)* 1987;66(2):114–125.
70. Desousa AL, Muller J, Campbell R, et al. Atrial myxoma: A review of the neurological complications, metastases, and recurrences. *J Neurol Neurosurg Psychiatry* 1978;41(12):1119–1124.
71. Koo YH, Kim TG, Kim OJ, et al. Multiple fusiform cerebral aneurysms and highly elevated serum interleukin-6 in cardiac myxoma. *J Korean Neurosurg Soc* 2009;45(6):394–396.
72. Orlandi A, Ciucci A, Ferlosio A, et al. Increased expression and activity of matrix metalloproteinases characterize embolic cardiac myxomas. *Am J Pathol* 2005;166(6):1619–1628.
73. Knepper LE, Biller J, Adams HP Jr, et al. Neurologic manifestations of atrial myxoma. A 12-year experience and review. *Stroke* 1988;19(11):1435–1440.
74. Marazuela M, Garcia-Merino A, Yebra M, et al. Magnetic resonance imaging and angiography of the brain in embolic left atrial myxoma. *Neuroradiology* 1989;31(2):137–139.
75. Mizutani T. Middle cerebral artery dissecting aneurysm with persistent patent pseudolumen. Case report. *J Neurosurg* 1996;84(2):267–268.
76. Krings T, Geibprasert S, terBrugge KG. Pathomechanisms and treatment of pediatric aneurysms. *Childs Nerv Syst* 2010;26(10):1309–1318.
77. Sasaki O, Ogawa H, Koike T, et al. A clinicopathological study of dissecting aneurysms of the intracranial vertebral artery. *J Neurosurg* 1991;75(6):874–882.
78. Mizutani T, Aruga T, Kirino T, et al. Recurrent subarachnoid hemorrhage from untreated ruptured vertebrobasilar dissecting aneurysms. *Neurosurgery* 1995;36(5):905–911; discussion 912–903.
79. Caplan LR, Estol CJ, Massaro AR. Dissection of the posterior cerebral arteries. *Arch Neurol* 2005;62(7):1138–1143.
80. Leibowitz R, Do HM, Marcellus ML, et al. Parent vessel occlusion for vertebrobasilar fusiform and dissecting aneurysms. *AJNR Am J Neuroradiol* 2003;24(5):902–907.
81. Rabinov JD, Hellinger FR, Morris PP, et al. Endovascular management of vertebrobasilar dissecting aneurysms. *AJNR Am J Neuroradiol* 2003;24(7):1421–1428.
82. Kim CH, Son YJ, Paek SH, et al. Clinical analysis of vertebrobasilar dissection. *Acta Neurochir (Wien)* 2006;148(4):395–404.
83. Sakata N, Takebayashi S, Kojima M, et al. Different roles of arteriosclerosis in the rupture of intracranial dissecting aneurysms. *Histopathology* 2001;38(4):325–337.
84. Songsaeng D, Srivatanakul K, Krings T, et al. Symptomatic spontaneous vertebrobasilar dissections in children: Review of 29 consecutive cases. *J Neurosurg Pediatr* 2010;6(3):233–243.
85. Scott GE, Neubuerger KT, Denst J. Dissecting aneurysms of intracranial arteries. *Neurology* 1960;10:22–27.
86. Clower BR, Sullivan DM, Smith RR. Intracranial vessels lack vasa vasorum. *J Neurosurg* 1984;61(1):44–48.
87. Kitani R, Itouji T, Noda Y, et al. Dissecting aneurysms of the anterior circle of Willis arteries. Report of two cases. *J Neurosurg* 1987;67(2):296–300.
88. Piepgras DG, McGrail KM, Tazelaar HD. Intracranial dissection of the distal middle cerebral artery as an uncommon cause of distal cerebral artery aneurysm. Case report. *J Neurosurg* 1994;80(5):909–913.
89. Chang V, Rewcastle NB, Harwood-Nash DC, et al. Bilateral dissecting aneurysms of the intracranial internal carotid arteries in an 8-year-old boy. *Neurology* 1975;25(6):573–579.
90. Pozzati E, Andreoli A, Padovani R, et al. Dissecting aneurysms of the basilar artery. *Neurosurgery* 1995;36(2):254–258.
91. Matschke J. Fatal ischemic stroke due to dissecting aneurysm of the intracranial arteries presenting as sudden unexpected death in childhood. *Am J Forensic Med Pathol* 2010;31(4):364–369.
92. Kocaeli H, Chaalala C, Andaluz N, et al. Spontaneous intradural vertebral artery dissection: A single-center experience and review of the literature. *Skull Base* 2009;19(3):209–218.
93. Kitanaka C, Tanaka J, Kuwahara M, et al. Nonsurgical treatment of unruptured intracranial vertebral artery dissection with serial follow-up angiography. *J Neurosurg* 1994;80(4):667–674.
94. Kitanaka C, Sasaki T, Eguchi T, et al. Intracranial vertebral artery dissections: Clinical, radiological features, and surgical considerations. *Neurosurgery* 1994;34(4):620–626; discussion 626–627.
95. Yamaura A, Watanabe Y, Saeki N. Dissecting aneurysms of the intracranial vertebral artery. *J Neurosurg* 1990;72(2):183–188.

96. Durward QJ. Treatment of vertebral artery dissecting aneurysm by aneurysm trapping and posterior inferior cerebellar artery reimplantation. Case report. *J Neurosurg* 1995;82(1):137–139.
97. Higashida RT, Halbach VV, Cahan LD, et al. Detachable balloon embolization therapy of posterior circulation intracranial aneurysms. *J Neurosurg* 1989;71(4):512–519.
98. Hodes JE, Aymard A, Gobin YP, et al. Endovascular occlusion of intracranial vessels for curative treatment of unclippable aneurysms: Report of 16 cases. *J Neurosurg* 1991;75(5):694–701.
99. Steinberg GK, Drake CG, Peerless SJ. Deliberate basilar or vertebral artery occlusion in the treatment of intracranial aneurysms. Immediate results and long-term outcome in 201 patients. *J Neurosurg* 1993;79(2):161–173.
100. Tsukahara T, Wada H, Satake K, et al. Proximal balloon occlusion for dissecting vertebral aneurysms accompanied by subarachnoid hemorrhage. *Neurosurgery* 1995;36(5):914–919; discussion 919–920.
101. Binning MJ, Khalessi AA, Siddiqui AH, et al. Stent placement for the treatment of a symptomatic intracranial arterial dissection in an adolescent. *J Neurosurg Pediatr* 2010;6(2):154–158.
102. Jeon P, Kim BM, Kim DI, et al. Emergent self-expanding stent placement for acute intracranial or extracranial internal carotid artery dissection with significant hemodynamic insufficiency. *AJNR Am J Neuroradiol* 2010;31(8):1529–1532.
103. Lee JM, Kim TS, Joo SP, et al. Endovascular treatment of ruptured dissecting vertebral artery aneurysms—Long-term follow-up results, benefits of early embolization, and predictors of outcome. *Acta Neurochir (Wien)* 2010;152(9):1455–1465.
104. Ohta H, Natarajan SK, Hauck EF, et al. Endovascular stent therapy for extracranial and intracranial carotid artery dissection: Single-center experience. *J Neurosurg* 2011;115(1):91–100.
105. Yoon WK, Kim YW, Kim SR, et al. Angiographic and clinical outcomes of stent-alone treatment for spontaneous vertebrobasilar dissecting aneurysm. *Acta Neurochir (Wien)* 2010;152(9):1477–1486; discussion 1486.
106. Halbach VV, Higashida RT, Dowd CF, et al. Endovascular treatment of vertebral artery dissections and pseudoaneurysms. *J Neurosurg* 1993;79(2):183–191.
107. Aoki N, Sakai T. Rebleeding from intracranial dissecting aneurysm in the vertebral artery. *Stroke* 1990;21(11):1628–1631.
108. Yamaura A. Diagnosis and treatment of vertebral aneurysms. *J Neurosurg* 1988;69(3):345–349.
109. Zhao WY, Krings T, Alvarez H, et al. Management of spontaneous haemorrhagic intracranial vertebrobasilar dissection: Review of 21 consecutive cases. *Acta Neurochir (Wien)* 2007;149(6):585–596; discussion 596.
110. Nakagawa K, Touho H, Morisako T, et al. Long-term follow-up study of unruptured vertebral artery dissection: Clinical outcomes and serial angiographic findings. *J Neurosurg* 2000;93(1):19–25.
111. Yoshimoto Y, Wakai S. Unruptured intracranial vertebral artery dissection. Clinical course and serial radiographic imagings. *Stroke* 1997;28(2):370–374.
112. Collier J. Cerebral haemorrhage due to causes other than atherosclerosis. *Br Med J* 1931;2:519–521.
113. Stebbens WE. Aneurysms and anatomical variations of cerebral arteries. *Arch Pathol* 1963;75:45–64.
114. Suzuki J, Ohara H. Clinicopathological study of cerebral aneurysms. Origin, rupture, repair, and growth. *J Neurosurg* 1978;48(4):505–514.
115. Schievink WI, Katzmann JA, Piepgras DG, et al. Alpha-1-antitrypsin phenotypes among patients with intracranial aneurysms. *J Neurosurg* 1996;84(5):781–784.
116. Lach B, Nair SG, Russell NA, et al. Spontaneous carotid-cavernous fistula and multiple arterial dissections in type IV Ehlers–Danlos syndrome. Case report. *J Neurosurg* 1987;66(3):462–467.
117. Desal HA, Toulgoat F, Raoul S, et al. Ehlers–Danlos syndrome type IV and recurrent carotid-cavernous fistula: Review of the literature, endovascular approach, technique and difficulties. *Neuroradiology* 2005;47(4):300–304.
118. Zilocchi M, Macedo TA, Oderich GS, et al. Vascular Ehlers–Danlos syndrome: Imaging findings. *AJR Am J Roentgenol* 2007;189(3):712–719.
119. Mettinger KL. Fibromuscular dysplasia and the brain. II. Current concept of the disease. *Stroke* 1982;13(1):53–58.
120. Mettinger KL, Ericson K. Fibromuscular dysplasia and the brain. I. Observations on angiographic, clinical and genetic characteristics. *Stroke* 1982;13(1):46–52.
121. Schievink WI, Schaid DJ, Rogers HM, et al. On the inheritance of intracranial aneurysms. *Stroke* 1994;25(10):2028–2037.
122. Vlak MH, Algra A, Brandenburg R, et al. Prevalence of unruptured intracranial aneurysms, with emphasis on sex, age, comorbidity, country, and time period: A systematic review and meta-analysis. *Lancet Neurol* 2011;10(7):626–636.
123. Xu HW, Yu SQ, Mei CL, et al. Screening for intracranial aneurysm in 355 patients with autosomal-dominant polycystic kidney disease. *Stroke* 2011;42(1):204–206.
124. Schievink WI, Parisi JE, Piepgras DG. Familial intracranial aneurysms: An autopsy study. *Neurosurgery* 1997;41(6):1247–1251; discussion 1251–1242.
125. Nakagawa T, Hashi K. The incidence and treatment of asymptomatic, unruptured cerebral aneurysms. *J Neurosurg* 1994;80(2):217–223.
126. Obuchowski NA, Modic MT, Magdinec M. Current implications for the efficacy of noninvasive screening for occult intracranial aneurysms in patients with a family history of aneurysms. *J Neurosurg* 1995;83(1):42–49.
127. Lozano AM, Leblanc R. Familial intracranial aneurysms. *J Neurosurg* 1987;66(4):522–528.
128. Leblanc R. Familial cerebral aneurysms. A bias for women. *Stroke* 1996;27(6):1050–1054.
129. Leblanc R, Melanson D, Tampieri D, et al. Familial cerebral aneurysms: A study of 13 families. *Neurosurgery* 1995;37(4):633–638; discussion 638–639.
130. Dyste GN, Beck DW. De novo aneurysm formation following carotid ligation: Case report and review of the literature. *Neurosurgery* 1989;24(1):88–92.
131. Hassler O. Experimental carotid ligation followed by aneurysmal formation and other morphological changes in the circle of Willis. *J Neurosurg* 1963;20:1–7.
132. Fujiwara S, Fujii K, Fukui M. De novo aneurysm formation and aneurysm growth following therapeutic carotid occlusion for intracranial internal carotid artery (ICA) aneurysms. *Acta Neurochir (Wien)* 1993;120(1–2):20–25.
133. Timperman PE, Tomsick TA, Tew JM Jr, et al. Aneurysm formation after carotid occlusion. *AJNR Am J Neuroradiol* 1995;16(2):329–331.
134. Schievink WI, Wijdicks EF, Piepgras DG, et al. The poor prognosis of ruptured intracranial aneurysms of the posterior circulation. *J Neurosurg* 1995;82(5):791–795.
135. Wiebers DO, Piepgras DG, Meyer FB, et al. Pathogenesis, natural history, and treatment of unruptured intracranial aneurysms. *Mayo Clin Proc* 2004;79(12):1572–1583.
136. Sonobe M, Yamazaki T, Yonekura M, et al. Small unruptured intracranial aneurysm verification study: SUAVE study, Japan. *Stroke* 2010;41(9):1969–1977.
137. Wiebers DO, Whisnant JP, Huston J 3rd, et al. Unruptured intracranial aneurysms: Natural history, clinical outcome, and

- risks of surgical and endovascular treatment. *Lancet* 2003; 362(9378):103–110.
138. Sato K, Yoshimoto Y. Risk profile of intracranial aneurysms: Rupture rate is not constant after formation. *Stroke* 2011; 42(12):3376–3381.
 139. Schievink WI, Piepgras DG, Wirth FP. Rupture of previously documented small asymptomatic saccular intracranial aneurysms. Report of three cases. *J Neurosurg* 1992;76(6): 1019–1024.
 140. Juvela S, Porras M, Heiskanen O. Natural history of unruptured intracranial aneurysms: A long-term follow-up study. *J Neurosurg* 1993;79(2):174–182.
 141. Sacco RL, Wolf PA, Bharucha NE, et al. Subarachnoid and intracerebral hemorrhage: Natural history, prognosis, and precursive factors in the Framingham Study. *Neurology* 1984; 34(7):847–854.
 142. Bell BA, Symon L. Smoking and subarachnoid haemorrhage. *Br Med J* 1979;1(6163):577–578.
 143. Petitti DB, Wingerd J. Use of oral contraceptives, cigarette smoking, and risk of subarachnoid haemorrhage. *Lancet* 1978;2(8083):234–235.
 144. Fogelholm R. Subarachnoid hemorrhage in middle-Finland: Incidence, early prognosis and indications for neurosurgical treatment. *Stroke* 1981;12(3):296–301.
 145. King JT Jr, Glick HA, Mason TJ, et al. Elective surgery for asymptomatic, unruptured, intracranial aneurysms: A cost-effectiveness analysis. *J Neurosurg* 1995;83(3):403–412.
 146. Greving JP, Rinkel GJ, Buskens E, et al. Cost-effectiveness of preventive treatment of intracranial aneurysms: New data and uncertainties. *Neurology* 2009;73(4):258–265.
 147. Ljunggren B, Saveland H, Brandt L, et al. Early operation and overall outcome in aneurysmal subarachnoid hemorrhage. *J Neurosurg* 1985;62(4):547–551.
 148. Whisnant JP, Sacco SE, O’Fallon WM, et al. Referral bias in aneurysmal subarachnoid hemorrhage. *J Neurosurg* 1993; 78(5):726–732.
 149. Longstreth WT Jr, Nelson LM, Koepsell TD, et al. Clinical course of spontaneous subarachnoid hemorrhage: A population-based study in King County, Washington. *Neurology* 1993;43(4):712–718.
 150. Le Roux PD, Elliott JP, Downey L, et al. Improved outcome after rupture of anterior circulation aneurysms: A retrospective 10-year review of 224 good-grade patients. *J Neurosurg* 1995;83(3):394–402.
 151. Kassell NF, Torner JC, Haley EC Jr, et al. The International Cooperative Study on the Timing of Aneurysm Surgery. Part 1: Overall management results. *J Neurosurg* 1990;73(1): 18–36.
 152. Kassell NF, Torner JC, Jane JA, et al. The International Cooperative Study on the Timing of Aneurysm Surgery. Part 2: Surgical results. *J Neurosurg* 1990;73(1):37–47.
 153. Hunt WE, Hess RM. Surgical risk as related to time of intervention in the repair of intracranial aneurysms. *J Neurosurg* 1968;28(1):14–20.
 154. Vermeulen M, van Gijn J, Hijdra A, et al. Causes of acute deterioration in patients with a ruptured intracranial aneurysm. A prospective study with serial CT scanning. *J Neurosurg* 1984;60(5):935–939.
 155. Leblanc R. The minor leak preceding subarachnoid hemorrhage. *J Neurosurg* 1987;66(1):35–39.
 156. Fisher CM, Kistler JP, Davis JM. Relation of cerebral vasospasm to subarachnoid hemorrhage visualized by computerized tomographic scanning. *Neurosurgery* 1980;6(1): 1–9.
 157. Kistler JP, Crowell RM, Davis KR, et al. The relation of cerebral vasospasm to the extent and location of subarachnoid blood visualized by CT scan: A prospective study. *Neurology* 1983;33(4):424–436.
 158. Graff-Radford NR, Torner J, Adams HP Jr, et al. Factors associated with hydrocephalus after subarachnoid hemorrhage. A report of the Cooperative Aneurysm Study. *Arch Neurol* 1989;46(7):744–752.
 159. Hasan D, Wijdieks EF, Vermeulen M. Hyponatremia is associated with cerebral ischemia in patients with aneurysmal subarachnoid hemorrhage. *Ann Neurol* 1990;27(1): 106–108.
 160. Yuki K, Kodama Y, Onda J, et al. Coronary vasospasm following subarachnoid hemorrhage as a cause of stunned myocardium. Case report. *J Neurosurg* 1991;75(2):308–311.
 161. Ehrifai AM, Bailes JE, Shih SR, et al. Characterization of the cardiac effects of acute subarachnoid hemorrhage in dogs. *Stroke* 1996;27(4):737–741; discussion 741–732.
 162. Cantore G, Santoro A, Guidetti G, et al. Surgical treatment of giant intracranial aneurysms: Current viewpoint. *Neurosurgery* 2008;63(4 suppl 2):279–289; discussion 289–290.
 163. Christiano LD, Gupta G, Prestigiacomo CJ, et al. Giant serpentine aneurysms. *Neurosurg Focus* 2009;26(5):E5.
 164. Lee SJ, Ahn JS, Kwun BD, et al. Giant serpentine aneurysm of the middle cerebral artery. *J Korean Neurosurg Soc* 2010; 48(2):177–180.
 165. Drake CG. Giant intracranial aneurysms: Experience with surgical treatment in 174 patients. *Clin Neurosurg* 1979;26: 12–95.
 166. Heros RC, Nelson PB, Ojemann RG, et al. Large and giant paraclinoid aneurysms: Surgical techniques, complications, and results. *Neurosurgery* 1983;12(2):153–163.
 167. Morley TP, Barr HW. Giant intracranial aneurysms: Diagnosis, course, and management. *Clin Neurosurg* 1969;16:73–94.
 168. Dehdashti AR, Le Roux A, Bacigaluppi S, et al. Long-term visual outcome and aneurysm obliteration rate for very large and giant ophthalmic segment aneurysms: Assessment of surgical treatment. *Acta Neurochir (Wien)* 2011;154(1): 43–52.
 169. Sughrue ME, Saloner D, Rayz VL, et al. Giant intracranial aneurysms: Evolution of management in a contemporary surgical series. *Neurosurgery* 2011;69(6):1261–70.
 170. Jahromi BS, Mocco J, Bang JA, et al. Clinical and angiographic outcome after endovascular management of giant intracranial aneurysms. *Neurosurgery* 2008;63(4):662–674; discussion 674–665.
 171. Ito M, Yoshihara M, Ishii M, et al. Cerebral aneurysms in children. *Brain Dev* 1992;14(4):263–268.
 172. Jian BJ, Hetts SW, Lawton MT, et al. Pediatric intracranial aneurysms. *Neurosurg Clin N Am* 2010;21(3):491–501.
 173. Fulkerson DH, Voorhies JM, Payner TD, et al. Middle cerebral artery aneurysms in children: Case series and review. *J Neurosurg Pediatr* 2011;8(1):79–89.
 174. Sanai N, Auguste KI, Lawton MT. Microsurgical management of pediatric intracranial aneurysms. *Childs Nerv Syst* 2010;26(10):1319–1327.
 175. Moore CH, Murchison C. On a new method of procuring the consolidation of fibrin in certain incurable aneurysms. *Med Chir Trans, London* 1864;47:129–149.
 176. Gallagher JP. Obliteration of intracranial aneurysms by pilocarpine. *JAMA* 1963;183:231–236.
 177. Alksne JF, Fingerhut AG, Rand RW. Magnetic probe for the stereotactic thrombosis of intracranial aneurysms. *J Neurol Neurosurg Psychiatry* 1967;30(2):159–162.
 178. Blakemore AH, King BG. Electrothermic coagulation of aortic aneurysms. *JAMA* 1938;111:1821–1827.
 179. Werner SC, Blakemore AH, King BG. Aneurysm of the internal carotid artery within the skull. Wiring and electrothermic coagulation. *JAMA* 1941;116:578–582.
 180. Mullan S. Experiences with surgical thrombosis of intracranial berry aneurysms and carotid cavernous fistulas. *J Neurosurg* 1974;41(6):657–670.

181. Serbinenko FA. Balloon catheterization and occlusion of major cerebral vessels. *J Neurosurg* 1974;41(2):125–145.
182. Vanninen R, Koivisto T, Saari T, et al. Ruptured intracranial aneurysms: Acute endovascular treatment with electrolytically detachable coils—A prospective randomized study. *Radiology* 1999;211(2):325–336.
183. Koivisto T, Vanninen R, Hurskainen H, et al. Outcomes of early endovascular versus surgical treatment of ruptured cerebral aneurysms. A prospective randomized study. *Stroke* 2000;31(10):2369–2377.
184. Molyneux A, Kerr R, Stratton I, et al. International Subarachnoid Aneurysm Trial (ISAT) of neurosurgical clipping versus endovascular coiling in 2143 patients with ruptured intracranial aneurysms: A randomised trial. *Lancet* 2002;360(9342):1267–1274.
185. Molyneux AJ, Kerr RS, Yu LM, et al. International subarachnoid aneurysm trial (ISAT) of neurosurgical clipping versus endovascular coiling in 2143 patients with ruptured intracranial aneurysms: A randomised comparison of effects on survival, dependency, seizures, rebleeding, subgroups, and aneurysm occlusion. *Lancet* 2005;366(9488): 809–817.
186. Molyneux AJ, Kerr RS, Birks J, et al. Risk of recurrent subarachnoid haemorrhage, death, or dependence and standardised mortality ratios after clipping or coiling of an intracranial aneurysm in the International Subarachnoid Aneurysm Trial (ISAT): Long-term follow-up. *Lancet Neurol* 2009;8(5):427–433.
187. Scott RB, Eccles F, Molyneux AJ, et al. Improved cognitive outcomes with endovascular coiling of ruptured intracranial aneurysms: Neuropsychological outcomes from the International Subarachnoid Aneurysm Trial (ISAT). *Stroke* 2010; 41(8):1743–1747.
188. Flett LM, Chandler CS, Giddings D, et al. Aneurysmal subarachnoid hemorrhage: Management strategies and clinical outcomes in a regional neuroscience center. *AJNR Am J Neuroradiol* 2005;26(2):367–372.
189. Qureshi AI, Janardhan V, Hanel RA, et al. Comparison of endovascular and surgical treatments for intracranial aneurysms: An evidence-based review. *Lancet Neurol* 2007;6(9): 816–825.
190. Lee T, Baytion M, Sciacca R, et al. Aggregate analysis of the literature for unruptured intracranial aneurysm treatment. *AJNR Am J Neuroradiol* 2005;26(8):1902–1908.
191. Brilstra EH, Rinkel GJ, van der Graaf Y, et al. Quality of life after treatment of unruptured intracranial aneurysms by neurosurgical clipping or by embolisation with coils. A prospective, observational study. *Cerebrovasc Dis* 2004;17(1):44–52.
192. Kahara VJ, Seppanen SK, Kuurne T, et al. Patient outcome after endovascular treatment of intracranial aneurysms with reference to microsurgical clipping. *Acta Neurol Scand* 1999; 99(5):284–290.
193. Lot G, Houdart E, Cophignon J, et al. Combined management of intracranial aneurysms by surgical and endovascular treatment. Modalities and results from a series of 395 cases. *Acta Neurochir (Wien)* 1999;141(6):557–562.
194. Johnston SC, Dudley RA, Gress DR, et al. Surgical and endovascular treatment of unruptured cerebral aneurysms at university hospitals. *Neurology* 1999;52(9):1799–1805.
195. Johnston SC, Zhao S, Dudley RA, et al. Treatment of unruptured cerebral aneurysms in California. *Stroke* 2001;32(3): 597–605.
196. Gallas S, Pasco A, Cottier JP, et al. A multicenter study of 705 ruptured intracranial aneurysms treated with Guglielmi detachable coils. *AJNR Am J Neuroradiol* 2005;26(7):1723–1731.
197. Raymond J, Guilbert F, Weill A, et al. Long-term angiographic recurrences after selective endovascular treatment of aneurysms with detachable coils. *Stroke* 2003;34(6):1398–1403.
198. Tamatani S, Ito Y, Abe H, et al. Evaluation of the stability of aneurysms after embolization using detachable coils: Correlation between stability of aneurysms and embolized volume of aneurysms. *AJNR Am J Neuroradiol* 2002;23(5):762–767.
199. Park HK, Horowitz M, Jungreis C, et al. Periprocedural morbidity and mortality associated with endovascular treatment of intracranial aneurysms. *AJNR Am J Neuroradiol* 2005; 26(3):506–514.
200. Niskanen M, Koivisto T, Rinne J, et al. Complications and postoperative care in patients undergoing treatment for unruptured intracranial aneurysms. *J Neurosurg Anesthesiol* 2005;17(2):100–105.
201. Biondi A. Diffusion-weighted imaging of thromboembolic events associated with coil embolization of intracranial aneurysms. *AJNR Am J Neuroradiol* 2004;25(10):1861; author reply 1861–1862.
202. Soeda A, Sakai N, Murao K, et al. Thromboembolic events associated with Guglielmi detachable coil embolization with use of diffusion-weighted MR imaging. Part II. Detection of the microemboli proximal to cerebral aneurysm. *AJNR Am J Neuroradiol* 2003;24(10):2035–2038.
203. Rordorf G, Bellon RJ, Budzik RE Jr, et al. Silent thromboembolic events associated with the treatment of unruptured cerebral aneurysms by use of Guglielmi detachable coils: Prospective study applying diffusion-weighted imaging. *AJNR Am J Neuroradiol* 2001;22(1):5–10.
204. Albayram S, Selcuk D. Thromboembolic events associated with Guglielmi detachable coil embolization of asymptomatic cerebral aneurysms: Evaluation of 66 consecutive cases with use of diffusion-weighted MR imaging. *AJNR Am J Neuroradiol* 2004;25(1):159–160; author reply 160.
205. Fiorella D, Thiabolt L, Albuquerque FC, et al. Antiplatelet therapy in neuroendovascular therapeutics. *Neurosurg Clin N Am* 2005;16(3):517–540, vi.
206. Reavey-Cantwell JF, Fox WC, Reichwage BD, et al. Factors associated with aspirin resistance in patients premedicated with aspirin and clopidogrel for endovascular neurosurgery. *Neurosurgery* 2009;64(5):890–895; discussion 895–896.
207. Sullivan J, Amarshi N. Dual antiplatelet therapy with clopidogrel and aspirin. *Am J Health Syst Pharm* 2008;65(12): 1134–1143.
208. Muller I, Besta F, Schulz C, et al. Prevalence of clopidogrel non-responders among patients with stable angina pectoris scheduled for elective coronary stent placement. *Thromb Haemost* 2003;89(5):783–787.
209. Chen WH, Lee PY, Ng W, et al. Aspirin resistance is associated with a high incidence of myonecrosis after non-urgent percutaneous coronary intervention despite clopidogrel pretreatment. *J Am Coll Cardiol* 2004;43(6):1122–1126.
210. Matetzky S, Shenkman B, Guetta V, et al. Clopidogrel resistance is associated with increased risk of recurrent atherothrombotic events in patients with acute myocardial infarction. *Circulation* 2004;109(25):3171–3175.
211. Montalescot G, Wiviott SD, Braunwald E, et al. Prasugrel compared with clopidogrel in patients undergoing percutaneous coronary intervention for ST-elevation myocardial infarction (TRITON-TIMI 38): Double-blind, randomised controlled trial. *Lancet* 2009;373(9665):723–731.
212. Wiviott SD, Braunwald E, McCabe CH, et al. Prasugrel versus clopidogrel in patients with acute coronary syndromes. *N Engl J Med* 2007;357(20):2001–2015.
213. Ding YH, Dai D, Lewis DA, et al. Angiographic and histologic analysis of experimental aneurysms embolized with platinum coils, Matrix, and HydroCoil. *AJNR Am J Neuroradiol* 2005;26(7):1757–1763.
214. Murayama Y, Tateshima S, Gonzalez NR, et al. Matrix and bioabsorbable polymeric coils accelerate healing of intracranial aneurysms: Long-term experimental study. *Stroke* 2003; 34(8):2031–2037.

215. Cloft HJ. HydroCoil for Endovascular Aneurysm Occlusion (HEAL) study: Periprocedural results. *AJNR Am J Neuroradiol* 2006;27(2):289–292.
216. Gaba RC, Ansari SA, Roy SS, et al. Embolization of intracranial aneurysms with hydrogel-coated coils versus inert platinum coils: Effects on packing density, coil length and quantity, procedure performance, cost, length of hospital stay, and durability of therapy. *Stroke* 2006;37(6):1443–1450.
217. White PM, Lewis SC, Gholkar A, et al. Hydrogel-coated coils versus bare platinum coils for the endovascular treatment of intracranial aneurysms (HELPS): A randomised controlled trial. *Lancet* 2011;377(9778):1655–1662.
218. Fiorella D, Albuquerque FC, Han P, et al. Preliminary experience using the Neuroform stent for the treatment of cerebral aneurysms. *Neurosurgery* 2004;54(1):6–16; discussion 16–17.
219. Higashida RT, Halbach VV, Dowd CF, et al. Initial clinical experience with a new self-expanding nitinol stent for the treatment of intracranial cerebral aneurysms: The Cordis Enterprise stent. *AJNR Am J Neuroradiol* 2005;26(7):1751–1756.
220. Pumar JM, Blanco M, Vazquez F, et al. Preliminary experience with Leo self-expanding stent for the treatment of intracranial aneurysms. *AJNR Am J Neuroradiol* 2005;26(10):2573–2577.
221. Biondi A, Janardhan V, Katz JM, et al. Neuroform stent-assisted coil embolization of wide-neck intracranial aneurysms: Strategies in stent deployment and midterm follow-up. *Neurosurgery* 2007;61(3):460–468; discussion 468–469.
222. Mocco J, Fargen KM, Albuquerque FC, et al. Delayed thrombosis or stenosis following enterprise-assisted stent-coiling: Is it safe? Midterm results of the interstate collaboration of enterprise stent coiling. *Neurosurgery* 2011;69(4):908–914.
223. Wajnberg E, de Souza JM, Marchiori E, et al. Single-center experience with the Neuroform stent for endovascular treatment of wide-necked intracranial aneurysms. *Surg Neurol* 2009;72(6):612–619.
224. Moret J, Cognard C, Weill A, et al. Reconstruction technic in the treatment of wide-neck intracranial aneurysms. Long-term angiographic and clinical results. Apropos of 56 cases. *J Neuroradiol* 1997;24(1):30–44.
225. Pierot L, Cognard C, Spelle L, et al. Safety and efficacy of balloon remodeling technique during endovascular treatment of intracranial aneurysms: Critical review of the literature. *AJNR Am J Neuroradiol* 2011;33(1):12–15.
226. Shapiro M, Babb J, Becske T, et al. Safety and efficacy of adjunctive balloon remodeling during endovascular treatment of intracranial aneurysms: A literature review. *AJNR Am J Neuroradiol* 2008;29(9):1777–1781.
227. Sluzewski M, van Rooij WJ, Beute GN, et al. Balloon-assisted coil embolization of intracranial aneurysms: Incidence, complications, and angiography results. *J Neurosurg* 2006;105(3):396–399.
228. van Rooij WJ, Sluzewski M, Beute GN, et al. Procedural complications of coiling of ruptured intracranial aneurysms: Incidence and risk factors in a consecutive series of 681 patients. *AJNR Am J Neuroradiol* 2006;27(7):1498–1501.
229. Piske RL, Kanashiro LH, Paschoal E, et al. Evaluation of Onyx HD-500 embolic system in the treatment of 84 wide-neck intracranial aneurysms. *Neurosurgery* 2009;64(5):E865–E875; discussion E875.
230. Simon SD, Eskioglu E, Reig A, et al. Endovascular treatment of side wall aneurysms using a liquid embolic agent: A US single-center prospective trial. *Neurosurgery* 2010;67(3):855–860; discussion 860.
231. Tevah J, Senf R, Cruz J, et al. Endovascular treatment of complex cerebral aneurysms with Onyx HD-500((R)) in 38 patients. *J Neuroradiol* 2011;38(5):283–290.
232. Weber W, Siekmann R, Kis B, et al. Treatment and follow-up of 22 unruptured wide-necked intracranial aneurysms of the internal carotid artery with Onyx HD 500. *AJNR Am J Neuroradiol* 2005;26(8):1909–1915.

Vascular Malformations of the Brain

Key Points

- Most procedural problems during embolization of brain arteriovenous malformations (AVMs) occur at the time of microcatheter withdrawal. Intensive management of the patient following the procedure is also essential to avoid complications related to sudden adjustment of flow in the setting of chronic adaptations of the autoregulatory curve.
- Mechanisms of gene regulation and angiogenesis that are responsible for the dynamic nature of brain AVMs over time likely have much in common with those found in other hypervascular conditions such as tumors, dural vascular disease, and chronic occlusive Moya-Moya disease.

The conventional description of vascular malformations of the intracranial blood vessels begins with McCormick from 1966 (1,2) and describes four distinct categories:

1. Capillary telangiectasis
2. Cavernous malformation
3. AVM malformation
4. Anomaly of venous drainage

While this classification is still reasonably valid for most clinical purposes, an understanding is emerging that thinking about vascular malformations in this categorical way is a blinkered perspective. Many malformations do not fit into one exclusive category raising the question of what the mechanisms of pathogenesis for these lesions might be and how they might impact the treatment of vascular malformations.

It is generally accepted without much controversy that in the case of dural AVMs or fistulas, a preceding venous abnormality such as venous sinus thrombosis or venous hypertension frequently plays a role in the opening of AVM shunts and recruitment of vessels into the developing lesion (3). Since the 1970s cases of dural sinus thrombosis or head trauma leading to subsequent development of dural AVMs have been recognized (4,5). Patients with dural AVMs are more commonly found to have thrombogenic risk factors than the general population, such as factor V

Leiden, protein S deficiency, antithrombin III deficiency, and the G20210A prothrombin mutation (6–12), supporting the contention that venous thrombotic states likely precede a significant number or most cases of dAVMs. It is understandable, therefore, that endovascular obliteration of the venous side of a dural AVM is considered to be an obligatory component of the endovascular cure of a dural AVM, whether the treatment is transarterial or transvenous (see Chapter 20). Similarly, in facial or syndromic AVMs of the extremities, treatment strategies for endovascular obliteration or sclerosis of vascular lesions has come more and more to emphasize the need to gain total control of the lesion by dwelling on obliteration of the venous side (13). The conventional wisdom hitherto with reference to pial AVMs of the brain has been that the fragility and propensity to rupture of the cortical veins would preclude any such primary emphasis in the endovascular treatment of AVMs. This concern is still realistic. However, veins likely play a big role in the genesis of AVMs in the first place and probably have a big influence on factors favoring recanalization or growth of the AVM (see below).

► TELANGIECTASIS (CAPILLARY ANGIOMAS)

These are common, incidental findings at autopsy, found particularly in the pons. They cannot be seen by angiography and are considered, with cavernous malformations, among the *angiographically occult vascular malformations*. They consist of ill-defined areas of thin-walled capillaries without smooth muscle or elastic fibers. Normal brain tissue may be found within the interstices of these areas. When saccular dilatations and surrounding gliosis with abundant mineralization are present, pathologic differentiation from cavernous malformations can be difficult (1). However, they are usually not associated with evidence of surrounding gliosis or pigment deposition. Their exact borders can be difficult to discern, even microscopically (14). Occasional reports of symptomatic capillary telangiectasis have been published (15,16), but most studies represent these lesions as incidental curiosities (Fig. 19-1). Hemorrhage in the setting of a capillary telangiectasis is more likely due to the co-existence of a developmental venous anomaly and/or features of a cavernous malformation (17,18).

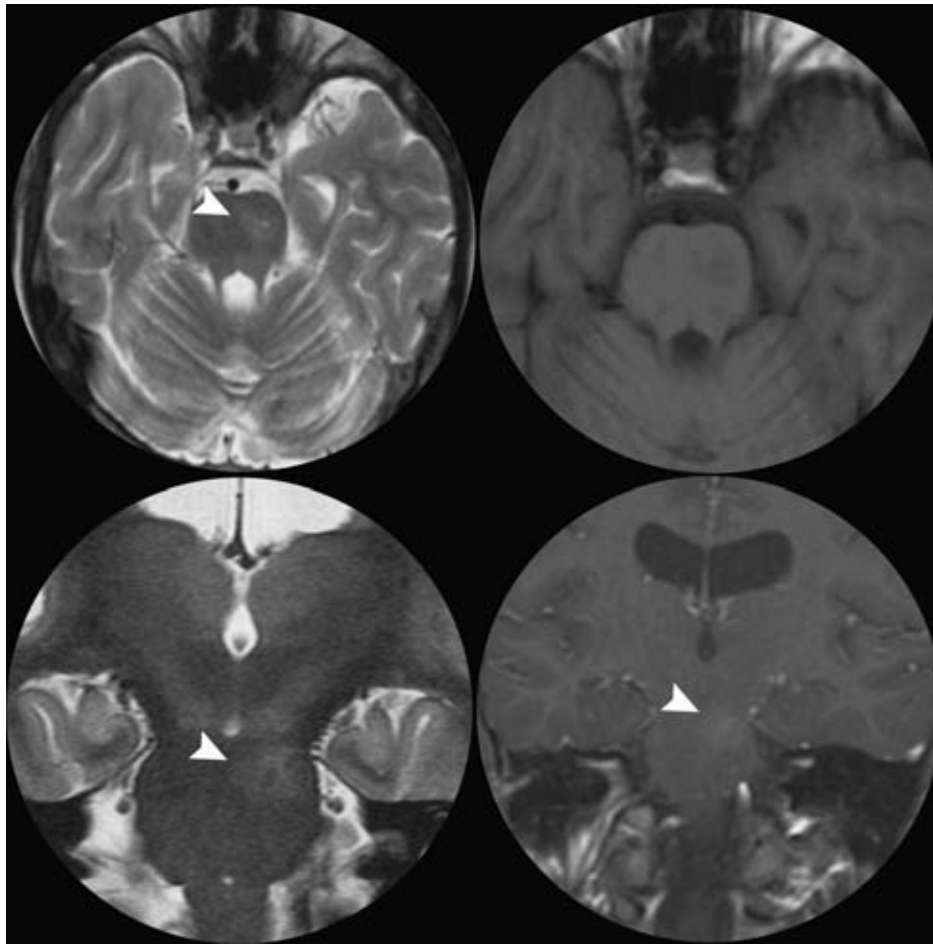


FIGURE 19-1. Presumed capillary telangiectasis of the pons in a 12-year-old female. A child imaged for other indications demonstrates a faint area of signal abnormality (*arrowheads*) in the left side of the basis pontis. In the lower right-hand image, T1 weighted with gadolinium, faint enhancement is seen. This is a very typical location and appearance for this entity, which, as stated in the text, is probably best regarded as an imaging curiosity.

► CAVERNOUS MALFORMATIONS OF THE BRAIN

Cavernous malformations of the brain are described as hamartomatous lesions that are characterized by the presence of sinusoidal, thin-walled vessels. They are usually not seen angiographically unless they are extremely large. They have a more circumscribed or defined border than that seen in capillary telangiectasis and are unlikely to have intervening normal brain tissue (1). The recognition of de novo appearance of cavernous malformations in the brain and the dynamic, changing quality of the disease, particularly in familial forms, has brought an understanding that these lesions are not classified easily as hamartomatous or static (19,20). The gross appearance has been likened to a cluster of mulberries.

Cavernous malformations have a prevalence of less than 1% in the general population and account for approximately 5% to 16% of vascular malformations of the nervous system (21,22). They can be found anywhere in the brain (Figs. 19-2–19-4) and may also occur in the spinal cord (Fig. 19-5), dura, optic nerve, optic chiasm, and pineal gland. Histologically, they demonstrate a simple endothelial lining and a thin fibrous adventitia devoid of elastin, smooth muscle, or other elements characteristic of mature

vascular walls. Although the absence of intervening normal brain tissue is one of the hallmarks of a cavernous malformation, occasionally satellite lesions may give a more complex appearance to their apparent configuration. Foci of maturing thrombosis, hyalinization, calcification, cysts, and cholesterol granules are characteristic, with an absence of large afferent or efferent vessels and of AVM shunting. Surrounding gliosis with ferritin and hemosiderin deposition from repeated hemorrhages or calcification from repeated episodes of thrombosis give the appearance of encapsulation and contribute to the typical MRI ring appearance.

Coexistence of a cavernous malformation with an adjacent anomaly of venous drainage is common, particularly infratentorially, seen in 24% to 86% of lesions (23–25). Cavernous malformations associated with a venous malformation can have a more aggressive clinical course (20). The possibility of an associated venous anomaly is of particular concern when surgery is planned, as it is important not to disturb the pattern of venous flow in the associated anomaly (26,27).

Cavernous malformations are multiple in approximately 33% of sporadic cases and in up to 73% of familial cases (19). Familial cases may also demonstrate an increase in the number of detectable lesions when followed over time. De novo genesis of cavernous malformations has been seen in

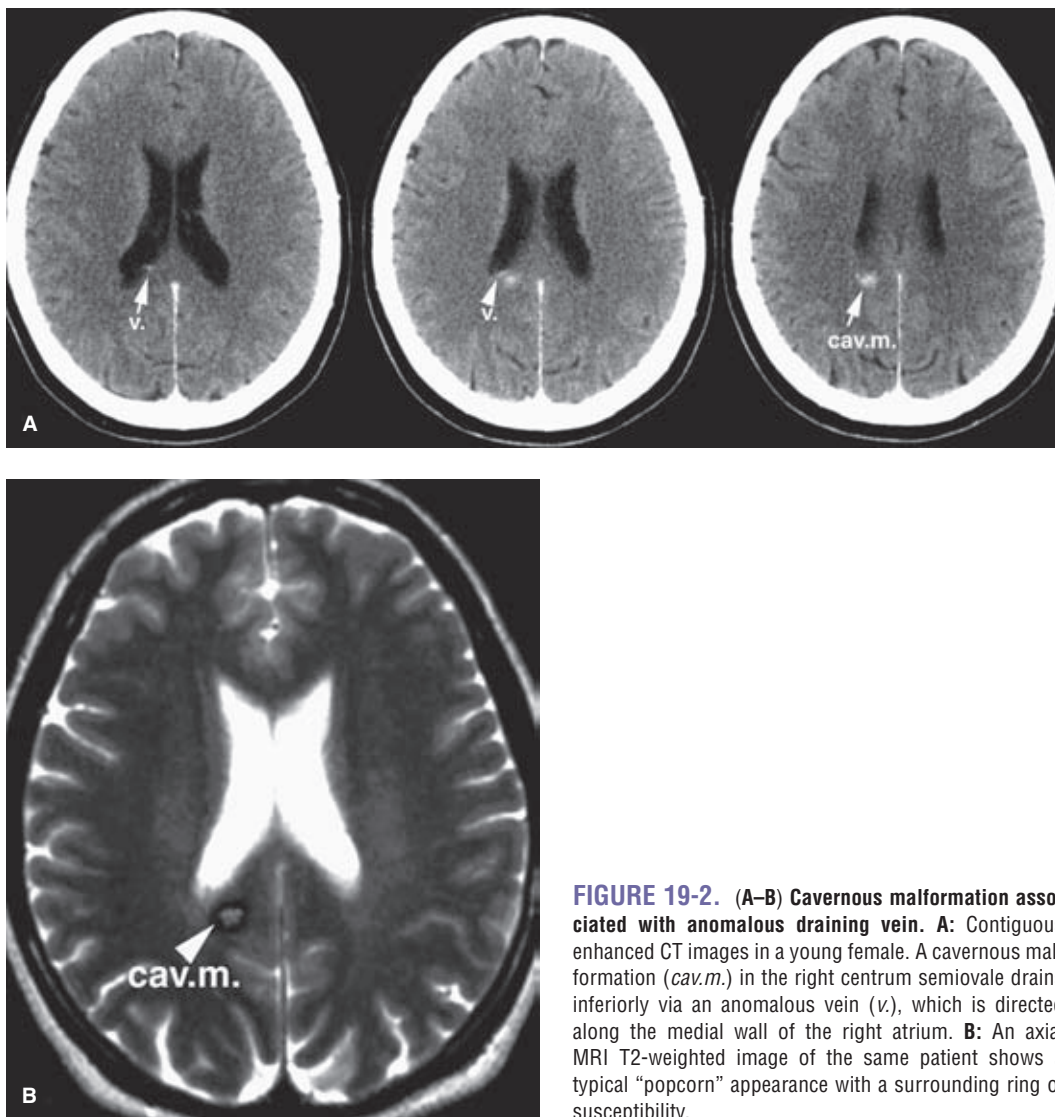
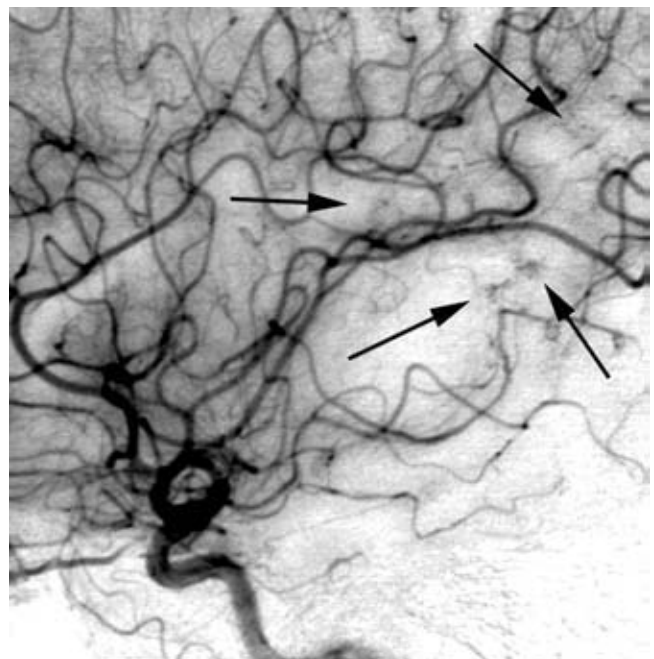


FIGURE 19-2. (A–B) Cavernous malformation associated with anomalous draining vein. **A:** Contiguous enhanced CT images in a young female. A cavernous malformation (*cav.m.*) in the right centrum semiovale drains inferiorly via an anomalous vein (*v.*), which is directed along the medial wall of the right atrium. **B:** An axial MRI T2-weighted image of the same patient shows a typical “popcorn” appearance with a surrounding ring of susceptibility.

FIGURE 19-3. Unusual angiographic evidence of a cavernous malformation. The majority of cavernous malformations are angiographically occult. In this adult female with a large cavernous malformation of the left hemisphere, there is displacement of the adjacent branches of the left middle cerebral artery. Subtle puddling of contrast within the cavernous malformation is seen (*arrows*). This is seen in only a minority of such lesions. The angiogram was performed to exclude an accompanying AVM following a symptomatic hemorrhage.



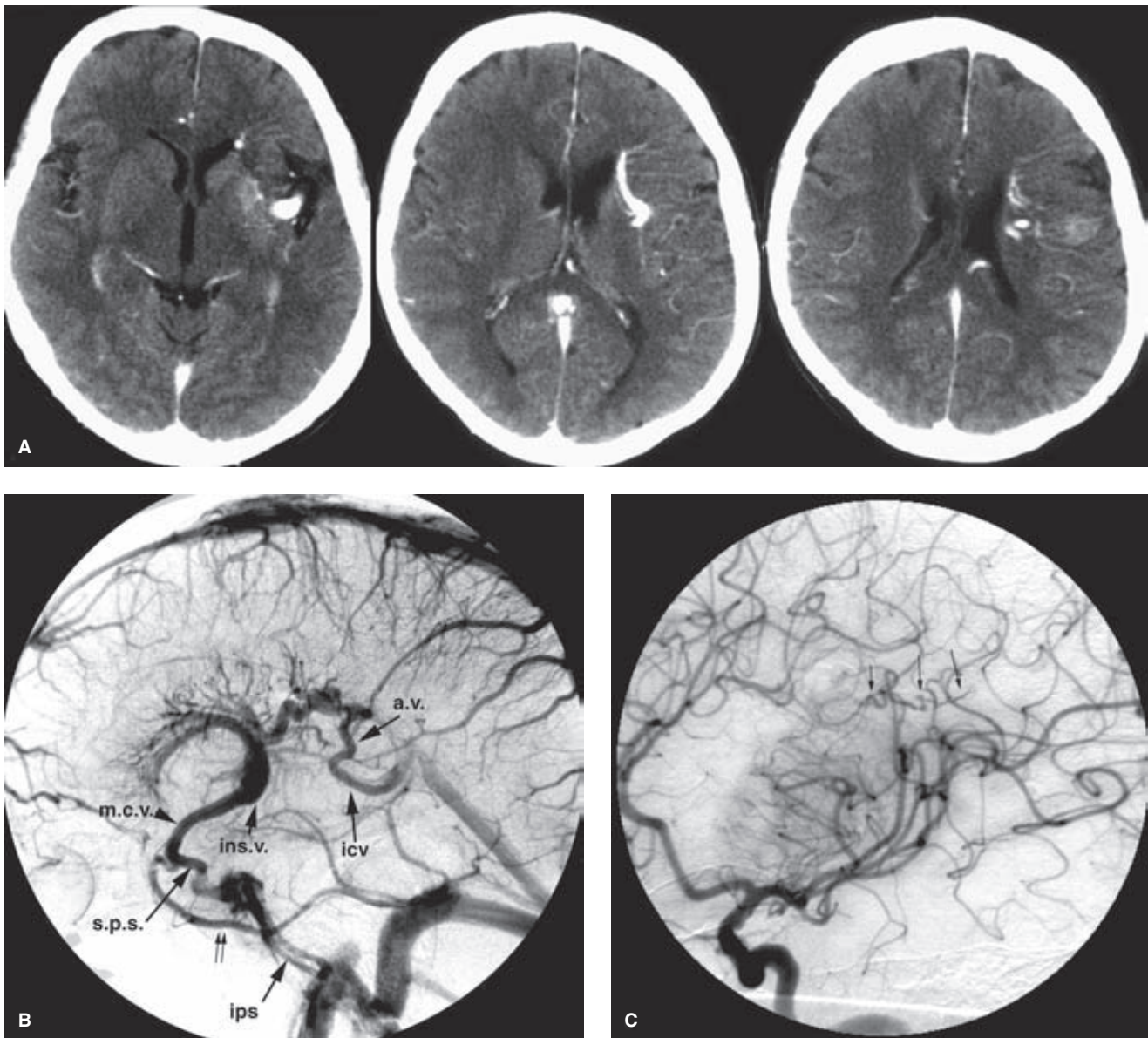


FIGURE 19-4. (A–C) Mixed vascular lesion. A: A contrast-enhanced CT demonstrates a typical appearance of a venous anomaly of the left frontal lobe draining centrifugally to an insular vein. The patient presented with a large subarachnoid hemorrhage in the left Sylvian fissure some weeks prior to this CT. **B:** The venous phase of a left internal carotid artery injection, lateral view, confirms the finding. An extensive anomaly of venous drainage in the left hemisphere drains to an insular vein (*ins.v.*) and the middle cerebral vein (*m.c.v.*). The anterior components of the anomaly drain to the cavernous sinus via the ipsilateral sphenoparietal sinus (*s.p.s.*). The cavernous sinuses drain posteriorly via the inferior petrosal sinuses (*ips*). The sphenoparietal sinus also drains to the sigmoid sinus via an alternative channel (*double arrow*), which probably represents a variant dural sinus along the floor of the middle cranial fossa. The posterior aspect of the anomaly drains via an atrial vein (*a.v.*) to the internal cerebral vein (*icv*). **C:** An oblique magnification view of the Sylvian area from the arterial phase of the study (same patient) demonstrates fistulous opacification of a venous structure (*arrows*) directed medially. This represents a micro-AVM associated with a larger anomaly of venous drainage. The micro-AVM was almost certainly the source of the patient's Sylvian hemorrhage.

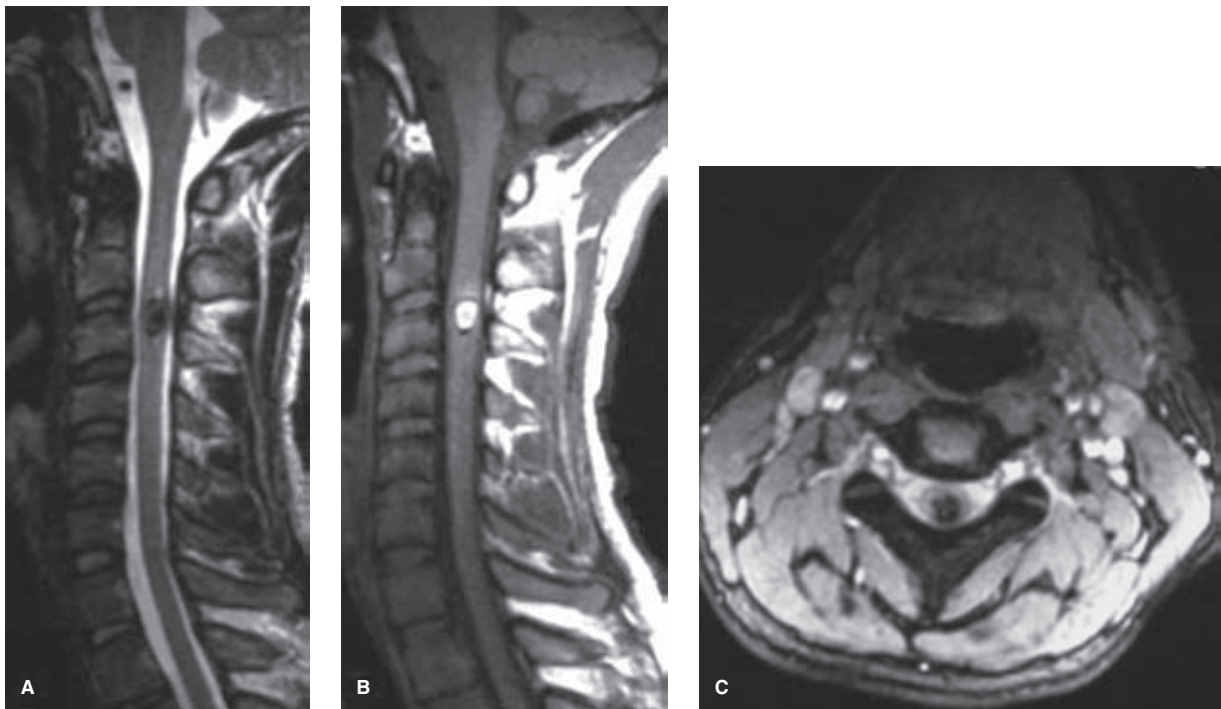


FIGURE 19-5. (A–C) Presumed cavernous malformation of the cervical spine. A young adult with abrupt onset of long tract signs demonstrates a typical appearance of acute hemorrhage into a cavernous malformation of the upper cervical spine. Sagittal T2 (A) and nonenhanced T1 (B) images indicate the presence of intracellular methemoglobin with surrounding expansion of the cord. An axial gradient echo sequence (C) demonstrates prominent susceptibility artifact within the center of the cord.

association with capillary telangiectasis from which they may evolve (28), with venous anomalies (26), at sites of stereotactic biopsy (29), and in patients who have undergone radiation therapy (30).

The natural history of cavernous malformations before they become symptomatic is difficult to evaluate. The best predictor for bleeding in a particular lesion is a history of previous bleeding (31). Asymptomatic lesions that have not previously hemorrhaged have an annual hemorrhage rate of less than 1% per year (32,33). For those lesions with previous bleeding, the annual figure for rebleeding may be as high as 4.5% (34), with a cumulative risk as high as 20% to 80% over a period of weeks to years. Patients who present with nonspecific neurologic symptoms have a risk of developing seizures of approximately 1.5% per year (32).

Cavernous malformations that become symptomatic present with hemorrhage, seizure, or other focal neurologic deficit. Seizures may be simple, complex partial, or generalized, and when found in the temporal lobes may be medically difficult to manage. Considering their size and location, cavernous malformations are considerably more epileptogenic than are AVMs, possibly a reflection of the reactive gliosis and iron deposition, which occur in the periphery of cavernous malformations (34,35).

In addition to seizures, bleeding is a common complication of cavernous malformations. A distinction is drawn between the more common, slow, repeated microhemorrhages associated with cavernous malformations and overt or major hemorrhage, which is reported in 8% to 37% of

symptomatic lesions. Significant hemorrhage from a cavernous malformation can be identified by CT or MRI with blood outside the confines of the hemosiderin ring, in the subarachnoid space, or with clinical evidence of apoplectic hemorrhage (31). Hemorrhage may rarely be fulminant and life-threatening but is usually milder than that associated with AVMs. Hemorrhage from a cavernous malformation is usually associated with onset of severe headache and clinical signs and has a stepwise pattern of worsening deficits according to the location of hemorrhage. Lesions in the brainstem are most likely to present with severe cranial nerve or long tract deficits, as they are particularly likely to affect multiple pathways. Intraventricular cavernous malformations can cause obstructive hydrocephalus and hypothalamic symptoms (36,37). Cerebellar lesions present with nausea, vomiting, nystagmus, ataxia, and diplopia.

The clinical behavior of particular cavernous malformations changes with time in response to the effects of cumulative intralesional hemorrhage, thrombosis, and mineralization. Age is a significant factor in the natural history of these lesions, with most patients presenting in the second to fourth decades. Children who are symptomatic with such lesions have a greater likelihood of significant hemorrhage and of acute neurologic deficits than young male adults who present with seizures. Female adults and children tend to demonstrate significant hemorrhage and neurologic deficits (31,33,35,38), and the clinical course of cavernous malformations in women is adversely affected during pregnancy (20,21). Hormonal factors may influence the behavior of

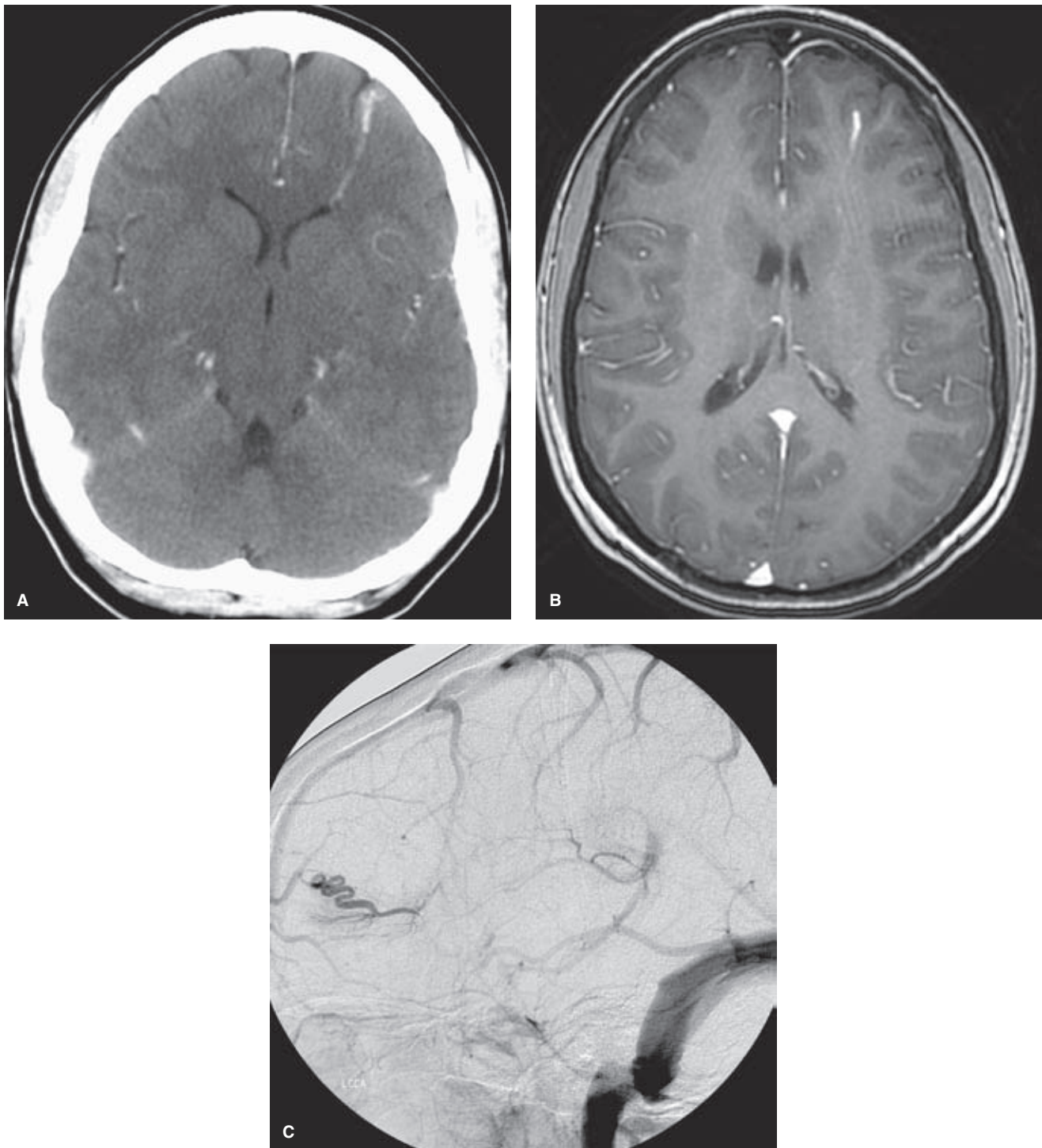


FIGURE 19-6. (A–C) Venous anomaly. A teenaged patient presenting with a questionable seizure episode demonstrated a linear enhancing abnormality of the left frontal lobe on contrast-enhanced CT (**A**). The MRI gadolinium-enhanced study (**B**) indicated no other evidence of pathology other than that demonstrated on the CT scan, but, nevertheless, an angiogram was requested to exclude the possibility of a micro-AVM. The angiogram of the left common carotid artery (**C**) shows that the lesion, seen only in the late venous phase, was much more extensive than the noninvasive imaging portrayed. Questions to ask oneself when an indeterminate lesion is being analyzed on angiography: appearance and phase of filling of the supplying vessels; rate of opacification of the lesion; early washout versus late lingering contrast. In this case, the lesion filled late in a posterior to anterior direction. There was no evidence of fistulous flow or of an early draining vein. It is most likely an incidental finding of no relevance to the patient's symptoms.

cavernous malformations because they are more likely to become hemorrhagic in females. A more aggressive clinical course has been reported also for patients with familial forms of the disease, patients with multiple lesions, patients with previous whole brain or stereotactic radiotherapy, and patients with lesions with an intraventricular location or an associated venous anomaly.

► ANOMALIES OF VENOUS DRAINAGE

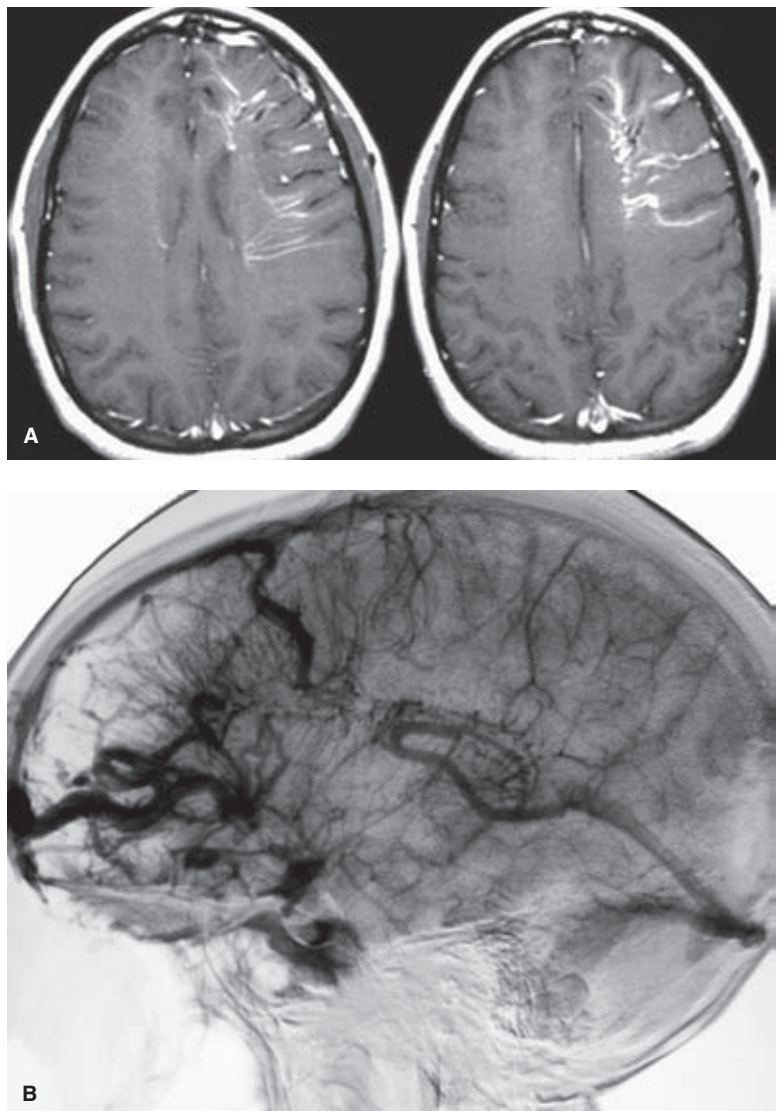
The venous angioma, venous malformation, or anomaly of venous drainage represents, at a basic level, an apparently innocuous developmental aberration of venous arborization. On a more abstract level, these commonplace findings may provide a useful insight into the mechanism of development of brain AVMs.

Venous anomalies are commonly found at autopsy, identified in 2.5% of a large autopsy series (2,39). Surrounded by normal neural parenchyma, they consist in a converging pattern of abnormally prominent medullary veins draining to a single trunk (Figs. 19-6 and 19-7). Frequently

disposed in a radial or star pattern, the appearance of these prominent veins is likened to the “caput medusae.” Occasional instances of this lesion are seen where the draining vein has a particularly distended and indolent aspect, earning the qualification of an “intracerebral varix” (40,41). Although rare, an intra-axial varix can constitute a diagnostic hazard, as it can resemble a cystic mass on CT or MRI (42) (Fig. 19-8).

Usually, these anomalies appear small on axial imaging, with vessel components extending over an area measuring 2 to 3 cm or less in maximal dimensions. Although they are so small, such dimensions amplify into considerably larger venous territories paying tribute to a venous anomaly. The significance of this observation is evident in the consequences of extensive venous infarction and hemorrhage which can follow surgical excision of these lesions. Therefore, they are now conceptualized as developmental anomalies. They are thought to involve little if any innate risk and do not warrant any specific treatment in most circumstances, with an innate risk of hemorrhage estimated to be less than 1% per year (43–46).

FIGURE 19-7. (A–B) Incidental anomaly of venous drainage. An incidentally discovered anomaly of venous drainage is seen throughout the left frontal lobe. Radially disposed transmedullary veins with a characteristic straight appearance are seen on the axial MRI T1-enhanced images (A). The disposition of the transmedullary veins is thought to emulate the migration of the primitive germinal layer of the brain. The accompanying angiogram (B) illustrates a typical “caput medusae” draining anteriorly to the superior sagittal sinus.



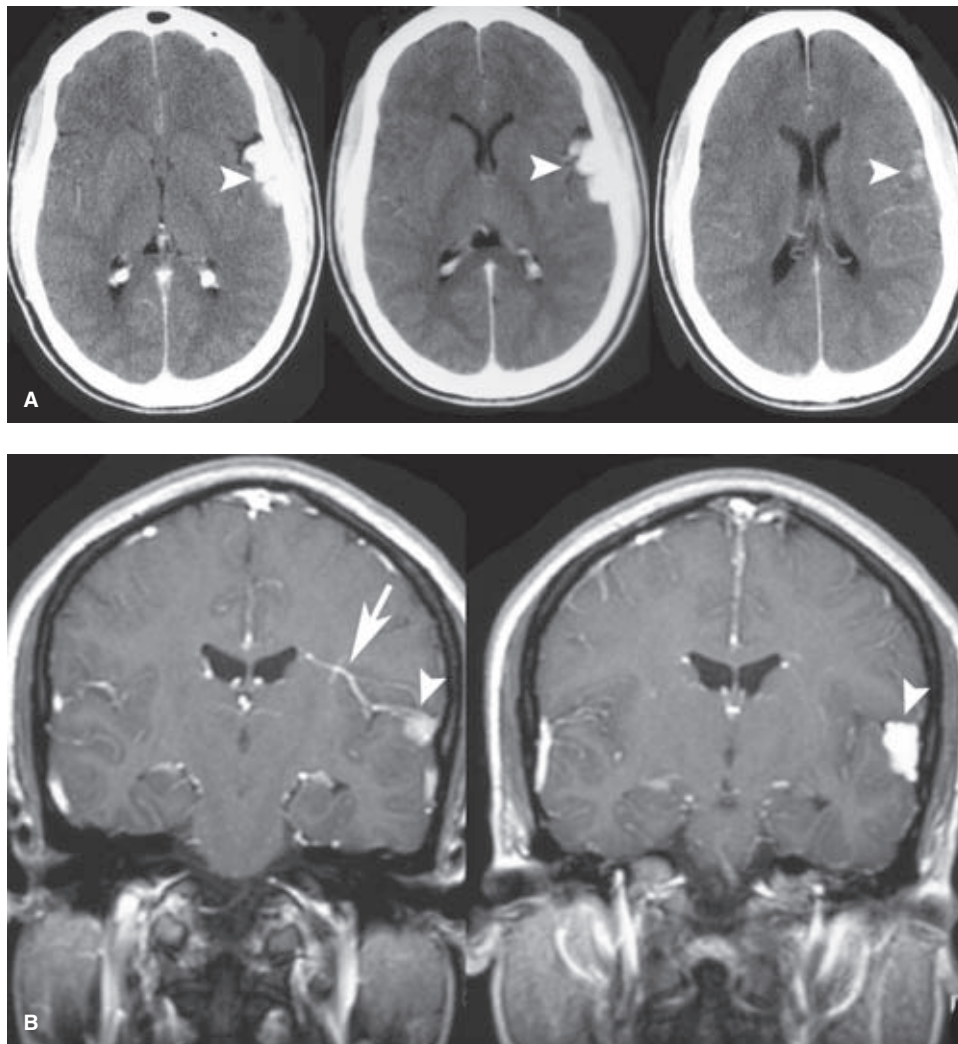


FIGURE 19-8. (A–B) Subarachnoid venous varix associated with anomalous veins. A 28-year-old female with complaints of headache was evaluated at another hospital and referred with a diagnosis of brain AVM. The CT scan with contrast (**A**) demonstrates a brightly enhancing structure in the left Sylvian region, which appears to be extra-axial (*arrowheads* in **A**). The contrast enhancement MRI confirms these findings and suggests that there are prominent intramedullary vessels (*arrows* in **B**) associated with this lesion. During the course of investigation, a left common carotid artery angiogram was performed to evaluate for the possibility of pial and dural disease together. (*continued*)

The clinical significance of venous anomalies is first to recognize them as distinct from AVMs and to treat conservatively. Second, the anomaly of venous drainage has a propensity to occur in association with more symptomatic lesions, particularly with cavernous malformations (47). The latter agent is thought responsible when venous anomalies are seen in close proximity to small intraparenchymal areas of hemorrhage. If treated surgically, it is important to preserve the integrity of the venous components of the anomaly and to confine the resection procedure to the cavernous malformation.

Venous anomalies are frequently associated with aberrations or deficiencies of adjacent pial veins and dural sinuses, similar to those seen with AVMs of the brain. Mullan et al. (48) have suggested that cerebral venous anomalies and AVMs may have a related mechanism of genesis, arguing cogently that an AVM represents a fistulization of a venous anomaly

(Fig. 19-4). Time and a greater understanding of cell signaling have supported the prescience of this insight. Venous hypertension within the territory of a venous anomaly can occasionally be suspected when parenchymal signal changes are seen on FLAIR and T2 imaging, presumably representing the first stages of complications of venous thrombosis or compromise of venous flow. Analogous to the pathophysiology of dural AVMs following venous sinus thrombosis, there is a persuasive body of evidence that suggests that brain AVMs and cavernous malformations may be generated as de novo lesions in a similar way (3). Gene expression of vascular endothelial growth factor (VEGF), and angiogenic factors such as integrin receptors, matrix metalloproteinases (particularly MMP-9), angiopoietin, and basic fibroblast growth factor (bFGF) can be altered in a sustained manner by physiologic changes in blood flow, shear stress, and venous pressure, leading in the long term to anatomic and

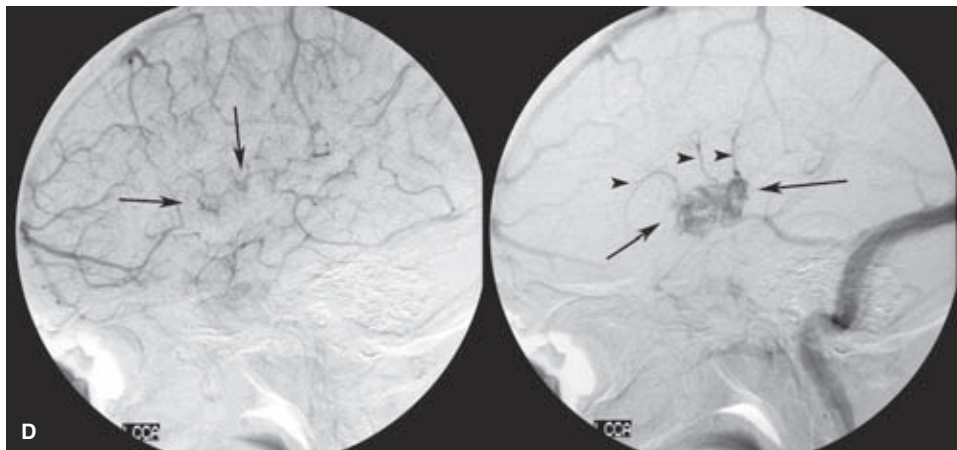
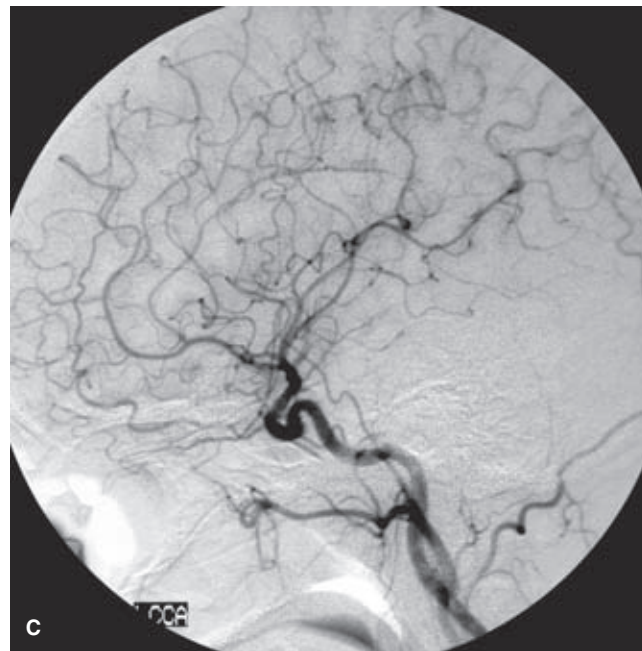


FIGURE 19-8. (CONTINUED) The arterial phase (**C**) is normal, with no evidence of early venous opacification or abnormal shunting. The parenchymal and venous phases (**D**) show gradual appearance of a patchy vascular structure in the left Sylvian region, which becomes more opacified with time (*arrows* in **D**) and drains eventually via anomalous medullary veins (*arrowheads* in **D**). The most likely diagnosis is an anomaly of venous drainage that has incorporated some element of pial veins into its structure. The long-standing nature of the lesion is suggested by the relative hypoplasia of the opercular structures on the CT and MRI. No treatment is warranted in a case like this. In fact, surgical removal or tinkering with these veins would likely induce venous infarction of normal tissue in the dominant hemisphere.

vascular alterations that become clinically recognized as one type of malformation or another. Depending on the nature of the initial insult, the particular genetic profile of the patient, and the timing in life of the event, complications of venous pathology could lead to expression of an AVM, a cavernous malformation, or a mixed type of lesion. Pial AVMs, for instance, are thought to have a slightly more mature endothelial profile with higher ratio of laminin to fibronectin and thus a greater stability of the basement membrane compared with the more friable and immature composition of cavernous malformations where fibronectin predominates and laminin is deficient (49–52).

▶ ARTERIOVENOUS MALFORMATIONS OF THE BRAIN

AVM malformations of the brain are vascular lesions in which an abnormal tangle or nidus of vessels permits pathologic shunting of blood flow from the arterial to the venous tree without an intervening capillary bed (Figs. 19-9 and 19-10). They are frequently described as congenital, but this is questionable. Incidental brain AVMs are rarely seen in children, even with the endemic use of CT scanning currently in vogue for every minor trauma. Furthermore, an unusual

(text continues on page 305)

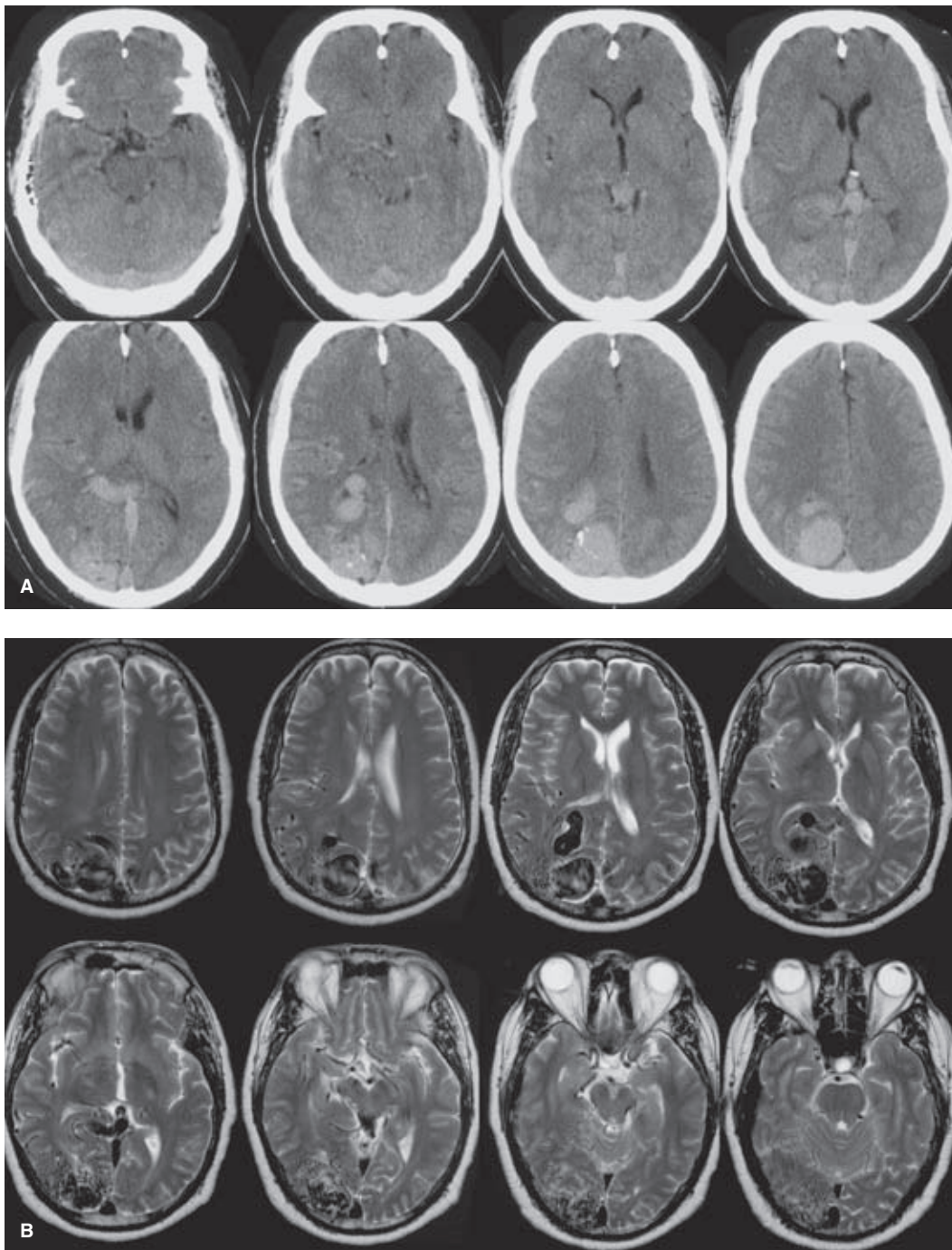


FIGURE 19-9. (A–B) Large brain AVM. An untreated brain AVM of the right occipital lobe illustrates the gamut of imaging findings typically associated with larger, easy-to-identify lesions. The contrast-enhanced CT (**A**) and T2-weighted MRI (**B**) demonstrate the massive distension of veins within the parenchyma and ventricle associated with this lesion. There is gliosis and involution of adjacent parenchymal structures, perhaps in response to “steal phenomenon,” that is, relative ischemia due to the sump of the AVM. Previous hemorrhage could account for this finding as well but was not known in this patient. Venous pressure is so great that there is distortion and mass effect on the brainstem and adjacent structures. (*continued*)

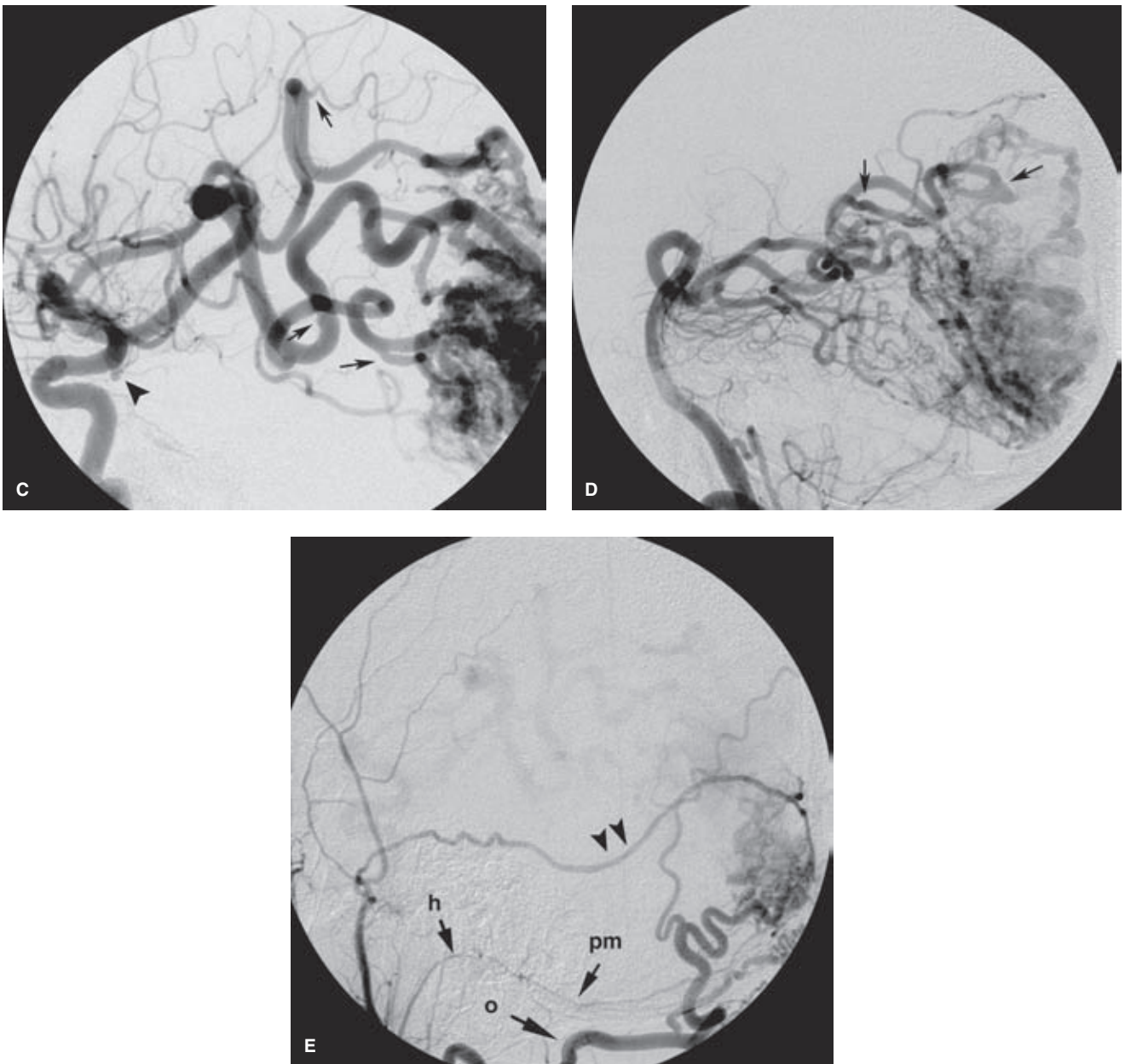


FIGURE 19-9. (CONTINUED) The right internal carotid artery angiogram (C) illustrates the markedly overgrown and slightly dysplastic feeding vessels (focal dysplasia marked with *arrows* in C) of the middle cerebral artery. A small, flow-related aneurysm on the right posterior communicating artery is present (*arrowhead* in C). The left vertebral artery injection (D) shows areas of focal dysplasia, but some of the feeding vessels appear to have a less direct route of access to the AVM than was the case with the middle cerebral artery. This is probably in part a reflection of “angiomatous change” in the branches of the right posterior cerebral artery, where arteries perfusing normal adjacent tissue undergo hyperplasia in response to the demand for flow from the AVM. The right external carotid artery injection (E) shows a component of dural supply to the AVM as well. This is mediated via an enlarged middle meningeal artery (*double arrowheads*), the occipital artery (*o*), and the posterior meningeal artery (*pm*), which derives from the hypoglossal branch (*h*) of the ascending pharyngeal artery.

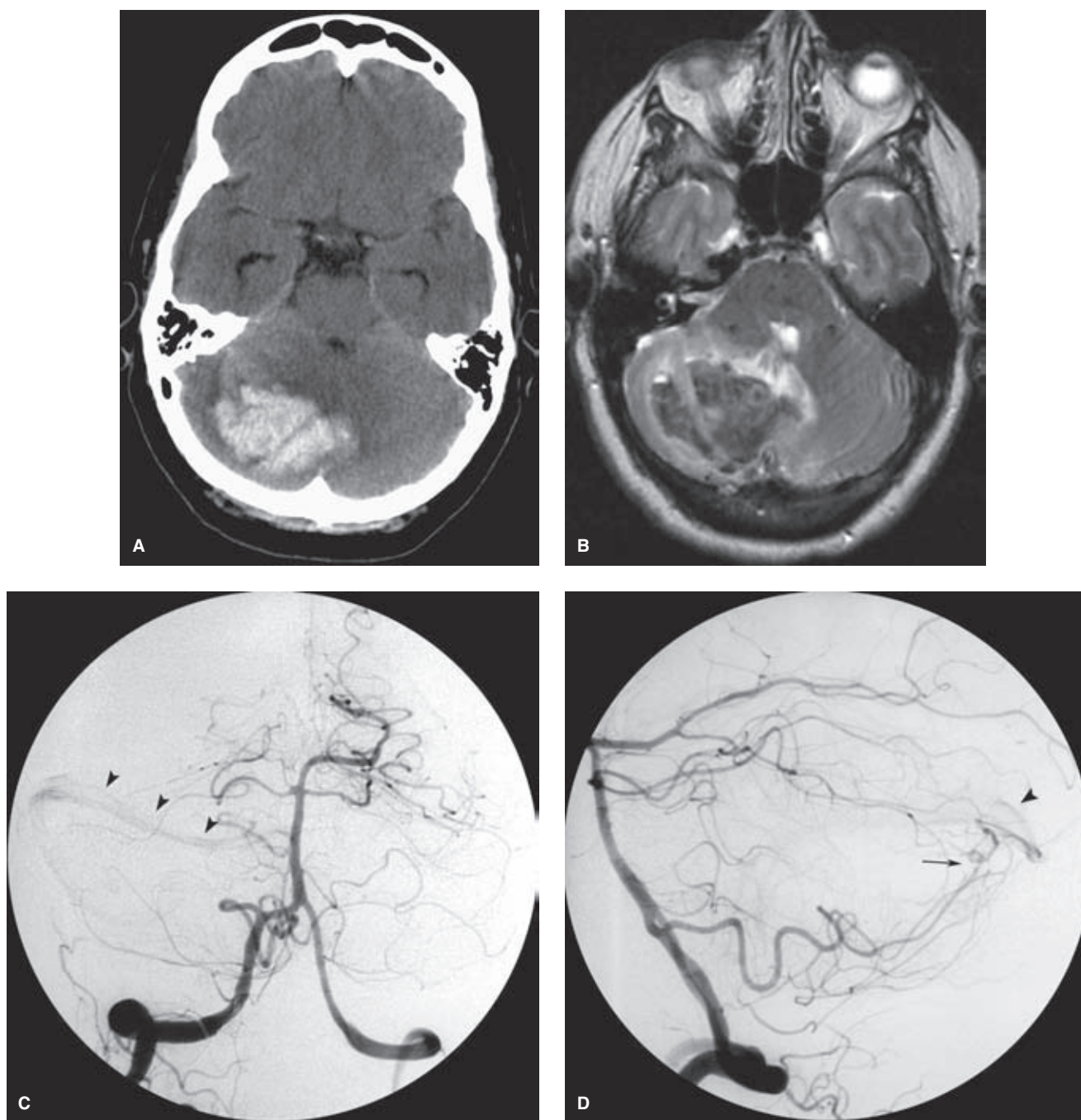


FIGURE 19-10. (A–N) Big bleeds do not necessarily mean big AVMs. (Four Cases.) While anybody can suspect that all is not well with the images demonstrated in Figure 19-9, the points are scored in cases of micro-AVMs that are much more subtle in their angiographic appearance. Parenthetically, it is worth remembering that in the angiographic evaluation of intracranial hemorrhage dural AVMs are frequently overlooked by neuroradiologists who confine their angiographic workup to the intracranial vessels and who neglect the external carotid artery in some cases. A dural AVM with venous hypertension or infarction might well be considered in presentations of intracerebral hemorrhage such as the cases under discussion here, but for the purposes of this chapter, pial AVMs will be illustrated.

Case 1. A–D: A 68-year-old female presented with a large right cerebellar hemorrhage (A, noncontrast CT). Evaluation with CT angiography and MRI (B, T2-weighted MRI) showed no evidence of an underlying mass or lesion. The possibility of a hypertensive etiology was entertained. However, a carefully interpreted angiogram showed evidence of early venous opacification of the right transverse sinus. This is not always easy to see, particularly when the patient is uncooperative or agitated, as was the case here. The images of the left vertebral artery injection under anesthesia (C, D) during subsequent endovascular treatment of this lesion show a tiny pial fistula or micro-AVM distally from the right posterior inferior cerebellar artery (arrow) with early opacification of the right transverse sinus (arrowheads). One must always be vigilant in neuroangiographic interpretation for subtle early veins because they frequently are not the type of finding that will leap out actively from the film. Their identification often requires analytic searching on the film. This is true also in the angiographic evaluation of veins in the investigation of dural AVMs. (continued)

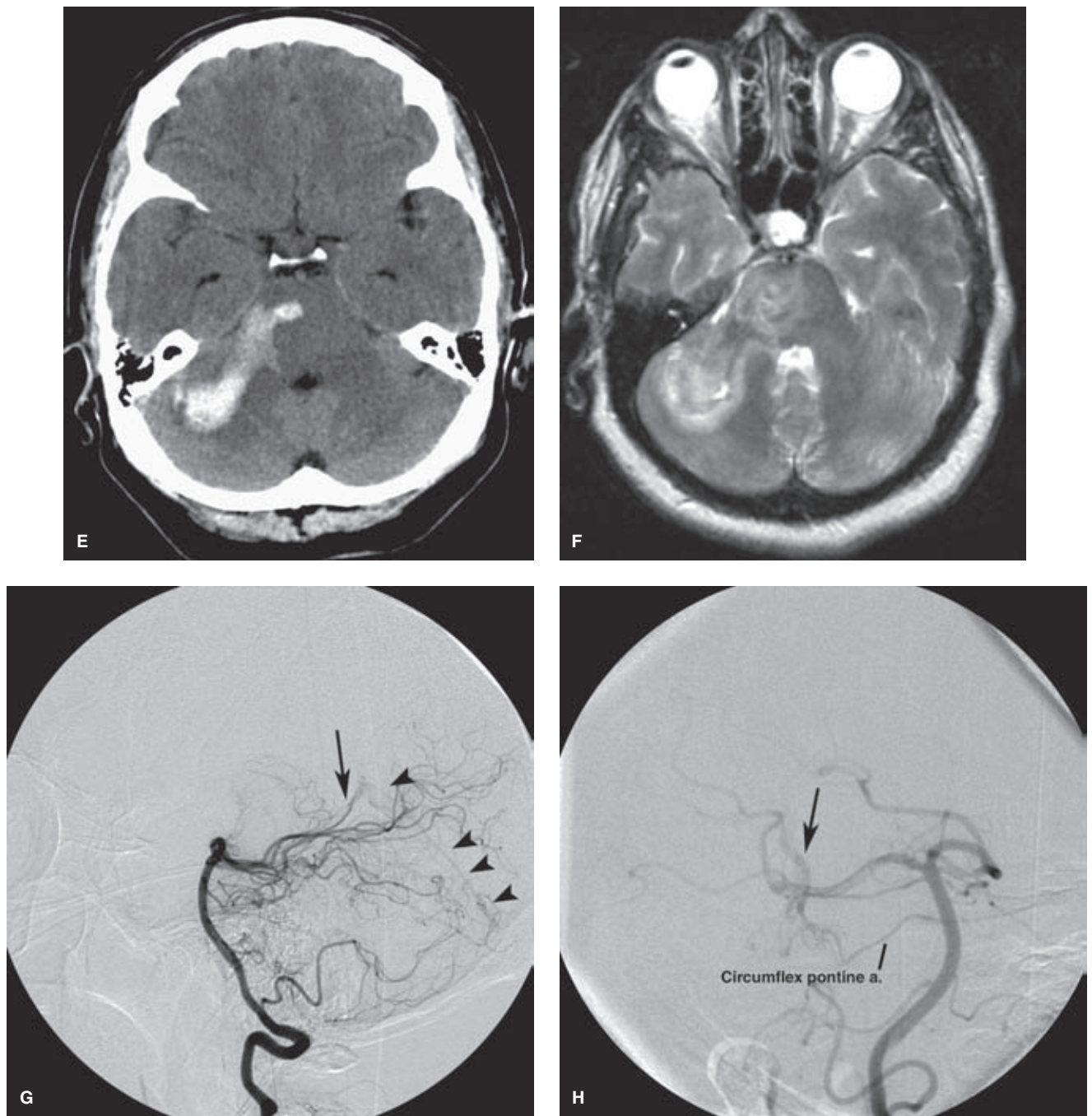


FIGURE 19-10. (CONTINUED) Case 2. E–H: A 54-year-old female presented with a large cerebellar hemorrhage of the right hemisphere dissecting into the right middle cerebellar peduncle illustrated on the noncontrast CT (E) and T2-weighted MRI (F). This patient has multiple aneurysms of the anterior circulation identified on earlier runs, so with the suspicion of aneurysms in mind, one has to be very careful to recognize the early opacification of the straight sinus (arrowheads in G) on the left vertebral artery injection. A magnification oblique view (H) shows that the AVM is feeding from a circumflex pontine branch of the basilar artery and draining via the lateral mesencephalic vein (arrow in G and H) to the straight sinus. (continued)

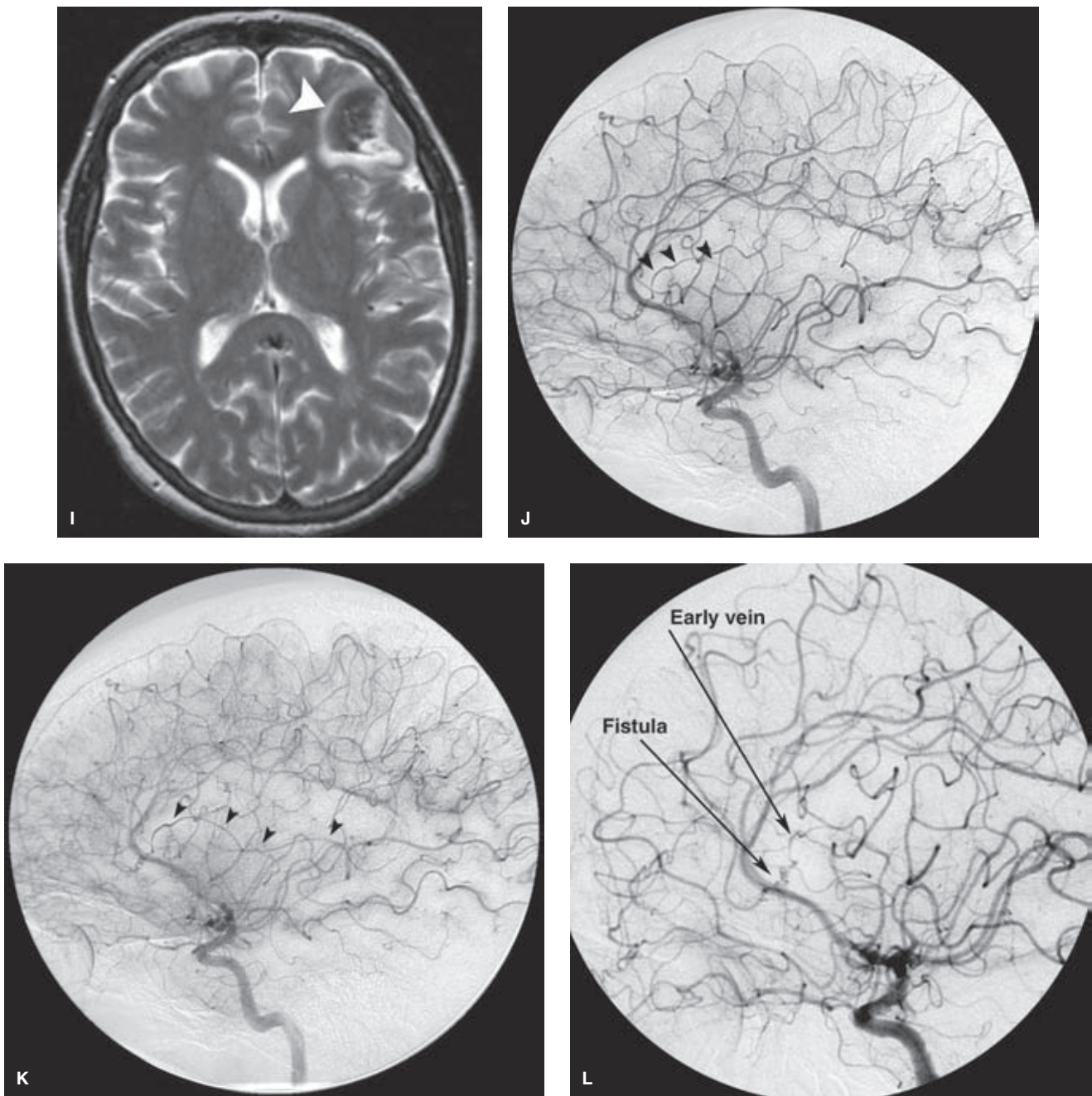


FIGURE 19-10. (CONTINUED) Case 3. I–L: A 45-year-old female presented with a left frontal hemorrhage (*arrowhead* in I, T2-weighted MRI). At first glance, the angiogram of the left internal carotid artery shows no major abnormality, but a more careful review of the lateral angiogram (arterial phase J, early parenchymal phase K) reveals that an abnormal vessel (*arrowheads*) appears early and courses posteriorly to join the left transverse sinus. This is an early draining vein, and one must always be on the qui vive for subtle findings of this nature because they can imply as much risk to the patient as do the florid findings shown in Figure 19-9. Magnification oblique view (L) demonstrated the microfistula more clearly. (*continued*)

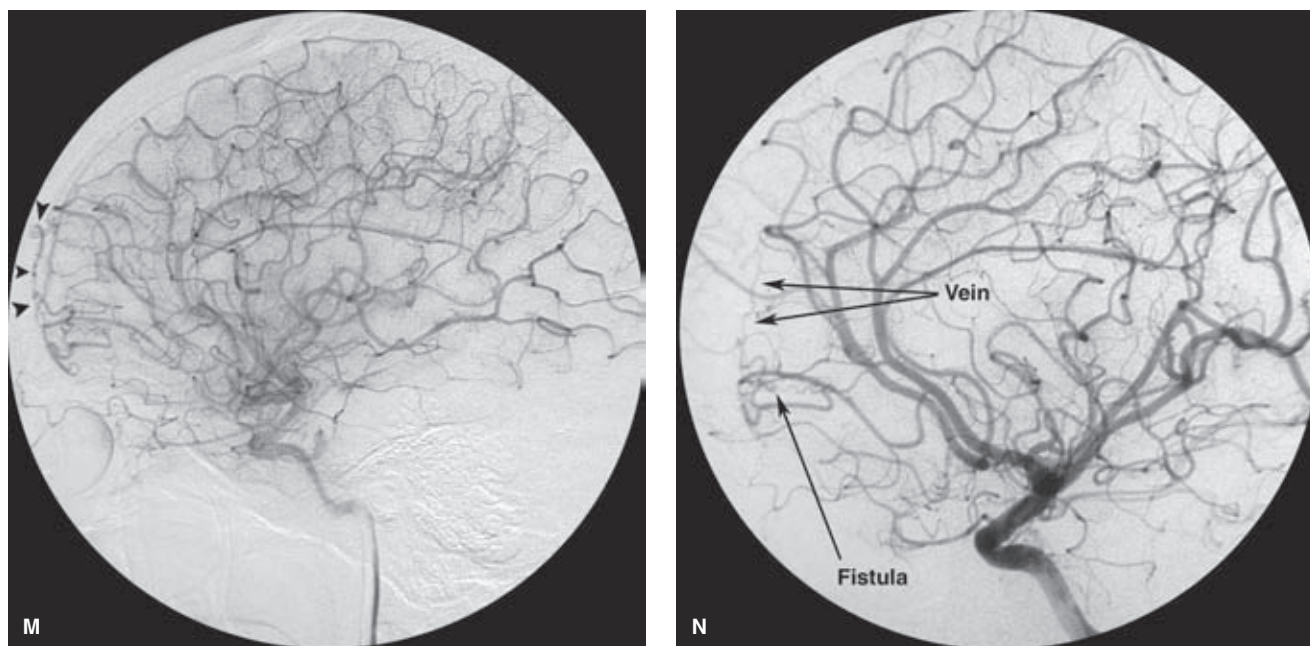


FIGURE 19-10. (CONTINUED) Case 4. M–N: A 33-year-old female was admitted with nausea, vomiting, and visual disturbances. A CT and MRI (not shown) demonstrated a moderate-sized left frontal intraparenchymal hemorrhage. The left internal carotid artery injection shows a subtle tangle of vessels in the late arterial phase (*arrowheads in M*) with subsequent early opacification of the superior sagittal sinus. The magnification oblique view demonstrates the precise fistula to better advantage (*N*).

Conclusion: The common denominator to these cases is the necessity for careful screening of the images for subtle appearance of an early vein. The AVM itself in such cases is too small to see on conventional images and may consist, in some patients, of a single fistula. Once found, the vein can be traced retrogradely to its provenance on the magnification images.

form of AVM can be seen in children, specifically a pial AV fistula, which is very rare in adults, raising the question of whether a single vessel AVF would mature over the years and grow with the child into a more complex nidal type of AVM in adulthood (53–55) (Figs. 19-11 and 19-12).

AVM malformations remain the most controversial and difficult of lesions in the field of endovascular treatment. The natural history of asymptomatic lesions is uncertain, and that of symptomatic lesions is thought by many to be unrepresentative of the entire AVM population. Moreover, their treatment is hazardous and often unpredictable. Even elective cases are vulnerable to the type of catastrophic procedural and postprocedural complications not seen in other diagnostic categories. Published papers on the reasonable rates of complications following endovascular and microsurgical treatment of AVMs are almost invariably written by highly experienced operators. Nobody, on the other hand, wants to publish or read about the cumulative train of disasters related to the first year in practice phenomenon. For this reason, the question has been raised whether treatment of asymptomatic brain AVMs should be pursued lest the danger of doing more harm than good be courted (56), a question that is highly individualized for each patient, depending on presentation, age, anatomy, and other circumstances.

Natural History of Brain Arteriovenous Malformations

Symptomatic brain AVMs present usually either with hemorrhage (40%) or with seizure (40%). The more serious complication is intracranial hemorrhage, parenchymal and/

or subarachnoid, portending a raised yearly risk of hemorrhage thereafter for patients who survive and recover. Typically, the yearly risk of hemorrhage is quoted as between 6% and 17% in the first year after a hemorrhage, and declining somewhat thereafter (57–59). After a second bleed, the risk per year rises to 25% (60). The question of the risk of hemorrhage *before* the first hemorrhage occurs, however, is a more controversial one. Typically, this figure is given as 2% to 4.6% per year (58,59,61–64), with even higher rates of hemorrhage and gravity of neurologic outcome or mortality in Spetzler–Martin Grade IV and V patients (see Table 19-1) (65). With reference to all of these studies, however, the same point has been made that an inductive extrapolation of prognosis cannot be performed on future patients (66), due to the large number of variables involved in a question like this and the heterogeneity of the patient population in different centers. Furthermore, evidence can be invoked from the literature to suggest that a realistic figure for treatment-related complications of brain AVMs could be anywhere between 5% and 19% meaning that the risk of treatment could match or outweigh the natural course of the disease (67).

When hemorrhage does occur the mortality rate is about 10% to 29% during the first hemorrhage, or more than 50% in instances of posterior fossa hemorrhage (57–59,68). Pregnancy is not a specific risk factor for hemorrhage. Mortality with rehemorrhages is even higher than with initial hemorrhages. Other patients may present with headache, complications of hydrocephalus, and focal or progressive neurologic deficits.

(text continues on page 308)

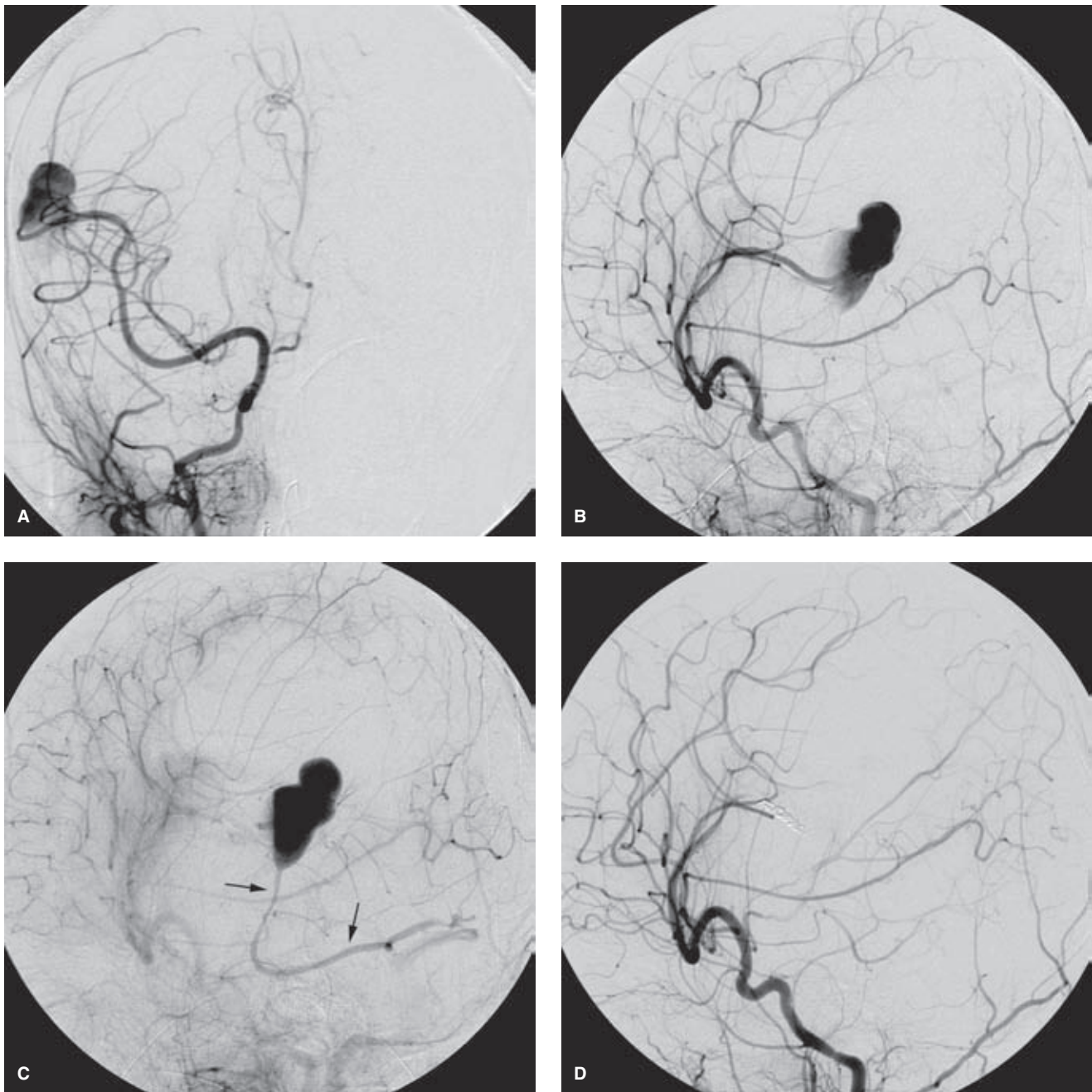


FIGURE 19-11. (A–D) Single vessel direct fistula in an infant. A five-month-old child presented with a large intraparenchymal and subarachnoid hemorrhage. The fistula seen on this angiogram is a type of lesion very rarely seen in adults, begging the question whether these lesions evolve into more “typical” AVMs before presenting in the third and fourth decades. The AP (A) and early lateral angiogram (B) show the single MCA feeder to the large pouch or possibly pseudoaneurysm, with extensive mass effect on MCA and ACA branches. The later venous phase (C) shows the same phenomena and now the single draining vein of Labbé is seen (*arrows*). The postembolization image (D) shows occlusion of the fistula with coils and complete elimination of the fistula. The patient was going to have surgical evacuation of the hematoma, so using a liquid agent for a more permanent cure was not necessary. Furthermore, one has to consider the extreme young age of this patient. How much stress could the arteries take during microcatheter retrieval if the microcatheter got stuck in the Onyx plug? How can one explain to young parents that the microcatheter ruptured during NBCA injection or a small droplet of NBCA withdrew with the microcatheter and caused an MCA occlusion? How safe is DMSO in children this young, if an alternative agent is available?

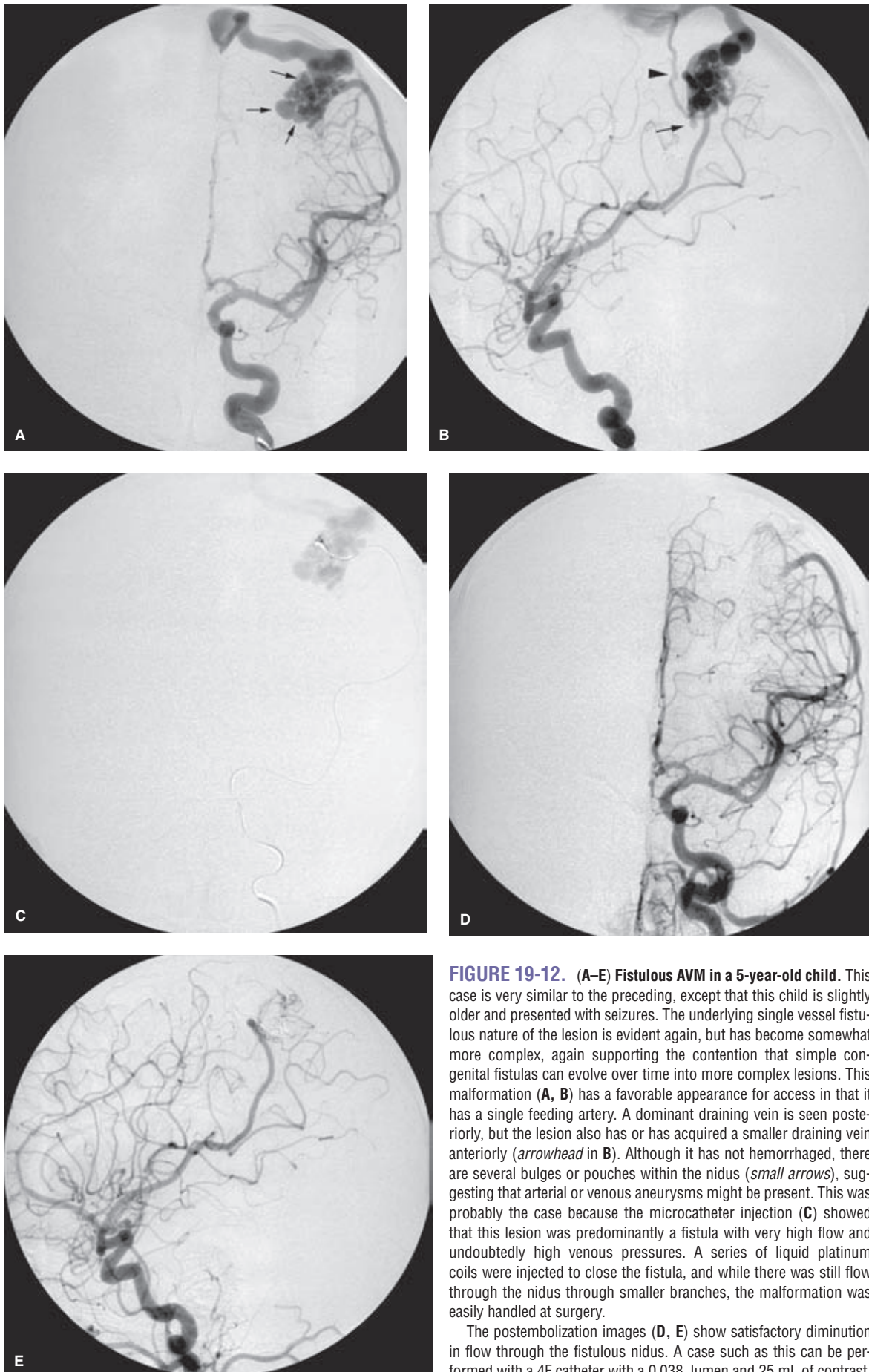


FIGURE 19-12. (A–E) **Fistulous AVM in a 5-year-old child.** This case is very similar to the preceding, except that this child is slightly older and presented with seizures. The underlying single vessel fistulous nature of the lesion is evident again, but has become somewhat more complex, again supporting the contention that simple congenital fistulas can evolve over time into more complex lesions. This malformation (A, B) has a favorable appearance for access in that it has a single feeding artery. A dominant draining vein is seen posteriorly, but the lesion also has or has acquired a smaller draining vein anteriorly (*arrowhead* in B). Although it has not hemorrhaged, there are several bulges or pouches within the nidus (*small arrows*), suggesting that arterial or venous aneurysms might be present. This was probably the case because the microcatheter injection (C) showed that this lesion was predominantly a fistula with very high flow and undoubtedly high venous pressures. A series of liquid platinum coils were injected to close the fistula, and while there was still flow through the nidus through smaller branches, the malformation was easily handled at surgery.

The postembolization images (D, E) show satisfactory diminution in flow through the fistulous nidus. A case such as this can be performed with a 4F catheter with a 0.038 lumen and 25 mL of contrast.

TABLE 19-1 Spetzler–Martin Scale for Prediction of Surgical Risk for AVM

GRADED FEATURE	POINTS
<i>Maximum Diameter of AVM</i> Measured from the angiogram and correcting for magnification.	
Small <3 cm	1
Medium 3–6 cm	2
Large >6 cm	3
<i>Eloquence of Adjacent Brain</i> Eloquent brain includes primary sensorimotor, language, and visual cortex, hypothalamus, thalamus, internal capsule, brainstem, cerebellar peduncles, and the deep cerebellar nuclei.	
Eloquent	1
Noneloquent	0
<i>Pattern of Venous Drainage</i> Deep veins are considered those that drain to the internal cerebral vein, the basal vein of Rosenthal, or the precentral cerebellar vein.	
Superficial	0
Deep	1

Characteristics of AVMs associated with a higher propensity for bleeding include a periventricular or intraventricular location, a central location in the basal ganglia or thalamus, arterial aneurysms, intranidal aneurysms, central (deep) venous drainage, a single venous drainage outlet, venous restrictions or stenoses, delay in venous drainage, feeding by perforator vessels or by the vertebrobasilar artery, and poorer grade on the Spetzler–Martin scale (65,69–71). Smaller AVMs that become symptomatic are most likely to do so by hemorrhage rather than by provoking a nonhemorrhagic neurologic deficit. The question of whether smaller AVMs represent a higher risk of hemorrhage than big ones is somewhat confusing, as it is counterintuitive to think that one might prefer to have a large AVM than a small one. The true variable in question here might be more related to mean arterial pressure in the feeding pedicle and intranidal pressure than the actual size of the AVM. Lesions presenting with hemorrhage tend to have higher pressure readings and slower transit time within the nidus than do patients presenting with seizures (72–74). This phenomenon could also explain why partial embolization of an AVM does not reduce the risk of hemorrhage and may, in fact, increase the risk, if one were to posit that sudden or sustained elevation of the pedicular pressure could alter the patient's risk profile for the worse.

Aneurysms Associated with Arteriovenous Malformations

A major focus of concern for sources of hemorrhage in patients with AVMs is the presence of aneurysms in the nidus, on the feeding arteries (Fig. 19-13), or in the circle of Willis. Aneurysms of major or feeding vessels are seen in approximately 10% of AVMs (75). When one includes small intranidal aneurysms, the incidence increases to more than 20% (76), and as high as 58% (71) with superselective microcatheter injections. Interpretation of superselective angiography of the nidus can be difficult, and therefore,

what constitutes an intranidal aneurysm can be a matter of subjectivity.

Aneurysms are considered to be a primary site of hemorrhage in the course of the natural history of the disease and during surgery or embolization (77,78). In certain instances, treatment may be initially directed toward an aneurysm on

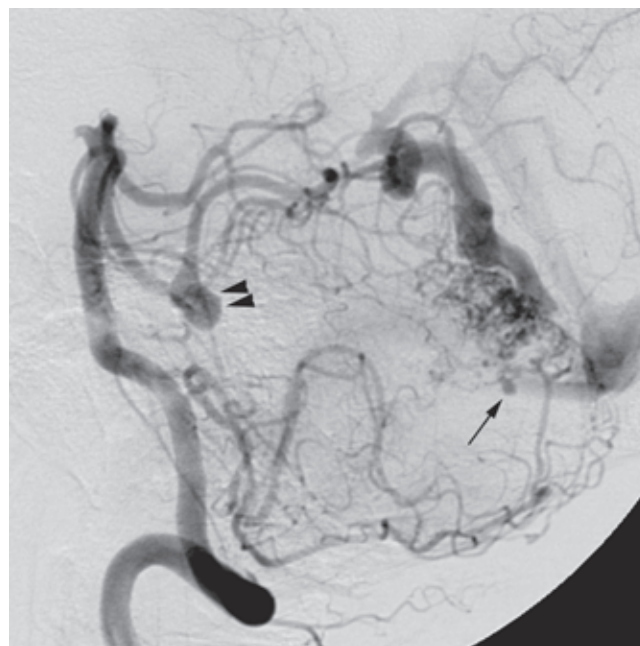


FIGURE 19-13. Aneurysms associated with AVMs. The lateral view of this recently hemorrhaged AVM shows a substantial aneurysm (*arrowheads*) of the right superior cerebellar artery and at least one intranidal aneurysm (*arrow*) more distally. Where to concentrate one's initial efforts in the treatment of a lesion like this can be difficult if the noninvasive images do not give a clue as to the precise origin of the hemorrhage. In the event of uncertainty, treating the aneurysm of the feeding artery first is probably the safer course.

a feeding pedicle before attention is turned to the AVM. In a patient presenting with hemorrhage, a quandary can arise over whether to treat the AVM or an aneurysm of the feeding pedicle first. Obviously, it is better to treat the site of hemorrhage first, but this can be difficult to determine. When the exact site of hemorrhage is uncertain, part of the argument for treating the aneurysm first is that the risk of immediate rehemorrhage is far greater with a ruptured aneurysm than with a bleeding AVM. Aneurysms on major or accessible vessels can be clipped or can be treated by endovascular coil embolization. When they are close to the nidus, they can sometimes be embolized with the nidus by including the aneurysm site in the cast of embolic material.

Arterial or venous pseudoaneurysms are seen with an incidence of approximately 8% in acutely ruptured AVMs (79). They are recognized by their irregular contour, development since a previous angiogram, and relationship on axial imaging to the site of hematoma. Endovascular treatment of an AVM with an arterial pseudoaneurysm should focus on the pedicle feeding the pseudoaneurysm first. Initial embolization of other pedicles might cause hemodynamic changes that could rupture the pseudoaneurysm anew.

Grading of Arteriovenous Malformations

Every AVM is unique. Although it is impossible to predict exactly the risk of hemorrhage or other complication, the presence of some of the angiographic features described would prompt more concern toward treatment for a particular patient. A slightly alternative approach used by many neurosurgeons is to predict the perioperative and postsurgical outcome by using a scale or grading system (80–82). These scales score each AVM based on size, relationship to critical tissue, venous drainage, and surgical accessibility. The Spetzler–Martin scale (80) is one of the most commonly used and correlates with the risk of surgical intervention (Table 19-1). Patients are assigned points on three features and categorized into Grades I to VI.

Prospective application of the Spetzler–Martin grading scheme demonstrates a strong correlation between the pretreatment grade of an AVM and the risks of surgical excision of the AVM, with or without preoperative embolization (76). AVM malformations of Grades I to III have extremely low rates of surgically related morbidity and mortality, but these rates rise considerably for higher-grade malformations. Patients in Grade VI are considered to be inoperable (83,84).

► ENDOVASCULAR TREATMENT OF BRAIN ARTERIOVENOUS MALFORMATION

Arteriovenous malformations of the brain are consistently among the most treacherous lesions for endovascular treatment. Several references could be cited to show a complication and death rate for endovascular treatment that is within reasonable or prudent limits, but it can be safely assumed that everyone in the field with experience treating AVMs can recall one or more cases that they wish had turned out differently. The reality of clinical practice may be somewhat divergent from that of peer-reviewed publications. The New York Islands AVM Study, a population-based incidence and case-control study, suggests that clinical bias may have pre-

vailed disproportionately in the past in treatment decision making concerning brain AVMs. Certain data suggest that half of AVM patients may suffer intracranial hemorrhage (85). However, the older data (57,59,60) stating that once a patient with an AVM has hemorrhaged then he or she has a 3% to 4% risk of hemorrhage per year thereafter until successful treatment is now being questioned. Moreover, among those undergoing treatment, the risk of treatment-related deficits in patients without previous hemorrhage may be higher than among those who have previously hemorrhaged (86). Disabling deficits can afflict 5% of those treated, and new treatment-related nondisabling deficits can be observed in 42% more (86). This raises the question of the risk–benefit ratio of treating brain AVMs, particularly those that are asymptomatic, and whether all such patients should be treated (87). There are still unresolved issues concerning the significance of an asymptomatic, incidentally discovered, or nonhemorrhagic AVM, the natural history, and prognosis.

The dangerous quality of brain AVMs from an endovascular and surgical viewpoint derives principally from their dynamic, almost feral, nature. Most of the endovascular lesions we deal with elsewhere are static—stenoses, aneurysms, occlusions. Even when there is a bleeding point with extravasation in the external carotid artery or a fistula in the vertebral artery or cavernous carotid artery, we conceive of the lesion as fixed in space and approach it accordingly. Brain AVMs are not so simple. They tend to have multiple arterial feeders, one affecting the other. The particular location of an AVM within the brain can have a significant impact on the nature of potential complications through procedural misadventure (Fig. 19-14). The autoregulatory effects of AVMs on the surrounding brain are variable, meaning that risks of hyperperfusion or normal pressure breakthrough bleeding after treatment can be difficult to predict. Where the arteries end and the veins begin within an AVM nidus is difficult to discern under the best of circumstances. Inadequate penetration of the nidus with embolic agent will mean an ineffective embolization, but excessive nidal penetration into the venous side will induce new pressure fluxes and gradients that are often unsustainable to the vessels of the nidus. The result, unfortunately, will sometimes be a catastrophic hemorrhage following an apparently successful embolization procedure.

Gene Regulation of Angiogenesis: The Common Thread of Cerebrovascular Disorders

It is easily and frequently observed that AVMs have a strong capacity to regenerate or reestablish themselves in a short period of time following a partial embolization (Figs. 19-15 and 19-16). Furthermore, several cases of complete angiographic elimination of brain AVMs have been documented where subsequent regrowth of the AVM can be seen, and several sources have posited the possibility that partial embolization of an AVM may increase the risk of subsequent hemorrhage. While it is very frustrating clinically, this phenomenon may be an interesting insight into the pathophysiology of brain AVMs at a very basic level. It is known that the regulation of over 900 genes affect the behavior and growth of brain AVMs (88), and chief among these are the regulatory mechanisms governing the angiogenic cytokines and proteins known to play a prominent role in normal brain physiology, tumor regulation, and immune

(text continues on page 312)

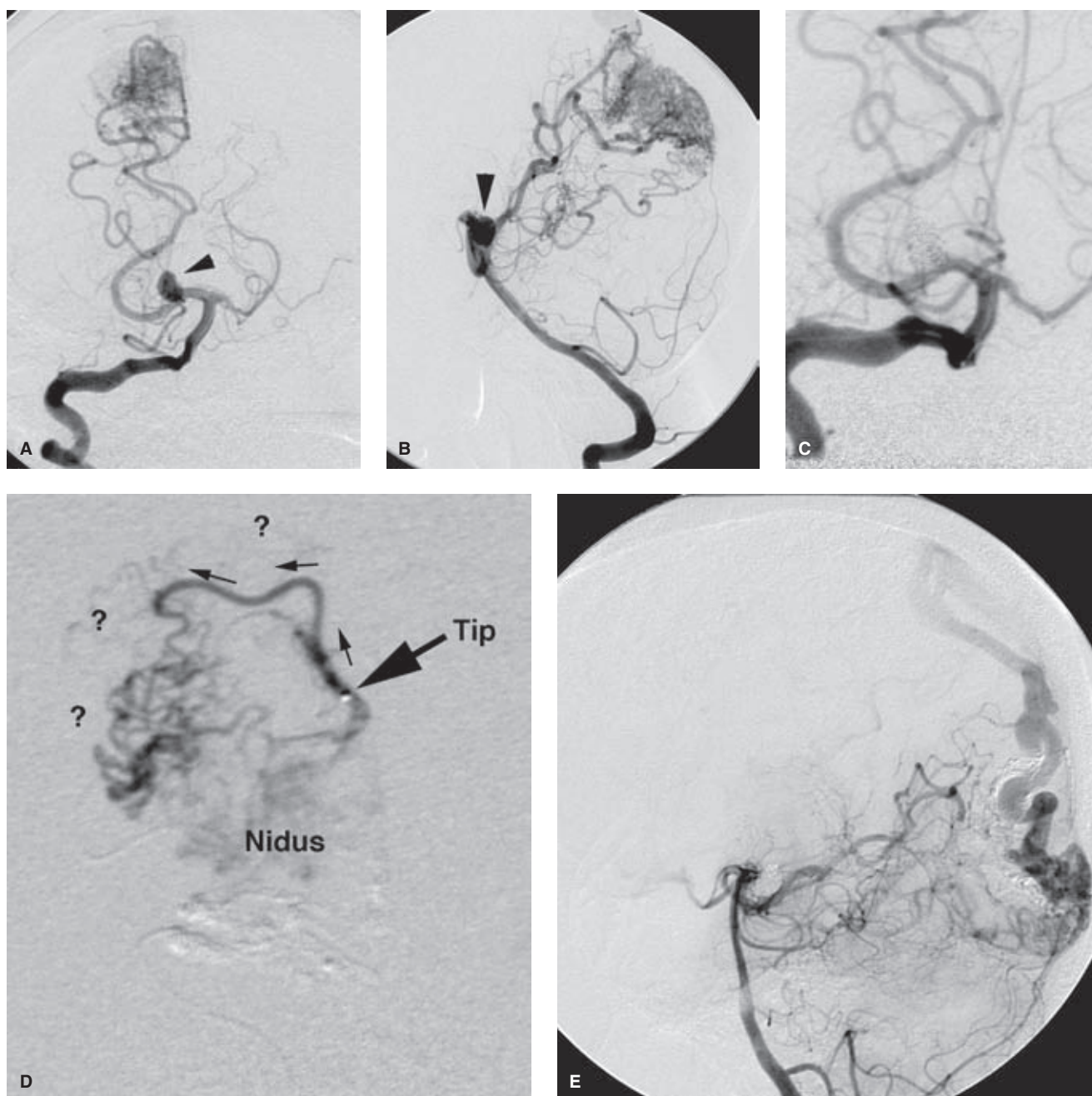


FIGURE 19-14. (A–E) Embolization of a right occipital AVM with an aneurysm on the right posterior cerebral artery. A middle-aged female patient presented with a subarachnoid hemorrhage in the right occipital and perimesencephalic region. The right vertebral artery angiogram AP (A) and lateral (B) show the malformation distally in the right occipital cortex and a 9-mm aneurysm (arrowhead) projecting directly posteriorly from the proximal P1–P2 segment, embedded in the right mesencephalon. Although the hemorrhage was most likely from the AVMs, it was thought prudent to tend to the aneurysm first, which was embolized satisfactorily with coils (C). Two embolization sessions were scheduled for the AVM with reasonably satisfactory results. An intraprocedural microcatheter injection (D) shows one of the dilemmas that may be encountered in AVM morphology. The microcatheter (tip labeled with arrow) is probably somewhat short of the AVM, and the contrast traverses (small arrows) unknown territory (?) to reach the nidus proper. In all likelihood, there is a danger of injuring normal tissue (close to the primary visual cortex) by attempting to push liquid embolic agent from this location to the nidus. This vessel is probably an example of angiomatous change in the region of the periphery of an AVM, an appearance exaggerated by the effects of previous embolizations incompletely penetrating the nidus. The final lateral view (E) shows a reasonably satisfactory appearance of the aneurysm. While opacification of the posterior aspect of the AVM persists, no complications to the visual pathways were sustained.

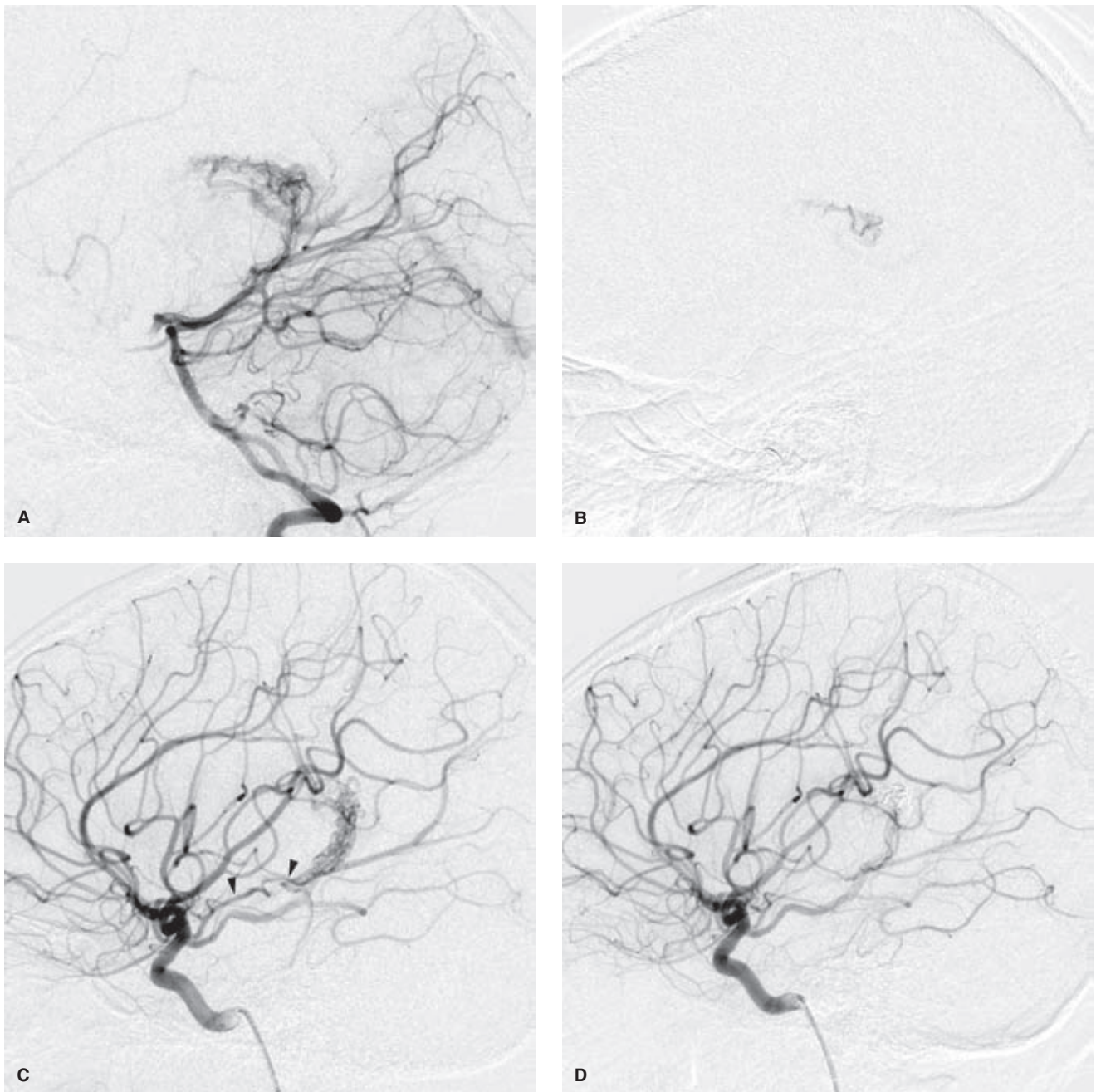


FIGURE 19-15. (A–D) Prompt recurrence after partial embolization of a choroidal AVM in a 5-year-old female. This young child presented with an intraventricular hemorrhage due to a choroidal AVM feeding from the left anterior choroidal artery and left posterior lateral choroidal arteries. It was unclear what the safest course of treatment for her might be, and the risk of a surgical exploration of her ventricle for AVM resection was considered high. An angiogram with an intention to embolize was undertaken. The left vertebral artery injection lateral view (A) shows the AVM filling from posterior choroidal vessels and draining to the internal cerebral vein. Image (B) is the lateral view of the microcatheter injection taken prior to the Onyx embolization. This was far from being a complete treatment, but it would have been better to stop at that point. The left carotid injection, lateral view (C), shows the hypervascular choroid filling from the left anterior choroidal artery (*arrowheads*). This was catheterized but not as distally as would have been thought possible from this image and then embolized with a *tiny* drop of Onyx. The postembolization view of the left internal carotid artery appears satisfactory, although just how far the anterior choroidal artery is flowing at this point is a concern. Faint opacification of the choroidal AVM persists, but appears much diminished. At this point, before the patient awoke from anesthesia, it appeared like a worthwhile procedure. Certainly, some of the AVM must be sclerosed and stabilized, one would argue, to reduce the risk of rehemorrhage while the patient was being prepared for definitive surgery or gamma-knife therapy.

The trouble was that the child did not wake up, at least not for a whole week. The embolization caused a tiny medial left thalamic infarction that induced an unusual state of profound somnolence, from which she could barely be roused even momentarily. Needless to say, when she did finally wake up it was an occasion of some relief, to say the least. She also had a fluctuating quadrantanopsia, which fortunately resolved completely. When she came back for her gamma-knife-targeting angiogram 2 months later, the AVM had almost completely recanalized, begging the question of whether the embolization procedure had been of any merit whatsoever, considering the extreme risk and narrow margin of safety. The other lesson of a case such as this is to try to recognize when a potentially foolhardy or futile embolization is pursued simply because the juggernaut has been put in motion and one feels a pressure to deliver a result. Perhaps the embolization in this little girl stabilized some portion of the AVM and prevented a second bleed, but the converse situation wherein she might not have recovered so completely from an iatrogenic injury to the anterior choroidal artery territory would be difficult to justify.

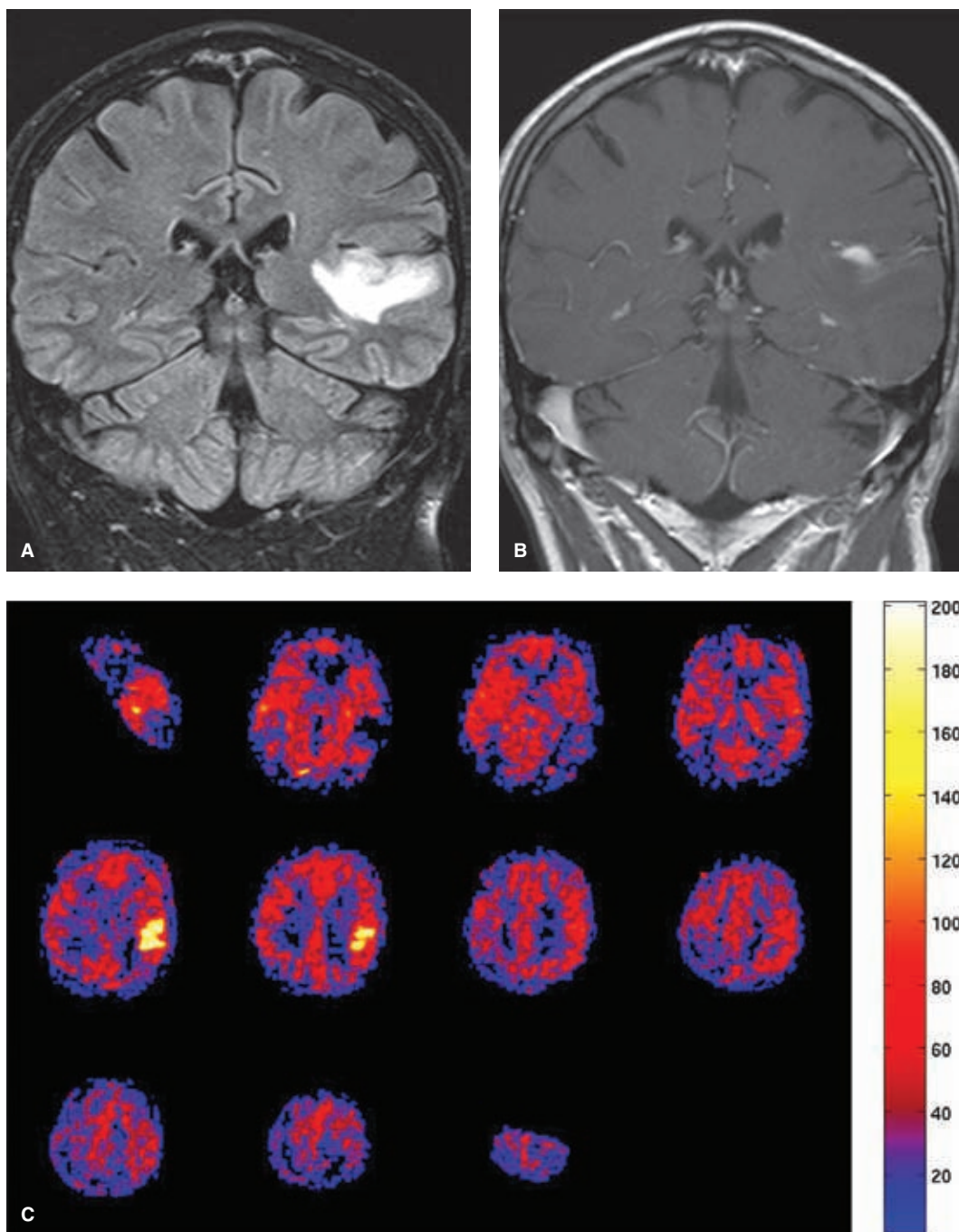


FIGURE 19-16. (A–F) Presumed de novo origin of a fistulous vascular malformation from a venous anomaly.

This late middle-aged patient presented initially at an outside hospital with nonspecific neurologic symptoms. His MRI FLAIR (A) and gadolinium-enhanced T1 images (B) showed an enhancing mass-like lesion with vasogenic edema in the left Sylvian region. This was biopsied but yielded only nonspecific gliosis and normal tissue. A year later, a follow-up MRI PASL sequence (C) showed hypervascularity in the region of previously seen abnormality, but the follow-up T1 image (D) and FLAIR (E) showed involution of the previously seen area of abnormality with no findings to suggest progression of a tumor or features of generalized demyelination. (continued)

surveillance, such as VEGF, interleukin 6, hypoxia-inducible-factor $HIF\alpha$, transforming growth factor $TFG\alpha$, bFGF, and several proteins of the angiopoietin family (52,88–90). In conditions such as Moya-Moya (Chapter 22), several of these factors have been implicated in the genesis of the friable collateral pathways so prominently seen in that condition, and it is not surprising, therefore, that many of these agents are prominently expressed in brain AVMs too. Syn-

dromic conditions known to be associated with brain AVMs such as ataxia telangiectasia, Wyburn–Mason syndrome, Osler–Rendu–Weber syndrome, and Sturge–Weber syndrome demonstrate prominent markers of gene expression for these agents in skin and other tissues. Brain AVMs that have been partially embolized prior to surgery demonstrate increased expression of markers for endothelial proliferation and neoangiogenesis, particularly VEGF and $HIF\alpha$ (91,92),

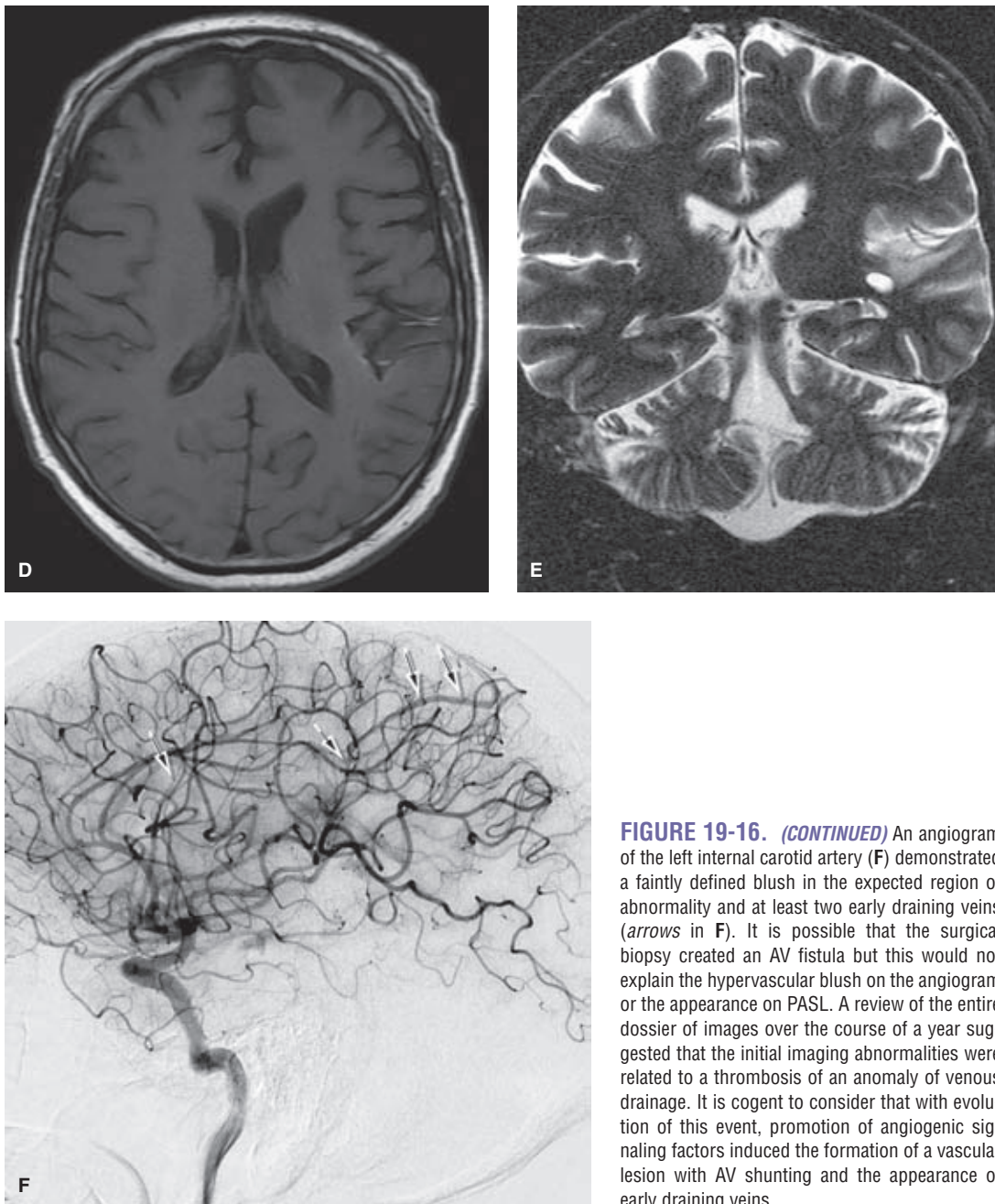


FIGURE 19-16. (CONTINUED) An angiogram of the left internal carotid artery (F) demonstrated a faintly defined blush in the expected region of abnormality and at least two early draining veins (arrows in F). It is possible that the surgical biopsy created an AV fistula but this would not explain the hypervascular blush on the angiogram or the appearance on PASL. A review of the entire dossier of images over the course of a year suggested that the initial imaging abnormalities were related to a thrombosis of an anomaly of venous drainage. It is cogent to consider that with evolution of this event, promotion of angiogenic signaling factors induced the formation of a vascular lesion with AV shunting and the appearance of early draining veins.

compared with AVMs that were not embolized or that were treated with radiation only (93). A possible explanation is that localized hypoxia within the brain AVM or alterations in flow kinetics following partial embolization result in upregulation of mRNA production to promote regrowth of the AVM.

The alterations of gene expression seen in diverse cerebrovascular conditions such as pial AVMs, hypoxia, Moya-Moya, dural AVMs and in conditions such as malignant glioma form a common thread that may explain many of the shared angiographic features of these conditions (Figs. 19-17 and 19-18). Angiographic evidence of AVM shunting was a common finding in the setting of high-grade gliomas when angiography was used for diagnostic evaluation of these patients. Occasional cases of “collision” phenomena may also be seen, for example, coexistence

of a dural AVM in immediate propinquity to a glioblastoma multiforme (Fig. 20-14), or co-existence of a dural and pial component of an AVM, which is difficult to categorize into one exclusive label. The shared immunohistologic and gene expression basis for these phenomena in various diseases illustrates the point made at the beginning of the chapter, not that these diseases are all the same, but that they are not so different from one another. Modulation of gene expression is already a successful therapeutic option for brain tumors rich in VEGF markers. The possibility of similar therapeutic options for cerebrovascular disorders such as brain or dural AVMs may become clinically relevant, for instance, the capacity of doxycycline or minocycline to suppress the expression of matrix metalloproteinase MMP-9 might be effective for stabilizing brain AVMs (94–96).

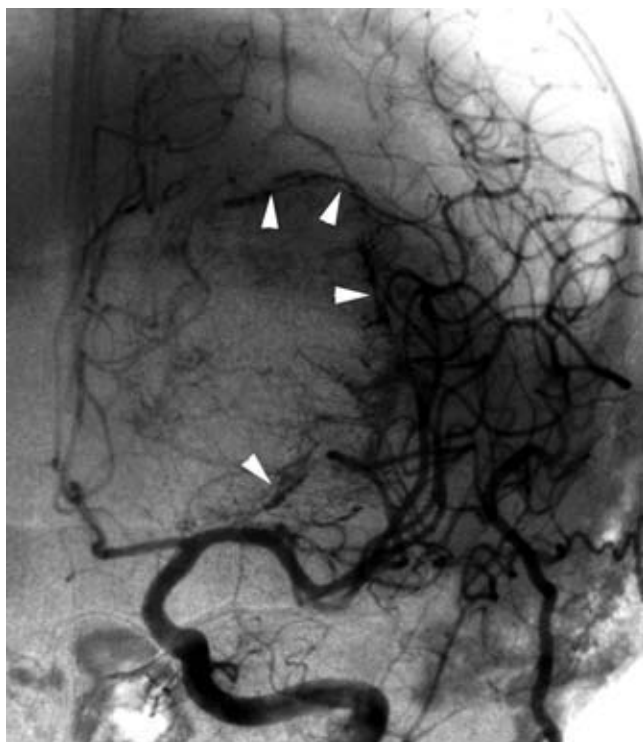


FIGURE 19-17. Hypervascular glioblastoma multiforme. A left common carotid artery injection demonstrates the hypervascular periphery of a glioblastoma in the left hemisphere. An AVM that has recently hemorrhaged with compression of peripheral vessels might be considered in the differential diagnosis for such a lesion. However, AV shunting is not clearly seen in this patient. On later images, centripetal progression of contrast was evident, a pattern not likely to be seen with an AVM.

Embolic Agents for Brain AVM Malformation Embolization

NBCA (*N-Butylcyanoacrylate*) (Trufill) “Glue”

NBCA is an extremely effective embolic agent, but the risk of inadvertent glue embolization of normal tissue can make the use of this agent extremely dangerous. Acrylate glue, NBCA, is supplied in a liquid form. It is diluted with Ethiodol to render it radiographically visible and is occasionally mixed with tungsten or tantalum powder (Fig. 19-19). This must be done at a separate tray or table to prevent inadvertent premature initiation of the polymerization process. When NBCA comes in contact with an ionic solution of alkali pH, it solidifies quickly into a hard paste by an exothermic reaction. To prevent this from happening within the delivery system or too quickly within the body, the bolus of glue is preceded by a low pH, nonionic flush solution such as 5% dextrose or glacial acetic acid. The approximate angiographic point at which the glue solidifies is ideally controlled by altering the mixture and dilution of the glue. More Ethiodol is added when more distal migration of the glue is desired. The microcatheter must be lavaged thoroughly beforehand with several syringes of 5% dextrose, and the glue injected carefully either as a continuous column or as a small bolus pushed with a column of dextrose. Concentrations of 25% to 30% are commonly used, but ranges from 17% for distant penetration to 100% (nonopacified) for a direct fistula are occasionally used. To prevent gluing the microcatheter in place, the assistant will usually be directed to “PULL!” the microcatheter at the appropriate moment. The operator should be anticipating this moment, and therefore, the valve on the catheter should be loosened to allow free passage of the microcatheter when the moment comes.

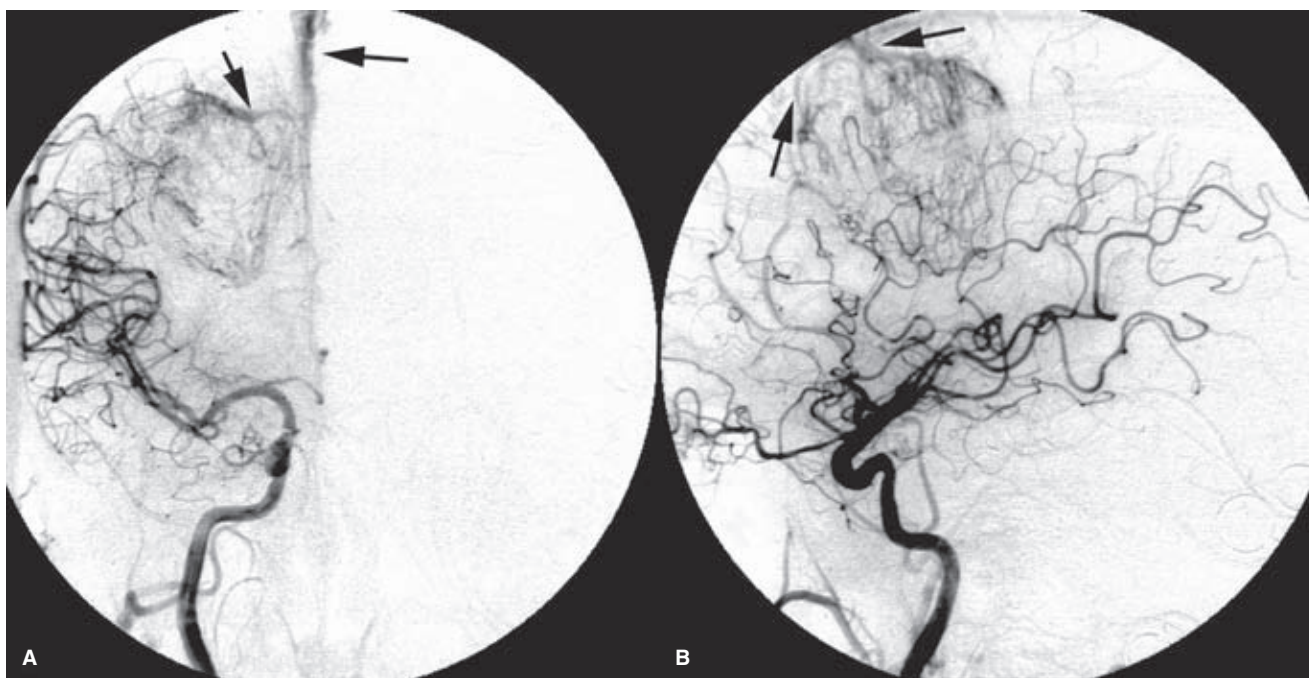


FIGURE 19-18. (A–B) AVM shunting in an astrocytoma. An injection of the right internal carotid artery demonstrates a hypervascular mass in the center of the right hemisphere with a centripetal pattern of opacification. Early venous opacification due to shunting (arrows in **A** and **B**) is present, but the angiographic appearance is dominated by a mass-like arrangement of radially arranged vessels.

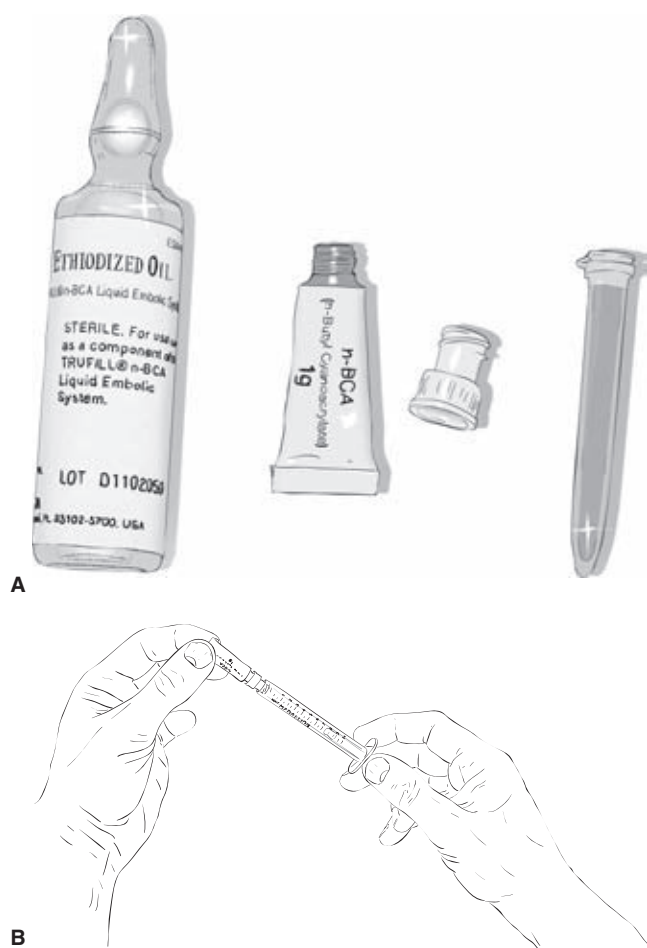


FIGURE 19-19. (A–B) Preparation of NBCA. Trufill is provided in a 1-mL metal tube with a sealed tip (A). A vial of Ethiodol for dilution and opacification is included with the package as well as a minivial of tantalum (optional). The mixture is usually performed in a glass-mixing jar on a separate clean tray away from any possibility of contamination with contrast or saline. A fresh set of gloves is donned. A plastic adaptor is provided (B) for perforating the seal on the NBCA vial and withdrawing the 1 mL within, but it is easier to use an 18G needle for the same purpose with less likelihood of spillage. Thorough lavage of the microcatheter with dextrose ahead of the embolization is necessary to prevent premature polymerization. NBCA should not be used without extensive supervised experience.

Some operators still prefer to pull the whole microcatheter-catheter combination in one piece to avoid shaving a piece of glue off the tip as the microcatheter enters the catheter.

Onyx

Ethylene-vinyl alcohol (EVOH) was released on the US market in 2005 and fills a niche for embolizations where previously use of NBCA had connotations of being difficult to predict or control (Figs. 19-20 and 19-21). The EVOH copolymer is suspended with tantalum particles in dimethylsulfoxide (DMSO), which leaches from the embolus after injection, allowing the soft paste-like material to precipitate and conform to the vessel lumen. Onyx is supplied in three concentrations: Onyx 18, Onyx 34, and Onyx HD500 (97). Onyx 18 is composed of 6% EVOH and 94% DMSO for a viscosity of 18 centipoise (cps). Onyx 34 is composed of 8% EVOH and has a viscosity of 34 cps. Onyx HD500, which is designed for use in recurrent aneurysms, has an EVOH

concentration of 20% and a viscosity of 500 cps, which in itself requires considerable modification of technique, larger-bore microcatheters, and larger-bore needles for drawing it up into syringes. Onyx has several impositions on the routine of the procedure that must be anticipated.

1. The vials of Onyx must be agitated in a dedicated mixer for 20 minutes prior to use.
2. A DMSO-compatible microcatheter must be used to prevent incompatibilities with the materials of other catheters.
3. Syringes used to draw up the material must be DMSO compatible and are provided with the kit.
4. The microcatheter must be primed ahead of the embolus with liquid DMSO (analogous to the use of 5% dextrose for NBCA). Therefore, one must know the volume of the microcatheter in use beforehand to facilitate this part of the procedure. When the injection of Onyx begins, it must be done knowing that the embolus is pushing a column of DMSO ahead of it, and the rate for this extrusion is limited to less than 0.25 mL over 1.5 minutes.
5. The patient and family might wish to be warned ahead of time that there will be an odd personal odor for a day or two due to the halitotic effects of DMSO residuum.

Several very creative techniques for injecting Onyx into brain AVMs have been described with the goal of enhancing the complete penetration of the nidus and reduction of the risk of injury to adjacent normal tissue through reflux. These include use of parallel microcatheters, one of which is used to form a proximal plug of Onyx 34 and the distal one is then used for injecting Onyx 18 beyond the protective plug. Alternatively, a single catheter might achieve the same goal, by switching from Onyx 34 to Onyx 18 after the initial plug has been formed. A double-catheter technique can be used with simultaneous or alternating injections of Onyx into the nidus to achieve greater filling of the nidus, the argument being that the second pedicle would not be as easily accessed due to the “spoiling” effect of the first embolization, if the same thing was one in a sequential manner, rather than parallel (98,99). Adjunctive balloons can be used to plug arteries and to control flow when the Onyx is being injected, or the balloon may be inserted transvenously and used to control the venous outflow during transarterial or transvenous embolizations (100).

Success rates of achieving a total angiographic cure of AVMs with transvascular treatment alone using Onyx vary, but generally speaking the higher rates of total occlusion are achieved with longer injection times and thus higher complication rates. The complications are frequently due to the difficulty of extracting the microcatheter at the end of the injection, and considerable distortion of the brain can be inferred from the deflection of the Onyx nidus, which frequently accompanies this difficult component of the procedure. This problem can be addressed by using a microcatheter with an intentionally detachable tip designed to break at a junction proximal to the embedded end of the microcatheter (101). Alternatively, several coaxial rescue techniques have been described for guiding an outer microcatheter (akin to the old double-catheter technique for detachable balloons) or snare over the shaft of the embedded microcatheter up close to the AVM to allow countertraction or direct local traction on the stuck microcatheter (102–104).

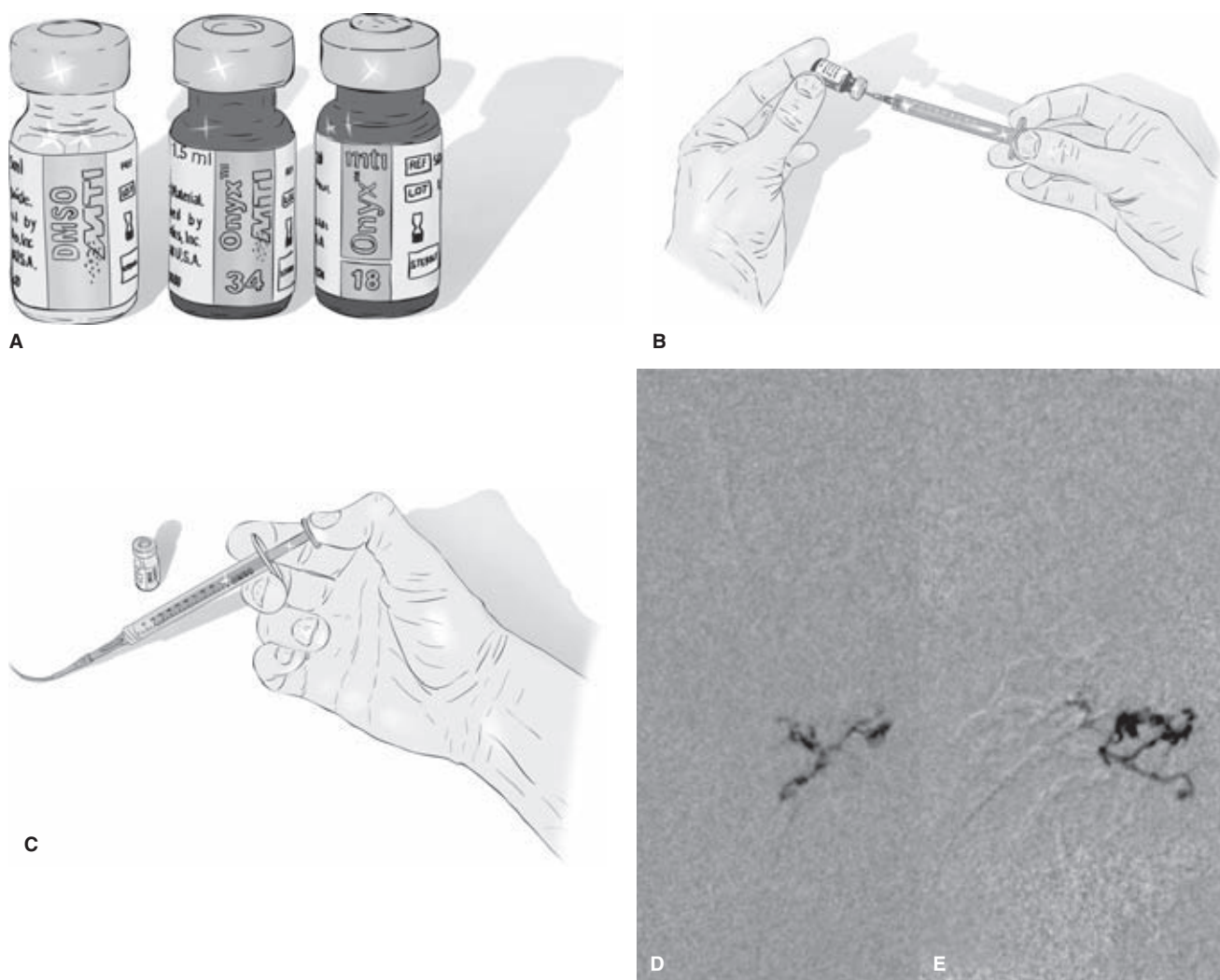


FIGURE 19-20. (A–D) **Onyx.** Onyx is supplied in minivials of 18 and 34 denomination, the former being more commonly used. Each kit comes with a vial of DMSO (1 mL = 1.1 g) for priming the microcatheter ahead of time and with DMSO-compatible syringes. These vials are not on the sterile field because the Onyx must be agitated ahead of time for 20 minutes. An assistant holds the vial while the gowned operator siphons the material into a sterile syringe (B). The microcatheter must be primed ahead of the Onyx with pure DMSO, which is then extruded from the microcatheter by the embolic column at a rate not exceeding 0.25 mL per 1.5 minutes. Onyx is watched carefully on a roadmap mask (D) as it extrudes until some reflux around the catheter tip or toward an undesirable location is seen. The injection is then paused and a fresh mask is obtained that zeroes out the cast of Onyx from previous injections (E), allowing greater conspicuity of the next extrusion. The maximum dose of DMSO per session can be a concern in small children, with the highest permissible dose according to manufacturer's recommendations being 600 mg/kg, but the highest doses in children in actual clinical practice being more in the order of less than 300 mg/kg (105,106).

Dehydrated Alcohol

Use of liquid alcohol in neurointerventional procedures tends not to receive as much attention as other agents and is used in fewer departments. Those who use it a great deal tend to profess that it has some safety and efficacy features missing from the profiles of other agents. Its efficacy is based on its immediate cytotoxic effect on the endothelium of vessels near the tip of the microcatheter, and when it is successful, the damaged intimal lining induces a thrombosis of the vessel that becomes apparent over the course of 5 to 10 minutes after the embolization. Proponents maintain that by virtue of the dilution of the alcohol that takes place within the nidus of the AVM, compromise or early thrombosis of the veins

on the other side of the nidus is not likely to happen, at least not early in the procedure. The technique for its use is easy with the operator rehearsing with contrast ahead of time to gain a sense of what force of injection is needed to lavage the entire wall of the feeding vessel when the time comes to inject the nonopacified alcohol. Problems with alcohol include its extreme toxicity in high concentrations to brain parenchyma and a possibility of induction of catastrophic pulmonary hypertension when the rate of volumetric return to the heart is excessive. Volume limitations for treatment at one session are recommended not to exceed 1 mL/kg of body weight, and a Swan-Ganz catheter is recommended if the anticipated rate of injection exceeds 10% of this total

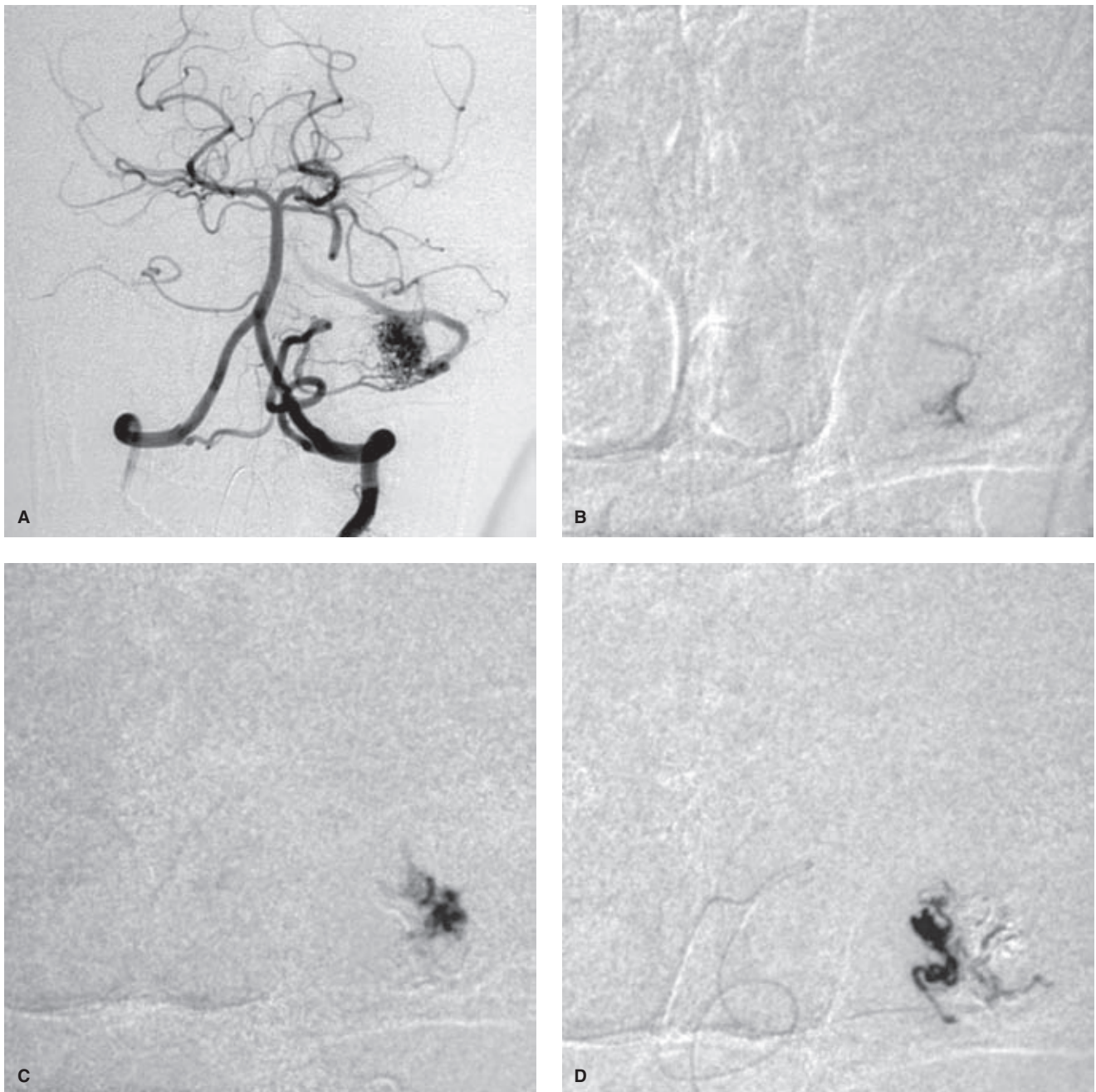


FIGURE 19-21. (A–E) Onyx embolization of a left cerebellar AVM. This young adult presented with a left cerebellar hemorrhage from this AVM feeding predominantly from the left posterior inferior cerebellar artery. The pre-embolization AP image (A) shows the pretreatment appearance, while images (B) through (E) show the AP mask images as progressive Onyx embolization was performed through several branches, with the final nonsubtracted appearance of the mass of Onyx, and the final postembolization angiogram (F). It is important to realize that complete or near-complete penetration of an AVM with Onyx is wrought with the risk of increasing time that the microcatheter is embedded within the plug of Onyx. While this type of result is technically very satisfactory, the risk to the patient comes at the time of withdrawal of the microcatheter and the distortion of vascular anatomy inherent in overcoming the resistance of the anchored microcatheter tip. In this patient's case one has to consider the tortuosity of the posterior inferior cerebellar artery, but also what the effect of a distortion of the left vertebral artery will be on the medullary perforators of the brainstem. Most procedural bleeds that happen with Onyx embolization occur at the time of microcatheter withdrawal, and it is probably prudent to reverse anticoagulation of the patient as a routine precautionary measure prior to that maneuver.

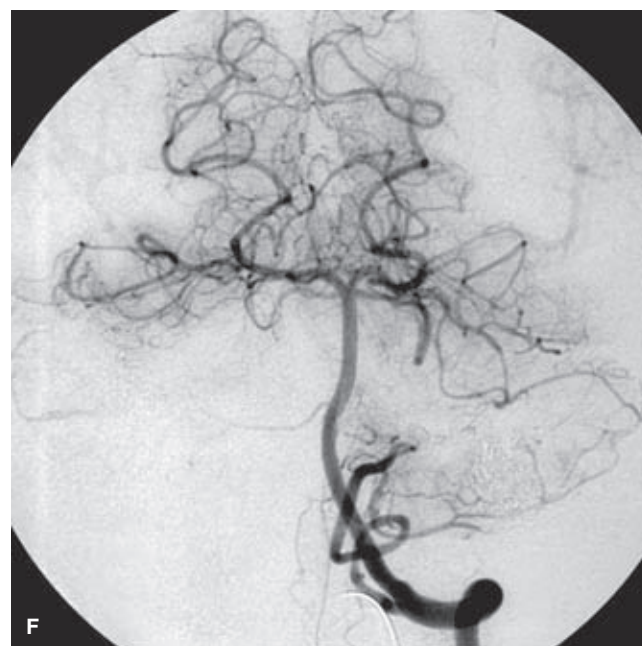
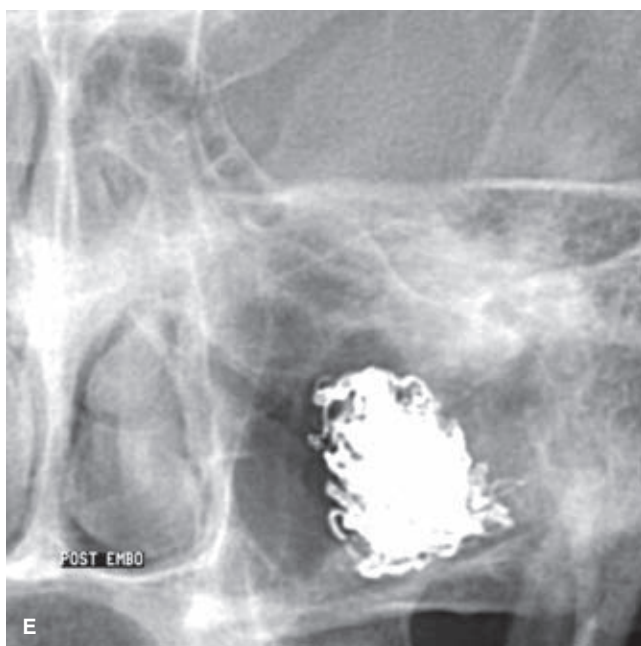


FIGURE 19-21. (CONTINUED)

dose per 10-minute period. Liquid alcohol is supplied in 5 mL vials and has no compatibility problems with any of the currently available microcatheters.

Coils

Coils are easy to use in brain AVMs but tend to be thought of as ineffective by virtue of the proximal deposition site achieved with them because they do not tend to penetrate the nidus. However, for exclusively presurgical embolization, the use of coils is safe and highly effective. Fibered coils require insertion of a larger-lumen microcatheter, most of which are a little stiff and potentially hazardous for the very distal access involved with most AVMs. A series of fibered or unfibered coils can slow down flow in a feeding vessel considerably and make use of a subsequent embolic agent more controlled or more effective. Even when used by themselves, they can achieve a very respectable result at low risk.

Other Materials

Polyvinyl alcohol has too great a capacity to shunt its way to the lungs through most AVMs and has fallen out of use in this domain. Moreover, its effect is transient and will be invariably followed by recanalization of the vessel over subsequent weeks. Other agents such as threads and Gelfoam have similarly fallen into disuse.

Procedural Dangers of Brain Arteriovenous Malformation Embolization

In addition to the standard concerns with neurointerventional cases, particular attention during AVM embolization is due to the following features:

1. As mentioned above, the biggest risk to the patient is excessive or early venous penetration of the venous side of the AVM. If this happens, consideration may need to be given to either completely closing down the arterial side straight away or sending the patient for early

surgery. Blood-pressure management in the ICU afterward is obviously necessary but will not remove the risk of this complication substantially.

2. Risks following a substantial embolization include normal perfusion breakthrough bleeding, akin to the hyperperfusion syndrome seen following carotid stenosis procedures where the autoregulatory curve has been adjusted so far that immediate correction is not feasible. Again, ICU blood-pressure management is the single controllable variable afterward.
3. The microcatheters used for AVM embolization have improved considerably over the past 10 years, but there is still a risk that a tear or microperforation could have developed during a long and taxing navigation. This would mean that the embolus would exit the microcatheter very proximally, for example, in the basilar artery or internal carotid artery, and shower the brain with material before the operator who is focused on a magnified view of the catheter tip would have a chance to realize what was going on. The last safeguard against this catastrophic event is to look very carefully at the last microcatheter injection performed before the embolization and be sure that no flashes of contrast are seen coming from somewhere other than the tip of the microcatheter.
4. The process of wire navigation to a very distal AVM can be either very easy or very tedious and frustrating. In the latter instance, several passages back and forth of the wire, milking and coaxing the microcatheter forward and back can place a great deal of stress not just on the microcatheter but also on the walls of the feeding arteries. If these walls are dysplastic or have flow-generated aneurysms along their course, there will be limitations in how much abuse they can withstand, and the possibility of inducing an arterial tear or perforation must always be borne in mind.
5. Reflux of embolic material into normal proximal branches is a constant danger. When performing an embolization

into an AVM, it is very important to know exactly where one's margin for safe reflux, if any, is exactly. Injection of Onyx depends very frequently on generating a sufficient "plug" around the distal end of the catheter to use as a base for pushing the embolus more distally. Some writers have advocated use of selective Wada testing with injections of barbiturates into locations of uncertainty in awake patients. However, the difficulties of performing brain AVM embolization on awake patients are considerable, and the results of such testing have not always been dependable.

6. Backthrombosis of a larger feeding vessel rendered stagnant by the effects of the procedure is occasionally seen. In some cases, it is hypothesized that retrograde thrombosis of a feeder can propagate back to a junction with a normal proximal branch. Continuation of heparinization after a procedure can sometimes be necessary for this reason. A similar phenomenon may be possible on the venous side of a malformation where flow has been substantially impacted by the procedure.

References

1. McCormick WF. The pathology of vascular ("arteriovenous") malformations. *J Neurosurg* 1966;24(4):807–816.
2. McCormick WF, Hardman JM, Boulter TR. Vascular malformations ("angiomas") of the brain, with special reference to those occurring in the posterior fossa. *J Neurosurg* 1968;28(3):241–251.
3. Aboian MS, Daniels DJ, Rammos SK, et al. The putative role of the venous system in the genesis of vascular malformations. *Neurosurg Focus* 2009;27(5):E9.
4. Houser OW, Baker HL Jr, Rhoton AL Jr, et al. Intracranial dural arteriovenous malformations. *Radiology* 1972;105(1):55–64.
5. Houser OW, Campbell JK, Campbell RJ, et al. Arteriovenous malformation affecting the transverse dural venous sinus—An acquired lesion. *Mayo Clin Proc* 1979;54(10):651–661.
6. Gerlach R, Boehm-Weigert M, Berkefeld J, et al. Thrombophilic risk factors in patients with cranial and spinal dural arteriovenous fistulae. *Neurosurgery* 2008;63(4):693–698; discussion 698–699.
7. Kraus JA, Stuper BK, Nahser HC, et al. Significantly increased prevalence of factor V Leiden in patients with dural arteriovenous fistulas. *J Neurol* 2000;247(7):521–523.
8. Kraus JA, Stuper BK, Muller J, et al. Molecular analysis of thrombophilic risk factors in patients with dural arteriovenous fistulas. *J Neurol* 2002;249(6):680–682.
9. Safavi-Abbasi S, Di Rocco F, Nakaji P, et al. Thrombophilia due to Factor V and Factor II mutations and formation of a dural arteriovenous fistula: Case report and review of a rare entity. *Skull Base* 2008;18(2):135–143.
10. Saito A, Takahashi N, Furuno Y, et al. Multiple isolated sinus dural arteriovenous fistulas associated with antithrombin III deficiency—Case report. *Neurol Med Chir (Tokyo)* 2008;48(10):455–459.
11. Voorberg J, Roelse J, Koopman R, et al. Association of idiopathic venous thromboembolism with single point-mutation at Arg506 of factor V. *Lancet* 1994;343(8912):1535–1536.
12. Wenderoth JD, Phatouros CC. Incidental discovery of a dural arteriovenous fistula in a patient with activated protein C resistance. *AJNR Am J Neuroradiol* 2003;24(7):1369–1371.
13. Legiehn GM, Heran MK. A step-by-step practical approach to imaging diagnosis and interventional radiologic therapy in vascular malformations. *Semin Intervent Radiol* 2010;27(2):209–231.
14. Challa VR, Moody DM, Brown WR. Vascular malformations of the central nervous system. *J Neuropathol Exp Neurol* 1995;54(5):609–621.
15. Farrell DF, Forno LS. Symptomatic capillary telangiectasia of the brainstem without hemorrhage. *Neurology* 1960;20:341–360.
16. Teilmann K. Hemangiomas of the pons. *AMA Arch Neurol Psychiatry* 1953;69(2):208–223.
17. McCormick PW, Spetzler RF, Johnson PC, et al. Cerebellar hemorrhage associated with capillary telangiectasia and venous angioma: A case report. *Surg Neurol* 1993;39(6):451–457.
18. Pozzati E, Marliani AF, Zucchelli M, et al. The neurovascular triad: Mixed cavernous, capillary, and venous malformations of the brainstem. *J Neurosurg* 2007;107(6):1113–1119.
19. Zabramski JM, Wascher TM, Spetzler RF, et al. The natural history of familial cavernous malformations: Results of an ongoing study. *J Neurosurg* 1994;80(3):422–432.
20. Pozzati E, Acciarri N, Tognetti F, et al. Growth, subsequent bleeding, and de novo appearance of cerebral cavernous angiomas. *Neurosurgery* 1996;38(4):662–669; discussion 669–670.
21. Sage MR, Brophy BP, Sweeney C, et al. Cavernous haemangiomas (angiomas) of the brain: Clinically significant lesions. *Australas Radiol* 1993;37(2):147–155.
22. Simard JM, Garcia-Bengochea F, Ballinger WE Jr, et al. Cavernous angioma: A review of 126 collected and 12 new clinical cases. *Neurosurgery* 1986;18(2):162–172.
23. Abdulrauf SI, Kaynar MY, Awad IA. A comparison of the clinical profile of cavernous malformations with and without associated venous malformations. *Neurosurgery* 1999;44(1):41–46; discussion 46–47.
24. Clatterbuck RE, Elmaci I, Rigamonti D. The juxtaposition of a capillary telangiectasia, cavernous malformation, and developmental venous anomaly in the brainstem of a single patient: Case report. *Neurosurgery* 2001;49(5):1246–1250.
25. Roberson GH, Kase CS, Wolpaw ER. Telangiectases and cavernous angiomas of the brainstem: "Cryptic" vascular malformations. Report of a case. *Neuroradiology* 1974;8(2):83–89.
26. Rigamonti D, Spetzler RF. The association of venous and cavernous malformations. Report of four cases and discussion of the pathophysiological, diagnostic, and therapeutic implications. *Acta Neurochir (Wien)* 1988;92(1–4):100–105.
27. Zimmerman RS, Spetzler RF, Lee KS, et al. Cavernous malformations of the brain stem. *J Neurosurg* 1991;75(1):32–39.
28. Rigamonti D, Johnson PC, Spetzler RF, et al. Cavernous malformations and capillary telangiectasia: A spectrum within a single pathological entity. *Neurosurgery* 1991;28(1):60–64.
29. Ogilvy CS, Moayeri N, Golden JA. Appearance of a cavernous hemangioma in the cerebral cortex after a biopsy of a deeper lesion. *Neurosurgery* 1993;33(2):307–309; discussion 309.
30. Wilson CB. Cryptic vascular malformations. *Clin Neurosurg* 1992;38:49–84.
31. Robinson JR Jr, Awad IA, Magdinec M, et al. Factors predisposing to clinical disability in patients with cavernous malformations of the brain. *Neurosurgery* 1993;32(5):730–735; discussion 735–736.
32. Del Curling O Jr, Kelly DL Jr, Elster AD, et al. An analysis of the natural history of cavernous angiomas. *J Neurosurg* 1991;75(5):702–708.
33. Robinson JR, Awad IA, Little JR. Natural history of the cavernous angioma. *J Neurosurg* 1991;75(5):709–714.
34. Kondziolka D, Lunsford LD, Kestle JR. The natural history of cerebral cavernous malformations. *J Neurosurg* 1995;83(5):820–824.

35. Aiba T, Tanaka R, Koike T, et al. Natural history of intracranial cavernous malformations. *J Neurosurg* 1995;83(1):56–59.
36. Sinson G, Zager EL, Grossman RI, et al. Cavernous malformations of the third ventricle. *Neurosurgery* 1995;37(1):37–42.
37. Katayama Y, Tsubokawa T, Maeda T, et al. Surgical management of cavernous malformations of the third ventricle. *J Neurosurg* 1994;80(1):64–72.
38. Robinson JR Jr, Awad IA, Masaryk TJ, et al. Pathological heterogeneity of angiographically occult vascular malformations of the brain. *Neurosurgery* 1993;33(4):547–554; discussion 554–545.
39. Sarwar M, McCormick WF. Intracerebral venous angioma. Case report and review. *Arch Neurol* 1978;35(5):323–325.
40. Handa J, Suda K, Sato M. Cerebral venous angioma associated with varix. *Surg Neurol* 1984;21(5):436–440.
41. Kelly KJ, Rockwell BH, Raji MR, et al. Isolated cerebral intraaxial varix. *AJNR Am J Neuroradiol* 1995;16(8):1633–1635.
42. Uchino A, Hasuo K, Matsumoto S, et al. Varix occurring with cerebral venous angioma: A case report and review of the literature. *Neuroradiology* 1995;37(1):29–31.
43. Numaguchi Y, Kitamura K, Fukui M, et al. Intracranial venous angiomata. *Surg Neurol* 1982;18(3):193–202.
44. Numaguchi Y, Nadell JM, Mizushima A, et al. Cerebral venous angioma and a varix: A rare combination. *Comput Radiol* 1986;10(6):319–323.
45. Rigamonti D, Spetzler RF, Medina M, et al. Cerebral venous malformations. *J Neurosurg* 1990;73(4):560–564.
46. Kondziolka D, Dempsey PK, Lunsford LD. The case for conservative management of venous angiomata. *Can J Neurol Sci* 1991;18(3):295–299.
47. Wilms G, Bleus E, Demaerel P, et al. Simultaneous occurrence of developmental venous anomalies and cavernous angiomata. *AJNR Am J Neuroradiol* 1994;15(7):1247–1254; discussion 1255–1247.
48. Mullan S, Mojtahedi S, Johnson DL, et al. Cerebral venous malformation–arteriovenous malformation transition forms. *J Neurosurg* 1996;85(1):9–13.
49. Dejana E, Lampugnani MG, Giorgi M, et al. Fibrinogen induces endothelial cell adhesion and spreading via the release of endogenous matrix proteins and the recruitment of more than one integrin receptor. *Blood* 1990;75(7):1509–1517.
50. Kittelberger R, Davis PF, Stehens WE. Distribution of type IV collagen, laminin, nidogen and fibronectin in the haemodynamically stressed vascular wall. *Histol Histopathol* 1990;5(2):161–167.
51. Krum JM, More NS, Rosenstein JM. Brain angiogenesis: Variations in vascular basement membrane glycoprotein immunoreactivity. *Exp Neurol* 1991;111(2):152–165.
52. Kilic T, Pamir MN, Kullu S, et al. Expression of structural proteins and angiogenic factors in cerebrovascular anomalies. *Neurosurgery* 2000;46(5):1179–1191; discussion 1191–1172.
53. Lv X, Jiang C, Li Y, et al. Clinical outcomes of endovascular treatment for intracranial pial arteriovenous fistulas. *World Neurosurg* 2010;73(4):385–390.
54. Lee JY, Son YJ, Kim JE. Intracranial pial arteriovenous fistulas. *J Korean Neurosurg Soc* 2008;44(2):101–104.
55. Yang WH, Lu MS, Cheng YK, et al. Pial arteriovenous fistula: A review of literature. *Br J Neurosurg* 2011;25(5):580–585.
56. Mohr JP, Moskowitz AJ, Stapf C, et al. The ARUBA trial: Current status, future hopes. *Stroke* 2010;41(8):e537–540.
57. Brown RD Jr, Wiebers DO, Forbes G, et al. The natural history of unruptured intracranial arteriovenous malformations. *J Neurosurg* 1988;68(3):352–357.
58. Graf CJ, Perret GE, Torner JC. Bleeding from cerebral arteriovenous malformations as part of their natural history. *J Neurosurg* 1983;58(3):331–337.
59. Ondra SL, Troupp H, George ED, et al. The natural history of symptomatic arteriovenous malformations of the brain: A 24-year follow-up assessment. *J Neurosurg* 1990;73(3):387–391.
60. Brown RD Jr, Flemming KD, Meyer FB, et al. Natural history, evaluation, and management of intracranial vascular malformations. *Mayo Clin Proc* 2005;80(2):269–281.
61. Crawford PM, West CR, Chadwick DW, et al. Arteriovenous malformations of the brain: Natural history in unoperated patients. *J Neurol Neurosurg Psychiatry* 1986;49(1):1–10.
62. Mast H, Young WL, Koennecke HC, et al. Risk of spontaneous haemorrhage after diagnosis of cerebral arteriovenous malformation. *Lancet* 1997;350(9084):1065–1068.
63. Hernesniemi JA, Dashti R, Juvela S, et al. Natural history of brain arteriovenous malformations: A long-term follow-up study of risk of hemorrhage in 238 patients. *Neurosurgery* 2008;63(5):823–829; discussion 829–831.
64. van Dijk JM, Terbrugge KG, Willinsky RA, et al. The natural history of dural arteriovenous shunts: The Toronto experience. *Stroke* 2009;40(5):e412; author reply e413–414.
65. Laakso A, Dashti R, Juvela S, et al. Risk of hemorrhage in patients with untreated Spetzler–Martin grade IV and V arteriovenous malformations: A long-term follow-up study in 63 patients. *Neurosurgery* 2011;68(2):372–377; discussion 378.
66. Raymond J, Naggara O, Guilbert F, et al. Assessing prognosis from nonrandomized studies: An example from brain arteriovenous malformations. *AJNR Am J Neuroradiol* 2011;32(5):809–812.
67. Stapf C, Mohr JP, Choi JH, et al. Invasive treatment of unruptured brain arteriovenous malformations is experimental therapy. *Curr Opin Neurol* 2006;19(1):63–68.
68. Wilkins RH. Natural history of intracranial vascular malformations: A review. *Neurosurgery* 1985;16(3):421–430.
69. Marks MP, Lane B, Steinberg GK, et al. Hemorrhage in intracerebral arteriovenous malformations: Angiographic determinants. *Radiology* 1990;176(3):807–813.
70. Miyasaka Y, Yada K, Ohwada T, et al. An analysis of the venous drainage system as a factor in hemorrhage from arteriovenous malformations. *J Neurosurg* 1992;76(2):239–243.
71. Turjman F, Massoud TF, Vinuela F, et al. Correlation of the angioarchitectural features of cerebral arteriovenous malformations with clinical presentation of hemorrhage. *Neurosurgery* 1995;37(5):856–860; discussion 860–852.
72. Spetzler RF, Hargraves RW, McCormick PW, et al. Relationship of perfusion pressure and size to risk of hemorrhage from arteriovenous malformations. *J Neurosurg* 1992;76(6):918–923.
73. Norris JS, Valiante TA, Wallace MC, et al. A simple relationship between radiological arteriovenous malformation hemodynamics and clinical presentation: A prospective, blinded analysis of 31 cases. *J Neurosurg* 1999;90(4):673–679.
74. Moftakhar P, Hauptman JS, Malkasian D, et al. Cerebral arteriovenous malformations. Part 2: Physiology. *Neurosurg Focus* 2009;26(5):E11.
75. Fults D, Kelly DL Jr. Natural history of arteriovenous malformations of the brain: A clinical study. *Neurosurgery* 1984;15(5):658–662.
76. Cunha Sa MJ, Stein BM, Solomon RA, et al. The treatment of associated intracranial aneurysms and arteriovenous malformations. *J Neurosurg* 1992;77(6):853–859.
77. Abe T, Nemoto S, Iwata T, et al. Rupture of a cerebral aneurysm during embolization for a cerebral arteriovenous malformation. *AJNR Am J Neuroradiol* 1995;16(9):1818–1820.
78. Lasjaunias P, Piske R, Terbrugge K, et al. Cerebral arteriovenous malformations (C. AVM) and associated arterial aneurysms (AA). Analysis of 101 C. AVM cases, with 37 AA in 23 patients. *Acta Neurochir (Wien)* 1988;91(1–2):29–36.

79. Garcia-Monaco R, Rodesch G, Alvarez H, et al. Pseudoaneurysms within ruptured intracranial arteriovenous malformations: Diagnosis and early endovascular management. *AJNR Am J Neuroradiol* 1993;14(2):315–321.
80. Spetzler RF, Martin NA. A proposed grading system for arteriovenous malformations. *J Neurosurg* 1986;65(4):476–483.
81. Shi YQ, Chen XC. A proposed scheme for grading intracranial arteriovenous malformations. *J Neurosurg* 1986;65(4):484–489.
82. Spetzler RF, Ponce FA. A 3-tier classification of cerebral arteriovenous malformations. Clinical article. *J Neurosurg* 2011;114(3):842–849.
83. Hamilton MG, Spetzler RF. The prospective application of a grading system for arteriovenous malformations. *Neurosurgery* 1994;34(1):2–6; discussion 6–7.
84. Heros RC, Korosue K, Diebold PM. Surgical excision of cerebral arteriovenous malformations: Late results. *Neurosurgery* 1990;26(4):570–577; discussion 577–578.
85. Stapf C, Mast H, Sciacca RR, et al. The New York Islands AVM Study: Design, study progress, and initial results. *Stroke* 2003;34(5):e29–33.
86. Hartmann A, Mast H, Mohr JP, et al. Determinants of staged endovascular and surgical treatment outcome of brain arteriovenous malformations. *Stroke* 2005;36(11):2431–2435.
87. Lawton MT, Du R, Tran MN, et al. Effect of presenting hemorrhage on outcome after microsurgical resection of brain arteriovenous malformations. *Neurosurgery* 2005;56(3):485–493; discussion 485–493.
88. Lim M, Cheshier S, Steinberg GK. New vessel formation in the central nervous system during tumor growth, vascular malformations, and Moyamoya. *Curr Neurovasc Res* 2006;3(3):237–245.
89. Hjelmeland AB, Lathia JD, Sathornsumetee S, et al. Twisted tango: Brain tumor neurovascular interactions. *Nat Neurosci* 2011;14(11):1375–1381.
90. Konya D, Yildirim O, Kurtkaya O, et al. Testing the angiogenic potential of cerebrovascular malformations by use of a rat cornea model: Usefulness and novel assessment of changes over time. *Neurosurgery* 2005;56(6):1339–1345; discussion 1345–1336.
91. Sure U, Battenberg E, Dempfle A, et al. Hypoxia-inducible factor and vascular endothelial growth factor are expressed more frequently in embolized than in nonembolized cerebral arteriovenous malformations. *Neurosurgery* 2004;55(3):663–669; discussion 669–670.
92. Sure U, Butz N, Siegel AM, et al. Treatment-induced neovascularization in cerebral arteriovenous malformations. *Clin Neurol Neurosurg* 2001;103(1):29–32.
93. Kilic K, Konya D, Kurtkaya O, et al. Inhibition of angiogenesis induced by cerebral arteriovenous malformations using gamma knife irradiation. *J Neurosurg* 2007;106(3):463–469.
94. Frenzel T, Lee CZ, Kim H, et al. Feasibility of minocycline and doxycycline use as potential vasculostatic therapy for brain vascular malformations: Pilot study of adverse events and tolerance. *Cerebrovasc Dis* 2008;25(1–2):157–163.
95. Hashimoto T, Matsumoto MM, Li JF, et al. Suppression of MMP-9 by doxycycline in brain arteriovenous malformations. *BMC Neurol* 2005;5(1):1.
96. Lee CZ, Xue Z, Zhu Y, et al. Matrix metalloproteinase-9 inhibition attenuates vascular endothelial growth factor-induced intracerebral hemorrhage. *Stroke* 2007;38(9):2563–2568.
97. Ayad M, Eskioglu E, Mericle RA. Onyx: A unique neuroembolic agent. *Expert Rev Med Devices* 2006;3(6):705–715.
98. Lopes DK, Bagan B, Wells K. Onyx embolization of arteriovenous malformations using 2 microcatheters. *Neurosurgery* 2010;66(3):616–618; discussion 618–619.
99. Abud DG, Riva R, Nakiri GS, et al. Treatment of brain arteriovenous malformations by double arterial catheterization with simultaneous injection of Onyx: Retrospective series of 17 patients. *AJNR Am J Neuroradiol* 2011;32(1):152–158.
100. Dalyai RT, Schirmer CM, Malek AM. Transvenous balloon-protected embolization of a scalp arteriovenous fistula using Onyx liquid embolic. *Acta Neurochir (Wien)* 2011;153(6):1285–1290.
101. Maimon S, Strauss I, Frolov V, et al. Brain arteriovenous malformation treatment using a combination of Onyx and a new detachable tip microcatheter, SONIC: Short-term results. *AJNR Am J Neuroradiol* 2010;31(5):947–954.
102. Kelly ME, Turner Rt, Gonugunta V, et al. Monorail snare technique for the retrieval of an adherent microcatheter from an onyx cast: Technical case report. *Neurosurgery* 2008;63(1 suppl 1):ONSE89; discussion ONSE89.
103. Alamri A, Hyodo A, Suzuki K, et al. Retrieving microcatheters from Onyx casts in a series of brain arteriovenous malformations: A technical report. *Neuroradiology* Oct 26 2011.
104. Newman CB, Park MS, Kerber CW, et al. Over-the-catheter retrieval of a retained microcatheter following Onyx embolization: A technical report. *J Neurointerv Surg* Jun 16 2011.
105. Jankowitz BT, Vora N, Jovin T, et al. Treatment of pediatric intracranial vascular malformations using Onyx-18. *J Neurosurg Pediatr* 2008;2(3):171–176.
106. Thiex R, Williams A, Smith E, et al. The use of Onyx for embolization of central nervous system arteriovenous lesions in pediatric patients. *AJNR Am J Neuroradiol* 2010;31(1):112–120.

Cranial Dural Vascular Malformations

Key Points

- The physiologic impact of dural arteriovenous malformations (DAVMs) is determined almost exclusively by the pattern of venous drainage.
- Treatment of DAVMs must strive to preserve normal parenchymal venous drainage in order to avoid complications of venous infarction and venous hypertension.

Vascular malformations or fistulas of the dura are uncommon diseases, but they have the potential to develop severe complications. They account for 10% to 15% of intracranial arteriovenous malformations of all types. They can occur in the brain or spine (Chapter 21) with characteristic patterns of pathophysiology in both locations.

The cranial dura consists of two tightly apposed layers, an outer periosteal layer and an inner meningeal layer, separated by a rich vascular layer of meningeal or dural veins and arterioles. Where the two layers of dura become separated, a larger venous space forms the dural sinuses. Along the cranial dura, any meningeal artery that perforates the dura usually does so in close relationship to surrounding venous plexuses. The artery penetrates the dura through or may run for a while within a venous structure or sinus. Venous thrombosis or other injuries, including surgery (1–3), may occasion a process of inflammation, neovascularization, and angiogenesis (4). The adjacent arterioles are thought to become involved with the formation of pathologic shunts to venous channels (5). In some instances, the fistulous connection could be the initiating event, as might happen with acute trauma, and the high-flowing lesion is then hypothesized to recruit additional arterial supply through the angiogenic mediators. In most patients, an acquired etiology is certain, in view of well-documented cases of such lesions soon after surgery, trauma, or mastoid air-cell infection. Metachronous formation of dural arteriovenous malformations (DAVMs) has also been seen, supporting the assumption of an acquired etiology (6). Patients with systemic syndromes involving abnormalities of vascular fragility, such as neurofibromatosis type I, fibromuscular dysplasia, and Ehlers–Danlos syndrome (7–10), are reported to be

slightly more prone to develop these disorders of the cranial dura or spine.

An acquired dural fistula may be single, multifocal, or complex. The terms *DAVMs* and *dural arteriovenous fistulas* are interchangeable and synonymous. Fistulous malformations of the dura can be seen in young children as well. In children, long-standing changes suggest that some rare instances of congenital DAVMs occur.

In the cranial dura, the pathophysiology and significance of these lesions derive from their effects on venous flow (Figs. 20-1 and 20-2). Various classification schemes have been proposed to categorize these lesions (11–16). The quintessence of all of these schemes is an analysis of the state of disruption of venous outflow from the malformation, and the patency and direction of flow in adjacent dural sinuses, dural veins, and subarachnoid veins. The particular arterial feeders involved with a dural vascular malformation are usually not of primary importance for analysis of risks or treatment options (Figs. 20-3 and 20-4). An interesting classification scheme (16) on the basis of the homologous embryologic origins of segments of dura of the spine and cranium has been proposed with the predictive value that clinical complications are more likely to be seen with certain types, but the process of clinical decision making is not influenced, regardless of the perspective.

Uncomplicated DAVMs are occasionally seen as incidental findings (Fig. 20-5). They may be single or multiple, resulting in arterialization of flow in an orthograde fashion in a major dural sinus. Symptomatic patients present with pulsatile tinnitus, audible bruit, or cranial nerve deficits, depending on location of the lesion. Pulsatile tinnitus may be reported in 20% to 70% of patients, some of whom will volunteer a history of being able to suppress the bruit by manual compression of the neck. Visual symptoms and headache are also common (17). Hydrocephalus due to impaired resorption of CSF in more advanced cases can be seen, progressing in extreme instances to a state of dementia, parkinsonism, seizure, or movement disorders which can be reversible with treatment of the vascular lesion (18–22). Patients with symptomatic DAVMs are reported to have a recurrence rate of hemorrhage or non-hemorrhagic complications of at least 15% to 19% per year, necessitating urgent treatment (23,24). Thus, the presence of cortical reflux of venous flow has been represented as an angiographic

(text continues on page 326)

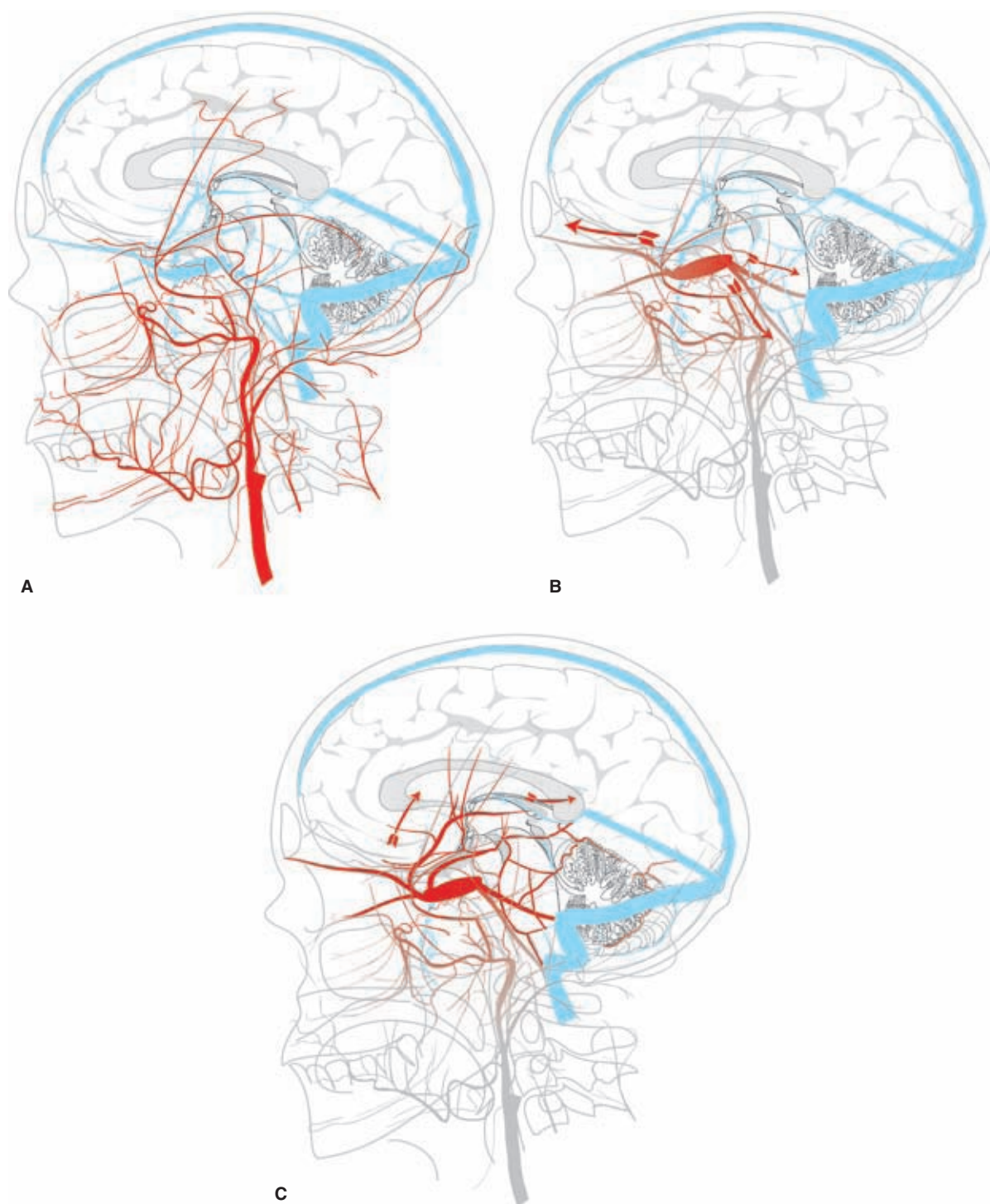


FIGURE 20-1. (A–C) Cavernous sinus DAVMs. The arterial and venous anatomy in the region of the cavernous sinus is illustrated (A), as depicted in preceding chapters. Most commonly, DAVMs in this region involve a degree of flow that is easily handled by the multitude of venous connections around the cavernous sinus bilaterally (B) so that exiting arterialized venous flow is seen as opacification of the superior ophthalmic vein (SOV), the superior petrosal sinus, or the IPS (*arrows*). When the flow is too voluminous or when there are anatomic constrictions on venous connections (C), arterialized flow can be diverted intracranially to the ipsilateral temporal lobe, the deep venous system, the superficial Sylvian vein, or even to the posterior fossa (either via the basal vein of Rosenthal or via the petrosal venous connection between the superior petrosal sinus and the cerebellar veins). The manifestation of these venous fields can be very subtle but of enormous moment to the patient, and therefore, the angiographic images must be examined thoroughly for the possibility of these findings.

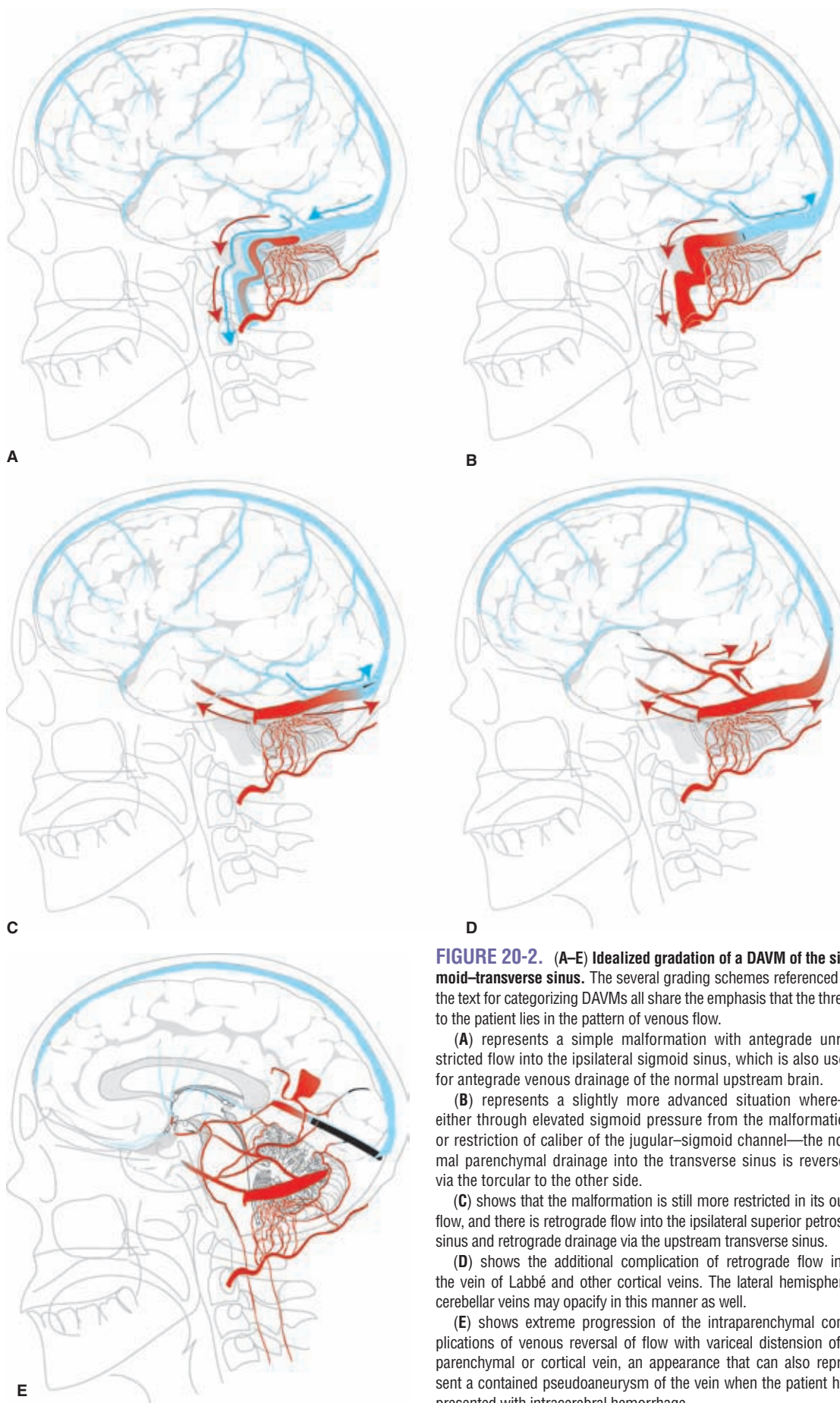


FIGURE 20-2. (A–E) Idealized gradation of a DAVM of the sigmoid–transverse sinus. The several grading schemes referenced in the text for categorizing DAVMs all share the emphasis that the threat to the patient lies in the pattern of venous flow.

(A) represents a simple malformation with antegrade unrestricted flow into the ipsilateral sigmoid sinus, which is also used for antegrade venous drainage of the normal upstream brain.

(B) represents a slightly more advanced situation where—either through elevated sigmoid pressure from the malformation or restriction of caliber of the jugular–sigmoid channel—the normal parenchymal drainage into the transverse sinus is reversed via the torcular to the other side.

(C) shows that the malformation is still more restricted in its out-flow, and there is retrograde flow into the ipsilateral superior petrosal sinus and retrograde drainage via the upstream transverse sinus.

(D) shows the additional complication of retrograde flow into the vein of Labbé and other cortical veins. The lateral hemispheric cerebellar veins may opacify in this manner as well.

(E) shows extreme progression of the intraparenchymal complications of venous reversal of flow with variceal distension of a parenchymal or cortical vein, an appearance that can also represent a contained pseudoaneurysm of the vein when the patient has presented with intracerebral hemorrhage.

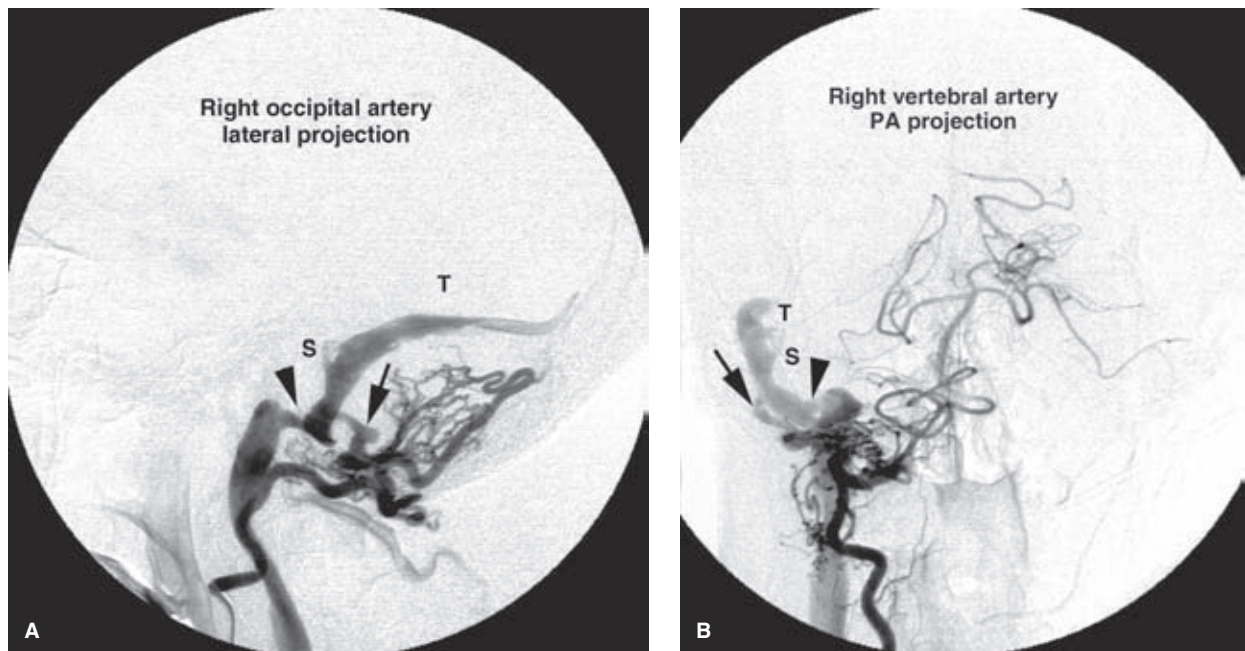


FIGURE 20-3. (A–B) DAVM of right sigmoid sinus. An elderly patient presented with a 3-month history of pulsatile tinnitus. Angiography demonstrated a DAVM of the right sigmoid sinus supplied by the ipsilateral occipital (A) and vertebral (B) arteries. All avenues of fistulous flow converge on a single venous channel (arrow), which empties into the sigmoid sinus. Although this DAVM is confined and simple on its arterial side, there is constriction (arrowhead) in the sigmoid sinus (S) with bidirectional flow to the jugular bulb and transverse sinus (T). This suggests that the DAVM has passed the early stages of evolution and is developing signs of sinus hypertension.

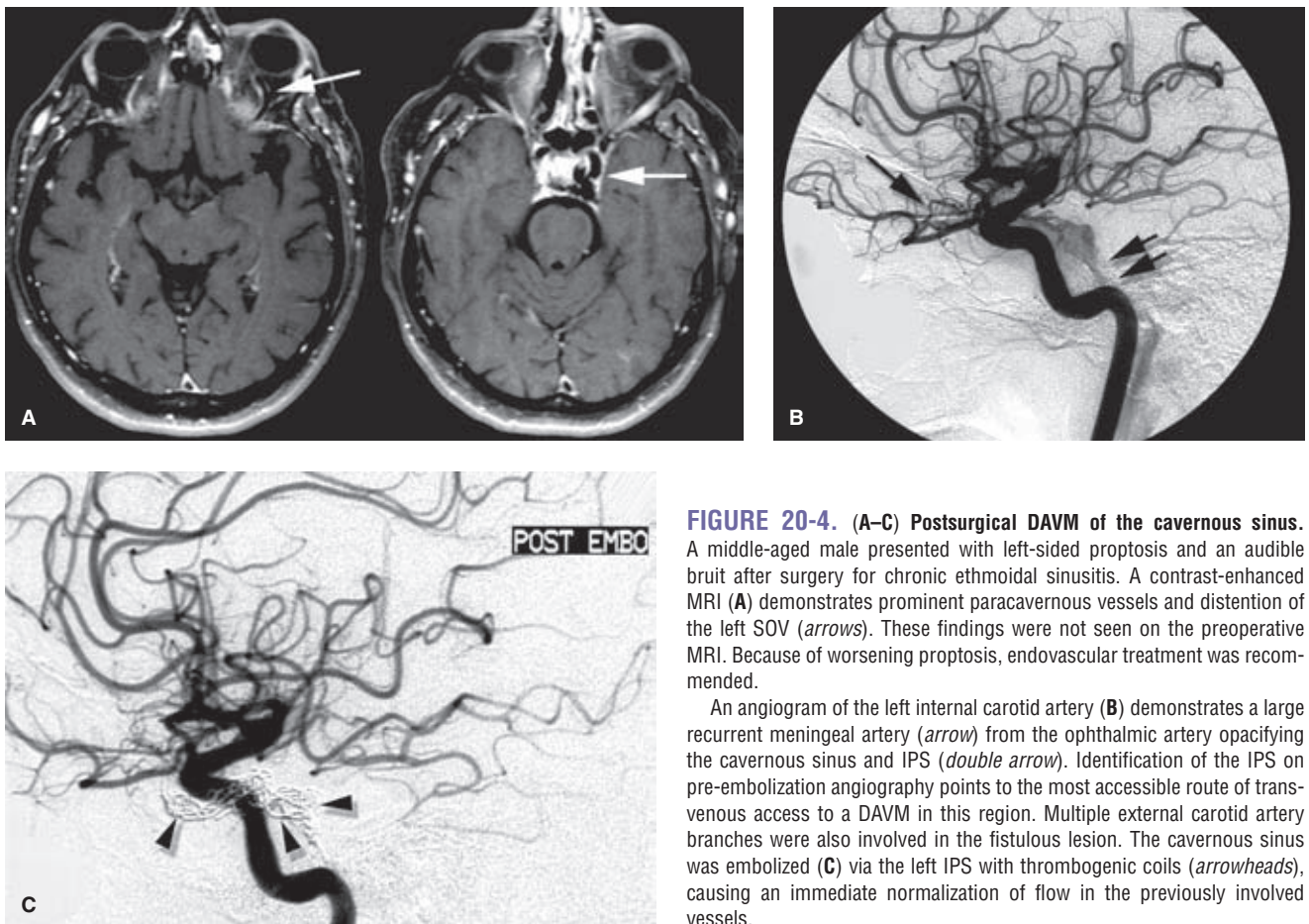


FIGURE 20-4. (A–C) Postsurgical DAVM of the cavernous sinus. A middle-aged male presented with left-sided proptosis and an audible bruit after surgery for chronic ethmoidal sinusitis. A contrast-enhanced MRI (A) demonstrates prominent paracavernous vessels and distention of the left SOV (arrows). These findings were not seen on the preoperative MRI. Because of worsening proptosis, endovascular treatment was recommended.

An angiogram of the left internal carotid artery (B) demonstrates a large recurrent meningeal artery (arrow) from the ophthalmic artery opacifying the cavernous sinus and IPS (double arrow). Identification of the IPS on pre-embolization angiography points to the most accessible route of trans-venous access to a DAVM in this region. Multiple external carotid artery branches were also involved in the fistulous lesion. The cavernous sinus was embolized (C) via the left IPS with thrombotic coils (arrowheads), causing an immediate normalization of flow in the previously involved vessels.

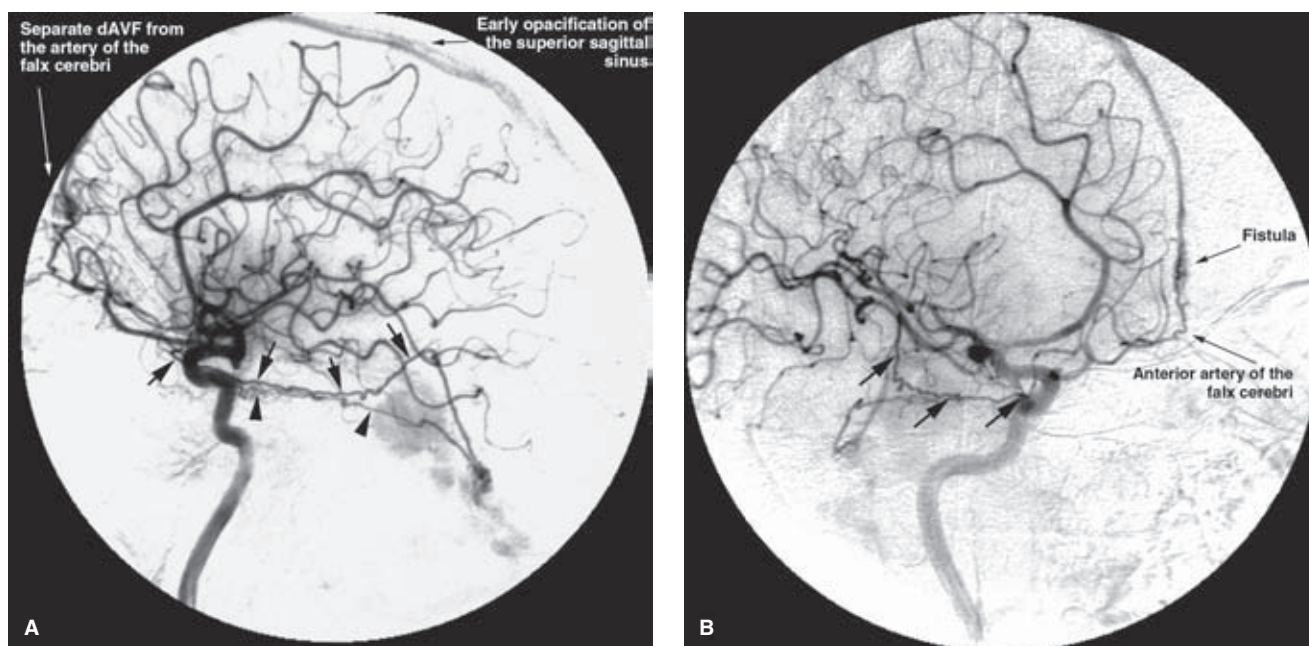


FIGURE 20-5. (A–B) Synchronous DAVMs. An elderly male presented with headaches. Two separate DAVMs were demonstrated on lateral (A) and oblique (B) images of the right internal carotid artery. A DAVM of the tentorium causing the patient's symptoms opacifies greatly distended veins in the posterior fossa. It is supplied by the marginal tentorial artery (*arrows*) arising from the ophthalmic artery and tentorial arteries (*arrowheads*) from the cavernous internal carotid artery. A separate fistula of the superior sagittal sinus is supplied by the anterior artery of the falx cerebri.

indicator for urgent intervention, but it is likely that such a sense of urgency is not always valid. DAVMs with cortical reflux which are asymptomatic at the time of detection have a much lower rate of complication, <2% (25,26), implying that a more tempered approach should be advocated in advising asymptomatic patients for whom an endovascular treatment may involve significant risk.

Dural arteriovenous fistulas are most commonly seen in the cavernous, sigmoid, and transverse sinuses (Figs. 20-6–20-10). Dural arteriovenous fistulas in the early stages may undergo spontaneous remission, although the likelihood of this in a well-established lesion is low (14,27,28). The dural sinus in early or uncomplicated cases may be completely normal in appearance or may show evidence of only partial thrombosis at the time of presentation. Depending on the patient's tolerance of symptoms, expectant management of patients with uncomplicated DAVMs may be reasonable (Fig. 20-11). Training the patient to perform manual contralateral carotid compression at home has been advocated to eliminate smaller lesions over a few weeks, but the efficacy of this home remedy is dubious.

The venous pattern changes as the pressure in the venous system increases due to intimal flow-related changes in the main venous channels or recruitment of arterial feeders. Diversion of flow away from the involved sinus is seen angiographically with retrograde flow in the dural sinuses. It can be difficult to identify the presence of incipient cortical venous hypertension unless a careful examination of the entire angiogram is performed. For example, an internal carotid arteriogram in which opacification of the DAVM is not seen may still demonstrate very ominous signs in the patterns of flow in the venous stages.

(text continues on page 331)

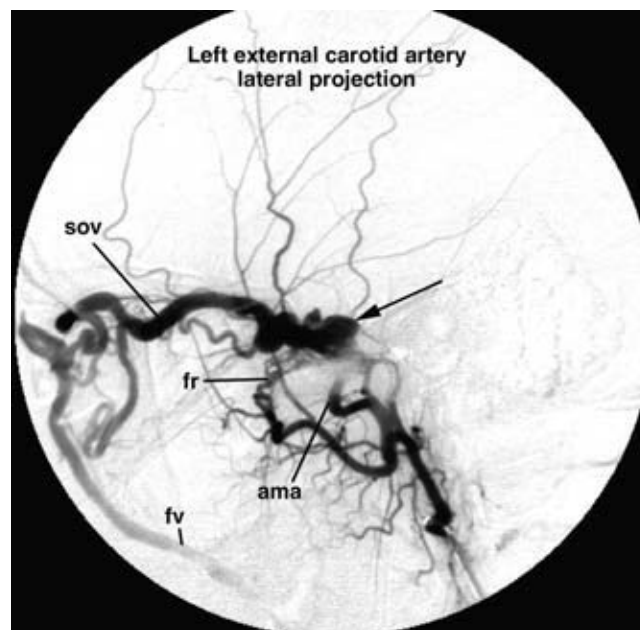


FIGURE 20-6. DAVM of the cavernous sinus. A lateral view of a left internal maxillary artery injection demonstrates opacification of a distended and tense cavernous sinus (*arrow*) via the accessory meningeal artery (*ama*) and artery of the foramen rotundum (*fr*). The cavernous sinus drains anteriorly to the SOV and subsequently to the facial vein (*fv*). In contrast to the patient in Figure 20-4, the IPS is not seen in this patient, which implies that transvenous access to the lesion through that route may not be possible. In a patient with a lesion such as this, urgency of treatment is guided primarily by concerns for the patient's vision. An ophthalmologist's involvement to monitor the intraocular pressure and visual acuity is imperative. The likelihood of such complications depends in part on the anastomoses of the ophthalmic veins with other drainage routes.

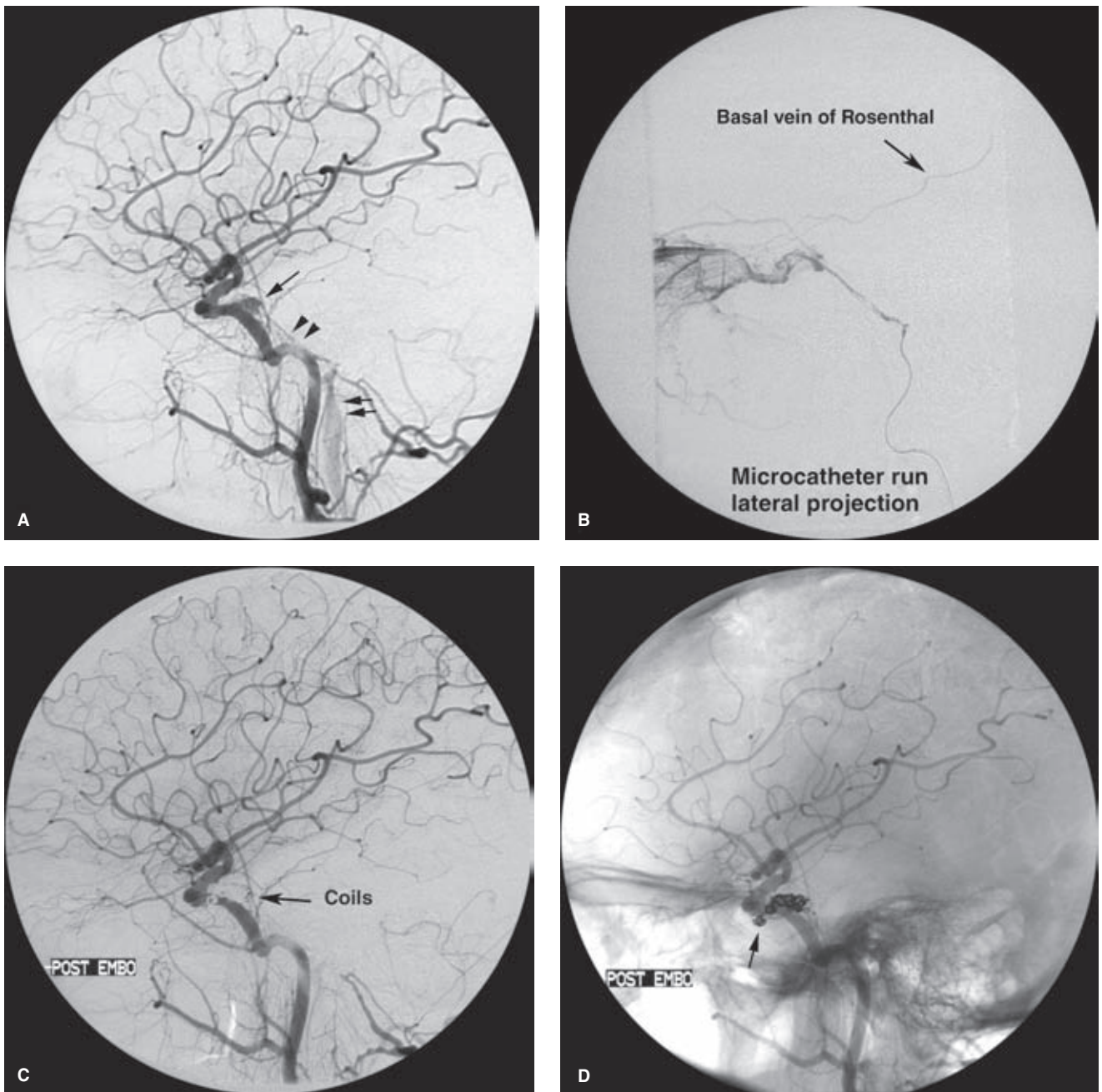


FIGURE 20-7. (A–D) A “simple” DAVM of the cavernous sinus. A lateral common carotid arteriogram (A) shows an apparently straightforward malformation of the cavernous sinus (*arrow*) with drainage via the ipsilateral IPS (*double arrowheads*) to the jugular vein (*double arrows*). There is no evidence of sinister intracranial complications. Treatment was undertaken because of the patient’s presentation with orbital chemosis and III and VI nerve palsies. The described route of venous drainage was used to access the cavernous sinus retrogradely with a microcatheter through which an angiographic run was performed (B). This image shows the connection to the ophthalmic vein responsible for the appearance of chemosis and also how this straightforward lesion has nevertheless the potential to develop serious complications through small, previously unseen connections to the basal vein of Rosenthal. A misadventurous endovascular treatment could end up diverting flow from the cavernous sinus to these deep channels and induce deep venous cerebral hypertension. The cavernous sinus was occluded with coils (C, D) to eliminate the fistulous flow, but with care taken to include the junction between the cavernous sinus and the SOV (*arrow*) so as to prevent diversion of flow into this channel with induction of complications in the eye.

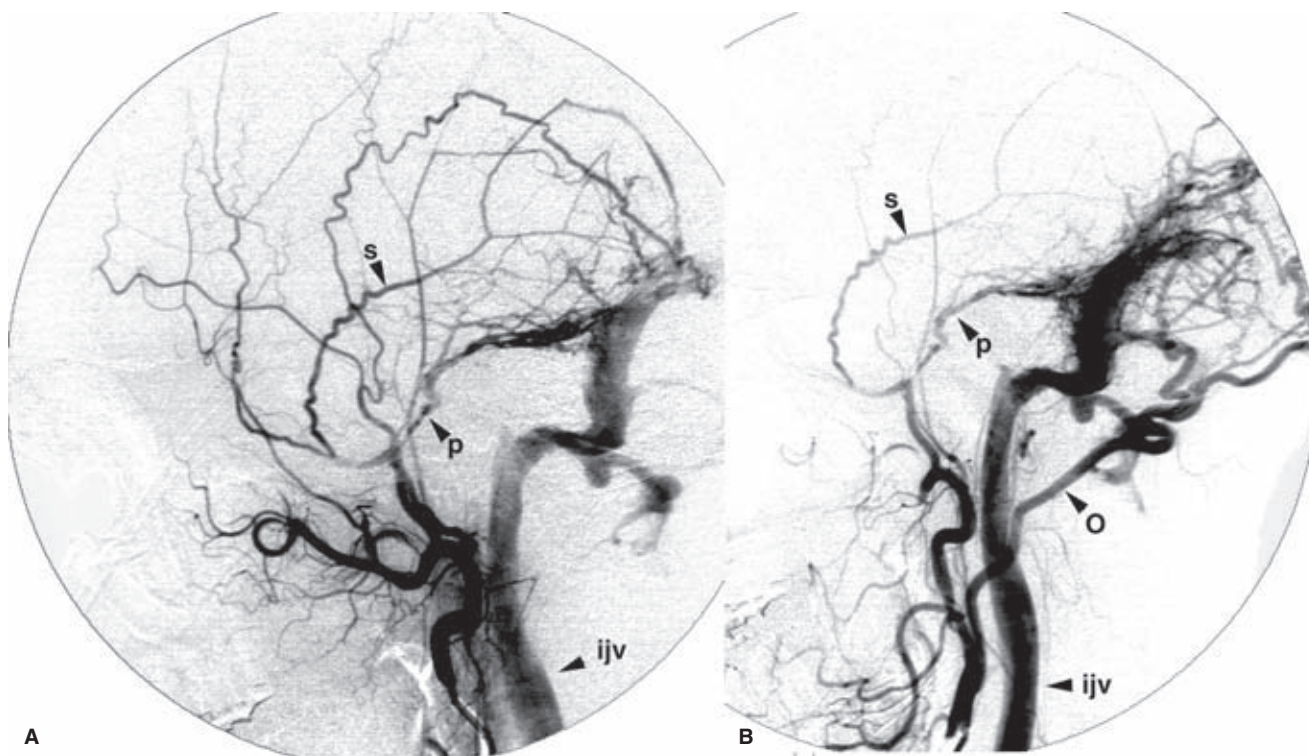


FIGURE 20-8. (A–B) DAVM of the transverse and sigmoid sinuses. **A:** Lateral view of a distal external carotid artery injection. **B:** Lateral view of the proximal external carotid artery. A DAVM in a prolonged segment of the transverse and sigmoid sinuses is opacified by squamous (*s*) and petrosal (*p*) branches of the middle meningeal artery and transosseous branches of the occipital artery (*O*). Flow is antegrade into the internal jugular vein (*ijv*). The transverse sinus is occluded between the DAVM and the torcular.

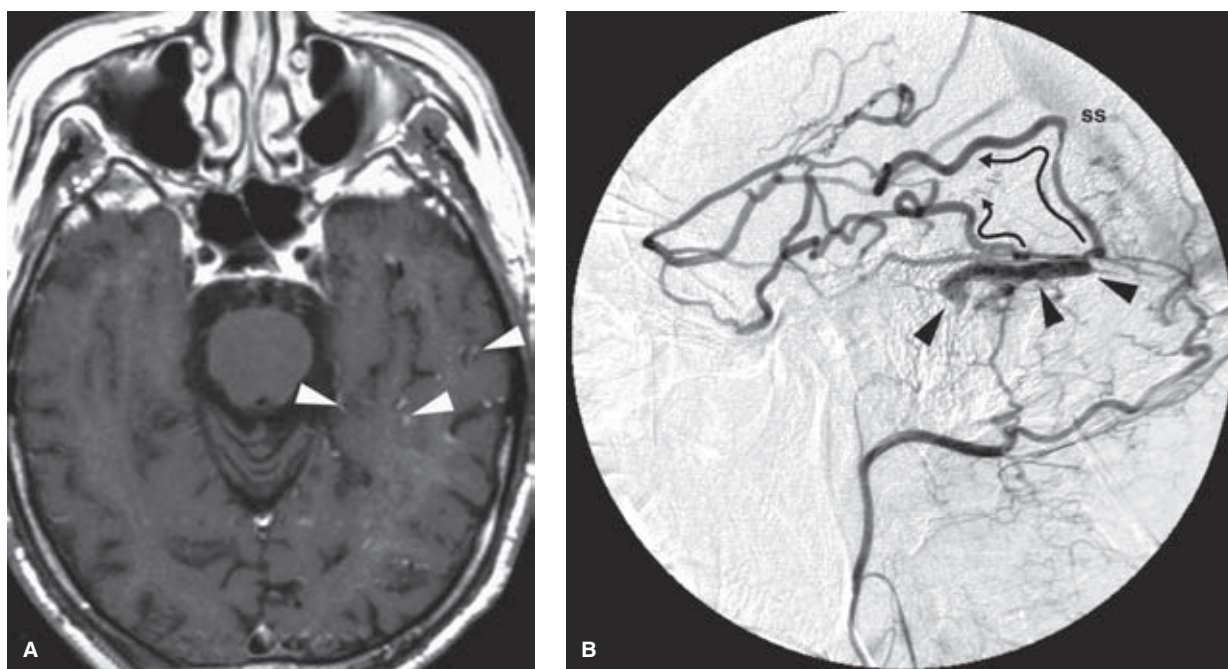


FIGURE 20.9 (A–B) Venous hypertension due to a DAVM. An elderly male presented with sudden loss of consciousness and seizure. A CT scan (not shown) demonstrated a small intraparenchymal bleed of the left occipital lobe. An axial image from a T1-weighted contrast-enhanced MRI sequence (**A**) shows a profusion of enhancing vessel-like structures (*arrowheads*) through the left hemisphere. A DAVM of the left transverse sinus was found by angiography. A lateral view of the left occipital artery injection (**B**) shows that the involved segment of transverse sinus (*arrowheads*) is isolated from the remainder of the sinus. Therefore, this segment of transverse sinus decompresses via cortical veins to the occipital and temporal lobes (*curved arrows* indicating direction of flow). This causes an extreme elevation of venous pressure throughout the left cerebral hemisphere, which resulted in the patient's condition of venous infarction and hemorrhage (*ss*, straight sinus).

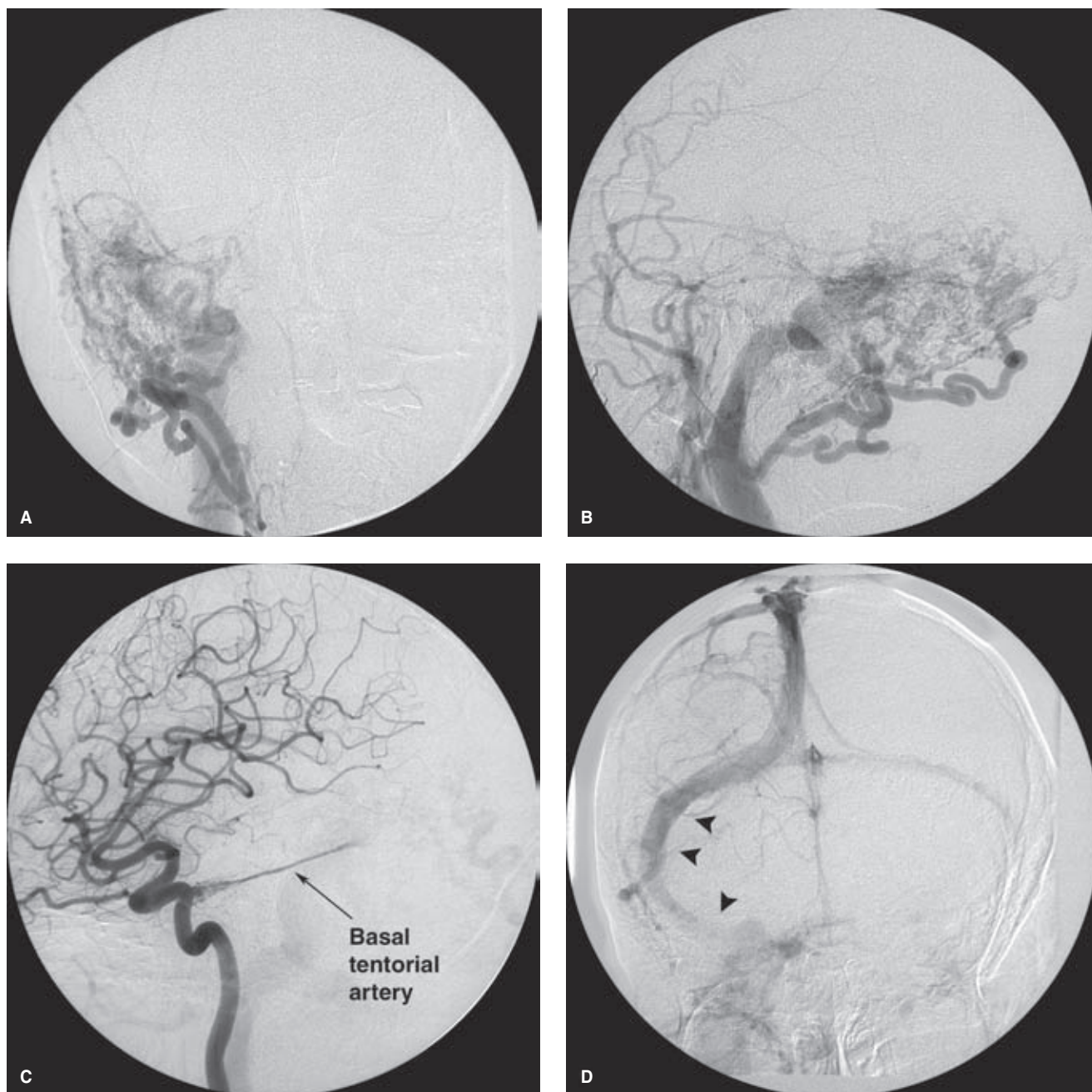


FIGURE 20-10. (A–D) Angiographically uncomplicated DAVM of the right sigmoid sinus. An elderly patient presented with tinnitus behind the right ear. The right external carotid artery AP (A) and lateral (B) views show a rapidly flowing but otherwise uncomplicated angiographic appearance with antegrade flow down the jugular vein. There is no evidence of intracranial venous hypertension. For the reader's interest, an image of the right internal carotid artery injection (C) is provided, showing a nice example of basal tentorial artery from the meningohypophyseal trunk also feeding the malformation. The most important information is provided on the venous-phase AP view of the right ICA injection (D), where the normal brain parenchymal flow is preserved through the disease segment of sinus (*arrowheads*). This implies that a transvenous procedure to occlude this sinus is out of the question.

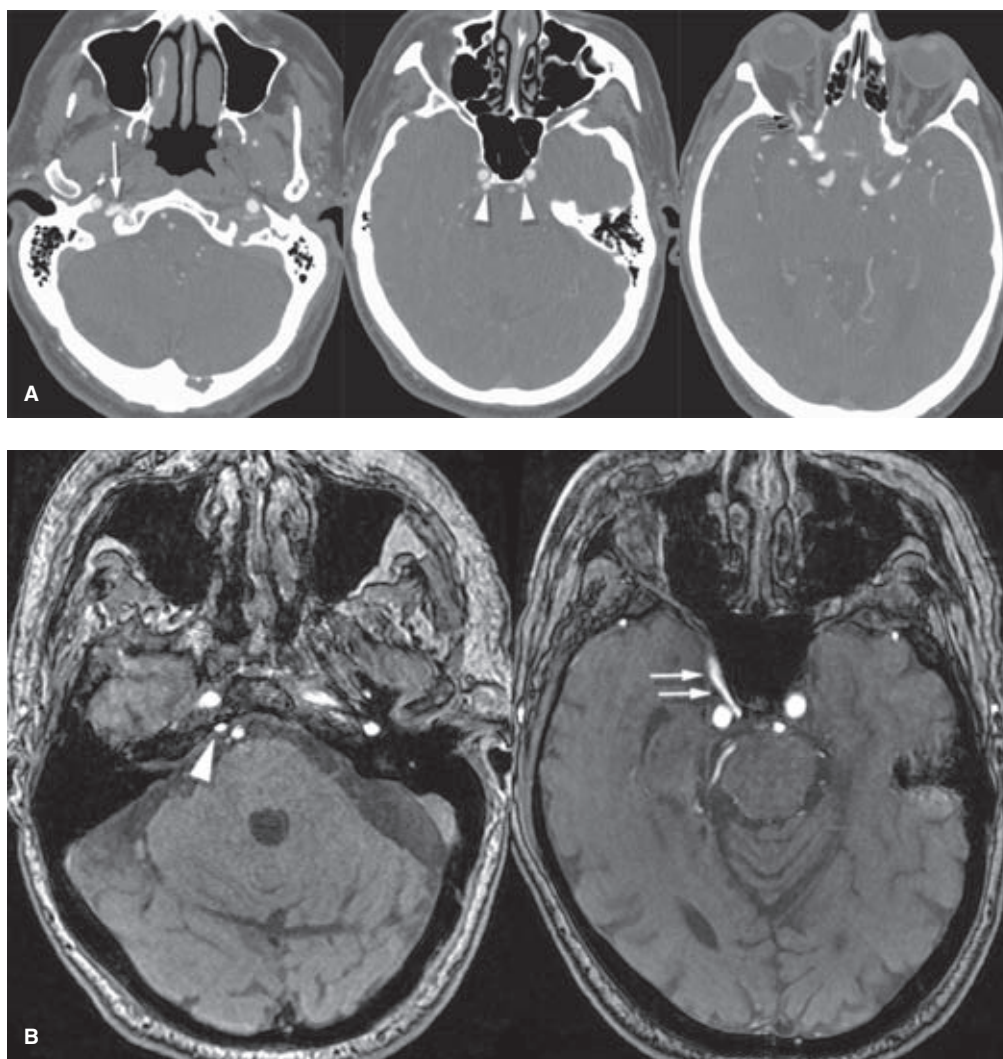


FIGURE 20-11. (A–D) The case of the disappearing DAVM. The initial CTA on this patient (A) demonstrates the reason for his right-sided orbital proptosis and chemosis. An unusual state of venous opacification is seen near the right hypoglossal canal (arrow) with a similar appearance in the inferior petrosal sinuses (arrowheads) and right ophthalmic vein (small double arrows). The exact location of the fistula is unclear from this study, but the TOF MRA with a superior saturation band (B) demonstrates that the flow signal within the right IPS (arrowhead) and right cavernous sinus (double white arrows) is flowing from caudad to craniad, that is, the fistula is not likely to be in the cavernous sinus. The first angiogram (C, right common carotid artery) demonstrated no evidence of a fistula, but the patient happened to mention that his symptoms had started improving a few days before the angiogram, about the time that his Coumadin was discontinued in preparation for the study. His symptoms resumed after the angiogram, a few days after his Coumadin had been restarted. His second angiogram (D, AP view of right ascending pharyngeal artery; E, lateral view) demonstrated that the fistula was related to the neuromeningeal trunk of that vessel, likely the hypoglossal branch with opacification of the predicted structures on the basis of the initial non-invasive images. This case illustrates the potential for spontaneous closure of some DAVMs and an explanation for fluctuation of symptoms in some patients depending on extraneous factors such as anticoagulation. (continued)

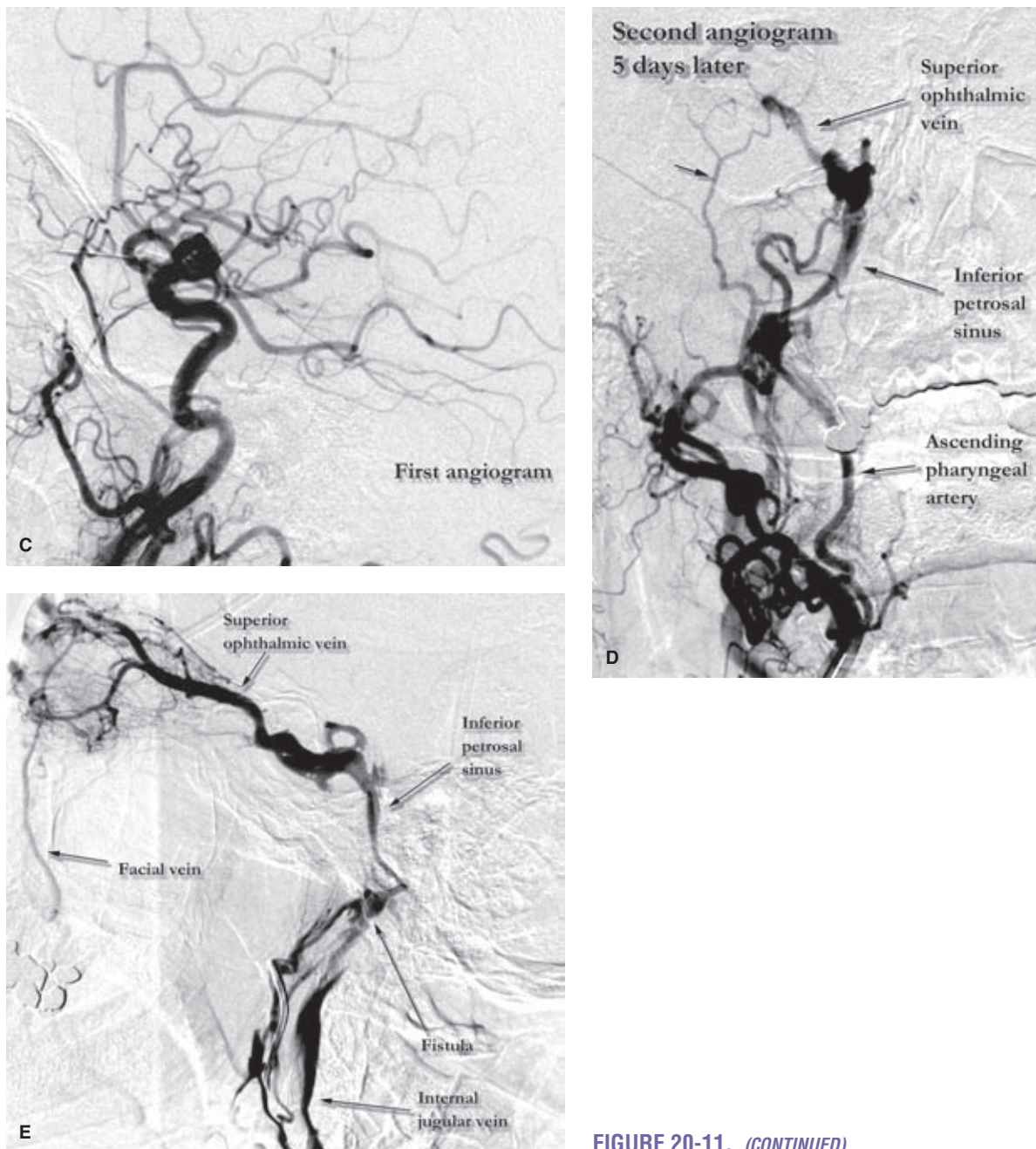


FIGURE 20-11. (CONTINUED)

With increasing venous and sinus hypertension, retrograde flow of contrast from the sinuses into leptomeningeal (cortical) veins becomes evident. With elevation of venous pressure in the cortical veins, new symptoms related to seizure, headache, venous hemorrhage, elevated intracranial pressure, and focal neurologic deficits can emerge. Depending on the venous territory involved, patients may present with focal hemispheric symptoms, motor weakness, and brainstem or cerebellar symptoms. Cranial nerve deficits may also be seen, particularly ophthalmoplegia in the setting of a cavernous sinus DAVM. Interestingly, it is during this stage of diversion of flow away from the sinuses into cortical veins, perhaps with progressive occlusion of the main

sinus, that patients may experience a subjective improvement in tinnitus. Thus, such a report from a patient with a known DAVM is a concern, as it may bode an ominous turn of events. Immediate treatment is indicated when complications appear imminent. Urgent treatment is required also for patients with DAVMs near the cavernous sinus who are developing complications of exophthalmos, secondary glaucoma, or visual deterioration.

The gravest progression of the disease occurs when venous outflow is completely restricted to cortical veins due to complete occlusion of the sinuses. In these instances, the arterial flow may be directed exclusively into the subarachnoid veins or into an isolated segment of sinus that drains only through

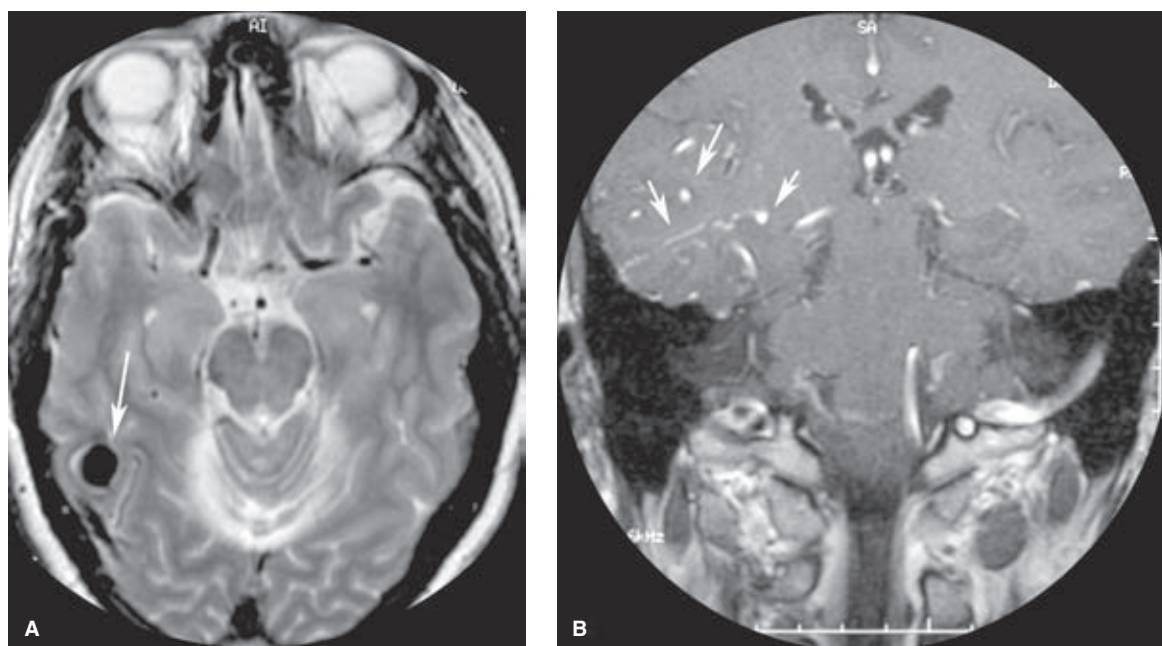


FIGURE 20-12. (A–H) A dural vascular malformation with parenchymal venous hypertension. An elderly patient presented with right hemispheric and subarachnoid hemorrhage. A T2-weighted MRI (A) and contrast-enhanced T1 coronal image (B) show a large aneurysmal flow void within the right temporo-occipital area and distension of intraparenchymal vessels through the region (arrows). A right common carotid arteriogram (C) and right external carotid arteriogram (D) demonstrate that the offending lesion is a DAVM with arterial feeders from the right middle meningeal artery and right occipital artery.

The entire scope of the fistula itself is very small (enclosed by the ring on D), but there is a variceal dilatation of the draining parenchymal veins, including the intraparenchymal venous pseudoaneurysm seen on (A). Later venous-phase images showed extensive venous distension throughout the right hemisphere. The first embolization with 25% n-butyl-cyanoacrylate was done from the right middle meningeal artery (E), but it failed to penetrate the nidus completely. A change in the density of contrast in (E) shows that there is an unseen feeder coming in (from the occipital artery). The postembolization image of the middle meningeal artery looked fine of course but deceptive (F), and because the column of NBCA did not penetrate fully enough to the venous side, flow persisted from the occipital injection (G). Fortunately, a column of NBCA was able to penetrate from the occipital feeder to finish the remaining nidus (H). At follow-up 1 month later, the patient's intraparenchymal pseudoaneurysm had resolved completely with no residuum of the lesion other than some traces of NBCA. (continued)

cortical veins. These patients present with severe neurologic deficits, extensive cortical venous hypertension (Fig. 20-12), venous hemorrhages or infarcts, and hydrocephalus. DAVMs of the anterior cranial fossa or of the tentorium represent a particular risk of sudden massive frontal lobe or subarachnoid hemorrhage, which may be the presenting symptom in more than 70% to 80% of cases (Fig. 20-13) (29–33). DAVMs in the anterior cranial fossa are usually close to the cribriform plate and have a propensity to develop venous aneurysms or varices adjacent to the site of fistulous flow from the ethmoidal branches of the ophthalmic arteries (34,35). Prompt surgical clipping of the DAVM is the treatment of choice for this particular subgroup of patients. Embolization usually is not favored for lesions in this location, given the risks and difficulties involved in catheterization and embolization of ophthalmic artery branches.

The natural history of DAVMs is variable (Fig. 20-14). Certain anatomic locations are typically more likely to develop serious complications. The presence of venous aneurysms at angiography, and a location close to the tentorial incisura, or venous drainage to the galenic system, the superior petrosal sinus, or straight sinus should prompt con-

cern for an unfavorable disease progression (31,36). Patients with these features seem particularly prone to severe neurologic complications and intracranial hemorrhage. The locations of the shunt and the pattern of venous flow have a far greater bearing on the significance of the lesion than the particular arterial feeders involved or the volume of flow.

► TREATMENT OF DURAL ARTERIOVENOUS MALFORMATIONS

The first decision concerning a patient with a DAVM is whether treatment is warranted at all. Some lesions are small or their physiologic profile is benign and inconsequential, the patients are asymptomatic, and therefore, automatic treatment of every lesion is not predetermined. Treatment is, however, warranted for the following circumstances:

- Cerebral complications, including headache, or incipient complications of intracranial venous hypertension (Fig. 20-15);

(text continues on page 336)

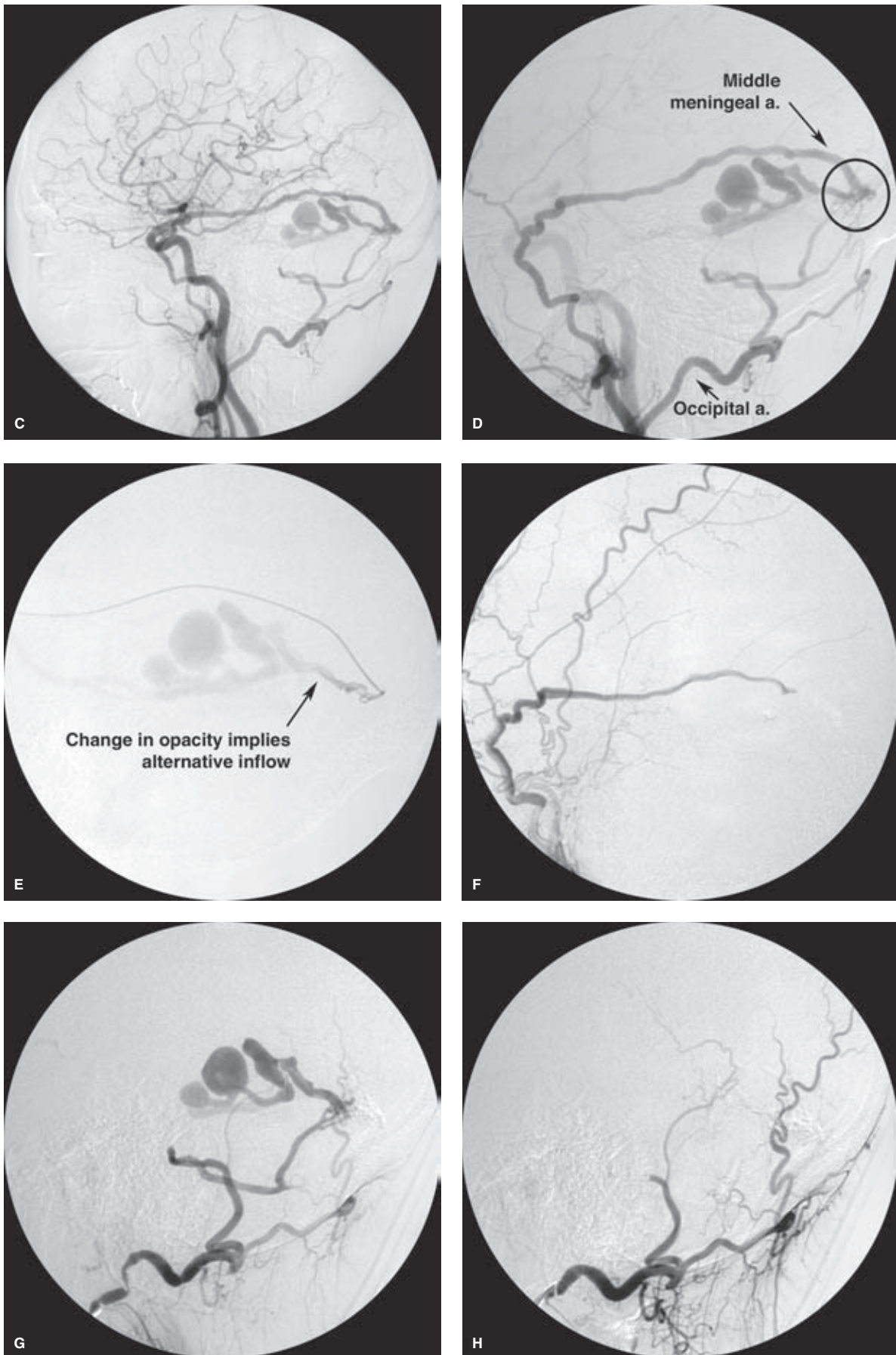


FIGURE 20-12. (CONTINUED)

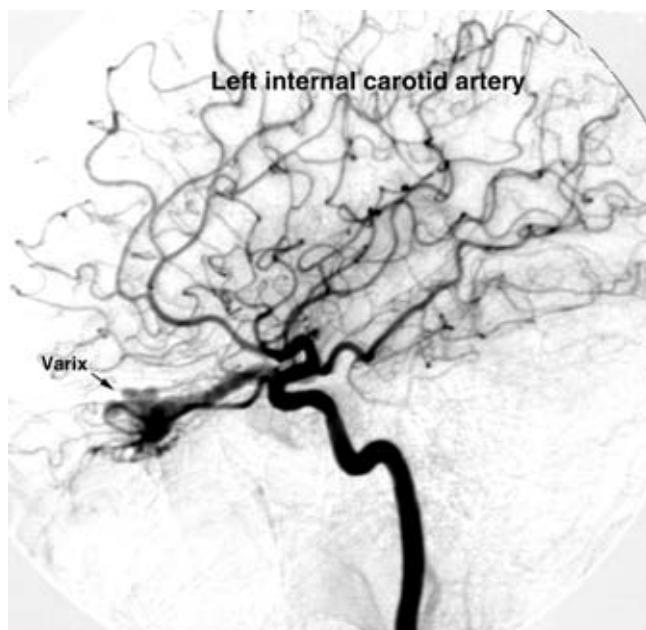


FIGURE 20-13. DAVM of the anterior cranial fossa. A middle-aged patient presented with headaches. A DAVM of the cribriform plate is opacified by ethmoidal branches of the left ophthalmic artery. Venous drainage from this malformation is posteriorly to the lesser wing of the sphenoid bone. In this patient, most of the subsequent drainage was via the cavernous sinuses.

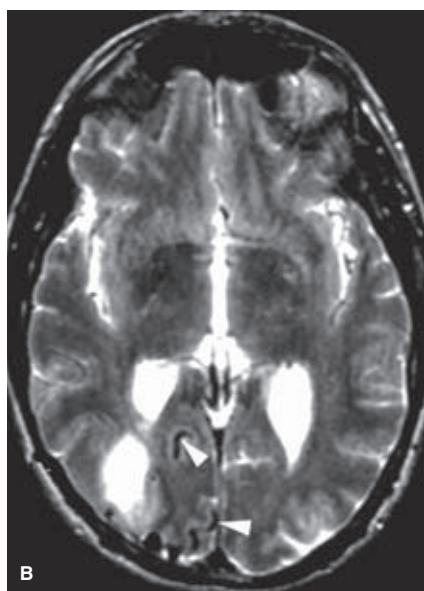
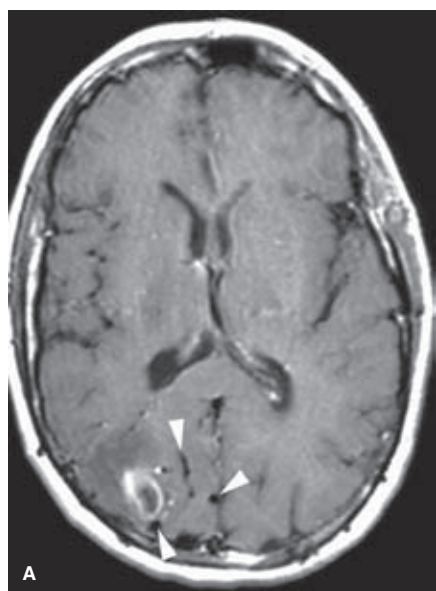
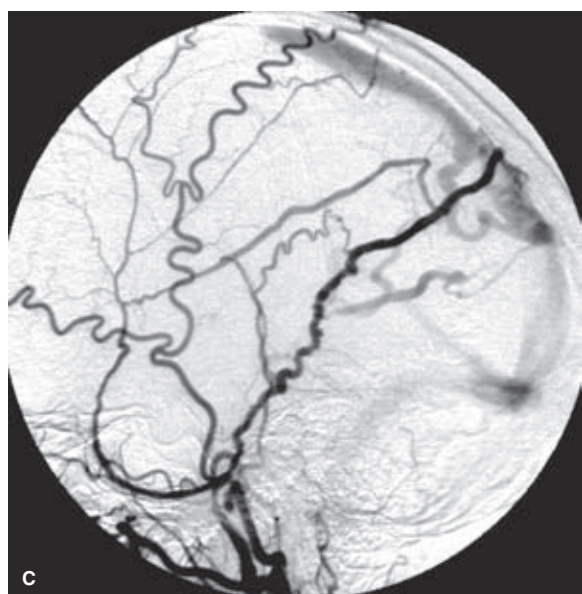


FIGURE 20-14. (A–C) “Collision” DAVM with underlying Glioblastoma Multiforme. A middle-aged patient presented with sudden onset of seizures and headaches. MRI demonstrated a right parieto-occipital parenchymal hematoma with mass effect, edema, and prominent surrounding flow voids (*arrowheads* in **A**, **B**). A diagnosis of a DAVM of the right parasagittal convexity was confirmed with angiography of the external carotid arteries (**C**). Transarterial embolization of the external carotid artery feeders was performed before surgical resection of the DAVM. Unfortunately, the parenchymal signs of complications from the DAVM masked signs that the patient had a coexistent glioblastoma multiforme in the same location. It is intriguing to wonder if the angiogenic factors discussed in Chapter 19 associated with the pathophysiology of GBM were responsible for inducing a secondary adjacent DAVM in this patient.



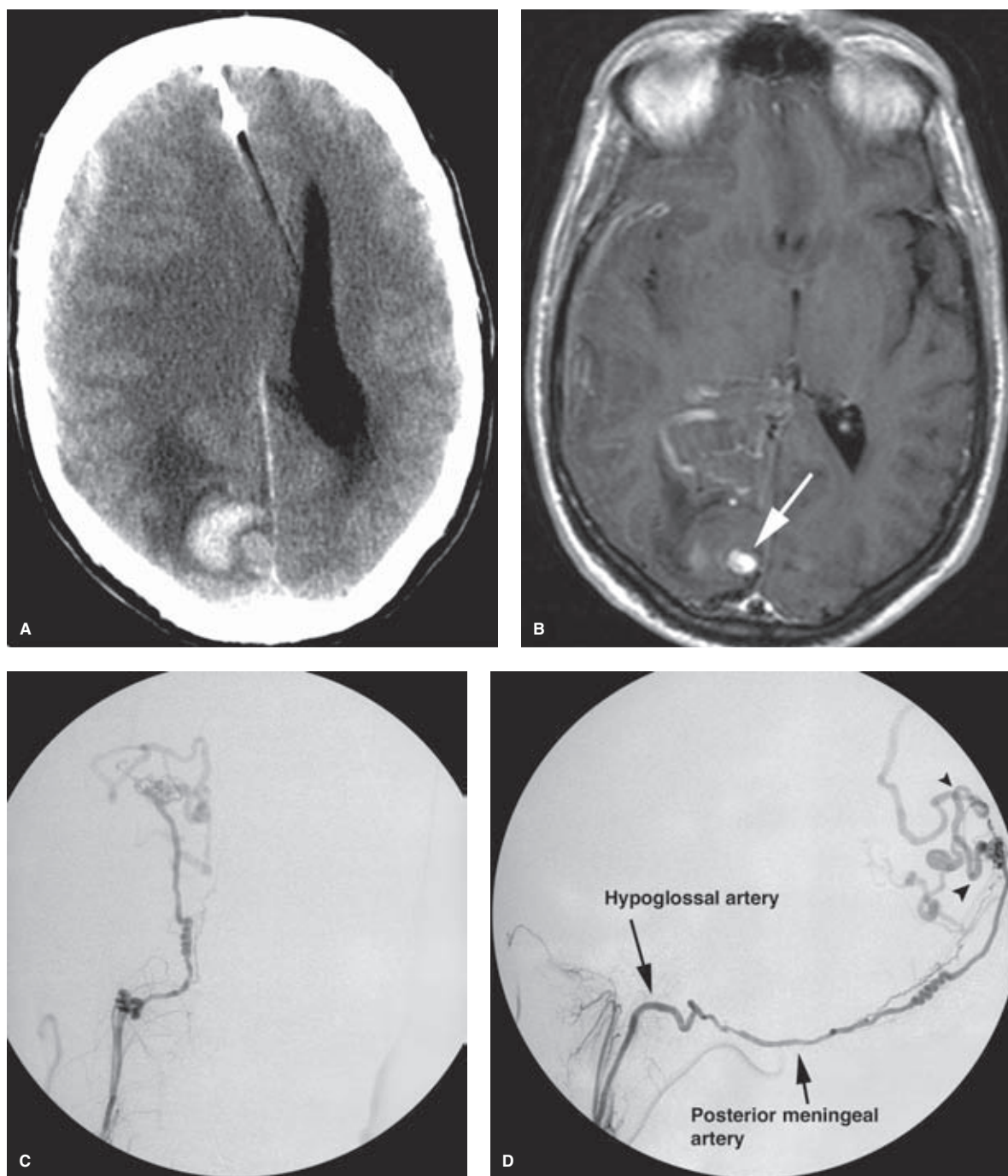


FIGURE 20-15. (A–D) Small dural AVF presenting with massive intracranial complications. This elderly patient presented with abrupt onset of a right intraparenchymal bleed and a large right subdural hematoma, which had to be evacuated emergently, shown on a noncontrast CT (A). A postoperative MRI T1-weighted image with gadolinium shows numerous right occipital enhancing vessels with a large enhancing aneurysmal structure (arrow in B). The eventual diagnosis was nailed down to a tiny (<1 cm²) area of the occipital calvarium, where a dural AVF was deriving supply from the right ascending pharyngeal artery (C, AP view; D, lateral view) via the hypoglossal branch of the neuromeningeal trunk, which in turn became the posterior meningeal artery of the posterior fossa extending to the AVF. From the AVF, two pial veins extend centripetally, causing venous hypertension with a ruptured pseudoaneurysm, explaining the original presentation. An endovascular treatment was attempted, but access along the posterior meningeal artery proved too difficult due to tortuosity not well seen on these images. The patient was successfully treated surgically by disconnection of the AVF from the pial veins.

- Patterns of venous drainage suggesting that progressive involvement of the intracranial venous pattern seems imminent or likely (Figs. 20-16–20-18);
- Elevation of intraocular pressure (Fig. 20-19);
- Proptosis of the orbit;
- For most patients, chemosis of the eye, even though painless, would be a reasonable indication for treatment (Fig. 20-20);
- Intolerable bruit (Fig. 20-21).

Surgical treatment of cranial DAVMs is accomplished by techniques such as clipping of the malformation, surgical isolation (skeletonization) of the involved sinus, or cauterization of involved vessels. For some lesions, such as DAVMs

of the anterior fossa, treatment is exclusively surgical due to the easy accessibility of the ethmoidal vessels by craniotomy. Other DAVMs, particularly of the cavernous, transverse, and sigmoid sinuses, lend themselves exclusively to endovascular treatment (37–40). Sometimes, a combination of surgical and endovascular techniques is necessary (41–44). In recent years, radiation therapy has emerged as an additional modality capable of curing lesions suitable for this method in over 50% of cases (45–48). However, this treatment modality requires 3 to 6 months for the full effect to occur, an option that precludes its use in many patients presenting with acute symptoms.

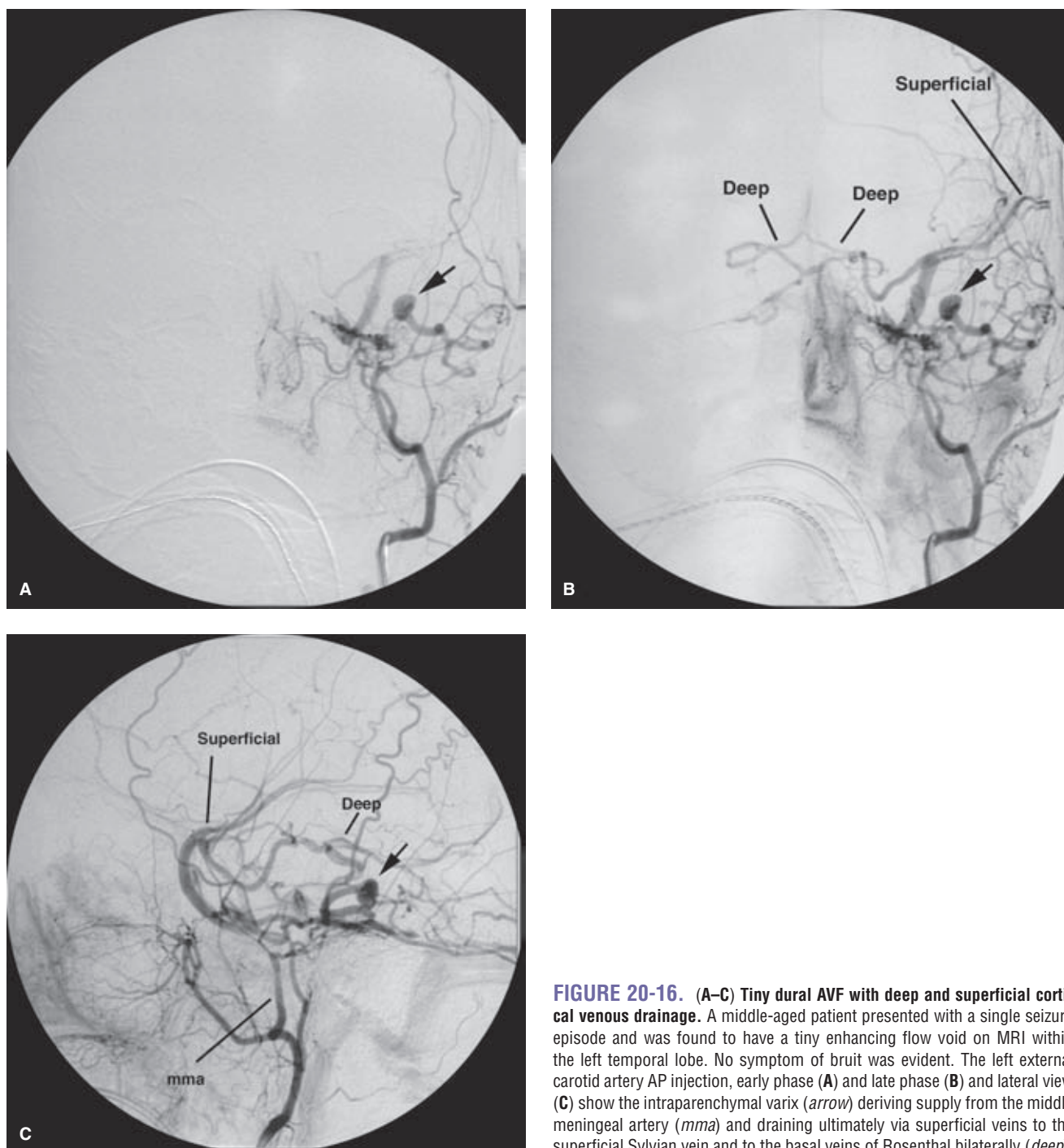


FIGURE 20-16. (A–C) Tiny dural AVF with deep and superficial cortical venous drainage. A middle-aged patient presented with a single seizure episode and was found to have a tiny enhancing flow void on MRI within the left temporal lobe. No symptom of bruit was evident. The left external carotid artery AP injection, early phase (A) and late phase (B) and lateral view (C) show the intraparenchymal varix (arrow) deriving supply from the middle meningeal artery (*mma*) and draining ultimately via superficial veins to the superficial Sylvian vein and to the basal veins of Rosenthal bilaterally (*deep*).

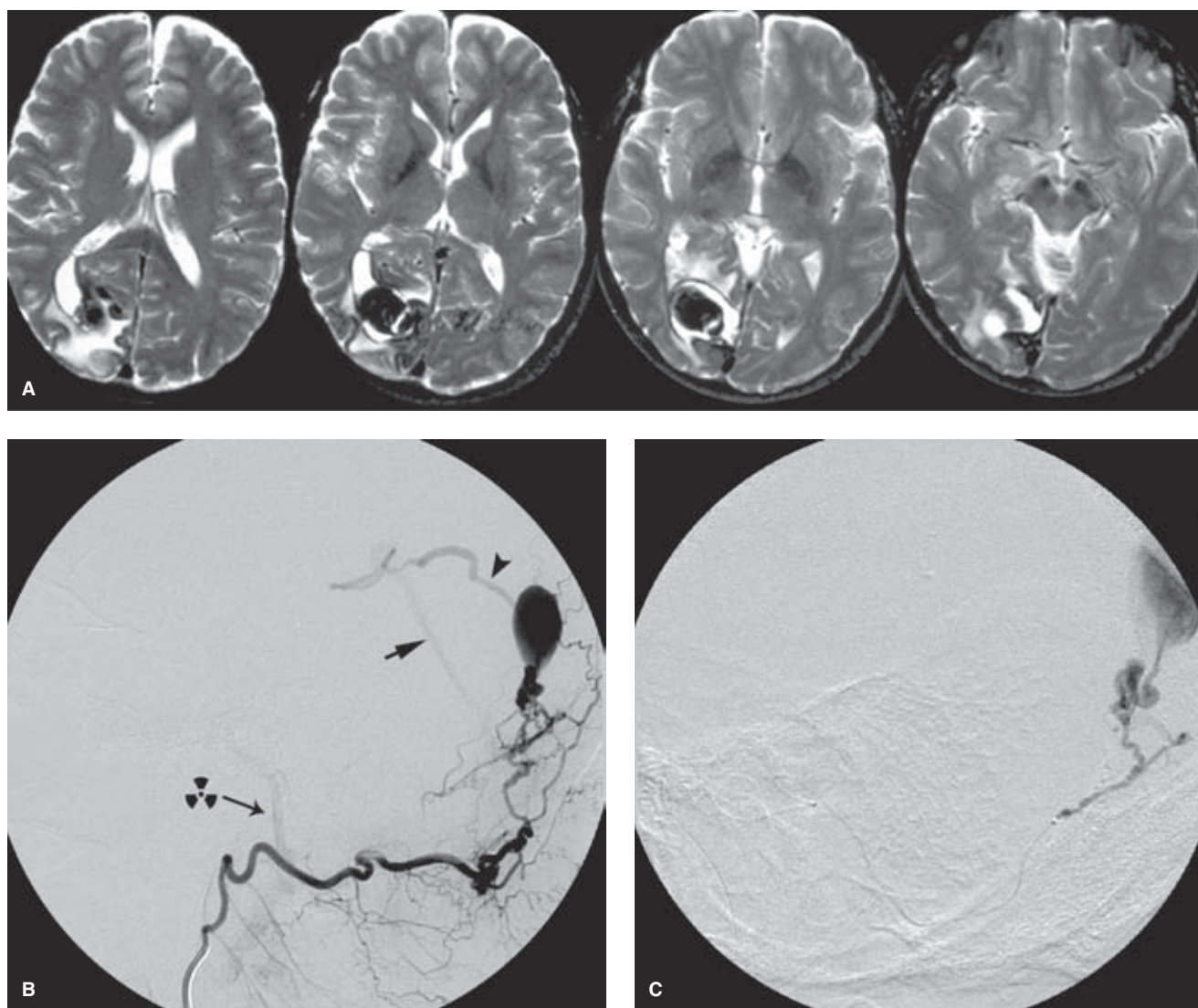


FIGURE 20-17. (A–C) Dural AVF mimicking the appearance and clinical presentation of a pial arteriovenous malformation. This middle-aged male patient suffered several hemorrhages of the right occipital lobe over several years before agreeing to endovascular treatment. The T2-weighted MRI (A) shows a profusion of abnormal flow voids, gliosis, and evidence of previous hemorrhage in the right occipital lobe. Note the pulsation artifact in the phase-encoding direction from the dominant intralobar varix. The right occipital artery injection (B) shows the dural AVF to be situated along the posterior tentorium with venous drainage to the right occipital parenchymal veins, including the dominant varix seen on the MRI. A single draining vein (arrowhead) connects the abnormal venous field with the straight sinus (arrow). Notice the transient opacification of the basilar artery (nuclear danger sign) from the occipital artery, a reminder of importance of potential dangerous anastomoses during embolizations. An NBCA embolization from the occipital artery was only partially successful, but the lesion was finished off with a distal NBCA embolization from a dural branch of the right anterior inferior cerebellar artery (C, microcatheter injection showing persistent AVF opacification prior to final embolization with 17% NBCA via a Spinnaker Elite microcatheter).

Prior to the advent of Onyx, the endovascular treatment of DAVMs relied most heavily on transvenous obliteration of the venous side of the malformation with thrombogenic coils (Figs. 20-22 and 20-23), liquid NBCA, or balloons. Transarterial treatment was difficult, hazardous, or ineffective with transarterial NBCA, alcohol, particles, or coils. Transarterial Onyx has altered the field dramatically allowing successful transarterial treatment of lesions which might have been previously inaccessible or untreatable (14,15,36,49,50). Transarterial Onyx has become the primary modality for endovascular therapy at many centers (51), primarily because it allows a prolonged, somewhat controlled penetration of the entire arte-

rial rete extending to a DAVM and, most importantly from the point of view of a permanent cure, penetration and obliteration of the venous side of the fistula while preserving normal venous parenchymal drainage.

Generally speaking, DAVMs in which the venous sinus system remains patent will have the predominant component of venous flow through that sinus, meaning that the grade of the lesion on the Cognard or Borden classification schemes will be relatively mild and that the sinus will be accessible for retrograde venous access and transvenous occlusion with coils or Onyx. Milder or lower grade DAVMs have, therefore, a high rate of cure (>70%) on the initial endovascular

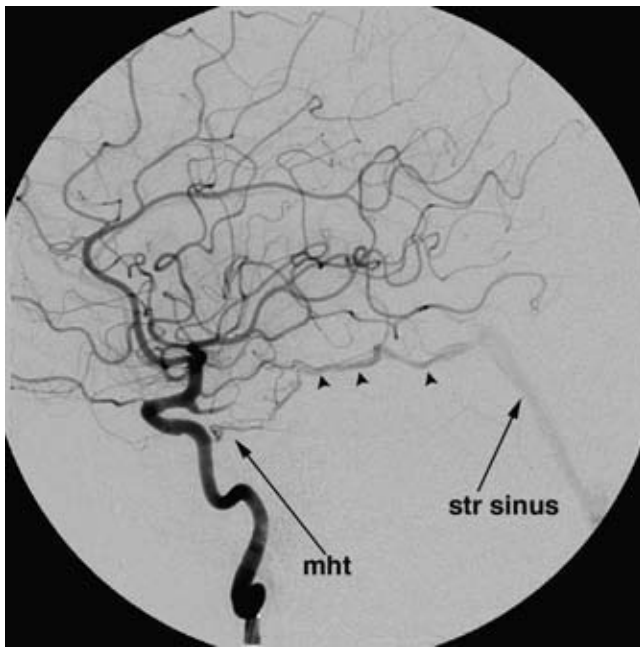


FIGURE 20-18. Tiny AVF from the meningo-hypophyseal trunk. This selective internal carotid injection shows a tiny fistula from the meningo-hypophyseal trunk (*mht*) with opacification of the basal vein of Rosenthal (*arrowheads*) and subsequently the straight sinus (*labeled*). Although this is a tiny lesion and its volume of flow is negligible, the impact on the deep venous system is potentially serious.

attempt (52–54). For higher-grade lesions where the native venous drainage has become occluded or stenotic, retrograde venous access is by definition hampered, and cure rates in these lesions have always been lower. In particular, the risks of transarterial embolization in the region of the cavernous sinus have limited the options for treatment.

However, transarterial embolization with Onyx in safe locations and transvenous embolization with Onyx in locations where coils are suboptimal such as a multicompartamental cavernous sinus, have significantly improved the outcome of embolization for many patients (52,55).

(text continues on page 342)

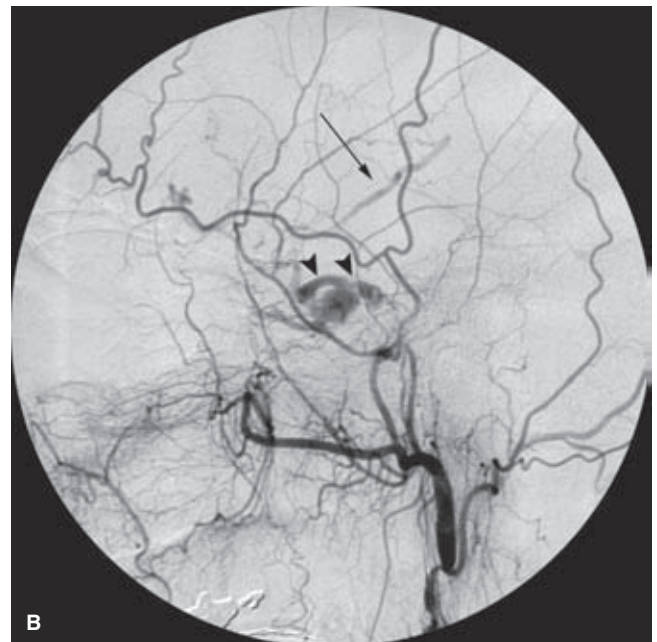
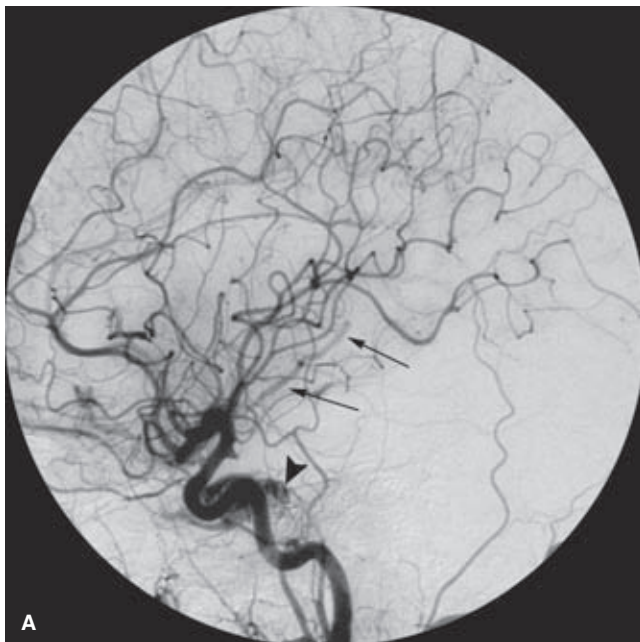


FIGURE 20-19. (A–B) Deep venous drainage can be subtle to identify. This middle-aged female was referred reluctantly by her ophthalmologist, on the recommendation of the consulting neurosurgeon, for cerebral angiography for evaluation of a chemotic left eye. The early-phase lateral projection of the left common carotid artery (**A**) shows dense opacification of the left cavernous sinus (*arrowhead*), confirming the diagnosis of a small, low-flow dural AVF of the left cavernous sinus region. However, the important finding is an abnormal venous structure, a deep vein (*arrows*) filling during the arterial phase of the injection. The late-phase lateral projection of the left external carotid artery injection (**B**) shows the same findings to better advantage, indicating that although the patient's eye symptoms are minimal, the implications of the angiogram are potentially serious.

FIGURE 20-20. Chemotic injected eye from a dural AVF of the cavernous sinus. Orbital venous hypertension looks painful but is not so. However, the critical finding is whether the intraocular pressure is elevated, indicating a greater need for treatment. Patients do not like to have a look of permanently blood-shot eyes and usually opt for treatment.

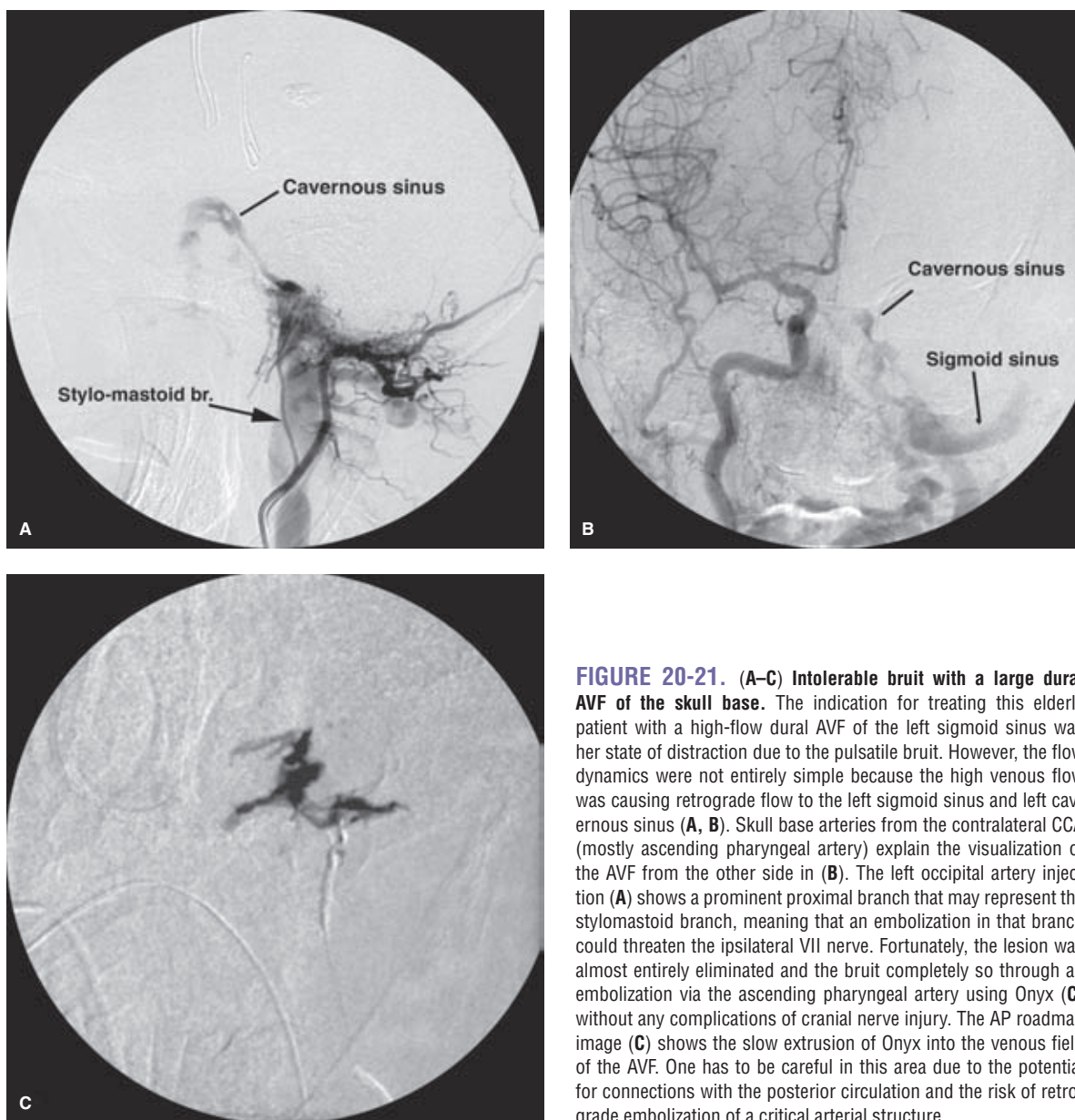


FIGURE 20-21. (A–C) Intolerable bruit with a large dural AVF of the skull base. The indication for treating this elderly patient with a high-flow dural AVF of the left sigmoid sinus was her state of distraction due to the pulsatile bruit. However, the flow dynamics were not entirely simple because the high venous flow was causing retrograde flow to the left sigmoid sinus and left cavernous sinus (A, B). Skull base arteries from the contralateral CCA (mostly ascending pharyngeal artery) explain the visualization of the AVF from the other side in (B). The left occipital artery injection (A) shows a prominent proximal branch that may represent the stylomastoid branch, meaning that an embolization in that branch could threaten the ipsilateral VII nerve. Fortunately, the lesion was almost entirely eliminated and the bruit completely so through an embolization via the ascending pharyngeal artery using Onyx (C) without any complications of cranial nerve injury. The AP roadmap image (C) shows the slow extrusion of Onyx into the venous field of the AVF. One has to be careful in this area due to the potential for connections with the posterior circulation and the risk of retrograde embolization of a critical arterial structure.

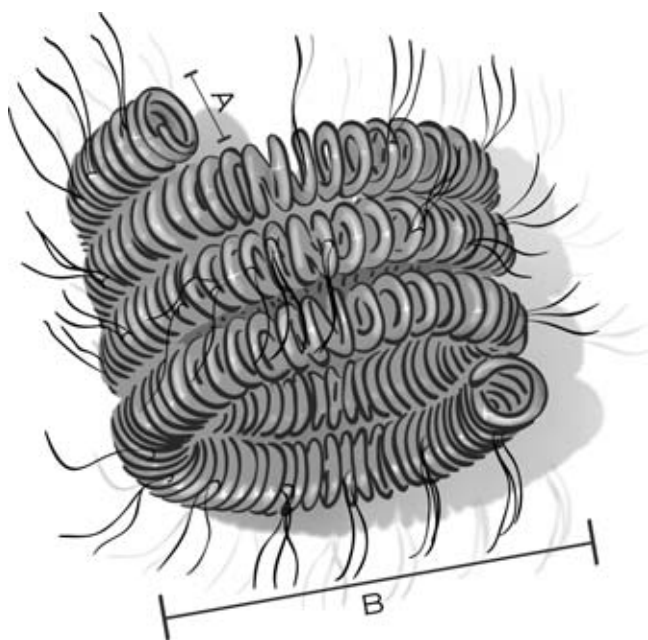


FIGURE 20-22. Fibred push coils. Push coils rendered more thrombogenic by virtue of the addition of Dacron fibers are generally of a more robust and stiffer construction than those intended for aneurysm embolization. Diameter (**A**) determines the necessary lumen of the microcatheter for use with these coils. Generally, for the larger diameter and longer coils, a larger lumen microcatheter, such as a Renegade or Rapid Transit, is necessary. Diameter (**B**) is the diameter of the reconfigured coil within the vessel. Obviously, a coil that is too small will be loose and unstable, whereas a large coil will not curl within the vessel and will tend to back the microcatheter out.

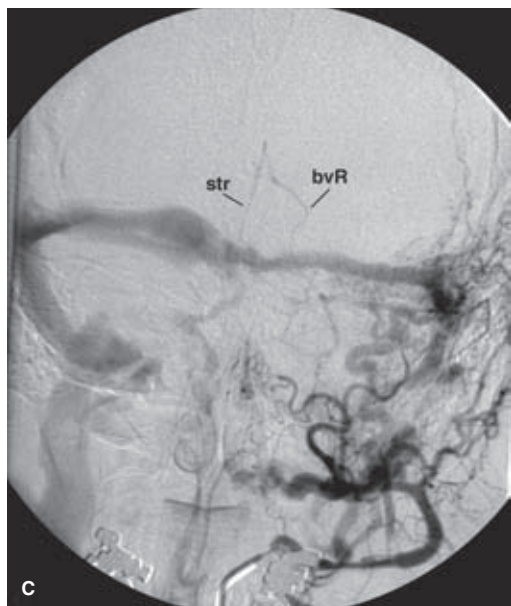
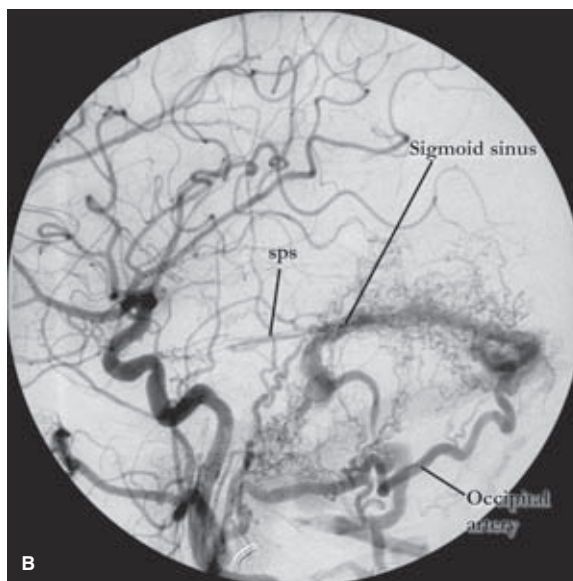
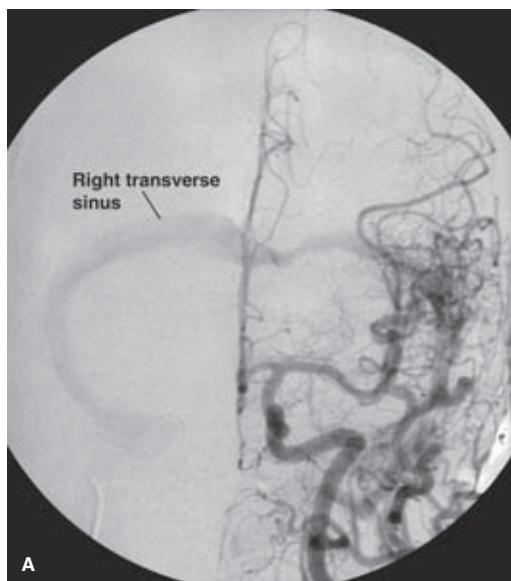


FIGURE 20-23. Transvenous coil embolization of a DAVM. A late-middle-aged female patient presents with a loud pulsatile bruit behind the left ear for over a year. The symptom is causing her mild distress, but she believes that she can live with the noise, provided that the lesion is of no serious implication.

The left common carotid artery (**A, B**) and left external carotid artery (**C**) injections demonstrate the expected findings of a DAVM of the left transverse sinus. The malformation is supplied on the arterial side by a profusion of branches from the left external carotid artery and dural branches of the left internal carotid artery. The important information concerning DAVMs is usually on the venous side. In this instance, there is occlusion of the left jugular bulb with retrograde venous flow from the left sigmoid and transverse sinuses via the torcular to the right side. However, the pivotal information is that there is already establishment of venous drainage to the deep venous system with opacification of the ipsilateral superior petrosal sinus (*sps*) and thence drainage to the basal vein of Rosenthal (*bvR*) and straight sinus (*str*). This changes the classification of this malformation to a more sinister category with the potential for development of deep venous hypertension, venous infarction, and venous hemorrhage. (*continued*)

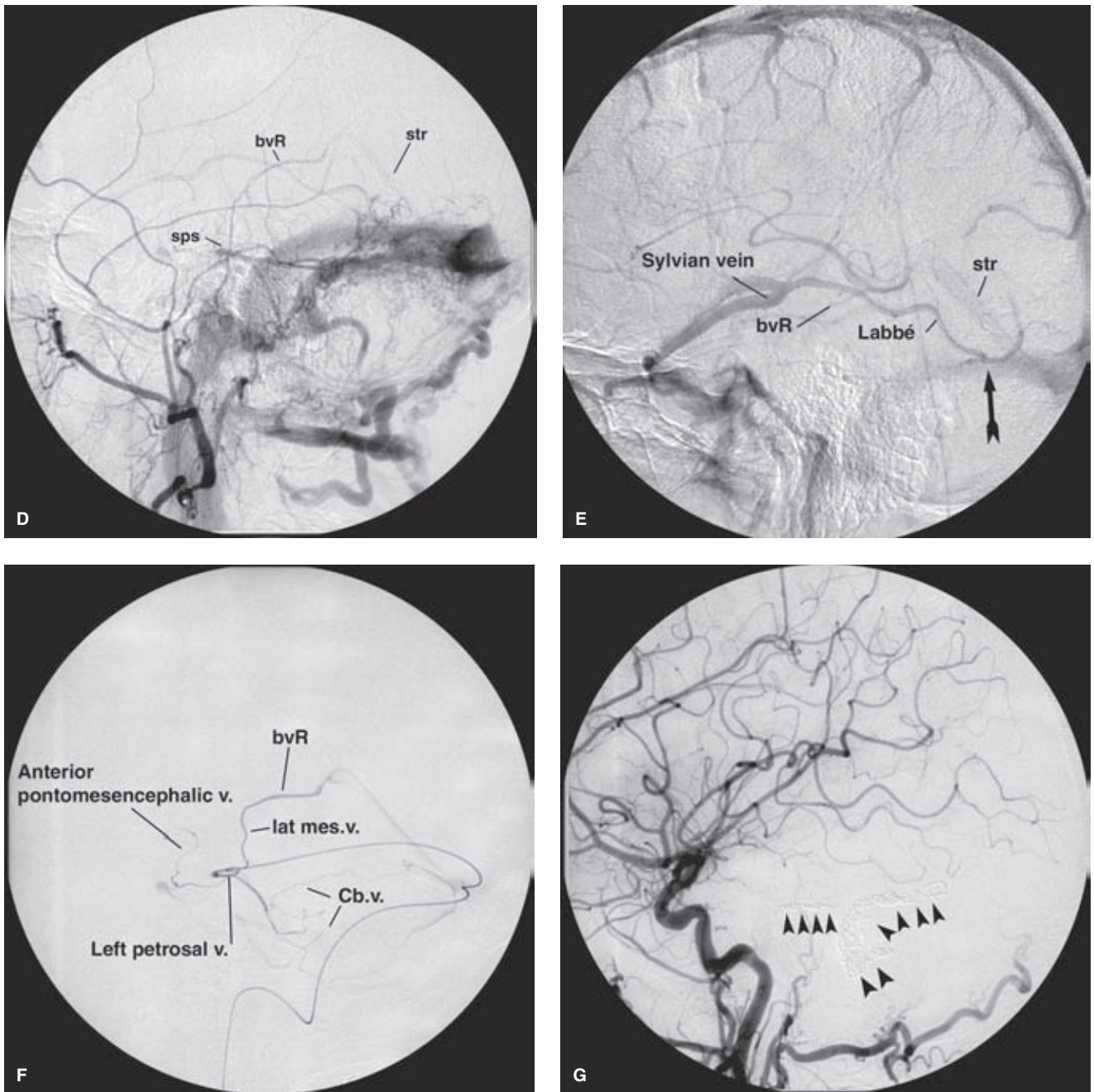


FIGURE 20-23. (CONTINUED) The endovascular treatment for this patient was a transvenous occlusion of the venous side of the malformation using fibered thrombogenic coils. During transvenous embolization of this type of lesion, several particular risks must be avoided. The classic peril of a transvenous embolization in this location is inadvertent occlusion of the ipsilateral vein of Labbé, precipitating venous infarction of the ipsilateral cerebral hemisphere. Therefore, the location of the vein of Labbé must be studied in advance with skewed lateral views of the transverse sinuses (the better to discern left from right) and a transvenous embolization of a diseased segment of sinus must leave the status of the vein of Labbé intact and undisturbed (E). A microcatheter injection (F, lateral view) into the left superior petrosal sinus illustrates the venous connections already mentioned, with additional opacification of the anterior pontomesencephalic vein, the cerebellar veins (*Cb.v.*) and the lateral mesencephalic vein (*lat mes.v.* in F lateral view, venous phase). The final lateral common carotid artery injection (G, lateral view) shows complete elimination of the malformation with coils (*arrowheads*) in the superior petrosal sinus and sigmoid sinus anterior to the point of insertion of the vein of Labbé.

For lesions in the cavernous sinus, much of the frustration and technical difficulties with the cases relates to access. Ideally, successful treatment consists of retrograde cannulation of the ipsilateral inferior petrosal sinus (IPS), navigation through the cavernous sinus to its junction with the ipsilateral superior ophthalmic vein (SOV), and obliteration of the sinus by an anterior-to-posterior packing of the cavernous sinus with fibered coils (Fig. 20-24). However, matters are this simple only in a minority of cases, and the following technical caveats and modifications are frequently encountered:

1. The ipsilateral IPS can be absent or difficult to cannulate. This is a frequent obstacle because if the patient had

a large, promptly draining IPS, the pressure in the cavernous sinus would not have been transmitted to the eye and the patient would not be having obvious symptoms, or so one is sometimes tempted to think. This observation may be also due to the pathogenesis of the DAVM itself, affecting the IPS through thrombosis and the subsequent processes that caused the DAVM to arise in the cavernous sinus. In these cases, it is still often possible to get through the diseased or thrombosed IPS with a microwire, but one has to be careful not to try too hard. Potential complications include injuring the ipsilateral VI nerve in the Dorelo canal, perforation of the adjacent petrosal or posterior fossa veins, or dural injury.

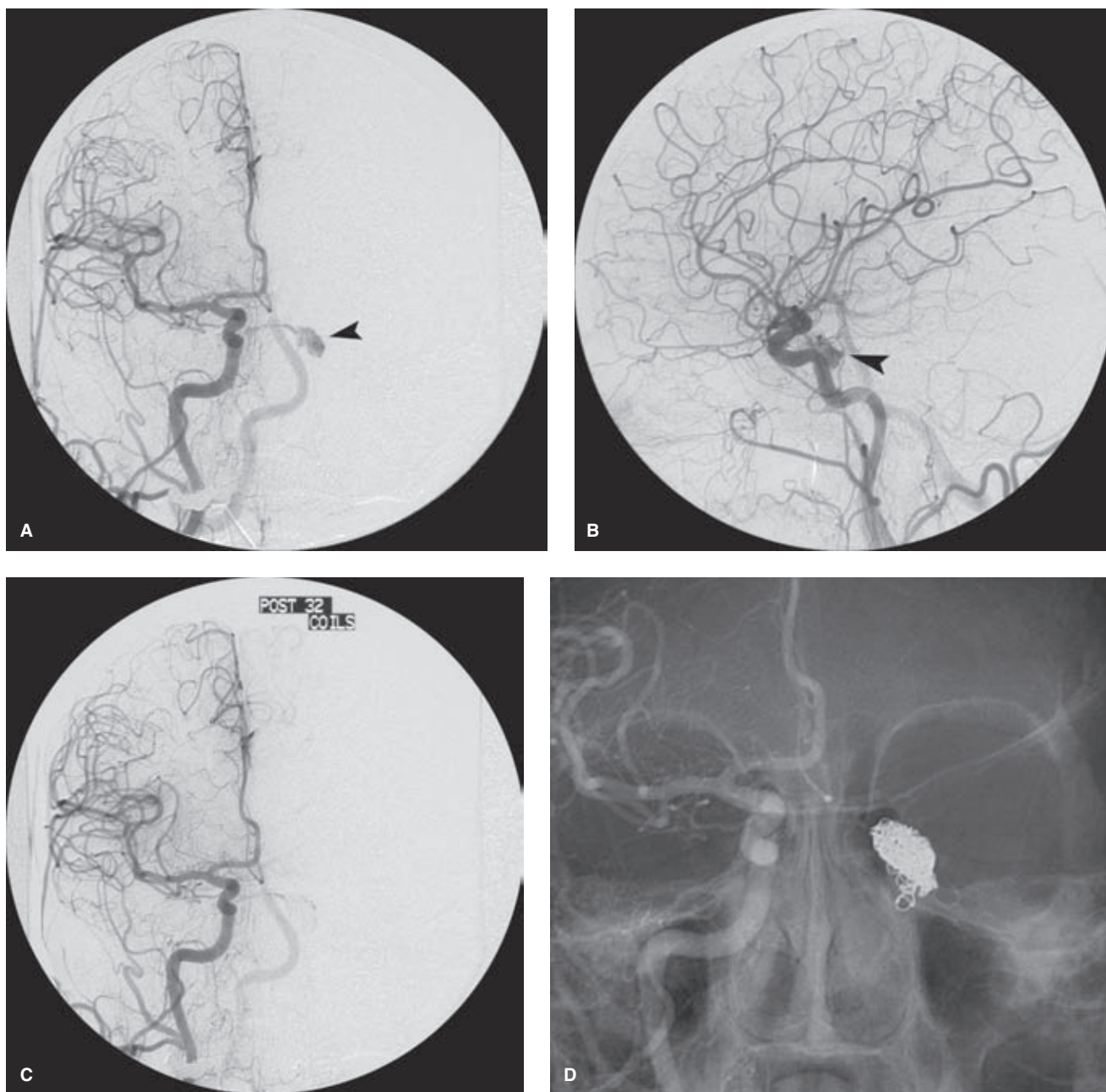


FIGURE 20-24. (A–D) “Simple” dural AVF of the left cavernous sinus. This relatively straightforward lesion—from the point of view of treatment—was unusual nonetheless in that the entire supply to the left-sided lesion was from the contralateral internal carotid artery (A). The left cavernous sinus was filling slowly (arrowheads in A, B) and although an IPS could not be seen, retrograde access from the jugular bulb was gained with a Renegade microcatheter. A series of coils was deposited tightly in the left cavernous sinus (C, D) with complete elimination of the lesion and of the patient’s ocular symptoms.

2. The compartmented nature of the cavernous sinus may prevent one from gaining access from the posterior compartments to the anterior. Again, trying too hard in this situation can be fraught with risk. The adjacent cranial nerves III, IV, and VI are prone to injury through device-related trauma. The ipsilateral internal carotid artery is running through the cavernous sinus and could be injured by injudicious wire manipulation or misadventure.
3. The packing of the cavernous sinus with fibered coils can be done in a manner that can inadvertently aggravate the patient's symptoms or provoke complications. If the coils are deposited in a manner that leaves the arteriovenous shunt intact but with venous access to a critical vein, previously negligible or nonflowing communications can open up, and venous diversion to the uncal veins (Fig. 20-25) or intensification of pressure in the SOV can result. Studying the anatomy of the cavernous sinus with microcatheter injections before starting the coil insertion to identify such dangers and obtaining a tightly occlusive packing are therefore very important.
4. Ipsilateral IPS access is sometimes impossible, and options then include ipsilateral superior petrosal sinus

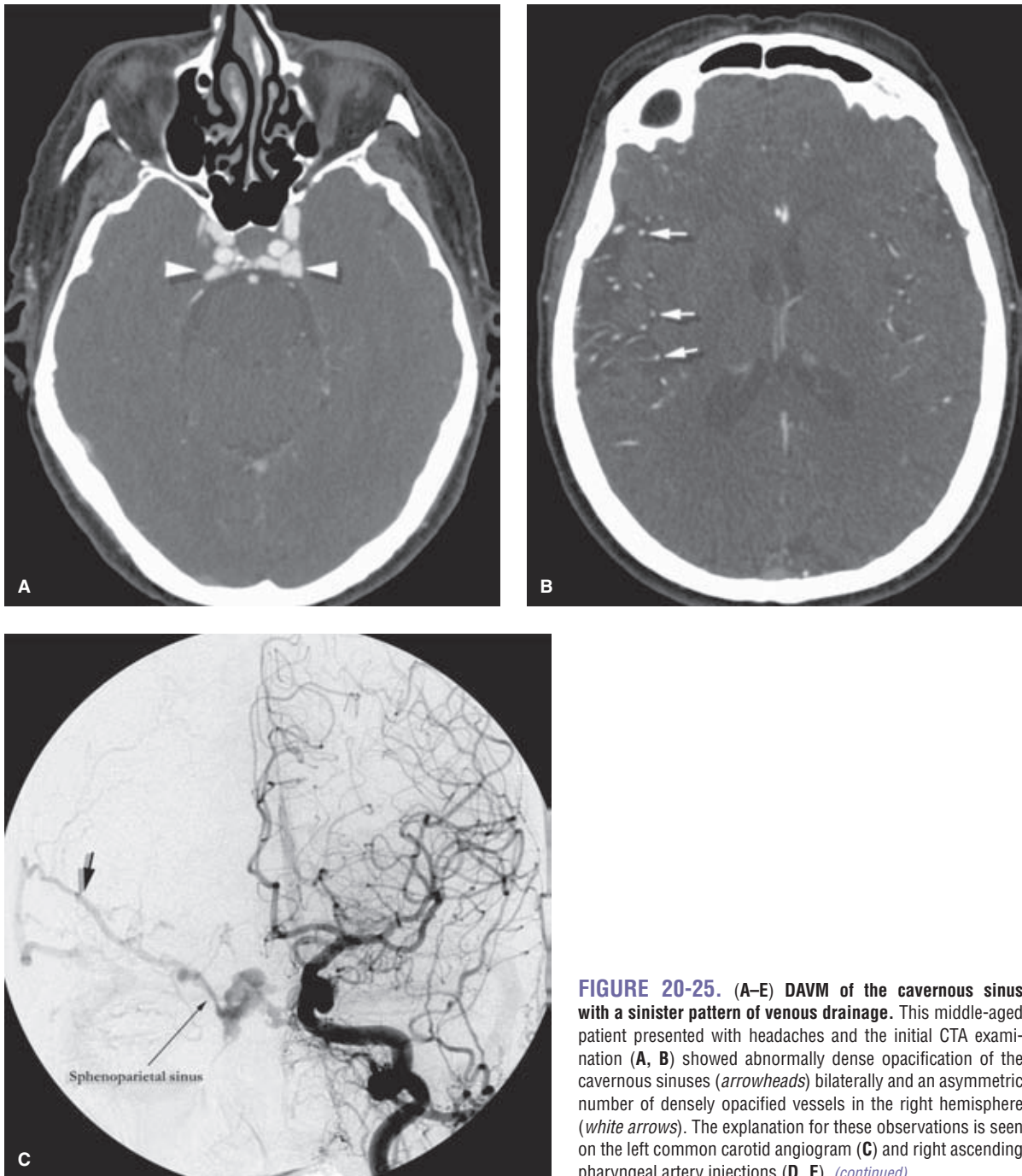


FIGURE 20-25. (A–E) DAVM of the cavernous sinus with a sinister pattern of venous drainage. This middle-aged patient presented with headaches and the initial CTA examination (A, B) showed abnormally dense opacification of the cavernous sinuses (*arrowheads*) bilaterally and an asymmetric number of densely opacified vessels in the right hemisphere (*white arrows*). The explanation for these observations is seen on the left common carotid angiogram (C) and right ascending pharyngeal artery injections (D, E). (*continued*)

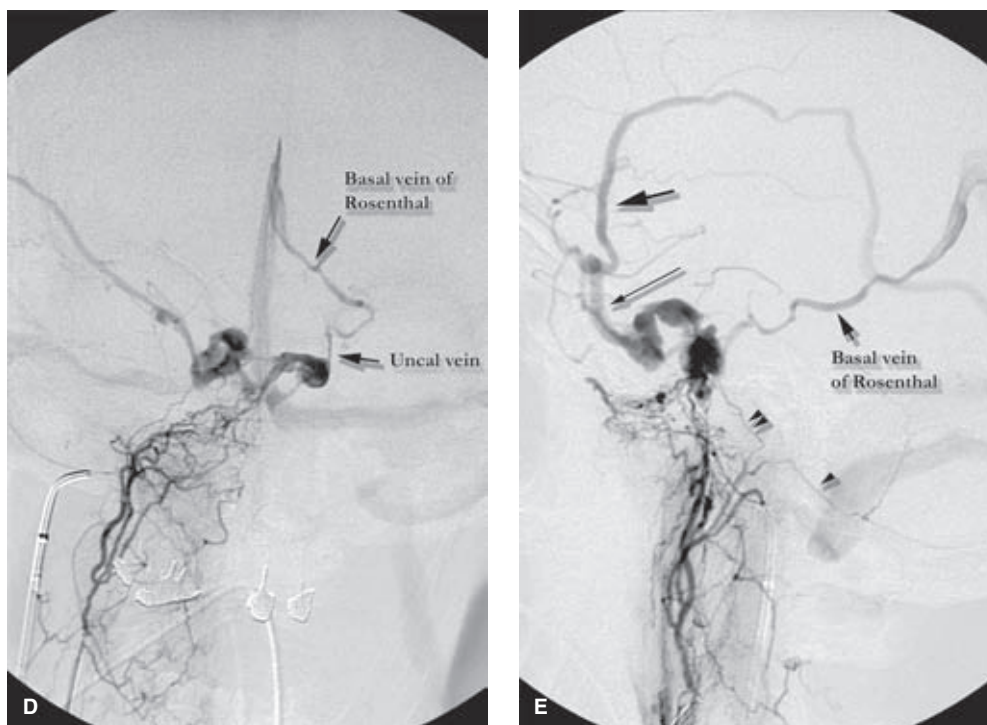


FIGURE 20-25. (CONTINUED) The malformation is bilateral, but predominantly left sided. Nevertheless, most of the drainage is via the right cavernous sinus to the sphenoparietal sinus and right Sylvian veins (*arrows*). Left-sided drainage is even more concerning via the left uncal vein to the basal vein of Rosenthal. Clival branches (*double arrowheads*) and the posterior meningeal artery (*single arrowhead*) filling from the ascending pharyngeal artery are labeled for clarity. A transvenous catheter is also present in the right jugular bulb in anticipation of transvenous treatment.

access and the contralateral IPS with crossing of the midline at the level of the pituitary gland or along a clival vein. Access via the ipsilateral SOV via the facial vein, either from a direct stick of the facial vein or via a transfemoral approach is sometimes possible but is frequently confounded by the restriction of the venous anastomoses between the SOV and the angular vein through the orbital septum (Figs. 20-26 and 20-27). (By a similar logic to that mentioned above, if the patient had prompt venous connections, the intraorbital pressure would not be nearly so high and would possibly not require treatment). When the facial vein approach fails, direct exposure of the SOV with retrograde cannulation to the cavernous sinus works very well but requires a very competent orbital surgeon for collaboration (56) (Fig. 20-28). Direct exposure and needle puncture of the cavernous sinus or the sphenoparietal sinus at craniotomy may sometimes be necessary in extreme cases.

DAVMs of the transverse sinus can be very difficult to treat (13). Overly or necessarily aggressive use of NBCA or Onyx via a transarterial route runs the risk of lower cranial nerve injury (Fig. 20-29), such as ipsilateral VII nerve injury in the stylomastoid canal or brainstem injury (53,57). Transvenous embolization of the fistula can sometimes be accomplished when one is fortunate enough to catheterize retrogradely a venous tributary of the sinus and find that this single channel is the final common pathway for the fistula. Frequently, however, one is left with the dilemma of deciding between some sort of palliative or partial procedure and a transvenous occlusion of the diseased segment of sinus with

coils. The latter is an easy decision when the state of venous flow is so advanced that the diseased sinus is no longer being used for normal parenchymal brain drainage. One can obliterate it with impunity, taking care not to obliterate an antegradely flowing vein of Labbé or other parenchymal vein (Fig. 20-30). When the diseased sinus is flowing antegrade, *(text continues on page 349)*

TABLE 20-1 Categorization Schemes for Dural Arteriovenous Malformations

TYPE	VENOUS DRAINAGE PATTERN
Borden Classification of Dural AVMs (15)	
1	Dural sinus venous drainage only
2	Some reflux into cortical veins
3	Cortical venous drainage predominates
Cognard Classification of Dural AVMs (14)	
I	Antegrade flow within dural sinus
IIa	Retrograde flow within dural sinus
IIb	Antegrade flow in sinus with some cortical venous reflux
IIa and IIb	Retrograde flow in sinus with some cortical venous reflux
III	Cortical venous drainage without ectasia
IV	Cortical venous drainage with ectasia
V	Spinal medullary vein drainage

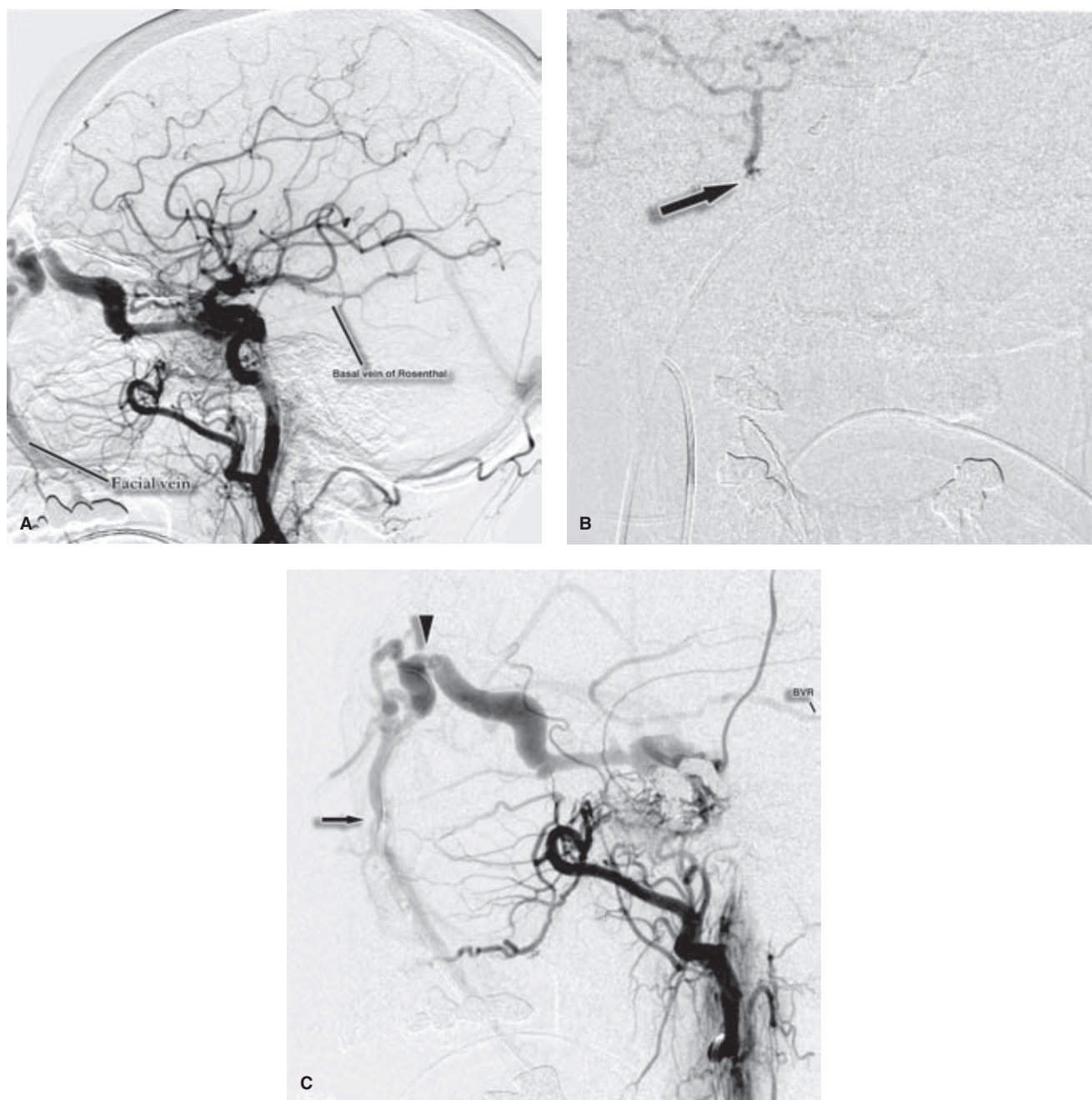


FIGURE 20-26. (A–C) Dangers during transvenous embolization of cavernous DAVM. This case demonstrates that even with anticipation of certain difficulties, they cannot always be averted. The right common carotid artery lateral view (**A**) shows a typical DAVM of the right cavernous sinus with massive opacification of the ophthalmic vein draining to the ipsilateral facial vein. More concerning for the possibility of intracranial complications there is also a prominent connection to the basal vein of Rosenthal. The first goal of endovascular transvenous therapy is to find and disconnect the critical veins to the deep system before obliterating the rest of the cavernous sinus (and one's access to it at the same time). Image (**B**) is an AP projection of the microcatheter injection into the uncal vein (*arrow* in **B**) of the anterior aspect of the cavernous sinus, inserted retrogradely via the IPS. This was disconnected early in the procedure with coils. Even with this caution, access to the lesion was still lost due to unfavorable compartmentation of the cavernous sinus and an incomplete treatment resulted. Image (**C**) shows the right external carotid artery injection lateral view after access had been lost via the IPS. The deep venous system is still filling through some other undiscovered vein. The microcatheter (*arrow* in **C**) is now being navigated retrogradely via the facial vein to gain access to the ophthalmic vein for eventual retrograde access to the cavernous sinus. This is not as easy as it sometimes looks. The orbital septum almost consistently narrows and kinks the connection (*arrowhead* in **C**) between the ophthalmic veins and the facial vein and makes retrograde access very difficult. It can be easy to perforate the vein in this situation of frustration, in which case the patient will get a nasty hematoma and the case will have to be discontinued for another day or an alternative route of access planned.

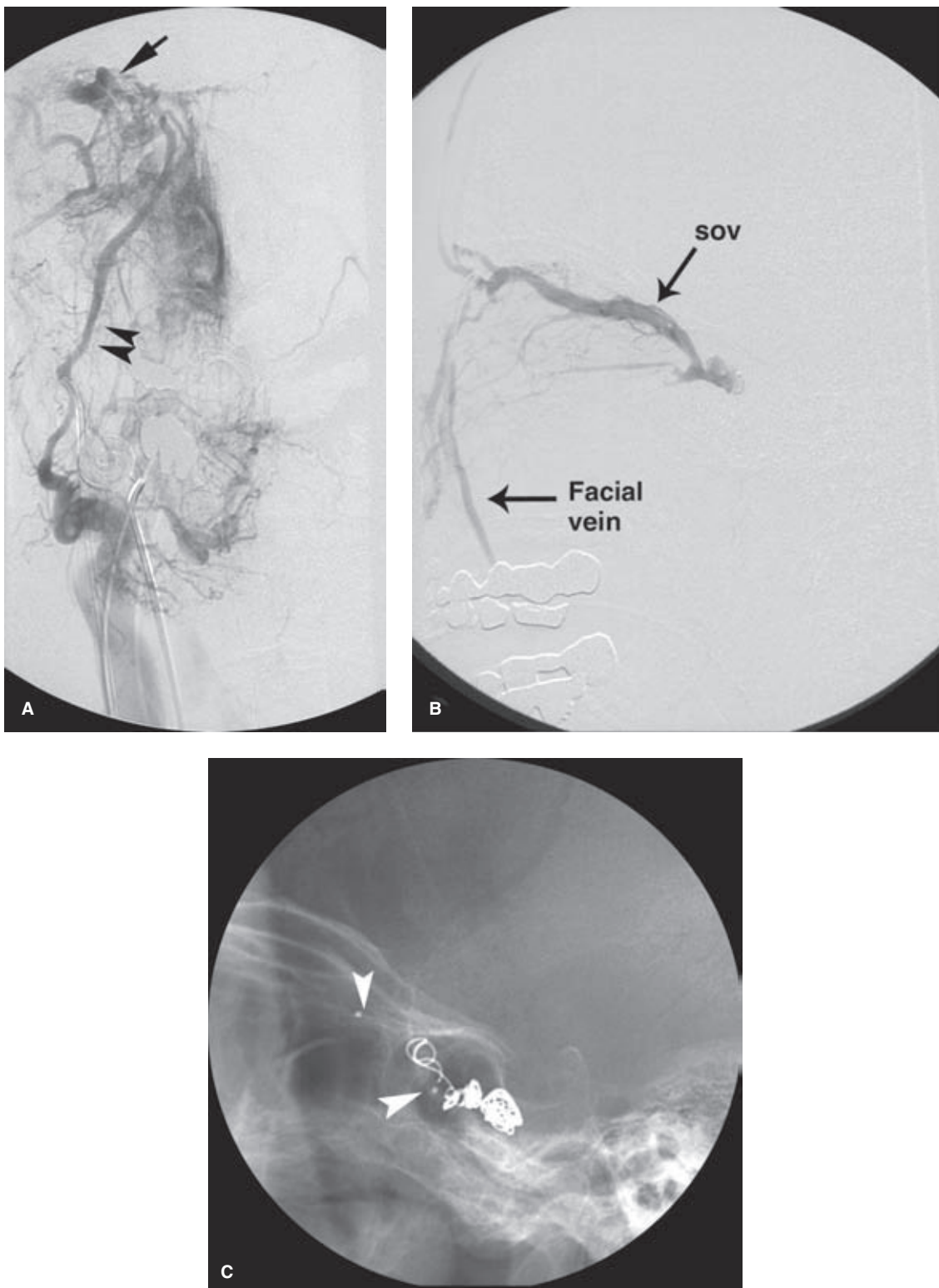


FIGURE 20-27. (A–C) **Retrograde access via the right facial vein.** A dural AVF of the right cavernous sinus proved difficult to access until an attempt was made to catheterize the ipsilateral facial vein to reach the massively distended SOV (*arrow*). To find the facial vein (*arrowheads*) a run (A, AP plane, venous phase) or roadmap centered on the angle of the mandible to identify the junction of the retromandibular vein with the internal jugular vein is usually necessary. Even when the veins are moderately developed, such as here, this approach is difficult. A lateral view run (B) of the microcatheter in the cavernous sinus shows the subtracted artifact of the 5F introducer catheter in the facial vein all the way up to the angular vein. The appearance of the fibered coils within the cavernous sinus is shown in lateral view (C). The two markers of the microcatheter are indicated with *white arrowheads*. Fibered retractable are exceptionally good for cases such as this where one wishes to avoid getting pushed out by stiff fibered coils.

FIGURE 20-28. Retrograde access via the SOV. An intraoperative photograph of an incision above the eyebrow, taken from vantage of the patient's head facing toward the feet, shows how difficult it is to see what is what without the aid of an expert orbital surgeon. Vascular ties are securing the vein, which has been punctured with a 4F micropuncture sheath system. This is secured to the skin and fitted with a flush valve for retrograde access with a microcatheter to the cavernous sinus. The big potential for complications with this approach is rupture or losing control of the pressurized vein, with development of an intraorbital hematoma, secondary glaucoma, and even optic nerve damage. Even when the vein appears enormous on an angiogram, the surgical exposure of the vein can be very confusing and understated.

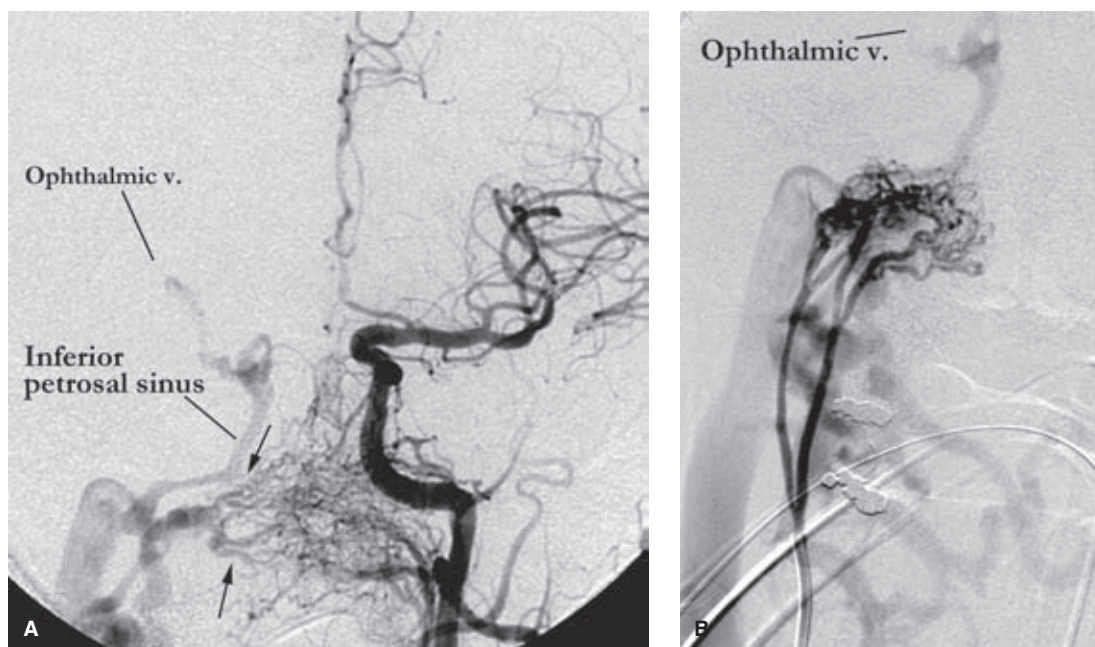


FIGURE 20-29. (A–B) Cranial nerve injury following Onyx embolization. This case of a young adult male presenting with a bruit and a red right eye had many lessons to be learned from it. Firstly, the DAVM appeared overwhelming complex with a multitude of feeders from both vertebral arteries and a countless number of arterial inputs from the external carotid arteries bilaterally. However, the two images selected (A, AP view of left common carotid artery; B, AP view of right ascending pharyngeal artery) show that the malformation can be condensed into a geographically confined set of fistulas in the region of the right petro-clival fissure (between the two long arrows on A) from which point venous opacification emanates to include the retrograde opacification of the rightSOV. This very intimidating malformation was then embolized completely using Onyx predominantly through several branches of the right ascending pharyngeal artery with a very satisfactory angiographic appearance. About an hour after waking up from the procedure the patient developed hoarseness of his voice due to a progressive paresis of the right laryngeal nerve. This made a very slow recovery over many months, although his right XII nerve palsy and XI palsy improved less satisfactorily and constituted a particular loss to him due to the interference of the latter with his right shoulder strength. Whether this injury was specifically linked to a neurotoxic effect of the DMSO or a generic devascularization following embolization is difficult to say. It is most likely the former. Awake patients experience exquisite pain when DMSO solvent is injected into scalp or facial tissue as prelude to an Onyx injection, and a similar noxious effect on the cranial nerves seems likely. When the embolization with Onyx around the skull base is extensive, as was the case here, the likelihood of cranial nerve injury should be considered.

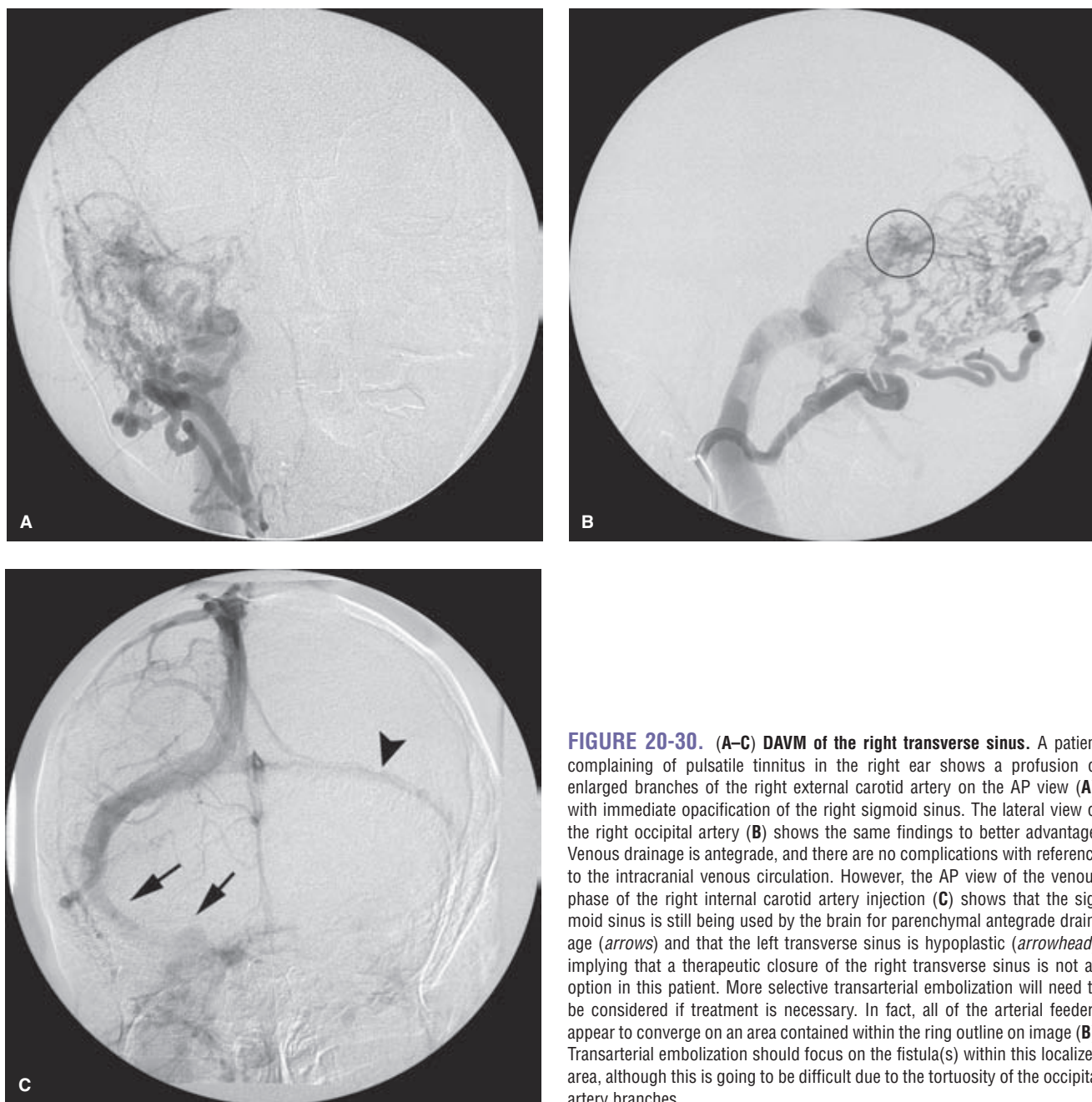


FIGURE 20-30. (A–C) DAVM of the right transverse sinus. A patient complaining of pulsatile tinnitus in the right ear shows a profusion of enlarged branches of the right external carotid artery on the AP view (A), with immediate opacification of the right sigmoid sinus. The lateral view of the right occipital artery (B) shows the same findings to better advantage. Venous drainage is antegrade, and there are no complications with reference to the intracranial venous circulation. However, the AP view of the venous phase of the right internal carotid artery injection (C) shows that the sigmoid sinus is still being used by the brain for parenchymal antegrade drainage (arrows) and that the left transverse sinus is hypoplastic (arrowhead), implying that a therapeutic closure of the right transverse sinus is not an option in this patient. More selective transarterial embolization will need to be considered if treatment is necessary. In fact, all of the arterial feeders appear to converge on an area contained within the ring outline on image (B). Transarterial embolization should focus on the fistula(s) within this localized area, although this is going to be difficult due to the tortuosity of the occipital artery branches.

one must attempt to evaluate the risk of inducing postprocedural venous complications. The state of the parenchymal veins and the capacity of the retrograde route via the torcular to carry the necessary flow must be evaluated. Some have advocated using a balloon-test occlusion of the sinus in question and observing whether an elevation of pressure above the balloon occurs with inflation as a predictor of intolerance. However, the reliability of this test is not established.

Classification schemes, and particularly it seems those with Roman numerals, and very particularly those with Roman numerals and subscripted lower case codicils, are an odious imposition on one's memory, but seem to be unavoidable. The two principal schemes (Table 20-1) for categorizing DAVMs described by Borden (15) and Cognard (14) are useful mainly as a line of buckets for lumping clinical cases for *post hoc* statistical analysis. The process of clinical

treatment decision making is very much individualized for the particular lesion in hand, its idiosyncratic risks related to adjacent dangerous arterial anastomoses, and a careful analysis of the venous physiology in the site of proposed occlusion. As mentioned in the text, whether there already is a history of hemorrhage or other neurologic complications seems to be a greater predictor of subsequent clinical complications than the grade of angiographic complexity.

References

1. Nabors MW, Azzam CJ, Albanna FJ, et al. Delayed postoperative dural arteriovenous malformations. Report of two cases. *J Neurosurg* 1987;66(5):768–772.
2. Watanabe A, Takahara Y, Ibuchi Y, et al. Two cases of dural arteriovenous malformation occurring after intracranial surgery. *Neuroradiology* 1984;26(5):375–380.

3. Sakaki T, Morimoto T, Nakase H, et al. Dural arteriovenous fistula of the posterior fossa developing after surgical occlusion of the sigmoid sinus. Report of five cases. *J Neurosurg* 1996; 84(1):113–118.
4. Sundt TM Jr, Piepgras DG. The surgical approach to arteriovenous malformations of the lateral and sigmoid dural sinuses. *J Neurosurg* 1983;59(1):32–39.
5. Mullan S. Reflections upon the nature and management of intracranial and intraspinal vascular malformations and fistulae. *J Neurosurg* 1994;80(4):606–616.
6. Yamashita K, Taki W, Nakahara I, et al. Development of sigmoid dural arteriovenous fistulas after transvenous embolization of cavernous dural arteriovenous fistulas. *AJNR Am J Neuroradiol* 1993;14(5):1106–1108.
7. Desal HA, Toulgoat F, Raoul S, et al. Ehlers-Danlos syndrome type IV and recurrent carotid-cavernous fistula: review of the literature, endovascular approach, technique and difficulties. *Neuroradiology* 2005;47(4):300–304.
8. Graf CJ. Spontaneous carotid-cavernous fistula. Ehlers-Danlos syndrome and related conditions. *Arch Neurol* 1965;13(6):662–672.
9. Lach B, Nair SG, Russell NA, et al. Spontaneous carotid-cavernous fistula and multiple arterial dissections in type IV Ehlers-Danlos syndrome. Case report. *J Neurosurg* 1987; 66(3): 462–467.
10. Zilocchi M, Macedo TA, Oderich GS, et al. Vascular Ehlers-Danlos syndrome: imaging findings. *AJR Am J Roentgenol* 2007; 189(3):712–719.
11. Barrow DL, Spector RH, Braun IF, et al. Classification and treatment of spontaneous carotid-cavernous sinus fistulas. *J Neurosurg* 1985;62:248–256.
12. Djindjian R, Merland JJ. *Superselective Arteriography of the External Carotid Artery*. Berlin: Springer-Verlag; 1978.
13. Lalwani AK, Dowd CF, Halbach VV. Grading venous restrictive disease in patients with dural arteriovenous fistulas of the transverse/sigmoid sinus. *J Neurosurg* 1993;79(1):11–15.
14. Cognard C, Gobin YP, Pierot L, et al. Cerebral dural arteriovenous fistulas: clinical and angiographic correlation with a revised classification of venous drainage. *Radiology* 1995; 194(3): 671–680.
15. Borden JA, Wu JK, Shucart WA. A proposed classification for spinal and cranial dural arteriovenous fistulous malformations and implications for treatment. *J Neurosurg* 1995;82(2):166–179.
16. Geibprasert S, Pereira V, Krings T, et al. Dural arteriovenous shunts: a new classification of craniospinal epidural venous anatomical bases and clinical correlations. *Stroke* 2008;39(10): 2783–2794.
17. Lasjaunias P, Chiu M, ter Brugge K, et al. Neurological manifestations of intracranial dural arteriovenous malformations. *J Neurosurg* 1986;64(5):724–730.
18. Zeidman SM, Monsein LH, Arosarena O, et al. Reversibility of white matter changes and dementia after treatment of dural fistulas. *AJNR Am J Neuroradiol* 1995;16(5):1080–1083.
19. Ito M, Sonokawa T, Mishina H, et al. Reversible dural arteriovenous malformation-induced venous ischemia as a cause of dementia: treatment by surgical occlusion of draining dural sinus: case report. *Neurosurgery* 1995;37(6):1187–1191; discussion 1191–1192.
20. Nencini P, Inzitari D, Gibbs J, et al. Dementia with leucoaraiosis and dural arteriovenous malformation: clinical and PET case study. *J Neurol Neurosurg Psychiatry* 1993;56(8):929–931.
21. Miura S, Noda K, Shiramizu N, et al. Parkinsonism and ataxia associated with an intracranial dural arteriovenous fistula presenting with hyperintense basal ganglia in T1-weighted MRI. *J Clin Neurosci* 2009;16(2):341–343.
22. Noqueira RG, Baccin CE, Rabinov JD, et al. Reversible parkinsonism after treatment of dural arteriovenous fistula. *J Neuroimaging* 2009;19(2):183–184.
23. Duffau H, Lopes M, Janosevic V, et al. Early rebleeding from intracranial dural arteriovenous fistulas: report of 20 cases and review of the literature. *J Neurosurg* 1999;90(1):78–84.
24. van Dijk JM, terBrugge KG, Willinsky RA, et al. Clinical course of cranial dural arteriovenous fistulas with long-term persistent cortical venous reflux. *Stroke* 2002;33(5):1233–1236.
25. Satomi J, van Dijk JM, Terbrugge KG, et al. Benign cranial dural arteriovenous fistulas: outcome of conservative management based on the natural history of the lesion. *J Neurosurg* 2002; 97(4):767–770.
26. Strom RG, Botros JA, Refai D, et al. Cranial dural arteriovenous fistulae: asymptomatic cortical venous drainage portends less aggressive clinical course. *Neurosurgery* 2009;64(2):241–247; discussion 247–248.
27. Bitoh S, Sakaki S. Spontaneous cure of dural arteriovenous malformation in the posterior fossa. *Surg Neurol* 1979; 12(2):111–114.
28. Magidson MA, Weinberg PE. Spontaneous closure of a dural arteriovenous malformation. *Surg Neurol* 1976;6(2):107–110.
29. Baskaya MK, Suzuki Y, Seki Y, et al. Dural arteriovenous malformations in the anterior cranial fossa. *Acta Neurochir (Wien)* 1994;129(3–4):146–151.
30. Grisoli F, Vincentelli F, Fuchs S, et al. Surgical treatment of tentorial arteriovenous malformations draining into the subarachnoid space. Report of four cases. *J Neurosurg* 1984;60(5): 1059–1066.
31. Awad IA, Little JR, Akarawi WP, et al. Intracranial dural arteriovenous malformations: factors predisposing to an aggressive neurological course. *J Neurosurg* 1990;72(6):839–850.
32. Kikuchi K, Kowada M. Anterior fossa dural arteriovenous malformation supplied by bilateral ethmoidal arteries. *Surg Neurol* 1994;41(1):56–64.
33. Kobayashi H, Hayashi M, Noguchi Y, et al. Dural arteriovenous malformations in the anterior cranial fossa. *Surg Neurol* 1988;30(5):396–401.
34. Espinosa JA, Mohr G, Robert F. Dural arteriovenous malformations of the ethmoidal region: report of two cases. *Br J Neurosurg* 1993;7(4):431–435.
35. Kaplan SS, Ogilvy CS, Crowell RM. Incidentally discovered arteriovenous malformation of the anterior fossa dura. *Br J Neurosurg* 1994;8(6):755–759.
36. Brown RD Jr, Wiebers DO, Nichols DA. Intracranial dural arteriovenous fistulae: angiographic predictors of intracranial hemorrhage and clinical outcome in nonsurgical patients. *J Neurosurg* 1994;81(4):531–538.
37. Halbach VV, Higashida RT, Hieshima GB, et al. Transvenous embolization of direct carotid cavernous fistulas. *AJNR Am J Neuroradiol* 1988;9(4):741–747.
38. Halbach VV, Higashida RT, Hieshima GB, et al. Transvenous embolization of dural fistulas involving the transverse and sigmoid sinuses. *AJNR Am J Neuroradiol* 1989;10(2):385–392.
39. Halbach VV, Higashida RT, Hieshima GB, et al. Dural fistulas involving the cavernous sinus: results of treatment in 30 patients. *Radiology* 1987;163(2):437–442.
40. Halbach VV, Higashida RT, Hieshima GB, et al. Treatment of dural fistulas involving the deep cerebral venous system. *AJNR Am J Neuroradiol* 1989;10(2):393–399.
41. Jung HH, Chang JH, Whang K, et al. Gamma Knife surgery for low-flow cavernous sinus dural arteriovenous fistulas. *J Neurosurg* 2010;113(suppl):21–27.
42. Loumiosis I, Lanzino G, Daniels D, et al. Radiosurgery for intracranial dural arteriovenous fistulas (DAVFs): a review. *Neurosurg Rev* 2011;34(3):305–315; discussion 315.
43. Matsushige T, Nakaoka M, Ohta K, et al. Tentorial dural arteriovenous malformation manifesting as trigeminal neuralgia treated by stereotactic radiosurgery: A case report. *Surg Neurol* 2006;66(5):519–523; discussion 523.
44. Yang HC, Kano H, Kondziolka D, et al. Stereotactic radiosurgery with or without embolization for intracranial dural arteriovenous fistulas. *Neurosurgery* 2010;67(5):1276–1283; discussion 1284–1285.
45. O’Leary S, Hodgson TJ, Coley SC, et al. Intracranial dural arteriovenous malformations: results of stereotactic radiosurgery in 17 patients. *Clin Oncol (R Coll Radiol)* 2002;14(2):97–102.

46. Pan DH, Chung WY, Guo WY, et al. Stereotactic radiosurgery for the treatment of dural arteriovenous fistulas involving the transverse-sigmoid sinus. *J Neurosurg* 2002;96(5): 823–829.
47. Lewis AI, Tomsick TA, Tew JM Jr. Management of tentorial dural arteriovenous malformations: transarterial embolization combined with stereotactic radiation or surgery. *J Neurosurg* 1994;81(6):851–859.
48. Guo WY, Pan DH, Wu HM, et al. Radiosurgery as a treatment alternative for dural arteriovenous fistulas of the cavernous sinus. *AJNR Am J Neuroradiol* 1998;19(6):1081–1087.
49. Liu HM, Wang YH, Chen YF, et al. Long-term clinical outcome of spontaneous carotid cavernous sinus fistulae supplied by dural branches of the internal carotid artery. *Neuroradiology* 2001;43(11):1007–1014.
50. Ricolfi F, Manelfe C, Meder JF, et al. Intracranial dural arteriovenous fistulae with perimedullary venous drainage. Anatomical, clinical and therapeutic considerations. *Neuroradiology* 1999; 41(11):803–812.
51. Natarajan SK, Ghodke B, Kim LJ, et al. Multimodality treatment of intracranial dural arteriovenous fistulas in the Onyx era: a single center experience. *World Neurosurg* 2010;73(4):365–379.
52. Macdonald JH, Millar JS, Barker CS. Endovascular treatment of cranial dural arteriovenous fistulae: a single-centre, 14-year experience and the impact of Onyx on local practise. *Neuroradiology* 2010;52(5):387–395.
53. Cognard C, Januel AC, Silva NA Jr, et al. Endovascular treatment of intracranial dural arteriovenous fistulas with cortical venous drainage: new management using Onyx. *AJNR Am J Neuroradiol* 2008;29(2):235–241.
54. Noqueira RG, Dabus G, Rabinov JD, et al. Preliminary experience with onyx embolization for the treatment of intracranial dural arteriovenous fistulas. *AJNR Am J Neuroradiol* 2008; 29(1):91–97.
55. van Rooij WJ, Sluzewski M. Curative embolization with Onyx of dural arteriovenous fistulas with cortical venous drainage. *AJNR Am J Neuroradiol* 2010;31(8):1516–1520.
56. Baldauf J, Spuler A, Hoch HH, et al. Embolization of indirect carotid-cavernous sinus fistulas using the superior ophthalmic vein approach. *Acta Neurol Scand* 2004;110(3):200–204.
57. Lv X, Jiang C, Li Y, et al. Results and complications of transarterial embolization of intracranial dural arteriovenous fistulas using Onyx-18. *J Neurosurg* 2008;109(6):1083–1090.

Vascular Malformations of the Spine

Key Points

- All of the available sources of supply to the anterior spinal artery may not declare themselves readily on the initial angiographic evaluation. Care should always be exercised when using particulate or liquid agents near the spinal cord, lest an unsuspected pedicle to the anterior spinal artery be present.
- Manifestations of spinal venous hypertension may be very subtle, particularly on nonenhanced MRI examinations.

► INTRODUCTION

Spinal cord vascular malformations represent about 2% to 3% of spinal masses and typically present with myelopathic symptoms related to compromise of long tract function (bowel and bladder dysfunctions, motor and sensory losses) but can also present with back pain, radicular symptoms, subarachnoid or intraspinal hemorrhage, or spinal deformity.

Spinal arteriovenous malformations are rare. With the exception of spinal dural arteriovenous malformations, there are probably almost as many publications and classification systems for spinal vascular disease in the literature as there are patients with these disorders. The most helpful way to understand these lesions is by their location with reference to the dura and the spinal cord. Secondarily, they can be categorized into simple fistulous lesions (AVF) or multivessel lesions (AVM). Intramedullary AVMs are classified into juvenile type (whole cross-sectional area of the cord involved) or glomus type (a more restricted pea-like configuration). Pial fistulas are usually on the surface of the cord or just below and are sometimes graded according to the degree or absence of ectasia of the feeding arteries.

Spinal AVMs can alternatively be classified from a genetic point of view:

1. Genetic hereditary lesions of the vascular germinal cells, such as seen in hereditary hemorrhagic telangiectasia.
2. Genetic nonhereditary lesions with metamereric expression, such as Cobb syndrome where patients have multiple shunts and malformations of the spine, muscles, paraspinous and cutaneous tissues.

3. Single lesions of the cord, nerve roots, or filum terminale (1,2).

Dural arteriovenous fistulas, on the other hand, are tiny, slowly flowing lesions, which with rare exceptions represent an acquired disease of later adulthood (>40 years). They are supplied by dural arteries and typically affect the lower spine and lower extremities. They cause a more progressive slow decline compared with intramedullary vascular malformations. They do not typically cause subarachnoid hemorrhage.

Intradural Spinal Arteriovenous Malformations

Intradural, intramedullary spinal arteriovenous malformations occur most commonly in the cervical or thoracic cord and are classified into three types (Figs. 21-1–21-5).

Juvenile-type Spinal Arteriovenous Malformations

The juvenile type of spinal arteriovenous malformations occupies the entire spinal canal at the involved level(s) and can have normal spinal parenchyma present within the interstices of its components. There may be multiple medullary arterial feeders, most prominently the anterior spinal artery, which, like the arterial feeders to arteriovenous malformations in the brain, may have a dysplastic appearance. Feeding pedicle or intranidal aneurysms may be seen in approximately 20% of intramedullary arteriovenous malformations (3,4), as can venous ectasia or venous aneurysms. A minority of patients show a widened interpedicular distance and may even emit an audible spinal bruit (Fig. 21-6). They can present with gradual or abrupt onset of motor and sensory symptoms related to the level of involvement or with spinal subarachnoid hemorrhage.

Glomus-type Spinal Arteriovenous Malformations

Glomus-type spinal arteriovenous malformations are more compact and defined than the juvenile type. They do not have intermingled normal spinal tissue, are confined to a shorter segment of cord, and are usually fed by a single arterial pedicle. They have a risk of subarachnoid hemorrhage higher than that of other types of intradural vascular malformations, seen in 85% of symptomatic patients (3).

Intramedullary and Perimedullary Arteriovenous Fistulas

Fistulas of the spinal cord may be intramedullary or perimedullary. Flow is usually from an anterior or posterior
(text continues on page 356)

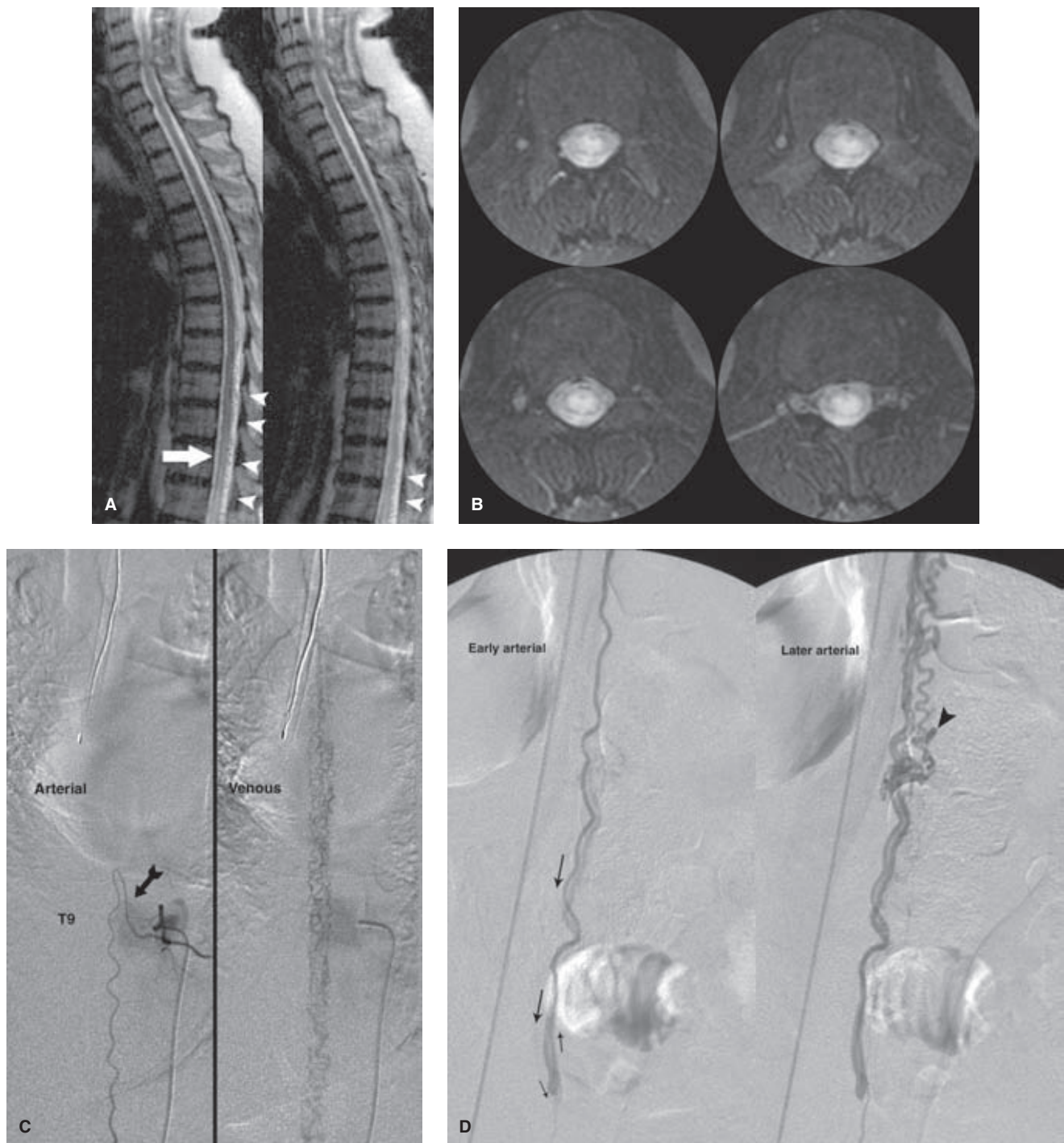


FIGURE 21-1. (A–D) Intradural spinal arteriovenous malformation presenting with venous infarction (Foix–Alajouanine). A 53-year-old female presented with a 3- to 4-year history of progressive lower extremity weakness, incontinence, and ascending sensory disturbances. Her presentation was confounded by a remote history of surgical release of a tethered cord. However, her sagittal (A) and axial (B) T2-weighted MRI images at the time of presentation show findings not likely related to the previous surgery. The conus is hyperintense in signal (arrow), and numerous flow voids (arrowheads) are seen along the dorsal surface. The axial appearance is that of a “hyper-round” cord, which could be seen with an arterial infarction of the artery of Adamkiewicz or a tumor of the conus. In this instance, however, the appearance is that of a venous infarction with chronic venous hypertension in the lower cord. This could be due to either a dural AVF along the cord or a pial AVM on or in the cord itself. The diagnostic spinal arteriogram must find and analyze the lesion accordingly in order to plan treatment. In this particular patient, the lesion was an intramedullary arteriovenous malformation of the cord deriving supply from the anterior spinal artery. This vessel was found at left T9 (arrow in C) and was injected (2mL/s × 2s) with the intensifier centered over the catheter tip as shown. The arterial phase was significant for marked conspicuity of the anterior spinal artery, implying that it was enlarged, but was otherwise normal. However, the venous phase demonstrates that the venous plexus of the cord is markedly distended and exhibits prolonged stagnation. This is an illustration of the importance of the entire angiographic sequence for critical vessels. A subsequent run centered over the conus (D) shows that the arteriovenous malformation is located on the dorsum of the cord. The anterior spinal artery descends along the anterior median sulcus, wraps around the tip of the conus—centered at L3 in this patient—and ascends the dorsum of the cord to opacify the arteriovenous malformation (arrows indicate sequential progress of flow). An intracanalicular aneurysm is noted (arrowhead in D). The venous structures then emanate cephalad to allow eventually the opacification seen on image (C). Technique is very important in spinal angiography because the findings can be so elusive that they can easily escape attention due to oversight or technical shortfalls.

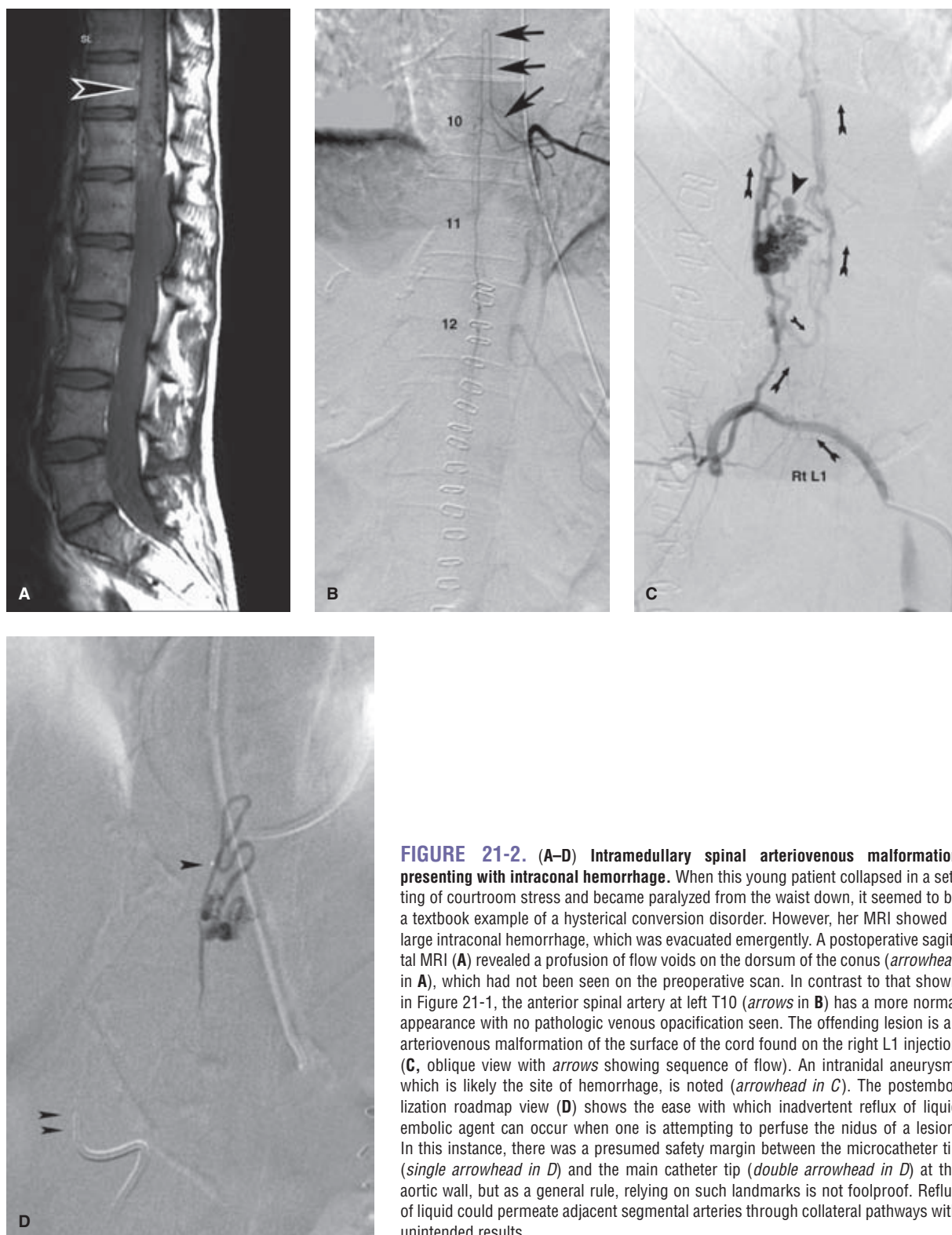


FIGURE 21-2. (A–D) Intradural spinal arteriovenous malformation presenting with intracanal hemorrhage. When this young patient collapsed in a setting of courtroom stress and became paralyzed from the waist down, it seemed to be a textbook example of a hysterical conversion disorder. However, her MRI showed a large intraconal hemorrhage, which was evacuated emergently. A postoperative sagittal MRI (A) revealed a profusion of flow voids on the dorsum of the conus (arrowhead in A), which had not been seen on the preoperative scan. In contrast to that shown in Figure 21-1, the anterior spinal artery at left T10 (arrows in B) has a more normal appearance with no pathologic venous opacification seen. The offending lesion is an arteriovenous malformation of the surface of the cord found on the right L1 injection (C, oblique view with arrows showing sequence of flow). An intranidal aneurysm, which is likely the site of hemorrhage, is noted (arrowhead in C). The postembolization roadmap view (D) shows the ease with which inadvertent reflux of liquid embolic agent can occur when one is attempting to perfuse the nidus of a lesion. In this instance, there was a presumed safety margin between the microcatheter tip (single arrowhead in D) and the main catheter tip (double arrowhead in D) at the aortic wall, but as a general rule, relying on such landmarks is not foolproof. Reflux of liquid could permeate adjacent segmental arteries through collateral pathways with unintended results.

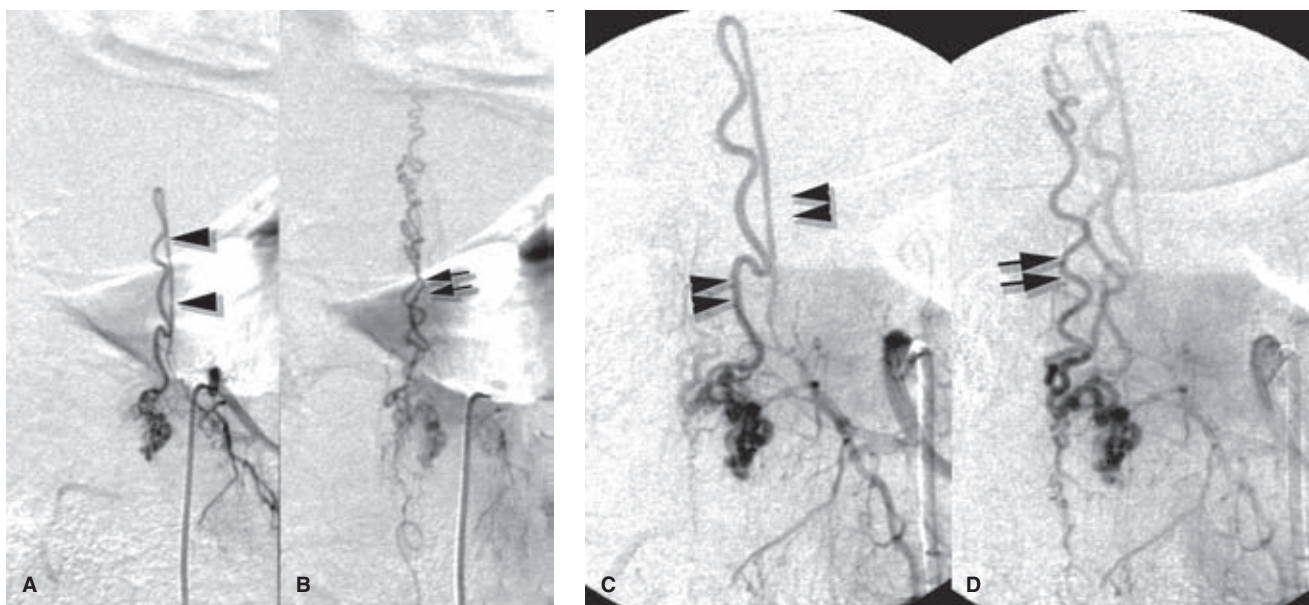


FIGURE 21-3. (A–D) Perimedullary spinal arteriovenous malformation. An elderly male presented with a clinical history of gait disturbance and urinary incontinence. MRI and myelographic findings (not shown) suggested spinal venous hypertension. A left T12 injection demonstrates an enlarged posterior spinal artery (*arrowheads in A*) supplying a perimedullary arteriovenous malformation of the surface of the cord. The early venous phase of the PA view (**B**) shows drainage of the arteriovenous malformation superiorly through the tortuous venous plexus of the spine. An oblique magnification view of the same pedicle (**C**, early; **D**, late) helps to clarify the surgical anatomy. The posterior spinal artery (*arrowheads in C*) behind the cord makes a hairpin turn on the posterior surface to supply the perimedullary nidus. A slightly later image (**D**), taken when the posterior spinal artery is almost washed out, demonstrates the most prominent vein (*double arrow in D*) draining along the surface of the cord.

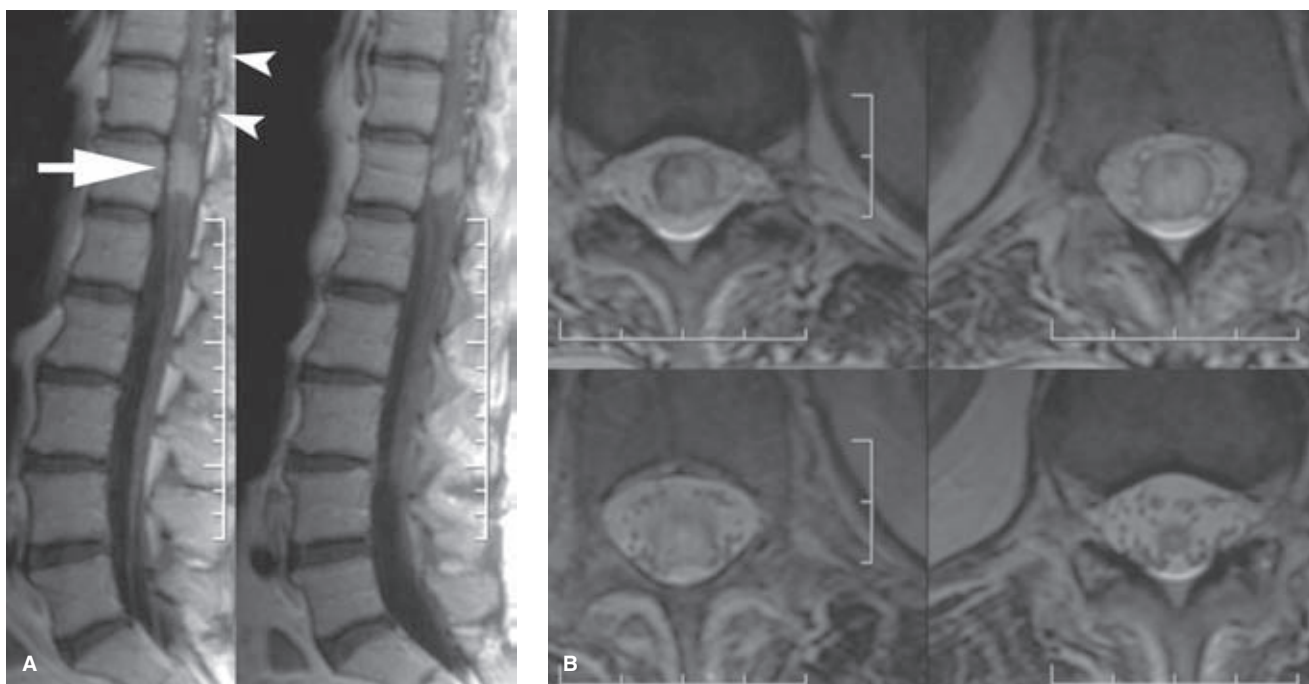


FIGURE 21-4. (A–E) Spinal arteriovenous malformation with venous hypertension (Foix–Alajouanine) mimicking a conal mass. An 83-year-old female with a remote history of breast carcinoma presented with progressive lower extremity weakness and sensory disturbance. An enhancing mass on her sagittal T1 gadolinium-enhanced MRI (*arrow in A*) prompted the diagnosis of metastatic carcinoma to the cord. The axial T2 MRI (**B**) seemed to confirm the expansile hyperintense appearance of the cord. However, she had no other history of metastatic disease, and a prominence of vascular structures (*arrowheads in A*) on the dorsum of the cord suggested that an arteriovenous malformation might be a consideration. The anterior spinal artery at left T9 shows indirect signs of disease. (*continued*)

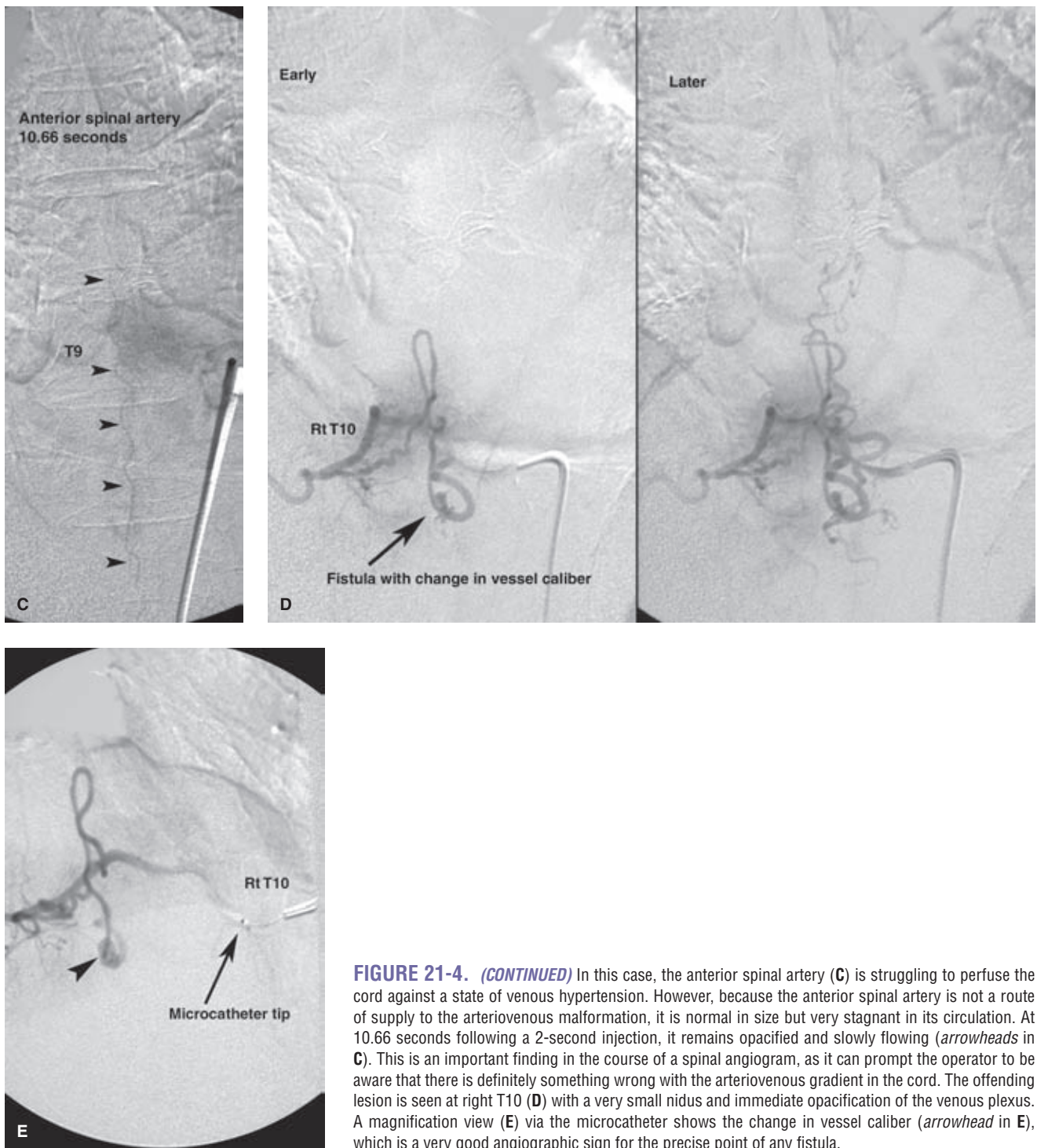


FIGURE 21-4. (CONTINUED) In this case, the anterior spinal artery (C) is struggling to perfuse the cord against a state of venous hypertension. However, because the anterior spinal artery is not a route of supply to the arteriovenous malformation, it is normal in size but very stagnant in its circulation. At 10.66 seconds following a 2-second injection, it remains opacified and slowly flowing (*arrowheads* in C). This is an important finding in the course of a spinal angiogram, as it can prompt the operator to be aware that there is definitely something wrong with the arteriovenous gradient in the cord. The offending lesion is seen at right T10 (D) with a very small nidus and immediate opacification of the venous plexus. A magnification view (E) via the microcatheter shows the change in vessel caliber (*arrowhead* in E), which is a very good angiographic sign for the precise point of any fistula.

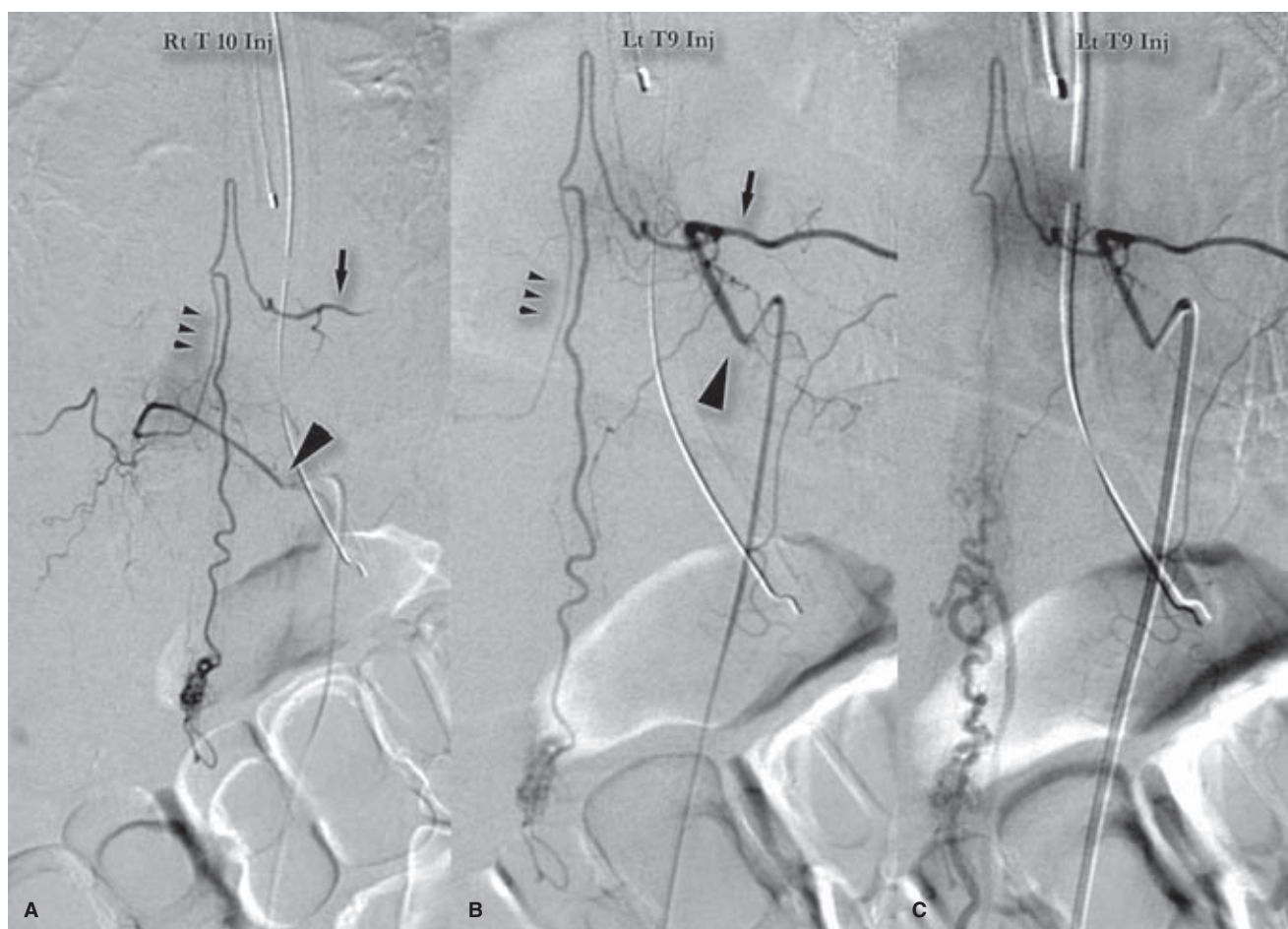


FIGURE 21-5. (A–C) Be wary of unexpected anatomic variants in the anterior spinal artery. These images from the diagnostic evaluation of a perimedullary AVM or fistula on the dorsum of the conus illustrate the variability of the input to the anterior spinal artery. The right T10 injection (A) catheter tip indicated with *arrowhead* shows a small pedicle (*triple arrowhead* in A) extending up to the midline, with retrograde reflux to the larger contributor to the anterior spinal axis from left T9 (*arrow* in A). The subsequent direct injection of left T9 (B) shows the same anatomy, with a slightly different emphasis in conspicuity. A slightly later image (C) demonstrates the centrifugal veins emanating from the region of the AVM extending caudad along the lumbar nerve roots. The images from this case are relatively clear in what they demonstrate but are selected here to make the point that the anatomy of the anterior spinal axis can be very unpredictable, and may even have seemingly redundant feeders. In some circumstances these can pose a substantial risk for misadventure through particle or liquid embolization of unexpected pedicles.

spinal artery, which connects directly to a vein without an identifiable nidus. Flow is faster than that seen in dural arteriovenous fistulas. They can present with intramedullary or subarachnoid hemorrhage, but this appears to be a minority of cases. As is the case for dural arteriovenous fistulas, venous hypertension with cord edema appears to be an important pathophysiologic mechanism for symptoms of intradural arteriovenous shunts (5). Aneurysms of the feeding pedicles are not as likely to be present with perimedullary fistulas compared with intramedullary arteriovenous malformations (4).

Paraspinal and Epidural Arteriovenous Malformations

Paraspinal AVMs are rare lesions that can affect the paravertebral muscles, nerve root foramina, or prevertebral structures (6). They can be seen posttraumatically, but most are considered to be congenital lesions presenting in children with back pain, paraparesis, high-output cardiac failure, or

an audible bruit (Fig. 21-7). Most of them seem to exert their functional effect through venous congestion transmitted to the intradural veins.

Hypervascular Tumors Simulating Arteriovenous Malformations

Arteriovenous shunting or early venous opacification can be seen with vascular intra-axial tumors such as glioblastoma multiforme (Figs. 21-8 and 21-9) or hemangioblastoma. Extra-axial vascular tumors, such as hemangiopericytoma and extra-axial or spinal hemangioblastoma, may also give an appearance that could be confused with that of an arteriovenous malformation. Usually, the vascularity of such tumors is easily recognized as subordinate in prominence to other evidence of a mass lesion. Arteriovenous shunting is rarely as fast in a tumor as that seen in arteriovenous malformations. A parenchymal blush characteristically seen in vascular tumors is not seen in arteriovenous malformations.

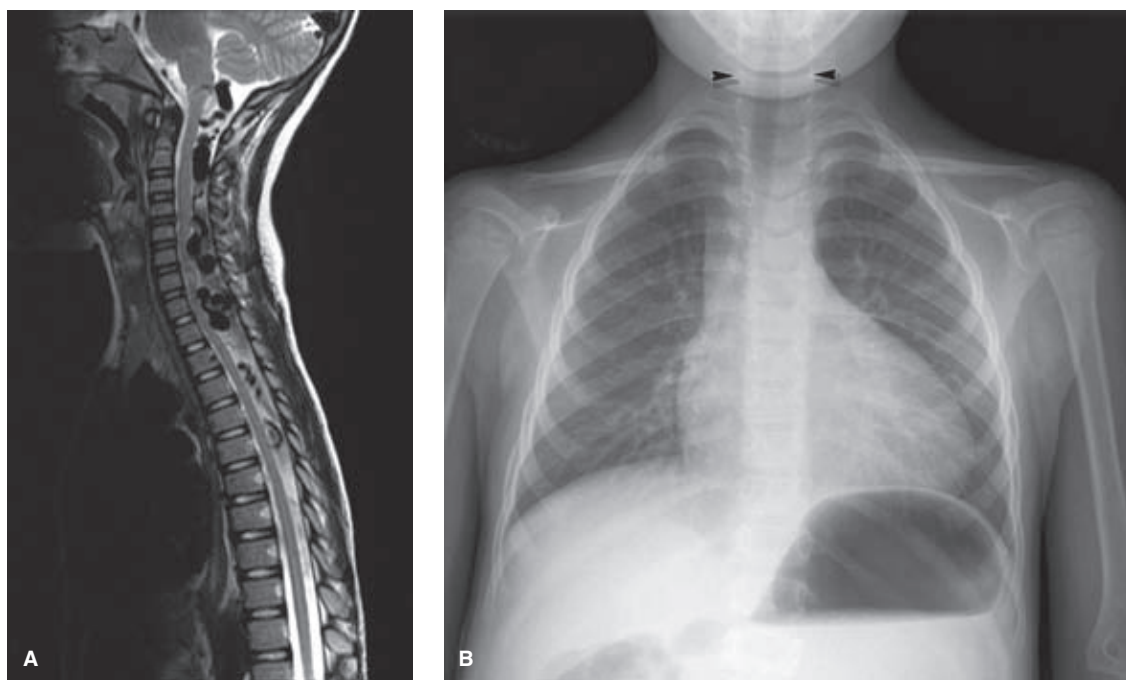


FIGURE 21-6. (A–B) **Syndromic spinal AVM in a small child.** This presumably congenital AVM of the cervical spine was characterized by a number of high-flow fistulas that had resulted in massive distention of the veins of the spinal cord draining upward via the foramen magnum (A). In fact the distended appearance of the basal vein of Rosenthal and mesencephalic veins gave the appearance at first glance that this might be a vein of Galen type of malformation in the tectal region, until one realized the fact that these veins were emerging out of the spinal canal into the cranial vault, instead of vice versa. The chest x-ray in this child (B), who had an audible bruit over his neck and suboccipital area, shows the widened interpedicular distance (*arrowheads*) wrought by such lesions when they occur early in development.

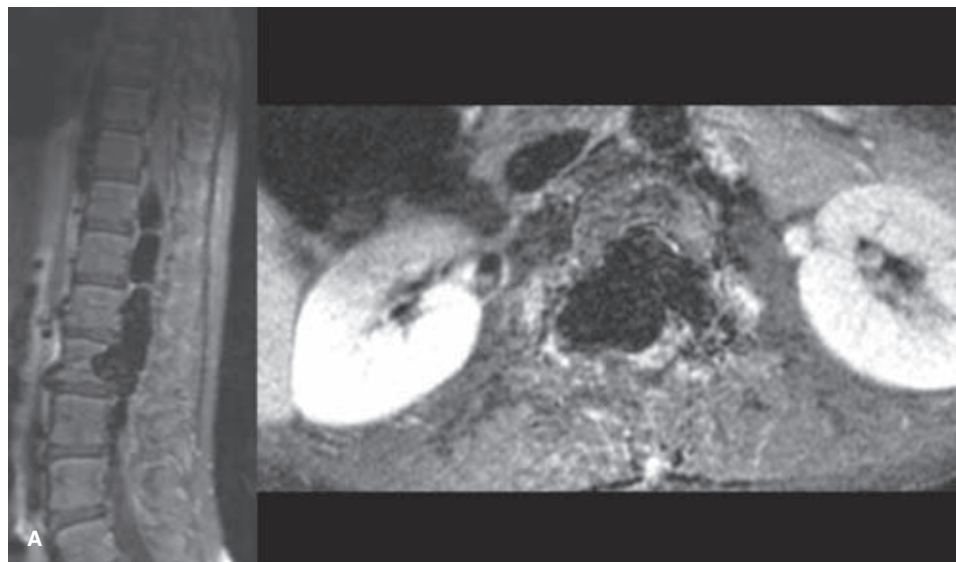


FIGURE 21-7. (A–E) **Paraspinal AVM in a young child.** This girl presented with high-output cardiac failure, a bruit over the lower back, and scoliotic deformity. Her cardiologist astutely noted that the contrast from her ventriculogram returned to the heart more quickly than normal, leading to the eventual discovery of this large lumbar paraspinal malformation. The treatment for this lesion predated the availability of Onyx and was staged over several years. The initial MRI (A) showed massive distention of the intracanalicular veins and permeative remodeling of the lumbar bodies, particularly L2. (*continued*)

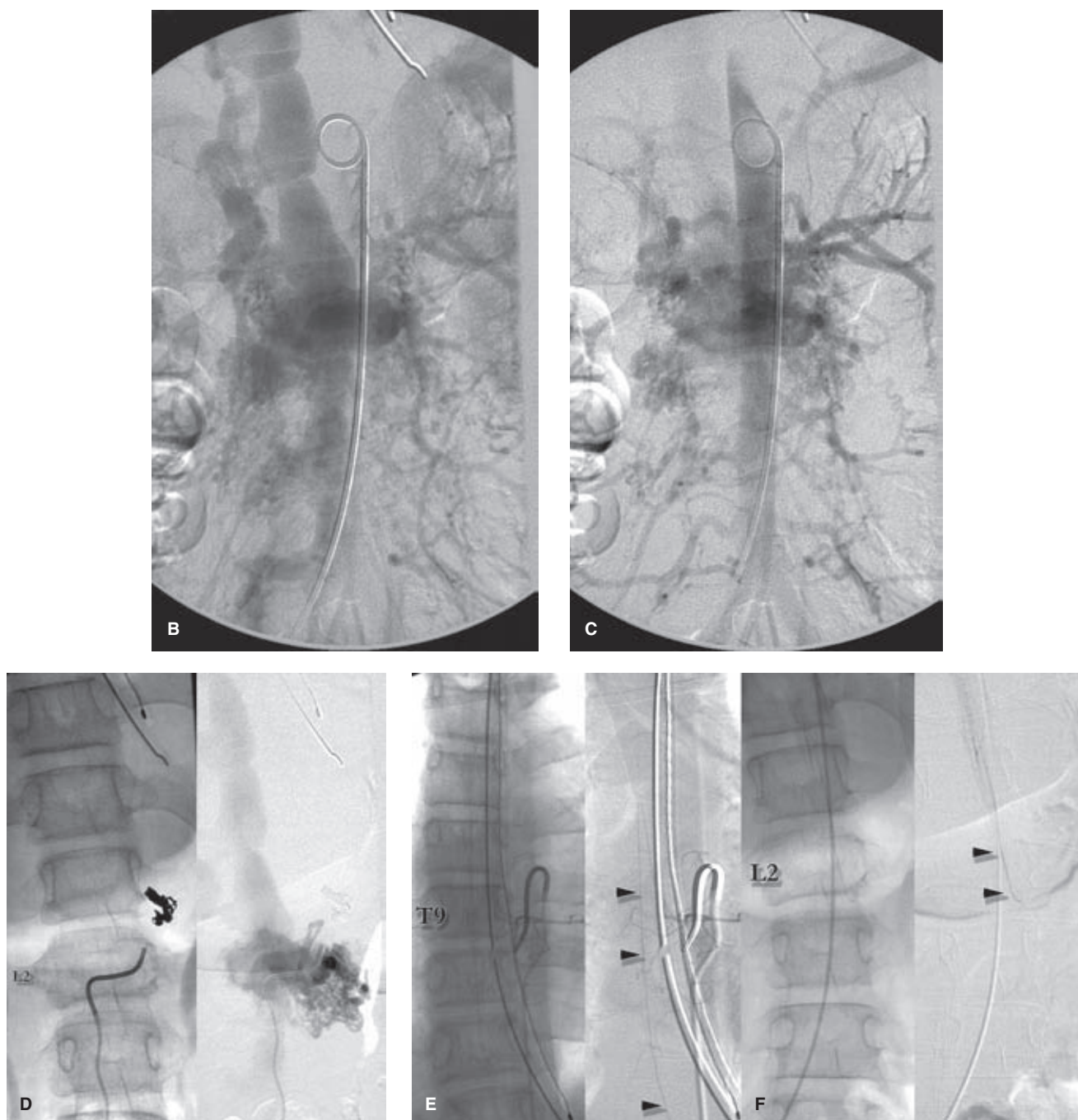


FIGURE 21-7. (CONTINUED) The first aortogram AP projection (image **B** early, image **C** venous) shows the numerous enlarged lumbar and paraspinal arteries involved with this lesion, and the massively enlarged intracanalicular vein that ascended to enter the azygous vein in the thorax. Among the many concerns with this child who is obviously in need of significant reduction of flow in this lesion is where to begin and how to embolize this lesion without injuring the anterior spinal artery? Image (**D**) places native and subtracted views from the left L2 injection side by side during the initial tentative embolization using coils in some of the direct fistulas. A large component of AVM is opacified from left L2 draining immediately to the intracanalicular vein. A different set of images indicates the hidden dangers that can lurk in cases like these. The left T9 injection (**E**, native and subtracted) demonstrates the normal-sized anterior spinal artery (*arrowheads*), which takes an unusual sweep toward the left as it descends along the cord, perhaps reflecting displacement by the massive vein within the canal. A second image (**F**, native and subtracted) with the catheter still in Left T9 but centered lower over L2 shows that mass effect is not the entire explanation. The anterior spinal artery bevels away from the cord itself and descends to the left L2–L3 foramen and then is cut off at a precise point. The image is telling us that there is a major input to the anterior spinal axis at left L2, but it has become *reversed* due to the sump effect of the AVM. In other words, the anterior spinal axis is supplying the AVM with flow (to a small degree) through the reversed L2 ramus. One needs to be very careful with this discovery. A sudden, effective embolization of left L2 (or even some of its immediate neighbors) with a liquid agent could eliminate the sump of the AVM in this local area, causing the left L2 ramus to the anterior spinal artery to reverse itself suddenly. This could result in transmission of liquid agent to the cord.



FIGURE 21-8. Spinal hemangioblastoma. A patient with Von Hippel–Lindau syndrome and multiple hemangioblastomas of the posterior fossa and cervical spine. A tumor of the lumbar spine opacified via the anterior spinal artery from left T8 injection is demonstrated. Hemangioblastomas typically give a dense immediate blush that reaches prominence during the early arterial phase of an injection, and are thus easily distinguished from vascular malformations.

▶ ENDOVASCULAR TREATMENT OF SPINAL VASCULAR MALFORMATIONS

The prognosis for an untreated symptomatic spinal AVM is poor with 36% of patients younger than 40 years progressing to severe impairment of function within 3 years (7). Safe endovascular embolization of spinal vascular lesions hinges on the ability to distinguish between a posterior spinal artery and an anterior spinal artery. Typically an average-sized PSA supplies a small rim of peripheral tissue centripetally in the posterior third of the cord and its loss, inadvertent or otherwise, is thought to be well tolerated due to the proclivity to develop collateral pathways of supply (8). The anterior spinal artery is a different story. Typically it supplies the greater portion of the cross-sectional territory of the spine at any one level due to penetrating branches from the anterior median sulcus, the sulco-commissural branches, which measure between 400 and 100 μm in size (9) tapering to approximately 60 μm as they penetrate the cord parenchyma centrifugally (10).

The anterior spinal artery (artery of Adamkiewicz (11,12)) is difficult to embolize safely for several reasons. The nature of a juvenile vascular malformation of the spine is such that normal traversing tracts might be expected to be intermingled with many such lesions and thus be vulnerable to ischemic injury from an embolic agent. Furthermore, the adjacent sulco-commissural branches emanating centrifu-

gally to normal tissue will be subject to injury if any inadvertent reflux or collateral misdirection of embolic agent should occur. Finally, the hairpin curvature of the anterior spinal artery is vulnerable to severe injury through the effect of a sudden tug on a microcatheter embedded in NBCA or Onyx. The latter agents are probably more straightforward to use in a posterior spinal artery, while in the anterior spinal artery most experience has been with PVA particles (4,13). PVA embolization while benefiting the majority of patients is associated with a recanalization rate within a year of embolization as high as 80%. NBCA embolization is probably more effective, but has a procedural morbidity of at least 14% even in highly experienced hands (14).

▶ SPINAL DURAL ARTERIOVENOUS MALFORMATIONS

Various types of vascular malformations of the spine or related dura result in a myelographic appearance of distention of the pial spinal venous plexus and of the medullary veins. However, this is the final common pathway or outcome of a variety of disparate processes. To understand these diseases, it is necessary to discern clearly between arteriovenous fistulas of the dura and intradural vascular malformations of the spinal cord itself. The pathophysiology, epidemiology, mechanism of cord injury, and treatment of these disorders differ substantially. Although both categories are rare diseases, dural vascular fistulas are much more common than intradural vascular malformations (3,15).

▶ PATHOPHYSIOLOGY OF SPINAL DURAL VASCULAR DISEASE

The pathophysiology of dural or peridural arteriovenous malformations along the spine is similar to those of the cranial dura mater. The cranial dural layers separate at the foramen magnum to become the spinal dura and the periosteal dura of the spinal canal separated by the epidural space. Within the subarachnoid space, a venous reticulum or plexus covers the medullary surface of the spinal cord. In the normal state, the pial venous plexus of the spinal cord is protected against reflux from the epidural venous plexus, so there is no generalized state of connection between the vascular supply of the spinal dura or dura-covered nerve roots on the one hand, and that of the cord on the other. In other words, the venous territory of the spinal cord normally serves only the radiculomedullary (anterior spinal) or radiculopial (posterior spinal) arteries. A valve mechanism has been proposed as an explanation for the insulation of the pial venous plexus from pressure fluctuations in the epidural venous plexus (16).

Normal venous drainage away from the cord is via medullary veins, running in association with nerve roots, which drain normally in a centrifugal fashion to the epidural venous plexus (Fig. 21-10). Medullary veins are more common on the posterior aspect of the cord, and the posterior longitudinal vein is usually larger than its anterior counterpart (17,18).

Dural-related vascular malformations or fistulas result in an abnormal state of slow arteriovenous shunting into the medullary veins and pial venous plexus of the cord. This results in venous hypertension in the cord. There is

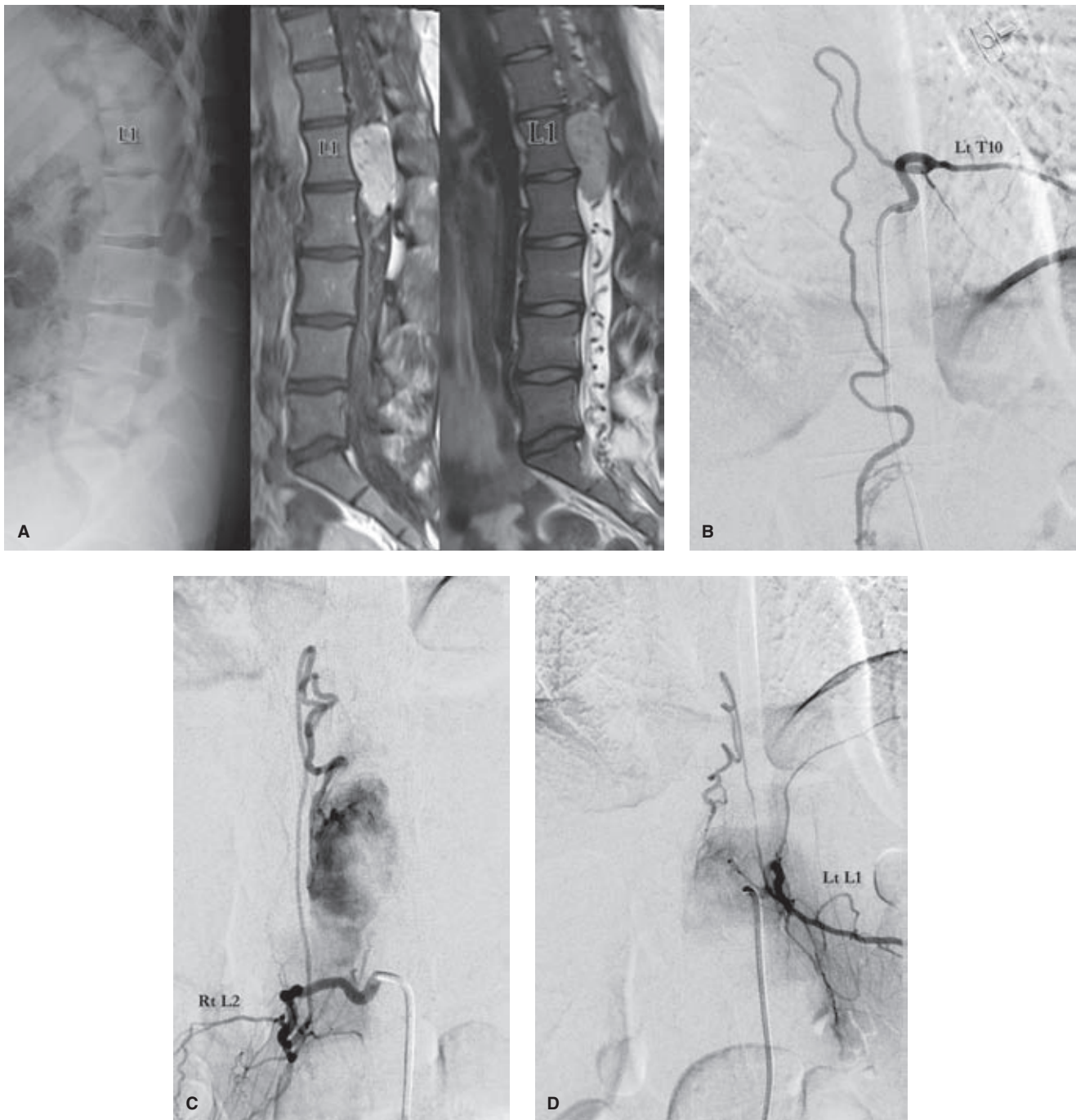


FIGURE 21-9. (A–D) Spinal hemangioblastoma presenting with bladder dysfunction and paraparesis. A young adult presented with precipitate decline of spinal function and back pain over a period of some weeks. Her MRI examination (A) showed an enhancing mass where the plain film demonstrated scalloping and remodeling of the posterior margin of L1. A profusion of large vessels in the canal raised the question of a spinal AVM, but the solid appearing nature of the lesion favored a hypervascular tumor. Preoperative angiography (images B–D) showed numerous enlarged arterial feeders from the anterior spinal artery (B) and posterior spinal arteries (D). The artery at right L2 was a little more difficult to analyze at first glance, but two factors classify it as an anterior spinal artery. Firstly, the ascending loop of the hairpin extends over three full vertebral body heights, very unusual for a posterior spinal artery. Secondly, careful review of the images showed that the inferior reaches of this vessel connected with those of the left T10 injection, forming a rete on the periphery of the tumor.

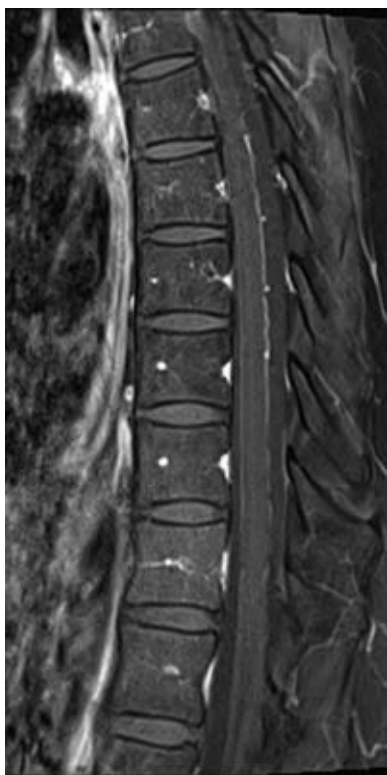


FIGURE 21-10. Normal MRI. Occasionally in a young patient who remains exceptionally still during an MRI examination, the conspicuity of normal vessels can be remarkable, as in this case. The distinguishing features from those of a patient with venous hypertension of the cord include the clinical history, absence of cord expansion or enhancement, absence of T2 signal hyperintensity within the cord, and a general *gestalt* of absence of tension (tortuosity) within the veins. Sometimes it can be difficult, but more generally the problem is not false-positive interpretation of normal MRIs, but rather the blurring of pathologic MRIs by patient motion and restlessness.

enlargement of the perimedullary veins, cord edema, and progressive myelomalacia. The MRI appearance is one of prominently enlarged, enhancing intrathecal vessels, cord T2 hyperintensity, cord enhancement, and a variable appearance of mass effect within the cord (19).

Although most spinal dural arteriovenous fistulas are centered primarily within the spinal dura, epidural and intradural variants are seen occasionally (3,20,21). Fistulas form at the points where arterioles pierce the dura mater in close relation to dural veins and can occur at any level from the foramen magnum to the sacrum (22). The malformation or fistula forms most commonly near the intervertebral foramen along the dural sleeve of a nerve root. The fistula is most commonly, but not always, located on the dorsal aspect of the nerve root near the axilla of the dural sleeve.

Intracranial dural arteriovenous malformations with restricted venous egress draining to the spinal veins can give an identical clinical presentation due to venous hypertension and edema of the spinal cord. Therefore, the intracranial vessels are included in the evaluation of patients with suspected spinal dural arteriovenous malformations (23,24). Similarly, the internal iliac arteries are included to evaluate the sacral nerve roots (24) (Figs. 21-11 and 21-12, 3-2).

Microangiographic studies of the most common type of dural arteriovenous malformation by McCutcheon et al. (25) demonstrate that the lesion is usually a true arteriovenous

fistula with one or two arterial feeders and a single draining medullary vein. Occasionally, the site of the shunt may be intradural or extradural (26). Venous drainage may also involve the epidural venous plexus in a supplementary or exclusive manner (27–29). Paravertebral or pelvic vascular tumors, posttraumatic fistulous injuries, and other conditions with arteriovenous shunting or high flow may connect to the medullary veins, causing a radiographic and clinical presentation similar to that seen with dural vascular malformations (30–32).

Clinical Manifestations of Spinal Venous Hypertension and Dural Vascular Disease

It is a singular observation how minuscule and slow a spinal dural fistula may be in relation to the advanced incapacitation of the patient. The potential for clinical deterioration with such a small fistula rests in the relative physiologic restriction of venous outflow from the pial plexus. This restriction limits the ability of the system to adapt to the pathologically increased state of venous flow. The veins of the spine normally drain out of the dural sac by a limited number of medullary centrifugal veins.

With increasing pressure and distention of the spinal veins, a decrease in the arteriovenous gradient of the spinal circulation takes place. Circulation time becomes prolonged. The effects of such an altered gradient are maximal at the farthest reach of the circulation, that is, the conus (Fig. 21-13). Therefore, patients will present with symptoms of a conal syndrome, although their fistulas may be remote from the conus.

Rare cases of paravertebral fistulas with exclusively epidural venous drainage have been described in which the pial plexus is of normal pressure and caliber. In these instances, the symptoms of the fistula may be caused by compression of the cord or nerve roots by distended, tense epidural vessels (29,33).

A shared feature of both dural and intradural arteriovenous malformations is the presence of distended draining subarachnoid veins on myelographic images. Publications describing spinal vascular diseases before the advent of selective spinal arteriography were therefore imprecise in terminology. Spinal dural arteriovenous malformations are epidemiologically, pathophysiologically, anatomically, and clinically distinguishable from parenchymal arteriovenous malformations of the spine. Patients with spinal dural arteriovenous fistulas present in late middle age or older (>40 years) and are more often male. They frequently have a history of progressive decline in gait, sensory function, strength, and loss of bladder and bowel control. Paresthesiae and subjective sensations of spasm in affected limbs are common, and muscle wasting with fasciculation is frequently seen (3). Patients frequently demonstrate an unusual clinical phenomenon whereby they deteriorate after administration of steroids, possibly due to effects of the intravascular blood volume (34). Hemorrhage into the epidural or subarachnoid spaces from a spinal dural arteriovenous fistula is rare. Symptoms may be aggravated by activity, although this is not constant. The period of decline can range from a few months to 2 to 3 years. They can have a more rapid deterioration over some weeks, but it usually does not have the saltatory, episodic quality seen with intranidal hemorrhage of parenchymal arteriovenous malformations (35,36). Frequently, patients with advanced

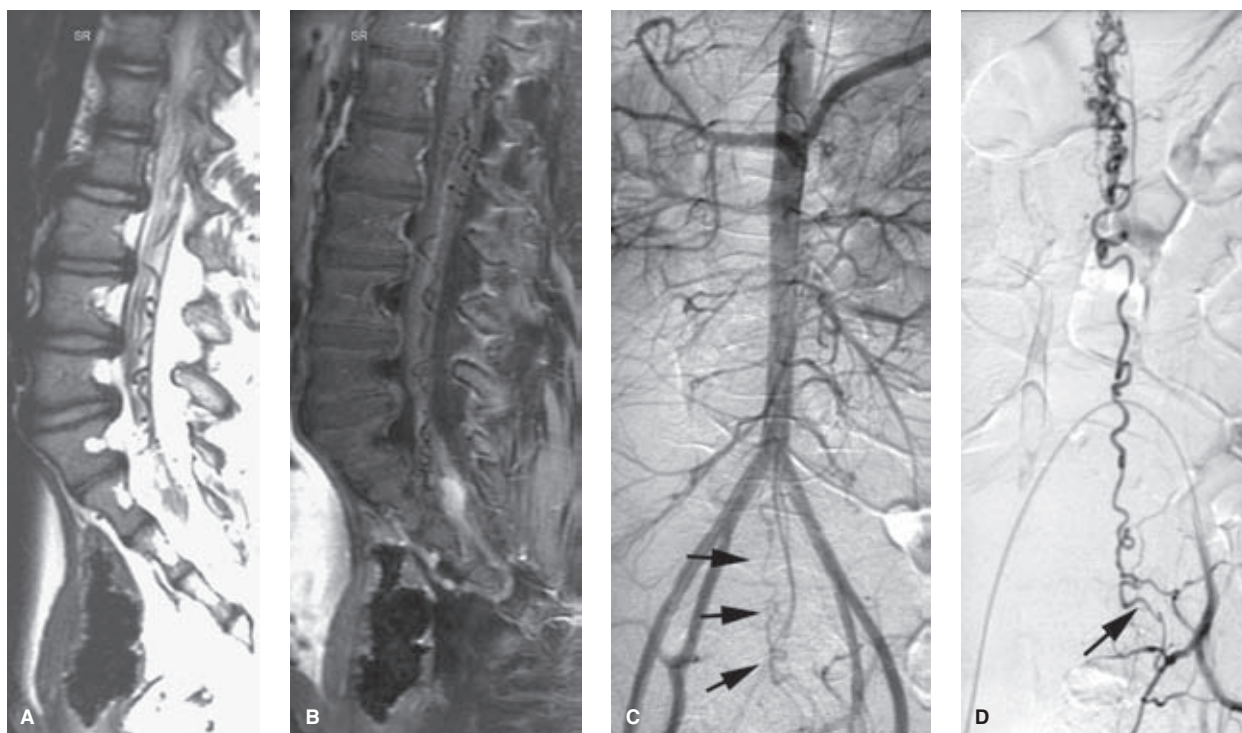


FIGURE 21-11. (A–D) Sacral dural A-V fistula. A 7-year-old boy with Proteus syndrome suffered rapidly progressive deterioration of gait and sensory disturbance over several weeks, and an MRI examination showed abnormal flowing vessels on the surface of the cord. The sagittal T2 image (A) and T1 image with gadolinium (B) show syndromic scalloping of the vertebral bodies, a tethered cord that had been previously operated on, and a lipoma of the filum terminale, in addition to several tortuous intrathecal vessels. A diagnosis of spinal dural AVF was suggested, and a spinal angiogram was planned. Fortunately, the volume of contrast for the procedure did not become a problem (34 mL total), and the lesion was seen on the initial aortogram (arrows in C) as a fistula from the left lateral sacral artery from the left internal iliac artery. The selective injection of the offending artery (D) is a cumulative image over an entire run for the purposes of illustration, with the fistula indicated (arrow) at the point of caliber change between the artery and vein. A single 25% NBCA injection via a microcatheter permanently eliminated the fistula, with a satisfactory recovery by the patient.

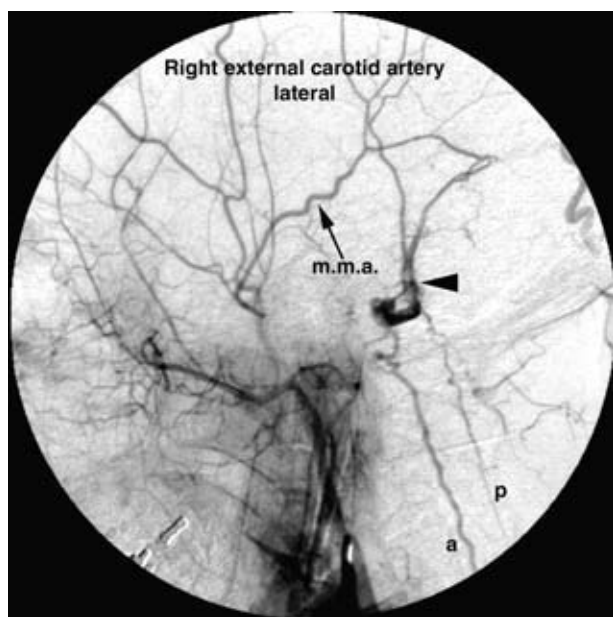


FIGURE 21-12. Intracranial dural arteriovenous malformation presenting with a myelopathic syndrome. A lateral view of the right external carotid artery injection performed at the end of a complete spinal angiogram in a middle-aged patient complaining of lower extremity weakness and MRI findings suggesting venous hypertension of the cord. A tiny dural fistula (arrowhead) from the distal middle meningeal artery (m.m.a.) is seen along the right sigmoid sinus draining into a restricted venous compartment. This results in distention of the anterior (a) and posterior spinal vein (p), causing the patient's symptoms.

symptoms may spontaneously report a sensory level below which sensation is dulled. Hyperesthesia may be experienced as the disease process ascends along the trunk. Formerly, such a subacute myelopathy would have been termed *Foix–Alajouanine syndrome* (35,37). This syndrome was described as a progressive myelopathy and was thought to be due to vascular thrombosis. However, in this context, the term is imprecise and not commonly used.

Because the MRI and myelographic signs can be subtle and symptoms of dural vascular disease can be similar to more common conditions such as degenerative disc disease or spinal stenosis, these patients frequently are misdiagnosed. By the time of final angiographic diagnosis, they often have had multiple imaging studies, myelograms, and even surgical procedures for symptoms of presumed spinal stenosis, disc compression, or spinal tumor. Myelography is sometimes insensitive to the presence of the serpentine intrathecal vessels, which are the hallmark of this disease. MRI is the most sensitive noninvasive test for diagnosing dural vascular disease. MRI demonstrates high T2 signal and patchy gadolinium enhancement in the conus, ascending in the cord. Gadolinium enhancement also accentuates the conspicuousness of distended venous structures. T2-weighted images and gadolinium-enhanced images demonstrate a characteristic pattern of serpentine vessels more numerous along the posterior aspect of the cord. However, motion artifact or too large a field of view will reduce the sensitivity of MRI to this disease.

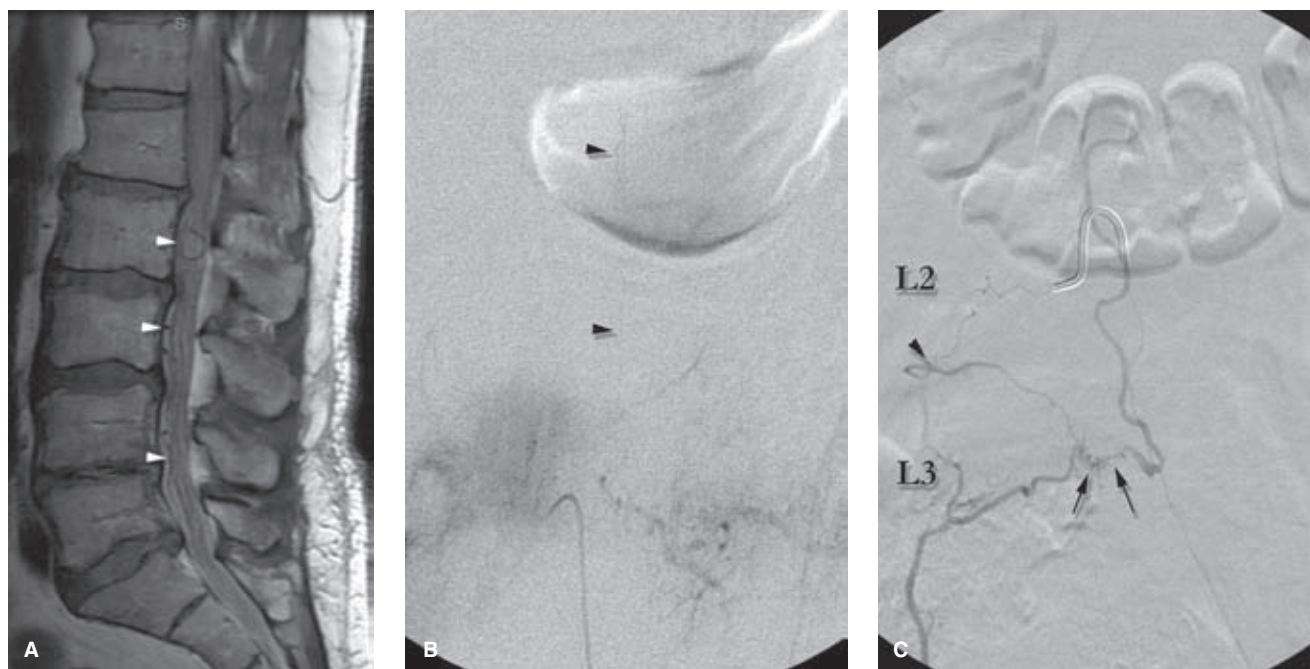


FIGURE 21-13. (A–C) Spinal dural AVF in a postsurgical spine. This unfortunate case of a middle-aged patient who lost a great deal of spinal function due to a SdAVF illustrates several lessons. Firstly, even though the patient was presenting with a postoperative spine for MRI, it is important to remain vigilant for this diagnosis in all spinal MRI examinations. The preoperative MRI in retrospect showed many of the findings of venous distension and cord expansion (*arrowheads* in A) evident in the postoperative MRI. Secondly, the findings on the spinal angiogram at right L1 (B) are important because they are so difficult to see. The A-V gradient of the anterior spinal axis was so greatly altered in this patient that only minimal opacification of his anterior spinal artery was possible. Moreover, the little contrast that did enter the anterior spinal artery lingered there for much longer than would be normally expected (*arrowheads* in B). This is an important sign to watch for during spinal angiograms for suspected SdAVF. An abnormally prolonged stain of the anterior spinal artery can be a good spur to keep searching during a long and difficult study because it confirms the suspicions raised by the previous studies as well grounded. The magnified images at right L2 in this patient (C) illustrate the archetypal anatomy of these lesions. The injection of right L2 via a microcatheter (*arrowhead*) opacifies the adjacent right L3 pedicle that is feeding the lesion. The fistula typically has a speckled or rete appearance (*arrows*) just before the caliber change into a single draining vein.

Treatment of Spinal Dural Arteriovenous Malformations

Early surgical techniques for patients with spinal dural arteriovenous fistulas sometimes involved stripping an extended segment of vein from the spinal cord. This technique inherently involved a risk of depriving the cord of its normal venous drainage. Therefore, the results were not favorable. Selective surgical clipping or cauterization of the single draining medullary vein identified at spinal angiography is the current treatment of choice (36,38), particularly as it is not always easy to penetrate the tiny dural fistula with permanently occlusive embolic material, even with Onyx. Depending on the degree and duration of preoperative decline, patients have variable prospects for recovery of premorbid function.

Given the tedious and protracted nature of spinal arteriography needed to identify a single, tiny offending fistula, there is a strong desire to derive a double benefit from this procedure by combining it with therapeutic embolization. If successful, this can avoid the need for surgery and its attendant morbidity. However, to be effective, the embolization needs to be permanent and safe without occluding the anterior or posterior spinal arteries. Early embolization techniques of spinal dural arteriovenous malformations using particulate matter such as polyvi-

nyl alcohol, muscle fragments, or collagen were effective only in the short term (Figs. 21-14 and 21-15). After initial clinical improvement, patients experienced relapse after 2 to 8 months. Recanalization was seen at repeat angiography in most cases following use of these agents. Embolization with liquid acrylate or Onyx carries the possibility of permanent sclerosis of the draining medullary vein in 70% or more of selected cases (39–44). Propinquity of spinal arteries precluding embolization or capricious behavior of the acrylate gives a success rate for embolization somewhat less than that of surgery. However, when appended to a planned diagnostic procedure or as an interventional procedure with surgery as a fallback in the event of failure, it is a worthwhile undertaking. In situations where embolization is avoided due to the presence of dangerous connections, a radiographically dense coil can be placed in the feeding pedicle as a fluoroscopic landmark for subsequent surgery.

Concern about recanalization of the fistula should be prompted when a patient does not improve clinically after embolization or surgery. Transient improvement followed by relapse may also indicate that recanalization has taken place. Prompt repeat angiography is indicated for these patients. Rare cases of synchronous or metachronous anatomically separate lesions have been described (45).

(text continues on page 366)

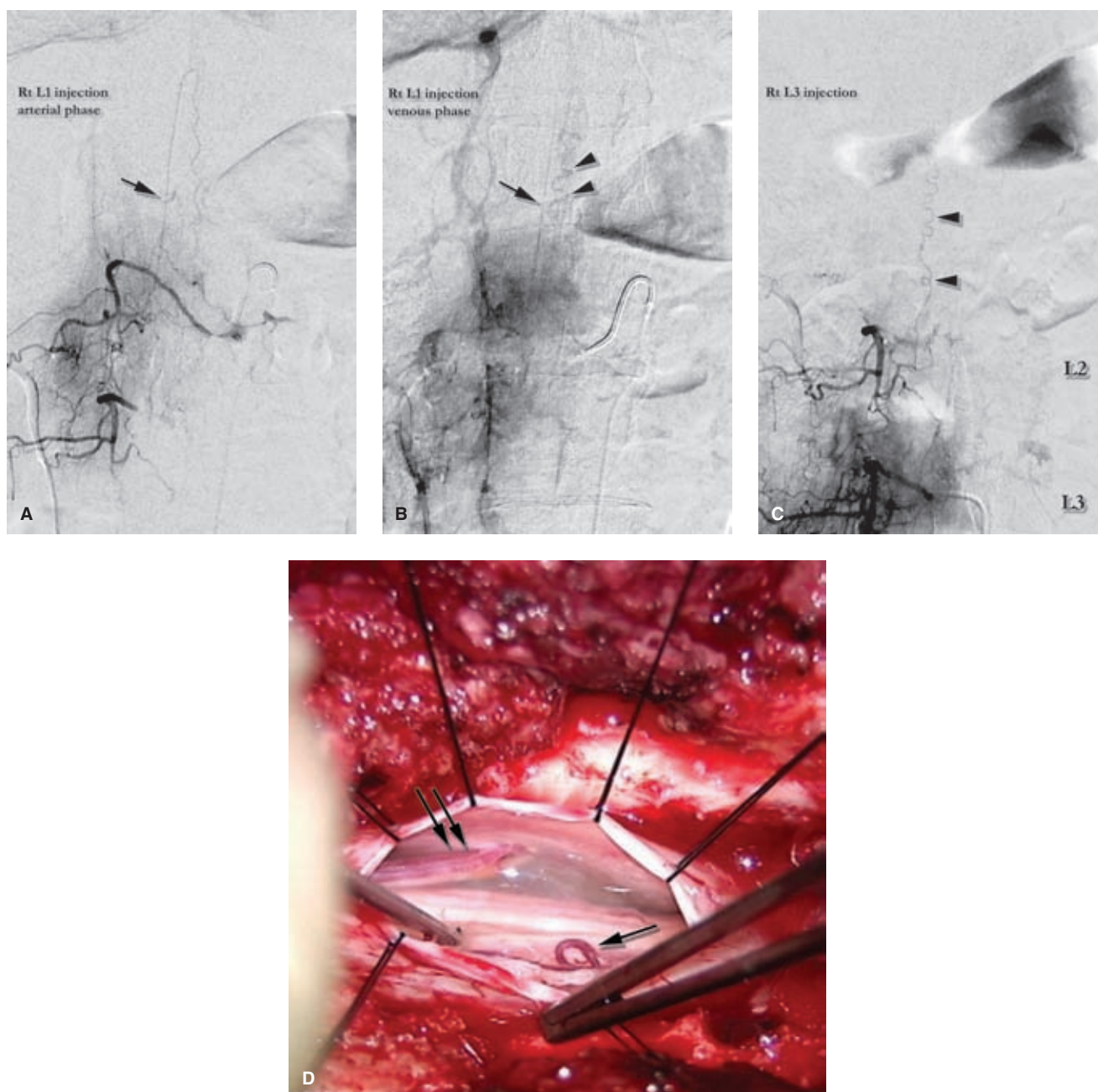


FIGURE 21-14. (A–D) Spinal dural AVF immediately adjacent to an anterior spinal artery. The selected images from this case illustrate several important points in the angiographic evaluation of SdAVF patients. The right L1 injection (A) opacifies the adjacent right L2 pedicle (which turned out to be hemodynamically compromised at its origin from the aorta). There is also opacification of an anterior spinal artery (*arrow* in A) from right L1 on the arterial image. Later in the venous phase of right L1 (B) there is sustained abnormal opacification of the anterior spinal artery (see discussion for Fig. 21-13) indicating the abnormal A-V gradient in the anterior spinal axis. There is also late opacification of an abnormal vein (*arrowheads* in B) suspicious for unsatisfactory opacification of the expected abnormality. The right L2 injection (not shown) was technically unsatisfactory due to poor opacification from stenosis. The right L3 injection (C) showed the abnormality again (*arrowheads*) as arising from the elusive right L2 level again filled through collateral routes. A still image (D) from the intraoperative video (patient's head on reader's left) shows the opened dura with a prominent arterialized vein (*single arrow*) immediately inside the thecal sac. The vein draining cephalad from the fistula (i.e., the vein primarily the focus of surgical or therapeutic interest) is a little more difficult to see on this image (*double arrow*) as it emerges from the right lateral wall of the dura accompanying the right L2 nerve route ascending toward the conus.

The difficulties encountered with immediate propinquity of the anterior spinal artery in this case in close association with the fistula, the prolonged opacification of the anterior spinal artery, the fleeting glimpse of the fistula on its first view, and the inaccessibility of direction opacification of the fistula are all common problems in this patient population. *Video images kindly provided by John Wilson MD.*

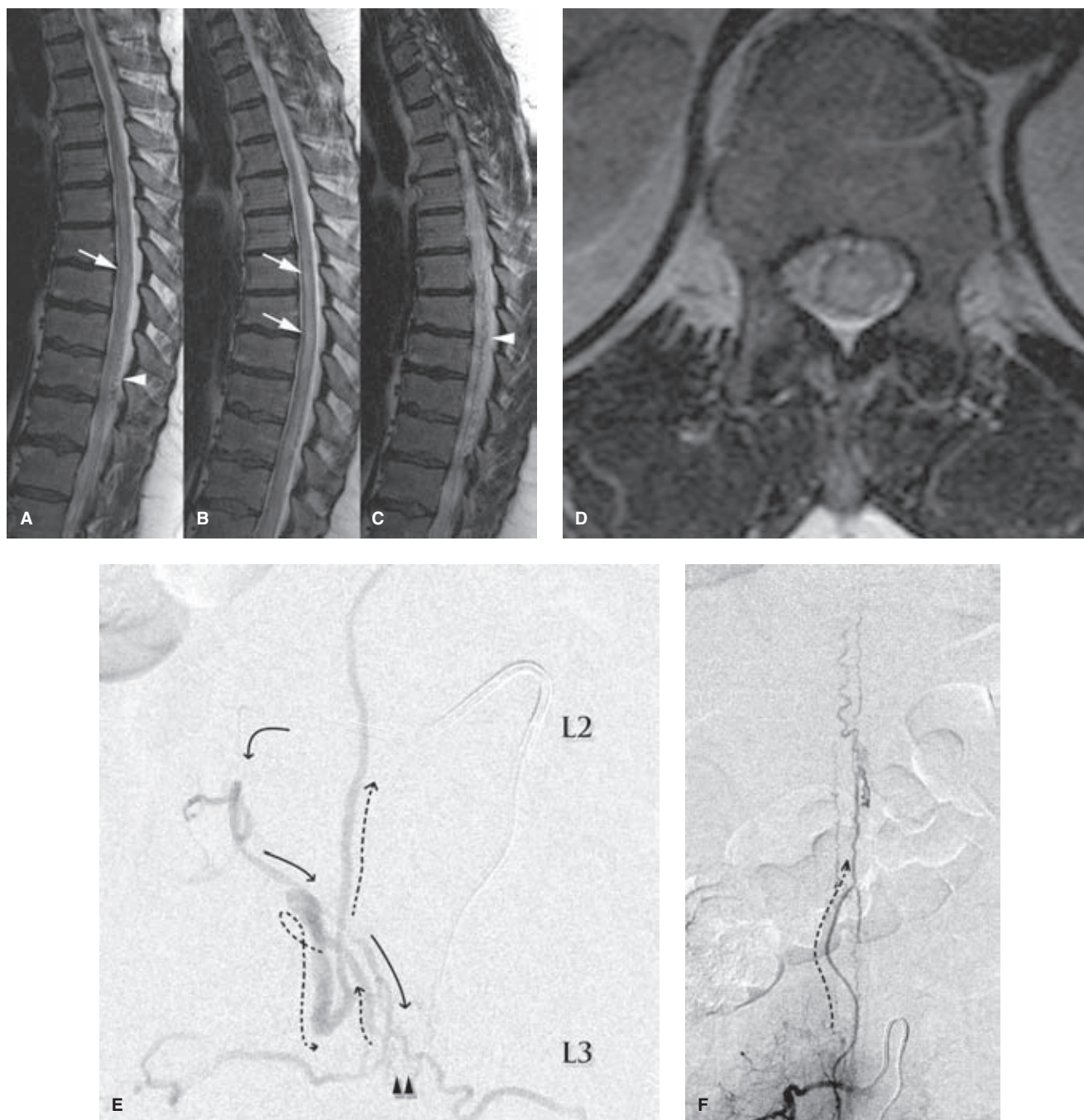


FIGURE 21-15. (A–F) Spectrum of findings in SdAVF. This case is selected to demonstrate firstly that the MRI findings in a clinically advanced case can be much more subtle than those in previous cases. Many spinal MRI examinations will be performed without gadolinium, leaving one to rely on detection of subtle T2 signal within the cord (arrows in **A**, **B**, and **C**), venous distension (arrowheads), or conus expansion (**D**). As was the case in Figure 21-14, direct injection of the fistula was not possible, and the abnormality at midline L3 was seen via the right L2 injection (**E**). The direction of arterial flow is indicated with solid arrows extending to the fistulous rete itself (double arrowheads) and thence the venous drainage to the cord traced with the broken arrows. Reflux into the compromised L3 arterial pedicles bilaterally is evident on this image too. A run performed from the same catheter position but with the imaging panel centered on the conus (**F**) demonstrates the pattern of venous opacification on the cord once the draining vein reaches the conus. Endovascular embolization of a fistula must penetrate adequately into the venous side to achieve a complete and reliable cure. This could extend anywhere along the intradural course of the offending vein, but penetration all the way up to and along the cord would be undesirable.

References

- Rodesch G, Hurth M, Alvarez H, et al. Classification of spinal cord arteriovenous shunts: Proposal for a reappraisal—The Bicêtre experience with 155 consecutive patients treated between 1981 and 1999. *Neurosurgery* 2002;51(2):374–379; discussion 379–380.
- Krings T, Thron AK, Geibprasert S, et al. Endovascular management of spinal vascular malformations. *Neurosurg Rev* 2010; 33(1):1–9.
- Rosenblum B, Oldfield EH, Doppman JL, et al. Spinal arteriovenous malformations: A comparison of dural arteriovenous fistulas and intradural AVM's in 81 patients. *J Neurosurg* 1987; 67(6):795–802.
- Biondi A, Merland JJ, Hodes JE, et al. Aneurysms of spinal arteries associated with intramedullary arteriovenous malformations. II. Results of AVM endovascular treatment and hemodynamic considerations. *AJNR Am J Neuroradiol* 1992;13(3): 923–931.
- Tomlinson FH, Rufenacht DA, Sundt TM Jr, et al. Arteriovenous fistulas of the brain and the spinal cord. *J Neurosurg* 1993;79(1):16–27.
- Kitagawa RS, Mawad ME, Whitehead WE, et al. Paraspinal arteriovenous malformations in children. *J Neurosurg Pediatr* 2009;3(5):425–428.
- Aminoff MJ, Logue V. The prognosis of patients with spinal vascular malformations. *Brain* 1974;97(1):211–218.
- Patsalides A, Knopman J, Santillan A, et al. Endovascular treatment of spinal arteriovenous lesions: Beyond the dural fistula. *AJNR Am J Neuroradiol* 2011;32(5):798–808.
- Suh TH, Alexander L. Vascular System of the human spinal cord. *Arch Neurol Psychiatry* 1939;41:659–677.
- Herren RY, Alexander L. Sulcal and intrinsic blood vessels of the human spinal cord. *Arch Neurol Psychiatry* 1939;41: 678–687.
- Pawlina W, Maciejewska I. Albert Wojciech Adamkiewicz 1850–1921. *Clin Anat* 2002;15(5):318–320.
- Adamkiewicz A. Die Blutgefäße des menschlichen Rückenmarkes II Theil. Die Gefäße der Rückenmarks-Oberflächens. *Sitzungsberichte der Kaiserlichen Akademie des Wissenschaften, Mathematisch-naturwissenschaftliche Classe* 1882; 85:101–130.
- Biondi A, Merland JJ, Reizine D, et al. Embolization with particles in thoracic intramedullary arteriovenous malformations: Long-term angiographic and clinical results. *Radiology* 1990; 177(3):651–658.
- Rodesch G, Hurth M, Alvarez H, et al. Embolization of spinal cord arteriovenous shunts: morphological and clinical follow-up and results—Review of 69 consecutive cases. *Neurosurgery* 2003;53(1):40–49; discussion 49–50.
- Kendall BE, Logue V. Spinal epidural angiomatous malformations draining into intrathecal veins. *Neuroradiology* 1977;13 (4):181–189.
- Tadie M, Helias A, Thiebot J, et al. Lumbar phlebography without catheterization. Technique, indications and results in the diagnosis of intervertebral disk herniation. *Rev Rhum Mal Osteoartic* 1979;46(11):601–605.
- Fried LC, Doppman JL, Di Chiro G. Venous phase in spinal cord angiography. *Acta Radiol Diagn (Stockh)* 1971;11(4): 393–401.
- Thron AK. *Vascular Anatomy of the Spinal Cord*. New York, NY: Springer-Verlag; 1988.
- Gilbertson JR, Miller GM, Goldman MS, et al. Spinal dural arteriovenous fistulas: MR and myelographic findings. *AJNR Am J Neuroradiol* 1995;16(10):2049–2057.
- Oldfield EH, Di Chiro G, Quindlen EA, et al. Successful treatment of a group of spinal cord arteriovenous malformations by interruption of dural fistula. *J Neurosurg* 1983;59(6): 1019–1030.
- Oldfield EH, Doppman JL. Spinal arteriovenous malformations. *Clin Neurosurg* 1988;34:161–183.
- Gaensler EH, Jackson DE Jr, Halbach VV. Arteriovenous fistulas of the cervicomedullary junction as a cause of myelopathy: Radiographic findings in two cases. *AJNR Am J Neuroradiol* 1990;11(3):518–521.
- Gobin YP, Rogopoulos A, Aymard A, et al. Endovascular treatment of intracranial dural arteriovenous fistulas with spinal perimedullary venous drainage. *J Neurosurg* 1992;77(5): 718–723.
- Partington MD, Rufenacht DA, Marsh WR, et al. Cranial and sacral dural arteriovenous fistulas as a cause of myelopathy. *J Neurosurg* 1992;76(4):615–622.
- McCutcheon IE, Doppman JL, Oldfield EH. Microvascular anatomy of dural arteriovenous abnormalities of the spine: A microangiographic study. *J Neurosurg* 1996;84(2):215–220.
- Arnaud O, Bille F, Pouget J, et al. Epidural arteriovenous fistula with perimedullary venous drainage: Case report. *Neuroradiology* 1994;36(6):490–491.
- Heier LA, Lee BC. A dural spinal arteriovenous malformation with epidural venous drainage: A case report. *AJNR Am J Neuroradiol* 1987;8(3):561–563.
- Cahan LD, Higashida RT, Halbach VV, et al. Variants of radiculomeningeal vascular malformations of the spine. *J Neurosurg* 1987;66(3):333–337.
- Willinsky R, terBrugge K, Montanera W, et al. Spinal epidural arteriovenous fistulas: arterial and venous approaches to embolization. *AJNR Am J Neuroradiol* 1993;14(4):812–817.
- Cognard C, Gobin YP, Pierot L, et al. Cerebral dural arteriovenous fistulas: clinical and angiographic correlation with a revised classification of venous drainage. *Radiology* 1995; 194(3):671–680.
- Han SS, Love MB, Simeone FA. Diagnosis and treatment of a lumbar extradural arteriovenous malformation. *AJNR Am J Neuroradiol* 1987;8(6):1129–1130.
- Kim DI, Choi IS, Berenstein A. A sacral dural arteriovenous fistula presenting with an intermittent myelopathy aggravated by menstruation. Case report. *J Neurosurg* 1991;75(6):947–949.
- Kohn M, Takahashi H, Ide K, et al. A cervical dural arteriovenous fistula in a patient presenting with radiculopathy. Case report. *J Neurosurg* 1996;84(1):119–123.
- Cabrera M, Paradis C, Marquez C, et al. Acute paraparesis following intravenous steroid therapy in a case of dural spinal arteriovenous fistula. *J Neurol* 2008;255(9):1432–1433.
- Symon L. Foix–Alajouanine syndrome. *Neurosurgery* 1990; 27(1):168–169.
- Symon L, Kuyama H, Kendall B. Dural arteriovenous malformations of the spine. Clinical features and surgical results in 55 cases. *J Neurosurg* 1984;60(2):238–247.
- Crisuolo GR, Oldfield EH, Doppman JL. Reversible acute and subacute myelopathy in patients with dural arteriovenous fistulas. Foix–Alajouanine syndrome reconsidered. *J Neurosurg* 1989;70(3):354–359.
- Saladino A, Atkinson JL, Rabinstein AA, et al. Surgical treatment of spinal dural arteriovenous fistulae: A consecutive series of 154 patients. *Neurosurgery* 2010;67(5):1350–1357; discussion 1357–1358.
- Warakaulle DR, Aviv RI, Niemann D, et al. Embolisation of spinal dural arteriovenous fistulae with Onyx. *Neuroradiology* 2003;45(2):110–112.

40. Song JK, Gobin YP, Duckwiler GR, et al. *N*-butyl 2-cyanoacrylate embolization of spinal dural arteriovenous fistulae. *AJNR Am J Neuroradiol* 2001;22(1):40–47.
41. Niimi Y, Berenstein A, Setton A, et al. Embolization of spinal dural arteriovenous fistulae: Results and follow-up. *Neurosurgery* 1997;40(4):675–682; discussion 682–673.
42. Nogueira RG, Dabus G, Rabinov JD, et al. Onyx embolization for the treatment of spinal dural arteriovenous fistulae: Initial experience with long-term follow-up. Technical case report. *Neurosurgery* 2009;64(1):E197–E198; discussion E198.
43. Schmidt C, Lonjon J, Costalat V, et al. Paraspinal arteriovenous malformations with perimedullary venous drainage. *J Neuroradiol* 2008;35(3):165–172.
44. Sivakumar W, Zada G, Yashar P, et al. Endovascular management of spinal dural arteriovenous fistulas. A review. *Neurosurg Focus* 2009;26(5):E15.
45. Pierot L, Vlachopoulos T, Attal N, et al. Double spinal dural arteriovenous fistulas: Report of two cases. *AJNR Am J Neuroradiol* 1993;14(5):1109–1112.

Pediatric Ischemic Stroke and Arteriopathy

Key Points

- The spectrum of transient or progressive cerebral arteriopathy of childhood may not be familiar to those with a predominantly adult-based practice.
- Intracranial dissection is a potentially fatal condition in the differential diagnosis for childhood stroke that can mimic angiographically the more benign condition of focal cerebral arteriopathy (FCA).

Pediatric stroke, ischemic or hemorrhagic, is no longer considered to be a rare disease with a recognized incidence of 2 to 6/100,000 (1). The risk factors and epidemiology of pediatric stroke differ from those of the adult population, with some particular phenomena evident on imaging that have substantial bearing on the likely prognosis and risk of recurrence. Furthermore, pediatric stroke has well-recognized associations with several syndromic disorders that have other imaging features that warrant specific evaluation during noninvasive and angiographic imaging.

► PERINATAL STROKE

Pediatric stroke is considered in two time periods, perinatal and late childhood. Perinatal stroke occurs between 20 weeks of fetal life and the 28th postnatal day, and has an incidence of about 1/4,000 births (1,2). Risk factors include any causes of chorioamnionitis, premature membrane rupture, cardiac anomalies, and birth asphyxia (3,4). Venous sinus compression and thrombosis have an association with maternal or fetal factor V Leiden, antiphospholipid antibody activity, and protein C deficiency. Arteriopathy is considered rare in this subgroup, and catheter angiographic evaluation is rarely warranted.

► CHILDHOOD STROKE

The risk factors for childhood stroke demonstrate significant genetic and geographic variabilities, and broadly speaking include trauma, infection, arteriopathy (abnormal looking vessels of any cause), cardiac anomalies, prothrombotic conditions, and rarer genetic conditions including Menke's disease, Fabry's disease, and incontinentia pigmenti (4).

Stroke accounts for approximately 10% of childhood mortality in some series, and has substantial impacts on cognitive and psychomotor development, particularly if it is recurrent. Childhood strokes also have a greater propensity to present with seizure than is the case with adults.

Congenital cardiac anomalies account for between 20% and 40% of childhood strokes (5). The remaining 60% to 80% demonstrate an abnormal appearance of the intracranial or extracranial vessels, generically termed "arteriopathy" (6,7). It is in the parsing of the latter group that imaging and angiography can play an important role.

► PEDIATRIC CEREBRAL ARTERIOPATHY

In most series, some form of arteriopathy will be demonstrated in the dominant majority (80%) of pediatric patients with childhood stroke. The most commonly recognized entities are *Focal Cerebral Arteriopathy of Childhood* (also termed *Transient Cerebral Arteriopathy*) (8,9), arterial dissection, primary Moya-Moya disease particularly in Asian populations in whom it can account for a majority of cases of arteriopathy, and Moya-Moya syndrome secondary to other entities discussed below.

Focal Cerebral Arteriopathy (FCA) accounts for approximately half of all stroke related to arterial abnormalities in the pediatric group, and is itself a heterogeneous group (Fig. 22-1). Most cases are ascribed to an immunologic reaction to antecedent varicella infection (10–12), or other infections such as Lyme disease or enterovirus (13). FCA is defined as a unilateral, nonprogressive, somewhat localized vasculopathy, usually confined to the region of the carotid terminus and its major branches. It most commonly presents with ischemic complications of lenticulostriate compromise, or ipsilateral hemispheric watershed infarctions. It generally runs its course in 1 to 3 months and most patients (75%) recover well (14). Due to its presumed immunologic basis, it may represent a transient or localized form of primary angitis of the central nervous system, although this is debated. Focal or transient arteriopathy is discerned from the 25% of patients who demonstrated signs at presentation or develop subsequent more diffuse findings suggesting the presence of *Progressive Arteriopathy of Childhood*. Progressive arteriopathy is associated with a worse prognosis and outcome, due to a recurrent and worsening clinical pattern of strokes.

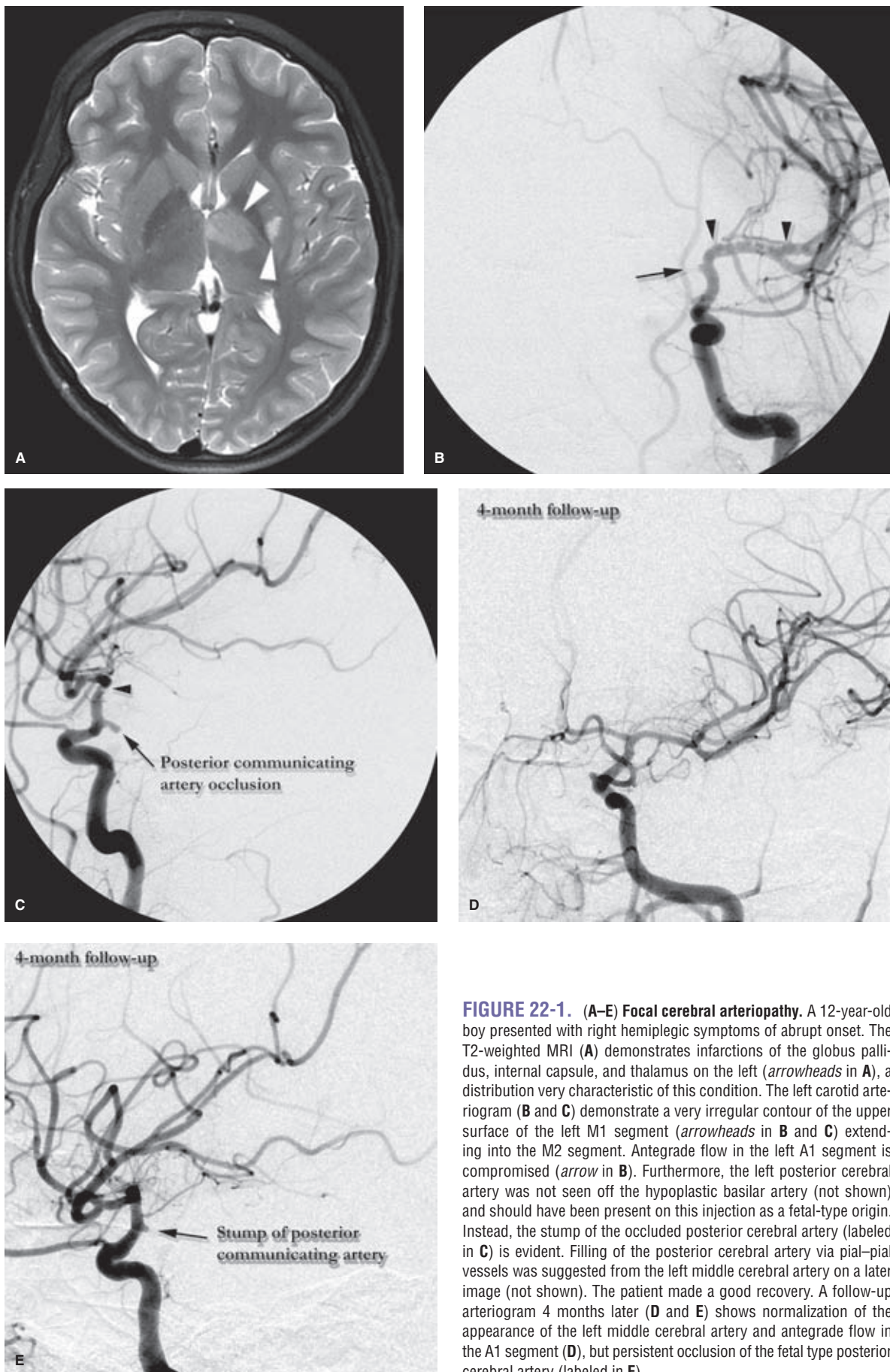


FIGURE 22-1. (A–E) Focal cerebral arteriopathy. A 12-year-old boy presented with right hemiplegic symptoms of abrupt onset. The T2-weighted MRI (**A**) demonstrates infarctions of the globus pallidus, internal capsule, and thalamus on the left (*arrowheads* in **A**), a distribution very characteristic of this condition. The left carotid arteriogram (**B** and **C**) demonstrate a very irregular contour of the upper surface of the left M1 segment (*arrowheads* in **B** and **C**) extending into the M2 segment. Antegrade flow in the left A1 segment is compromised (*arrow* in **B**). Furthermore, the left posterior cerebral artery was not seen off the hypoplastic basilar artery (not shown) and should have been present on this injection as a fetal-type origin. Instead, the stump of the occluded posterior cerebral artery (labeled in **C**) is evident. Filling of the posterior cerebral artery via pial–pial vessels was suggested from the left middle cerebral artery on a later image (not shown). The patient made a good recovery. A follow-up arteriogram 4 months later (**D** and **E**) shows normalization of the appearance of the left middle cerebral artery and antegrade flow in the A1 segment (**D**), but persistent occlusion of the fetal type posterior cerebral artery (labeled in **E**).

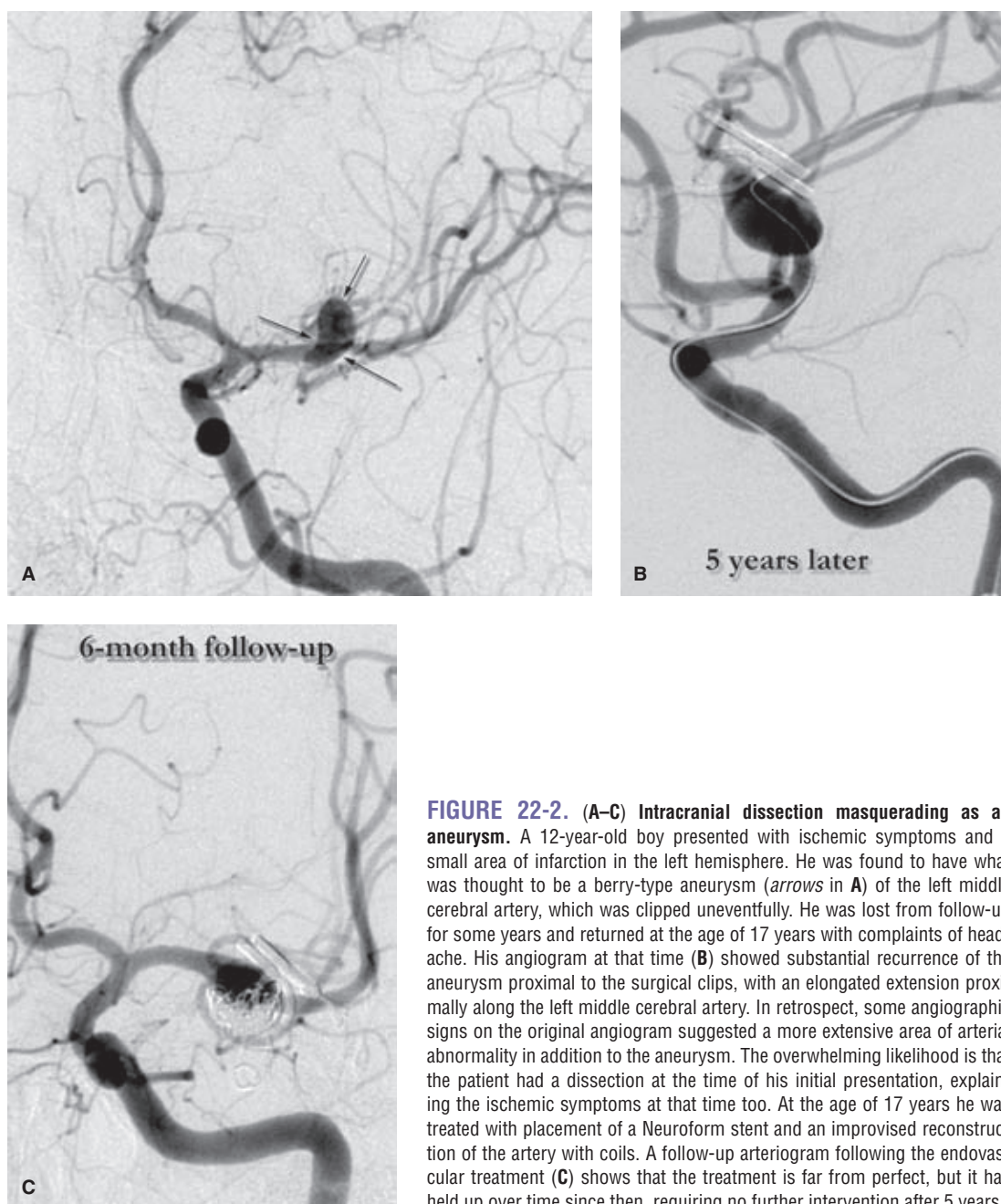


FIGURE 22-2. (A–C) Intracranial dissection masquerading as an aneurysm. A 12-year-old boy presented with ischemic symptoms and a small area of infarction in the left hemisphere. He was found to have what was thought to be a berry-type aneurysm (arrows in A) of the left middle cerebral artery, which was clipped uneventfully. He was lost from follow-up for some years and returned at the age of 17 years with complaints of headache. His angiogram at that time (B) showed substantial recurrence of the aneurysm proximal to the surgical clips, with an elongated extension proximally along the left middle cerebral artery. In retrospect, some angiographic signs on the original angiogram suggested a more extensive area of arterial abnormality in addition to the aneurysm. The overwhelming likelihood is that the patient had a dissection at the time of his initial presentation, explaining the ischemic symptoms at that time too. At the age of 17 years he was treated with placement of a Neuroform stent and an improvised reconstruction of the artery with coils. A follow-up arteriogram following the endovascular treatment (C) shows that the treatment is far from perfect, but it has held up over time since then, requiring no further intervention after 5 years.

Sometimes it is not possible on the first angiogram to be specific in the diagnosis of FCA, and a second study at a second time point after 6 months may be necessary. Early Moya-Moya disease may present initially with unilateral findings. Particular caution is warranted not to overlook the possibility of intracranial dissection which can easily mimic and imaging findings of FCA.

Intracranial Dissection is a well-recognized disease of childhood, accounting for approximately 10% of non-cardiac-related strokes (Figs. 22-2). It seems to have a higher association in younger children with trauma, including child abuse, whereas in older children, it may be seen following normal effortful behavior, similar to the presentation in young adults. It seems questionable to include dissection with the category of nonprogressive arteriopathy, but it is likely that

most dissections heal spontaneously. Some, however, can present with or progress to intracranial occlusions or rupture with pseudoaneurysm formation. Complicated intracranial dissection tends to have a poor prognosis and can be initially diagnosed as more benign FCA (15).

Progressive Cerebral Arteriopathy of Childhood encompasses the 25% of pediatric stroke patients who have disease more extensive than FCA and who generally tend to have a high likelihood of stroke recurrence and neurologic impairment. Chief among these entities are primary Moya-Moya disease, and secondary Moya-Moya syndromes due to sickle cell disease (16,17), previous brain irradiation (18), neurofibromatosis type 1 (4), neurofibromatosis type 2, hemolytic-uremic syndrome, Down syndrome (19–21), and even rarer entities such as PHACES (posterior fossa abnormalities,

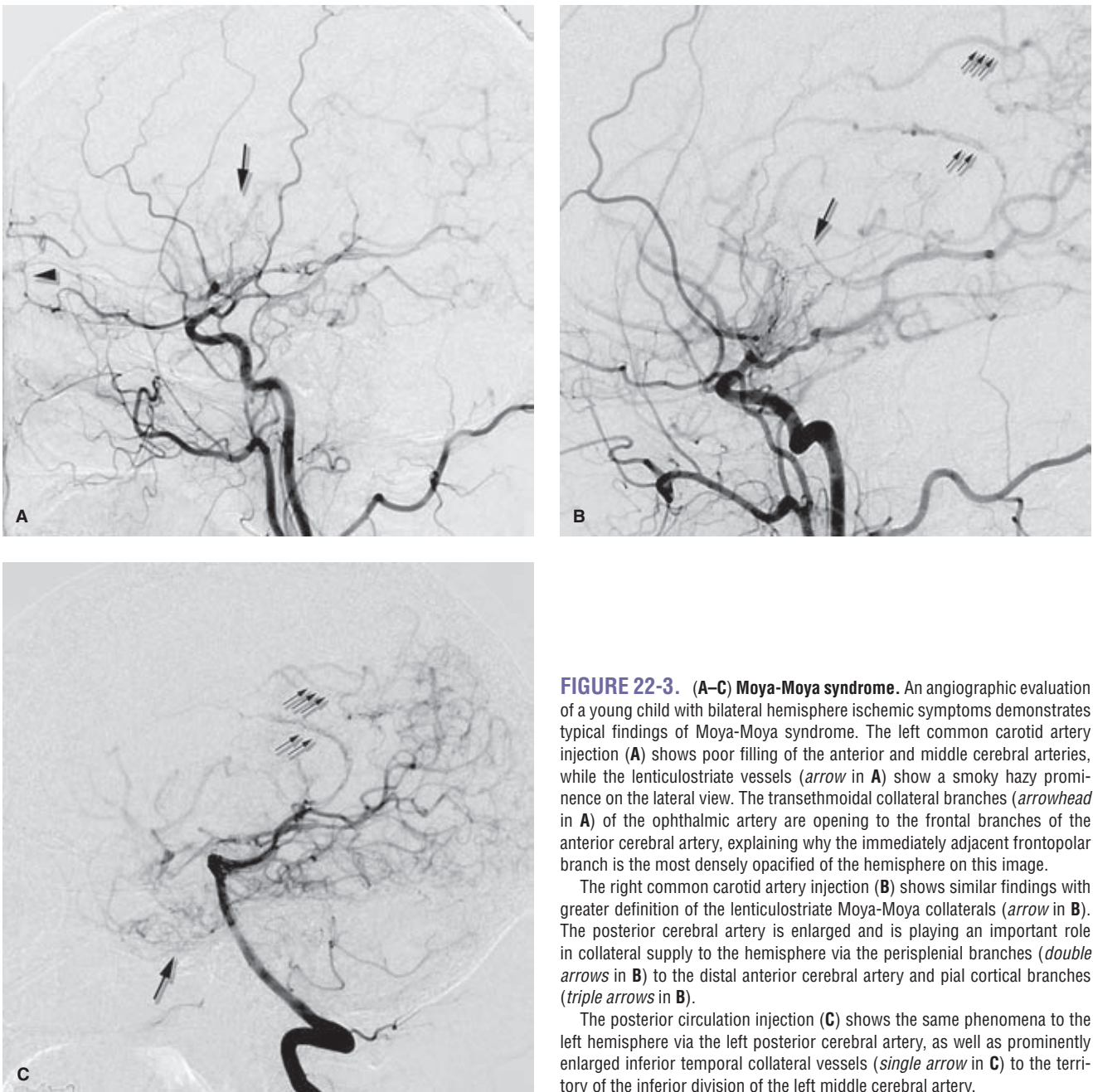


FIGURE 22-3. (A–C) Moya-Moya syndrome. An angiographic evaluation of a young child with bilateral hemisphere ischemic symptoms demonstrates typical findings of Moya-Moya syndrome. The left common carotid artery injection (**A**) shows poor filling of the anterior and middle cerebral arteries, while the lenticulostriate vessels (*arrow* in **A**) show a smoky hazy prominence on the lateral view. The transthemoidal collateral branches (*arrowhead* in **A**) of the ophthalmic artery are opening to the frontal branches of the anterior cerebral artery, explaining why the immediately adjacent frontopolar branch is the most densely opacified of the hemisphere on this image.

The right common carotid artery injection (**B**) shows similar findings with greater definition of the lenticulostriate Moya-Moya collaterals (*arrow* in **B**). The posterior cerebral artery is enlarged and is playing an important role in collateral supply to the hemisphere via the perisplenial branches (*double arrows* in **B**) to the distal anterior cerebral artery and pial cortical branches (*triple arrows* in **B**).

The posterior circulation injection (**C**) shows the same phenomena to the left hemisphere via the left posterior cerebral artery, as well as prominently enlarged inferior temporal collateral vessels (*single arrow* in **C**) to the territory of the inferior division of the left middle cerebral artery.

hemangiomas, arterial anomalies, cardiac anomalies, coarctation, eye abnormalities, sternal defects) (22), Robinow syndrome (23), and Seckel syndrome (24,25).

► MOYA-MOYA DISEASE AND SYNDROME

Moya-Moya disease is a rare condition characterized by idiopathic, progressive, occlusive disease of the terminal carotid arteries and major branches. It was first described in Japan (26,27) where its incidence is approximately $\times 10$ that seen in the United States and Europe. Approximately 12% of cases are familial. Early in the disease course, overgrowth of the lenticulostriate and anterior thalamoperforator collateral vessels leads to the characteristic hazy appearance from which the name “Moya-Moya” from the Japanese is derived

(Figs. 22-3 and 22-4). The angiographic stages of Moya-Moya are described in the Japanese literature as having a typical progression beginning with narrowing of the carotid artery, development of Moya-Moya collaterals, growth of ethmoidal collaterals from the ophthalmic artery, hyperplasia of dural collateral vessels, and finally disappearance of the original Moya-Moya collaterals with complete closure of the carotid arteries (28).

The primary form of the disease presents in two age groups, childhood around the age of 5 years and patients in their mid-40s (29). Left untreated, the disease is progressive in at least two thirds of patients (30–32). Among those with unilateral presentation, at least 40% develop bilateral changes (21). Approximately 25% involve the posterior cerebral arteries in later stages.

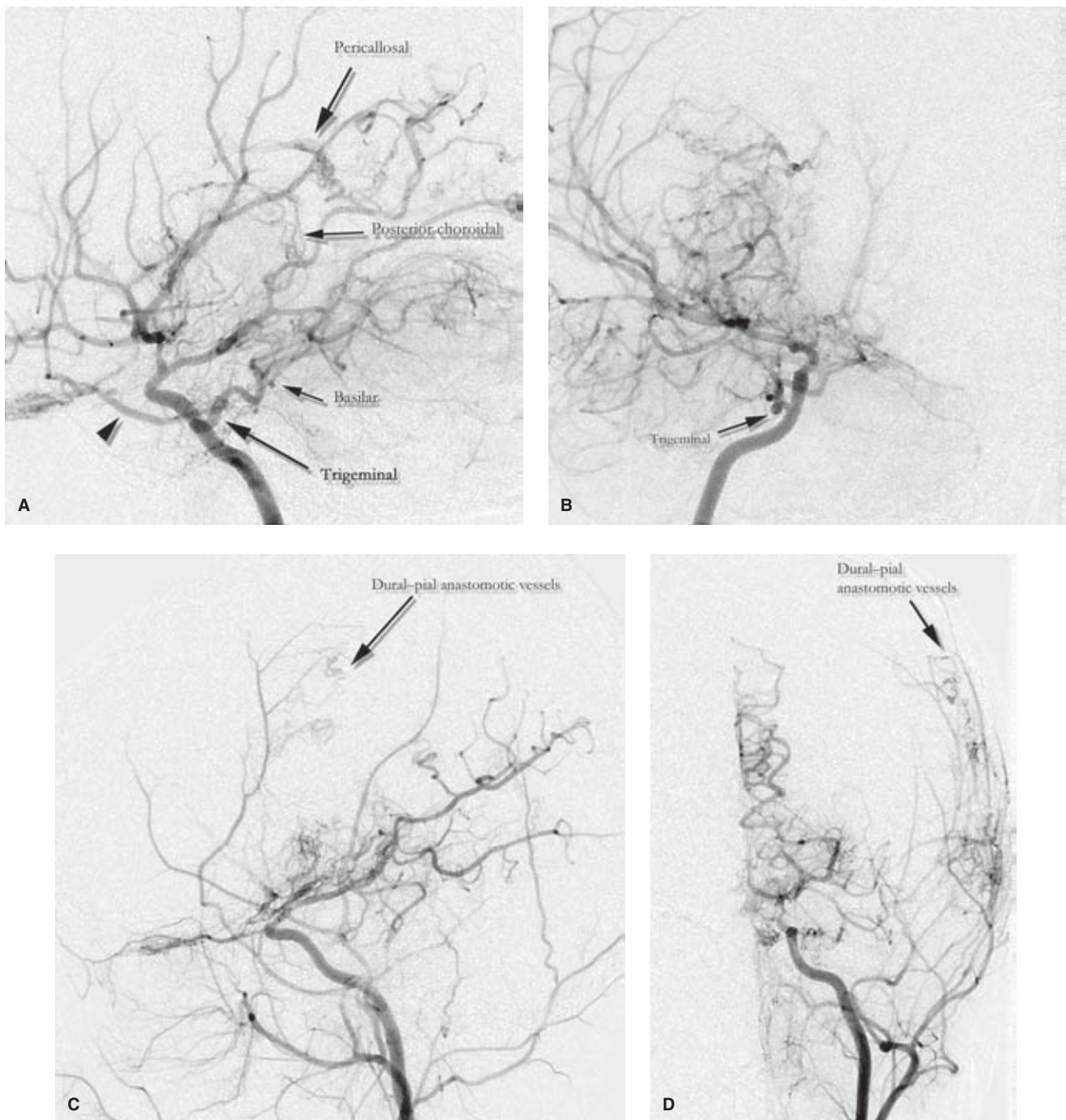


FIGURE 22-4. (A–D) Moya-Moya syndrome. The right internal carotid artery injection (**A** and **B**) in this child with multiple previous ischemic episodes shows changes of advanced Moya-Moya syndrome. The preserved trigeminal artery is labeled and gives rise to an unusual collateral vessel (*arrowhead* in **A**) taking over the role of the otherwise missing ophthalmic artery. The right M1 segment is still patent, but substantially narrowed, while the A1 segment is effectively occluded. The basilar artery, posterior choroidal, and perisplenial collateral branches from the right posterior cerebral artery are labeled. Faint opacification of the A2 segments is seen in (**B**) due to collateral supply via the lenticulostriate collaterals.

Changes within the left hemisphere (**C** and **D**) are more advanced, with more severe narrowing of the supraclinoid left carotid artery and virtually complete absence of antegrade flow in the left anterior cerebral and left middle cerebral arteries. Lenticulostriate and thalamoperforator collaterals and collaterals from the left ophthalmic artery are more developed. Dural-pial collateral routes (labeled in **C** and **D**) have developed spontaneously, but appear inadequate.

Children with Moya-Moya disease present with ischemic complications and focal neurologic deficits, choreiform movements, seizures, and an abnormal response on EEG to hyperventilation called “rebuild-up” thought to be due to cerebrovascular steal phenomenon. Symptoms in children can be precipitated by episodes of effortful hyperventilation. The disease produces characteristic signs of collateral networking of vessels on MRI including a profusion of lenticulostriate arteries and leptomeningeal enhancement on T1 or hyperintensity on FLAIR imaging (“ivy sign”) (33–35).

Adults with Moya-Moya have a higher likelihood of presenting with parenchymal or intraventricular hemorrhage (20%) in addition to ischemic complications. The hemorrhage is thought to be related to a friability of the collateral vessels and can sometimes be seen over the cerebral convexities. Cognitive, psychiatric, and personality decline can be seen in adult and pediatric patients (36). Due to abnormal rheologic stress patterns and the overstimulation of angiogenic cytokines in this condition, it is now recognized that adults with Moya-Moya have an increased vulnerability to development of cerebral aneurysms and arteriovenous malformations, which can also be a source of hemorrhage. Occult microbleeds are evident at presentation on MRI of up to 44% of adult patients (36). Headache is also a significant problem for adult patients, likely due to nociceptive changes in the dura related to collateral signaling (21).

At present there is no established medical treatment for Moya-Moya. Research into pathophysiology and histopathology has identified the process as a fibrocellular thickening of the tunica intima, excessive migration of vascular smooth muscle cells, and extreme tortuosity of the internal elastic lamina leading eventually to thrombosis and occlusion of the middle cerebral and anterior cerebral artery (37). Several angiogenic factors, presumably in response to local hypoxia, are present in supraphysiologic levels including vascular endothelial growth factor (VEGF), basic fibroblast growth factor (bFGF), hepatocyte growth factor (HGF), transforming growth factor ($TGF\beta_1$), matrix metalloproteinases MMP-2 and MMP-9, and E-selectin (37–43). A polygenic inheritance is thought likely, but environmental factors such as exposure to Epstein–Barr virus may also trigger the disease (44).

Effective treatment for Moya-Moya lies with surgical intervention, which aims to improve intracranial flow through a variety of bypass and grafting procedures: encephaloduroarteriosynangiosis, encephalomyosynangiosis, encephalogaleosynangiosis, ECA–MCA bypass, and stimulation of dural–pial anastomoses by the drilling of multiple burr holes (45,46). Surgical outcome studies (47–49) appear to indicate a significant efficacy at reducing the symptoms of Moya-Moya, including ischemic and hemorrhage complications. Interestingly, when surgical intervention is effective the imaging features of the Moya-Moya vessels on angiography and the “ivy sign” on MRI appear to regress (33).

Although it is a rare arteriopathy, Moya-Moya patients and those with related syndromes present for cerebral angiography with a disproportionately high familiarity due to the preference of most surgeons for mapping the external carotid anatomy prior to surgical intervention. Most of these cases, at least in the pediatric age group, will be conducted under general anesthesia. It is important to avoid hypotension, variations in body temperature, hypocarbia, and hypercarbia

during anesthesia, as is the case during surgery. Hydration in both circumstances should be much more aggressive than for routine cases, and should be continued for a prolonged period afterward (21,50,51). Patients with Moya-Moya syndrome and other risk factors for angiography, such as sickle cell disease, warrant especial pre- and postprocedure caution (52).

References

- Lynch JK, Hirtz DG, DeVeber G, et al. Report of the National Institute of Neurological Disorders and Stroke workshop on perinatal and childhood stroke. *Pediatrics* 2002;109(1):116–123.
- Lynch JK, Nelson KB. Epidemiology of perinatal stroke. *Curr Opin Pediatr* 2001;13(6):499–505.
- Raju TN, Nelson KB, Ferriero D, et al. Ischemic perinatal stroke: Summary of a workshop sponsored by the National Institute of Child Health and Human Development and the National Institute of Neurological Disorders and Stroke. *Pediatrics* 2007;120(3):609–616.
- Dlamini N, Kirkham FJ. Stroke and cerebrovascular disorders. *Curr Opin Pediatr* 2009;21(6):751–761.
- Domi T, Edgell DS, McCrindle BW, et al. Frequency, predictors, and neurologic outcomes of vaso-occlusive strokes associated with cardiac surgery in children. *Pediatrics* 2008;122(6):1292–1298.
- Braun KP, Bulder MM, Chabrier S, et al. The course and outcome of unilateral intracranial arteriopathy in 79 children with ischaemic stroke. *Brain* 2009;132(pt 2):544–557.
- Fullerton HJ, Wu YW, Sidney S, et al. Risk of recurrent childhood arterial ischemic stroke in a population-based cohort: The importance of cerebrovascular imaging. *Pediatrics* 2007;119(3):495–501.
- Sebire G. Transient cerebral arteriopathy in childhood. *Lancet* 2006;368(9529):8–10.
- Sebire G, Fullerton H, Riou E, et al. Toward the definition of cerebral arteriopathies of childhood. *Curr Opin Pediatr* 2004;16(6):617–622.
- Gilden D, Cohrs RJ, Mahalingam R, et al. Varicella zoster virus vasculopathies: Diverse clinical manifestations, laboratory features, pathogenesis, and treatment. *Lancet Neurol* 2009; 8(8):731–740.
- Amlie-Lefond C, Jubelt B. Neurologic manifestations of varicella zoster virus infections. *Curr Neurol Neurosci Rep* 2009; 9(6):430–434.
- Amlie-Lefond C, Sebire G, Fullerton HJ. Recent developments in childhood arterial ischaemic stroke. *Lancet Neurol* 2008;7(5):425–435.
- Ribai P, Liesnard C, Rodesch G, et al. Transient cerebral arteriopathy in infancy associated with enteroviral infection. *Eur J Paediatr Neurol* 2003;7(2):73–75.
- Danchavijit N, Cox TC, Saunders DE, et al. Evolution of cerebral arteriopathies in childhood arterial ischemic stroke. *Ann Neurol* 2006;59(4):620–626.
- Dlamini N, Freeman JL, Mackay MT, et al. Intracranial dissection mimicking transient cerebral arteriopathy in childhood arterial ischemic stroke. *J Child Neurol* 2011;26(9):1203–1206.
- Bitzer M, Topka H. Progressive cerebral occlusive disease after radiation therapy. *Stroke* 1995;26(1):131–136.
- Anson JA, Koshy M, Ferguson L, et al. Subarachnoid hemorrhage in sickle-cell disease. *J Neurosurg* 1991;75(4):552–558.
- Kim TG, Kim DS, Chung SS, et al. Moyamoya syndrome after radiation therapy: case reports. *Pediatr Neurosurg* 2011;47(2):138–142.
- Vila-Herrero E, Padilla-Parrado F, Vega-Perez J, et al. Moya-Moya syndrome and arterial dysplasia associated to Down syndrome. *Rev Neurol* 2004;39(10):943–945.

20. Cornelio-Nieto JO, Davila-Gutierrez G, Ferreyro-Irigoyen R, et al. Acute hemiplegia in childhood and alternating hemiconvulsions secondary to Moya-Moya disease. Report of a case associated with Down's syndrome. *Bol Med Hosp Infant Mex* 1990;47(1):39–42.
21. Scott RM, Smith ER. Moyamoya disease and Moyamoya syndrome. *N Engl J Med* 2009;360(12):1226–1237.
22. Heyer GL, Dowling MM, Licht DJ, et al. The cerebral vasculopathy of PHACES syndrome. *Stroke* 2008;39(2):308–316.
23. Qaiser R, Scott RM, Smith ER. Identification of an association between Robinow syndrome and Moyamoya. *Pediatr Neurosurg* 2009;45(1):69–72.
24. Rahme R, Crevier L, Dubois J, et al. Moyamoya-like vasculopathy and Seckel syndrome: Just a coincidence? *Childs Nerv Syst* 2010;26(7):983–986.
25. Codd PJ, Scott RM, Smith ER. Seckel syndrome and Moyamoya. *J Neurosurg Pediatr* 2009;3(4):320–324.
26. Takeuchi K, Shimizu K. Hypoplasia of the bilateral internal carotid arteries. *Brain Nerve* 1957;9:37–43.
27. Suzuki J, Takaku A. Studies on diseases showing an abnormal vascular network at the base of brain frequently found in the Japanese. 4. Cases in the earlier stage and the authors' opinion. *No To Shinkei* 1968;20(1):35–40.
28. Suzuki J, Takaku A. Cerebrovascular "Moyamoya" disease. Disease showing abnormal net-like vessels in base of brain. *Arch Neurol* 1969;20(3):288–299.
29. Ibrahimi DM, Tamargo RJ, Ahn ES. Moyamoya disease in children. *Childs Nerv Syst* 2010;26(10):1297–1308.
30. Choi JU, Kim DS, Kim EY, et al. Natural history of Moyamoya disease: Comparison of activity of daily living in surgery and non surgery groups. *Clin Neurol Neurosurg* 1997;99(suppl 2):S11–S18.
31. Kobayashi E, Saeki N, Oishi H, et al. Long-term natural history of hemorrhagic Moyamoya disease in 42 patients. *J Neurosurg* 2000;93(6):976–980.
32. Yoshida Y, Yoshimoto T, Shirane R, et al. Clinical course, surgical management, and long-term outcome of Moyamoya patients with rebleeding after an episode of intracerebral hemorrhage: An extensive follow-up study. *Stroke* 1999;30(11):2272–2276.
33. Mori N, Mugikura S, Higano S, et al. The leptomeningeal "ivy sign" on fluid-attenuated inversion recovery MR imaging in Moyamoya disease: A sign of decreased cerebral vascular reserve? *AJNR Am J Neuroradiol* 2009;30(5):930–935.
34. Ohta T, Tanaka H, Kuroiwa T. Diffuse leptomeningeal enhancement, "ivy sign," in magnetic resonance images of Moyamoya disease in childhood: Case report. *Neurosurgery* 1995;37(5):1009–1012.
35. Yoon HK, Shin HJ, Chang YW. "Ivy sign" in childhood Moyamoya disease: Depiction on FLAIR and contrast-enhanced T1-weighted MR images. *Radiology* 2002;223(2):384–389.
36. Kuroda S, Houkin K. Moyamoya disease: Current concepts and future perspectives. *Lancet Neurol* 2008;7(11):1056–1066.
37. Weinberg DG, Arnaout OM, Rahme RJ, et al. Moyamoya disease: A review of histopathology, biochemistry, and genetics. *Neurosurg Focus* 2011;30(6):E20.
38. Derynck R, Jarrett JA, Chen EY, et al. Human transforming growth factor-beta complementary DNA sequence and expression in normal and transformed cells. *Nature* 1985;316(6030):701–705.
39. Fujimura M, Watanabe M, Narisawa A, et al. Increased expression of serum Matrix metalloproteinase-9 in patients with Moyamoya disease. *Surg Neurol* 2009;72(5):476–480; discussion 480.
40. Hojo M, Hoshimaru M, Miyamoto S, et al. A cerebrospinal fluid protein associated with Moyamoya disease: Report of three cases. *Neurosurgery* 1999;45(1):170–173; discussion 173–174.
41. Hojo M, Hoshimaru M, Miyamoto S, et al. Role of transforming growth factor-beta1 in the pathogenesis of Moyamoya disease. *J Neurosurg* 1998;89(4):623–629.
42. Sakamoto S, Kiura Y, Yamasaki F, et al. Expression of vascular endothelial growth factor in dura mater of patients with Moyamoya disease. *Neurosurg Rev* 2008;31(1):77–81; discussion 81.
43. Takekawa Y, Umezawa T, Ueno Y, et al. Pathological and immunohistochemical findings of an autopsy case of adult Moyamoya disease. *Neuropathology* 2004;24(3):236–242.
44. Takanashi J. Moyamoya disease in children. *Brain Dev* 2011;33(3):229–234.
45. Ausman JI, Diaz FG, Ma SH, et al. Cerebrovascular occlusive disease in children: A survey. *Acta Neurochir (Wien)* 1988;94(3–4):117–128.
46. Onesti ST, Solomon RA, Quest DO. Cerebral revascularization: a review. *Neurosurgery* 1989;25(4):618–628; discussion 628–619.
47. Rhee JW, Magge SN. Moyamoya disease and surgical intervention. *Curr Neurol Neurosci Rep* 2011;11(2):179–186.
48. Scott RM, Smith JL, Robertson RL, et al. Long-term outcome in children with Moyamoya syndrome after cranial revascularization by pial synangiosis. *J Neurosurg* 2004;100(2 suppl Pediatrics):142–149.
49. Guzman R, Lee M, Achrol A, et al. Clinical outcome after 450 revascularization procedures for Moyamoya disease. Clinical article. *J Neurosurg* 2009;111(5):927–935.
50. Nomura S, Kashiwagi S, Uetsuka S, et al. Perioperative management protocols for children with Moyamoya disease. *Childs Nerv Syst* 2001;17(4–5):270–274.
51. Smith ER, McClain CD, Heeney M, et al. Pial synangiosis in patients with Moyamoya syndrome and sickle cell anemia: Perioperative management and surgical outcome. *Neurosurg Focus* 2009;26(4):E10.
52. Hankinson TC, Bohman LE, Heyer G, et al. Surgical treatment of Moyamoya syndrome in patients with sickle cell anemia: Outcome following encephaloduroarteriosynangiosis. *J Neurosurg Pediatr* 2008;1(3):211–216.

Carotid-Cavernous Fistulas

Key Points

- The intraocular pressure is an important datum in the deliberation on when it is necessary to treat a patient with a carotid-cavernous fistula urgently, particularly when there are conflicting clinical concerns due to other injuries.
- Intracranial venous drainage may be clinically silent, but is a significant concern for the development of intracranial venous hypertension.

Carotid-cavernous fistulas used to be among the most dramatic of angiographic diagnostic and interventional procedures, but since the advent of airbags in cars they have become a rarity, at least in the Occident. They are still common in countries where scooter transportation at high speed and without helmets is prevalent, and most acutely where such transportation comes to a sudden stop. A descriptive scheme for carotid-cavernous fistulas and dural arteriovenous malformations of the cavernous sinus that is frequently invoked is the Barrow classification (1). This describes the direct type of fistula, that is, a tear of the internal carotid artery as a Type A, and describes three categories, Types B to D, of indirect fistulas depending on arterial supply. Other than the fact that it discerns between direct and indirect fistulas, this classification scheme, particularly in its subcategorization of dural arteriovenous malformations according to this feature, is of little utility, and is mentioned here only because it is referred to frequently in papers and lectures. This chapter deals with direct fistulas with direct communication between the internal carotid artery and the paracavernous venous structures. Dural arteriovenous malformations and lesser fistulous lesions are discussed in Chapter 20.

Although the term “carotid-cavernous fistula” is often applied in the vernacular to dural arteriovenous malformations of the cavernous sinus, the two conditions are distinct with several implications for treatment. Carotid-cavernous fistula is the consequence of a transmural tear in the cavernous carotid artery establishing a fistula to the ipsilateral venous structures, usually the cavernous sinus. It is most commonly seen in young males following trauma, or in older females following spontaneous rupture of a pre-existent cavernous aneurysm (2). Occasional iatrogenic cases can be seen following transphenoidal surgery. Typically, onset is acute with a loud orbital bruit, proptosis, chemosis,

eversion of the conjunctiva, corneal abrasions, and palsy of the VI or other cranial nerves. With rapid maturation of the fistulous rent in the arterial wall, the volume of flow and venous hypertensive complications can escalate quickly leading to secondary glaucoma, intracranial venous hypertension, venous infarcts, and cerebrovascular compromise due to steal (Fig. 23-1). For this reason, treatment can frequently be necessary on an emergency basis, posing a conflict in many patients with other aspects of treatment for traumatic injuries to viscera or intracranial structures (3–5).

Angiographic diagnosis of carotid-cavernous fistulas is easy as the abnormality is usually fairly prominent (Figs. 23-2–23-6). What is not so straightforward is identifying precisely the location and extent of the arterial tear. This is because the volume of flow to the venous side engulfs the artery with venous contrast and obscures the view of the leakage point. Bumping up the frame rate per second for the DSA run can help enormously, but the most useful images are frequently those obtained of the fistula indirectly through the circle of Willis, particularly the vertebral artery. Reflux via the ipsilateral posterior communicating artery with retrograde flow to the fistula is often the best indicator of the upper edge of the tear, information that can be very useful in planning an endovascular treatment.

Secondly, information from the diagnostic angiogram relevant to the salvageability or otherwise of the carotid artery is important for evaluating the therapeutic options for a particular patient. Almost invariably, if there is reflux down the supraclinoidal carotid artery from the circle of Willis, the patient will have effectively undergone a successful test occlusion of the injured internal carotid artery, that is, the carotid artery can be sacrificed as a therapeutic option. However, occasional cases can be seen where continued intracranial flow past the fistula is necessary and in these patients the carotid artery has to be preserved.

► TREATMENT OF CAROTID-CAVERNOUS FISTULAS

Some carotid-cavernous fistulas do not need to be treated immediately if, for instance, there are other more pressing problems in hand with a multitrauma patient with a low-flow lesion and clinical contraindications to heparinization during an endovascular procedure. A very tiny fistula may be of no immediate consequence and some undergo

(text continues on page 379)



FIGURE 23-1. Ocular findings of carotid-cavernous fistula.

This patient experienced a trivial traffic accident that occasioned deployment of his airbag against his chest and face. Within a few days of the accident he became aware of a gathering bruit on the right side of his head and progressive proptosis and swelling around the right eye. Elevation of his intraocular pressure on the right prompted urgent treatment of his carotid-cavernous fistula. Compared with the ocular findings of dural arteriovenous malformations, which are usually more subdued than those illustrated, the findings in the presence of a carotid-cavernous fistula are sometimes almost grotesque due to the extremely high pressure within the veins. Due to the anatomic distortion of the globe, evaluation of the extraocular muscles can often be difficult. These findings regress very quickly after treatment, and within 24 hours of his procedure, his right eye had almost normalized in appearance.

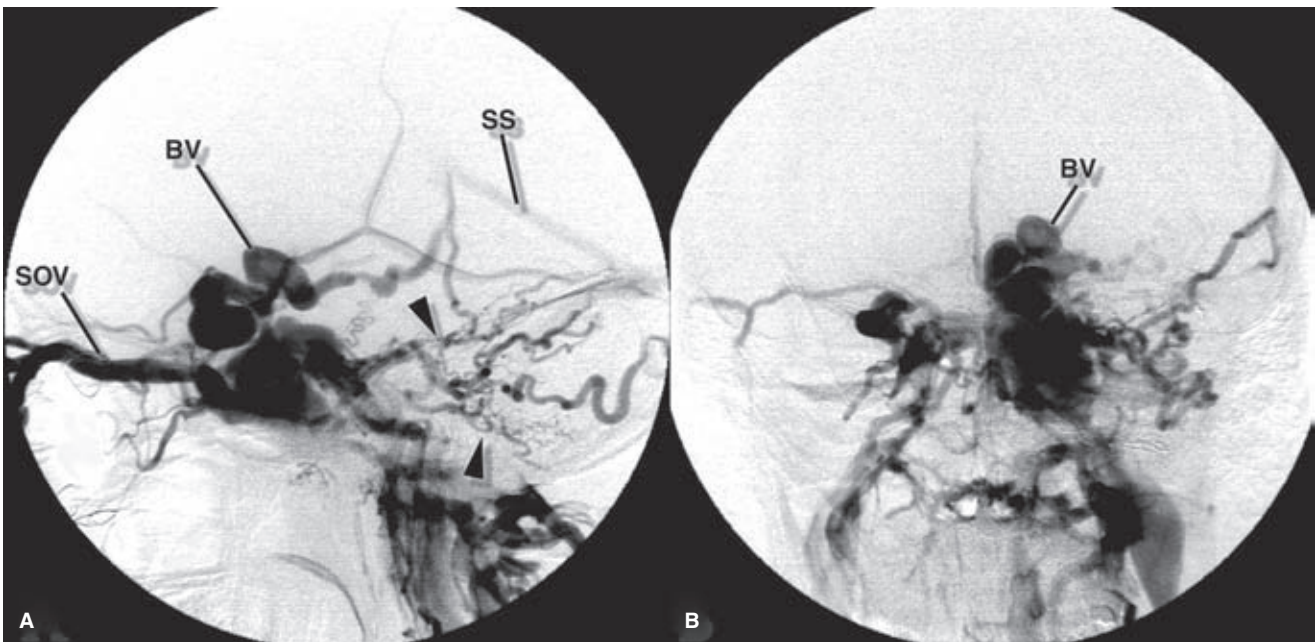


FIGURE 23-2. (A–B) Carotid-cavernous fistula following trauma. Lateral (A) and PA (B) views of the left internal carotid artery injection in a young adult following severe head trauma. There is immediate and profuse opacification of venous structures due to fistulous flow from the cavernous internal carotid artery. Intercavernous connections fill the contralateral cavernous sinus. Although his symptoms were relatively mild, the angiographic appearance of varicose distention of the anterior segment of the basal vein (BV) and opacification of parenchymal veins of the posterior fossa (arrowheads) suggest that complications of venous hypertension may be imminent. (Labels: SOV, superior ophthalmic vein; SS, straight sinus.)

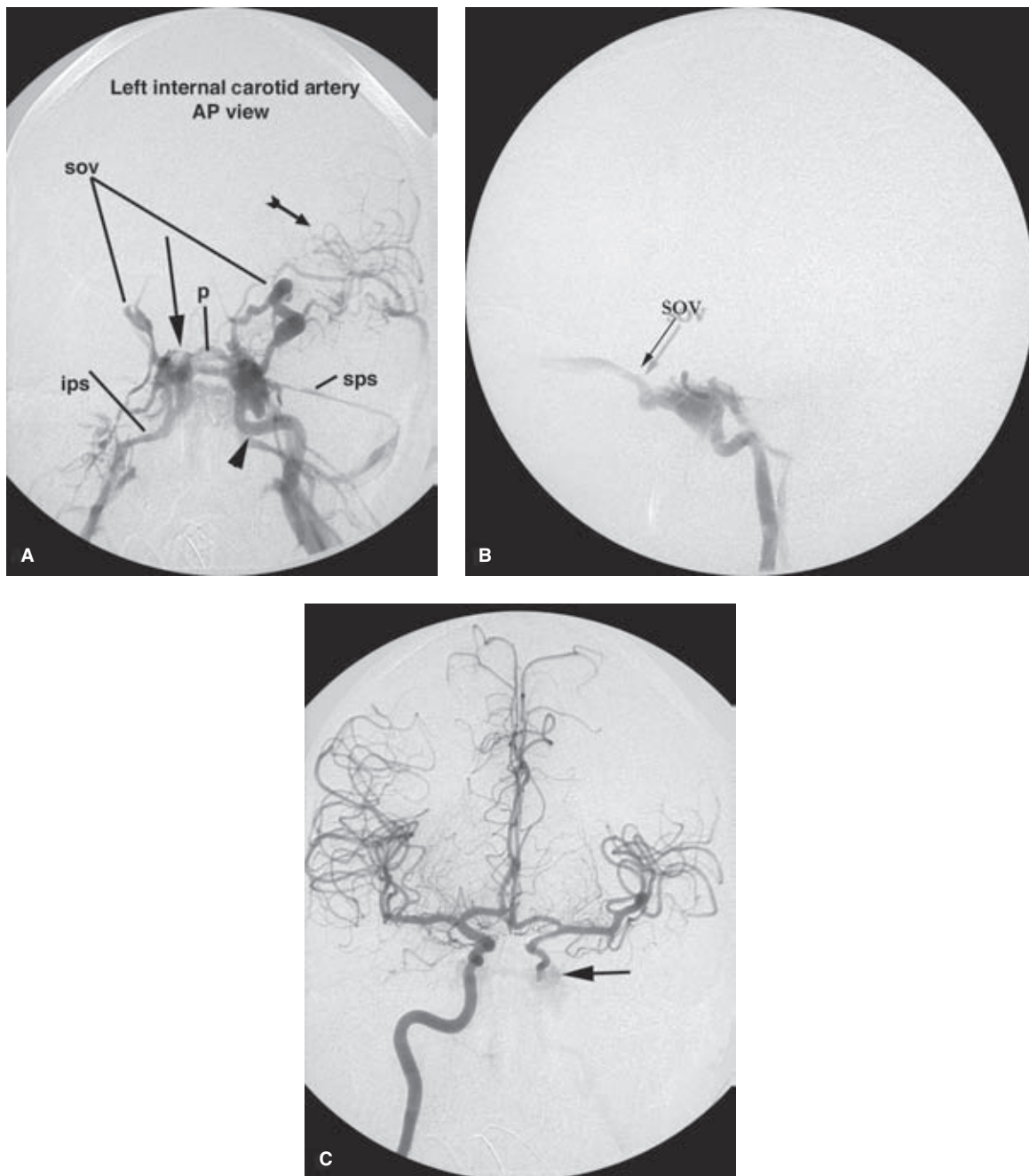


FIGURE 23-3. (A–C) Carotid-cavernous fistula with compromise of the left internal carotid artery. A carotid-cavernous fistula in the left cavernous internal carotid artery shows features commonly seen with this lesion. First, the left internal injection (A, AP view; B, lateral view) shows that there is narrowing of the cavernous segment, probably related to the patient's trauma and a dissection of that site. Second, the flow is fulminant with extensive opacification of the cavernous sinuses bilaterally, with visualization of a lucency created by the unopacified contralateral right internal carotid artery (long arrow in A), the ophthalmic veins bilaterally (SOV), and the superior and inferior petrosal sinuses (sps and ips). Note the midline lucency created by the pituitary gland (p). Most of the vascular structures projecting over the left hemisphere (feathered arrow in A) are venous, not arterial, from retrograde venous flow. Finally, the right internal carotid artery injection (C) shows retrograde flow down to the fistula (arrow in C), an indirect way of seeing the fistula that can be very important in some patients. Several considerations arise:

- The brain is obviously well perfused without the left internal carotid artery, and therefore, sacrifice of the left internal carotid artery, a technically easy procedure with the correct devices, is an option for this patient.
- Struggling for hours to obtain a satisfactory closure of the fistula on the left may not be worthwhile because the resumption of antegrade flow across the dissected segment into the brain may transpire to be concerning at the end of the procedure, due to risks of emboli from the dissected segment or from cerebral hyperperfusion syndrome.

Therefore, while preservation of vessels is generally laudable, it is not necessarily always the best treatment for this type of lesion.

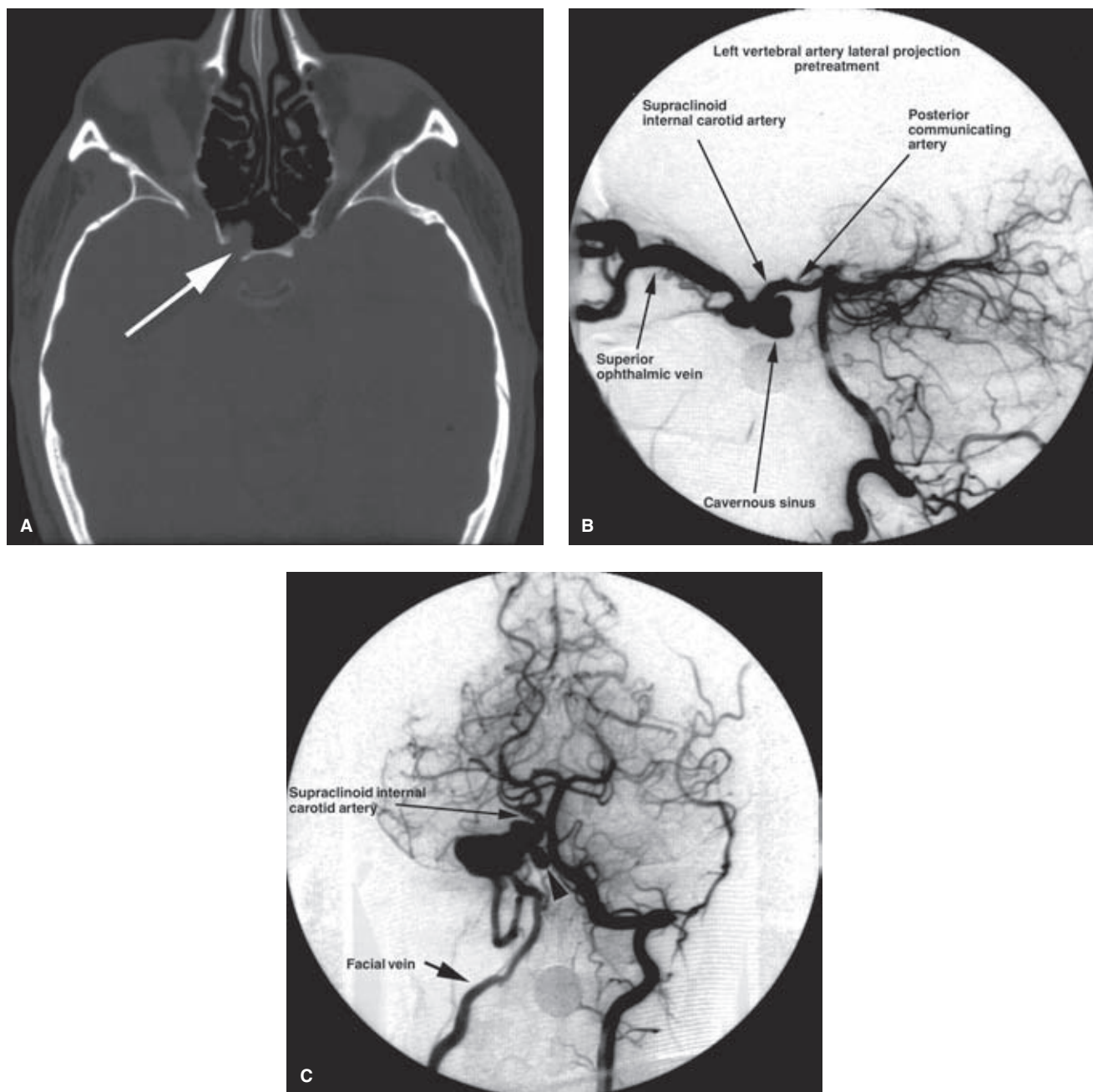


FIGURE 23-4. (A–C) Posttraumatic carotid-cavernous fistula with ipsilateral carotid dissection. A young adult male presented with history of mild right-sided proptosis and a pulsatile bruit following an assault with a lead pipe. A CT examination demonstrated prominent vascular structures in the region of the right cavernous sinus. A most significant finding on the bone windows was a breach (*arrow* in **A**) in the bony wall of the sphenoid sinus with protrusion of a soft tissue density from the cavernous sinus. With a history of trauma and a diagnosis of carotid-cavernous fistula, the possibility of a pseudoaneurysm or tense venous pouch expanding into the sphenoid sinus must be considered, raising the risk of life-threatening epistaxis from that site. The right common carotid artery arteriogram (not shown) demonstrated complete occlusion of the right internal carotid artery. The carotid-cavernous fistula filled via the right posterior communicating artery from the left vertebral artery injection (**B**). Contrast flows from the right posterior cerebral artery to the supraclinoid internal carotid artery. A distended cavernous sinus drains exclusively to a massively distended superior ophthalmic vein. Despite the torrential rate of flow in the superior ophthalmic vein, the patient's proptosis was mild. This was because of prompt drainage to the facial vein, seen on the Townes view (**C**). On this view, a medially projecting pouch (*arrowhead* in **C**) from the genu of the internal carotid artery is seen, correlating with the CT appearance in (**A**). Because of the possibility of massive epistaxis from the pouch or pseudoaneurysm, urgent embolization was undertaken.

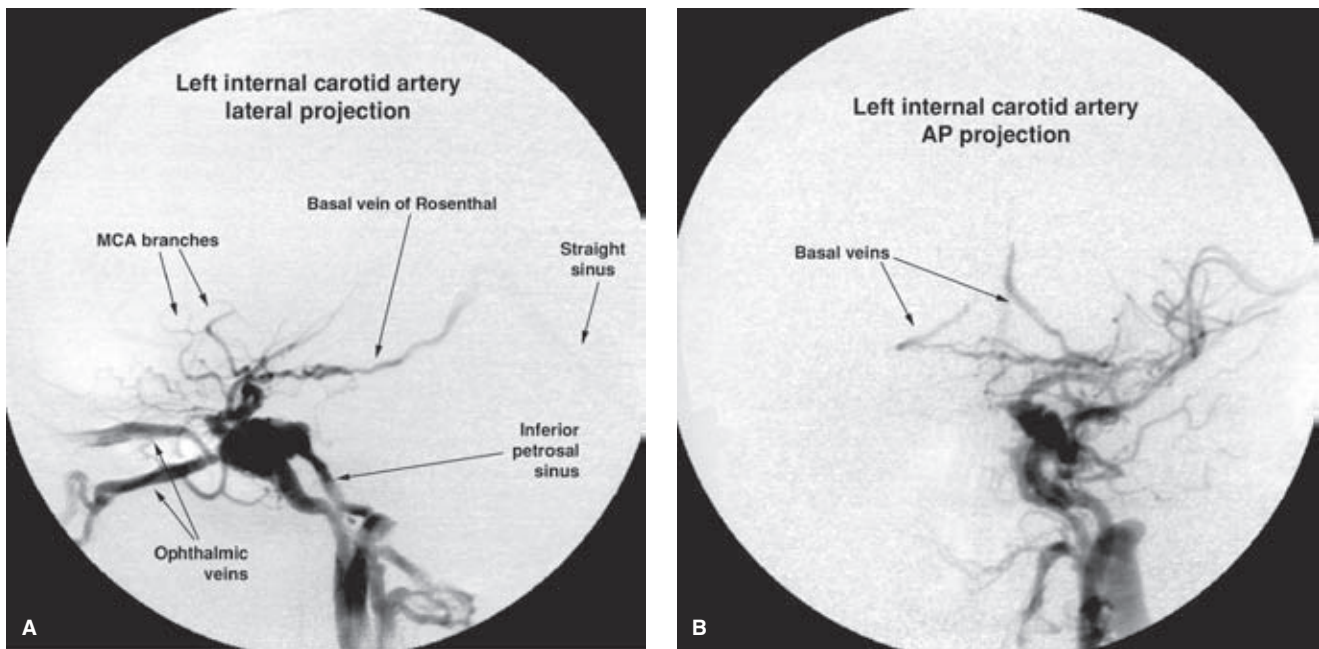


FIGURE 23-5. (A–B) Carotid-cavernous fistula after a motor vehicle accident. A carotid-cavernous fistula of the right internal carotid artery in a young adult after severe head trauma. In contrast to the case of Figure 23-4, this patient demonstrates opacification of the subarachnoid basal veins of Rosenthal, an alarming finding because of its implications for the risks of complications from venous hypertension and hemorrhage. The inferior petrosal sinus is also opacified. Antegrade arterial flow to the middle cerebral artery branches is diminished, but present. This is likely an instance where preservation of flow in the internal carotid artery after occlusion of the fistula will be necessary.

spontaneous regression (Fig. 23-7). Imaging and clinical features of carotid-cavernous fistulas that indicate a need for urgent treatment include evidence of venous hypertension affecting the intracranial venous system, increasing proptosis or diminishing visual acuity, increasing intracranial pressure, elevated intracranial pressure, rupture into the subarachnoid space, and extension of a pseudoaneurysm or venous varix from the cavernous sinus into the subarachnoid space (5).

The treatment of choice for carotid-cavernous fistulas used to be endovascular occlusion of the fistula with a detachable latex or silicon balloon, while preserving flow in the internal carotid artery. Since the withdrawal of detachable balloons from the US market, this therapeutic option has joined the historical ranks of autologous muscle embolization and carotid ligation (6,7). Although several reference papers point to detachable balloon therapy as being the treatment of choice, there were several problems with this technology that were difficult to deal with. Firstly, premature detachment of the balloon from the microcatheter allowing it to migrate intracranially or migration of an inflated balloon during detachment (accomplished by tugging gently on the microcatheter) back into the artery were very undesirable events. Failure of the balloon, or balloons, to fit into or to occlude fully the fistula was common, and premature deflation of the balloon after treatment or rupture against an adjacent shard of fractured bone would allow immediate resumption of fistulous flow. Finally, longer-term studies suggested that even with successful treatment, the healing pattern of the carotid artery allowed persistence of a pseudoaneurysm in 30% to 44% of cases (2,8).

Currently in the US treatment of carotid-cavernous fistulas relies on two main approaches. Firstly, the artery can be sacrificed above and below (“trapping”) the fistula with coils or other devices. Secondly, the artery can be preserved by transarterial, transvenous, or combined approaches for occlusion of the fistula with liquid agents, coils or bare metal, and covered stents. Transvenous coil packing of the cavernous sinus is more challenging in the setting of a direct carotid-cavernous fistula compared with a dural arteriovenous malformation due to the high volume of flow and the need therefore to achieve a very dense packing of the venous space to induce thrombosis. Fibered coils have an advantage in this respect, although their stiffness and tendency to kickback one’s microcatheter from a hard-won venous space can be very frustrating. Migration of coils or liquid agents from the venous side to the artery is definitely a big consideration in many patients, and this problem can be addressed by transarterial placement of a temporary balloon across the mouth of the fistula or placement of a bare metal stent (9,10) (Figs. 23-8 and 23-9). As with the transvenous treatment of dural arteriovenous malformations, a complete elimination of the fistula is desirable, but, above all, an outcome that results in *diversion* of venous flow to the intracranial veins must be avoided. This can easily happen if the outflow to the ophthalmic veins or petrosal sinuses is occluded but access from the cavernous sinus to the uncal veins or sphenoparietal sinus is left intact, resulting in aggravation of intracranial venous hypertension with attendant risks of venous infarction and hemorrhage.

Covered stents have been used in carotid-cavernous fistulas by several authors (11–15) when alternatives have

(text continues on page 383)

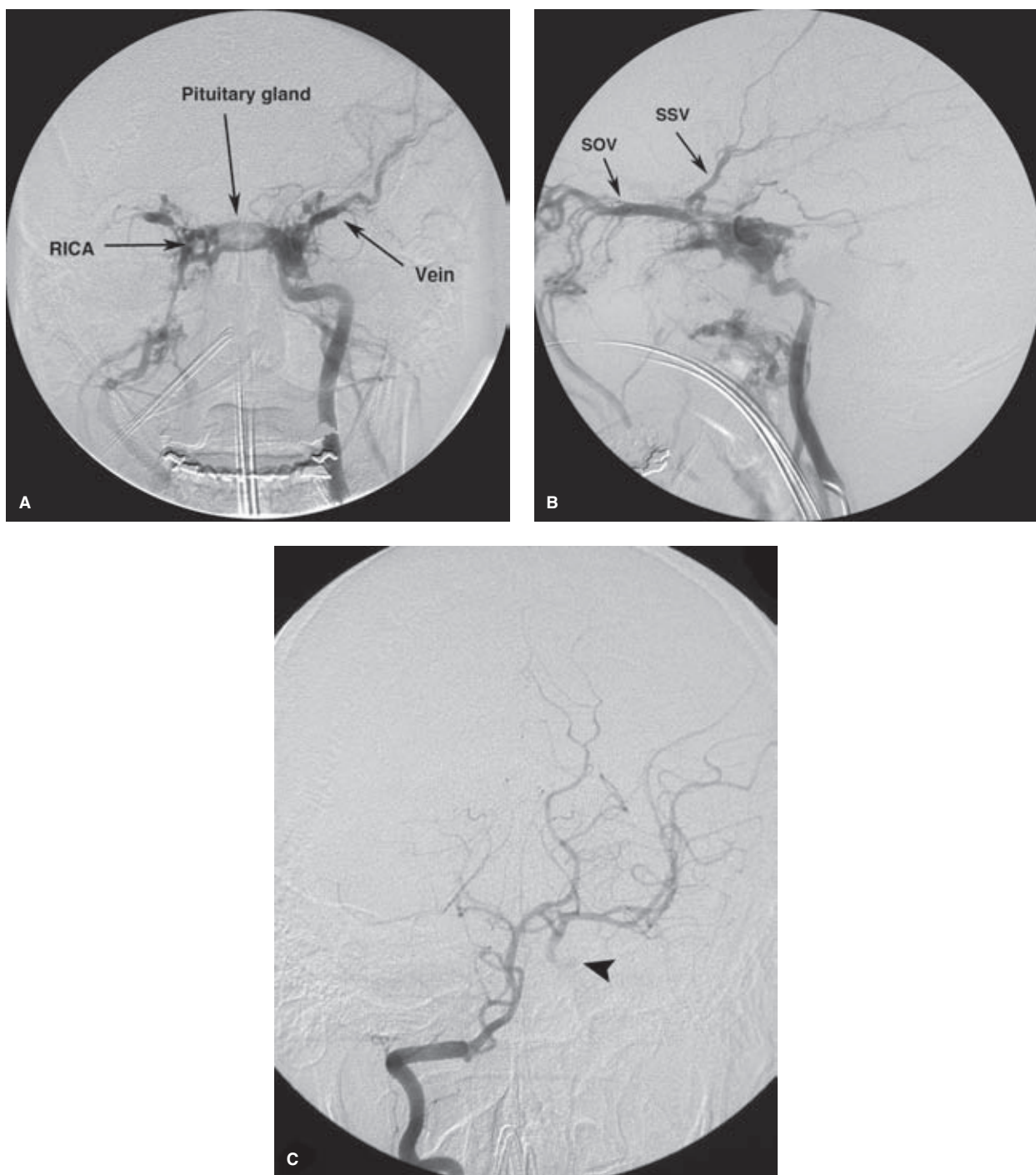


FIGURE 23-6. (A–C) Carotid-cavernous fistulas after a motor vehicle accident. The degree of trauma associated with precipitation of a carotid-cavernous fistula is almost always substantial, of a magnitude associated with vehicular accidents. Even so, these specific lesions are uncommon and may be diminishing in frequency since the advent of air bag restraints. In Asian countries where transport by scooter or motorbike is commonplace, these injuries are more common and correlate with the neglect of wearing a protective helmet. The left internal carotid artery injection in this young adult shows immediate opacification of both cavernous sinuses (A) within which the lucencies created by the pituitary gland and nonopacified right internal carotid artery are nicely demonstrated (labeled). The important findings here are that there is little if any antegrade arterial flow in the left internal carotid artery past the fistula. Virtually all of the intracranial opacification is to the sphenoparietal sinus and the superficial Sylvian vein on the left, implying that the patient is at risk for developing complications of venous hypertension in the left hemisphere. The lateral view (B) shows the same complications with prominent drainage to the superficial Sylvian vein (SSV) and the superior ophthalmic vein (SOV). The right vertebral artery injection (C) demonstrates the precise point of the fistula through reflux via the left supraclinoid carotid artery (arrowhead in C). This is useful for planning the site of therapeutic occlusion, which was attempted unsuccessfully using balloons in this patient. The left internal carotid artery was occluded above and below the fistula after several unsuccessful attempts. With the advent of covered stents, consideration might be given to using these devices in a patient such as this, but the risk of embolic complications would need to be considered carefully when the patient has already demonstrated that her cerebral perfusion is not dependent on the left internal carotid artery for flow. Approximately 1 week after her carotid occlusion procedure the patient developed ischemic symptoms in the left hemisphere and a left vertebral arterial injection showed a small embolus in the left MCA bifurcation (not shown), the result of a presumed stump embolus, a lesson since applied to other patients with a similar propensity (see Fig. 23-11).

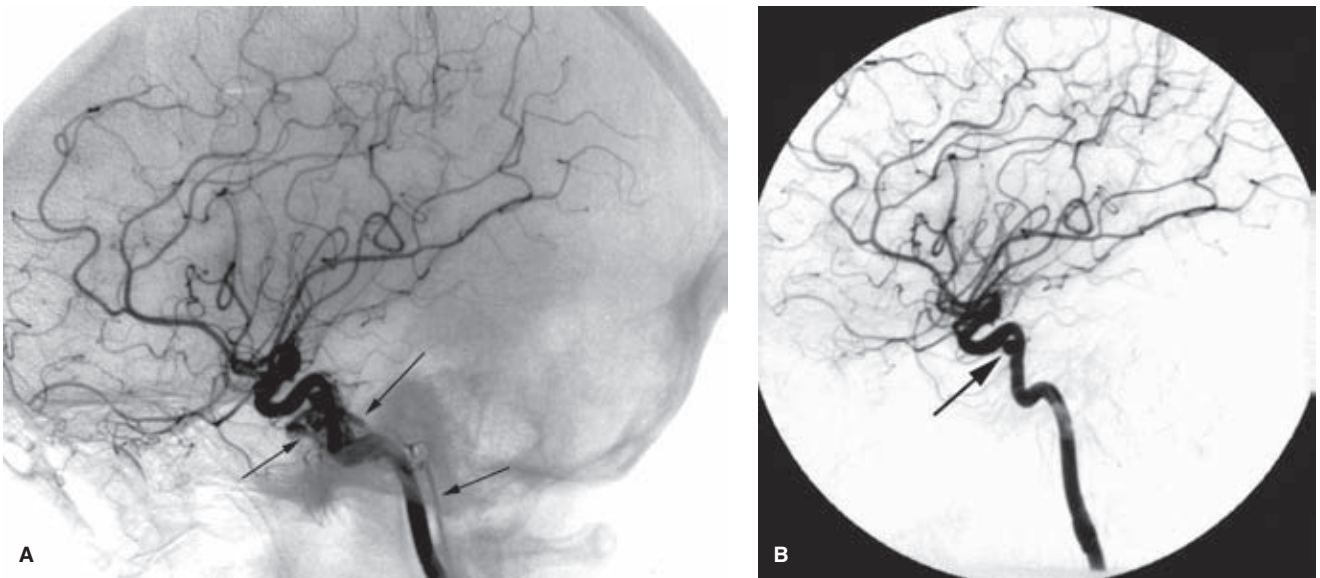


FIGURE 23-7. (A–B) Spontaneous regression of a carotid-cavernous fistula. A left internal carotid artery angiogram (A) in an elderly female with bruit and headaches after head trauma. A fistula from the precavernous internal carotid artery to the paracavernous veins and inferior petrosal sinus was present (arrows in A). Three weeks later (B), the fistula has closed spontaneously, leaving a residual pseudoaneurysm (arrow in B) at the site of the traumatic tear in the internal carotid artery. A small pouch or pseudoaneurysm of this appearance is thought to be a common long-term event after balloon occlusion of a carotid-cavernous fistula because most balloons undergo a slow deflation over time.

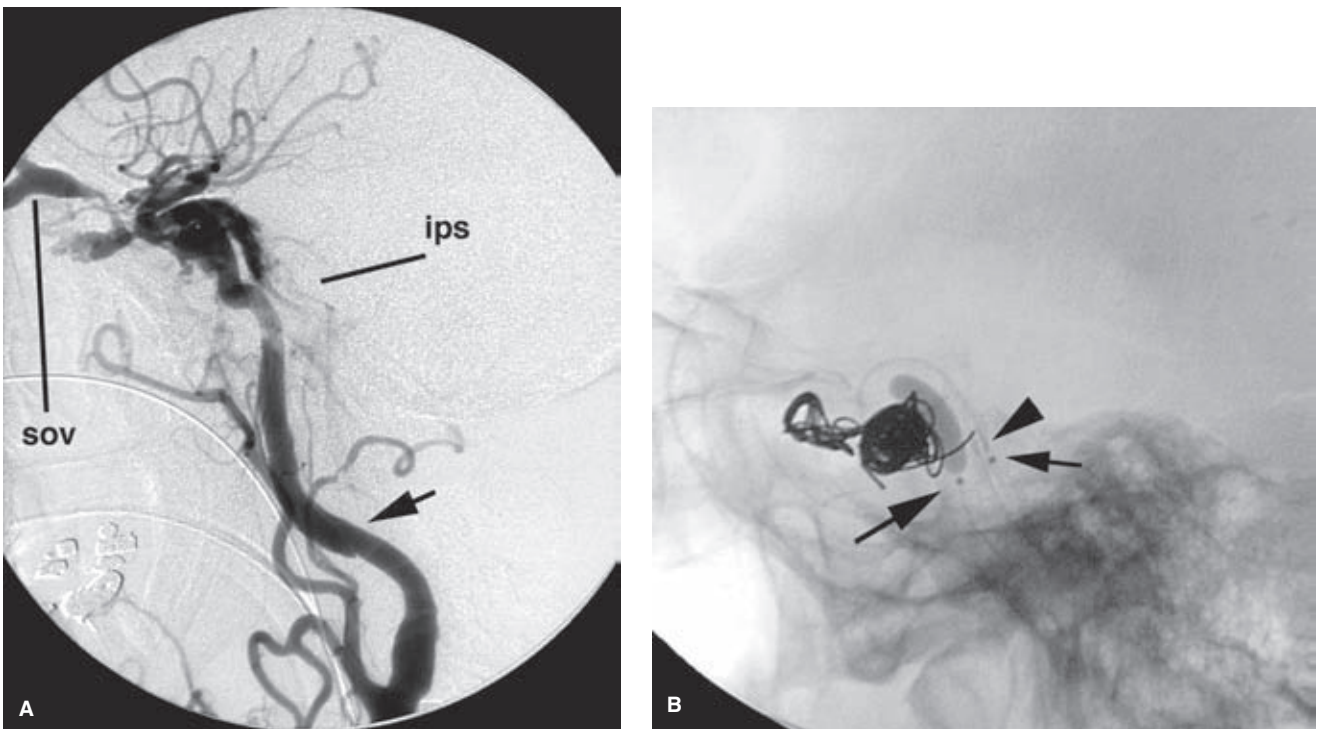


FIGURE 23-8. (A–C) CCF with combined transarterial and transvenous treatment. A middle-aged male patient sustained a right CCF in a car accident. The lateral view of the right common carotid artery (A) shows a spiral dissection (arrow in A) in the midcervical segment with immediate opacification of the superior ophthalmic vein (SOV) and inferior petrosal sinus (ips). Prolonged attempts with several balloon sizes were pursued fruitlessly to obtain an occlusion of the fistula. On the final treatment attempt, a combined transarterial placement of a non-detachable balloon and transvenous placement via the IPS of a microcatheter to place coils in the cavernous sinus was successful. Image (B) is the lateral view during coiling; Image (C) is the AP view. (continued)

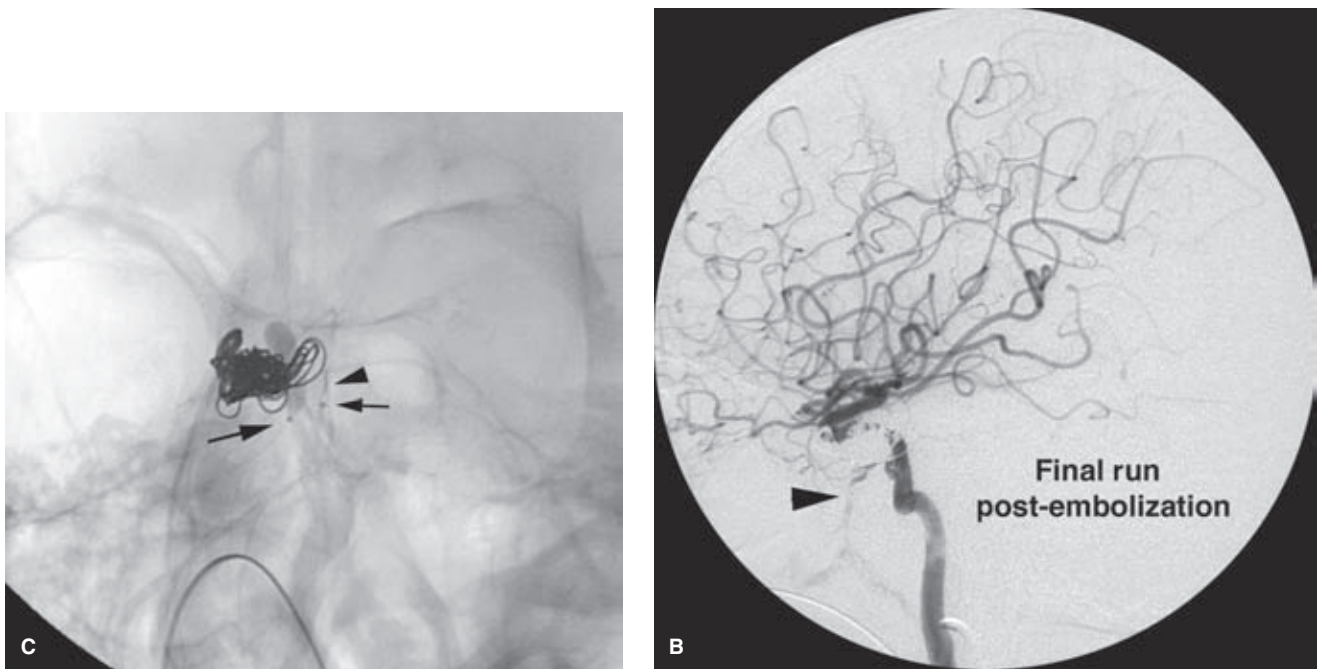


FIGURE 23-8. (CONTINUED) The arrowhead indicates the detachment marker of the coil within the microcatheter; the smaller arrow is the proximal marker of the microcatheter and the longer arrow is the metallic marker on the proximal end of the balloon catheter. The balloon was necessary because the coils prolapsed freely from the cavernous sinus to the artery without this adjunctive protection. The balloon guaranteed the integrity of the artery, which could not be seen in profile view without superimposed coils as the case progressed. The final view (**D**) shows only a tiny trickle of flow (*arrowhead* in **D**) to the pterygoid plexus with a complex nidus of coils surrounding the carotid artery. A follow-up angiogram some days later confirmed complete elimination of the fistula.

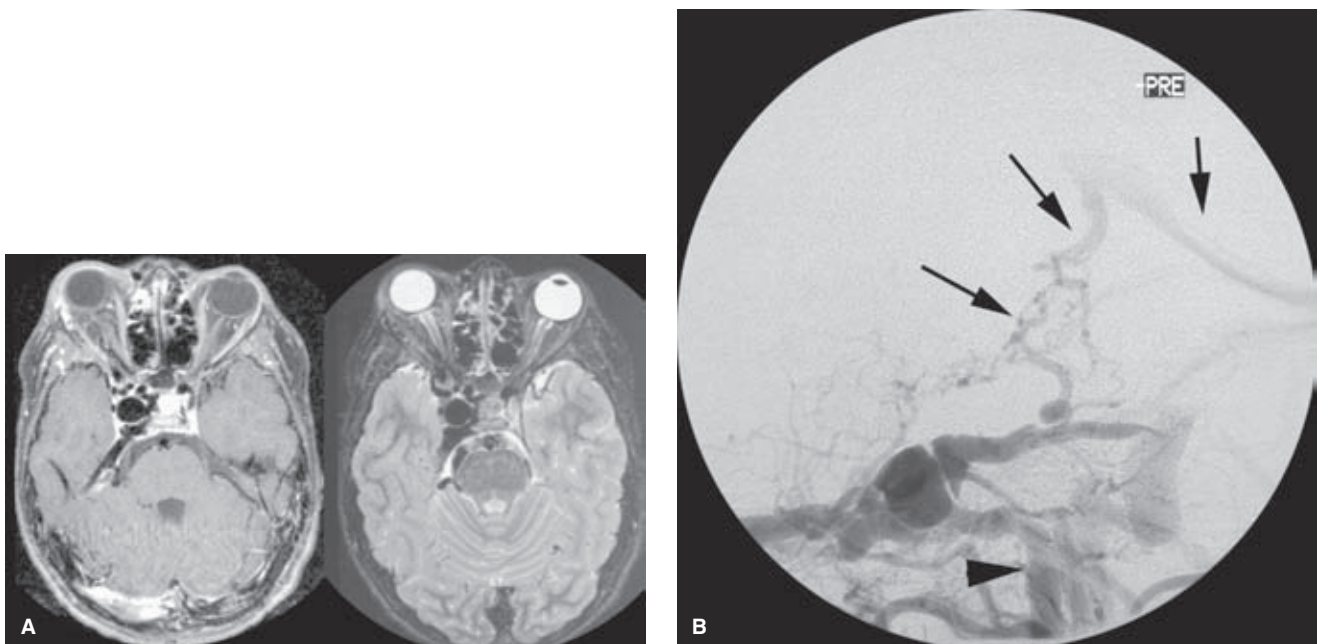


FIGURE 23-9. (A-E) CCF in a 14-year-old boy. A teenager sustained severe head injuries when his family car was rear-ended at a traffic light by an inattentive driver. During 6 months of recovery, his right eye became proptotic, and a pulsatile bruit developed. The MRI (**A**) shows massive distension of the right cavernous sinus and adjacent venous structures. The right carotid artery angiogram (**B**, lateral view centered on the head) shows no intracranial opacification of arteries beyond the fistula. The right cervical internal carotid artery itself (*arrowhead* in **B**) is irregular, having been dissected at the time of the original trauma. There is deep venous drainage involving the basal vein of Rosenthal and the veins of the posterior fossa (*arrows* in **B**). (*continued*)

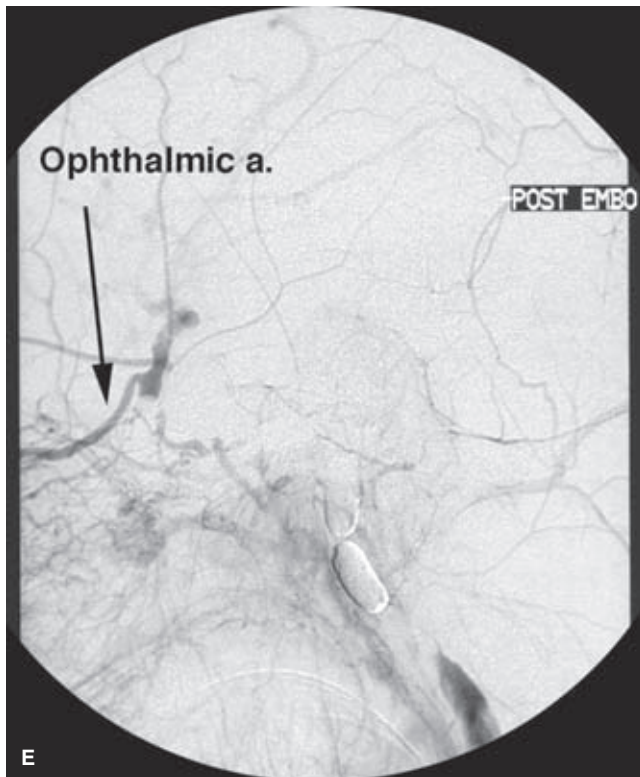
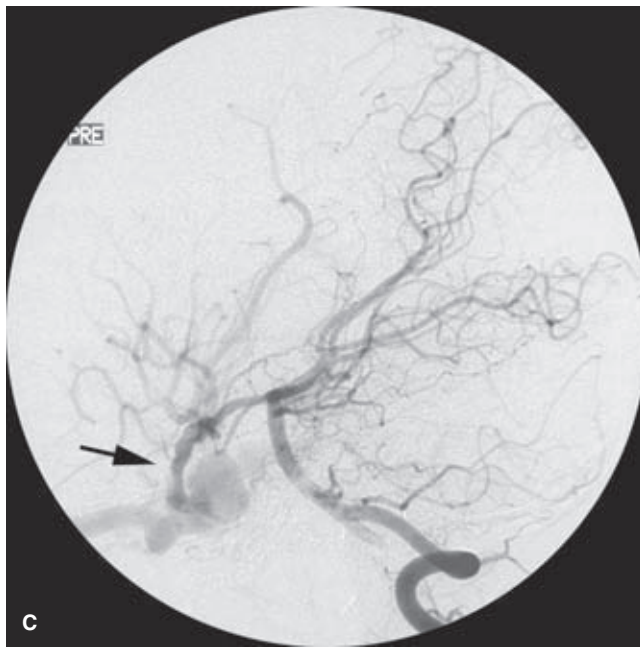


FIGURE 23-9. (CONTINUED) The lateral view of the vertebral artery injection (**C**) shows retrograde opacification to the fistula, providing important information on the location of the fistula with reference to the ophthalmic artery. The latter is not seen directly on this view, but it creates an indentation on the column of contrast (*arrow in C*) by virtue of retrograde flow of unopacified blood via this route to the carotid. A prolonged attempt was made to preserve this carotid artery, but the aneurysmal dilatation of the cavernous sinus was too much for any available balloons. Moreover, when an attempt was made to occlude the artery above the fistula with a balloon in the genu, the retrograde pressure from the artery pushed the balloon back into the fistula. Finally, a combined deployment of a balloon in the genu stabilized prior to its detachment by a large nidus of coils in the fistula and artery and supported by further balloons worked (**D**, lateral postembolization unsubtracted view). The lateral common carotid injection (**E**) postembolization shows the enlarged ophthalmic artery now flowing retrogradely to the brain. In retrospect, preserving the orifice of the ophthalmic artery was not necessary in this case because the collateral flow to the area was excellent. Part of the concern about keeping the initial balloon position low, however, was related to the unknown factor of how much stress the supraclinoidal (intradural) segment of the artery could sustain from a balloon inflated enough to gain a firm grip on the intima.

failed. These stents are usually constructed with a membrane of polytetrafluoroethylene (PTFE) and are much stiffer than conventional bare stents. Advancing such a stent all the way to the cavernous-carotid artery is probably an option only in young patients with relatively straight vessels and will require a much larger introducer catheter or sheath. Furthermore, the risks and unknown outcome problems of such a procedure, particularly long-term patency, must be balanced against the tried and true option of arterial sacrifice, which can be an option for most patients (Fig. 23-9).

Following successful occlusion of a carotid-cavernous fistula, several management considerations remain:

1. Vigilance for recanalization of the fistula (Fig. 23-10).
2. When the artery is sacrificed, the possibility of “stump emboli” emanating intracranially from above the occlusion may need to be considered and treated with antiplatelet or anticoagulant medication (Fig. 23-11).
3. A long-established carotid-cavernous fistula may have altered the hemodynamics of cerebral blood flow sufficiently, such that after sudden elimination of the sump, the patient is vulnerable to an effective hyperperfusion syndrome. This may need to be managed with hypotensive and anticonvulsant medication, similar to such situations following endarterectomy or carotid stenting.

(text continues on page 386)

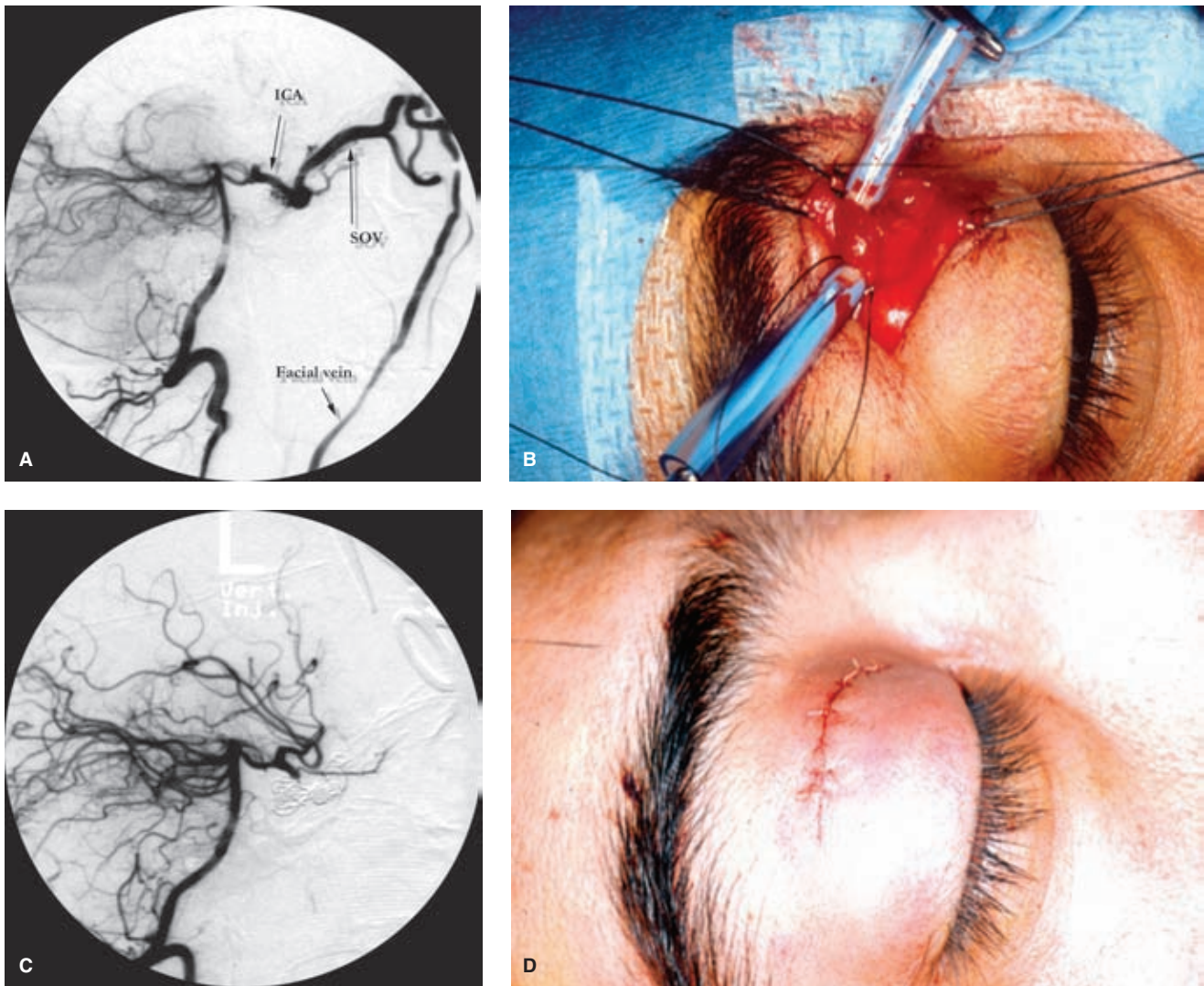


FIGURE 23-10. (A–D) Recanalization of previously treated carotid-cavernous fistula. This patient's presentation was described in Figure 23-4 at which time he was treated by navigation of a microcatheter to the cavernous sinus via the right posterior communicating artery and occlusion of the fistula with coils. The right internal carotid artery was already occluded below this level by the traumatic dissection. Although the treatment was seemingly successful, the patient returned approximately 2 weeks later with recurrence of his bruit and deterioration of his right-sided proptosis. A left vertebral arteriogram (a lateral view) shows recanalization from the supraclinoid carotid (*ICA*) to the superior ophthalmic vein (*SOV*) and draining to the ipsilateral facial vein (labeled). A number of options could have been employed for the second treatment, including another attempt at catheterization of the posterior communicating artery, or retrograde catheterization of the facial vein. In this instance, surgical exposure of the superior ophthalmic artery was employed for direct catheterization with a microcatheter. Image (**B**) shows the ophthalmic vein secured between two vascular ties and ready for puncture. The surgical anatomy can be very confusing during such procedures and the guidance of the orbital surgeon to know which direction is anterior and posterior in the vein is imperative. Image (**C**) is a vertebral artery injection following successful retrograde closure of the recurrent fistula, now demonstrating antegrade flow in the ipsilateral middle cerebral artery (absent in image **A**) and preservation of the ophthalmic artery. Once the fistula is depressurized, closure of the vein becomes more straightforward, and a clinically and esthetically pleasing result can be obtained (**D**). However, losing control of the vein during the procedure while the pressure within is still high could result in a very unpleasant orbital hematoma.

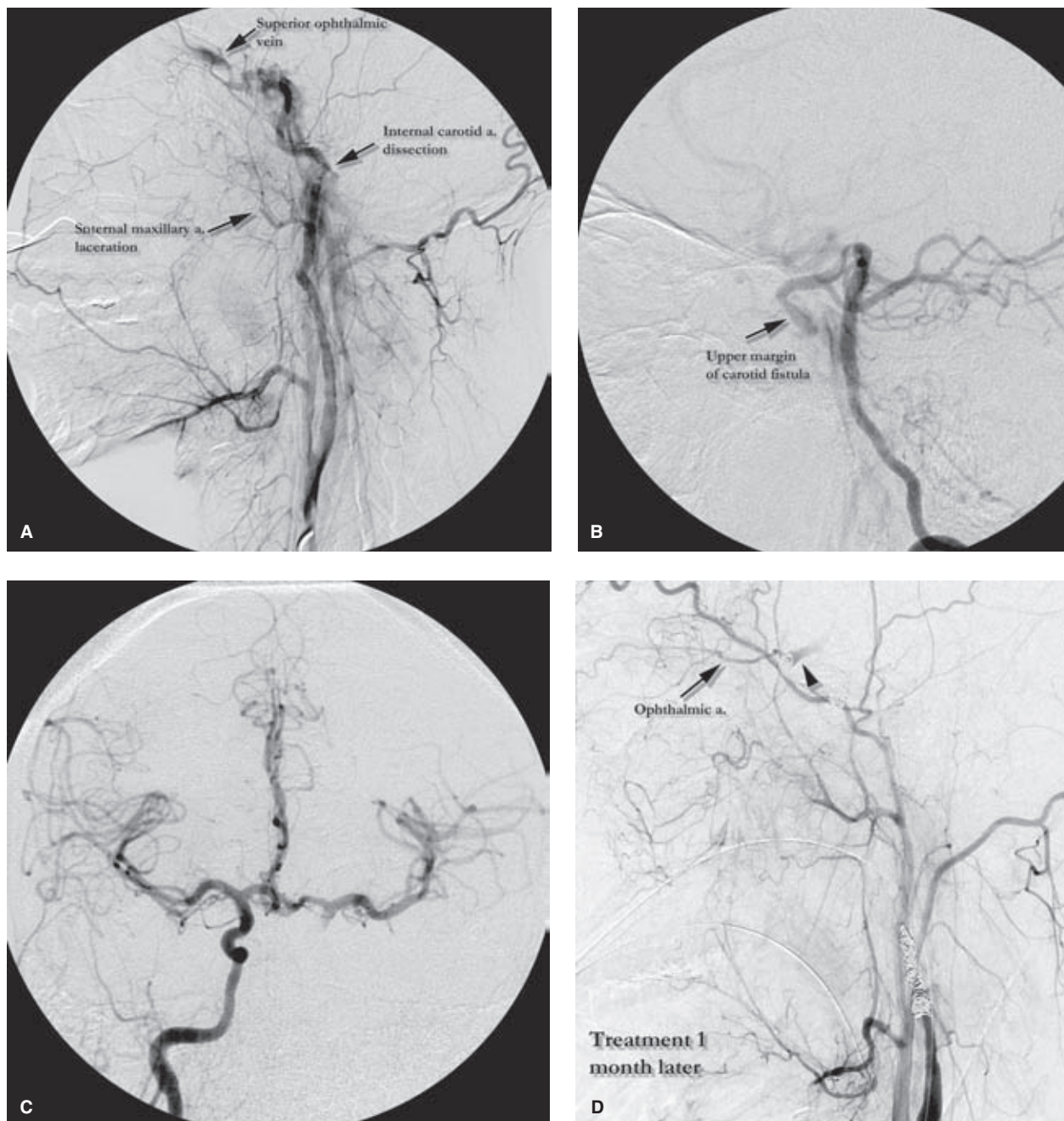


FIGURE 23-11. (A–E) Carotid-cavernous fistula in a teenager: delayed treatment and concern for stump emboli.

This teenager was involved in a severe car accident due to inattentive driving on his part and was studied angiographically for evaluation of uncontrolled facial bleeding. The first study (A) of the left common carotid artery showed laceration of several external carotid artery branches, a severe dissection of the internal carotid artery, fistulous opacification of the superior ophthalmic vein, and absence of antegrade intracranial flow from the left carotid system. The vertebral artery injection (B) showed the upper margin of the fistula accurately, and also showed that the supraclinoid carotid artery on the side of the fistula was still patent. The right carotid artery injection (C) demonstrated excellent perfusion of the left hemisphere via the anterior communicating artery. His lacerated external carotid artery was embolized with particles and gelfoam, and his CCF treatment was deferred. He has no immediate neurologic indications for treatment, but had several other injuries of a more pressing nature.

Approximately 1 month later, his CCF embolization was performed. The fistula had enlarged slightly in the interim, but its dynamics were broadly unchanged otherwise. Due to the dissected nature of the left internal carotid artery, preservation of that artery with a covered stent, or coil occlusion of the fistula only, would have reversed flow in the supraclinoid carotid artery with attendant risks of antegrade generation of thromboembolic complications. Therefore a trapping procedure of the fistula by sacrificing the left internal carotid artery with coils was undertaken. The final images (D and E) via the left common carotid artery and left vertebral artery, respectively, appear reasonably satisfactory. *(continued)*

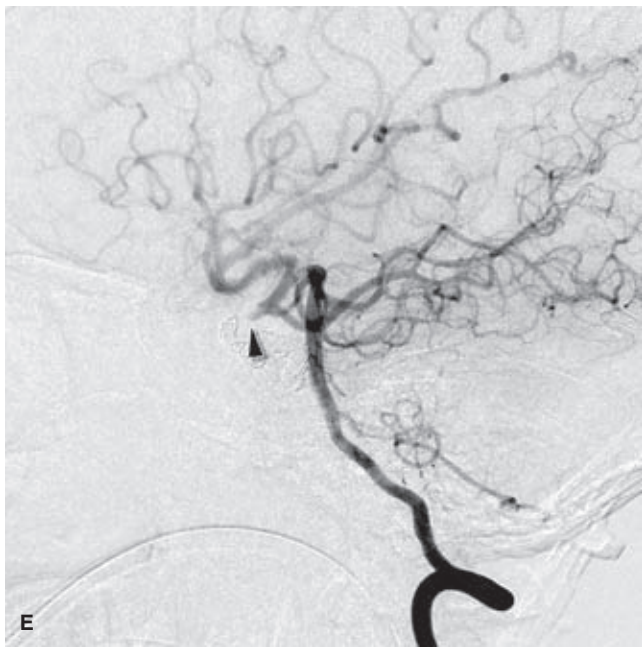


FIGURE 23-11. (CONTINUED) There is retrograde opacification of the ophthalmic artery (labeled) via the left external carotid artery, which results in some stagnation of contrast in the supraclinoid carotid artery (arrowheads in **D** and **E**) with bidirectional flow. Because of this the patient was placed on Coumadin for a 3-month period to discourage any possibility of stump embolization (a complication seen in the young patient in Fig. 23-6, a patient of very similar age and angiographic characteristics).

4. The mass effect of a thrombosed venous sac in the cavernous sinus following occlusion of the fistula may result in aggravation of pressure on the local cranial nerves. The need for prophylactic analgesic and glucocorticoid medication should be anticipated.

References

1. Barrow DL, Spector RH, Braun IF, et al. Classification and treatment of spontaneous carotid-cavernous sinus fistulas. *J Neurosurg* 1985;62:248–256.
2. Lewis AI, Tomsick TA, Tew JM Jr. Management of 100 consecutive direct carotid-cavernous fistulas: Results of treatment

with detachable balloons. *Neurosurgery* 1995;36(2):239–244; discussion 244–235.

3. Halbach VV, Higashida RT, Hieshima GB, et al. Transvenous embolization of direct carotid cavernous fistulas. *AJNR Am J Neuroradiol* 1988;9(4):741–747.
4. Lin TK, Chang CN, Wai YY. Spontaneous intracerebral hematoma from occult carotid-cavernous fistula during pregnancy and puerperium. Case report. *J Neurosurg* 1992;76(4):714–717.
5. Halbach VV, Hieshima GB, Higashida RT, et al. Carotid cavernous fistulae: Indications for urgent treatment. *AJR Am J Roentgenol* 1987;149(3):587–593.
6. Boyes TL, Ralph FT. Carotid-cavernous fistula. *Am J Ophthalmol* 1954;37(2):262–266.
7. Locke CE. Intra-cranial arteriovenous aneurysms or pulsating exophthalmos. *Ann Surg* 1924;80:1–24.
8. Lewis AI, Tomsick TA, Tew JM Jr, et al. Long-term results in direct carotid-cavernous fistulas after treatment with detachable balloons. *J Neurosurg* 1996;84(3):400–404.
9. Moron FE, Klucznik RP, Mawad ME, et al. Endovascular treatment of high-flow carotid cavernous fistulas by stent-assisted coil placement. *AJNR Am J Neuroradiol* 2005;26(6):1399–1404.
10. Lee CY, Yim MB, Kim IM, et al. Traumatic aneurysm of the supraclinoid internal carotid artery and an associated carotid-cavernous fistula: Vascular reconstruction performed using intravascular implantation of stents and coils. Case report. *J Neurosurg* 2004;100(1):115–119.
11. Archondakis E, Pero G, Valvassori L, et al. Angiographic follow-up of traumatic carotid cavernous fistulas treated with endovascular stent graft placement. *AJNR Am J Neuroradiol* 2007;28(2):342–347.
12. Gomez F, Escobar W, Gomez AM, et al. Treatment of carotid cavernous fistulas using covered stents: midterm results in seven patients. *AJNR Am J Neuroradiol* 2007;28(9):1762–1768.
13. Tiewei Q, Ali A, Shaolei G, et al. Carotid cavernous fistulas treated by endovascular covered stent grafts with follow-up results. *Br J Neurosurg* 2010;24(4):435–440.
14. Saatci I, Cekirge HS, Ozturk MH, et al. Treatment of internal carotid artery aneurysms with a covered stent: Experience in 24 patients with mid-term follow-up results. *AJNR Am J Neuroradiol* 2004;25(10):1742–1749.
15. Vanninen RL, Manninen HI, Rinne J. Intracranial iatrogenic carotid pseudoaneurysm: Endovascular treatment with a polytetrafluoroethylene-covered stent. *Cardiovasc Intervent Radiol* 2003;26(3):298–301.

Nonaneurysmal Perimesencephalic Subarachnoid Hemorrhage

Key Points

- Approximately 5% of nontraumatic subarachnoid hemorrhages conform to the benign pattern of nonaneurysmal subarachnoid hemorrhage.
- Even with this pattern of hemorrhage however, there is still a 3% to 9% probability of finding a cerebral aneurysm.

In approximately 15% to 30% of patients with spontaneous subarachnoid hemorrhage, no cause of bleeding can be identified on the initial cerebral angiogram (1–5). While patients with negative angiography after a subarachnoid hemorrhage have a benign overall prognosis with a low yield from repeated angiography, it is important to discern between the subgroups of patients within this population to avoid missing potentially serious or treatable lesions. Within this population of patients with negative cerebral angiography, a particular subgroup was first described in 1985 in the Netherlands (6) with an almost universally benign and favorable outcome. Extent and volume of hemorrhage is mild and confined to the prepontine and perimesencephalic area, and the clinical condition is characterized by headache and signs of meningeal irritation only (Figs. 24-1–24-3). The clinical entity of “nonaneurysmal perimesencephalic subarachnoid hemorrhage” (alternatively named “pretruncal nonaneurysmal hemorrhage”) has since been validated in other countries (7,8). This group probably accounts for 5% of all patients presenting with nontraumatic SAH (9) or a third of the angiogram-negative nonaneurysmal population, with the following features:

- Onset of subarachnoid hemorrhage is spontaneous and presents with severe headache and meningeal irritation. Focal neurologic deficits, focal signs, and diminished levels of consciousness are not seen.
- The CT pattern of hemorrhage is symmetric or virtually so, confined to the perimesencephalic area, the prepontine cistern and interpeduncular fossa, the posterior part of the suprasellar cistern, the posterior part of the interhemispheric

fissure, and to a minimal degree the medial aspects of the Sylvian fissures. Dense clots of blood are uncharacteristic. Extension into the anterior extent of the interhemispheric fissure, into the lateral aspects of the Sylvian fissures, and into the ventricles, or intraparenchymal hematoma are not seen with this entity, and such findings would qualify the condition as diffuse nonperimesencephalic nonaneurysmal hemorrhage (see below) (10). The CT images used to define this pattern must be obtained within 48 hours of the bleed.

- Hydrocephalus may develop in a minority of patients with nonaneurysmal perimesencephalic subarachnoid hemorrhage but is usually mild and resolves spontaneously (4,10). Hydrocephalus can occur in patients in whom encirclement of the mesencephalon by blood obstructs flow of CSF through the tentorial incisura (11).
- A familial or genetic predisposition seems likely as several instances of siblings or first-degree relatives with this condition have been recognized (12,13).
- The prognosis for patients with this pattern of hemorrhage and with negative cerebral angiography is excellent with a low risk of vasospasm, rehemorrhage, or of neurologic sequelae (5,6,14,15).

It is thought that the source of hemorrhage in this group of patients may be venous, possibly from a ruptured prepontine vein or an angiographically occult vascular malformation at the pial surface, arterial microaneurysms of the basilar perforators (16,17), or venous stenotic disease due to congenital causes or acquired narrowings (18). The combination of a typical CT pattern of perimesencephalic subarachnoid hemorrhage and a negative angiogram in a patient with a good clinical grade is very reassuring that the prognosis for the patient is favorable. The likelihood of vasospasm in this group of patients is also very low and rarely of clinical concern. Several publications suggest rates of significant hydrocephalus or clinically symptomatic vasospasm can be seen in up to 25% of patients, but it is likely that many papers have included in their analysis patients with more diffuse patterns of nonaneurysmal subarachnoid hemorrhage (19,20).

The chance of finding an aneurysm in the setting of this pattern of hemorrhage is between 3% and 9% (20,21).

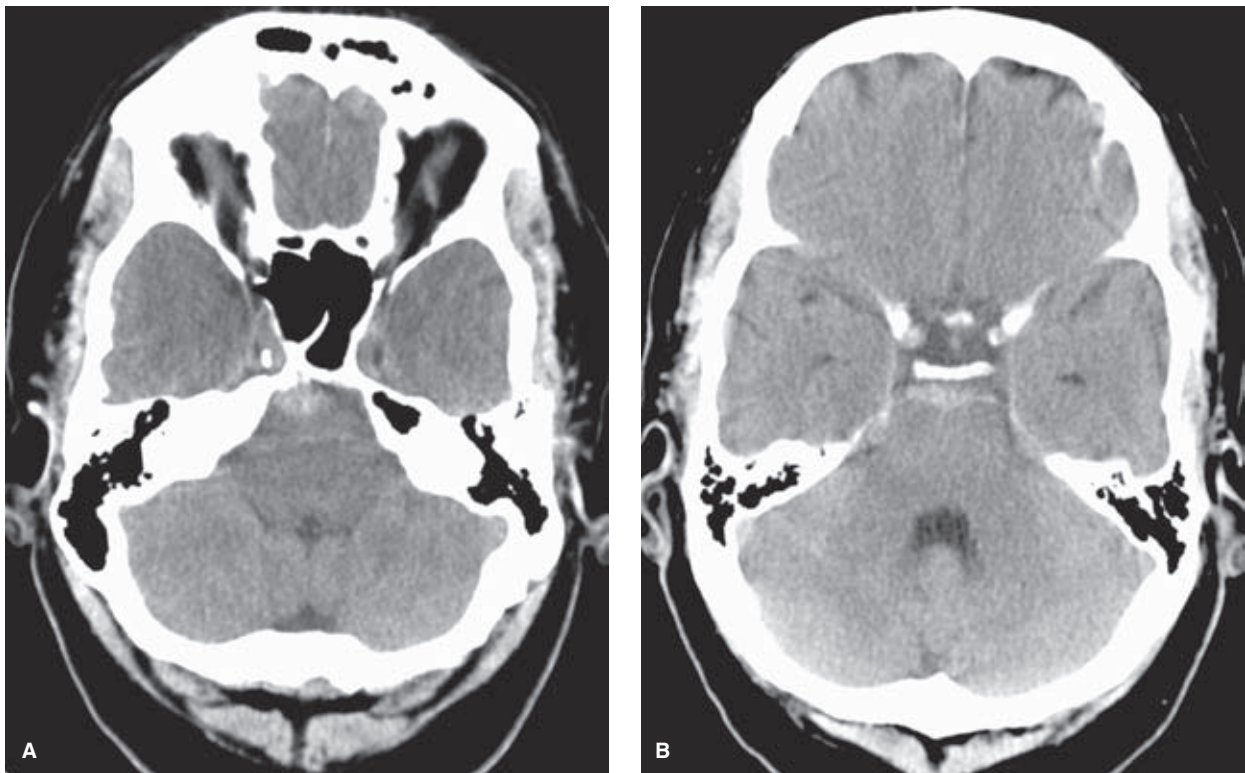


FIGURE 24-1. (A–B) Pretruncal subarachnoid hemorrhage. A typical pattern of “pretruncal” or prepontine hemorrhage is demonstrated in this 55-year-old patient presenting with headache and a stiff neck. Angiographic workup was negative, and recurrence of hemorrhage did not occur.



FIGURE 24-2. Perimesencephalic hemorrhage. This 29-year-old patient presented with typical clinical symptoms of headache and nuchal rigidity. Angiography was normal. The hemorrhage is localized in the left perimesencephalic region, although a small quantity of blood rests dependently in the interpeduncular fossa.



FIGURE 24-3. Symmetric distribution of perimesencephalic hemorrhage. A CT image demonstrates a typical appearance of nonaneurysmal perimesencephalic subarachnoid hemorrhage. The anterior interhemispheric and Sylvian fissure are clear. There is mild dilatation of the temporal horns, indicating hydrocephalus.

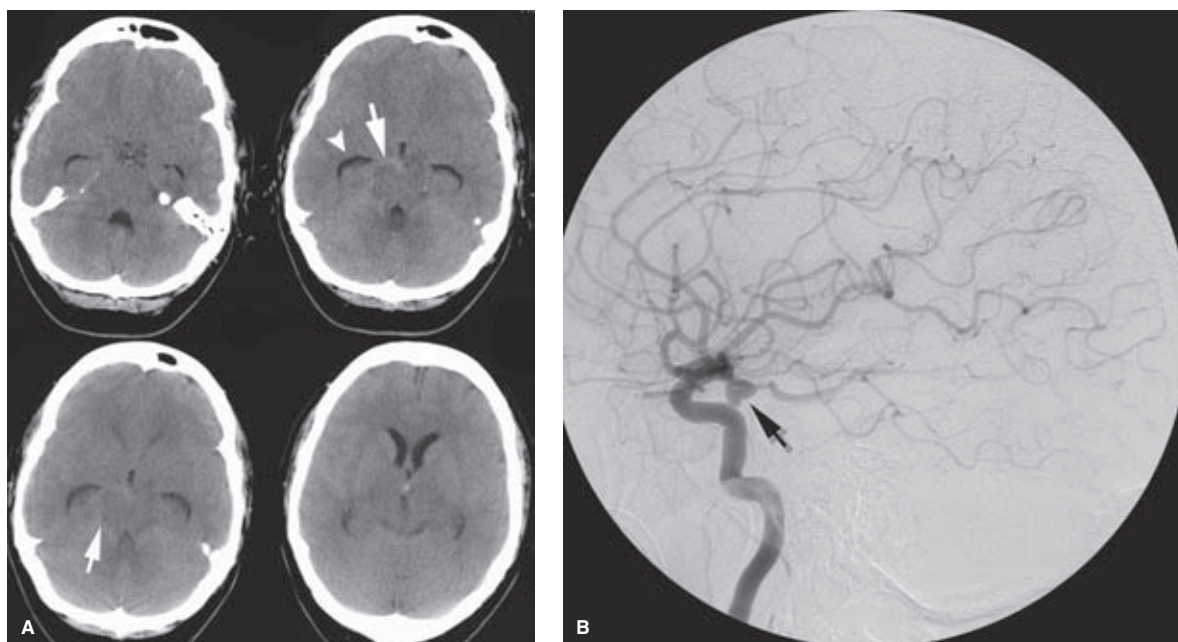


FIGURE 24-4. (A–B) **Aneurysm in the setting of apparent perimesencephalic bleed.** A young adult presented with very mild symptoms and a CT scan (A) showing a very typical appearance of perimesencephalic bleeding (arrows) and mild hydrocephalus (arrowhead). However, the angiogram (B) shows an irregular aneurysm of the right posterior communicating artery with lobulation of the dome (arrow), representing either an indentation of the tentorium on the dome or the presence of a ruptured daughter sac. The perimesencephalic pattern of subarachnoid hemorrhage on CT cannot be relied on to preclude the need for further investigation.

Fewer than 2% of aneurysms present with this pattern of hemorrhage according to most publications (11,22,23), but up to 16.6% of ruptured aneurysms of the posterior circulation can do so (21). Therefore, most authors still agree on the need for at least one cerebral angiogram even when the initial CT pattern is typical for nonaneurysmal perimesencephalic subarachnoid hemorrhage (24), and preferably two angiograms when the pattern of hemorrhage is exten-

sive or atypical (21). Aneurysms typically found hiding under a perimesencephalic pattern of hemorrhage include the tip of the basilar artery; the vertebrobasilar junction possibly associated with a fenestration; the origin of the posterior inferior cerebellar artery contralateral to the side of vertebral artery injection; the distal posterior cerebellar artery; or the posterior communicating artery (Figs. 24-4–24-9) (25).

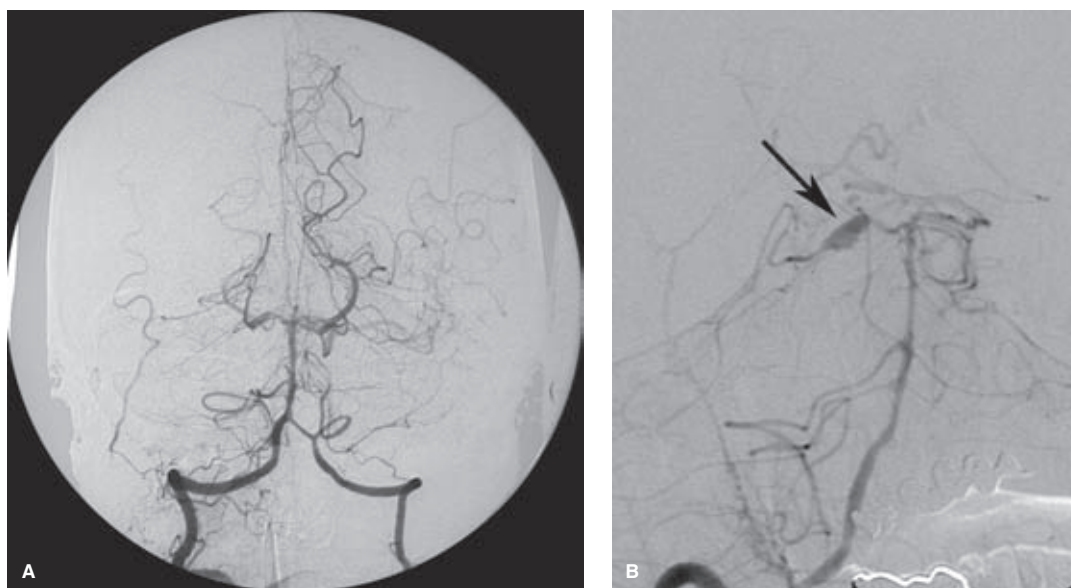


FIGURE 24-5. (A–B) **Angiographically negative subarachnoid hemorrhage.** A middle-aged patient presented with subarachnoid hemorrhage and had a negative arteriographic workup. Because of suspicion raised by the pattern of profuse hemorrhage on CT, an early follow-up angiogram was performed a few days later (Townes view of left vertebral artery in A). This shows subtle irregularity or complexity in the region of the overlap between the hypoplastic P1 segment and the right superior cerebellar artery. A magnification oblique view (B) demonstrates a dissection of the right superior cerebellar artery (arrow), which had eluded attention on the first angiogram. Its conspicuity on this second angiogram is accentuated by the presence of diffuse early vasospasm of the posterior circulation, not present on the first angiogram.

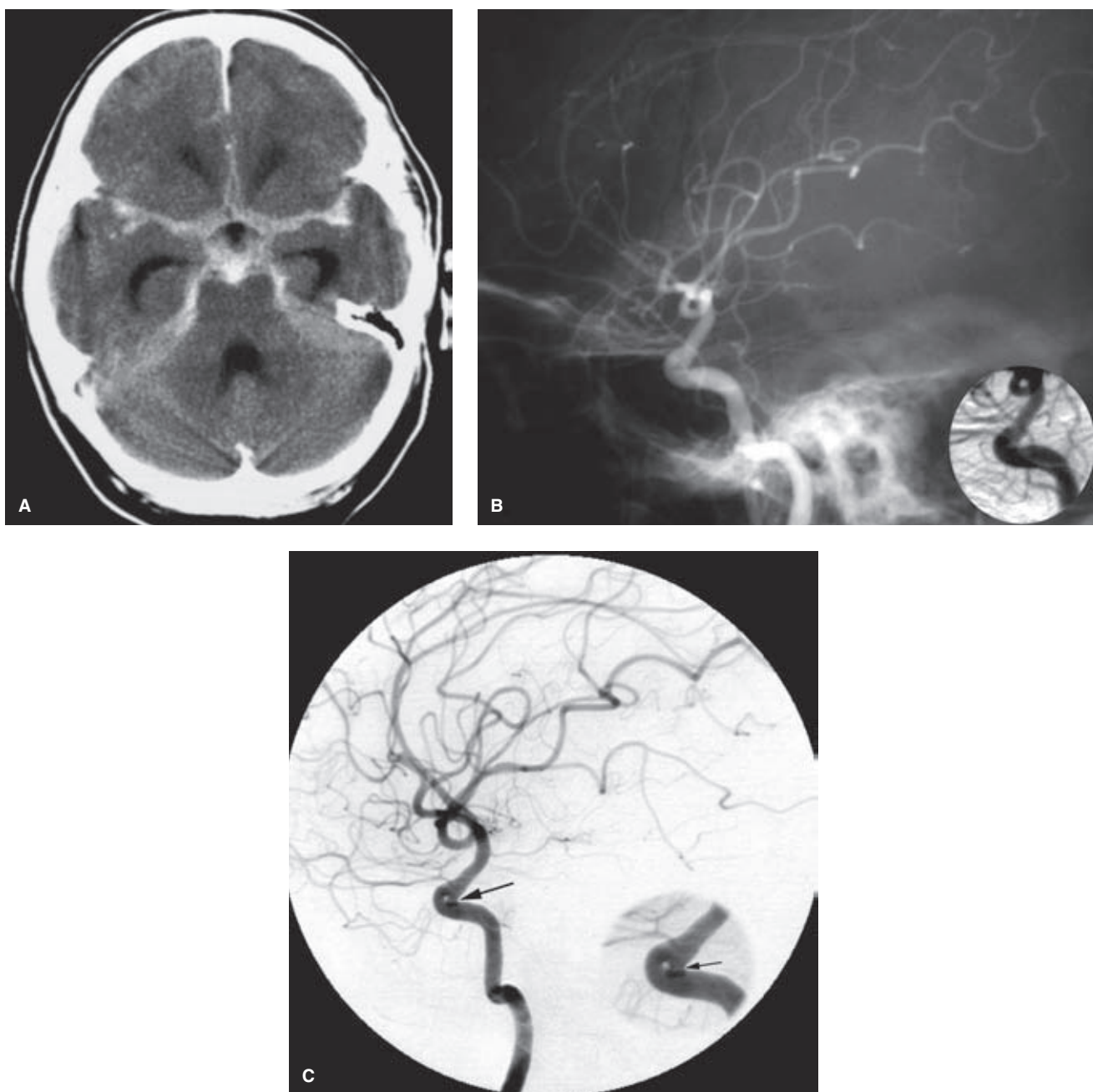
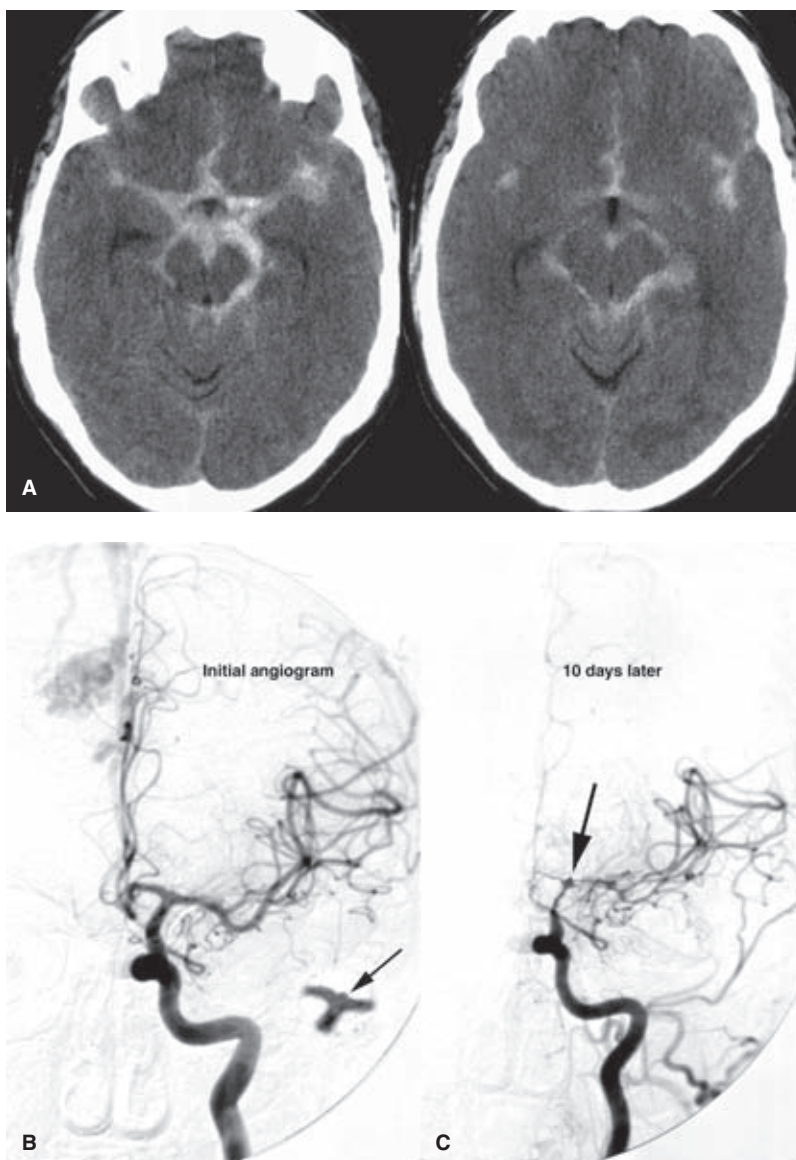


FIGURE 24-6. (A–C) Angiographically negative subarachnoid hemorrhage: importance of obliqued and skewed views. A CT examination (A) in an elderly female with Grade III subarachnoid hemorrhage demonstrates profuse subarachnoid hemorrhage and hydrocephalus. The initial angiogram (B) of the left internal carotid artery was interpreted as negative (*inset of subtracted image of left internal carotid artery siphon*). A follow-up angiogram showed an identical appearance on the first lateral view. A skewed view (C) of the left siphon demonstrated the aneurysm (*arrow*). On the magnified *inset*, a waist-like constriction of the aneurysm probably represents where this subarachnoid aneurysm enters the dura of the cavernous sinus. This aneurysm could not be seen on any PA or shallow oblique views because of its position directly behind the genu. Looking for a widening of the diameter of the genu (apparent on the initial lateral angiogram) can help to direct one to the presence of such an occult aneurysm. Because this aneurysm extends from the subarachnoid space to the extradural cavernous sinus, the term *transitional aneurysm* might be invoked. However, transitional aneurysms usually start on the cavernous segment and expand in the other direction. This case predates the availability of 3D rotational angiography which would have certainly demonstrated a hidden lesion of this nature and location. A low threshold for performing 3D rotational angiography in the work-up of occult SAH is a good policy.

FIGURE 24-7. (A–C) Angiographically negative subarachnoid hemorrhage II: importance of follow-up angiography and examining the images very closely.

A CT examination (A) in a young adult with Grade III subarachnoid hemorrhage and a right hemispheric AVM demonstrates extensive subarachnoid hemorrhage, more profuse on the left side of the suprasellar cistern. The initial angiogram (B) was interpreted as negative for the presence of aneurysm. A follow-up angiogram (C) demonstrated significant intracranial vasospasm. Serendipitously, the vasospasm allowed recognition of a 2-mm blister aneurysm of the internal carotid artery bifurcation (arrow), which was confirmed at surgery. In retrospect, a very subtle dimple of the internal carotid artery bifurcation was evident on the initial angiogram (inset on B).



These sites must be screened perfectly on the initial angiogram to allow discharge of the patient without further investigation. Most authors consider that there is not an indication for repeat cerebral angiography if the clinical appearance of the patient, the CT pattern of hemorrhage, and the technical quality of the angiogram (particularly that of the posterior fossa) are all satisfactory for the diagnosis of perimesencephalic hemorrhage. The final dilemma is a counterbalance between the small risk of an angiogram versus the risk of missing a subtle aneurysm or other lesion in this group of patients.

► **DIFFUSE NONPERIMESENCEPHALIC NONANEURYSMAL HEMORRHAGE**

Patients with diffuse nonaneurysmal subarachnoid hemorrhage in whom the pattern is more prominent and

widespread involving multiple cisterns, Sylvian, interhemispheric, perimesencephalic, and intraventricular blood are distinguished from those with simple perimesencephalic hemorrhage (Fig. 24-10). This is considered a benign entity too, although not quite as favorable as hemorrhage confined to the prepontine or perimesencephalic regions (26,27). Those patients with a more diffuse pattern are more prone to clinical complications such as a hydrocephalus, vasospasm, and ischemic complications from the hemorrhage, and in one study showed a 76% rate of complete recovery versus 97% for the perimesencephalic hemorrhage group (28). This nonperimesencephalic nonaneurysm group of patients is somewhat less likely to achieve a complete return to premorbid levels of professional and social well-being, performing less well on emotional and psychological batteries (27).

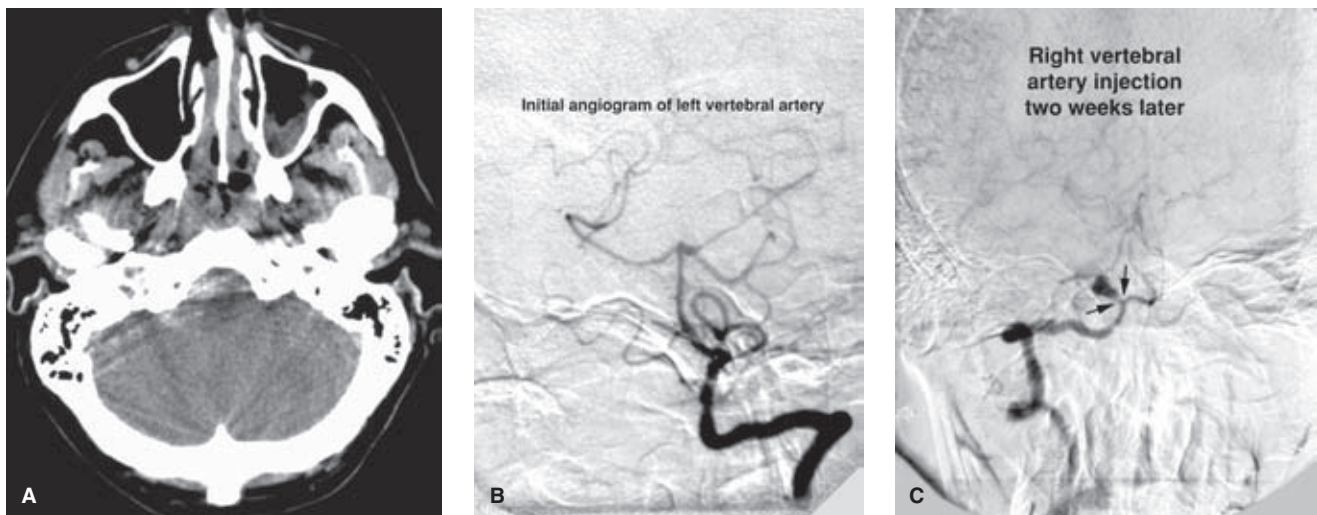


FIGURE 24-8. (A–C) **Angiographically negative subarachnoid hemorrhage III: importance of the distal right vertebral artery and right posterior inferior cerebellar artery.** An elderly male was admitted to the hospital with Grade II subarachnoid hemorrhage and a preponderance of blood on the right side of the posterior fossa (A). This CT appearance should prompt particular suspicion about the right posterior inferior cerebellar artery. Its omission from angiographic interrogation constitutes a major, and in this case fatal, oversight. Moreover, in the setting of a posterior fossa hemorrhage in which the right posterior inferior cerebellar artery origin has been seen by reflux, the possibility of a subarachnoid dissection of the right vertebral artery should not be forgotten when no other explanation for subarachnoid hemorrhage has been found. The initial angiogram (B) of the posterior fossa was performed via the left vertebral artery only, an injection that did not opacify the distal right vertebral artery. The patient made a complete clinical recovery. A follow-up angiogram (C) 2 weeks later included an injection of the right vertebral artery. This demonstrated an aneurysm of the origin of the right posterior inferior cerebellar artery (arrows). The patient was immediately scheduled for treatment, but the aneurysm ruptured fatally the next day.



FIGURE 24-9. **Siderosis of the subarachnoid tissues due to a spinal ependymoma.** An axial T2-weighted MRI image in a patient with recurrent angiogram-negative subarachnoid hemorrhage demonstrates outlining of the structures of the posterior fossa by susceptibility artifact due to deposition of hemosiderin. An ependymoma of the spine was subsequently identified as the cause of bleeding.

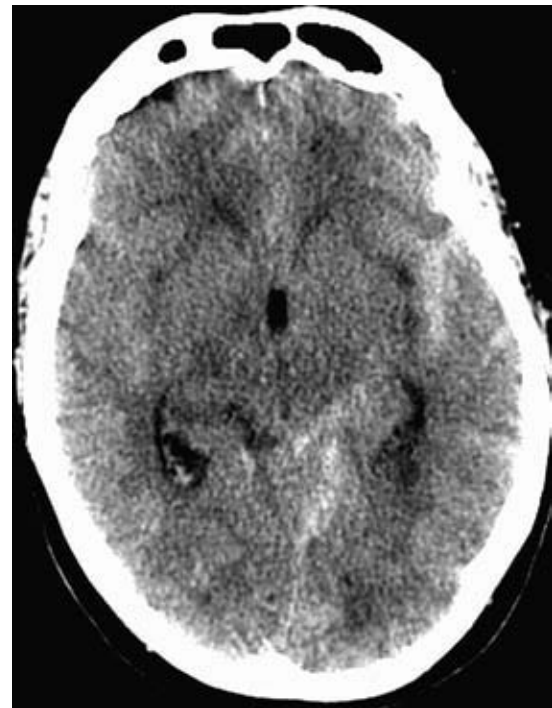


FIGURE 24-10. **Diffuse pattern of angiographically negative subarachnoid hemorrhage.** This 82-year-old patient presented with apparently spontaneous subarachnoid hemorrhage. The pattern is too diffuse to be considered consistent with the benign category of perimesencephalic hemorrhage. Although no cause for hemorrhage was identified on sequential cerebral angiograms and his subsequent clinical outcome was good, a high index of suspicion remains in cases of entities such as subtle dissections, microaneurysms, or blister aneurysms being present but eluding attention.

References

- Kassell NF, Torner JC, Jane JA, et al. The International Cooperative Study on the Timing of Aneurysm Surgery. Part 2: Surgical results. *J Neurosurg* 1990;73(1):37–47.
- West HH, Mani RL, Eisenberg RL, et al. Normal cerebral arteriography in patients with spontaneous subarachnoid hemorrhage. *Neurology* 1977;27(6):592–594.
- Shephard RH. Prognosis of spontaneous (non-traumatic) subarachnoid haemorrhage of unknown cause. A personal series 1958–1980. *Lancet* 1984;1(8380):777–779.
- Congia S, Carta S, Coraddu M. Subarachnoid hemorrhage of unknown origin. A 44 cases study. *Acta Neurol (Napoli)* 1994;16(4):177–183.
- Duong H, Melancon D, Tampieri D, et al. The negative angiogram in subarachnoid haemorrhage. *Neuroradiology* 1996;38(1):15–19.
- van Gijn J, van Dongen KJ, Vermeulen M, et al. Perimesencephalic hemorrhage: A nonaneurysmal and benign form of subarachnoid hemorrhage. *Neurology* 1985;35(4):493–497.
- Goergen SK, Barrie D, Sacharias N, et al. Perimesencephalic subarachnoid haemorrhage: Negative angiography and favourable prognosis. *Australas Radiol* 1993;37(2):156–160.
- Canhao P, Ferro JM, Pinto AN, et al. Perimesencephalic and nonperimesencephalic subarachnoid haemorrhages with negative angiograms. *Acta Neurochir (Wien)* 1995;132(1–3):14–19.
- Flaherty ML, Haverbusch M, Kissela B, et al. Perimesencephalic subarachnoid hemorrhage: Incidence, risk factors, and outcome. *J Stroke Cerebrovasc Dis* 2005;14(6):267–271.
- Rinkel GJ, Wijdicks EF, Vermeulen M, et al. Nonaneurysmal perimesencephalic subarachnoid hemorrhage: CT and MR patterns that differ from aneurysmal rupture. *AJNR Am J Neuroradiol* 1991;12(5):829–834.
- Rinkel GJ, Wijdicks EF, Vermeulen M, et al. Acute hydrocephalus in nonaneurysmal perimesencephalic hemorrhage: Evidence of CSF block at the tentorial hiatus. *Neurology* 1992;42(9):1805–1807.
- Tieleman AA, van der Vliet TA, Vos PE. Two first-degree relatives with perimesencephalic nonaneurysmal hemorrhage. *Neurology* 2006;67(3):535–536.
- Lazaridis C, Bodle J, Chaudry I, et al. Familial nontraumatic, nonaneurysmal subarachnoid hemorrhage: A report on three first-degree siblings. *J Neurosurg* 2011;115(3):621–623.
- Alexander MS, Dias PS, Uttley D. Spontaneous subarachnoid hemorrhage and negative cerebral panangiography. Review of 140 cases. *J Neurosurg* 1986;64(4):537–542.
- Juul R, Fredriksen TA, Ringkjøb R. Prognosis in subarachnoid hemorrhage of unknown etiology. *J Neurosurg* 1986;64(3):359–362.
- Park SQ, Kwon OK, Kim SH, et al. Pre-mesencephalic subarachnoid hemorrhage: Rupture of tiny aneurysms of the basilar artery perforator. *Acta Neurochir (Wien)* 2009;151(12):1639–1646.
- White JB, Wijdicks EF, Cloft HJ, et al. Vanishing aneurysm in pretruncal nonaneurysmal subarachnoid hemorrhage. *Neurology* 2008;71(17):1375–1377.
- Shad A, Rourke TJ, Hamidian Jahromi A, et al. Straight sinus stenosis as a proposed cause of perimesencephalic nonaneurysmal haemorrhage. *J Clin Neurosci* 2008;15(7):839–841.
- Samaniego EA, Dabus G, Fuentes K, et al. Endovascular treatment of severe vasospasm in nonaneurysmal perimesencephalic subarachnoid hemorrhage. *Neurocrit Care* 2011;15(3):537–541.
- Whiting J, Reavey-Cantwell J, Velat G, et al. Clinical course of nontraumatic, nonaneurysmal subarachnoid hemorrhage: A single-institution experience. *Neurosurg Focus* 2009;26(5):E21.
- Alen JF, Lagares A, Lobato RD, et al. Comparison between perimesencephalic nonaneurysmal subarachnoid hemorrhage and subarachnoid hemorrhage caused by posterior circulation aneurysms. *J Neurosurg* 2003;98(3):529–535.
- Pinto AN, Ferro JM, Canhao P, et al. How often is a perimesencephalic subarachnoid haemorrhage CT pattern caused by ruptured aneurysms? *Acta Neurochir (Wien)* 1993;124(2–4):79–81.
- Van Calenbergh F, Plets C, Goffin J, et al. Nonaneurysmal subarachnoid hemorrhage: Prevalence of perimesencephalic hemorrhage in a consecutive series. *Surg Neurol* 1993;39(4):320–323.
- Dupont SA, Lanzino G, Wijdicks EF, et al. The use of clinical and routine imaging data to differentiate between aneurysmal and nonaneurysmal subarachnoid hemorrhage prior to angiography. Clinical article. *J Neurosurg* 2010;113(4):790–794.
- Schievink WI, Wijdicks EF, Piepgras DG, et al. Perimesencephalic subarachnoid hemorrhage. Additional perspectives from four cases. *Stroke* 1994;25(7):1507–1511.
- Gupta SK, Gupta R, Khosla VK, et al. Nonaneurysmal nonperimesencephalic subarachnoid hemorrhage: Is it a benign entity? *Surg Neurol* 2009;71(5):566–571; discussion 571, 571–562, 572.
- Beseoglu K, Pannes S, Steiger HJ, et al. Long-term outcome and quality of life after nonaneurysmal subarachnoid hemorrhage. *Acta Neurochir (Wien)* 2010;152(3):409–416.
- Hui FK, Tumialan LM, Tanaka T, et al. Clinical differences between angiographically negative, diffuse subarachnoid hemorrhage and perimesencephalic subarachnoid hemorrhage. *Neurocrit Care* 2009;11(1):64–70.

25

ENT Bleeding and Tumor Embolization

Key Points

- Airway protection is one of the biggest oversights or risk factors affecting patient safety and outcome during head and neck embolizations.
- Hazardous anastomotic connections in the region of the orbit and at the skull base are almost universally present to some degree and need to be considered carefully during craniofacial embolizations.

Head and neck embolizations for acute bleeding, preoperative tumor devascularization, or preoperative test occlusion share a common anatomic background and similar considerations with reference to technology and risk, and, therefore, to avoid repetition will be discussed together here. Fatal or debilitating complications from these procedures are rare, fortunately. Most patients are remarkably resilient and can pull through anything reasonable that the medical profession is apt to throw at them. It is with an uncommon or rare event that one's experience or diligence will make a difference to patient outcome. Adverse endovascular outcomes in the head and neck involve blindness, disfiguring skin necrosis, or intracranial ischemic strokes, so one has to conduct these and all neurointerventional procedures methodically and carefully with a view to preventing a rare or uncommon set of circumstances whereby such outcomes arise. There are two principal considerations for patient safety during these procedures.

The first consideration is airway protection. A patient who is propped up in bed talking to you before the procedure may have much more difficulty maintaining an airway when sedated and supine on the angiographic table. Furthermore, if bleeding resumes during the procedure into the oropharyngeal cavity this may escape the initial attention of staff in the room and the patient may easily aspirate a large clot. Clotted blood is much more difficult for patients to clear from the airway than phlegm or other secretion, and respiratory distress can quickly establish itself. Moreover, patients who have had laryngeal surgery may not be able to communicate their distress to the team, particularly when they are hidden from view under the drapes and behind the

lead shields. Therefore, a low threshold for using general anesthesia is recommended. It is a tedium waiting for the anesthesia team to arrive and to get all their lines set up, and the temptation is there to say that one can get along perfectly fine without them. That is true in 98% of cases, but it is the other 2% that counts.

Secondly, many disastrous or unnecessary complications of head and neck embolization procedures relate to variant or misperceived vascular anatomy. One must be very suspicious at all times that variant connections with the ophthalmic artery or intracranial vessels might be present, even if they do not show themselves on the initial angiogram. Dynamics of flow can change with relief of catheter-induced vasospasm or due to the effects of progressive embolization, meaning that injections that appeared safe early in the procedure become much more hazardous later. The commonest dangerous anastomotic junctures (1) where the external carotid and intracranial circulation interplay are:

- *The common carotid artery bifurcation.* During all embolizations in proximal branches of the external carotid artery the risk of inadvertent reflux of an errant coil or liquid agent into or even close to the external carotid artery trunk must be kept in mind. The biphasic pattern of flow in the external carotid trunk can pull a liquid device or loose coil into the stream of common carotid flow and thence to the head (Fig. 25-1).
- *The ascending pharyngeal artery.* The anastomotic connections of the ascending pharyngeal artery are many, and include the C3 anastomosis to the ipsilateral vertebral artery and laceral branch to the inferolateral trunk of the internal carotid artery, amongst others (Fig. 25-2).
- *The C1 and C2 anastomotic connections between the vertebral artery and the occipital artery.* These are consistently present in virtually all patients and are sometimes characterized by an immediacy of flow that can be alarming. Embolizations in the occipital artery should be conducted with an understanding that the ipsilateral vertebral artery is only millimeters away and readily accessible to the contents of one's syringe (Fig. 25-3).
- *The middle meningeal artery and ophthalmic artery.* The variant connections whereby the ophthalmic supply is partially or completely derived from variant branches of the middle meningeal artery have been covered in

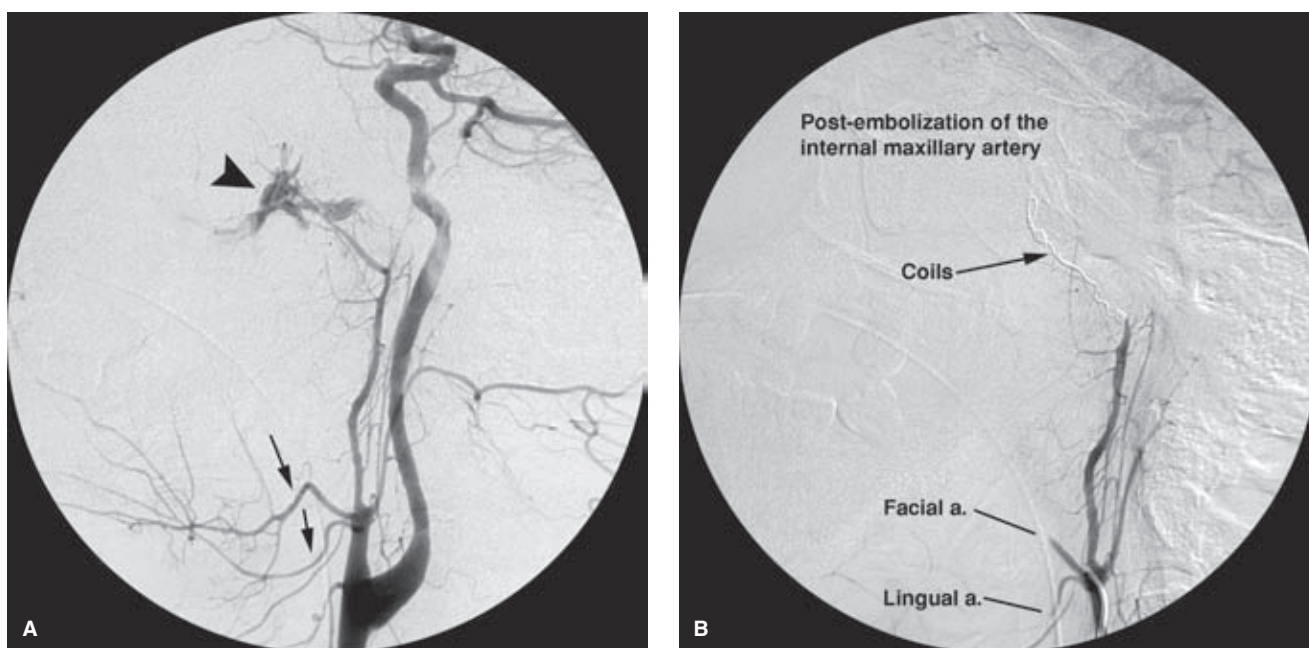


FIGURE 25-1. (A–B) Dangers of forceful injection of Gelfoam with proximal reflux. Here was a lucky escape and a lesson well learned by all involved. A middle-aged patient with penetrating facial injuries shows severe extravasation from the distal left internal maxillary artery (*arrowhead* in **A**) correlating with her state of near exsanguination evident from her appearance and clinical status. A rapid control of the hemorrhage with microcoils and Gelfoam pledgets via a microcatheter was performed. Due to the urgency of the moment, a Gelfoam pledget was injected forcefully, but it was unclear where it had lodged. A postembolization run (**B**) demonstrates satisfactory suppression of the extravasation. However, the fate of the refluxed Gelfoam is now apparent with occlusions of the facial artery and lingual artery (compare with the arteries indicated in **A**). Observe in (**A**) how easily it would have been from this episode of inadvertent reflux to carry the Gelfoam back into the ostium of the internal carotid artery, an event of potentially disastrous consequences for any patient. Fortunately, in this case, there was no angiographic or clinical evidence of intracranial occlusions, and the episode was inscribed in the annals of “All’s well that ends well, but don’t ever do this again.” Incidentally, with the internal maxillary artery and facial artery occluded on the left side, as long as the right external carotid artery is not embolized, there should be no significant risk of ischemic injury to the left face. However, one needs to be careful in patients in situations such as this because the external carotid artery circulation is not all forgiving, particularly in the distal facial artery and lingual artery where ischemic necrosis can follow even from PVA embolization performed in a heavy-handed manner.

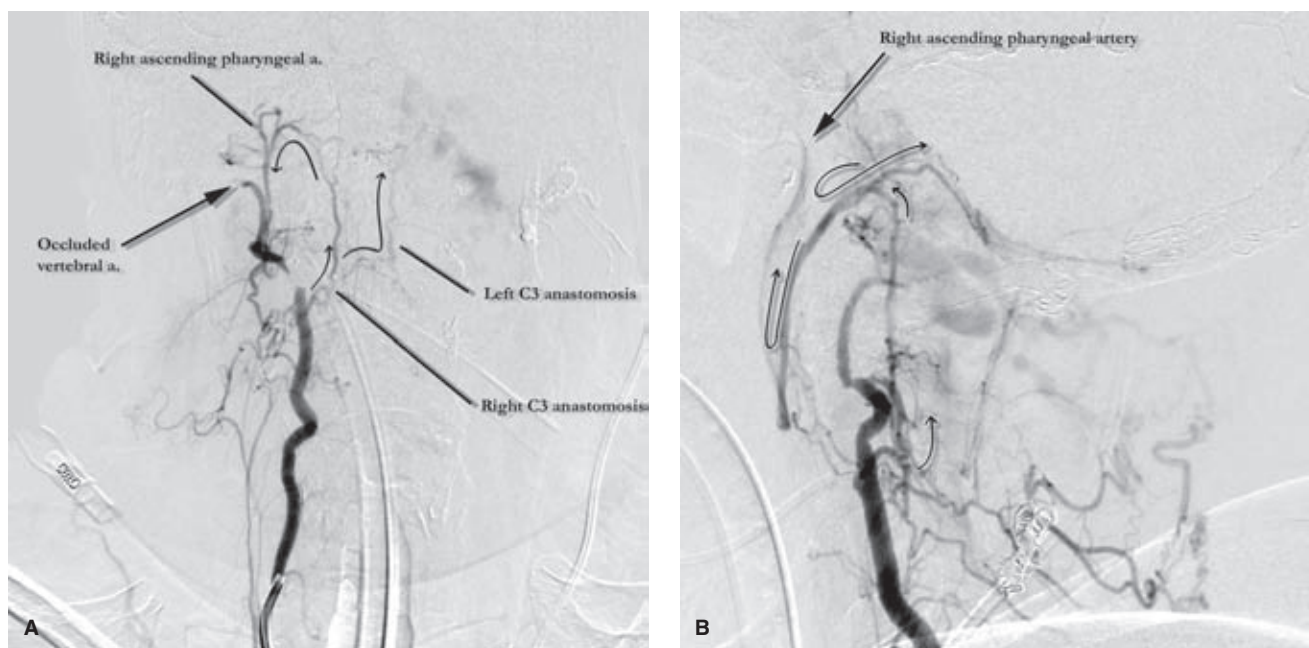


FIGURE 25-2. (A–B) Complex anatomic connections of the ascending pharyngeal artery. Several variations of the anatomy of this region are demonstrated elsewhere in the text. This example is taken from the treatment images of a complex skull base dural AVM where the right vertebral artery, previously occluded with coils at the skull base, is being injected. The AP (**A**) and lateral views (**B**) show bilateral opacification of the C3 anastomotic branches (*curved arrows* indicate direction of flow) connecting to the right ascending pharyngeal artery, and thence to the dural AVM via the posterior fossa dural branches along the skull base and dorsal surface of the clivus.

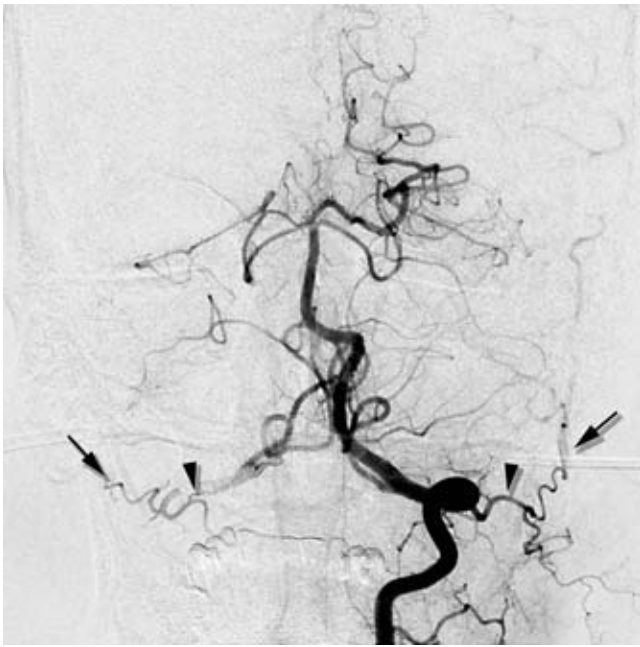


FIGURE 25-3. Vertebral artery to occipital artery C1 anastomoses. These connections are virtually universal and robust. Despite this they are seen only fleetingly under the effects of a power-injector run, during pathologic states, or during disruption of normal physiology by catheter-induced spasm. In this AP view the occipital artery (*arrows*) is seen bilaterally through the C1 anastomosis (*arrowhead*), that on the right being a very short connection of a few millimeters. On the next frame these arterial branches were no longer opacified.

previous chapters. Orbital pathology, such as vascular malformations, will tend to accentuate the likelihood of such anastomoses opening up to a physiologically significant degree. A good habit to cultivate is that one's first glance at every external carotid arteriogram should be for the presence of any component of the ophthalmic artery (Figs. 25-4 and 25-5).

- *Distal external carotid artery and internal carotid artery.* Anastomotic connections between the terminal branches of the external carotid artery and the intracranial circulation can flow readily via such routes as the foramen rotundum and the Vidian canal. Even when they are not seen angiographically, one has to bear them in mind when

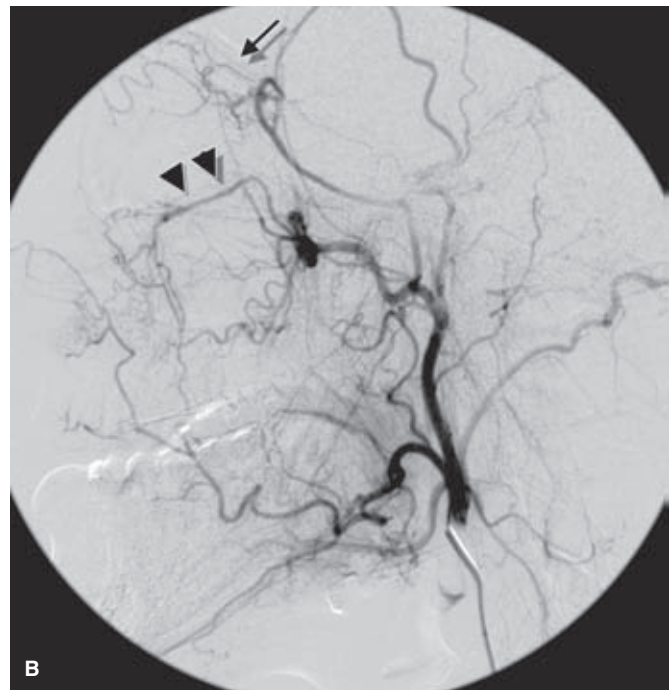
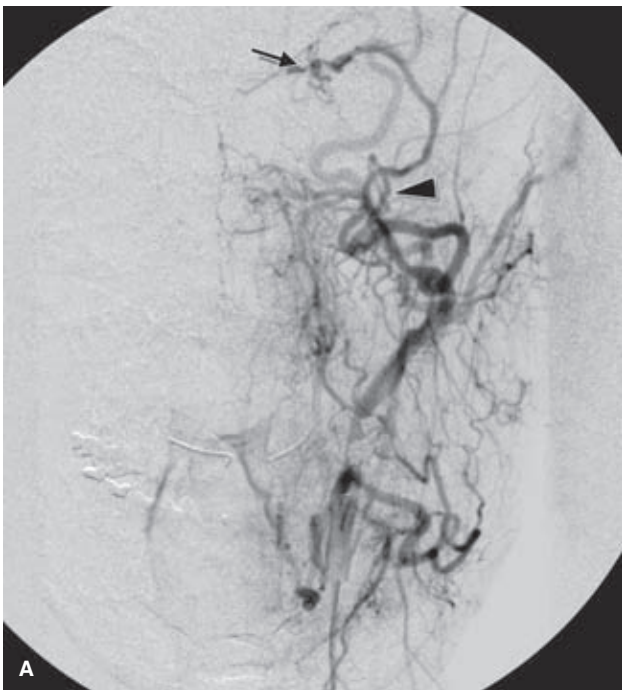


FIGURE 25-4. (A–B) Ophthalmic artery (arrow) supplied by middle meningeal artery (arrowhead). This young patient demonstrated bilateral anomalous supply to the ophthalmic artery from the middle meningeal artery, unrecognized by the physician performing an epistaxis embolization, as a result of which she lost vision in one eye (see Figure 5-1). The AP (**A**) and lateral views (**B**) of the left external carotid artery show the ophthalmic artery territory (*arrows*) perfused from the middle meningeal artery (*arrowhead* in **A**). The infraorbital artery (*double arrowheads* in **B**) serve as a reference for the orbital anatomy.

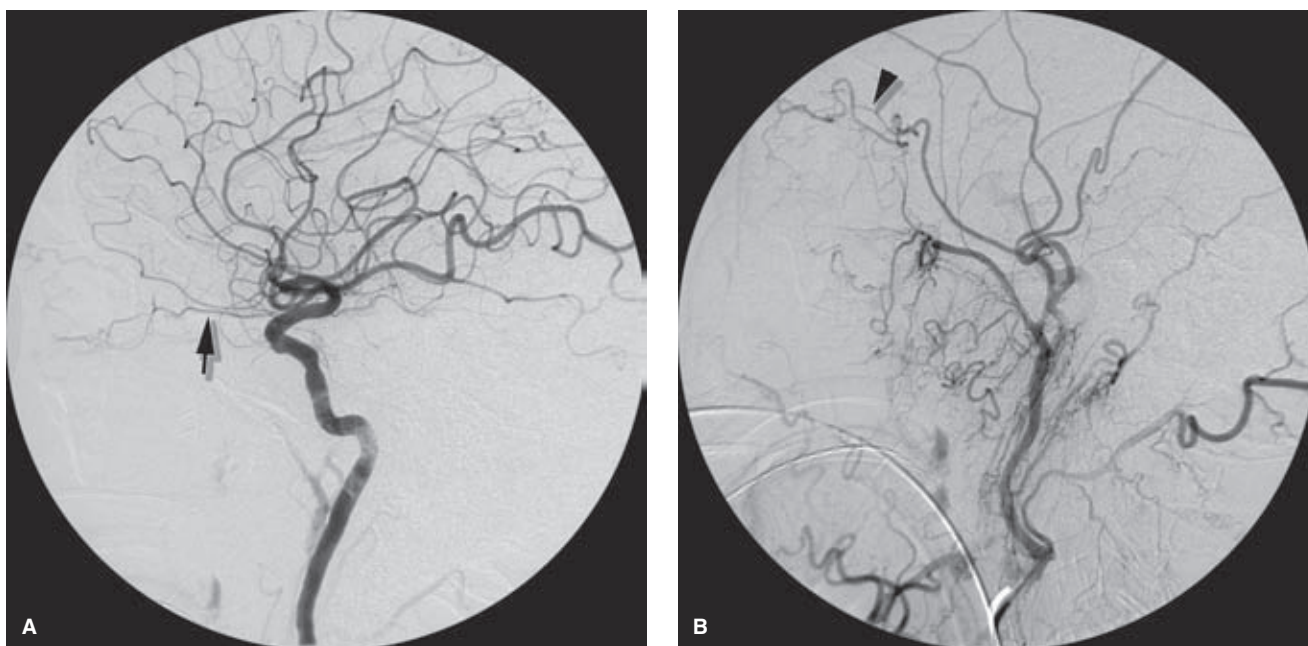


FIGURE 25-5. (A–B) Ophthalmic artery supplied in part by the middle meningeal artery. Simply identifying the ophthalmic artery (*arrow*) arising from the internal carotid artery (A) is not an assurance that the ophthalmic artery territory is not influenced by the middle meningeal artery. Here the external carotid artery injection (B) again shows an extensive middle meningeal-to-orbital territory (*arrowhead*) with a great risk to the eye from any embolization in that region.

using hazardous agents such as Onyx, nBCA, or small particles (Fig. 25-6).

► EPISTAXIS AND SINONASAL BLEEDING

Severe epistaxis of a degree warranting embolization is usually of the idiopathic posterior type, although this procedure will also be requested for epistaxis following trauma and epistaxis associated with tumor erosion, postsurgical complications, bleeding diathesis, and conditions such as hereditary hemorrhagic telangiectasia (HHT).

Posterior idiopathic epistaxis is a fulminant arterial type of bleeding seen in hypertensive adult patients and is thought to be related to a denudation of the nasal mucosa over the sphenopalatine arteries in the posterior nasal cavity. It is quite distinct from the minor venous oozing seen in children or young adults where the bleeding is coming from Little's area (Kiesselbach plexus) along the anterior nasal septum. The volume of bleeding from posterior epistaxis can be life-threatening, particularly when there are comorbidities. Primary treatment for posterior epistaxis consists of first-aid measures such as application of external pressure, endoscopic cauterization of the bleeding point, and packing of the nasal passage with gauze maintained under pressure with a clamped Foley balloon catheter (2). This is a most uncomfortable sensation for the patient, and most will willingly consent to endovascular embolization of the epistaxis if it involves the promise of expeditious removal of the balloon.

Embolization for control of epistaxis was described in 1974 by Sokoloff et al. (3) and has a technical success rate for controlling the bleeding of over 85% (4–8). Minor complications from the procedure occur in 8% to 21% of patients. While major complications such as neurologic

injury, septal perforation, blindness, CVA, or skin necrosis have been reported, the incidence is low—0% to 1.4% (9).

As mentioned previously, the incessant dripping of blood into the nasopharynx through the packing material

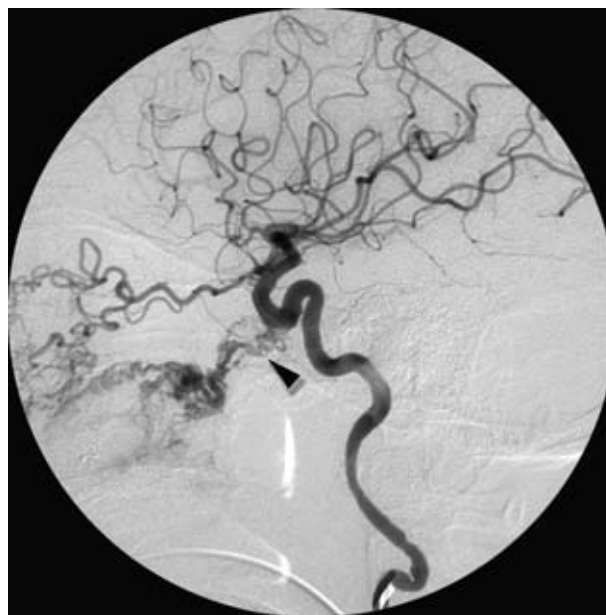


FIGURE 25-6. Inferolateral trunk to external carotid artery anastomoses. This patient with a large facial AVM shows marked enlargement of transosseous branches from the internal carotid artery, most likely running within the foramen rotundum or Vidian canal, reconstituting the distal external carotid artery that has been previously ligated. When flow is reversed within these vessels, that is, running back to the internal carotid artery, for whatever reason the possibility of embolizing the intracranial circulation from an external carotid location is very real.

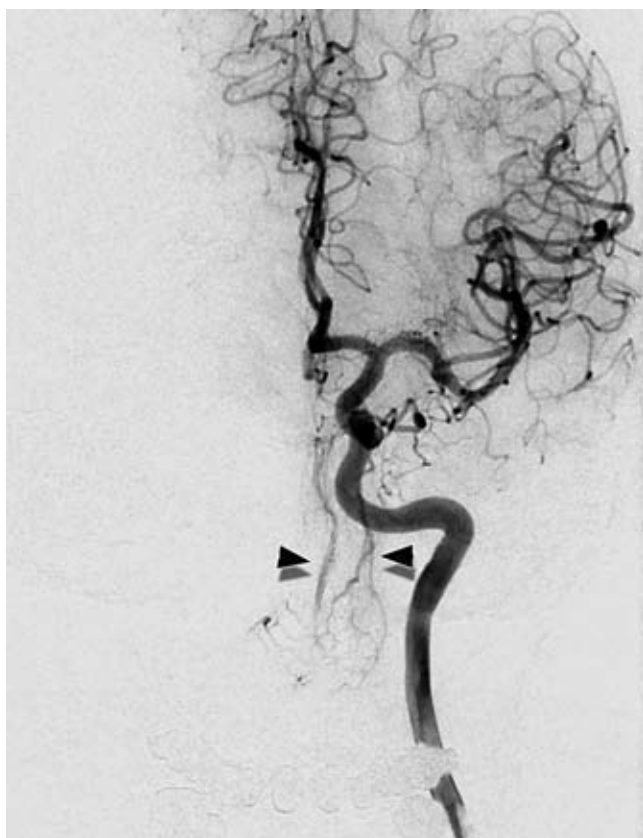


FIGURE 25-7. Prominent ethmoidal branches from the ophthalmic artery. A left internal carotid artery angiogram in a patient being studied for unrelated reasons shows large ethmoidal branches (*arrowheads*) along the nasal septum. In some patients with an appearance like this, a recurrence of bleeding would almost certainly prompt consideration of ethmoidal clipping.

represents a serious risk of aspiration and airway compromise for a patient who is about to undergo a procedure involving several hours supine under sedation. General anesthesia for airway protection is a prudent investment of time and resources for such patients.

As the prototypical neurointerventional “easy” case, epistaxis embolization exemplifies many of the procedures of this discipline in that it can be performed with a generous degree of latitude for safety and freedom from complications in most patients. However, this impression is deceptive. The potential for injury to the patient through use of inappropriate devices and materials, incorrect embolization technique, or lack of awareness of dangerous collateral branches to the internal carotid artery or ophthalmic artery is greater than the neophyte or pinch hitter neurointerventionalist-for-a-day supposes, and the learning curve, even for epistaxis embolization, is longer in retrospect than is apparent to the beginner with a half-dozen cases notched on his fuselage. Nevertheless, epistaxis embolization is a good starting point for a discussion of elementary techniques and use of polyvinyl alcohol (PVA) and Gelfoam, and how things can always go wrong even in the most foolproof situation.

The angiographic evaluation starts on the side ipsilateral to the bleeding and requires some initial review of the proximal intracranial internal carotid artery to ascertain that the bleeding is not from some pathology of the internal carotid artery (a very rare but important consideration) (10) and to evaluate the prominence of the ethmoidal branches of the ophthalmic artery. Should the ethmoidal branches be dominant in the supply of the nasal septum, resumption

of epistaxis after an otherwise successfully accomplished embolization may imply that surgical clipping of the ethmoidal branches may be necessary to control the bleeding (Fig. 25-7). Next, angiography of the external carotid artery is performed to map the anatomy of the internal maxillary artery, which is then navigated with a microwire and microcatheter to a point ideally just distal to the origin of the infraorbital artery. In reality, the infraorbital branch is often included in the embolization field either directly, for want of being able to catheterize the internal maxillary artery more distally, or through reflux of particles (Figs. 25-8–25-10). An angiographic run via the microcatheter in the internal maxillary artery runs the risk of redundancy at this point but it is, nevertheless, prudent to exclude the possibility of hitherto invisible critical collaterals. If all is well, the internal maxillary artery is then embolized carefully to the point of near stagnation of flow with PVA particles (250 to 1,000 μm) suspended in contrast. The vessel can be plugged finally with a pledget or two of Gelfoam. Coils should not be used in an epistaxis embolization because they are of limited efficacy in this instance and, more importantly, deny the possibility of a repeat procedure on that side if the patient should bleed again at a later date.

The facial artery—or very rarely the transverse facial artery—ipsilateral to the side of nasal bleeding may have the capacity to collateralize flow to the nasal mucosa of the lateral nasal wall via its angular branch (Fig. 25-11). Therefore, it is common to perform a very light (2 to 3 mL) particle embolization of the ipsilateral facial artery to suppress this tendency. However, this has to be done lightly to avoid the possibility of nasal skin or jugal necrosis in a field that

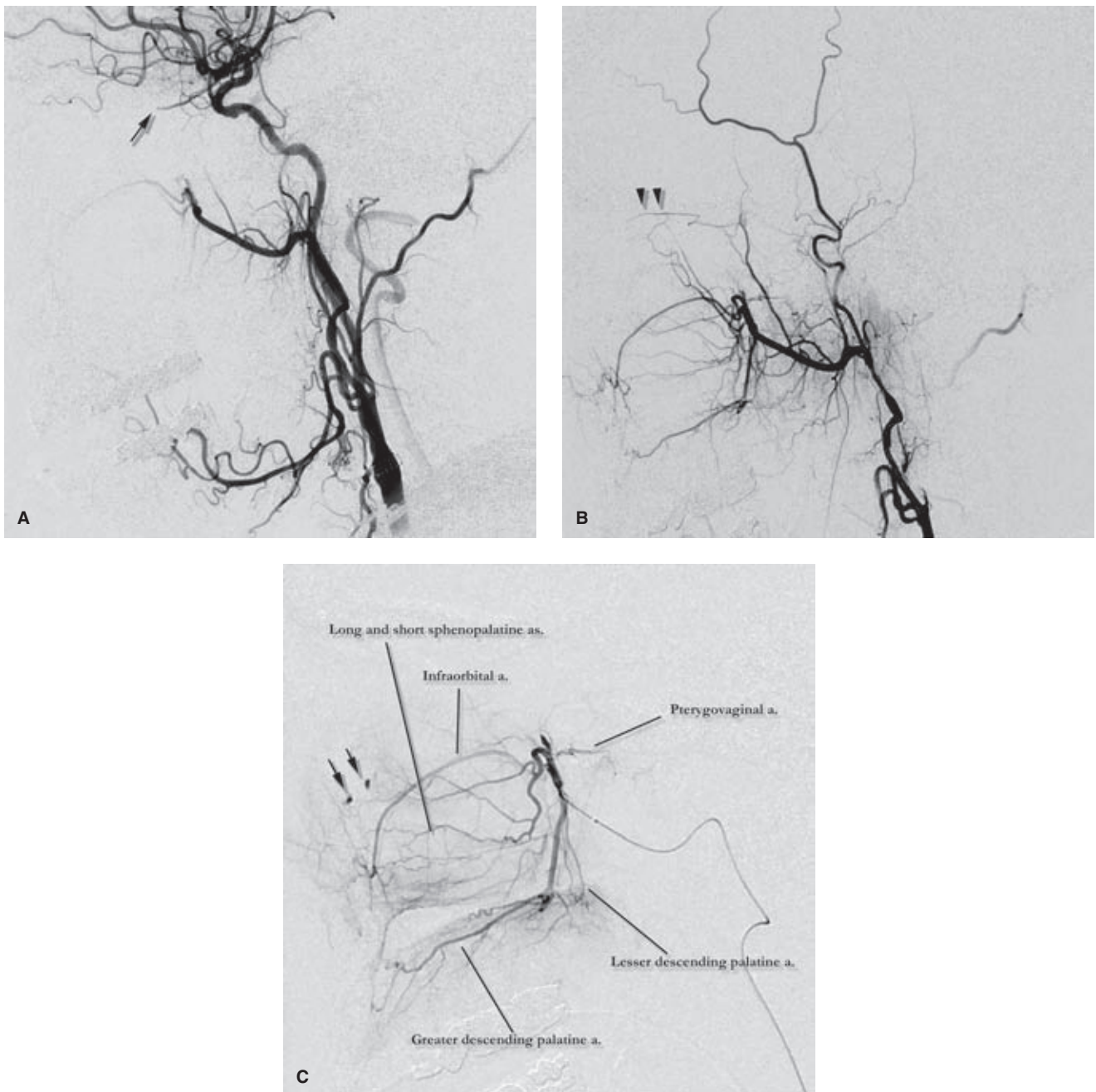


FIGURE 25-8. (A–C) Interruption of normal physiology with effects on the ophthalmic artery. This patient's left common carotid artery injection (A) shows a severe stenosis of the proximal left internal carotid artery, with the result that the filling of the ophthalmic artery (*arrow*) is bidirectional. A selective left external carotid artery injection (B) shows a standard anatomic configuration, but there is transient opacification of the ophthalmic artery (*arrowheads*) probably through deep temporal arteries. The superselective internal maxillary artery injection (C) is beyond the deep temporal origins and therefore the ophthalmic artery is not seen. The anatomy of the internal maxillary branches is exquisitely demonstrated and labeled in this instance, including some focal points of extravasation (*arrows*).

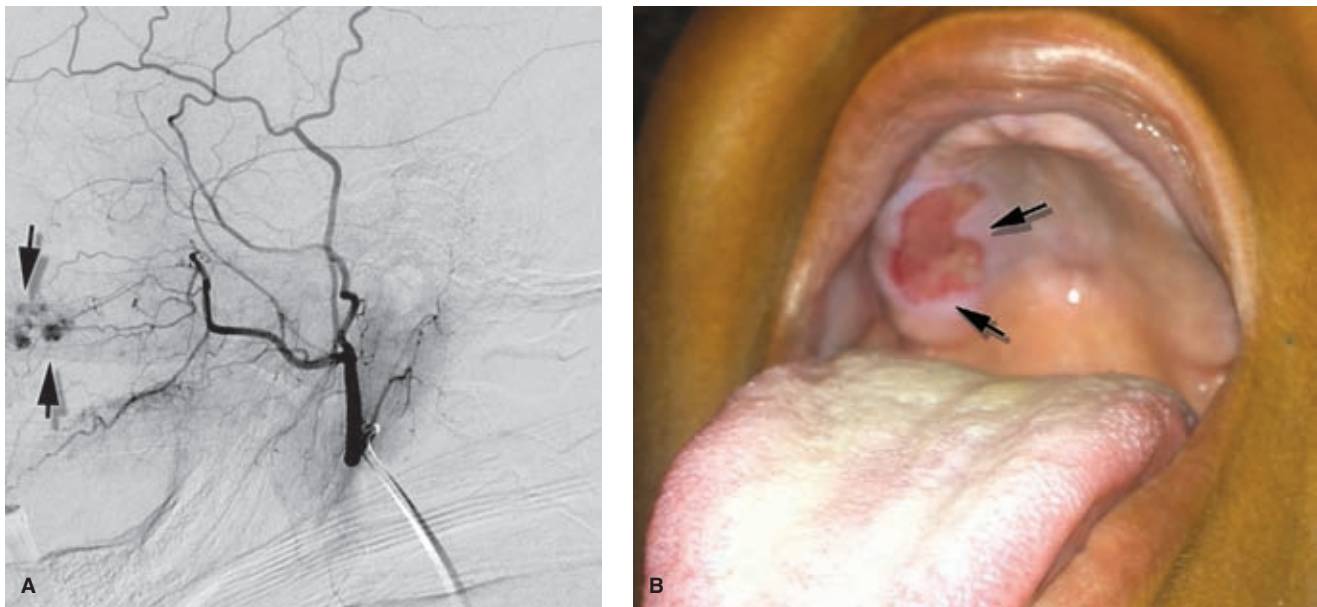


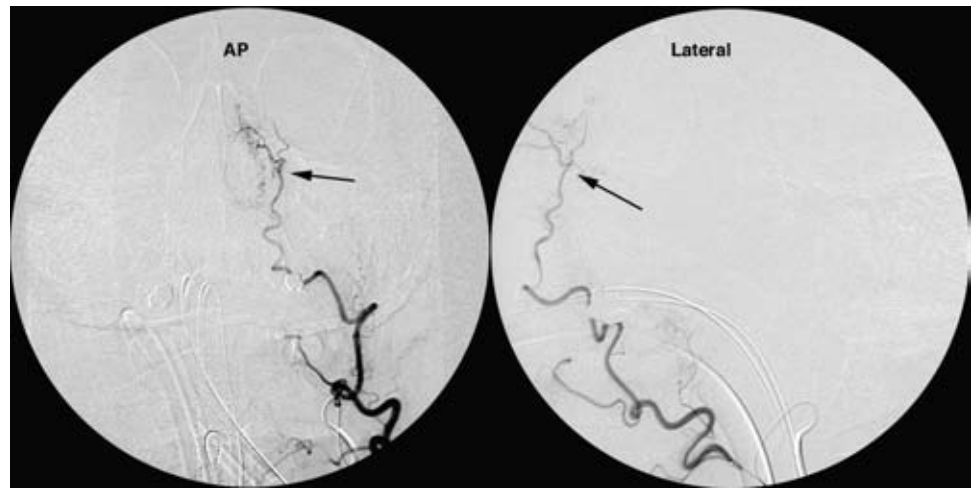
FIGURE 25-9. (A–B) Complications of embolization for epistaxis in hereditary hemorrhagic telangiectasia.

This patient had a history of prolonged nasal bleeds during her lifetime, and repeated gastrointestinal bleeding. Her internal maxillary artery injection (A) shows an unusual blush anteriorly (arrows) related to the dysplastic lesions characteristic of HHT. Her embolization was conducted in a standard fashion using PVA of 250 to 350 μm and Gelfoam pledgets in the internal maxillary artery bilaterally. Approximately a week later she returned with severe mouth pain and showed a sloughing ulcer (B) along her right alveolar ridge. This was treated symptomatically with mouthwashes and analgesics and resolved within a couple of weeks. The reason for this complication is unclear but may have been, in part, related to trauma of the palate against some poor dentition of the mandible. However, the entire hard palate has a pale ischemic appearance in the photograph. A widespread territorial ischemia is an inevitable consequence of the technique of epistaxis embolization as described in the text, and it is likely that more patients come close to developing this type of complication than we realize. Skin injuries are described in up to 2% of patients in some reviews, but tissue tenderness and nonnecrotic ischemic symptoms are probably more prevalent than that.



FIGURE 25-10. Pseudoaneurysm of the short sphenopalatine artery as a source of bleeding. Most patients do not demonstrate any focal bleeding injury other than the anatomic distortion induced by vigorous nasal packing. Often the vessels have a beaded or irregular appearance. This patient shows a small aneurysm (arrow) along the right lateral nasal wall, almost certainly the site of his recent bleed.

FIGURE 25-11. Nasal mucosal collateralization via the angular branch of the facial artery. A facial artery injection performed after ipsilateral internal maxillary artery embolization shows pronounced nasal blush on the lateral aspect of the nose through which repeat bleeding could occur. However, the artery cannot be catheterized very distally, and embolization of this branch, from whatever point of catheterization, will involve peppering an extensive territory of the facial artery. Therefore, this is done only gingerly and only with PVA.



has already been compromised through embolization of the infraorbital artery via the internal maxillary artery.

Finally, the contralateral internal carotid artery and external carotid artery are studied as above. The internal maxillary artery is catheterized and embolized with PVA and Gelfoam (Figs. 25-12–25-17) as on the previous side. The facial artery is not touched. For other causes of posttraumatic or postsurgical epistaxis, the embolization technique may have to be varied accordingly, following principles discussed in Box 25-1) that are more appropriate to emergency head and neck bleeding. In such cases, use of coils, for instance, might be entirely favorable because the lacerated vessel may be more proximal than those involved in posterior epistaxis (Figs. 25-18 and 25-19).

► **HYPERVASCULAR TUMORS OF THE HEAD AND NECK**

Embolization of head and neck tumors is frequently undertaken because of the surgeon's concern about inordinate or uncontrollable blood loss during proposed surgery. Most of

these cases are tumors idiosyncratic to this anatomic region, juvenile angiofibromas and paraganglioma, but other occasions present themselves such as metastatic thyroidal carcinoma or renal cell carcinoma.

(text continues on page 405)

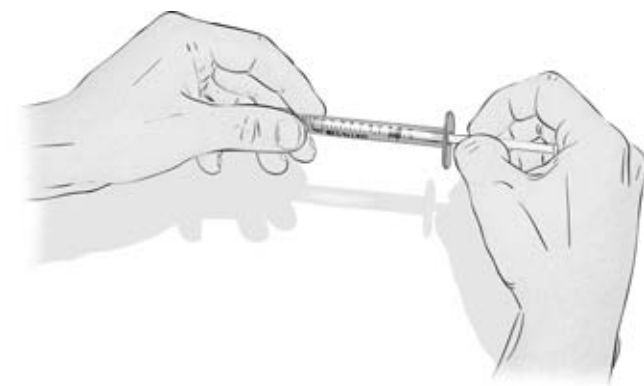


FIGURE 25-12. PVA push technique. PVA has a tendency to clump in the hub of the microcatheter, especially with larger particle sizes greater than 500 μm . To avoid buildup of resistance and sudden decompression with reflux at the tip of the microcatheter, get in the habit of holding the syringe as illustrated so that the thumb and index finger of the right hand have a firm grip on the piston of the syringe. Small, measured pulses of PVA can be given in this manner, and the grip will also act as a brake if there is sudden decompression of the syringe.



FIGURE 25-13. Gelfoam preparation. Gelfoam sponge is supplied as a small sheet from which tiny (2–3 \times 7–10 mm) slivers are cut with scissors. These are difficult to control, but if you leave your plastic-handled scalpel nearby, the static electricity in the handle will attract the slivers as they fall from the scissors.



FIGURE 25-14. Rolling a pledget. Tiny torpedoes are rolled as illustrated (but only with a dry clean glove).



FIGURE 25-15. Loading the pledget. The Gelfoam torpedo is loaded retrogradely and tamped snugly into a syringe containing 0.1 to 0.2 mL of contrast. Because the swelling of the Gelfoam begins immediately, this step is only taken when one is immediately ready to inject the Gelfoam. Any delay may imply that the Gelfoam has swelled to a point where it may no longer fit through the microcatheter.

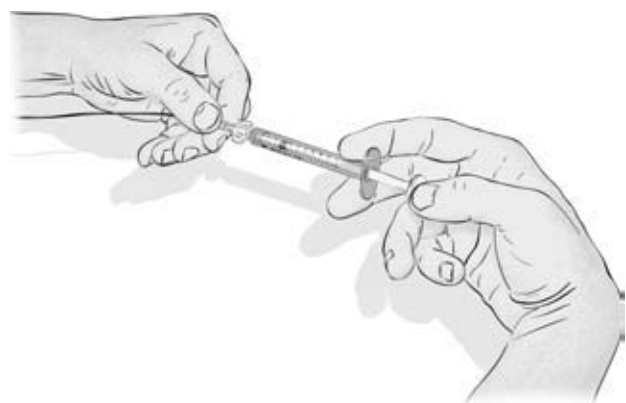


FIGURE 25-16. Launching the pledget. The microcatheter has been flushed with saline and the syringe containing contrast and Gelfoam is attached to the hub and injected immediately. Any of the usual tapping and inspection for microbubbles at this point will allow more time for the sodden Gelfoam to stick to the inner wall of the syringe and resist being pushed into the lumen of the microcatheter. The push must be fast and relatively forceful.

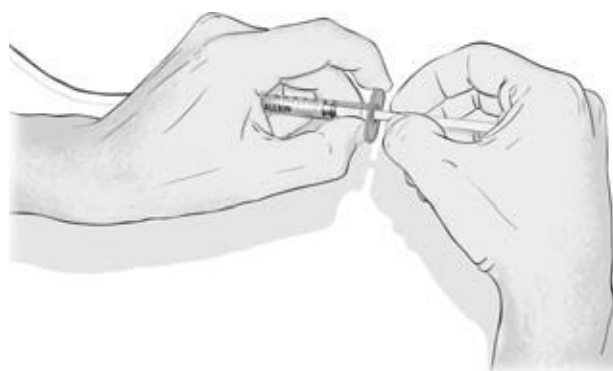


FIGURE 25-17. Injecting the Gelfoam pledget and contrast bolus with a saline syringe. The syringe is immediately switched for one of saline. As is the case for PVA, the injection of Gelfoam requires a controlled delivery. However, the resistance to advancing the pledget is considerable. The grip illustrated is as much for control as for heft. Small increments are necessary. The Gelfoam arrival at the microcatheter is announced by a spray of contrast and a sudden drop in the syringe resistance.

BOX 25-1 Polyvinyl Alcohol and Gelfoam

PVA particles are the staple of tumor and mass preoperative embolization in the head and neck. They are used only rarely now for transarterial embolization of arteriovenous malformations (AVMs) of the brain and dura because their effect is temporary.

Various commercial preparations of PVA are available, which are supplied in sizes between 45 and 1,000 μm . PVA particles of 50 to 150 μm have a more effective histopathologic outcome for inducing hemostasis and tumor necrosis than larger particles (11). However, this size range probably carries a greater risk of cranial neuropathy if inadvertent embolization of *vasa nervorum* occurs. Particles of this range could also cause skin and mucosal necrosis. Depending on operator preference, particle sizes of 250 to 750 μm are most commonly used in head and neck embolization because they constitute an adequate compromise between the need to penetrate the vascular bed of a preoperative tumor, on the one hand, and the need to avoid ischemic necrosis of target tissue and possible delay of healing in the surgical bed, on the other hand.

Particles are prepared as a dilute suspension in radiographic contrast and injected as punctuated miniboluses that are monitored on a fluoroscopic roadmap while being carried to their destination by antegrade arterial flow (Fig. 25-12). Careful monitoring of the pattern of flow is maintained throughout the embolization to avoid reflux of particles and to identify the development of vasospasm or opening of potentially dangerous anastomoses.

In situations in which small anastomoses are suspected or arteriovenous shunting is evident on the angiogram, larger particles may be preferred. The chances of obstructing a microcatheter with clumps of particles are greater with bigger particles. Microcatheters of the 0.010" series are usually limited to PVA particles up to 250 μm .

Biologic Effects of PVA

PVA particles impair blood flow by adherence to the vessel wall in clumps, with preservation of some luminal flow in many vessels (12,13). They also provoke variable degrees of acute inflammatory reaction. Foreign body giant-cell reaction, mural angioneurosis, and necrotizing vasculitis can be seen in the acute phase (days) after embolization of AVMs and other lesions. However, the behavior of PVA is still relatively inert compared with other embolic agents, particularly compared with acrylic materials (14).

After PVA embolization of an AVM, there is usually preservation of some flow in large- and medium-sized vessels, and a tendency of embolized territories to recanalize slowly, over a period of weeks to months (11,15). This has suggested to some authors that PVA embolization of brain AVMs provides only a temporary improvement in the angiographic appearance. The size of an AVM nidus may be underestimated after PVA

embolization. Radiotherapy planning based on this angiographic appearance runs the risk of recurrence of the AVM in those regions not included in the radiation port (9). The preservation of some minimal degree of flow in a tissue bed embolized with PVA is an important safety feature of this embolization agent. Embospheres, an alternative particle embolic material marketed for fibroid embolization, has been used in the head and neck for epistaxis and other embolizations but has an anecdotally higher risk of tissue necrosis due to the lubricious smooth texture of the particles and its tendency to occlude completely a target vessel.

Gelfoam

Gelfoam is a pliable, water-insoluble embolic agent prepared from purified pork skin gelatin granules. It is supplied in the form of a white powder or as a sponge that can be cut to required sizes. Its utility lies in a physical hemostatic effect due to its ability to hold up to 45 times its weight of blood within its interstices. It is resorbed by the body within 2 to 6 weeks and does not have a significant sclerosing effect (16).

Gelfoam sponge can be cut easily with a scissors into small pledgets that can be injected via a microcatheter to occlude a small vessel, usually after the distal field has been embolized with PVA (Figs. 25-13–25-17). One should err on the small side in cutting pledgets to avoid obstructing the microcatheter. The pledgets are injected in a bolus of contrast. A reduction in resistance in the microcatheter confirms delivery of the Gelfoam. Gelfoam pledgets are useful in situations in which ultimate recanalization of the vessel might be acceptable or desired, for example, posttraumatic small vessel bleeding or epistaxis embolization.

Due to the small quantity of force needed to deliver the pledget via a microcatheter, pledgets should be used in safe situations only, that is, where a degree of inadvertent reflux would not have disastrous complications. Gelfoam pledgets are typically used in a distal branch of the external carotid artery. Use of the pledgets close to the origin of the external carotid artery would threaten the internal carotid artery.

Gelfoam powder has particle dimensions of 40 to 60 μm . Mixed with radiographic contrast for fluoroscopic visualization, it has the ability to penetrate an arterial field to the level of the distal arterioles. Therefore, in contrast to embolization with larger PVA particles, in which preservation of distal tissue or mucosa is maintained through small vessel collateral flow, Gelfoam powder embolization produces a powerful, ischemic lysis of the targeted tissue. It is used in safe situations for preoperative tumor embolization, where the possibility of reflux or of dangerous anastomoses is not present, and where flow from the microcatheter is directed exclusively toward the tumor.

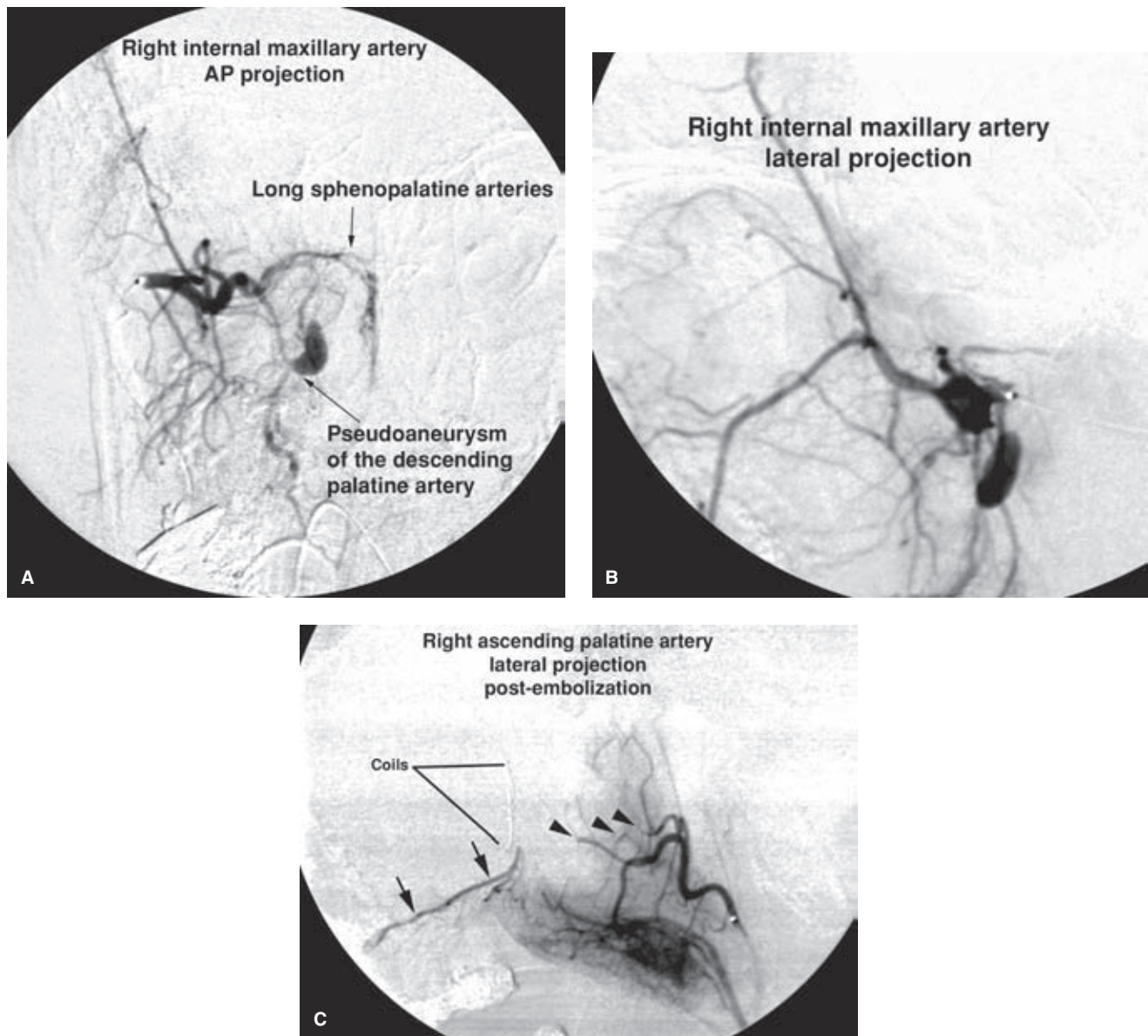


FIGURE 25-18. (A–C) Bleeding after LeFort osteotomy. A young adult developed severe bleeding 8 days after a LeFort osteotomy performed for a congenital facial deformity and dental malocclusion. A right external carotid arteriogram, AP projection (**A**) and lateral projection (**B**), demonstrates a pseudoaneurysm of the descending palatine artery along the plane cut by the osteotomy saw. A microcatheter was navigated into the descending palatine artery and steered past the pseudoaneurysm. Fibered coils were then laid down distal to, across, and proximal to the neck of the pseudoaneurysm. A postembolization injection of the ascending palatine artery (**C**, lateral projection) demonstrates the necessity of occluding the torn vessel on both sides of the pseudoaneurysm. There is immediate reconstitution of the descending palatine artery along its horizontal segment (*arrows*). This could have potentially filled the pseudoaneurysm from below if an incomplete occlusion had been performed. Notice other vessels (*arrowheads*) of the ascending palatine region that have been severed by the saw.

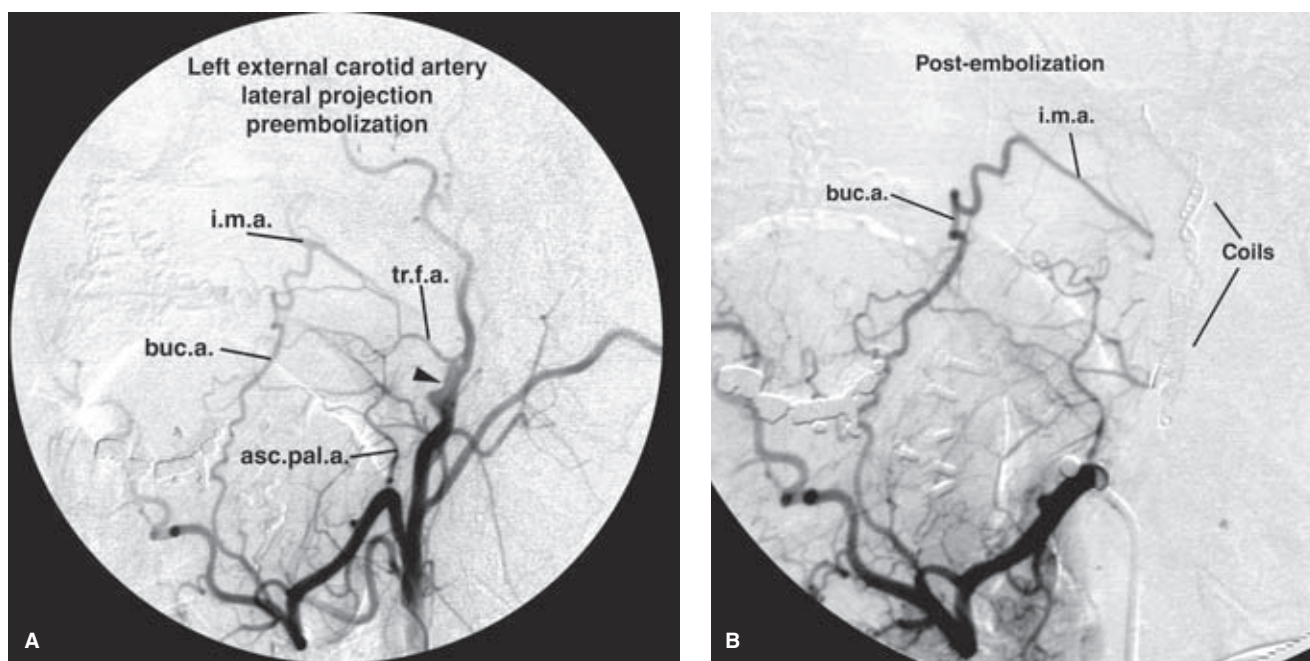


FIGURE 25-19. (A–B) Bleeding after LeFort osteotomy: Case II. This middle-aged patient had a LeFort osteotomy and maxillary reconstruction for intractable airway obstruction. Ten days after surgery, he developed severe bleeding. A lateral external carotid artery (A) injection demonstrates a pseudoaneurysm (arrowhead) of the external carotid artery at the level of the origin of the internal maxillary artery (*i.m.a.*). The internal maxillary artery is occluded proximally and fills via the buccal artery (*buc.a.*) from the facial artery. The transverse facial artery (*tr.f.a.*) and ascending palatine artery (*asc.pal.a.*) are labeled. The external carotid artery was occluded with fibered coils along the lacerated segment. A postembolization lateral projection of the facial artery (B) demonstrates filling of the internal maxillary artery via the buccal artery, but there is no evidence of opacification of the pseudoaneurysm.

Paragangliomas of the head and neck are highly vascular tumors of neural crest elements that usually occur in typical locations in the skull base or along the neurovascular structures of the carotid sheath. Unlike sympathetic derived paragangliomas elsewhere in the body, paragangliomas of the head and neck are parasympathetic in derivation and rarely demonstrate catecholamine secretion. Approximately 40% of paragangliomas overall have malignant potential, and these will tend to be more aggressive and invasive in appearance on noninvasive imaging. In the head and neck they present with mass effect in the neck, cranial nerve dysfunction, or middle-ear disturbance. Genetic-related and syndromic paragangliomas, such as those seen in von Hippel–Lindau syndrome, have a greater incidence of multiplicity.

Juvenile angiofibromas are unusual tumors of endothelial and spindle cell stromal composition and their exact origin is unclear. They are seen almost exclusively in young males and present with symptoms related to expansion and destruction about the pterygomaxillary fissure and posterior nasopharynx where they originate. Slow evolution of a change in voice, mouth breathing, and nasal stuffiness are commonly reported by the patients and their parents, but the diagnosis seems frequently elusive early in the development of the tumor. With progressive growth intracranial invasion can be seen in 10% to 20% of cases.

Paragangliomas and juvenile angiofibromas are interesting tumors from the vantage of cytokine and cell-signaling pathways. The dramatic opacification that they demonstrate

represents the angiographic correlate of cell-biology processes of great relevance in the world of cancer treatment. The vascular pattern of a typical paraganglioma tends to be more chaotic and disorganized, with a wide variability in vessel caliber and contour, compared with the striated, finer vessels of a juvenile angiofibroma, but the two tumor types share many features (Figs. 25-20 and 25-21). With immunostaining techniques it is now established that the hypervascular nature of both relates significantly to a marked upregulation in the expression of angiogenic factors familiar to oncologists and that provide the basis for many recent advances in oncologic chemotherapy (17,18). Cytokines including vascular endothelial growth factor (VEGF) protein, VEGF receptors, transforming growth factors beta-1 (TGF β -1), angiopoietin 2, hypoxia induced factor (HIF) and platelet-derived growth factors (PDGF-A and PDGF-B) are expressed at high levels in these tumors, likely accounting for the marked hypervascularity that is their angiographic hallmark (19–21). These tumors exist in an effective state of “pseudo-hypoxia” meaning that their drive to stimulate the formation of new vessels is pathologically high (22). Interestingly, there is evidence that embolization of a JNA tumor with induction of actual hypoxia along its still viable edges may lead to even greater upregulation of the expression of these cytokines (17), but the clinical significance of this is not yet known.

Embolization of hypervascular tumors of the head and neck can be performed with a classical endovascular approach using a variety of particles, coil, and liquid agents. (text continues on page 408)

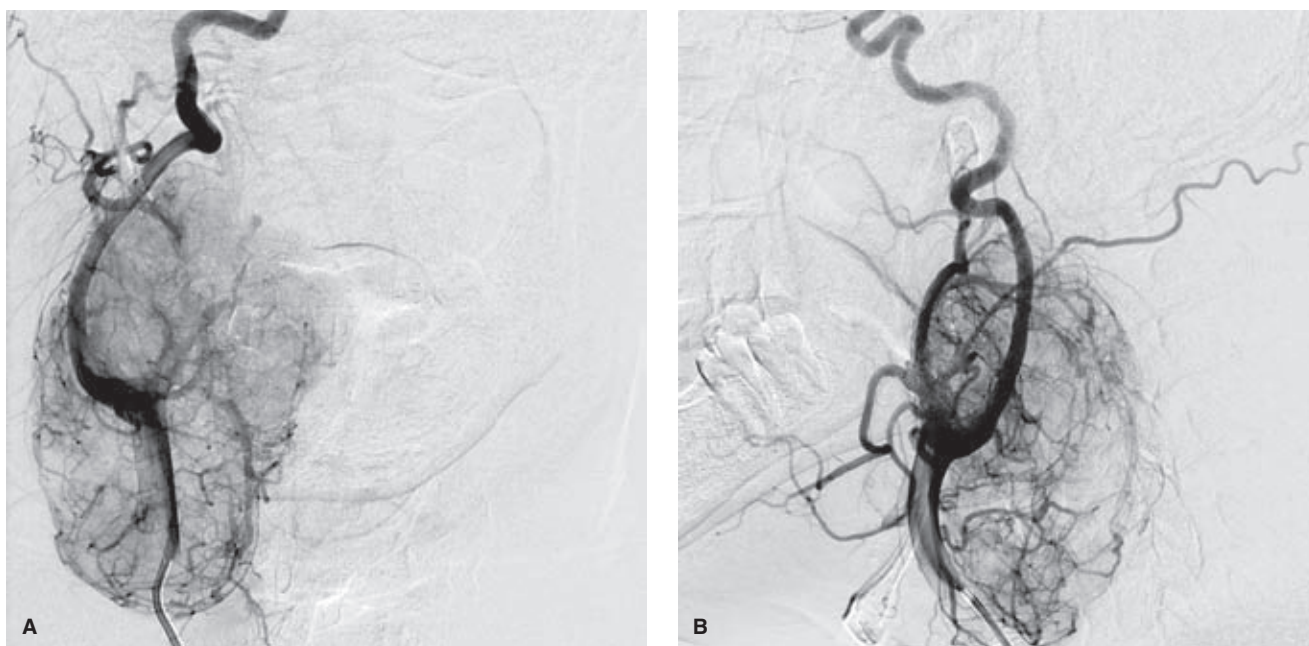


FIGURE 25-20. (A–B) Typical appearance of advanced carotid paraganglioma. One of the epiphenomena of the obesity epidemic is that large neck masses may escape detection until they are quite advanced. In cases such as this the viability of the carotid artery may be seen to be lost at the time of surgery due to direct mural invasion. This patient succumbed to a carotid blowout some days after surgery, likely due to a spontaneous rupture of the carotid wall. The angiographic images show the typical wild appearance of the vessels in an aggressive paraganglioma in contrast to the finer vessels seen in juvenile angiofibromas.

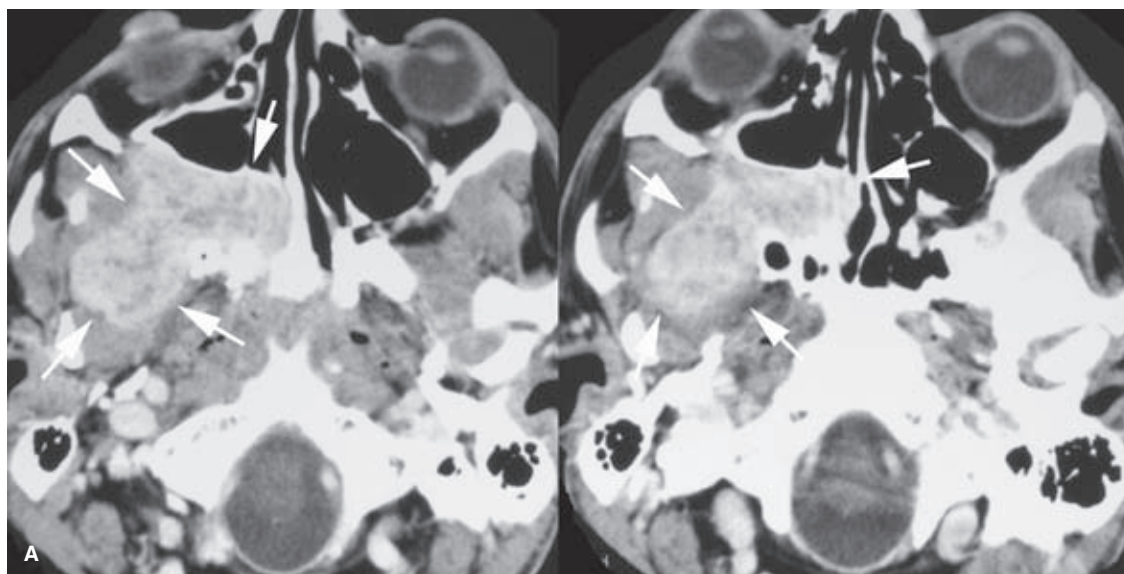


FIGURE 25-21. (A–E) Typical computed tomography (CT) and angiographic appearance of a JNA. A contrast-enhanced CT examination (A) demonstrates the hypervascular nature of this JNA in a teenaged male patient (arrows). There is expansion of the pterygomaxillary fissure and extension of tumor into the infratemporal fossa. Patients with this disorder typically present with nasal stuffiness or epistaxis. With more advanced tumor growth, expansion into the nasal passage will be expected and bone erosion of the skull base will allow intracranial invasion. (continued)

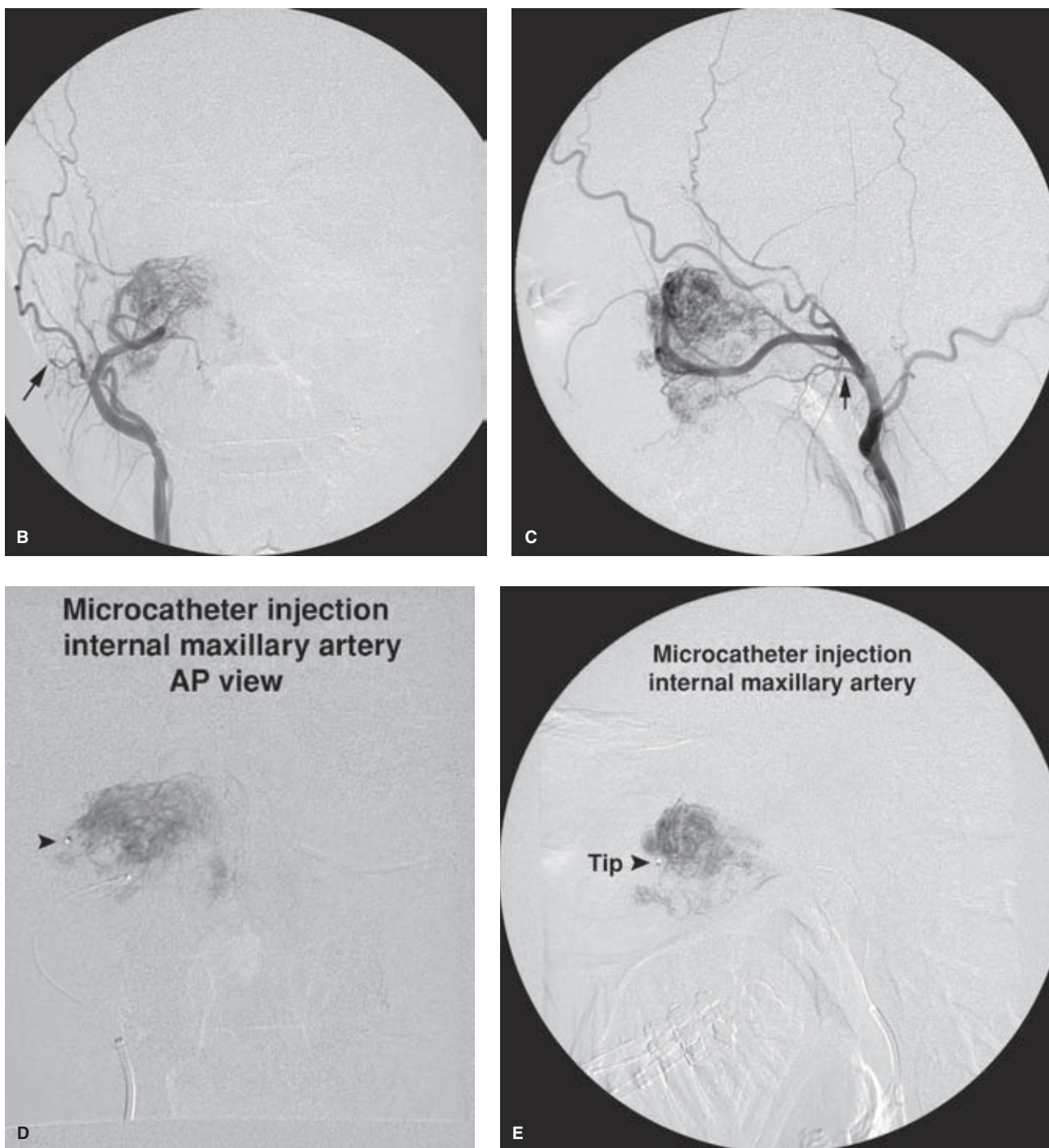


FIGURE 25-21. (CONTINUED) The AP (**B**) and lateral (**C**) angiographic images of the external carotid artery show the typically striated and hypervascular nature of this tumor deriving supply from the terminal branches of the internal maxillary artery. For the reader's interest, the vessel on the lateral view (marked with an *arrow*) running parallel to the internal maxillary artery is in a more lateral plane on the AP view (*arrow*) and not involved with the tumor. This is a nice incidental example of the transverse facial artery. Microcatheter runs (**D** and **E**) in the distal internal maxillary artery confirm the absence of dangerous collateral branches to the internal carotid artery, and an embolization performed in this location is usually quite satisfactory. In many patients, the accessory meningeal and ascending pharyngeal arteries will need to be embolized as well due to recruitment into the nasopharyngeal component of the tumor. In addition to the usual dangerous collaterals from the external carotid artery to the internal carotid artery, JNA patients frequently demonstrate enlargement of the mandibulovidian artery from the petrous carotid segment. Intratumoral retrograde passage of particles via this route is a possibility, therefore, in some patients.

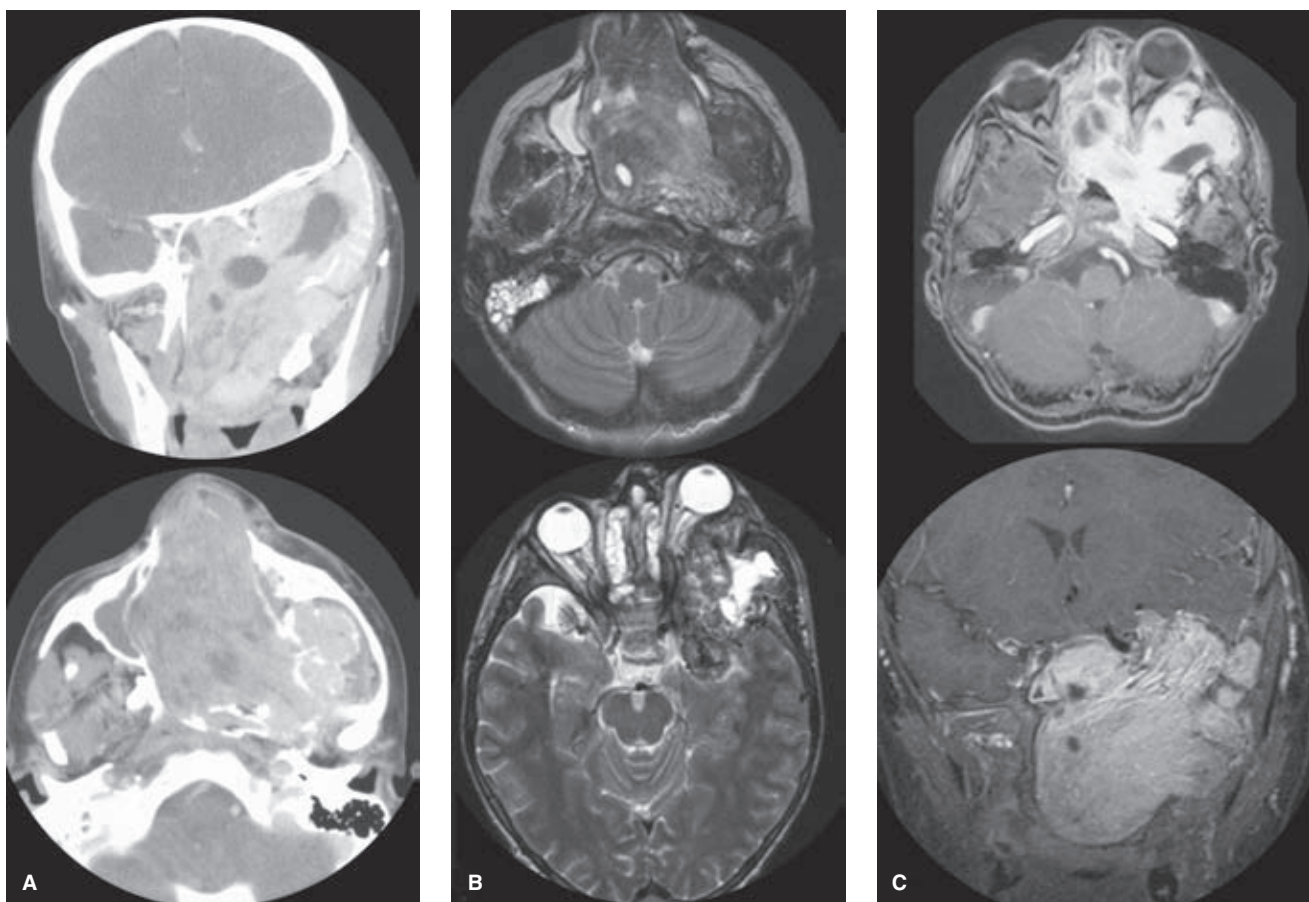


FIGURE 25-22. (A–G) Recurrent JNA with intracranial invasion. An 18-year-old male patient from overseas presented for surgery with an extensively invasive JNA that had been embolized and treated with proximal vessel ligation on several occasions previously. These previous procedures compounded the difficulty of proposed pre-operative embolization.

The contrast-enhanced CT (A), T2-weighted MRI (B), and gadolinium-enhanced T1-weighted images (C) show the grotesque extent of this uncontrolled tumor to a degree rarely seen in the Occident. There is invasion of the left cavernous sinus, protrusion of the left globe, threatened invasion of the petrous left internal carotid artery, and complete obstruction of the nasal passages, which dripped incessantly of blood while the patient struggled for breath through a compromised airway. (continued)

Recently, a combination of endovascular techniques, endoscopically guided direct tumor puncture (23), and percutaneous ultrasound-guided injection of Onyx or nBCA have demonstrated very impressive levels of safe devascularization of tumors (24–26) (Fig. 25-22). Concern about extrusion of Onyx into the internal carotid artery, injury to the adjacent cranial nerves (27), or embolization to the posterior circulation is foremost in all such procedures, and protection of the internal carotid artery with an endovascular balloon may be necessary for procedures close to the bifurcation (28).

The principal risks involved in head and neck tumor embolization are as follows:

- *Inadvertent particle/coil/liquid embolization of a critical vessel either through reflux or through dangerous collateral pathways.* Even very simple-looking cases can carry uncommon but grave risks of embolization to the internal carotid artery, ophthalmic artery, or vertebral artery (Figs. 25-23–25-28) (29–32).
- *Lower cranial nerve injury around the skull base.* For example, the VII nerve is vulnerable when glomus tympanicum or jugulotympanicum tumors are being embolized around the middle ear, and the X and XII nerves are similarly at risk for any kind of embolization around the hypoglossal and jugular foramina (27,33).
- *Facial skin or mucosal necrosis through excessively aggressive technique or inappropriate agents.*
- *Shunting of embolic material through the tumor in the setting of a patent foramen ovale permitting paradoxical embolization to occur systemically.* This is a particular risk for juvenile nasal angiofibroma (JNA) where transit of 50 μm radiolabeled particles through the tumor to the lungs has been demonstrated (34).
- *Tumor swelling postembolization.* Airway compromise might be a concern with this phenomenon, and it might be necessary to intubate a patient prophylactically on this account. Intracranial mass effect can worsen when a very large intracranial meningioma or other mass is embolized (text continues on page 413)

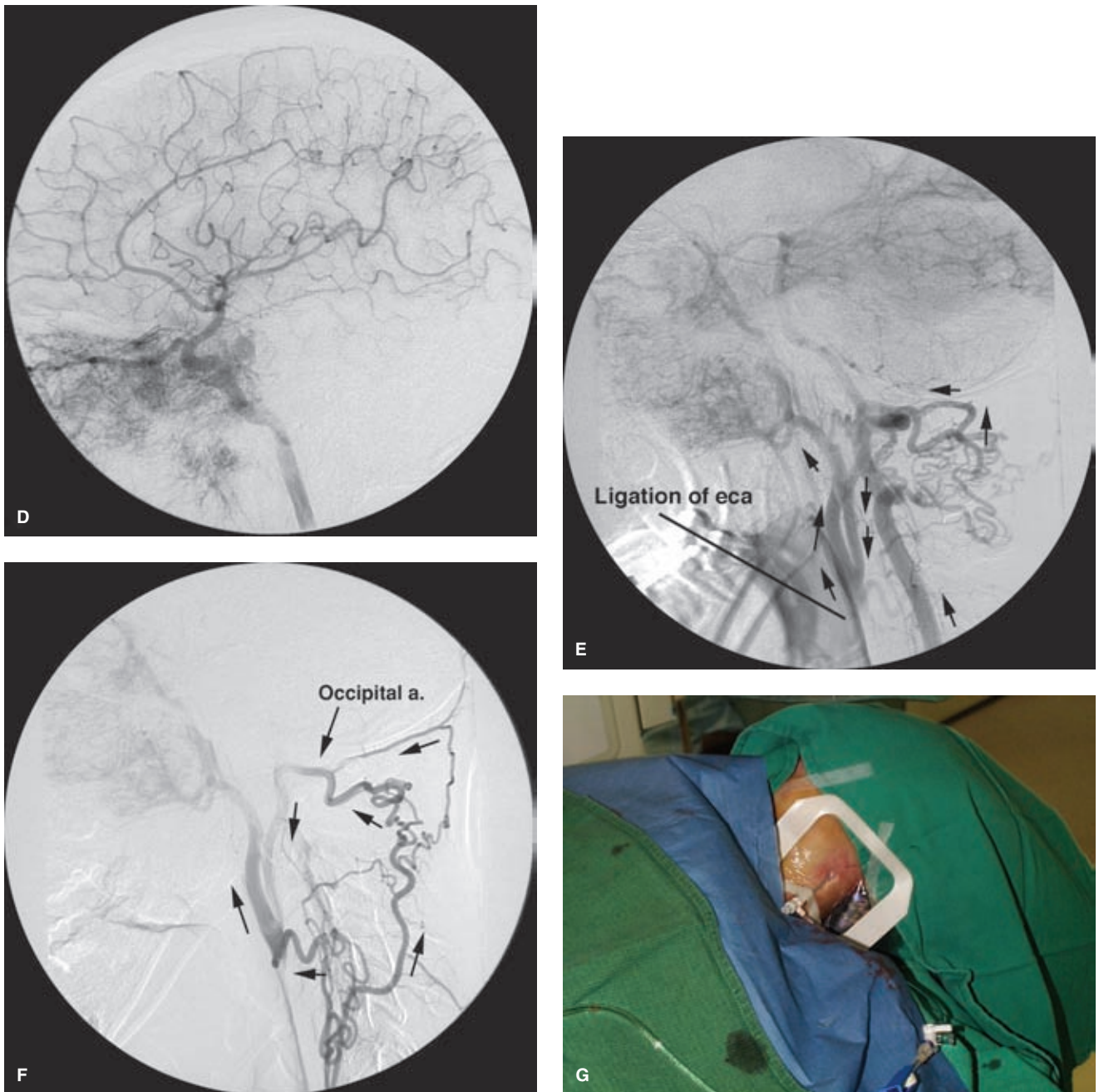


FIGURE 25-22. (CONTINUED) The left common carotid injection (D) showed that the left external carotid artery had been ligated during a previous procedure with extensive tumor opacification from the cavernous branches of the internal carotid artery extending into the orbit and adjacent nasopharyngeal region. The left vertebral artery injection (E) shows that the external carotid artery is reconstituted promptly via the occipital artery, which flows retrogradely (arrows) from the C1 and C2 anastomoses to the reversed occipital artery. Alternative access to the external carotid artery was sought through the ascending cervical artery via a thyrocervical injection (F), but this proved equally inaccessible. The external carotid artery was cannulated using a micropuncture kit (G) by roadmapping from a vertebral artery injection and puncturing the neck using the roadmap as a guide. The major bulk of tumor was embolized with PVA via this route, but the component of tumor from the internal carotid artery could not be safely catheterized. Despite these efforts in the external carotid artery, the bleeding at surgery was torrential with a rocky course over many weeks for the patient, who made a fully cured recovery.

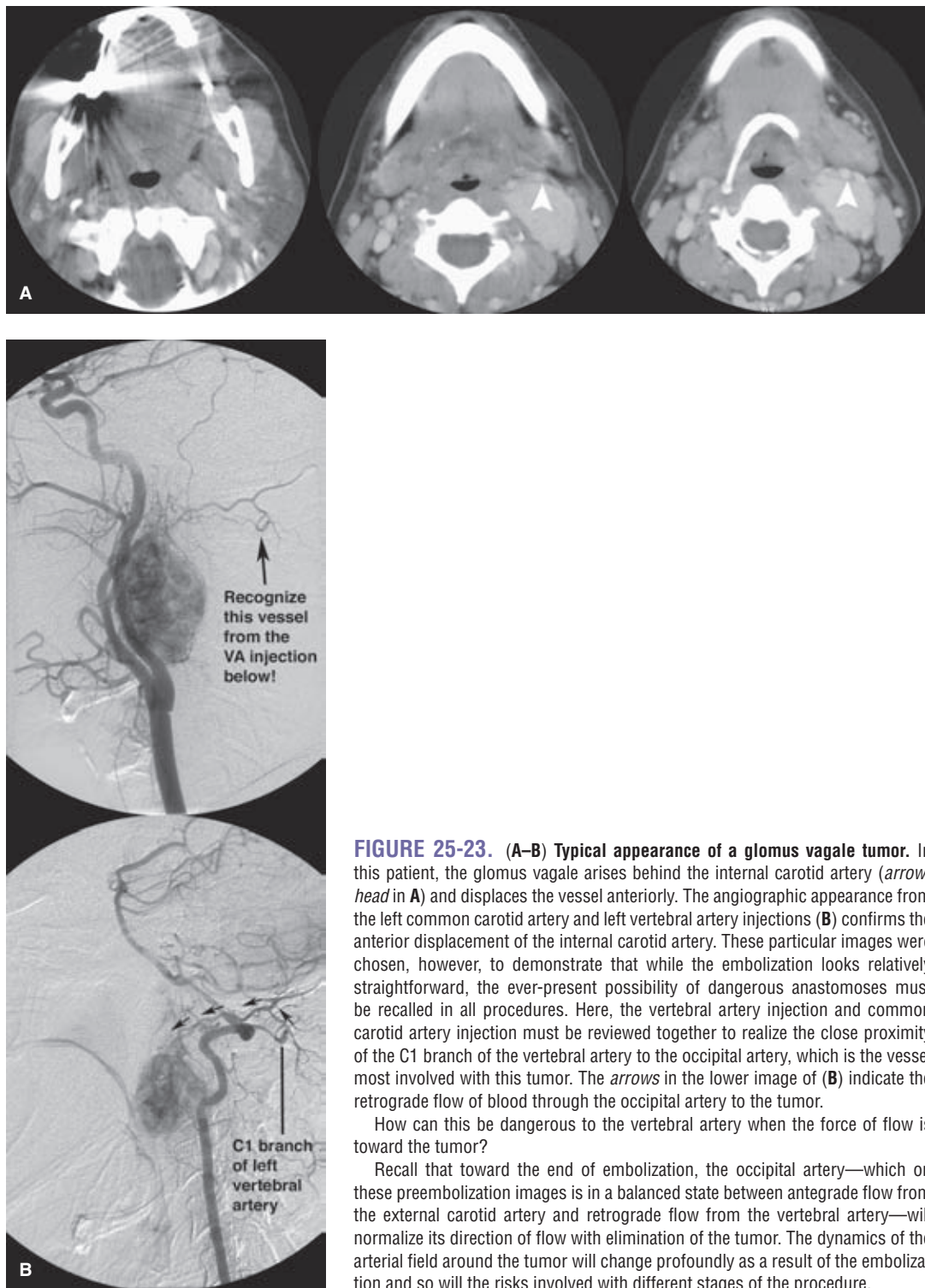


FIGURE 25-23. (A–B) Typical appearance of a glomus vagale tumor. In this patient, the glomus vagale arises behind the internal carotid artery (*arrow-head* in **A**) and displaces the vessel anteriorly. The angiographic appearance from the left common carotid artery and left vertebral artery injections (**B**) confirms the anterior displacement of the internal carotid artery. These particular images were chosen, however, to demonstrate that while the embolization looks relatively straightforward, the ever-present possibility of dangerous anastomoses must be recalled in all procedures. Here, the vertebral artery injection and common carotid artery injection must be reviewed together to realize the close proximity of the C1 branch of the vertebral artery to the occipital artery, which is the vessel most involved with this tumor. The *arrows* in the lower image of (**B**) indicate the retrograde flow of blood through the occipital artery to the tumor.

How can this be dangerous to the vertebral artery when the force of flow is toward the tumor?

Recall that toward the end of embolization, the occipital artery—which on these preembolization images is in a balanced state between antegrade flow from the external carotid artery and retrograde flow from the vertebral artery—will normalize its direction of flow with elimination of the tumor. The dynamics of the arterial field around the tumor will change profoundly as a result of the embolization and so will the risks involved with different stages of the procedure.

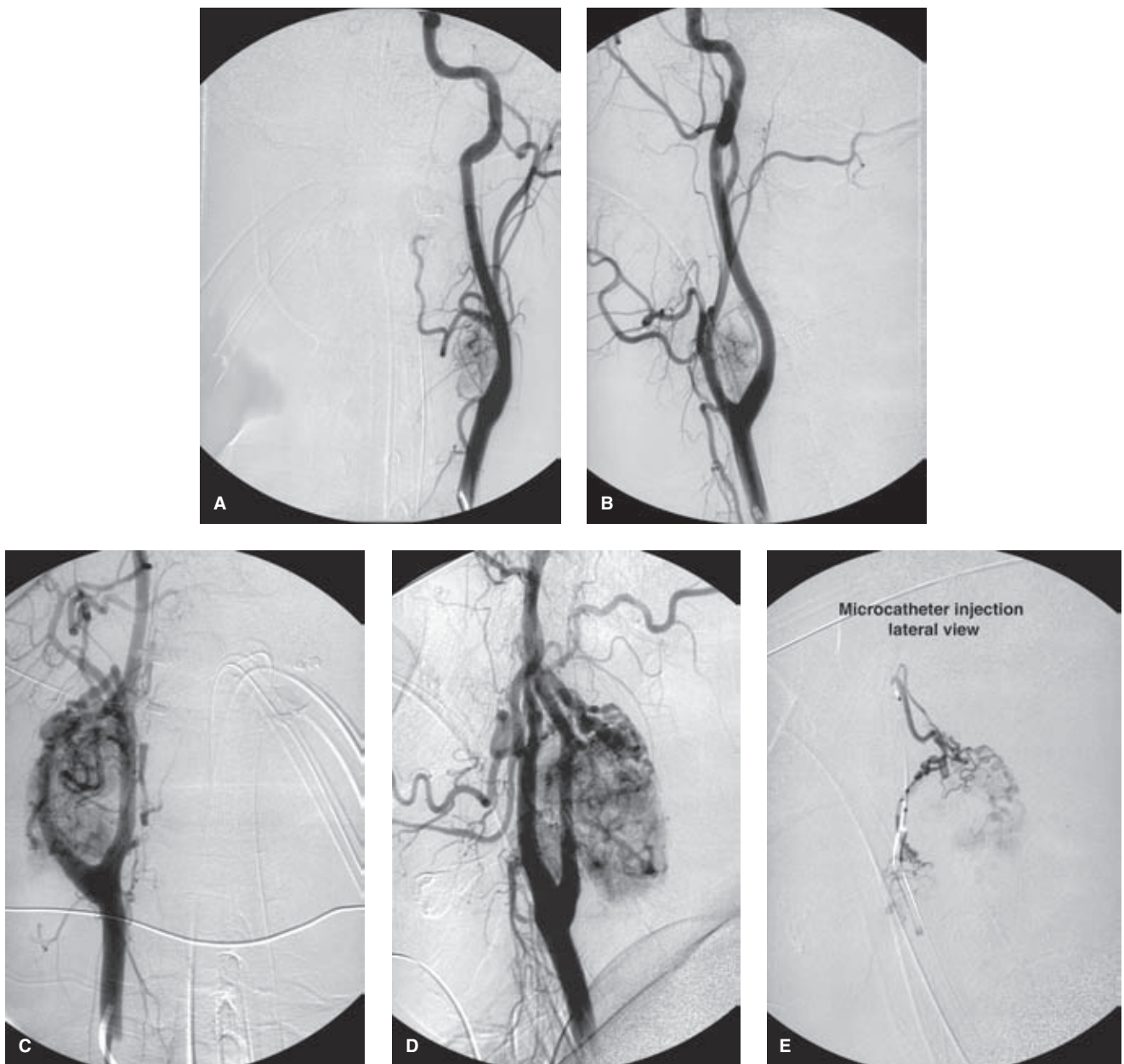


FIGURE 25-24. (A–E) Two cases of glomus tumors referred for preoperative embolization. Images (A) and (B) are from a patient with a relatively small carotid body tumor, while images (C) and (E) are from a much larger glomus vagale. One of these cases is a considerably higher risk for embolization than the other. Which one and why?

The smaller carotid body tumor (A and B) lies closer to the carotid bifurcation and derives its blood supply from vessels quite close to the bifurcation. Furthermore, it could be argued that such a small tumor probably does not need to be embolized at all and should be easily manageable in the hands of a competent surgeon. Its branches are smaller and more difficult to access, and are more prone to reflux particles into the internal carotid artery during embolization. Despite all of this, scheduled cases like these have a momentum of their own, and it is very difficult to resist the compulsion to do *something* when the patient has come so far and the family is waiting for tidings of the procedure. This is how accidents can happen.

The larger tumor (C and D) is a glomus vagale arising behind the carotid artery. Atypically, in this case, it splays the internal carotid artery from the external carotid artery, a feature more usually associated with carotid body tumors. The main feeding artery for this tumor enters the upper pole (microcatheter injection shown in (E)) and is most likely the musculospinal branch of the ascending pharyngeal artery. Very typical of these tumors, the feeding vessels branch along the surface of the tumor, which means that it can be possible to embolize nearly the entire tumor from a single position. However, it also means that feeding vessels to the lower pole of the tumor will be similarly along the periphery of the tumor and in free communication with those seen here. When the lower pole vessels are immediately adjacent to the carotid bifurcation, the distance back to the internal carotid artery through peritumoral reflux is very short. This is a situation in which one should be careful and avoid forceful pushing of the embolic material.

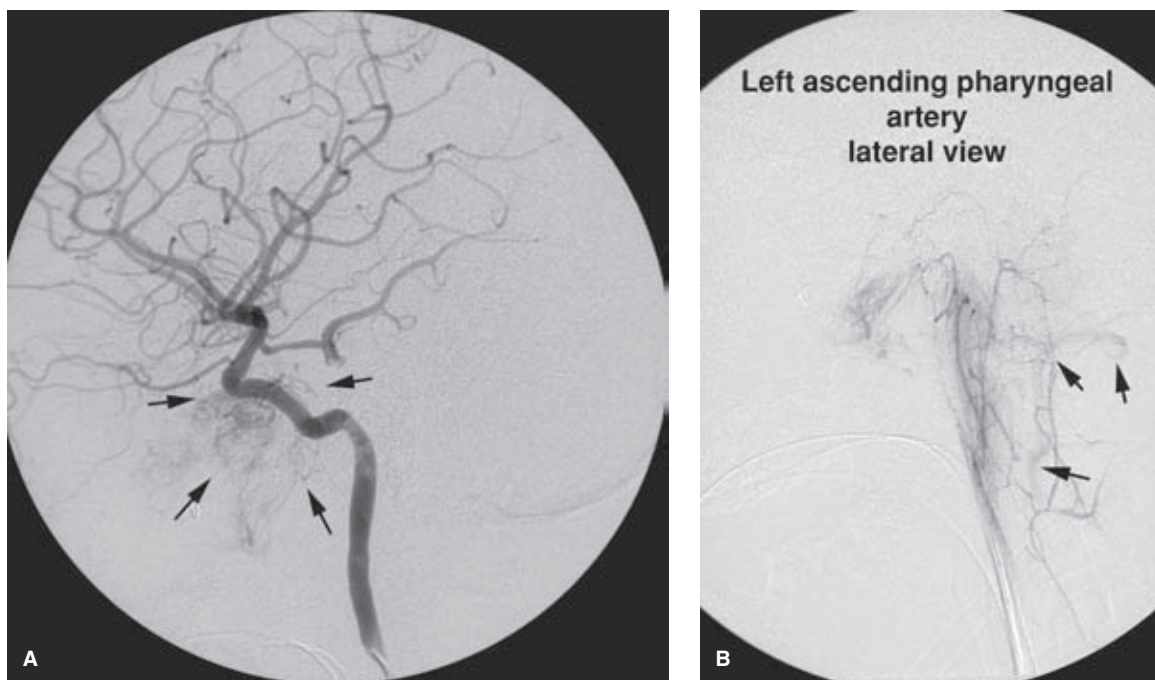


FIGURE 25-25. (A–B) Recurrent JNA with dangerous anastomoses. A left internal carotid artery angiogram (A) in a patient with recurrence of a JNA following surgery some years previously shows a substantial component of tumor supplied by arterial branches of the cavernous and precavernous carotid artery (arrows). These are very dangerous to catheterize due to their short length and the risk of reflux to the internal carotid artery. Furthermore, intratumoral reflux to these vessels during embolization of the external carotid artery is another hazard. The left ascending pharyngeal artery injection (B) shows relatively minor tumor blush in the nasopharynx through this route but reminds one of the ever-present risk and ease of inadvertent embolization to the vertebral artery (arrows) via this route.

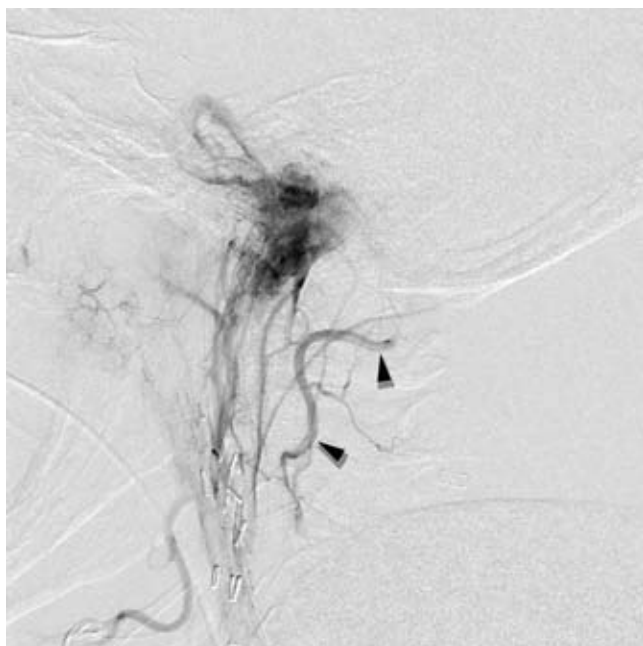


FIGURE 25-26. Dangerous anastomosis. This patient demonstrates a recurrence of a jugular paraganglioma. The lateral view of the ascending pharyngeal artery injection refluxes into the ipsilateral vertebral artery (arrowheads). This injection is performed with approximately 0.5 mL of contrast and without much force, indicating the ease with which embolic material might be pushed into the intracranial circulation.

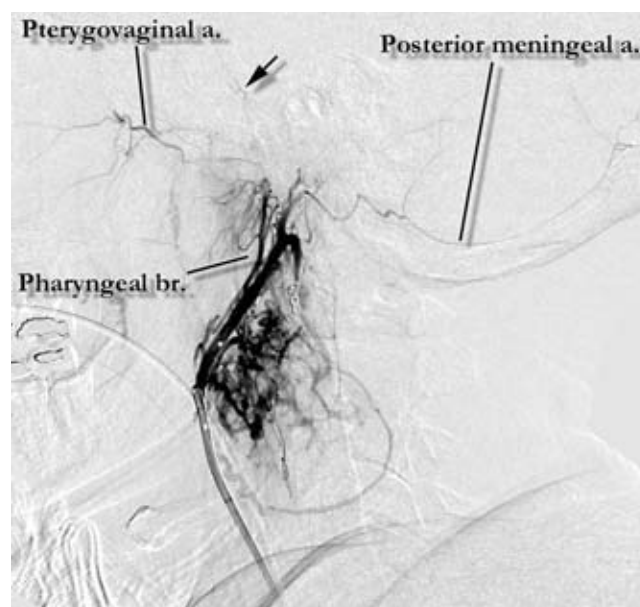
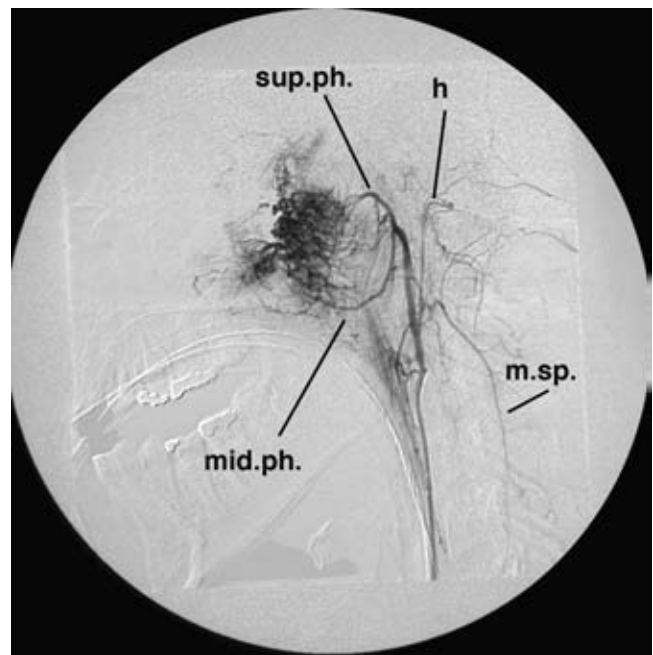


FIGURE 25-27. Anastomotic connections of the ascending pharyngeal artery around a glomus vagale. Some typical anastomoses are illustrated. Contrast refluxes into the pharyngeal trunk of the ascending pharyngeal artery and opacifies the pterygovaginal artery and thus the internal maxillary artery. The posterior meningeal artery is also seen. Although it is not seen here, one can assume that the vertebral artery is not far away. In fact, coils have been already placed in a large posterior branch on the periphery of the tumor, precisely to obstruct a peritumoral anastomosis to the vertebral artery and thus allow particle embolization to continue. Clival anastomoses (arrow) are also present extending up towards the internal carotid artery.

FIGURE 25-28. Anatomy of the ascending pharyngeal artery supplying a juvenile angiofibroma. The superior, middle, and inferior branches of the pharyngeal trunk are nicely demonstrated on this lateral view, as is the hypoglossal branch (*h*) of the neuromeningeal trunk, and the musculospinal artery (*m.sp.*).



(Fig. 25-29). Preprocedure steroid medication or, better yet, immediate surgery following the procedure may be considered.

- *Risk to the anterior spinal artery.* With tumors in the lower neck and shoulder it is easy to forget the many possible origins of the anterior spinal artery that can be

easily obscured by the overgrown vessels of a large tumor (Fig. 25-30).

- *Hypertensive response to release of vasoactive peptides from large chemodectomas.* Although this is a concern in only 3% of chemodectomas, there are reports of death from this complication (35). Advance screening of

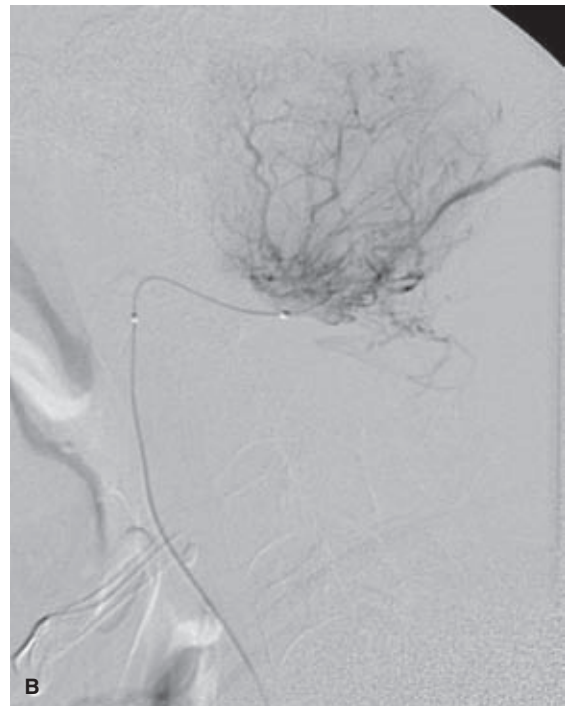
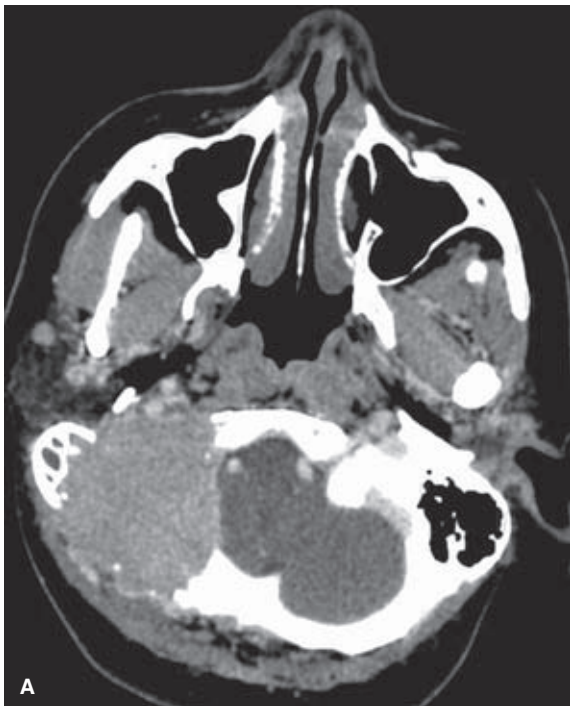


FIGURE 25-29. (A–B) Sometimes, the obvious is not so easy to see. This elderly patient was billed as a preoperative embolization of a posterior fossa meningioma. There is a smoothly enhancing lesion on the contrast-enhanced CT scan (A) conforming with this diagnosis. The lateral occipital artery angiogram was interpreted as showing a typical “sunburst” radial pattern of vasculature consistent with meningioma, although in retrospect the vessels look a little more disorganized than is typical of meningioma. The pathology report stated plasmacytoma. In retrospect, the CT scan shows a great deal more bone replacement by tumor than should be the case for simple meningioma.

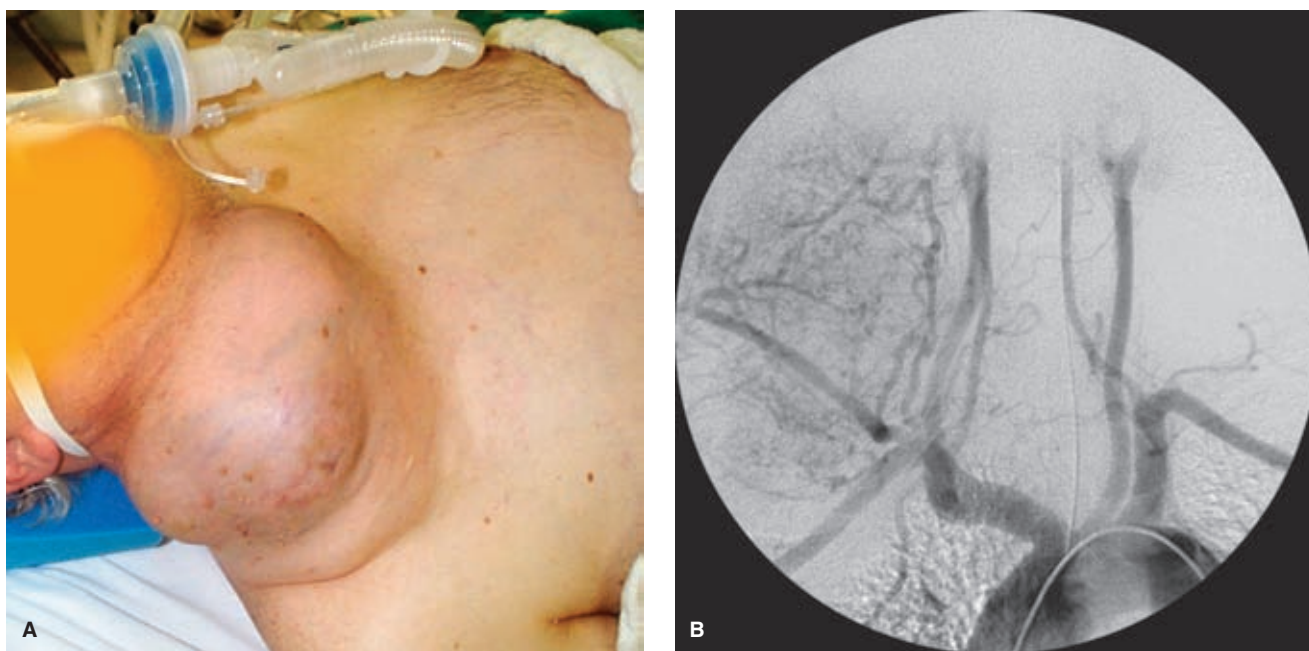


FIGURE 25-30. (A–B) Large thyroidal papillary carcinoma. This elderly gentleman neglected his health until his thyroid carcinoma began to affect his airway. This case is selected for two reasons. Firstly, airway protection should always be a paramount consideration, if not before the embolization, then possibly afterward. A large tumor may swell only a small degree after embolization but that could well be sufficient to cause a disaster. An intratumoral hemorrhage after embolization could cause the same problem. Secondly, the image of the patient (A) before his procedure is included to demonstrate the point that when confronted with such a tumor, one of the first things to come to mind should be concern for the anterior spinal artery. Any time an embolization in the region of the lower neck or supraclavicular fossa is considered, the possibility of the anterior spinal branch arising from the thyrocervical trunk or adjacent vessels should be thought of. The arch aortogram (B) on this patient demonstrates how easily such a tiny, critical vessel could be overlooked or hidden in the course of such a challenging case.

hypertensive patients for secretion of vanillyl-mandellic acid and catecholamines to predict the need for intraprocedural and intraoperative blockade with alpha-blockading agents may be necessary.

► NECK AND FACE BLEEDING AND ARTERIAL INJURIES

The general principles and repertoire of devices available for dealing with the other types of head and neck arterial injuries are no different from those described previously (36). Airway protection (Fig. 25-31) and hemodynamic stabilization or resuscitation of the patient are of paramount importance. Some particular aspects of dealing with bleeding patients and other arterial injuries deserve emphasis.

1. It is surprisingly difficult—considering what pains one takes to avoid inadvertent vessel thrombosis in all other cases—to stop bleeding or extravasation when one needs to do so. This is probably due to the fact that in the angiography suite, one sees only a tiny minority of trauma patients. Most patients stop bleeding with simple first-aid maneuvers, and, therefore, those sent for endovascular management likely have an unusual set of prevailing circumstances, physiologic, anatomic, or otherwise.
2. It is also surprisingly difficult to find the site of hemorrhage unless the patient is actively extravasating at the time of the angiographic run. Therefore, the more

information one has before the case about where exactly the bleeding is coming from, the better will one be able to focus the examination. If possible, mark the outside of the patient with a radiographically dense indicator of the site of bleeding.

3. Bleeding patients referred for endovascular management have invariably been through a triage of standard procedures in the emergency room and/or the operating room. Only those patients who fail this screening are referred to radiology, and, therefore, the patients in the angiography suite are several hours into their bleeding episode by the time the technologists start swabbing down the femoral arterial site. The point to remember is that the margin between apparent stability and incipient decompensation and shock is often very thin for these patients, and working with all haste, even at the cost of compromising some standards of room preparation, is absolutely imperative.
4. Smaller distal vessels are usually responsive to PVA particles or Gelfoam. Larger, more proximal vessels that are torn or have pseudoaneurysms will need to be occluded with fibered coils. For the internal carotid artery, common carotid artery, or vertebral artery, covered or uncovered stents (Figs. 25-32–25-34) with coils may be the only option to repair the vessel while preserving flow to the brain (37,38).
5. When working in the vertebral artery, care must always be given to the possibility that the anterior spinal artery is nearby and thus in jeopardy. The only way to avoid
(text continues on page 417)

FIGURE 25-31. Gunshot wound with active extravasation from the tongue. This lateral common carotid artery view shows active extravasation from the lingual artery following a gunshot wound. The image is a cumulative one, spanning the arterial and venous phases of the run, hence the visualization of venous structures. The image was saved in this manner for photographic purposes, to capture the high rate of extravasation better than could be achieved on a single image. This is a serious injury and must be embolized as quickly as possible, before the patient decompensates into hemodynamic shock. Gelfoam, liquid agents, or a very distal coil would be preferable. Small particle PVA would probably not occlude a bleeder of this size, and, besides, the tongue is vulnerable to ischemic injury from aggressive particle embolization (having no collateral flow except weakly from its contralateral fellow moiety). The obvious risk posed by a bleeder of this type to the airway is evident.

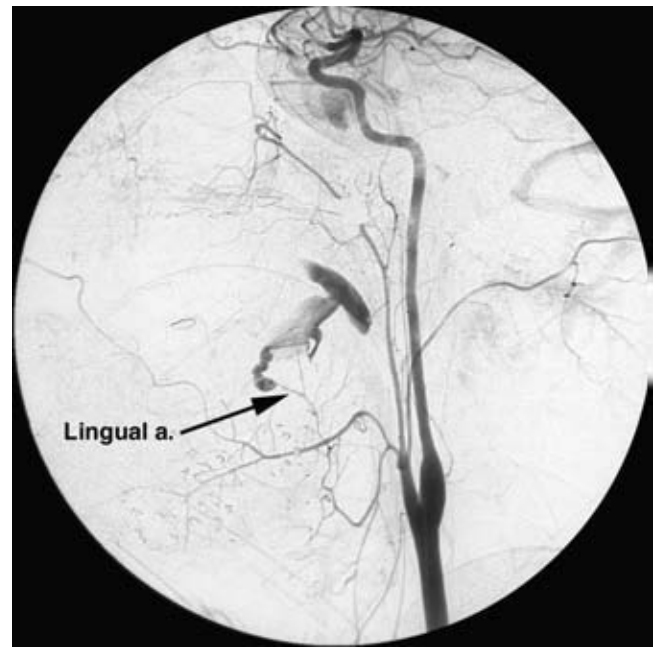


FIGURE 25-32. Covered stent for treatment of a vertebral artery pseudoaneurysm. Images from before and after treatment of a pseudoaneurysm of the right vertebral artery induced by an attempted central line placement. The patient developed a massive hematoma of the lower neck. The pseudoaneurysm (*arrowhead*) represents only a tiny component of the hematoma. The lateral wall of the vertebral artery (*arrows*) shows additional intimal injury or mural thrombus. After placement of a 4-mm covered stent the artery demonstrates a much improved appearance with elimination of the pseudoaneurysm.

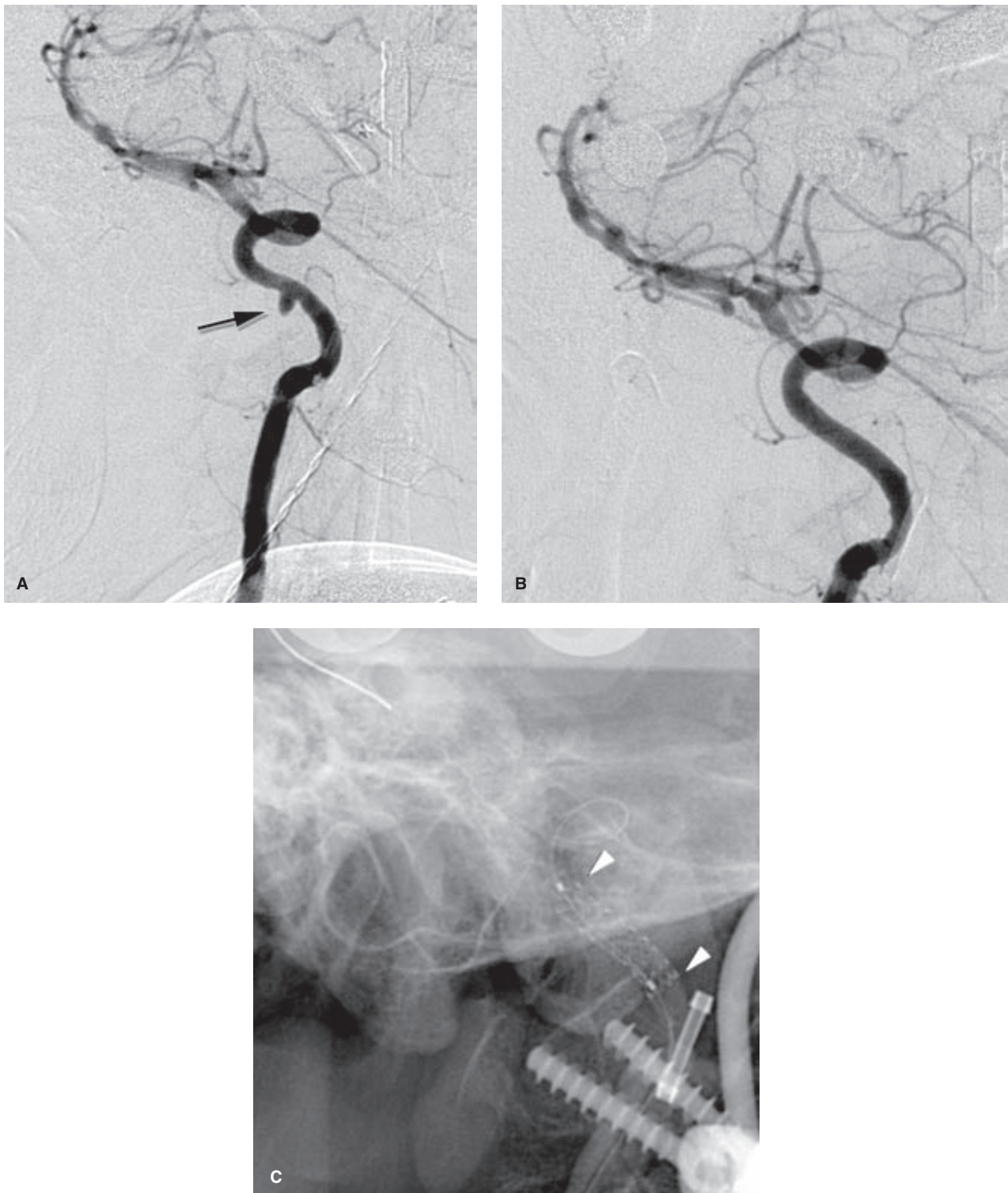


FIGURE 25-33. (A–C) Covered stent for treatment of a postsurgical vertebral artery pseudoaneurysm (*arrow*). This patient developed bleeding complications from a difficult skull base fixation procedure for spinal decompression in the setting of an anomalous craniocervical junction. The lateral views before (A) and after (B) deployment of a covered stent show the immediate normalization of vessel contour characteristic of these devices, when things go well. The nonsubtracted view (C) shows the extent of the short device (*arrowheads*), which can be placed very precisely and balloon-inflated in place. These images do not show the tremendous spasm of the posterior circulation induced by the wire during the procedure but which responded immediately afterward to wire removal and spasmolytics.

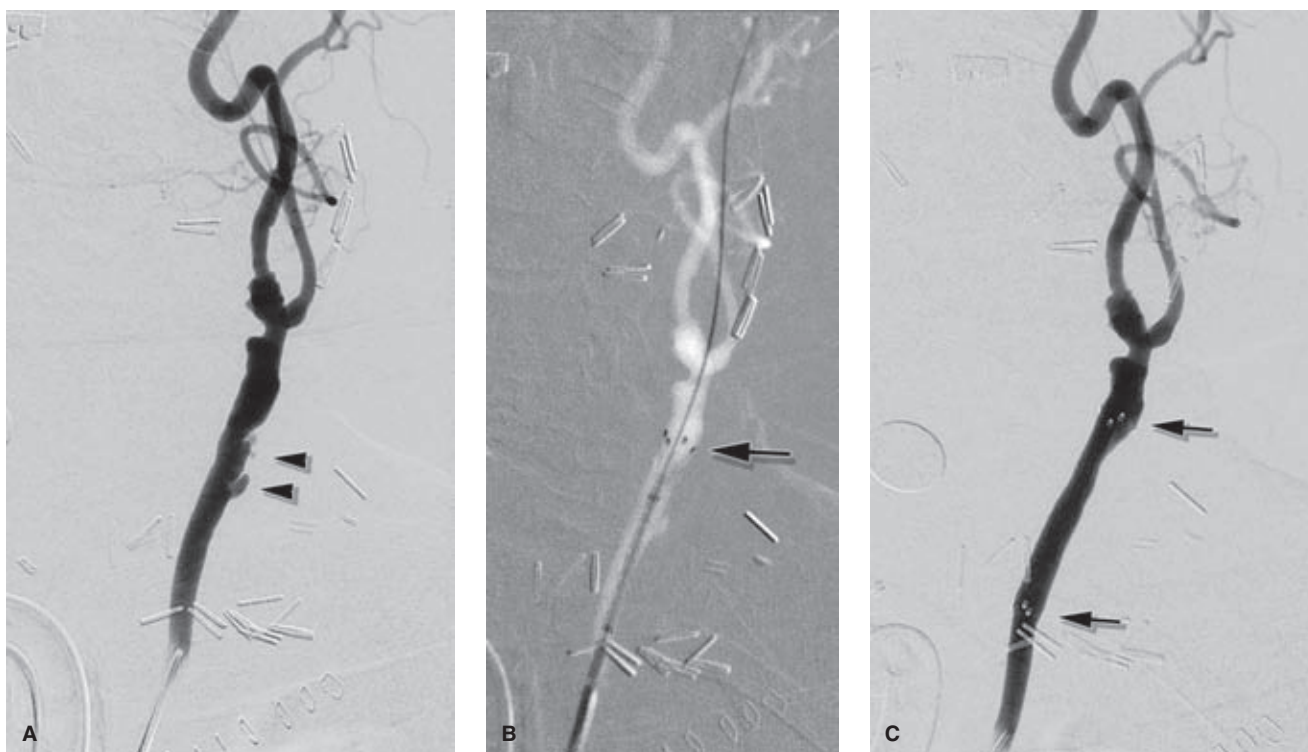


FIGURE 25-34. (A–C) Repair of a carotid pseudoaneurysm with covered stent. Covered stents have supplanted the role previously played by balloons or coils for endovascular arterial sacrifice when major bleeding occurred in the setting of an inoperable arterial injury. These devices are bulkier than their noncovered counterparts. For example, an 8-mm noncovered stent fitting through an 8F catheter or 6F introducer sheath will translate when covered into a 10F catheter or 8F introducer sheath. In this instance, an 8F short sheath was placed at the groin, a roadmap made of the common carotid artery, and an exchange-length wire was then placed above the pseudoaneurysm (*arrowheads*) into the external carotid artery. This was used to advance the delivery catheter for the covered stent seen partially deployed in (**B**) (*arrow*). The exchange-length wire was then used to reintroduce the diagnostic catheter for a final image (**C**) showing immediate elimination of the pseudoaneurysm and satisfactory apposition of the tines against the arterial wall (*arrows*).

this calamity is to identify the anterior spinal artery with certainty before performing a therapeutic occlusion (Figs. 25-35–25-41).

6. Vessel occlusion in the external carotid artery proximally, that is, close to the bifurcation and thus the origin of the internal carotid artery, carries special risks. The possibility of refluxing a pledget of Gelfoam has already been discussed, and when one does this close to the bifurcation, the risk to the internal carotid artery is self-evident. Therefore, Gelfoam should be used only with extreme caution close to the bifurcation. Similarly, pushed coils are notoriously capricious in how they will either curl nicely within a vessel (desirable) or extrude themselves rigidly (due to an oversizing in choice relative to the vessel) and will push the microcatheter back toward the bifurcation. Therefore, there is a risk of a fibered coil backing itself into the origin of the internal carotid artery. To avoid this, choose coils deliberately so that they are close in size to the vessel diameter. Coils that are too small will be ineffective or will be insecure within the artery, also at risk for falling into the internal carotid artery. Overlapping or interweaving of the fibered coils is the optimal situation.

► POSTTONSILLECTOMY BLEEDING

Posttonsillectomy bleeding is a much-feared complication of tonsillectomy and adenoidectomy, occurring in approximately 3% of elective cases, more frequently in up to 13% of emergency cases performed for quinsy or abscess (39,40). Fatal outcomes are still reported in the western hemisphere (41), and the magnitude of such a tragedy in a child suggests that it may be worthy of specific reference here (Figs. 25-42 and 25-43). Occasionally, the complication is due to aberrant vasculature (42), but generally, the problem arises 5 to 10 days postsurgery, when a breakdown of the surgical bed exposes underlying arteries. Patients commonly respond well to repeated cauterization of the tonsillectomy bed, but sometimes, persistent bleeding will require emergency interventional assistance (43).

1. These cases are always performed, even in adults, under general anesthesia to protect the airway.
2. The first task of such an angiogram is to clarify whether any major injury to the internal carotid artery or main trunk of the external carotid artery is present.
3. For faucial bleeding, the most typical site of injury is the ascending palatine artery, small tonsillar branches from
(*text continues on page 422*)

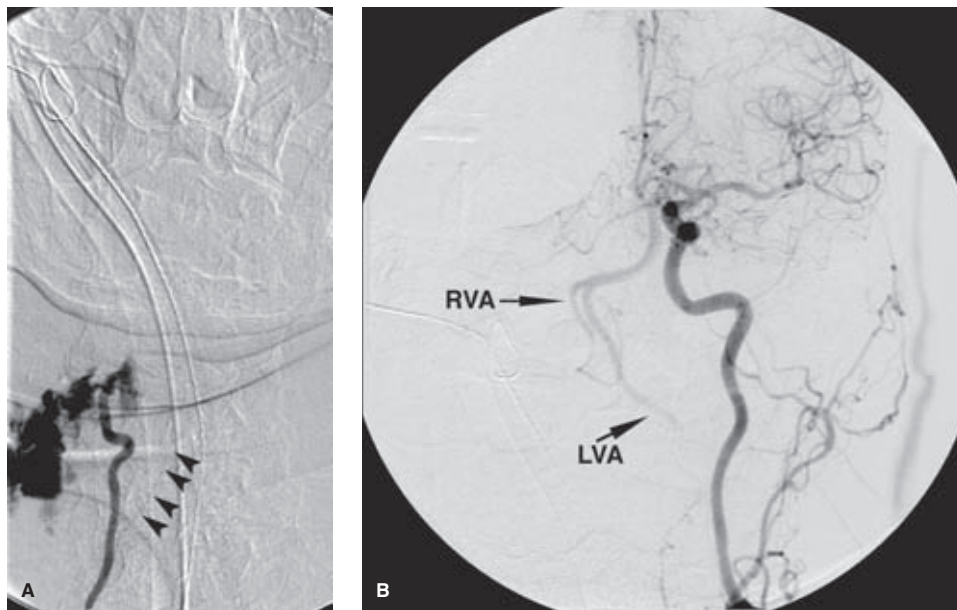


FIGURE 25-35. (A–B) Transection of the right vertebral artery. A penetrating injury with rapidly accumulating hematoma was related to this complete transection of the right vertebral artery (A). Although there is unfortunately motion artifact on the image, the anterior spinal artery (*arrowheads*) is present below the tear and must on all accounts be preserved to avoid spinal infarction. The left carotid injection (B) shows retrograde flow down the vertebral arteries bilaterally due to a coexistent injury of the left vertebral artery. A risk with coil occlusion of the right vertebral artery in this patient might be persistent bleeding from the top-down direction if the right vertebral artery is patent and flowing above the tear. This was not the case here, and the right vertebral artery was occluded with 0.018” coils placed via a microcatheter, preserving the segment below with the anterior spinal artery.

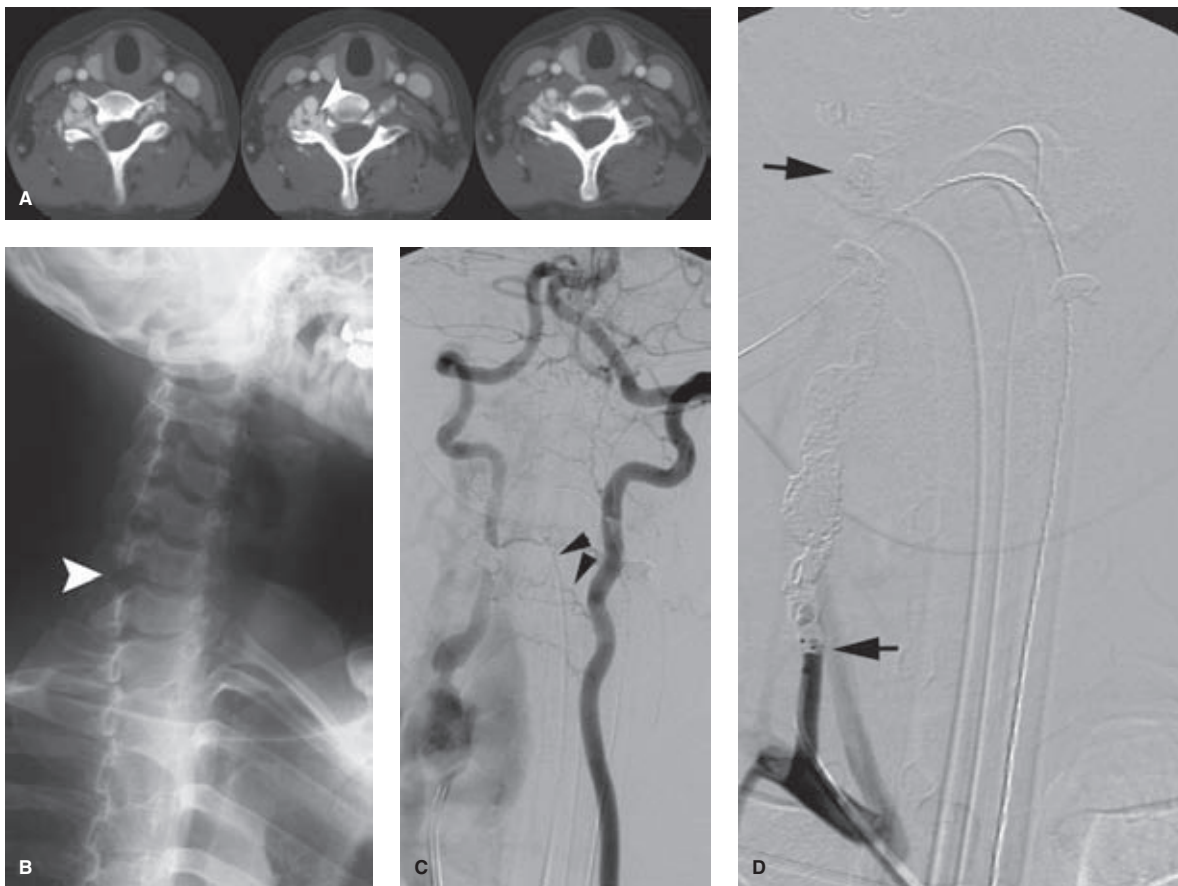


FIGURE 25-36. (A–D) Spontaneous right vertebral artery fistula. A young adult with subtle manifestations of neurofibromatosis Type I developed a loud bruit in association with right brachial plexus symptoms. Her CTA examination (A) showed the precise point of the spontaneous fistula (*arrowhead* in A), while the plain film (B) showed enlargement of the ipsilateral C6–C7 neural foramen (*arrowhead* in B). The left vertebral artery injection (C) with a second catheter in the right vertebral artery shows the obvious fistula, but the most important finding is the location of the anterior spinal artery (*arrowheads*) arising from the left and flowing retrogradely, through an arrangement of bilateral pedicles, to the right. This clears the way from a complete occlusion of the right vertebral artery with 0.018” and 0.038” coils (*arrows* in D) deployed from C1 to below the fistula in order to avoid antegrade transmission of thrombus from the stump above the occlusion site. Balloons would have been better for this case but were unavailable. A covered stent would also have worked possibly but would not have been as tested in terms of long-term safety compared with this simple treatment.



FIGURE 25-37. (A–E) Dangers of the anterior spinal artery. In the context of a big dramatic production that frequently accompanies patients with rapidly expanding hematoma and other ICU problems, it is easy to forget the most critical vessel in the body that can often be waiting to snare the unwary. This patient with extensive metastatic laryngeal carcinoma (A) and a neck hematoma shows the anterior spinal artery (*arrowhead*) on the neck CT as the least conspicuous finding on this axial image. The left thyrocervical trunk injection (B) shows the anterior spinal artery (*arrowheads*) or at least part of it (its presence on the left does not preclude the possibility of another pedicle on the right).

The second lesson of this case is the difficulty of opacifying even big pseudoaneurysms with nonselective injections. The innominate artery injection (C) barely hints at the presence (*arrow*) of an abnormal blush somewhere near the midline, but without much specific hint as to where it might be arising. The right thyrocervical injection (D) demonstrates the pseudoaneurysm (*long arrow*), but also shows the ease with which collaterals can cross the midline (*arrowheads*) where the anterior spinal artery has already been seen. (*continued*)

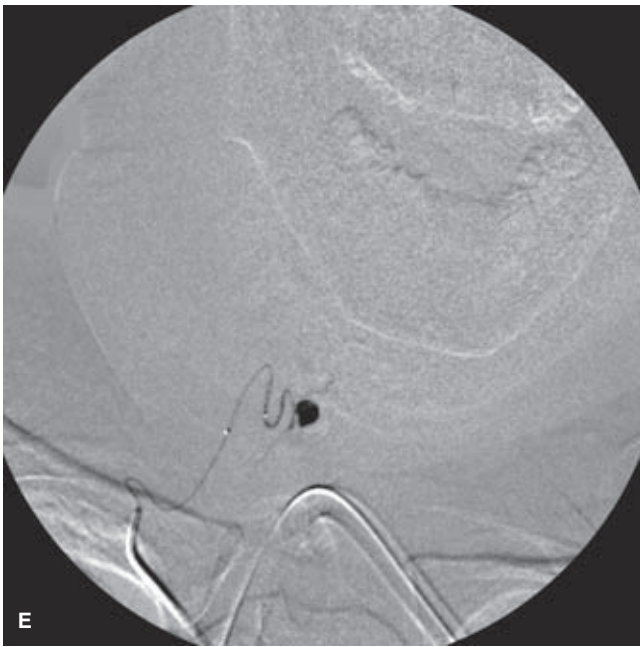


FIGURE 25-37. (CONTINUED) The leak was sealed with an injection of nBCA (E), which would not have been advisable if the anterior spinal artery were on the ipsilateral side or otherwise close to the lesion.

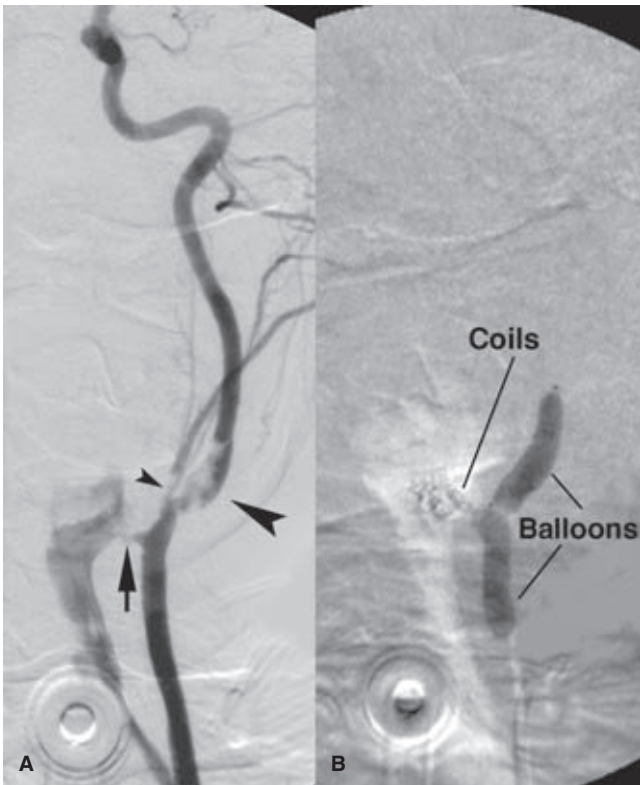


FIGURE 25-38. (A–B) Balloon occlusion of a carotid injury. An elderly patient with laryngeal carcinoma had severe oral bleeding on the day of this study. This improbable diagnosis is a carotid–esophageal fistula (arrow), occasioned by the erosion of carcinomatous tissue (arrowheads) into her left carotid bulb. The neuroradiologist performing this case was understandably concerned about abruptly sacrificing her carotid artery because flow past the carcinoma to the intracranial circulation continued to be robust. A hastily conducted study of the collateral circulation was inconclusive as to whether she would tolerate loss of the left carotid artery. Therefore, an initial attempt was made to occlude the fistula by using fiberoed coils. These were ineffective, and the patient required cardiopulmonary resuscitation three times on the table, prompting immediate closure of the artery with detachable latex balloons.

Her unusual diagnosis and long odds of survival were trumped only by her appearance the next morning sitting up in bed, nonchalantly reading the *Boston Globe* while leisurely taking the lightly boiled. In a glass specimen jar by her bed, she proudly displayed one of the still inflated latex balloons, which she had regurgitated uneventfully during the night! This case is from some years ago and would be handled more effectively today with a covered stent.

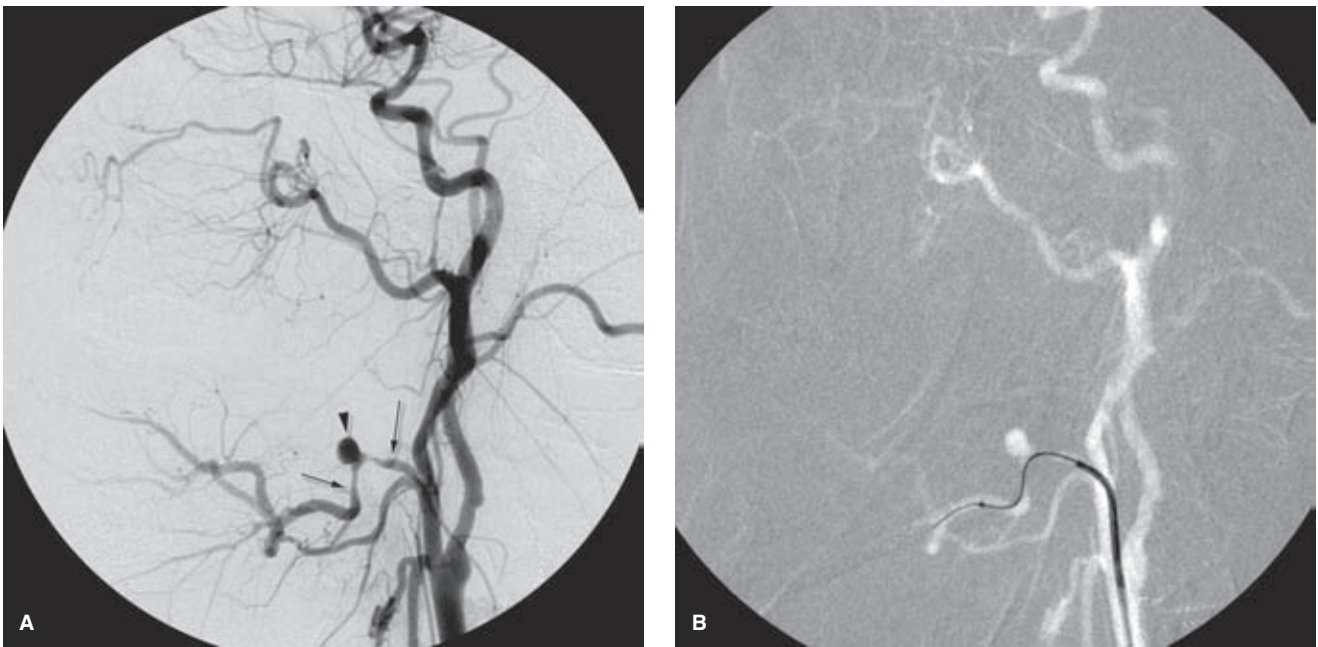


FIGURE 25-39. (A–B) Facial artery pseudoaneurysm: importance of “trapping.” When a pseudoaneurysm cannot safely be obliterated with a liquid agent, coils are a simple and usually safer alternative. However, the capacity for the external carotid artery to reconstitute itself distal to an occlusion is such that a proximal occlusion for a bleeding site is often ineffective. Trapping the pseudoaneurysm by navigating past the pseudoaneurysm is usually necessary. Obviously this involves a risk of perforating the pseudoaneurysm anew. One should be ready to work fast when this happens, the first reaction being to ram the introducer catheter into the feeding vessel to obturate it, if possible, while the microcatheter is used to occlude the leak.

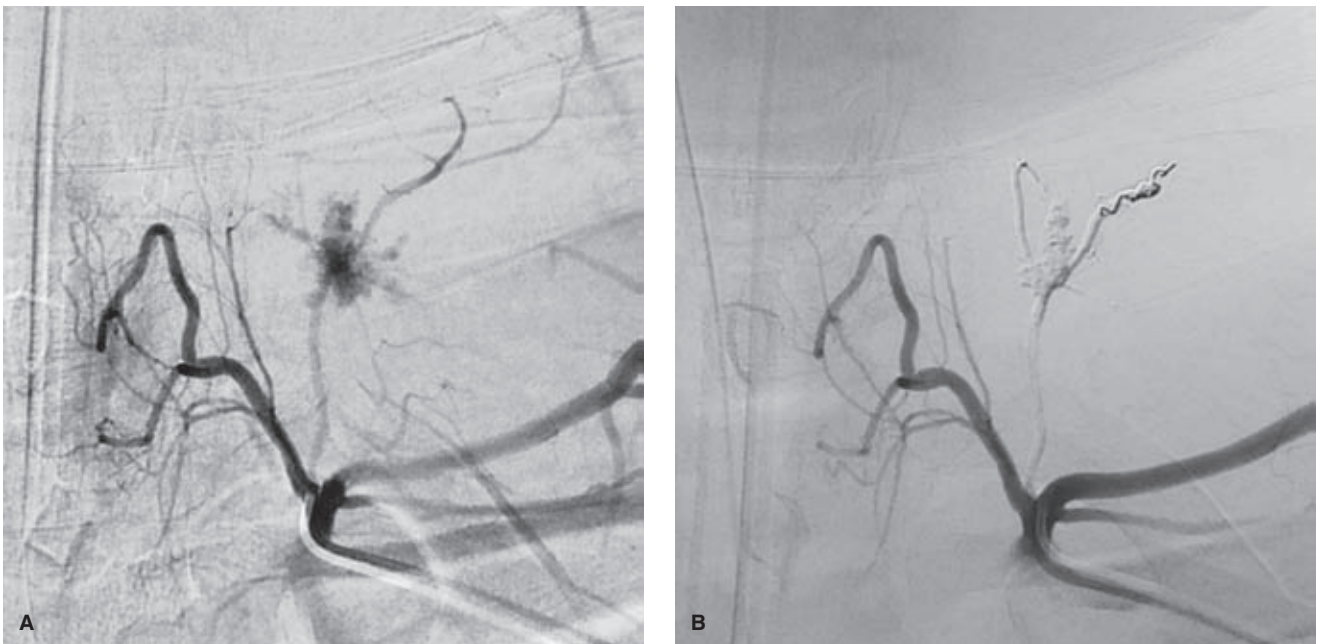


FIGURE 25-40. (A–B) Trapping a pseudoaneurysm with liquid embolic agent. This patient suffered an injury to the thyrocervical trunk in the ICU and when he was transported to radiology for endovascular treatment it became apparent that he had both groins heavily spoken for with multiple central lines of every ilk. A left transradial approach was used, but even at that, as mentioned in Figure 25-37, the bleeding site was extremely difficult to see. The thyrocervical trunk appears to show a possible anterior spinal artery, while the leak is from a transected ascending cervical branch. Coils were placed distal to the leak, but the patient was so coagulopathic that the coils failed to staunch the flow. The lesion was then embolized with nBCA distally, within the pseudoaneurysm by pulling back the microcatheter, and at the entrance point. The final subtracted image (B) shows the cast of nBCA. The stump below is filled with test contrast giving the impression that the nBCA extends all the way back to the origin of the ascending cervical artery, but due to the possible presence of the anterior spinal artery, this would have been extremely hazardous. Finally, the transradial approach proved to be a blessing in disguise as the coagulopathic state of the patient would have made femoral artery control potentially problematic. Two hours of prolonged application of the Terumo wrist-band (with Doppler confirmation of the palmar arch and clinical evaluation to exclude venous occlusion) took care of hemostasis after the case.

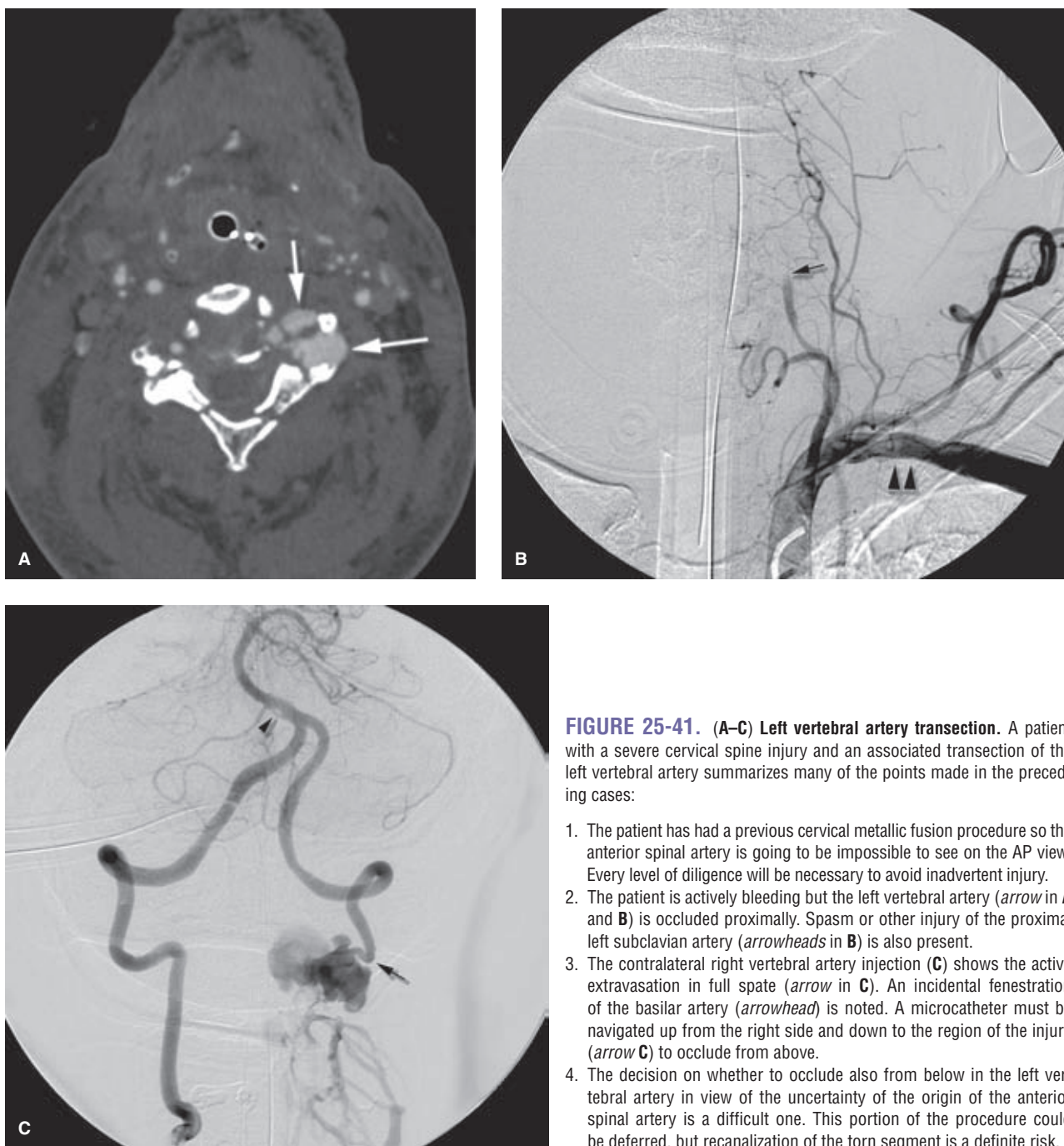


FIGURE 25-41. (A–C) Left vertebral artery transection. A patient with a severe cervical spine injury and an associated transection of the left vertebral artery summarizes many of the points made in the preceding cases:

1. The patient has had a previous cervical metallic fusion procedure so the anterior spinal artery is going to be impossible to see on the AP view. Every level of diligence will be necessary to avoid inadvertent injury.
2. The patient is actively bleeding but the left vertebral artery (*arrow* in **A** and **B**) is occluded proximally. Spasm or other injury of the proximal left subclavian artery (*arrowheads* in **B**) is also present.
3. The contralateral right vertebral artery injection (**C**) shows the active extravasation in full spate (*arrow* in **C**). An incidental fenestration of the basilar artery (*arrowhead*) is noted. A microcatheter must be navigated up from the right side and down to the region of the injury (*arrow C*) to occlude from above.
4. The decision on whether to occlude also from below in the left vertebral artery in view of the uncertainty of the origin of the anterior spinal artery is a difficult one. This portion of the procedure could be deferred, but recanalization of the torn segment is a definite risk.

proximal facial artery, or from the segment of the external carotid close to the origin of the facial artery (44). These can be embolized selectively with short-fibered coils. Extravasation will probably not be obvious. A cut-off or truncated vessel may be the only clue. When the bleeding is adenoidal, the ascending pharyngeal artery and the pterygogovaginal artery will be the primary sites of interest (45).

4. Occasionally, the ascending palatine artery arises directly from the external carotid artery just beyond the origin of the facial artery. The injury may cut quite close to or involve the external carotid artery itself here, and in many such patients, the torn or bleeding vessel will be

in temporary spasm at the time of the angiogram. Examine the images *very closely* for a vessel that looks odd or truncated.

▶ TEST OCCLUSION OF THE CAROTID OR VERTEBRAL ARTERIES

Test occlusion of the internal carotid artery with or without radionuclide injection for SPECT scanning can be performed in a variety of ways depending on institutional protocols. The question is whether the patient's circle of Willis is competent to sustain cerebral perfusion following

FIGURE 25-42. Posttonsillectomy bleeding I. A young adult female developed recurrent severe bleeding 2 weeks after a routine tonsillectomy. A left external carotid artery injection demonstrates irregularity of the proximal facial artery (*arrowhead*). At the same level, a small palatine or tonsillar branch (*arrow*) of the facial artery has a cut-off appearance. In this patient, the ascending palatine artery (*asc.pal.*) appears unremarkable, and it was assumed that the tonsillar artery represented the most likely site of bleeding. It was occluded with coils placed through a microcatheter.

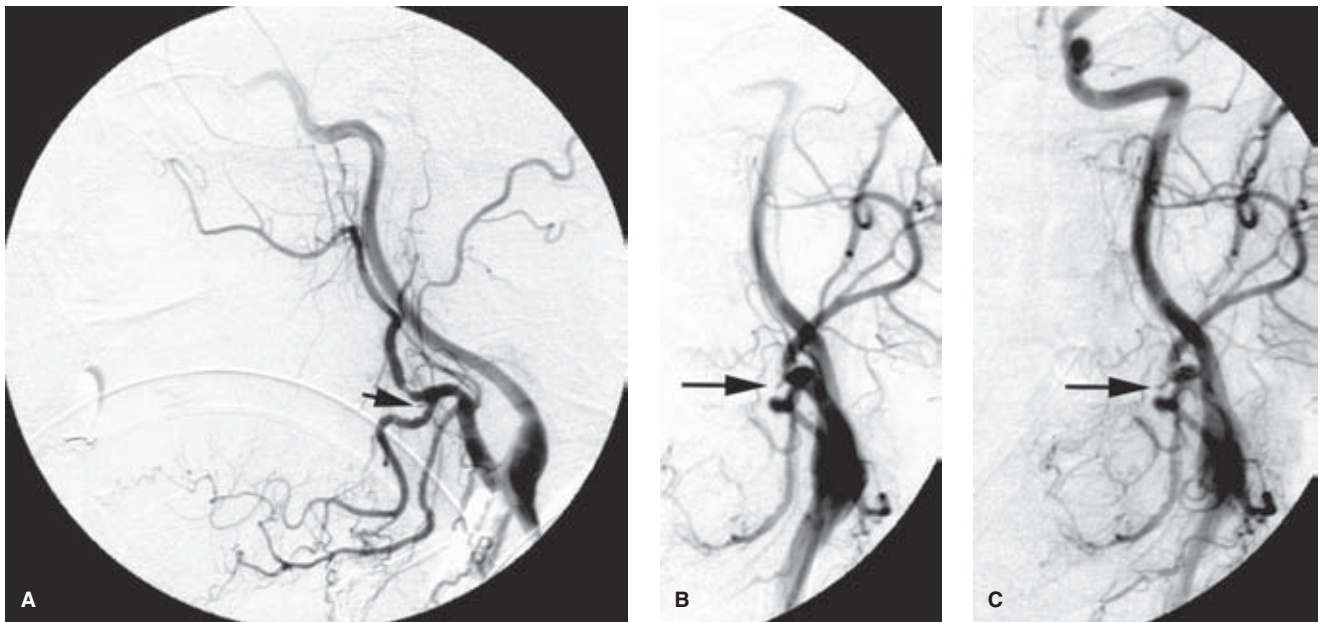
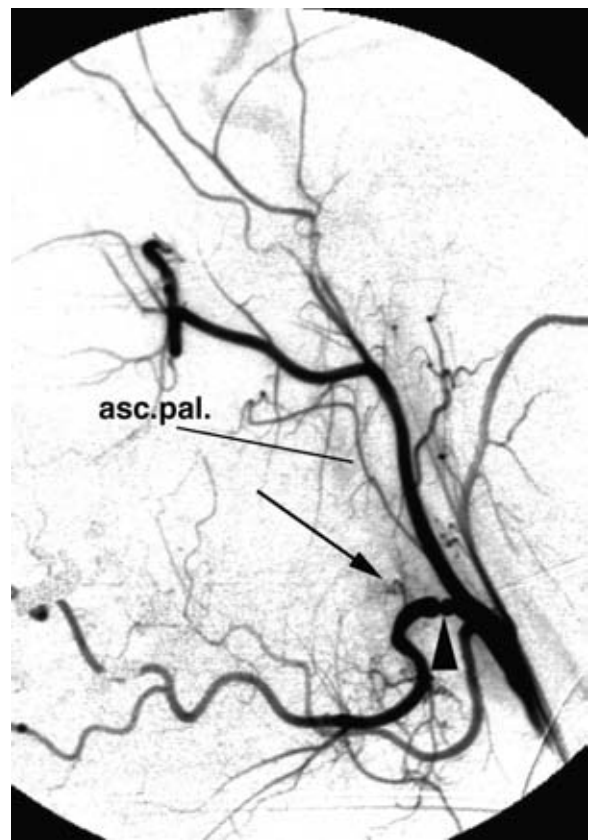


FIGURE 25-43. (A–C) Posttonsillectomy bleeding II. A young adult male developed severe bleeding 4 days after a tonsillectomy. Left common carotid arteriography (**A** and **B**) demonstrates subtle extravasation from a rent or torn vessel between the external carotid artery and the facial artery (*arrows* in **A** and **B**). The blush of extravasation becomes more prominent in the late arterial phase (**C**). Above this level, there is spasm of the external carotid artery, best seen on the lateral view (**A**). The area of extravasation was cannulated with a microcatheter and occluded with a push coil.

anticipated endovascular or surgical sacrifice of the vessel (46). Therefore, the physiologic conditions under which the test occlusion is performed must be noted for a meaningful interpretation of the results. Sometimes dropping the patient's systemic blood pressure during the test occlusion period (usually around 20 minutes) to stress the competence of the collateral channels can increase the sensitivity of the procedure to potential problems after the definitive sacrifice, but the reliability of such additional sensitivity is uncertain (47–49). Even with an auspicious result from a test occlusion procedure hypotensive or orthostatic ischemic symptoms are common in dehydrated or long-recumbent patients who are suddenly lifted upright in bed. Gradual mobilization and elevation of the head of the bed over several days is necessary to allow a gradual adjustment of the autoregulatory curve.

Test occlusion of the carotid arteries is performed with a compliant soft-balloon under full heparinization. A double-lumen balloon catheter is most desirable to allow saline lavage of the carotid artery above and below the balloon throughout the procedure. Usually the balloon is placed in cavernous segment just below the ophthalmic artery. Occasionally, in order to avoid a false-negative or false-positive test, some critical thought must be given to where to place the balloon, particularly in the vertebral arteries, so that the collateral state of flow through alternative routes during the test procedure emulates those that will be present after the vessel is sacrificed. During the test period repeated neurologic checks of motor function and language ability are conducted with particular reliance on an examination for pronator drift toward the end of the occlusion period.

References

- Geibprasert S, Pongpech S, Armstrong D, et al. Dangerous extracranial-intracranial anastomoses and supply to the cranial nerves: Vessels the neurointerventionalist needs to know. *AJNR Am J Neuroradiol* 2009;30(8):1459–1468.
- Schlosser RJ. Clinical practice. Epistaxis. *N Engl J Med* 2009; 360(8):784–789.
- Sokoloff J, Wickbom I, McDonald D, et al. Therapeutic percutaneous embolization in intractable epistaxis. *Radiology* 1974; 111(2):285–287.
- Andersen PJ, Kjeldsen AD, Nepper-Rasmussen J. Selective embolization in the treatment of intractable epistaxis. *Acta Otolaryngol* 2005;125(3):293–297.
- Fukutsuji K, Nishiike S, Aihara T, et al. Superselective angiographic embolization for intractable epistaxis. *Acta Otolaryngol* 2008;128(5):556–560.
- Layton KF, Kallmes DF, Gray LA, et al. Endovascular treatment of epistaxis in patients with hereditary hemorrhagic telangiectasia. *AJNR Am J Neuroradiol* 2007;28(5):885–888.
- Strach K, Schrock A, Wilhelm K, et al. Endovascular treatment of epistaxis: Indications, management, and outcome. *Cardiovasc Intervent Radiol* 2011;34(6):1190–1198.
- Willems PW, Farb RI, Agid R. Endovascular treatment of epistaxis. *AJNR Am J Neuroradiol* 2009;30(9):1637–1645.
- Christensen NP, Smith DS, Barnwell SL, et al. Arterial embolization in the management of posterior epistaxis. *Otolaryngol Head Neck Surg* 2005;133(5):748–753.
- Jao SY, Weng HH, Wong HF, et al. Successful endovascular treatment of intractable epistaxis due to ruptured internal carotid artery pseudoaneurysm secondary to invasive fungal sinusitis. *Head Neck* 2011;33(3):437–440.
- Weaver EM, Chaloupka JC, Putman CM, et al. Effect of internal maxillary arterial occlusion on nasal blood flow in swine. *Laryngoscope* 1999;109(1):8–14.
- Davidson GS, Terbrugge KG. Histologic long-term follow-up after embolization with polyvinyl alcohol particles. *AJNR Am J Neuroradiol* 1995;16(4 suppl):843–846.
- Quisling RG, Mickle JP, Ballinger WB, et al. Histopathologic analysis of intraarterial polyvinyl alcohol microemboli in rat cerebral cortex. *AJNR Am J Neuroradiol* 1984;5(1):101–104.
- Vokes DE, McIvor NP, Wattie WJ, et al. Endovascular treatment of epistaxis. *ANZ J Surg* 2004;74(9):751–753.
- Gurney TA, Dowd CF, Murr AH. Embolization for the treatment of idiopathic posterior epistaxis. *Am J Rhinol* 2004; 18(5):335–339.
- Diaz-Daza O, Arraiza FJ, Barkley JM, et al. Endovascular therapy of traumatic vascular lesions of the head and neck. *Cardiovasc Intervent Radiol* 2003;26(3):213–221.
- Ngan BY, Forte V, Campisi P. Molecular angiogenic signaling in angiofibromas after embolization: Implications for therapy. *Arch Otolaryngol Head Neck Surg* 2008;134(11):1170–1176.
- Zhang X, Xu W, Sun J, et al. VEGF mRNA expression in jugulotympanic paraganglioma. *Eur J Cancer Care (Engl)* 2010; 19(6):816–819.
- Nagai MA, Butugan O, Logullo A, et al. Expression of growth factors, proto-oncogenes, and p53 in nasopharyngeal angiofibromas. *Laryngoscope* 1996;106(2 pt 1):190–195.
- Coutinho-Camillo CM, Brentani MM, Nagai MA. Genetic alterations in juvenile nasopharyngeal angiofibromas. *Head Neck* 2008;30(3):390–400.
- Brieger J, Wierzbička M, Sokolov M, et al. Vessel density, proliferation, and immunolocalization of vascular endothelial growth factor in juvenile nasopharyngeal angiofibromas. *Arch Otolaryngol Head Neck Surg* 2004;130(6):727–731.
- Favier J, Igaz P, Burnichon N, et al. Rationale for anti-angiogenic therapy in pheochromocytoma and paraganglioma. *Endocr Pathol* 2011;23(1):34–42.
- Herman B, Bublik M, Ruiz J, et al. Endoscopic embolization with onyx prior to resection of JNA: A new approach. *Int J Pediatr Otorhinolaryngol* 2011;75(1):53–56.
- Santaolalla F, Araluce I, Zabala A, et al. Efficacy of selective percutaneous embolization for the treatment of intractable posterior epistaxis and juvenile nasopharyngeal angiofibroma (JNA). *Acta Otolaryngol* 2009;129(12):1456–1462.
- Elhannady MS, Johnson JN, Peterson EC, et al. Preoperative embolization of juvenile nasopharyngeal angiofibromas: Transarterial versus direct tumoral puncture. *World Neurosurg* 2011;76(3–4):328–334; discussion 263–325.
- Elhannady MS, Peterson EC, Johnson JN, et al. Preoperative Onyx embolization of vascular head and neck tumors by direct puncture. *World Neurosurg* Nov 10 2011.
- Wiegand S, Kureck I, Chapot R, et al. Early side effects after embolization of a carotid body tumor using Onyx. *J Vasc Surg* 2010;52(3):742–745.
- Yang TH, Ou CH, Yang MS, et al. Preoperative embolization of carotid body tumor by direct percutaneous intratumoral injection of N-butyl cyanoacrylate glue assisted with balloon protection technique. *J Chin Med Assoc* 2011;74(2):91–94.
- Ahmed Ashrafi SK, Suhail Z, Khambaty Y. Postembolization infarction in juvenile nasopharyngeal angiofibroma. *J Coll Physicians Surg Pak* 2011;21(2):115–116.
- Ramezani A, Haghightakhah H, Moghadasi H, et al. A case of central retinal artery occlusion following embolization procedure for juvenile nasopharyngeal angiofibroma. *Indian J Ophthalmol* 2010;58(5):419–421.
- Gupta AK, Purkayastha S, Bodhey NK, et al. Preoperative embolization of hypervascular head and neck tumours. *Australas Radiol* 2007;51(5):446–452.
- Sawlani V, Browning S, Sawhney IM, et al. Posterior circulation stroke following embolization of glomus tympanicum? Relevance of anatomy and anastomoses of ascending pharyngeal artery. A case report. *Interv Neuroradiol* 2009;15(2):229–236.

33. Bentson J, Rand R, Calcatera T, et al. Unexpected complications following therapeutic embolization. *Neuroradiology* 1978; 16:420–423.
34. Schroth G, Haldemann AR, Mariani L, et al. Preoperative embolization of paragangliomas and angiofibromas. Measurement of intratumoral arteriovenous shunts. *Arch Otolaryngol Head Neck Surg* 1996;122(12):1320–1325.
35. Pandya SK, Nagpal RD, Desai AP, et al. Death following external carotid artery embolization for a functioning glomus jugulare chemodectoma. Case report. *J Neurosurg* 1978; 48(6): 1030–1034.
36. Schrock A, Jakob M, Strach K, et al. Transarterial endovascular treatment in the management of life-threatening intra- and postoperative haemorrhages after otorhinolaryngological surgery. *Eur Arch Otorhinolaryngol* Nov 12 2011.
37. Pyun HW, Lee DH, Yoo HM, et al. Placement of covered stents for carotid blowout in patients with head and neck cancer: Follow-up results after rescue treatments. *AJNR Am J Neuroradiol* 2007;28(8):1594–1598.
38. Zussman B, Gonzalez LF, Dumont A, et al. Endovascular management of carotid blowout: Institutional experience and literature review. *World Neurosurg* Nov 7 2011.
39. Lehnerdt G, Senska K, Jahnke K, et al. Post-tonsillectomy haemorrhage: A retrospective comparison of abscess- and elective tonsillectomy. *Acta Otolaryngol* 2005;125(12):1312–1317.
40. Giger R, Landis BN, Dulguerov P. Hemorrhage risk after quinsy tonsillectomy. *Otolaryngol Head Neck Surg* 2005;133(5): 729–734.
41. Windfuhr JP. Lethal post-tonsillectomy hemorrhage. *Auris Nasus Larynx* 2003;30(4):391–396.
42. Hofman R, Zeebregts CJ, Dijkers FG. Fulminant post-tonsillectomy haemorrhage caused by aberrant course of the external carotid artery. *J Laryngol Otol* 2005;119(8):655–657.
43. Windfuhr JP. Indications for interventional arteriography in post-tonsillectomy hemorrhage. *J Otolaryngol* 2002;31(1):18–22.
44. Opatowsky MJ, Browne JD, McGuiert WF Jr, et al. Endovascular treatment of hemorrhage after tonsillectomy in children. *AJNR Am J Neuroradiol* 2001;22(4):713–716.
45. Borden NM, Dungan D, Dean BL, et al. Posttraumatic epistaxis from injury to the pterygogaginal artery. *AJNR Am J Neuroradiol* 1996;17(6):1148–1150.
46. Lesley WS, Rangaswamy R. Balloon test occlusion and endosurgical parent artery sacrifice for the evaluation and management of complex intracranial aneurysmal disease. *J Neurointerv Surg* 2009;1(2):112–120.
47. Dare AO, Chaloupka JC, Putman CM, et al. Failure of the hypotensive provocative test during temporary balloon test occlusion of the internal carotid artery to predict delayed hemodynamic ischemia after therapeutic carotid occlusion. *Surg Neurol* 1998;50(2):147–155; discussion 155–146.
48. Standard SC, Ahuja A, Guterman LR, et al. Balloon test occlusion of the internal carotid artery with hypotensive challenge. *AJNR Am J Neuroradiol* 1995;16(7):1453–1458.
49. Wong GK, Poon WS, Chun Ho Yu S. Balloon test occlusion with hypotensive challenge for main trunk occlusion of internal carotid artery aneurysms and pseudoaneurysms. *Br J Neurosurg* 2010;24(6):648–652.

Reversible Cerebral Vasoconstriction Syndrome

Key Points

- Reversible cerebral vasoconstriction syndrome (RCVS) is a relatively common disorder, sharing pathophysiologic features with a spectrum of disorders, including posterior reversible encephalopathy syndrome (PRES), drug-related arteriopathies, and others.
- The clinical presentation of “thunderclap” headache is typical of this disorder, but not specific.

Reversible cerebral vasoconstriction syndrome (RCVS) is a group of diverse disorders characterized by acute onset, often with a thunderclap headache and an acute course of illness spanning 2 to 8 weeks during which complications of cerebral vasoconstriction may become clinically evident. About 40% of cases can be termed primary, that is, no known cause or precipitant, and about 60% have well-recognized antecedent risk factors. Within this entire group of disorders, an undefined dysregulation of arterial tone is a common feature, leading to significant overlap in clinical features with other disorders such as posterior reversible encephalopathy syndrome (PRES). It is important to be familiar with the entity of RCVS as it is not as rare a condition as it was once considered. Furthermore, some of the features of RCVS can lend itself to being confused with primary angiitis of the central nervous system (PACNS), a distinct condition with a very different prognosis and specific treatment requirements.

► BACKGROUND

The recognition of RCVS as a distinct, although heterogeneous, group of related conditions has evolved over the past two decades. A paper in 1988 (1) by Call and Fleming drew attention to a group of patients presenting with sudden severe headaches and proceeding to variable patterns of cerebral ischemia associated with multivessel, scattered vasoconstriction of the circle of Willis and its major branches (Figs. 26-1–26-3). Over the years since then, many reports and case series of patients with disparate backgrounds have appeared, all of whom shared many features with the

patients in the 1988 paper. These were variably described as having benign angiopathy of the central nervous system (CNS), postpartum angiopathy, migrainous vasospasm, drug-related CNS arteritis, pheochromocytoma-induced arteritis, hypertensive encephalopathy, or variants of PRES. The clinical, prognostic, and treatment similarities among all these groups, as distinct from patients with other conditions, particularly PACNS (see Chapter 27) and aneurysmal subarachnoid hemorrhage, make the categorical labeling with RCVS useful and valid. Primary RCVS remains a diagnosis of exclusion, after other entities have been considered, but because this is not a rare phenomenon, and is in fact more common than PACNS, patients with primary RCVS need to be spared the more drastic immunosuppressive therapy warranted for PACNS. Thunderclap headache is not pathognomonic of RCVS, even in the absence of a cerebral aneurysm ruptured or otherwise. Entities such as intracranial dissection, ischemic stroke, acute hypertensive crisis, acute obstruction by a colloid cyst, or intracranial infection are all considered in the differential diagnosis initially (2).

► CLINICAL PRESENTATION OF RCVS

Several large case series of patients with RCVS report a consistent clinical appearance and course of this condition (3–6). Typically this condition is seen in its primary form, or with minimal risk factors, in middle-aged women (80%), while younger male patients have a greater likelihood of associated risk factors. Less commonly, the condition has been identified in children (7,8). The presentation is abrupt, most frequently with a thunderclap headache in 82% to 100% of patients, which may be recurrent during the first week. By the 2nd or 3rd week, neurologic complications of vasoconstriction declare themselves, and about 80% of patients develop brain lesions on MRI or CT. About 40% develop ischemic strokes usually in a watershed distribution and frequently with a pattern similar to that seen in PRES (9,10), subarachnoid hemorrhage 30% to 40%, lobar hemorrhage, cortical blindness (Anton’s syndrome), or seizure. Cerebrospinal fluid (CSF) analysis is normal except where xanthochromia from hemorrhage is to be expected. Segmental, multivessel irregularities with a “bead and string” appearance will be seen in the majority of patients on CTA or MRA, although the initial study may frequently be normal. In the published papers,

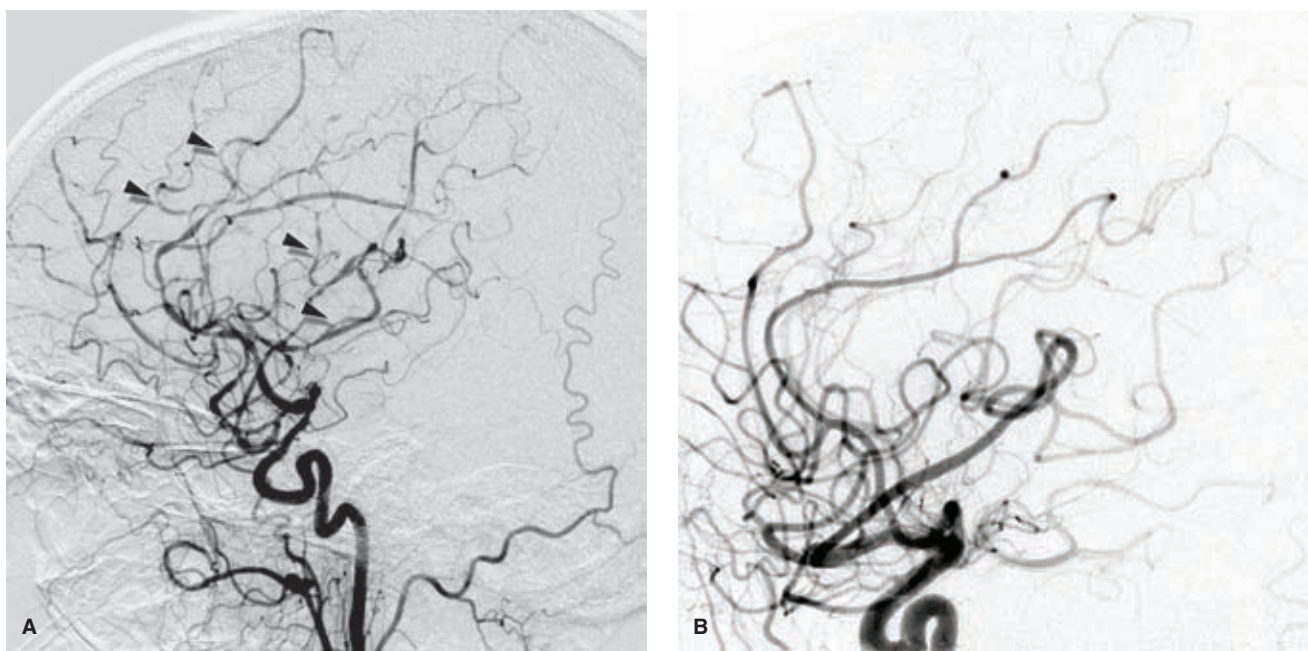


FIGURE 26-1. (A–B) RCVS. A right common carotid arteriogram lateral view (A) in a young adult admitted with thunderclap headache demonstrates the typical “bead and string” appearance of RCVS. Multiple sites of involvement are labeled with arrowheads, but the extent of involvement is virtually universal, including the supraclinoidal carotid artery. The extracranial vessels are not affected. A follow-up arteriogram 3 months later (B) shows that the vessels have virtually normalized in the interim.

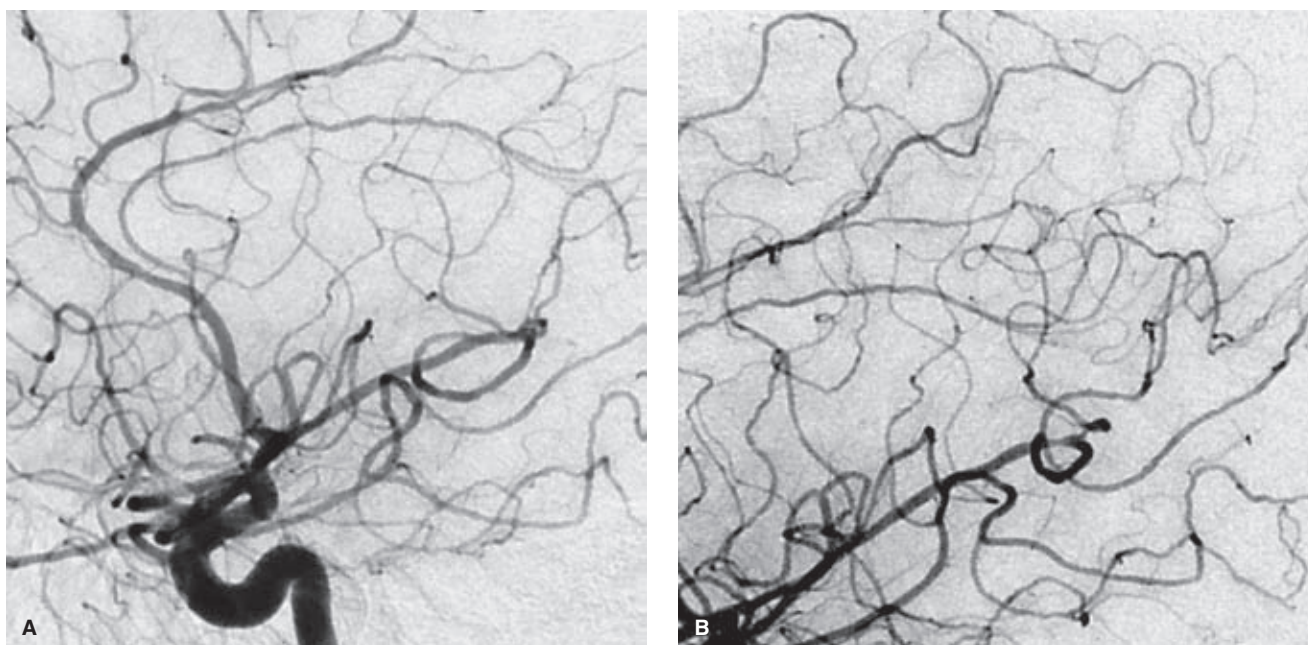


FIGURE 26-2. (A–C) Marijuana-related RCVS. A middle-aged patient with a long history of heavy marijuana use was admitted with headache and mental status changes. The angiogram of the right internal carotid artery (A, lateral view; B, magnification view; C, magnification oblique view) shows a more subtle appearance of RCVS than that seen in Figure 26-1, but with, nevertheless, diffuse involvement of the medium-sized and more distal arteries. The corrugated appearance of the distal vessels gives an irregular, almost cork-screw aspect to many of the vessels. (continued)

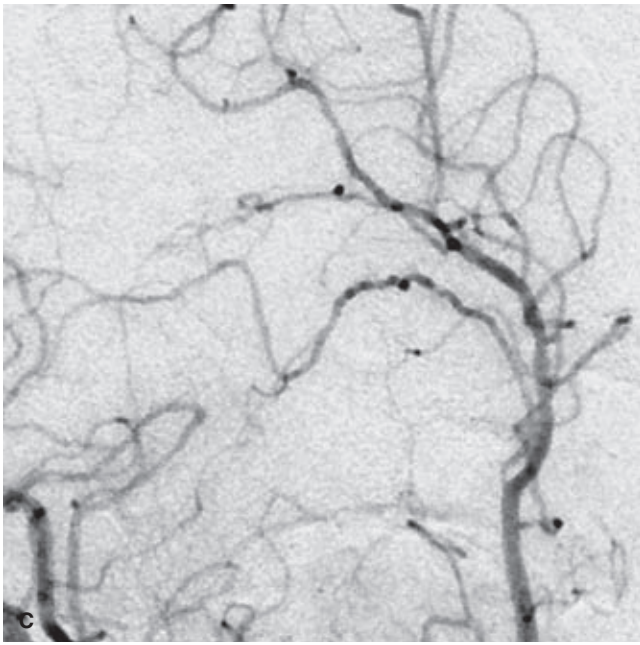


FIGURE 26-2. (CONTINUED)

catheter angiography shows abnormalities in 100% of patients. About 80% of patients or more have a very favorable outcome, provided that severe complications of ischemic stroke are not present, and the condition runs its course within 6 to 12 weeks with complete normalization and reversal of imaging features of vasoconstriction.

PACNS, by contrast, tends to present with a more insidious onset of dull headache, with a step-wise neurologic deterioration and course. The course of illness is prolonged, frequently over months or longer until a diagnosis

is reached. Patients present due to difficulties with paresis, cognitive or personality change, visual problems, dysphasia, or ataxia. No gender predisposition is seen. Ischemic lesions are not confined to the watershed territories (Fig. 27-2). CSF findings are abnormal in the great majority of patients with pleocytosis and elevated protein count. Even with orthodox immunosuppressive therapy, angiographic findings do not reverse themselves acutely (11,12).

It seems cogent to argue that RCVS and PRES are closely related and overlapping disorders that share many

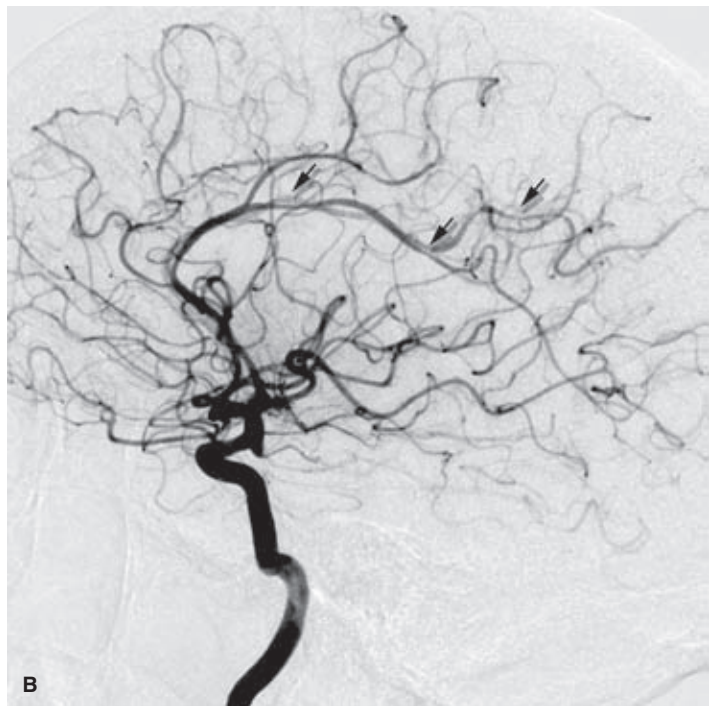
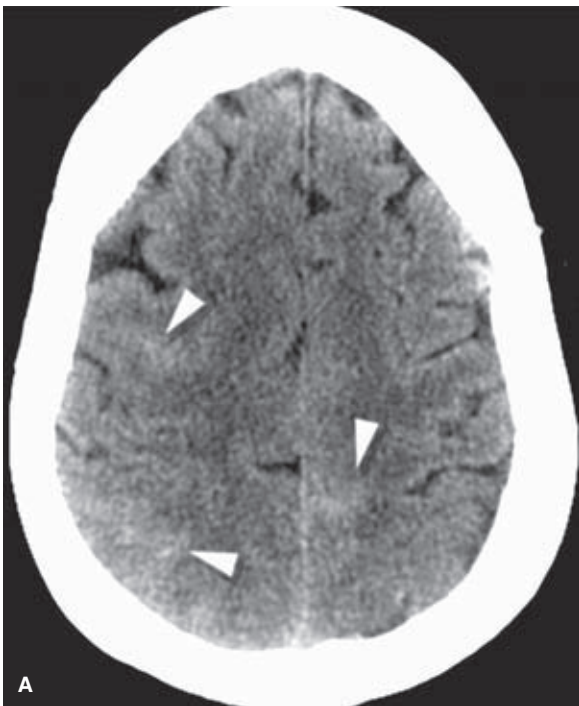


FIGURE 26-3. (A–B) Nonperimesencephalic subarachnoid hemorrhage. A female patient in her early fifties complained of a week of crescendo headache and was found to have evidence of subarachnoid hemorrhage on CT (*arrowheads* in **A**) over the convexities. No aneurysm was found and no history of substantial head trauma was forthcoming. Angiography demonstrated (*arrowheads* in **B**) multiple areas of luminal constriction in the medium-sized vessels of the anterior and posterior circulation. These findings and her clinical symptoms were ascribed to RCVS.

clinical and imaging features (9,10). The risk factors for both conditions are virtually identical (Table 26-1), except that the lists for PRES cast a wider net to encompass a range of complex immunologic conditions such as posttransplant immunotherapy, cancer chemotherapy, transfusion, and autoimmune disease, but it is possible that these entities are part of a shared spectrum of common pathophysiologic processes. The most discerning shibboleth between the two diagnoses appears to be the prominence of vasogenic edema within white matter with PRES. Otherwise, a description of what separates the two conditions might be captious. PRES has been associated with findings suggesting the importance of endothelial activation, reactive astrocytosis, and T-cell migration with increased vascular endothelial growth factor (VEGF) activity on biopsy (13), and at least 10% to 17% of RCVS patients are recognized as having archetypal PRES findings (4,6), although the figure is likely even higher. Within the realm of RCVS, clinical differences between groups of patients described by different authors can be ascribed to their being recruited variably from headache clinics versus inpatient stroke services, for example (3,5). It is very likely that the recognition and labeling of patients as having either PRES or RCVS is influenced by a similar bias.

► ANGIOGRAPHIC APPEARANCE OF RCVS

The angiographic findings of RCVS are not necessarily specific or pathognomonic to the condition, and a deal of overlap with other vasoconstrictive conditions is inevitable. The appearance of RCVS declares itself in the major branches of the circle of Willis intradurally, and does not show itself in the extracranial or extradural vessels. Typically it starts at the level of dural perforation. It has a multifocal, beaded appearance proximally on the circle of Willis, while the appearance of PACNS is considered more likely to be a disease of distal vessels and smaller

arteries. The angiographic abnormalities of RCVS are thus more dramatic and easier to see on an angiogram than those of PACNS. While some patients with RCVS may have a normal or nondiagnostic MRA or CTA, 100% of those studied with catheter angiography have angiographic findings of vasoconstriction. Typically the angiographic findings of RCVS resolve completely within 8 to 12 weeks of onset.

The question of the sensitivity of catheter angiography in the setting of PACNS is a little more difficult to answer. A review of PACNS in 1992 (11) reported that almost 40% of cerebral angiograms were normal in this condition, but in retrospect this study contained a substantial number of patients who would now be categorized as RCVS, and therefore the sensitivity of angiography to PACNS is probably less than 60%. Other studies in which biopsy was used as the gold standard for establishing the diagnosis have reported a surprisingly limited sensitivity of catheter angiography to the presence of PACNS, ranging from 56% to 75% (14–16), but with the caveat that the specificity or diagnostic utility of this procedure was probably only in the range of 25% to 27%.

► TREATMENT OF RCVS

Even with just symptomatic management, over 80% of RCVS patients have a favorable outcome with short-term (8 to 12 weeks maximum) resolution of symptoms and imaging findings. Use of glucocorticoids has been associated with an unfavorable outcome (3), but several authors have recommended oral or intravenous calcium channel blockers, nifedipine, nimodipine, or verapamil, for relief of headache and reversal of vasospasm (3,5,8). Several reports of favorable response in patients with RCVS to intra-arterial administration of calcium-channel blockers and/or balloon angioplasty have been published (Fig. 26-4) (17,18–21), and *(text continues on page 432)*

TABLE 26-1 Etiologies and Associations of RCVS

Primary RCVS

- Idiopathic thunderclap headache, emotional stress, bath-time induced (22)
- Cough
- Exertional headache
- Migraine associated
- Carriers of brain-derived neurotrophic factor BDNF gene Val66Met polymorphism (4)

Secondary RCVS

- Postpartum (23–25)
- Eclampsia or preeclampsia

Drug-related

- Marijuana (“reefer madness”) (Fig. 26-5)
- Cocaine, amphetamine, ecstasy
- Ergot-derived drugs, ergotamine tartrate, bromocriptine, lisuride
- Sympathomimetics, ephedrine, pseudoephedrine, phenylpropanolamine
- Serotonin and norepinephrine uptake inhibitors, SSRI (Fig. 26-6)
- Immunosuppressants, tacrolimus, cyclophosphamide, cyclosporin-A, IFN-alpha
- Nicotine, liquorice (26), indomethacin, binge alcohol

Catecholamine Secreting Tumors

- Carcinoid, paraganglioma, pheochromocytoma

Others

- High altitude (27), tonsillectomy, intravenous immunoglobulin, graft-versus-host disease (GVHD) (28) (Fig. 26-7).

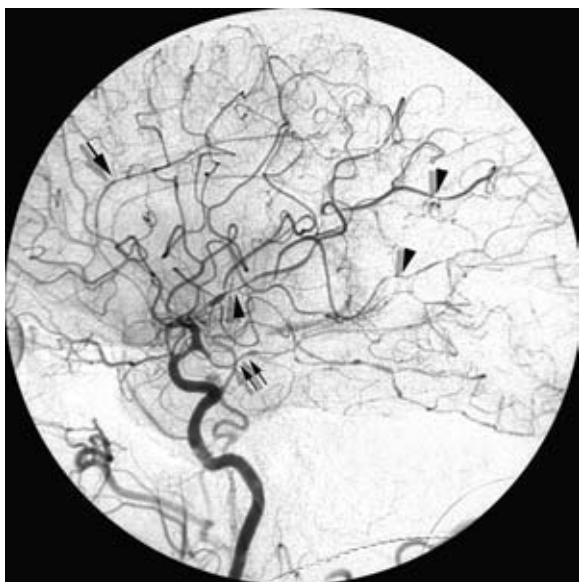


FIGURE 26-4. Postpartum RCVS treated with endovascular angioplasty and spasmolytic infusion. A 10-day postpartum patient in her mid-twenties was admitted with severe headache, mental status changes, and evidence of mild subarachnoid hemorrhage on CT. No aneurysm was identified. Her declining condition prompted repeated angiographic evaluation and eventual endovascular treatment of the proximal vasospastic vessels with balloon angioplasty and infusion of papaverine. The pattern of RCVS involvement of the middle cerebral artery (arrowheads) is multifocal and segmental, whereas that of the anterior cerebral artery (single arrow) and fetal posterior cerebral artery (double arrow) is more severe and generalized. Her clinical outcome was good.

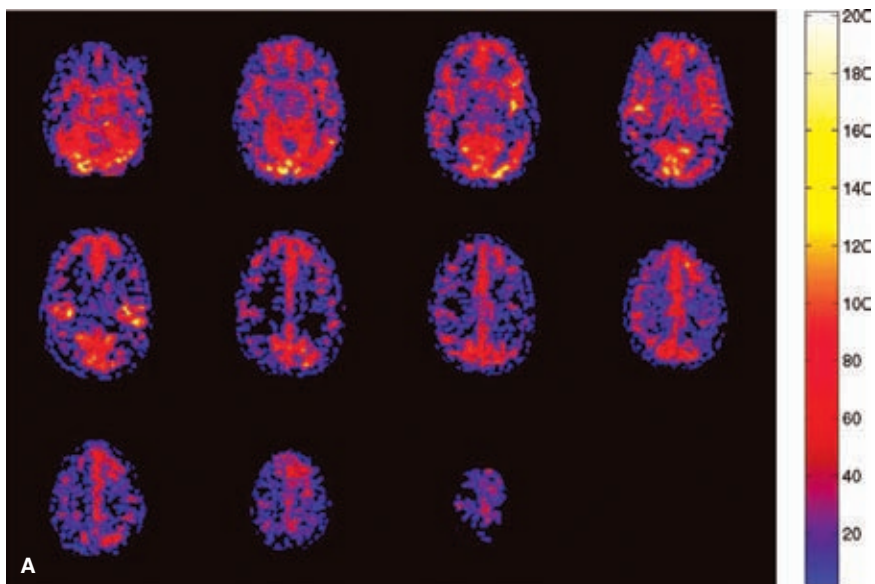
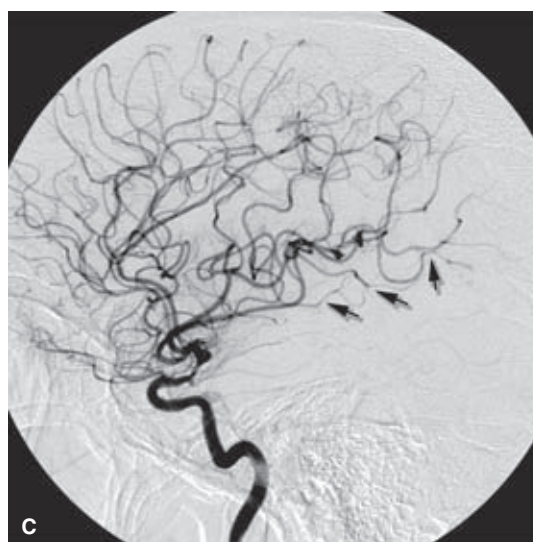
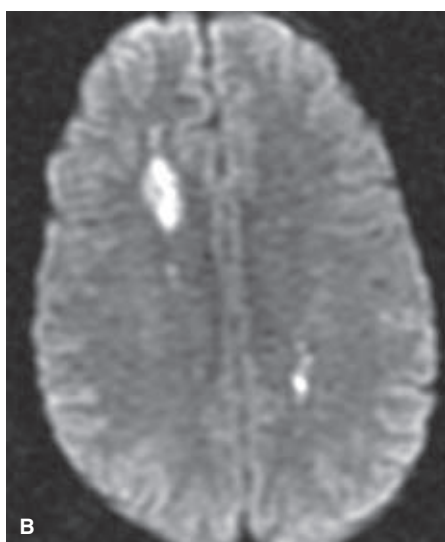


FIGURE 26-5. Marijuana-related RCVS. A young adult was admitted with an acute history of headache, heavy marijuana use, and fluctuating neurologic deficits. Her arterial spin labeling study (A) demonstrated global, multiregional hypoperfusion. Her MRI demonstrated a watershed pattern of infarction bilaterally on DWI (B). The angiogram of the right internal carotid artery (C) showed severe narrowing of the supraclinoidal carotid artery and scattered more distal areas of vessel narrowing (arrows in C). A repeat angiogram 3 months later (not shown) was normal.



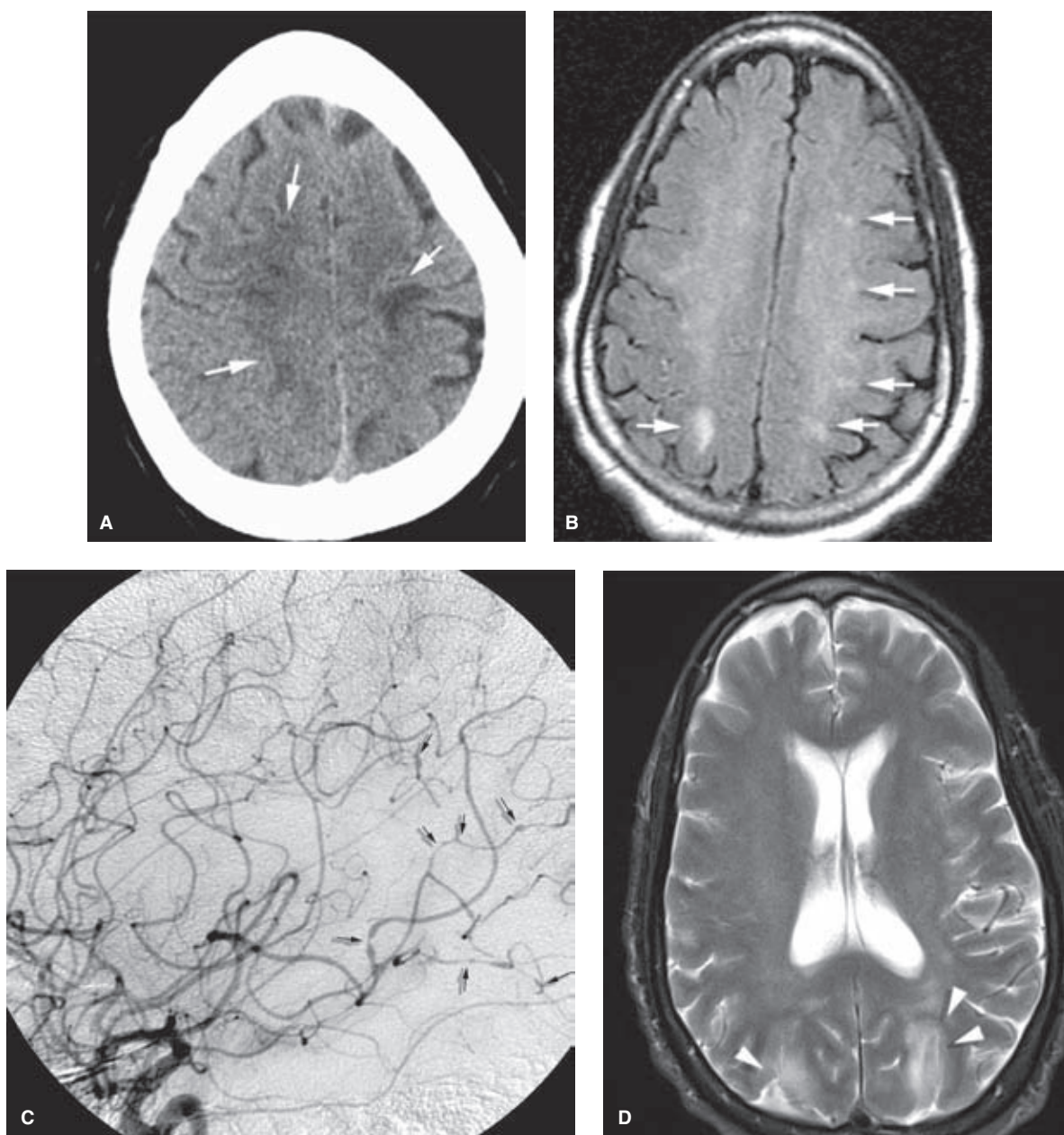


FIGURE 26-6. (A–D) RCVS associated with selective serotonin uptaker inhibitor use. A female patient in her sixties who had been prescribed an SSRI agent for treatment of depression presented with acute seizure and changes in mental status. During the diagnostic evaluation, her clinical condition and the extent of the imaging findings deteriorated on sequential examinations. Her CT (**A**) initially demonstrated nonspecific white matter lesions over the convexities (*arrows* in **A**), while FLAIR showed similar findings (*arrows* in **B**). Her initial angiogram (**C**) showed multiple irregularities (*small arrows* in **C**) in the left internal carotid artery territory and other vessels. Two weeks later her T2-weighted MRI (**D**) showed bilateral occipital lesions similar to those seen in PRES (*arrowheads* in **D**). Biopsy was considered, but cancelled when her condition finally began to improve, seemingly related to withdrawal of the SSRI medication. Her condition was ascribed to the SSRI agent, a recognized association and her improved clinical condition has been sustained without relapse. The long biologic half-life of most of the SSRI agents may be a factor in delaying recovery, as was the case in this patient.

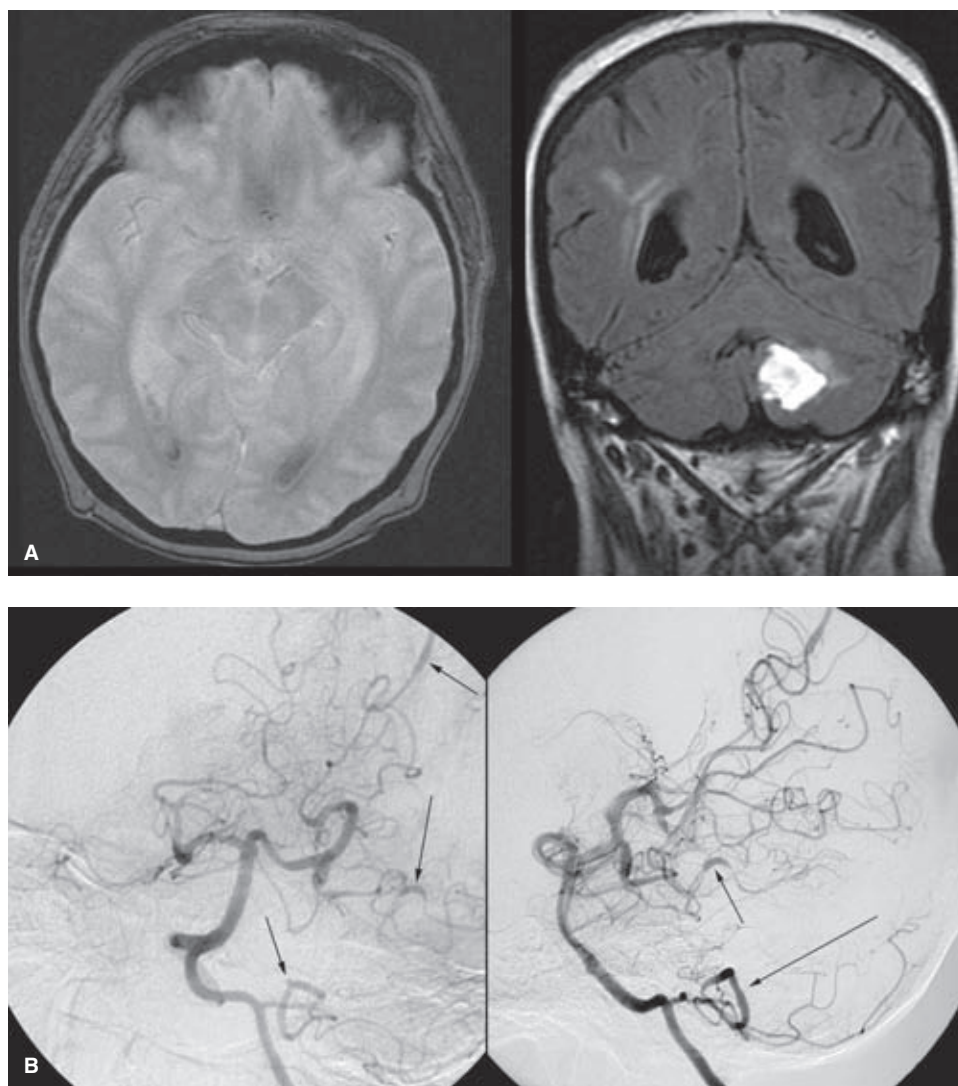


FIGURE 26-7. (A–B) Intracranial vasculitis versus RCVS as an expression of graft-versus-host-disease (GVHD). A female patient in her mid-fifties presented with a peripheral vasculitis 2 years following a bone marrow transplant complicated by GVHD affecting the skin, gastrointestinal tract, and liver. Sudden onset of intracranial hemorrhage (A) with intracerebellar and subarachnoid hemorrhage prompted the performance of a cerebral angiogram. The left vertebral artery injection (B) demonstrates multiple areas of vessel irregularity in the posterior circulation (arrows) and the possibility of a microaneurysm on the left posterior inferior cerebellar artery. RCVS is a recognized association of GVHD, but the diagnostic and treatment decision in this case was complicated by her previous rheumatologic diagnosis of peripheral vasculitis. The patient was treated successfully by a reinstatement of her immunosuppressant regimen, which had been previously tapered (28).

it is likely that endovascular treatment of this disorder will gain more acceptance in the future.

References

1. Call GK, Fleming MC, Sealfon S, et al. Reversible cerebral segmental vasoconstriction. *Stroke* 1988;19(9):1159–1170.
2. Agostoni E, Rigamonti A, Aliprandi A. Thunderclap headache and benign angiopathy of the central nervous system: A common pathogenetic basis. *Neurol Sci* 2011;32 suppl 1:S55–S59.
3. Singhal AB, Hajj-Ali RA, Topcuoglu MA, et al. Reversible cerebral vasoconstriction syndromes: analysis of 139 cases. *Arch Neurol* 2011;68(8):1005–1012.
4. Chen SP, Fuh JL, Wang SJ. Reversible cerebral vasoconstriction syndrome: Current and future perspectives. *Expert Rev Neurother* 2011;11(9):1265–1276.
5. Ducros A, Boukobza M, Porcher R, et al. The clinical and radiological spectrum of reversible cerebral vasoconstriction syndrome. A prospective series of 67 patients. *Brain* 2007;130(pt 12):3091–3101.
6. Ducros A, Fiedler U, Porcher R, et al. Hemorrhagic manifestations of reversible cerebral vasoconstriction syndrome: Frequency, features, and risk factors. *Stroke* 2010;41(11):2505–2511.
7. Kirton A, Diggle J, Hu W, et al. A pediatric case of reversible segmental cerebral vasoconstriction. *Can J Neurol Sci* 2006;33(2):250–253.
8. Liu HY, Fuh JL, Lirng JF, et al. Three paediatric patients with reversible cerebral vasoconstriction syndromes. *Cephalalgia* 2010;30(3):354–359.
9. Bartynski WS. Posterior reversible encephalopathy syndrome, part 2: Controversies surrounding pathophysiology of vasogenic edema. *AJNR Am J Neuroradiol* 2008;29(6):1043–1049.

10. Bartynski WS. Posterior reversible encephalopathy syndrome, part 1: Fundamental imaging and clinical features. *AJNR Am J Neuroradiol* 2008;29(6):1036–1042.
11. Calabrese LH, Furlan AJ, Gragg LA, et al. Primary angiitis of the central nervous system: Diagnostic criteria and clinical approach. *Cleve Clin J Med* 1992;59(3):293–306.
12. Calabrese LH, Dodick DW, Schwedt TJ, et al. Narrative review: Reversible cerebral vasoconstriction syndromes. *Ann Intern Med* 2007;146(1):34–44.
13. Horbinski C, Bartynski WS, Carson-Walter E, et al. Reversible encephalopathy after cardiac transplantation: Histologic evidence of endothelial activation, T-cell specific trafficking, and vascular endothelial growth factor expression. *AJNR Am J Neuroradiol* 2009;30(3):588–590.
14. Harris KG, Tran DD, Sickels WJ, et al. Diagnosing intracranial vasculitis: The roles of MR and angiography. *AJNR Am J Neuroradiol* 1994;15(2):317–330.
15. Salvarani C, Brown RD Jr, Calamia KT, et al. Primary central nervous system vasculitis: Analysis of 101 patients. *Ann Neurol* 2007;62(5):442–451.
16. Vollmer TL, Guarnaccia J, Harrington W, et al. Idiopathic granulomatous angiitis of the central nervous system. Diagnostic challenges. *Arch Neurol* 1993;50(9):925–930.
17. Ringer AJ, Qureshi AI, Kim SH, et al. Angioplasty for cerebral vasospasm from eclampsia. *Surg Neurol* 2001;56(6):373–378; discussion 378–379.
18. Elstner M, Linn J, Muller-Schunk S, et al. Reversible cerebral vasoconstriction syndrome: A complicated clinical course treated with intra-arterial application of nimodipine. *Cephalalgia* 2009;29(6):677–682.
19. Farid H, Tatum JK, Wong C, et al. Reversible cerebral vasoconstriction syndrome: treatment with combined intra-arterial verapamil infusion and intracranial angioplasty. *AJNR Am J Neuroradiol* 2011;32(10):E184–E187.
20. Klein M, Fesl G, Pfister HW, et al. Intra-arterial nimodipine in progressive postpartum cerebral angiopathy. *Cephalalgia* 2009;29(2):279–282.
21. Linn J, Fesl G, Ottomeyer C, et al. Intra-arterial application of nimodipine in reversible cerebral vasoconstriction syndrome: A diagnostic tool in select cases? *Cephalalgia* 2011;31(10):1074–1081.
22. Wang SJ, Fuh JL, Wu ZA, et al. Bath-related thunderclap headache: A study of 21 consecutive patients. *Cephalalgia* 2008;28(5):524–530.
23. Singhal AB, Bernstein RA. Postpartum angiopathy and other cerebral vasoconstriction syndromes. *Neurocrit Care* 2005;3(1):91–97.
24. Bogousslavsky J, Despland PA, Regli F, et al. Postpartum cerebral angiopathy: Reversible vasoconstriction assessed by transcranial Doppler ultrasounds. *Eur Neurol* 1989;29(2):102–105.
25. Chandrashekar S, Parikh S, Kapoor P, et al. Postpartum reversible cerebral vasoconstriction syndrome. *Am J Med Sci* 2007;334(3):222–224.
26. Chatterjee N, Domoto-Reilly K, Fecci PE, et al. Licorice-associated reversible cerebral vasoconstriction with PRES. *Neurology* 2010;75(21):1939–1941.
27. Neil WP, Dechant V, Urtecho J. Pearls & oysters: Reversible cerebral vasoconstriction syndrome precipitated by ascent to high altitude. *Neurology* 2011;76(2):e7–e9.
28. Campbell JN, Morris PP. Cerebral vasculitis in graft-versus-host disease: A case report. *AJNR Am J Neuroradiol* 2005;26(3):654–656.

27

Vasculitides Involving the Central Nervous System

Key Points

- Primary angiitis of the central nervous system (PACNS) is a rare disorder, far less common than mimics such as reversible vasoconstriction syndrome or secondary CNS involvement by systemic vasculitis.
- Cerebral angiography is of very limited sensitivity in the evaluation of PACNS, a disorder usually manifest in the distal arterioles beyond the limits of angiographic sensitivity.

The understanding, categorization, and treatment of vasculitides affecting the CNS have progressed substantially in the past two decades, and therefore clinical requests for cerebral angiography to “rule out vasculitis” are much more frequent. While it should seem intuitively obvious that a good-quality angiogram would be highly relevant to the diagnosis of CNS vasculitis, the question of the sensitivity, specificity, and predictive values of angiography in this group of patients warrants some elucidation.

Vasculitides are a heterogeneous group of disorders characterized by inflammatory and necrotic changes in the blood vessel wall. When dealing with a neurologic patient, the first question to consider is whether the disorder in question is systemic or confined to the CNS.

► SYSTEMIC VASCULITIDES

Rheumatologists tend to categorize systemic vasculitic disorders according to whether the vessel involvement is large (giant cell arteritis, Takayasu arteritis), medium (polyarteritis nodosa, Kawasaki disease), or small. The small vessel vasculitides are separated into those positive for ANCA (anti-neutrophil cytoplasmic antibodies), including Churg–Strauss, and Wegener’s granulomatosis, and negative for ANCA (lupus Fig. 27-1, Sjogren’s syndrome, and cryoglobulinemic vasculitis) (1). A multitude of other conditions are associated with vasculitic changes and CNS involvement including arteriopathic complications of HIV infections, neurosyphilis, hepatitis C, herpes zoster complications, Lyme disease, (2), and so on. Even rarer entities will need to be considered in particular patients, for example, cerebral autosomal dominant

arteriopathy with subcortical infarcts and leukoencephalopathy (CADASIL) (3), or Eale’s syndrome (4). Susac syndrome (5,6) may need to be considered in ophthalmology patients, Köhlmeier–Degos syndrome (malignant atrophic papulosis) (7) in patients with spontaneous gastrointestinal infarctions or perforations with CNS involvement, or Behçet’s disease when there is basal ganglia or brainstem involvement (8,9). Angiocentric fungal infections, nocardia, or intravascular lymphoma (10) may all present with imaging features identical to those of CNS vasculitis.

Systemic vasculitis with secondary involvement of the CNS occurs with a prevalence of approximately 15/100,000 to 30/100,000, and while these diseases are rare, this prevalence far exceeds that of primary angiitis of the CNS (PACNS). The role of angiography in the setting of a known systemic vasculitis will be determined by the particular circumstances in hand, and may include evaluation of the great vessels of the aortic arch, renal angiography, and evaluation of the extracranial carotid and vertebral arteries.

► PRIMARY ANGIITIS OF THE CNS (PACNS)

PACNS is a rare disorder with a peak presentation around the age of 50 years, more commonly seen in males (11), but sometimes seen even in children (12). Older papers dealing with CNS vasculitis include a substantial number of patients who would now be distinctly categorized under reversible cerebral vasoconstriction syndrome (see Chapter 26), and therefore a deal of confusion can arise in describing the entity of PACNS when this distinction is not clear. The symptoms and manifestations of PACNS likely relate in part to the size of vessel involvement. Proximal involvement close to the circle of Willis tends to give a picture of focal deficits, infarctions, transient ischemic attacks, and ataxia (Fig. 27-2). More distal small vessel involvement tends to cause vague, nonspecific complications such as personality and cognitive impairment. The distinction is relevant to the diagnostic angiographic evaluation of the patient, because there is a higher likelihood that with the latter pattern of small vessel involvement the angiogram will be normal (Fig. 27-3).

There may be different subtypes of PACNS, but the most classic presentation is that sometimes referred to as “granulomatous angiitis,” which is seen in more distal vessels, causing a multitude of infarctions of different sizes and ages,

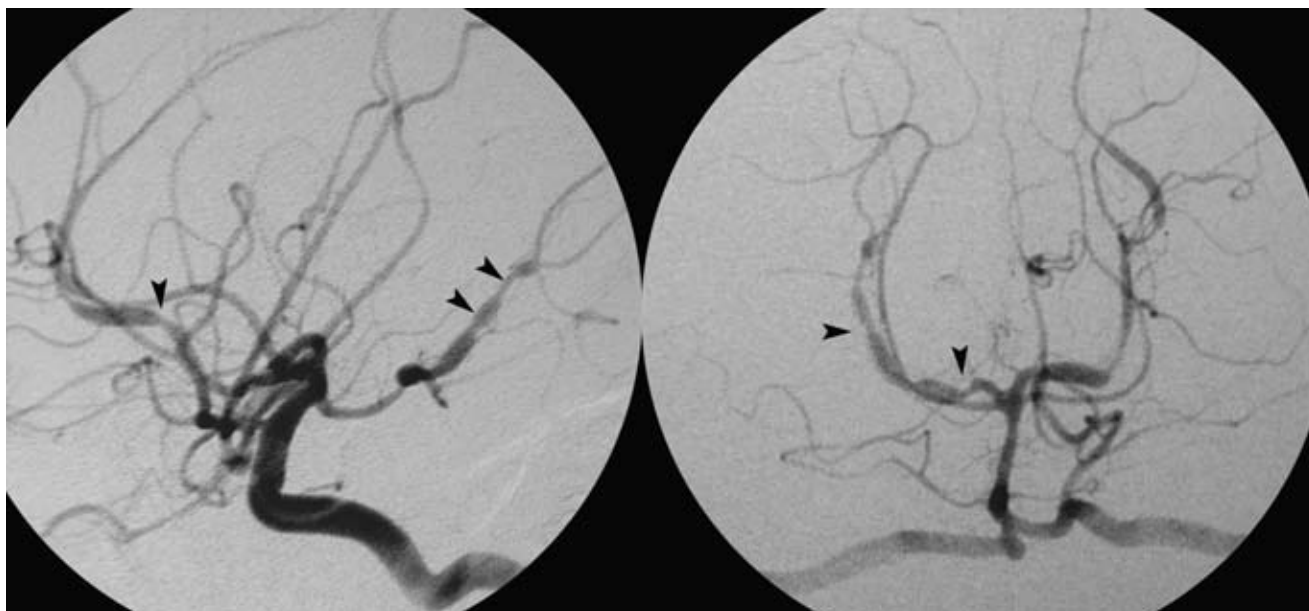


FIGURE 27-1. Angiographic appearance of intracranial vasculitis. A patient with fluctuating neurologic deficits in the course of treatment for systemic lupus erythematosus demonstrates a profusion of intracranial irregularities of the anterior and posterior circulation (*arrowheads*). The question is always asked, how do you tell the difference between this and intracranial atherosclerotic disease? There are several answers to this question, including the acknowledgment that at times one cannot tell. Atherosclerotic lesions are classically taught to be eccentric on the vessel, arteritis concentric. On the other hand, modern understanding of the genesis of atherosclerosis would suggest that the difference between inflammatory arteritis and atherosclerotic narrowing is specious, as they both represent overlapping pathophysiologic mechanisms.

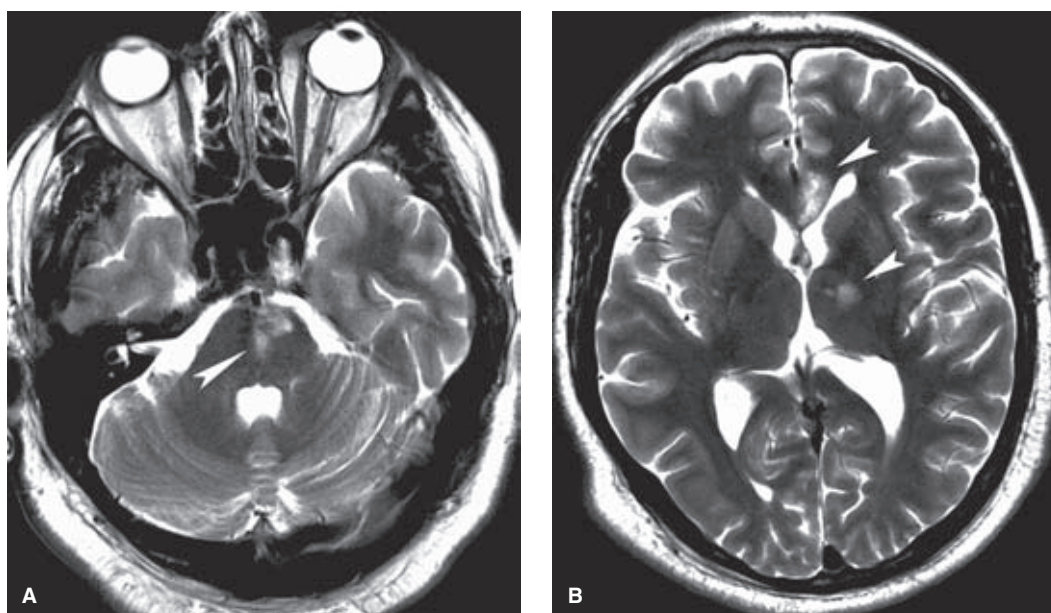


FIGURE 27-2. (A–D) Intracranial presumed vasculitis presenting with multiple ischemic infarcts. A young adult presented with multiple scattered infarctions of the posterior and anterior circulations. The presumptive diagnosis was PACNS. The distribution of ischemic lesions on MRI is more scattered and involves perforator vessels, in contrast to the watershed infarction pattern more typically seen in RCVS in Chapter 26. Notice how the pontine perforator infarct (*arrow* in **A**, T2-weighted MRI) respects the midline, a reflection of the anatomic configuration of the brainstem perforators. (*continued*)

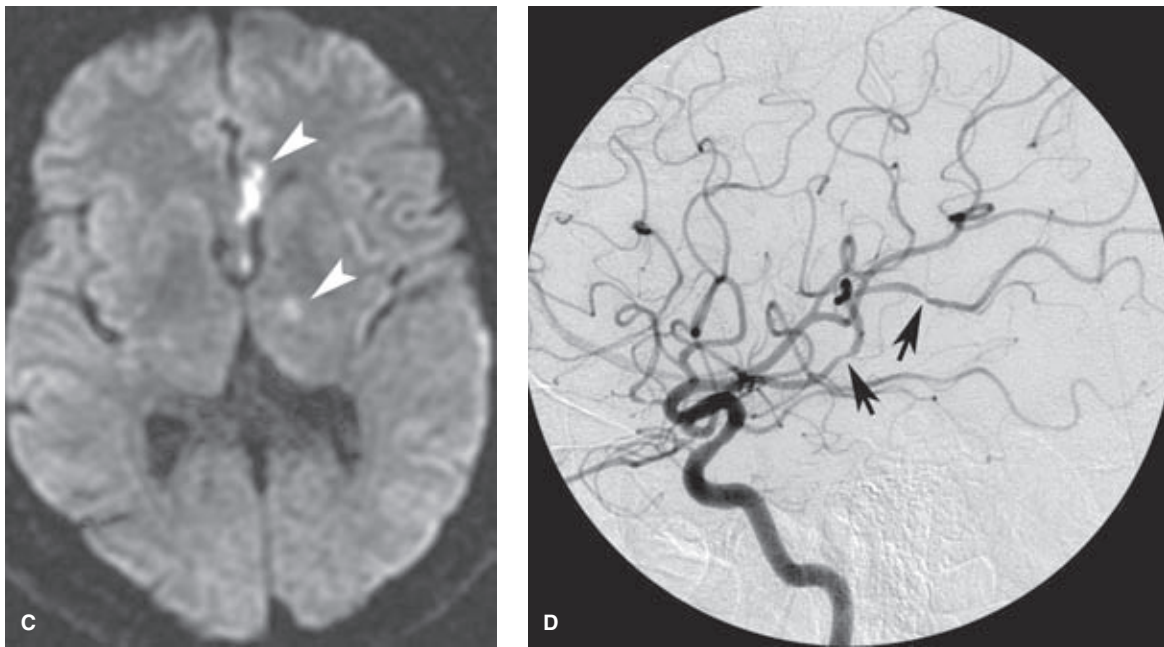


FIGURE 27-2. (CONTINUED) Other infarcts (*arrowheads* in **B**, T2 MRI, and **C**, DWI scan) are seen in the forebrain and thalamus. A cerebral angiogram of the left internal carotid artery (**D**) shows that the angiographic confirmation of vasculitis (*arrows*) can be relatively subtle, even when other manifestations of the disease are florid.

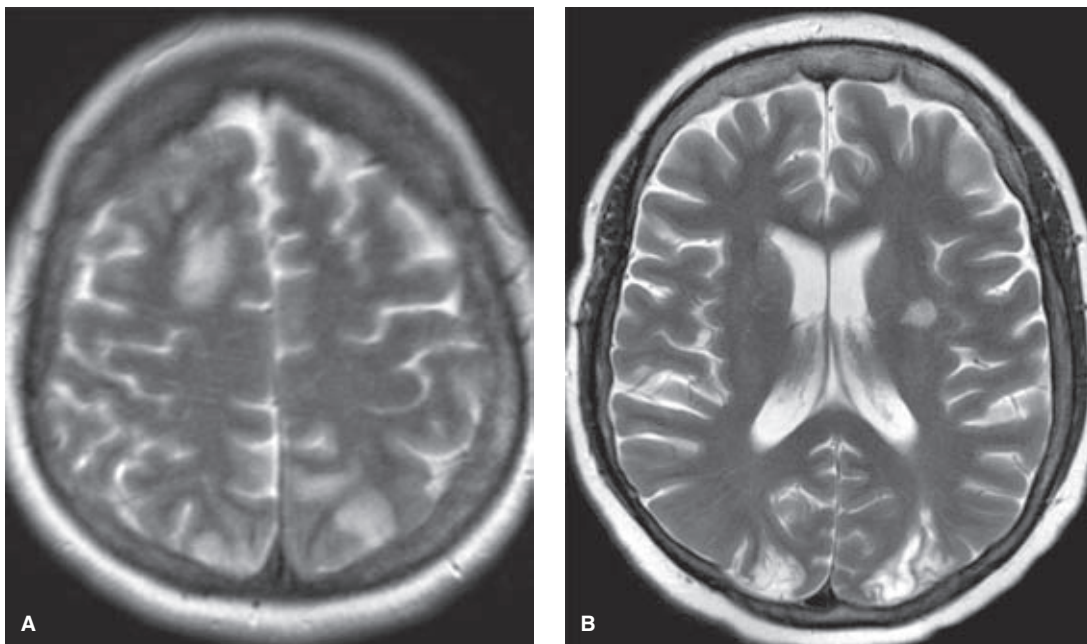


FIGURE 27-3. (A–E) Biopsy-proven PACNS. A middle-aged female presented with a right frontal parenchymal hemorrhage, seizure, and headache. Her condition deteriorated while in hospital, but her imaging features, seen in isolation, are not particularly distinguishable from many of the patients with RCVS illustrated in Chapter 26. Her T2-weighted images (**A** and **B**) showed progressive gray and white matter nonenhancing lesions. (*continued*)

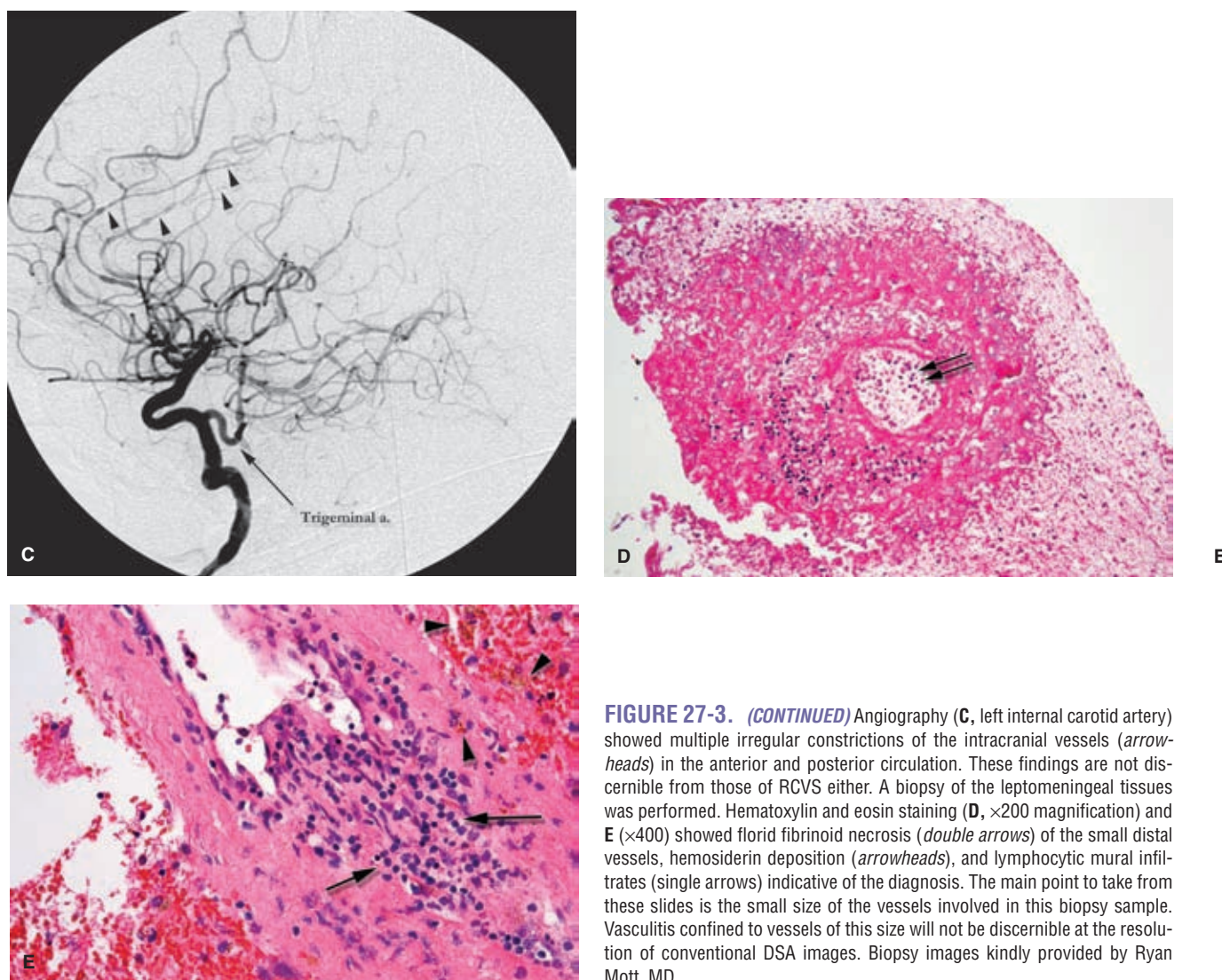


FIGURE 27-3. (CONTINUED) Angiography (**C**, left internal carotid artery) showed multiple irregular constrictions of the intracranial vessels (*arrowheads*) in the anterior and posterior circulation. These findings are not discernible from those of RCVS either. A biopsy of the leptomeningeal tissues was performed. Hematoxylin and eosin staining (**D**, $\times 200$ magnification) and **E** ($\times 400$) showed flurid fibrinoid necrosis (*double arrows*) of the small distal vessels, hemosiderin deposition (*arrowheads*), and lymphocytic mural infiltrates (*single arrows*) indicative of the diagnosis. The main point to take from these slides is the small size of the vessels involved in this biopsy sample. Vasculitis confined to vessels of this size will not be discernible at the resolution of conventional DSA images. Biopsy images kindly provided by Ryan Mott, MD.

diffuse dull headache, and abnormal CSF. MRI demonstrates ischemic lesions and sometimes leptomeningeal enhancement (10% to 15%) (13), which can serve as a target for biopsy. Cerebral angiography is normal in some series, most likely when the disease is exclusively confined to the small distal vessels (11), but other series of biopsy-proven granulomatous angiitis demonstrate consistently abnormal, although nonspecific, findings of vessel irregularity and beading (14). Other subsets of patients with primarily lymphocytic perivascular infiltrates or PACNS featuring histologic overlap with cerebral amyloid angiopathy are also described (15,16).

PACNS is sometimes a diagnosis of exclusion. The commoner entities such as a systemic vasculitis with CNS manifestations must be considered on the basis of a rheumatologic workup, and the possibility of RCVS can be considered with the appropriate clinical presentation (acute symptomatology often with thunderclap headache, normal CSF, associated risk factors in the history). When the symptoms are more difficult to categorize and appear to correlate with odd patterns of parenchymal or leptomeningeal enhancement (17), ischemic lesions not confined to a particular pattern or vas-

cular territory, and dull headache with CSF findings consistent with aseptic meningitis, then the possibility of PACNS is more likely. About 5% of patients develop myelopathic symptoms and signs from spinal involvement (18,19). PACNS is probably a reasonable option to consider whenever one is tempted to use the word “bizarre” in describing an MRI (Fig. 27-4). The phenomenon of PACNS presenting with a solitary mass looking very suggestive of an aggressive tumor is also well recognized (20) (Figs. 27-5 and 27-6). Furthermore, the diagnostic evaluation of this entity is complicated by a significant false-negative rate on brain or leptomeningeal biopsy (11,16,21).

The question at this point is how useful is a cerebral arteriogram in the support or rejection of such a diagnosis of “true” PACNS (Fig. 27-7). Several references suggest a very limited sensitivity of 70% or less (13,22,23), and a specificity of <30% (21,24). Furthermore, some references state that in the setting of “true” granulomatous angiitis, small vessel PACNS cerebral angiography will be normal, but the balance of evidence is against this extreme opinion. Lie (14), for instance, *(text continues on page 440)*

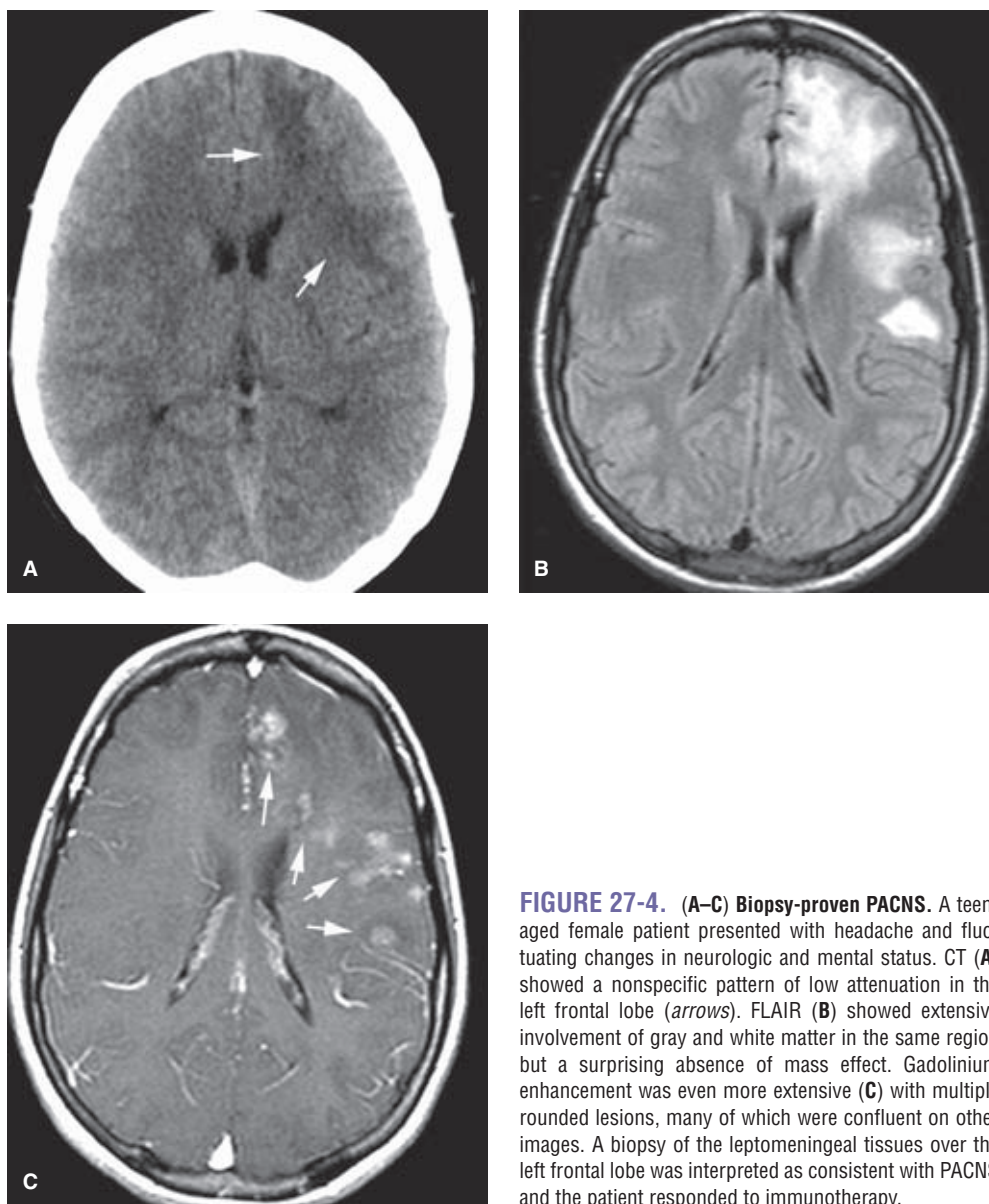


FIGURE 27-4. (A–C) Biopsy-proven PACNS. A teenaged female patient presented with headache and fluctuating changes in neurologic and mental status. CT (A) showed a nonspecific pattern of low attenuation in the left frontal lobe (arrows). FLAIR (B) showed extensive involvement of gray and white matter in the same region but a surprising absence of mass effect. Gadolinium enhancement was even more extensive (C) with multiple rounded lesions, many of which were confluent on other images. A biopsy of the leptomeningeal tissues over the left frontal lobe was interpreted as consistent with PACNS and the patient responded to immunotherapy.

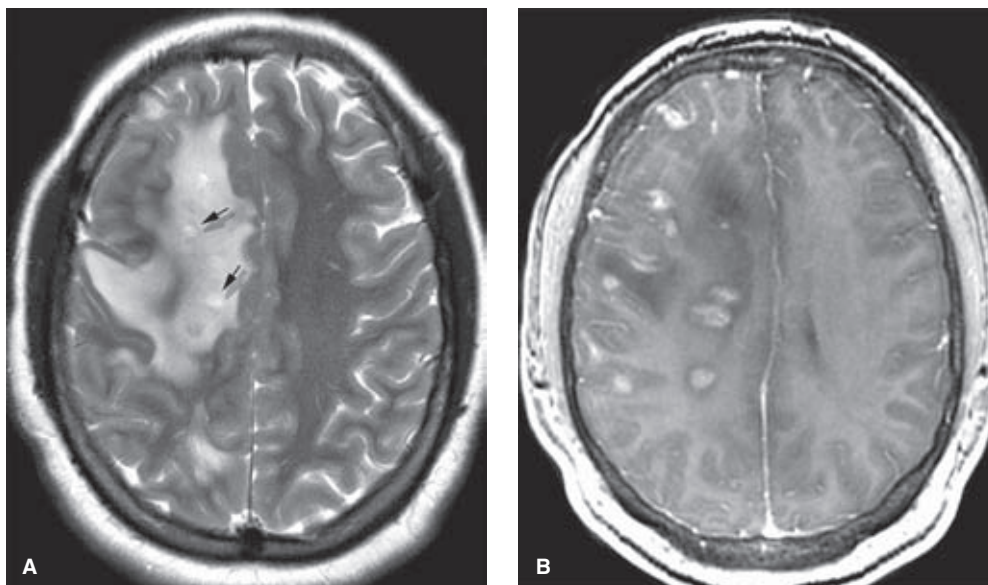


FIGURE 27-5. (A–C) Biopsy-proven PACNS. A teenaged female patient presented with recurrent seizure. T2-weighted MRI (A) showed extensive white matter confluent changes with unusual internal ring-like lesions (arrows in A), which demonstrated focal enhancement after administration of gadolinium (arrows in B). (continued)

FIGURE 27-5. (CONTINUED) The arterial spin labeling study (**C**) showed a predominantly hypoperfused appearance (*arrowheads* in **C**) compared with the contralateral side. Biopsy was consistent with necrotic vasculitis.

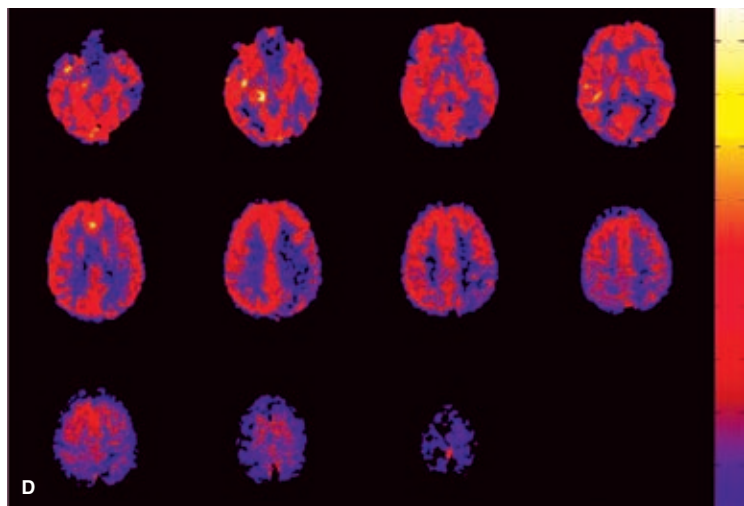
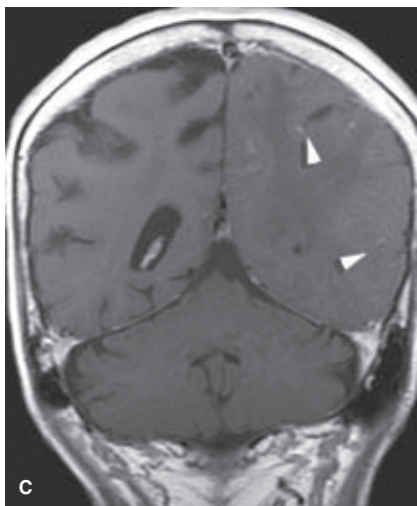
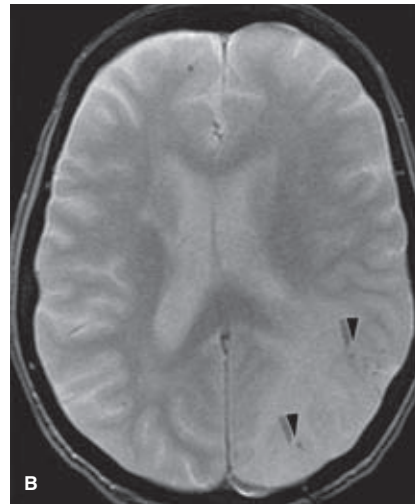
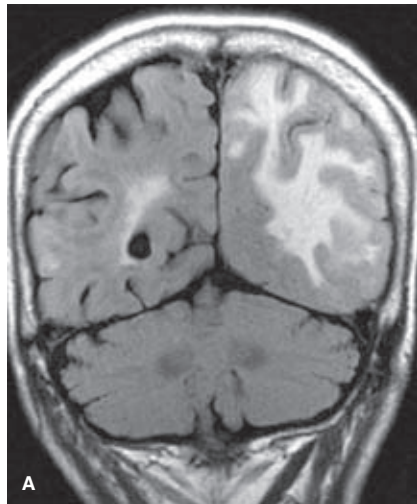
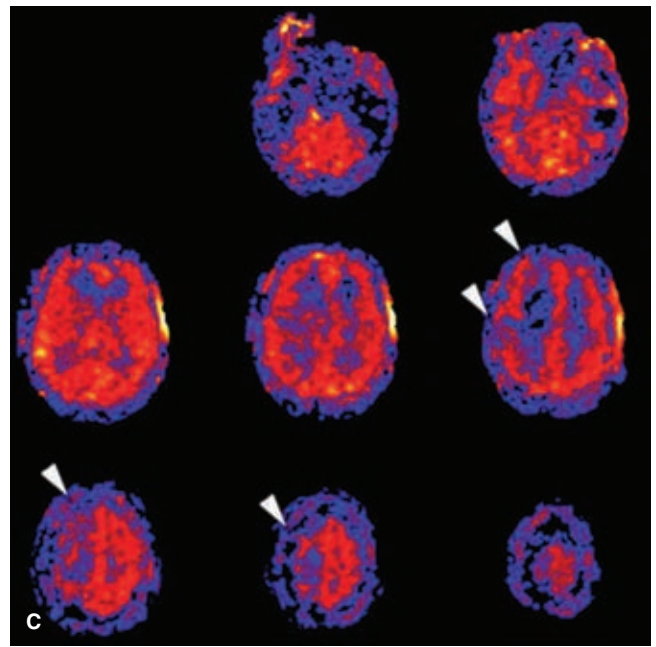


FIGURE 27-6. (A–D) Presumed tumor, with final diagnosis of CNS vasculitis. An elderly patient presented with onset of generalized weakness and was transferred from another hospital with a presumed brain tumor. FLAIR (**A**) showed severe white matter disease and swelling in the posterior left hemisphere. Gradient echo imaging demonstrated small foci of susceptibility (*arrowheads* in **B**) within the left hemispheric abnormality suggesting internal microhemorrhages. Contrast enhancement after gadolinium (**C**) was relatively minor and for the most part appeared to be intravascular (*arrowheads* in **C**). Arterial spin-labelling (ASL) images showed hypoperfusion in the region of the presumed tumor (**D**). A biopsy showed no evidence of tumor, only features of necrosis and gliosis suggesting the diagnosis of vasculitis. The patient was treated accordingly with clinical improvement in his condition.

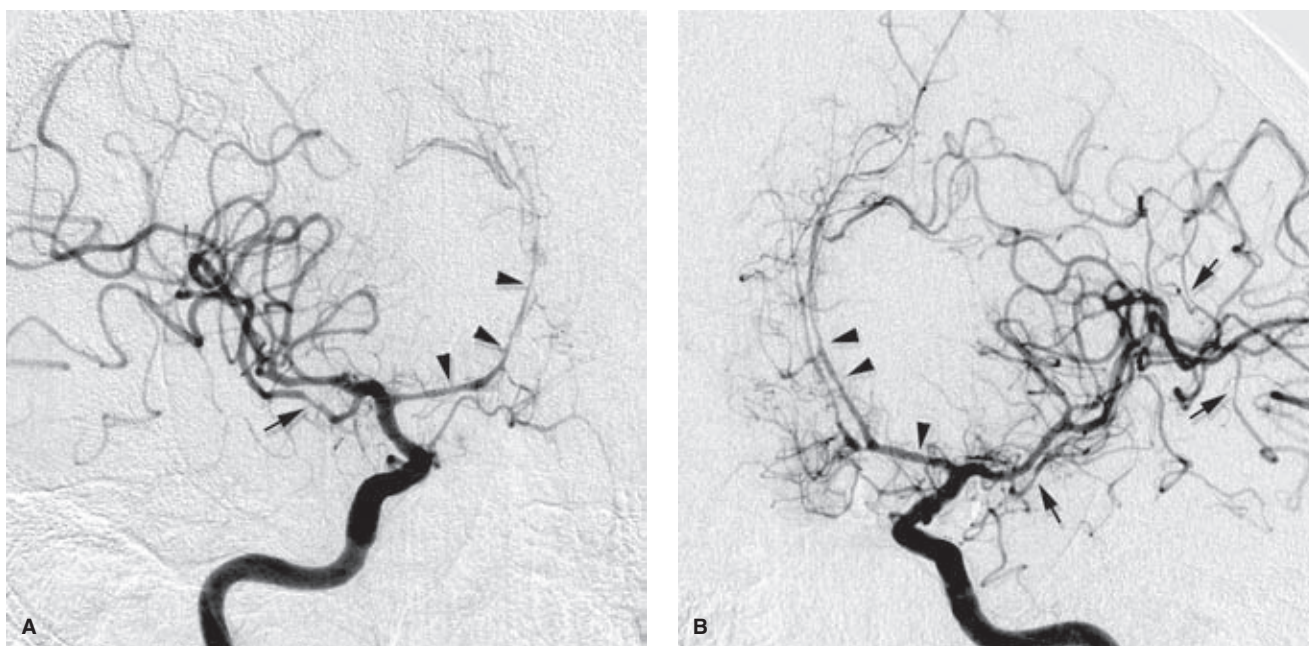


FIGURE 27-7. (A–B) Presumed PACNS in a young adult. A patient in his early thirties who presented with multiple infarctions of varying ages in multiple territories demonstrated evidence of abnormal vessels intracranially, including the right internal carotid artery (A, oblique view) and left internal carotid (B, oblique view). These abnormalities appeared to be multifocal in the middle cerebral arteries (arrows) and more diffuse in the anterior cerebral arteries (arrowheads).

published a series of 15 cases, proven to be granulomatous or lymphocytic angiitis by biopsy or autopsy, in which angiography was consistently, albeit nonspecifically, abnormal. Evidence from a large Mayo Clinic series even suggests that among patients with PACNS, those with rapidly progressive disease and a worse prognosis are more likely to have large vessel involvement and thus positive findings on angiography (25). In conclusion, the prudent course might be to assume that cerebral angiography is an investigative tool with some limitations of sensitivity and specificity in the evaluation of patients with difficult diagnostic dilemmas. A positive result is a help to the clinician to narrow his/her differential consideration, but a negative or normal result does not appear to exclude the possibility of PACNS (as is also true of biopsy (16)).

References

- Berlit P. Diagnosis and treatment of cerebral vasculitis. *Ther Adv Neurol Disord* 2010;3(1):29–42.
- Pipitone N, Salvarani C. The role of infectious agents in the pathogenesis of vasculitis. *Best Pract Res Clin Rheumatol* 2008;22(5):897–911.
- Ringelstein EB, Kleffner I, Dittrich R, et al. Hereditary and non-hereditary microangiopathies in the young. An up-date. *J Neurol Sci* 2010;299(1–2):81–85.
- Biswas J, Sharma T, Gopal L, et al. Eales disease—An update. *Surv Ophthalmol* 2002;47(3):197–214.
- Bitra RK, Eggenberger E. Review of Susac syndrome. *Curr Opin Ophthalmol* 2011;22(6):472–476.
- Susac JO, Egan RA, Rennebohm RM, et al. Susac's syndrome: 1975–2005 microangiopathy/autoimmune endotheliopathy. *J Neurol Sci* 2007;257(1–2):270–272.
- Burrow JN, Blumberg PC, Iyer PV, et al. Kohlmeier–Degos disease: A multisystem vasculopathy with progressive cerebral infarction. *Aust N Z J Med* 1991;21(1):49–51.
- Taylor S, Islam O, Joneja M, et al. The imaging spectrum of neuro-Behcet disease. *Neurology* 2009;73(11):903.
- Borhani Haghghi A, Sharifzad HR, Matin S, et al. The pathological presentations of neuro-Behcet disease: A case report and review of the literature. *Neurologist* 2007;13(4):209–214.
- Lie JT. Malignant angioendotheliomatosis (intravascular lymphomatosis) clinically simulating primary angiitis of the central nervous system. *Arthritis Rheum* 1992;35(7):831–834.
- Hajj-Ali RA, Singhal AB, Benseler S, et al. Primary angiitis of the CNS. *Lancet Neurol* 2011;10(6):561–572.
- Cellucci T, Benseler SM. Diagnosing central nervous system vasculitis in children. *Curr Opin Pediatr* 2010;22(6):731–738.
- Birnbaum J, Hellmann DB. Primary angiitis of the central nervous system. *Arch Neurol* 2009;66(6):704–709.
- Lie JT. Primary (granulomatous) angiitis of the central nervous system: A clinicopathologic analysis of 15 new cases and a review of the literature. *Hum Pathol* 1992;23(2):164–171.
- Salvarani C, Brown RD Jr, Calamia KT, et al. Primary central nervous system vasculitis: Comparison of patients with and without cerebral amyloid angiopathy. *Rheumatology (Oxford)* 2008;47(11):1671–1677.
- Miller DV, Salvarani C, Hunder GG, et al. Biopsy findings in primary angiitis of the central nervous system. *Am J Surg Pathol* 2009;33(1):35–43.
- Salvarani C, Brown RD Jr, Calamia KT, et al. Primary central nervous system vasculitis with prominent leptomeningeal enhancement: A subset with a benign outcome. *Arthritis Rheum* 2008;58(2):595–603.
- Manara R, Schiavon F, Carraro V, et al. Angiographic diagnosis of primary central nervous system vasculitis with spinal cord involvement. *Arch Neurol* 2009;66(4):532–533.
- Salvarani C, Brown RD Jr, Calamia KT, et al. Primary CNS vasculitis with spinal cord involvement. *Neurology* 2008;70(24 pt 2):2394–2400.

20. You G, Yan W, Zhang W, et al. Isolated angiitis of the central nervous system with tumor-like lesion, mimicking brain malignant glioma: A case report and review of the literature. *World J Surg Oncol* 2011;9(1):97.
21. Duna GF, Calabrese LH. Limitations of invasive modalities in the diagnosis of primary angiitis of the central nervous system. *J Rheumatol* 1995;22(4):662–667.
22. Salvarani C, Brown RD Jr, Calamia KT, et al. Primary central nervous system vasculitis: Analysis of 101 patients. *Ann Neurol* 2007;62(5):442–451.
23. Vollmer TL, Guarnaccia J, Harrington W, et al. Idiopathic granulomatous angiitis of the central nervous system. Diagnostic challenges. *Arch Neurol* 1993;50(9):925–930.
24. Harris KG, Tran DD, Sickels WJ, et al. Diagnosing intracranial vasculitis: The roles of MR and angiography. *AJNR Am J Neuroradiol* 1994;15(2):317–330.
25. Salvarani C, Brown RD Jr, Calamia KT, et al. Rapidly progressive primary central nervous system vasculitis. *Rheumatology (Oxford)* 2011;50(2):349–358.

Bow Hunter's Stroke

Key Points

- Bow hunter's stroke is probably not as rare as the literature would suggest but requires an observant history from the patient.
- Patients are very reluctant to induce these unpleasant symptoms during angiographic evaluation and need to be encouraged strongly by making them realize that their medical care depends on it.

Rotational vertebral artery insufficiency (bow hunter's stroke) is the phenomenon of vertebrobasilar ischemia induced by passive or active head rotation, usually in the setting of contralateral vertebral artery compromise or occlusion. First described in a patient who experienced this phenomenon during archery (1), it was once considered a very rare condition, but has been described in several recent reports. Suspicion of the disorder is dependent upon an observant history from the patient. It is difficult to image well angiographically. Furthermore, some compromise of one or both vertebral arteries may be seen with extreme head rotation in a sizeable proportion of the normal population, which diminishes the physiologic reserve when additional pathologic extrinsic compression of the artery supervenes (2,3). It is likely, therefore, that this is an underdiagnosed condition.

Typically, the occlusion or stenosis of the vertebral artery is described as occurring at the C1 to C2 level due to prominence of a bony spur or outgrowth impinging on the course of the artery (Figs. 28-1 and 28-2). However, it can happen anywhere in the cervical spine related to a variety of developmental bony anomalies, big uncovertebral osteo-

phytes, fibrous bands, thyroid cartilage, or herniated discs (4–10). The posterior circulation is usually isolated and the contralateral vertebral artery is small or occluded, leaving the posterior circulation vulnerable to compromise of the only arterial supply remaining. The phenomenon has also been described in nondominant vertebral arteries where the artery terminates in an ipsilateral posterior inferior cerebellar artery (11). While the condition is most commonly seen in adults with degenerative uncovertebral disease, it may also present in children or young adults with anomalous bony cervical configurations (12,13). In children it is thought likely that transient ischemia of the posterior circulation does not occur due to greater resilience of collateral pathways, and therefore the phenomenon is more likely to present in children with established infarctions due to thromboembolic complications or arterial dissection (14). With repetitive injuries or sudden nonphysiologic movement, such as in chiropractic manipulation, complications of dissection and thromboembolic ischemia are well-recognized events (1,15–17). Similar dynamic states of compromise and ischemia can be seen with the internal carotid artery but are likely much rarer (18), due to the anatomic mobility of the carotid artery.

Angiographic confirmation of bow hunter's phenomenon is difficult unless one impresses on the patient the absolute need to induce his or her symptoms during the angiographic injection. Furthermore, the onset of posterior circulation ischemic symptoms is likely to cause patient movement, which will degrade imaging. The condition is treated with a variety of surgical fixation or decompressive procedures (15,19). Intraoperative angiography has been used successfully in coordination with surgical fixation to confirm the location of the occlusion and efficacy of surgery (19–21).

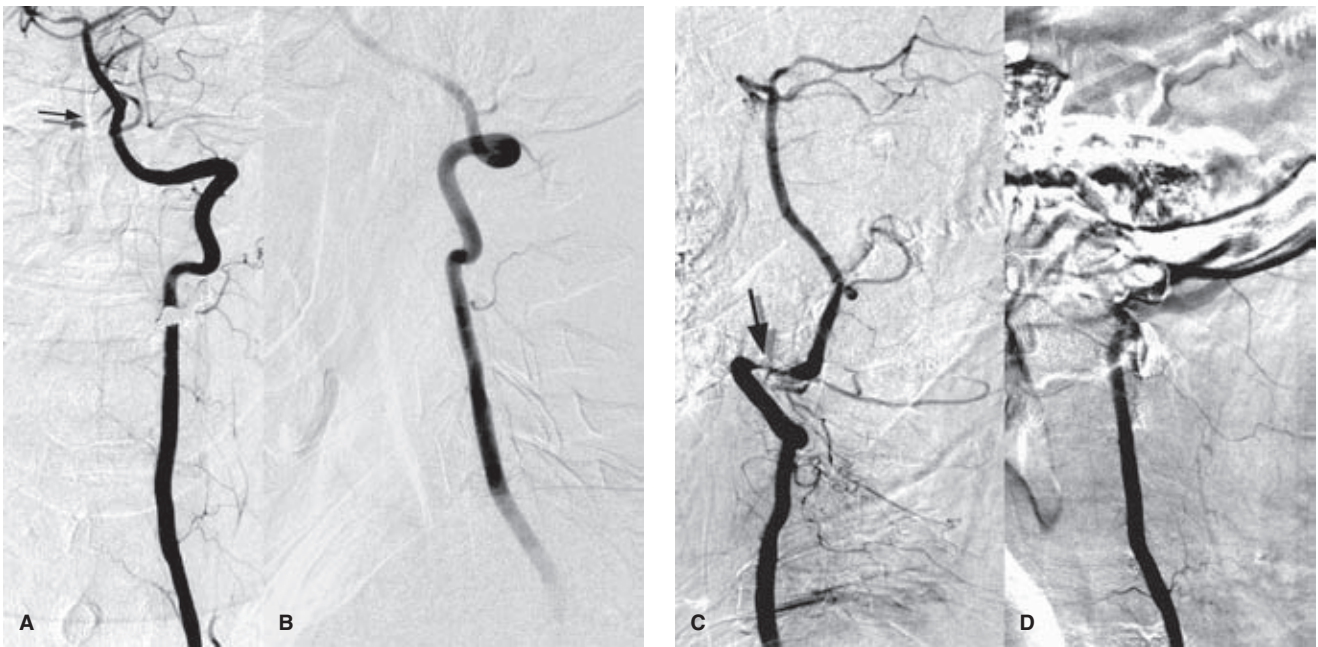


FIGURE 28-1. (A–D) **Bow hunter's phenomenon I.** This middle-aged patient presented with a history of imbalance, double-vision, clouding of vision, and loss of consciousness when he turned his head to the right. While his symptoms are certainly typical of vertebrobasilar ischemia, there would have been no hint of the cause of the problem on the standard AP (A) and lateral (B) views, and without the patient's observation of the context of his symptoms, his diagnosis would have proved elusive. There was some sustained reflux into the distal right vertebral artery (arrow in A) indicating occlusion of that vessel, but this by itself would not be a very unusual finding in posterior circulation angiography. Furthermore, he was reluctant to induce his symptoms voluntarily during the course of the angiographic examination. Initial attempts with serial angiography were not helpful due to the restraint he placed on his own movement. Finally, when coached that it was pivotal to his own welfare, he was willing to turn his head sufficiently to reveal the narrowing of the vertebral artery at the occiput–C1 level (arrow in C), and complete occlusion with slightly more rotation (D) at which point he lost consciousness (hence the motion artifact in D). He was treated surgically by upper cervical to occiput fusion with elimination of his symptoms.

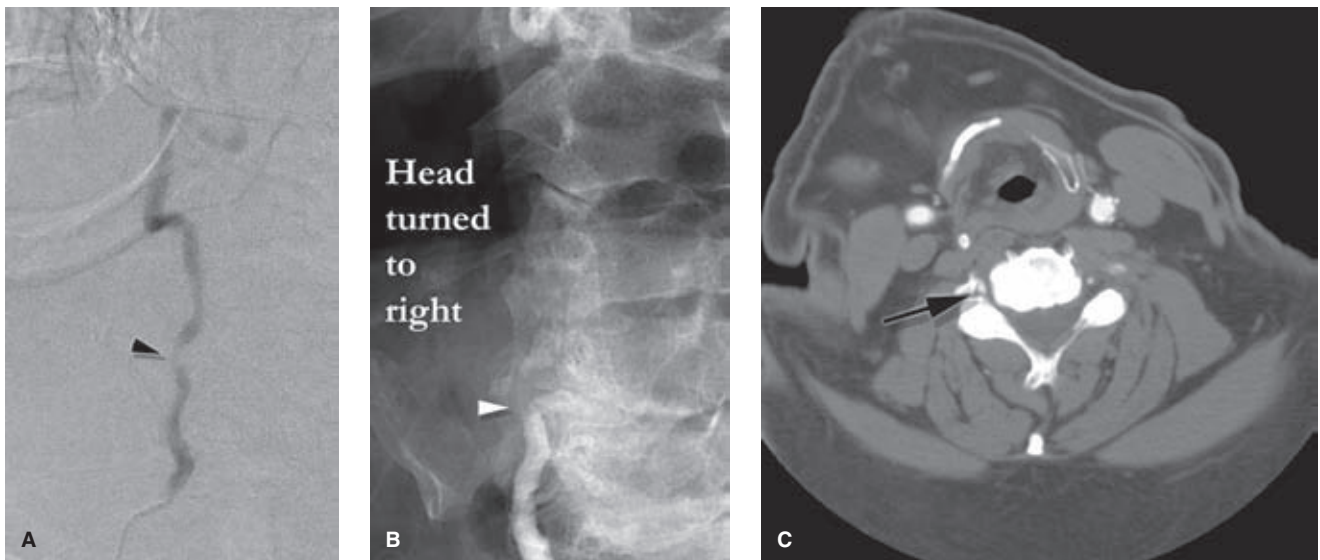


FIGURE 28-2. (A–C) **Bow hunter's phenomenon II.** This patient presented with a similar clinical appearance as the patient described in Figure 28-1. A roadmap mask (A) taken in a state of rotation not quite at the level expected to induce symptoms shows compression of the lumen of the midright vertebral artery (arrowhead in A). With more neck rotation toward the right, there is complete occlusion of the vessel (arrowhead in B) associated with diffuse mild atherosclerotic disease of the vessel and prominent hypertrophic degenerative disease of the adjacent uncovertebral joints of the cervical spine. An image from his CTA examination (taken in a state of mild rotation to the right, the patient was not willing to induce his symptoms for the sustained period necessary for the CTA examination) shows the distortion and compression of the right vertebral artery (arrow in C) at the level of the C4 to C5 disc.

References

1. Sorensen BF. Bow hunter's stroke. *Neurosurgery* 1978;2(3):259–261.
2. Faris AA, Poser CM, Wilmore DW, et al. Radiologic visualization of neck vessels in healthy men. *Neurology* 1963;13:386–396.
3. Toole JF, Tucker SH. Influence of head position upon cerebral circulation. Studies on blood flow in cadavers. *Arch Neurol* 1960;2:616–623.
4. Dadsetan MR, Skerhut HE. Rotational vertebrobasilar insufficiency secondary to vertebral artery occlusion from fibrous band of the longus colli muscle. *Neuroradiology* 1990;32(6):514–515.
5. Hardin CA, Poser CM. Rotational obstruction of the vertebral artery due to redundancy and extraluminal cervical fascial bands. *Ann Surg* 1963;158:133–137.
6. Dabus G, Gerstle RJ, Parsons M, et al. Rotational vertebrobasilar insufficiency due to dynamic compression of the dominant vertebral artery by the thyroid cartilage and occlusion of the contralateral vertebral artery at C1–2 level. *J Neuroimaging* 2008;18(2):184–187.
7. Lu DC, Gupta N, Mummaneni PV. Minimally invasive decompression of a suboccipital osseous prominence causing rotational vertebral artery occlusion. Case report. *J Neurosurg Pediatr* 2009;4(3):191–195.
8. Ohsaka M, Takgami M, Koyanagi I, et al. [Cerebral ischemia originating from rotational vertebral artery occlusion caused by C5/6 spondylotic changes: A case report]. *No Shinkei Geka* 2009;37(8):797–802.
9. Ujifuku K, Hayashi K, Tsunoda K, et al. Positional vertebral artery compression and vertebrobasilar insufficiency due to a herniated cervical disc. *J Neurosurg Spine* 2009;11(3):326–329.
10. Vates GE, Wang KC, Bonovich D, et al. Bow hunter stroke caused by cervical disc herniation. Case report. *J Neurosurg* 2002;96(1 suppl):90–93.
11. Matsuyama T, Morimoto T, Sakaki T. Bow hunter's stroke caused by a nondominant vertebral artery occlusion: Case report. *Neurosurgery* 1997;41(6):1393–1395.
12. Saito K, Hirano M, Taoka T, et al. Juvenile bow hunter's stroke without hemodynamic changes. *Clin Med Insights Case Rep* 2010;3:1–4.
13. Saito K, Hirano M, Taoka T, et al. Artery-to-artery embolism with a mobile mural thrombus due to rotational vertebral artery occlusion. *J Neuroimaging* 2010;20(3):284–286.
14. Greiner HM, Abruzzo TA, Kabbouche M, et al. Rotational vertebral artery occlusion in a child with multiple strokes: A case-based update. *Childs Nerv Syst* 2010;26(12):1669–1674.
15. Fox MW, Piepgras DG, Bartleson JD. Anterolateral decompression of the atlantoaxial vertebral artery for symptomatic positional occlusion of the vertebral artery. Case report. *J Neurosurg* 1995;83(4):737–740.
16. Tsutsumi S, Ito M, Yasumoto Y. Simultaneous bilateral vertebral artery occlusion in the lower cervical spine manifesting as bow hunter's syndrome. *Neurol Med Chir (Tokyo)* 2008;48(2):90–94.
17. Yoshimura K, Iwatsuki K, Ishihara M, et al. Bow hunter's stroke due to instability at the uncovertebral C3/4 joint. *Eur Spine J* 2011;20 suppl 2:S266–S270.
18. Bauer R, Sheehan S, Meyer JS. Arteriographic study of cerebrovascular disease. II. Cerebral symptoms due to kinking, tortuosity, and compression of carotid and vertebral arteries in the neck. *Arch Neurol* 1961;4:119–131.
19. Hanakita J, Miyake H, Nagayasu S, et al. Angiographic examination and surgical treatment of bow hunter's stroke. *Neurosurgery* 1988;23(2):228–232.
20. Velat GJ, Reavey-Cantwell JF, Ulm AJ, et al. Intraoperative dynamic angiography to detect resolution of bow hunter's syndrome: Technical case report. *Surg Neurol* 2006;66(4):420–423; discussion 423.
21. Matsuyama T, Morimoto T, Sakaki T. Usefulness of three-dimensional CT for bow hunter stroke. *Acta Neurochir (Wien)* 1997;139(3):265–266.

Dural Sinus Occlusive Disease

Key Points

- Dural sinus stenotic disease may be a common cause of benign intracranial hypertension and idiopathic headache. Endovascular treatment for this condition may play a greater role in the future.
- Dural sinus thrombotic disease might be amenable to endovascular therapy in some patients, but the efficacy or outcome of this treatment has not been established.

Formerly, neurointerventionalists were familiar with venous navigation of the dural sinuses only in the course of transvenous embolization of dural arteriovenous malformations. In the past few years, however, endovascular technology has lent itself to potentially helpful procedures for the treatment of idiopathic venous hypertension and acute dural sinus thrombosis (DST).

► IDIOPATHIC INTRACRANIAL HYPERTENSION

Idiopathic intracranial hypertension (IIH) (“pseudotumor cerebri,” “benign intracranial hypertension”) is a condition characterized by elevation of intracranial pressure in the absence of a mass-occupying lesion or hydrocephalus, and with normal CSF composition (1). The cause of this condition is not known. It may be related to a disruption of CSF dynamics, and it is characteristically a disease of overweight young females of childbearing age.

The symptoms of this disorder are typically severe headache of prolonged duration, transient or permanent visual disturbances of various types, pulse synchronous tinnitus, retrobulbar pain, and double vision (2). This group of headache patients is set apart from other nonspecific headache patients by the ophthalmologic finding of papilledema, which generally leads to performance of a lumbar puncture, identification of elevated CSF pressure (>200 mm H₂O in nonobese patients, >250 mm H₂O in obese patients), and establishment of the diagnosis. There is some evidence and speculation that this disorder may be more common than hitherto suspected by virtue of the observation that a substantial proportion of IIH patients, probably those with milder pressures, may not demonstrate papilledema (3,4), and that this condition could account for as many as 25% of chronic headache patients.

Most patients respond well to treatment with weight loss, serial lumbar punctures, and pharmacologic therapy with acetazolamide, topiramate, or furosemide, but about 20% of patients are refractory to conventional treatments (5,6). About 3% to 10% develop serious visual complications, and 25% develop milder but significant visual impairment, from prolonged disruption of axonal transport and ischemic complications in the optic nerves (7–9). As many as 50% of cases of “fulminant” IIH lose substantial vision to the point of permanent legal blindness. A variety of CSF-diverting procedures including lumboperitoneal shunting and optic nerve fenestration have been demonstrated to be effective for some patients, and have become the established treatment when medical therapy has failed.

Idiopathic intracranial hypertension is one of those disorders that, depending on its manifestations and complications, can show up in clinics of varying specialties and, accordingly, evokes different anecdotal biases and perspectives when treatment is discussed. In the past decade several case series (10–17) have been published advocating endovascular treatment, specifically stenting of the transverse sinuses, as a potential therapy for selected patients with refractory IIH, but it has not yet been generally embraced and has not been ratified by any type of randomized trial (Figs. 29-1–29-3).

The core issue is the pathophysiology of the disease, which is not understood. Approximately 90% of patients with IIH demonstrate evidence of narrowing, compression, or stenosis of the transverse sinuses on gadolinium-enhanced MRV. This area is typically prone to artifact on time-of-flight MRV, and thus many radiologists are accustomed to seeing “narrowing” in this particular area and dismissing the finding as normal variation or in-plane artifact. The sensitivity of gadolinium-enhanced MRV has changed this standard. The narrowing of the sinuses and the localization of a pressure gradient to that site is consistently seen on subsequent venography in patients with IIH. The debate and controversy surrounding endovascular therapy for IIH depends on one’s interpretation of these findings.

If the narrowing of the transverse sinuses in patients with IIH is epiphenomenal and a consequence of the elevated ICP, then insertion of a stent to prop open the sinus should not reverse the disease. Moreover, it is well recognized in some patients that medical therapy or shunting procedures can improve the disease and cause normalization of the appearance of the transverse sinus (18,19). On the other hand, however, it is possible and cogent that the compression

(text continues on page 450)

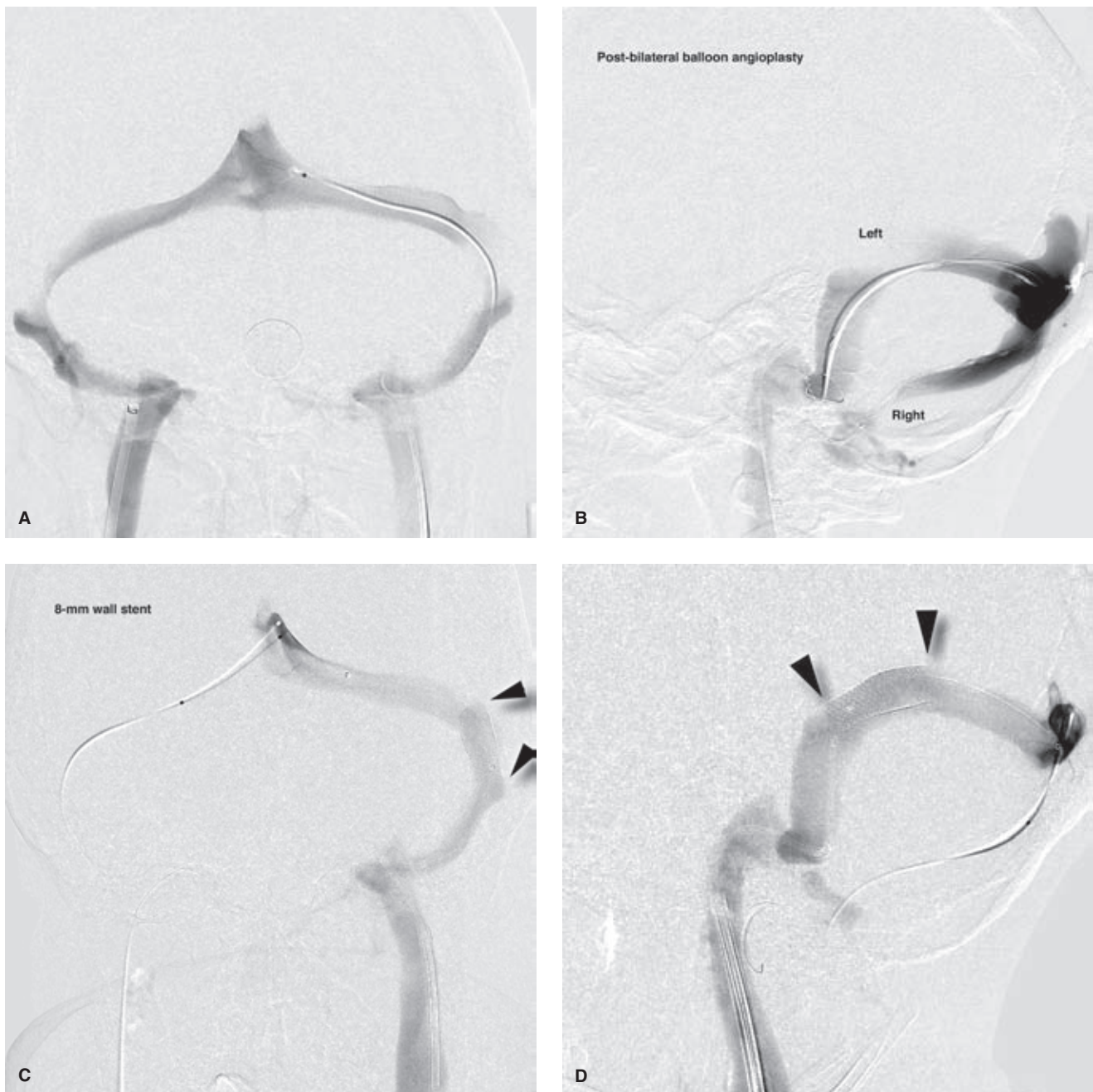


FIGURE 29-1. (A–F) Idiopathic intracranial hypertension refractory to medical therapy. This young adult female presented with intractable headaches and visual deterioration over a period of days. Her MRI and MRV (not shown) demonstrated marked bulging of the optic discs and bilateral narrowing of the transverse sinuses. Even on direct retrograde venography (**A**) the indentations on the course of the transverse sinuses bilaterally are subtle. The venous gradient across these regions was greater than 40 mm Hg and did not change post venous angioplasty with an 8-mm balloon (**B**). Notice in image (**B**) that skewing the lateral view allows a view of the transverse sinuses separated from one another. In images (**C**) and (**D**) an 8-mm Wallstent (*arrowheads*) has been placed in the left transverse sinus eliminating the appearance of compression of the sinus contour and also reducing the venous gradient to <10 mm Hg. (*continued*)

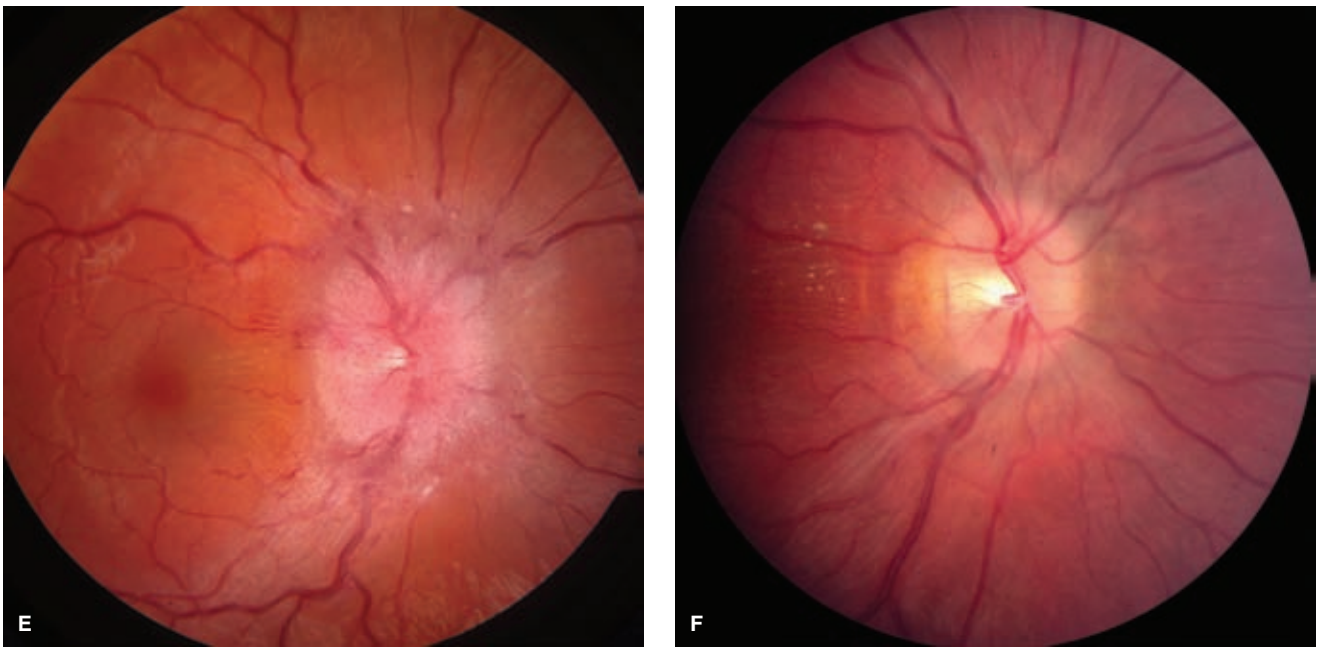


FIGURE 29-1. (CONTINUED) The patient's extreme papilledema before the stenting procedure (E) contrasts with the improved appearance in the right eye 4 weeks later (F). Although her clinical response with improvement of headache and of visual complaints of blurring and tunnel vision was immediate and sustained, it takes several weeks for the ophthalmoscopic findings of this disorder to reverse themselves.

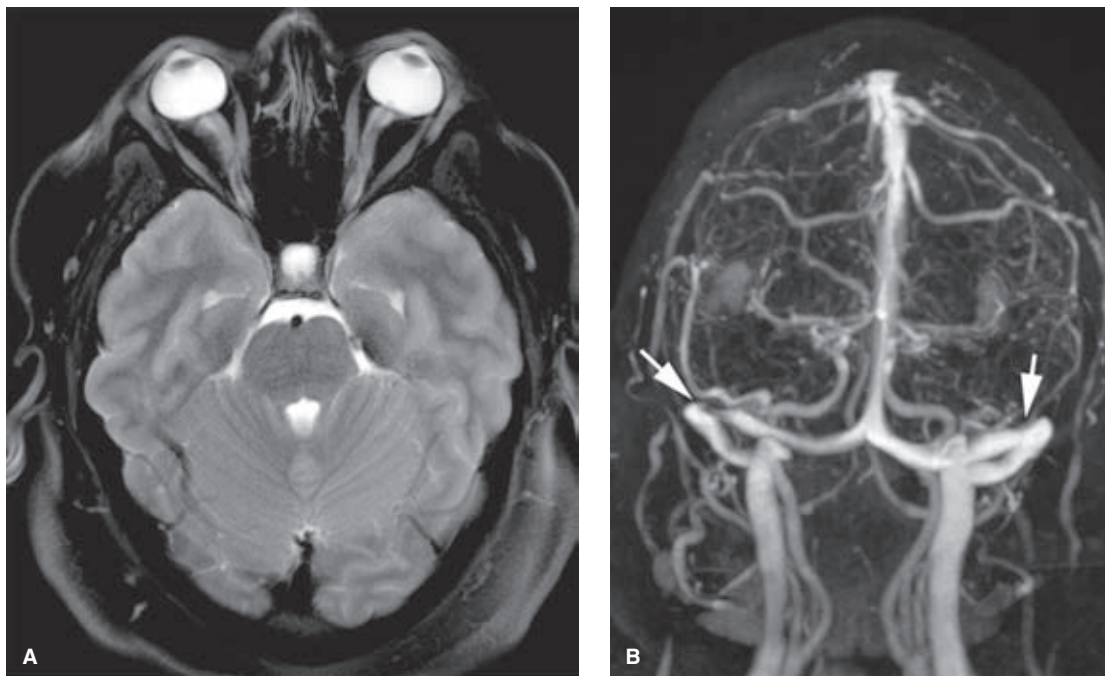


FIGURE 29-2. (A–F) Idiopathic intracranial hypertension treated with emergency endovascular stenting. This young female presented with precipitate loss of vision and severe headache. Her MRI (A) showed prominent bulging of the optic discs and redundancy of the optic sheaths. The gadolinium-enhanced venogram (B) demonstrates bilateral narrowing of the transverse sinuses (arrows) although the appearance is not impressive and the finding on the left has to be sought diligently on different projections in order to be seen. (continued)

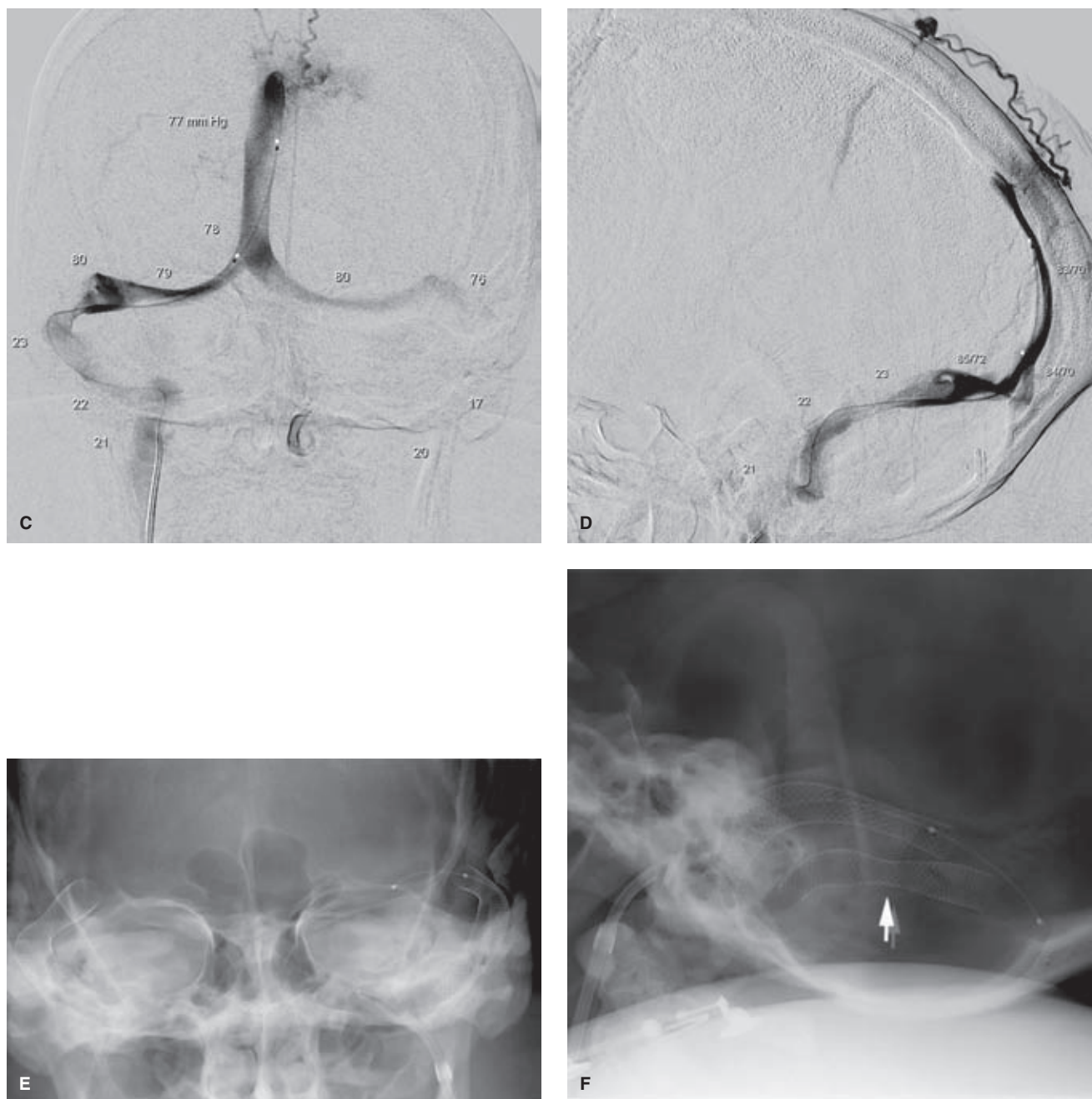


FIGURE 29-2. (CONTINUED) The retrograde venogram (C and D) also shows that the venous compression/narrowing tends not to be a visually dramatic finding. Transvenous pressure readings are annotated indicating a venous gradient of greater than 50 mm Hg bilaterally at the midtransverse sinus. Transosseous venous rerouting to the scalp is evident on the lateral view. In this patient a satisfactory unilateral stent placement did not eliminate the gradient, which was difficult to explain. A second stent was placed on the other side (E and F), which did reduce the gradient to approximately 10 mm Hg. Some deformity of the stents is still evident on the lateral view (*arrow*). The patient's headaches improved dramatically after the procedure, but her vision remained poor.

Cases such as described in Figures 29-1 and 29-2 are almost always performed under general anesthesia due to patient discomfort. The use of general anesthesia can distort venous pressure readings, so in elective or semielective cases the declaration of a venous gradient may be more valid when performed in advance when the patient is awake. Delivery of the stent is unquestionably the most difficult component of this procedure. A triaxial catheter and sheath system is invariably necessary. The 8-mm Wallstent has favorable flexibility and low-profile advantages compared to most other similarly sized stents. Initial catheter access to the sinus can be difficult too. A hydrophilic 4F catheter over an 0.035" wire can sometimes be more helpful than a microcatheter and microwire system. Care should always be taken to be gentle and measured in one's manipulation of the wire. Subdural bleeding can be seen in a small number of patients after transvenous procedures and could be ascribed to a number of causes, including inadvertent retrograde perforation of subdural veins entering the sinuses.

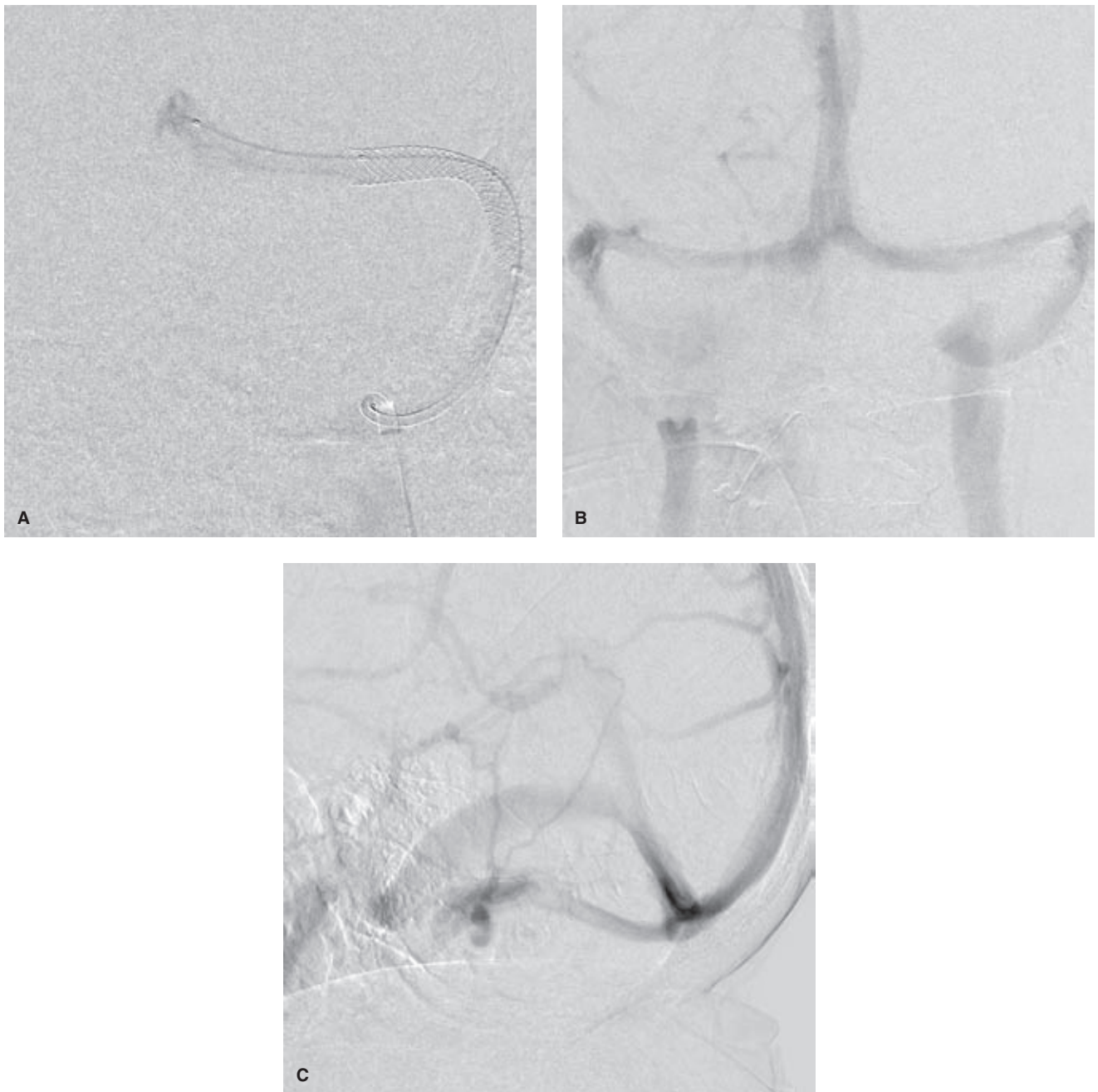


FIGURE 29-3. (A–C) Idiopathic intracranial hypertension: insensitivity of transarterial images for venous stenosis. This case of a young adult female is virtually identical to those given in Figures 29-1 and 29-2, with a similar therapeutic outcome. The poststenting image (A) shows some persistent narrowing of the stent in the midtransverse sinus, but the gradient was much improved by the procedure. The original study for this patient was an arteriogram, which was nondiagnostic. Even when the diagnosis is suspected, the AP (B) and lateral (C) venous phase images from the arteriogram are not helpful in identifying any degree of venous obstruction. Direct retrograde venography with manometry is necessary to confirm the diagnosis and to document the severity.

of the dural sinuses might be effectively a positive feedback mechanism of self-sustaining pathophysiology, the interruption of which might explain why a substantial number of severely affected patients have a remarkable and sustained improvement of their symptoms with a transvenous stenting procedure. Due to the success of the published case series and the dire consequences of permanent visual loss in the most fulminant of cases of ITH, usually having already demonstrated a nonresponsiveness to medical therapy, it is likely that transvenous stenting of this condition will see a surge in practice in the future.

Two types of deformities of the contours of the transverse sinuses are described: a focal obstruction may be related to hyperplasia or prominence of an arachnoid granulation (20) or to a dural fold or web; more commonly, in ITH a smoothly tapered nondescript flattening of the sinus is evident (14). Coronal MRI images may demonstrate frank herniation of brain into the expected location of the sinus, again arguing for a patulous or weakened dura as part of the spectrum of changes seen in this disorder.

Part of the persuasiveness of the efficacy of the endovascular approach to this disorder is the ability to image these lesions with high-flow venography, and especially the ability to demonstrate a pressure gradient specifically related to the narrowing lesion. Published series of endovascular treatment report a success rate of between 80% and 100% in symptom relief and disappearance of papilledema. These studies undoubtedly have a recruitment bias of patients treated with this modality, but they generally detected a gradient of at least 10 mm Hg, usually much higher, at the targeted lesion, and were able to show a substantial reduction or elimination of the gradient after treatment. With subsequent regression of the patients' symptoms and of findings of papilledema, it is tempting to see a cause and effect from the procedure, and furthermore to read into the mechanism of the disease the fundamental importance of the physical compromise of the dural sinus. However, all of these conjectures remain to be validated.

In a large case series, Ahmed et al. (14) reported on 52 patients of whom all had tried or failed medical therapy and who demonstrated a mean gradient in the transverse sinus of 20 mm Hg. The patients had an initial 100% response rate to unilateral transverse sinus stenting, with relapse in a small number of patients being ascribed to recurrent stenosis followed by subsequent successful retreatment. Significant intracranial complications due to wire perforations and extravasations were seen in two patients and were managed surgically with a good outcome. Other smaller series of similar patients and treatments report low complications rates including stent thrombosis (11), recurrent stenosis away from the stent site, or inconsequential extravasations (15). Premedication of the patients with aspirin and clopidogrel and continuation of antiplatelet therapy for at least 3 months or longer following the procedure appears to be successful in published series in maintenance of stent patency. All published series report a consistently high level of symptomatic response to endovascular treatment in 80% or more of patients.

► DURAL SINUS THROMBOSIS

The most important lesson to draw concerning DST is not to miss it on MRI or CT because its signs can be subtle or inconspicuous. Delay in radiologic diagnosis of this condi-

tion is still common (21) due to the fact that the classic signs of a hyperdense sinus and the associated "cord sign" or "delta sign" are not present in all patients (22). Symptoms of the condition are frequently vague and nonspecific. Younger patients less than 65 years tend to present with headache and elevated intracranial pressure, while older patients tend to have nonspecific changes in mental status, meaning that in both instances the given clinical history with the imaging study will be very vague and not particularly alerting to the diagnosis in hand.

In older studies, it was reported that DST had an expected mortality of up to 50%, but a more realistic figure with modern in-hospital management is in the region of 5% to 8% for all patients with this diagnosis (23–26), but with some modern references as high as 36% (27,28). Grouping of patients tends to dilute the statistical outcomes due to the preponderance of patients with mild disease. Poorer prognosis was seen in a large international study in patients with age >37 years, male gender, hemorrhagic complications, altered mental status, deep cerebral venous thrombosis, and superimposed CNS infection (26,29). Older patients are more likely to develop serious neurologic complications such as lobar hemorrhage, herniation, diffuse edema, or subarachnoid hemorrhage. Precipitating conditions include disseminated malignancies, use of oral contraceptive agents or hormone replacement therapy (approximately 50% in cases of young females) (30), proteins S and C deficiency, antiphospholipid antibodies, treatment with L-asparaginase, postpuerperal status, generalized sepsis, or any hypercoagulable state.

The standard of treatment for this disorder is anticoagulation, although the rate of spontaneous improvement in a certain proportion of patients has meant that even this treatment has failed to demonstrate an unimpeachable benefit in some studies (31,32). Nevertheless, anticoagulation with heparin and warfarin are now the accepted standard of care.

Despite optimal medical management with anticoagulation, as many as 22% of younger patients and 32% of older patients will show neurologic deterioration or progressive complications after admission to the hospital (24). Furthermore, in those patients who die, the mean time from admission to expiry is approximately 6 days with a median of 2 days, meaning that when a patient does decline, a quick decision on what to do next must be made. Predictors of death include seizure, progressive decline in consciousness, Glasgow Coma Scale score of less than 9 at admission, right-sided hemorrhage or lesions in the posterior fossa, and occurrence of new focal lesions after admission (23).

Therefore, when confronted with a patient who is not responding favorably to treatment with anticoagulation or whose neurologic status is profoundly impaired by hemorrhagic or other complications, it may be reasonable to attempt percutaneous mechanical and pharmacologic thrombolysis of the affected sinuses. The limited case reports on this topic have been universally favorable (24–27,33–40), but no controlled studies have been performed to date, and the value of this treatment is therefore still not established.

The entire panoply of interventional devices can be put to service in cases such as this—microwire for clot maceration, angioplasty balloons, microcatheters for drug infusion, rheolytic catheters, and loop snares (Figs. 29-4–29-7). The sigmoid sinus can be surprisingly difficult to traverse and often depends on pointing the introducer catheter posteriorly

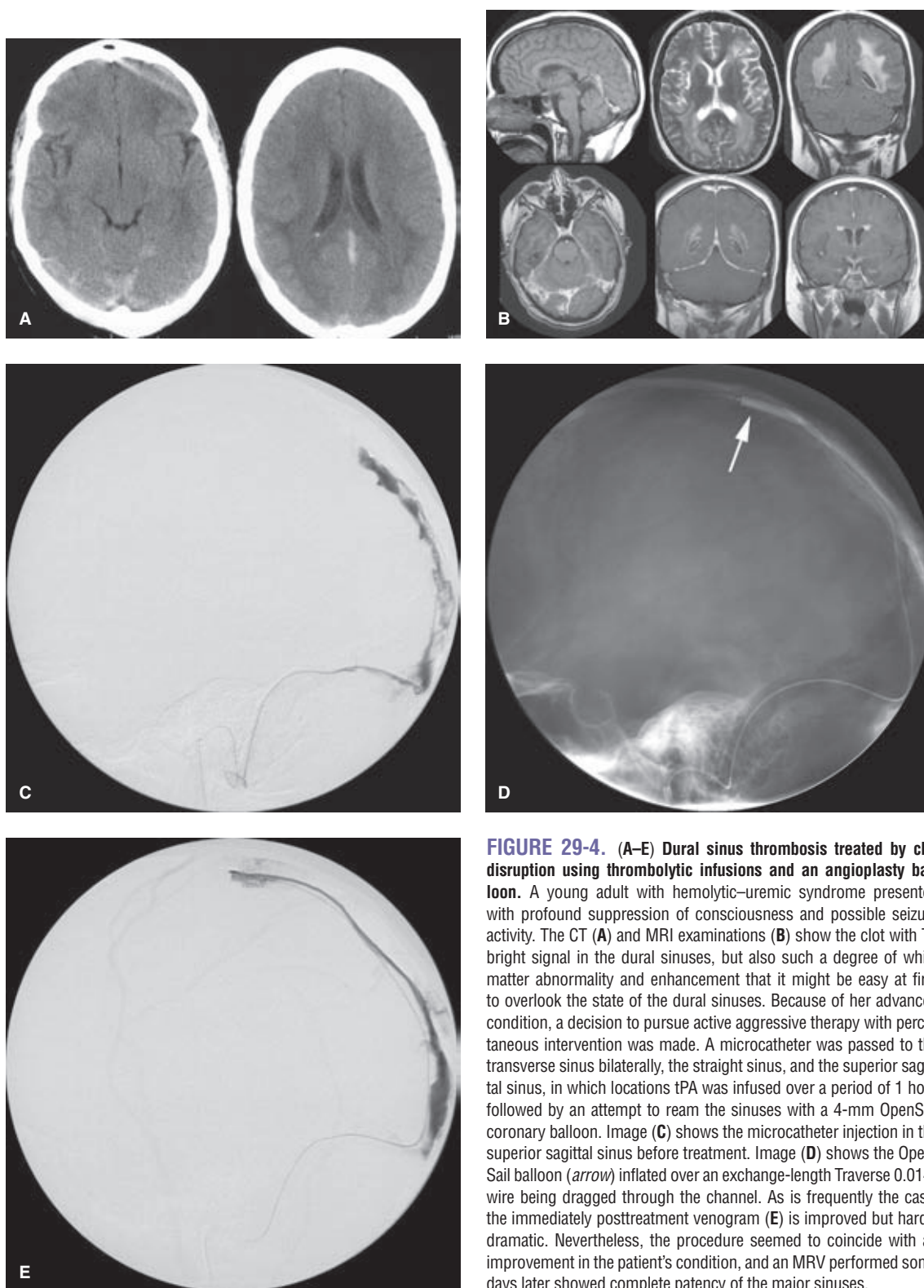


FIGURE 29-4. (A–E) Dural sinus thrombosis treated by clot disruption using thrombolytic infusions and an angioplasty balloon. A young adult with hemolytic–uremic syndrome presented with profound suppression of consciousness and possible seizure activity. The CT (A) and MRI examinations (B) show the clot with T1 bright signal in the dural sinuses, but also such a degree of white matter abnormality and enhancement that it might be easy at first to overlook the state of the dural sinuses. Because of her advanced condition, a decision to pursue active aggressive therapy with percutaneous intervention was made. A microcatheter was passed to the transverse sinus bilaterally, the straight sinus, and the superior sagittal sinus, in which locations tPA was infused over a period of 1 hour followed by an attempt to ream the sinuses with a 4-mm OpenSail coronary balloon. Image (C) shows the microcatheter injection in the superior sagittal sinus before treatment. Image (D) shows the OpenSail balloon (*arrow*) inflated over an exchange-length Traverse 0.014” wire being dragged through the channel. As is frequently the case, the immediately posttreatment venogram (E) is improved but hardly dramatic. Nevertheless, the procedure seemed to coincide with an improvement in the patient’s condition, and an MRV performed some days later showed complete patency of the major sinuses.

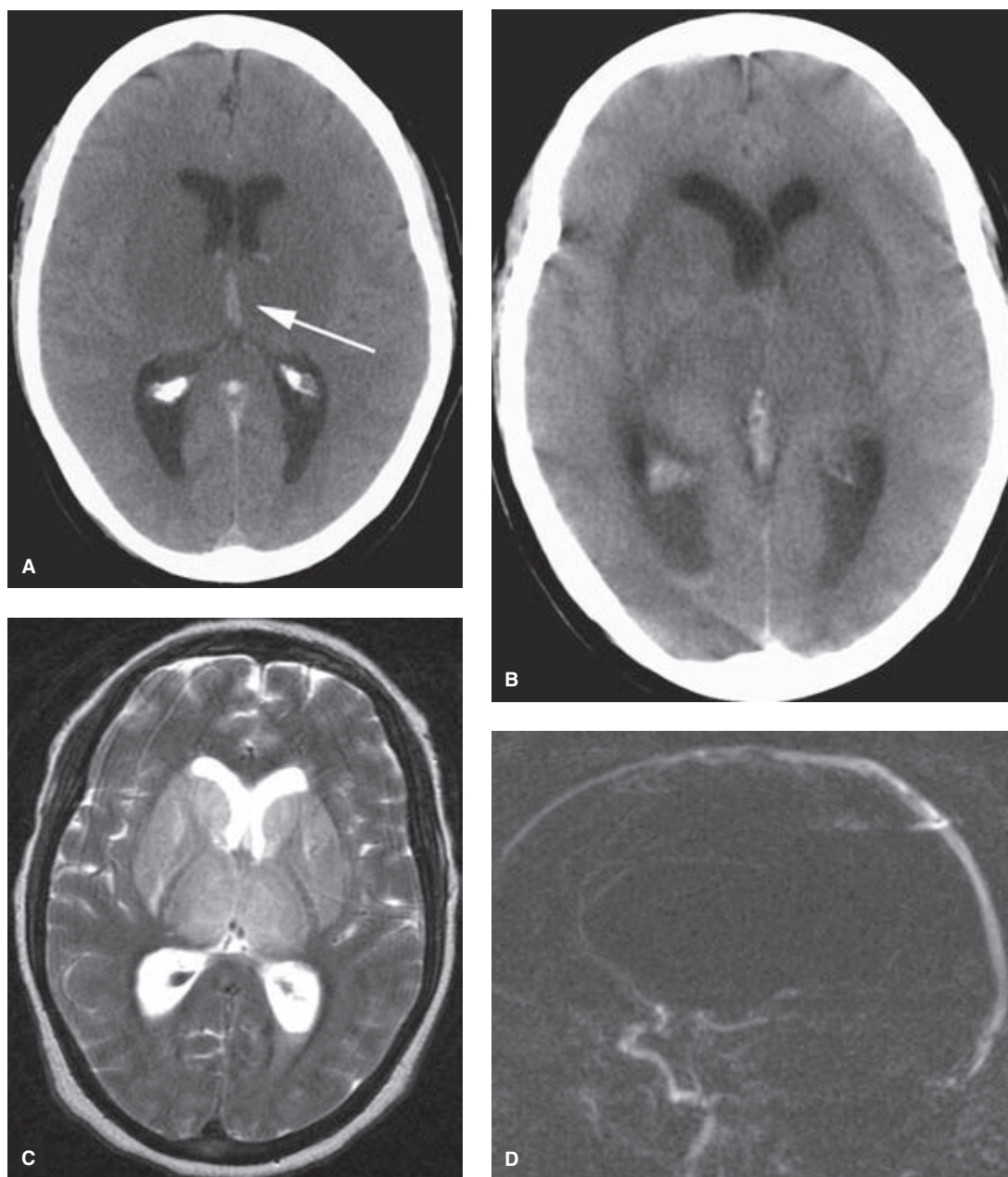


FIGURE 29-5. (A–G) Extensive DVT with profound neurologic decline. An elderly female patient living alone was found unconscious by her neighbors following a 2- to 3-day period during which she had been taking antibiotics for a minor urinary infection. Her first CT scan (**A**) and follow-up scan the next day (**B**) show extensive brain edema, intraventricular hemorrhage, hydrocephalus, and dense thrombus in the internal cerebral veins (*arrow* in **A**). The T2-weighted MRI (**C**) shows layering blood in the ventricles and diffuse hyperintense signal in the basal ganglia and thalami, an appearance that could be mistaken for a variety of toxic or infective encephalitides. The phase-contrast MRV (**D**) and left common carotid arteriogram (**E**) show no evidence of filling of the internal cerebral vein, minimal filling of the straight sinus with a linear filling defect (*arrow* in **E**), and drainage only via the left transverse sinus. (*continued*)

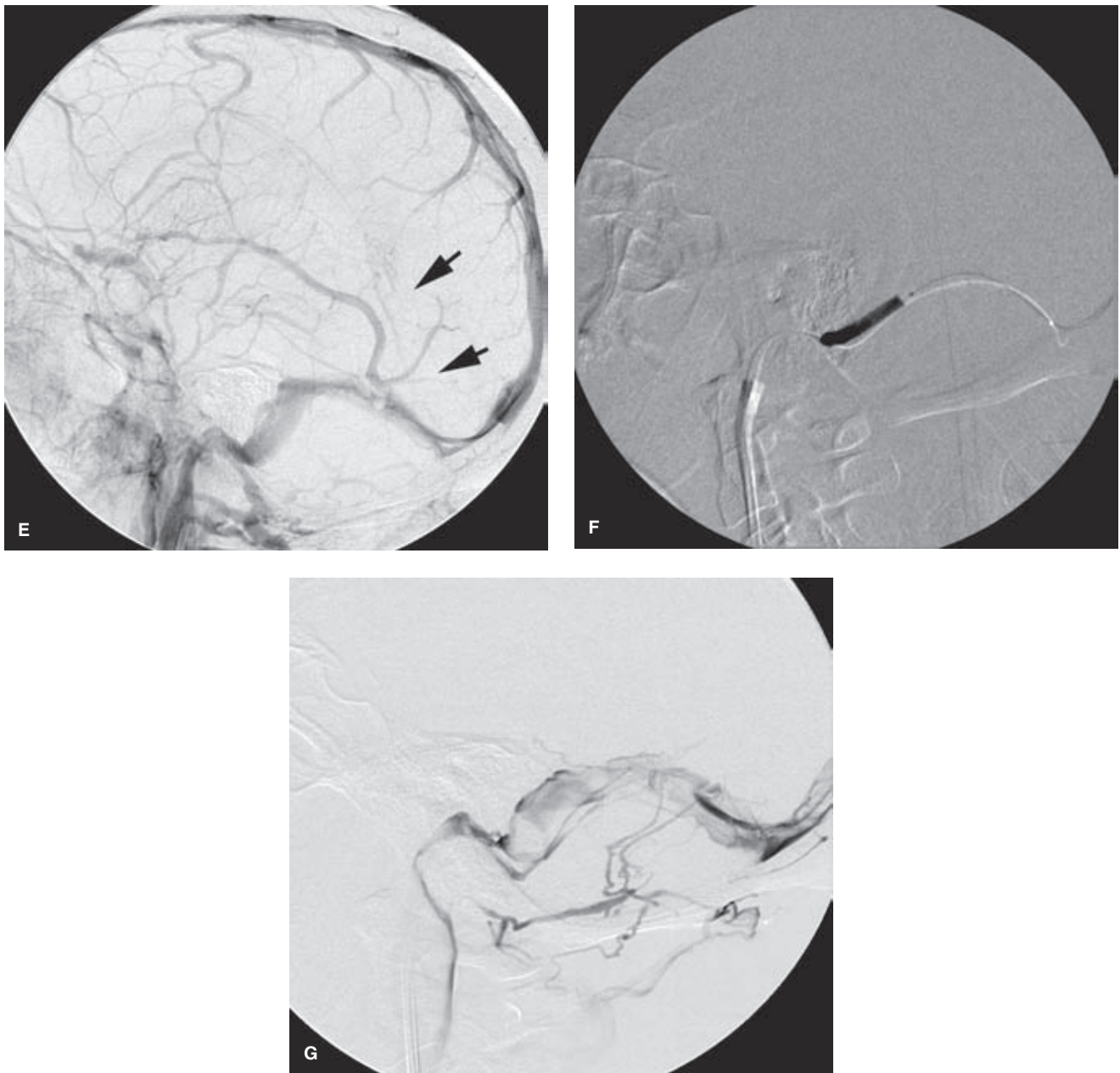


FIGURE 29-5. (CONTINUED) The right transverse and sigmoid sinuses were reamed as much as possible using urokinase 500,000 units via a microcatheter and a 4-mm balloon (F) but despite prolonged efforts, the straight sinus could not be accessed. The posttreatment venogram (G) shows that while flow has been reestablished in the right transverse sinus, a colossal burden of thrombus remains. Several treatment attempts were made on this patient with seemingly little impact on her comatose state. She was transferred to a nursing home for terminal care, where despite all odds, she made a remarkable recovery to near-baseline condition over the course of several months.

Since this case was performed some years ago, several distal access catheters have become available that would lend themselves well to an aggressive suction thrombectomy of cases such as this (see later cases).

and laterally to launch the microcatheter and microwire in the right direction. A triple coaxial system of catheters and sheaths can be very helpful to prevent prolapse into the right atrium. As one traverses the thrombosed sinuses retrogradely, a wide J-shape on the wire can be most helpful to cleave the thrombus and to stay out of cortical veins, which might otherwise be prone to perforation by the tip of the wire. For this same reason, staying shy of the internal cerebral veins is undoubtedly advisable when the target of treatment is the deep system

with straight sinus occlusion. Confining one's manipulations to the dural sinuses themselves might be prudent, as it would be very difficult to catheterize an internal cerebral vein retrogradely through clot without running a risk of perforation. Authors have described protocols for thrombolytic infusion either all at the acute setting, urokinase 1 M units or equivalent tPA of approximately 10 mg, or prolonged infusions of tPA at 1 to 2 mg/hour (41).

(text continues on page 456)

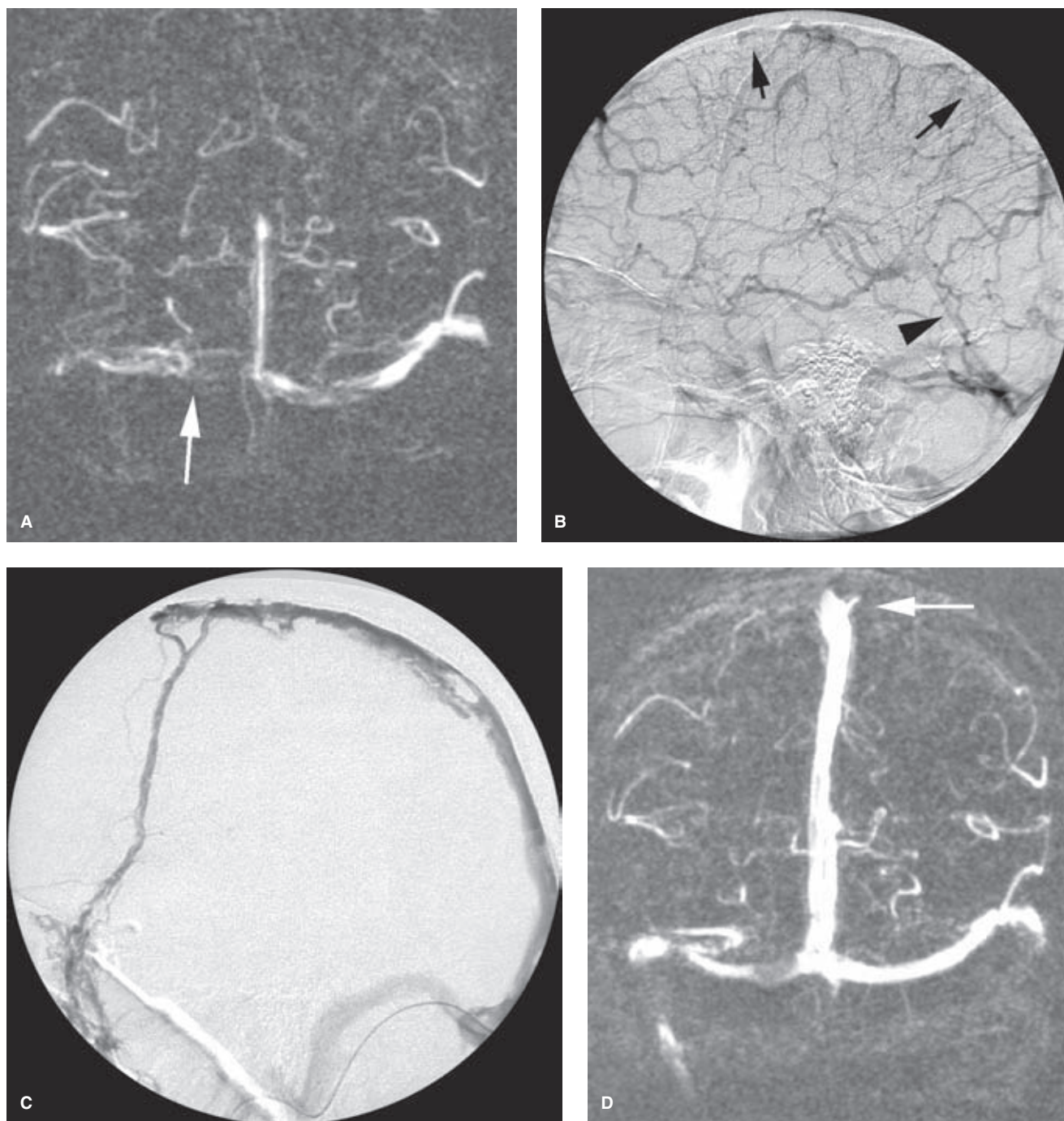


FIGURE 29-6. (A–D) Dural sinus thrombosis treated with AngioJet Rheolytic Catheter. A middle-aged female with extensive sinus thrombosis due to protein C deficiency showed signs of neurologic deterioration despite adequate anticoagulation. A decision was made to improve her venous flow through endovascular means. A phase-contrast MRV (A) shows absence of the superior sagittal sinus and poor filling of the right transverse sinus (*arrow*). These findings are confirmed on the venous phase of the left common carotid arteriogram (B). Note the distended abnormal pattern of the cortical veins with nonopacification of the superior sagittal sinus (*arrows*) and poor filling of the straight sinus (*arrowhead*). After several passes with a 5F Angiojet (Possis) catheter device, a venogram (C) shows marked improvement in the caliber of the draining sinus, although a considerable clot remains. A repeat MRV performed some days later shows filling of the superior sagittal sinus (*arrow*) and improvement in the appearance of the right transverse sinus.

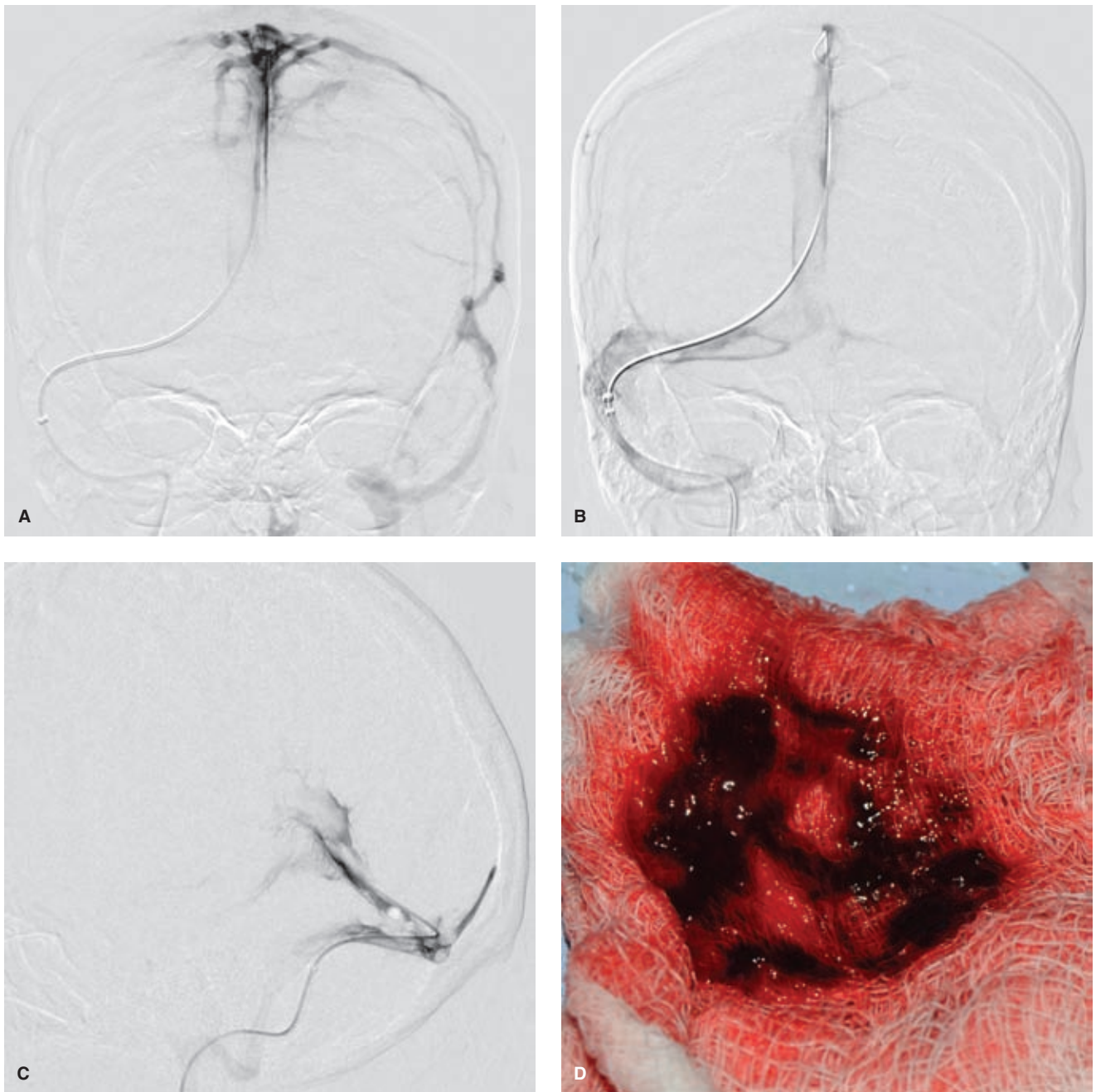


FIGURE 29-7. (A–D) Suction thrombectomy for dural sinus and straight sinus thrombosis. Among the techniques described in this chapter for endovascular treatment of DST, suction thrombectomy with a large-caliber distal access catheter seems to be the most timely and angiographically effective by far. These images from a middle-aged patient show extensive superior sagittal sinus thrombosis (A) partially relieved (B) after just one pass with the catheter suctioned by hand with a 60 mL syringe. Even retrograde triaxial access to the straight sinus (C) was immediately fruitful, with several iterations resulting in large volumes of clot being aspirated (D). With such a degree of clot burden the likelihood of pulmonary emboli of clinical significant magnitude must be considered. Suction thrombectomy seems to offer the best effect with immediate relief of venous obstruction, at least in the major venous channels, while minimizing the pulmonary risks, compared to other clot disrupting techniques.

References

- Fraser C, Plant GT. The syndrome of pseudotumour cerebri and idiopathic intracranial hypertension. *Curr Opin Neurol* 2011; 24(1):12–17.
- Wall M. Idiopathic intracranial hypertension. *Neurol Clin* 2010; 28(3):593–617.
- Bono F, Messina D, Giliberto C, et al. Bilateral transverse sinus stenosis and idiopathic intracranial hypertension without papilledema in chronic tension-type headache. *J Neurol* 2008; 255(6):807–812.
- De Simone R, Ranieri A, Montella S, et al. Sinus venous stenosis-associated IIHWOP is a powerful risk factor for progression and refractoriness of pain in primary headache patients: A review of supporting evidences. *Neurol Sci* 2011;32(suppl 1): S169–S171.
- Burgett RA, Purvin VA, Kawasaki A. Lumboperitoneal shunting for pseudotumor cerebri. *Neurology* 1997;49(3):734–739.
- Garton HJ. Cerebrospinal fluid diversion procedures. *J Neuroophthalmol* 2004;24(2):146–155.
- Liu GT, Volpe NJ, Schatz NJ, et al. Severe sudden visual loss caused by pseudotumor cerebri and lumboperitoneal shunt failure. *Am J Ophthalmol* 1996;122(1):129–131.
- Thambisetty M, Lavin PJ, Newman NJ, et al. Fulminant idiopathic intracranial hypertension. *Neurology* 2007;68(3):229–232.
- Baheti NN, Nair M, Thomas SV. Long-term visual outcome in idiopathic intracranial hypertension. *Ann Indian Acad Neurol* 2011;14(1):19–22.
- Donnet A, Metellus P, Levrier O, et al. Endovascular treatment of idiopathic intracranial hypertension: Clinical and radiologic outcome of 10 consecutive patients. *Neurology* 2008;70(8): 641–647.
- Higgins JN, Cousins C, Owler BK, et al. Idiopathic intracranial hypertension: 12 cases treated by venous sinus stenting. *J Neurol Neurosurg Psychiatry* 2003;74(12):1662–1666.
- Higgins JN, Owler BK, Cousins C, et al. Venous sinus stenting for refractory benign intracranial hypertension. *Lancet* 2002; 359(9302):228–230.
- Owler BK, Parker G, Halmagyi GM, et al. Cranial venous outflow obstruction and pseudotumor cerebri syndrome. *Adv Tech Stand Neurosurg* 2005;30:107–174.
- Ahmed RM, Wilkinson M, Parker GD, et al. Transverse sinus stenting for idiopathic intracranial hypertension: A review of 52 patients and of model predictions. *AJNR Am J Neuroradiol* 2011;32(8):1408–1414.
- Bussiere M, Falero R, Nicolle D, et al. Unilateral transverse sinus stenting of patients with idiopathic intracranial hypertension. *AJNR Am J Neuroradiol* 2010;31(4):645–650.
- Owler BK, Parker G, Halmagyi GM, et al. Pseudotumor cerebri syndrome: Venous sinus obstruction and its treatment with stent placement. *J Neurosurg* 2003;98(5):1045–1055.
- Levrier O, Metellus P, Fuentes S, et al. Use of a self-expanding stent with balloon angioplasty in the treatment of dural arteriovenous fistulas involving the transverse and/or sigmoid sinus: Functional and neuroimaging-based outcome in 10 patients. *J Neurosurg* 2006;104(2):254–263.
- Rohr A, Dorner L, Stingele R, et al. Reversibility of venous sinus obstruction in idiopathic intracranial hypertension. *AJNR Am J Neuroradiol* 2007;28(4):656–659.
- De Simone R, Marano E, Fiorillo C, et al. Sudden re-opening of collapsed transverse sinuses and longstanding clinical remission after a single lumbar puncture in a case of idiopathic intracranial hypertension. Pathogenetic implications. *Neurol Sci* 2005;25(6):342–344.
- Zheng H, Zhou M, Zhao B, et al. Pseudotumor cerebri syndrome and giant arachnoid granulation: Treatment with venous sinus stenting. *J Vasc Interv Radiol* 2010;21(6):927–929.
- Provenzale JM, Kranz PG. Dural sinus thrombosis: Sources of error in image interpretation. *AJR Am J Roentgenol* 2011; 196(1):23–31.
- Virapongse C, Cazenave C, Quisling R, et al. The empty delta sign: Frequency and significance in 76 cases of dural sinus thrombosis. *Radiology* 1987;162(3):779–785.
- Canhao P, Ferro JM, Lindgren AG, et al. Causes and predictors of death in cerebral venous thrombosis. *Stroke* 2005;36(8): 1720–1725.
- Ferro JM, Canhao P, Bousser MG, et al. Cerebral vein and dural sinus thrombosis in elderly patients. *Stroke* 2005;36(9): 1927–1932.
- de Bruijn SF, Stam J. Randomized, placebo-controlled trial of anticoagulant treatment with low-molecular-weight heparin for cerebral sinus thrombosis. *Stroke* 1999;30(3):484–488.
- Ferro JM, Canhao P, Stam J, et al. Prognosis of cerebral vein and dural sinus thrombosis: Results of the International Study on Cerebral Vein and Dural Sinus Thrombosis (ISCVT). *Stroke* 2004;35(3):664–670.
- Cantu C, Barinagarrementeria F. Cerebral venous thrombosis associated with pregnancy and puerperium. Review of 67 cases. *Stroke* 1993;24(12):1880–1884.
- Ben Hamouda-M'Rad I, Mrabet A, Ben Hamida M. [Cerebral venous thrombosis and arterial infarction in pregnancy and puerperium. A series of 60 cases]. *Rev Neurol (Paris)* 1995; 151(10):563–568.
- Ferro JM, Canhao P, Bousser MG, et al. Cerebral venous thrombosis with nonhemorrhagic lesions: Clinical correlates and prognosis. *Cerebrovasc Dis* 2010;29(5):440–445.
- Coutinho JM, Ferro JM, Canhao P, et al. Cerebral venous and sinus thrombosis in women. *Stroke* 2009;40(7):2356–2361.
- de Bruijn SF, de Haan RJ, Stam J. Clinical features and prognostic factors of cerebral venous sinus thrombosis in a prospective series of 59 patients. For the Cerebral Venous Sinus Thrombosis Study Group. *J Neurol Neurosurg Psychiatry* 2001; 70(1):105–108.
- Einhaupl KM, Villringer A, Meister W, et al. Heparin treatment in sinus venous thrombosis. *Lancet* 1991;338(8767): 597–600.
- Baker MD, Opatowsky MJ, Wilson JA, et al. Rheolytic catheter and thrombolysis of dural venous sinus thrombosis: A case series. *Neurosurgery* 2001;48(3):487–493; discussion 493–484.
- Dowd CF, Malek AM, Phatouros CC, et al. Application of a rheolytic thrombectomy device in the treatment of dural sinus thrombosis: A new technique. *AJNR Am J Neuroradiol* 1999; 20(4):568–570.
- Cicccone A, Canhao P, Falcao F, et al. Thrombolysis for cerebral vein and dural sinus thrombosis. *Cochrane Database Syst Rev* 2004;(1):CD003693.
- Curtin KR, Shaibani A, Resnick SA, et al. Rheolytic catheter thrombectomy, balloon angioplasty, and direct recombinant tissue plasminogen activator thrombolysis of dural sinus thrombosis with preexisting hemorrhagic infarctions. *AJNR Am J Neuroradiol* 2004;25(10):1807–1811.
- Kumar S, Rajshekher G, Reddy CR, et al. Intrasinus thrombolysis in cerebral venous sinus thrombosis: Single-center experience in 19 patients. *Neurol India* 2010;58(2):225–229.
- Blackham KA. Extensive dural sinus thrombosis: Successful recanalization with thrombolysis and a novel thrombectomy device. *J Neurosurg* 2011;114(1):133–135.
- Filippidis A, Kapsalaki E, Patramani G, et al. Cerebral venous sinus thrombosis: Review of the demographics, pathophysiology, current diagnosis, and treatment. *Neurosurg Focus* 2009; 27(5):E3.
- Tsai FY, Kostanian V, Rivera M, et al. Cerebral venous congestion as indication for thrombolytic treatment. *Cardiovasc Intervent Radiol* 2007;30(4):675–687.
- Frey JL, Muro GJ, McDougall CG, et al. Cerebral venous thrombosis: Combined intrathrombus rtPA and intravenous heparin. *Stroke* 1999;30(3):489–494.

Cerebral Vasospasm

Key Points

- Cerebral vasospasm following subarachnoid hemorrhage is a poorly understood phenomenon with an unclear correlation with the delayed ischemic neurologic deficits (DINDs) seen in a subgroup of patients with this disorder.
- Mechanisms other than simple regional hypoperfusion and ischemic injury may be at play in declining patients exhibiting angiographic evidence of cerebral vasospasm.

► INTRODUCTION

Patients who are severely ill with the sequelae of aneurysmal subarachnoid hemorrhage encounter significant setbacks even after their aneurysm has been secured by open clipping or endovascular occlusion. Chief amongst these is the onset of delayed ischemic neurologic deficits (DINDs) related to stroke or stroke-like lesions throughout the brain, usually seen within the first 2 weeks after the bleed. This overlaps with the long recognized period of risk of vasospasm following subarachnoid hemorrhage, and for many years conventional wisdom has held that the two phenomena are directly and causally related (1,2), that is, that ischemia of the brain during this period of critical illness is related to regional cerebral perfusion deficits induced by arterial spasm. Recent work has drawn this direct 1:1 relationship into question (3,4). It is likely that angiographic evidence of vasospasm or altered indices on transcranial Doppler imaging are just one facet of a complex physiologic storm at play in these severely ill patients (5). Still, vasospasm of the major branches of the circle of Willis and of the distal arterioles likely makes a substantial contribution to the onset of ischemia in some patients and endovascular relief of severe vasospasm is likely to continue to play a role in their management.

► VASOSPASM AND CEREBRAL ISCHEMIA

Delayed vasospasm requiring endovascular intervention is usually seen 3 to 14 days following a severe subarachnoid hemorrhage, but can also be seen in postpartum patients, trauma, arteriovenous malformations, and tumors (6). The biochemical mechanisms of vasospasm are not completely understood, with various hypotheses explaining its pathogenesis (7):

- A role for increased production of protein kinase C with increased production of vasoconstricting prostaglandins and inhibition of production of prostacyclin (a vasodilator) (8,9).
- Increased protein kinase C leads to excessive intracellular activity of free calcium in smooth muscle, causing phosphorylation of contractile proteins (10).
- Local depletion of nitric oxide (NO), which is an important tonic dilator of cerebral arteries by virtue of its activation of cyclic guanosine monophosphate (cGMP). Inactivation of NO by oxyhemoglobin or superoxide radicals may initiate this process (11,12).
- Oxidative stress may lead to activation of calcium channels and of vasoactive proteins such as arachidonic acid to produce vasoactive lipids or, alternatively, bilirubin oxidation products causing vessel wall contraction (3).
- Increased availability and potency of endothelin-1 (ET-1), a potent vasoconstrictor (13). ET-1 levels rise in response to shear stress, hypoxia, catecholamines, insulin, and angiotensin II and are counteracted by NO through the intermediary roles of endothelin-3, prostaglandin E₂, and prostacyclin (14).

Angiographic evidence of vasospasm can be seen in 30% to 87% of patients following subarachnoid hemorrhage, but only about half of these will require specific management, and only the most severely affected of the latter group will require endovascular intervention (15–17). However, with recent use of diffusion imaging on MRI it is evident that the proportion of patients who develop infarctions may be much higher than previously believed, possibly as many as 50% to 80% even with optimal ICU management (17). Even with optimal Triple-H therapy (hemodilution, hypertension, hypervolemia) with nimodipine, as many as 13.5% of patients with subarachnoid hemorrhage die or become disabled from vasospasm, and among those disabled following a subarachnoid hemorrhage, DIND can account for almost 40% of the disabilities (18). Previously, these complications were ascribed primarily to the effects of vasospasm, although this is now in question. Nevertheless, a strong correlation exists between the severity of vasospasm and the likelihood of a bad clinical outcome due to ischemic deficits (19). Particular risk factors predicting a risk of severe vasospasm include a heavy burden of clot in the CSF, as categorized by the Fisher scale (20), and in female patients who smoke (21–23).

Microstructural changes in the vessel wall have been described in animal experiments and anecdotally in human patients, suggesting that the onset of vasospasm and

decreased wall compliance correlates with the development of smooth muscle vacuolation, myonecrosis, periaventricular inflammation, and medial and subendothelial fibrosis (24–27). The timeline of these events is clinically significant because it is a well-recognized phenomenon that spastic cerebral arteries become less compliant and responsive to intra-arterial drug instillation as the course of severe spasm evolves. Correlation between histologic mural changes and decreasing responsiveness to papaverine have been confirmed in monkeys (28,29); experiments also confirmed the transience of the response to papaverine with the effect lasting less than 24 hours and possibly as short as 10 minutes (30,31). These observations in animals dovetail with clinical anecdotal experience that the most intractable cases of persistent spasm become more difficult and hazardous to treat as the days elapse.

► CORTICAL SPREADING DEPRESSION AND OTHER CAUSES OF DELAYED CEREBRAL ISCHEMIA

Despite the emphasis for many decades on treating vasospasm as a means of reducing the likelihood of delayed ischemic deficits in patients with subarachnoid hemorrhage, several anomalous observations indicate that the cause-and-effect relationship between vasospasm and ischemia is not direct. With the exception of nimodipine, many drug trials with tightly argued hypotheses have succeeded in reversing the severity and extent of vasospasm but have failed to demonstrate an improvement in clinical outcome (32,33). For instance, clazosentan, an endothelin receptor antagonist, can reduce the severity of vasospasm by half in a dose-dependent manner compared with placebo, but does not improve clinical outcome at 3 months (34,35). At a more fundamental level, the correlation between the distribution and timing of vasospasm and the onset and location of cerebral infarctions is not consistent (36–38), and even the effects of Triple-H therapy on cerebral blood flow are unclear and not correlated with an impact on clinical outcome at 1 year (39,40). Quantitative studies of vasospasm using CT perfusion and PET suggest that even in territories with angiographically severe vasospasm, the ischemic threshold of cerebral blood flow (CBF) of 25 mL/100 g/min may not be reached in many severely ill patients, raising the question of why ischemic infarctions occur in this patient population (41,42).

The failure to detect a clear therapeutic effect on clinical outcome from systemic or intra-arterial drugs known to reverse cerebral vasospasm as well as other inconsistencies in the patterns of ischemic deficits following severe subarachnoid hemorrhage has shifted attention to other pathophysiologic mechanisms. These include microvessel spasm, distal microthrombosis (36,43), platelet activation (44), and the phenomenon of cortical spreading depression (45) (“killer waves of depolarization”) (46). Histologic *postmortem* evidence of thromboembolic mediation of cerebral ischemia in patients who have succumbed after subarachnoid hemorrhage is well-recognized, and transcranial Doppler evidence of microcirculatory emboli following open surgery or endovascular coiling appears to support the hypothesis that distal ischemia may be related to spontaneous platelet activation (37,43,44).

Cortical spreading depolarization (or depression) is a self-propagating mass depolarization of cells resulting in massive activity of sodium and calcium pumps requiring substantial increases in regional CBF and oxygen delivery (47). The influx of cations and of extracellular fluid that characterize the initial stages of cortical spreading depression are familiar as the imaging findings of cytotoxic edema. The normal brain responds with a marked increase in blood flow to meet the metabolic requirements of the affected area of cortex. Under certain pathologic conditions an uncoupling or inverse response of blood flow occurs following the onset of cortical spreading depression, which results in a confluence of diminished CBF and increased metabolic requirements of neuronal tissue, thus resulting in an aggravation of the metabolic neuronal insult. On electroencephalography this sequence of events leads to suppression of high-frequency activity, hence the name of the condition, leading to a paradoxical state of suppressed electrical activity and markedly elevated metabolic requirements. Intriguingly, nimodipine, the one calcium channel blocker associated with an improved clinical outcome in subarachnoid patients, is known in laboratory animals to have an effect on the sequelae of cortical spreading depression by partially normalizing the response of vasomotor tone and of blood flow, raising the possibility that part of the therapeutic response to nimodipine may be mediated through this effect rather than through a simple vasodilatory response.

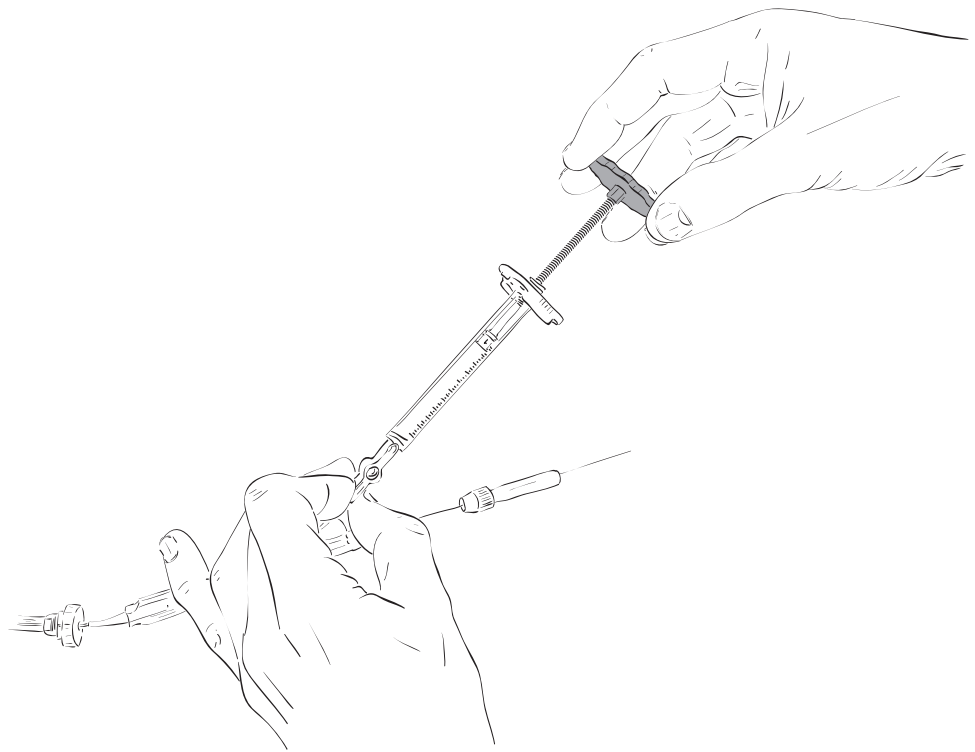
► ENDOVASCULAR TREATMENT OF CEREBRAL VASOSPASM

Until the pathophysiology of critically ill patients with aneurysmal subarachnoid hemorrhage is understood more fully and better therapeutic alternatives become available, it is likely that endovascular relief of vasospasm will continue to be used for patients with progressive neurologic decline despite maximal medical therapy. It is likely that the phenomena of DIND are multifactorial or that even moderate vasospasm may decrease cerebral blood flow by a degree conducive to lowering the threshold for spreading cortical depolarization or other processes that result in permanent ischemic injury. Therefore, in the absence of satisfactory alternatives, endovascular therapy to relieve vasospasm is likely reasonable and may be helpful in a certain number of patients. The options available include direct intra-arterial drug infusion and balloon angioplasty.

Intra-arterial Drugs

Papaverine, a benzyloquinoline alkaloid opioid derivative, was for many years the staple of intra-arterial treatment for vasospasm. However, as mentioned earlier, its effect is marginal and transient, and the drug has fallen into disfavor in recent years. Significant concerns over neurologic deterioration in some patients, elevation of intracranial pressure following its use, and the neurotoxic effects of papaverine have been raised (48–50). Specifically, MRI changes following papaverine infusions with histologic changes of laminar necrosis or direct neuronal toxicity have been reported in a small series of patients. Papaverine has a wide array of physiologic and pharmacologic effects that could account for these changes, including a direct opening effect on the blood–brain barrier (51), direct toxicity to endothelial cells

FIGURE 30-1. Graduated cadence syringe (MTI) for vasospasm angioplasty. For intracranial angioplasty for vasospasm, single-lumen balloon catheters such as the Hyperform (MTI) and Hyperglide (MTI) are usually excellent. Unfortunately, the range of diameters for these balloons is limited, and one has to be very careful not to overinflate the balloon and rupture a vessel. The manufacturers suggest loading a syringe on the balloon with only the maximal volume of the balloon contained in the syringe. Alternatively, the Cadence syringe (MTI) is a superb device for controlling the degree of balloon inflation. It has a threaded piston that clicks with movement, and five clicks is the equivalent of 0.1 mL of inflation. When blood gets into the balloon shaft, or if the contrast preparation is too dilute, it can be very difficult to see the balloon and whether it is inflating. Some sort of safeguard to prevent overinflation is essential.



(52), and other intracellular mitochondrial and metabolic effects (53).

Calcium blocker drugs have been gaining increasing acceptance as an intra-arterial agent for endovascular relief of vasospasm. Oral or intravenous nimodipine has an established efficacy at improving clinical outcome following subarachnoid hemorrhage, with 34% reduction in vasospasm-induced cerebral infarction and 40% reduction in the rate of poor outcomes (54). However, as mentioned above it is not clear that the therapeutic effect of nimodipine is related to a vasodilation effect. Nevertheless, several intra-arterial calcium blocker agents have gained currency in the intra-arterial treatment of vasospasm, including nimodipine (55,56), milrinone (57), and verapamil (58,59).

In the United States, nicardipine is the foremost agent available in parenteral form tested in this application (60). Nicardipine is a dihydropyridine calcium channel blocker with good water-solubility properties and a relatively specific affinity for cardiac and cerebral vascular smooth muscle. At physiologic pH it has neutral molecular charge, but in ischemic tissue it becomes protonated and a theoretical tendency, thus, to accumulate in the areas where it is needed most (61). The dose used varies between 0.5 and 10 mg per arterial tree, with very diligent attention to the intracranial pressure, systemic blood pressure, EKG, and heart rate during the procedure, changes that can call for an adjustment in the rate of dosage. Nicardipine is formulated by adding a 25-mg vial to 250 mL of saline for a concentration of 0.1 mg/mL, although higher concentrations up to 1 mg/mL are sometimes used.

Balloon Angioplasty

In 1984, Zubkov et al. (62) described the use of balloon angioplasty in the endovascular treatment of vasospasm, and the technique has gained general acceptance since that time.

In contrast to the evanescent effect of intra-arterial papaverine, it is perceived that the effect of balloon percutaneous transluminal angioplasty (PTA) on vasospastic vessels is sustained and more likely to endure for the remainder of the vasospastic period, and therefore, most authors profess a preference for this technique when it can be used safely. However, for inaccessible, hypoplastic, or distal vessels, drug instillation remains the only intra-arterial option.

Several small balloons with differing compliance characteristics are available from vendors and are currently used for intracranial angioplasty of vasospasm (Fig. 30-1). Non-compliant balloons have the theoretical advantage of having a fixed diameter of expansion, but they tend to be stiffer to advance through tortuous anatomy and different vessels' diameters require several size exchanges. No difference in clinical outcome is obvious when compliant and noncompliant balloons are compared (63), and most operators tend to prefer compliant balloons for this purpose. Compliant and noncompliant balloons all have the potential to be used with excessive zeal and a risk of vessel rupture, and their small size and volume of expansion mean that the conspicuity of the inflated balloon is very low on the monitor (Figs. 30-2 and 30-3). Certain precautions in the use of balloons for this purpose are useful:

- Visibility of the balloon and of the artery is of paramount importance. Setting up one's view, for instance, of the A1 or M1 segment without an overlying orbital rim or other bony obstacle is helpful. A rehearsal inflation of the balloon in the proximal carotid or vertebral artery to assess the adequacy of contrast opacification and to practice balloon deflation is sometimes vitally important (64).
- As is the case for atherosclerotic angioplasty, slow inflations are much safer than rapid inflations. Impatient inflation of the balloon can only end badly.

(text continues on page 462)

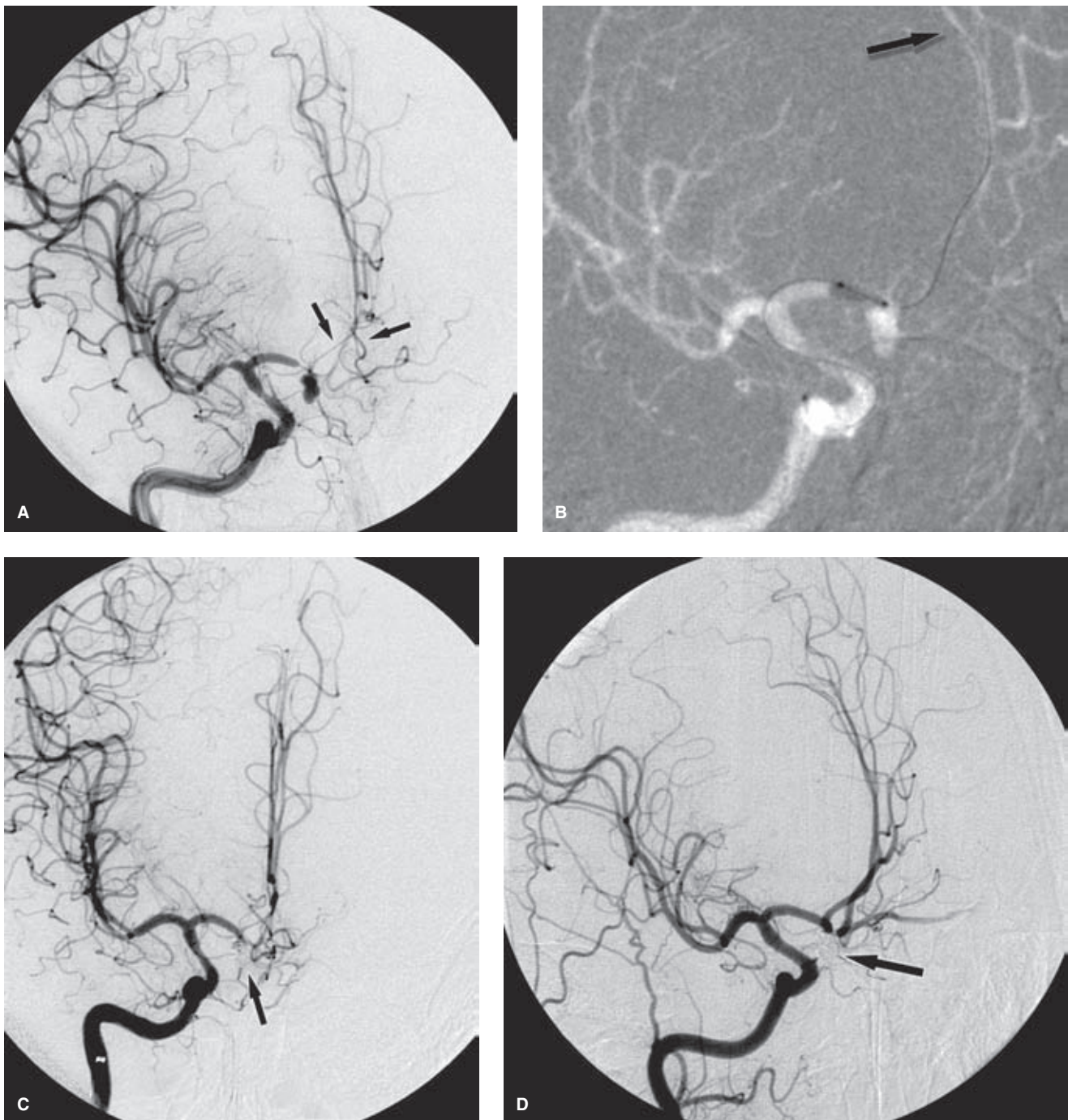


FIGURE 30-2. (A–D) Balloon angioplasty as a reluctant prelude to aneurysm coiling. Sometimes when a patient presents in a delayed manner or when there is hyperacute vasospasm present the degree of vessel narrowing can be so extreme that it interferes with the ability to treat the offending aneurysm. Ideally, one would prefer to secure the aneurysm before opening up the spastic vessels, but sometimes even that is impossible. In this middle-aged patient there is severe spasm adjacent to a recently ruptured aneurysm of the anterior communicating artery (**A**) including the distal A2 segments (*arrows*). The aneurysm was catheterized with an SL10 microcatheter but this maneuver eliminated flow in both anterior cerebral arteries due to obturation of the distal right A1 spastic segment. The microcatheter was withdrawn and angioplasty of the A1 and later the M1 segments was undertaken (**B**). For greatest stability and control of the balloon catheter the wire was advanced distally in the left A2 segment, that is, through the anterior communicating artery itself. The postcoiling image (**C**) suggests that the aneurysm might be incompletely packed with coils, and the anticipation was that with relaxation of vasospasm the neck of the aneurysm, at least, would reopen. However, follow-up angiography (**D**) shows a satisfactory appearance. The left A1 segment, like the rest of the circle of Willis, is now patent but this was not the case at the initial treatment due to severe vasospasm on the left as well at that time.

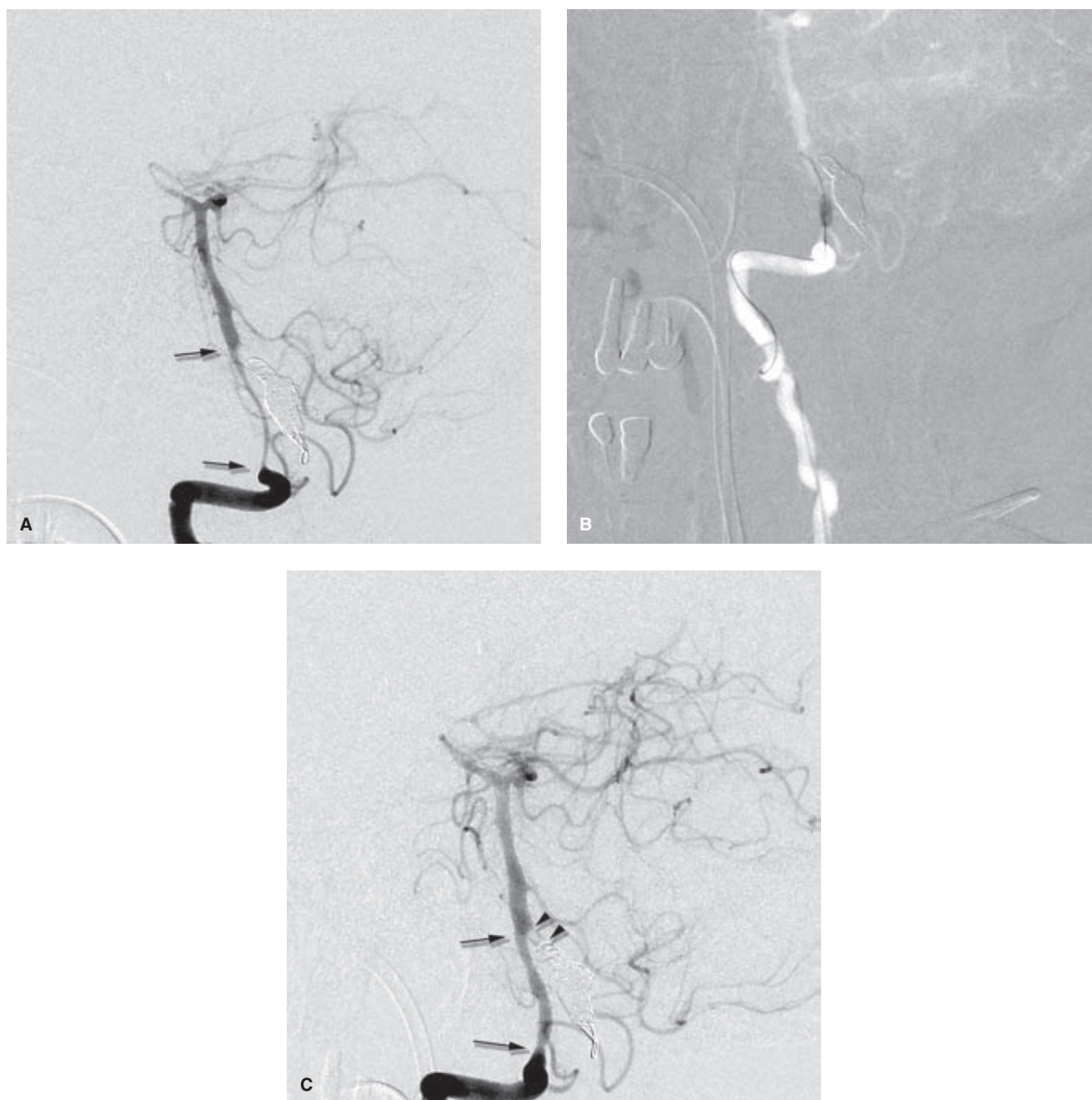


FIGURE 30-3. (A–C) Posterior circulation vasospasm angioplasty. This young patient presented with a severe hemorrhage of the posterior fossa related to an intracranial dissection of the dominant right vertebral artery. This was treated by coil occlusion of the dissected segment, leaving the patient's posterior circulation dependent on the nondominant but adequate left vertebral artery. Despite an initial rally in her condition, she deteriorated clinically and was treated endovascularly on several occasions for vasospasm of the intradural left vertebral artery (*arrows in A*). Due to extreme tortuosity of the left vertebral artery, balloon angioplasty was performed from a very proximal position (*B*) using a compliant Hyperform balloon. A reasonably satisfactory response was obtained from the angioplasty (*arrows in C*) but despite this, the patient did not respond, suggesting that factors other than simple limitation of perfusion pressure were responsible for her deterioration (see text). Furthermore, on the postangioplasty image (*C*) thrombus (*arrowheads*) can be seen within the distal coil-occluded right vertebral artery. This segment had been left intact at the time of coil placement as there was a ramus to the anterior spinal artery in that region on the initial angiogram. The possibility of stump emboli can sometimes present itself in this situation where thrombus edges into the stream of flow and gets carried distally. This patient also later demonstrated one of the difficulties in dealing repeatedly with patients on hyperdynamic therapy in the setting of prolonged and difficult vessel catheterizations, which is the complication of catheter-related intimal injury. Although it is an uncommon event, this particular clinical scenario is a set of circumstances in which the risk of iatrogenic catheter injury is more likely to be seen.

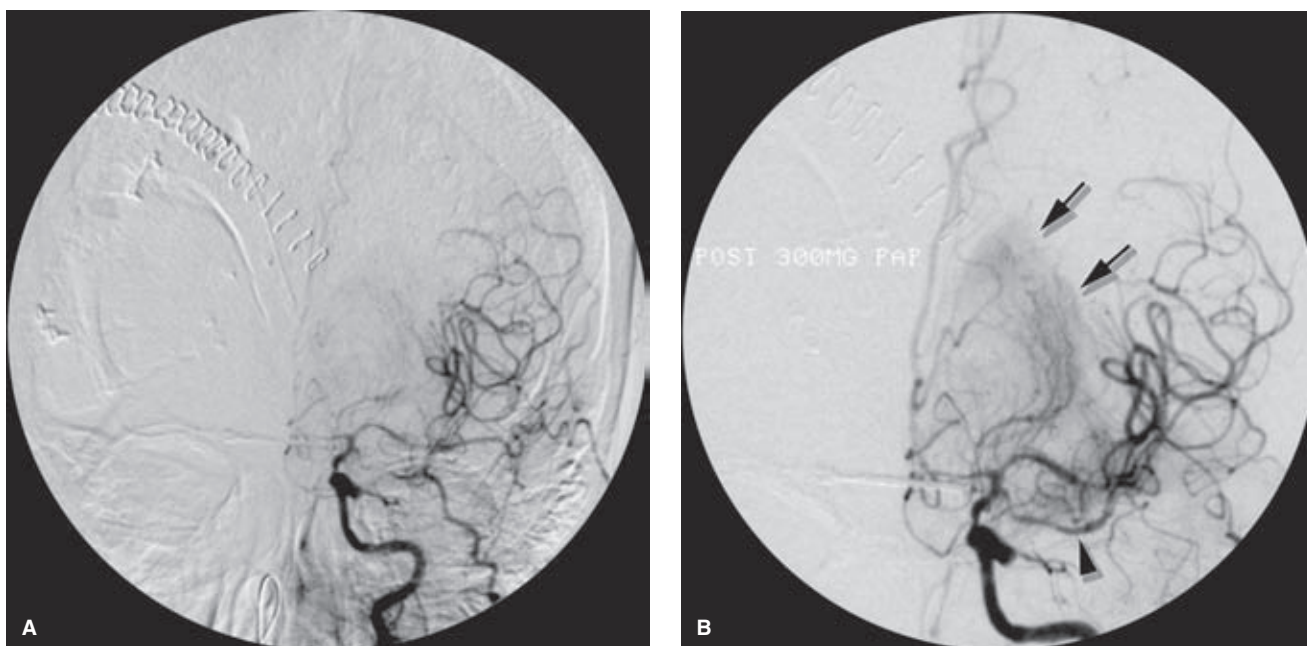


FIGURE 30-4. (A–B) Vasospasm treatment in the setting of variant anatomy. This case was treated some years ago when papaverine was still being used for infusion therapy of vasospasm. The first image before treatment (A) shows the extremely limited perfusion of the anterior cerebral artery territory and marked attenuation of the proximal and distal middle cerebral artery branches. The patient had been treated with a clipping procedure for a ruptured anterior communicating artery. The posttreatment image (B) after instillation of 300 mg of papaverine shows a number of interesting features. Firstly, there is a duplicated middle cerebral artery present (*arrowhead*), which means that a balloon angioplasty of that vessel or of even the main middle cerebral artery would have been even more risky than usual due to native vessel size. Secondly, there is a pronounced blush of the lenticulostriate region (*arrows*). This could be a direct effect of the papaverine itself, but this type of blush is commonly seen in any kind of procedure where short-term or longer-term ischemia of the brain has been reversed, for example, atherosclerotic balloon angioplasty, or acute ischemic stroke therapy. In this instance the presence of blush seems to confirm that the brain was indeed physiologically ischemic prior to the procedure and has been temporarily relieved by the papaverine infusion, as suggested by the generalized improvement in the appearance of the vessels compared with the earlier image.

- Great care is needed when performing an angioplasty close to a surgical clip. It may be prudent to avoid angioplasty entirely immediately next to a recently clipped aneurysm.
- It is possible for an uninflated balloon to get trapped above an area of proximal spasm or by going through a fenestrated aneurysm clip. It is generally technically easier to allow the balloon to travel distally and perform the angioplasty as one pulls back, but when spasm is extremely tight, advance infusion of vasodilators may open the vessel up in a helpful way or angioplasty in a proximal to distal progression might be considered to avoid the disquietude of a stuck balloon.
- Care is always necessary to avoid angioplasty of a hypoplastic variant, duplicated middle cerebral arteries (Fig. 30-4), and so on, or inadvertent inflation in a small posterior communicating artery or anterior choroidal artery into which vessels the wire insinuates itself with almost predictable tenacity in these cases. Therefore, familiarity with the previous angiographic studies to avoid interpreting hypoplastic vessels as spastic is important.
- In the posterior circulation, the posterior inferior cerebellar artery origin has a remarkable capacity to lure in the wire during passage of the balloon catheter.
- For balloon angioplasties of the proximal posterior cerebral arteries, care should always be given to the possibility of having inadvertently selected a tiny perimesencephalic circumflex branch that is running parallel to the P1 or P2 segment and thus giving the appearance on roadmap of the balloon being in the main branch of the posterior cerebral artery itself.

Despite the sometimes excellent angiographic responses that can be obtained with PTA of vasospastic vessels, outcome studies validating the use of these techniques over infusion therapy are still wanting (65–67).

References

1. Kassell NF, Sasaki T, Colohan AR, et al. Cerebral vasospasm following aneurysmal subarachnoid hemorrhage. *Stroke* 1985; 16(4):562–572.
2. Nishioka H, Torner JC, Graf CJ, et al. Cooperative study of intracranial aneurysms and subarachnoid hemorrhage: A long-term prognostic study. III. Subarachnoid hemorrhage of undetermined etiology. *Arch Neurol* 1984;41(11):1147–1151.
3. Pluta RM, Hansen-Schwartz J, Dreier J, et al. Cerebral vasospasm following subarachnoid hemorrhage: Time for a new world of thought. *Neurol Res* 2009;31(2):151–158.
4. Strong AJ, Macdonald RL. Cortical spreading ischemia in the absence of proximal vasospasm after aneurysmal subarachnoid

- hemorrhage: evidence for a dual mechanism of delayed cerebral ischemia. *J Cereb Blood Flow Metab* 2012;32(2): 201–202.
5. Naidech AM, Drescher J, Tamul P, et al. Acute physiological derangement is associated with early radiographic cerebral infarction after subarachnoid haemorrhage. *J Neurol Neurosurg Psychiatry* 2006;77(12):1340–1344.
 6. Mayberg MR. Cerebral vasospasm. *Neurosurg Clin N Am* 1998;9(3):615–627.
 7. Koliass AG, Sen J, Belli A. Pathogenesis of cerebral vasospasm following aneurysmal subarachnoid hemorrhage: Putative mechanisms and novel approaches. *J Neurosci Res* 2009; 87(1):1–11.
 8. Pasqualin A. Epidemiology and pathophysiology of cerebral vasospasm following subarachnoid hemorrhage. *J Neurosurg Sci* 1998;42(1 suppl 1):15–21.
 9. Findlay JM, Macdonald RL, Weir BK. Current concepts of pathophysiology and management of cerebral vasospasm following aneurysmal subarachnoid hemorrhage. *Cerebrovasc Brain Metab Rev* 1991;3(4):336–361.
 10. Takenaka K, Yamada H, Sakai N, et al. Induction of cytosolic free calcium elevation in rat vascular smooth-muscle cells by cerebrospinal fluid from patients after subarachnoid hemorrhage. *J Neurosurg* 1991;75(3):452–457.
 11. Wolf EW, Banerjee A, Soble-Smith J, et al. Reversal of cerebral vasospasm using an intrathecally administered nitric oxide donor. *J Neurosurg* 1998;89(2):279–288.
 12. Fathi AR, Bakhtian KD, Pluta RM. The role of nitric oxide donors in treating cerebral vasospasm after subarachnoid hemorrhage. *Acta Neurochir Suppl* 2011;110(pt 1):93–97.
 13. Kikkawa Y, Matsuo S, Kameda K, et al. Mechanisms underlying potentiation of endothelin-1-induced myofilament Ca(2+) sensitization after subarachnoid hemorrhage. *J Cereb Blood Flow Metab* 2012;32(2):341–352.
 14. Levin ER. Endothelins. *N Engl J Med* 1995;333(6):356–363.
 15. Kassell NF, Peerless SJ, Durward QJ, et al. Treatment of ischemic deficits from vasospasm with intravascular volume expansion and induced arterial hypertension. *Neurosurgery* 1982;11(3):337–343.
 16. Hunt WE, Hess RM. Surgical risk as related to time of intervention in the repair of intracranial aneurysms. *J Neurosurg* 1968;28(1):14–20.
 17. Weidauer S, Lanfermann H, Raabe A, et al. Impairment of cerebral perfusion and infarct patterns attributable to vasospasm after aneurysmal subarachnoid hemorrhage: A prospective MRI and DSA study. *Stroke* 2007;38(6):1831–1836.
 18. Kassell NF, Torner JC, Haley EC Jr., et al. The International Cooperative Study on the Timing of Aneurysm Surgery. Part 1: Overall management results. *J Neurosurg* 1990;73(1):18–36.
 19. Crowley RW, Medel R, Dumont AS, et al. Angiographic vasospasm is strongly correlated with cerebral infarction after subarachnoid hemorrhage. *Stroke* 2011;42(4):919–923.
 20. Fisher CM, Kistler JP, Davis JM. Relation of cerebral vasospasm to subarachnoid hemorrhage visualized by computerized tomographic scanning. *Neurosurgery* 1980;6(1):1–9.
 21. Winn HR, Richardson AE, Jane JA. The long-term prognosis in untreated cerebral aneurysms: I. The incidence of late hemorrhage in cerebral aneurysm: A 10-year evaluation of 364 patients. *Ann Neurol* 1977;1(4):358–370.
 22. Lasner TM, Weil RJ, Riina HA, et al. Cigarette smoking-induced increase in the risk of symptomatic vasospasm after aneurysmal subarachnoid hemorrhage. *J Neurosurg* 1997;87(3): 381–384.
 23. Weir BK, Kongable GL, Kassell NF, et al. Cigarette smoking as a cause of aneurysmal subarachnoid hemorrhage and risk for vasospasm: A report of the Cooperative Aneurysm Study. *J Neurosurg* 1998;89(3):405–411.
 24. Hughes JT, Schianchi PM. Cerebral artery spasm. A histological study at necropsy of the blood vessels in cases of subarachnoid hemorrhage. *J Neurosurg* 1978;48(4):515–525.
 25. Fujiwara N, Ohkawa M, Tanabe M, et al. [The effect of PTA on cerebral vessels in experimental vasospasm: A histopathological study]. *Nippon Igaku Hoshasen Gakkai Zasshi* 1994; 54(5): 378–388.
 26. Ohkawa M, Fujiwara N, Tanabe M, et al. Cerebral vasospastic vessels: Histologic changes after percutaneous transluminal angioplasty. *Radiology* 1996;198(1):179–184.
 27. Kobayashi H, Ide H, Aradachi H, et al. Histological studies of intracranial vessels in primates following transluminal angioplasty for vasospasm. *J Neurosurg* 1993;78(3):481–486.
 28. Kazan S. Effects of intra-arterial papaverine on the chronic period of cerebral arterial vasospasm in rats. *Acta Neurol Scand* 1998;98(5):354–359.
 29. Fujiwara N, Honjo Y, Ohkawa M, et al. Intraarterial infusion of papaverine in experimental cerebral vasospasm. *AJNR Am J Neuroradiol* 1997;18(2):255–262.
 30. Nagai H, Noda S, Mabe H. Experimental cerebral vasospasm. Part 2: Effects of vasoactive drugs and sympathectomy on early and late spasm. *J Neurosurg* 1975;42(4):420–428.
 31. Kuwayama A, Zervas NT, Shintani A, et al. Papaverine hydrochloride and experimental hemorrhagic cerebral arterial spasm. *Stroke* 1972;3(1):27–33.
 32. Zhang S, Wang L, Liu M, et al. Tirilazad for aneurysmal subarachnoid haemorrhage. *Cochrane Database Syst Rev* 2010(2): CD006778.
 33. Velat GJ, Kimball MM, Mocco JD, et al. Vasospasm after aneurysmal subarachnoid hemorrhage: Review of randomized controlled trials and meta-analyses in the literature. *World Neurosurg* 2011;76(5):446–454.
 34. Macdonald RL, Higashida RT, Keller E, et al. Clazosentan, an endothelin receptor antagonist, in patients with aneurysmal subarachnoid haemorrhage undergoing surgical clipping: A randomised, double-blind, placebo-controlled phase 3 trial (CONSCIOUS-2). *Lancet Neurol* 2011;10(7):618–625.
 35. Macdonald RL, Kassell NF, Mayer S, et al. Clazosentan to overcome neurological ischemia and infarction occurring after subarachnoid hemorrhage (CONSCIOUS-1): Randomized, double-blind, placebo-controlled phase 2 dose-finding trial. *Stroke* 2008;39(11):3015–3021.
 36. Vergouwen MD, Vermeulen M, Coert BA, et al. Microthrombosis after aneurysmal subarachnoid hemorrhage: An additional explanation for delayed cerebral ischemia. *J Cereb Blood Flow Metab* 2008;28(11):1761–1770.
 37. Stein SC, Levine JM, Nagpal S, et al. Vasospasm as the sole cause of cerebral ischemia: How strong is the evidence? *Neurosurg Focus* 2006;21(3):E2.
 38. Dankbaar JW, Rijdsdijk M, van der Schaaf IC, et al. Relationship between vasospasm, cerebral perfusion, and delayed cerebral ischemia after aneurysmal subarachnoid hemorrhage. *Neuroradiology* 2009;51(12):813–819.
 39. Egge A, Waterloo K, Sjöholm H, et al. Prophylactic hyperdynamic postoperative fluid therapy after aneurysmal subarachnoid hemorrhage: A clinical, prospective, randomized, controlled study. *Neurosurgery* 2001;49(3):593–605; discussion 605–606.
 40. Lennihan L, Mayer SA, Fink ME, et al. Effect of hypervolemic therapy on cerebral blood flow after subarachnoid hemorrhage: a randomized controlled trial. *Stroke* 2000;31(2):383–391.
 41. Sviri GE, Britz GW, Lewis DH, et al. Dynamic perfusion computed tomography in the diagnosis of cerebral vasospasm. *Neurosurgery* 2006;59(2):319–325; discussion 319–325.
 42. Wintermark M, Ko NU, Smith WS, et al. Vasospasm after subarachnoid hemorrhage: utility of perfusion CT and CT angiography on diagnosis and management. *AJNR Am J Neuroradiol* 2006;27(1):26–34.
 43. Stein SC, Browne KD, Chen XH, et al. Thromboembolism and delayed cerebral ischemia after subarachnoid hemorrhage: An autopsy study. *Neurosurgery* 2006;59(4):781–787; discussion 787–788.

44. Romano JG, Forteza AM, Concha M, et al. Detection of microemboli by transcranial Doppler ultrasonography in aneurysmal subarachnoid hemorrhage. *Neurosurgery* 2002;50(5):1026–1030; discussion 1030–1021.
45. Leng LZ, Fink ME, Iadecola C. Spreading depolarization: A possible new culprit in the delayed cerebral ischemia of subarachnoid hemorrhage. *Arch Neurol* 2011;68(1):31–36.
46. Iadecola C. Bleeding in the brain: Killer waves of depolarization in subarachnoid bleed. *Nat Med* 2009;15(10):1131–1132.
47. Dreier JP, Major S, Manning A, et al. Cortical spreading ischemia is a novel process involved in ischaemic damage in patients with aneurysmal subarachnoid haemorrhage. *Brain* 2009;132(pt 7):1866–1881.
48. Katoh H, Shima K, Shimizu A, et al. Clinical evaluation of the effect of percutaneous transluminal angioplasty and intra-arterial papaverine infusion for the treatment of vasospasm following aneurysmal subarachnoid hemorrhage. *Neurol Res* 1999; 21(2):195–203.
49. Andaluz N, Tomsick TA, Tew JM Jr., et al. Indications for endovascular therapy for refractory vasospasm after aneurysmal subarachnoid hemorrhage: Experience at the University of Cincinnati. *Surg Neurol* 2002;58(2):131–138; discussion 138.
50. Smith WS, Dowd CF, Johnston SC, et al. Neurotoxicity of intra-arterial papaverine preserved with chlorobutanol used for the treatment of cerebral vasospasm after aneurysmal subarachnoid hemorrhage. *Stroke* 2004;35(11):2518–2522.
51. Bhattacharjee AK, Kondoh T, Ikeda M, et al. MMP-9 and EBA immunoreactivity after papaverine mediated opening of the blood–brain barrier. *Neuroreport* 2002;13(17):2217–2221.
52. Yoshimura S, Hashimoto N, Goto Y, et al. Intraarterial infusion of high-concentration papaverine damages cerebral arteries in rats. *AJNR Am J Neuroradiol* 1996;17(10):1891–1894.
53. Urakov AL, Baranov AG. [Effect of papaverine on the energy processes of myocardial mitochondria]. *Farmakol Toksikol* 1979; 42(2):132–136.
54. Pickard JD, Murray GD, Illingworth R, et al. Effect of oral nimodipine on cerebral infarction and outcome after subarachnoid haemorrhage: British aneurysm nimodipine trial. *BMJ* 1989; 298(6674):636–642.
55. Biondi A, Ricciardi GK, Puybasset L, et al. Intra-arterial nimodipine for the treatment of symptomatic cerebral vasospasm after aneurysmal subarachnoid hemorrhage: Preliminary results. *AJNR Am J Neuroradiol* 2004;25(6):1067–1076.
56. Cho WS, Kang HS, Kim JE, et al. Intra-arterial nimodipine infusion for cerebral vasospasm in patients with aneurysmal subarachnoid hemorrhage. *Interv Neuroradiol* 2011;17(2):169–178.
57. Schmidt U, Bittner E, Pivi S, et al. Hemodynamic management and outcome of patients treated for cerebral vasospasm with intraarterial nicardipine and/or milrinone. *Anesth Analg* 2010;110(3):895–902.
58. Feng L, Fitzsimmons BF, Young WL, et al. Intraarterially administered verapamil as adjunct therapy for cerebral vasospasm: safety and 2-year experience. *AJNR Am J Neuroradiol* 2002;23(8):1284–1290.
59. Sehy JV, Holloway WE, Lin SP, et al. Improvement in angiographic cerebral vasospasm after intra-arterial verapamil administration. *AJNR Am J Neuroradiol* 2010;31(10):1923–1928.
60. Badjatia N, Topcuoglu MA, Pryor JC, et al. Preliminary experience with intra-arterial nicardipine as a treatment for cerebral vasospasm. *AJNR Am J Neuroradiol* 2004;25(5):819–826.
61. Weant KA, Ramsey CN 3rd., Cook AM. Role of intraarterial therapy for cerebral vasospasm secondary to aneurysmal subarachnoid hemorrhage. *Pharmacotherapy* 2010;30(4):405–417.
62. Zubkov YN, Nikiforov BM, Shustin VA. Balloon catheter technique for dilatation of constricted cerebral arteries after aneurysmal SAH. *Acta Neurochir (Wien)* 1984;70(1–2):65–79.
63. Miley JT, Tariq N, Souslian FG, et al. Comparison between angioplasty using compliant and noncompliant balloons for treatment of cerebral vasospasm associated with subarachnoid hemorrhage. *Neurosurgery* 2011;69(2 suppl Operative):ons161–168; discussion ons168.
64. Santillan A, Knopman J, Zink W, et al. Transluminal balloon angioplasty for symptomatic distal vasospasm refractory to medical therapy in patients with aneurysmal subarachnoid hemorrhage. *Neurosurgery* 2011;69(1):95–101; discussion 102.
65. Rabinstein AA, Friedman JA, Nichols DA, et al. Predictors of outcome after endovascular treatment of cerebral vasospasm. *AJNR Am J Neuroradiol* 2004;25(10):1778–1782.
66. Polin RS, Coenen VA, Hansen CA, et al. Efficacy of transluminal angioplasty for the management of symptomatic cerebral vasospasm following aneurysmal subarachnoid hemorrhage. *J Neurosurg* 2000;92(2):284–290.
67. Zwieneberg-Lee M, Hartman J, Rudisill N, et al. Effect of prophylactic transluminal balloon angioplasty on cerebral vasospasm and outcome in patients with Fisher grade III subarachnoid hemorrhage: Results of a phase II multicenter, randomized, clinical trial. *Stroke* 2008;39(6):1759–1765.

Angioplasty and Stenting of Atherosclerotic Disease

Key Points

- Carotid endarterectomy is the established treatment of choice for symptomatic carotid artery bifurcation disease in most patients.
- Intracranial angioplasty/stenting with bare or drug-eluting stents has a role to offer in some patients, although the hazardous nature of the procedure warrants extreme caution.

► CAROTID ARTERY ANGIOPLASTY AND STENTING

Carotid artery atheromatous disease accounts for approximately 10% to 20% of ischemic stroke (1,2). Several randomized controlled trials have established that carotid endarterectomy is the standard of care for symptomatic carotid artery disease of moderate or severe degree, compared with best medical management (3–5). Timely endarterectomy of severe (>70%) stenosis within 2 weeks of onset of symptoms brings about an absolute risk reduction of 15.6% and a relative risk reduction of 52% over medical therapy. For symptomatic carotid artery stenosis >50% in degree, the benefit of endarterectomy is a reduction in the absolute risk of stroke of approximately 8% per year. The relative risk reduction of approximately 52% compared with medical management sounds substantial, but this is a reduction of an uncommon event, and thus the absolute benefit to an asymptomatic patient in whom this event is even less common than among symptomatic patients is even more marginal (6,7). In fact at the time of these studies, endarterectomy could only be rationally recommended for the symptomatic and asymptomatic populations if perioperative (30 day) death and stroke risks could be confined below 6% and 3%, respectively. Moreover, it is worth realizing that the margin of benefit to patients from endarterectomy has probably narrowed significantly since the 1990s because of substantial improvements in the medical and pharmaceutical options which have become mainstream since that time. This would imply that the stringent performance standards for endarterectomy complications, <6% complication rates for symptomatic, <3% for asymptomatic patients, have been

shaved down substantially since the time when these landmark studies were completed.

Since it was first approved under stringent conditions by the U.S. Food and Drug Administration in 2004 for patients at high risk for endarterectomy, carotid artery angioplasty and stenting has grown substantially in use as an alternative definitive revascularization procedure for carotid occlusive disease. The reasons for this change are unclear, but likely manifold. The novelty of the procedure, the wider pool of participating physicians interested in the procedure, the general conventional wisdom that minimally invasive procedures are better and less costly than surgical procedures especially for older patients, the perception that avoidance of general anesthesia must be a good thing especially for older patients, and the presumption that the improved technology surrounding carotid stenting must translate into safer outcomes are likely all part of the explanation for the change in this standard of practice. None of these factors or assertions has been shown to be valid in the case of carotid stenting, but this trend away from endarterectomy shows every sign of gaining even more momentum in the foreseeable future.

There is no evidence that carotid artery stenting for symptomatic or asymptomatic carotid disease represents an improvement in patient welfare over carotid endarterectomy, and most evidence suggests that stenting is less safe under typical clinical circumstances (1,8,9). It seems reasonable to ask if there might be a place for this procedure in particular situations of risk, for example, radiation injury where surgical dissection and tissue healing are problematic, previous endarterectomy where surgical dissection is hampered by scar tissue, or unusual situations where a contralateral lower cranial nerve injury already exists and the addition of a new nerve injury would represent a significant injury to the patient. However, these situations represent a minority of patients with moderate or severe carotid disease.

Several randomized trials have been performed comparing endarterectomy and carotid stenting (with or without angioplasty) (10–17). All, or virtually all, of these studies of endarterectomy versus stenting have come up with the same answer, which is that under the strict conditions of a rigorously monitored trial with experienced surgeons and thoroughly screened interventionalists, carotid artery stenting is not as safe as endarterectomy (1). Overall stroke

and death rates within 120 days of carotid artery stenting are in the range of 8.9%, whereas endarterectomy patients show a rate of 5.8% based on data from several studies (18). While results for patients under 70 years are more equivalent between the two procedures, these pooled numbers reflect the extreme discrepancy of adverse events in the age group >70 years, 12% complication rates following stenting versus 5.9% following endarterectomy. One major trial was discontinued by its safety committee (15) due to the unacceptably high 30-day incidence of death or any stroke during the progress of the trial, 3.9% following endarterectomy, and 9.6% following carotid stenting. The major trial in the United States, CREST (16,19), evaluated clinical outcome on the basis of an aggregate of the incidence of stroke, death, and myocardial infarction, and found no significant difference between the stenting and endarterectomy groups. However, myocardial infarction was defined as any rise in the postprocedure enzyme assay, which skewed the aggregate score in favor of stenting. Setting cardiac enzymes aside, the risk of stroke or death in the CREST study was significantly higher in the stenting group 6.4% versus 4.7% for the endarterectomy group, while myocardial infarction or enzyme elevations were more common in the surgical group.

The conclusion taken from these trials and editorial critiques often seems to be that “carotid stenting is almost as good as carotid endarterectomy and with the correct protective devices and rigorous screening of interventionalists, carotid stenting might come out on top eventually,” or so one might conclude from the observation that ordering still more trials seems to be the outcome whenever carotid stenting fails to outrun endarterectomy. Even at that, however, trial conditions are currently still biased in favor of carotid stenting. The clinical events examined in the trials to date, death and stroke, have dominated attention in this field. Relatively little attention has been paid to more subtle or comprehensive neurocognitive markers of brain performance following one procedure or the other. One randomized study of symptomatic patients (11) with results along the lines of those already discussed found significantly higher clinical rates of stroke within 30 days following stenting (7.4%) versus endarterectomy (4%). However, they also found that DWI brain injuries 1-day posttreatment were seen in 50% of stent patients and only 17% of endarterectomy patients. At 1-month posttreatment FLAIR injuries were present in 33% of stent patients and 8% of endarterectomy patients (20). Within this study, these numbers were even worse (73% of stent patients had DWI findings postprocedure) at centers where cerebral protection devices had been used during the stenting procedures. Several other authors have made similar observations in the comparison of stenting and carotid endarterectomy to the effect that clinically silent DWI injuries are much more common following stenting procedures, 34% to 71% of stent patients, compared with <10% of endarterectomy patients (21–29). Furthermore, the extent and number of lesions are greater in the stenting group, with substantial numbers of lesions showing up in alternative arterial distributions following stenting, in contrast to endarterectomy where the lesions are more typically confined to the artery undergoing surgery. The presumed explanation for this observation is the risk posed to the patient by aortic arch disease and navigation of devices across the ostia of major vessels.

So far, the different question of whether carotid stenting is more effective or safer than best medical management, akin to the question asked about endarterectomy in the original ACAS and NASCET studies, has not been addressed.

There are two separate and distinct worlds. There is the domain of rigorously controlled trials in which some attempt at standardization of the patients and the level of training of operating physicians is made, and from this world the data cited above are generated. The real world of medical practice is not the same. When carotid endarterectomy was first demonstrated to be effective, the major paper of the NASCET trial concluded: “Our final results do not justify a large increase in the rate of endarterectomy. We recommend restraint” (3). Such restraint was not forthcoming in the years that followed, and substantial correction to the excessively liberal practice of endarterectomy among Medicare patients, particularly in some geographic areas, eventually proved necessary, reducing the rate of inappropriate surgery from 32% to 8% (30). Based on less convincing evidence than that shown in the NASCET trial, the same phenomenon is likely to take place with carotid stenting in the years to come. Already 30-day mortality rates among Medicare patients undergoing carotid stenting (1.9%) exceed mortality rates in the CREST trial (0.7%) (8). More than 80% of Medicare patients undergoing carotid stenting are >70 years in age, the very group least suited for this procedure in the randomized trials referenced above (31), and nearly one-third of them are >80 years, a group very prone to complications following stenting in controlled trials.

From the point of view of the physician who simply wishes to do a good job for his/her individual patients, there is little to guide one in technical or procedural recommendations (Figs. 31-1–31-9). Some authors are adamantly in

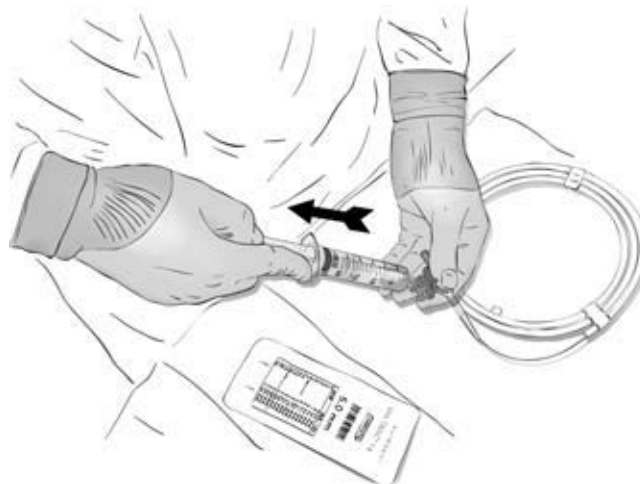


FIGURE 31-1. Preparation of an angioplasty balloon. A common error is made in preparing a double-lumen angioplasty balloon by pushing the solution of 50% contrast into the balloon and extracting it out again with the syringe. This will destroy the slick, factory-made profile of the balloon, which can be critical for very tight stenoses. Using a winker or jabster on a contrast syringe, fill the hub of the balloon catheter with contrast, and attach the syringe with a three-way stopcock. Use only extraction force to place the balloon lumen under negative pressure, and by working the syringe back and forth, most or all of the air within the balloon can be extracted without inflating the balloon.



FIGURE 31-2. Angioplasty balloon inflation. Balloon inflation is performed extremely slowly, particularly for intracranial cases. The vessels needs to be *stretched*, not cracked open. As the contrast appears within the balloon on screen and the waist of the target stenosis becomes evident in the contour of the balloon, slow the rate of inflation down to fractions of an atmosphere per minute. It is infinitely easier to come back repeatedly during a procedure for several iterations of a timid inflation technique than it is to undo a ruptured vessel. For carotid stenosis lesions where the patient is awake, slow inflations are preferable as well, in order to avoid trauma to the stenosis or induction of a carotid body vagal reflex bradycardia. There is no need to panic if the patient becomes ischemic during the inflation because an immediate deflation will relieve the symptoms straight away. For patients with complete and abrupt intolerance of any measure of carotid occlusion, an infusion of sodium amytal immediately prior to a balloon PTA will buy a minute or two of suppression of hemispheric metabolic requirements, similar to that seen in Wada testing, while the balloon angioplasty is performed. Notice that the diagram was inadvertently drawn with omission of the three-way stopcock between the inflation handle and the balloon shaft. The stopcock is vital for the deflation portion of the procedure.

favor of using cerebral protection in the form of balloons or filters and their argument seems cogent (32). It seems to make sense that a 100 μm filtering mesh or complete arrest of flow above the stent site must lend some protection to the brain. Others have analyzed their data and concluded that protection devices have no impact on outcome and could represent a risk of complications independently of other factors (33). Their argument is that crossing an atherosclerotic plaque of dubious integrity with a complex device, deploying that device in the carotid artery, retrieving that device through the stent afterward, or in the case of balloon arrest of flow, advancing a 9F catheter in the aorta and common carotid artery have all got to be hazardous to the welfare of the patient. Use of a filter certainly adds to the complexity of a carotid stent case and may be associated with more showering of hits on transcranial Doppler and DWI changes than unprotected procedures (34–36). Even the safest design of stent is not clear. A closed-cell design is advocated by those who believe in the theoretical capacity of the metal struts to pinion down (“scaffolding”) potentially itinerant

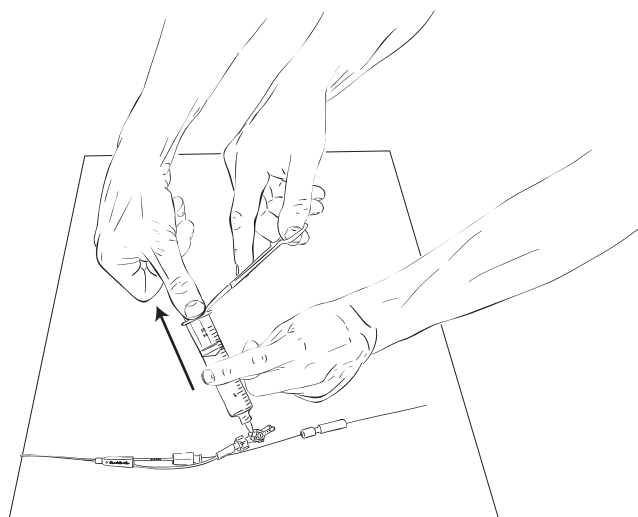


FIGURE 31-3. Angioplasty balloon deflation. Depending on the size of the inflated balloon, deflation is usually performed with a 20-mL or 60-mL syringe attached to the side port of the three-way stopcock. Due to viscosity of contrast, the deflation is often slower than one would desire, especially when the patient has become ischemic and the proverbial Three Ring Circus atmosphere suddenly prevails. Sustained negative pressure can be achieved by having an assistant clamp the piston of the evacuating syringe with a forceps in the withdrawn position.

plaque during vessel expansion or postdilation (32). However, closed-cell design stents have other features such as diminished flexibility and pliability compared with open-cell design, which might be theoretically disadvantageous from the point of view of vessel compliance and distortion of native anatomy, particularly in a tortuous vessel. Comparison of closed- and open-cell design stents on the basis of clinical complications shows no major differences between the two designs in immediate complications or MRI findings (37). Hemodynamic and rheologic differences between closed- and open-cell design stents are measurable, however, in that peak systolic velocities in the carotid artery are more than twice as likely to be in the elevated range following closed-cell design stent placement compared with open-cell design (38). Whether this differential impact of stent designs on vessel compliance and on the hemodynamics of flow has a significant outcome on long-term cerebrovascular health is not known.

▶ EXTRACRANIAL VERTEBRAL ARTERY ANGIOPLASTY AND STENTING

Symptomatic extracranial vertebral artery atherosclerotic occlusive disease is a condition with a poor natural history (39). While it has not received the detailed scientific scrutiny accorded to “typical” carotid artery disease in the form of randomized controlled trials, some differences between carotid and vertebral artery disease are evident and are relevant to the clinical decision-making process of whether to attempt endovascular repair in a symptomatic patient.

Symptomatic posterior circulation atherosclerotic disease has an incidence of stroke or death within 1 year of approximately 5% to 11%, and transient ischemic attacks related

(text continues on page 470)

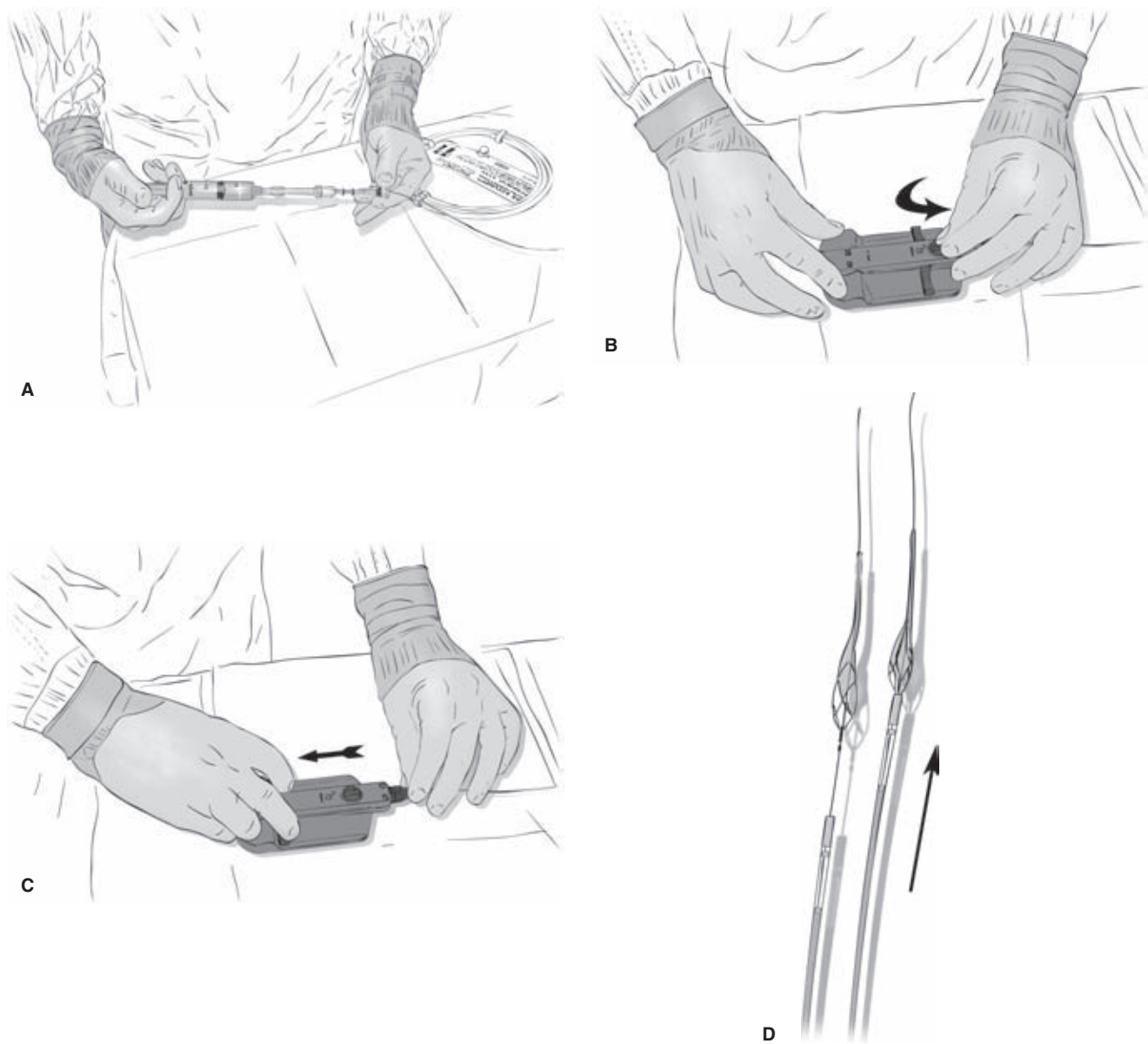


FIGURE 31-4. (A–D) Preparation and deployment of the Acculink stent and Accunet protective device. The Accunet protection device requires a very diligent preparation through flushing in advance (A) to avoid binding of the elements within the patient when one attempts to deploy the protective filter. The stent (Acculink) deployment system is easy to use and stable. A protective lock on the handle is rotated according to provided instructions, (B) and the stent is deployed by retraction of two handles on the base (C). The Acculink stent series includes the option of using tapered stents, that is, flared proximally to a wider diameter to accommodate the likelihood that the distal common carotid artery will be included in the stent site in most patients. Ideally, one wishes to choose a stent that nominally is 1 mm or, preferably, 2 mm wider than the estimated diameter of the target vessel. After deployment of the stent, the resheathing catheter is inserted through the stent up to the base of the protective filter, which is then constrained and withdrawn through the stent (D). All of these steps, even with well-designed and manufactured equipment, are fraught with potential problems, and the learning curve is steep and long.

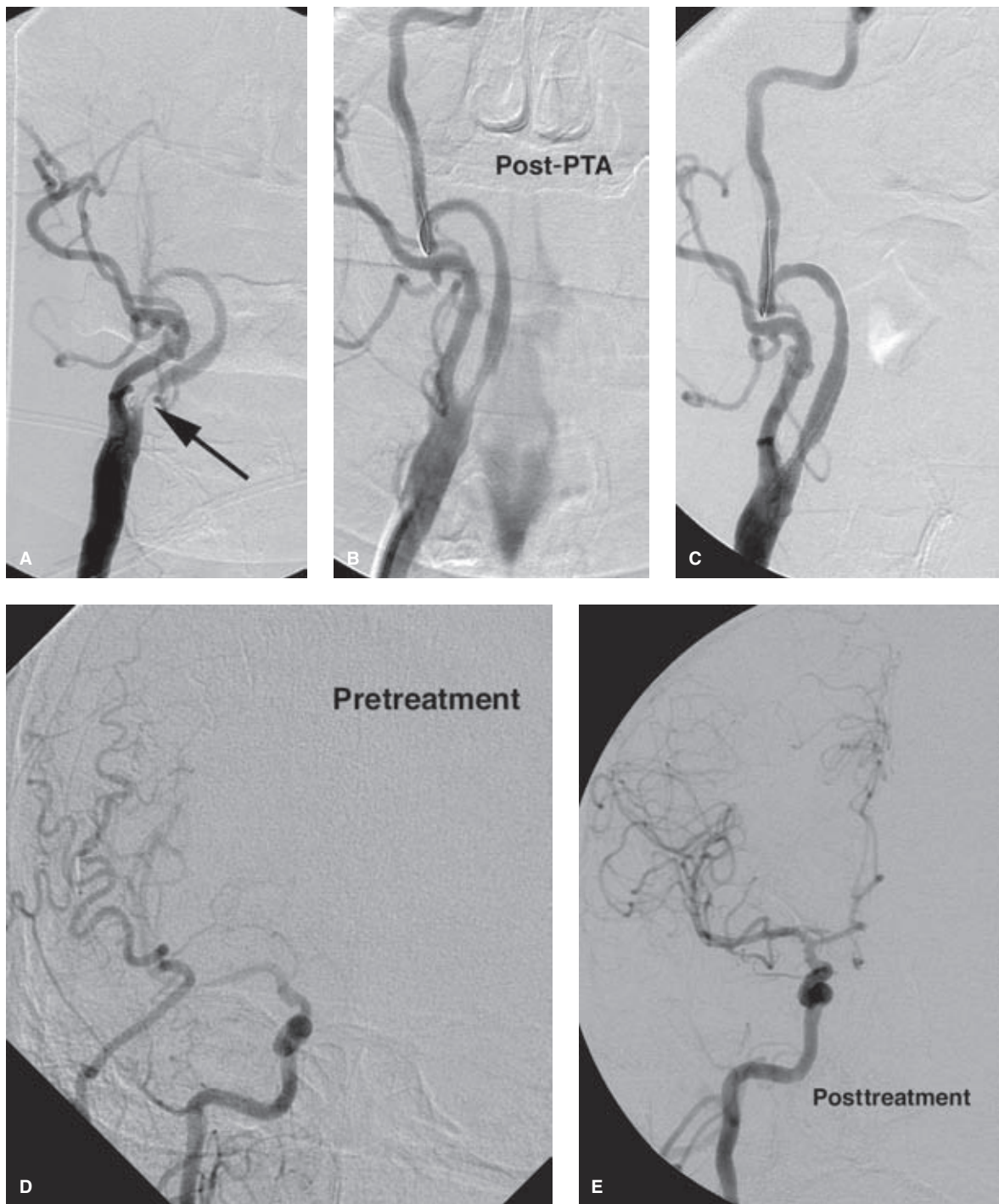


FIGURE 31-5. (A–E) Unprotected carotid angioplasty and stenting in a tortuous vessel. This patient presented with watershed infarctions in the right hemisphere due to a severe stenosis (>90%) of the right internal carotid artery (*arrow* in **A**). The cervical right internal carotid artery is slow and compromised. The tortuosity of the cervical carotid artery made deployment of a protective device difficult, and although the artery could be straightened out using the “buddy wire” system, that is, making it an offer it cannot refuse with a stiffer wire, it was opted to treat the stenosis in this case without the protective system. The initial angioplasty results (**B**) with a 4-mm coronary balloon were auspicious. After deployment of an 8 × 30 stent, a persistent waist on the stent was evident (**C**) but was not pursued due to the risks of postdilation, particularly without cerebral protection. The pre- and post-treatment intracranial images (**D** and **E**) show the substantial changes in intracranial hemodynamics brought about through this procedure.

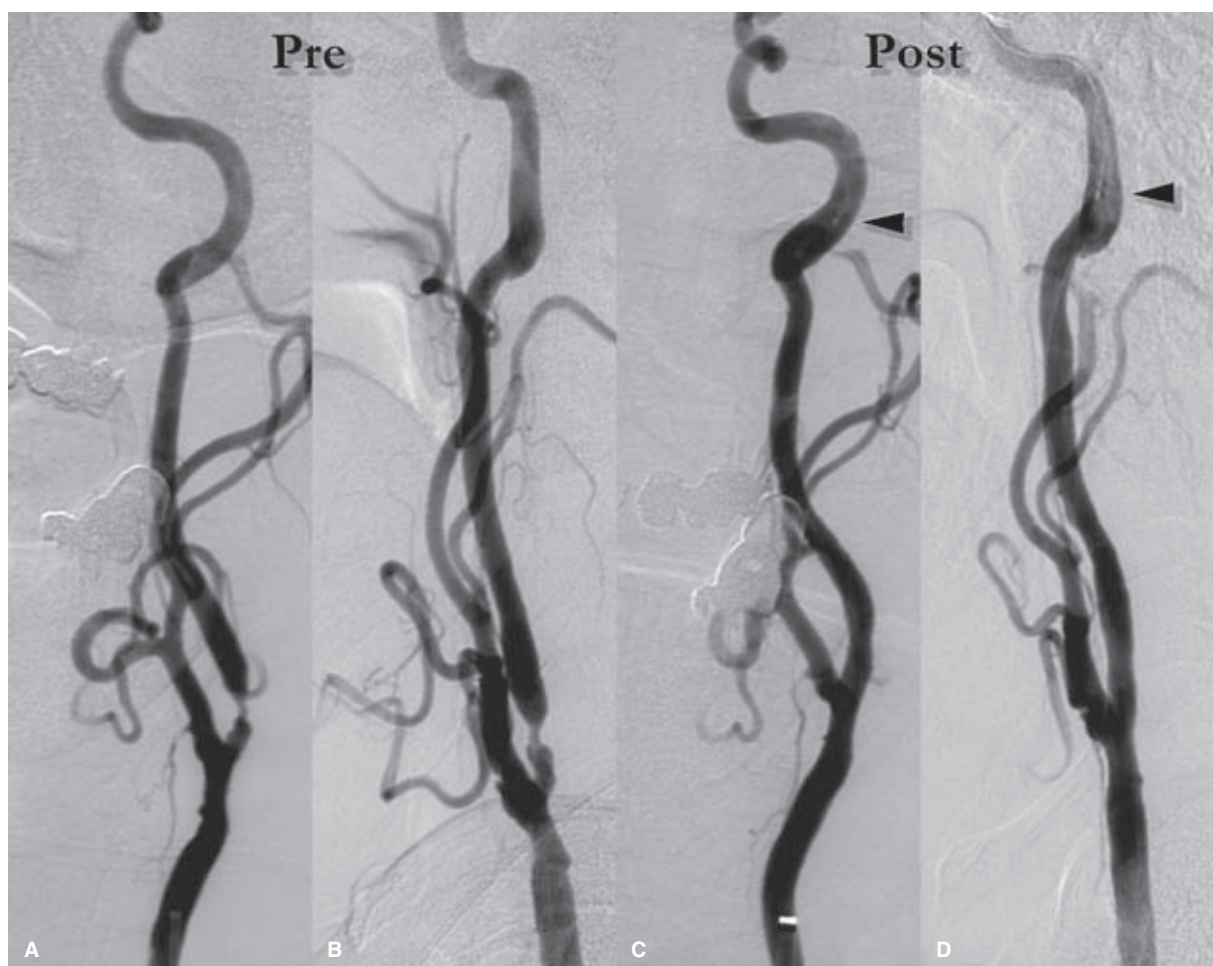


FIGURE 31-6. (A–D) Protected carotid angioplasty and stenting. AP and lateral images of the pretreatment (A and B) and posttreatment (C and D) angiograms of the left carotid artery in what appears to be a relatively straightforward case. The cervical carotid artery above the lesion is smooth and straight and offers no obvious obstruction to passage of the protection device. Nevertheless, some hazards are inevitable. Crossing the lesion initially may prove difficult with any of the protective devices that offer less control than does a standard microwire. Therefore, an initial unprotected angioplasty might still prove necessary before navigation of a protective device is possible. Adequate room above the lesion must be allowed for lest the stent-delivery system should run into the protection device too soon (*arrowheads*), thus preventing the stent itself from straddling the lesion adequately.

to extracranial vertebral artery disease portend a stroke rate of approximately 30% over 5 years (40–43). The neurologically debilitating nature of even small strokes in the posterior circulation compared with the carotid circulation is not reflected in these numbers, but adds to the urgency of efforts to help patients with these conditions (39).

Furthermore, the surgical options available for carotid revascularization are not freely available in the case of vertebral artery disease. Open surgical procedures involving reimplantation of the vertebral artery origin or ostial endarterectomy are associated with complications rates of 10% to 20% and these procedures are generally not viewed favorably even by surgeons (41,44).

An additional major feature of contrast with isolated carotid artery disease is the strong association between vertebral artery occlusive disease and symptomatic arterial

disease elsewhere (45). This population of patients tends to demonstrate more consistent patterns of generalized arterial disease of the carotid arteries, the coronary circulation, the intracranial vessels, and peripheral arterial system. This translates into a high association with morbidity and mortality elsewhere in the body not primarily ascribed to the symptomatic vertebral artery lesion.

In the absence of randomized trials, several case series indicate a favorable risk and efficacy profile for angioplasty and stenting of the proximal vertebral arteries in symptom relief and extended clinical outcome (10,45–52). Technical feasibility of the revascularization procedure with either bare-metal or drug-eluting stents approaches 100% with procedural complication rates of <2% and almost universally satisfactory angiographic restoration of luminal patency. The problems with vertebral artery procedures of

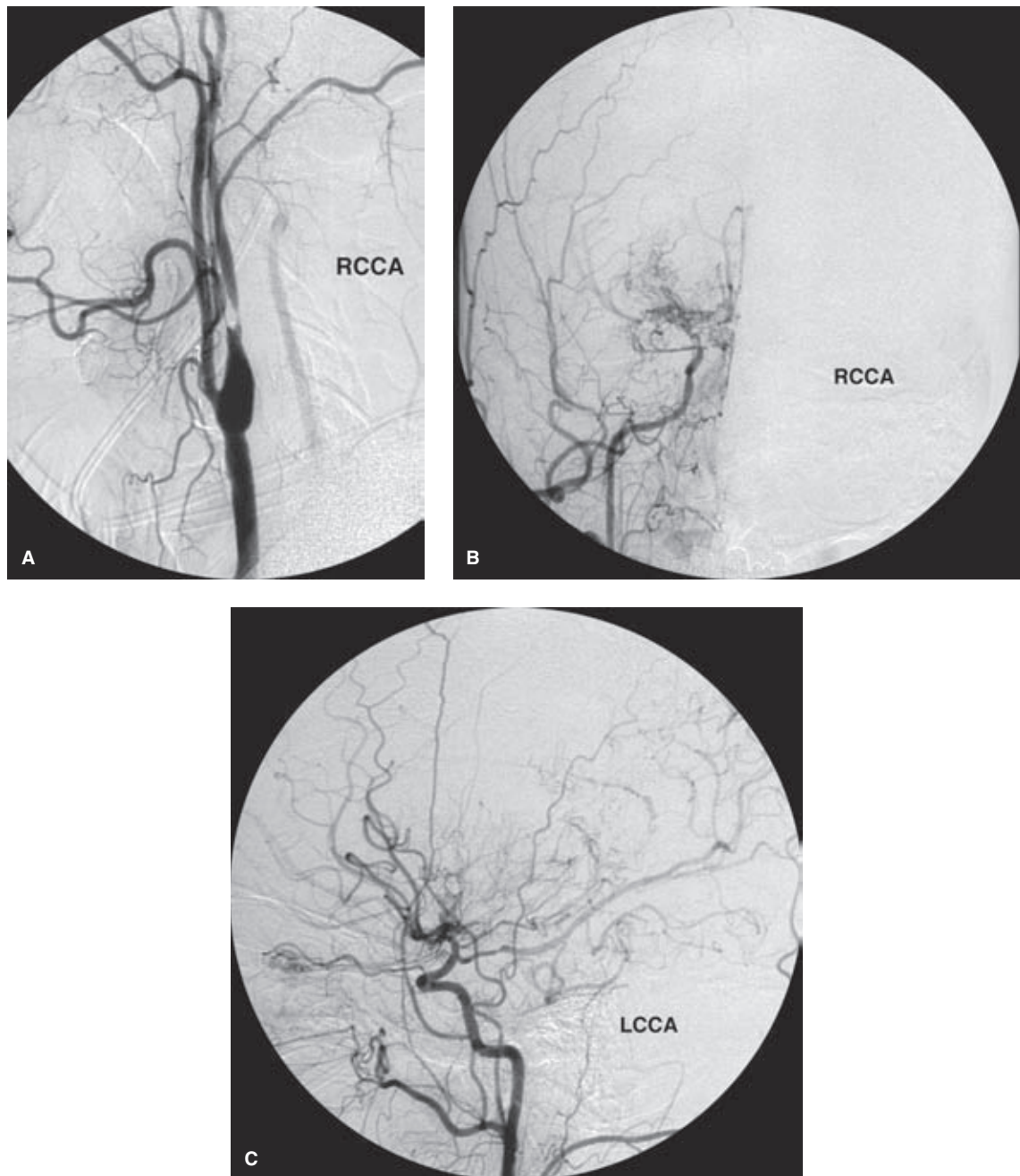


FIGURE 31-7. (A–C) Symptomatic carotid stenosis possibly better not treated by stenting. A 46-year-old female with right amaurosis fugax and left hemispheric ischemic symptoms, 5 years status post previous right carotid endarterectomy, was referred for treatment of the right carotid artery and evaluation of the left. The right carotid bifurcation (A) shows a severe stenosis as predicted from the Doppler examination, but the surprising finding was the unsuspected Moyamoya pattern of intracranial flow bilaterally (B and C). While an angioplasty and stent of the right internal carotid artery might relieve the symptoms of amaurosis fugax on that side, the significance of those symptoms lies in their prediction of the risk of stroke. These data from NASCET are probably not applicable to a patient with Moyamoya occlusive disease. Furthermore, the question of whether reopening the right carotid system might induce a hyperperfusion injury in the right hemisphere needs to be considered. A 2-mm angioplasty of the right internal carotid artery was performed, but this did not seem to suggest the opening of a middle or anterior cerebral artery intracranially, and more definitive endovascular treatment was therefore not pursued in this patient as a result.

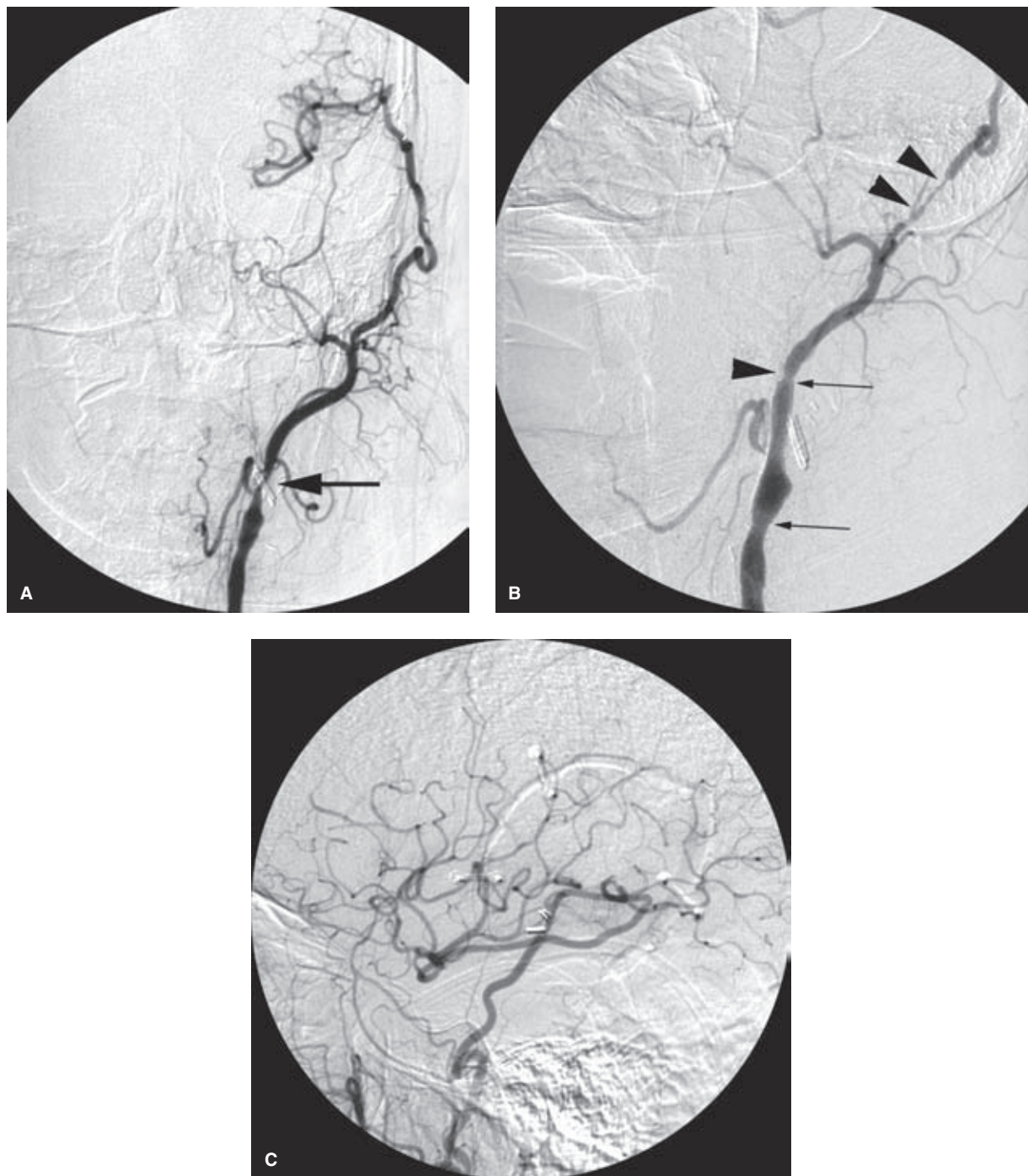


FIGURE 31-8. (A–C) Symptomatic external carotid artery stenosis proximal to an ECA–MCA bypass. A patient with a previously successful left external carotid endarterectomy for restoration of a left ECA–MCA bypass presented after several years with new ischemic deficits in the left hemisphere thought to be related to hypoperfusion from recurrent stenosis (*arrow* adjacent to surgical clip in **A**). The case was conducted with the same routine that one would apply to a stenotic left internal carotid artery lesion—a 4-mm angioplasty followed by deployment of a 6–8 × 30 mm Acculink stent extending into the common carotid artery using a 4.5-mm AccUNET protective device. The poststent image (**B**) was satisfactory (*arrows* mark the position of the stent), but there was a good deal of spasm in the superficial temporal artery and above the stent site (*arrowheads*). This was relieved immediately with nitroglycerin 400 mcg IA, and the intracranial lateral view poststenting (**C**) showed no angiographic complications.

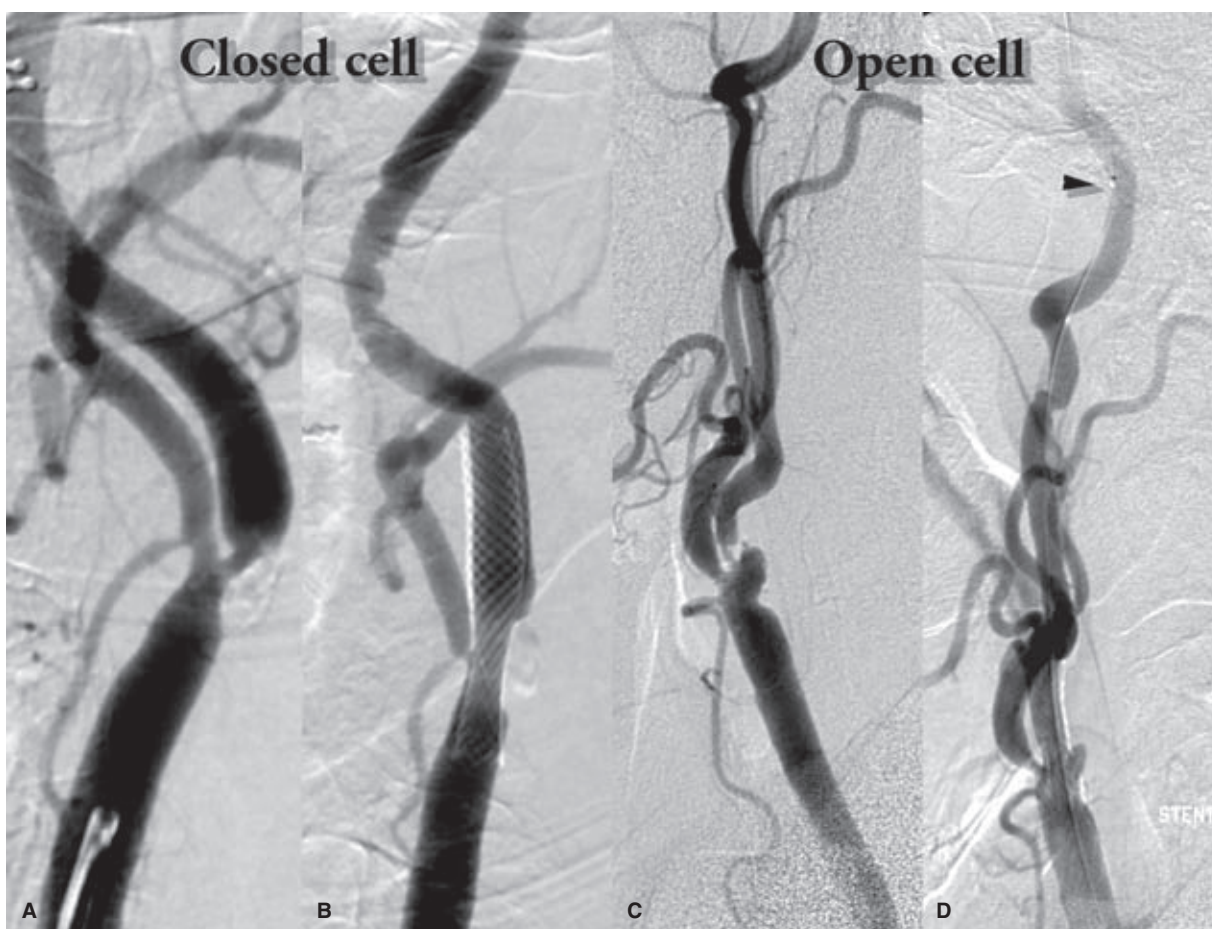


FIGURE 31-9. (A–D) Open-cell versus closed-cell design stents. The pre- and posttreatment images of two patients treated with different stents are shown. The more complex lesion (C and D) has been treated with an open-cell design stent and a protection device (arrowhead). Despite the complexity of the second case, wall apposition is better in the case of the second stent (open-cell) both in the internal carotid and in the common carotid artery. Furthermore, the extent of straightening of the native anatomy is more starkly evident in the case of the closed-cell stent. Notice the prominent spasm of the carotid artery (D), a common and easily reversed problem encountered with protection devices. One must be careful, however, not to dissect the carotid intima when retrieving the protection devices in a situation such as this or in tortuous anatomy.

this nature, particularly those related to the vertebral artery ostium, lie with long-term patency, stent fracture due to the shearing motion induced by the adjacent subclavian artery, stent recoil and compression, and in-stent stenosis (Figs. 31-10 and 31-11). Significant restenosis rates within 2 years of 43% or greater can be seen with bare-metal stents (48,50,52), with some authors reporting reduced rates of restenosis with use of drug-eluting stents, but other reporting no significant differences in outcome (51).

Vertebral artery stenting is generally easier to perform than is the case in the carotid artery. Protection devices are not used, simplifying the procedure from a technical point of view. Procedural difficulties can arise with achieving a stable position for the introducer catheter in the subclavian artery (Fig. 31-12), a problem sometimes circumvented by retrograde radial artery access. A self-expanding stent of a size and radial strength appropriate for the vertebral artery origin (3.5 to 4.5 mm) is not available, and most cases are performed with a balloon-expandable stent. Landing the stent very precisely so that it opens the ostial lesion to a sufficient degree but without ungainly protrusion of tines into

the subclavian artery lumen can be difficult. The motion of the subclavian artery with the cardiac cycle makes road-mapping invalid as a guide in this situation. The best course is to deploy the stent slowly, puffing contrast through the introducer catheter intermittently and adjusting the stent catheter position until the expanding balloon lodges against the arterial wall. Postdilation of the stent site to achieve maximal expansion and intimal apposition is generally encouraged and does not appear to carry as many risks as poststent dilation in the carotid artery. Using a drug-eluting stent will require continuation of dual-antiplatelet agents for a minimum of 1 year.

▶ INTRACRANIAL ANGIOPLASTY AND STENTING

Symptomatic intracranial atherosclerotic stenosis is one of the commonest causes of stroke worldwide with a natural history of high probability of recurrence in the short and long term (53–56). The prevalence among certain ethnic

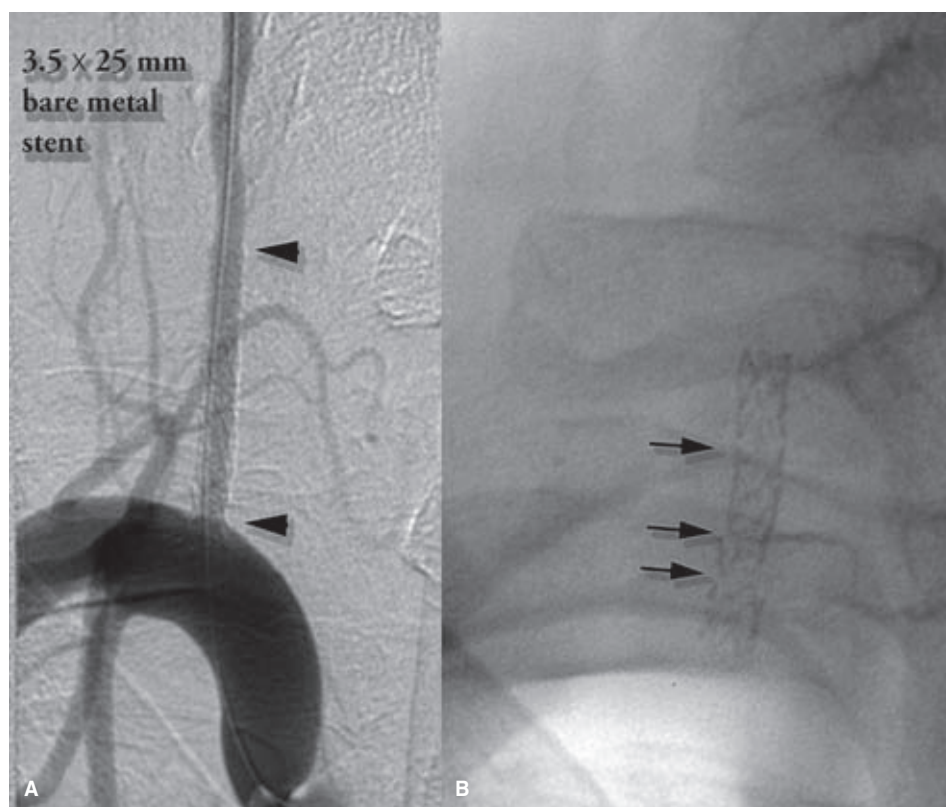


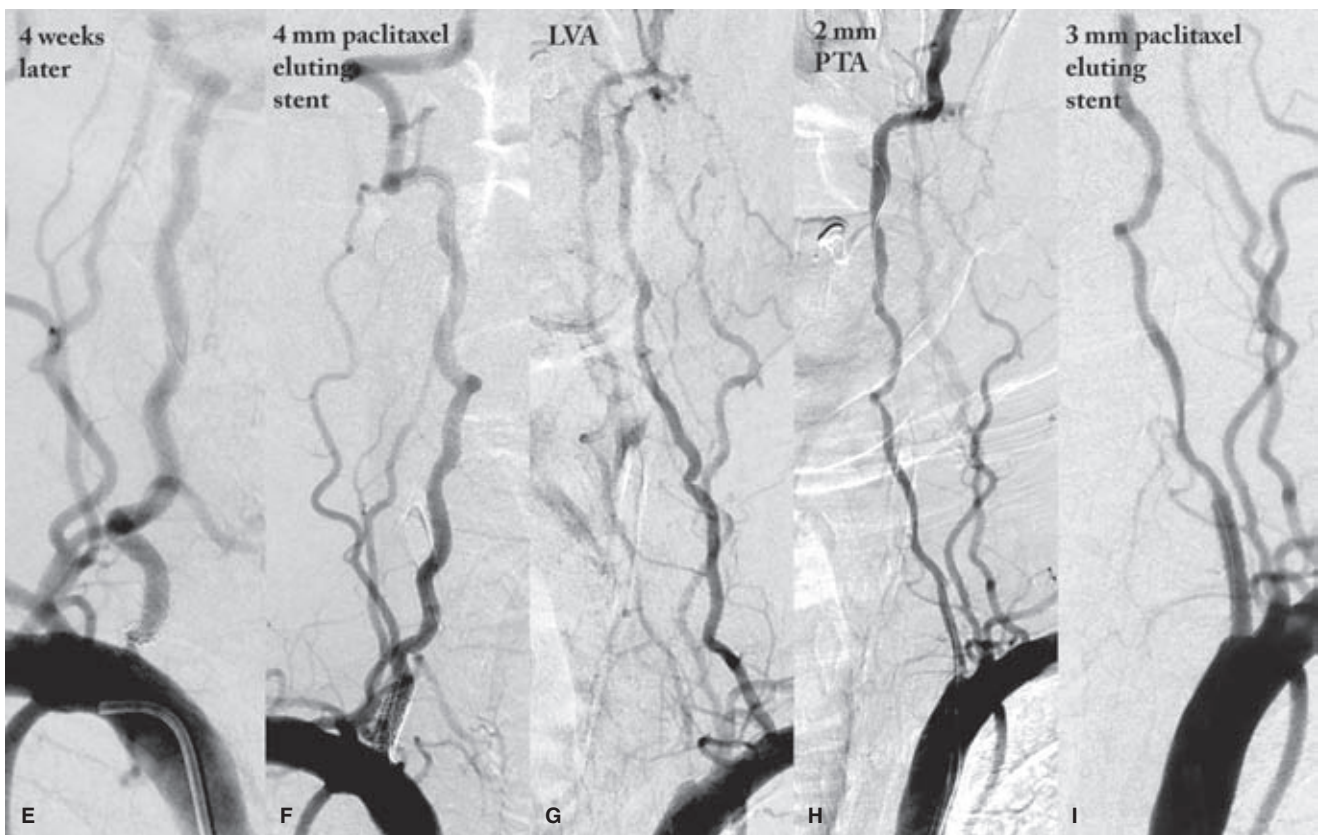
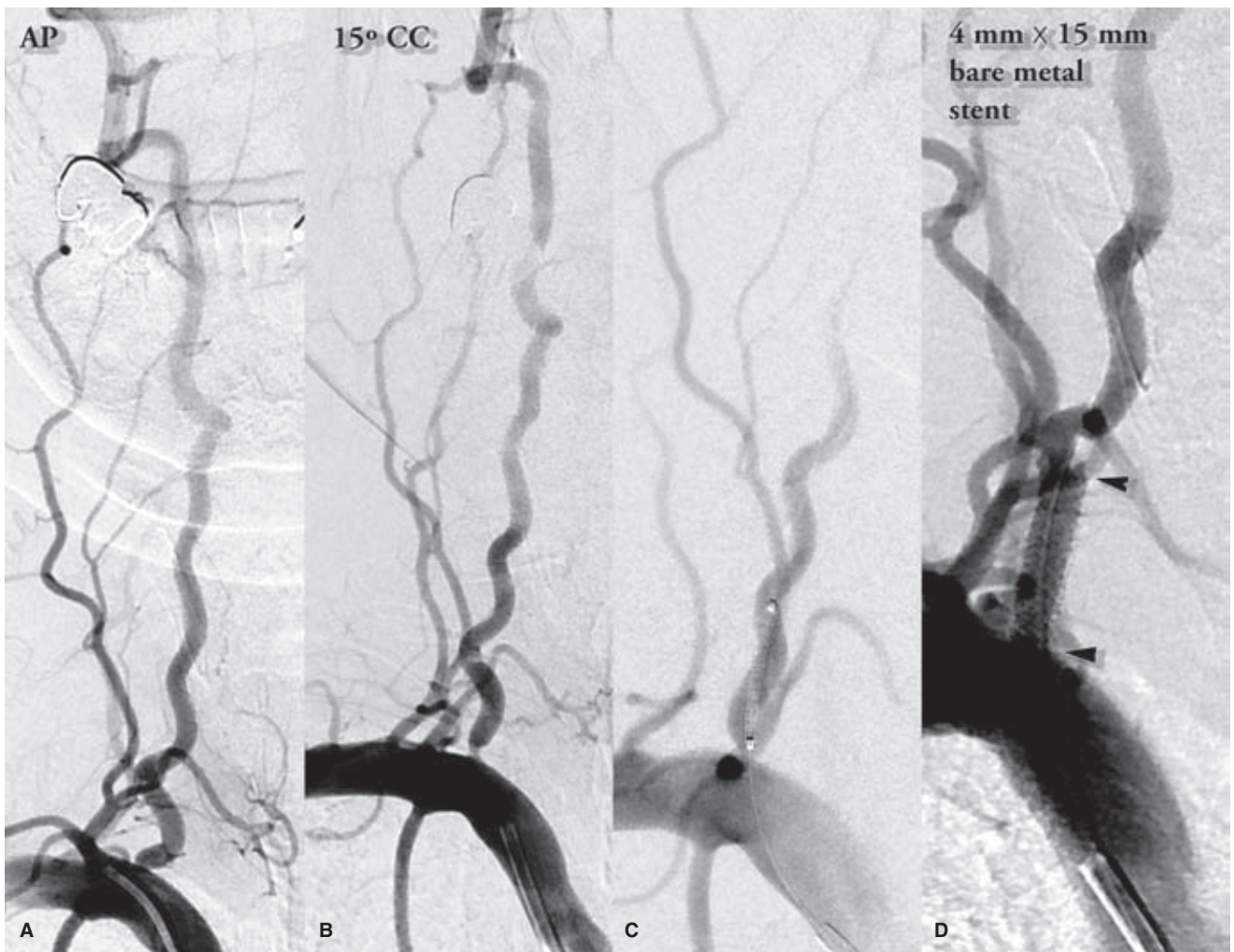
FIGURE 31-10. (A–B) Fragmentation of a vertebral artery ostium stent. Short-term follow-up (<12 months) in this patient shows a common problem with the stenting of the vertebral artery origin. A very esthetically pleasing result was obtained (A) with a coronary stent with good relief of symptoms immediately. At the time of stent placement, it was noted that an extraordinary degree of movement of the stent was present with each cardiac cycle. The patient returned some time later (B) with recurrent 70% stenosis and multisegmental fragmentation (arrows) of the stent.

groups is particularly high, making this more of a global medical challenge than is immediately evident in the West.

For many years patients with symptomatic intracranial atherosclerotic disease were treated with warfarin anticoagulation. This ended in 2005 when the WASID study randomized treatment of symptomatic patients with 50% to 99% intracranial stenoses to either warfarin or aspirin and found that warfarin was associated with significantly higher rates of adverse events for no benefit. Strokes, hemorrhages, and nonvascular deaths were all higher in the warfarin-treated group (57).

In 2011 the SAMMPRIS study demonstrated that optimized medical therapy for symptomatic intracranial stenoses >70% far surpassed percutaneous angioplasty and stenting in safety and efficacy (40). Patients were randomized to aggressive medical management alone, including dual-antiplatelet therapy, or to a combination of medical management and endovascular intervention using the Wingspan stent system. Enrollment was stopped when it became evident that the 30-day stroke or death rate was 14.7% for the endovascular group versus 5.8% for the medical group. The results of the SAMMPRIS study are not surprising to

FIGURE 31-11. (A–I) Short-term recurrence of right vertebral artery stenosis and virtual occlusion of the left vertebral artery origin treated with drug-eluting stents. This patient demonstrates many features commonly encountered in vertebral artery stenting. Firstly, the patient had multivessel disease, such that most of his intracranial circulation depended upon the right vertebral artery. Secondly, images (A) and (B) show that it can be easy to overlook a significant stenosis of the vertebral artery ostium unless a profile view is sought out. In this instance inclining the AP plane 15 degrees cranio-caudad was critically important both for measuring the stenosis and for a clear target whereon to land the stent. Image (C) is included to demonstrate how little room there is for error in where to land the stent at the vertebral artery origins in contrast to the carotid arteries. Repeated short DSA runs or injections of contrast as the balloon inflation starts will be necessary, and in this case very slight retraction of the stent was necessary. Due to vessel motion with the cardiac cycle, relying on road-map images will not be adequate. In this instance, using a bare-metal 4-mm coronary stent, a very satisfactory angiographic result (D) was obtained. The patient returned within 4 weeks with recurrent symptoms, even before his appointment in the clinic had time to happen. A significant recurrence of stenosis within the first stent (E) is evident, treated on this occasion with a drug-eluting stent (F) within the first. Because of his bad overall prognosis—the patient has previously failed an ECA–MCA bypass on the right—an attempt to probe the left vertebral artery (G) proved fruitful, with a 2-mm angioplasty (H) followed by a 3-mm drug-eluting stent resulting in complete reconstitution of the left vertebral artery (I). Whether drug-eluting stents will prove better for craniocervical procedures than bare-metal stents remains to be seen. One could argue that drug-eluting stents at least could not be worse than the efficacy of bare-metal stents as illustrated in cases 31.10 and 31.11, but there is one circumstance in which they could do much worse, which is if the patients are noncompliant with dual-antiplatelet medication. Many patients cannot afford all the medications that we prescribe for them but are reluctant to admit it. Frequently, the most costly drugs are the ones dropped by patients out of consideration of expense (e.g., Plavix), and in the case of drug-eluting stents the likelihood of complications and stent closure are much higher. It is very important to clarify with patients ahead of time that the proposed use of a drug-eluting stent requires a firm commitment from them to a year of dual-antiplatelet agents.



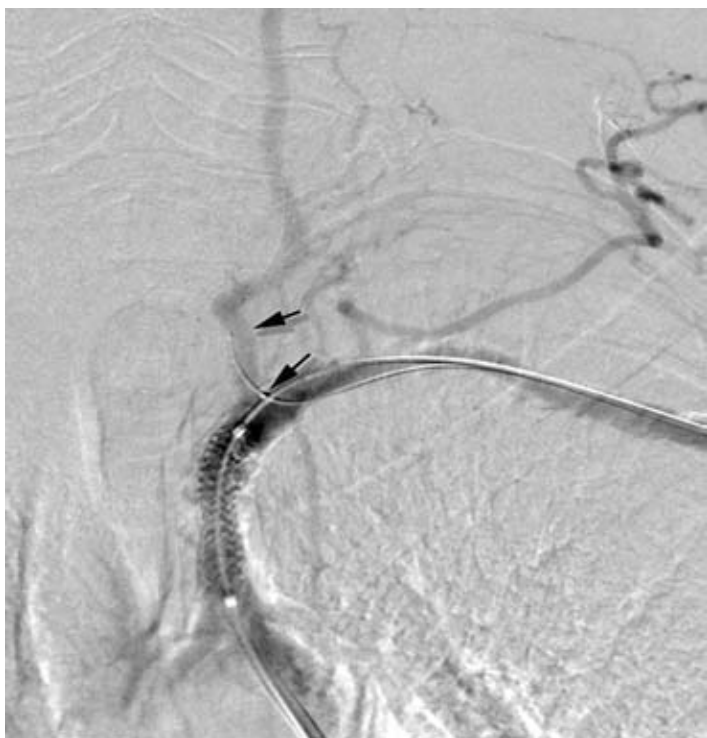


FIGURE 31-12. Transradial catheterization during subclavian artery stenting. In this patient a subclavian artery stenosis has been stented via a trans-femoral approach. A retrograde left transradial approach has been used to catheterize the left vertebral artery with a 4-mm Ascent balloon (*arrows*) on a Synchro wire to protect the left vertebral artery during angioplasty and stent delivery. The transradial approach (Chapter 2) is extremely valuable in many similar procedures, particularly for otherwise inaccessible right vertebral artery origins, either for stenting procedures or for intracranial procedures.

authors who have examined the safety and complication rates of intracranial stenting procedures and who found very similar results (58,59). For instance, a review of intracranial angioplasty and stenting outcomes in 2009 showed a periprocedural stroke or death rate between 0% and 50%, higher rates of procedural complications in the posterior circulation than in the anterior, and restenosis rates of 17% within 6 months (60). Moreover, one needs to consider the publication bias that exists in the literature toward positive or good outcomes, with very few authors of case series or institutional review or even journal editors being eager to publish litanies of disasters, of which there are many in the category of intracranial stenting (Figs. 31-13–31-16).

Although the treatment for symptomatic intracranial atherosclerotic disease is clearly medical for the overwhelming majority of patients, it would, nevertheless, be a mistake to consider that for some patients endovascular procedures should never be considered. This technology is still critically necessary for situations where acute revascularization is imperative, for example, in the course of an acute ischemic stroke intervention or management of a patient with crescendo TIA's and imminent decompensation of the cerebrovascular autoregulatory curve. Short focal lesions in a straight segment of vessel likely lend themselves more to safe intervention, for instance, meaning that the outcome statistics of the SAMMPRIS trial do not necessarily apply to every patient when such interventions are necessary. Furthermore, outcome statistics along the lines of the SAMMPRIS results for endovascular procedural complications might seem very favorable compared with the apparent natural history of some particular patients.

The following technical considerations will be of paramount concern during all intracranial stenting and angioplasty procedures:

1. *Access and support.* Much of the difficulty of these procedures comes late in the case when advancing a stent-delivery catheter or balloon along a wire proves very difficult. Without taking the precaution of placing a robust supporting sheath or even a coaxial support system, the heartbreak of watching one's delivery catheter collapse in the aortic arch dragging the intracranial wire down with it below the lesion is inevitable in some patients.
2. *Wire technique.* Exchanging devices over an exchange-length wire is stressful and difficult (Fig. 31-17). Many hemorrhagic strokes following intracranial stenting procedures are unquestionably due to microperforations related to excessive forward play of the wire. On the other hand, slewing or bowing of the wire outside the body results in retraction of the tip below the stenotic lesion. Lubricate the wire well before all exchanges. Keep the table tidy to minimize snagging during advancement.
3. *Stent Delivery.* The component of the procedure most likely to give trouble is delivery of the stent. Therefore, it is prudent to get as much of the case accomplished in advance of this, that is, with angioplasty, lest ultimate failure of stent delivery be the outcome. In addition, counting on getting a balloon back up into a deployed stent to perform a postdilation is not going to work in many patients. Friction between the balloon and the stent will result in failure to advance the balloon, or worse will cause the stent to move forward, or worse still for the stent to enmesh itself on the balloon. Therefore, if the postangioplasty lumen size is very small and there is no prominent intimal dissection necessitating a stabilizing stent, it might be worth asking if placing the stent on that particular day is really necessary. Intracranial angioplasty alone for atherosclerotic disease is frequently considered
(text continues on page 482)

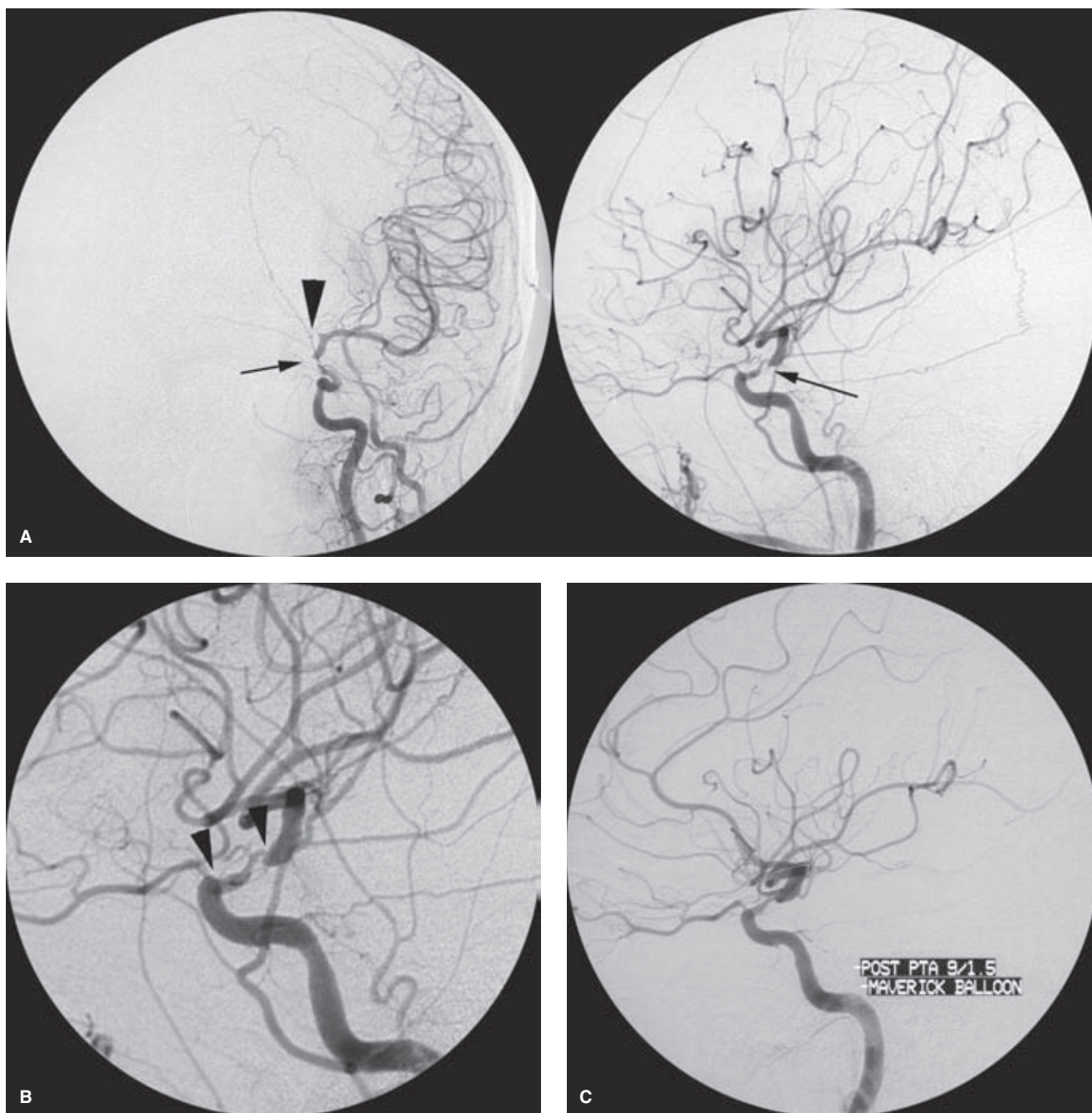


FIGURE 31-13. (A–F) Symptomatic supraclinoid stenosis. A middle-aged female patient presented with ischemic deficits in the left hemisphere. The left internal carotid artery angiogram (A) shows a severe supraclinoid stenosis (arrows) distal to the ophthalmic artery, with no filling of the ipsilateral anterior cerebral artery (arrowhead). The magnified view (B) shows the irregular nature of the stenosis (arrowheads) and the potential for difficulties in crossing it with a wire. An ACS Traverse wire was navigated to the M2 segment through a microcatheter and used to perform angioplasties at 0.5-mm increments, starting with a 1.5-mm Maverick balloon (C) and ending with deployment of a 4 × 9 mm coronary stainless-steel stent (D). (continued)

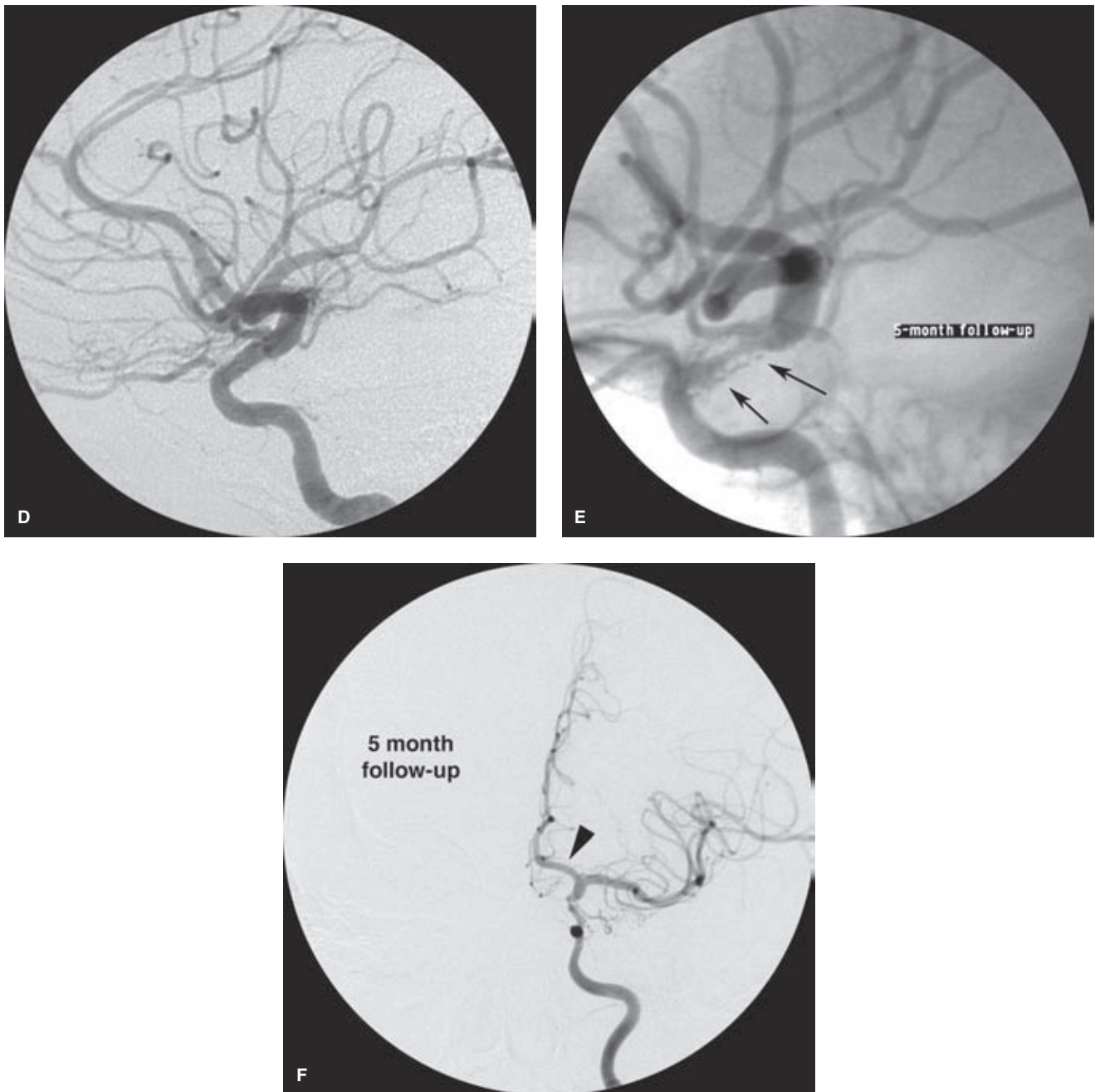


FIGURE 31-13. (CONTINUED) The patient was asymptomatic following the procedure, and although the lateral view at 5-month follow-up (E) shows significant in-stent restenosis, the AP view (F) shows continued robust filling of the anterior cerebral artery (*arrowhead*). The patient has not required retreatment in the 7 years since the original procedure. Drug-eluting stents may have a role in the future for prevention of intracranial recurrent stenosis.

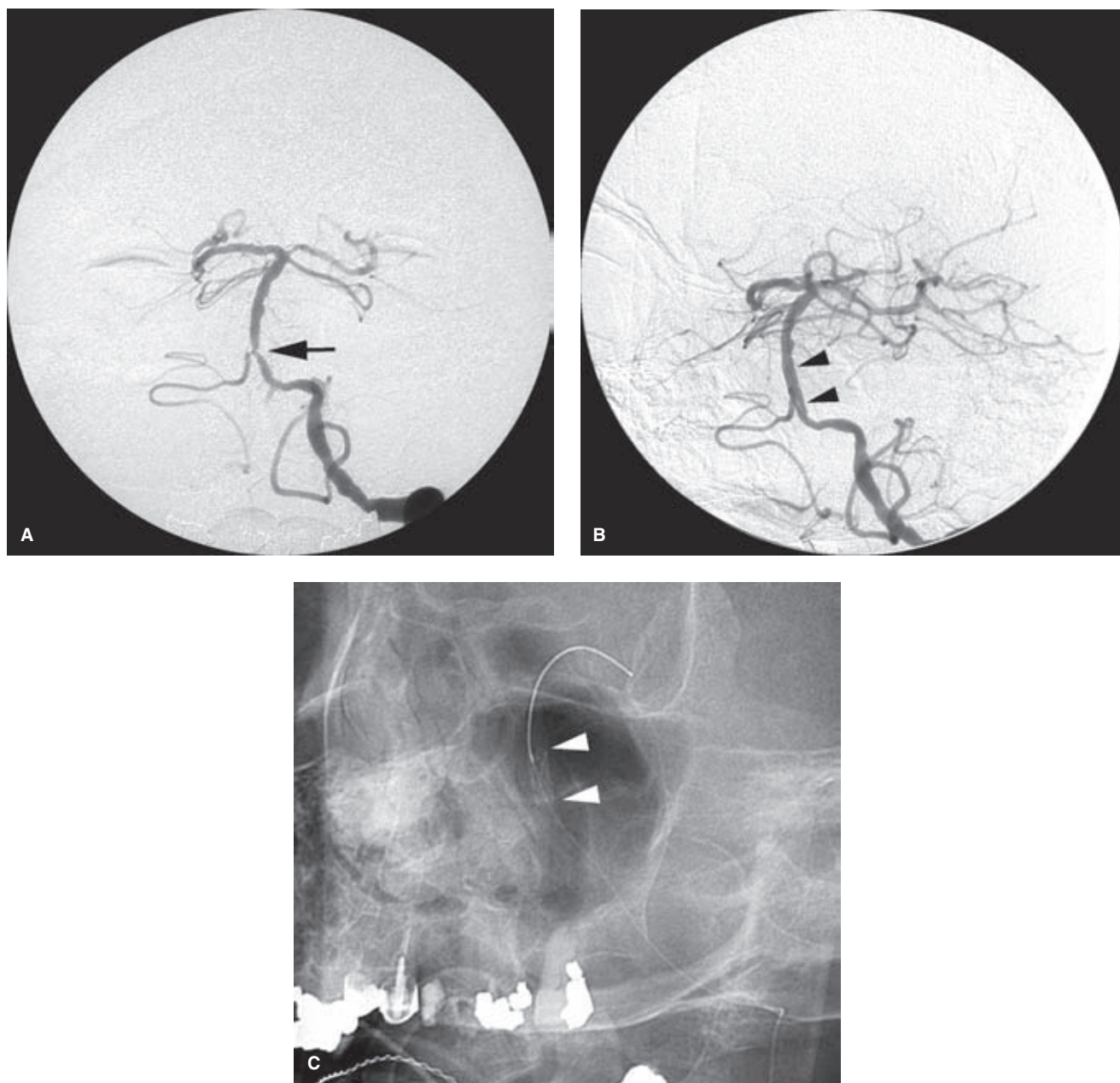


FIGURE 31-14. (A–C) Symptomatic midbasilar stenosis. An elderly patient with intermittent brainstem ischemic symptoms was treated successfully with angioplasty and stenting. The pretreatment image (**A**) shows that the focal stenosis (*arrow*) involves the origin of the right AICA/PICA artery. Despite being jailed by the stent (**B**), the branch artery seems intact after the procedure, an observation that holds through in the experience of most authors with particular reference to the small brainstem perforators involved in cases such as this. The unsubtracted image of the stent (*arrowheads* in **C**) is provided as a reminder of how it can be very helpful to position the target lesion in a lucency of the field so that bone density and subtraction artifact do not impair visualization during the procedure.

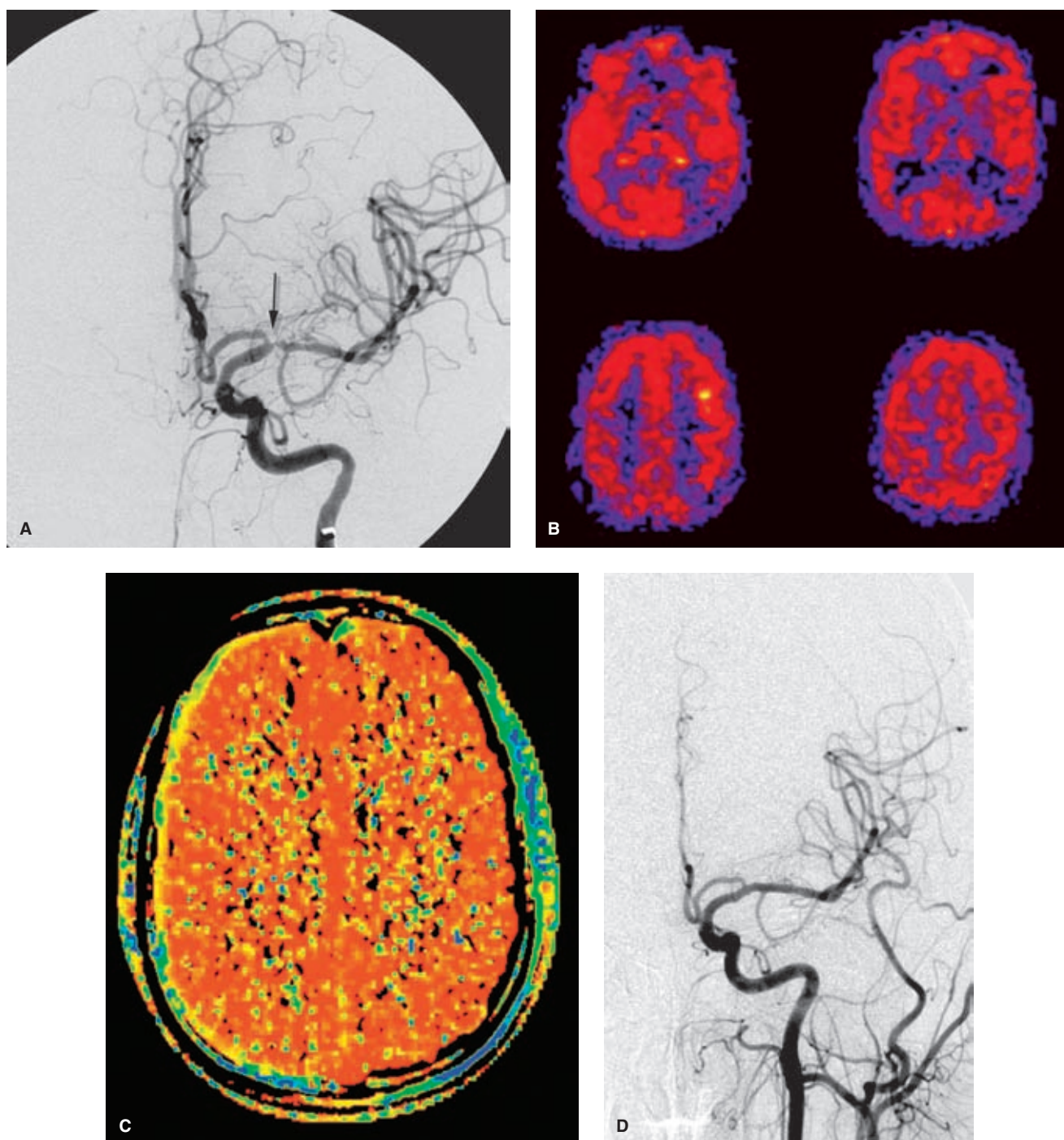


FIGURE 31-15. (A–D) Focal middle cerebral artery stenosis treated with Wingspan stent. A symptomatic middle-aged male patient presented with a focal lesion (*arrow* in **A**) of the left middle cerebral artery, treated with angioplasty and subsequent placement of a Wingspan stent spanning the supraclinoid carotid artery and left M1 segment, thus jailing the left A1 ostium. The patient's pulsed arterial spin labelling (PASL) images (**B**) prior to treatment show a hyperemic lesion in the left frontal area related to a recent ischemic insult and hypoperfusion in a watershed distribution posteriorly in the left cerebral hemisphere. At 6 months posttreatment the patient was asymptomatic with virtual normalization of his perfusion imaging. The MTT image (**C**) from a CTP examination shows no asymmetry between the hemispheres. A follow-up angiogram 1 year after treatment (**D**) shows a very favorable sustained effect of the procedure with normalization of the M1 contour. The Mori classification (61–63) of intracranial stenotic lesions divides lesions into three categories: Type A < 5 mm long and concentric, mildly eccentric; Type B 5 to 10 mm, long or tubular, moderately eccentric, or moderately angulated; Type C > 10 mm, tortuous, angulated > 90 degrees. Technical feasibility, safety, and long-term outcome are all correlated with the type of lesion.

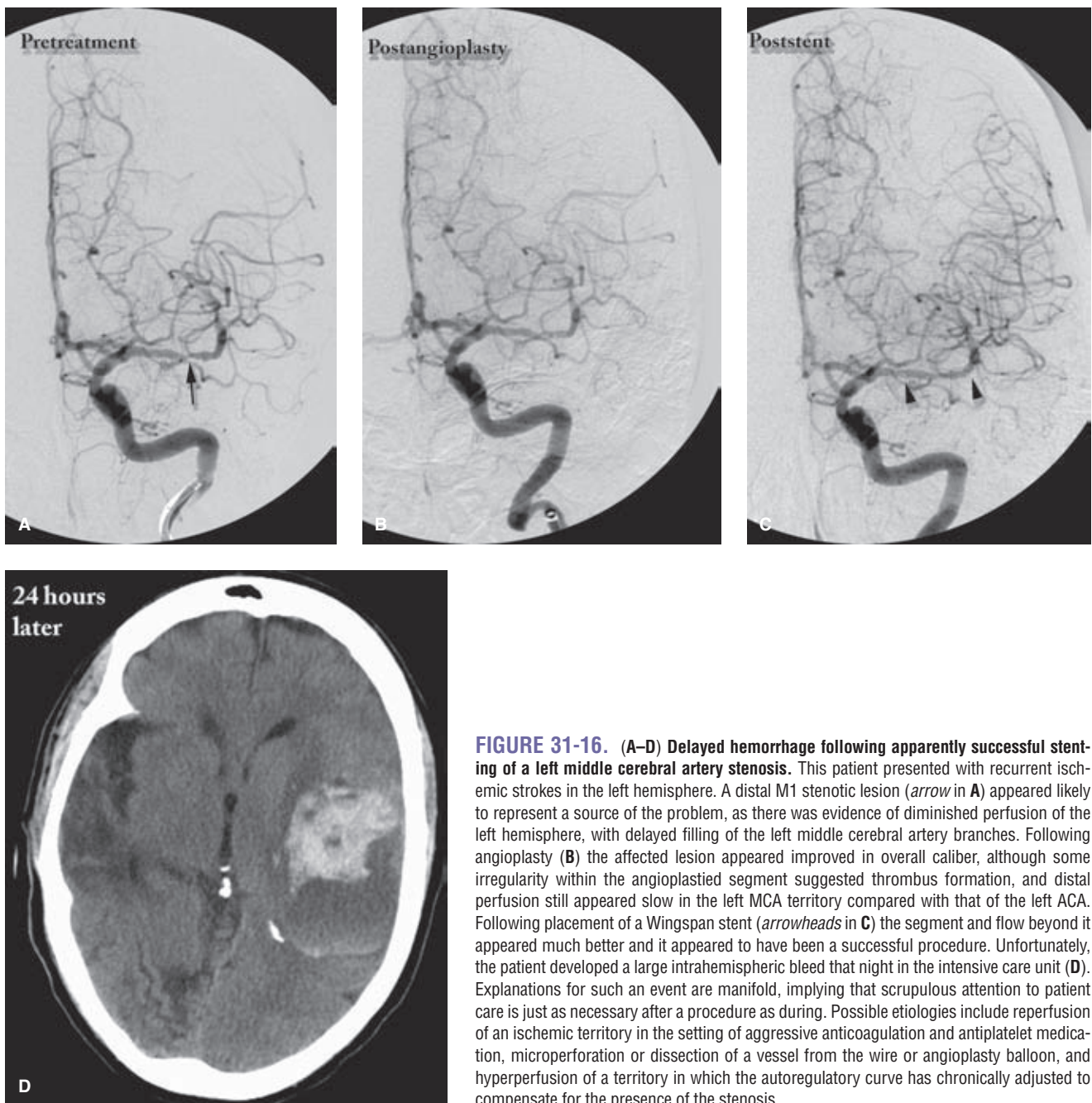


FIGURE 31-16. (A–D) Delayed hemorrhage following apparently successful stenting of a left middle cerebral artery stenosis. This patient presented with recurrent ischemic strokes in the left hemisphere. A distal M1 stenotic lesion (arrow in A) appeared likely to represent a source of the problem, as there was evidence of diminished perfusion of the left hemisphere, with delayed filling of the left middle cerebral artery branches. Following angioplasty (B) the affected lesion appeared improved in overall caliber, although some irregularity within the angioplastied segment suggested thrombus formation, and distal perfusion still appeared slow in the left MCA territory compared with that of the left ACA. Following placement of a Wingspan stent (arrowheads in C) the segment and flow beyond it appeared much better and it appeared to have been a successful procedure. Unfortunately, the patient developed a large intrahemispheric bleed that night in the intensive care unit (D). Explanations for such an event are manifold, implying that scrupulous attention to patient care is just as necessary after a procedure as during. Possible etiologies include reperfusion of an ischemic territory in the setting of aggressive anticoagulation and antiplatelet medication, microperforation or dissection of a vessel from the wire or angioplasty balloon, and hyperperfusion of a territory in which the autoregulatory curve has chronically adjusted to compensate for the presence of the stenosis.

ineffective or suboptimal due to restenosis rates, but the evidence for this is anecdotal. An okay angioplasty result is better by far than a stent-related disaster. If the stent does not want to go, don't force it, and don't put a stent up where there is not room for it.

4. *Angioplasty technique.* The intracranial vessels are uniquely deficient in adventitia and in surrounding support by connective tissue, compared with extracranial vessels. Therefore, one must bear their delicacy in mind during all intracranial procedures. Movements should be slow and controlled. It is quite possible, for instance, to slice a curved segment of intracranial vessel longitudinally through excessive repetitive or hurried wire motion, akin to a cheese slicer. While inflating an angioplasty balloon, consider the vessel wall as a *visco-elastic solid*. The likeli-

hood of cracking as opposed to stretching the wall, assuming a correct balloon diameter choice, is entirely related to the rate of application of the deformity. Therefore, the balloon inflation should be *tediously slow*, measured in fractions of an atmosphere per minute or slower. Most patients are under general anesthesia for these procedures and concern about brain ischemia can be managed by breaks in the inflation process with resumption of flow, blood pressure elevation, or reduction of the metabolic needs of the brain territory by injecting small doses of Amytal immediately prior to the angioplasty.

5. *Postprocedure management.* It is likely that most disasters related to intracranial stenting either occur or at least become evident in the postprocedure period. Management of the patient in the intensive care unit can therefore have

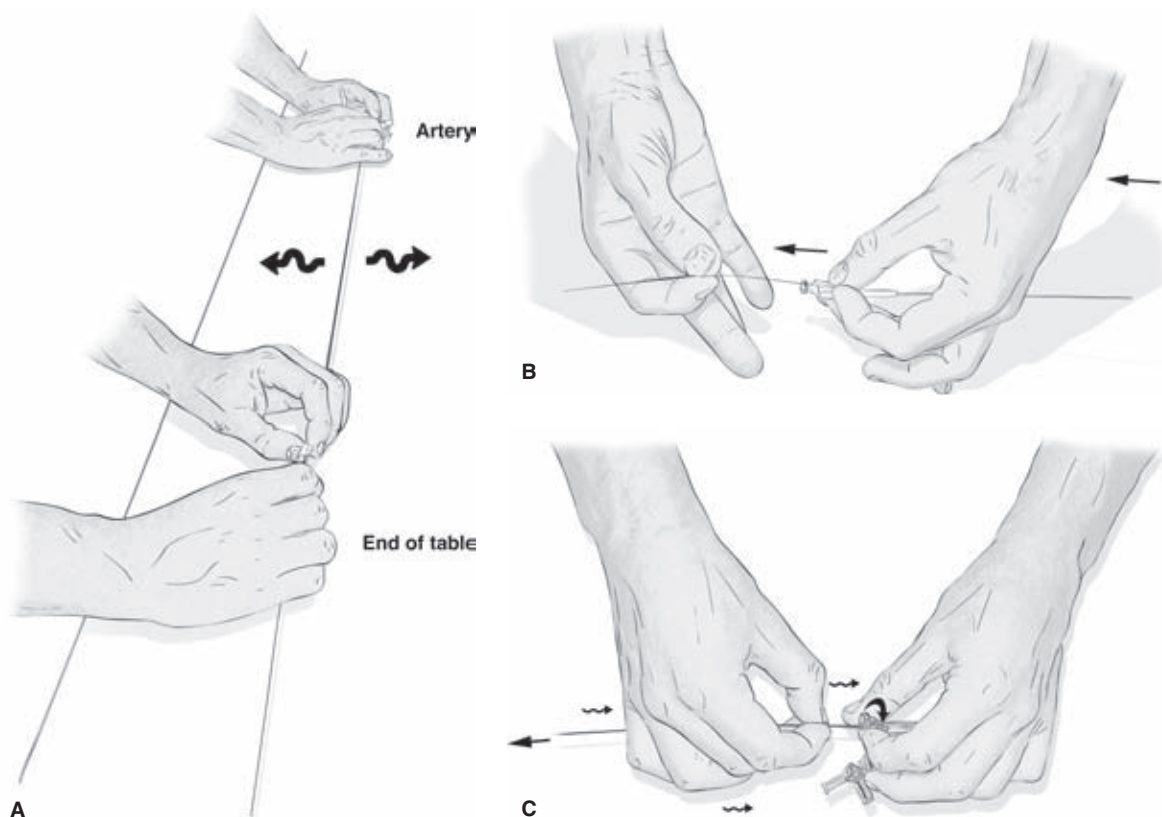


FIGURE 31-17. (A–C) Exchange-wire maneuvers. Despite what one hears at sales pitches or from colleagues at national meetings (“29 minutes, skin-to-skin”) these cases are often not easy. A large measure of the difficulty is imposed by the need to avoid movement of the tip of the exchange wire in a distal intracranial artery or of the protection device in the high cervical carotid artery. Although some aspects of the exchanges can be faster with monorail or “Rapid Exchange” devices, the same difficulties apply. The extraction of the device is performed by two operators keeping the shaft and wire absolutely straight between them (A). Any slewing of the device from side to side during the exchange will translate into retraction or advances of the wire tip within the patient. The extraction is performed primarily by the operator who controls the catheter hub (B), who keeps the right hand fixed to a reference point on the table while withdrawing the catheter with the left in smooth increments. The role of the operator (C) at the head of the table is twofold: first, the left hand regulates the valve to eliminate undue resistance on the catheter as it is withdrawn, and second and most importantly the shaft of the catheter is pinched with the right hand to provide sufficient countertraction to the movements of the primary operator so that the device remains taut and straight on the wire during the extraction.

a big impact on mitigating the effects of procedural misadventure. Blood pressure according to the outcome of the treatment may have to be elevated to maintain perfusion when stent patency is suboptimal, or may need to be reduced to prevent hyperperfusion syndrome when a chronically stenotic vessel becomes widely patent. Combinations of heparin, oral antiplatelet medication, and glycoprotein IIb-IIIa inhibitors appear attractive when one is focused completely on keeping the stent patent, but likely lead to excessive rates of hemorrhagic complications, particularly in patients who have had recent cerebral ischemic injuries, preceding or even during the procedure.

References

1. Young KC, Jain A, Jain M, et al. Evidence-based treatment of carotid artery stenosis. *Neurosurg Focus* 2011;30(6):E2.
2. White H, Boden-Albala B, Wang C, et al. Ischemic stroke subtype incidence among whites, blacks, and Hispanics: The Northern Manhattan Study. *Circulation* 2005;111(10):1327–1331.
3. Barnett HJ, Taylor DW, Eliasziw M, et al. Benefit of carotid endarterectomy in patients with symptomatic moderate or severe stenosis. North American Symptomatic Carotid Endarterectomy Trial Collaborators. *N Engl J Med* 1998;339(20):1415–1425.
4. Randomised trial of endarterectomy for recently symptomatic carotid stenosis: Final results of the MRC European Carotid Surgery Trial (ECST). *Lancet* 1998;351(9113):1379–1387.
5. Mayberg MR, Wilson SE, Yatsu F, et al. Carotid endarterectomy and prevention of cerebral ischemia in symptomatic carotid stenosis. Veterans Affairs Cooperative Studies Program 309 Trialist Group. *JAMA* 1991;266(23):3289–3294.
6. Endarterectomy for asymptomatic carotid artery stenosis. Executive Committee for the Asymptomatic Carotid Atherosclerosis Study. *JAMA* 1995;273(18):1421–1428.
7. Halliday A, Mansfield A, Marro J, et al. Prevention of disabling and fatal strokes by successful carotid endarterectomy in patients without recent neurological symptoms: Randomised controlled trial. *Lancet* 2004;363(9420):1491–1502.
8. Halm EA. Carotid stenting at the crossroads: Practice makes perfect, but some may be practicing too much (and not enough). *JAMA* 2011;306(12):1378–1380.
9. Halm EA. The good, the bad, and the about-to-get ugly: National trends in carotid revascularization: Comment on “Geographic variation in carotid revascularization among

- Medicare beneficiaries, 2003-2006". *Arch Intern Med* 2010; 170(14):1225-1227.
10. Coward LJ, McCabe DJ, Ederle J, et al. Long-term outcome after angioplasty and stenting for symptomatic vertebral artery stenosis compared with medical treatment in the Carotid And Vertebral Artery Transluminal Angioplasty Study (CAVATAS): A randomized trial. *Stroke* 2007;38(5):1526-1530.
 11. Ederle J, Dobson J, Featherstone RL, et al. Carotid artery stenting compared with endarterectomy in patients with symptomatic carotid stenosis (International Carotid Stenting Study): An interim analysis of a randomised controlled trial. *Lancet* 2010;375(9719):985-997.
 12. Gurm HS, Yadav JS, Fayad P, et al. Long-term results of carotid stenting versus endarterectomy in high-risk patients. *N Engl J Med* 2008;358(15):1572-1579.
 13. Rockman C, Loh S. Carotid endarterectomy: Still the standard of care for carotid bifurcation disease. *Semin Vasc Surg* 2011; 24(1):10-20.
 14. Mas JL, Trinquart L, Leys D, et al. Endarterectomy Versus Angioplasty in Patients with Symptomatic Severe Carotid Stenosis (EVA-3S) trial: Results up to 4 years from a randomised, multicentre trial. *Lancet Neurol* 2008;7(10):885-892.
 15. Mas JL, Chatellier G, Beysses B, et al. Endarterectomy versus stenting in patients with symptomatic severe carotid stenosis. *N Engl J Med* 2006;355(16):1660-1671.
 16. Brott TG, Hobson RW 2nd, Howard G, et al. Stenting versus endarterectomy for treatment of carotid-artery stenosis. *N Engl J Med* 2010;363(1):11-23.
 17. Mantese VA, Timaran CH, Chiu D, et al. The Carotid Revascularization Endarterectomy versus Stenting Trial (CREST): Stenting versus carotid endarterectomy for carotid disease. *Stroke* 2010;41(10 suppl):S31-34.
 18. Bonati LH, Dobson J, Algra A, et al. Short-term outcome after stenting versus endarterectomy for symptomatic carotid stenosis: A preplanned meta-analysis of individual patient data. *Lancet* 2010;376(9746):1062-1073.
 19. Silver FL, Mackey A, Clark WM, et al. Safety of stenting and endarterectomy by symptomatic status in the Carotid Revascularization Endarterectomy Versus Stenting Trial (CREST). *Stroke* 2011;42(3):675-680.
 20. Bonati LH, Jongen LM, Haller S, et al. New ischaemic brain lesions on MRI after stenting or endarterectomy for symptomatic carotid stenosis: A substudy of the International Carotid Stenting Study (ICSS). *Lancet Neurol* 2010;9(4):353-362.
 21. Faraglia V, Palombo G, Stella N, et al. Cerebral embolization in patients undergoing protected carotid-artery stenting and carotid surgery. *J Cardiovasc Surg (Torino)* 2007;48(6):683-688.
 22. Flach HZ, Ouhlous M, Hendriks JM, et al. Cerebral ischemia after carotid intervention. *J Endovasc Ther* 2004;11(3):251-257.
 23. Garcia-Sanchez S, Millan-Torne M, Capellades-Font J, et al. [Ischemic brain lesions following carotid revascularisation procedures: A comparative study using diffusion-weighted magnetic resonance imaging]. *Rev Neurol* 2004;38(11):1013-1017.
 24. Iihara K, Muraio K, Sakai N, et al. Outcome of carotid endarterectomy and stent insertion based on grading of carotid endarterectomy risk: A 7-year prospective study. *J Neurosurg* 2006;105(4):546-554.
 25. Lacroix V, Hammer F, Astarci P, et al. Ischemic cerebral lesions after carotid surgery and carotid stenting. *Eur J Vasc Endovasc Surg* 2007;33(4):430-435.
 26. Poppert H, Wolf O, Theiss W, et al. MRI lesions after invasive therapy of carotid artery stenosis: A risk-modeling analysis. *Neurol Res* 2006;28(5):563-567.
 27. Roh HG, Byun HS, Ryoo JW, et al. Prospective analysis of cerebral infarction after carotid endarterectomy and carotid artery stent placement by using diffusion-weighted imaging. *AJNR Am J Neuroradiol* 2005;26(2):376-384.
 28. Skjelland M, Krohg-Sorensen K, Tennoe B, et al. Cerebral microemboli and brain injury during carotid artery endarterectomy and stenting. *Stroke* 2009;40(1):230-234.
 29. Tedesco MM, Coogan SM, Dalman RL, et al. Risk factors for developing postprocedural microemboli following carotid interventions. *J Endovasc Ther* 2007;14(4):561-567.
 30. Halm EA, Tuhim S, Wang JJ, et al. Has evidence changed practice?: Appropriateness of carotid endarterectomy after the clinical trials. *Neurology* 2007;68(3):187-194.
 31. Nallamothu BK, Gurm HS, Ting HH, et al. Operator experience and carotid stenting outcomes in Medicare beneficiaries. *JAMA* 2011;306(12):1338-1343.
 32. Hart JP, Peeters P, Verbist J, et al. Do device characteristics impact outcome in carotid artery stenting? *J Vasc Surg* 2006;44(4):725-730; discussion 730-731.
 33. Barbato JE, Dillavou E, Horowitz MB, et al. A randomized trial of carotid artery stenting with and without cerebral protection. *J Vasc Surg* 2008;47(4):760-765.
 34. Macdonald S, Evans DH, Griffiths PD, et al. Filter-protected versus unprotected carotid artery stenting: A randomised trial. *Cerebrovasc Dis* 2010;29(3):282-289.
 35. Schluter M, Tubler T, Steffens JC, et al. Focal ischemia of the brain after neuroprotected carotid artery stenting. *J Am Coll Cardiol* 2003;42(6):1007-1013.
 36. Tallarita T, Rabinstein AA, Cloft H, et al. Are distal protection devices 'protective' during carotid angioplasty and stenting? *Stroke* 2011;42(7):1962-1966.
 37. Grunwald IQ, Reith W, Karp K, et al. Comparison of Stent Free Cell Area and Cerebral Lesions after Unprotected Carotid Artery Stent Placement. *Eur J Vasc Endovasc Surg* 2011.
 38. Pierce DS, Rosero EB, Modrall JG, et al. Open-cell versus closed-cell stent design differences in blood flow velocities after carotid stenting. *J Vasc Surg* 2009;49(3):602-606; discussion 606.
 39. Savitz SI, Caplan LR. Vertebrobasilar disease. *N Engl J Med* 2005;352(25):2618-2626.
 40. Chimowitz MI, Lynn MJ, Derdeyn CP, et al. Stenting versus aggressive medical therapy for intracranial arterial stenosis. *N Engl J Med* 2011;365(11):993-1003.
 41. Hopkins LN, Budny JL. Complications of intracranial bypass for vertebrobasilar insufficiency. *J Neurosurg* 1989;70(2):207-211.
 42. Coward LJ, Featherstone RL, Brown MM. Percutaneous transluminal angioplasty and stenting for vertebral artery stenosis. *Cochrane Database Syst Rev* 2005;(2):CD000516.
 43. Wityk RJ, Chang HM, Rosengart A, et al. Proximal extracranial vertebral artery disease in the New England Medical Center Posterior Circulation Registry. *Arch Neurol* 1998;55(4): 470-478.
 44. Koskas F, Kieffer E, Rancurel G, et al. Direct transposition of the distal cervical vertebral artery into the internal carotid artery. *Ann Vasc Surg* 1995;9(6):515-524.
 45. Jenkins JS, Patel SN, White CJ, et al. Endovascular stenting for vertebral artery stenosis. *J Am Coll Cardiol* 2010;55(6):538-542.
 46. Dabus G, Gerstle RJ, Derdeyn CP, et al. Endovascular treatment of the vertebral artery origin in patients with symptoms of vertebrobasilar ischemia. *Neuroradiology* 2006;48(12):917-923.
 47. Weber W, Mayer TE, Henkes H, et al. Efficacy of stent angioplasty for symptomatic stenoses of the proximal vertebral artery. *Eur J Radiol* 2005;56(2):240-247.
 48. Wehman JC, Hanel RA, Guidot CA, et al. Atherosclerotic occlusive extracranial vertebral artery disease: Indications for intervention, endovascular techniques, short-term and long-term results. *J Interv Cardiol* 2004;17(4):219-232.
 49. Levy EI, Horowitz MB, Koebe CJ, et al. Transluminal stent-assisted angioplasty of the intracranial vertebrobasilar system for medically refractory, posterior circulation ischemia: Early

- results. *Neurosurgery* 2001;48(6):1215–1221; discussion 1221–1213.
50. Werner M, Braunlich S, Ulrich M, et al. Drug-eluting stents for the treatment of vertebral artery origin stenosis. *J Endovasc Ther* 2010;17(2):232–240.
 51. Raghuram K, Seynaeve C, Rai AT. Endovascular treatment of extracranial atherosclerotic disease involving the vertebral artery origins: A comparison of drug-eluting and bare-metal stents. *J Neurointerv Surg* 2012;4(3):206–210.
 52. Stayman AN, Nogueira RG, Gupta R. A systematic review of stenting and angioplasty of symptomatic extracranial vertebral artery stenosis. *Stroke* 2011;42(8):2212–2216.
 53. Arenillas JF. Intracranial atherosclerosis: Current concepts. *Stroke* 2011;42(1 suppl):S20–S23.
 54. Gorelick PB, Wong KS, Bae HJ, et al. Large artery intracranial occlusive disease: A large worldwide burden but a relatively neglected frontier. *Stroke* 2008;39(8):2396–2399.
 55. Sacco RL, Roberts JK, Boden-Albala B, et al. Race-ethnicity and determinants of carotid atherosclerosis in a multiethnic population. The Northern Manhattan Stroke Study. *Stroke* 1997;28(5):929–935.
 56. Wong LK. Global burden of intracranial atherosclerosis. *Int J Stroke* 2006;1(3):158–159.
 57. Chimowitz MI, Lynn MJ, Howlett-Smith H, et al. Comparison of warfarin and aspirin for symptomatic intracranial arterial stenosis. *N Engl J Med* 2005;352(13):1305–1316.
 58. Lanfranconi S, Bersano A, Branca V, et al. Stenting for the treatment of high-grade intracranial stenoses. *J Neurol* 2010; 257(11):1899–1908.
 59. Lu PH, Park JW, Park S, et al. Intracranial stenting of subacute symptomatic atherosclerotic occlusion versus stenosis. *Stroke* 2011;42(12):3470–3476.
 60. Groschel K, Schnaudigel S, Pilgram SM, et al. A systematic review on outcome after stenting for intracranial atherosclerosis. *Stroke* 2009;40(5):e340–347.
 61. Mori T, Fukuoka M, Kazita K, et al. Follow-up study after intracranial percutaneous transluminal cerebral balloon angioplasty. *AJNR Am J Neuroradiol* 1998;19(8):1525–1533.
 62. Mori T, Fukuoka M, Kazita K, et al. Follow-up study after percutaneous transluminal cerebral angioplasty. *Eur Radiol* 1998;8(3):403–408.
 63. Mori T, Kazita K, Chokyu K, et al. Short-term arteriographic and clinical outcome after cerebral angioplasty and stenting for intracranial vertebrobasilar and carotid atherosclerotic occlusive disease. *AJNR Am J Neuroradiol* 2000;21(2): 249–254.

Endovascular Treatment of Ischemic Stroke

Key Points

- Techniques for endovascular revascularization of acute ischemic stroke are capable of achieving consistent success rates of over 90%.
- Angiographic revascularization of ischemic stroke has become conflated with clinical efficacy. These are two entirely separate, and often unrelated, phenomena.

More than 80% of strokes worldwide are ischemic in origin and one in five of these affect the posterior circulation. Ischemic stroke is a heterogeneous diagnostic categorization involving a multitude of variables including age, cardiovascular health status, location and nature of the ischemic lesion, and the physiologic impact of the lesion in each individual patient. Identifying a single treatment modality that can improve outcomes in the setting of so many diverse circumstances has been and continues to be difficult.

► INTRAVENOUS THROMBOLYSIS

Intravenous thrombolysis for acute ischemic stroke was described as far back as the 1950s (1). However, the first trials of intravenous thrombolytic agents administered within 6 hours of onset of ischemic stroke were not auspicious. Hemorrhage rates were unacceptably high with intravenous streptokinase, and a defined therapeutic impact was not evident with early trials of tPA probably due to the late timing of treatment (2–4). Finally, in 1995 with publication of the NINDS rt-PA study FDA approval was gained for use of intravenous recombinant tissue plasminogen activator (rt-PA) within 3 hours of onset of symptoms (5). A modest improvement in 90-day outcome was seen in patients treated with rt-PA compared with placebo. Patients treated with tPA were 30% more likely to have a good outcome at 90 days compared with patients treated with placebo. Symptomatic hemorrhage within 36 hours of administration of tPA was seen in 6.4% of tPA patients, while mortality rates in the tPA and placebo groups were similar at 17% and 21%, respectively. In 2008 the ECASS-III study additionally demonstrated a small but statistically significant effect

of intravenous rt-PA in stroke patients during the 3- to 4.5-hour period since onset (6). Patients treated in this time window were 28% more likely to have a favorable outcome on the Modified Rankin Scale compared with placebo. Rates of symptomatic hemorrhage were higher with tPA (2.4% vs. 0.3%) and overall hemorrhage rates were substantially higher (27% vs. 17.6%) but without any difference in mortality rates (7.7% vs. 8.4%).

From trials of intravenous thrombolytic agents and other studies it was inferred that clinical improvement of the patient bore some relationship to the success of recanalization, although this correlation was difficult to define precisely. Independent of any thrombolytic agent, approximately 25% of all ischemic strokes will recanalize spontaneously within 24 hours and more than 50% will do so within 1 week (7–9). Administration of thrombolytic drugs improves acute recanalization rates to approximately 46% overall, and the chances of a good outcome at 3 months are increased by a factor of 4 or 5 in patients with immediate and sustained recanalization (7). Nevertheless, a good therapeutic outcome following intravenous thrombolytics is seen in substantially less than half of treated patients, and a sizeable proportion of patients deteriorate even in the absence of contraindications to administration of the drug (10).

In summary, intravenous thrombolytic therapy by itself helps at best only about a third of those ischemic stroke patients who are eligible for its strictly defined criteria, even when stretched to include presentation within 4.5 hours. Timing of administration is a factor, being twice as efficacious within the first 1.5 hours after onset of a stroke as it is when administered within 1.5 to 3 hours (6). Symptomatic intracranial hemorrhage occurs in 1.7% to 8% of treated patients (5,6,11), and many patients are ineligible for this treatment due to late presentation or other reasons.

► INTRA-ARTERIAL TREATMENT OF ISCHEMIC STROKE

Due to the shortcomings and limitations of intravenous thrombolytic therapy for acute ischemic stroke the drive to develop intra-arterial techniques of recanalization has been strong since the method was first described (12,13). Intra-arterial therapy offers several theoretical and actual advantages compared with bedside drug administration including

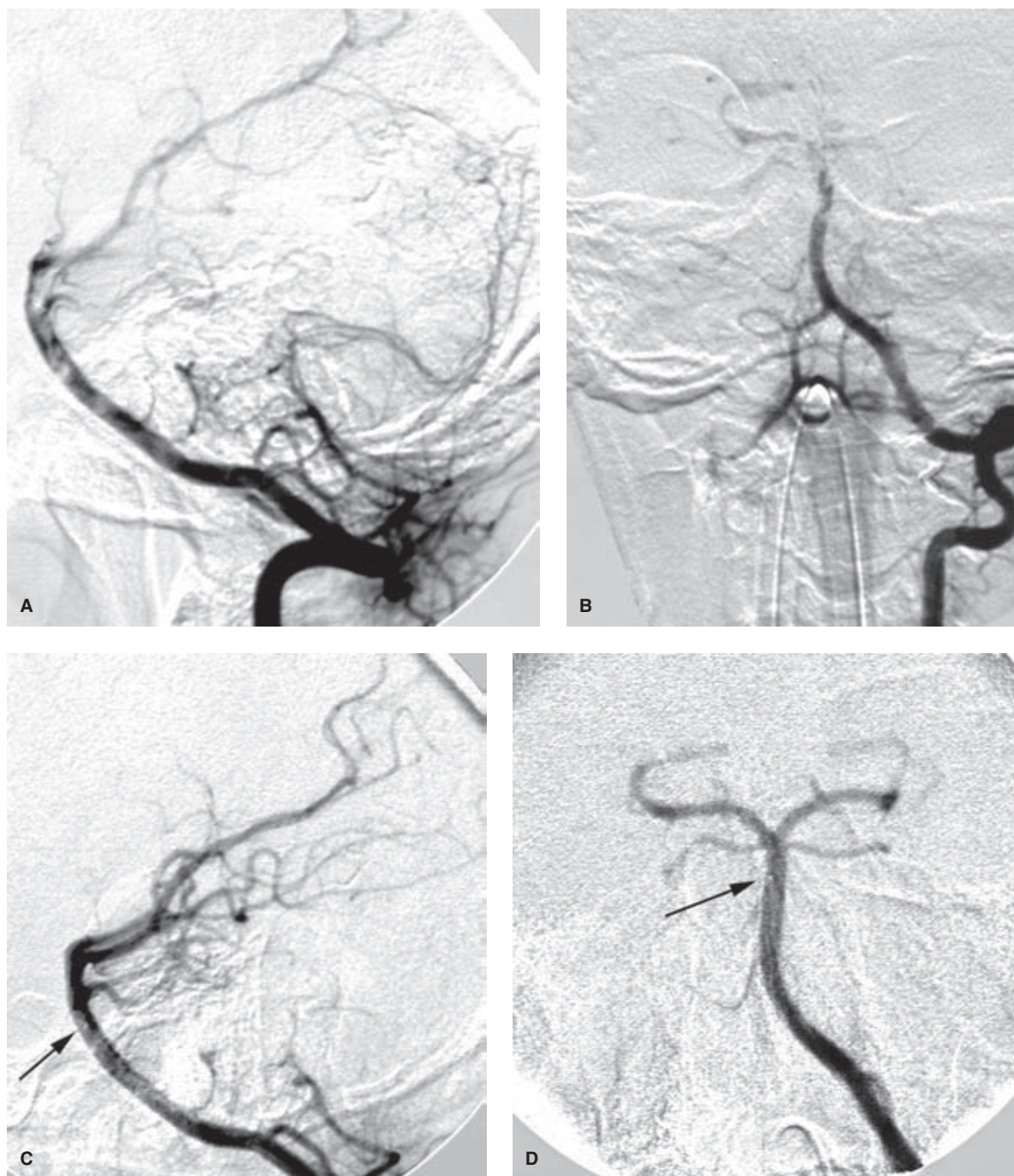


FIGURE 32-1. (A–D) Acute basilar artery thromboembolism during pregnancy. A young female who was 8 weeks pregnant presented following a long air flight with signs of posterior fossa ischemia. Her MRA demonstrated attenuation of flow signal in the basilar artery. She responded well to heparin at first but after approximately 18 hours became suddenly obtunded and hemiparetic. Left vertebral angiography, lateral (A) and PA (B) views, demonstrated an elongated filling defect in the upper two-thirds of the basilar artery with poor filling of the left posterior cerebral artery and superior cerebellar arteries. Thrombolysis was performed at various points within the thrombus through a microcatheter using a total of 600,000 units of urokinase. Lateral (C) and PA (D) views after urokinase show complete filling of the previously nonvisualized branches. The microcatheter tip is indicated with an arrow; the injection of contrast was made through the introducer catheter. The patient left the hospital with a residual deficit of a mild VI palsy. Her pregnancy was apparently unaffected, and she subsequently had an endovascular repair of a patent foramen ovale, which had been instrumental to the genesis of this paradoxical embolus. Pregnancy is mentioned as a contraindication to the use of urokinase, but under circumstances such as these, all contraindications are relative.

the capacity to deliver higher concentrations of local fibrinolytic agents into the clot itself and to monitor the state of vessel recanalization angiographically (Fig. 32-1). Furthermore, there is the potential to use several different mechanical techniques and devices sequentially until a winning solution is achieved (Figs. 32-2 and 32-3). However, it must

be emphasized that the overarching focus on arterial recanalization in the literature dealing with intra-arterial therapy as a biomarker for successful therapy is potentially misleading. Given the correct circumstances endovascular recanalization of an ischemic lesion can be helpful, but recanalization
(text continues on page 490)

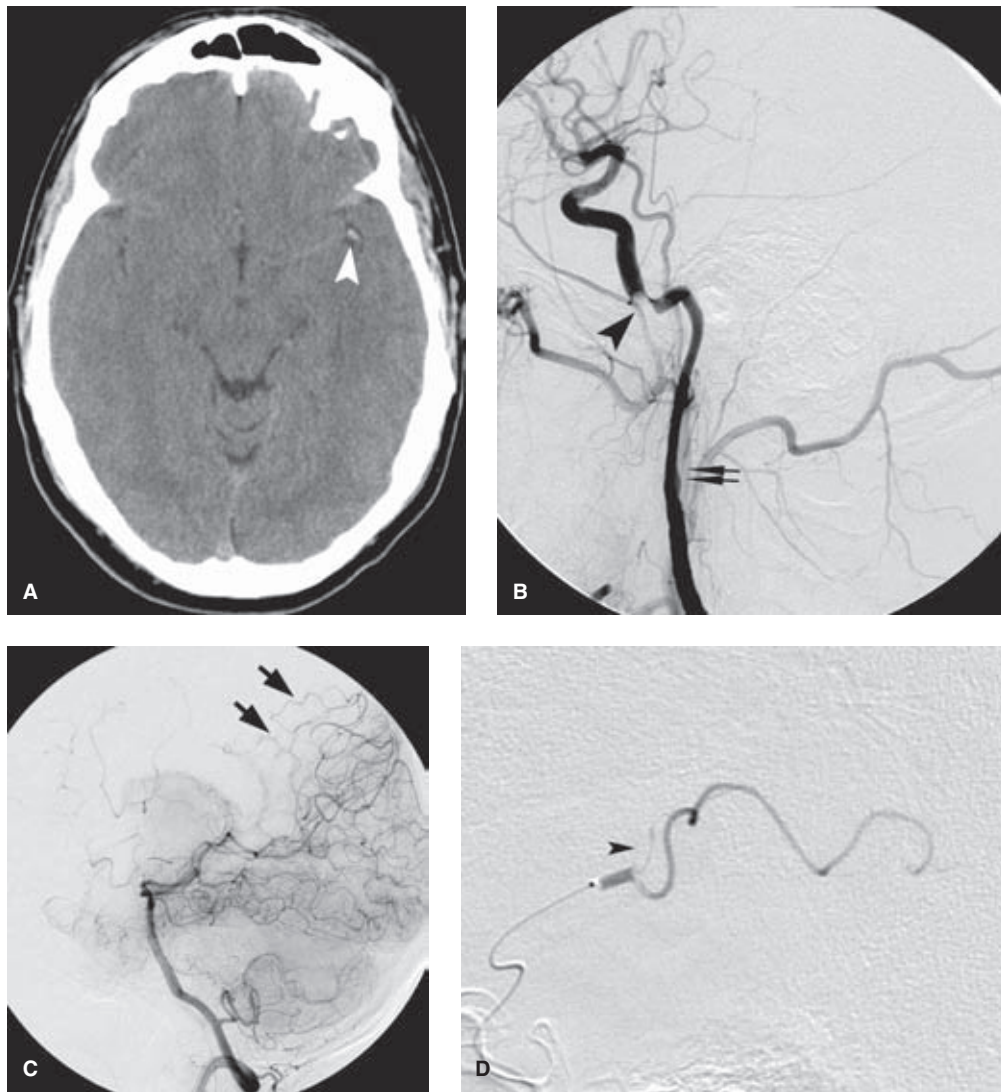


FIGURE 32-2. (A–I) Successful thrombolysis in the left middle cerebral artery outside of the 0- to 6-hour window, undoubtedly due to the large role played by the pial–pial collateral vessels. A young father of three children sustained a trivial sports injury to the neck at approximately 7 PM and soon thereafter developed a fluctuating aphasia and right-sided hemiparesis. Largely due to the insistence of his wife despite temporary spontaneous improvement, his discharge home from an outside hospital was countermanded, and he was transferred to our hospital by which time his condition had deteriorated again. His initial 1 A.M. CT (A) demonstrated no evidence of extensive ischemic injury in the left hemisphere, but the left middle cerebral artery trunk and bifurcation show a “dense MCA sign” (arrowhead). His left common carotid artery injection (B) shows an extensive dissection of the left internal carotid artery (double arrows) with a near-occlusive intimal sock (arrowhead) in the petrous section. The posterior division of the left middle cerebral artery is not filling. The superior division is filling well, implying that the embolus seen on the initial CT that caused his presenting aphasia has broken up and moved distally. A left vertebral artery injection taken later during the procedure (C) shows that the patient has some collateral flow (arrows in C) to the distal branches of the affected territory. In one of those instances of inexplicable good fortune, a microcatheter seemed to find its own way past the dissection to the main residual site of occlusion (D), where a saddle embolus (arrowhead in D) sits astride the bifurcation between the angular branch and the parietal branches. This responded very well to an infusion of 250,000 units of urokinase, following which the territorial perfusion was much improved (E). (continued)

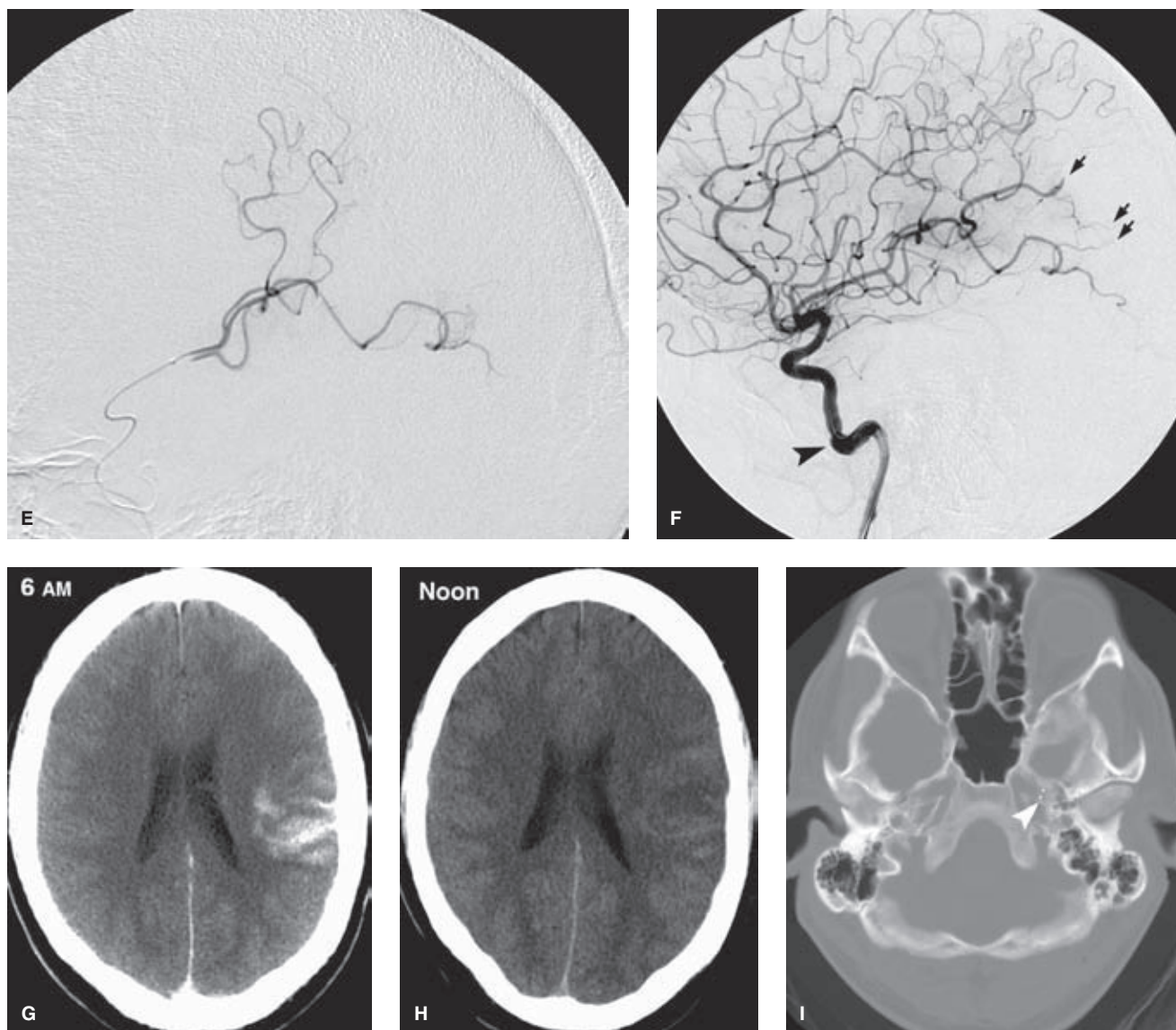


FIGURE 32-2. (CONTINUED) An attempt to stent the petrous carotid artery with a coronary stent precipitated a calamitous complete occlusion of the carotid artery, and for several minutes, the left hemisphere was dependent on collateral flow via the left ophthalmic artery. The situation was rescued by placement of a Neuroform stent in the artery (*arrowhead* in **F**). Distal microemboli are still evident in posterior hemisphere (*small arrows* in **F**), but this territory is rescued by the pial–pial collaterals from the posterior circulation in (**C**). His CT postprocedure at 6 A.M. (**G**) shows extensive patchy high attenuation in the left hemisphere, a finding easily confused for hemorrhage by those unfamiliar with this phenomenon. However, there is no mass effect associated with it and no fluid–fluid levels, and one can predict with reasonable confidence that the next CT (**H**) would demonstrate fading of this contrast staining that occurred in the territory of compromise of the blood–brain barrier. The bone windows (**I**) show that only the platinum tines (*arrowhead*) of the Neuroform stent can be discerned.

A thrombolytic nihilist's interpretation of these images would say that the patient was spontaneously improving anyway, that the embolus was breaking up and moving distally, and that the pial–pial collateral vessels were responsible for sustaining him during the period of occlusion, and that this case proves nothing. Certainly, the role of the collateral vessels is very important in a case such as this, but it is doubtful that they were sufficient to compensate completely for the occlusion. His clinical state of hemiparesis and aphasia were quite profound by the start of the procedure. Furthermore, it must be pointed out that the patient did make a very good recovery starting immediately after the procedure, considering that the affected territory involved his dominant hemisphere, and that this could not have been predicted to happen with IV thrombolytic from the NINDS data even if IV treatment had been started in the first 3 hours. It must also be allowed that the natural history of his near-occlusive dissection might not have been so good, considering that it had already induced cerebral thromboembolic complications once and might well have done so again without intervention.

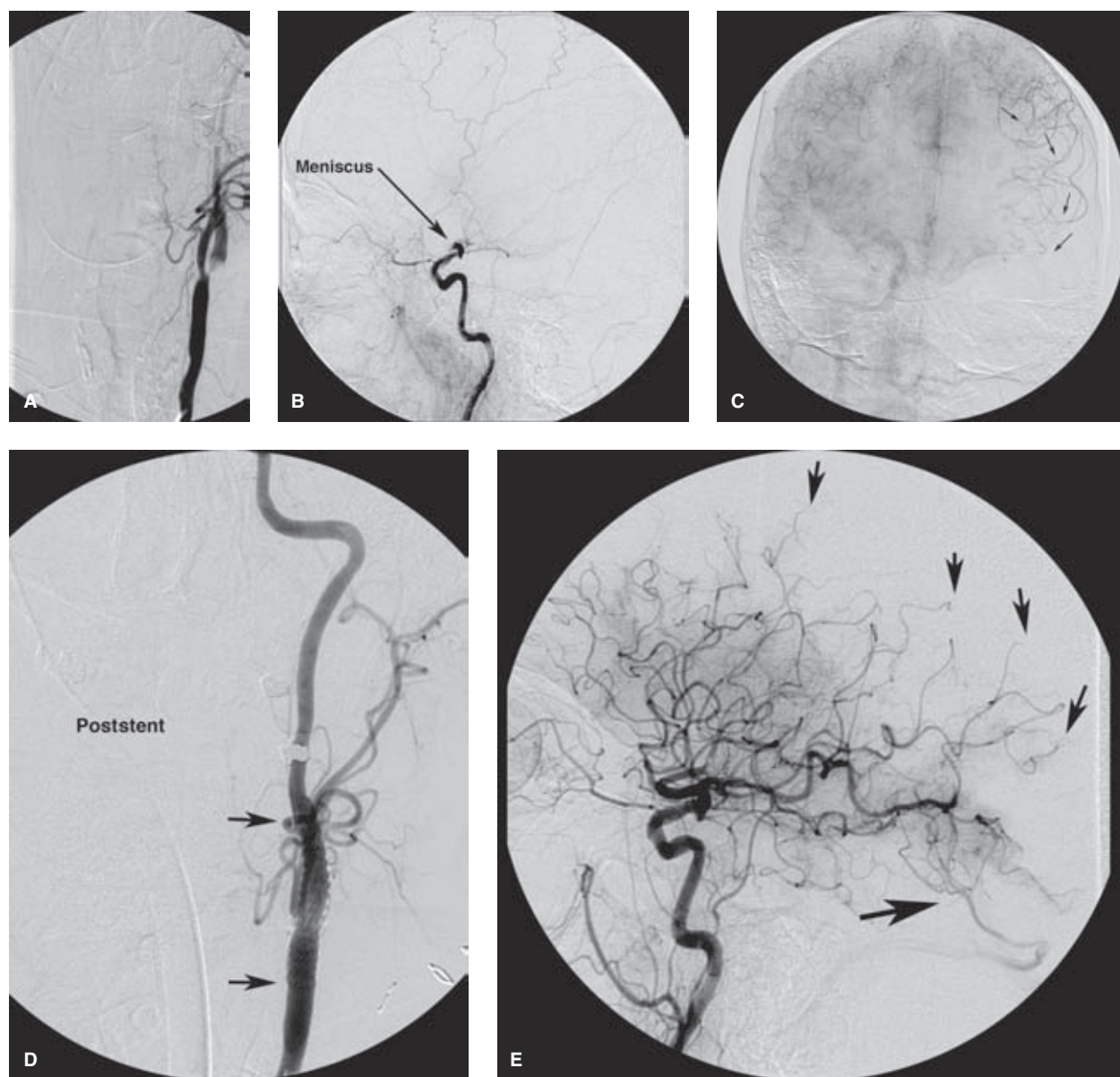


FIGURE 32-3. (A–E) Successful left carotid thrombolysis showing the importance of pial collateral flow, the illusion of a fixed “window” for all patients, and of preparedness to perform emergency carotid stenting. A middle-aged female was scheduled for elective head and neck surgery, for which her aspirin medication was discontinued. In the recovery unit after surgery at approximately 9 A.M., she developed a fluctuating neurologic deficit of aphasia and right-sided weakness. Between one thing and another, despite a progressive trend toward deterioration during the day, the first left common carotid arteriogram (A and B) was not performed until approximately 4.30 P.M., by which time she was well outside the much touted 6-hour window for intervention. The AP view of the neck (A) and lateral view of the intracranial circulation (B) showed a critical stenosis of the left internal carotid artery origin with likely thrombus in the lumen and poor intracranial perfusion through this route. There is an apparent complete occlusion of the left middle cerebral artery with a meniscus sign (*label* in B). Most importantly, the right internal carotid artery (C) perfuses the left anterior cerebral artery territory from which several prominent pial–pial collateral pathways extend to reconstitute the left middle cerebral artery (*arrows*).

An attempt was made at first to lyse the thrombus in the left middle cerebral artery by snaking a microcatheter through the stenosis and instilling tPA into the clot, but the effort was fruitless. Thinking that if we opened the carotid proximally we might be able to balloon angioplasty the clot in the left middle cerebral artery, we performed an angioplasty of the clotted stenosis and were surprised to see what an effect that had on the intracranial circulation. This site was then stented with the results shown on the left common carotid arteriogram (D) and lateral projection of the head (E). While some distal branches of the left middle cerebral artery show occlusions (*small arrows*), the overall appearance is dramatically different from that of a few minutes previously without addition of any more thrombolytic drug. Note the early venous opacification (*larger arrow* in E) indicating the likely establishment of infarction. The patient made a virtually complete recovery and was living a normal life within a month.

The lessons from this case are manifold. First, what saved her was the fact that either through the effects of a long-standing stenosis or through some other mechanism, this patient had an unusual propensity to form pial–pial collateral channels to the affected territory. Second, the effect of a standard dose of thrombolytic drugs was miserable until flow was established by opening the stenosis proximally, a potential lesson for other situations where balloon angioplasty of clot might be considered. Third, her outstanding recovery in the time frame described underscores that the 6-hour rule does not apply to everybody.

is not synonymous with reversal of ischemia or with the assurance of a good outcome.

Three randomized trials of intra-arterial administration of thrombolytic drug for M1 or M2 occlusion have been published. The PROACT-II study identified a favorable outcome in 40% of patients treated with IA r-pro-UK versus 25% of placebo (heparin) patients, with a recanalization rate of 66% versus 18%, respectively (14). The Japanese MELT study also focused on MCA occlusions and found similar results (15). These studies were limited in scope and by the specific avoidance of mechanical disruption of the clot in the PROACT studies and only wire disruption in the MELT study, so the favorable outcome they describe is an indication of the power of even limited endovascular techniques in achieving recanalization. Since then, the expanding technologic capabilities of endovascular therapy have outraced and left behind the possibility of performing comprehensive randomized trials. Establishing vessel recanalization has become the de facto goal of treatment, with lesser attention paid to clinical outcome or complication rates, or so one might perceive from a review of the literature.

Endovascular intervention can achieve consistent rates of recanalization of 90% to 100% using a variety of snare, aspiration, balloon-angioplasty, and stent devices, particularly when multiple modalities are employed (16,17–20). These rates represent a considerable improvement over the recanalization rates seen with intravenous therapy alone (30% to 46%) and rates seen with exclusive use of intra-arterial thrombolytics or one mechanical device alone (60% to 70%) (21–23). Intra-arterial treatment of ischemic stroke can be performed on pediatric patients (24) and octogenarians sometimes with margins of safety and angiographic success comparable to those in other age groups, sometimes not (25,26), with only an occasional question being raised as to whether this is sustainable from a medical resource point of view, cost efficacy, or clinical outcome. The phenomenon of “futile recanalization” is well recognized and commonplace, that is, the acknowledgment that reopening an ischemic vessel really does not accomplish anything positive for the patient and may do a great deal of economic and medical harm. It is not uncommon for high double-digit published rates of futile recanalization (90%) or triple-digit rates of successful stent deployment to be juxtaposed with extremely modest rates of clinical improvement (27,28). The illusory success of achieving recanalization at such a high rate compounded with the phenomenon that aggressive stroke therapy is being touted as a showcase or marketing tool for many medical institutions means that the likelihood of rationalization or triage of stroke patients *away* from intra-arterial therapy seems even more improbable.

Aggressive and difficult intra-arterial procedures for acute stroke, or those delayed even beyond 8 hours after onset, are not minor procedures. Published accounts report complication rates with symptomatic hemorrhage of 16%, wire perforations 10%, and overall mortality of 33% (22,28), while real-life unsung numbers are probably even higher (Figs. 32-4 and 32-5). A half of all angiographically successful procedures are futile, that is, recanalization gained for no clinical improvement (29), while the proportion in older patients is likely even higher. In the >80 years age group, at best only about 25% of patients have a favorable outcome while mortality rates are in excess of 40%, twice that seen in younger patients (25,26). Furthermore,

economic data suggest that for patients >82 years the cost-effectiveness of IA mechanical thrombectomy is very dubious (30).

The contraindications to intravenous administration of thrombolytic agents are clearly indicated by the FDA. No such list of contraindications to intra-arterial treatment of stroke exists, but it is becoming evident that patients of a certain profile will not do well with the procedure. Attempts have been made to predict which patients might do well or badly using factors such as time since onset of symptoms, extent of infarction on the noncontrast CT, DWI changes on MRI, or mismatched perfusion parameters on CTP. Others have taken a simpler clinical approach by defining this risk profile with simple predictive scoring systems (31–33) based on demographic and clinical criteria. The THRIVE (Total Health Risks in Vascular Events) score (32), for instance, assigns a score of 0 to 9 points on the basis of the NIHSS score at presentation, age, and presence of complicating medical risks. A score of 0 to 2 predicts a good outcome in 65% of cases, a score of 3 to 5 points predicts a good outcome in 44% of cases, while only 11% of those with a higher score have a good outcome. Patients with a high THRIVE score (6 to 9) had a 90-day mortality rate of 56% while those with a low score of 0 to 2 had a mortality of 6% following endovascular thrombectomy. The factors incorporated into the THRIVE score seem to trump the importance of whether recanalization was achieved during the procedure. Low-score patients with recanalization had a good outcome in 83% of cases, while high-score patients even with recanalization had a good outcome in only 18.5% of cases, while low-score patients even *without* recanalization had a good outcome in 27% of cases. An even simpler scale, the Houston Intra-arterial Therapy (HIAT) scale, ranks patients on a score of 0 to 3 based on age >75 years, admission glucose >150 mg/dL, and NIHSS >18 (33). On this four-point scale poor outcome ranges from 44% to 100% and mortality from 11% to 44% respectively, without being influenced by the rates of recanalization that were constant within the different groups. Clearly, recanalization alone is not an adequate goal or justification for the use of this treatment in all patients, even within the 6-hour window.

The challenge of intra-arterial stroke therapy, therefore, is not to achieve recanalization of an occluded vessel, but rather to do so only in those patients for whom a reasonable risk–benefit–cost analysis can be proposed and with a reasonable prospect of a meaningful clinical outcome. Guidelines are necessary on when to withhold this procedure. Without them the bleakness of the clinical situation in which decisions are made one patient at a time becomes overwhelming and the procedure is thus offered to all. (This situation is analogous to that encountered with infants suffering from advanced complications of vein of Galen malformations as rated on the Bicêtre Vein of Galen Assessment Scale, where a score below a certain futile level contraindicates treatment (34). See Chapter 33.)

Characteristics associated with likelihood of a bad outcome from intra-arterial therapy of ischemic stroke are given below:

- Age >80 years (25,26,32,33)
- High NIHSS score >18 (32,33)
- Large infarct on DWI or CTP >100 mL or on noncontrast CT as defined by ASPECTS score (35)

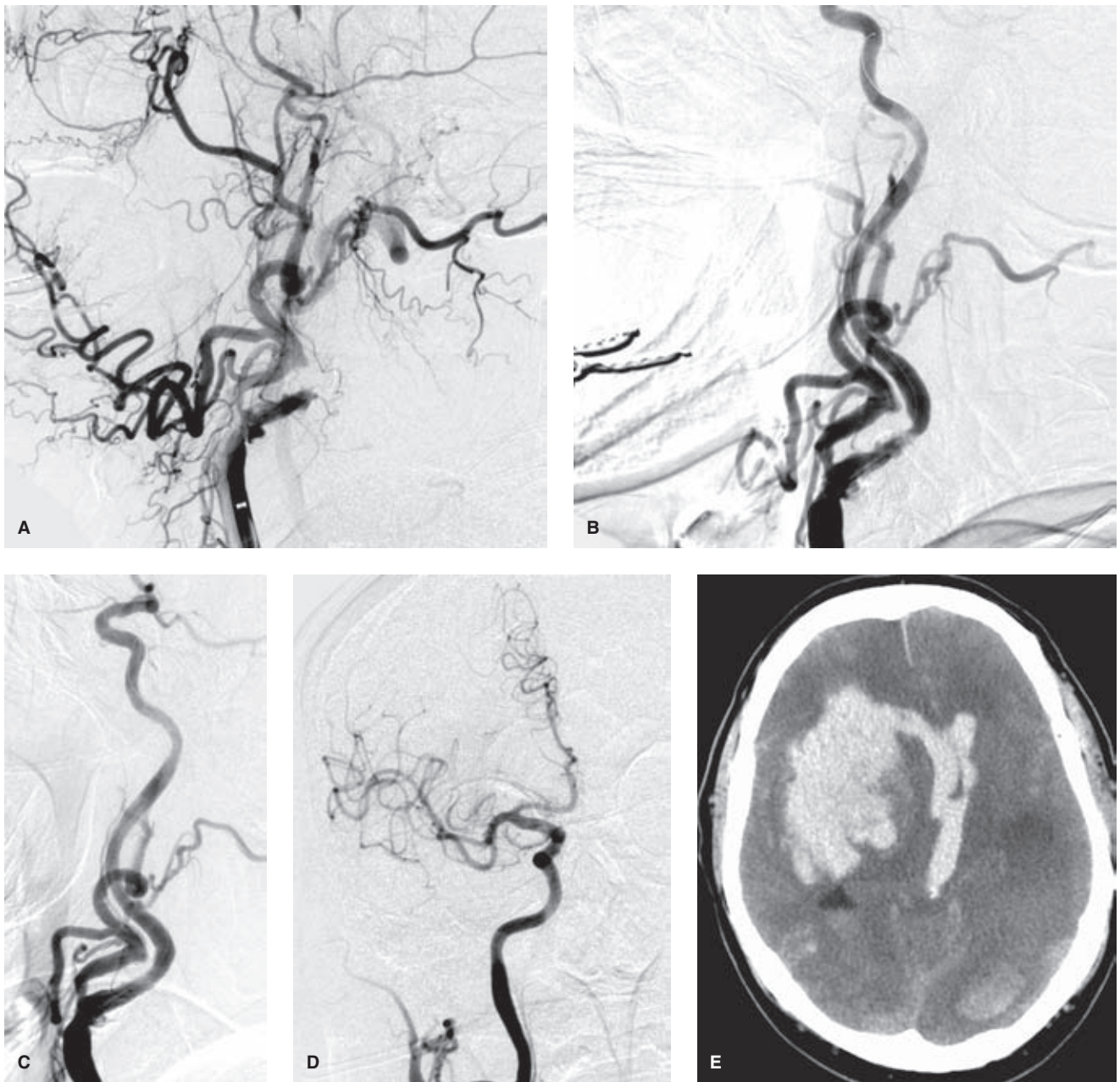


FIGURE 32-4. (A–E) Catastrophic outcome following a successful angiographic procedure. An elderly patient presented with an NIHSS score >20 and evidence of both infarcted tissue and extensive penumbra in the right hemisphere on CTP. The decision to treat him was not undertaken with a great deal of optimism. The right common carotid artery injection (A) showed complete occlusion of the right internal carotid artery with faint distal reconstitution at the cavernous level via ophthalmic and lesser collaterals, but poor intracranial collateral flow. An angioplasty (B) of the proximal right internal carotid artery was initially successful, but progressed to complete occlusion soon thereafter. A loading dose of eptifibatide was administered and the right internal carotid artery was stented (C) with a satisfactory appearance. The intracranial circulation was then revascularized (D) using a combination of balloon angioplasty (Hyperform), MERCI, and Penumbra devices. The patient's status did not improve dramatically following the procedure and the next day his condition deteriorated precipitately with massive hemorrhage evident on CT (E). The possible explanations for this hemorrhage are manifold and possibly interactive. These include overly aggressive antiplatelet measures prompted by the necessity for the stent, microwire perforations during the intracranial manipulations, or reperfusion of already infarcted tissue.

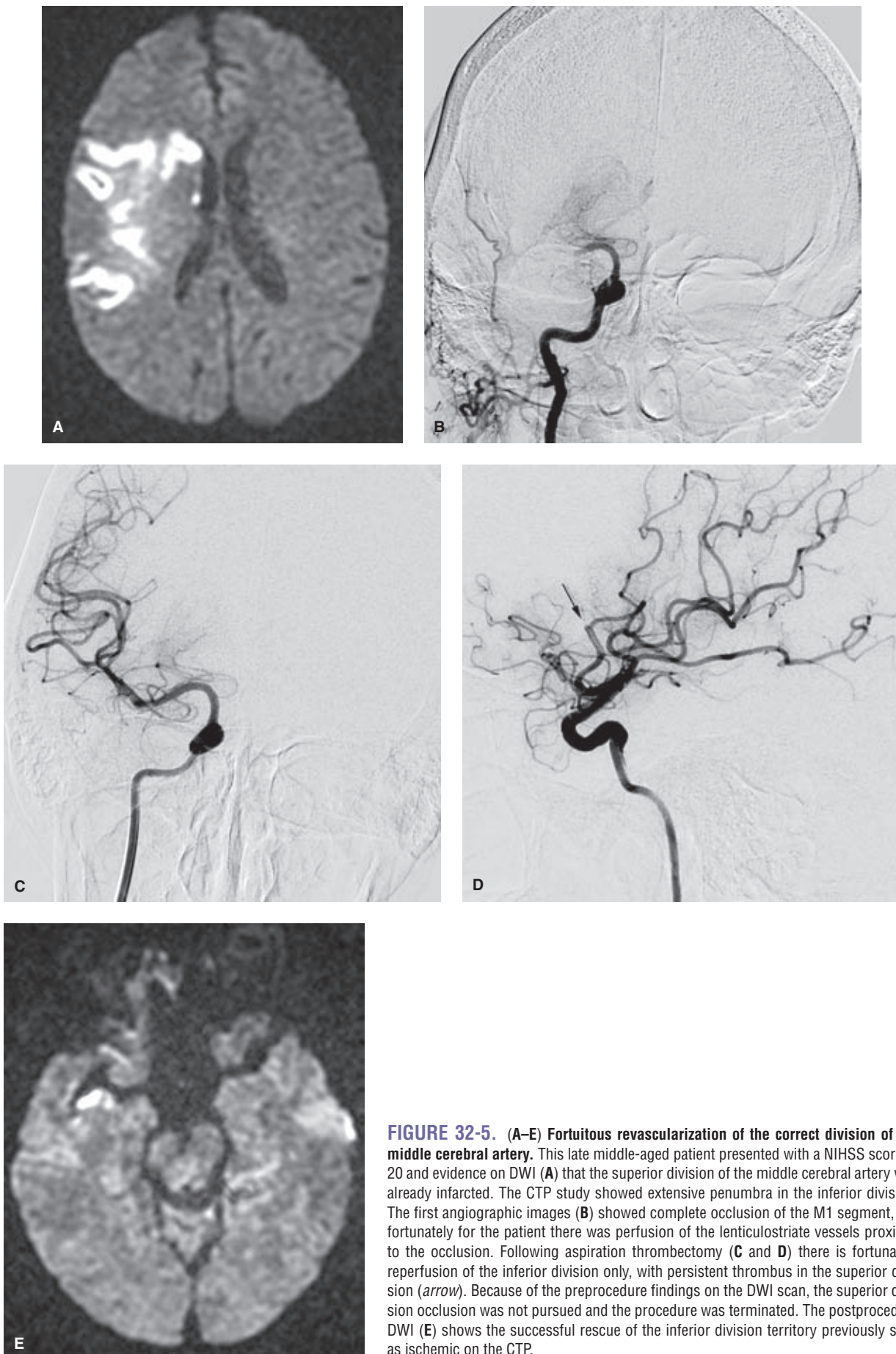


FIGURE 32-5. (A–E) Fortuitous revascularization of the correct division of the middle cerebral artery. This late middle-aged patient presented with a NIHSS score of 20 and evidence on DWI (A) that the superior division of the middle cerebral artery was already infarcted. The CTP study showed extensive penumbra in the inferior division. The first angiographic images (B) showed complete occlusion of the M1 segment, but fortunately for the patient there was perfusion of the lenticulostriate vessels proximal to the occlusion. Following aspiration thrombectomy (C and D) there is fortunately reperfusion of the inferior division only, with persistent thrombus in the superior division (*arrow*). Because of the preprocedure findings on the DWI scan, the superior division occlusion was not pursued and the procedure was terminated. The postprocedure DWI (E) shows the successful rescue of the inferior division territory previously seen as ischemic on the CTP.

- Hyperglycemia at presentation (with or without a history of diabetes) (10,32,33,36)
- Coexistent medical risks: Hypertension, atrial fibrillation, diabetes mellitus (10,32,33)
- Hemorrhage evident on initial CT
- Failure of recanalization (6,37)

► PIAL COLLATERAL CIRCULATION: THE PRIMARY VITAL COMPONENT

A list of factors associated with the likelihood of a favorable outcome following intra-arterial therapy of ischemic stroke could be drawn up which could be the converse of the list above for bad outcomes (37). While these factors are important, the single greatest factor for determining the clinical response to a successful revascularization is the phenomenon of pial–pial collateral flow (or stuttering flow via the circle of Willis in the setting of incomplete occlusions). This is the starting point from which all other discussions emanate. Without preservation of threatened tissue during the period between onset of symptoms and success of treatment, a meaningful recovery is not possible (38). Some patients may be fortunate and recover well even without recanalization when pial collateral flow is robust, but usually recanalization of the occlusion is the second vital *sine qua non* without which ischemic tissue will progress substantially to infarction (38,39). On the other hand, however, recanalization without substantial prior sustenance by collateral flow is most often futile. One study correlated CTP metrics at presentation and clinical outcome at 3 months following intra-arterial treatment and estimated that while recanalization was certainly desirable and resulted in a fivefold likelihood of a favorable ultimate outcome, this was trumped by whether good collateral flow was present initially, which translated into a sevenfold likelihood (40)

(Figs. 32–6–32–8). Time as a factor influencing stroke treatment outcome has been identified in several studies, meaning that earlier treatment results in better outcomes (6,14,41), but again this presupposes the presence of underlying collateral flow (42). Moreover, cases of presentation at 12 or even 24 hours and treated with intra-arterial therapy with a good outcome are well recognized, implying once again that collateral status trumps time in determination of outcome (22).

Pial collateral flow is easy to identify and recognize angiographically, but difficult to quantitate accurately. However, pial collateral flow is the element that determines many of the metrics familiar from perfusion imaging and is largely the determinant of the NIHSS score for otherwise identical anatomic lesions. The state of collateral flow is virtually synonymous with the likelihood of identifying a substantial penumbra and thus of the size of infarction (39). Moreover, it has been shown also that rate of growth of an established infarction is slower in the setting of good collateral flow (43). The factors determining a patient's propensity to having good pial collateral vessels are not known, although ischemic preconditioning, for example, a slowly progressive critical carotid stenosis, is one feature that can be used to explain this phenomenon in some patients (44).

► PRACTICAL CONCLUSIONS

The state of the art for intra-arterial therapy of ischemic stroke will likely evolve rapidly in the coming years. Devices already on the market with FDA approval such as the Penumbra and MERCI catheters with recanalization rates in the 70% to 100% range (21,23,27,45) are being superseded by consistent recanalization rates of 95% to 100% achieved with techniques such as vigorous suction thrombectomy (46) or stent (temporary or permanent) deployment (16,19,28,47–49,50).

(text continues on page 496)

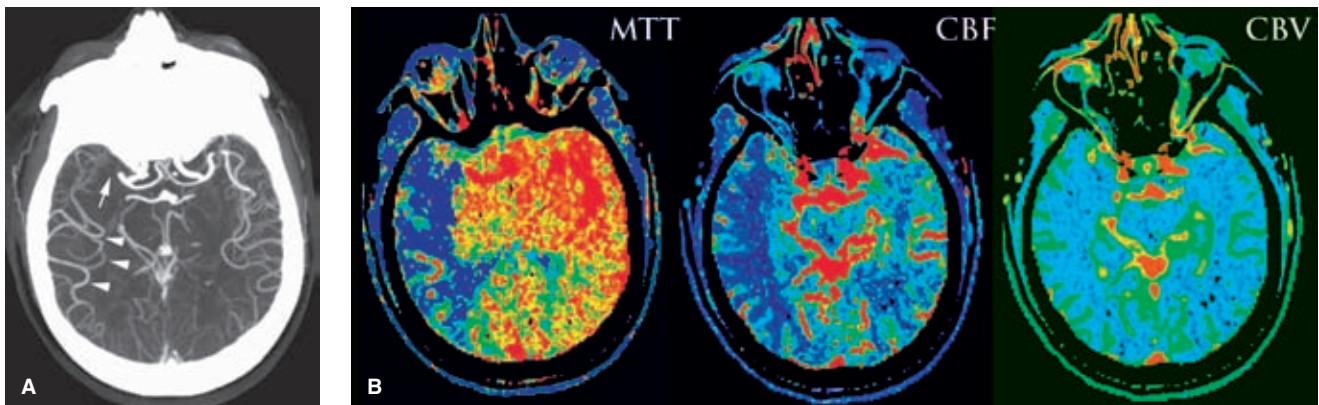


FIGURE 32-6. (A–F) Importance of pial–pial collateral flow I. The MIP thick slice image through the circle of Willis on the CTA is frequently one of the most helpful overall views of the study. The right M1 segment (*arrow*) is completely occluded. A defect in the distal left M1 segment is due to plane selection. The distal branches of the right middle cerebral artery territory are not just well seen, but they appear larger and more densely opacified than their left-sided equivalents. These findings are suggestive of excellent collateral flow to the right middle cerebral artery. The CTP images (**B**) confirm this with the MTT and CBF indicating an extensive ischemic territory in the right hemisphere with symmetry of the CBV map. (*continued*)

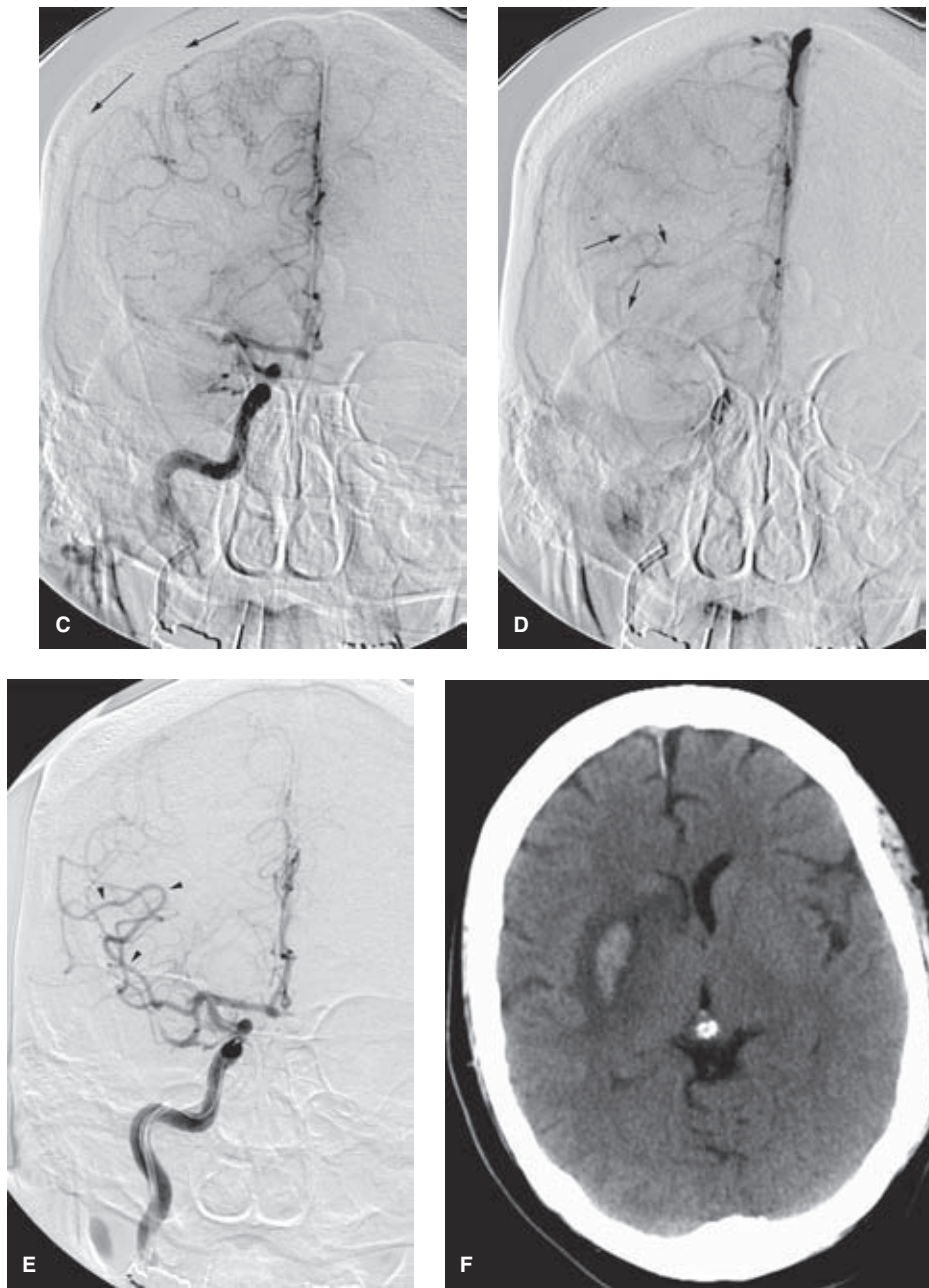


FIGURE 32-6. (CONTINUED) The angiographic images of the right internal carotid artery in the early phase (**C**) and late venous phase (**D**) show a complete M1 occlusion with prompt progressive pial collateral flow (*arrows*) allowing retrograde arterial opacification all the way back to the region of occlusion. A Penumbra 041 microcatheter was advanced with the help of a coaxial 170-cm microcatheter over a Synchro 014 wire and vigorous syringe aspiration was applied as the catheter was withdrawn back through the region of occlusion. This resulted in much improved flow (**E**) in the right middle cerebral artery allowing visualization of the M2 branch (*arrowheads* in **E**) faintly seen on image (**D**). The postprocedure CT (**F**) shows some swelling and high-density opacification in the region of the basal ganglia with an excellent clinical recovery. In most patients such high-density opacification is related to staining by contrast and not necessarily hemorrhagic change.

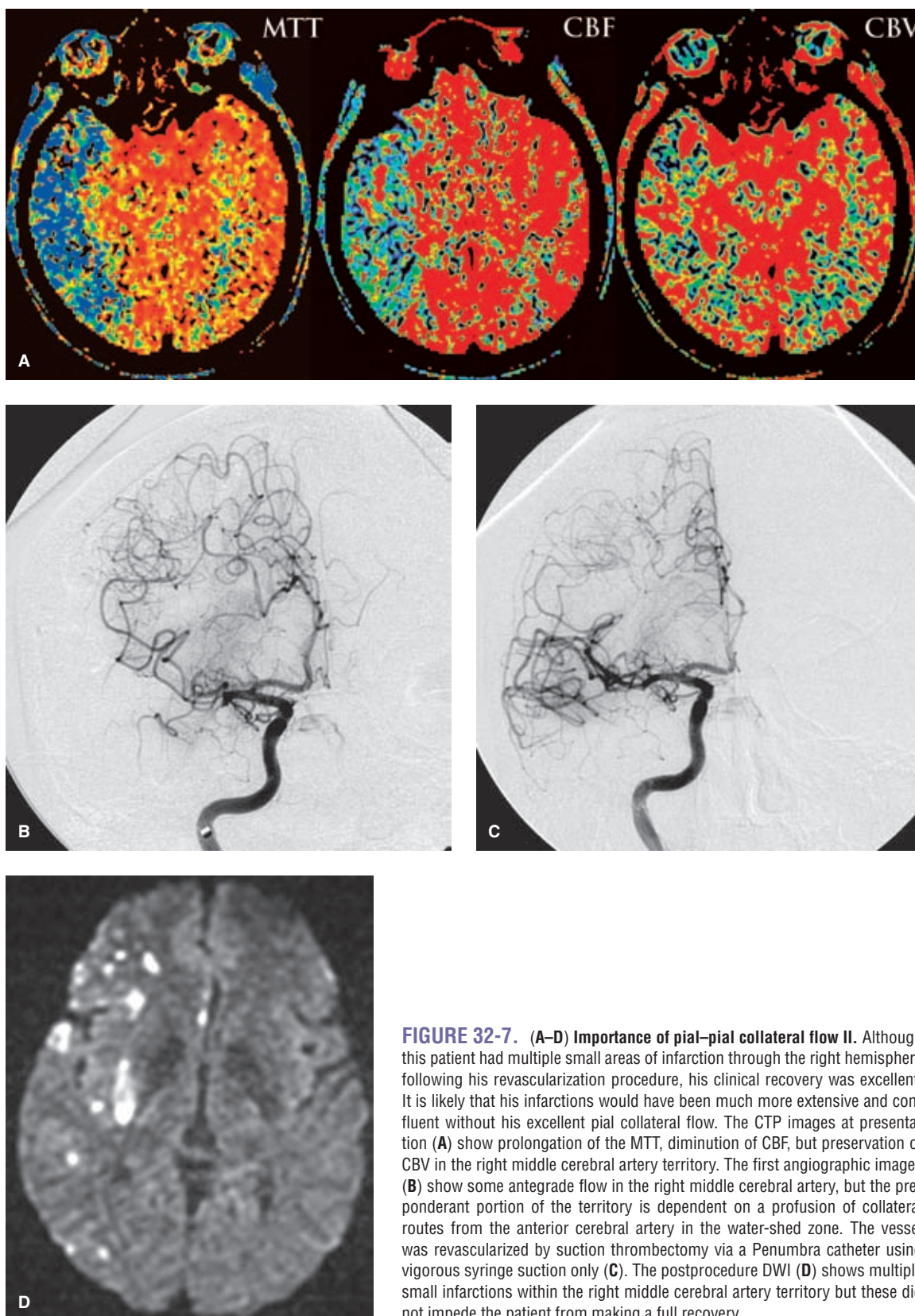


FIGURE 32-7. (A–D) Importance of pial–pial collateral flow II. Although this patient had multiple small areas of infarction through the right hemisphere following his revascularization procedure, his clinical recovery was excellent. It is likely that his infarctions would have been much more extensive and confluent without his excellent pial collateral flow. The CTP images at presentation (A) show prolongation of the MTT, diminution of CBF, but preservation of CBV in the right middle cerebral artery territory. The first angiographic images (B) show some antegrade flow in the right middle cerebral artery, but the preponderant portion of the territory is dependent on a profusion of collateral routes from the anterior cerebral artery in the water-shed zone. The vessel was revascularized by suction thrombectomy via a Penumbra catheter using vigorous syringe suction only (C). The postprocedure DWI (D) shows multiple small infarctions within the right middle cerebral artery territory but these did not impede the patient from making a full recovery.

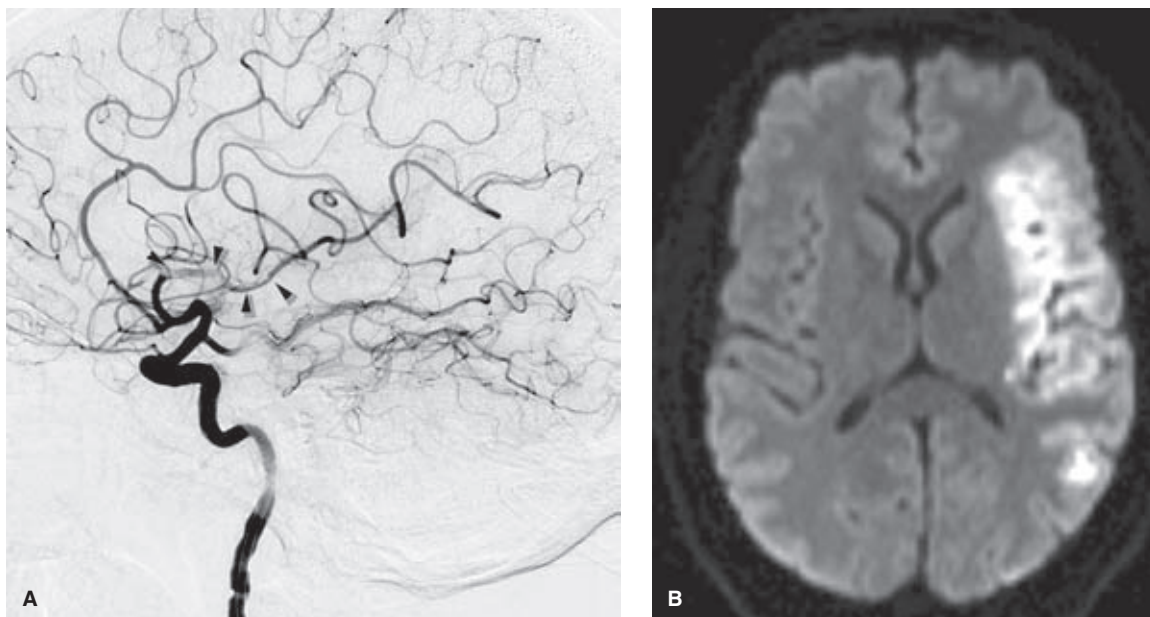


FIGURE 32-8. (A–B) Pial collateral flow without revascularization is not sufficient. This patient illustrates the point that although profuse collateral flow is desirable, it may not be sufficient in all patients in the absence of revascularization. This patient shows extensive elongated thrombus (*arrowheads* in **A**) in the left middle cerebral artery that despite prolonged attempts could not be substantially extracted or broken up. Nevertheless, there are multiple collateral vessels in the compromised territory and it seemed at the time that based on the angiographic images that the patient should do reasonably well. However, the postprocedure DWI (**B**) shows a complete infarction of the left middle cerebral artery territory. It is possible that this degree of infarction might have been established before the procedure and that the angiographic appearance represents a spontaneously revascularized state following a previous more extensive occlusion. Nevertheless, the evolution of this case suggests that collateral flow alone may not be sufficient in all patients to avoid progression to spreading infarction in the absence of recanalization of the compromised artery.

As stated previously, however, endovascular recanalization of an occluded vessel is not the technical challenge in most patients that it was some years ago. “Patient selection” is not likely to be a major force in the determination of practice habits either, in the absence of regulatory proscription of intra-arterial therapy in certain defined circumstances. Occasional patients with good outcomes in defiance of all rational predictions become formative anecdotal experiences, which then have a disproportionate influence on the decision-making process for subsequent patients, particularly when no treatment alternatives are available in an apparently gloomy clinical situation. Furthermore, institutional policies and competitive forces likely play a greater role in this field than is acknowledged, while few if any oversight or internal review procedures exist to dampen the near-universal use of this therapy. What constitutes an acceptable rate of futile recanalization, the cost–benefit analysis of performing this procedure in the face of bad prognostic features, and the degree to which mortality rates in excess of the natural history of ischemic stroke should be tolerated are all factors awaiting future consensus.

References

1. Sussman BJ, Fitch TS. Thrombolysis with fibrinolytic in cerebral arterial occlusion. *J Am Med Assoc* 1958;167(14):1705–1709.
2. Hacke W, Kaste M, Fieschi C, et al. Intravenous thrombolysis with recombinant tissue plasminogen activator for acute hemispheric stroke. The European Cooperative Acute Stroke Study (ECASS). *JAMA* 1995;274(13):1017–1025.
3. Hacke W, Kaste M, Fieschi C, et al. Randomised double-blind placebo-controlled trial of thrombolytic therapy with intravenous alteplase in acute ischaemic stroke (ECASS II). Second European-Australasian Acute Stroke Study Investigators. *Lancet* 1998;352(9136):1245–1251.
4. Clark WM, Wissman S, Albers GW, et al. Recombinant tissue-type plasminogen activator (Alteplase) for ischemic stroke 3 to 5 hours after symptom onset. The ATLANTIS Study: A randomized controlled trial. Alteplase thrombolysis for acute non-interventional therapy in ischemic stroke. *JAMA* 1999;282(21):2019–2026.
5. Tissue plasminogen activator for acute ischemic stroke. The National Institute of Neurological Disorders and Stroke rt-PA Stroke Study Group. *N Engl J Med* 1995;333(24):1581–1587.
6. Hacke W, Kaste M, Bluhmki E, et al. Thrombolysis with alteplase 3 to 4.5 hours after acute ischemic stroke. *N Engl J Med* 2008;359(13):1317–1329.
7. Rha JH, Saver JL. The impact of recanalization on ischemic stroke outcome: A meta-analysis. *Stroke* 2007;38(3):967–973.
8. Kaps M, Damian MS, Teschendorf U, et al. Transcranial Doppler ultrasound findings in middle cerebral artery occlusion. *Stroke* 1990;21(4):532–537.
9. Zanette EM, Roberti C, Mancini G, et al. Spontaneous middle cerebral artery reperfusion in ischemic stroke. A follow-up study with transcranial Doppler. *Stroke* 1995;26(3):430–433.
10. Leigh R, Zaidat OO, Suri MF, et al. Predictors of hyperacute clinical worsening in ischemic stroke patients receiving thrombolytic therapy. *Stroke* 2004;35(8):1903–1907.
11. Wechsler LR. Intravenous thrombolytic therapy for acute ischemic stroke. *N Engl J Med* 2011;364(22):2138–2146.
12. Zeumer H, Hacke W, Kolmann HL, et al. Local fibrinolysis in basilar artery thrombosis. *Dtsch Med Wochenschr* 1982;107(19):728–731.

13. Hacke W, Zeumer H, Ferbert A, et al. Intra-arterial thrombolytic therapy improves outcome in patients with acute verte-brobasilar occlusive disease. *Stroke* 1988;19(10):1216–1222.
14. del Zoppo GJ, Higashida RT, Furlan AJ, et al. PROACT: A phase II randomized trial of recombinant pro-urokinase by direct arterial delivery in acute middle cerebral artery stroke. PROACT Investigators. Prolyse in Acute Cerebral Thrombo-embolism. *Stroke* 1998;29(1):4–11.
15. Ogawa A, Mori E, Minematsu K, et al. Randomized trial of intraarterial infusion of urokinase within 6 hours of middle cerebral artery stroke: The middle cerebral artery embolism local fibrinolytic intervention trial (MELT) Japan. *Stroke* 2007;38(10):2633–2639.
16. Gupta R, Tayal AH, Levy EI, et al. Intra-arterial thrombolysis or stent placement during endovascular treatment for acute ischemic stroke leads to the highest recanalization rate: Results of a multicenter retrospective study. *Neurosurgery* 2011;68(6):1618–1622; discussion 1622–1613.
17. Park H, Hwang GJ, Jin SC, et al. A retrieval thrombectomy technique with the Solitaire stent in a large cerebral artery occlusion. *Acta Neurochir (Wien)* 2011;153(8):1625–1631.
18. Seifert M, Ahlbrecht A, Dohmen C, et al. Combined interven-tional stroke therapy using intracranial stent and local intraar-terial thrombolysis (LIT). *Neuroradiology* 2011;53(4):273–282.
19. Stampfl S, Hartmann M, Ringleb PA, et al. Stent placement for flow restoration in acute ischemic stroke: A single-center expe-rience with the Solitaire stent system. *AJNR Am J Neuroradiol* 2011;32(7):1245–1248.
20. Wehrsuetz M, Wehrsuetz E, Augustin M, et al. Early single center experience with the solitaire thrombectomy device for the treatment of acute ischemic stroke. *Interv Neuroradiol* 2011;17(2):235–240.
21. Smith WS, Sung G, Saver J, et al. Mechanical thrombectomy for acute ischemic stroke: Final results of the Multi MERCI trial. *Stroke* 2008;39(4):1205–1212.
22. Natarajan SK, Snyder KV, Siddiqui AH, et al. Safety and effec-tiveness of endovascular therapy after 8 hours of acute isch-emic stroke onset and wake-up strokes. *Stroke* 2009;40(10):3269–3274.
23. Bose A, Henkes H, Alfke K, et al. The Penumbra System: A mechanical device for the treatment of acute stroke due to thromboembolism. *AJNR Am J Neuroradiol* 2008;29(7):1409–1413.
24. Arnold M, Steinlin M, Baumann A, et al. Thrombolysis in childhood stroke: Report of 2 cases and review of the litera-ture. *Stroke* 2009;40(3):801–807.
25. Mono ML, Romagna L, Jung S, et al. Intra-Arterial Throm-bolysis for Acute Ischemic Stroke in Octogenarians. *Cerebro-vasc Dis* 2011;33(2):116–122.
26. Kim D, Ford GA, Kidwell CS, et al. Intra-arterial thrombolysis for acute stroke in patients 80 and older: A comparison of results in patients younger than 80 years. *AJNR Am J Neuroradiol* 2007;28(1):159–163.
27. Taschner CA, Treier M, Schumacher M, et al. Mechanical thrombectomy with the Penumbra recanalization device in acute ischemic stroke. *J Neuroradiol* 2011;38(1):47–52.
28. Linfante I, Samaniego EA, Geisbusch P, et al. Self-expandable stents in the treatment of acute ischemic stroke refractory to current thrombectomy devices. *Stroke* 2011;42(9):2636–2638.
29. Hussein HM, Georgiadis AL, Vazquez G, et al. Occurrence and predictors of futile recanalization following endovascular treatment among patients with acute ischemic stroke: A multi-center study. *AJNR Am J Neuroradiol* 2010;31(3):454–458.
30. Patil CG, Long EF, Lansberg MG. Cost-effectiveness analysis of mechanical thrombectomy in acute ischemic stroke. *J Neu-rosurg* 2009;110(3):508–513.
31. Ishkanian AA, McCullough-Hicks ME, Appelboom G, et al. Improving patient selection for endovascular treatment of acute cerebral ischemia: A review of the literature and an external validation of the Houston IAT and THRIVE predictive scoring systems. *Neurosurg Focus* 2011;30(6):E7.
32. Flint AC, Cullen SP, Fageles BS, et al. Predicting long-term outcome after endovascular stroke treatment: The totaled health risks in vascular events score. *AJNR Am J Neuroradiol* 2010;31(7):1192–1196.
33. Halleivi H, Barreto AD, Liebeskind DS, et al. Identifying patients at high risk for poor outcome after intra-arterial ther-apy for acute ischemic stroke. *Stroke* 2009;40(5):1780–1785.
34. Lasjaunias P, Hui F, Zerah M, et al. Cerebral arteriovenous mal-formations in children. Management of 179 consecutive cases and review of the literature. *Childs Nerv Syst* 1995;11(2):66–79; discussion 79.
35. Hill MD, Rowley HA, Adler F, et al. Selection of acute isch-emic stroke patients for intra-arterial thrombolysis with pro-urokinase by using ASPECTS. *Stroke* 2003;34(8):1925–1931.
36. Natarajan SK, Dandona P, Karmon Y, et al. Prediction of adverse outcomes by blood glucose level after endovascular therapy for acute ischemic stroke. *J Neurosurg* 2011;114(6):1785–1799.
37. Nogueira RG, Liebeskind DS, Sung G, et al. Predictors of good clinical outcomes, mortality, and successful revascular-ization in patients with acute ischemic stroke undergoing thrombectomy: Pooled analysis of the Mechanical Embolus Removal in Cerebral Ischemia (MERCI) and Multi MERCI Trials. *Stroke* 2009;40(12):3777–3783.
38. Christoforidis GA, Mohammad Y, Kehagias D, et al. Angio-graphic assessment of pial collaterals as a prognostic indicator following intra-arterial thrombolysis for acute ischemic stroke. *AJNR Am J Neuroradiol* 2005;26(7):1789–1797.
39. Roberts HC, Dillon WP, Furlan AJ, et al. Computed tomo-graphic findings in patients undergoing intra-arterial throm-bolysis for acute ischemic stroke due to middle cerebral artery occlusion: Results from the PROACT II trial. *Stroke* 2002;33(6):1557–1565.
40. Miteff F, Levi CR, Bateman GA, et al. The independent predic-tive utility of computed tomography angiographic collateral sta-tus in acute ischaemic stroke. *Brain* 2009;132(pt 8):2231–2238.
41. Khatiri P, Abruzzo T, Yeatts SD, et al. Good clinical outcome after ischemic stroke with successful revascularization is time-dependent. *Neurology* 2009;73(13):1066–1072.
42. Kucinski T, Koch C, Eckert B, et al. Collateral circulation is an independent radiological predictor of outcome after thrombolysis in acute ischaemic stroke. *Neuroradiology* 2003;45(1):11–18.
43. Bang OY, Saver JL, Buck BH, et al. Impact of collateral flow on tissue fate in acute ischaemic stroke. *J Neurol Neurosurg Psychiatry* 2008;79(6):625–629.
44. Kitagawa K, Yagita Y, Sasaki T, et al. Chronic mild reduction of cerebral perfusion pressure induces ischemic tolerance in focal cerebral ischemia. *Stroke* 2005;36(10):2270–2274.
45. Smith WS, Sung G, Starkman S, et al. Safety and efficacy of mechanical embolectomy in acute ischemic stroke: Results of the MERCI trial. *Stroke* 2005;36(7):1432–1438.
46. Kang DH, Hwang YH, Kim YS, et al. Direct thrombus retrieval using the reperfusion catheter of the penumbra system: Forced-suction thrombectomy in acute ischemic stroke. *AJNR Am J Neuroradiol* 2011;32(2):283–287.
47. Levy EI, Mehta R, Gupta R, et al. Self-expanding stents for recanalization of acute cerebrovascular occlusions. *AJNR Am J Neuroradiol* 2007;28(5):816–822.
48. Suh SH, Kim BM, Roh HG, et al. Self-expanding stent for recanalization of acute embolic or dissecting intracranial artery occlusion. *AJNR Am J Neuroradiol* 2010;31(3):459–463.
49. Machi P, Costalat V, Lobotesis K, et al. Solitaire FR thrombec-tomy system: Immediate results in 56 consecutive acute isch-emic stroke patients. *J Neurointerv Surg* 2012;4(1):62–66.
50. Cohen JE, Gomori JM, Leker RR, et al. Preliminary experi-ence with the use of self-expanding stent as a thrombectomy device in ischemic stroke. *Neurol Res* 2011;33(4):439–443.

Vein of Galen Malformations

Key Points

- The age of presentation, gravity of the condition, and difficulty of treatment of vein of Galen malformations are highly linked to the angioarchitectural subtypes of this disorder.
- Most intraprocedural complications during treatment of these lesions can be ascribed to the extreme delicacy of the intracranial vessels in neonates and infants who require treatment in early life. Mundane endovascular maneuvers are not as easily tolerated by these thin-walled, distended structures.

The treatment of vein of Galen malformations is among the most difficult of neuroendovascular challenges, requiring intensive collaboration between obstetrical, neonatal intensivist, pediatric cardiology, and anesthesia staff, often beginning with a prenatal diagnosis. The most effective ultimate treatment modality is endovascular closure of the shunting vessels, but the welfare of the patient is best served by deferring this procedure for as long as is safely possible.

► INTRODUCTION

The first description of a vein of Galen malformation/aneurysm dates to 1937 (1). Fortunately, these are extremely rare lesions, and it has been estimated that a neurosciences center serving a population of 3 million will see a patient with this diagnosis less than once per year (2). This group of lesions is characterized by the midline presence of enlarged arteries in the region of the quadrigeminal cistern shunting into a massively enlarged venous sac, previously thought to represent the vein of Galen. The embryonic origins of this lesion have been clarified by Raybaud and subsequent authors (3) as a shunt that becomes established between 6 and 11 weeks of gestation resulting in persistence of the median vein of the prosencephalon and secondary failure of development of the normal deep venous drainage system. Therefore, in most patients with this disorder the venous drainage pattern, which at a glance can look similar to an enlarged version of the vein of Galen and straight sinus, actually represents a primitive precursor of the usual venous system, with variant channels of drainage through falx and tentorial sinuses that would have regressed under otherwise normal circumstances. The practical implications of this nice point are two-fold:

1. The brain does not therefore develop the usual system of deep venous drainage, and alternative venous pathways persist resulting often in enlargement of venous routes on the face, subcutaneous tissues, or scalp.
2. The presumption that the brain does not drain to the venous sac of the malformation would imply that therapeutic venous occlusion of the sac should be possible without risking venous infarction of the brain (although this presumption is questioned as not entirely reliable in all patients by some authors).

The patterns of arterial feeders to the malformation fall into two categories with significant implications on the clinical presentation of the patient and on the challenges of endovascular treatment.

Mural type of vein of Galen malformations account for about 30% to 40% of lesions and are the better type to deal with in every way (4,5). The number of arterial feeders is limited and usually confined to discrete, enlarged posterior choroidal arteries from the proximal posterior cerebral arteries (Fig. 33-1). They are named according to the discrete nature of the shunt in the wall of the venous sac. The volume of flow is not quite as high as the choroidal type of lesion, and thus angiographic images tend not to be quite so washed out, with better definition and visualization of the arterial feeders and venous sac. These children are less likely to develop immediate problems with cardiac output and tend to present later in childhood—or reach a point of needing treatment later—with macrocephaly, developmental delay, and seizures.

Choroidal type of vein of Galen malformations account for the majority of cases in most series. Their appearance is wilder on the angiogram with extremely rapid flow, markedly sinuous vessels, and involvement of choroidal vessels from the posterior circulation, thalamoperforator branches, and also the distal choroidal branches of the anterior cerebral artery (Fig. 33-2) (6). Occasionally, dural branches from the tentorium or falx can be recruited too, originating from the cavernous segment of the internal carotid artery or external carotid artery.

► CLINICAL PRESENTATION AND MANAGEMENT

The near universal practice of prenatal ultrasonography means that these lesions are now sometimes detected *in utero* with a midline cystic intracranial lesion demonstrating color Doppler flow. Prenatal MRI has the same capacity

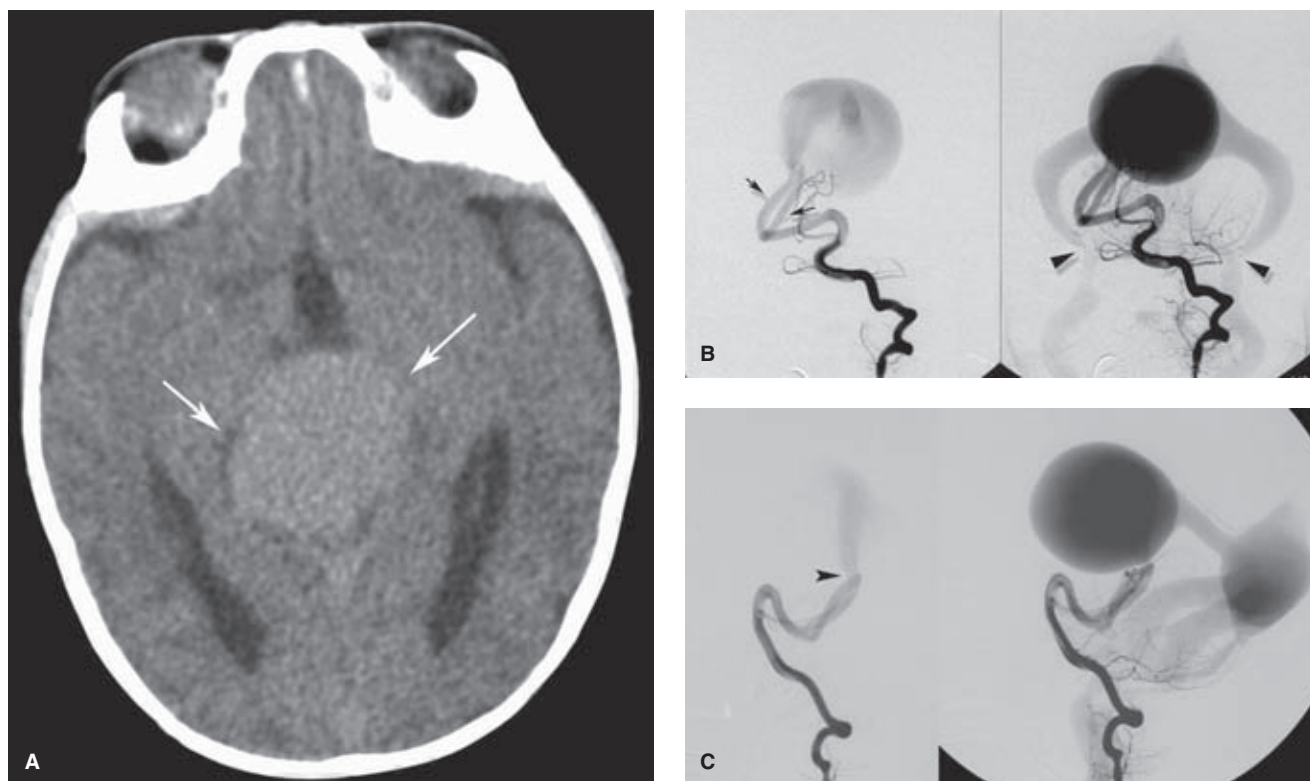


FIGURE 33-1. (A–C) Mural-type vein of Galen aneurysm in a 2-month-old child. This vein of Galen aneurysm was detected on a prenatal ultrasound. After birth, the patient had moderate problems with respiratory distress and congestive heart failure that were managed medically with the hopes that treatment could be postponed as long as possible. By 2 months of age, however, there was progressive decline in the capacity of medical measures to control his heart failure, and it was decided to go ahead with endovascular treatment. His pretreatment CT (**A**) shows mild hydrocephalus with massive distension of the venous sac (*arrows*) of the malformation. Of note particularly is the absence of any signs of irreversible brain damage such as parenchymal calcification or involucional gliosis. The AP views (**B**) and lateral views (**C**) of the left vertebral artery injection show that all or most of the flow is via two fistulous choroidal branches on the right side (*arrows*). The force of egress of flow from the arterial to the venous side generates a pronounced jet on the lateral view (*arrowhead*). Relative restriction of size of the straight sinus accounts in part for the marked distension of the “galenic” sac. The jugular confluences of the sigmoid and occipital sinuses demonstrate pronounced restriction of caliber, an observation of debated significance frequently found with this disorder (*arrowheads* in **B**). This lesion was treated successfully with complete closure of the fistulas using fibered coils. However, 2 years later, the patient returned with a small intraventricular hemorrhage of the III ventricle and was found to have a small degree of recanalization of the lesion requiring further embolization of tiny choroidal feeders. He ultimately needed gamma-knife therapy for unreachable arterial branches, and has since had a normal childhood with no neurologic sequelae.

and also allows an evaluation of the condition of the rest of the brain. Most prenatales with this disorder tolerate the shunting well due, it is thought, to the extremely low resistance of the placental circulation, meaning that the shunting within the malformation does not become relevant until after birth. Children with large volume shunts, typically those with choroidal-type malformations, tend to become symptomatic within a few days of birth or early in the neonatal period with high-output cardiac failure. With as much as 70% or more of the cardiac output shunting through the lesion, return to the heart is overwhelming and pulmonary hypertension with persistent right-to-left shunting in the heart and ductus arteriosus quickly becomes a dominant management problem. Reduced arterial systemic diastolic pressure, with biphasic reversal of flow in the aorta, results in hypoperfusion of the coronary, renal, and hepatic circulations. Tachypnea and difficulty feeding quickly leads to failure to thrive and eventual multiorgan failure in many

patients, with a virtual 100% mortality rate documented in older papers before effective treatment was a possibility (7). The cerebral circulation is particularly vulnerable due to the combination of hypoperfusion from cardiac failure, physiologic arterial steal due to the size of the shunts, and elevated venous pressure secondary to the effects on venous outflow. Early changes of parenchymal calcification progressing to more advanced “brain-melting” syndrome likely constitute an effective deterrent to treatment and most of the time indicate a poor prognosis.

Patients with milder type of choroidal malformations or mural-type malformations are less severely affected in the neonatal period and may remain asymptomatic or be managed medically until they have grown older (>6 months) at which time they can tolerate an endovascular procedure more safely. Frequent clinical and MRI evaluations during this time of waiting are advised, with any evidence of progression of macrocephaly or developmental delay being

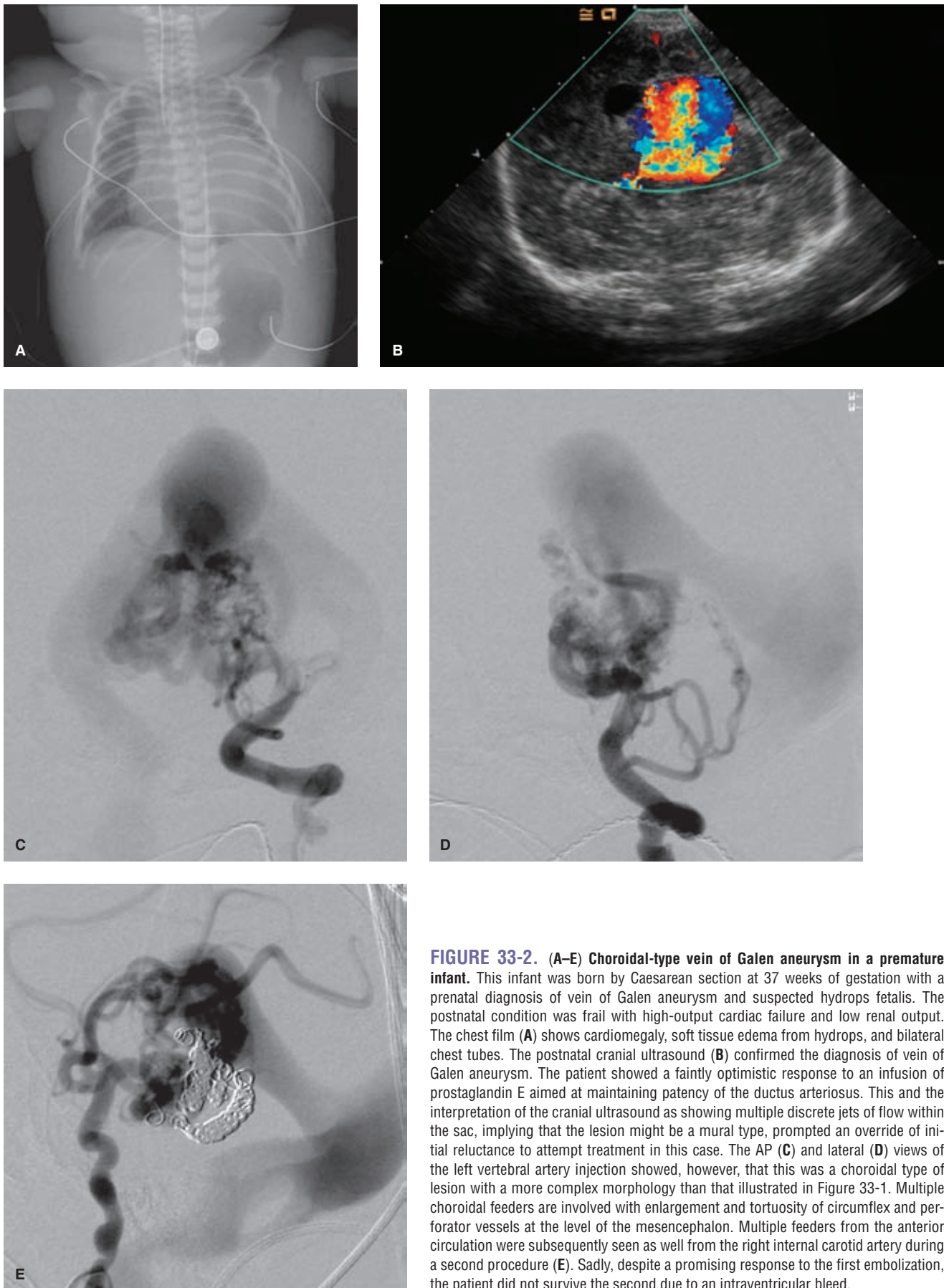


FIGURE 33-2. (A–E) Choroidal-type vein of Galen aneurysm in a premature infant. This infant was born by Caesarean section at 37 weeks of gestation with a prenatal diagnosis of vein of Galen aneurysm and suspected hydrops fetalis. The postnatal condition was frail with high-output cardiac failure and low renal output. The chest film (A) shows cardiomegaly, soft tissue edema from hydrops, and bilateral chest tubes. The postnatal cranial ultrasound (B) confirmed the diagnosis of vein of Galen aneurysm. The patient showed a faintly optimistic response to an infusion of prostaglandin E aimed at maintaining patency of the ductus arteriosus. This and the interpretation of the cranial ultrasound as showing multiple discrete jets of flow within the sac, implying that the lesion might be a mural type, prompted an override of initial reluctance to attempt treatment in this case. The AP (C) and lateral (D) views of the left vertebral artery injection showed, however, that this was a choroidal type of lesion with a more complex morphology than that illustrated in Figure 33-1. Multiple choroidal feeders are involved with enlargement and tortuosity of circumflex and perforator vessels at the level of the mesencephalon. Multiple feeders from the anterior circulation were subsequently seen as well from the right internal carotid artery during a second procedure (E). Sadly, despite a promising response to the first embolization, the patient did not survive the second due to an intraventricular bleed.

taken as a trigger to initiate endovascular treatment (8). Typically mural-type malformations present with macrocephaly, hydrocephalus, seizures, or developmental delay, with cardiac failure being a less prominent feature as the age of presentation increases. Occasionally a vein of Galen malformation may escape detection completely during childhood and may present in adulthood, typically with a subarachnoid bleed or macrocrania (Figs. 33-3 and 33-4).

For severely ill neonatal patients with this disorder, severe cardiac failure and impending multiorgan failure may imply that deferring the endovascular treatment until later in childhood may not be an option. The question of whether to treat these poorly faring infants at all has been addressed by the Bicêtre Vein of Galen rating scale according to the renal, cardiac, respiratory, hepatic, and neurologic status of the patient. A score of 0 to 8 points, in the recommendations of the late Dr. Lasjaunias, implies a futile outlook and a withholding of treatment, a score of 8 to 12 implies a need for urgent treatment, whereas treatment can be deferred for the present on scores >12/21 (9). However, several series have since commented that a small number of their cases with low Bicêtre scores (<8/21) have done well, suggesting that some reconsideration may be warranted for those children with low scores in whom extensive brain injury is not evident (5,10,11).

▶ ENDOVASCULAR TREATMENT

Microsurgical management of vein of Galen has little to offer for definitive treatment with historical mortality rates of 80% to 100% (7,12). Ventriculoperitoneal shunting has also been associated consistently with abrupt clinical decline of the patient. Endovascular management has had a profound impact on the previously bleak long-term prognosis for these children led by the few centers with the most cumulative experience including Paris (7), Toronto (8), London (5), New York (13), and others (14–17). Of those patients who undergo treatment, a good long-term outcome is seen in 39% to 74% of patients with an overall mortality rate of 10% to 20%. Children who fare best are those who are well enough to wait for treatment until after 5 months of age, with good outcomes seen in 67% to 100% of this group and a mortality rate of <6.5% (12). Outcomes of those with multisystem failure or early evidence of cerebral injury and who undergo treatment in the neonatal period have less encouraging outcomes, even in highly experienced hands, with a mortality rate still ranging as high as 50% (8).

The obliteration of the shunt can be approached from the venous or transarterial side. Older papers detailed inventive transvenous approaches via the torcular on occasion, while transarterial cannulation via the umbilical artery was

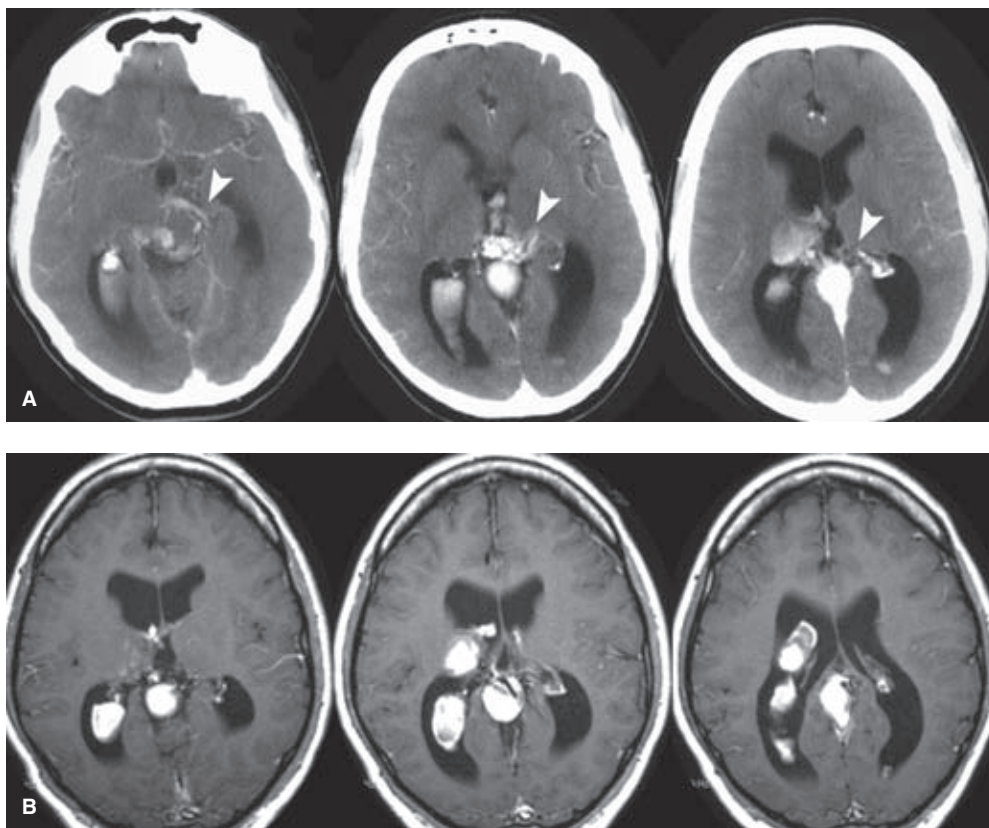


FIGURE 33-3. (A–E) Choroidal-type vein of Galen aneurysm in a 28-year-old adult. A 28-year-old male who had been seen in childhood at a major pediatric center and told that he had a malformation in his brain best left untreated at that time presented in adulthood with his first complication, a mild intraventricular hemorrhage. His contrast-enhanced CT scan (A) shows moderate ventriculomegaly with intraventricular hemorrhage and a profusion of enhancing vessels in the perimesencephalic and quadrigeminal cisterns (*arrowheads*). The distended “galenic” sac is evident on the CT scan. The contrast-enhanced T1-weighted MRI (B) and T2-weighted MRI (C) demonstrate the same findings with a complexity of vascular findings suggesting that this is a choroidal type of lesion. (*continued*)

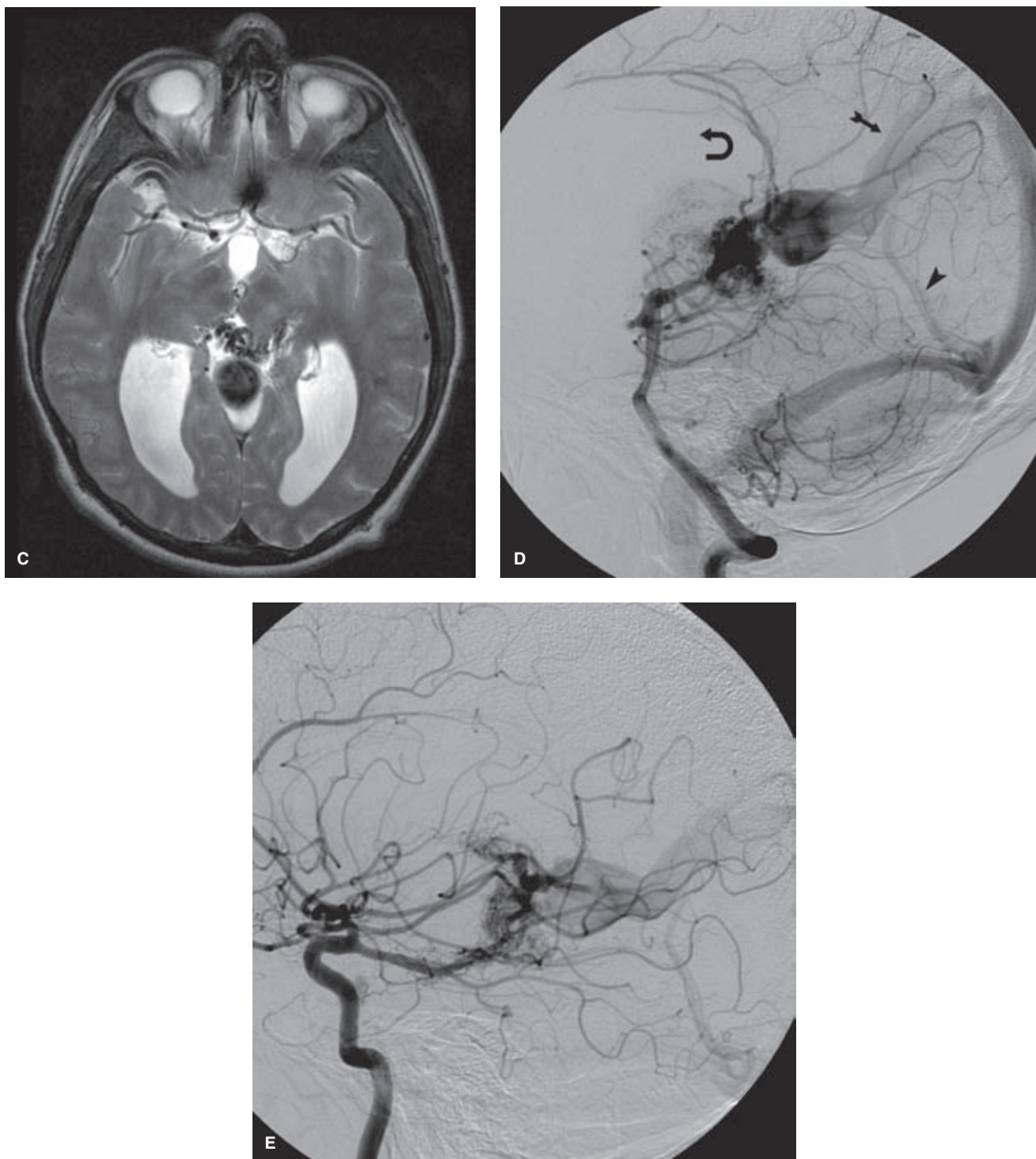


FIGURE 33-3. (CONTINUED) The lateral vertebral artery injection (**D**) and right internal carotid artery injection (**E**) demonstrate that fortunately for the patient, this was a relatively low-flow lesion, accounting for his being able to reach adulthood without a need for treatment. Notice the relatively deficient appearance of the straight sinus in (**D**) (*arrowhead*) and the large falcine sinus (*arrow*). There is angiographic evidence of hydrocephalus with taut rounding of the lateral course of the anterior cerebral artery. Furthermore, there is prominent retrograde flow into the perisphenal-to-pericallosal route of flow (*curved arrow*) from the posterior circulation, a finding that was difficult to explain. One possibility is that the lesion had been in a state of higher flow when he was younger and thus had encouraged development of anterior to posterior circulation via this route. With hypothesized diminution of flow in later life, the demand for flow via this route might have diminished, but the connection may have persisted in a nonphysiologic pattern of flow. The patient opted for treatment by placement of a ventriculoperitoneal shunt and gamma-knife irradiation of the malformation. An angiogram 3 years later showed no evidence of remaining fistulous flow.

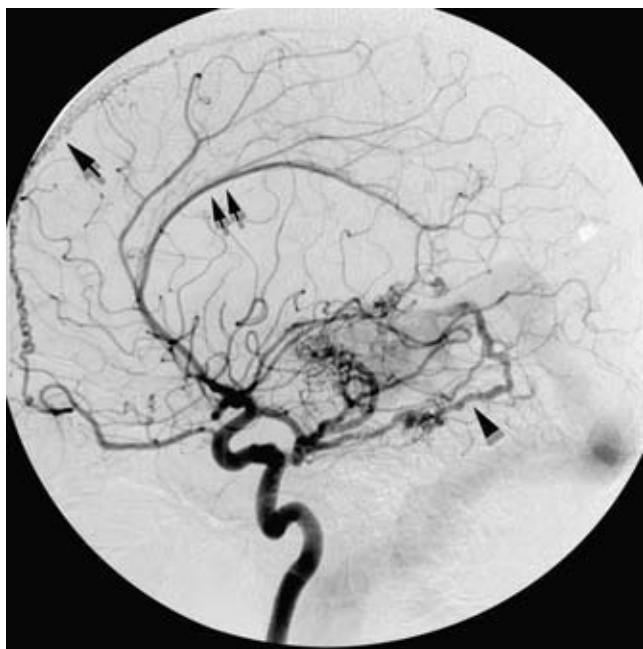


FIGURE 33-4. Vein of Galen malformation presenting in adulthood. A lateral internal carotid angiogram in this young adult who had eluded medical detection until the time of his presentation with hydrocephalus—note the splayed appearance of the anterior cerebral artery (*double arrows*). In this patient the straight sinus has developed in a relatively mature configuration, and the volume of flow is relatively low although it is impossible to know what the situation was when this patient was younger. There is a complex rete of pial and dural arteries supplying this lesion, including enlarged tentorial dural vessels (*arrowhead*). The effect of prominent dural arterial involvement is seen remotely in the enlargement of the anterior artery of the falx (*single arrow*).

sometimes used too. However, these techniques are rarely necessary in modern experience. Transarterial femoral access using ultrasound assistance is almost universally successful, although occasionally inventive alternatives such as transaxillary cannulation prove necessary. Transvenous coil obliteration of the venous sac is still used by some authors (10), but the majority of modern sources highly favor a piece-meal transarterial approach using liquid embolic agents, sometimes with coil assistance (8,12,18). One major argument in favor of the transarterial approach is that it can be done over several embolization sessions, allowing some measure of autoregulatory adjustment over time, whereas a transvenous embolization is a single all-or-none abrupt closure of the lesion. Furthermore, occasional instances of hemolysis or disseminated intravascular coagulopathy have been ascribed to the presence of a rapidly flowing shunt through a partially occlusive mesh of venous coils placed via a transtorcular approach (19,20).

In addition to the challenges of repeated transarterial femoral access in these patients, technical challenges of the procedure include the following:

- Contrast load. The recommended dose of contrast per session should not exceed 5 to 10 mL/kg body weight (18,21), but even this might have to be rescaled when renal function is impaired.
- The fragility of the intracranial arteries and veins, particularly in the neonate, means that much of the latitude to which one has become accustomed in dealing with adults

is not present in neonatal and infant cases. Therefore, minor events such as deploying a coil in an artery or vein or pulling a slightly embedded microcatheter are much more risky in this group of patients, and likely explain the common difficulty with procedural bleeding seen in many published series.

- The rapidity of arterial flow in the shunts is such that only the highest concentration of nBCA 80% to 100% mixed with tantalum can be used for embolization, a skill that is not generally being passed on to a new generation due to its having been supplanted by Onyx.
- An alternative strategy is to partially embolize the artery with coils and then deploy Onyx 18 or Onyx 34, but the major limitation with this device is the volume of DMSO that can be used for catheter lavage (22). A maximum dose of DMSO (1 mL = 1.1 g) per session should not exceed 600 mg/kg and preferably should be closer to 205 mg/kg (the average adult dose in FDA trials) (21,23), which would significantly limit the number of pedicles that could be embolized at one session in small children.
- The radiation dose from the procedure and the presumed increased sensitivity of a neonate's or infant's skin to levels of ESD that might be well tolerated in adults or older children is another factor to consider. Published recommendations suggest stopping at 1,000 mGy.
- Partial treatment of a vein of Galen malformation may not at all be a suboptimal outcome and may, in fact, represent the safest strategy (11,21). This might diminish the risk of hyperperfusion phenomenon or choroidal bleeding after an abrupt total closure of the malformation. Furthermore, a small residual remnant may respond well to gamma-knife treatment with less risk than an endovascular embolization of small tortuous vessels might represent (24,25).

Finally, a distinction must be drawn between true vein of Galen malformations on the one hand and other rare lesions such as pial AVMS) or dural malformations in which there is secondary involvement of the vein of Galen proper ("aneurysmal dilatation of the Vein of Galen"). In the latter instance, a transvenous occlusion of the vein of Galen could have catastrophic complications.

References

1. Jaeger JR, Forbes RP, Dandy WE. Bilateral congenital cerebral arteriovenous communication aneurysm. *Trans Am Neurol Assoc* 1937;63:173–176.
2. Bhattacharya JJ, Thammaroj J. Vein of Galen malformations. *J Neurol Neurosurg Psychiatry* 2003;74 (suppl 1):i42–44.
3. Raybaud CA, Strother CM, Hald JK. Aneurysms of the vein of Galen: Embryonic considerations and anatomical features relating to the pathogenesis of the malformation. *Neuroradiology* 1989;31(2):109–128.
4. Halbach VV, Dowd CF, Higashida RT, et al. Endovascular treatment of mural-type vein of Galen malformations. *J Neurosurg* 1998;89(1):74–80.
5. McSweeney N, Brew S, Bhate S, et al. Management and outcome of vein of Galen malformation. *Arch Dis Child* 2010; 95(11):903–909.
6. Wolfram-Gabel R, Maillot C, Koritke JG. The vascular pattern in the tela choroidea of the prosencephalon in man. *J Neuroradiol* 1987;14(1):10–26.
7. Lasjaunias PL, Chng SM, Sachet M, et al. The management of vein of Galen aneurysmal malformations. *Neurosurgery* 2006;59(5 suppl 3):S184–194; discussion S3–13.

8. Li AH, Armstrong D, TerBrugge KG. Endovascular treatment of vein of Galen aneurysmal malformation: Management strategy and 21-year experience in Toronto. *J Neurosurg Pediatr* 2011;7(1):3–10.
9. Lasjaunias P, Ter Brugge K. *Vascular Diseases in Neonates, Infants and Children*. Berlin: Springer; 1997:167–202.
10. Frawley GP, Dargaville PA, Mitchell PJ, et al. Clinical course and medical management of neonates with severe cardiac failure related to vein of Galen malformation. *Arch Dis Child Fetal Neonatal Ed* 2002;87(2):F144–F149.
11. Jones BV, Ball WS, Tomsick TA, et al. Vein of Galen aneurysmal malformation: Diagnosis and treatment of 13 children with extended clinical follow-up. *AJNR Am J Neuroradiol* 2002;23(10):1717–1724.
12. Khullar D, Andeejani AM, Bulsara KR. Evolution of treatment options for vein of Galen malformations. *J Neurosurg Pediatr* 2010;6(5):444–451.
13. Berenstein A, Ortiz R, Niimi Y, et al. Endovascular management of arteriovenous malformations and other intracranial arteriovenous shunts in neonates, infants, and children. *Childs Nerv Syst* 2010;26(10):1345–1358.
14. Heuer GG, Gabel B, Beslow LA, et al. Diagnosis and treatment of vein of Galen aneurysmal malformations. *Childs Nerv Syst* 2010;26(7):879–887.
15. Fullerton HJ, Aminoff AR, Ferriero DM, et al. Neurodevelopmental outcome after endovascular treatment of vein of Galen malformations. *Neurology* 2003;61(10):1386–1390.
16. Geibprasert S, Krings T, Armstrong D, et al. Predicting factors for the follow-up outcome and management decisions in vein of Galen aneurysmal malformations. *Childs Nerv Syst* 2010;26(1):35–46.
17. Gupta AK, Rao VR, Varma DR, et al. Evaluation, management, and long-term follow up of vein of Galen malformations. *J Neurosurg* 2006;105(1):26–33.
18. Berenstein A, Fifi JT, Niimi Y, et al. Vein of Galen malformations in neonates: New management paradigms for improving outcomes. *Neurosurgery* 2012;70(5):1207–1213.
19. Charafeddine L, Numaguchi Y, Sinkin RA. Disseminated coagulopathy associated with transtorcular embolization of vein of Galen aneurysm in a neonate. *J Perinatol* 1999;19(1):61–63.
20. Rosenberg EM, Nazar GB. Neonatal vein of Galen aneurysms: Severe coagulopathy associated with transtorcular embolization. *Crit Care Med* 1991;19(3):441–443.
21. Thiex R, Williams A, Smith E, et al. The use of Onyx for embolization of central nervous system arteriovenous lesions in pediatric patients. *AJNR Am J Neuroradiol* 2010;31(1):112–120.
22. Germanwala AV, Vora NA, Thomas AJ, et al. Ethylenevinylalcohol copolymer (Onyx-18) used in endovascular treatment of vein of Galen malformation. *Childs Nerv Syst* 2008;24(1):135–138.
23. Jankowitz BT, Vora N, Jovin T, et al. Treatment of pediatric intracranial vascular malformations using Onyx-18. *J Neurosurg Pediatr* 2008;2(3):171–176.
24. Payne BR, Prasad D, Steiner M, et al. Gamma surgery for vein of Galen malformations. *J Neurosurg* 2000;93(2):229–236.
25. Tomsick TA, Ernst RJ, Tew JM, et al. Adult choroidal vein of Galen malformation. *AJNR Am J Neuroradiol* 1995;16(4 suppl):861–865.

Index

A

- Aberrant internal carotid artery, 151–152, 153f
Aberrant right subclavian artery, 109, 110f, 111f
ACAS. *See* Asymptomatic carotid artery stenosis
Accessory meningeal artery, 237, 240–242, 241f–244f
Accessory middle cerebral artery
 from A1 segment, 181f
 bilateral, 181f
Activated clotting time (ACT), 272
 systemic heparinization, dose measurement of, 26
Adamson–Kienbock procedure, 88
Agraphia
 angular gyrus of dominant lobe and, 179
Aica–pica complex, 213
Air bubbles, cerebral angiography and, 73
Allen test, 17
 of palmar arch, 17f
Ambient segment, of posterior cerebral artery, 183
American Society of Neuroradiology, 68
Amplatz wire, arterial puncture and, 13
Anastomotic vein of Labbé, 223
Anastomotic vein of Trolard, 223, 224f
Anesthesia
 spinal angiography and, 52
Aneurysmal rupture
 cerebral angiography and, 75–77, 76f
 endovascular treatment for, efficacy of, 267–269, 268f
Aneurysm(s)
 A1 fenestration and, 163f
 of anterior cerebral artery, 168
 AVM and, 44, 45f–50f
 bacterial, 253
 basilar apex, 50f
 basilar artery, 213f
 blister, 49f
 of carotid cave, 149f
 carotid–ophthalmic, 48f
 cavernous, 12, 249
 cavernous carotid, 143, 145f, 146
 cerebral, 249, 266–267
 circle of Willis and, 114
 of distal anterior cerebral artery, 169f
 of distal posterior cerebral artery, 193f
 dysplastic, 12
 embolization, 269
 endovascular treatment of, 267
 extradural, 249
 false, 249–252
 formation, sites of, 264–265
 fusiform, 250f
 fusiform intradural, 252–253
 giant, 266
 giant fusiform, 253
 giant serpentine, 179f
 inflammatory, 253, 256
 intracranial, 42, 249–284
 intraoperative angiography, 43
 intrasellar, 144f
 left carotid–ophthalmic, 280f
 left middle cerebral artery, 46f
 mycotic, 253, 255f
 oncotic intracranial, 256–257
 of petrous internal carotid artery, 139f
 of posterior cerebral artery II, 188f
 proximal basilar artery, 119f
 recurrence of, 46f–47f
 rupture, 76f
 ruptured intracranial, 265–266
 saccular, 264–265
 serpentine, 254f
 superior hypophyseal, 148f
 of supraclinoid internal carotid artery, 148
 surgical clipping of, 43
 unruptured intracranial, 265
 vein of Galen, 107
Angiocentric fungal infections, 434
Angioplasty technique, 481
Angiogenesis, gene regulation of, 309, 312–313
Angiography
 cerebral, 6, 14t
 neurologic complications of, 66–77
 intraoperative, 43
 spinal, 52–57
Anterior cerebral artery, 161–173
 branches of the distal, 168–169
 branches of the proximal, 164–167
 callosal branches of, 170–171
 cortical branches of, 169, 170f, 171f
 distal, 168, 169f
 dural branches of, 171
 ophthalmic artery from, 161
 pial–pial collaterals and, 171f
 segmental anatomy of, 161, 162f
 shift, 172–173, 172f, 173f
 variations in distal, 171–172
 variations of, 161, 162f–164f, 164, 165f–167f
Anterior choroidal artery, 118
 origin of, 148–150, 150f
 territory of, 150, 151f
Anterior inferior cerebellar artery, 214
Anterior perforator vessels, 164–165
Anterior spinal artery, risks, 413
Anterior spinal communicating artery, 206
Anterior temporal branch, 178f
Antineutrophil cytoplasmic antibodies (ANCA), 434
Anton syndrome, 191
Aortic aneurysmal disease, 18
Aortic arch, 109–113
 carotid catheterization and, 112
 navigation, catheter and, 18–19, 18f–21f
 variations and anomalies, 110f
Arcade of odontoid process, 236
Arterial embryology, 100
 4-mm fetal stage, 101–102, 102f
 5- to 6-mm fetal stage, 102, 103f
 7- to 12-mm fetal stage, 102–103, 104f
 12- to 14-mm fetal stage, 103–104, 105f
 16- to 18-mm fetal stage, 104–106, 105f
Arterial injuries, neck/face bleeding, 414–417
Arterial puncture
 landmark palpation, 13f
 sheath placement, 13–14, 15f–17f
Arteries of posterior fossa, 206–216, 211f, 212f
Arteriopathy, 368
Arteriotomy, 15f
 pediatric neuroangiography and, 58, 59f
Arteriovenous malformation (AVM), 12, 89, 138, 224
 aneurysms associated with, 308–309, 308f
 of brain, 299, 300f–305f, 305, 306f–307f, 308–309
 dural, 186, 344t
 of foramen of Monro, 189f
 grading of, 309
 intracranial dural, 362f
 intradural spinal, 351, 352f–356f, 356
 occipital, 192f
 parieto-occipital, 191f
 shunting in astrocytoma, 314f
 Spetzler–Martin Scale for, 308t
 spinal dural, 359
 volume of, 44, 45f–50f

Note: Page numbers followed by f denote figures; those followed by t denote tables; those followed by b indicate a box.

- Arteriovenous shunting, 356
 Artery of Adamkiewicz, 359
 Artery of cervical enlargement, 199
 Artery of foramen rotundum, 245
 Artery of Percheron, 186
 Ascending palatine artery, 237
 Ascending pharyngeal artery, 150, 152, 231, 234–236, 235f–236f, 236, 237, 394
 anatomic connections, 395f
 in upper cervical vascular system, 247
 Aspirin
 for thromboembolic complications reduction, 272
 Asymptomatic carotid artery stenosis (ACAS), 67
 Atherosclerotic disease, 465
 accunet protective device preparation, 468f
 angioplasty balloon
 deflation, 467f
 inflation, 467f
 preparation of, 466f
 carotid artery angioplasty and stenting, 465–467
 ECA–MCA bypass
 symptomatic external carotid artery stenosis, 472f
 exchange-wire maneuvers, 482f
 extracranial vertebral artery angioplasty, 467–473
 intracranial angioplasty and stenting, 473–482
 middle cerebral artery stenosis
 delayed hemorrhage, 481f
 open-cell *versus* closed-cell design stents, 473f
 protected carotid angioplasty and stenting, 470f
 right vertebral artery stenosis, 474f–475f
 symptomatic carotid stenosis, 471f
 symptomatic midbasilar stenosis, 479f
 symptomatic supraclinoid stenosis, 477f–478f
 tortuous vessel
 unprotected carotid angioplasty, 469f
 transradial catheterization
 during subclavian artery stenting, 476f
 vertebral artery ostium stent, fragmentation of, 474f
 Wingspan stent, 480f
 AVM. *See* Arteriovenous malformation
- B**
- Bacterial aneurysms, 253
 Balloon remodeling technique, 275, 282
 Balloon-test occlusion of sinus, dural arteriovenous malformations, 349
 Barrow classification, 375
 Basal cerebral vein of Rosenthal, 227–228, 227f
 Basal hemispheric superficial veins, 224–226
 Basal vein, 227
 anatomic variants in, 227–228, 228f
 Basal vein of Rosenthal, 107, 183, 223, 224
 Basic fibroblast growth factor (bFGF), 298, 373
 Basilar apex aneurysm, 50f
 Basilar artery, 106, 210–213
 aneurysm and perforator vessels, 213f
 bifurcation, 210, 213
 brainstem branches of, 210
 spinal artery collateral flow to, 210f
 Basilar tip aneurysms, projections of, 207f
 Benign intracranial hypertension, 445
 Bentson wire, 43
 Berry aneurysm, 114
 bFGF. *See* Basic fibroblast growth factor
 Bicarotid trunk, 109, 111f
 Bi-innominate artery, 109, 110f
 Bleeding, acute
 head and neck embolizations for, 394
 Blister aneurysm, of right carotid terminus, 49f
 Blood pressure, 482
 Borden classification scheme, 337
 Bow hunter's stroke, 442, 443f
 angiographic confirmation, 442
 Brachial vein, 229
 Brain
 arteriovenous malformations of, 299, 300f–305f, 305, 306f–307f, 308–309
 embolic agents for, 314–319
 endovascular treatment of, 309, 310f–313f, 312–319
 history of, 305, 308
 cavernous malformations of, 292–297, 293f–295f
 vascular malformations of, 291–319
 Brain-melting syndrome, 499
 Brainstem, surface of, 229
 Brainstem syndromes, 207
 Bridging veins, 223
 Buccal artery, 244
- C**
- Calcarine artery, 191
 Calcium blocker drugs, 459
 Callosomarginal artery, 170
 Candelabra group, 179
 Capillary angiomas, 291, 292f
 Capillary telangiectasis, 291
 Capsular arteries of McConnell, 143, 144f
 Caput medusae, 297
 Cardiac enzymes, 466
 Carotid arteries
 test occlusion, 424
 Carotid artery stenosis
 measurement of, 133f
 Carotid–basilar anastomoses, 154–159
 Carotid bifurcation, 112
 Carotid cave, 148
 aneurysms of, 149f
 Carotid-cavernous fistula (CCF), 154, 249, 380f, 382f–386f
 cavernous aneurysm rupture *v.*, 375
 combined transarterial and transvenous treatment, 381f–382f
 endovascular treatment of, 375
 with ipsilateral carotid dissection, 378f
 of left internal carotid artery, 377f
 ocular findings of, 376f
 post-trauma, 378f
 spontaneous regression of, 381f
 trauma and, 375, 376f
 treatment of, 375, 379, 383, 386
 Carotid endarterectomy (CEA), 75
 Carotid–ophthalmic aneurysm, 48f
 Carotid pseudoaneurysm, 256f
 Carotid pseudoaneurysm repair
 with covered stent, 417f
 Carotid revascularization, 470
 Carotid ulceration, 134f
 Carotid/vertebral arteries
 advanced carotid paraganglioma, appearance of, 406f
 test occlusion, 422–424
 Catheter
 cerebral, 12f
 choosing, angiographic study and, 12
 flushing, 19, 22–26, 22f–30f
 induced arterial spasm, 32f
 measurement, 12
 for spinal angiography, 57f
 Cavernous aneurysms, 249
 Cavernous carotid aneurysms, 143, 145f, 146
 Cavernous malformation, 291
 of brain, 292–297, 293f–295f
 Cavernous sinus, 218
 CCF. *See* Carotid-cavernous fistula
 Centigrays (cGy), 7
 Central nervous system (CNS), 434
 infection, 450
 intracranial vasculitis
 angiographic appearance of, 435f
 with multiple ischemic infarcts, 435f–436f
 presumed tumor, 439f
 primary angitis of CNS (PACNS), 426, 428, 434–440
 biopsy-proven, 436f–439f
 Mayo Clinic series, 440
 presumed in young adult, 440f
 systemic vasculitides, 434
 Cerebellar veins, 229
 Cerebellum, arteries of, 213–215
 anterior inferior, 214
 posterior inferior, 213–214
 superior, 214–215
 Cerebral aneurysm, 249, 266–267
 in children, 266–267
 Cerebral angiography, 109
 aneurysmal rupture and, 75–77, 76f
 and contrast agents, 13, 13t, 14t
 dangers of, 68f
 neurologic complications of, 66–77, 68f, 70f, 71f
 nonneurologic complications of, 77
 principles, 69t
 transient global amnesia and, 75
 Cerebral angiography, 434, 437
 Cerebral arteries, territories of, 122, 128f–130f
 Cerebral arteriogram, performing, 11–50
 Cerebral catheter, 12f
 Cerebral circulation, 499
 Cerebral vasospasm, 457
 balloon angioplasty
 to aneurysm coiling, 460f
 calcium blocker drugs, 459
 cortical spreading depression, 458
 delayed ischemia neurologic deficits (DINDs), 457
 endovascular treatment
 balloon angioplasty, 459–462
 intra-arterial drugs, 458–459
 posterior circulation vasospasm angioplasty, 461f
 treatment in, 462f
 vasospasm and cerebral ischemia, 457–458
 Cervical anastomoses, 246f
 Cervical arteries, 245–247, 245f–247f

- Cervical embolization, dangers of, 246f
 Cervical vertebral artery, 195
 Chernobyl
 radiation exposure risks and, 86
 Childhood stroke, 368
 Children
 cerebral aneurysms in, 266–267
 Choroidal veins, 226
 Cingulate gyrus, 223
 Circle of Willis, 114–130
 aneurysm and, 264–265
 anomaly categories, 118–120, 119f–124f
 dissections in, 114
 evolution of, 116
 fenestrations of, 120–122, 125f–127f
 surrounding structures, anatomic relationship to, 114, 115f, 116f
 variations in, 114–122, 117f–119f
 vessel size, 116–118, 267
 Cistern of the velum interpositum, 227
 Clopidogrel
 for thromboembolic complications reduction, 272
 CNS. *See* Central nervous system
 Cobb syndrome, 351
 Cockcroft–Gault formula, for creatinine clearance, 78t
 Coexistent medical risks, 493
 Cognard classification scheme, 337
 Coil
 brain AVM and, 318
 Compton effect, X-rays and, 84
 Contrast agents
 cerebral angiography and, 13, 13t, 14t
 Contrast-induced nephropathy, 78–79
 bicarbonate protocol for, 78t
 prevention of, 78
 Contrast reaction, premedication for, 77
 Convexity hemispheric veins, 223–224
 Cranial circulation, embryology of, 100–107
 Cranial dura, 322
 Cranial dural vascular malformations, 322–349
 Craniocervical junction, 237
 Craniocervical foramen, 106
 Cerebrospinal fluid (CSF) analysis, 426
 CREST trial, 466
- D**
- DAVM. *See* Dural arteriovenous malformations
 Deep supratentorial veins, 224–226, 225f, 226f
 Deep temporal arteries, 243–244
 Deep venous filling, sequence of, 228
 Deep venous system, choroidal veins of, 226
 Dehydrated alcohol, AVM embolization and, 316–318
 Delayed ischemia neurologic deficits (DINDs), 457
 Detective quantum efficiency (DQE), 92
 Deterministic effects, radiation and, 86
 Diffuse nonperimesencephalic nonaneurysmal hemorrhage, 391
 Diffusion-weighted imaging (DWI), 74–75
 Dimethylsulfoxide (DMSO), 315
 Distal anterior cerebral artery, 168, 169f
 Distal external carotid artery, anatomy of, 239f, 396f
 Doppler imaging, 457
 Doppler sonography, of cerebral artery flow, 76.
 See also Aneurysmal rupture
- Dorello canal, 236, 342
 Dose–area product (DAP), 86
 Double aortic arch, 109, 111f
 Down syndrome, 370
 DQE. *See* Detective quantum efficiency
 Duplicated posterior cerebral artery, 118
 Duplicated posterior communicating artery. *See*
 Duplicated posterior cerebral artery
 Dural arteriovenous fistula, 351. *See also* Dural
 arteriovenous malformations (DAVM)
 Dural arteriovenous malformations (DAVM)
 of anterior cranial fossa, 332, 334f
 of cavernous sinus, 323f, 326f, 327f, 339f,
 343f–344f
 circumstances for treatment, 332, 336–338,
 342–344, 349
 disappearing, 330f–331f
 embolization, procedure for, 332
 endovascular treatment of, 336
 with Glioblastoma Multiforme, 334f
 intracranial complications, 335f
 of left transverse sinus, carotid artery
 injections and, 328f
 meningohypophyseal trunk, 338f
 with parenchymal venous hypertension, 332f
 pial arteriovenous malformation, 337f
 post surgical, of cavernous sinus, 325f
 of right sigmoid sinus, 325f, 329f
 of right transverse sinus, 348f–349f
 schemes for, 344t
 of sigmoid sinus, 336
 of sigmoid-transverse sinus, grading schemes,
 324f
 subarachnoid hemorrhage and, 332f–333f
 superficial cortical venous drainage, 336f
 transvenous coil embolization of, 340f–341f
 transvenous embolization of cavernous, 345f
 of transverse and sigmoid sinuses, 328f
 uncomplicated, 322
 venous hypertension and, 328f
 Dural sinuses, 217–221, 219f–222f
 Dural sinus occlusive disease, 445–455
 AngioJet rheolytic catheter, treatment by,
 454f
 extensive DST with profound neurologic
 decline, 452f–453f
 idiopathic intracranial hypertension, 445–450
 with emergency endovascular stenting,
 447f–448f
 to medical therapy, 446f–447f
 venous stenosis, insensitivity, 449f
 suction thrombectomy
 straight sinus thrombosis, 455f
 thrombosis, 450–455
 clot disruption, treatment by, 451f
 Dural sinus thrombosis (DST), 445, 450
 Dural vascular disease
 clinical manifestations of, 361–362
 Dural vascular disease, angiographic study and,
 12
 DWI brain injuries, 466
 DWI. *See* Diffusion-weighted imaging
- E**
- Eale’s syndrome, 434
 ECASS-III study, 485
 Ectasia, 249
 Ehlers–Danlos syndrome, 322
 Electrocardiogram (EKG), 41
- Encephaloduroarteriosynangiosis, 373
 Encephalomyosynangiosis, 373
 Endocranial branches, 238
 Endovascular coil embolization
 safety concerns for, 269, 270f–282f, 272, 275,
 282–284
 Endovascular intervention
 in mycotic aneurysms management, 256
 Endovascular intervention, 490
 Endovascular treatment
 of brain arteriovenous malformations, 309,
 310f–313f, 312–319
 ENT bleeding. *See also* Head; Neck
 after LeFort osteotomy, 404f, 405f
 common carotid artery bifurcation, 394
 epistaxis, 397–401
 head and neck embolizations for, 394
 head and neck tumors
 hypervascular tumors, 401–414
 principal risks, 408
 nasal mucosal collateralization, 401f
 short sphenopalatine artery, pseudoaneurysm
 of, 400f
 sinonasal bleeding, 397–401
 Epidural arteriovenous malformation, 356
 Epistaxis, 397–401
 embolization for control, 397
 gelfoam pledget, injecting, 402f
 in hereditary hemorrhagic telangiectasia, 400f
 launching, pledget, 402f
 loading, pledget, 402f
 posterior idiopathic, 397
 rolling, pledget, 402f
 and sinonasal bleeding, 397–401
 Epstein–Barr virus, 373
 Estimated skin dose (ESD), 86
 Ethylene-vinyl alcohol (EVOH), 315
 External carotid artery, 232f–234f
 branches of, 231, 234–245
 inferolateral trunk, 397f
 External carotid artery injection
 angiographic study and, 11–12
 External jugular vein, 217
 Extracranial veins, 217, 218f–221f
 Extradural aneurysms, 249
 Extradural vertebral arteries, 195–204,
 196f–204f
- F**
- Face bleeding, 414–417
 Facial artery, 237, 237f, 398
 nasal mucosal collateralization, 401f
 False aneurysms
 of intracranial circulation, 249–252
 Falx cerebelli, artery of, 209f
 FCA. *See* Focal Cerebral Arteriopathy
 Femoral arterial puncture, 16f
 Femoral artery pseudoaneurysms, 77
 Fetal posterior communicating artery, 183
 Fisher scale, 266
 FLAIR injuries, 466
 Flat detector (FD), 82
 Focal Cerebral Arteriopathy (FCA), 368, 369f
 Foley balloon catheter, 397
 Foix–Alajouanine syndrome, 362
 Foramen cecum, 206
 Foramen lacerum, 236
 Foramen meningoorbitale, 106
 Foramen of Hyrtl, 106

- Foramen of Vesalius, 107, 242
 Foramen of Vicq d'Azyr, 206
 Foramen rotundum, artery of, 245
 Fröhlich–Babinski syndrome, 6
 Fusiform aneurysm, 250f
 intradural, 252–253, 253f
 Futile recanalization, 490
- G**
- Galenic system, 107
 Galen malformations, vein of, 498–503
 in adulthood, 503f
 catastrophic complications, 503
 categories, 498
 choroidal type, 498
 mural type, 498
 choroidal type, 500f
 premature infant, 500f
 in 28-year-old adult, 501f–502f
 clinical presentation and management, 498–501
 endovascular treatment, 501–503
 microsurgical management, 501
 pial AVMS, 503
 radiation dose, 503
 transarterial femoral access, challenges, 503
- G20210A prothrombin mutation, 291
 Gelfoam
 proximal reflux, forceful injection, 395f
 Gelfoam powder, 74
 Giant aneurysm, 266
 Giant fusiform aneurysm, 253
 Giant serpentine aneurysm, 266
 Glasgow Coma Scale, 450
 Glomus tympanicum tumors, 236
 Glomus vagale tumor
 pharyngeal artery, anastomotic connections, 412f
 for preoperative embolization, 411f
 typical appearance of, 410f
 Glossopharyngeal nerve, Jacobson branch of, 236
 Gray (Gy), 86
 Great cerebral vein of Galen, 227
 Greater descending palatine artery, 242
 Great vessel catheterization, wire manipulation
 and, 34–35, 35f–41f, 39–43
 Groin compression
 pediatric neuroangiography and, 58, 60f
 Gunshot wound
 with active extravasation from tongue, 415f
- GVHD
 reversible cerebral vasoconstriction syndrome (RCVS)
 intracranial vasculitis, 432f
- H**
- Head. *See also* ENT bleeding
 airway protection, 414
 hemodynamic stabilization, 414
 paragangliomas, 405
 tumor, 408
 Hemangioblastoma of right cerebellar hemisphere, 216f
 Hemiplegia, 150
 Hemochron System, 26
 Heparin
 protamine sulfate reversal and, 26–43, 31f–41f
 Hepatocyte growth factor (HGF), 373
 Heubner arteritis, 253
 Hippel–Lindau syndrome, 405
 Hippocampal artery, 191
 HIV infections, 434
 Hormesis, 84
 Horner syndrome, 6
 Human immunodeficiency virus (HIV), 253
 Hunt and Hess Scale
 for clinical grading of subarachnoid hemorrhage, 266b
 Hydration
 contrast-induced nephropathy, 78
 and diabetic patients, 77
 Hydrocephalus
 management of, 266
 nonaneurysmal perimesencephalic subarachnoid hemorrhage, 387
 Hyoid artery, fetal stage, 101
 5 mm–6 mm, 102
 Hyoid–stapedial artery, development of, 105f
 Hyperglycemia, 493
 Hypervascular glioblastoma multiforme, 314f
 Hypervascular tumors
 embolization of, 405
 head and neck tumors, 401–414
 Hypoglossal artery, 127f, 159, 236
 Hypoplasia, 206
 Hypoxia induced factor (HIF), 405
- I**
- ICRP. *See* International Commission on Radiological Protection
 Idiopathic intracranial hypertension, 445
 Idiopathic venous hypertension
 treatment of, 445
 IHH
 transverse sinuses, 445
 visual loss, 450
 Inferior alveolar (dental) artery, 244
 Inferior choroidal vein, 226
 Inferior ophthalmic vein, 221
 Inferior petrosal sinus (IPS), 218, 342
 Inferior sagittal sinus, 223
 Inferior temporal branches, 191
 Inferior tympanic artery, 234, 236
 Inferolateral trunk, 138, 141f–145f, 143
 Inflammatory aneurysm, 253, 256
 Infraorbital artery, 237, 243
 Infraorbital ramus, of stapedial artery, 16 mm–18 mm and, 106
 Infratentorial venous system, 228–229
 Injection rates, angiogram and, 43, 44f
 Injury. *See also* Arterial injuries
 Internal carotid artery, 132–159, 133f–136f
 agenesis of, 151, 151f, 152f
 anatomic variants of, 150–154
 anatomy of, segments of, 132, 137–150, 137f
 aneurysm, 249
 angiogram, 132
 anterior choroidal artery, 148–150
 cavernous segment of, aneurysms of, 249
 cervical segment of, aneurysms of, 249
 children and, catheter positioning, 138
 clinoidal segment of, 146
 dissecting pseudoaneurysms of, 136f
 giant aneurysms and, 146
 head position and, 135f
 laceration segment of, 132, 137, 139f
 laceration of, 135f
 meningohypophyseal trunk of, 138, 141f
 occipital artery, 138f
 occlusions of, 135f
 ophthalmic segment of, 146–148, 146f–147f
 petrous segment of, aneurysms of, 249
 pseudoaneurysms of, 136f
 reconstitution of, 143f
 segmental nomenclature of, 137f
 stapedial artery variant, 140f
 Townes view of, 150f
 Internal cerebral veins, 227
 Internal jugular vein, 217
 Internal maxillary artery, 238–239, 239f
 International Commission on Radiological Protection (ICRP), 87
 International Study of Unruptured Intracranial Aneurysms (USUIA), 265, 269
 International Subarachnoid Trial (ISAT), 267, 269
 Interpeduncular fossa, 229
 Interventional reference point (IRP), 93f
 Intracerebral varix, 297
 Intracranial aneurysm
 anterior cerebral artery and, 267
 familial history, 264
 risk factors for, 264
 ruptured
 left atrial myxoma and, 257
 natural history and outcome of, 265–266
 Intracranial circulation
 false aneurysms of, 249–252
 Intracranial dissections
 and dissecting aneurysms, 257–258, 258f–263f, 264
 Intracranial dural arteriovenous malformation with myeloplastic syndrome, 362f
 Intracranial dural sinuses and veins, 219f–221f
 Intracranial pseudoaneurysms, 250
 Intracranial saccular aneurysms, 114, 210, 264
 Intradural spinal arteriovenous malformation, 352f–356f
 glomus-type, 351
 hypervascular tumors simulating, 356, 359f, 360f
 intramedullary and perimedullary arteriovenous fistula, 351, 356
 juvenile type, 351, 357f
 paraspinal and epidural, 356, 357f–358f
 Intraparenchymal hemorrhage, 257
 Intrasellar aneurysm, 144f
 Intravenous thrombolytic therapy, 485
 Iodixanol, contrast-induced nephropathy, 78
 IPS. *See* Inferior petrosal sinus
 IRP. *See* Interventional reference point
 ISAT. *See* International Subarachnoid Trial
 Ischemic stroke, endovascular treatment, 485
 intra-arterial treatment, 485–493
 acute basilar artery thromboembolism, 486f
 catastrophic outcome, angiographic procedure, 491f
 emergency carotid stenting, 489f
 left carotid thrombolysis, 489f

- middle cerebral artery, fortuitous revascularization, 492f
thrombolysis in left middle cerebral artery, 487f–488f
intravenous thrombolysis, 485
pial collateral circulation, 493
importance of, 493f–496f
- J**
- Jabbe, 28f
Jacobson branch of glossopharyngeal nerve, 236
Joint Commission for Accreditation of Healthcare Organizations (JCAHO), 88
Jugal vessels, 237
Juvenile angiofibroma
pharyngeal artery supplying, anatomy of, 413f
Juvenile nasal angiofibroma (JNA), 408
computed tomography (CT) and angiographic appearance, 406f–407f
dangerous anastomosis, 412f
intracranial invasion, recurrent, 408f–409f
recurrent with with dangerous anastomoses, 412f
- K**
- Kernohan notch, 183
Kiesselbach plexus, 242
Kiesselbach plexus, 397
Klippel–Feil syndrome, 195
Köhlmeier–Degos syndrome, 434
- L**
- Labial vessels, 237
Lateral clival artery, 143
Lateral medullary infarct, 202
Lateral medullary syndrome, 213
Lateral posterior choroidal arteries, 190
Lenticulostriate arteries, 177f
Lesser descending palatine artery, 243
Lingual artery, 236–237, 237
Linguo-facial trunk and buccal artery, 237f
Longitudinal neural arteries, 102
Longitudinal neural plexi, 4 mm fetal stage of, 102
Lumbar segmental arteries, catheter and, 55
- M**
- Magnification errors, angiogram and, 43–44
Mandibular artery, fetal stage, 101
Mandibulovidian artery, 242, 245
Marginal and basal tentorial arteries, 138, 142f
Marginal sinus, 218
Masseteric arteries, branches of, 244
Matrix metalloproteinases (MMP), 298
Maxillomandibular branch, 106
Medial hemispheric superficial veins, 223
Medial posterior choroidal arteries, 186, 189f, 190
Median artery of the corpus callosum, 171
Megadolichobasilar anomaly, 253, 254f
- MELT study, 490
Meningeal veins, 217
Meningioma, sunburst radial pattern, 413f
Meningohypophyseal trunk, 138, 236
Meningolacrimal artery, 106
MERC1 catheters, 493
Microbubbles
during cerebral angiography, 72f, 73–75, 73f, 74f
Microcatheter angiography, in infant, 62f–63f
Microemboli
during cerebral angiography, 72f, 73–75, 73f, 74f
Middle cerebral artery, 175–181
anomalies of, 180f–181f, 181
anterior temporal branch of, 178, 178f
bilateral accessory, 181f
branching patterns of, 175, 177f
cortical branches of, 176–179, 177f, 178f, 179f
duplicated, 180f
fenestrations of, 180f
fetal stage, 7 mm–12 mm, 103
giant serpentine aneurysm of, 179f
perforating branches of, 175–176, 177f
segmental anatomy of, 175, 176f
trifurcation pattern, 175
Middle meningeal artery, 239–240, 240f, 394, 396
ophthalmic artery supplied, 397f
orbital branch of, 106
Mikaelsson catheter, segmental artery and, 55
Military personnel, radiation exposure and, 82
Modified Rankin Scale, 485
Moniz, Égas
life history of, 5–6, 5f
Moore–Corradi technique, 267
Moya–Moya disease and syndrome, 371–373, 371f, 372f
Musculospinal artery, 234
Mycotic aneurysms
incidence and presentation of, 253, 255f, 257f
management of, 256
of right middle cerebral artery, 255f
- N**
- N-acetylcysteine (Mucomyst), contrast-induced nephropathy, 78
NASCET trial, 466
Nasopharynx, 397
N-Butylcyanoacrylate (NBCA), 314–315
preparation of, 315f
Neck. *See also* ENT bleeding
airway protection, 414
bleeding, 414–417
hemodynamic stabilization, 414
paragangliomas, 405
tumor, 408
Neuromeningeal trunk, 234, 236
Nicardipine, calcium blocker drugs, 459
NIHSS score, 493
Nimodipine, treating vasospasm, 458
NINDS rt-PA study, 485
Nitinol Neuroform stent, 277f
- O**
- Occipital artery, 150, 237–238
Occlusive diseases
angiographic study and, 12
Oculomotor nerve, 114, 117
Oncotic intracranial aneurysms, 256–257, 257f
Onyx
AVM embolization and, 315, 316f–318f
Onyx HD-500, 282, 284
technique and complications, 284f
treatment of recurrent carotid–ophthalmic aneurysm, 283f
Ophthalmic artery, 394, 396f, 398f
dural branches of, 147f
meningeal artery and, 147f
normal physiology, interruption of, 399f
prominent ethmoidal branches, 398f
Ophthalmomeningeal sinus, 107
Orbital anastomoses, 240f
Osler–Rendu–Weber syndrome, 312
Otic artery, 107, 159
- P**
- Paragangliomas
head and neck, 405
and juvenile angiofibromas, 405
Paraspinal arteriovenous malformation, 356
Paraterminal gyrus, 223
Parieto-occipital arteriovenous malformation, 191f
Parieto-occipital artery, 191
Parkinson disease, 150
Papaverine, pharmacologic effects, 458
Patient
evaluation, Doppler and, 11
Pediatric cerebral arteriopathy, 368–371
Pediatric neuroangiography, 58–64
arteriotomy and sheath, 58, 59f
catheter and wire length, 60
contrast volume, 60, 61f–63f, 64
groin compression, 58, 60f
radiation protocol, 58
Pediatric stroke, 368
Peduncular segment, of posterior cerebral artery, 183, 185f
Pelvic vascular tumor, 361
Percutaneous transluminal angioplasty (PTA), 75
Pericallosal artery, 169–170, 171f
Perimedullary spinal arteriovenous malformation, 354f
Perimesencephalic hemorrhage, 388f
Perinatal stroke, 368
Persistent hypoglossal artery, 156f–158f, 157–159, 158f
Persistent stapedia artery, 152
Persistent trigeminal artery, 143, 154, 154f–156f
Petrosal sinuses, 229
Petrous internal carotid artery
caroticotympanic branch of, 137
mandibulovidian branch of, 137, 140f
Pharyngeal trunk, 234
Pial collateral flow, 493
Pial fistula, 351
Platelet-derived growth factors (PDGF), 405
Polyarteritis nodosa, 253, 254f
Polytetrafluoroethylene (PTFE), 383

- Polyvinyl alcohol (PVA)
 biologic effects, 403
 catheterized and embolized, 401
 embolization, of AVM, 318
 gelfoam sponge, 403
 push technique, 401f
 use of, 398
- Pontomedullary junction, 210
- Pontomesencephalic vein, 229
- Posterior auricular artery, 238
- Posterior cerebral artery, 183–193, 184f
 brainstem branches of, 186
 branches, 186
 circumflex branches of, 186
 collateral potential of, 185f
 cortical branches of, 190–193, 190f–193f
 dissecting aneurysm of, 187f, 188f
 Hippocampal branches of, 191
 peduncular perforating branches of, 186
 segmental nomenclature of, 183
 temporal branches of, 191
 thalamic branches of, 186
 thalamic perforator arteries of, 186, 187f, 188f
 thalamoperforator arteries of, 186
 ventricular branches of, 186, 190
- Posterior choroidal arteries
 lateral, 190
 medial, 186, 190
- Posterior fossa
 arteries of, 206–216, 211f, 212f
 Townes projection of, 208f
- Posterior inferior cerebellar artery
 cervical origin of, 198f
 duplicated origin of, 76f
 meningeal branches of, 214
 Townes projection of, 198f
- Posterior inferior hypophyseal artery, 138, 143
- Posterior meningeal artery, 214
- Posterior pericallosal artery, 191
- Posterior reversible encephalopathy syndrome (PRES), 426
- Posttonsillectomy bleeding, 417–422, 423f
- Posterior temporal artery, 191
- Posterior thalamic veins, thalamus and, 227
- Post-tonsillectomy bleeding, 237
- Precentral cerebellar vein, 229
- Pregnancy
 basilar artery thromboembolism, acute, 486f
 Premamillary artery, 114
- Preocclusive carotid disease, sign of, 134f
- Prenatal MRI, 498
- Primitive aortic arches, 101f
 pairs of, 100
- Primitive dorsal ophthalmic artery, 102
- Primitive hypoglossal artery, 4 mm fetal stage of, 102
- Primitive internal carotid artery
 caudal division, 102
 cranial division, 102
- Primitive maxillary artery, 102, 152–154
- Primitive trigeminal artery, 102
- PROACT studies, 490
- Proatlantal and otic arteries, etymology of, 107
- Proatlantal artery, 107, 157f
- Proatlantal intersegmental artery, 154–157, 156f–157f, 195, 237
- Proatlantal type II artery, 113
- Prominent occipital sinus, 222f
- Protamine sulfate reversal
 and heparin, 26–43, 31f–41f
- Pseudoaneurysm, 249
- Pseudomeningeal appearance, 244
- Pterygoid plates, 237
- Pterygoid plexus, 217, 218
- Pterygopalatine Fossa, 240t
- Pterygovaginal artery, 244–245
- Pterygovaginal branch of internal maxillary artery, 242
- Pulse oximetry, 17
- ## Q
- Quadrigeminal segment, of posterior cerebral artery, 183
- ## R
- Radial artery access, 14–18
- Radial artery compression, Terumo band for, 17f
- Radiation
 biologic responsiveness to, quantification of, 86–87
 dose and exposure quantification, 86–88
 dose-response curve, 83–84, 83f
 effects of, 82–83
 exposure in neuroangiographic procedures, 88–89
 partial body exposure and, 87
 pediatric patient exposure, 89–91
 reducing, 95t
 risks, safety and, 82–95
 stochastic effects of, 85–86, 85t
 x-rays, 84–85
- Radiation protocol
 pediatric neuroangiography and, 58
- Radiologic diagnosis, 450
- Radio-opaque microcatheter, 42
- Radium dial painters, radiation exposure risks and, 82
- Rathké pouch, 102
- Recoil electron, 84
- Recurrent artery of Heubner, 103, 165–167, 168f
- Recurrent artery of the foramen lacerum, 143
- Recurrent meningeal artery, 106
- Renal failure, contrast-induced nephropathy, 78
- Retromandibular vein, 217
- Reversible cerebral vasoconstriction syndrome (RCVS), 426
 angiographic abnormalities, 429
 angiographic appearance, 429
 angiographic findings, 429
 clinical presentation, 426–429
 endovascular angioplasty, 430f
 etiologies and associations, 429t
 intracranial vasculitis, 432f
 marijuana-related, 427f–428f, 430f
 non-perimesencephalic subarachnoid hemorrhage, 428f
 right common carotid arteriogram lateral view, 427f
 serotonin uptake inhibitor, uses, 431f
 spasmodic infusion, 430f
 symptomatic management, 429
 treatment of, 429–432
- Right aortic arch, 109, 112, 112f
- Right cerebellar hemisphere, hemangioblastoma of, 216f
- Robinow syndrome, 371
- Roentgen equivalent man (REM), 86
- Rosenmuller fossa, 132
- Ruptured aneurysm. *See* Aneurysmal rupture
- Ruptured intracranial aneurysms, history of, 265–266, 266b
- ## S
- Saccular (Berry) aneurysms, 264–265
- SAMMPRIS study, 474
- Schwalbe foramen, 206
- Seckel syndrome, 371
- Seldinger technique, 13
- Septal vein, 228
- Serpentine aneurysm, 254f
- Sheath/dilator advancement, 16f
- Sheath placement, arterial puncture and, 13–14, 15f–17f
- Sievert (Sv), 86
- Simmons curve, 17
- Simmons-type catheter, 43
- Sinonasal bleeding, 397–401
 angiographic evaluation, 398
- Sodium bicarbonate, contrast- induced nephropathy, 78–79
- Source image distance (SID), 58
- SOV. *See* Superior ophthalmic vein
- SPECT scanning, 422
- Spetzler–Martin Scale
 for arteriovenous malformation, 308t
- Sphenobasal sinus, 107
- Sphenoidal artery, 106
- Sphenoid wing meningioma, 147f
- Sphenopalatine arteries, 242
 ethmoidal branches of, 239f
- Sphenopalatine fossa, 238, 242
- Sphenoparietal sinus, 218, 223
- Sphenotemporal sinus, 107
- Spinal angiography, 52–57
 anesthesia during, 52
 diagnostic, setup for, 53f
 indications, 52, 53t
 technical aspects, 52–54, 53f–55f
 vessel selection during, 54–57, 56f, 57f
- Spinal arteriovenous malformation, 351
 with venous hypertension, 354f–355f
- Spinal cord vascular malformation, 351
- Spinal dural arteriovenous malformation, 52, 351, 359
 treatment of, 363, 364f, 365f
- Spinal dural vascular disease, pathophysiology of, 359–365
- Spinal hemangioblastoma, 359f
 with bladder dysfunction and paraparesis, 360f
- Spinal vascular malformations, 351–365
 endovascular treatment of, 359
- Spinal venous hypertension
 clinical manifestations of, 361–362
- Splenic artery, 191–193
- Stapedial artery
 fate of, 104–106
 fetal stage
 12 mm–14 mm, 103
 16 mm–18 mm, 104–106
 infraorbital ramus of, 16 mm–18 mm and, 106
 supraorbital ramus of, 16 mm–18 mm and, 106
- Stroke
 childhood, 368

- incidence, 466
 intra-arterial procedures, 490
 pediatric, 368
 perinatal, 368
 risk, 465
- Sturge-Weber syndrome, 312
- Stylomastoid artery, 238
- Subarachnoid hemorrhage, 387–392
 angiographically negative, 389f–392f
 causes of, 387
 cerebral angiography and, 387
 negative cerebral angiography and, 387
 pretruncal, 388f
- Subclavian artery and cervical trunk variations, 112f
- Sulcus limitans of Reil, 176
- Superficial anastomotic veins, 224f
- Superficial supratentorial cortical veins, 223
- Superficial temporal artery, 238, 238f, 239f
- Superior alveolar (dental) artery, 244
- Superior anterior communicating artery, 118, 172
- Superior cerebellar artery, 214–215, 214f–216f
- Superior choroidal vein, 226
- Superior hypophyseal arteries, 148, 148f
- Superior labial arteries, 237
- Superior ophthalmic vein (SOV), 221, 342, 347f
- Superior petrosal sinus, 218
- Superior sagittal sinus, 223
- Superior thyroidal artery, 231, 232f–234f, 234f
- Supraorbital ramus, of stapedial artery, 16 mm–18 mm and, 106
- Supratentorial intradural venous system, 223–224, 223f
- Swan-Ganz catheter, 316
- Sylvian fissure, 223
- Sylvian triangle, 176, 177f
- Sylvian vein, 217, 218, 223
- Symptomatic carotid artery stenosis, 465
- Symptomatic intracranial atherosclerotic disease
 stenosis, 473
 treatment for, 476
 warfarin anticoagulation, 474
 hemorrhage, 485
- Symptomatic posterior circulation atherosclerotic disease, 467
- T**
- TCD. *See* Transcranial Doppler
- Tela choroidea, 227
- Telangiectasis, 291, 292f
- Tentorial arteries, 138, 142f
- Tentorial incisura, herniation through, 183
- Tentorium cerebelli, 229, 240
- Terumo band, for radial artery compression, 17f
- Thalamic veins, 226–227
 anterior, 227
 inferior, 227
 posterior, 227
- Thalamostriate vein, 226
- Thalamotuberal artery. *See* Premamillary artery
- Thalamus
 posterior thalamic veins and, 227
- Thyroid cartilage, 442
- Thorotrast, 6–10, 7f
 carotid angiography with, 8f, 9f
 exposure, Townes view of vertebral artery and, 9f
 patients, follow-up studies of, 8–10
- Tic douloureux, 215
- Tissue-weighting factor (W_T), 87
- Torcular Herophili, 107, 217, 218
- Tortuous vessels, 35
- Townes projection of posterior fossa, 208f
- Transcranial Doppler (TCD), 73
- Transient global amnesia, cerebral angiography and, 75
- Transmastoid branch, 238
- Transverse sinuses
 IHH, 445
 types of deformities, 450
- Transverse facial artery, 238, 238f
- Traumatic intracranial aneurysms, 250–252, 251f, 252f. *See also* False aneurysms
- Trigeminal artery, 127f, 155f, 207
- Trigeminal nerve, 215
- Tuohy-Borst valve, 60
 system, 22, 23f
- U**
- Unruptured aneurysm, endovascular treatment for, efficacy of, 269
- Unruptured intracranial aneurysms, history of, 265
- Uranium miners, radiation exposure risks and, 82
- USUIA. *See* International Study of Unruptured Intracranial Aneurysms
- V**
- Vascular endothelial growth factor (VEGF), 298, 373
- Vascular malformation
 brain, 291–319
 spine, 351–365
- Vascular endothelial growth factor (VEGF), 429
 protein, 405
- Vasculitides. *See* Central nervous system (CNS)
- Vasoactive peptides, hypertensive response, 413f
- Vasospasm
 angiographic evidence, 457
 management of, 266
 triple-H therapy for, 266
- Vasospasm angioplasty
 graduated cadence syringe (MTI) for, 459f
- VEGF. *See* Vascular endothelial growth factor
- Vein of Galen, 170, 218, 223, 224
- Vein of Galen aneurysm, 107
- Vein of Labbé, 218, 223, 344
- Vein of Rosenthal, 107
- Vein of Trolard, 218, 223
- Venous angioma, 297
- Venous drainage, anomalies of, 296f, 297–299, 297f–299f
- Venous embryology, 106–107
- Venous hypertension and cavernous sinus, 222f
- Venous malformation, 297
- Venous sinus compression, 368
- Venous system, 217–229
- Ventral pharyngeal artery, 102
- Ventral pharyngeal system, 102
- Ventral primitive ophthalmic artery, 103
- Venturi effect, 32
- Vertebral arteries, 53t, 473
 dissection of, 200–202, 201f–204f
 extradural, 195–204
 intracranial segment of, 206–207, 210
 occipital artery
 C1 and C2 anastomotic connections, 394, 396f
 variants, 112–113, 112f
- Vertebral artery dissection
 with presumed fibromuscular dysplasia, 202f
 unruptured left, 260f
- Vertebral artery pseudoaneurysm
 covered stent for treatment, 415f
 postsurgical
 covered stent for treatment, 416f
- Vertebrobasilar junction, 206
- Vertebrobasilar systems, 120
- Vessel
 selection, during spinal angiography, 54–57, 56f, 57f
- Vidian artery, 137
- Vidian canal, 101, 245
- Vidian nerve, 132
- W**
- Wada testing, 154
 trigeminal artery in, 154f
- Wallenberg infarct, vertebral artery dissection and, 202
- Wallenberg syndrome, 213
- WASID study, 474
- Watershed zone, 176
 shift of, 176
- Weighting factor (W_R), 86
- Willis, Thomas
 life history of, 2–4, 3f, 4f
- Wire technique, 476
- Wyburn-Mason syndrome, 312
- X**
- X-rays
 children, tinea capitis and, 88
 coherent scattering, 84
 Compton effect with, 84
 effective doses of, 87t
 energy and, 84
 HE and, 87
 photoelectric effect and, 84
 radiation, 84–85
 thyroid gland and, childhood tinea capitis and, 88
 tinea capitis and, 88–94, 88f, 90f–94f
- Z**
- Zygomatiko-orbital artery, 238